ABSTRACT BOOK

Association for Research in Otolaryngology

39th Annual MidWinter Meeting

Saturday, February 20-

Wednesday, February 24, 2016

Manchester Grand Hyatt

San Diego, CA

ARO OFFICERS FOR 2015-2016

PRESIDENT

Lawrence R. Lustig, MD (15-16)
Columbia University Medical Center
Department of Otolaryngology-HNS
Harkness Pavillion, Suite 818
180 Fort Washington Avenue
New York, NY 10032 USA

PRESIDENT ELECT

Matthew W. Kelley. PhD (15-16)
NIDCD/NIH-Porter Neuroscience
Research Center
Building 35, Room ID-993, 35 Convent Drive
Bethesda, MD 20892 USA

PAST PRESIDENT

Ruth Anne Eatock, PhD (15-16)
University of Chicago
Department of Neurobiology
947 East 58th Street, Mail Code 0928
Chicago, IL 60637 USA

SECRETARY/TREASURER

Elizabeth S. Olson, PhD (14-17)
Columbia University
Otolaryngology & HNS
630 West 168th Street
New York, NY 10032 USA

EDITOR

Barbara G. Shinn-Cunningham, PhD (15-18)
Boston University
Center for Computational Neuroscience & Neural Technology
677 Beacon Street
Boston, MA 02215 USA

HISTORIAN

David J. Lim, MD
UCLA Geffen School of Medicine
Department of Head & Neck Surgery
2100 West Third Street
Los Angeles, CA 90057 USA

COUNCIL MEMBERS AT LARGE

Howard Francis, MD (13-16)
Johns Hopkins School of Medicine
Department of Otolaryngology – HNS
601 North Caroline Street
Baltimore, MD 21287-0910 USA

Sharon G. Kujawa, PhD (14-17)
Massachusetts Eye and Ear Infirmary
Department of Otology and Laryngology
243 Charles Street
Boston, MA 02114 USA

Jennifer S. Stone, PhD (15-18)
Research Associate Professor
Department of Otolaryngology
VM Bloedel Hearing Research Center
CHDD CD 176 Box 357923
University of Washington
Seattle, WA 98195 USA

Haley Brust
Talley Management Group
19 Manna Road
Mt. Royal, NJ 08061 USA
Ph: 1 (856) 423-7222 EXT. 103
Fax: 1 (856) 423-0041
Email: hbrust@TALLEY.com
headquarters@aro.org

ABSTRACTS OF THE 39TH ANNUAL MIDWINTER MEETING OF THE

On behalf of the ARO Council, I would like to welcome you to the 39th ARO MidWinter Meeting in San Diego! Thanks to the work of the Program Committee under the direction of Dr. Ruth Litovsky, we have a truly exciting program lined up. There are over 1168 submitted presentations, 215 symposia, and 952 posters spanning the entire range of auditory and vestibular basic, clinical and translational science. This year in particular we would also like to welcome the members of the NHCA who have decided to join us.

The **Presidential Symposium** *(Saturday 8:00am–12:00pm),*"Cochlear Gene Therapy" will summarize the current state of progress of using virally-mediated gene therapy to treat disorders of hearing and balance. These will include a lecture on gene therapy for eye diseases by one of the world's top researchers in this field (Dr. Jean Bennett). Additional speakers will discuss the regulatory landscape (Dr. Dan Salomon), the perspective from industry (Douglas Brough from GenVec), the status of genetic testing for hearing disorders (Dr. Richard Smith), and current applications of gene therapy for hearing disorders in animals (Dr. Jeff Holt and Dr. Christine Petit). Lastly, the experiences of the first gene therapy study for hearing loss in humans will be summarized by Dr. Hinrich Staecker.

At the **ARO Business Meeting** *(Sunday 6:00pm-7:00pm),* we will update the state of the Association, transfer leadership from the 2015 Council to the 2016 Council, including the new President, Dr. Matt Kelley, and hand out prizes – you can enter the prize draw when you visit the exhibits.

This year we have arranged a special combined program with the **San Diego Symphony** scheduled for Saturday evening *(7:30pm–9:30pm).* The evening will begin with a special lecture by Dr. Charles Limb, who will be discussing the relationship between music and hearing, featuring his research in patients with hearing loss and cochlear implants. We have arranged a special reduced admission for this event and would strongly encourage you to look into attending this very special evening.

At daily **Mentoring Sessions** for young investigators (*Saturday, Sunday and Monday 4:30–5:30pm and 12:15–1:30pm on Tuesday*), mentors and peers exchange ideas on different topics in navigating careers. We hope you take advantage of this unique program geared towards students, post-docs and junior faculty.

At the **Awards** ceremony *(Monday 6:00-7:30 pm)* and reception *(7:30-8:30 pm)*, we celebrate the people and work that merited several awards, including the **Young Investigator Award** and the **ARO Award of Merit**: **Dr. Geoffrey Manley** for pioneering research in cochlear physiology across vertebrate species.

We are also proud to announce the return of the **Hair Ball** *(Tuesday 8:00pm–12:00am).* This popular event began in 2006 as an offsite "Patch-Clampers Ball" instigated by those hair cell and dance enthusiasts Bill Roberts, Mark Rutherford and Paul Fuchs and remains one of the most fun traditions of the MidWinter meeting.

Each MidWinter Meeting depends on the hard work and innovative contributions of many ARO members in various committees, especially the Program Committee, with energetic and thoughtful assistance from Talley Management. Without the combined efforts of each and every one of them, this meeting would not continue to be the success it has been. To help us continue to improve, please respond to a survey you will be sent after the meeting, and consider joining a committee - see "About Us" at www.aro.org for the options and contact headquarters@aro.org to volunteer.

Best wishes for a productive, and more importantly, fun meeting.

Lawrence Lustig
ARO President, 2015-2016

CONFERENCE OBJECTIVES
At the conclusion of the MidWinter Meeting, participants should be better able to:

- Explain current concepts of the function of normal and diseased states of the ear and other head and neck structures
- Recognize current controversies in research questions in auditory neuroscience and otolaryngology
- Describe key research questions and promising areas of research in otolaryngology and auditory neuroscience

REGISTRATION

The 2016 MidWinter Meeting Registration Desk is located in the Harbor Foyer and Terrace and will be open and staffed during the following hours:

Friday, February 19	4:00 PM-7:00 PM
Saturday, February 20	7:00 AM-6:00 PM
Sunday, February 21	7:00 AM-6:00 PM
Monday, February 22	7:00 AM-6:00 PM
Tuesday, February 23	7:00 AM-6:00 PM
Wednesday, February 24	7:30 AM-12:00 PM

SPEAKER READY ROOM

The 2016 Program Committee is committed to providing attendees cutting edge technology and coordinated presentations at the MidWinter Meeting. To be fully prepared for your session, each presenter is requested to visit the Speaker Ready Room at least 24 hours prior to your presentation. The Speaker Ready Room is located in the **Show Office 5** and will be open the following days and times:

Friday, February 19	4:00 PM - 7:00 PM
Saturday, February 20	7:00 AM-6:00 PM
Sunday, February 21	7:00 AM-6:00 PM
Monday, February 22	7:00 AM-6:00 PM
Tuesday, February 23	7:00 AM-6:00 PM
Wednesday, February 24	7:00 AM-10:00 AM

ADMISSION

Conference name badges are required for admission to all activities related to the 39th Annual MidWinter Meeting, including the Exhibit Hall and social events.

PROGRAM AND ABSTRACT BOOKS

A limited supply of the abstract will be available for purchase at the ARO MidWinter Meeting Registration Desk. Electronic copies of the books are also available online at www.aro.org.

MOBILE DEVICES

As a courtesy to the speakers and your fellow attendees, please switch your mobile device(s) to silent while attending the sessions.

RECORDING POLICY

ARO does not permit audio or photographic recording of any research data presented at the meeting.

BREAKS

Complimentary coffee and tea will be available in the morning and at selected breaks.

ASSISTED LISTENING DEVICES

A limited amount of assisted listening devices are available at the ARO MidWinter Meeting Registration Desk, courtesy of Phonak.

A SPECIAL NOTE FOR THE DISABLED

ARO wishes to take steps that are required to ensure that no individual with a disability is excluded, denied services, segregated or otherwise treated differently than other individuals because of the absence of auxiliary aids and services. If you need any auxiliary aids or services identified in the American with Disabilities Act, or any assistance in registering for this course please contact ARO Meetings Department at meetings@aro.org; via telephone at 1 (856) 423-0041, option 2; or write to ARO Meetings Department, 19 Mantua Road, Mt. Royal, NJ 08061 USA.

FAMILY ACTIVITIES / CHILD CARE

Please contact the Hotel Concierge for information about off-site activities and tourism needs. Subsidized onsite day care is being offered through an experienced, accredited company, KiddieCorp. The child care room is located in **Mission Beach**.

Shilo Harris came from a family with deep roots in military service. As a son of a Vietnam veteran, Shilo always knew he wanted to be a soldier. On September 11th his life changed forever and shortly afterward he enlisted as a Cavalry Scout in the US Army. His first deployment was to Schweinfurt, Germany with the 1st Infantry Division. From Germany Shilo headed to war-torn Iraq.

On his second deployment with the 10th Mountain Division he was assigned and worked near southern Baghdad. On February 19, 2007, Harris' armored vehicle was struck by an improvised explosive device (IED). The explosion injured the driver and ended the lives of three of his fellow soldiers. Shilo survived but with severe third degree burns on 35% of his body. The severity of the burns meant the loss of Shilo's ears, the tip of his nose and three fingers. The crushing explosion fractured his left collarbone and C-7 vertebrae.

The devastating injuries required that Shilo remain in a medically induced coma for 48 days; after, he spent nearly three years recovering and undergoing intensive physical therapy at the burn unit of Brooklyn Medical Center (BAMC) in San Antonio, TX. While at BAMC, he was the first soldier to participate in cutting-edge regenerative stem-cell research to regrow his fingers, and later received prosthetic ears. Shilo's recovery has involved more than 75 surgeries, which required his family to spend up to six hours a day on wound care. Shilo also struggled from PTSD. In 2010 he was medically retired from the Army. Shilo reflects on his time in the service and his injuries: "Everything in life is a gift. Sometimes it may not be the gift you want but you realize that your challenges are a new beginning."

Shilo is a family man who is committed to five children, and also a devout Christian. In 2012, the Harris family was the recipient of ABC's *Extreme Makeover: Home Edition* and was provided with a new home equipped to serve the needs of Shilo's unique medical and physical circumstances. Today, Shilo is a motivational speaker, sharing his story with groups around the country, raising awareness for PTSD and serving as an inspiration to fellow soldiers.

PROGRAM

CHAIR:

Ruth Y. Litovsky, PhD (3/14-2/17)

MEMBERS:
Carolina Abdala, PhD (3/14-2/17)
Kumar Alagramam, PhD (3/13-2/16)
Jennifer Bizley, PhD (3/14-2/17)
Alan Cheng, MD (3/13-2/16)
Rick Friedman, MD, PhD (3/15-2/18)
Erick Gallun, PhD (3/14-2/17)
Ronna Hertzano, MD, PhD (3/15-2/18)
Larry Hoffman, PhD (3/12-2/17)
Philip X. Joris, MD, PhD (3/13-2/16)
Brian McDermott, PhD (3/15-2/18)u
Jeff Lichtenhan, PhD (3/13-2/16)
Barbara Shinn-Cunningham, PhD (3/14-2/17)
Jenny Stone, PhD (3/13-2/16)
Xiaoqin Wang, PhD (3/14-2/17)
Council Liaison: Ruth Y. Litovsky, PhD (3/14-2/17)
spARO Representative: Michelle Valero

ANIMAL RESEARCH

CHAIR:

Claus-Peter Richter, MD, PhD (3/13-2/16)

MEMBERS:
Wei Dong, PhD (3/14-2/17)
Steve Eliades, MD, PhD (3/15-2/18)
James Fallon, PhD (3/14-2/17)
Rudolf Glueckert, PhD (3/14-2/17)
Andrej Kral, MD, PhD (3/13-2/16)
Stéphane Maison, PhD (3/14-2/17)
Chandrakala Puligilla, PhD (3/13-2/16)
Sonja Pyott, PhD (3/15-2/18)
Suhrud Rajguru, PhD (3/14-2/17)
Maike Vollmer, MD, PhD (3/13-2/16)
Council Liaison: Sharon Kujawa, PhD (3/15-2/16)
spARO Representative: Rebecca Curry

AWARD OF MERIT

CHAIR:

Eric D. Young, PhD (3/13-2/16)

MEMBERS:
Catherine E. Carr, PhD (3/14-2/17)
David P. Corey, PhD (3/13-2/16)
Ana Belen Elgoyhen, PhD (3/15-2/18)
Stefan Heller, PhD (3/14-2/17)
Michael McKenna, MD (3/15-2/18)
John Middlebrooks, PhD (3/14-2/17)
Chris Schreiner, MD, PhD (3/15-2/18)
Karen P. Steel, PhD (3/13-2/16)
Steve D. Rauch, MD (3/13-2/16)
Council Liaison: Past-President Ruth Anne Eatock (3/15-2/16)

DIVERSITY & MINORITY AFFAIRS

CHAIR:

Avril Genene Holt, PhD (3/13-2/16)

MEMBERS:
Deniz Başkent, PhD (3/13-2/16)
Evelyn Davis-Venn, PhD (3/15-2/18)
Michael Hoa, MD (3/14-2/17)
Mirna Mustapha, PhD (3/14-2/17)
Diana Peterson, PhD (3/14-2/17)
J. Tilak Ratnanather, DPhil (3/13-2/16)
Shurud Rajguru, PhD (3/13-2/16)
Lina Reiss, PhD (3/13-2/16)
Astin Ross, PhD (3/15-2/18)
Council Liaison: Howard W. Francis (3/15-2/16)
spARO Representative: Chang Liu

EXTERNAL RELATIONS

CHAIR:

Dan Lee, MD (3/15-2/18)

MEMBERS:
Julie Bierer, PhD (3/13-2/16)
Keith Duncan, PhD (3/15-2/18)
Jonathan Fritz, PhD (3/13-2/16)
Hubert Lim, PhD (3/15-2/18)
Yunxia (Yesha) Wang Lundberg, PhD (3/15-2/18)
Cynthia Morton, PhD (3/14-2/17)
Debara Tucci, MD (3/14-2/17)
Shinichi Someya, PhD (3/15-2/18)
Beverly Wright, PhD (3/13-2/16)
Jinsheng Zhang, PhD (3/13-2/16)
Council Liaison: Sharon Kujawa, PhD (3/15-2/16)
spARO Representative: Karolina Charaziak

FINANCE AND INVESTMENT

CHAIR:

Paul Fuchs, PhD (3/14-2/17)

MEMBERS:
John P. Carey, MD (3/14-2/17)
Erick Gallun, PhD (3/15-2/18)
Matt Kelley, PhD (3/14-2/17)
Neil Segil, PhD (3/15-2/18)
Christopher Shera, PhD (3/14-2/17)
Ex-officio: *Secretary-Treasurer* Elizabeth S. Olson, PhD (3/14-2/17)

INTERNATIONAL

CHAIR:

Andrej Kral, MD, PhD: Germany (3/13-2/16)

MEMBERS:
Alan Brichta, PhD: Australia (3/14-2/17)
Alain Dabdoub, PhD: Canada (3/13-2/16)
Andy Forge, PhD: UK (3/13-2/16)
Juichi Ito, MD, PhD: Japan (3/14-2/17)
Christian Lorenzi, PhD: France (3/13-2/16)
ShiNae Park, MD, PhD: Korea (3/15-2/18)
Yilai Shu, MD, PhD: China (3/15-2/18)
Joris Soons, PhD: Belgium (3/15-2/18)
Jan Wouters, PhD: Belgium (3/13-2/16)
Council Liaison: Jennifer Stone, PhD (3/15-2/16)

JARO – JOURNAL OF THE ASSOCIATION FOR RESEARCH IN OTOLARNYGOLOGY

JARO EDITORIAL BOARD
Paul B. Manis, PhD, Editor-in-Chief (2011-2016)
University of North Carolina at Chapel Hill
Department of Otolaryngology – HNS
G127 Physician's Office Building CB #7070
Chapel Hill, NC 27599-7070 USA
Ph: 1 (919) 843-9318
Fax: 1 (919) 966-7656
E-mail: pmanis@med.unc.edu

ASSOCIATE EDITORS
Julie Bierer, PhD (2015-2018)
Alan Brichta, PhD (2015-2018)
Christian Chabbert, PhD (2012-2015)
Bertrand Delgutte, PhD (2013-2016)
Mark Eckert, PhD (2013-2016)
Ana Belén Elgoyhen, PhD (2013-2016)
W. Robert J. Funnell, PhD (2013-2016)
Elisabeth Glowatzki, PhD (2015-2018)
Ronna Hertzano, MD, PhD (2015-2018)
Richard Lewis, MD (2015-2018)
Ruth Litovsky, PhD (2013-2016)
Brigette Malgrange, (2015-2016)
John Middlebrooks, PhD (2015-2018)
Donata Oertel, PhD (2013-2016)
Christopher Plack, PhD (2013-2016)
Adrian Rees, PhD (2015-2018)
Xiaorui Shi, MD, PhD (2013-2016)
Susan Shore, PhD (2015-2018)
George A. Spirou, PhD (2014-2017)
Marcel van der Heijden, PhD (2014-2017)
Marianne Vater, PhD (2013-2016)

LONG RANGE PLANNING

CHAIR:

Steven H. Green, PhD (3/14-2/17)

MEMBERS:
Karina Cramer, PhD (3/15-2/18)
Amy Donahue, PhD, *NIDCD Rep.*
Judy Dubro, PhD (3/15-3/18)
Lisa Goodrich, PhD (3/14-2/17)
Ana Kim, MD (3/15-2/18)
KC Lee, ScD (3/13-2/16)
Tobias Moser, MD (3/14-2/17)
Sunil Puria, PhD (3/13-2/16)
Mark Rutherford, PhD (3/15-2/18)
Council Liaison: President-Elect: Matt Kelley (3/15-2/16)
Chair, International Cmte: Andraj Kral, MD, PhD (3/14-2/17)
spARO Representative: Anna Diedesch

MEMBERSHIP

CHAIR:

Chris J. Sumner (3/14-2/17)

MEMBERS:
Deniz Başkent, PhD (3/15-2/18)
Bernd Fritzsch, PhD (3/15-2/18)
Sam Gubbels, MD (3/14-2/17)
Colleen Le Prell, PhD (3/14-2/17)
Dan Polley, PhD (3/14-2/17)
William H. Slattery, MD (3/15-2/18)
Council Liaison: Jennifer Stone, PhD (3/15-2/16)

NOMINATING

CHAIR:

Ruth Anne Eatock, PhD (3/15-2/16)

MEMBERS:
Paul Fuchs, PhD (3/15-2/16) (elected position)
Mark Warchol, PhD (3/15-2/16) (elected position)
(appointed position) – TBA
(appointed position) – TBA

PUBLICATIONS

CHAIR:

Anil K. Lalwani, MD (3/13-2/16)

MEMBERS:

Yuri M. Agrawal, MD (3/13-2/16)
Maria Chait, PhD (3/14-2/17)
Gestur B. Christianson, PhD (3/15-2/18)
Gregory I. Frolenkov, PhD (3/15-2/18)
Elisabeth Glowatzki, PhD (3/14-2/17)
Kuni H. Iwasa, PhD (3/15-2/18)
Charles J. Limb, MD (3/13-2/16)
Hinrich Staecher, MD, PhD (3/15-2/18)
Chris Stecker, PhD (3/13-2/16)
Kelly L. Tremblay, PhD (3/13-2/16)
JARO Editor: Paul B. Manis, PhD, *ex officio*
Springer Representative: Ann Avouris, *ex officio*
Secretary/Treasurer: Elizabeth S. Olson, PhD (3/14-2/17)
Council Liaison: Barbara G. Shinn-Cunningham, PhD (3/15-2/16)
spARO Representative: David Morris

TRAVEL AWARDS

CHAIR:

Ronna Hertzano, MD, PhD (3/14-2/17)

MEMBERS:

Karen Banai, PhD (3/15-2/18)
Mike Bowl, PhD (3/14-2/17)
Benjamin Crane, MD PhD (3/14-2/17)
Elizabeth Driver, PhD (3/14-2/17)
Matt Goupell, PhD (3/14-2/17)
Michael Anne Gratton, PhD (3/15-2/18)
Hainan Lang, MD, PhD (3/15-2/18)
Tomoko Makishima, MD, PhD (3/15-3/18)
Chandrakala Puligilla, PhD (3/14-2/17)
Felipe Santos, MD (3/13-2/16)
Robert Withnell, PhD (3/15-2/18)
Jong Ho Won, PhD (3/13-2/16)
Norio Yamamoto, MD, PhD (3/15-2/18)
James F. Battey, MD, PhD, *NIDCD Dir exofficio*
Council Liaison: Howard W. Francis (3/15-2/16)
spARO Representative: Jeremy Duncan

EXECUTIVE OFFICES
ASSOCIATION FOR RESEARCH IN OTOLARYNGOLOGY
19 Mantua Road
Mt. Royal, New Jersey 08061
Phone: 1 (856) 423-0041
Fax: 1 (856) 423-3420
E-Mail: headquarters@aro.org
Meetings E-Mail: meetings@aro.org

AWARD OF MERIT

2016 Award of Merit Recipient
Geoffrey A. Manley
Cochlear and Auditory Brainstem Physiology
Department of Neuroscience
School of Medicine and Health Sciences
Research Centre Neurosensory Science
Carl von Ossietzky University Oldenburg

AWARD OF MERIT LECTURE ABSTRACT

Comparative auditory neuroscience: Understanding the evolution and function of ears.

Geoffrey A. Manley

The great variety of both extinct and living vertebrate organisms is of incalculable scientific value, since it enables us to study the function of the ear and the auditory brain in organisms related to ourselves. Our current understanding of the history of life through the study of fossils together with the comparative anatomy and physiology of a wide variety of extant animals shows clearly how humans and other mammals are related and how auditory systems evolved in these and other vertebrates. The characteristically different middle ears and auditory end-organs of, e.g., lizards, birds and mammals (amniotes) are the result of their unique evolutionary trajectories since they diverged from a common ancestor more than 200 million years ago. Comparative studies of the hearing abilities of modern representatives of these groups have shown how structure can determine function and which components of hearing systems are essential for sensitivity, selectivity and time processing. Examples of convergent evolution, such as in the division of labor between two groups of hair cells, help us understand the selection pressures behind evolutionary changes. Remarkably, despite huge differences in size and clear and systematic differences in structure, most features of inner-ear physiology in all groups of amniotes are the same or very similar. In particular, more recent studies of spontaneous and evoked otoacoustic emissions have brought such similarities to light and show clearly how auditory processing is, at the most basic level of the hair cells, very similar indeed in all groups. Interestingly, the characteristics of otoacoustic emissions do not permit direct and quantitative conclusions concerning frequency selectivity at the level of the auditory nerve. Further comparative studies should help find the vital link that is still needed to fully understanding cochlear processing.

AWARD OF MERIT BIOSKETCH

Geoff Manley is recognised with the Award of Merit for his tremendous contributions through comparative studies on hearing in vertebrates. He creatively used the diversity of middle ears, cochlear anatomy and physiology in lizards and birds to analyse the evolution of hearing and to show how structure correlates with function in the middle ear and cochlea. A fundamental contribution was the demonstration that many of the characteristics of the mammalian cochlea are found in non-mammals, including sharp frequency tuning, sensitivity to soft sounds, tonotopic organisation, two-tone interactions, otoacoustic emissions, and the different roles of the subtypes of hair cells (inner vs. outer, short vs. tall, etc.). This work showed convincingly that cochlear amplification and many other features of hearing are ancestral for vertebrates. Geoff has also helped to bridge understanding of the paleontology and function of the middle and inner ears of mammals for the benefit of the auditory community.

Geoff grew up in England just after the second world war in a poor environment with no particular academic tradition. Nevertheless, he excelled in school and, in particular, landed on his early academic feet in an innovative London comprehensive school. Geoff became their first pupil to enter “Oxbridge” – a fact that made headlines in local newspapers! He read botany, zoology and geology at Cambridge University and graduated with a BA in 1967. Following his then wife to the USA, he started his PhD with a young professor in Princeton working in hearing, Mark Konishi. Geoff was Mark’s first graduate student and pretty independently pursued his own line of work on the evolution of hearing, recording from the cochlear nucleus of different lizards, of a turtle, and of a crocodilian species. He was later the first to carry out recordings from the auditory nerves of lizards and birds. Geoff finished his MA in 1969 and his PhD in 1970. At the age of 25, he was appointed Assistant Professor at McGill University in Montreal – only to almost immediately take leave of absence for a Queen Elisabeth II fellowship, to work with Brian Johnstone in Perth, Australia. Using the new Mössbauer technique that Brian had pioneered, they carried out the first measurements above 10 kHz on guinea pig and bat middle ears, using a home-made amplifier and loudspeaker to obtain data up to 115 kHz. The nature of Australia – especially the hundreds of lizard species - also enchanted Geoff forever and he has returned many times since then. After six years in Montreal, Geoff went on Sabbatical to Germany and there found a more permanent home. While working in Eberhard Zwicker’s lab at the Technical University in Munich, he was offered and after long negotiations finally took the Chair of Zoology in 1979. Building up the newly-founded department of Zoology was a monumental task, but also a great opportunity that Geoff seized to create an environment that was both unorthodox in German terms and very stimulating. Everyone, from students to senior scientists, enjoyed great freedom to develop their interests.

Over the next 31 years, until his retirement in 2011, Geoff’s lab was a hotspot of comparative auditory research, with a string of international guests and fellows enriching the experience, among them the Humboldt prize winners Peter Narins, Bob Dooling and Catherine Carr, to name just a few. Geoff’s main interests always revolved around the relation of structure and function of the inner ear and the relevance for the evolution of the hearing organ in terrestrial vertebrates:

mammals, lizards and birds. The group initially focussed on birds, studying a wide variety of species: starling, pigeon, zebra finch, canary (including the Waterslager mutants), budgerigar, chicken, tufted duck, emu and barn owl. Their work made it clear that the specialisations of inner and outer hair cells in mammals on the one hand, and tall and short hair cells in birds on the other, were independent evolutionary innovations – a classic example of convergent evolution demonstrating the importance of the division of labour in specialised hair cells. Perhaps the most dramatic discovery was that avian short hair cells are not afferently innervated. This led Geoff to a very productive line of research on the evolution of hair-cell amplification mechanisms. Back in Perth, Australia for a Sabbatical, he discovered spontaneous otoacoustic emissions in lizards and opened up a new non-invasive toolbox for investigating the relation of structure and function in the inner ear. Across lizard species, Geoff showed that the variety of anatomical features of the tectorial structures in the inner ear correlates with the spectral properties of spontaneous otoacoustic emissions. In an ingenious experiment on the Australian bobtail lizard, he, Christine Köppl and the late Graeme Yates showed that the motor responsible for otoacoustic emissions must be in the hair bundles. Geoff also exposed some real oddities of the evolution in hearing. He showed, e.g., that the tonotopy in geckos is reversed, with the higher frequencies being apical in the cochlea - a finding that would have delighted von Békésy – and also how this might be explained by the pattern of papillar evolution in lizards. Despite retirement, Geoff maintains a keen interest in everything evolutionary-auditory and now actively continues as a guest scientist at the University of Oldenburg. Most recently, he applied his long-standing interests in paleontology to review for the auditory community the exciting new analyses of mammalian fossils and their implications for the evolution of mammalian middle ears and cochleae, especially with regard to high-frequency hearing.

These are just some examples where Geoff's work has highlighted the value of evolutionary and comparative research for understanding basic mechanisms in hearing. He taught us that putting findings in an evolutionary context enables us to distinguish what are shared features and principles in the evolution of hearing on the one hand, and to recognize just how much independent evolution and specialization has occurred in the auditory periphery (middle and inner ear) on the other hand. His work has inspired many students and colleagues to explore auditory mechanisms across species.

Our heartfelt congratulations to Geoff for receiving the 2016 Award of Merit!

Pim van Dijk and Christine Köppl

Past Presidents

1973-74 David L. Hilding, MD
1974-75 Jack Vernon, PhD
1975-76 Robert A. Butler, PhD
1976-77 David J. Lim, MD
1977-78 Vicente Honrubia, MD
1978-80 F. Owen Black, MD
1980-81 Barbara Bohne, PhD
1981-82 Robert H. Mathog, MD
1982-83 Josef M. Miller, PhD
1983-84 Maxwell Abramson, MD
1984-85 William C. Stebbins, PhD
1985-86 Robert J. Ruben, MD
1986-87 Donald W. Nielsen, PhD
1987-88 George A. Gates, MD
1988-89 William A. Yost, PhD
1989-90 Joseph B. Nadol, Jr., MD
1990-91 Ilsa R. Schwartz, PhD
1991-92 Jeffrey P. Harris, MD, PhD
1992-93 Peter Dallos, PhD
1993-94 Robert A. Dobie, MD
1994-95 Allen F. Ryan, PhD
1995-96 Bruce J. Gantz, MD
1996-97 M. Charles Liberman, PhD
1997-98 Leonard P. Rybak, MD, PhD
1998-99 Edwin W. Rubel, PhD
1999-00 Richard A. Chole, MD, PhD
2000-01 Judy R. Dubno, PhD
2001-02 Richard T. Miyamoto, MD
2002-03 Donata Oertel, PhD
2003-04 Edwin M. Monsell, MD, PhD
2004-05 William E. Brownell, PhD
2005-06 Lloyd B. Minor, MD
2006-07 Robert V. Shannon, PhD
2007-08 P. Ashley Wackym, MD
2008-09 Paul A. Fuchs, PhD
2009-10 Steven Rauch, MD
2011-12 Karen B. Avraham, PhD
2012-13 Debara L. Tucci, MD
2013-14 John C. Middlebrooks, PhD
2014-15 Jay T. Rubinstein, MD, PhD
2015 -16 Lawrence R. Lustig, MD

Award Of Merit Recipients

1978 Harold Schuknecht, MD
1979 Merle Lawrence, PhD
1980 Juergen Tonndorf, MD
1981 Catherine Smith, PhD
1982 Hallowell Davis, MD
1983 Ernest Glen Wever, PhD
1984 Teruzo Konishi, MD
1985 Joseph Hawkins, PhD
1986 Raphel Lorente de Nó, MD
1987 Jerzy E. Rose, MD
1988 Josef Zwislocki, PhD
1989 Åke Flóck, PhD
1990 Robert Kimura, PhD
1991 William D. Neff, PhD
1992 Jan Wersäll, PhD
1993 David Lim, MD
1994 Peter Dallos, PhD
1995 Kirsten Osen, MD
1996 Ruediger Thalmann, MD & Isolde Thalmann, PhD
1997 Jay Goldberg, PhD
1998 Robert Galambos, MD, PhD
1999 Murray B. Sachs, PhD
2000 David M. Green, PhD
2001 William S. Rhode, PhD
2002 A. James Hudspeth, MD, PhD
2003 David T. Kemp, PhD
2004 Donata Oertel, PhD
2005 Edwin W. Rubel, PhD
2006 Robert Fettiplace, PhD
2007 Eric D. Young, PhD
2008 Brian C. J. Moore, PhD
2009 M. Charles Liberman, PhD
2011 Robert V. Shannon, PhD
2012 David P. Corey, PhD
2013 Karen P. Steel, PhD
2010 Ian Russell, PhD
2011 Robert V. Shannon, PhD
2012 David P. Corey, PhD
2013 Karen P. Steel, PhD
2014 H. Steven Colburn, PhD
2015 Thomas B. Friedman, PhD
2016 Geoffrey T. Manley

2016 TRAVEL AWARD RECIPIENTS

Sean Anderson
Aaron Apawu
Huriye Atilgan
Vasiliki(Vaso) Basinou
David Brown
Lorcan Browne
Brian Buechel
Annalisa Buniello
Jane A. Burton
Francisco Cervantes Constantino
Maxin Chen
Elise Cheng
Nikola Ciganovic
Donatella Contini
Rebecca Curry
Laura D'Aquila
Mishaela DiNino
Ysabel Domingo
Edward Doyle
Daniel Dudley
Vijayalakshmi Easwar
Karen Eliott Thompson
Gregory Ellis
Anastasia Filia
Farzad Forouzandeh
Darcy Frear
Fei Gao
Christopher Giardina
Ana Claudia Goncalves
Stefania Goncalves
Suhasini Gopal
Jackson Graves
Ariel Grobman
Xiying Guan
Kristin Hageman
Nicol Harper
Amarins Heeringa
Erica Hegland
Ann Hogan
Hui Hong
Hamish Innes-Brown
Lauren Javier
Aryn Kamerer
Robert Keller
Fatemeh Khatami
Mi-Jung Kim
Doo Hee Kim
Jinkyung Kim
Shin Hye Kim
Anastasiya Kobrina
Tess Koerner
Elliott Kozin
Veronique Kraaijenga
Benjamin Krueger
Karina Leal
Choongheon Lee
Chun Liang
Alejandro Lopez Valdes
Annika Luckmann
Elena Mahrt
Zoe Mann
Elisa Martelletti
Melissa McGovern
Louise Menendez
Giedre Milinkeviciute
Mark Miller
Gabrielle (Elle) O'Brien
Dominik Peus
Mariangela Panniello
Brandon Paul
Jeroen P.M. Peters
Melissa Polonenko
Rachel Reetzke
Christopher Rose
Nicole Rosskothen-Kuhl
Alexis Roy
Mark Rudolf
Thore Schade-Mann
Tina Schluter
Katrina Schrode
Adam Sheppard
Brikha Shrestha
Sumi Sinha
Roozbeh Soleymani
Aleta Steevens
Michelle Stoller
Yaqing Su
Vishal Tandon
Litao Tao
Ankita Thawani
Ann Todd
Roberto Valdizon-Rodriguez
Katrien Vermeire
Angela Vong
Dragana Vuckovic
Guoqiang Wan
Yi Wang
Tian Wang
Ammaar Wattoo
Angela Wenzel
Katherine Wood
Wenqing Yan
Yael Zaltz
Ladan Zamaninezhad
Katharina Zenke
Xin Zhou
Yan Zhu

ISSN-0742-3152

The *Abstracts of the Association for Research in Otolaryngology* is published annually and consists of abstracts presented at the Annual MidWinter Research Meeting. A limited number of copies of this book are available, after the meeting this publication will be added to the electronic library on the ARO website (1978-2015). Please address your order or inquiry to Association for Research in Otolaryngology Headquarters by calling 1 (856) 423-0041 or emailing headquarters@aro.org.

This book was prepared from abstracts that were entered electronically by the authors. Authors submitted abstracts over the World Wide Web using Omnipress Abstract Management System. Any mistakes in spelling and grammar in the abstracts are the responsibility of the authors. The Program Committee performed the difficult task of reviewing and organizing the abstracts into sessions. The Program Committee; Program Committee Chair, Dr. Ruth Litovsky; the President, Dr. Ruth Anne Eatock; and the Editor, Dr. Linda J. Hood constructed the final program. Omnipress electronically scheduled the abstracts and prepared Adobe Acrobat pdf files of the Program and Abstract Books. These abstracts and previous years' abstracts are available at www.aro.org.

Citation of these abstracts in publications should be as follows: **Authors, year, title, Assoc. Res. Otolaryngol. Abs.: page number.**

Table of Contents

PRES SYMP 1

Seeing the light with retinal gene therapy: Behind the scenes perspectives

Jean Bennett, MD, PhD*

F.M. Kirby Professor of Ophthalmology and Cell & Developmental Biology; Director, Center for Advanced Retinal and Ocular Therapeutics (CAROT), University of Pennsylvania Perelman School of Medicine; Scientist, The Children's Hospital of Philadelphia, Philadelphia, PA

Gene therapy has the potential to reverse disease or prevent further deterioration of sensory organs in patients with incurable degenerative diseases. The demonstration of safe and stable recovery of retinal/visual function in children and adults with congenital blindness due to *RPE65* mutations in gene therapy trials being carried out at The Children's Hospital of Philadelphia (CHOP) and in Iowa provide great hope for people with other more common blinding diseases. The CHOP Phase 1-2 study is now >8 years past initiation and a Phase 3 (pivotal) trial is well underway. The first set of results from the Phase 3 studies revealed robust improvements in retinal and visual function as well as a high degree of safety, thereby placing this reagent as the frontrunner for being the first approved gene therapy drug in the USA. This presentation will describe the path we established for translational studies. Finally, it will describe some of the challenges presented by the nature of the targeted disease itself, hurdles that have been navigated in order to conduct gene therapy studies, and issues of importance for eventual approval of gene augmentation as a therapy for sensorineural diseases, such as those causing vision or hearing loss.

*on behalf of the CHOP-Penn-Iowa-Spark LCA2 Consortium

Funding

Supported by The Children's Hospital of Philadelphia, Spark Therapeutics, FFB, NEI/NIH grants R21EY020662, R24EY019861, and 8DP1EY023177, Clinical Translational Science Award NIH/NCRR UL1-RR-024134, RPB, the Mackall Foundation Trust, the Scheie Eye Institute, CAROT, the F.M. Kirby Foundation, the grants from the National Center for Research Resources, and the Howard Hughes Medical Institute

PRES SYMP 2

Taking gene therapy from bench to bedside

Daniel R. Salomon, M.D.

Professor

Director, Laboratory for Functional Genomics

Program Medical Director, Scripps Center for Organ Transplantation

Department of Molecular and Experimental Medicine

The Scripps Research Institute

Summary

The last three decades have seen tremendous progress in new vector designs and preclinical models for using gene therapies to cure a number of devastating human diseases. This scientific success has not been equally matched to new clinical trials and clinical success. The objective of this talk is to examine the current challenges facing clinical translation of preclinical cell and animal model results to human patients. The challenges include the selection of disease targets and whether to emphasize relatively rare inherited diseases or tackle complex medical complications like heart failure and cancer. Another challenge is the difference between how well animal models reflect real disease states in human patients. The immune response to gene vectors and to the delivered gene payloads is another major obstacle and we will discuss the issues and possible options for immunosuppressive therapy. Finally, the field faces a number of regulatory hurdles that must be addressed in the design of the preclinical studies to have any relevance to supporting a human clinical trial. In other words, it is not just about science and compelling diseases to treat, but success is also about strategy and having the right preclinical data.

PRES SYMP 3

From Petri Dish to Patient

Douglas E. Brough Ph.D., Chief Scientific Officer

GenVec, Inc., Gaithersburg, MD, USA.

Translation of early research findings into product candidates is the bridge between discoveries and clinical application. GenVec's proprietary gene delivery platform, which is based upon a diverse array of human and non-human adenoviral vectors, has provided the means by which several product candidates have been moved to proof of concept clinical studies, including the first gene therapy in the inner ear. To accomplish this we have taken a directed–translational medicine approach to identify a problem in patients, design a solution that can be tested in the laboratory, test that solution for proof of principle in early experiments and work through the basic, non–clinical and clinical research necessary to test in the patients. Examples from our portfolio of gene therapy, cell therapy and molecular vaccine product candidates will illustrate the key points along this path.

PRES SYMP 4

Personalized Medicine and Deafness – Revolutionizing the Care of Persons with Hearing Loss

Richard J.H. Smith[2], Paul J. Abbas[1], Hela Azaiez[2], Amanda Bierer[2], Ann Black-Ziegelbein[2], Kevin T. Booth[2], Terry A. Braun[3], Colleen A. Campbell[2], Thomas L. Casavant[3], Sean S. Ephraim[2], Kathy L. Frees[2], Emily N. Glanz[3], Shawn S. Goodman[1], Alexander T. Goodwin[2], Jeffrey R. Holt[4], Patrick L. M. Huygen[5], Diana L. Kolbe[2], Hideaki Moteki[5], Carla J. Nishimura[2], Bifeng Pan[4], Paul T. Ranum[2], Todd E. Scheetz[3], A. Eliot Shearer[2], Seiji B. Shibata[2], Christina M. Sloan-Heggen[2], Kyle R. Taylor[3], Donghong Wang[2], Amy E. Weaver[2]

[1] Department of Communication Sciences and Disorders, College of Liberal Arts and Sciences, University of Iowa, Iowa City, IA 52242, USA

[2] Molecular Otolaryngology and Renal Research Laboratories, Carver College of Medicine, University of Iowa, Iowa City, IA 52242, USA

[3]Department of Electrical and Computer Engineering, University of Iowa, Iowa City, IA 52242, USA

[4] Department of Otolaryngology, F.M. Kirby Neurobiology Center, Boston Children's Hospital and Harvard Medical School, Boston, MA 02115, USA

[5]Department of Otorhinolaryngology, Radboud University Nijmegen Medical Centre, 6500 HB Nijmegen, The Netherlands

[6] Department of Otorhinolaryngology, Shinshu University School of Medicine, Matsumoto, Japan

Targeted genomic enrichment with massively parallel sequencing (TGE+MPS) has revolutionized human genetics and promises to be the harbinger of personalized medicine. In the treatment of deaf and hard-of-hearing persons, this technology has made comprehensive genetic testing possible and as a result, it has changed the clinical evaluation of these persons. We have developed three complementary tools to facilitate TGE+MPS for deafness: The first, a TGE+MPS platform, allows us to sequence all exons of all genes implicated in non-syndromic hearing loss; The second, a bioinformatics platform, facilitates variant identification by incorporating a number of filtering strategies in the analysis pipeline; The third, a software system employing machine-learning techniques to extract phenotypic information from audiograms, allows us to correlate phenotypic and genotypic data.

Using these tools in 1119 sequentially accrued patients, we show that an underlying genetic cause for hearing loss can be identified in 39% of patients (440 patients). 49 genes carried pathogenic variants that included missense variants (49%), large copy number changes (18%), small insertions and deletions (18%), nonsense variants (8%), splice-site alterations (6%), and promoter variants (<1%). The diagnostic rate varied based on phenotype and was highest for patients with a positive family history of hearing loss or when the loss was congenital and symmetric. The spectrum of implicated genes showed wide ethnic variability. These results support the early use of TGE+MPS in algorithms for the diagnosis of hearing loss as an evidence-based test that optimizes the utilization of medical resources.

A genetic diagnosis underpins the foundation upon which novel therapies are being developed to personalize habilitation for hearing loss. For example, missense variants underlie 85% of all human autosomal dominant non-syndromic hearing loss, suggesting that selective suppression of mutant alleles using RNA interference may be broadly applicable to prevent this type of deafness. In a proof-of-principle study supporting this possibility, we show that a single intra-cochlear injection of an artificial micro-RNA can rescue the progressive hearing-loss phenotype in the Beethoven mutant mouse, a model of human autosomal dominant non-syndromic hearing loss at the DFNA36 locus. This study is the first to demonstrate that long-term suppression of an endogenous deafness-causing allele is feasible and prevents progressive hearing loss.

PRES SYMP 5

Gene Therapy for Hearing and Balance defects: How close are we ?

Christine Petit [1,2,3,8], Alice Emptoz[1,2,3], Sedigheh Delmaghani,[1,2,3] Omar Akil[4] , Paul Avan [5,6], Lawrence Lustig[7], and Saaid Safieddine[1,2,3]

[1]Unité de Génétique et Physiologie de l'Audition, Institut Pasteur, 75015 Paris, France

[2]UMRS 1120, Institut National de la Santé et de la Recherche Médicale (INSERM), 75015 Paris, France

[3]Sorbonne Universités, UPMC Université Paris 06, Complexité du Vivant, 75005 Paris, France

[4] Otorinolaringology-Head & Neck Surgery, University of California San Francisco, 2380 Sutter Street, San Francisco

[5]Laboratoire de Biophysique Sensorielle, Université d'Auvergne, 63000 Clermont-Ferrand, France

[6]UMR 1107, Institut National de la Santé et de la Recherche Médicale (INSERM), 63000 Clermont-Ferrand, France

[7]Columbia University School of Medicine and New York Presbyterian Hospital, New-York

[8]Collège de France, 75005 Paris, France

Since the initial report on hearing restoration by cochlear gene transfer in a mouse mutant defective for vesicular glutamate transporter-3 (VGLUT3-/-), a growing number of studies tackle similar objectives in the perspective of developing inner ear gene therapy in humans. This presentation will focus on our main approaches to inner ear gene therapy, including the prevention of noise-induced hearing loss and the restoration of balance in vestibulopathies.

The first issue was addressed upon the finding that the mutations in the gene encoding pejvakin (Pjvk) result in an hypervulnerability to sound in mice and humans caused by a marked oxidative stress; this stress develops as a consequence of the defect in the adaptive peroxisome proliferation in response to noise exposure. The results of a comparative analysis of the prevention of noise-induced hearing loss by anti-oxidant drugs and adeno-associated virus (AAV) gene transfer of the murine Pjvk cDNA in Pjvk-/- mice will be discussed.

The second issue was addressed in a mouse model for Usher syndrome of type 1G (USH 1G), that is characterized by congenital profound deafness, vestibular dysfunction, and retinitis pigmentosa. This gene encodes Sans, a scaffolding protein expressed in the cochlear and the vestibular hair-bundles. The results of the cure of hearing and vestibular disorders of Ush1g-/- mutant mice by an recombinant AAV2/8 carrying the Ush1g cDNA will be presented with a special focus on the vestibulopathy of the syndrome.

PRES SYMP 6

TMC gene therapy restores hearing in mouse models of genetic deafness

Jeffrey R. Holt, Ph.D.
Associate Professor, Boston Children's Hospital, Harvard Medical School

Genetic hearing loss accounts for up to 50% of prelingual deafness worldwide, yet there are no biologic treatments currently available. Our research group is working to develop gene therapy strategies to treat genetic deafness. We have focused on DFNB7/11 and DFNA36, which are autosomal recessive and dominant deafnesses, respectively, caused by mutations in Transmembrane channel-like 1 (*TMC1*). We use mice that carry targeted deletion of *Tmc1*, or mice with a dominant point mutation, known as *Beethoven*, which are good models for human DFNB7/11 and DFNA36, respectively. We engineered adeno-associated viral (AAV) serotype AAV2/1 together with the chicken beta-actin (*Cba*) promoter as an efficient combination for driving expression of exogenous *Tmc1* or *Tmc2* in inner hair cells *in vivo*. Exogenous *Tmc1* or its closely related ortholog, *Tmc2*, were capable of restoring sensory transduction, partial auditory brainstem responses, and acoustic startle reflexes in otherwise deaf mice. These proof-of-principle data suggest that gene therapy with *Tmc1* or *Tmc2* is well-suited for further development as a strategy for restoration of auditory function in deaf patients who carry *TMC1* mutations.

PRES SYMP 7

Developing molecular therapeutics for human inner ear disease

Hinrich Staecker, MD PhD
Department of Otolaryngology Head and Neck Surgery University of Kansas School of Medicine Rainbow Blvd, MS 3010 Kansas City KS 66160 hstaecker@kumc.edu

The last 30 years have seen an explosion in our understanding of the molecular basis of hearing loss. The pathways underlying the development of the year as well as the numerous molecular components that make hearing work have been extensively explored. So far this has not translated into the development of new types of therapeutics for what is actually the most common neurodegenerative disease in man. A significant portion of our focus has been on understanding the pathways that control the genesis of auditory and vestibular hair cells in an effort to apply this in patients. Despite all of this work, moving a molecule forward that tackles this problem into the clinic is a daunting task. We will review the development process and initial trial of CGF166, which uses an Ad5 based vector to deliver hath1, the human homolog of atonal into the inner ear. Finally we will discuss how this phase I trial provides an important bridge for translating other potential molecular therapeutics into products that are usable in the human inner ear.

SYMP 1

Defective Protein Complex Assembly and ER Stress as the Proximal Cause and Key to Therapeutics for Usher syndrome

Monte Westerfield; Bernardo Blanco-Sanchéz; Aurélie Clément
University of Oregon

Human Usher syndrome, the most frequent cause of deaf blindness, is a genetically heterogeneous recessive disease. Patients present with congenital deafness and progressive retinal degeneration. Fourteen loci and eleven genes have been linked to Usher syndrome to date. Surprisingly, these genes encode a wide range of different kinds of proteins including transmembrane adhesion and signaling molecules, intracellular scaffold proteins, and a myosin motor. In vitro binding studies suggest that the scaffold proteins bind the other Usher proteins into a macromolecular complex. Although this model that Usher proteins act together in a complex is an appealing explanation for how the human disease can result from mutation of any one of a number of different genes, it is still controversial. Moreover, the effects of mutations on protein complex formation, subcellular transport, and stability are completely unknown. We have developed an in situ proximity assay to identify if, where, and when Usher proteins form complexes. We find that a subset of Usher proteins preassemble into a complex in the endoplasmic reticulum (ER). In Usher mutants, transport of this complex to the Golgi is disrupted, leading to ER stress and, in some cases, apoptosis. We propose that improper assembly of the Usher complex is the proximal cause of cell death in Usher syndrome. This link between ER stress and apoptosis suggests that therapeutics being developed for the treatment of other neurodegenerative diseases, such as Alzheimer's and Parkinson's diseases, will be useful in managing the progression of symptoms in Usher syndrome patients. Although hearing defects are typically congenital due to defects in the mechanoreceptors, hair cells ultimately die, and vision loss is progressive as photoreceptors degenerate over decades. Treatments that delay or reduce cell loss will provide time to patients, while therapies that address the defects are developed and applied to non-degenerating cell populations.

SYMP 2

Stress-Induced Protection of Sensory Hair Cells: Basic and Translational Studies

Lisa Cunningham[1]; Elyssa Monzack[2]; Lindsey May[2]; Soumen Roy[3]; Matthew Ryals[2]; Tiffany Baker[4]; Shimon Francis[2]
[1]NIH; [2]NIDCD; [3]NCI; [4]Medical University of South Carolina

Mechanosensory hair cells are sensitive to death from a variety of stresses, including noise trauma, aging, and exposure to therapeutic drugs with ototoxic side effects. Studies of stress signaling suggest that cells under stress activate signal transduction pathways that will promote the cell's survival while simultaneously activating pathways that will promote the cell's death. It is often the balance (or imbalance) of

these death *vs.* survival signals that determines whether the cell under stress ultimately lives or dies. While severely stressful stimuli result in hair cell death, moderately-stressful "preconditioning" stimuli can trigger a robust protective response in the inner ear. Examples of moderate stresses that induce this preconditioned state include heat stress, sound stress ("sound conditioning"), and treatment with low-dose kanamycin. Each of these preconditioning stresses results in a period of resistance to hearing loss caused by later traumatic noise. In addition, preconditioning sound can also protect against hearing loss caused by ototoxic drugs, suggesting that the preconditioned state is a generalized response that can protect the inner ear against a variety of stresses that would otherwise cause permanent hearing loss. The molecular and cellular mechanisms underlying these protective responses are poorly understood, but emerging evidence suggests that signals from surrounding cell types, including supporting cells and resident macrophages, play important roles as mediators of stress-induced conditioning. Harnessing these intrinsic protective responses may allow the development of clinical therapies to reduce hearing loss and balance disturbances caused by noise trauma or ototoxic drug exposure.

SYMP 3

ER stress inhibitor attenuates hearing loss and hair cell death in Cdh23 mutant mice

Qing Zheng[1]; Jing Yuan[1]; Bo Li[2]; Juan Hu[1]; Heping Yu[1]; Shami Entenman[1]

[1]Case Western Reserve University; [2]Binzhou Medical University

Hearing loss is one of the most common sensory impairments in humans. Research on the hair bundle structures of cochlear hair cells has elucidated clear mechanisms for hearing generation and sensorineural deafness. However, no effective hearing-loss therapeutics have been identified. We recently discovered the erlong (*erl*) mutation of the Cadherin23 (*Cdh*23) gene and suggested that hair cell apoptosis is one of the pathological mechanisms leading to hearing loss in this mutation. In this study, we sought to reveal the upstream apoptosis pathway of hair cells. Our results suggest that endoplasmic reticulum (ER) stress-induced apoptosis might be the earliest molecular event leading to hair cell death in a mouse model of postnatal onset hearing loss. We also report that the ER stress inhibitor of apoptosis, Salubrinal (Sal), could delay the progression of hearing loss and preserve hair cells in *Cdh23*$^{erl/erl}$ mice. Our results provide evidence that therapies targeting upstream molecules prevent hair cell apoptosis at an early stage and lead to more effective outcomes, rather than targeting downstream factors such as tip-link degeneration and apoptosis.

SYMP 4

Advancement in the Mechanisms and Prevention of Noise-induced Hearing Loss

Suhua Sha

Medical University of South Carolina

Background

Although animal research has delineated potential pathomechanisms related to oxidative stress and influx of calcium after noise exposure, there is no clinical treatment to prevent or mitigate the auditory consequences of noise exposure, which include loss of sensory hair cells, synaptic connections to the auditory nerve and, consequently, loss of auditory function. Our laboratory has recently established ATP depletion as an initial response to noise in inner ear, suggesting AMPK-related mechanisms involved in noise-induced hearing loss (NIHL).

Methods

Male CBA/J mice and breeding pairs of CaMKKβ C57BL6 heterozygous mice, AMPKα knockout mice and wild-type C57BL6 mice were purchased from the Jackson Laboratory. CBA/J mice at 12 weeks of age were exposed to a broadband noise (BBN) with a frequency spectrum from 2–20 kHz for 2 h at either 106 dB SPL to induce permanent threshold shifts (PTS) with losses of both outer hair cells (OHCs) and inner hair cells (IHCs) or 98 dB SPL to induce PTS with only loss of OHCs and IHC synaptic ribbons. Due to the *ahl* gene present in the C57BL6 strain, all knockout and wild-type mice were exposed to noise at age of 7 weeks to induce PTS. Auditory thresholds were determined by auditory brainstem responses (ABRs). OHC loss was quantified from surface preparations labeled with myosin VII and then stained with DAB. Cochlear surface preparations, cryosections, silencing techniques, and specific inhibitors were utilized to elucidate the detailed molecular and cellular mechanisms responsible for noise-induced losses of hair cells and synaptic ribbons and NIHL.

Results

Our results revealed that levels of p-AMPKα increased in cochlear hair cells in a noise intensity-dependent manner. Inhibition of AMPK via administration of siRNA or a pharmacological blocker attenuated noise-induced losses of OHCs and synaptic ribbons, and preserved auditory performance. Noise exposure also increased p-LKB1 in cochlear tissues and p-CaMKI/IV in OHCs, while inhibition of LKB1 or CaMKKβ by siRNA or gene knockout reduced OHC loss and NIHL. Finally, the increased p-AMPKα after noise exposure in OHCs was attenuated by silencing LKB1 or using CaMKKβ-knockout mice.

Conclusions

These results indicate that noise exposure leads to hair cell loss by activating AMPK via LKB1- and CaMKKβ-mediated pathways. Targeting these pathways may provide a novel route to prevent NIHL and noise-induced cochlear synaptopathy.

The research project described was supported by the grant R01 DC009222 from the National Institute on Deafness

and Other Communication Disorders, National Institutes of Health.

PD 9

Hidden Hearing Loss In Children With 'Auditory Processing Disorder' (APD)?

David Moore[1]; Stephanie Sieswerda[1]; Michael Smith[1]; Rola Farah[1]; Maureen Grainger[1]; Nicholette Smith[1]; Lisa Hunter[1]; Leonard Varghese[2]; Barbara Shinn-Cunningham[2]; Andrew Dimitrijevic[1]

[1]Cincinnati Children's Hospital; [2]Boston University

Children with listening difficulties (LiD), but normal audiometric thresholds, are sometimes diagnosed with APD. Two main current hypotheses of APD are that it derives from abnormal function of the central auditory system, or that it is a consequence of a generalized, top-down, supra-modal cognitive dysfunction. Previously (Moore et al., Pediatrics, 2010), we showed that LiD in children was more closely associated with a range of impaired cognitive abilities and with response variability on hearing tasks than with response threshold, suggesting that LiD/APD was 'top-down'. Based on recent evidence showing sub-clinical hearing loss deriving from cochlear pathology (e.g. synaptopathy), we asked in this study whether 'hidden hearing loss' contributes to communication difficulties in children diagnosed with APD.

Children (6-12 y.o.) were recruited from the Audiology service at Cincinnati Children's Hospital (APD; n=7) and through advertisements (Typically developing, TD; n=20). Each child received a wide range of audiological, electrophysiological and behavioral tests. Here we focus on two measures of synaptopathy, Wave I of the auditory brainstem response (ABR-WI), recorded with 'tiptrodes', and the brainstem envelope following response (EFR; Bharadwaj et al., 2014). We also report speech-in-noise hearing (LiSN-S).

For ABR-WI, we found robust, click-evoked, extra-tympanic ear canal responses in TD children that were 2x larger than mastoid recorded responses. Responses increased with sound level (100-120 dB pSPL), but did not differ significantly between groups. For EFR, half-wave rectified, amplitude-modulated (80 Hz) tones (4000 Hz) produced variable responses that increased with modulation depth (40 – 100%). Response amplitudes and phase locking values were, on average, smaller in children with APD than in TD children. However, those differences were not significant. LiSN-S speech reception thresholds increased with age in both groups, achieving published mature levels by 9 y.o. TD children, age matched to the children with APD, had better thresholds on all indices (SRT, Talker, Spatial and Total advantage) but none of those differences were significant.

These data, based on a small sample of children with APD, do not thus far support the hypothesis that those children have hidden hearing loss, relative to a larger sample of TD children. They do suggest, however, that further investigation is warranted. The LiSN-S derived, 'advantage' measures of speech hearing in noise also showed variable results between individual children. Further research will extend these data sets, compare them with other indices of ear and brain function, and provide data from children with LiD lacking a diagnosis of APD.

Funding

Cincinnati Children's Hospital, NIH R01DC014078

PD 11

Imbalance in Excitation and Inhibition in Ventral Cochlear Nucleus (VCN) of Mice Exposed to Damaging Noise

Katrina Schrode[1]; Michael Muniak[2]; Brian McGuire[1]; Amanda Lauer[1]

[1]Johns Hopkins University; [2]Garvin Institute of Medical Research

While it is well-documented that noise overexposure causes damage to hair cells and auditory nerve fibers, the consequences of noise exposure on the central auditory system are less well understood. There is evidence for a loss of inhibition and a corresponding increase in neural activity in the inferior colliculus and dorsal cochlear nucleus after noise exposure, and it is assumed these changes are related to tinnitus and hyperacusis. There is also physiological evidence of hyperactivity in the ventral cochlear nucleus (VCN), but very little quantitative information describing the underlying changes in synaptic organization is available. In patients with tinnitus and hyperacusis, waves III and IV of the auditory brainstem response (ABR) tend to be larger than in normal-hearing individuals, suggesting there may be neural hyperactivity in bushy cell-driven pathways. Anatomical studies of a very small region of posterior VCN have noted degeneration of both excitatory and inhibitory axons and terminals in the VCN following unilateral noise exposure. We investigated the effects of noise exposure on the imbalance of excitation and inhibition in the VCN of CBA/CaJ mice exposed to moderately loud noise. We found that the wave III/I and wave IV/I ratios of ABR amplitudes were larger in subjects that had been exposed to damaging broadband noise one month prior compared with unexposed controls. These larger amplitudes suggest either that excitation in bushy cell driven pathways is increased, that inhibition is decreased, or both. When we quantified the presence of glutamate decarboxylase (GAD65), a protein localized to GABAergic synaptic terminals, we found a substantial and widespread loss of GAD65 in the VCNs of noise-exposed subjects relative to unexposed individuals, indicating a massive loss of inhibition in VCN. In contrast, excitatory vesicular glutamate transporter 1 (VGLUT1)-positive puncta, representing auditory nerve terminals, were less affected by noise exposure. We conclude that the imbalance of excitation and inhibition in the VCN is largely attributable to loss of inhibition, but changes in excitatory synapses at the ultrastructural level cannot be ruled out.

Funding

Supported by NIH R03 DC012352, NIH T32 DC000023, and NHMRC grant #1080652.

PD 12

The Contribution of Inferior Colliculus Activity to the Auditory Brainstem Response (ABR) in Mice

Rüdiger Land; Alice Burghard; Andrej Kral
Hannover Medical School

The diagnostic value of the auditory brainstem response (ABR) increases with knowledge about the anatomical sources of its characteristic waves. In mice, the ABR is frequently used to assess hearing status. However, the contribution of the inferior colliculus (IC) to the ABR is not clear. Here, we studied the relation between the click-evoked IC response and the ABR in C57Bl/6 mice. We compared the depth profile of spiking activity and electric fields recorded with multi-electrode arrays in the IC to the scalp ABR.

The IC response was reflected in the non-invasive scalp ABR recording as a slow positive wave with peak latency ~8 ms. The slow wave in the ABR corresponded to the evoked LFP in the IC, which correlated in amplitude and duration with the spiking response in the central nucleus. The onset of the click-evoked IC response (~5 ms) was related to ABR wave V. However, the relation between the onset activity within the IC and ABR wave V was ambiguous. Small amplitude 'hash' spiking activity within the central nucleus preceded ABR wave V, whereas most large spiking activity occurred after ABR wave V. When measuring the ABR at different positions within the IC, the amplitude of ABR wave V was most influenced by position within the IC. This supports a near-field origin of wave V close or within the IC. In contrast amplitude of ABR waves I-IV changed only little with recording position within the IC.

In conclusion, the IC response can be visualized in the non-invasive scalp ABR in mice, when recording with reduced high-pass filter settings. The slow wave IC component in the ABR represents a marker for IC functionality in screening mouse hearing models. Further, IC onset activity in mice is fast enough to contribute to the fast ABR wave V. However, similar to previous studies in other species, our results were not conclusive about a direct role of the IC in the generation of ABR wave V in mice.

Funding
Supported by the German Research Foundation (SPP 1608) and MED-EL.

PD 13

Implications for Presynaptic Modulation of the BK Channel by Targeted Custom Peptides

Elliott Brecht; Brent Beck; Luisa Scott; Joseph Walton
University of South Florida

Slow, Ca^{2+}-activated, BK-type-channels contribute to action-potential duration, firing frequency, and spike frequency adaptation. BK-channels can be found in the axon terminal, somata, and dendrites of neurons and open in response to a rise in intracellular Ca^{2+}. We've previously reported that application of a general pore-blocker, paxilline, to the auditory midbrain affected not only temporal processing properties but also decreased receptive field (RF) formation and maintenance of young animals producing results similar to findings seen in aged animals. Similarly, our previous work utilizing BMS191011, a channel opener, increased excitatory drive within the RF and improved temporal processing.

Expanding these findings, we utilized current source density (CSD) analysis of local field potentials (LFPs), a method of classification that allows us to examine the net ionic flow across neural cortical tissue layers. CSD analysis has largely been used to analyze the primary auditory cortex to discern the variations in average ion flow between different cortical layers. This study investigates the use of CSD analysis to study the effects of a custom-peptide BK-channel opener on the transfer of information within the inferior colliculus (IC).

LFPs and CSDs were derived from responses to both pure-tones and broadband-noise (BBN) using custom designed software. Calculations were derived from a 16-channel vertical array having 150uM electrode spacing and placed within the central nucleus of the IC in old CBA/CaJ mice. Peptides were applied (4uL) to the surface of the IC in 3 dosages (0.1, 1, and 10μM). Each stimulus series was presented pseudo-randomly in the contralateral hemifield, with 25ms pure-tones presented at frequencies from 4-64 kHz and 0-80dB, in 5-dB steps, replicated 5 times. Noise rate-level functions were determined using 50ms duration BBNs in 10-dB steps, replicated 50 times.

CSDs revealed a dose dependent effect of the peptide upon sinks and sources, and this occurred over several hours. Following peptide application a significant and steady decline in the amplitudes of both the sinks and sources were observed for both the 0.1 and 10μM concentrations. However, the 1μM concentration included an initial decrease in amplitudes, which eventually recovered to baseline after 24 hrs. In many ways these findings are similar to the effect of synthetic BK-channel openers, though unique because increasing concentration of the peptide did not intensify effects. CSD analysis allows for the simultaneous examination of inputs driving IC activity and the result (output) and these results indicate that a custom peptide may modulate BK-channel at presynaptic targets.

Funding
Work Supported by NIH_NIA Grant PO1 AG009524 and NIAAA R01 AA020992

PD 14

Neurodegeneration and Cell Death Mechanisms in the Mouse Central Auditory System after Single or Repeated Noise Trauma

Moritz Gröschel; Felix Fröhlich; Ira Strübing; Arne Ernst; Dietmar Basta
Unfallkrankenhaus Berlin

Beside peripheral pathologies of neuronal structures, noise trauma leads to changes in central neuroanatomy and neurophysiology. Several studies have shown an impact on

the auditory pathway either by acoustic deprivation or acoustic overstimulation. Our group has found a significant loss of cells in central structures of the ascending auditory pathway after a noise trauma (Gröschel et al., JNeurotrauma 2010). Moreover, we were able to detect cell death mechanisms after traumatizing single noise exposure, particularly in the auditory brainstem (Coordes et al., JNeurotrauma 2012), which started immediately postexposure and lasted for several days. Therefore, recent data indicate that apoptosis seem to play a key role in the underlying pathologies. Here, we describe the time course of neurodegeneration and cell death mechanisms in the central auditory system after a single or repeated noise trauma using histological and immunohistochemical techniques. Normal hearing mice (NMRI strain) were exposed to a broadband noise (5-20 kHz) at a sound pressure level of 115 dB for 3 hours. Cell densities were measured in brain slices after hemalum eosin (HE) staining. Further, cell death mechanisms were visualized via TUNEL-staining (terminal deoxynucleotidyl transferase dUTP nick-end labelling). Data have been analysed at different time points (1, 7 or 14 days) after a first or a second noise exposure. The focus was put on the ventral and dorsal cochlear nucleus (VCN, DCN), inferior colliculus (IC), medial geniculate body (MGB) and primary auditory cortex (AI). Data showed a strong decrease in cell densities within the central auditory system as well as a significant increase of TUNEL-positive cells. The effects were particularly present in the brainstem and midbrain structures (VCN, DCN, IC) and, to a lesser extent, in the MGB and AI after a single noise trauma compared to normal hearing controls. In contrast, a second noise trauma had a much stronger impact on higher auditory brain structures compared to a single exposure, whereas the lower pathway was less affected. A single noise trauma seems to induce early apoptosis mainly in the basal structures of the central auditory system, whereby the amount of cell death mechanisms in MGB and AI was somewhat weaker. Possibly, afferent inhibitory projections from hierarchically lower auditory areas protect higher structures from a direct acute noise impact during the first exposure. However, the effects after a second trauma could be due to a reduction of protective mechanisms as a result of pre-existing damage as well as deprivation-induced neurodegeneration.

Funding
This work was supported by the Deutsche Forschungsgemeinschaft DFG (GR 3519/3-1)

PD 15

Integration of Pontine Nuclei Inputs in Dorsal Cochlear Nucleus

Calvin Wu; Susan Shore
University of Michigan

The pontine nuclei (PN) complex mediates information transfer from the cerebral cortex to the cerebellum, where cortical motor signals are integrated with proprioceptive and vestibular inputs. Anatomical studies in rats have shown that PN neurons also send projections to the contralateral cochlear nucleus (CN) (Ohlrogge, Doucet, & Ryugo, J Comp Neurol, 2001), suggesting that CN likely receives a copy of cortico-pontine motor signals in addition to peripheral somatosensory inputs (Zhou & Shore, J Neurosci Res, 2004). The CN granule cells (GCs) relay somatosensory information to the apical dendrites of fusiform cells, the principal output neurons of the dorsal cochlear nucleus (DCN) via parallel-fiber axons. Fusiform cells integrate parallel fiber inputs with auditory inputs on their basal dendrties to perform auditory-somatosensory integration via stimulus-timing-dependent plasticity (STDP) (Koehler & Shore, J Neurosci, 2012). Similar to the somatosensory inputs, PN projections to CN co-localize to the GC domain, and likely utilize similar circuits to facilitate motor integration in fusiform cells. To study this possibility in guinea pigs, we first electrically stimulated the PN while recording from DCN fusiform cells. Fusiform cell responses to PN stimulation alone (unimodal stimulation) consisted of an early inhibitory phase (5–10 ms) followed by a delayed excitatory phase (>20 ms). In order to avoid activation of the longer latency, indirect projections, we adopted an optogenetic technique to achieve temporal and spatial specificity. Guinea pigs were transfected with channelrhodopsins (ChR2) via injections of viral vectors in the PN. After four weeks, a hybrid optical stimulation/recording electrode was positioned in the DCN. Fusiform cells responded to 5–20 Hz laser stimulation with latencies of 0.8–3.5 ms, corresponding to activation of ChR2-transfected axonal terminals of PN direct-projection neurons. Paired auditory and laser stimulation induced stimulus-timing dependent enhancement and suppression of fusiform cell responses, consistent with previous studies of auditory-somatosensory stimulation. These results suggest that the PN–CN projections are functionally active, and likely transmit integrated motor information to fusiform cells. Future work using targeted viral transfection and optical stimulation will determine whether PN neurons relay cortical efferent information, and whether motor information affects somatosensory integration in fusiform cells.

Funding
NIH R01-DC004825 (SES), NIH T32-DC00011 (CW)

PD 16

Localization of Components of the Atrial Natriuretic Peptide System in the Mouse Cochlear Nucleus

Janet Fitzakerley[1]; Teia Koopmeiners[2]; George Trachte[1]
[1]University of Minneosta Medical School; [2]University of Minnesota Duluth

Atrial natriuretic peptide (ANP) and its receptor, NPR-A, regulate fluid and electrolyte balance in many tissues. ANP is synthesized extracellularly by corin, and circulates as a paracrine or endocrine hormone. Activation of NPR-A increases intracellular cGMP concentrations and can have many downstream effects, depending upon the tissue. Previous work in our laboratory has shown that administration of ANP significantly improves hearing in normal mice and that NPRA knockout mice exhibit an early onset, high frequency hearing loss. Additionally, NPRA and corin were found in several cells of the cochlear potassium recycling pathways of

the cochlea, and in spiral ganglion neurons. More specifically, NPR-A was observed both the cell body and the central and peripheral processes of spiral ganglion neurons, suggesting that this receptor could be trafficked to the cochlear nucleus (CN). The experiments in this study were designed to test the hypothesis that corin and NPR-A are found in the cochlear nucleus.

NPRA and corin were localized using standard immunohistochemical techniques. CBA/J mice under 100 days old with normal hearing were perfused with a 4% paraformaldehyde/0.05% picric acid solution and brainstem sections were cut at a thickness of 10 microns on a cryostat. Commercially available antibodies against NPRA, corin and MAP2 (a marker for neuronal cell bodies and dendrites) were used and visualized via confocal microscopy.

NPR-A and corin were found in cell bodies and in the neuropil of all 3 major regions of the cochlear nucleus, as well in the nerve root. Corin staining was consistently weaker and less extensive compared to that of NPR-A. In all regions, projection neurons were the most densely labelled, including bushy and stellate cells in the anteroventral CN, octopus cells of the posterventral CN, and fusiform and giant cells of the dorsal CN (DCN). Some, but not all interneurons were labelled. Corin and NPR-A labelling was largely absent from the granule cell domains, although cartwheel cells were labelled in the molecular layer of DCN. There was some evidence that the nerve terminals of auditory nerve fibres contained NPR-A reaction product, predominantly in the ventral regions of CN. There is increasing evidence that natriuretic peptides mediate diverse physiological functions, in addition to their role in the regulation of endocrine and cardiovascular homeostasis. The results of this study support the hypothesis that ANP and NPR-A are positioned to influence neuronal function in the auditory system.

PD 1

Molecular Mechanisms for Human Otic Placode Cell Lineage Specification

Megan Ealy; Andres Plata Stapper; Robert Durruthy-Durruthy; Mohammad Ronaghi; Stefan Heller
Stanford University

The ability to produce human cell types of interest from pluripotent stem cells requires efficient guidance protocols that reliably produce the desired cell types. The generation of sensory epithelia of the human inner ear is hampered by a lack of data about the molecular mechanisms that lead to human cranial placode development and subsequent otic lineage development. In-depth understanding of the molecular events that give rise to specific lineages, however, is a prerequisite for downstream applications such as phenotype studies, disease models, screens for disease ameliorating drugs or treatments, or cell transplantation. To gain better insight into human cranial placode development, we utilize both monolayer and three-dimensional cell culture of human embryonic stem cells (hESCs) that undergo a stepwise induction. First hESCs are guided to non-neural ectoderm using a combination of BMP signaling with TGF-β inhibition with or without WNT inhibition to reduce primitive streak formation, thereby promoting ectodermal cell fates. In monolayer culture this guidance is sufficient to produce SIX1-expressing cells indicative of pre-placodal ectoderm. We show that further inhibition of BMP signaling along with bFGF produces a limited number of potential otic cells expressing PAX2 or PAX8 in both monolayer and three-dimensional culture. The number of PAX2 and PAX8 expressing cells increases with the addition of retinoic acid.

Overall, three-dimensional culture is more efficient and reliable for producing PAX2 and PAX8 expressing cells, which we consider to be presumptive human otic progenitors. Because PAX2 generally is considered a significant otic marker in many vertebrate and mammalian species, we focus on the PAX2-expressing population. The majority of the PAX2 cells also express E-cadherin, indicative of a developing epithelium. Using a combination of immunolabeling, fluorescence-activated cell sorting, and single cell multiplex qRT-PCR gene expression profiling, we analyze PAX2/E-cadherin double positive cells from the three-dimensional culture. Single cell gene expression analysis reveals whether the generated presumptive human otic lineage cells are a homogeneous or heterogeneous population. Furthermore, we will present our first assessment whether the gene expression profiles of the hESC-derived presumptive human otic progenitors are closely related to native otic placode or otocyst cells isolated from the developing early mouse inner ear. Other ongoing work focuses on whether the three-dimensional cultures are capable of producing pro-sensory cells as well as hair cells and supporting cells. Progress along all these lines of investigation will be presented.

Funding
Supported by the NIDCD (R01 DC012250, P30 DC010363, F32 DC014176) and the European Union (FP7-HEALTH-2013-INNOVATION).

PD 2

Tbx1 and Jag1 Modulate the Neurosensory Progenitor Cell Population Required for Development in the Mouse Inner Ear

Stephania Macchiarulo; Bernice Morrow
Albert Einstein College of Medicine

The hair cells of the utricle and saccule, as well as the neurons that form the cochleovestibular ganglion (CVG), are derived from a common pool of cells within the neurosensory domain (NSD) of the otic vesicle (OV) competent to differentiate into both neurons and hair cells. Little is known about the genetic regulation of the NSD progenitor pool. In this study we focused on two genes, the transcription factor *Tbx1* and the Notch ligand, *Jag1* (*Jagged1*) in maintaining a balance of cells in the NSD in the mouse. *Tbx1* is expressed in a complementary location with respect to the NSD while the CVG rudiment forms. Inactivation of *Tbx1* in the mouse leads to an expansion of the neurogenic domain as marked by increased expression of *NeuroD*, *Notch1*, *Sox2* and *Jag1* in the NSD. When *Tbx1* is over-expressed, the neurogenic domain is smaller, but the utricle and saccule do not develop.

Sox2 is a key factor in determining neurosensory competence in the NSD and *Jag1* is required for maintaining its expression, though inactivation of *Jag1* does not affect early CVG size. We observed that *Tbx1* and *Jag1* were surprisingly co-expressed early in development of the otic epithelium, but as expected, were complementary during mid-OV stages. To test whether inactivation of *Jag1* in the *Tbx1* domain can suppress the CVG phenotype observed in *Tbx1* loss-of-function mutants, we inactivated one and both alleles of *Jag1* using a knock-in $Tbx1^{Cre}$ allele. Surprisingly, we found that expression of *NeuroD* and *Sox2* was expanded in the NSD and this phenotype was greatly enhanced on a *Tbx1* null background. When we over-expressed *Tbx1* using a gain-of-function allele (*Pax2-Cre/+;*$Rosa26^{Tbx1GFP/+}$) we found that *Jag1* and *Sox2* expression was reduced, potentially accounting for the hypoplastic utricle, saccule, and CVG observed in these mutants. These findings suggest that *Tbx1* may act to limit the pool of neurosensory progenitor cells within the NSD by restricting *Jag1* expression, which may then in turn act on *Sox2* downstream to regulate the formation of the CVG and sensory organs.

Funding
NIH

PD 3

Antagonistic Interactions Between Notch and Lmx1 Regulate Sensory Patch Segregation in the Embryonic Inner Ear

Hector Galvez-Garcia[1]; David Pedreno-Fernandez[1]; Zoe Mann[1]; Elena Chrysostomou[1]; Elachumee Canden[1]; Beatriz Lorente-Canovas[2]; Karen Steel[2]; Berta Alsina[3]; **Nicolas Daudet**[1]
[1]University College London; [2]King's College London; [3]Universitat Pompeu Fabra-PRBB

The inner ear contains multiple sensory organs responsible for sound and balance perception, whose number and morphology vary among vertebrates. Some sensory patches appear to form during ear development by segregation from a common prosensory domain, but this process remains poorly understood at a cellular and molecular level. An early phase of Notch activity, mediated by lateral induction and the ligand Jagged1 (Jag1), is known to promote the formation of the sensory domains. The LIM-homeodomain transcription factor Lmx1a (cLmx1b in chick) is expressed in non-sensory cells, in a complementary manner to Jag1, and has been shown to be essential for the proper segregation of sensory patches. In this study, we found that increasing the strength of lateral induction in the early developing chicken inner ear induces defects in sensory patch boundaries and segregation similar to those occurring in the Lmx1a mutant mice. Furthermore, results from genetic labelling experiments in the embryonic chick inner ear show that some of the prosensory cells switch off Notch activity and commit to a non-sensory fate. On the other hand, overexpression of cLmx1b antagonizes Jag1 expression and commitment to a sensory fate, whilst the absence of Lmx1a results in an expansion of the Jag1-positive prosensory domain.These results suggest that the balance of Notch versus Lmx1 activities regulate the commitment of the prosensory cells to either a sensory or non-sensory fate, which ultimately defines sensory patch location and boundaries. Although the molecular details of the antagonistic interactions between Notch and Lmx1 are unclear, it is conceivable that their modification could have played a role in the emergence of new sense organs in the course of inner ear evolution.

Funding
BBSRC

PD 4

Elp3 Lysine Acetyl-Transferase Controls Neuronal Survival in the Developing Inner Ear and is Crucial to Balance and Hearing

Laurence Delacroix; Susana Mateo Sanchez; Stephen Freeman; Laurent Nguyen; Brigitte Malgrange
University of Liege

Elp3 lysine acetyl-transferase, the catalytic subunit of the Elongator complex, has been assigned multiple roles in gene transcription, DNA methylation and protein translation efficiency. Given the importance of acetylation homeostasis in controlling developmental processes together with recent reports implicating Elp3 in cortical neurogenesis, we investigated its role during inner ear formation.

In the inner ear, we detected Elp3 transcript in the sensory epithelia of the entire otic vesicle at embryonic day E11.5. At later stages, Elp3 mRNA is strongly expressed in the vestibular and spiral ganglion neurons. To investigate the role of Elp3 *in vivo*, we used a conditional knock-out mice (Foxg1Cre) in which the expression of the acetyl-transferase is lost in early otocyst. These mice show obvious vestibular defects as indicated by a stereotyped circling ambulation, head bobbing, retropulsion and the absence of a reaching response in the tail-hanging test. Furthermore, we identified a severe hearing loss in Elp3cKO mice through Auditory Brainstem Responses. We show that Elp3 enzyme is crucial for neuronal survival in the spiral ganglion and in the vestibule and that it ensures a correct innervation pattern in the developing inner ear. In the absence of Elp3, a drastic increase in the number of apoptotic neurons was detected by active Caspase-3 and pH2AX immunostainings, particularly during the early stages of development (between E12.5 and E14.5). Postnatally, the neurons remaining in Elp3cKO cochleae seem to establish synaptic contacts with the sensory cells but show obvious signs of cell damage as evidenced by Transmission Electron Microscopy.

Taken together, these data support a role for Elp3 in hearing and balance and point out an important role for acetylation homeostasis during inner ear formation. We are currently investigating the molecular mechanisms underlying Elp3 effect on neuronal survival and pathfinding.

Funding
FRS-FNRS Belgium Fonds Leon Fredericq

PD 5

Overexpression of Sponge bHLH and Mouse Neurod1 mRNA in Xenopus laevis Disrupts Inner Ear Neurosensory Development

Karen Elliott; Hannah Maher; Charles Holliday; Ning Pan; Bernd Fritzsch
University of Iowa

Background

Three proneural basic helix-loop-helix (bHLH) transcription factors, Neurog1, Neurod1, and Atoh1, play crucial roles in neurosensory development of the inner ear. Overexpression of these genes in embryos of the frog *Xenopus laevis* was used to define their function and Neurod1 and Neurog1 were both shown to convert ectoderm into ectopic neurons. Comparative data suggest an early metazoan origin of these transcription factors. Consistent with the hypothetical conserved function, overexpression of the presumed ancestral bHLH gene found in the sponge in *X. laevis* also results in the formation of ectopic neurons in the ectoderm. However, none of these studies examined later stages or how overexpression of bHLH genes affects neurosensory development of the ear in *X. laevis,* known to be critically dependent on the right level and timing of expression of several bHLH transcription factors.

Methods

Various concentrations of sponge bHLH mRNA or mouse Neurod1 mRNA were injected into one cell at the two-cell stage in *X. laevis* embryos. Animals were kept until stage 46 (tadpole), at which point inner ear neurosensory development was assessed using immunohistochemistry.

Results

Overexpression of sponge bHLH mRNA in *X. laevis* resulted in a dose-dependent reduction of ears. At concentrations less than previously found to convert ectoderm into neurons we found that the inner ear neurosensory development consisted sometimes of only a few scattered hair cells in a single-layer epithelia. As the degree of inner ear neurosensory development decreased, there was an increase in branching of other cranial neurons, as well as an increased number of Mauthner cells in the hindbrain. Furthermore, the projections of both cranial neurons and hindbrain neurons were disorganized. We also injected mouse Neurod1 at concentrations previously shown to effectively convert ectoderm into neurons. However, there were no effects on ear development with these concentrations. Even at concentrations at least an order of magnitude higher compared to the sponge bHLH mRNA, the effect of Neurod1 was at best mild, suggesting a very potent anti-neurosensory activity of this ancestral bHLH protein.

Conclusions

We show that overexpressing two bHLH genes, sponge bHLH and mouse Neurod1, both negatively affect inner ear neurosensory development and general neuronal pathfinding abilities. However, the effect of Neurod1 may relate to unspecific effects associated with high concentrations. In contrast, sponge bHLH mRNA derailed ear development nearly completely at levels where Neurod1 had no noticeable effect, indicating a specific anti-neuronal effect of this ancestral proneural bHLH protein.

Funding

NASA Base Grant No. NNX10AK63H NIH Grant Nos. R01 DC055095590, P30 DC010362, and R01 GM083999

PD 6

Isl1 and Pou4f1 synergistically regulate the differentiation and survival of inner ear sensory neurons

Lin Gan
University of Rochester

Inner ear sensory neurons play pivotal roles in auditory processing and balance control. Though significant progress has been made, the underlying mechanisms that control the differentiation and survival of inner ear sensory neurons remain largely unknown. Previously, we have shown that ISL1 plays important roles in determining neuron type identities, regulating axon pathfinding, and maintaining neuronal survival in the retina. Moreover, ISL1 and the Class IV POU-homeodomain transcription factor POU4F2 cooperate in controlling the differentiation and survival of retinal ganglion cells. Here we show that *Isl1* and *Pou4f1* synergistically regulate the differentiation and survival of inner ear sensory neurons. *Isl1* is expressed in the developing inner ear sensory neurons and inactivation of *Isl1* resulted in a significant loss of cochleovestibular ganglion (CVG) cells. In the absence of *Isl1*, the differentiation of CVG is delayed and CVG neurons are defective in migration and pathfinding. Targeted deletion of *Isl1* in adult mice lead to a significant loss of spiral ganglion neurons and hearing deficit. Furthermore, compound deletion of *Isl1* and *Pou4f1* causes more severe CVG defects, with a loss of nearly all CVG neurons. We have further demonstrated that ISL1 and POU4F1 act synergistically in regulating the expression of a common set of spiral ganglion-specific genes through co-binding to the promoters of target genes. Our results demonstrate ISL1's essential role along with POU4F1 in the development and survival of inner ear neurons during embryogenesis and in adults.

Funding

National Institute of Health Grants 1R01 DC008856

PD 7

Macrophage migration inhibitory factor (MIF) induces the formation of neuron-like cells with cellular, molecular, and physiological similarity to spiral ganglion neurons (SGN)

Kate Barald[1]; Poornapriya Ramamurthy[1]; Fumi Ebisu[2]; Flor Mendez[1]
[1]University of Michigan; [2]University of Osaka

Background

Improved treatments for hearing loss, including mechanisms for improving the function of the only known "cure" for severe or total hearing loss, the cochlear prosthesis or cochlear implant (CI) are urgently needed. In order for the CI to send meaningful acoustic information to the brain, it must become

closely coupled to the processes of as large and as healthy a population of remaining Spiral Ganglion Neurons (SGN) as possible. In 2012, we made the surprising discovery that the inner ear's first developmentally important "neurotrophin" is not a classical neurotrophin, but an immune system "inflammatory" cytokine, which is made by the inner ear's supporting cells (SuC) and acts as a neurotrophic cytokine in the inner ear: Macrophage Migration Inhibitory Factor (MIF) (Bank et al., 2012, cited in Faculty of 1000). We showed that MIF also induces mouse embryonic stem cells (mESC) to differentiate into neuron-like cells (Bank et al., 2012). Earlier work from this laboratory also demonstrated that mESC could be induced to become Schwann cell-like by exposure to Neuregulin (Roth et al., 2007, 2008) and that such Sc secrete MIF. Both the neuron-like cells that could replace SGN and the SC-like cells that could provide directional cues for a remaining population of SGN or the mESC-derived neuron like cells can be derived from the same population of mESC.

Results

MIF-induced mESC-derived neurons (Fig. 1c) bear significant resemblance to inner ear statoacoustic ganglion (SAG) and SGN, both molecularly and physiologically; Docosahexaenoic acid (DHA) enhances their maturation. MIF-expressing mESC Neuregulin-derived Schwann Cell-like cells have been used to "coat" a cochlear prosthesis/cochlear implant (CI) (Fig. 2). In vitro, extensive directional outgrowth of both immature and mature mouse inner ear primary neurons as well as MIF-induced mESC-derived neurons to the "coated" CI is seen.

Conclusions

These findings could provide a novel stem cell-based approach to the problem of Sensorineural Hearing Loss (SNHL). MIF-induced stem cell derived "neurons" could be used to replace lost or damaged SGN. An ESC-derived Sc-coated CI could provide trophic support and neuron-directing molecular cues to attract existing SGNs to improve contact and function.

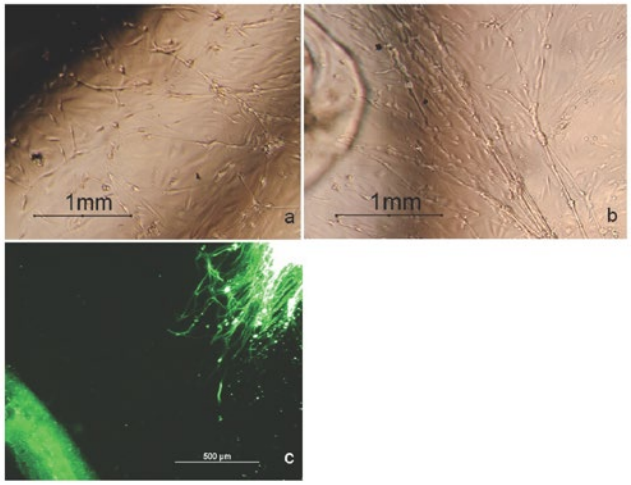

Figure 1: Neuron-like cells derived from mESC exposed to MIF as a differentiation factor and DHA as a maturation factor co-cultured with a: a bare CI showed no directional neurite outgrowth and exhibited few processes extending from the explant itself (experimental control); b: mESC-derived Schwann cell coated CI showed directional outgrowth of neuronal processes towards the CI, part of which is seen in shadow at left; c) a wild type excised mouse O of C (green, lower left) with clusters of fasciculated neurites (upper right/green) growing towards the O of C after a week in coculture

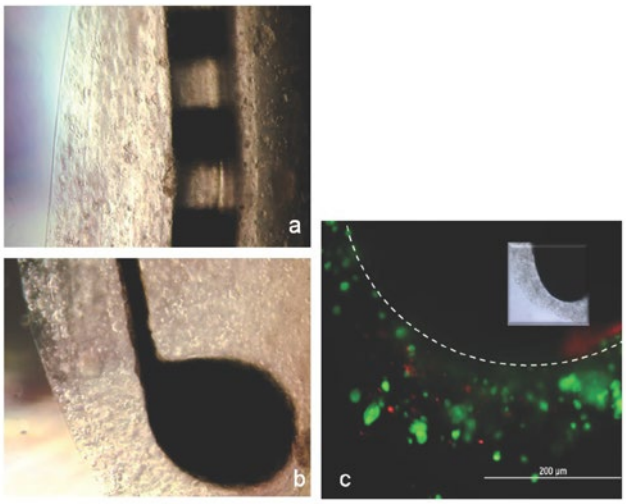

Figure 2: Two different types of electrodes coated with encapsulated mESC-derived SC-like cells are shown: a. Platinum iridium eight array electrode. b. Platinum iridium ball electrode. Differentiated Schwann cells were grown in layers on the electrode in sodium alginate hydrogels for 2wks; c: Photograph of Live/Dead staining (ethidium homodimer for dead cells- orange/calcein AM for live cells-green) of a CI coated with hydrogel-encapsulated mESC-derived Sc, maintained for 2 wks. Insert shows a phase contrast image of the Sc encapsulated CI

Funding

National Science Foundation IOS1146132 (KFB)

PD 8

En1 Deletion Alters Eph and Ephrin Expression in the Developing Superior Olivary Nucleus

Stefanie Altieri; **Stephen Maricich**; Allison Graine
University of Pittsburgh

The molecules that control auditory brainstem neuron migration, positioning and nucleogenesis have not been identified. We recently showed that the homeobox transcription factor *En1* is required for neuronal survival and nucleogenesis in the developing superior olivary complex (SOC). To identify potential mechanisms for the nucleogenesis defects, we investigated members of the Eph family of receptor tyrosine kinases because they are regulated by *En1*, direct neuronal migration in other regions of the developing CNS, and are expressed by and play roles in axon guidance within the developing auditory brainstem. SOC expression of EphA4, ephrin B1 and ephrin B2 was reduced in *En1*-null compared to littermate control mice at embryonic day E14.5 and at birth (P0), suggesting that expression of these proteins depends on *En1*. Ephrin B3 immunolabeling was unchanged at E14.5 but reduced at P0, indicating that *En1* is required for maintained expression. Finally, EphB2 expression was unaffected by *En1* deletion. These data implicate *En1* in regulating Eph and ephrin expression in the developing SOC and present a possible mechanism for nucleogenesis defects seen in *En1*-null mice. These data are potentially relevant for understanding SOC malformations in human disease states such as autism.

Funding
This work was supported by the Richard King Mellon Institute for Pediatric Research at the University of Pittsburgh (SMM) and the NIDCD F32DC014896 (SCA).

PS 1

Progress Report on the Roles of Mitochondrial Thioredoxin 2 in Age-related Hearing Loss

Mi-Jung Kim[1]; Chul Han[1]; Hyo-Jin Park[1]; Karessa White[1]; Logan Walker[1]; Anamaria Parus[1]; Jiyeon Koo[1]; Kap Owens[1]; Christiaan Leeuwenburgh[1]; Dalian Ding[2]; Richard Salvi[2]; Paul Linser[1]; Shinichi Someya[1]
[1]University of Florida; [2]State University of New York at Buffalo

Background
Hearing loss is the third most prevalent chronic health condition in adults and affects more than 40% of people over 65 years of age in the US. Yet, currently there is no treatment or preventative intervention for this common disorder. The overall goal of this project is to investigate the roles of mitochondrial thioredoxin 2 (TXN2) in the auditory system under normal conditions and/or during aging. The TXN2 system is one of the major antioxidant defense systems in mitochondria. There are three major players in the TXN2 system: thioredoxin 2 (Txn2), thioredoxin reductase 2 (Txnrd2), and peroxiredoxin 3 (Prdx3). In mitochondria, NADPH-dependent Txnrd2 catalyzes the reduction of oxidized Txn2 (oxiTxn2) to regenerate reduced Txn2 (redTxn2). Subsequently, redTxn2 catalyzes the reduction of oxidized Prdx3 (oxiPrdx3) to regenerate reduced Prdx3 (redPrdx3) which plays a role in the removal of hydrogen peroxide (H2O2), one of the major reactive oxygen species (ROS) in cells. In this project, we hypothesize that a decline in the mitochondrial TXN2 antioxidant defense system results in increased oxidative stress and mitochondrial dysfunction which in turn promotes cochlear degeneration and hearing loss.

Methods
To investigate if knockdown of Txn2, Txnrd2, or Prdx3 increases oxidative stress-induced cell death, we conducted oxidative stress tests followed by cell viability tests in the mouse auditory cell line HEI-OC1 (House Ear Institute-Organ of Corti 1) transfected with si-Txn2, si-Txnrd2, or si-Prdx3. To investigate if knockdown of Txn2 causes mitochondrial dysfunction, we measured oxygen consumption rates (OCRs), an indicator of mitochondrial respiration, in Txn2 knockdown HEI-OC1 cells. We also measured mRNA expression levels of mitochondrial biogenesis markers (Tfam, Pgc1α, Nrf-1, and Nrf-2) in Txn2 knockdown HEI-OC1 cells. To investigate Txn2 localization and sub-cellular localization in mouse cochlea, we performed colocalization analysis of Txn2 protein in the cochlea of CBA/CaJ mice using immunofluorescence confocal microscopy.

Results
Knockdown of Txn2, Txnrd2, or Prdx3 did not decrease cell viability in HEI-OC1 cells under oxidative stress conditions. Consistent with these results, Txn2 knockdown did not decrease OCRs in HEI-OC1 cells. There were no significant differences in mRNA expression levels of mitochondrial biogenesis markers between control and Txn2 knockdown HEI-OC1 cells. Immunostaining observations showed that Txn2 protein primarily resides in the pillar cells within the organ of Corti, spiral ganglion neurons, and basal cells of stria vascularis in mouse cochlea.

Conclusions
We are currently measuring mitochondrial function parameters including cyclooxygenase (COX) activity, mitochondrial DNA copy number, and mitochondrial DNA deletion/point mutation frequencies in Txn2 knockdown HEI-OC1 cells. We are also investigating if Txn2 deficiency or Txn2 overexpression affects cochlear and auditory function in mice during aging using Txn2 heterozygous knockout mice or inner ear-specific Txn2-overexpressing conditional transgenic mice at 5, 12, and 24 months of age. The results of this project will provide an enhanced understanding of the fundamental molecular mechanisms underlying age-related hearing loss (AHL).

Funding
Supported by NIH/NIDCD grants R01 DC012552 (S.S.).

PS 2

Progress Report on the Roles of Glutathione Reductase in the Auditory System

Chul Han[1]; Hyo-Jin Park[1]; Mi-Jung Kim[1]; Logan Walker[1]; Austin Sowers[1]; Kap Owens[1]; Cole Slade[1]; Tatsuya Yamasoba[2]; Dalian Ding[3]; Richard Salvi[3]; Paul Linser[1]; Shinichi Someya[1]
[1]University of Florida; [2]University of Tokyo; [3]University at Buffalo The State University of New York

Backgrounds

Glutathione acts as the major small molecule antioxidant and is found mostly in the reduced form (GSH) in healthy cells. During aging, oxidized glutathione (GSSG) accumulates, and hence an altered ratio of GSH:GSSG is thought to be a marker of both oxidative stress and aging. Glutathione reductase (GSR) plays a critical role in preventing accumulation of GSSG and maintaining the appropriate redox environment in cells through regeneration of GSH, thereby enhancing the glutathione antioxidant defense system. We have previously shown that calorie restriction delays the onset of age-related hearing loss (AHL), reduces oxidative DNA damage and cochlear cell loss, and increases the activity of glutathione reductase and the GSH/GSSG ratio in mouse cochlea. The goal of this project is to investigate whether GSR plays an essential role in maintaining cochlear and auditory function under normal conditions or during aging in mice.

Methods

To investigate whether GSR deficiency promotes oxidative stress-induced cell death, we conducted in vitro oxidative stress tests using H2O2 and paraquat in mouse inner ear cells (HEI-OC1) or human neuroblastoma cells (SHSY-SY) that are transfected with siRNA targeted to Gsr (Gsr-knockdown) or scrambled siRNA (Control). To investigate whether Gsr-knockdown affects mitochondrial function, we measured mitochondrial oxygen consumption rates using a mito-stress test in Gsr knockdown and control mouse inner ear cells. To investigate whether Gsr deficiency results in the early onset of hearing loss, we conducted ABR hearing test in 3-5 month-old Gsr+/+ and Gsr+/- mice that were backcrossed onto the CBA/CaJ strain for 6 generations.

Results

Gsr-knockdown increased susceptibility to oxidative stress-induced cell death in cultured mouse inner ear cells and human neuroblastoma cells and displayed lower oxygen consumption rates compared to control cells. ABR hearing test revealed that young Gsr+/- mice displayed significantly higher hearing thresholds at high frequencies (48 and 64 kHz) when compared to age-matched Gsr+/+ mice. However, there were no significant differences in the numbers of inner hair cells or outer hair cells between Gsr+/+ and Gsr+/- mice. We are currently measuring glutathione antioxidant defense and mitochondrial function parameters in the cochlea of Gsr+/+ and Gsr+/- mice

Conclusions

These results suggest that GSR may play a key role in protecting cochlear cells against oxidative stress in mice.

Funding

Supported by NIH/NIDCD grants R03 DC011840 (S.S.), R01 DC012552 (S.S.), and R01 R01DC014437.

PS 3

Progress Report on the Roles of Mitochondrial Isocitrate Dehydrogenase in the Auditory System

Karessa White; Mi-Jung Kim; Chul Han; Hyo-Jin Park; Kap Owens; Austin Sowers; Paul Linser; Shinichi Someya
University of Florida

Background

Age-related hearing loss (AHL) is the third most common chronic condition among the elderly. By 2030, 19.3% of the population will be over 65 years of age and the prevalence of AHL is expected to increase as well. However, there are no treatments or preventative interventions for this irreversible sensory disorder and only about 20% of individuals receive benefit from amplification devices. Drugs targeting the NADPH system are a key interest towards treatment. IDH2 (isocitrate dehydrogenase 2) plays a crucial role in the TCA cycle through the conversion of isocitrate to alpha ketoglutarate and the reduction of NADP+ to NADPH. IDH2 supplies NADPH for the regeneration of mitochondrial glutathione and thioredoxin for protection against oxidative stress, cell loss, and resulting hearing loss. Our central hypothesis is that mitochondrial IDH2 plays an essential role in maintaining cochlear and auditory function during aging.

Methods

To determine whether knockdown of Idh1 or Idh2 promotes oxidative stress induced cell death, we performed in vitro oxidative stress tests and cell viability tests in mouse inner ear cells (HEI-OC1) transfected with siRNA targeted to Idh1 or Idh2. To determine whether Idh2 is essential for maintaining mitochondrial function, we performed mitochondrial stress test in Idh2 knockdown HEI-OC1 cells. To determine whether Idh2 is essential for auditory function in normal conditions and during aging, we performed auditory brainstem response (ABR) and distortion product otoacoustic emission (DPOAE) tests in Idh2+/+, Idh2+/-, and Idh2-/- male and female mice at 3-5 and 12-15 months of age.

Results

Knockdown of Idh2 increased susceptibility to oxidative stress-induced cell death in HEI-OC1 cells when treated with either H2O2 or paraquat; however, knockdown of Idh1 decreased cell viability only when treated with paraquat. We found that knockdown of Idh2 in HEI-OC1 cells decreased oxygen consumption rates compared to control cells.

Conclusions

Idh2 is essential for protection against oxidative stress and maintaining mitochondrial function in HEI-OC1 cells. We are currently investigating whether Idh2 deficiency promotes cochlear degeneration in young, middle-aged and old mice that were backcrossed onto the CBA/CaJ strain. The results of this study will enrich current knowledge of the mechanisms of AHL.

Funding
Supported by American Federation for Aging Research Grant 12388 (S.S.), R01 DC012552 (S.S.) and McKnight Doctoral Fellowship Program (K.W.)

PS 4

Analysis of the Genomic Response to Cochlear Lateral Wall Injury in an Adult Mouse Model

Robert Keller; Mary Bridges; Michael Moore; Yazhi Xing; Jeremy Barth; Judith Dubno; Hainan Lang
Medical University of South Carolina

Background
Age related hearing loss (presbyacusis) is a highly prevalent condition in adult humans. Degeneration of the cochlear lateral wall (CLW) is a key feature of metabolic presbyacusis and may be linked to diminished regenerative capacity of specialized non-sensory cells within the CLW over time. MicroRNAs (miRNAs) modulate as much as 60% of the mammalian genome and are important regulators of cellular proliferation in various tissues. We hypothesize that miRNAs regulate cellular recovery and proliferation in the CLW after ototoxic injury, ultimately facilitating its structural and functional restoration.

Methods
Using a surgical approach, mice were subjected to round window application of heptanol, a gap-junction inhibitor that provides a specific ototoxic insult to the CLW. On post-operative days (POD) 3 and 7, auditory brainstem responses (ABRs) were recorded to assess post-operative changes in neural thresholds. CLWs were subsequently harvested and processed for mRNA and miRNA microarray analysis. RNAs differentially expressed between heptanol-treated mice and non-treated controls were analyzed using Ingenuity Pathway Analysis software to identify mRNA targets, highest-ranking canonical pathways, and predicted interaction networks.

Results
Heptanol exposure resulted in differential expression of 63 miRNAs and 960 mRNAs at POD3. Nine of the miRNAs had putative mRNA targets that significantly changed with heptanol (65 total targets). Cellular growth and proliferation ranked as a top molecular function category to which 350 of the 960 mRNAs mapped, including 28 of the predicted targets. Further analysis revealed a 33-gene network related to DNA replication and repair and a 29-gene network pertaining to cell cycle and assembly. Initial validation analysis confirmed upregulation of two high-ranked candidates, mir-216a and mir-155. Both of these candidates are known to regulate cell proliferation and both had multiple predicted mRNA targets that changed significantly and belonged to cellular proliferation networks. At POD7, 39 miRNAs and 225 mRNAs were differentially expressed. Five miRNAs had putative mRNA targets with demonstrated expression change (22 total targets); 101 of the 225 mRNAs are linked to cellular growth and proliferation. Network analysis revealed a 22-gene group pertaining to humoral immune response and hematological system development and a 19-gene group relating to inflammation and cell signaling.

Conclusions
Numerous miRNAs and their putative mRNA targets are differentially expressed following acute CLW damage with heptanol exposure. These molecules are linked to cellular function recovery, proliferation, and inflammatory network activation. Further validation and functional analyses will continue to illuminate the how these miRNAs constitute the genomic response to CLW injury.

Funding
This work is supported, in part, by NIH Grants R01DC012058, P50DC00422, P30GM103342, and P20GM103499

PS 5

Cochlear Perivascular Integrity and Auditory Function Require Cholesterol Homeostasis

Michelle Seymour; **Fred Pereira**
Baylor College of Medicine

Animal models and human studies support a link between altered cholesterol homeostasis and sensorineural hearing loss. However, mechanistic understanding of how circulating lipids modulate cochlear cellular activities is lacking. The rising prevalence of obesity and hypercholesterolemia demands a clearer model of how systemic cholesterol homeostasis influences cochlear cholesterol homeostasis and hearing function. We seek to define the relationships between systemic and cochlear cholesterol homeostasis during hearing development and adulthood, as well as how elevations of systemic cholesterol affect cochlear and hearing function.

Systemic cholesterol levels should influence the levels of cholesterol within cochlear tissues, yet they do not correspond exactly, in part, due to a regulated permeability of the cochlear blood-labyrinth barrier (cBLB). We discovered that the low-density lipoprotein receptor knock-out (LDLR KO) mice display elevated hearing thresholds, indicative of hearing loss, concomitant with elevations in serum cholesterol by 1 month of age. The cBLB is mostly intact at this age and only becomes completely permeable by 4 months of age in LDLR KO mice, allowing circulating cholesterol to enter the cochlear duct. However, cochlear cholesterol levels do not significantly increase in LDLR KO mice until 8-12 months of age, which reflects a complex mechanism of cochlear homeostasis in combination with the integrity of the cBLB. The vascular organization within the *stria vascularis* (SV), the metabolic engine of the cochlea, is also altered in LDLR KO mice. Perivascular-resident macrophage-like melanocytes (PVM/Ms), which contribute to the maintenance of the structural integrity of the cBLB in the SV vessels, are decreased in LDLR KO mice. The loss of PVM/Ms and alterations in SV vascular organization occur prior to elevations in cochlear cholesterol, suggesting that cholesterol-induced hearing loss may initially result from strial damage and compromise of cBLB integrity.

Funding
DC00354 and DC009622 NIH/NIA 5T32 AG00183 NIDCD/ NIH NRSA F31DC012503

PS 6

MicroRNAs as Regulators of Senescence in the Cochlear Lateral Wall of Aged Mouse

Mary Bridges; Robert Keller; Yazhi Xing; Jeremy Barth; Michael Moore; Hainan Lang
The Medical University of South Carolina

Background
Age-related hearing loss (presbycusis) affects greater than one-third of the population over 60 years old. Pathological alterations to the cochlear lateral wall (CLW) disrupting the maintenance of endocochlear potential (EP) are a major cause of presbycusis. In an animal model of presbycusis, we observed an age-dependent decline in spiral ligament fibrocyte turnover. Senescent cells accumulate in aged tissues, leading to a loss of tissue regenerative capacity. With the emergence of microRNAs (miRNAs) as key regulators of senescence and cell cycle, we investigated miRNA expression in the CLW as a function of age.

Methods
RNAs isolated from CLW tissues of young-adult (2-3M) and aged (1.5-2Y) CBA/CaJ mice were used in Affymetrix mRNA and miRNA microarray analyses. Biologically significant miRNA-mRNA relationships and potential downstream functional effects were evaluated with differentially expressed (DE) genes using Ingenuity Pathway Analysis software. MicroRNA Target Filter was applied to predict miRNA targets from DE mRNAs; BioProfiler was used to analyze relationships between DE mRNAs and biological processes. In situ hybridization (ISH) was conducted to detect spatial expression patterns of identified miRNAs in young-adult and aged cochleae.

Results
Microarray analysis identified 79 DE miRNAs in aged CLWs. Two of these, miR-17 (F.C.: -2.04) and miR-19b (F.C.: -1.85), are downregulated in > 6 human/mouse models of aging and have been implicated in controlling transcriptional regulation of senescence. Additionally, four DE miRNAs (miR-497, miR-141, miR-449b, miR-3473) have roles in cell cycle arrest in multiple species/tissues. Microarray analysis detected 1074 DE mRNAs in aged CLWs. Evaluation of putative miRNA-mRNA relationships linked 30 of the DE miRNAs with 195 of the DE mRNAs. Enrichment analysis of the 195 predicted mRNAs targets identified cell cycle regulation as one of the top significant functions. Further analysis of the 195 DE mRNAs identified 26 targets whose expression change correlated with an increase in senescence and cell cycle arrest, including four transcription factors and a D-type cyclin involved in the cdk/pRb/E2F pathway. Differential expression of 6 miRNAs was validated by qRT-PCR. ISH showed that miR-351 and miR-762 were highly expressed in strial marginal cells, and that miR-762 was highly expressed in spiral ligament root cells; each of these miRNAs has multiple senescence-associated predicted targets.

Conclusion
Our investigation reveals age-related alterations in miRNA and mRNA expression in the CLW that are predicted to influence cellular senescence. These results implicate miRNAs as determinants in maintaining normal CLW homeostasis and as candidates in influencing CLW degeneration and presbycusis.

Funding
This work is supported, in part, by NIH Grants R01DC012058, P50DC00422, P30GM103342, and P20GM103499.

PS 7

Age-Related Modulation of BK Channel Phosphorylation and the Effects of Using Specific Peptides That Modulate BK Function

Bo Ding[1]; Luisa Scott[2]; Xiaoxia Zhu[1]; Yuan Yuan[1]; Yoshihisa Sakai[1]; Joseph Walton[1]
[1]University of South Florida; [2]University of Texas-Austin

The molecular mechanisms that regulate BK channel function in the auditory pathway are highly complex. The BK channel plays an essential role in neuronal excitability and is expressed in both the auditory midbrain and cortex. To infer the likely relationship among protein expression, phosphorylation and function in these brain regions, we first measured BK channel expression as a function of age. BK channels from young (3 mon. N=3) and old (30 mon. N=3) mouse brains showed that protein expression of the α subunit decreased with age in the inferior colliculus and auditory cortex. Next, to begin to uncover how these age-related changes could be manipulated, we employed BK channel-specific peptides (pskan1, 3 and 10) and BK channel phosphorylation mutants. The peptides modulated both gating of heterologously expressed BK channels and function of BK channels *in vivo*. BK channel phosphorylation mutants were made on a WT background. S869A and S869D mimicked dephosphorylation and phosphorylation by protein kinase A (PKA). The phosphor-(ser) 14-3-3 binding motif was mutated to the dephosphomemitric 4E2A and phosphomemitric 4E2D. BK channels were immunoprecipitated from clu196 cells transfected with wild type (WT) and mutant BK**a** channels and subjected to the blotting with anti-phosphorylation antibodies. The BK channel-directed peptides dynamically reduced serine/threonine phosphorylation of WT BK channels. The reduction in phosphorylation was found after treatment with pskan3. In contrast, the peptides did not alter tyrosine phosphorylation. Mutation at S869 and 4E2 influenced serine/threonine phosphorylation, with A (Alanine) mutations decreasing and D (Aspartic Acid) mutations increasing phosphorylation relative to the wild type. Additionally, 14-3-3 motif mutants presented the same degree of change vs. wild-type as BK channel-PKA mutants. These data suggest a shared molecular pathway between modifications at these two sites. Pskan1 and 3 exerted similar effects on the wild-type channel as S869A and 4E2A, consistent with the idea that these peptides dephosphorylate the channel. These data support the hypothesis that BK channel function is regulated by S869 phosphorylation, and 14-3-3 binding through a

shared pathway modulated by BK channel-directed peptides . These novel BK channel peptide modulators can be used as a tool to probe how BK channel phosphorylation contributes to age-related changes in central auditory processing in our future studies.

Funding
Work Supported by NIH_NIA Grant PO1 AG009524 and NIAAA R01 AA020992

PS 8

Loss of inner hair cell afferent synapses in aging gerbils

Lichun Zhang; Roksana Stachowiak; Christine Köppl
Carl von Ossietzky University Oldenburg

Background
Age-related hearing loss is well documented in gerbils more than 2 years old. Outer hair cell (OHC) loss, mostly used as an indicator of age-dependent hearing loss, is scattered and mainly found in apical and basal half-turns. However, loss of OHC is not well correlated with hearing loss, as assessed by CAP thresholds. In addition, inner hair cells (IHC) are rarely missing. A reduction in the number of synapses between afferent neurons and IHC has been reported in ageing mice (Sergeyenko, et al., J Neurosci., 2013, 33:13686-13694). In gerbils, few studies have focused on synapses, mainly due to technical difficulties with labeling (Meyer AC, et al. Nat Neurosci, 2009, 12:444-453). In this study, we present reliable pre- and postsynaptic immunoloabeling of afferent synapses in gerbils of different ages. We followed changes in the synapses with ageing, to investigate a potential mechanism for age-related hearing loss.

Methods
Quiet-aged gerbils, 2 to 43 months old, were perfused transcardially with 4% paraformaldehyde under deep anesthesia with sodium pentobarbital. Cochleae were harvested immediately after perfusion and decalcified in 0.5 M EGTA for 2 days at 4°C. An anti-CTBP2 antibody (BD Biosciences, No. 612044) and an anti-GluR2 (Millipore MAB 397) were used to label presynaptic ribbons and postsynaptic receptors, respectively. An anti-Myosin VIIa antibody (Proteus Biosciences 25-6790) labeled hair cells. Four different regions, located at 3.8, 5.19, 6.64, and 8.13 mm from the apex, corresponding to 2, 4, 8 and 16 kHz respectively (Müller M, Hear Res, 1996, 94:148–156) were examined with confocal microscopy. At each location, structures co-labeled with anti-CtBP2 and anti-GluA2 were defined as functional afferent synapses and quantified.

Results
The staining methods for both pre- and post-synaptic markers were reliable and repeatable at all ages. The total length of 6 cochleae analyzed to date was 11.6 ±0.45 mm. Preliminary data showed that both the pre- and post- synaptic markers decreased with age. At the 2 kHz region, afferent synapse numbers changed from 21/IHC in gerbils between 2 and 17 months of age, to 10.6/IHC in 43 months old animals. At the regions corresponding to 4, 8, and 16 kHz, synapse numbers decreased more gradually with age.

Discussion
In conclusion, synapse loss occurs much earlier than OHC loss in ageing gerbils and therefore could be a more reliable indicator of age-related hearing loss. However, the relation between synapse loss and age-related hearing loss still needs clarification.

Funding
This research is supported by the program of Cluster of Excellence “Hear4all”.

PS 9

Activation of TRAIL-DR5 Pathway Promotes Sensorineural Degeneration in the Inner Ear

Shyan-Yuan Kao; Vitor Soares; Arthur Kristiansen; Konstantina Stankovic
Massachusetts Eye and Ear Infirmary

Background
We have previously shown that osteoprotegerin (OPG) is involved in the survival of cochlear neurons and that loss of OPG causes progressive sensorineural hearing loss, in addition to the previously reported conductive hearing loss. In order to further elucidate the mechanism underlying the sensorineural degeneration, we have studied molecules involved in OPG signaling, especially the TNF-related apoptosis-inducing ligand (TRAIL), which is known to interact with OPG and play a role in cell death.

Methods
The cochlear expression of TRAIL and its signaling Death Receptor 5 (DR5) was analyzed using quantitative real-time RT-PCR, western blot analysis and in situ hybridization. The function of TRAIL-DR5 signaling was analyzed by treating cochlear explants and auditory neuroblast cells with recombinant TRAIL.

Results
Expression of Trail mRNA was stable in postnatal day (P) 5-12 cochleae, then increased significantly at 7 weeks. A similar trend was present at the protein level. Expression of Dr5 mRNA decreased during postnatal development and maturity. In contrast, DR5 protein expression increased from P5 to 7 weeks, suggesting post-transcriptional modifications. Trail and Dr5 expression localized to specific cochlear cells in 6 week old mice – primarily hair cells and supporting cells of the organ of Corti.

The treatment of cochlear explants with TRAIL reduced the number of inner hair cells. The damage was partly prevented by pre-treatment with an anti-DR5 neutralizing antibody, αDR5 Ab. TRAIL treatment also reduced the number of outer hair cells, which was not prevented with αDR5 Ab. Nonetheless, the morphology of outer hair cells was greatly improved with DR5 neutralization. Although TRAIL treatment did not significantly reduce the number of spiral ganglion neurons, it caused shrinkage of neuronal somata, which was prevented by αDR5 Ab. Studies in auditory neuroblast VOT33 cells

showed that TRAIL treatment induced cell death, which was prevented by pre-treatment with αDR5 Ab and recombinant OPG.

Discussion

Our discovery of TRAIL and the death receptor DR5 in the cochlea is novel and may have therapeutic implications. We show that the TRAIL-DR5 pathway induces degeneration of cochlear sensorineural structures in vitro. These results motivate future studies to determine whether inhibition of the TRAIL-DR5 signaling in the cochlea in vivo can prevent sensorineural death and the associated hearing loss.

Research Funding

DoD grant W81XWH-15-1-0472, the Bertarelli Foundation, Nancy Sayles Day Foundation, and the Lauer Tinnitus Center (all to K.M.S.).

PS 10

Age-Related Modulation of BK Channel Phosphorylation and the Effects of Using Specific Peptides That Modulate BK Function

Bo Ding[1]; Luisa Scott[2]; Xiaoxia Zhu[1]; Yuan Yuan[1]; Yoshihisa Sakai[1]; Joseph Walton[1]

[1]University of South Florida; [2]University of Texas-Austin

The molecular mechanisms that regulate BK channel function in the auditory pathway are highly complex. The BK channel plays an essential role in neuronal excitability and is expressed in both the auditory midbrain and cortex. To infer the likely relationship among protein expression, phosphorylation and function in these brain regions, we first measured BK channel expression as a function of age. BK channels from young (3 mon. N=3) and old (30 mon. N=3) mouse brains showed that protein expression of the α subunit decreased with age in the inferior colliculus and auditory cortex. Next, to begin to uncover how these age-related changes could be manipulated, we employed BK channel-specific peptides (pskan1, 3 and 10) and BK channel phosphorylation mutants. The peptides modulated both gating of heterologously expressed BK channels and function of BK channels in vivo. BK channel phosphorylation mutants were made on a WT background. S869A and S869D mimicked dephosphorylation and phosphorylation by protein kinase A (PKA). The phosphor-(ser) 14-3-3 binding motif was mutated to the dephosphomemitric 4E2A and phosphomemitric 4E2D. BK channels were immunoprecipitated from clu196 cells transfected with wild type (WT) and mutant BKa channels and subjected to the blotting with anti-phosphorylation antibodies. The BK channel-directed peptides dynamically reduced serine/threonine phosphorylation of WT BK channels. The reduction in phosphorylation was found after treatment with pskan3. In contrast, the peptides did not alter tyrosine phosphorylation. Mutation at S869 and 4E2 influenced serine/threonine phosphorylation, with A (Alanine) mutations decreasing and D (Aspartic Acid) mutations increasing phosphorylation relative to the wild type. Additionally, 14-3-3 motif mutants presented the same degree of change vs. wild-type as BK channel-PKA mutants. The data suggested a shared molecular pathway between modifications at these two sites. Pskan1 and 3 exerted similar effects on the wild-type channel as S869A and 4E2A, consistent with the idea that these peptides dephosphorylate the channel. The data supported the hypothesis that BK channel function is regulated by S869 phosphorylation, and 14-3-3 binding through a shared pathway modulated by BK channel-directed peptides. The novel BK channel peptide modulators can be used as a tool to probe how BK channel phosphorylation contributes to age-related changes in central auditory processing in our future studies.

Funding

Work supported by: NIH-NIA Grant P01 AG009524 and NIAAA R01 AA020992

PS 11

Co-deficiency of Lysosomal Mucolipins 3 and 1 in Cochlear Hair Cells Diminishes Outer Hair Cell Longevity and Accelerates Age-Related Hearing Loss

Teerawat Wiwatpanit; Natalie Remis; Aisha Ahmad; Yingjie Zhou; Mary Ann Cheatham; Jaime García-Añoveros

Northwestern University

Background

Mucolipins are lysosomal calcium channels of the transient receptor potential family that regulate endolysosomal organelle trafficking. Although mucolipin 1 is ubiquitously expressed, we found mucolipin 3 exclusively in inner ear hair cells, marginal cells of the stria vascularis and very few other cell types. This selective expression implies that hair cells have specialized lysosomes. Cochlear hair cells endure sustained mechanical stimulation and potentially harmful energetic demands, yet they can last up to a century in humans. This resilience is not associated with most other epithelial cells where survival can be a matter of days to weeks. Given that one function of lysosomes is cellular repair and turnover of damaged organelles, we hypothesize that hair cells use their specialized lysosomes to enhance survival.

Methods

Mice lacking mucolipin 3 (*Trpml3*$^{-/-}$), mucolipin 1 (*Trpml1*$^{-/-}$), and both in all cells (*Trpml3*$^{-/-}$;*Trpml1*$^{-/-}$) were created along with mice lacking both mucolipins in hair cells only (*Gfi1*$^{Cre/+}$;*Trpml3*$^{Flox/Flox}$;*Trpml1*$^{-/-}$). Auditory function was assessed using DPOAEs and ABRs at ~1 and ~3 months of age. We also constructed cytocochleograms, and examined lysosomes using immunohistochemistry and electron microscopy.

Results

Mice lacking both mucolipins in all cells, but not mice lacking either one alone, experienced hearing loss at 1 month at higher frequencies (27 kHz) and progressing in severity and towards lower (12 kHz) frequencies with increasing age. This loss was similar in magnitude for both ABRs and DPOAEs, suggesting an outer hair cell (OHC) defect. Cytocochleograms also revealed a loss of OHCs especially in the base where the more severe high frequency hearing loss was encountered. To confirm a sensory loss independent of any strial

component, we subsequently characterized a conditional knockout (*Gfi1*$^{Cre/+}$;*Trpml3*$^{Flox/Flox}$;*Trpml1*$^{-/-}$), in which mucolipin co-deficiency is restricted to hair cells and does not occur in any other cochlear cell type. A similar auditory phenotype was recorded, demonstrating that the loss of hearing and OHCs results from lysosomal mucolipin impairment in hair cells. Finally, we detected a severe lysosomal augmentation and accumulation in the apical third of the OHC cytoplasm.

Conclusions
The progressive loss of sensitivity and OHCs from base to apex is characteristic of age-related hearing loss, but with a much earlier onset. The conditional ablation of mucolipins in hair cells reveals that these channels are required in these cells (particularly OHCs) for their long-term survival. The lysosomal abnormalities in mucolipin co-deficient OHCs further support the notion that lysosomes are required for their remarkable longevity.

Funding
Knowles Hearing Center (JG-A), R01 DC000089 (MC) and R31 DC010529 (NNR)

PS 12

Mechanisms of Protection from Premature Age-Related Hearing Loss Mediated via Mitochondrial Protein Fus1

Alla Ivanova; Amy Shettino; Joseph Santos-Sacchi; Lei Song
Yale University

Mitochondrial protein Fus1 is a crucial regulator of inflammatory response and tumorigenesis at systemic level. At cellular and molecular levels we showed that Fus1 is a protein indispensable for maintenance of mitochondrial health via modulation of calcium and reactive oxygen species (ROS) levels in mitochondria and in the entire cell.

Recently, we convincingly showed that the Fus1 KO mouse is a mechanistically novel model of premature Age-Related Hearing Loss (ARHL). Progressive hearing loss in Fus1 KO mice was identified by measuring Auditory Brainstem Response (ABR) in young, adult and aging groups of mice. While 2 mo old mice showed similar to WT mice hearing levels, 100% of 8-11 mo old mice (corresponding to ~40 years old for humans) showed profound threshold elevations across all frequencies possibly suggesting the loss of cochlear amplification, a strong indicator of inner ear pathology. In comparison, wild type mice showed such level of hearing decline only by 18-24 mo of age (~80 years old for humans). To more precisely determine the source of auditory dysfunction, we analyzed details of the ABR waves in 2 mo and 8-11 mo old WT and KO animals.

Interestingly, while we did not find differences in the peak latencies between young WT and KO mice, significant increase in the peak amplitude of waves I, II and IV was observed in young KO mice. This indicates a higher excitability or synchronicity in inner ear as well as in auditory ascending pathway of young KO mice. In contrast, 8-11 mo old KO mice demonstrated a dramatic decrease in the peak amplitudes of all four waves. In addition, KO mice also showed prominent increase in peak latencies of all four waves. Since histopathological analysis showed no severe signs of cochlear degeneration (severe outer hair cells or spiral ganglion cells loss) in older KO mice and taking into account our data on peak analysis, we suggest that the hearing loss in Fus1 KO mice is based on the premature and prominent drop in excitability or synchronicity in both inner ear and ascending pathway. Experiments on deciphering the molecular mechanisms of such premature loss of excitability are underway. At the moment we focus on age-dependent mitochondrial changes in cochlear cells of Fus1 KO and WT mice that could affect this parameter including energy production, ROS production and associated oxidative stress, mitochondrial biogenesis and intracellular/mitochondrial calcium levels that could affect release of glutamate to synapses.

Funding
R01DC 007894; DC000273

PS 13

A physiologically-based method for prescribing amplification for sensorineural hearing loss

Lucia Schnetzer[1]; Joshua Alexander[2]; Larry Humes[1]; Robert Withnell[1]
[1]Indiana University; [2]Purdue University

Background
Popular threshold-based prescriptive algorithms for setting hearing aid gain across a wide range of input levels attempt to balance user needs for audibility and user preferences for loudness. This study compares a physiologically-based algorithm to two threshold-based prescriptive algorithms. Methods: Amplification requirements were calculated for nine different audiogram configurations using NAL NL2, DSL v5.0a, and a physiologically-based algortihm. The latter used the formula Gain = HTL - Input + Input/CR, where HTL is the hearing threshold in dB, and CR is the compression ratio, CR = 105/(105-HTL_60), 0 < HTL_60 < 60. The 60 dB upper limit for HTL_60 assumes that 60 dB is the cut-off for OHC loss, IHC loss being present for hearing losses greater than 60 dB. The physiologically-based algorithm was high-pass filtered to account for upward spread of masking. Results: The physiologically-based algorithm was similar to NAL-NL2, although it provided more gain for losses in excess of 80 dB HL. DSL did not provide a good match to either of the other methods. Conclusion: Differential gain requirements for outer versus inner hair cell loss, based on loss of compression versus linear loss, may provide an alternative to threshold-based formulae for hearing aids.

PS 14

Fractalkine Signaling Influences the Survival of Auditory Afferent Neurons After Aminoglycoside Ototoxicity

Tejbeer Kaur; Mark Warchol
Washington University, Saint Louis

Background

Auditory hair cells are vulnerable to a variety of insults such as acoustic trauma and ototoxic drugs. Such injury can also lead to degeneration of spiral ganglion neurons (SGNs), but this occurs over a period of months to years. Neuronal survival is necessary for the function of cochlear prosthetics, so it is of great interest to understand the mechanisms that regulate neuronal survival after cochlear injury. We have recently demonstrated that selective hair cell ablation in $Pou4f3^{DTR/+}$ mice is sufficient to recruit macrophages into the spiral ganglion, and that disruption of fractalkine signaling (by genetic deletion of the fractalkine receptor CX_3CR1) results in diminished survival of afferent neurons (Kaur et al., 2015). The present study examined the role of fractalkine signaling in macrophage recruitment and survival of auditory afferents after aminoglycoside ototoxicity.

Methods

Experiments utilized mature $CX_3CR1^{GFP/+}$ and $CX_3CR1^{GFP/GFP}$ mice. The $CX_3CR1^{GFP/+}$ line expresses GFP in all macrophages and monocytes and retains fractalkine signaling, while mice homozygous for GFP ($CX_3CR1^{GFP/GFP}$) lack fractalkine signaling. Hair cell death was induced by administrating a single dose of kanamycin (1000 mg/kg) followed 30-45 min later by a single injection of furosemide (250 mg/kg). Animals were sacrificed at different time points after these injections and cochleae were fixed and processed for immunohistochemistry as either whole mounts or frozen sections to label either hair cells, macrophages or neurons. Saline-injected animals served as controls.

Results

Consistent with previous studies, systemic treatment with single dose of kanamycin/furosemide resulted in nearly-complete ablation of outer hair cells and a partial loss of inner hair cells along the length of the cochlea. This lesion was accompanied by a ~2-fold increase in macrophage numbers within the cochlea and spiral ganglion and these numbers remained elevated at 60 days after ototoxic injury. Deletion of CX_3CR1 did not affect macrophage recruitment into the cochlear sensory epithelium and spiral ganglion, but resulted in increased macrophage accumulation in the spiral ligament. At 2 months after hair cell injury, we observed a tonotopic reduction in the numbers of SGN cell bodies in $CX_3CR1^{-/-}$ mice (~30% reduction), when compared to $CX_3CR1^{+/-}$ littermate controls.

Conclusions

Our results indicate that disruption of fractalkine signaling leads to reduced survival of SGNs after aminoglycoside-induced hair cell death. These results complement our previous findings and point to a key role for macrophages can influence the long term survival of target-deprived afferent neurons.

Funding

NIH RO1 and P30

PS 15

Central Connectivity of Auditory Neurons after Selective Hair Cell Ablation

Takaomi Kurioka; Min Young Lee; Amarins Heeringa; Lisa Beyer; Donald Swiderski; Ariane Kanicki; Susan Shore; Yehoash Raphael
University of Michigan, Ann Arbor

Background

In experimental animal models of hair cell (HC) loss, the insults often lead to neural changes and degeneration. In the DTR mouse, the primary insult is specific to the HC, leaving the cochlear neural components intact and providing a model for studies of the response of the auditory pathways to loss of HCs. Here we studied changes of central synapses of the auditory nerve (AN) in the cochlear nucleus (CN) using the vesicular glutamate transporter-1 (VGLUT-1), which packages glutamate into synaptic vesicles and is the prime marker for glutamatergic terminals of the AN (Zhou et al., 2014). We examined expression of VGLUT-1 and morphological changes of CN after selective HC ablation in DTR mice.

Materials and Methods

DTR mice express diphtheria toxin (DT) receptor (DTR) selectively in HCs (Golub et al 2012). A single systemic injection of DT into these mice causes selective loss of cochlear HCs. DTR and wild type (WT) mice were injected with DT (15 ng/g) at 3 weeks of age and allowed to survive 1 or 2 months after injection. ABRs were measured 1 week after DT injection to confirm HC loss. Cochleae were examined to confirm HC loss, and transverse sections of the brainstem through the CN were examined for VGLUT1-expression and Nissl staining.

Results

Baseline ABRs were normal for both WT and DTR mice. One week after injection, DTR mice were profoundly deaf but WT mice had normal thresholds. DTR mice treated with DT exhibited extensive HC loss, with inner hair cells completely absent 4 weeks after DT injection. Their supporting cells remained intact. In the ventral CN, injection of DT did not influence the number of neurons. VGLUT-1 expression in the ventral CN and the molecular layer of the dorsal CN also was not changed by selective HC loss in DT treated DTR mice.

Conclusions

Morphology and number of central synapses of AN in the CN did not change despite complete loss of HCs. These results suggest HCs are not required for the maintenance of central auditory synapses in mature animals, at least in the time-frame studied here. As such, the DTR mouse is useful for studying the influence of HC death on neural pathways as well as for regenerative work in the auditory periphery.

Funding
Supported by NIDCD grants R01 DC004825, R01-DC010412 and P30-DC05188.

PS 16

Chd7 regulates non-coding RNA expression during otic neuronal differentiation

Azadeh Jadali[1]; Jennifer Skidmore[2]; Donna Martin[2]; **Kelvin Kwan**[1]
[1]Rutgers University; [2]University of Michigan

Encased in a bony labyrinth, the cochlea that resides within the inner ear allows us to discriminate and hear complex sounds. Hair cells in the cochlea are the sensory cells that convert sound into neural signals, which are then relayed to the brain by spiral ganglion neurons (SGN). CHARGE patients frequently suffer from sensorineural hearing loss resulting from hair cells or SGN dysfunction. Mutations in Chd7, a chromatin remodeling protein, have been associated with CHARGE syndrome. Immunolabeling of Chd7 in the early developing inner ear shows Chd7 expression in neurosensory progenitors. To determine the genome-wide downstream targets of Chd7 during SGN development, we employed an immortalized otic progenitor (iMOP) cell line. Using chromatin immunoprecipitation followed by deep sequencing (ChIP-seq), we identified a specific subset of non-coding RNAs (ncRNA) as targets of Chd7. One of these ncRNA is miR9-2, which has previously been implicated in neurogenesis of mouse telencephalon. We propose that Chd7 modulates expression of non-coding RNAs to ensure proper development of SGNs.

PS 17

Neurotrophins, Potassium Currents and High Frequency Stimulation in Primary Auditory Neurons

Karina Needham[1]; Tess Wright[1]; Lisa Gillespie[1,2]
[1]University of Melbourne; [2]Bionics Institute

Background
Brain-derived neurotrophic factor (BDNF) and neurotrophin-3 (NT3) are key neurotrophic factors for the survival of primary auditory neurons (spiral ganglion neurons; SGNs). Our previous study (Needham et al. Hearing Research 2012) revealed that exposure to both BDNF and NT3 *in vitro* increases the contribution of hyperpolarization-activated currents (I_h) in SGNs. This work also hinted at a concurrent increase in voltage-dependent potassium currents (I_K). Here we compare I_K in SGNs grown in the presence or absence of exogenous BDNF and NT3, and examine the impact of neurotrophin exposure on firing entrainment during high frequency pulse trains.

Methods
Dissociated SGNs were prepared from early post-natal rats. Untreated (UT) SGNs were grown in Neurobasal media alone, while neurotrophin-treated (NT) cultures were supplemented with both BDNF and NT3 at 10 ng/ml each. Whole-cell patch-clamp recordings (n>130) were made in both current- and voltage-clamp modes. Channel blockers used included Tetrodotoxin (TTX), ZD7288, Dendrotoxin-I (DTX-I) and Phrixotoxin-I (PaTX-1).

Results
Voltage-clamp recordings comparing the overall outward currents evoked with membrane depolarization revealed no significant difference in either peak or steady-state portions with exposure to neurotrophins in the presence of TTX and ZD7288. In both UT and NT neurons, the presence of either DTX-I (blocker of KV1.1 and KV1.2) or PaTX-1 (blocker of KV4.2) reduced I_K. Whilst there was no difference in the contribution of PaTX-1-sensitive currents between the two groups, DTX-I-sensitive currents were responsible for a greater percentage of the steady-state portion of I_K in NT neurons when compared to the UT population. Differences were also observed between the groups in current-clamp mode. NT neurons had a lower firing threshold, and action potentials activated by suprathreshold stimulation had longer latency and shorter duration than UT neurons. SGNs in both groups showed similar entrainment to pulse trains presented between 2.5 and 33.3 pulses per second (pps). NT neurons showed slightly better firing entrainment at higher frequencies (>50 pps).

Conclusion
Exposure to combined BDNF and NT3 alters the contribution of DTX-I-sensitive potassium currents, and induces a subtle shift in firing entrainment to pulse trains presented at higher frequencies.

Funding
This work was supported by the Senior Wagstaff Fellowship in Otolaryngology (Royal Victorian Eye & Ear Hospital).

PS 18

Neuregulin-1 effects spiral ganglion neuritogenesis and Schwann cell proliferation

Stefan Hansen[1]; Diana Lang[2]; Laura Holtmann[3]; Stephan Lang[3]
[1]University Hospital Essen; [2]University of Duesseldorf; [3]Department for Otorhinolaryngology

Introduction
After peripheral nerve crush Schwann cells play a critical role in the axonal regeneration process by providing trophic support. They can dedifferentiate and promote neurite outgrowth by releasing various neurotrophins and adhesion molecules. One important factor for the neuron-glial interaction is neuregulin-1 (NRG1). It is an essential axo-glial signal protein that contains an epidermal growth factor (EGF)-like domain that signals by stimulating ErbB receptor tyrosine kinases. In the cochlea of rodents clear expression of NRG1 has only been demonstrated in spiral ganglion neurons while expression in the organ of Corti is less reconfirmed. Furthermore, neuregulin/ErbB signaling is essential in long-term functional regulation of the auditory nerve, maybe through reciprocal neuron-glial interactions.

Methods
Immunohistochemical expression analysis of NRG1 during hearing development in the mouse were performed in

cryosections. Furthermore, the effect of NRG1 administration on neurite outgrowth and Schwann cell development in vitro as well as blocking of ErbB-receptor by a panErbB (CI-1033) inhibitor was evaluated in a spiral ganglion/Schwann cell co-culture.

Results
The immunohistochemical analysis showed time-dependent expression of NRG1 also in supporting cells and hair cells. In the cell culture the addition of NRG1 caused a concentration-dependent increase in axonal outgrowth and proliferation of immature Schwann cells, while the panErbB receptor blocker induced a neurite growth inhibition.

Conclusion
NRG1 seems to be a relevant factor in the development of the auditory nerves by Schwann cell interaction and could play a critical role in future regenerative therapeutic strategies in the inner ear.

PS 19

Effect of Temporary Neurotrophin Treatment on Peripheral and Central Processes of the Spiral Ganglion Cells in Deafened Guinea Pigs

Dyan Ramekers; Patrick Buitenhuis; Steven Kroon; Sjaak Klis; **Huib Versnel**; Wilko Grolman
University Medical Center Utrecht

Background
Exogenous neurotrophin treatment prevents degeneration of spiral ganglion cells (SGCs) after severe hair cell loss. Recently we demonstrated a long-lasting effect with brain-derived neurotrophic factor (BDNF) after cessation of treatment (Ramekers et al., J. Neurosci. 35:12331-45, 2015). In that study the survival of the cell bodies was examined. Using the same cochleas of that study we address here the question whether BDNF protects the peripheral processes and central processes (axons) as well.

Methods
Guinea pigs were deafened by co-administration of kanamycin and furosemide. Two weeks after deafening the right cochleas were implanted with an intracochlear electrode array with a cannula connected to an osmotic pump filled with BDNF. The left cochleas served as untreated control. Four weeks later the treatment was stopped by surgically removing the osmotic pump. At that point, or another 4 or 8 weeks later, the animals were sacrificed for histological analysis. Cochleas were sectioned along different planes of interest including (1) myelinated portion of peripheral processes in the osseous spiral lamina, (2) the cell bodies in Rosenthal's canal, and (3) central processes in the internal auditory meatus. Packing densities and cross-sectional areas of cell or process were determined using light microscopical analyses of basal, middle and apical cochlear regions.

Results
After BDNF treatment the number of peripheral and central processes was significantly higher than in untreated cochleas. Whereas the number of cell bodies did not decrease after cessation of treatment, the peripheral processes slowly degenerated, most notably in the apical turn. The central processes appeared to be well protected by BDNF, to a similar extent as the cell bodies.

Conclusion
Protection against degeneration with BDNF was less effective for the peripheral process than for the SGC soma and central processes. Strategies to prevent SGC degeneration after hair cell loss should consider the differential effects on the various neural elements.

Funding
This study was supported by MED-EL GmbH and Heinsius-Houbolt foundation

PS 20

Does p75NTR Play a Role in Control of the Number of Cochlear Afferent Synapses and/or in Noise-induced Synaptopathy?

Ning Hu; Steven Green
University of Iowa

The research background
Signaling by the pan-neurotrophin receptor ($p75^{NTR}$) is diverse and complex, depending on cell type, physiological or pathological conditions, receptor-ligand interactions and stoichiometry. In non-neuronal cells, $p75^{NTR}$ can be proapoptotic or associated with cell division, either promoting cell survival or death depending on the ligands that $p75^{NTR}$ binds. In view of previous studies showing expression and function of $p75^{NTR}$ in the cochlea after various neuropathic traumas, we have begun investigating a possible role of $p75^{NTR}$ in noise-induced cochlear synaptopathy, a condition in which neurotrophins have already been shown to potentially therapeutic.

Methods
We crossed a $p75^{NTR}$ knockout (KO) into a CBA/CaJ background. Both male and female mice were used. 12-14 week old mice were exposed to 8-16 kHz octave band noise at 100 dB SPL for 2 hours. ABRs at 8, 16 and 32 kHz were assessed prior to noise exposure, 1 day and 12-14 days post-noise to obtain baseline, noise-induced temporary threshold shift (TTS) and permanent threshold shift (PTS) measures. Synapses on inner hair cells (IHCs) were counted at the 8, 16 and 32 kHz locations. A "synapse" is operationally defined as a colocalized ribbon (labeled with anti-Ribeye/CtBP2) and a postsynaptic density (PSD, labeled with anti-PSD95). Hair cells were visualizd with anti-myosin VI and VIIa; spiral ganglion neuron (SGN) axons with anti-neurofilament antibodies.

Results
Homozygous KO mice generally show 15-20% lower body weight and higher activity than wild-type (WT) CBA/CaJ mice. Thus far, most of the KO mice we obtained have been female. KO females tend to have higher ABR amplitudes than WT females, nevertheless, thresholds are similar. Correspondingly, KO mice tend to have a larger number of

synapses than do WT mice. Also, there are a larger number of PSDs than of ribbons. Most of these “orphan” PSDs are located on SGN “dendrites” below the base of the IHC. After noise exposure, KO and WT mice show similar TTS and both genetypes show no PTS measured 12-14 days post-noise. The number of synapses per IHC in KO mice remains higher than that in WT mice after noise exposure. However, the average percentage loss is approximately the same in KO female mice as in WT female mice.

Conclusions

Loss of $p75^{NTR}$ results in increased numbers of PSDs in SGNs. $P75^{NTR}$ may be involved in negative regulation of synthesis, assembly or transport of PSDs in SGNs, but does not appear to significantly affect acute noise induced cochlear synaptopathy.

Funding

Supported by NIH/NIDCD grants R01DC009405, P30DC010362 and DoD grant W81XWH-14-1-0494

PS 21

Function deficits of auditory nerve are developed with synapse repair in noise-induced hidden hearing loss: implication to cochlear synaptopathy in aging

Hengchao Chen[1]; **Jian Wang**[2]; Qiang Song[1]; Lijuan Shi[3]

[1]6th Affiliated Hospital, Shanghai Jiaotong University; [2]Dalhousie University; [3]Southeast University, Nanjing China

Background

The synapse between inner hair cells (IHCs) and spiral ganglion neurons (SGNs) in the cochlea is characterized as ribbon synapse due its special presynaptic structure. It has been identified as a new locus of noise induced cochlear lesions. Massive damage to this synapse may occur after noise exposures insufficient to cause permanent threshold shifts, resulting in many SGNs losing their connections to IHCs. The SGNs that permanently lost their synapses with IHCs was found to slowly degenerate. However, there is a debate whether the synapses are repairable. Furthermore, the functional consequences of the synapse loss/repair are predicted but remain to be explored in detail.

Methods

Single unit recording from ANFs was done in guinea pigs at 3 different time points after a brief noise exposure (105 dB SPL, broad band noise, 2h) and compared with the control group. Morphologic observations for synapse counts and structures were performed across the same groups.

Results

The noise exposure preferentially but not exclusively damaged the ribbon synapses innervating ANFs with low spontaneous spike rate. A massive but incomplete repair of ribbon synapses was evident by in both functional tests and morphological data. A transient change in the distribution of low- and SR ANFs suggested disproportionate damage to low-SR units. Coding functions were found to be changed in many aspects including: (1) a reduction in driven spike rate, (2) an elongation in response latency, (3) a reduction in peak/sustained spike ratio, (4) poorer recovery of spike rate to the second click in a paired click paradigm. Those changes were more severe in the low-SR units and appeared with a later onset.

The ABR threshold changes induced by the exposure to the broadband noise at 105 dB SPL for two hours were summarized in Figure 1, which showed a temporal threshold shift 1 day after noise (1DPN) as compared with the threshold from the control animals. The threshold curves obtained later (1WPN and 1MPN) were overlapped with the control. The two-way ANOVA against the factor of noise treatment and frequency shows a significant effect of noise ($F3=318.57$, $p<0.01$), but only due to the elevated thresholds in 1DPN group (1DPN vs ctrl: $q=34.943$, $p<0.001$, Post-hoc test, Tukey method). In Figure 1, significant difference between the control and 1DPN groups was indicated by the asterisks based upon the post-hoc test within every frequency.

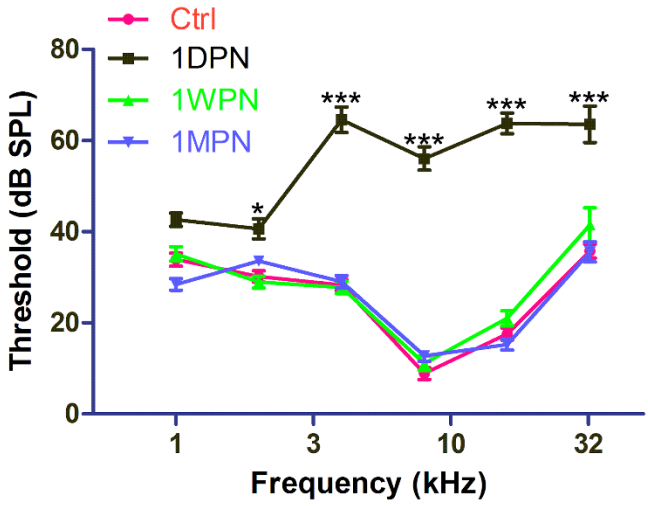

Figure 1. ABR thresholds. Significant threshold elevations were seen one day post noise exposure (1DPN). The thresholds measured at one week post noise (1WPN) and 1 month post noise (1MPN) were not significantly different from the control. *: p,0.05, ***: p<0.001.

DPOAE

Figure 2A compares the ribbon-count cochleograms across groups, in which the reduction in ribbon counts was seen across the whole cochlear region observed, more in the high frequency region. In order to see the regional difference in the ribbon count changes after the noise exposure, the averaged ribbon counts were converted into percentage against the values of the control cochleae separately for the upper and lower half of the cochlea. In the lower half, the initial loss of ribbon counts was more than 50%, but was recovered to less than 20% at 1MPN.

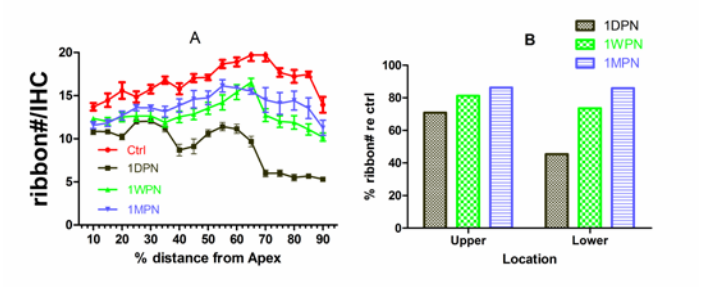

Figure 2. Noise induced changes of ribbon counts. A: ribbon-count cochleogram. B: the % ribbon (using control values as 100%) for both upper and lower half of the cochlea.

Corresponding to the reduction in ribbon counts, the CAP amplitude was also reduced in animals exposed to noise. In the present study, the CAP was tested in response to clicks of different levels. Figure 3 compares the input/output functions of CAP amplitude as a function of sound level across groups. A huge decrease of CAP was seen one day after noise exposure (1DPN), much larger than the overall reduction of ribbon counts, suggesting that the survived ribbon synapses were functionally impaired. Later after the noise exposure, the CAP amplitude IO function was largely recovered. At the highest sound level tested (90 dB peSPL), the CAP amplitude was 335.56 ± 21.78 μV in 1MPD group, 22.6% lower than that of the control group (433.60 ± 12.89 μV), larger than the % loss of ribbon counts at that time point.

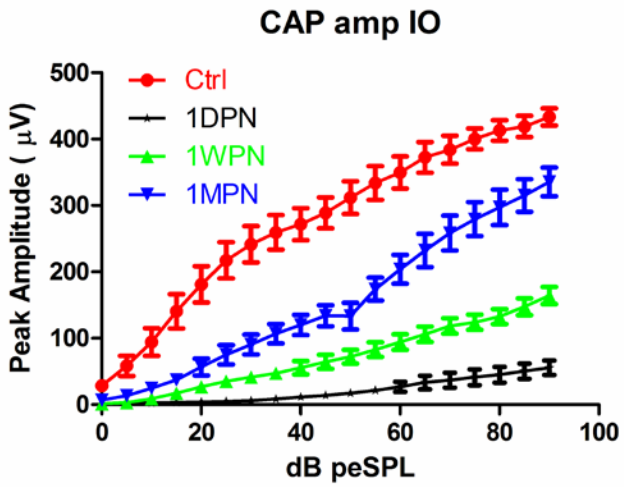

Figure 3. CAP amplitude input/output functions. A large reduction in CAP amplitude was seen in 1DPN group as compared with the control. The reduction was recovered with time. At every time point, the reduction in CAP amplitude was larger than the loss of ribbon counts shown in Figure 2.

The Results of Single Unit Recording

In this part of the experiment, we first examined impact of noise exposure on SR. One-way ANOVA of rank (Kruskal-Wallis test) was performed respectively on SR changes for the total units, and low/high BF units separated by BF=4 kHz. Significant changes in SR was seen only in high-BF units (H3=13.314, p=0.004). More importantly, the difference was only significant between the control units and those units obtained at 1DPN (Post-hoc test, Q=3.176, P<0.05, Fig. 4A). In the high-BF units, the ratio between low and high SR units (cut of 20 sp/sec) was 1.2 (55 versus 47 units) in the control and was reduced to 0.35 (18 versus 52 units) at 1DPN. The ratio was largely recovered at 1WPN (0.75) and 1MPN (0.86). The result suggests that the exposure produced more damage on synapses innervating low SR fibers. However, the change in SR distribution was a transient event and was largely recovered later, probably by the repair of the synapses.

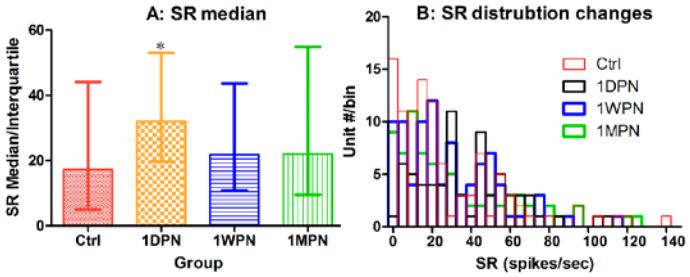

Figure 4. Noise-induced SR changes in units with BF >4kHz. A: the changes in SR median. B: the changes in SR distribution. One-way ANOVA of rank shows that a significant increase in SR exists only for those high BF units at 1DPN. *: p<0.05.

To examine the impact of noise exposure on the responses of single auditory nerve fibers to sound in the sense of intensity coding, we examined the potential changes of driven spike rate, which was further specified as the peak rate, sustained rate and total rate in responses to 50-ms tone bursts. Figure 5A shows the differences in peak spike rates across groups. The three curves represent the results from all units (green), and low (blue)/high (red) SR units respectively. Since large variations were seen in low SR units, a one-way ANOVA was performed for those units and the result showed a significant effect of noise exposure on the peak rate (F3=22.86, p<0.0001). Post-hoc pairwise tests (Tukey method) against the control showed significant decreases in the peak rate at 1WPN (q=8.554, p<0.001) and 1MPN (q=10.66, p<0.001), but not at 1DPN (q=2.069, p>0.05). Therefore, it is clear that (1) the noise exposure impact the peak spike rate only in low SR units and (2) the reduction in peak rate in the low SR units were significant at later time points (1WPN and 1MPN) but not shortly after the noise (1DPN). Figure 5B shows the cross-group difference in the total spike rate, in which it is also clear that the noise impact was significant only in low SR units and at later time points. One-way ANOVAs show a significant effect of noise only in those low-SR units (F3=14.03, p<0.001), but not in the high-SR units (F3=1.16, p>0.05). Post-hoc pairwise tests (Tukey Method) shows the significant reduction in total spike rate at 1WPN (q=7.759, p<0.01) and 1MPN (q=4.562, p<0.01). Those results suggest that the response ability of the synapses to sound was reduced especially in those low SR units that were presumably repaired after the silencing by the noise. For the changes in both peak rate and total rate, we did not see a significant difference related to BF.

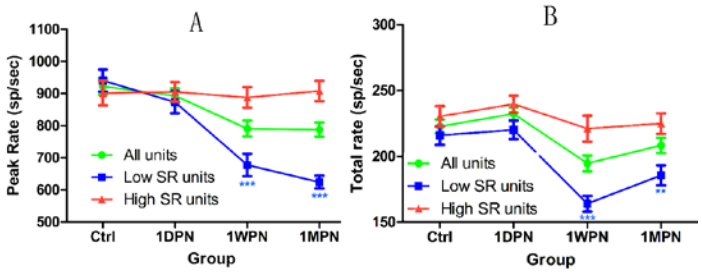

Figure 5. Noise-induced changes of driven spike rate. Significant effects were seen only in low-SR units and appeared later after noise exposure. A: peak rate, B: total rate. **: p<0.01, ***: p<0.001.

To examine the potential impact of the noise exposure on the response properties of the auditory nerve fibers that are likely related to the temporal coding, we evaluated (1) peak latency and (2) peak-to-sustained spike ratio in PSTH in response to tone bursts (Figure 6A and B). One-way ANOVAs performed for peak latency showed a significant effect of noise on low SR units (F3=7.061, p=0.0001), but not on high-SR units (F3=1.239, p>0.05) although the latency was increased (Figure 6A). Post-hoc tests (Tukey method) for low-SR units show significant latency increase at 1DPN (q=4.624, P<0.01 against the control), 1WPN (q=4.921, p<0.01) and 1MPN (q=5.603, p<0.001). ANOVAs also show significant decreases in peak-sustained ratio after noise, in both in low SR units (F3=117.0, p<0.0001) as well as the high-SR units (F3=12.01, p<0.0001). However, the post-hoc tests (Tukey method) show that significant changes appears only at 1WPN and 1MPN, but not at 1DPN in both low- and high-SR units (indicated by the arterisks in Fig. 6B). Again, we did not see BF related differences in noise induced changes in peak latency and peak-sustained spike ratio. These results suggest a broad impact of noise on these two criteria, to which more changes were seen in low SR units and later after the noise exposure.

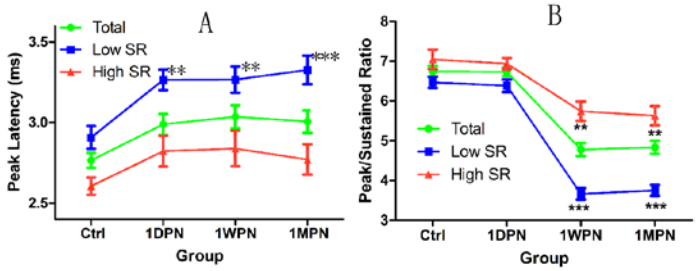

Figure 6. Noise induced prolongation in peak latency (A) and reduction in peak-sustained spike ratio (B). **: p<0.01, ***: p<0.001.

To further evaluate the impact of the noise exposure on the temporal response properties of auditory nerves, we used paired clicks with varied inter click interval (ICI, from 2 to 20 ms). As shown in Figure 7A, the spike rate to click 2 was suppressed by the preceding click 1 when the ICI was short; and it was recovered with increasing ICI and approached to the rate to click 1 for ICI > 10 ms. Figure 7B and C shows the recovery of both the click2 spike rate and click2/click1 spike rate ratio, as a function of ICI for all auditory nerve fibers recorded in the control group. The comparison between low- and high-SR units shows an overall high spike rate in low-SR units, the recovery functions with ICI in ratio are overlapped between the two types (Fig. 7C).

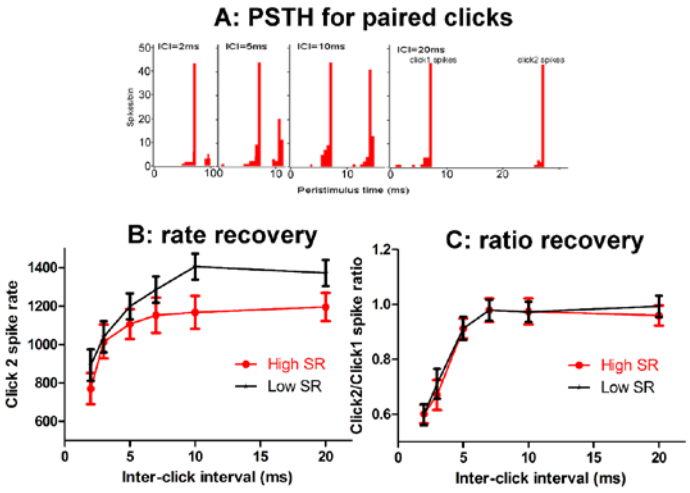

To examine the impact of the noise exposure on the recovery function, we compares them across the groups and separately for both high- and low-SR units (Figure 8 and 9). Overall, we found a slower recovery of click2 spike rate and ratio was seen after the noise and the changes were clearly shown later (at 1MPN) but not immediately after the noise. Furthermore, this deterioration in recovery function was worse in low-SR units.

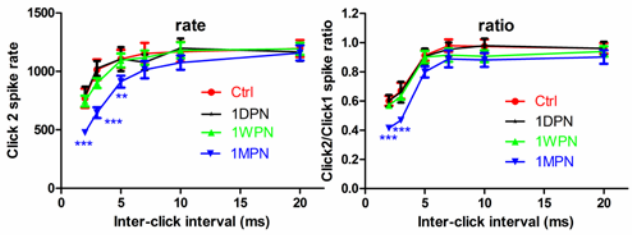

Figure 8. Paired click recovery functions of high-SR units. Left: click2 spike rate-ICI functions. Right: click2/click1 ratio-ICI functions. Two-way ANOVA on the factors of groups (noise-treatment) and ICI shows significant effect of noise. Post-hoc tests (Tukey method) within ICI shows significant differences only between 1MPN and the control groups. ***: p<0.001, **: p<0.01.

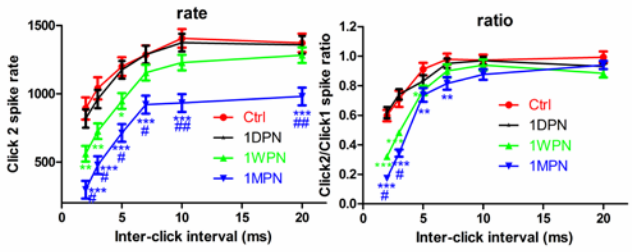

Figure 9. Paired click recovery functions of low-SR units. Left: click2 spike rate-ICI functions. Right: click2/click1 ra-

tio-ICI functions. Two-way ANOVA on the factors of groups (noise-treatment) and ICI shows significant effect of noise, which is further identified by the post-hoc tests (Tukey method) within ICI factor between the control and 1WPN/1MPN groups respectively (by *s), as well as between 1WPN and 1MPN groups (by #s). ***: $p<0.001$, **/##: $p<0.01$, and */#: $p<0.05$.

Conclusions
The synapses damaged by noise are largely repairable. The repaired synapses (mostly the low-SR units) are not functionally healthy and show deficits in both intensity and temporal coding.

Funding
This study was supported by the grants from Natural Science and Engineering Research Council of Canada (RGPIN-2014-05437), Natural Science Foundation of China (81271086, 81400464, 81170920) and the State Key Development Program for Basic Research of China (2014CB541705).

PS 22

Voltage-gated Na+ and K+ Channel Topographies in Auditory Nerve Fibers

Kyunghee Kim; Mark Rutherford
Washington University in St. Louis

In response to sound or in response to stimulation by a cochlear implant, excitation of the auditory nerve and thus hearing as well depend on action potential initiation and propagation in the individual auditory nerve fibers (ANFs). Action potential initiation and propagation in turn depend on spatially organized voltage-gated ion channels in axonal membranes. Although several voltage-gated ion channels are expressed by ANFs somatically, their native axonal locations are largely unknown. Here, we studied voltage-gated Na^+ and voltage-gated K^+ channel topographies in peripheral axons of ANFs in the rat cochlea with immunohistochemistry and confocal microscopy. The peripheral axon of each ANF has a heminode adjacent to the habenula perforata (HP) in the osseous spiral lamina (OSL), one or more node(s) in the OSL, and soma-flanking structures in the spiral ganglion. We focused on the heminode in the distal OSL where spikes are thought to initiate (Liberman, 1980; Hossain et al., 2005; McLean et al., 2009; Rutherford et al., 2012). The fast delayed rectifier $K_V3.1b$ was strictly localized to nodes and hemindoes while the slower delayed rectifier $K_V2.2$ was expressed in a mutually exclusive domain beginning on the juxtaparanode and continuing uniformly along the first internode toward the middle of the OSL. In contrast to these high-voltage activated channels, the low-voltage activated $K_V1.1$ was enriched at juxtaparanodes. However, $K_V1.1$ was enriched at juxtaparanodes only after approximately p13, the onset of hearing. Colocalization analysis suggested that voltage-gated Na^{2+} and K^+ channel co-localization with ankyrin-G increased through postnatal development at heminodal spike generators. In contrast, channels were already maximally co-localized with ankyrin-G before hearing onset at spike propagating nodes, suggesting that heminodes and nodes follow distinct developmental programs in relation to ankyrin-G. The spike generator at the HP is tightly coupled to the glutamatergic ribbon synapse approximately 20–40 µm away. The topographies of these voltage-gated Na^+ and K^+ channels are expected to influence ANF overall firing properties and their heterogeneities likely influence the diversity of firing properties among individual ANFs.

Funding
This work was funded by an International Project Grant from Action on Hearing Loss to M.A.R. and startup funds from the Dept. of Otolaryngology at Washington University in St. Louis.

PS 23

Shaping Action Potentials in the Auditory Nerve: Recruitment of Kv Channels to Specialized Microdomains in Spiral Ganglion Neurons

Katie Smith; Brikena Hoxha; Dan Jagger
University College London

Background
Type I spiral ganglion neurons (SGNs), transmit acoustic information from inner hair cells to the auditory brainstem. Action potentials which are generated at the first heminode (Hossain et al., J. Neurosci, 2005) must be propagated via saltatory conduction in the peripheral and central neurites towards the brainstem. Recently, we identified specific localization of voltage-gated K^+ channels within key SGN microdomains associated with action potential initiation and propagation (Smith et al., J. Neurosci, 2015). Here we examined the recruitment of ion channels to these microdomains during postnatal development in the mouse cochlea.

Methods
Immunofluorescence experiments were performed on 4% paraformaldehyde fixed mouse cochlear sections (C57Bl/6; postnatal day P8-P20). Antibodies were used to determine the subcellular localization of voltage-gated K^+ channel subunits (Kv1.1, Kv1.2, and Kv3.1b) and ankyrin-G which is known to anchor certain ion channels within the membrane at nodes of Ranvier and other key sites.

Results
At around one week post-hearing onset (P20), Kv1.1 and Kv1.2 subunits were localized to key SGN subcellular microdomains: the first heminode, juxtaparanodes adjacent to nodes of Ranvier in the peripheral neurites, the somatic membrane, and juxtaparanodes of central neurites. With the exception of the somatic membrane, Kv3.1b subunits localized to the same microdomains but were spatially distinct from Kv1.1/Kv1.2. At the first heminode Kv3.1b localized more proximally to the inner hair cell synapse, and it also targeted specifically to nodes of Ranvier. Earlier in development, ankyrin-G appeared at the nodes prior to the Kv subunits. The nodal appearance of Kv1 and Kv3.1b subunits was first observed around P10-P12, with their expression at the first heminode occurring later (~P12-14), and later still in the somatic membrane (P16 onwards).

Conclusions
Kv subunits are not evenly distributed throughout the membrane of SGNs. The targeting of Kv1 and Kv3.1b subunits to SGN microdomains points to key roles in both the generation and propagation of action potentials. Their relatively late appearance during development, particularly at the first heminode and somatic membrane, suggests that refinements in ion channel expression continue after hearing onset in mice. These refinements may underlie the exquisite temporal precision of spike coding in mature hearing. This spatio-temporal mapping of ion channel distribution may lead to improved accuracy of models of sound coding in the auditory nerve.

Funding
This work was funded by an Action on Hearing Loss Grant (P35021).

PS 24

Fatty Acids as Native Modulators of Coding in the Auditory Nerve

Lorcan Browne; Katie Smith; David McAlpine; David Selwood; Dan Jagger
University College London

Background
Rapid spike adaptation in auditory neurons ensures high temporal precision and fidelity to code excitatory inputs (Rutherford et al, J Neurosci 2012). Rapid adaptation in Spiral Ganglion Neurons (SGNs) is established by Kv1.1/Kv1.2 heteromeric channels that mediate low-threshold voltage-activated (LVA) K+ currents (Smith et al, J Neurosci 2015). These LVA currents are strongly dependent on the membrane phospholipid phosphatidylinositol-4,5-bisphosphate (PIP2), which binds preferentially to Kv1.2 subunits (Kruse 2013). Here we have assessed the effects of other membrane lipids on Kv1.2, to identify other native modulators of SGN function.

Methods
Whole-cell patch clamp recordings were made from HEK293 cells stably-transfected with the Kv1.2 subunit. Commercially available fatty acids (Sigma) and lab-synthesized analogues were bath applied.

Results
Homomeric Kv1.2 channels mediated non-inactivating outward K+ currents. Arachidonic acid (AA),which constitutes ~20% of membrane phospholipid fatty acid content, inhibited the currents in a dose-dependent manner and accelerated the inactivation kinetics. 100 μM AA decreased current amplitudes by >90%, and negatively shifted the voltage-dependence of activation. These effect could be reproduced by the related poly-unsaturated fatty acids docosahexaenoic acid and linoleic acid. However, mono-unsaturated fatty acids were less effective modulators of Kv1.2, reducing current amplitudes by <25%. Non-fatty acid chemical analogues of AA also strongly modulated Kv1.2-mediated currents. Anandamide (100 μM), decreased the current by >75% and accelerated the inactivation kinetics. Fatty acids effective on Kv1.2 subunits are presently being tested on SGN voltage-gated currents and spike adaptation.

Conclusions
Kv1.2 homomeric channels are highly-sensitive to poly-unsaturated fatty acids. In SGNs, Kv1.2 channel subunits are targeted to microdomains that regulate action potential generation and propagation, such as the spike initiation site, the somatic membrane and juxtaparanodes (Smith et al, J Neurosci 2015). Fatty acid modulation of Kv1.2 subunits identifies a potential mechanism of local control of membrane excitability in SGNs. Further, such molecules could form the basis of novel approaches to pharmaco-therapeutics in the auditory nerve.

Funding
This project was funded by a UCL Crucible Foundation Studentship and an Action on Hearing Loss Grant (Grant #: P35021)

PS 25

A Revised Model of Synaptic Release Accounts for Interspike-Interval Distributions, Spike-Count Distributions, and Non-Renewal Properties of Spontaneous Spike Trains of Auditory-Nerve Fibers

Adam Peterson; Peter Heil
Leibniz Institute for Neurobiology

In mammals, the spiking characteristics of each primary auditory afferent (type-I auditory-nerve fiber; ANF) are mainly determined by a single ribbon synapse in a single inner hair cell, with evidence that each transmitter release event evokes a postsynaptic spike unless the ANF is refractory. ANF spike trains therefore provide indirect information about the release statistics of these synapses in vivo. Heil et al. (J Neurosci 2007) demonstrated that the ISI distributions obtained from the spontaneous activity of cat ANFs likely result from brief refractoriness operating on a non-Poisson stochastic point process of excitation. Peterson et al. (J Neurosci 2014) proposed a 3-parameter model of vesicle-pool depletion and replenishment with non-Poisson release statistics. They demonstrated that, combined with refractoriness, it can account for the ISI distributions and also for the non-renewal properties (negative serial ISI correlations) of the spontaneous spike trains, with maximum pool size (n_{max} = 4) and replenishment time constant (t_{repl} ~13 ms) held constant, and only the release probability varying between synapses.

At rates higher than those used to fit the model (up to ~100 spikes/s), however, simulated trains of synaptic release events and spikes turned out to be excessively regular, due to modeling the vesicle-pool replenishment using a deterministic exponential recovery function. A solution to this problem is to model the replenishment of each release site independently, such that after each release event, the associated site remains depleted for a duration drawn from an exponential distribution. This revised model better accounts for spike trains having high rates, while not substantially affecting the results for low rates. We also extend the model to account for

observed long-range temporal dependences in spike trains, incorporated as fractional Gaussian noise (modified after Jackson and Carney, JARO 2005). We demonstrate that the revised model accounts for the non-renewal properties of cat spontaneous spike trains, the ISI distributions of cat, chinchilla, and guinea pig spontaneous spike trains (even with rates >100/s), and the long-range temporal dependences in cat and chinchilla spontaneous spike trains. Finally, we show that the popular models of Zilany et al. (JASA 2014) and Meddis et al. (JASA 2006) do not precisely account for these properties.

Because our revised synapse model accounts for all major properties of mammalian ANF spontaneous spike trains, we suggest that it can serve as a strong foundation upon which to base detailed explorations of responses to sounds.

Funding
This work was supported by a grant of the Deutsche Forschungsgemeinschaft to PH (He1721/11-1) within the Priority Program 1608.

PS 26

Spectro-Temporal Tuning of Suppressive Non-Linearities Measured from Chinchilla Auditory-Nerve-Fiber Responses Following Noise-Induced Hearing Loss

Mark Sayles[1]; Michael Heinz[2]
[1]Katholieke Universiteit Leuven; [2]Purdue University

Background
The compressive nonlinearity of healthy cochlear signal transduction manifests as suppressive spectral interactions. These frequency-dependent nonlinearities are important for neural coding of complex sounds. Acoustic-trauma-induced outer-hair-cell damage is associated with loss of nonlinearity, which auditory prostheses attempt to restore with, e.g., "multi-channel dynamic compression" algorithms. Quantitative descriptions of suppression for broadband sounds in hearing-impaired (HI) mammals are lacking. Here we used singular-value decomposition of the second-order Wiener kernel (h_2) to quantify suppression in normal-hearing (NH) and HI chinchilla auditory-nerve-fiber (ANF) responses to broadband Gaussian noise.

Methods
To induce hearing loss, chinchillas were exposed to a 500-Hz-centered octave-band noise at 116-dB SPL for 2 hours under ketamine-xylazine anesthesia and allowed to recover for at least 2 weeks. ANF spike-train responses to broadband noise (16-kHz bandwidth; 138 NH, and 148 HI fibers) were recorded under terminal barbiturate anesthesia. Stimuli were presented at equal sensation level (SL; ~15 dB), and in a subset of fibers at equal sound pressure level (~70-dB SPL). We computed h_2 as the scaled spike-triggered covariance matrix. We factored h_2 into excitatory ($h_2\varepsilon$) and suppressive ($h_2\sigma$) sub-kernels. The noise floor of each sub-kernel was computed using bootstrap resampling. To quantify the relative spectro-temporal tuning of suppression and excitation we computed a normalized 2-dimensional cross-correlation matrix between the significant $h_2\varepsilon$ and $h_2\sigma$ matrices.

Results
HI animals had elevated ANF excitatory thresholds (by ~20-40 dB), broadened frequency tuning, and reduced-magnitude distortion-product otoacoustic emissions. NH fibers showed strong even-order suppressive non-linearities. In NH fibers, singular-value decomposition of h_2 typically revealed several significant suppressive quadrature-phase vector pairs (*z-score* >3). Suppressive effects were observed for frequencies above, below, and within the excitatory band. At equal SL, HI fibers showed characteristic-frequency-(CF)-dependent changes in suppression magnitude and spectro-temporal dynamics. For mid-CF fibers (2-5 kHz), suppression above and below CF was absent; only weak suppression remained at CF. High-CF fibers (>5 kHz) showed a large increase in suppression magnitude below CF, and a loss of suppression above CF. Low-CF fibers (<2 kHz) showed similarly weak suppression in NH and HI animals. At equal SPL, spectro-temporal tuning and strength of suppression appear more similar between NH and HI animals.

Conclusions
Overall, suppression in ANF responses to broadband noise was reduced, but less than expected. Moreover, our data demonstrate important CF-dependent differences between NH and HI responses at equal SL. These data will help guide improvements in novel amplification strategies for complex listening situations (e.g., speech in noise).

Funding
Supported by NIH (NIDCD) R01-DC009838 (MGH) and an Action on Hearing Loss Fulbright scholarship (MS).

PS 27

A Multi-Compartment Neuronal Model of Spiral Ganglion Neurons Developed for NANOCI

Heval Benav; Carolyn Garnham
MED-EL Medical Electronics

Background
The NANOCI project aims at creating a gapless electrode-neuron interface for cochlear implants (CI) by pharmacologically induced growth of peripheral processes towards electrode contacts. We here present the development of a custom-made computational model for investigation of neuronal responses with the gapless electrode neuron-interface created by NANOCI.

Methods
For modelling of extracellular stimulation, an analytical approach assuming a point-source or a disk-electrode was selected for calculation of voltages generated by the electrode within the scala tympani. The mean resistivity of the extracellular medium was set to 300 Ωcm (Rattay et al. 2001). A multi-compartment model was developed for a morphologically correct representation of type I spiral ganglion neurons (SGNs) in the human. The SGN model had 52 compartments and a length of ~600µm. Diameters were set to 10µm for the soma, 1µm for the peripheral process and

2µm for the central process (Spoendlin and Schrott 1989). Peripheral and central process had 40 layers of myelin, however, somatic regions were assumed to be unmyelinated according to previous findings in human tissue (Liu et al. 2012). Na^+ channels, low threshold K^+ channels and high threshold K^+ channels were distributed across all nodes of Ranvier and unmyelinated perisomatic regions. The voltage-dependency was calculated with a biophysical model based on Negm et al. 2008. We calculated the neuronal response in dependence of the distance of the electrode to the terminal of the peripheral process (0µm to 100 µm). Biphasic current controlled stimuli with 40µs phase duration were applied with increasing amplitudes from 0µA to 150µA. A stimulation was considered to be successful if the membrane potential was raised from the resting potential of -80mV to above -20mV.

Results

The figure depicts the simulation results for distance dependency of the simulated SGN. Threshold values ranged from 15µA for 0µm distance to 130µA for 100µA distance. We observed a tendency of the SGN model in which the unmyelinated soma acted as a barrier and action potential were significantly weakened when crossing the soma.

Conclusion

The model delivered results for distance dependency which were qualitatively in agreement with similar in-vitro experiments (Hahnewald et al. 2015, submitted to JNE). The resulting threshold amplitudes suggest that not only SGNs which terminate directly at the electrode would be stimulated with stimuli in an operating range of 0µA to 150µA, but also peripheral processes of SGNs terminating in the vicinity of the stimulating electrode.

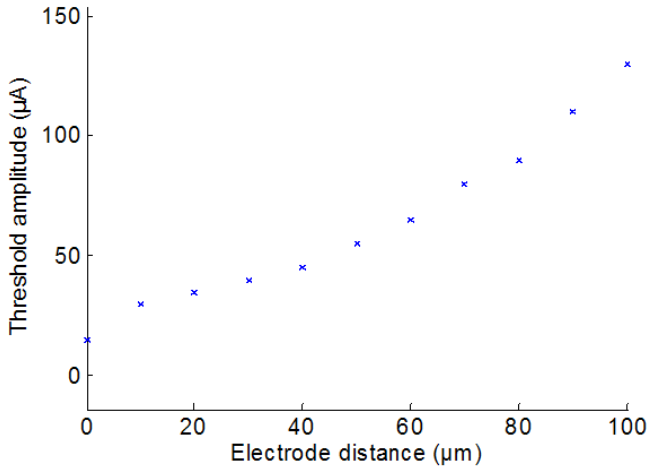

Funding

The research leading to these results has received funding from the European Union's Seventh Framework Programme under grant agreement No. 281056 (Project NANOCI)

PS 28

Bayesian Nonparametric Gaussian Mixture Modeling for Estimating Instantaneous Neural Firing Rate

Christopher Boven; Jont Allen; Robert Wickesberg
University of Illinois at Urbana-Champaign

Analysis of electrophysiological data often involves estimation of the instantaneous firing rate in the neuron's response. A common solution uses the peristimulus time histogram (PSTH) computed from the spike trains that the neuron produces during multiple repetitions of the stimulus. Using a PSTH requires the selection of a bin width, which could introduce undesirable temporal quantization error, can require numerous presentations of the stimulus across multiple experiments to reduce noise, and may involve the application of an arbitrary smoothing function. Kernel density estimation, a more recent alternative technique, has similar issues. Instead, we propose a computational statistics approach using the Dirichlet Process Gaussian Mixture Model (DPGMM) and Bayesian inference.

Our method assumes that each spike is a sample drawn from some unknown one-dimensional multi-modal probability distribution function whose shape represents the instantaneous firing rate. This probability distribution can be modeled by a mixture of Gaussian distributions, each with its own set of parameters (weight, mean and variance). Bayesian inference is used to compute the posterior distribution of these parameters given the data, while the need for specifying the number of Gaussians to include a priori is obviated by using a nonparametric prior distribution (the Dirichlet process) which contains information about the number of components in the model (Rasmussen, 2000). Collapsed Gibbs sampling, a well-known Markov Chain Monte Carlo method that generates samples from complicated posterior distributions, is used to perform the actual inference.

This machine learning approach describes the precise time-varying spike densities typically observed with electrophysiological recordings. The transient periods of high activity (such as onsets), as well as relative periods of inactivity (e.g., the spontaneous firing rate), are both accurately represented. The method is automatic, involves no specification of the parameters of the Gaussian Mixture Model by the investigator, and there is no overfitting of the data. The result is an estimate of the neuron's instantaneous firing rate that minimizes noise, allowing for a more confident and in-depth analysis of the spiking activity than is possible with PSTHs or kernel density estimates.

Funding

National Science Foundation; Department of Psychology, University of Illinois Urbana-Champaign

PS 29

A Comparative Study of Human Inner Hair Cell- Auditory Nerve Models.

Amin Saremi; Mathias Dietz; Rainer Beutelmann; Sarah Verhulst; Jutta Kretzberg
University of Oldenburg

Background

Despite the large variety of existing auditory models, it is often unknown how they respond to stimuli they were not primarily designed for, or how well they compare to other auditory models in reproducing the relevant experimental data. We aim to quantitatively investigate the performance of several mainstream auditory models in response to a set of common stimuli and understand their respective advantages and limitations. After comparing seven publicly-available models of the basilar membrane (BM) mechanics in our previous work, we now focus on the models of the human inner hair cell (IHC) – auditory nerve (AN) complex.

Methods

Six publicly available models of the IHC-AN complex were compared: **(1)** the computational model of Heinz and Carney (2001), **(2)** the IHC-AN stage of the MAP model of Meddis et al. (2010), **(3)** the IHC-AN stage of the phenomenological model of Zilany et al. (2014), **(4)** The IHC stage of the CASP model (Jepsen et al., 2008), (**5**) The IHC stage of the PEMO model (Dau et al., 1997), and (**6**) a biophysical lumped-element model of the IHC-AN stage (Lopez-Poveda and Eustaquio-Martin, 2006; Sumner et al., 2002). These six models were studied at characteristic frequencies (CFs) of 0.5, 1, 2 and 4 kHz. The IHC stages of the models were excited by sinusoids at 30 dB SPL at frequencies between 0.1 and 10 kHz to assess the characteristics of the IHC filtering.

Results

The IHC stages of the five functional models commonly showed a low-pass behavior estimated as the membrane potential relative to the hair bundle deflection. However, the 3-dB cut-off frequencies were different between the models, ranging from 440 to 1000 Hz at the CF of 1 kHz. The biophysical IHC model, on the other hand, showed a band-pass behavior with a peak at approximately 250 Hz and also relatively shallower low-pass slopes at higher frequencies. Furthermore, we are planning to simulate the hearing thresholds on the high-spontaneous rate AN fibers for CFs from 0.1 to 6 kHz and compare the predictions of these six models with the thresholds measured on the cat AN fibers (Liberman and Dodds, 1983).

Summary

The IHC-AN models are often used as pre-processors in hearing machines and speech processors. Therefore, the outcome of this ongoing project can provide important information for those seeking an appropriate model for a specific application.

Funding

This work is supported by the DFG Cluster of Excellence EXC 1077/1 “Hearing4all”, Germany.

PS 30

Quantifying envelope coding in the electrically stimulated auditory nerve: Effects of pulse rate and stimulus level

Suyash Joshi; Torsten Dau; Bastian Epp
Technical University of Denmark

Background

Cochlear implants (CI) stimulate the auditory nerve (AN) with a train of biphasic pulses modulated with the envelope of a desired acoustic signal. Since the envelope is the primary cue available to CI listeners, most stimulation strategies are developed with the goal to enhance this cue in the AN. It was hypothesized that one reason for the poor performance of CI listeners is due to phase-locking of the AN response to the carrier pulse train rather than to the stimulus envelope; High pulse rates would reduce the phase-locking to the carrier pulse train and hence improve the encoding of the stimulus envelope. Amplitude modulation detection thresholds (AMDT) showed, however, detrimental effects of higher pulse rates. Existing models of AN for electrical stimulation fail to predict such an effect.

Methods

A recently proposed two-neuron model of AN responses to electrical stimulation (Joshi et al., 2015, CIAP) was used to investigate the effect of carrier pulse rate on temporal coding in the AN. It consists of two exponential integrate-and-fire neurons that simulate peripheral and central sites of excitation along the AN neuron, that are preferentially excited by cathodic and anodic currents, respectively. This model was extended by inclusion of a stimulus-triggered adaptive current to account for temporal-context effects, like sub-threshold facilitation, adaptation and refractory effects. The model was stimulated with either unmodulated or sinusoidally modulated pulse train of carrier rates between 200 to 5000 Hz. Responses were analyzed using peri-stimulus-time histogram (PSTH) and inter-spike-interval (ISI).

Results

PSTH and ISI showed large differences for carrier pulse rates: Responses to low pulse rates showed a large degree of phase-locking to the carrier rate. Responses to high pulse rates were influenced by refractory properties, leading to broader ISI distributions. An interaction between the responses to the modulation frequency and the carrier pulse rate was found in the ISI. Most importantly, the ISI did not show a maximum at the period of the modulation frequency for any of the carrier pulse rates, particularly for low modulation depths.

Conclusion

The ability of the model to account for temporal-context effects makes it suitable for investigating temporal coding at the level of the electrically stimulated AN. The observed interaction between carrier pulse rate and the modulation frequency may be the reason underlying the detrimental effects on AMDT at high pulse rates. Separation of carrier and envelope contributions will help to understand the mechanisms underlying the behavioral data.

Funding
The work has been funded by grant from the People Programme (Marie Curie Actions) of the European Unionâ€™s 7th Framework Programme FP7/2007-2013/ under REA grant agreement number PITN-GA-2012-317521.

PS 31

Analysis of Simultaneous Multi-Electrode Stimulation Designs: creating independent channels

Florian Langner[1,2]; Aniket Saoji[3]; Leonid Litvak[3]; Andreas Büchner[2,4]; Waldo Nogueira[2,4]
[1]Hannover Medical School; [2]Medical University Hannover; [3]Advanced Bionics LLC; [4]Cluster of Excellence "Hearing4all"

In the last 30 years the field of cochlear implant (CI) sound coding strategies has seen a tremendous development, always in the prospect of improving speech intelligibility. These strategies can also be used to control the trade-off between speech performance and power consumption. For example multiple simultaneous electrode stimulation strategies can be used to lower the power consumption while affecting speech intelligibility in different ways. Most commercial CI strategies use sequential channel stimulation. One could add additional parallel stimulation channels such that the electrical interaction between the multiple simultaneous stimulated channels is increased. We hypothesize that electrical interaction will produce spectral/channel smearing and power savings because the electrical field of the simultaneous stimulated channels interact, producing a louder sensation than sequential stimulation. To test this hypothesis we implemented different strategies using the BEPS+ research interface from Advanced Bionics: (I) the commercial F120 strategy using sequential channel stimulation (each channel uses two simultaneous stimulated electrodes), (II) an extended version of F120, the Paired-F120 strategy, consisting of parallel stimulation with two channels. Here the electrical field of the two channels will interact, requiring less current on each channel to perceive the same loudness as with F120. However, channel interaction between theoretically independent channels may reduce speech performance. This can be diminished by adding an inverse-phased stimulation channel (flanking electrode) between the paired current-steered channels. This strategy is termed (III) Paired F120 with Flanks. For each strategy we measured speech intelligibility using two lists of the Hochmair-Schulz-Moser sentence test. Spectral smearing was assessed with spectral modulation depth detection (SMT) at two ripple per octave frequencies (0.5 Hz and 1 Hz). Initial results show that – compared to the F120 strategy - Paired stimulation provides similar performance whereas Paired with Flanks decreases in speech intelligibility (sole significant difference between F120 and Paired with Flanks with the highest flanking current, $p < 0.05$). In most subjects a higher threshold in the SMT task was observed (average decrease of 0.7 dB in the 0.5 Hz/Oct, 5 dB in the 1 Hz/Oct condition) with Paired stimulation. All subjects used lower current levels with Paired stimulation compared to F120 to reach equal loudness perception (average of 24 clinical units for Paired and 12 for Paired with Flanks; one unit equals 4.27 µA for a pulse width of 18 µs). Paired stimulation can therefore reduce power consumption while maintaining sufficient performance in terms of speech intelligibility and spectral smearing.

Funding
This work was supported by the DFG Cluster of Excellence EXC 1077/1 â€œHearing4allâ€ .

PS 32

Stapedotomy versus Cochlear Implantation for Advanced Otosclerosis: Systematic Review and Meta-analysis

Yasin Abdurehim[1,2]; Anthony Zeitouni[1]; Alexandre Lehmann[1]
[1]McGill University; [2]First Teaching Hospital, Xinjiang Medical University

Objectives
To compare the hearing outcomes of stapedotomy and cochlear implantation in patients with advanced otosclerosis.

Study Design
Systematic review of literature and meta-analysis.

Data Source
PubMed, EMBASE, and The Cochrane Library were searched for "otosclerosis", "stapedotomy" and "cochlear implantation" and their synonyms with no language restrictions on March 10, 2015.

Methods
Studies comparing the hearing outcomes of stapedotomy with cochlear implantation and studies comparing hearing outcomes of cochlear implantation with and without a previous stapes prothesis in patients with advanced otosclerosis were included. Postoperative speech recognition scores were compared using weighted mean difference and a 95% confidence interval, random effect model was used for data pooling.

Results
Only four studies met our inclusion criteria. Cochlear implantation leads to significantly better speech recognition scores than stapedotomy ($p< 0.00001$). However, cochlear implantation is no longer superior if compared with the subgroup of successful cases of stapedotomy ($p=0.47$). There is also no significant speech recognition difference between cochlear implantation with a previous stapes prothesis and those without a stapes prothesis ($p=0.22$).

Conclusions
Profound sensorineural hearing loss due to advanced otosclerosis should be distinguished from sensorineural hearing loss of distinct origin. Stapedotomy should be attempted before considering cochlear implantation in this particular group of patients. With stapedotomy and hearing aid, about 55% of such cases can achieve good hearing outcomes comparable to cochlear implantation. Cases of unsuccessful stapedotomy can still benefit from cochlear implantation without any negative effect.

PS 33

Randomized Controlled Trial on Cochlear Implantation versus Contralateral Routing of Sound Systems or Bone Conduction Devices in Patients with Single-Sided Deafness

Jeroen Peters; Anne Wendrich; Adriana Smit; Huib Versnel; Gijsbert Van Zanten; Inge Stegeman; Wilko Grolman
University Medical Center Utrecht

Background
Patients with single-sided deafness (SSD) have problems with speech perception in noise and localization of sounds. These tasks require binaural hearing, which is not improved by current treatment options: Contralateral Routing of Sound hearing aids (CROS) and Bone Conduction Devices (BCD). Moreover, SSD patients frequently suffer from tinnitus. In recent literature, cochlear implantation (CI) seems to be a promising treatment alternative for SSD. However, only low Level of Evidence (LoE) studies have been conducted so far. Our aim was to evaluate CROS, BCD and CI for SSD in a Randomized Controlled Trial (RCT).

Methods
We conducted an RCT at our tertiary referral cochlear implant center. Adult SSD patients (with a duration of deafness minimum 3 months – maximum 10 years and a pure tone average [0.5-4 kHz] of maximum 30 dB in the better ear and minimum 70 dB in the poor ear) were randomized into one of three groups: 1) CI, 2) 6 week trial periods of first BCD on headband, then CROS or 3) 6 week trial periods of first CROS, then BCD on headband. After the trial periods in groups 2 and 3, patients could choose with which treatment to proceed: CROS, BCD on abutment or No treatment. Outcomes of interest were speech perception in noise, sound localization, tinnitus suppression and quality of life (QoL).

Results
The results of 34 patients at 3 months follow up will be presented (CI, n = 9; BCD, n = 3; CROS, n = 11; No treatment, n = 11). Less patients than expected opted for a BCD. Patients in the CI and CROS groups had improved speech perception in noise with speech directed to the poor ear compared to baseline performance. However, CROS patients experienced a disadvantage with speech directed to the better ear, whereas the CI patients did not perform worse in this configuration. Sound localization improved most in CI patients. Mean tinnitus burden hardly changed in the BCD and CROS groups compared to baseline, whereas ot decreased siginifcantly in the CI group. QoL was most improved in CI patients.

Conclusions
Our current results of the RCT on treatment modalities for SSD confirmed that CI is a promising treatment alternative to improve hearing outcome, tinnitus and QoL.

Trial registration
Netherlands Trial Register (www.trialregister.nl): NTR4580.

Level of Evidence
1b.

Funding
Part of the costs of this study is funded by Cochlear Ltd. as a non-restrictive research grant.

PS 34

Evaluating a New Algorithm for Multi-Talker Babble Noise Reduction Using Q-Factor Based Signal Decomposition.

Roozbeh Soleymani; Ivan Selesnick; David Landsberger
New York University

Background
One of the key challenges for cochlear implant (CI) users is understanding speech in background noise. Previously, many different single-channel noise reduction algorithms have been introduced to address this issue. Typical algorithms have included applying a gain to the noisy envelopes, pause detection and spectral subtraction, feature extraction and splitting the spectogram into noise and speech dominated tiles. However, even with these algorithms, speech understanding in the presence of competing talkers (i.e. speech babble noise) remains difficult and additional artifacts are often introduced.

Algorithm
We have developed a new two-stage algorithm with the goal of improving intelligibility of speech in the presence of background noise (including multi-talker babble). The first stage decomposes the speech signal in to two components: a low Q-factor component and a high Q-factor component. The high Q-factor component exhibits more sustained oscillatory behavior than the low Q-factor component. The signal decomposition is achieved using a sparse optimization wavelet method. The second stage involves temporal and spectral cleaning of the signal using the information obtained from the two components derived in the first stage.

Methods
The algorithm was evaluated by measuring subject's understanding of IEEE standard sentences with and without processing by the algorithm. Sentences were presented against a background of 4-talker babble using four different signal to noise ratios (0, 3, 6, or 9 dB). Two randomly selected sentence sets (20 sentences) were presented for each of the 8 conditions (two processing conditions and 4 SNRs). The percentage of correct words in sentences was recorded. Prior to testing, subjects practiced with 20 processed sentences.

After completing the speech understanding test, subjects were asked to evaluate the sound quality of the sentences using a MUSHRA (MUltiple Stimuli with Hidden Reference and Anchor) scaling test.

Normal hearing subjects will be tested using a noise-vocoded simulation while CI users will be tested with un-vocoded stimuli.

Results
Preliminary results have been collected with 4 NH subjects. For all subjects, intelligibility and quality improved. While the improvement varied across subject and SNR, speech intelligibility improved between 10% to 20% while sound quality improved between 20% to 30%.

Conclusions
The new algorithm improves both speech understanding and sound quality for speech in multi-talker babble. Careful considerations must be taken to implement the strategy in real time if the strategy is to be clinically implemented.

Funding
NIH grant R01-DC12152

PS 35

Testing a New Cochlear Implant Stimulation Strategy With Dynamic Focusing

Julie Bierer[1]; Wendy Parkinson[1]; Heather Kreft[2]; Andrew Oxenham[2]; Chen Chen[3]; Leonid Litvak[3]
[1]University of Washington; [2]University of Minnesota; [3]Advanced Bionics

The standard, monopolar electrode configuration used in commercially available cochlear implants creates a broad electrical field, which can lead to unwanted channel interactions. Use of more focused configurations, such as tripolar and phased array, have led to mixed results for improving speech understanding and spectral resolution. Dynamic focusing, which uses focused tripolar stimulation at low levels and less focused stimulation at high levels, may better mimic cochlear excitation patterns in normal acoustic hearing, while reducing the current levels necessary to achieve sufficient loudness at high levels. Post-lingually deafened adults, implanted with the Advanced Bionics device participated in this study. Speech perception was assessed in quiet and in four-talker babble background noise. Speech stimuli were closed-set spondees in noise, and medial vowels in the hVd context at 60 and 50 dBA in quiet and in noise. The signal-to-noise ratio was adjusted such that performance was between 40 and 60% correct with the monopolar strategy. Subjects were fit with three experimental strategies matched for pulse duration, filter settings, clear voice level, and loudness on a channel-by-channel basis. The strategies included 14 channels programmed in monopolar, fixed partial tripolar (sigma = 0.8), and dynamic partial tripolar (sigma at 0.8 at threshold and 0.5 at the most comfortable level). Fifteen minutes of listening experience was given with each strategy by listening to the AZBio sentences. The results of speech perception scores were similar with all three strategies. However, most subjects rated the sound clarity and richness higher for the tripolar and dynamic focusing strategies. Longer experience with new strategies of stimulation might be necessary for subjects to learn how to use the potentially improved input to their auditory system.

Funding
This work was supported by NIH RO1 DC 012142 (JAB) and DC012262 (AJO).

PS 36

The Effects of Improved Sound Coding Strategy on the Voice Gender Identification in Cochlear Implant Users

Danijel Nejašmić[1]; Chris James[2]; **Damir Kovačić**[1]
[1]University of Split, Split; [2]Hôpital Purpan, Toulouse and Cochlear France

Enhanced spectral and temporal processing (STEP) was developed with the aim to improve the perception of indexical information carried by voice pitch, such as voice gender. A dual filter-bank approach was employed with a bank of narrow, good quality filters and a bank of parallel wide filters. The voice gender identification was compared with vowel pitch ranking task in 7 Nucleus CI recipients using two coding variants: ACE and STEP. The gender of the speaker was assessed in a 2-AFC task employing short 2-sec speech items extracted from 20 male and 20 female speakers. Vowel pitch ranking was evaluated in two frequency ranges, lower (LFR) in the 126 -164 Hz range and higher (HFR) in the 164-212 Hz range, roughly corresponding to a male to female F0 continuum.

Analysis of vowel pitch ranking indicated two of seven subjects having high performance with clear pattern for LFR and less clear pattern for HFR whether with ACE or STEP. One subject had very good performance in LFR, but in the HFR performance with ACE was clearer than for STEP. One subject had a clear pattern in LFR with STEP, but a poor pattern with ACE and a poor performance in the HFR with both variants. Preliminary data from regression bootstrap analysis indicates correlation tendency between cumulative d' (dee-prime) and gender accuracy for ACE (r=0,726; 95% CI=0,128-0,988) and STEP (r=0,651; 95% CI=0,285-0,993) coding variants in LFR. Same tendency is present between global d' and gender accuracy for ACE (r=0,739, 95% CI=0,176-0,988) and STEP (r=0,675, 95% CI=0,332-0,985) in LFR. However, data analysis did not show any correlation tendency between either cumulative d' or global d' and gender accuracy in HFR. Voice gender identification has not improved in CI subjects using STEP as a new sound coding variant. Six of seven CI subjects had high performance in voice gender identification with higher score when detecting female voices (F0 > 164 Hz). Lack of correlation tendency in HFR and gender accuracy indicates that CI subjects were good in both tasks: vowel pitch and gender discrimination. In LFR, the results show a trend between successful vowel pitch and gender discrimination. CI subjects who were good in gender discrimination using ACE also had good performance using novel sound coding strategy – STEP. Generally it appears that improving temporal pitch coding with STEP had some effect in the LFR but no effect in the HFR.

Funding
This research was supported by Cochlear, and a part of the work by DK was funded by the European Commission (FP7-CIG-2011-303927)

PS 37

Predicting Ear Differences in Speech Recognition using ECAP Data in Cochlear Implant Listeners

Kara Schvartz-Leyzac; Bryan Pfingst
University of Michigan

Introduction

While it seems logical that speech recognition abilities in human cochlear implant recipients should be related to auditory nerve survival, most post-mortem analyses of cochlear-implanted human temporal bones fail to demonstrate such a relationship. However, two potential confounds exist with most post-mortem studies to date: 1) uncontrolled time and events between speech recognition assessments and temporal bone analyses and 2) uncontrolled effects of top-down (e.g., cognitive) processing abilities that vary across patients and are known to affect speech recognition abilities. Here we approach the problem using electrophysiological measures to estimate nerve survival in life and a within-subject design to limit confounding across-subject variables. Previous studies demonstrate that more than 50% of the variance in SGN density in the deaf implanted guinea pig cochleae can be accounted for by the slope of the ECAP amplitude growth function (Pfingst et al., 2014 ARO Abstract 253). The current study investigated the relationship between characteristics of the ECAP response and speech recognition abilities across ears in human subjects with bilateral cochlear implants.

Methods

Participants were eight human subjects (23 – 76 years old) who were bilaterally implanted with Cochlear® CI24RE(CA), CI512, or CI24R (CA) implants. ECAP responses were recorded from each individual electrode in each ear using Neural Response Telemetry (NRT) and CustomSound™ EP software. ECAP amplitude-growth functions were collected using two interphase-gap conditions (7 and 30 μs IPG). Speech recognition testing was performed for each subject in each ear and included sentence recognition in noise, as well as vowel and consonant recognition in quiet and in noise.

Results

Results showed that characteristics of the ECAP recordings varied across-electrodes within each subject, and also across ears and across subjects. Within each subject, characteristics of the ECAP recordings correctly predicted the ear with better speech recognition. Specifically, characteristics of the slope of the ECAP amplitude-growth function are significantly related to the between-ear difference in sentence recognition in noise. Additional characteristics and their relationship with between-ear differences in speech recognition will be discussed.

Conclusions

When used in a well-controlled paradigm, characteristics of the ECAP response are related to speech recognition abilities in adult cochlear implant recipients. Based on animal data, it can be inferred that variability in outcomes among cochlear implant listeners can be explained, at least in part, by cochlear health status (largely SGN density). These ECAP measures can potentially be used to modify cochlear implant mapping to maximize performance outcomes.

Funding

NIH/NIDCD R01 DC010786 and P30 DC05188

PS 38

Cortical Evoked Potentials to Spectral Change in adults with Cochlear Implants: Relationships to Speech Perception Ability

Andrew Dimitrijevic; Michael Smith; Vairavan Manickam
Cincinnati Children's Hospital

Background

Speech perception outcomes after cochlear implant (CI) surgery are often variable and difficult to predict. Some have suggested that one source of this variability is related to cortical plasticity following surgery. Psychoacoustic studies have suggested that frequency discrimination ability in CI users is related to speech perception in noise. This observation provided the motivation for the current day and therefore we compared speech perception abilities in both quiet and in noise to auditory cortical measures of frequency discrimination.

Methods

Behavioral and electrophysiological data from 9 adult CI users were collected. Behavioral data included speech perception in quiet and noise for consonants, vowels, sentences, and words. 64-Channel EEG data were collected in response to spectral changes in an ongoing pure tone (250 Hz) presented in free field. The degrees of frequency change were based on the frequency allocation table of a default Cochlear CI program setting such that a 10% change (250 to 275 Hz, change in same channel), 50% change (250 to 375 Hz, change across one channel), and 100% change (250 to 500 Hz, change across two channels) were used.

Results

N1 amplitudes were opposite to what was expected, larger responses were observed in CI users with poor speech perception compared to those with higher speech perception performance. N1 latency changed as expected, i.e., more delayed in CI users with poor speech perception ability. Significant correlations between N1 amplitude and word perception (both in quiet and in noise) were observed. Additionally, the disruptive effect of noise masking for word perception as measured by the difference between quiet and noise was also significantly correlated to N1 amplitude. Other significant correlations between electrophysiology and speech perception were also observed.

Conclusions

These data demonstrate that the cortical potentials to frequency change is related to speech perception performance in CI users. The paradoxical increase in amplitude may reflect an altered cortical representation of frequency related to sub-optimal CI map settings or abnormal cortical plasticity.

PS 39

An eABR-based Estimation of Electrical Field Interactions Predicting Cochlear Implant Performance

Michel Hoen
Oticon Medical

Cochlear implants (CIs) are neural prostheses that have been used routinely in the clinic over the past 25 years. They allow children who were born profoundly deaf, as well as adults affected by hearing loss for whom conventional hearing aids are insufficient, to attain a functional level of hearing. An increasingly frequent and systematic use for less severe cases of deafness and bilateralization without strictly defined solid criteria, associated with a lack of reliable prognostic factors, has limited individual and societal optimization of deafness treatment.

Our aim was to develop a prognostic model for patients with unilateral cochlear implants. A novel method of objectively measuring electrical and neuronal interactions using electrical auditory brainstem responses (eABR) was used.

Speech recognition performance without lip reading was measured for each patient using a logatome test (64 “vowel-consonant-vowel”; VCV; by forced choice of 1 out of 16). eABRs were measured in 16 CIs patients (CIs with 20 electrodes, Digisonic SP; Oticon Medical ®, Vallauris, France). Two measurements were obtained: eABR measurements with stimulation by a single electrode at 70% of the dynamic range (four electrodes distributed within the cochlea were tested), followed by a summation of these four eABRs, measurement of a single eABR with stimulation from all four electrodes at 70% of the dynamic range.

A comparison of the eABRs obtained by these two methods indicated electrical and neural interactions between the stimulation channels. Significant correlations were found between speech recognition performance and the ratio of the amplitude of the V wave of the eABRs obtained with the two methods (Pearson’s linear regression model, parametric correlation: r2=0·33, p<0·05; n=16; non-linear regression model: r2=0·47, p=0·005).

This prognostic model allowed nearly half of the interindividual variance in speech recognition scores to be explained. The present study used measurements of electrical and neuronal interactions by eABR to assess patients’ bio-electric capacity to use multiple information channels supplied by the implant. This type of prognostic information is valuable in several ways. On the patient level, it allows for customization of individual treatments. More generally, it may also improve the distribution of health resources by allowing individual needs to be addressed more effectively.

Acknowledgements
The authors would like to thank the Nice University Hospital for financial support to this study.

PS 40

Development of Electric-Acoustic Pitch Comparisons in Single-Sided-Deaf Cochlear Implant Users

Silke Klawitter; Benjamin Krüger; Andreas Büchner; Waldo Nogueira
Medical University Hannover, Cluster of Excellence “Hearing4all”

Introduction
8 cochlear implant (CI) users with near-normal hearing in their non-implanted ear compared pitch percepts for pulsatile electric and acoustic pure-tone stimuli presented to the two ears. 2 CI users were implanted with the 28mm MED-EL FLEX, 1 with the Cochlear CI24RE(CA), 2 with the Cochlear CI512, 2 with the Cochlear CI522 and 1 with the AB MidScala electrode. The experiments were performed right after activation of the CI for the first time, 2 months, 5-8 months and 1 year after activation.

Method
After loudness balance the electric and acoustic stimuli, comparisons were performed between a 1000 pps pulse train and pure tones or between 12 pps electric pulse trains and bandpass-filtered acoustic pulse trains of the same rate. An interleaved adaptive procedure was used to obtain the match between the electric and the acoustic stimuli. In order to control for non-sensory biases potentially arising from the large range of acoustic stimuli presented during the pitch matching procedure sanity checks as proposed by [2] were applied.

Electrode position data for all 8 subjects were taken from Cone Beam Computer Tomography (CBCT) data. The angular positions of the intracochlear electrode contacts were determined postoperatively. The electrode position estimations were then used to estimate the frequency corresponding to each CI user’s electrode using Greenwood equation. Next the acoustic pitches matched to the electric pulse trains were compared to the Greenwood function estimations and the frequency allocation of the clinical map.

Conclusions
We observed that the 2 MedEL CI users matched the apical electrodes to lower frequencies than the Cochlear and AB CI users’ right after activation. The reason might be that the MedEl electrode array is inserted deeper in the cochlea. For one patient the acoustic matches to 12-pps or 1000-pps electric pulses were similar right after CI activation. Right after activation the results of the pitch matching deviate nearly by one octave and by 1.5 octaves with respect to the Greenwood predictions for the 1000 pps and for the 12 pps conditions respectively. For both conditions the mean pitch matching results are lying under the Greenwood predictions. In general the pitch elicited through electric stimulation seems to adapt to the frequency allocation of the clinical map.

Funding
This work was supported by the DFG Cluster of Excellence EXC 1077/1 “Hearing4all”.

References

1. Schatzer, R., Vermeire, K., Visser, D., Krenmayr, A., Kals, M., Voormolen, M., … Zierhofer, C. (2014). Electric-acoustic pitch comparisons in single-sided-deaf cochlear implant users: Frequency-place functions and rate pitch. Hearing Research, 309, 26–35. doi:10.1016/j.heares.2013.11.003.

2. Carlyon, R. P., MacHerey, O., Frijns, J. H. M., Axon, P. R., Kalkman, R. K., Boyle, P., … Dauman, R. (2010). Pitch comparisons between electrical stimulation of a cochlear implant and acoustic stimuli presented to a normal-hearing contralateral ear. JARO - Journal of the Association for Research in Otolaryngology, 11, 625–640. doi:10.1007/s10162-010-0222-7

PS 41

Characterization of Ipsilateral Masking between Acoustic and Electric Stimulation through Cochlear Implants

Benjamin Krüger; Andreas Büchner; Waldo Nogueira
Medical University Hannover, Cluster of Excellence "Hearing4all"

PS 42

Place-Dependent Stimulation Rates Improve Pitch Perception in Cochlear Implantees with Single-Sided Deafness

Tobias Rader[1]; Julia Doege[2]; Youssef Adel[2]; Tobias Weissgerber[2]; Uwe Baumann[2]
[1]University of Mainz; [2]University Hospital Frankfurt

Background

Pitch perception in cochlear implant users is mainly depending on place of stimulation. The perceived place pitch evoked of the electrical stimulation differs mostly with the stimulating rate and the corresponding rate pitch in the cochlear.

Method

A group of eleven unilateral implanted experienced CI users (CI experience 7-40 months; age 28-70, median 45 years) with acquired single-singled deafness and normal hearing in the contralateral ear ($PTA_{125\text{-}4000Hz}$ < 35 dB) were recruited in the present study. All uses implant devices manufactured by MED-EL (Innsbruck, Austria) with deep insertion (FLEXSOFT or FLEX28) electrode arrays. The task of the subjects was to adjust the frequency of a sinusoid presented at the non-implanted ear by means of an adjusting knob until they perceived the same pitch that was elicited by a reference stimulus at the implanted ear for the six most apical electrodes. Acoustical and electrical stimuli were presented in an alternating order. Six pitch matching trials per electrode were collected for each subject. A new method for improved (electrical) pitch perception was developed: The electrical stimulation rate for bilateral pitch comparisons was calculated by means of insertion angle assigned by postoperative imaging of the cochlea. The formula of Greenwood (1990) was combined with the findings of Stakhovskaya et al (2007) to calculate the individual stimulation rate for each subject's electrodes.

Results

1. Pitch-Function: In contrast to previous findings (Baumann and Rader 2011) the median of matched acoustic frequency with optimized stimulation rate is in line with the exponential predictions according to Greenwood for normal hearing.

2. Correlation between pitch and rate: A comparison between the median matched acoustic frequency and the pre-calculated stimulation rate results in a high significant correlation ($r = 0.937$; $p < 0.001$) in the double-logarithmic scale.

3. To performer: At the most apical electrodes, the best performing subjects show pitch matching skills comparable to normal hearing subjects.

Conclusion

These findings give the possibility to affect the preciseness of perceived pitch evoked by electrical stimulation in single-sided deafness patients.

PS 43

Bimodal Cochlear Implant and Hearing Aid Performance Using the Sung Speech Corpus

Joseph Crew[1]; John Galvin, III[2]; Qian-Jie Fu[2]
[1]University of Southern California; [2]University of California-Los Angeles

Previous work with electro-acoustic stimulation (EAS) patients has revealed the different contributions of pitch and timbre to speech and music perception, as well as different contributions of hearing aids (HAs) and cochlear implants (CIs) to speech and music. When evaluating the bimodal benefit for EAS listeners, pitch and timbre perception are typically measured independently, using very different stimuli and tasks that may obscure the sources of bimodal benefit. To address this, we created the Sung Speech Corpus (SSC), a database of acoustic stimuli that contains varying timbre (word) information as well as varying pitch (melody) information.

The SSC consists of 50 sung monosyllable words sung at 13 fundamental frequencies (F0s) from A2 (110 Hz) to and A3 (220 Hz) in semitone steps. Natural speech utterances were also produced for each word. All productions were normalized to have the same duration and amplitude; minor pitch adjustments were applied to obtain exact target F0s. The words were chosen to fit within a Matrix Sentence Test with the following syntax: "name" "verb" "number" "color" "clothing" (e.g., "Bob sells three blue ties."); each category contains ten words. As such, the constructed five-word sentence also contains a five-note melody, allowing word-in-sentence recognition to be measured alongside Melodic Contour Identification (MCI) using the same stimuli.

MCI was measured with fixed or variable words (i.e., timbres) and sentence recognition was measured with fixed or variable pitch cues (melodic contours) in EAS users. Preliminary data show that performance worsened as the stimuli became more complex. In general, a bimodal benefit was observed for both speech and music perception, compared to the better ear alone. For speech perception, performance with the CI+HA was slightly better than with the CI alone, and spoken words

were more intelligible than sung words. For MCI, performance with the CI+HA was slightly better than with the HA alone. MCI was much poorer with variable timbre than fixed timbre, suggesting that which suggests that EAS users still lack critical pitch processing abilities, despite the low-frequency pitch cues provided by the HA. The results suggest that combined device use can improve both speech and music perception relative to either device alone. Additionally, the SSC seems to better reveal complex interactions between CIs and HAs, pitch and timbre cues, and speech and music perception.

Funding
This work was supported by the NSF GK-12 Body Engineering Los Angeles program and NIDCD R01-DC004993 and R01-DC004792.

PS 44

Initial Enhancement and Later Decline of Absolute Pitch Identification in a Cochlear Implant User with Residual Hearing

Mario Svirsky; Elad Sagi; Annette Zeman; Chin-Tuan Tan; Mahan Azadpour; Arlene Neuman
NYU School of Medicine

Background
A professional pianist in his 60's received a cochlear implant in his left ear, which was severe-to-profoundly deaf after sudden hearing loss during childhood. His right ear had residual hearing with thresholds between 20-40 dB HL up to 1,000 Hz. The subject stated he had absolute pitch perception ability using this ear and claimed that this ability was enhanced when his newly activated cochlear implant (CI) was turned on.

Methods
This claim was tested over several sessions using note identification tests where single piano notes were presented one at a time in one of three conditions (acoustic hearing only, CI only, or binaural) and the subject had to indicate which note he heard.

Results
During the first session, two weeks after initial stimulation, his note identification was 83% correct in the acoustic ear, only 10% in the CI ear, and 96% in the binaural condition. The binaural score was significantly higher than in the acoustic only condition, ($p<0.001$) even though note identification was indistinguishable from chance in the CI only condition. In other words, the CI helped enhance the subject's remarkable absolute pitch perception ability, just as he reported. This happened despite the fact that note identification was very poor in the CI-only condition, where 78% of the notes that were played were labeled as G. Upon re-testing at 4 and 11 weeks after initial stimulation, the binaural absolute pitch enhancement effect disappeared: scores in the binaural condition were no better (and sometimes actually worse) than in the acoustic only condition. Furthermore, note identification using only the acoustic ear experienced a significant decline.

Discussion
We hypothesize that the initial enhancement of note identification may have been due to the listener's use of the CI signal as a reference, taking advantage of the relatively constant pitch percepts it produced. Detailed examination of responses in later sessions suggests that the subject may have changed his listening strategy by trying to use the CI signal as a source of pitch information rather than as a reference. Taken together, the observed longitudinal changes suggest that CI activation (which was successful for the main goal of enhancing speech perception) resulted in paradoxical effects on the subject's absolute pitch identification ability, as indexed by note identification.

Funding
This work was funded by NIH grants R01-DC003937 (PI: Svirsky), R01-DC011329 (PIs: Neuman, Svirsky), and K25-DC010834 (PI: Tan).

PS 45

Speech Intelligibility Benefits in a Model of Cochlear Implant Listeners with Ipsilateral Residual Acoustic Hearing

Ladan Zamaninezhad[1]; Volker Hohmann[1]; Andreas Büchner[2]; Tim Jürgens[1]
[1]Carl von Ossietzky Universität Oldenburg; [2]Hanover Medical School

Introduction
Speech perception in users of conventional cochlear implants (CI) degrades considerably in the presence of noise. Due to advances in surgical techniques, for a subgroup of CI candidates whose apical auditory nerves can still be stimulated acoustically, there is the possibility to preserve acoustic hearing even after implantation. Several clinical and vocoder studies reported on speech intelligibility benefits for electro-acoustic (EA-) listening condition in comparison with electric-only or acoustic-only conditions (termed EA-benefit) in these listeners.

Goals of the study
The goal of this study is to introduce an auditory model of speech intelligibility that can predict the EA-benefit. The model is used to assess the effect of different physiological factors on speech perception of electro-acoustic listeners.

Methods
Two different physiologically inspired auditory models are used to simulate the auditory nerve spiking pattern in response to electric and acoustic stimulation. The auditory model of Fredelake and Hohmann (2012) produces auditory nerve spikes in response to electric stimulation while the Meddis (2006) model simulates auditory nerve spikes in response to acoustic stimulation. Both spiking patterns were further processed by the central stage of the model of Fredelake and Hohmann (2012) to obtain internal representations of the stimuli, which may be present in the central part of the auditory system.

The back-end of the proposed model consists of a standard GMM/ HMM speech recognition system. The internal representations were fed into the classifier and the recognition rate determined the predicted speech reception thresholds (SRTs) for sentences in stationary speech-shaped noise. Predicted SRTs were compared to SRTs measured in 22 patients equipped with Nucleus Hybrid-L device.

Results
The model predicted EA-benefit (SRT-difference between electric-only and electro-acoustic listening condition) of up to 3 dB, which agrees with the EA-benefit observed in most of the patients. Changing the amount of residual acoustic hearing in the model resulted in an EA-benefit even if the speech intelligibility with acoustic-only stimulation was close to chance, which is in line with the results of some of the patients. Increasing the amount of electric field spatial spread in the model increased SRTs both in electric-only and electro-acoustic listening condition.

Conclusion
The model of speech intelligibility for electro-acoustic listeners can predict the EA-benefit that is observed in actual patients. The model has been used to assess the influence of different physiological parameters on speech reception thresholds and EA-benefit.

Funding
This work is supported by DFG cluster of excellence EXC 1077/1 â€œHearing4Allâ€ .

PS 46

Double Oblique Images In Temporal Bone CT To Approximate Microscopic Surgical Views

Haruka Nakanishi; Tetsuya Tono; Takeshi Nakamura
University of Miyazaki

Objectives
In this study, “Double Oblique (DO) images of temporal bone CT” were made based on the results from measurements of the angle between the visual axis under microscope and the axis of bony external auditory canal (EAC) . DO CT enabled cross section images to show the approximate surgical field of view under microscope.

Materials
11 cadaveric temporal bones were used in this study. CT images were taken using Cone beam CT.

Methods
Temporal bones were prepared in retro-auricular incision, and canal wall up procedure.

In order to visualize the direction of microscopic visual axis in CT, a fine piano wire (0.25×15 mm) was placed in the cadaveric temporal bones before CT scanning. The piano wire was precisely set parallel to the visual axis of the microscopic view. The obliquity of the piano wire in two different visual axis was measured, one along the visual axis in view of the tympanic membrane through the EAC and the other via the posterior tympanotomy opening.

The reference line for obliquity measurement was set to the axis of the bony external ear canal.

Based on results obtained from the obliquity measurements of the piano wire, DO images were made of the slices perpendicular to the piano wire using Multi-Planar Reconstruction (MPR) technique.

Results
The direction of the visual axis in view of the tympanic membrane through the external ear canal was virtually the same as the axis of the bony external ear canal.

The direction of the visual axis of the posterior tympanotomy was inclined backward in axial plane(ave.10.9 degree), and also inclined upward in coronal plane(ave.7.7 degree) toward the axis of the bony external ear canal.

Discussion
DO images which are based on the visual axis in view of the tympanic membrane through the external ear canal can provide anatomical information of the structure beneath the external ear canal. In addition, DO images based on the visual axis along the posterior tympanotomy via the facial recess opening provide anatomical information around facial recess, such as the distance between the facial nerve and the chorda tympani nerve.

Conclusion
DO images can be fused together to approximate the surgical view by conducting an appropriate rotation or making mirror-reversed images, and help to intuitively understand anatomical structures and their spatial relationships that are difficult to obtain from routine CT images using axial and/or coronal projections.

PS 47

Discrepancies of hearing examination results in patients with cerebellopontine angle meningioma

Teruyuki Sato; Kazuo Ishikawa
Akita university

Background
Meningioma is the most common tumor of the neuroaxis and is derived from meningothelial cells. Cerebellopontine angle (CPA) meningiomas are a relatively rare anatomical subgroup of meningiomas and comprise 6%–15% of all tumors in the region of the CPA.CPA meningioma may bring on hearing loss. Therefore, ENT specialists should be cautious before and after medical treatment. Recently we encountered a case which had greater disparity between auditory steady state response (ASSR) and pure-tone audiometry (PTA).

Aim
To investigate the characteristics of hearing level, comparing the difference of hearing level between PTA and ASSR in patients with CPA meningioma.

Study Design
Retrospective case series.

Methods
Five patients with unilateral CPA meningioma before treatment were candidate. They are one male, and four females, ranging from 47-68 years old with an average of 60.6. Opposite normal ear were used as normal control. We have compared those audio logical results on PTA, auditory brainstem response (ABR) and ASSR as objective audio logical examinations. In addition, we measured size of meningioma by MRI.

Result
the average differences of hearing level between PTA and ASSR were 12dB (0.5kHz), 8dB (1kHz), 1dB (2kHz), 7dB (4kHz) in opposite normal ear as control. It was not significant difference. The average differences of hearing level between PTA and ASSR were 56dB (0.5kHz), 39dB (1kHz), 30dB (2kHz), 37dB (4kHz) in ear on the affected side. We found significant difference in 0.5kHz and 1kHz. Then we compared the average differences of hearing level between PTA and ASSR in ear on the affected side, and that in opposite normal ear. Significant difference was found in 0.5kHz, 1kHz, 2kHz. **Latencies of wave V of ABR were found in all case of** ear on the affected side. We found the differences of hearing level between PTA and ASSR in meningioma cases which do not invade into the internal auditory canal, based upon the findings of MRI.

Discussion
The hearing levels of ASSR are 6~12dB greater than that of PTA was known in normal ear. We found much greater differences of hearing level between PTA and ASSR in CPA meningioma patients. Those discrepancies might reflect the complexity of pathogenesis of hearing impairment caused by meningioma. Details of those discrepancies were shown, and pathogenesis of hearing disorder by CPA meningioma will be discussed, referring pertinent papers.

PS 48

Submucosal Elastic Laminae of the Middle and Lower Pharynx: A Histological Study Using Elderly Cadaveric Specimens

Yukio Katori; Ai Kawamoto-Hirano; Yohei Honkura
Tohoku University Graduate School of Medicine

Purpose
The distribution of elastic fibers in the pharyngeal wall was investigated to consider the elasticity of the pharynx.

Method
Histological sections of the mid and lower pharynx from 15 elderly donated cadavers were observed, under the principles of the Declaration of Helsinki and the approval of institutional research ethics review committee.

Result
Two distinct submucosal tissue layers with a high content of elastic fibers (tentatively termed “laminae”) were identified. The inferolateral elastic lamina was restricted to the level from the upper part of the arytenoid to lower end of the inferior cornu of the thyroid cartilage. It originated from the pharyngeal submucosa, extended laterally along the inner aspect of the thyropharyngeal muscle, and inserted into the periosteum or perichondrium at posterior margin of the thyroid cartilage. The posteromedial lamina extended along the supero-inferior axis from a level above the greater horn of the hyoid bone to reach the muscularis mucosae of the cervical esophagus. The inferolateral and posteromedial laminae were connected at levels below the cricoarytenoid joint. Individual variations were evident in their thickness as well as the extent of connection between them.

Conclusion
Two distinct submucosal elastic laminae were newly described in the middle and lower pharynx. In association with striated muscle function, the inferolateral lamina seemed to suspend the lower pharyngeal mucosa, while the posteromedial lamina seemed to provide mucosal fold forcing smoothly peristaltic conveyance of a bolus during swallowing.

PS 49

Does Electrical Stimulation in Cochlear Implant Recipients Cause Acute Injury to Cochlear Structures?

Adrian Dalbert; Marco Hoesli; Christof Roosli; Flurin Pfiffner; Alexander Huber
University of Zurich, University Hospital Zurich

Background
Preservation of remaining intact cochlear structures is attempted in cochlear implant recipients nowadays. However, despite large progress regarding atraumaticity during surgery, loss of residual hearing still occurs in a majority of patients after cochlear implantation. The underlying mechanisms are controversial. Besides surgical trauma, postoperative mechanisms seem to contribute to the deterioration of cochlear function. Previous studies suggested that chronic as well as acute electrical stimulation could cause injury to cochlear structures and thereby contribute to post-implantation threshold shifts. Therefore, the aim of this study was to evaluate if after initial activation of the cochlear implant changes in cochlear function are detectable.

Method
Electrocochleography (ECoG) allows the detection of hair cell as well as neural responses to acoustic stimuli. In cochlear implant recipients, these signals represent the remaining cochlear function. To assess if acute injury to cochlear structures occurs after electrical stimulation, ECoG responses were recorded before and after initial activation of the cochlear implant immediately after surgery. ECoG responses to tone bursts at 250, 500, 750, 1000, 2000, and 4000 Hz and to click stimuli at suprathreshold intensities were recorded, using an extracochlear recording electrode.

Results
Ongoing ECoG responses in low frequencies and cochlear microphonics in high frequencies represent mainly hair cell responses. Changes of these ECoG responses were within the margin of error of approximately 3 dB. Compound action potentials represent responses of the cochlear nerve and

remained unchanged in response to click stimuli as well as tone bursts at all frequencies.

Conclusion
Short-term electrical stimulation as used in cochlear implant recipients seems to cause no acute injury to cochlear structures. Hair cell as well as neural components of the ECoG signal remained unchanged.

PS 50

The Mal de Debarquement Syndrome (MdDS) - Treatment Studies in 127 Cases

Sergei Yakushin; Mingjia Dai; Catherine Cho; Bernard Cohen
Icahn School of Medicine at Mount Sinai

The Mal de Debarquement Syndrome (MdDS) is a continuous feeling of swaying, rocking and/or bobbing that generally follows travel on the sea (the 'Classic' Form). It can also occur spontaneously (the 'Aberrant' Form). It is associated with many other debilitating symptoms. The underlying neural mechanisms of MdDS are unknown. Results in monkeys and humans suggested that MdDS was caused by maladaptation of the vestibulo-ocular reflex (VOR) to roll of the head during rotation. Current work is a continuation of our original study in treating this condition (Dai et al, Frontiers in Neurology. 2014; **5**:124). Patients were from North America and Europe.

Settings
Patients' heads were rolled while watching a rotating full-field visual surround. Each treatment session was about 2 – 3 minutes over 4 -5 days, 3–10 sessions each day.

Subjects
127 total (109 females; 18 males; Classic MdDS: 107; Aberrant MdDS: 20; Ages: 46±12 (20-81)).

Diagnosis was by: Physicians and PTs but 47 were self-diagnosed. **Duration**: 33.7±40.4 months (from 1 month to 20+ years; half were less than 3 years and the other half except 2 were less than 10 years).

Measures
1. Subjective score of severity on scales 0 – 10; 2. Static posturography. **Clinically significant Success**: Defined as a reduction of symptoms by at least 50%.

Results
For all classic and aberrant cases, the rate of success for a history of less than or equal to 3 years was 74% and for a history of more than 3 years was 66%, measured on the last day of intervention. When the two types of MdDS were separated, 76% of classic cases and 45% of aberrant cases were successfully treated. Fourteen males were treated successfully (79%), while only one out of 4 aberrant male patients was successfully treated. Both female patients with a history of more than 20 years scored a significant improvement (60% & 69%). The results demonstrate that the success rate with our treatment intervention is not dependent on the duration of MdDS or gender, but on the type of MdDS. The high rate of success demonstrated in this study indicates that MdDS should not be considered to be untreatable. Further results will be reported when the long term follow-up and postural analyses are completed.

Funding
DC012162

PS 51

Electrophysiological estimation of the intracochlear electrode position: Experiences and longterm reliability in perimodiolar and straight electrodes in a blinded multi-center study

Philipp Mittmann[1]; Ingo Todt[1]; Diana Arweiler-Harbeck[2]; Arneborg Ernst[1]; Florian Christov[2]
[1]Unfallkrankenhaus Berlin; [2]University of Essen

Introduction
The position of the cochlea electrode array within the scala tympani is essential for an optimal hearing benefit. An intraoperative NRT-ratio was established, which can provide information about the intraoperative intracochlear electrode array position for perimodiolar electrodes. The aims of this study were to verify the NRT-ratio for straight electrode arrays and the longterm reliability for the NRT-ratio in perimodiolar electrodes.

Materials and Methods
In a retrospective controlled study in a Tertiary Referral Center the electrophysiological data sets of 170 patients with measured intraoperative and up to one year follow up Auto-NRTs were evaluated. All patients were implanted either with a Nucleus Contour Advance electrode or a Nucleus slim straight electrode. The NRT-ratio was calculated by dividing the average Auto-NRT data from electrode 16-18 with the average from electrode 5-7. Using a flat panel tomography system, the position of the electrode array was certified radiological.

Results and Significance
77 patients with perimodiolar electrodes were detected electrophysiologically with a certain scalar tympani position. In 43 patients, a scalar change was probable. A significant correlation between the radiological results and the NRT-ratios was found intraoperatively. 109 patients were included in the one year follow-up group. The NRT-ratio remained stable in most of the cases. For the slim straight electrode group 38 patients showed a NRT-ratio indicating a scalar tympani position. 23 patients showed a NRT-ratio assuming a scalar translocation. In these patients the electrophysiological-radiological mismatch was higher than in the perimodiolar group.

Conclusion
The NRT-ratio can be used to determine the intracochlear position of the electrode array for perimodiolar and straight electrodes. Intraoperative the NRT-ratio predicts the array position within the cochlea highly reliable for perimodiolar electrodes. Sensitivity and specifity for the slim straight electrode are lower. We showed that after six months and a

year the NRT-ratio remains unchanged in most of the cases and shows a good correlation to the radiological determined position of the array. Nevertheless the condition of the neural structures is highly important for reproducible responses. Limited validity is given in patients with degenerative and structural neural disorders.

PS 52

Exploring Perilymphatic Fistula by Virtual Endoscopy combined to Density Threshold Variation on CT-Scan

Maxime Guyon[1]; Jean-Loup Bensimon[2]; Michel Toupet[1,3]; Alexis Bozorg Grayeli[1,4]
[1]Dijon University Hospital; [2]RMX Imaging center; [3]Centre d'Explorations Fonctionnelles Otoneurologiques; [4]CNRS UMR-6306, Le2i

Background
Virtual endoscopy on CT scan combined to variation of density threshold evaluates the radiological density of labyrinthine windows. We hypothesized that a perilymphatic fistula (PF) would decrease the density in the labyrinthine window region. In a previous study, we showed that this method could enhance the performance of CT-scan in detecting small perforation of otic capsula in human temporal bone specimen (Bensimon et al., 2005). The aim of this was to evaluate this method in detecting oval or round window fistula in a large population of patients.

Materials and Methods
Fourt-eight adult patients (mean age: 51 years, range : 18-78, sex ratio: 1.3) with a suspicion of PF defined by Portmann score > 7 (Portmann et al, 2005) and/or intra operative visualization of the fistula and/or resolution of the symptoms after surgery; and 103 control patients (mean age: 43 years, range : 20-86, sex ratio: 0,53) undergoing routine cranial high-resolution CT-scan for diseases other than otological disorders were included in this study. Labyrinthine windows were examined by virtual endoscopy and the reconstruction threshold was gradually increased until a virtual opening appeared (opening threshold, OT) This opening corresponded to the region with lowest density of the field. The OT difference between the suspected and contralateral side was calculated for each window in the same patient. The highest OT difference among round and oval windows in the same patient was chosen as the diagnostic criteria. The side of the fistula was indicated by the lowest OT value.

Results
OT difference was higher in patients than in control (60.7 ± 68.26, n=48 versus 26.7 ± 21.76 UH, n=103, $p<0.01$ unpaired t-test). A non parametric ROC analysis showed that at an OT difference of 31.5 UH had a sensitivity of 75 % (CI 95%: 60.4-86.4) and a specificity of 75% (CI95%: 65.2-82.8) for the PF diagnosis.

Conclusion
This method can be applied in routine and appears to be helpful with relatively high specificity and sensitivity in the diagnosis of PF.

Funding
Institut de Recherche en Otoneurologie (IRON) and Société ORL de Bourgogne

PS 53

The Analysis of Rehabilitation Effects in Children with Leukoencephalopathies after Cochlear Implantation

Haibo Shi; Peishu Fan; Yanmei Feng
The Sixth People's Hospital Affiliated to Shanghai Jiaotong University

Objective
To analysis the auditory and speech rehabilitation effects of the children with leukoencephalopathies after cochlear implantation (CI).

Material and Methods
Forty-six deaf children with mild to moderate leukoencephalopathies who received CI from January 2003 to December 2014 in our unit were investigated in this study. The pre and post-operative materials were collected and 37 (80.4%) were completed follow-up. Those CI children without leukoencephalopathies were served as the control group. Tools for assessment were Meaningful auditory integration scale (MAIS), Meaningful usage of speech scale (MUSS), Categories of auditory performance (CAP) and Speech intelligibility rating (SIR).

Results
All of the children had the CI surgery safely and used CI devices for virtually all their waking moments. Compared with the control group showing great progresses in MAIS, MUSS, CAP, and SIR scores during the first 2 years after CI, children with leukoencephalopathies acquired quick advance in these scores during 3 to 4 years after CI, but there was no statistical difference between two groups 4 years after CI. Post-operative language training is a main impact factor for the rehabilitation effects. Those with more than 2 years of language training got a higher score in SIR and MUSS ($P<0.05$).

Conclusion
Our results suggested that the deaf children with mild to moderate leukoencephalopathies may be recommended for CI. The early progresses in auditory and speech rehabilitations of these children were a bit poor compared with the general cases, but as the rehabilitation training continues, their long-term effects were nearly the same.

Funding
XBR2013085

PS 54

Hearing Impairment in U.S. Adults Is Associated with Loud and Very Loud Occupational Noise, Firearms Use, and Other Noise Exposures: The 2014 Hearing Supplement to the National Health Interview Survey (NHIS)

Howard Hoffman[1]; Robert Dobie[2]; Katalin Losonczy[1]; Christa Themann[3]; Greg Flamme[4]

[1]National Institute on Deafness and Other Communication Disorders (NIDCD), National Institutes of Health (NIH); [2]University of Texas Health Science Center at San Antonio; [3]National Istitute for Occupational Safety and Health (NIOSH), Centers for Disease Control and Prevention (CDC); [4]Western Michigan University

Background

Exposure to high-level sounds and noise is the major preventable cause of hearing impairment (HI) among adults in the United States and developed countries.

Objective

To estimate associations between HI and risk factors, including occupational and other noise exposures, based on a recent nationally-representative sample of the adult population.

Methods

The 2014 NHIS Hearing Supplement was sponsored by NIDCD/NIH and implemented by the National Center for Health Statistics (NCHS), CDC to collect updated national estimates on hearing health, including noise exposure and hearing ability, to track U.S. Healthy People 2020 goals. NCHS contracted with the U.S. Census Bureau for field staff to administer the hearing questions during personal interviews of the adult (aged 18 or more years) sample, n=36,697. Respondents were asked to describe their hearing as either "excellent", "good", "a little trouble", "moderate trouble hearing", "a lot of trouble", or "deaf". If hearing was worse in one ear, this question was repeated for the poorer-hearing ear; the Gallaudet hearing scale was also completed. Occupational noise was categorized by number of years of exposure to "very loud" (must shout to be understood by someone three feet away) or only "loud" (must speak with raised voice to be understood) sounds or noise. Firearms noise was categorized by the lifetime number of rounds fired. Frequency of hearing protection (ear plugs or ear muffs) use was also queried. Multivariable regression models in SAS and SUDAAN were used to calculate odds ratios (OR) and 95% confidence intervals (CI), while adjusting for national sampling weights.

Results

The prevalence of "very loud" occupational noise exposure was 20.4% (men: 32.3%; women: 9.4%) and of "loud" (but not "very loud") occupational noise was 3.9% (men: 5.2%; women: 2.3%). In multivariable models predicting "any hearing loss", we adjusted for race/ethnicity, education, income, smoking, and chronic illness (asthma, cardiovascular disease, diabetes, hypertension, and stroke) and found that age was the major risk factor, as expected. Nevertheless, when compared to respondents who were not exposed to high noise levels, "loud" occupational noise (OR=1.6, CI: 1.3-2.0), <5 years (OR=1.9, CI: 1.6-2.3) and ≥5 years "very loud" occupational noise (OR=2.9, CI: 2.5-3.2), firearms use (OR=1.3, CI: 1.2-1.4), and recurring "very loud" noise exposures outside of work (OR=1.7, CI: 1.5-1.9), were each independently associated with HI.

Conclusion

Since younger adults often have greater exposure to injurious noise, effective interventions aimed at them could substantially reduce the sex- and age-specific burden of HI.

Funding

Funding to support the implementation of the 2014 NHIS Hearing Supplement was provided to the NCHS, CDC, via an Interagency Agreement with the National Institute on Deafness and Other Communication Disorders (NIDCD), National Institutes of Health (NIH).

PS 55

A Nationwide Study on Enlargement of the Vestibular Aqueduct in Japan

Yoshihiro Noguchi[1]; Satoshi Fukuda[2]; Kunihiro Fukushima[3]; Kiyofumi Gyo[4]; Akira Hara[5]; Tsutomu Nakashima[6]; Kaoru Ogawa[7]; Makito Okamoto[8]; Hiroaki Sato[9]; Shin-ichi Usami[1]; Tatsuya Yamasoba[10]; Tetsuji Yokoyama[11]; Ken Kitamura[12]

[1]Shinshu University; [2]University of Hokkaido; [3]Fukuoka University; [4]Ehime University; [5]University of Tsukuba; [6]Nagoya University; [7]Keio University; [8]Kitasato University; [9]Iwate Medical University; [10]University of Tokyo; [11]National Institute of Public Health; [12]Tokyo Medical and Dental University

Background

Enlargement of the vestibular aqueduct (EVA) is the most common radiological anomaly of the inner ear. However, many controversies remain due to the paucity of large-scale studies. We conducted a nationwide survey in Japan to gather information on a large cohort of EVA patients. Clinical and demographic data were used for constructing a more detailed picture of symptomology and disease progression and identifying risk factors for EVA-related hearing loss (HL) and vestibular dysfunction.

Methods

A nationwide survey was performed using two questionnaires: the first was mailed in 2011 to 662 board-certified otolaryngology departments. A second questionnaire was mailed in 2012 to all facilities that reported treating EVA cases. EVA was defined as a vestibular aqueduct or endolymphatic duct diameter of ≥ 1.5 mm at the midpoint or ≥ 2 mm at the operculum on temporal bone. We analyzed clinical information, including gender, EVA side, age at onset, initial symptoms, etiology, and precipitating factors, from survey responses and assessed the degree of HL from accompanying pure-tone audiometry data. A multivariate

logistic regression analysis was applied to identify possible risk factors for fluctuating HL and repetitive vertigo/dizziness.

Results
Seventy-nine board-certified otolaryngology departments in Japan reported treating EVA patients. We identified a total of 387 EVA patients, who were enrolled to the present clinical survey. EVA was bilateral in 91.2% of patients, and the male-to-female ratio was 1:1.4. The most prevalent symptom was HL, followed by vertigo/dizziness/imbalance. Sudden HL occurred secondary to head trauma in 5.2% of patients and common cold in 5.2%. Pure-tone audiometry showed profound HL (pure-tone average ≥ 91 dB) in approximately 50% of the patients. The mean pure-tone average was 83.3 ± 27.4 dB and showed no statistical correlation with age. The mean air-bone gap was significantly higher at 250 Hz than at 500 Hz and 1000 Hz. Multivariate logistic regression identified bilateral HL and Pendred syndrome as significant risk factors for fluctuating HL and repetitive vertigo/dizziness, respectively.

Conclusions
Although EVA is rare, it is associated with early onset, sustained, and profound HL.

Funding
This study was supported by a grant-in-aid for scientific research from the Ministry of Health, Labour and Welfare in Japan (H23-kankaku-005).

PS 56

Image-guided implantation of the BonebridgeTM with a surgical navigation; a feasibility study

Young Joon Seo[1]; Kyurin Hwang[2]; Hyunmi Ju[3]
[1]Yonsei University Wonju College of Medicine, Wonju; [2]Yonsei University of Medicine; [3]Yonsei Wonju university

Objective
To access a method of fitting a designated location on the patient's temporal bone by surgically navigating to the Bonebridge implantation.

Study Design
A patient with unilateral profound hearing loss received early intervention with the Bonebridge implant for binaural hearing. The optimal implant site was determined from computed tomography (CT) images using a three-dimensional (3D) simulation software program before the surgery. The pre-calculated coordinates from the 3D simulation software program were moved to the Scopis Hybrid Navigation System. After using the surgical navigation system for the surgery, we evaluated the degree of mismatch of the center of the bone conduction-floating mass transducer (BC-FMT) between the computer simulation and the actual drilling.

Results
The time required to determine the implant location on the surface of the patient's temporal bone was shortened, and the accuracy of the implantation was high. The coordinates on the 3D simulation system were comparable to the surgical navigation system. The predicted coordinates were replicated exactly upon actual drilling during the surgery, and we could confirm this in preoperative and postoperative images.

Conclusions
Using an image-guided surgical navigation system to aid in the placement of the BC-FMT on the simulated location is a simple procedure and is more effective that finding the exact coordinates. It also shortens the decision time for applying the implant.

PS 57

Bone mineral density measurement in patients with benign paroxysmal positional vertigo and its relationship with recurrence

Hong Ju Park; **Chan Joo Yang**; Ji-Won Lee
University of Ulsan College of Medicine

Background
Osteoporosis has been reported to be a risk factor for benign paroxysmal positional vertigo (BPPV). The aim of this study was to evaluate the relationship between bone mineral density (BMD) and clinical features in patients with BPPV.

PS 58

Cochlear Implant in single sided deafness patients - are there benefits beyond speech perception?

Mark Praetorius; Maria Rösli-Khabas; Sebastian Hoth
University of Heidelberg

Background
Cochlear implants (CI) in patients with single sided deafness (SSD) become more common in some contries.The question of efficacy is still to be answered from the perspective of the funding.

Material and Methods
20 patients with normal pure tone audiogram (n=8) or moderate hearing loss (n=12) in one ear, were included. They were equipped with CI systems MED-EL SONATA/ CONCERTO + OPUS2 (n=12), COCHLEAR CI24RE(ST) + CP810 (n=7) and Advanced Bionics HiRes90K + Harmony (n=1) on the contralateral ear. When tested for this study, they had at least 6 months of CI experience. We tested them with respect to directional hearing, speech perception in noise, binaural loudness matching (ABLB) and binaural pitch matching. 26 normal hearing controls were included for normative references.

Results
Addition of the CI significantly improves in directional hearing (hit rate improved from 14.9% to 15.6%, RMS error decreased from 125° to 93°). Normal hearing controls performed better with values between 0 and 73° and a median of 12°. The thresholds are given as signal to noise ratio (snr), determined at a constant speech level of 65 dB HL with adaptive noise level in the spatial configuration S0N90 (noise from the side opposite to the CI). Here, speech perception in noise (SRT improved from -2.3 to -6.0 dBsnr median), equivalent

to a BILD = 3.7 dB). Alternate binaural loudness balancing (ABLB) showed that at levels between 48 and 55 dB HL (group averages) matching takes place. In the pitch matching experiment, the standard deviation of the relative interaural frequency difference at 0.5, 1 and 2 kHz amounted to 24.5%, 22.8% and 24.0% respectively (compared to 11.7%, 14.4% and 12.3% in the control group).

Conclusions
In the situation of single sided deafness, a CI can considerably improve the audiological performance in terms of directional hearing, binaural signal equivalence and speech perception.

Funding
Maria RÃ¶sli-Khabas recieved a personal fund from the DAAD (German academic exchange service)

PS 59

Long-Term Outcomes of Acute Low-Tone Hearing Loss

Eun Jin Son; **Kyung Jin Roh**; Eun Jung Lee; Jin Won Kim; Ah Young Park; Byeong Il Choi
Yonsei University College of Medicine

Background
Although acute low-tone hearing loss has been associated with cochlear hydrops or early stage Meniere's disease, its prognosis in the short-term has been reported to be better than sudden hearing loss. However, recurrence of hearing loss and possible progression to Meniere's disease remain important concerns in the clinical setting. This study aims to investigate the long-term audiological outcomes of acute low-tone hearing loss and to identify associated factors.

Subjects and Method
A retrospective review of patients presenting with a first attack of acute low-tone hearing loss was performed. Of the 77 patients, 33 were followed up for more than 3 months. Progression or recovery of hearing loss and recurrence of hearing loss were examined. Also, correlation between long-term outcomes and associated clinical factors were analyzed.

Results
Twenty-five patients (75.7%) had complete hearing recovery, five patients (15.1%) had partial recovery, two patients (6.0%) had no recovery, and one patient (3.0%) had progression of hearing loss 1 month after initial treatment. Thirty-three patients were followed up for more than 3 months (mean 22 months, range 3-79 months). Recurrence of acute low-tone hearing loss was observed in five patients (15.2%). All of the recurrences occurred during the first 12 months of follow-up. Long-term prognosis correlated with the initial therapy results (r^2=0.693).

Conclusions
Recurrence of hearing loss was documented in five patients (15.2%), and all of these cases occurred within one year of the first attack. Audiological outcomes after initial therapy may predict the recurrence of acute low-tone hearing loss.

Funding
This research was supported by a faculty research grant of Yonsei University College of Medicine (6-2012-0023 to E.J.S.).

PS 60

The Summating Potential in Clinical Assessment of Neural and Hair Cell Contributions to the Responses to Sound in Cochlear Implant Subjects

Tatyana Fontenot; Andrew Pappa; William Scott; Christopher Giardina; Harold Pillsbury; Kevin Brown; Douglas Fitzpatrick
University of North Carolina, Chapel Hill

Understanding the contributions of hair cells and neural sources to potentials recorded from the round window in response to sound can help to evaluate the cochlear physiology in clinical populations with various etiologies of hearing loss. Different parts of the response convey information about each of the sources. The summating potential (SP) to tones is the baseline shift that occurs for the duration of the tone, corresponding to the envelope of the response. Results of animal studies have suggested that this SP results from the overlap of hair cell and neural contributions. When neural activity is eliminated with kainic acid or blocked with neurotoxins including tetrodotoxin and CNQX, the resulting changes in the SP indicate removal of a neural contribution (Forgues et al., *J Neurophysiol.* 2014;111:580-593; Sellick P et al., *Hear Res.* 2003;176:42-58; van Emst et al., *Hear Res.* 1995;88(1-2):27-35.) The status of neural contributions in the residual physiology of cochlear implant recipients may be particularly important in understanding speech perception outcomes.

Recordings were performed intraoperatively from the round window using tone bursts (250-4000 Hz, 90 dB nHL), to determine if the SP morphology could be used to indicate cochlear neural status at the time of implantation. Typically, cases with a large compound action potential (CAP), and thus a clear neural component, had a small SP. In contrast, in many cases where there was little or no CAP, the SP had a large negative polarity. Finally, in some cases there was no CAP and no SP, despite the presence of a large cochlear microphonic (CM).

Based on the animal studies using neurotoxins, we interpret the cases with a large CAP as having a large neural contribution to the SP with a polarity that opposes that of the hair cell contribution, producing a small SP. In contrast, cases with a large negative SP and no CAP have little or no neural contribution. Several subjects with this response morphology had cochlear nerve deficiency, supporting this interpretation. Cases with a CM but no CAP and no SP may have intact outer hair cells but no functional inner hair cells, which would also prevent any neural responses. These results indicate that the SP can be a useful indicator of the site of lesion in cochlear implant subjects.

Funding
NIH T32 Training Grant: 5T32 DC 5360-12 Med El Corporation

PS 61

Energy output of outer hair cells

Kuni Iwasa
NIH

Electromotility of outer hair cells (OHCs) has been extensively studied with *in vitro* experiments because of its significance in the cochlear amplifier, which provides the exquisite sensitivity and frequency specificity of the mammalian ear. However, these studies have been performed largely under load-free conditions or with static load, while these cells function *in vivo* in a dynamic environment, using electrical energy to enhance mechanical oscillation in the inner ear by providing mechanical output. This gap in our knowledge leaves uncertainty in answering a key question, how much mechanical energy an OHC provides. The present report is an attempt of bridging the gap by introducing a simple one-dimensional model for electromotility of OHCs in a dynamic environment.

The model proposed here incorporates a feedback loop involving the receptor potential (RP) and the mechanical load on OHC. Specifically, the RP drives the motile mechanism by displacing the electric charge that is coupled with mechanical displacement, providing mechanical energy in the presence of a mechanical load. Such a load reciprocally reduces electrical displacement, and in turn, reduces the membrane capacitance, the main factor attenuating the RP. Such a feedback mechanism should improve the efficiency of OHCs for producing mechanical energy.

The simple model proposed enables writing down the equation of motion involving OHCs. It also leads to an expression for the membrane capacitance, which explicitly describes the dependence on the elastic load, viscous drag, frequency, and the mass. With the parameter values that reproduce *in vitro* experimental data, the model predicts that the mechanical output is maximal with an external elastic load, which is similar to the intrinsic elasticity of the OHC, provided that viscous drag is small. However, the optimal load is twice or more if the viscous drag is significant and increases with the frequency. With the reported experimental data on hair bundle gating, estimates of amplifier gain in elastic energy do not exceed factor three. However, the ratio of dissipative energy output to input can be much higher in the cellular scale.

PS 62

Voltage-dependent modulation of exocytotic event amplitudes at an auditory hair cell synapse

Owen Gross; Henrique von Gersdorff
Oregon Health & Science University

Background
Synaptic release patterns of auditory hair cells must be sufficiently complex to encode information about the timing, frequency, and amplitude of an acoustic stimulus. The signaling strategies employed by hair cells to maximize the information in their synaptic signals are crucial for downstream auditory processing but are not fully understood. We previously reported that stimulus intensity modulates the size of hair cell synaptic events, but the underlying mechanisms are still not well understood. We wondered whether this type of event amplitude modulation might supplement release rate modulation in order to increase the information capacity of the hair cell synapse.

Method
Paired voltage clamp recordings were obtained from auditory hair cells and afferent nerve fibers located in the bullfrog (*Rana catesbeiana*) amphibian papilla (Cho et al., 2011). Hair cells were stimulated with step depolarizations from -90 mV to voltages between -70 and -30 mV while excitatory postsynaptic currents (EPSCs) were measured in the afferent fiber. Instantaneous release rates (IRRs) were calculated from EPSCs using a new custom deconvolution algorithm. Event amplitude and rate statistics were determined from the IRR and were used to perform Monte Carlo simulations of synaptic release. We also implemented a leaky integrate-and-fire model based on previous whole cell current clamp recordings (Li et al., 2014).

Results
Different hair cell stimulation strengths consistently produced three qualitatively different EPSC types: sparse, non-sparse, and transiently large. These EPSC types exhibited significantly different event amplitude distributions, further characterized by best-fitting parameters of the log-normal function. Simulations of IRRs based on event rate and amplitude statistics were produced for a variety of discrete stimulus sets. We also generated comparison simulations in which the event amplitude distribution was fixed, while the event rate and total exocytosis were normalized. These simulations indicate that the information capacity of the hair cell synapse is increased by modulation of event amplitudes, with the largest effects observed for lower frequency (100-300 Hz) stimuli. Importantly, simulated spike trains show that gains in mutual information can be preserved when EPSCs are converted to spikes.

Conclusion
Stimulus-dependent modulation of event amplitudes can increase the rate of information transmitted by the synapse during low frequency stimulation by synchronizing release. The mechanism of event amplitude modulation is not known, though it is consistent with a scheme in which stronger stimuli produce larger presynaptic domains of elevated Ca^{2+}, thereby recruiting more vesicles per event.

Funding
We are grateful for support through NIH grants RO1-DC04274 (HvG) and F32-DC013917 (OPG).

PS 63

Force-Probing of the Adaptation Motors for Mechanotransduction

Corstiaen Versteegh; Tobias Bartsch; A. Hudspeth
The Rockefeller University

Mechanotransduction starts with the deflection of a hair cell's bundle, which increases the tension in each of the bundle's tip links and opens mechanically gated ion channels. In each stereocilium, myosin 1c motors that link the tip link through the insertional plaque to an actin paracrystal are thought to adjust the link's position along the stereocilium. By doing so they modify the open probability of the ion channels, the phenomenon of adaptation.

Although this model of adaptation has been inferred from the motion of hair bundles, direct measurements of the dynamics of the mechanosensitive channels and clusters of myosin molecules are lacking due to absence of appropriate single-molecule techniques. Here we show that a photonic-force microscope together with an *ex vivo* single-molecule assay can provide novel insights into the mechanics of adaptation.

In order to probe the dynamics of the adaptation-motor complex we attached a 1 μm-diameter bead to the upper end of an individual tip link in the hair bundle of a dissociated bullfrog hair cell. The bead was linked to the upper end of a cadherin-23 molecule through a 1 μm-long DNA tether and held in a weak optical trap. Using a custom-built, high-precision photonic-force microscope we then measured the position of the particle, which reflected the motion of the motor complex, with nanometer precision and megahertz bandwidth.

Funding
This work was partially supported by a NWO Rubicon grant to Corstiaen Versteegh, a Junior Fellow award from the Simons Foundation to Tobias Bartsch, and the Howard Hughes Medical Institute.

PS 64

Excitation and Inhibition of Semicircular Canal Type II Hair Cells by Pulsed Infrared Light

R. Rabbitt[1]; R. Lim[2]; H. Tabatabaee[2]; L. Poppi[2]; M. Fereck[1]; A. Brichta[2]
[1]University of Utah; [2]University of Newcastle

Background
Pulsed infrared (IR, 1862nm) optical stimulation applied to the crista ampullaris evokes robust semicircular canal afferent responses [1] and compensatory eye movements in mammals [2, 3]. Based on data from neurons, cellular responses are primarily due to the temperature rise (DT) and its time derivative (dT/dt) [4, 5] -- the former drives changes in ion-channel open probability, that can be excitatory or inhibitory, and the later drives excitatory changes in plasma membrane capacitance. The aim of the present study was to quantify the major mechanism(s) of IR excitability in mammalian type II vestibular hair cells.

Methods
Whole-cell voltage clamp was used to examine IR (1862nm, DT~0.1-4°C, dT/dt 50-500°C/s) evoked currents in mouse type II hair cells from semicircular canal cristae explants. The voltage-dependent thermo-electric capacitance and the classical temperature-dependent electrical capacitance were recorded using a 3-sine protocol to quantify transients evoked by IR heat pulses. Single-unit extracellular recordings quantified modulation of post-synaptic afferent spike trains to the same IR stimuli.

Results
Afferent recordings in mouse in response to pulsed IR were similar to those reported previously in fish, chinchilla, and rat, suggesting the mechanisms of action are ancestral. Capacitance recordings in type II hair cells demonstrate ultra fast thermo-electric and electrical components evoked by pulsed IR exciting the cell. Countering this were slower ionic currents altering hair cell impedance and excitability.

Conclusion
Data confirm that semicircular canal afferent responses to pulsed IR stimulation of the crista ampullaris are driven primarily by hair cell sensitivity to DT and dT/dt.

1. Rajguru, S.M., et al., *Infrared photostimulation of the crista ampullaris.* J Physiol, 2011. **589**(Pt 6): p. 1283-94.
2. Boutros, P., et al., *Vestibulo-Ocular Reflex Eye Movement Responses to Infra-Red Laser Stimulation of the Mammalian Labyrinth.* Association for Research on Otolaryngology, 2013.
3. Jaing, W., S. Angeil, and S. Rajguru, *Pulsed Infrared Stimulation of Vestibular System: Evoked Eye Movements.* Association for Research on Otolaryngology, 2015.
4. Liu, Q., et al., *Exciting cell membranes with a blustering heat shock.* Biophys J, 2014. **106**(8): p. 1570-7.
5. Shapiro, M.G., et al., *Infrared light excites cells by changing their electrical capacitance.* Nat Commun, 2012. **3**: p. 736.

Funding
NIDCD R01 DC006685 & R01 DC011481 (Rabbitt). University of Newcastle Visiting Fellowship, Australia.

PS 65

Characterization of Fluid Jet Stimulation of Mammalian Cochlear Hair Bundles

Anthony Peng[1]; Anthony Ricci[2]
[1]University of Colorado Denver; [2]Stanford University

In the auditory system, sensory hair cells convert mechanical stimuli into electrical signals at the hair bundle and pass the information onto the central nervous system. To study this mechanotransduction process, two mechanical stimulation methods predominate. The first is a stiff probe that is driven by a piezo-electric stack actuator, and the second is a fluid jet driven by a piezo-electric disc bender. The former is a

displacement stimulus, whereas the latter is a force stimulus. In multiple animal models, the sensory hair bundle is known exhibit mechanical changes during a sustained force stimulus (1–3). Therefore the mammalian auditory hair bundle is likely to change mechanics with a force stimulation, thus changing the position of the hair bundle over time. Current literature confirms this hypothesis, where the hair bundle exhibits a complex movement when stimulated with a fluid jet and imaged with a dual-photodiode (4, 5). Using patch clamp electrophysiology and high-speed video microscopy, we further characterize the fluid jet stimulation paradigm to delineate the complex motion of outer hair cell bundles resulting from a force step stimulation as compared to those obtained using a stiff probe stimulus. We measure the displacement of multiple points along the hair bundle during a step force stimulus by the fluid jet. We find that different parts of the hair bundle move different amounts. Additionally, we find sustained motion of the hair bundle after the force stimulus has plateaued, indicating a mechanical change in the hair bundle. These results show that the mammalian auditory hair bundle is a complex mechanical system and caution must be exercised when interpreting fluid jet stimulation data.

1. Howard J, Hudspeth A (1987) Mechanical relaxation of the hair bundle mediates adaptation in mechanoelectrical transduction by the bullfrog's saccular hair cell. *Proc Natl Acad Sci U S A* 84(9):3064–8.

2. Ricci AJ, Crawford AC, Fettiplace R (2000) Active hair bundle motion linked to fast transducer adaptation in auditory hair cells. *J Neurosci* 20(19):7131.

3. Kennedy HJ, Crawford AC, Fettiplace R (2005) Force generation by mammalian hair bundles supports a role in cochlear amplification. *Nature* 433(7028):880–883.

4. Kros CJ, et al. (2002) Reduced climbing and increased slipping adaptation in cochlear hair cells of mice with Myo7a mutations. *Nat Neurosci* 5(1):41–7.

5. Corns LF, Johnson SL, Kros CJ, Marcotti W (2014) Calcium entry into stereocilia drives adaptation of the mechanoelectrical transducer current of mammalian cochlear hair cells. *Proc Natl Acad Sci* 111:14918–14923.

Funding
This work was supported by NIDCD K99/R00 DC013299 to AWP, and R01 DC003896 to AJR.

PS 66

Structure of an Inner-Ear Protocadherin-15 Fragment with an Atypical Calcium-Free Linker

Raul Araya-Secchi; Marcos Sotomayor
The Ohio State University

Tip links are protein filaments essential for hearing and balance that convey force and gate inner-ear hair cell transduction channels to mediate sensory perception. Cadherin-23 and protocadherin-15 form tip links through a calcium-dependent heterophilic interaction of their extracellular domains, which are made of multiple modules called extracellular cadherin "EC" repeats. These EC repeats are similar but not identical to each other in terms of sequence and structure, often featuring highly-conserved calcium-binding sites at the linker region between them. Linker regions with bound calcium ions provide mechanical strength to the tip link and are often target of deafness-related mutations that prevent calcium binding. Here we present the X-ray crystal structure of protocadherin-15 EC8 to EC10, which shows an EC8-9 canonical-like calcium-binding linker, and an EC9-10 calcium-free linker that alters the linear arrangement of protocadherin-15's EC repeats. Molecular dynamics simulations and small angle X-ray scattering experiment supports the non-linear conformation observed in the structure. Simulations also suggest that the EC8 to EC10 fragment confers elasticity to the tip link during hair-cell mechanotransduction. The new structure provides a structural framework to understand hereditary deafness and to establish the role played by tip links during hair-cell mechanotransduction.

Funding
This work is supported by The Ohio State University and by the NIH (NIH-NIDCD R00-DC012534 to MS). RA is supported by the Pelotonia Postdoctoral Fellowship (Comprehensive Cancer Center - The Ohio State University).

PS 67

Probing the Active Process of Hair Cells: Adaptation & Spontaneous Oscillation Recovery after Overstimulation

Elizabeth Mills; Tracy-Ying Zhang; Dolores Bozovic
University of California, Los Angeles

In the inner ear, hair cells perform the transduction of mechanical input into electrical output. An energy-consuming process enhances their sensitivity to incoming auditory and vestibular stimuli. One manifestation of this active process is spontaneous oscillation of the mechano-sensitivie organelle, the hair bundle, which is at the apical surface of each hair cell. To attain this increased sensitivity, the hair bundle is postulated to operate near a bifurcation, where an internal control parameter, vital to the active process, determines whether the bundle shows limit cycle oscillations or is quiescent. This control parameter may be linked to *in vivo* phenomena, such as temporary threshold shifts, in response to prolonged high-intensity sounds. High amplitude, prolonged deflection of bullfrog sacculus bundles has been shown to temporarily suppress spontaneous oscillations, suggesting a readjustment of the control parameter through a bifurcation. The transition back from quiescence to limit cycle oscillations has been shown to depend on the duration of the imposed deflection and on calcium ion concentration around the mechanically gated transduction channels.

In the current study, we attach magnetic particles to the hair bundles and deflect them with an electromagnet. This technique allows us to impose strong stimuli on the bundles without risk of damage through physical contact with the stimulus probe, and without the associated hydrodynamic effects. We present experiments, performed on preparations

of the bullfrog sacculus, where we identify environmental factors that affect the suppression and recovery of active oscillations. We introduce various pharmacological agents to manipulate the mechano-electrical transduction process and the myosin motor activity inside the hair bundles. We compare how these agents affect particular components of the internal control parameter by measuring the duration of the induced quiescent intervals, time scales associated with the return of the bundle's position to equilibrium, and changes in oscillation frequency before, during, and after deflection.

Funding
This work was funded by AFOSR grant FA9550-12-1-0407.

PS 68

Optical Stimulation and Readout of Inner Hair Cell Vesicle Release

Stefanie Krinner; Lina Jaime; Rituparna Chakrabarti; Jakob Neef; SangYong Jung; Gerhard Hoch; Carolin Wichmann; Tobias Moser
University Medical Center Göttingen

Background
Until recently, patch-clamp provided the only means for time-resolved analysis of exo- and endocytosis of inner hair cells (IHCs). However, presynaptic or paired pre- and postsynaptic whole-cell patch-clamp recordings from IHC synapses do not assess Ca^{2+}-influx and synaptic vesicle (SV) fusion at a specific active zone (AZ) and hence, cannot measure the relative contribution of individual synapses. Here, we present two optical approaches that can be used to determine different aspects of the molecular physiology of IHC synaptic transmission with high spatiotemporal resolution.

Methods
Experiments were performed on freshly dissected mouse organs of Corti.

In the first approach, single synapse activity was examined by high-resolution fluorescence microscopy and electrophysiology. Ruptured patch-clamp was used to stimulate the IHC and record whole-cell Ca^{2+}-influx and capacitance changes. Simultaneous confocal imaging of Ca^{2+} signals and exocytosis through the pH-sensitive fluorophore mOrange2 provided an optical readout of Ca^{2+} triggered exocytosis.

In the second approach, optical stimulation of vesicle release was achieved by transgenic expression of channelrhodopsin-2 in IHCs. Light-induced currents, depolarization and exocytosis were determined by perforated patch-clamp. Optical stimulation protocols using different light intensities and durations were defined. In combination with high-pressure freezing we captured the ultrastructural correlates of exocytosis in a near native state.

Results
Fluorescence responses of the exocytosis reporter vGlut1-mOrange2 increased during IHC stimulation and co-localized with fluorescently-labeled synaptic ribbons. Preliminary data are shown on simultaneous two-color confocal imaging of vGlut1-mOrange2 and synaptic Ca^{2+}-influx to address the relative contributions of individual AZs, resulting in spatio-temporally confined co-localizing hotspots of both reporters.

In the presence of K+ channel blockers already 5 ms optogenetic stimulation of IHCs at high light intensity triggered a strong exocytic response that exceeded the size of the readily releasable pool. At the ultrastructural level we found that 10 ms optical pulse resulted in an increased fraction of docked vesicles and SV with shorter tether lengths.

Conclusions
Simultaneous imaging of presynaptic Ca^{2+}-influx and exocytosis has not yet been performed in mammalian IHCs in tissue, although it is a very sensitive method to approach the spatial coupling between the Ca^{2+} channels and release sites in near native environment. Optical methods in combination with electrophysiology increase the resolution to a single synapse level and might in the future provide new insights into the modes of IHC exocytosis. Further, optogenetic stimulation constitutes a non-invasive, fast and well-defined tool highly suitable for studying the ultrastructure of functional synapse states by electron microscopy.

Funding
This work has been supported by the Deutsche Forschungsgemeinschaft (DFG) trough the Collaborative Research Center 889 (project A2, A7 and A8), the Erasmus Mundus Consortium (Neurasmus) and the DFG Gottfried Wilhelm-Leibniz-Programme.

PS 69

Voltage-Mediated Control of Bundle Dynamics in Saccular Hair Cells

Patricia Quiñones; Sebastiaan Meenderink; Dolores Bozovic
University of California, Los Angeles

Introduction
Hair cells of the vertebrate vestibular and auditory systems convert mechanical inputs into electrical signals that are relayed to the brain. This mechano-electrical transduction (MET) involves mechanically gated ion channels that open following the deflection of hair bundles. The MET includes one or more active feedback mechanisms to keep the mechanically gated ion channels in their most sensitive operating range. Coupling between the gating of the mechanosensitive ion channels and this adaptation mechanism has been proposed to follow dynamics of a system that is close to a Hopf or other bifurcations. In the proximity of a critical point, the system exhibits high responsiveness to external stimuli, which could explain the sensitivity, dynamic range, and frequency selectivity of audition. This nonlinear system can cross the bifurcation into an unstable state, where it undergoes limit-cycle oscillations in the absence of input. We obtained simultaneous optical and electrophysiological recordings from bullfrog saccular hair cells with such spontaneously oscillating hair bundles.

Methods
For the experiments, we used sacculi from the American bullfrog (*R. catesbeiana*) that were placed in a two-compartment chamber such that a fluid separation between the apical and basolateral surfaces of the hair cells was maintained. Hair bundle position was tracked using a high-speed video camera system, and the hair cell membrane potential was controlled (voltage-clamp) or monitored (current-clamp) using patch-clamp techniques.

Results & Discussion
The spontaneous bundle oscillations allowed us to characterize several properties of MET without artificially loading the hair bundle with a mechanical stimulus probe. We show that the membrane potential of the hair cell can modulate or fully suppress innate oscillations, thus controlling the dynamic state of the bundle. We further demonstrate that this control is exerted by affecting the internal calcium concentration, which sets the resting open probability of the mechanosensitive channels. The auditory and vestibular systems could use the membrane potential of hair cells, possibly controlled via efferent innervation, to tune the dynamic states of the cells. Thus, a combination of mechanical stimulation and manipulation of the membrane potential are used to explore dynamics of sensitivity and tuning of the hair bundle.

Funding
This work was supported by NIH grant RO1DC011380 to DB.

PS 70

Evidence Supporting Direct Dopaminergic Innervation of Cochlear Hair Cells in the Adult Rat: Immunolocalization of Dopamine Receptors and Protein-Protein Interactions with Hair Cell Proteins

Christopher Rose; Marian Drescher; Neeliyath Ramakrishnan; Dakshnamurthy Selvakumar; Dennis Drescher
Wayne State University, Detroit

Background
Our original evidence supporting dopaminergic innervation of the organ of Corti (OC) was provided by detection of dopamine receptor D2L and D1B cDNA in an OC cochlear subfraction from adult rat cochlea, with receptor protein immunolocalized to olivocochlear efferent tunnel crossing fibers and cochlear outer hair cells, respectively (Kewson et al., ARO Abstr. 22:123, 1999). With protein-protein interaction (PPI) studies, dopamine D1A in OC was shown to input synaptic exocytosis pathways by interacting with NSF or alternatively, with snapin, otoferlin and AP2mu1 (Selvakumar et al., ARO Abstr. 37:107, 2014).

Methods
Organ of Corti, lateral wall, and spiral ganglion cochlear subfractions were microdissected from bony labyrinths of adult rats, total RNA extracted, and following DNase treatment, converted to cDNA with reverse transcriptase and analyzed with PCR for dopamine receptor subtypes. Primers were designed crossing introns for dopamine D4 and D3 receptors, D2 and D4 third intracellular loops, and dopamine D4 carboxy terminus. Yeast two-hybrid mating protocols identified direct PPI for OC-expressed dopamine receptors.

Results
Sequencing indicated expression of dopamine D4 receptor transcript in the OC, lateral wall, and spiral ganglion cochlear subfractions and dopamine D3 receptor in the lateral wall and spiral ganglion subfractions**.** D4 receptor protein was immunolocalized to the cochlear inner hair cells (IHC) in middle and apical turns, with IR filling the cell body. A line of D4 immunoreactivity was also observed in the basal cell layer of the stria vascularis. In addition to PPI of dopamine D2L with hair cell marker PCP4 in a CNGA3 pathway previously described (Selvakumar et al., 2014), OC dopamine D2L third intracellular loop, used as bait in yeast two-hybrid mating protocols, was found to directly interact with prey proteins snapin (a hair cell binding partner of D1A implicated in hair cell exocytosis via otoferlin), CtBP2 (ribeye), and ryanodine/calmyrin.

Conclusions
PPIs for mammalian OC D2L, along with D1 PPIs, represent corroborative evidence for dopaminergic input to HC vesicular transmitter exocytosis. Input to stereociliary HCN1 and CNGA3 cyclic-nucleotide pathways in HC potentially occurs via direct D2 PPI with filamin A. The intense and specific immunoreactivity for dopamine D4 in IHC would further support direct dopaminergic innervation of the IHC and involvement of D4 in basal-cell-directed trafficking in the stria vascularis. The carboxy terminus of D4 interacts directly with CLIC6, similar in molecular identity to CLIC5, implicated along with radixin in stabilizing membrane-actin filament linkages at the base of stereocilia (Salles et al., 2013).

Funding
Supported by Wayne State University Department of Oto-laryngology Resident Research Program and NIH R01 DC000156.

PS 71

GABAA Alpha-1 Direct Protein-Protein Interactions in the Organ of Corti Implicate GABAergic Input to Hair Cell Endocytosis

Angela Vong; Dakshnamurthy Selvakumar; Marian Drescher; Neeliyath Ramakrishnan; Dennis Drescher
Wayne State University, Detroit

Background
The neurotransmitter GABA has been identified as released in response to sound stimulation into perilymph of the mammalian cochlea (Drescher et al., 1983) and is recognized as an olivocochlear lateral efferent neurotransmitter with electron microscopic localization of GAD, the enzyme of synthesis, in efferent axonal synaptic endings on type I afferents and on cochlear inner hair cells in what was considered the adult configuration (Sobkowitz et al., 1997). Given that GABAA subunits are immunoprecipitated with the hair cell synapse marker ribeye (Kantardzhieva et al., 2012),

a role for GABAA molecular subunit interactions with hair cell synaptic proteins and function is predicted.

Methods
RT-PCR analysis was performed examining expression of GABAA channel subunit transcripts for GABAA channel subunits a1, a2, b1, b2, b3 and g2 in the microdissected mammalian organ of Corti. Direct protein-protein interactions (PPI) for GABAA a1 were identified by yeast two-hybrid mating protocols screening a rat organ of Corti cDNA library. Yeast two-hybrid co-transformation protocols were applied to OC proteins to ascertain whether the GABAA a1 subunit interacts directly with low-density lipoprotein receptor-related protein 1 (LRP-1), as determined with purified hair cells of the teleost saccule.

Results
RT-PCR demonstrated the presence of transcript for GABAA receptor subunits a1, a2, b1, b2, b3 and g2 in the microdissected mammalian organ of Corti. Further, yeast two-hybrid co-transformation protocols confirmed interaction of the intracellular M3-M4 domain of OC GABAA a1 and LRP-1. Yeast two-hybrid mating protocols with OC GABAA channel a1 as bait and a cDNA library as prey additionally identified 130 prey proteins in OC as direct binding partners: carcinoembryonic antigen-related cell adhesion molecule 16 and whirlin, both targeted in deafness, and kinectin, the kinesin receptor, calsyntenin-1, smoothelin, and alpha-2-macroglobulin, the ligand for LRP-1 and inhibitor of metallomatrix proteins, and protocadherin alpha 11.

Conclusions
GABAergic olivocochlear efferents innervating the organ of Corti exert functional control via a specific group of receptors comprising the GABAA ionotropic chloride channel expressed by hair cells. GABAA a-1, in particular, directly interacts with LRP-1, which mediates sorting of clathrin-coated vesicles in endocytosis accompanying neurotransmission. Direct PPI of GABAA a-1 with kinectin, the kinesin-1 receptor, and calsyntenin-1, which docks vesicular cargo to kinesin-1, further suggest mechanisms for GABAA molecular input to hair cell endocytosis. LRP-1, itself, directly interacts with cGMP-gated CNGA3, implicated in regulation of hair cell Ca^{2+} influx. Along with alpha-2-macroglobulin, LRP-1 controls extracellular levels of matrix metalloproteinases that regulate ligand-sensitivity of CNGA3.

Funding
Supported by The Lions Club of Southeastern Michigan, Wayne State University Department of Otolaryngology Resident Research Program and NIH R01 DC000156.

PS 72

Structural Changes in Inner Hair Cells and Surrounding Structures in a Mouse Model of Hidden Hearing Loss

Anwen Bullen; Warren Bakay
University College London

Research Background
Hidden hearing loss is a condition where patients exhibit symptoms of hearing dysfunction despite a normal audiogram. In humans, these patients were shown to have characteristic changes to their auditory brainstem response (ABR) measurements. An attenuation of Wave 1 was observed, which approximately correlates to the activity of the auditory nerve. Hidden hearing loss has been attributed at the level of the cochlea to a selective loss of high-threshold low-spontaneous rate afferent fibres at the inner hair cells, observed in both animal models and human patients. The aim of this work was to examine the spatial distribution of the lost fibres and to assess the effects of fibre loss on the structural organisation of inner hair cells.

Methods
Male CBA/Ca mice, 2-3 months old, were exposed to 100dB SPL octave band noise at 4-8kHz or 8-16kHz for 2 hours. ABR measurements were taken immediately after exposure. Mice were then left to recover for four weeks before a second ABR measurement was taken. Mice were accepted as suffering from hidden hearing loss if after the four week recovery period they showed attenuation of wave 1, recovery in wave 4, and no elevation in overall thresholds. Immediately following the final ABR mice were sacrificed and cochleae fixed. Cochleae were then prepared for electron microscopy. Samples were examined using TEM, Electron Tomography (ET) and Serial Block Face Scanning Electron Microscopy (SBF-SEM).

Results
3D electron microscopy showed the distribution of damaged and healthy terminals around IHCs in the noise-damaged region, as well as synaptic densities and ribbon synapses in the regions of damaged synapses. Changes to the intracellular contents of the IHC were also observed. Comparison of the cytoplasmic regions surrounding healthy and damaged synapses on the same cells indicated changes to cellular structures and organelles in the regions local to the synapses.

Conclusions
The results indicate that when synapses are lost after noise damage, concomitant changes occur in the inner hair cells. These changes may occur both at regions close to the synapse and in more distant parts of the cell. The results also suggest that synaptic ribbons and synaptic densities may persist for a while after degradation of the afferent terminal.

Funding
Action on Hearing Loss Pauline Ashley grant

PS 73

Short term synaptic plasticity of medial olivocochlear- hair cell synapses is altered by a point mutation in the α9α10 nAChR

Carolina Wedemeyer; Lucas Vattino; Jimena Ballestero; Eleonora Katz; Ana Belén Elgoyhen
Instituto de Investigaciones en Ingeniería Genética y Biología Molecular, INGEBI (CONICET)

Inner hair cells (IHCs) are involved in conveying acoustic information to the central nervous system through the auditory nerve, while OHCs are mainly responsible for the mechanical amplification of sound. Both hair cells are modulated through medial olivocochlear (MOC) neurons. IHCs receive transient MOC innervation from birth to the onset of hearing in the second postnatal week, while MOC fibers synapse with OHCs from the first postnatal week throughout adulthood. The MOC-hair cell synapse is cholinergic, inhibitory, and is mediated by activation of α9α10 nicotinic receptors (nAChRs).

We analyzed the properties of synaptic transmission in a knock-in mouse (Kin) bearing a mutation in the α9 nAChR subunit (L9´T) that prolongs cochlear inhibition and enhances noise protection (Taranda et. al 2009). Our aim was to determine if there is a consequent change in MOC-hair cell short term plasticity (STP) due to the presence of the L9'T mutation.

Synaptic currents (IPSCs) evoked by electrical stimulation of MOC fibers were recorded in IHCs from isolated mouse organ of Corti (apical turn) at postnatal days 9-11. High frequency stimulation, 100 Hz-trains, of MOC fibers caused depression of IPSC amplitudes in IHCs of both wt and Kin mice, (79% and 90% *n*=4, respectively). Interestingly, a low frequency stimulation of 10 Hz caused depression only in Kin mice (40%, *n*=5). Release probability analysis suggested that a reduction in the probability of release of synaptic vesicles contributed to depression at 10 Hz (p_{10}/p_1=0.77±0.3, *n*=3). In addition, the amplitude of single successful events decreased towards the end of the train, suggesting that a postsynaptic mechanism also contributed to synaptic decay (a_{10}/a_1=0.64±0.1, *n*=6). In order to determine the underlying causes for the drop in release probability in 10 Hz-trains we estimated the time course of recovery from synaptic depression. Following a 100 Hz-conditioning train a faster recovery was observed in wt compared to Kin mice (time constant of single-exponential fit wt= 1.21 ± 0.36 s, *n*=4; Kin: 2.36 ± 0.81 s, *n*=4.).

Results obtained strongly suggest that a change in the kinetic properties of the postsynaptic α9α10 hair cell nAChR is sufficient to alter release efficacy of MOC-IHC synapses. This could result from a homeostatic synaptic change such that presynaptic release probability drops during sustained physiological activity.

Funding
Support ANPCyT to ABE and R01 DC001508-24 to Paul Fuchs and ABE

PS 74

Transient and Sustained Exocytosis at the Auditory Hair Cell Ribbon Synapse Involve Different Cav1.3 Channel Isoforms

Philippe Vincent[1]; Yohan Bouleau[1]; Gilles Charpentier[1]; Alice Emptoz[2]; Saaid Safieddine[2]; Christine Petit[2]; Didier Dulon[1]
[1]University of Bordeaux; [2]Institut Pasteur

Introduction
The mechanisms orchestrating transient and sustained exocytosis in auditory inner hair cells (IHCs) remain essentially unknown. These two exocytotic regimes are believed to sequentially mobilize a readily releasable pool of vesicles (RRP) nearby the synaptic ribbons and a slowly releasable pool of vesicles (SRP) at farther distance from the ribbons. They are both controlled by Cav1.3 channels and require otoferlin as Ca^{2+} sensor but we don't know whether they use the same pool and spatial-organization of Ca^{2+}-channels.

Methods
Ca^{2+} currents and real-time changes in membrane capacitance were here recorded in mouse IHCs (P15-P17) in whole-cell voltage-clamp configuration. We used the property of UV-sensitivity of the dihydropyridine compound nifedipine, which can be transformed into an ineffective nitroso-compound, to instantaneously restore Ca^{2+} currents in cells incubated with 20 µM nifedipine. Brief UV-flashes were delivered with a Mic-LED 365. The Cav1.3 isoforms in Otof $^{+/-}$ and *Otof* $^{-/-}$ mice we identified by RT PCR on mRNA extract from organs of Corti or from isolated IHCs. Specific primers were designed to specifically amplify regions in the c-terminal domain of the pore forming α1D channel.

Results
Here, we show that only a small proportion (~25 %) of total Ca^{2+} current in IHCs, displaying fast inactivation and resistance to 20 µM nifedipine, is sufficient to trigger normal RRP exocytosis, but not SRP exocytosis. This transient nifedipine-resistant Ca^{2+} current is likely carried out by short C-term isoforms of Cav1.3 channels, notably Cav1.342a and Cav1.343s, since their mRNA were found strongly expressed in wild-type IHCs and poorly expressed in *Otof*$^{-/-}$ IHCs, showing Ca^{2+} currents with strongly reduced inactivation. The nifedipine-resistant RRP exocytosis was only slightly reduced by 5 mM intracellular EGTA suggesting that the Cav1.3 short-isoforms are closely associated with the site of release. Conversely, our results suggest that Cav1.3 long isoforms, Cav1.342L and Cav1.3Δ44, carrying ~80 % of total Ca^{2+} current, displaying poor inactivation and high sensitivity to nifedipine, are essential to trigger efficient Ca^{2+} diffusion and mainly involved in recruiting SRP vesicles. The strong sensitivity of SRP exocytosis to 5 mM EGTA suggested that the long Cav1.3 isoforms are localized at farther distance from the sites of release as compared to Cav1.3 short isoforms.

Conclusion
Our results strongly suggest that IHCs use different Cav1.3 isoforms to trigger and regulate both the dynamic of the RRP fusion and the vesicular recruitment.

PS 75

Vesicle Traffic in the Outer Hair Cell of the Guinea-Pig Cochlea

Csaba Harasztosi; Susanne Badum; Anthony Gummer
University of Tübingen

Background

Hair cells possess endocytic activity that can be visualized by fluorescent membrane markers. It has already been shown that outer hair cells (OHCs) possess rapid endocytic activity at their apical pole (Griesinger et al., 2004; Kachar et al., 1997; Kaneko et al., 2006; Meyer et al., 2001). It was demonstrated that membrane particles are intensively endocytosed at the apical pole of OHCs and transcytosed to different locations, namely into the basolateral membrane and along a central strand down to the nucleus (Griesinger et al., 2004; Kaneko et al., 2006). Endocytic vesicles have been demonstrated in the subnuclear region of OHCs using electron microscopy (Nadol, 1983). Horseradish peroxidase staining showed the presence of coated vesicles and small vacuoles in the synaptic zone of OHCs (Siegel & Brownell, 1986). We reported that vesicles formed at the basal pole are trancytosed towards the supranuclear area and endocytic activities at the opposite poles contribute equally to balance the exocytosis-evoked membrane surface increase - the membrane recycling (ARO 2013, #154).

Methods

In the current study confocal microscopy and styrylpyridinium dyes FM1-43 and FM4-64 were used to investigate the vesicle traffic of OHCs isolated from the guinea-pig cochlea. A local perfusion system was used to stain OHCs either only at one pole using FM1-43 or at both poles applying FM1-43 and FM4-64 independently to the opposite poles to investigate the apicobasal and the basoapical vesicle traffic simultaneously.

Results

Single-dye application demonstrated that vesicles endocytosed at the infranuclear pole are trancytosed up to the apex with a speed of ~0.44 and ~0.08 µm/s at the distances of 5 and 67 µm from the base of the cell, respectively (n=7). Double-dye application revealed, in general, that intracellular vesicle traffic becomes slower at distances longer away from the location of endocytosis. The calculated speed of basoapical traffic at the locations of 6 and 61 µm from the basal pole was ~0.54 and ~0.07 µm/s, respectively (n=5). At the same time in these cells at the locations of 5 and 31 µm from the apical pole of the cell the speed of the apicobasal traffic was ~0.18 and ~0.03 µm/s, respectively.

Conclusion

The data imply that the speed of the basoapical vesicle traffic is larger than the speed of the apicobasal traffic. Therefore, the experiments demonstrate that the dynamics of intracellular vesicle traffic is direction dependent and not homogeneous along the longitudinal axis of the OHC.

PS 76

Activation of Group I mGluRs Enhances Efferent Inhibition of Inner Hair Cells in the Developing Cochlea of the Rat

Zhanlei Ye[1]; Juan Goutman[2]; **Sonja Pyott**[3]; Elisabeth Glowatzki[4]
[1]Harvard University; [2]Instituto de Investigaciones en Ingeniería Genética y Biología Molecular (CONICET); [3]University Medical Center Groningen; [4]The Johns Hopkins University School of Medicine

Background

Before the onset of hearing, cholinergic neurons in the medial olivocochlear (MOC) nucleus in the brainstem supply inhibitory efferent innervation to the inner hair cells (IHCs) of the cochlea.

Methods

To examine this innervation, whole cell recordings for IHCs in excised cochlear coils (P7-11) were used to record evoked MOC-IHC efferent inhibitory postsynaptic currents (eIPSCs) in response to electrical stimulation of the efferent fibers (Goutman et al. 2005).

Results

Application of either the general mGluR agonist (t-ACPD, 100 µM) or a group I mGluR agonist (DHPG, 50 µM) enhanced the amplitude of the MOC-IHC eIPSCs. This enhancement was blocked by the continuous application of group I mGluR antagonists (CPCCOEt, 100 µM; MPEP, 10 µM). To determine whether group I mGluR activation targeted pre- or postsynaptic processes to enhance eIPSC amplitudes, changes in quantum size (the size of a single vesicle) and quantal content (the number of vesicles released per stimulation) were determined. Quantum sizes (calculated from the means of the sIPSC amplitude distributions) remained unchanged before and after agonist application. In contrast, the quantal content increased significantly when calculated using either the 'direct method' (in which m equals the ratio between the mean amplitudes of eIPSCs and the mean amplitude of sIPSCs) or by 'failures' (in which m equals the natural log of the ratio between the total number of stimuli and the total number of failures). These findings indicated that activation of group I mGluRs increases the number of vesicles released per stimulation without effecting the postsynaptic responsiveness to neurotransmitter release. Furthermore, conditions that maximized glutamate release from the IHCs and promoted the accumulation of glutamate were also able to enhance MOC-IHC eIPSCs. This enhancement could be blocked by application of CPCCOEt and MPEP. Finally, immunofluorescence indicated that IHC afferent ribbons (the sites of glutamate release) were located close enough to IHC efferent synapses to, in principle, allow for spillover of glutamate and activation of mGluRs on the efferent presynaptic terminals.

Conclusions

These findings suggest the presence of a local negative feedback loop: IHC activity enhances MOC efferent synaptic strength that, in turn, likely suppresses IHC activity. This

feedback loop has important implications for activity-dependent maturation of the cochlea.

Funding
Supported by Deafness Research Foundation (Hearing Health Foundation) to SJP and NIDCD R01DC006476 to EG

PS 77

Dominant-Negative Inhibition of the Retinoblastoma (Rb1) Gene in the Inner Ear

Shikha Tarang; Umesh Pyakurel; Sonia Rocha-Sanchez
Creighton University

Background
Retinoblastoma 1 (*Rb1*) is an essential gene regulating cellular proliferation, differentiation, and homeostasis. Complete germline or conditional *Rb1* deletion leads to abnormal cell proliferation, followed by massive apoptosis, making it difficult to fully address *Rb1*'s biochemical activities.

Methods
To overcome these limitations, we developed a tetracycline-inducible *TetO-CB-myc6-Rb1* (CBRb) mouse model to achieve transient and inducible dominant negative (DN) inhibition of the endogenous RB1 protein. Our strategy involved fusing the *Rb1* gene to the lysosomal protease pre-procathepsin B (CB), thus allowing for further routing of the DN-CBRb fusion protein and its interacting complexes for proteolytic degradation.

Results
DN-CBRb mice bred to a ubiquitous rtTA mouse line demonstrate a significant inhibition of the endogenous RB1 protein in the inner ear and in a number of other organs where RB1 is expressed. Histological analysis of cochleae isolated from CBRb mice show presence of supernumerary Hair Cells which persist up to ten days after discontinuation of Dox treatment. SEM analysis of cochlea obtained from $CBRb^{+}$ mice showed persistence of kinocilium and microvilli-like structures indicating developmental immaturity and higher potential for regeneration. *In situ-hybridization* using CBRb transgene specific probe showed the expression of transgene in the inner Hair Cell region which is consistent with the histological analysis on the presence of supernumerary cells in this region.

Conclusion
Our analyses so far support the notion that dominant-negative RB1 inhibition is low enough to trigger cell proliferation in HCs but high enough to prevent their death. Further analyses are underway to investigate the maturation and functional status of the newly generated Hair Cells.

Funding
Hearing Health Foundation (Tarang S), R21 (Rocha-Sanchez SM)

PS 78

Expression, Regulation and Function of Cannabinoid Receptor 2 in the Cochlea

Sumana Ghosh; Debashree Mukherjea; Kelly Sheehan; Srinivasn Tupal; Vikrant Borse; Asmita Dhukhwa; Vickram Ramkumar; Leonard Rybak
Southern Illinois University School of Medicine

Background
The pharmacological and therapeutic importance of cannabinoids has been gaining recognition in treatment of various pathological conditions. Natural and synthetic cannabinoids regulate inflammatory modulators and act as anti-oxidants. Recent data from our laboratory and others have shown that inflammation plays a central role in hearing loss. Ototoxicity occurs when the acute cochlear inflammation goes unabated and progress to cell apoptosis in regions of organ of Corti, such as stria vascularis (SV), spiral ligament (SL) and spiral ganglion (SG). There is very little information pertaining to cannabinoid receptors (CBRs) expression and function in cochlea. The current study examined the expression and regulation of CBRs in the cochlea. We show expression of the both cannabinoid receptor 1 and 2 (CB1R, CB2R) in the cochlea and cochlear-derived cell cultures. Cisplatin down regulated CB2R and increased apoptosis of UB/OC-1 cells, effects which are attenuated by activation of CB2R.

Methods
CB1R and CB2R expression was confirmed in the rat cochlea, mouse organotypic cultures and UB/OC1 cells using immunofluorescence, Western blotting and q-PCR techniques. The cytoprotective effect of the CB2 agonist (JWH-015) in UB/OC1 cells was investigated by MTS and LDH release assays and by assessing apoptotic markers.

Results
Both CB1R and CB2R are expressed in the outer and the inner hair cells, SG and SV in the rat and mouse cochleae. *In vitro* data indicate that CB2 specific agonist JWH-015 increases the expression of CB2R in UB/OC1 cells and attenuated cisplatin-induced reduction in expression of this receptor. Activation of CB2R decreased cisplatin-induced p53 and decreased the ratio of Bax:Bcl-xL, indicating an anti-apoptotic role of this receptor. CB2R agonist also decreased expression of pro-inflammatory genes, such as inducible nitric oxide synthase and cyclooxygenase2. In support of these findings, we show that CB2 agonist reduced cisplatin-induced activation of signal transducer and activator of transcription 1 (STAT1) and attenuated cisplatin-induced reduction in STAT3 activity. Furthermore, CB2R activation reduced cisplatin-induced activation of nuclear factor (NF) κB in UB/OC-1 cells.

Conclusions
We have shown the expression of CB1R and CB2R in the rat cochlea. Studies focusing on CB2R show that its expression is positively regulated by its agonist but negatively regulated by cisplatin. Activation of CB2R protected against cisplatin-induced inflammation and killing of hair cell cultures by suppressing STAT1 and possibly NF-κB, but by enhancing

STAT3 activity. These studies predict an otoprotective role of CB2R agonists against hearing loss, which will be evaluated in future experiments.

Funding
NIH grants : 1. RO1DC002396 (Leonard P Rybak) 2. RO-1CA166907 (Vickram Ramkumar)

PS 79

Hearing Loss in a Transgenic Mouse Model of HIV

Pamela Roehm; Lifan He; Taha Mur; Kamil Amer; Jennifer Gordon
Temple University School of Medicine

Background
35.3 million people were infected with HIV in 2012. Patients with human immunodeficiency type I (HIV) have a significantly increased rate of both sensorineural and conductive hearing loss. Causes of the increase in sensorineural hearing loss in this population could be the direct results of the virus, results of ototoxic damage due to highly active anti-retroviral therapy (HAART), due to opportunistic infections affecting the brain and ear, or due to medications used to treat opportunistic infections associated with HIV. Studies to determine the etiology of hearing loss in these patients are extremely difficult and ethically impossible. To better understand the role of viral proteins in hearing loss in HIV-infected patients, we have studied hearing in a transgenic model of HIV, the Tg26 mouse.

Methods
The Tg26trangenic mouse model contains nearly the entire HIV-1 genomic sequence except for the gag-pol region of the genome. These animals were maintained in a FVB background. Hearing was measured by auditory brainstem responses (ABR) and distortion-product otoacoustic emissions in Tg26 heterozygous mice and wild-type littermates at regular intervals from 2 to 18 months of age. At intervals, cochleas were harvested, immunostained with antibodies against for hair cell and neuronal proteins, and imaged with confocal microscopy. Cell counts of hair cells and spiral ganglion neurons were performed. Areas corresponding to accumulations of synapse protein markers were also counted. All data was analyzed using Mann-Whitney U tests and students t-tests as appropriate.

Results
An initial elevation of ABR thresholds by15-20 dB SPL was initially observed in Tg26+/- animals compared with wild-type littermates. This hearing loss increased gradually over time to a more severe loss. Defects in inner ear hair cells and hair cell-spiral ganglion synapses were observed in stained sections taken from Tg26+/- cochleas.

Conclusion
Further studies of this animal model will help us better understand hearing loss associated with HIV-1 infection.

Funding
CNAC/ NIMH, Development Grant, P30MH092177 Assessment of Hearing and Evaluation of Site of Pathology in Mouse Models of HIV

PS 80

Screening for Otoprotective Compounds using Multiple Assays in Zebra fish and Mouse.

Emma Kenyon; Marco Derudas; Nerissa Kirkwood; Molly O'Reilly; Sian Kitcher; Richard Goodyear; Simon Ward; Guy Richardson; Corne Kros
University of Sussex

Background
Aminoglycoside antibiotics are used in clinical practise to treat life-threatening bacterial infections such as septicaemia. As a side effect, they can cause the loss of sensory hair cells from the inner ear resulting in deafness and balance disorders. These ototoxic compounds are known to enter hair cells via the mechano-electrical transducer (MET) channels that are located in the hair bundle. Blocking these channels by non-toxic compounds is a potential strategy to stop aminoglycoside induced sensory hair cell damage.

Methods
To identify such agents we screened the Tocris Ion-Channel set, a library of 160 compounds. We used the zebra fish lateral line system in 3 different assays to identify any compounds that: 1) blocked entry of FM1-43, a fluorescent styryl dye that permeates hair cells via their MET channels, into hair cells, 2) blocked entry of Texas-red conjugated neomycin (TR-neo) into hair cells, 3) protected hair cells against longer-term aminoglycoside antibiotic exposure.

Results
We found 4 compounds that blocked and 33 compounds that reduced FM1-43 entry into hair cells, 8 that prevented and 25 compounds that diminished TR-neo entry and 24 compounds that completely and 15 compounds that partially protected hair cells against exposure to neomycin for 1 hour.

52 compounds were then selected to identify if any would protect hair cells in mouse cochlear cultures from aminoglycoside antibiotic induced damage. The purpose of this assay was to identify: 1) compounds that would protect mammalian hair cells against aminoglycoside antibiotic induced damage, 2) a zebra fish assay that predicts whether a compound can protect mammalian hair cells. Presently 3 compounds have been identified as protecting mouse cochlear culture hair cells from damage. Of the 10 compounds that were positive in all 3 zebra fish assays, 6 compounds have been tested to date, with no compounds protecting mouse cochlear hair cells.

Those compounds that protected mouse hair cells were subsequently assayed by electrophysiological methods for their ability to block the MET channels. Of the 3 compounds that protected in the mouse cochlear culture assay 2 have been tested by electrophysiological methods. Out of these,

one blocked MET channel currents in mouse cochlear hair cells.

Conclusions
This is the first step in identifying non-toxic therapeutic compounds that could be used to protect patients from deafness and balance disorders caused by the use of aminoglycosides.

This research is funded by the Medical Research Council.

Funding
This research is funded by the Medical Research Council.

PS 81

Protective effect of Astaxanthin nano emulsion against neomycin-induced hair cell damage in zebra fish.

Yousuke Takemoto; Yosinobu Hirose; Kazuma Sugahara; Makoto Hashimoto; Hiroshi Yamashita
Yamaguchi University

Introduction
The degeneration of mechanosensory hair cells of the inner ear sensory epithelia is the primary cause of deafness. Hair cells are commonly lost through drug-induced trauma, as well as noise-induced trauma and aging. The cause of those hair cells disorder is oxidative stress due to free radicals. In particular, hair cells are very susceptible to aminoglycosides. Antioxidant is known to reduce the generation of oxygen-derived free radicals. Various antioxidant is marketed, and different dosage form is developed with the same drug. For example, Coenzyme Q10, and Astaxanthin are fat-soluble, and there are the characteristics that are hard to be absorbed from intestinal tract and skin. However, it was more stable, and an absorbent good nanopreparation was developed. Using a zebra fish lateral-line, we report hair cell protection effect of Coenzyme Q10 and Astaxanthin from neomycin-induced trauma.

Materials and Methods
Zebra fish embryos were used in this study. Zebra fish larvae were exposed to Astaxanthin and CoenzymeQ10 (1-10000 ug/ml) for 1 hour before 200 uM neomycin to induce hair cell death for 1 hour. A bulk preparation and a nanopreparation were used. After that, they were fixed in 4% paraformaldehyde, incubated with anti-parvalbumin, Alexa 594, and hair cell damage was assessed.

Results
In zebra fish lateral line, the survival rate of hair cells in Neomycin + Nanoastaxanthin group Neomycin + NanocoenzymeQ10 group was significantly more than that in Neomycin group. The hair cell protection effect was not obtained with the bulk preparation.

Discussion
Zebra fish exhibit hair cells in the lateral-line neuromasts which are structurally and functionally similar to mammalian inner ear hair cells. Lateral line hair cells of zebra fish larvae are easily accessed making them ideal for experimental manipulation. The results of the current study, hair cell protection effect from neomycin-induced trauma was observed in only Coenzyme Q10 and Astaxanthin of the nanopreparation. But the hair cell protection effect was not obtained with the bulk preparation. We thought that it was not absorbed in zebra fish because the bulk sawing had a big particle diameter. It was suggested that particle diameter was involved in the absorption of the drug to a living body.

PS 82

Protective effect of Ceramide-1-Phosphate on apoptosis of cochlear hair cells induced by cisplatin

Keiji Tabuchi; Akira Hara; **Quang Le**
University of Tsukuba hospital

Background
Identification of effector molecules involving in the regulation of cell fate is crucial to develop a proper therapeutic strategy. In cochlear-hair-cell death induced by cisplatin, one of identified decisive factor is elevation of ceramide which is derived from activation of sphingomyelinase. Ceramide-1-phosphate (C1P) is a phosphorylated form of ceramide. The phosphorylation of ceramide is mediated by ceramide kinase. While ceramide is an inducer of apoptosis of hair cells in cisplatin ototoxicity, little is known about the function of C1P in the cochlear diseases. The present study was designed to show whether C1P could affect cisplatin-induced apoptosis of cochlear hair cells.

Method
Explants of cochlear basal turns collected from C57BL/6J mice at postnatal day 3 to 5 were used in all experiments. Cochlear explants were exposed to 10 or 5 μM cisplatin for 48 hours to assess the effects of C1P, NVP-231 (a ceramide kinase inhibitor) or ceramide. Western blotting of Akt/pAkt was conducted to check whether this pathway was modulated by C1P.

Results
C1P activated the Akt pathway and significantly reduced cochlear cell death induced by cisplatin. Next, when treating cochlear hair cells with NVP-231 under the present of cisplatin, a remarkable increase in apoptosis of hair cells was recognized. In addition, co-administration of cisplatin and ceramide decreased significantly residue of cochlear hair cells.

Conclusion
The present findings confirmed the anti-apoptotic function of C1P in the cisplatin ototoxicity. The balance between ceramide and C1P may play a critical role in determination of hair cell fate in cisplatin ototoxicity.

Funding
This work was supported by a Grant-in-aid for Scientific Research (C) 24592541 from the Ministry of Education, Culture, Sports, Science, and Technology of Japan

PS 83

Preventing HC Loss: An Epigenetic Approach

Alice Gervasoni; Mohi Ahmed; Cynthia Andoniadou; Andrea Streit
King's College London

Auditory hair cells are susceptible to ototoxicity from a multitude of drugs including aminoglycoside antibiotics such as gentamicin. Unlike non-mammalian vertebrates, damage or loss of hair cells results in permanent hearing loss. However, in the last few years it emerged that the neonatal mouse cochlea retains a limited regenerative potential during the first post-natal week. As the cochlea matures supporting and hair cells change their epigenetic profile. Here, we exploit this observation and ask whether drugs that modify histone modification enhance hair cell regeneration or survival after ototoxic damage. We find that indeed treatment of cochlear explants from postnatal day 8 with drugs that prevent deposition of repressive marks results in partial recovery of HCs after gentamicin treatment. There is a significant increase in Myo7a+ cells as compared to controls. Using Sox2 CreERt2/+; ROSA26CAG-td Tomato/+ and BrdU incorporation assays we show that recovered HCs do not arise from supporting cells or from cells, which have re-entered the cell cycle. This finding suggests that some changes in the epigenetic modifications affect HC survival rather than regeneration, and we are currently investigating the interaction between epigenetic modifiers and apoptosis.

Funding
Action On Hearing Loss; King's College London (KCL) ; BBRC.

PS 84

Actin Core Repair Underlies the Recovery of Overstimulation-Induced Stiffness Changes in Inner Hair Cell Stereocilia Bundles

J. Grossheim; Ruben Stepanyan; Gregory Frolenkov
University of Kentucky

Background
While the actin paracrystalline core determines the rigidity of the stereocilia shaft of auditory hair cells, actin filament organization in the rootlets allows the stereocilia to pivot at their base when deflected. Irreparable damage to the actin filaments at the stereocilia base was observed in cats exposed to acoustic stimulation sufficient to cause permanent noise-induced hearing loss (Liberman, 1987). Mechanical overstimulation of mammalian auditory hair cells *in vitro* results in a transient decrease of bundle stiffness (Saunders et al., 1986). Two mechanisms may be responsible for this change: 1) mechanical breakage of the tip-links and their subsequent regeneration; and 2) recoverable damage to the actin filaments near the base of stereocilia.

Methods
We used a fluid-jet to deflect inner hair cell (IHC) stereocilia in young postnatal cultured murine organ of Corti explants. Frame-by-frame analysis of video recordings of bundle displacements to small stimuli was used to estimate the stiffness of the IHC bundles before and after mechanical overstimulation with fluid-jet, as well as before and after breaking the tip-links with BAPTA-buffered Ca^{2+}-free media. We overstimulated the IHCs in a small, demarcated region of the explant. The unstimulated IHCs near that region served as undamaged controls. Explants were then fixed immediately, or after 24 hours at 37°C. After fixation, the samples were processed for scanning (SEM) and transmission (TEM) electron microscopy.

Results
Overstimulation with a fluid-jet caused increased displacements of stereocilia bundles to small mechanical stimuli, indicating a decrease in stiffness. After 24 hours at 37°C, the stiffness of IHC bundles showed significant recovery. Treatment with BAPTA did not alter bundle stiffness in young postnatal IHCs, indicating that decreased stiffness of the overstimulated hair bundles is not due to tip-link damage. Further, only a small decrease in the number of intact tip-links in overstimulated versus unstimulated IHC bundles was seen with SEM. TEM examination of the explants immediately after overstimulation revealed sub-micron breaks in the actin core of overstimulated IHC stereocilia which were not found in the unstimulated control IHC stereocilia. Additionally, after 24 hours of recovery, the actin core of overstimulated stereocilia showed no breaks but displayed some small areas with reduced actin filament density. These areas were not present in the unstimulated control IHCs.

Conclusion
The loss and recovery of IHC bundle stiffness after mechanical overstimulation occur due to sub-micron breaks in the actin filaments near the base of the stereocilia and their subsequent repair.

Funding
Supported by NIDCD/NIH (R01DC008861, R01DC014658)

PS 85

Generation of inner ear hair cells in vitro from mouse embryonic stem cells

Geping Wu
The first people hospital of ZhangJiaGang city

Background
Embryonic stem cells (ESCs) are key tools for genetic engineering and development of stem cell-based therapies. The investigation of ESCs pluripotency and early lineage commitment is an essential precondition for its translational use. In this study, we explored the ability of mouse ESC to differentiate into inner ear hair cell lineages. Method: Mouse embryonic stem cells (E14TG2A) were cultured on primary embryonic mouse fibroblasts (PMEF), and induced by successive steps with EGF and IGF-1 for 10 days to establish the formation of embryoid bodies (EBs), and then treated with bFGF for 8 days to induce potential inner ear hair cells. Results: Quantitative real-time PCR and immunofluorescence analysis were performed, which demonstrated that presence and significant increased expression of the specific biomarkers for inner ear hair cells, Espin, myosin VIIa, Math1,

α9 AchR proteins in the induced lineages. Conclusion: Our study provided the evidences that mESCs can be driven to express key genes in the development of inner ear hair cells and thereby promotes their status as candidate for regenerative therapies.

PS 86

Using Hearing in Noise Measures for Detecting Hidden Cochlear Damage

Edward Lobarinas[1]; Angela Fulbright[2]; Dalian Ding[3]; Colleen Le Prell[1]

[1]University of Texas at Dallas; [2]University of Florida; [3]State University of New York at Buffalo

The ability to hear in the presence of background noise can be substantially poorer than would be predicted by threshold measures for both the hearing impaired and those with normal threshold sensitivity. Here, we evaluated the effects of selective inner hair cell (IHC) damage on hearing in noise measures in carboplatin treated chinchillas. Nine chinchillas were trained to avoid a brief foot shock by breaking a photobeam when toneburst stimuli were presented in quiet or in competing noise. Prior to carboplatin treatment, thresholds (250-11,300 Hz) in quiet ranged from 2-8 dB SPL, thresholds in 50 dB SPL broadband noise (BBN) ranged from 30-38 dB, and thresholds in 70 dB SPL narrow band noise (NBN) centered at 500, 2000, and 4000 Hz varied as a function of the center frequency. Subjects were then treated with a single dose of 75 mg/kg carboplatin that produced a mean IHC loss of 64% with no evidence of outer hair cell loss. Following carboplatin treatment, thresholds in quiet remained unchanged whereas thresholds in BBN increased by 6-12 dB. Under the more intense NBN, thresholds increased at the center frequency and increased to an even greater extent at frequencies distal to the NBN masker, suggesting off-frequency listening deficits. The increases at both the high and low frequency tails of the NBN function ranged from 10 to as high as 15 dB. These studies suggest that substantial damage to IHC that does not produce any change in the audiogram can nonetheless result in substantially poorer thresholds in competing noise. Importantly, the presence of NBN at high intensities resulted in disproportionately poorer off-frequency hearing than would be predicted given the lack of changes in hearing sensitivity in quiet.

The difficulties observed with IHC loss here in chinchilla are consistent with suggestions that IHC/auditory nerve pathology may underlie human hearing in noise difficulties. However, the point at which functional deficits begin in chinchillas, and more importantly in humans, remain unknown. Additional studies are needed to determine if smaller IHC losses or other forms of deafferentation result in detectable functional deficits.

Funding

This study was funded by NIH-NIDCD 5 R03 DC011612-04 to E. Lobarinas.

PS 87

DNA demethylation stimulates human inner ear stem/progenitor cells differentiate into hair-like cells

Zhengqing Hu; Yang Zhou

Wayne State University

Background

Mammalian inner ear hair cells lack the ability of regeneration after damage. Recent studies suggest stem cell therapy is a possible approach for sensory hair cell replacement. Epigenetic modification, including DNA methylation and demethylaion, is a common method to regulate gene expression in various cell lines. 5-azacytidine (5-aza), a DNA methyltransferase (DNMT) inhibitor, is able to cause genomic DNA demethylation and regulate gene expression. Our previous studies suggested DNA demethylation can stimulate mouse inner ear stem cell to differentiate into sensory hair-like cells. However, it is unclear whether DNA demethylation is able to induce human inner ear stem/progenitor cells to differentiate into hair cells.

Aim

To investigate whether 5-aza induced DNA demethylation is able to regulate gene expression in human inner ear stem/progenitor cells and induce cell differentiation into sensory hair cells.

Methods: 5-aza was applied to human utricular sensory epithelial stem/progenitor cells (HUCs) for 5 days. Quantification of genomic methylated cytosine (5-mC%) of control and treated HUCs were measured to describe the methylation status. Gene expressions of DNMT1 and sensory hair cell gene were detected by reverse transcription PCR (RT-PCR) and real time quantitative PCR (quantitative PCR), whereas protein expression changes were tested by immunofluorescence. To investigate whether the gene expression change was caused by DNA demethylation, Nested methylation specific PCR (Nested-MSP) was performed.

Results

After 5-aza treatment, the 5-mC% was decreased from 0.45% ± 0.03% to 0.35% ± 0.03%. The expression of DNMT1 was remarkable decreased in treated HUCs. In addition, expressions of sensory hair cell gene including MYO7A and POU4F3 were significantly increased in both gene and protein levels. Nested-MSP demonstrated that up-regulation of sensory hair cell genes MYO7A and POU4F3 was induced by DNA demethylation.

Conclusion

These results reveal that genome-wide DNA demethylation can up-regulate sensory hair cell gene expression in human inner ear stem cells, which subsequently stimulates HUCs to possess a sensory hair-like cell fate. Our study provides an evidence for stem cell differentiation via epigenetic modification approach. Moreover, the results of this human stem cell study open avenues to develop human hair cell regeneration strategies for future clinical trials.

Funding
R01 NIDCD/NIH

PS 88

Transplanted H9-GFP stem cells survive in scala media of conditioned guinea pig cochlea

Min Young Lee; Sandra Hackelberg; Kari Green; Kelly Lunghamer; Takaomi Kurioka; R. Keith Duncan; Yehoash Raphael
Kresge Hearing Research Institute, University of Michigan

Background
Hair cells (HCs) in the mature mammalian cochlea are not spontaneously replaced once lost. One novel approach for restoring HCs and hearing in ears depleted of HCs is stem cell therapy. When cells are transplanted into scala media, they promptly die due to the high concentration of potassium in the endolymph. We previously designed a method for "conditioning" the scala media to make it more hospitable to implanted cells, and have shown that HeLa cells could survive for up to a week using this method. Here, we evaluated the survival of human embryonic stem cells (hESC) in deaf guinea pig cochleae that were conditioned to optimize survival of exogenous cells.

Materials and Methods
A modified hESC line (H9 Cre-Lox, WiCell Research Institute) was used for transplantation. In these cells, a floxed GFP transgene is constitutively expressed, sustained during differentiation, and suitable for tracing human cells in xenografts. Six guinea pigs were used for the transplantation surgery. The animals were deafened 1 to 4 weeks prior to surgery by infusing neomycin (10%) into the scala tympani. Just before stem cell transplantation, the animals were treated with the loop diuretic, furosemide, to block pumps in the stria vascularis, and endolymph was flushed with artificial perilymph (N=2) or stem cell media (N=4). Dissociated H9 cells, in the presence of ROCK inhibitor (Y-27632), were directly injected into scala media via cochleostomy (2^{nd} and 3^{rd} turn). Animals were sacrificed at 6 or 24 hours after the transplantation surgery and cochleae were harvested and stained with phalloidin (red) aid orienting the tissue. Epifluorescence microscopy was used to detect GFP-positive stem cells and determine their location in the tissue.

Results
Prior to implantation, the stem cells in the dish appeared round with bright GFP epifluorescence. Cochlea transplanted with stem cells had no surviving HCs but did have numerous GFP-expressing hESCs in the auditory epithelium. Stem cells were also visible in the lateral wall and spiral limbus area. GFP-positive cells appeared spherical or irregularly-shaped, and some were aggregated. GFP positive cells were found at 6 and 24 hours after surgery, with fewer positive cells at 24 hours. Irrigation with artificial perilymph and stem cell media yielded similar results.

Conclusion
Transplanted H9-GFP stem cells in to the cochlea can survive for at least 24 hours after pre-conditioning.

Funding
Supported by NIH/NIDCD grants R21-DC011631 and P30-DC05188.

PS 89

Innervation Patterns of Single Medial Olivocochlear Axons in the Cochlea

M. Christian Brown
Harvard Medical School

Background
Medial olivocochlear (MOC) neurons provide an efferent innervation to outer hair cells (OHCs), but the pattern of innervation of single axons onto the cochlea is incompletely known. Differences between activation of the OC reflex in response to ipsilateral vs. contralateral sound have been demonstrated (Lilaonitkul and Guinan, 2009) but the underlying anatomical and physiological mechanisms causing these differences have not been demonstrated. This study documents the innervation patterns of single axons of known characteristic frequency (CF) and response class (Ipsi, Contra, or Either Ear units).

Methods
In anesthetized guinea pigs, recordings were made using "sharp" electrodes and CFs were obtained from the unit's tuning curves. After physiological characterization, units were labeled with biocytin or in a few cases with horseradish peroxidase. Anatomical measures were obtained from examination of surface preparations of the cochlea.

Results
Labeled MOC axons (n=32) had a broad distribution of CFs (1.16 – 16.7 kHz). There was a large variability in the total numbers of OHCs innervated per axon (14 – 69), but high-CF axons tended to innervate lower numbers than low-CF axons. Each axon showed a "patchy" pattern with patches of OHCs innervated spaced by uninnervated regions. However, the sizes of the patches and the uninnervated regions were variable and did not show clear trends with CF or response class. The span of innervation (from the basalmost to apicalmost innervated OHC) for Contra units was significantly longer than for Ipsi units. The basalmost portion of the MOC innervation may be most closely associated with OHCs involved in the cochlear amplifier (since those OHCs are offset basally from the CF position). However, the basalmost portions of MOC innervation did not always preferentially innervate OHCs in row 1, which is the row thought to provide the most important contribution to the amplifier.

Conclusions
MOC axons showed large variability in the examined measures of innervation, with so far no consistent differences between Ipsi and Contra axons except that the latter had larger spans of innervation.

Funding
NIDCD grant 01089

PS 90

Contribution of Synaptic, Cisternal & Voltage-Gated Calcium to SK Channel Activation at the Efferent-Inner Hair Cell Synapse

Stephen Zachary; Paul Fuchs
Johns Hopkins School of Medicine

Background

Before postnatal day 14, cholinergic olivocochlear efferent neurons form synapses with inner hair cells (IHCs). Acetylcholine released from efferent terminals activates postsynaptic nicotinic acetylcholine receptors (nAChRs), which flux calcium into the IHC. Calcium entry leads to inhibition via the activation of small conductance calcium-activated (SK) potassium channels.

A feature of olivocochlear synapses is a postsynaptic cistern aligned with the efferent terminal. This structure has been thought to serve as a calcium store or sink, possibly in a manner that influences the extent of SK channel gating and therefore the strength of inhibition. Additionally, calcium entry through voltage-gated channels may contribute to the local calcium signal at the efferent-hair cell synapse. However, the manner in which synaptic calcium signals (through nAChRs), cisternal calcium, and voltage-gated calcium interact at the efferent synapse is not known.

Methods

We performed whole-cell patch clamp recordings from P7-10 rat IHCs in voltage clamp mode, using electrical stimulation to evoke release from efferent terminals. Evoked and spontaneous IPSC waveforms were analyzed.

Results

Stimulation in normal external solution evoked characteristic outward IPSCs at -60mV with an average decay time constant of 48.7 ms. At -20mV, stimulation produced outward events that were longer, decaying with an average time constant of 68.4 ms ($p<0.0001$), with many events having decay time constants over 100 ms. SK channels mediate these events at -20mV, as they were blocked by 400 nM apamin. To assess the contribution of voltage-gated calcium signals, we performed recordings in 10 µM nimodipine, which reduced IPSC amplitudes at -60mV and nearly abolished IPSCs at -20mV. Ryanodine (200 µM), which blocks calcium induced calcium release (CICR) from stores, had a similar effect. In both drug conditions and holding potentials, IHCs were still responsive to exogenously applied acetylcholine, suggesting that synaptic calcium signals through nAChRs were unaffected.

Conclusion

Synaptic, cisternal, and voltage-gated calcium can interact to mediate the gating of SK channels in response to efferent transmitter release. At -60 mV, synaptic calcium is sufficient to gate SK channels, but the strength of efferent inhibition is reduced without voltage-gated calcium and CICR. At -20 mV, voltage-gated calcium influx and release from internal stores play a larger role in SK channel gating.

Funding

NIDCD RO1 DC001508, T32 DC000023, P30 DC005211, F31 DC014184

PS 91

Connectivity of Dopaminergic Input to the Inner Ear and Hindbrain Auditory Efferent System of a Vocal Teleost

Jonathan Perelmuter[1]; Paul Forlano[1,2]
[1]Graduate Center, City University of New York; [2]Brooklyn College

Background

The natural biological function of dopaminergic innervation of the inner ear and its role in normal auditory processing and behavior remains unknown. The midshipman fish, *Porichthys notatus*, is an excellent model system for investigating the neural substrates of socio-acoustic communication, with well delineated auditory and dopaminergic circuitry that share homologies with other vertebrates. Females undergo a seasonal and steroid-dependent enhancement of hearing sensitivity, which facilitates detection and localization of males during the summer breeding season. Recently, we demonstrated that dopaminergic innervation of the midshipman inner ear changes seasonally, and that playbacks of male calls activate dopaminergic neurons in the cell group that project to the ear. We also observed catecholaminergic (CA) fibers surrounding the somata and dendrites of the hindbrain octavolateral efferent nucleus (OE), a major source of central cholinergic input to the inner ear. In the present study we used immunocytochemistry combined with electron microscopy to investigate the fine structure of CA innervation of the saccule and the OE.

Methods

The source of CA innervation of the OE was determined by DiI tract-tracing combined with immunofluorescence for tyrosine hydroxylase (TH), an enzyme marker for CA neurons, and colocalization was examined by confocal microscopy. To examine the fine structure of CA innervation, fixed saccular maculae and sections containing the OE were immunostained for TH, embedded in Epon resin, and serial ultrathin sections (60-70 nm) were examined with a transmission electron microscope.

Results

DiI filled, TH-immunoreactive (TH-ir) cells were found in the periventricular posterior tuberal nucleus (TPp), the same dopaminergic nucleus that projects to the saccule. In the saccule, TH-ir profiles containing synaptic vesicles were found in proximity to efferent and afferent synapses at the base of hair cells and interspersed between support cells and nerve processes. TH-ir profiles were not observed to form traditional synapses. In the OE, vesiculated TH-ir profiles were found in direct contact with somata and also made axoaxonic contact with unstained profiles synapsing on somata and dendrites.

Conclusion

Innervation of both the saccule and OE from the TPp points to coordinated dopaminergic modulation of peripheral auditory

processing. The lack of synaptic specializations in TH-ir profiles in the saccule is consistent with volume transmission of dopamine, with the potential to influence both afferent and efferent synapses. The variety of TH-ir profile morphologies in the OE suggests divergent mechanisms of modulation of the inner ear and the cholinergic efferent system by dopamine.

Funding
NIH Grant SC2DA034996, PSCCUNY Grant 6565000 43

PS 92

Developmental changes in CGRP and AChE expression in cochlear efferents in development of the rat cochlea

Dalian Ding; Kun Yang; Richard Salvi
University at Buffalo

The lateral olivocochlear (LOC) and medial olivocochlear (MOC) efferent neurons, which innervate afferent neurons beneath the inner hair cells (IHC) and outer hair cells (OHC), originate from within/around the lateral and medial superior olive respectively. The efferent neurons and fibers express the neurotransmitter acetylcholine (ACh) and calcitonin gene related peptide (CGRP), involved with vasodilation and pain. ACh and CGRP colocalize to LOC, but some MOC neurons seem to express ACh and CGRP. The efferent innervation of the cochlea changes during maturation and developmental changes in the spatiotemporal pattern of CGRP and ACh expression is poorly understood. To address this issue, we studied the pattern of CGRP and acetylcholinesterase (AChE) immunolabeling in the cochlea of postnatal (p3-15) and 4 months old rats. We found little evidence of CGRP and AChE immunolabeling in the organ of Corti until p15 at which time AChE was expressed in both the inner spiral bundles beneath the IHC and tunnel spiral bundles crossing the tunnel of Corti to the OHC. In contrast, CGRP was almost exclusively expressed in the efferent nerve endings of inner spiral bundle, but not in the tunnel spiral bundles. The presence of CGRP in the inner spiral bundle beneath the IHC leads to speculation that very high intensity sounds may trigger the release of CGRP from LOC terminals sufficient to reach the acoustic threshold of pain.

PS 93

Multivesicular Release of Glutamate Activates More AMPA Receptors with Higher Open Probability at the Hair Cell Ribbon Synapses

Fuu-Jiun Hwang; Daniil Frolov; Geng-Lin Li
University of Massachusetts Amherst

Multivesicular release (MVR), the simultaneous release of two or more synaptic vesicles from a single release site, results in higher concentration of neurotransmitter in the synaptic cleft when compared to single vesicle releases. While MVR has become a hallmark of the hair cell ribbon synapses, it is unknown how differently the higher concentration of glutamate would act upon postsynaptic AMPA receptors. In this study, we recorded spontaneous excitatory postsynaptic currents (EPSCs) from auditory afferent fibers in the bullfrog amphibian papilla, which have been previously shown to consist of both quantal and multiquantal events from single ribbon synapses, and performed non-stationary noise analysis to estimate the number of postsynaptic AMPA receptors ($N_{receptor}$) and the maximum open probability (P_m). For single vesicle releases (~50 pA), we estimated $N_{receptor}$ to be 79 and P_m to be 0.69. For MVR of two quanta (~100 pA), $N_{receptor}$ remains unchanged but P_m is increased to 0.85. For MVR of four quanta (~200 pA), $N_{receptor}$ is increased to 170 but P_m stays the same as MVR of two quanta. In a separate set of experiments, we applied 0.5 mM kainic acid, a non-desensitizing agonist for AMPA receptors, to auditory afferent fibers and performed stationary noise analysis on the resulting current responses, which yielded a total $N_{receptor}$ of ~7,000 per fiber. Given that each auditory afferent fiber makes ~35 ribbon contacts with a single hair cell (Graydon et al, 2011), we estimated an $N_{receptor}$ of ~200 per ribbon contact. This argues that MVR of more than 200 pA is likely due to spillover of glutamate to neighboring ribbon contacts. Consistent with this finding, spontaneous EPSCs of more than 300 pA are significantly slower in the rise time. In addition, the ratio of two adjacent EPSCs ($EPSC_{n+1}/EPSC_n$) is significantly smaller when they overlap significantly (i.e., with an interval of less than 1 ms), suggesting that AMPA receptors are likely to be shared between neighboring ribbon contacts. Taken together, we conclude that the higher concentration of glutamate from MVR in hair cells reaches more postsynaptic AMPA receptors in auditory afferent fibers and activates them with higher open probability.

Funding
This study was supported by a NIH/NIDCD R00 award (DC010198) and a university startup to G.-L. L.

PS 94

The Spike Generator of the Auditory Nerve Matures Anatomically After Hearing Onset

Mark Rutherford; Kyunghee Kim
Washington University in St. Louis

Sound localization and discrimination rely on precise temporal representation in the spike trains of auditory nerve fibers (ANFs). Precise temporal representation depends on reliable spike generation in each ANF peripheral axon. Here we examined the development of heminodal and nodal organization in the peripheral axons of auditory nerve fibers (ANFs) in the rat cochlea with immunohistochemistry and confocal microscopy. The scaffold protein Ankyrin-G, the nodal voltage-gated sodium channel $Na_V1.6$, and the paranodal contactin-associated protein Caspr emerged in a basal-to-apical gradient between postnatal days 5–7 (p5–7). These immature nodes presumably support action potentials, consistent with recordings of the auditory nerve-brainstem evoked response (ABR) by p7–8 in rats for bone conducted stimuli (Geal-Dor et al., 1993), and consistent with pre-sensory pattered electrical activity in ANFs that is necessary for development of the auditory brainstem (Tritsch and Bergles, 2010; Clause et al., 2014). Before the onset of acoustic hearing function, juxtaparanodes lacked the low-voltage activated $K_V1.1$. Because $K_V1.1$ may prevent

spike generation for slow depolarizations by enabling a dV/dT threshold, its absence in pre-hearing animals may allow the slower pre-sensory waveforms of synaptic transmission (Grant et al., 2010) to rigger spikes. External and middle-ear conductive immaturities disappear by p15; however, ANF threshold and synchrony improve through p30 (Geal-Dor et al., 1993). Presumably, continued development of unknown sensorineural mechanism(s) beyond p15 underlies this maturation of sound-response properties. With analysis of $Na_V1.6$ clusters in the distal osseous spiral lamina, we found that organization and alignment of the spike generator (i.e., the heminode) of ANFs continued until p25-30. Before hearing onset, nodal structures were evenly distributed along axons in the osseous spiral lamina. By p30, development of the first internodes appeared to be complete, most of the heminodes were centered within 10 µm of the habenula, and > 90% of heminodes were centered within 20 µm of the habenula. This alignment of spike generators at the habenula perforata couples them tightly to glutamatergic ribbon synapses only 20–40 µm away. This molecular-anatomical maturation of spike generators may underlie more precise spike-timing through reduction of temporal jitter within and among ANFs at sound onset and during periodic sounds. These results on ion channel localization may aid multicompartmental computational modeling of ANF responses to chemical transmission from hair cells or electrical stimulation by a cochlear implant.

Funding
This work was funded by an International Project Grant from Action on Hearing Loss to M.A.R. and startup funds from the Dept. of Otolaryngology at Washington University in St. Louis

PS 95

Independent component analysis recovers discrete cellular sources contributing to the electrical potential recorded at the round window.

Aryn Kamerer; Mark Chertoff
University of Kansas Medical Center

As medical and technological treatments for cochlear hearing loss become more available and sophisticated, there is a growing need for diagnostic techniques that can identify anatomical damage or dysfunction underlying a patient's hearing loss. The round-window cochlear response (CR) is an electrophysiologic signal comprised primarily of the cochlear microphonic: a reflection of current flow through outer hair cells (OHC), and an auditory nerve response. In our previous work in gerbils, we successfully used the CR to locate regions of OHC loss along the length of the cochlear partition, but found significant neural contamination to the response at 700 Hz. A follow-up study using near-infrasonic stimuli (45 Hz) yielded an atypical response waveform –uncharacteristic of OHCs yet highly consistent across animals –suggesting (an) additional cellular source(s) aside from OHC or auditory nerve. This study uses a blind source separation technique, independent component analysis (ICA), to separate the low-frequency CR into its distinct cellular sources.

The CR was recorded from an electrode on the round window of Mongolian gerbils to a 45 Hz tone burst embedded in 18 high-pass filtered noise conditions. Multiple trials were recorded for each animal at each noise condition, targeting apical to basal regions along the cochlear partition. The animals' trials at each condition served as a mixture, or linear combination of signals from multiple cellular contributors, which ICA used to recover statistically independent source signals. Using the estimated mixing coefficients from ICA, we compared the relative contribution of each cellular source of the CR at a particular region of the cochlear partition.

We thus conclude that ICA shows promise as a technique to recover distinct cellular source signals buried within the CR. An accompanying model combined with our previous data and existing literature, provide evidence that inner hair cell, as well as OHC and phase-locked auditory nerve potentials, are the primary sources of the low-frequency CR, and their relative contributions change as a function of location along the cochlear partition.

Funding
Supported by NIH R33DC011096

PS 96

Contributions of Inner and Outer Hair Cells and the Auditory Nerve to the Summating Potential Recorded at the Round Window

Andrew Pappa[1]; William Scott[1]; Kevin Fox[2]; Tatyana Fontenot[1]; Maheer Masood[1]; Ken Hutson[1]; Doug Fitzpatrick[1]
[1]University of North Carolina at Chapel Hill; [2]Campbell University

The summating potential (SP) to tones is a DC baseline shift that persists for the duration of the tone, corresponding to the envelope of the stimulus. Although the SP has been studied for many years, its sources are still poorly understood and controversial. Long considered to be produced by hair cells, particularly inner hair cells (IHCs), several studies show a neural contribution as well. In order to parse out these individual effects, cochlear recordings in Mongolian gerbils were performed following isolation of hair cell and neural contributions via exposure to ototoxic and neurotoxic chemicals.

An SP from hair cells can be produced from at least two mechanisms: 1) asymmetry in the operating point of the cochlear microphonic (CM) so that even harmonics, including DC, are produced and 2) high pass-filtering by hair cells that generate sustained currents from membrane capacitances. The first of these is expected to be associated primarily with outer hair cells (OHCs), and the second with IHCs. To separate OHC from IHC responses, gerbils were injected with varying doses of kanamycin (200-400 mg/kg, sc) followed 20 minutes later by furosemide (50-100 mg/kg, ip). The goal was to produce a model with absent or minimal OHCs and preserved IHCs. After 1 week, recordings were made before and after application of kainic acid (KA) to the round window niche to remove neural responses. Control animals received sham injections of vehicle only, here pre-KA recordings

correspond to normal hearing and post-KA recordings isolate total hair cell responses. After the recording session, animals were sacrificed and the cochleae harvested for hair cell counts.

Histology confirmed that different kanamycin/furosemide combinations removed some or all OHCs while leaving some or most IHCs. During ECochG, in the experimental group, a loss of asymmetry was seen upon onset of the SP, confirming that the contribution from OHCs was minimal or absent. After KA the change in the SP in both experimental and control groups was consistent with the removal of a neural contribution having a positive polarity. A substantial SP remained even after complete loss of OHCs and after KA, leaving IHCs as the only remaining source.

These studies reveal that by using the synergistic effects of kanamycin and furosemide, varying doses result in differential loss of OHCs and IHCs. The recordings show that both OHCs and IHCs, as well as neural activity, contribute to the SP recorded to tones.

Funding
NIH Grant 5 T32 DC 5360-12, MED-EL Coproration

PS 97

Direct Evidence of the Basilar Membrane Travelling Wave and Frequency-place Encoding of Sound in Humans

Stephen O'Leary; Luke Campbell; David Sly; Claire Iseli
University of Melbourne

The concept of the "travelling wave" was introduced by von Bekesy. The delay of sound travelling from the basal to apex of the cochlea has been measured in vivo by *indirect* methods from evoked, frequency-specific auditory responses such as brainstem responses (ABR) or extracochlear electrocochleography, usually by masking with high pass-filtered noise. Basilar membrane travelling wave characteristics have also been studied using otoacoustic emission delays and psychoacoustic experiments, which have reported velocities similar to ABR/OAE measures.

Recent advances in cochlear implant technology now allow high quality electrical recordings to be made from the implanted electrodes, and the retention of significant residual hearing is now possible. This means that for the first time we can *directly* measure components of auditory physiology in vivo. Here we used intracochlear electrocochleography measured from 10 electrodes spaced along the cochlea, to report the first human in vivo data directly demonstrating the travelling wave and place specific tonotopic tuning of the cochlea. These recordings were made from an adult with auditory neuropathy and significant residual hearing during cochlear implantation. The amplitude, latency and phase characteristics of the cochlear microphonic were recorded across the electrode array in response to fixed acoustic stimuli (500,1000,2000 Hz pure tones) and from these recordings the travelling wave was inferred. The position of the intracochlear electrodes was estimated from a post-operative cone-beam CT scan of the implanted cochlea.

As anticipated from von Bekesy's work, the amplitude of the wave grows as it travels up the cochlea until the point of resonance is reached, after which the amplitude rapidly diminishes as the wave moves more apically. Mean response latencies at the most basal electrode (radiologic 15 kHz region) and the tip electrode (radiologic 1 kHz region) were 0.6 and 3.1 ms respectively. Place specific encoding is best illustrated by the summating potentials, which present as a large voltage offset at the cochlear resonance point.

These recordings provide direct evidence for the basilar membrane travelling wave and frequency-specific encoding of sound. Delays measured here in the basal cochlea approximate those from other studies. The 1 kHz delay is 0.4 ms shorter than that expected in normal hearing. Some subjects with sensorineural hearing demonstrate shortened, low-frequency cochlea delays in the range we have measured here. Part of the difference may be that our method better estimates wavefront delay independent of cochlea filter delay, and that filter delay is longer at lower frequencies.

Funding
Garnett Passe and Rodney Williams Memorial Foundation, Australia

PS 98

Cytoarchitecture of the Gerbil Organ of Corti from the Apex, Determined Using In Situ Two-Photon Imaging

Gaby Steiner; Joris Soons; Anthony Ricci; Sunil Puria
Stanford University

Background
The mechanical interactions between different cell types within the Organ of Corti (OoC) are hypothesized to play a critical role in cochlear function. These interactions are shaped by the three dimensional organization and orientation of cells in the OoC. Therefore, precise knowledge of the OoC cytoarchitecture across the full length and width of the cochlea is critical for developing mathematical models and general understanding of how cells within the mammalian OoC, particularly the outer hair cells (OHC) and their Deiter cell (DC) and phalangeal process (PhP) attachments, produce high sensitivity and frequency selectivity (Yoon et al., 2011 BPJ). Quantitative information on how the lengths and longitudinal angles of the OoC cytoachitecture vary throughout the cochlea has only been reported from the mTmG mouse, genetically engineered to have their cell membranes autofluoresce (Soons et al, 2015 JARO). This project aims to similarly provide quantitative data on the gerbil OoC cytoarchitecture from cochlear base to apex. Because no genetically engineered gerbils are available, the difficulty lies in finding ways to fluoresce the gerbil OoC without damaging the cells.

Methods
In-situ two-photon microscopy images (Prairie Technologies) of the gerbil OoC were obtained through a hole in the cochlear duct at the apex. Cochleae are collected from adult gerbils under a dissection microscope. The sample is kept in an external solution containing glucose and sodium chloride to delay cell death. After extracting the cochlea, a small hole is poked in the cochlear duct at the location of imaging. We aim to keep the Stria Vascularis intact throughout the dissection. The sample is stained in a solution containing a fluorescent probe needed for two-photon imaging. Using a transfer pipette, the dye solution is perfused through the round window. The cochlea is positioned in a semi-solid agar solution prior to imaging.

Results
While several different approaches were attempted, the best results to date have been with FM4-64, a yeast-based fluorescent probe, introduced through the round window. This particular dye stains cell membranes with red fluorescence optimally at 850 nm, allowing differentiation between different cell types in the OoC. Thus far, image stacks of the OoC were obtained at the apex in 8 gerbil cochleae. The OHC, DC, and PhP and their interconnections will be segmented using Amira and analyzed with custom MATLAB software. In the future, we also aim to collect measurements from the base and mid-turn locations.

Funding
This research was funded by NIH NIDCD grants R01 DC007910 (to SP), R01 DC003896 (to AJR), Core Grant P30 44992, and shared instrumentation grant NIHS-10RR027267-01 as well as Research Foundation Flanders(F-WO) and Belgian American Educational Foundation(BAEF) grants (to JS).

PS 99

Tonotopical Gradient of Circadian Gene Expression in the Mouse Cochlea

Vasiliki Basinou[1]; Renate Buijink[2]; Stephan Michel[2]; Gabriella Lundqvist[1]; Christopher Cederroth[1]; Barbara Canlon[1]
[1]Karolinska Institutet; [2]Leiden University Medical Center

Mammalian physiology and behavior is subjected to a circadian regulation. Organ specific circadian rhythms are controlled by self-sustained oscillators, the peripheral clocks. Their rhythmicity is orchestrated by the central clock, located in the hypothalamic suprachiasmatic nucleus (SCN). The recently discovered clock in the mouse cochlea has been shown to exhibit robust circadian rhythms of the clock protein PER2, as evidenced by real-time tracking of the bioluminescent luciferase reporter PER2::LUC (Meltser *et al*., 2014). The capacity to recover from a noise trauma in a temporal manner appears to be regulated though the diurnal control of neurotrophin activation (Meltser *et al*., 2014). To identify the cellular origin of the PER2 rhythms within the cochlea, we developed a preparation that enabled us to monitor the dynamics of PER2::LUC expression at the single-cell level, with bioluminescence imaging and the use of a cooled CCD camera. CCD imaging revealed rhythms originating from sensory (outer hair cells and inner hair cells) and neuronal (spiral ganglion) cell populations with three distinct phase correlations. Luminescence signals first appeared in the outer hair cells, then radially propagated to the inner hair cells and eventually spread to the spiral ganglion neurons. Further analysis revealed a longitudinal gradient of cell rhythms in the cochlea. The apical region of the cochlea (low-frequency area) showed a pronounced phase advance compared to the middle region (higher frequency area). Surgical removal of the cochlear apex that appeared to generate the ‘’prime’’ oscillations did not affect the cochlea PER2::LUC rhythms. This suggests that the apex is not the sole generator of the circadian rhythms, but the cochlea rather contains cellular networks that oscillate with different phases. This topographic synchronicity in the cochlear molecular clock is a novel finding that could be very important for the auditory function, considering the tonotopical properties of the hearing organ and its circadian sensitivity to noise trauma.

Meltser I, Cederroth CR, Basinou V, Savelyev S, Lundkvist GS, Canlon B. (2014) TrkB-mediated protection against circadian sensitivity to noise trauma in the murine cochlea. *Curr Biol.* 24(6):658-63

Funding
AFA Insurance Company, Swedish Medical Research Council, National Institute on Deafness and other Communication Disorders of the National Institutes of Health, National Research Foundation of Korea grant, Knut and Alice Wallenberg , Karolinska Institutet, Tysta Skolan, Hörselforskningsfonden, Lars Hiertas Minne, Magnus Bergvalls, Lee och Hans Österman and Wenner Gren Stiftelse.

PS 100

Hair cells with reduced otoferlin lack a superlinear capacitance response

Michael Schnee; Anthony Ricci
Stanford University

Sensory hair cell ribbon synapses respond to graded stimulation in a linear, indefatigable manner requiring that vesicle trafficking to synapses be rapid and non-rate limiting. The two sine technique for tracking membrane capacitance in real time was used to follow Cm changes in inner hair cells of the *pachanga* mouse in which otoferlin is strongly reduced. Otoferlin is a six- C_2 domain protein that is expressed in inner, outer and vestibular hair cells and is required for hair cell exocytosis. A defect in vesicle trafficking has been proposed to be the major defect in pachanga thus otoferlin may be involved in replenishment of synaptic vesicles[2]. The two sine method allows for Cm measurements during depolarization where membrane conductance is varying. Using this technique we previously characterized two components of release, a linear saturable response that varied with the Ca load and a second superlinear component that had a constant rate with a Ca dependent onset[1]. Patch clamp recordings of inner hairs cells from homozygous *pachanga* mice showed a lack of superlinear release despite having a normal first component or readily releasable pool (RRP). Total release was reduced

70% compared to wild type (WT) even though Ca^{2+} currents were significantly larger in *pachanga*. To account for the Cm changes in superlinear release in a normal inner hair cell requires Ca^{2+} dependent recruitment of synaptic vesicles from a reserve pool thus the lack of a superlinear response in pachanga is evidence for the importance of vesicle trafficking in generating the superlinear Cm response.

References

1. Schnee ME, Santos-Sacchi J, Castellano-Munoz M, Kong JH, Ricci AJ**.** Calcium-dependent synaptic vesicle trafficking underlies indefatigable release at the hair cell afferent fiber synapse. *Neuron* 70: 326–338, 2011.

2. Pangrsic et. al. Hearing requires otoferlin-dependent efficient replenishment of synaptic vesicles in hair cells. Nat. Neurosci. 13(7) 2010

Funding

This work was funded by NIDCD Grant DC009913 and core grant P30 44992.

PS 101

Nanoparticle CT Molecular Imaging for Inner Ear Application

Lee Brake[1]; **Daqing Li**[2]

[1]University of Pennsylvania; [2]University of Pennsylvania School of Medicine

Inner ear pathology is responsible for the majority of hearing and balance disorders. With current technology, it is quite difficult for inner ear structures to be functionally and morphologically evaluated in living humans and animals. This is largely due to the presence of quite complicated structures within a small, compact, and sealed compartment such as the inner ear. In recent years, advances have been made in determining the molecular genetic etiologies for inner ear disorders. The potential effective treatment of such inner ear diseases requires precise determination of inner ear pathology at a molecular level.

The current study aims to develop molecular imaging strategies that target specific structures in the inner ear of a mouse model for potential clinical application, especially in the diagnosis of inner ear disorders with varying molecular genetic etiologies. In an *in vitro* study, increased binding specificity was observed between gold nanoparticles conjugated with the A665 peptide and CHO cells expressing prestin, a protein found exclusively in the outer hair cells of the inner ear. With our novel inner ear delivery system, targeted spherical gold nanoparticles (GNPs) capable of binding to prestin were used for inner ear computerized tomography (CT) contrast. Using these GNPs, typically non-visualized structures of the inner ear were detected using a standard microCT machine (Scanco *vivaCT 40*). The results indicate that this approach is able to detect molecular genetic defects of inner ear structures such as prestin. Further investigation is warranted towards targeting different molecular genetic etiologies using corresponding molecular biomarkers. The clinical application of this approach will positively impact diagnosis and treatment strategies for inner ear diseases.

Funding

NIH Grant 1R01DC014464-01

PS 102

Intratympanic Iodine Contrast Injection Diffuses Across the Round Window Membrane Allowing for Perilymphatic CT Volume Acquisition Imaging

Nicholas Abt; Mohamed Lehar; Carolina Guajardo; Richard Penninger; Bryan Ward; Monica Pearl; John Carey

Johns Hopkins University

Background

Imaging of hydrops in the living human ear has attracted recent interest. Intratympanic (IT) injection has shown gadolinium's ability to diffuse through the round window membrane (RWM), enhancing the perilymphatic space. Whether the RWM is permeable to iodine-based contrast agents (IBCA) is unknown; therefore, our goal was to determine if IBCAs could diffuse through the RWM using CT volume acquisition imaging.

Methods

Four unfixed human cadaver temporal bones underwent intratympanic IBCA injection using three sequentially studied methods. The first method was direct IT injection. The second method used direct RWM visualization via tympanomeatal flap for IBCA-soaked absorbable gelatin pledget placement. In the third method, the middle ear was filled with contrast after flap elevation. Volume acquisition CT images were obtained immediately post-exposure, and at 1, 6, and 24 hour intervals. Post-processing was accomplished using color ramping and subtraction imaging.

Results

Following the third method, positive RWM and perilymphatic enhancement were seen with endolymph sparing. Gray scale and color ramp multiplanar reconstructions displayed increased signal within the cochlea compared to pre-contrast imaging. The cochlea was measured for attenuation differences compared to pure water, revealing a pre-injection average of -1,103 HU and a post-injection average of 338 HU. Subtraction imaging shows enhancement remaining within the cochlear space, Eustachian tube, middle ear epithelial lining, and mastoid.

Conclusions

Iohexol iodine contrast is able to diffuse across the RWM. Volume acquisition CT imaging was able to detect perilymphatic enhancement at 0.5mm slice thickness. The clinical application of IBCA IT injection appears promising but requires further safety studies.

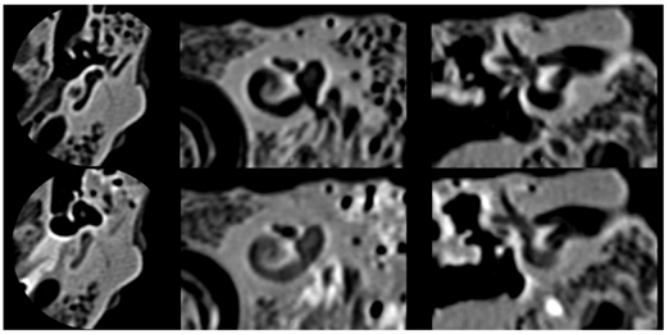

Figure 1. A human cadaver temporal bone represented as a multiplanar reconstruction of the volume acquisition CT. TOP ROW: Contains from left to right axial, oblique, and coronal sections pre-contrast injection. BOTTOM ROW: Post-contrast images with analogous sections as top row. Of note, the post-contrast imaging displays attenuation and enhancement within the cochlea. The Eustachian tube, middle ear epithelial lining, and mastoid air cells also contain contrast.

Figure 2. The images represent the same multiplanar CT slices as Figure 1, with color ramping for density mapping. The top row is pre-contrast and the bottom row is post-contrast injection.

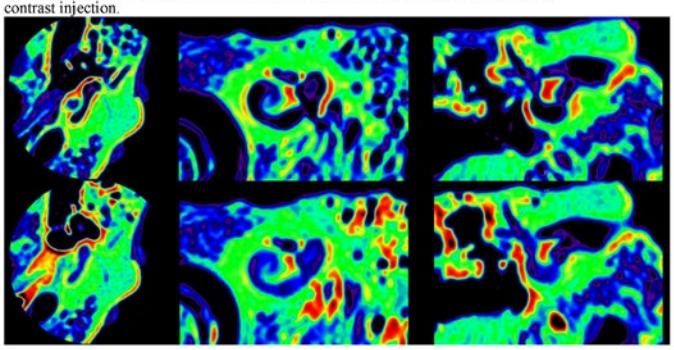

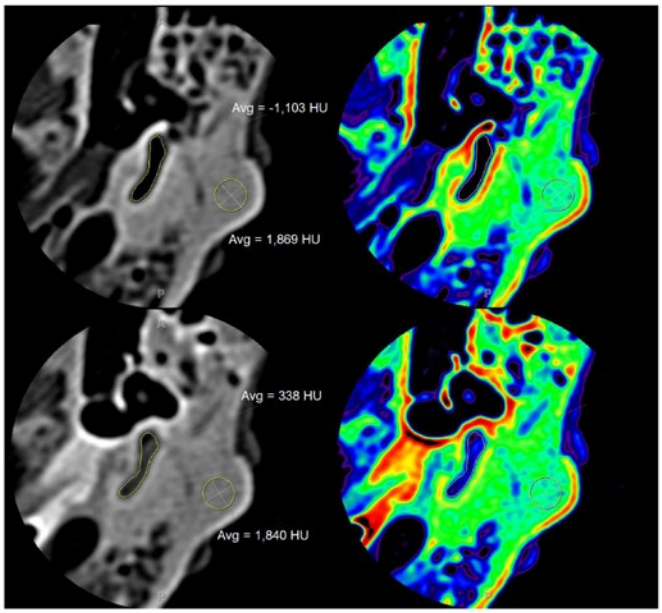

Figure 3. These images represent a 3.0x3.0cm view of the middle and inner ear. TOP ROW: Axial pre-contrast imaging with attenuation measured as average Hounsfield units (HU) within the cochlea. The attenuation averaged to -1,103 HU. BOTTOM ROW: Axial post-contrast imaging with average cochlear attenuation being 338 HU. Attenuation was also measured at the same spot within the bone marrow. The pre-contrast marrow measured 1,869HU with the post-contrast measuring 1,840HU. The Eustachian tube measured an average of 35 HU in 0.44cm^2 pre-contrast and an average of 3,157 HU in 0.42cm^2 post-contrast.

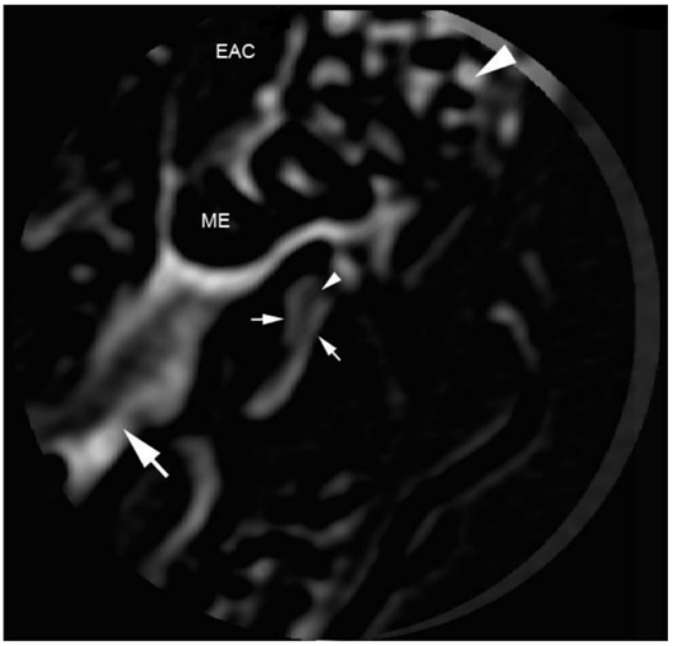

Figure 4. The post-contrast data was subtracted from the pre-contrast data, yielding this image. The cochlea can be seen with the small arrows and arrowhead. The small arrows point to the enhancing perilymphatic space while the small arrowhead shows the endolymph. The Eustachian tube (large arrow), mastoid air cells (large arrowhead), and middle ear epithelial lining have contrast media causing attenuation. EAC: external auditory canal, ME: middle ear.

Funding

Funding for temporal bone purchase from the Maryland State Anatomy Board was provided by the Center for Hearing and Balance Core Center at the Johns Hopkins University School of Medicine.

PS 103

Super-photostable GFP variant for superresolution imaging

Sheng Zhong; Dhasakumar Navaratnam; Joseph Santos-Sacchi

Yale University

Fluorescent proteins (FPs) have widespread uses in cell biology. However, the practical applications of FPs are significantly limited due to their rapid photobleaching and misfolding when fused to target proteins. Using a combination of novel and known mutations to eGFP, we developed a well folded photostable variant, SiriusGFP. It shows a 5 fold increase in photostability compared to the commonly used eGFP variant and folds well when fused to the N and C termini of cytoplasmic and membrane proteins. Using fusions to the mitochondrial outer membrane protein OMP25, we demonstrate its utility with marked improvements in resolution and image quality with SIM superresolution microscopy and in continuous confocal imaging in time and space (4D confocal). We also explore photobleaching mechanisms of this GFP variant by differing intensities of excitation light and its susceptibilities to oxidation. The location of these mutations raise important questions regarding the mechanisms of photobleaching. We propose to use GFP-Sirrius to monitor mitochondrial behaviors in transgenic mouse model TFB1

that shows progressive hearing loss as a result of the mutation in mitochondrial DNA A1555G.

Funding
NIH NIDCD R01 DC000273 (JSS) R01 DC 007894 (JSS/DN)

PS 104

Clearing of the mouse temporal bone using a modified SeeDB protocol

Tomoko Makishima; Rebecca Cook; Beau Vandiver; Naoki Shimizu; Adrian Perachio
University of Texas Medical Branch

Background
Histological and anatomical studies of the mouse inner ear are technically difficult due to its small size and its location embedded in the temporal bone. A recently published protocol, SeeDB (*Nat Neurosci* 16:1154-1161, 2013), allows the clearing and the visualization of the whole brain in mice in a 3D fashion. Our goal was to modify the SeeDB protocol to achieve 3D visualization of inner ear organs encased in the temporal bone.

Methods
Temporal bones were dissected from mice at different ages from postnatal day 1 – 2 (P1-2) to 8 months. The SeeDB protocol was modified for the mouse temporal bone. The adult temporal bones were decalcified before starting the clearing process. The cartilaginous temporal bone of younger mice was processed directly without decalcification. Labeling was carried out in two methods: using hair cell-specific markers with fluorescent dyes, or using colorimetric Xgal labeling on genetically engineered LacZ expression strains. Then the samples were incubated in a series of fructose solutions with increasing concentrations. Samples were mounted in sucrose solution and viewed using light microscopy, fluorescent microscopy, confocal microscopy and two-photon microscopy. The images were reconstructed in 3D using Fiji software.

Results
Successful clearing of cartilaginous temporal bone and partial clearing of decalcified temporal bone was achieved. We were able to successfully reconstruct the 3D image of some of the inner ear auditory and vestibular organs including the cochlea, posterior crista ampullaris and saccule.

Conclusion
The modified version of the SeeDB protocol was low-cost using readily available materials. Using this protocol, we were able to clear and visualize mouse temporal bones at younger and older ages. We hope to further optimize the protocol for immunofluorescent labeling that is specific to the individual inner ear cell populations.

Funding
K08DC011540 The University of Texas System Neuroscience and Neurotechnology Research Institute

PS 105

Spontaneous Calcium Transients in Interdental Cells of the Neonatal Mouse Cochlea

Thore Schade-Mann; Jutta Engel; Tobias Eckrich
Saarland University

Introduction
The tectorial membrane (TM) is essential for a normal hearing function. It is attached to the so-called spiral limbus and the sterocilia of the outer hair cells, stretching across the whole organ of Corti and spiraling along the longitudinal axis of the cochlea. It consists of collagens and glycoproteins (α- and β-tectorin and otogelin), the latter accounting for about 50% of TM material and exclusive to the inner ear. Mutations of these proteins not only lead to aberrant TM formation but also to severe hearing loss or deafness. During the first postnatal week, IDCs massively secrete TM proteins into the extracellular space. So far, little is known about the physiology of IDCs and about how they build up the TM.

Methods
Histological staining of cochlear cryosections with DAPI and live cell imaging of Corti explants using FM4-64 were used to get insight into the anatomy of IDCs in the spiral limbus. Ca^{2+} imaging experiments using the Ca^{2+} sensitive indicator Fluo-8 AM of acutely dissected organ of Corti explants at postnatal day 4-5 were performed. Whole cell patch-clamp recordings were used to characterize basic electrical properties of IDCs.

Results
In whole-mount preparations of the cochlear epithelium with the TM still attached, part of IDCs generated spontaneous Ca^{2+} transients at a low rate (≥1 event/10 min). However there were many IDCs in each specimen that did not exhibit activity within 10 min. Two principal types of spontaneous IDC Ca^{2+} transients were observed: a) single peaks with fast upstroke and decay and (b) longer, complex transients with double or multiple peaks. Applying 10 µM ATP evoked Ca^{2+} transients in all IDCs. Ca^{2+} transients were confined to single IDCs and did not spread to neighbouring cells, i.e. no intercellular propagation compared to Ca^{2+} waves in Koelliker's organ was observed between IDCs with or without ATP application. Whole cell voltage clamp recordings revealed a small membrane capacitance (5 - 7 pF) and a slow outward rectifier current in IDCs at the age of P3 - P9.

Conclusion
Spontaneous Ca^{2+} signals in IDCs were variable in shape and duration and were confined to individual IDCs. No wave-like propagation of Ca^{2+} signals was observed in IDCs, in contrast to intercellular Ca^{2+} waves in Koelliker's organ. The mechanisms behind the Ca^{2+} transients remain to be elucidated.

Funding
Supported by the DFG, SFB1027.

PS 106

Vesalius and the ear

Robert Ruben
Albert Einstein College of Medicine/ Montefiore Medical Center

Introduction: The publication De Humani Corporis Fabrica (The Fabric) in 1543 created a seismic change to the study of anatomy and to the practice of surgery. Vesalius wrote the text in ery stylistic Latin which, for many, was more than difficult to translate. The Fabrica has been called the most looked at and referenced but least read book. The arability of a new translation of the two editions allowed for the examination of how, if at all, did Vesalius' ideas about the ear develop over time?

Method

The text and illustrations concerning the anatomy of the ear in his two published editions, 1543 and 1555, of De Humani Corporis Fabrica and in marginalia, recently identified, in what is likely the author's copy of the second edition, that appear to anticipate a 3rd edition, never published were analyzed and compared. This study is based upon examination of the original editions in the New York Academy of Medicine, on the annotated English translations by D. H. Garrison and M. H. Hast (2013), and on Vivian Nutton's translation of Vesalius' marginalia concerning the ear in what is evidently Vesalius' own annotated copy of the 1555 edition. Vesalius' corrections and clarifications are noted and his final description is compared with current knowledge of the anatomy of the ear.

Results

Versalius's description of the ear and of hearing was not additive to existing knowledge with the exception of a more accurate description of the incus and the malleus. Galen's description of the labyrinth, fifth pair of cranial nerves and the styloidmastoid foramen are not noted in either of the two editions.

Discussion

Why does Vesalius's descriptions of the temporal bone, the styloidmastoid foramen and the 'filth' pair of cranial nerves omit these observations? He was aware of Galenic corpus as noted in his dedication to Charles the Fifth and in description of the cartilages of the pinnae. Versalius's quantal contribution specifically to the science of anatomy and science in general was that he only reported what he observed. He appears not to have seen the labyrinth nor explored the stylomastiod foramen. There are many other parts of the peripheral auditory system which are not noted. It was not until the 18th century that the stato acoustic facial nerve complex was identified and our present nomenclature was finalized in the 20th century.

PS 107

Deletion of Auxiliary Ca2+ Channel Subunit α2δ3 Affects Ca2+ Currents of Spiral Ganglion Neurons and Sizes of Auditory Nerve Fiber Terminals

Friederike Stephani[1]; Wenying Wang[2]; Stefan Münkner[1]; Jutta Engel[1]
[1]Saarland University; [2]University of Nevada

Introduction

Spiral ganglion neurons (SGNs) connect hair cells with central auditory neurons and therefore are indispensable for auditory signal transmission. Myelinated type I SGNs comprise 95% of all SGNs and make a precise 1 to 1 connection with inner hair cells. Proper function and morphology of auditory nerve fiber (ANF) synapses require the auxiliary Ca^{2+} channel subunit $\alpha_2\delta3$ (Pirone et al., J Neurosci 2014). To determine the role of $\alpha_2\delta3$ for SGNs, we analyzed Ca^{2+} currents in SGNs isolated from $\alpha_2\delta3^{+/+}$ and $\alpha_2\delta3^{-/-}$ mice. In addition we determined the effect of $\alpha_2\delta3$ deletion on ANF terminals.

Methods

Patch-clamp recordings of Ca^{2+} currents were performed on enzymatically dissociated SGNs isolated from neonatal (P5) or juvenile (P20) mice (cf. Lv et al., J Neurosci 2012). SGNs were cultured for 2-3 days. To label the active zones of ANF terminals, frozen brainstem sections were stained with anti-VGLUT1.

Results

Ca^{2+} currents of SGNs were isolated by blocking voltage-gated K^+ currents by TEA (30 mM), 4-AP (15 mM) and linopirdine (100 µM) in the bath and by 110 mM Cs^+ in the pipette solution. Large voltage-gated Na^+ currents were fully suppressed by extracellular NMDG (110 mM). L-type Ca^{2+} currents were blocked by superfusing SGNs with 10 µM nimodipine. The fraction of L-type Ca^{2+} currents was independent of the presence of $\alpha_2\delta3$. P/Q-type Ca^{2+} currents were blocked by superfusion with 1 µM ω-agatoxin IVA. $Ca_v2.1$ currents were not present in SGNs isolated from neonatal mice. In SGNs isolated from P20 $\alpha_2\delta3^{+/+}$ mice, $Ca_v2.1$ currents contributed 60% of the total Ca^{2+} current. Although total currents in mature SGN of $\alpha_2\delta3^{-/-}$ mice were similar to those of $\alpha_2\delta3^{+/+}$ mice, the fraction of $Ca_v2.1$ currents was reduced to only 20-30%. In brainstem sections of 20-day old mice, active zones of ANF terminals in the AVCN were labeled with anti-VGLUT1. The sizes of VGLUT1-positive boutons were significantly reduced in $\alpha_2\delta3^{-/-}$ mice.

Conclusion

Our data show that in P20 SGN, proper sizes of $Ca_v2.1$ Ca^{2+} currents required the presence of $\alpha_2\delta3$, whereas expression of L-type Ca^{2+} currents was independent of $\alpha_2\delta3$. The role of $\alpha_2\delta3$ for other Ca^{2+} current subtypes and for the sizes of ANF terminals in younger animals remains to be determined.

Funding

Supported by DFG-PP1608 (to JE).

PS 108

The Expression and Function of Connexin 43 in the Blood-Labyrinth-Barrier of the Stria Vascularis

Xiaohan Wang; Jing Cai; Xiaorui Shi
Oregon Health & Science University

Connexin 43 (Cx43) gap junctions are widely distributed in the central nervous and cardiac system, especially in the blood brain barrier (BBB). Cx43 mediates the exchange of ions, metabolites, and signaling molecules between cells under both physiological and pathological conditions. However, despite the importance of Cx43 in the BBB, not much attention has been given to the expression and function of Cx43 in the blood-labyrinth-barrier (BLB) of the stria vascularis. Using immunocytochemical techniques, we found Cx43 expressed in capillary endothelial cells (EC), perivascular resident macrophage-like melanocytes (PVM/Ms), and pericytes (PC) in adult C57/6 mouse cochlea. In particular, the PVM/Ms are extensively coupled to endothelium through Cx43 gap junctions. Suppression of Cx43 with small interfering RNA (*siRNA*) significantly increased hearing threshold and also caused the endocochlear potential (EP) to drop. Consistent with Cx43 expression *in vivo*, we found Cx43 expressed between ECs and ICs, ICs and ICs, ECs, and ECs, and PCs and PCs in the co-cultured cell line model. Using a patch clamp technique, we demonstrated that Alexa Fluor® 568 dye injected into PVM/Ms diffuses to neighboring ECs and ICs. The dye diffusion between PVM/Ms and ECs and between PVM/Ms and PCs was blocked when Cx43 was suppressed by siRNA. These results suggest the Cx43 mediates intracellular exchange between BLB component cells and may be important in integrating BLB function in the stria vascularis. Decreased expression of Cx43 may disrupt normal function of the strial BLB, attributing to Cx43 defect-induced hearing loss.

Funding
This work was supported by the National Institutes of Health grants NIH NIDCD R01-DC010844 (XS), DC R21DC1239801 (XS), and NIHP30-DC005983.

PS 109

Single-Cell RNA-Seq Analysis of Pre- and Postnatal Mouse Endolymphatic Sac

Keiji Honda[1]; Joseph Burns[1]; Michael Kelly[1]; Michael Hoa[1]; Matthew Kelley[1]; Philine Wangemann[2]; Robert Morell[1]; Andrew Griffith[1]
[1]National Institute on Deafness and Other Communication Disorders; [2]Kansas State University

Background
Mutations of the *SLC26A4* gene are a common cause of hearing loss associated with enlargement of the endolymphatic sac and duct and vestibular aqueduct (EVA). *SLC26A4* encodes a transmembrane anion exchanger, called pendrin, which is expressed in a subset of nonsensory epithelial cells in the cochlea, vestibular organs and endolymphatic sac (ES). Interestingly, for normal development and acquisition of hearing in mice, *Slc26a4* expression is required only in the ES and only between embryonic day 16.5 (E16.5) and postnatal day 2 (P2) (Choi et al., JCI. 2011; Li et al., PLOS genet. 2013). The physiological function of the ES is poorly understood but thought to involve homeostasis of endolymph. Histological analysis suggests that there are two major ES epithelial cell types: mitochondria-rich cells (MRCs) that express pendrin, and ribosome-rich cells (RRCs).

Objectives
(1) Obtain an unbiased classification of pre- and postnatal mouse ES epithelial cells based upon distinct mRNA expression signatures. (2) Generate and test hypotheses for ES epithelial development and function.

Methods
Suspensions of single cells were generated from C57BL/6J ES epithelium at E16.5 or P5. Cells were captured on a Fluidigm C1 microfluidic chip for lysis, reverse transcription, and PCR amplification. cDNA from each single cell was sequenced (RNA-seq on an Illumina HiSeq). Transcriptional profiles were analyzed using R softwares.

Results
Principal component analysis and hierarchical clustering of E16.5 and P5 data identified two major and several minor clusters of samples. The first major sample cluster was characterized by the expression of four genes (*Slc26a4*, *Foxi1*, *Atp6v0a4*, *Atp6v1b1*) known to be expressed in MRCs. Mutations of these four genes are known to cause EVA. This cluster also expressed many other genes encoding transporters, ion channels and pumps, and transcriptional regulators. The second major sample cluster was characterized by the absence of expression of the four MRC-specific genes and other genes encoding transporters or ion channels or pumps. This sample cluster may correspond to RRCs. A minor cluster in the P5 data featured a gene expression signature that overlapped with those of the two major clusters. Minor sample clusters in the E16.5 data featured gene expression signatures that include cell cycle and mitosis genes.

Conclusion
Single-cell RNA-seq provides an unbiased classification of endolymphatic sac epithelial cells. The results provide testable hypotheses for the molecular and cellular mechanisms of the development, structure and function of the ES epithelium.

Funding
This work was supported by NIH intramural research funds Z01-DC000059, Z01-DC000060 and Z01-DC000086. P.W. was supported by NIH grant R01-DC012151.

PS 110

No Relationship between Recreational Noise History and Performance on the Words-in-Noise (WIN) test in Normal Hearing Young Adults

Colleen Le Prell; Edward Lobarinas
University of Texas at Dallas

Background

Recent results from animal experiments have led to speculation that noise exposure may reduce hearing-in-noise performance even if it does not induce measurable permanent threshold changes. To evaluate whether noise exposure history was correlated with poorer hearing-in-noise, detailed noise histories were collected alongside threshold and supra-threshold measures. The dataset was analyzed to identify normal-hearing listeners with poorer than expected performance on a word-in-noise task in order to assess potential associations between noise history and word-in-noise performance. All study participants had a history of music player device use, and were exposed to other recreational sources of noise.

Method

Otoscopy, tympanometry, conventional pure-tone threshold audiometry (250-8000 Hz), distortion product otoacoustic emission (DPOAE) amplitude (F2=2-9 kHz, F1=35-55 dB SPL with F2 10-dB quieter than F1), and word-in-noise (WIN) test thresholds were measured in 70 participants between the ages of 18-27 years. Two participants were excluded from the current analysis due to thresholds that were greater than 25-dB HL at one or more frequencies. All participants completed detailed noise histories and listened to songs using a Nexus Asus tablet and eskuché on-ear headphones (13-20 songs per subject) to evaluate listening level preferences. A 30-sec sample at the preferred level for each individual song was measured using a Brüel and Kjær Type 4153 Artificial Ear Simulator and Pulse Spectrum Analyzer.

Results

Out of 68 subjects with thresholds within normal limits (<25 dB HL), 48 showed normal results on the WIN in both ears, 13 showed normal performance in one ear and mild deficits in the other ear, and 7 showed mild deficits in both ears. When ears were dichotomized as normal versus mild WIN deficits, there were no statistically significant differences in associated listening level, with approximately 1-dB difference between functional categories. Similarly, there were no significant differences in the total number of noise sources reported, with an average of 2.4 sources reported by participants in each WIN performance category. 7 of the 60 subjects reported having had a previous detectable temporary threshold shift; 6 out of 7 of those participants had normal WIN performance.

Conclusion

Music player use, total number of typical noise sources, and previous TTS history had no relationship with performance on the WIN test. The current study did not provide any evidence of deficits on a speech-in-noise task in normal hearing adults with a self-reported history of recreational noise exposure.

Funding

Data collection was funded by a contract from MaxSound to the University of Florida (PI: C. Le Prell).

PS 111

Modification of Histone H3 Lysine 9 in Noise-induced Hearing Loss and Cochlear Synaptopathy

Suhua Sha; Jun Chen; Haishan Long; Kayla Hill; Xianren Wang
Medical University of South Carolina

Background

Post-translational modification of histones is an important form of chromatin regulation. By altering the interactions of histones with DNA and nuclear proteins without changing the DNA sequence, local histone modifications impact the activation of gene transcription, including the transcription of genes related to stress response and cell fate. In this study, we investigated the effect of noise exposure on histone H3 lysine 9 acetylation (H3K9ac) and dimethylation (H3K9me2) in the inner ear of adult CBA/J mice.

Methods

CBA/J mice at age of 12 weeks were exposed to broadband noise (BBN) from 2–20 kHz for 2 hours at 98 dB SPL to induce permanent threshold shifts (PTS) with losses of outer hair cells (OHC) and inner hair cell (IHC) synaptic ribbons, but IHC maintained intact. Anti-H3K9ac, anti-H3K9me2, anti-HDAC1, 2, and 3, and anti-p300 antibodies were used on cochlear surface preparations and cryosections to determine the post-translational modifications of histones in the cochlea. Auditory thresholds were determined by auditory brainstem responses (ABRs). Sensory hair cells were quantified from surface preparations labeled with myosin VII and then stained with DAB. Treatments with the pharmacological inhibitors of HDAC, SAHA, and of methylation, BIX-01294, via intra-peritoneal injection were utilized to assess potential protective effects of inhibiting acetylation and methylation on noise-induced hearing loss (NIHL).

Results

Decreased H3K9ac was coupled with increased H3K9me2 in OHC nuclei in the basal region of the cochlear epithelium and marginal cells of the stria vascularis 1 h after 98 dB SPL noise exposure. Additionally, levels of histone deacetylase 2 (HDAC2) were increased, whereas HDAC1, HDAC3, and histone acetyltransferase (HAT) p300 were unchanged. Silencing HDAC2 with siRNA reduced its expression in OHCs, but did not attenuate noise-induced PTS. Treatment with the HDAC inhibitor SAHA diminished PTS-noise-induced p-JNK expression in OHCs, but only attenuated PTS at 16 kHz and marginally reduced OHC loss. Finally, inhibition of H3K9 methyltransferase G9a/GLP with its specific inhibitor BIX-01294 significantly attenuated noise-induced losses of OHCs and synaptic ribbons and prevented attenuation of wave I amplitudes and PTS.

Conclusions

These findings suggest that modification of histone H3 at lysine 9 is involved in the pathogenesis of NIHL. Pharmacological targeting of histone modification may afford a strategy for protection against NIHL and cochlear synaptopathy.

Funding

The research project described was supported by the grant R01 DC009222 from the National Institute on Deafness and Other Communication Disorders, National Institutes of Health.

PS 112

An ATP-purinergic receptor mediated gain control in active cochlear amplification and protection against noise stress

Ling Mei[1,2]; **Hong-Bo Zhao**[1]

[1]University of Kentucky Medical Center; [2]Xinhua Hospital, Shanghai Jiaotong University School of Medicine

Recently, it has been found that ATP purinergic signaling plays a critical role in the cochlear function and hearing. Mutations of the *P2RX2* gene, which encodes ATP-gated P2X2 purinergic receptors, can induce hearing loss and increase susceptibility to noise stress. Purinergic signaling can also mediate or control outer hair cell electromotility, hair cell adaptation process, and inner ear gap junctions. Here, we reported that ATP-purinergic signaling play a critical role in the gain control on active cochlear amplification. P2X7 is another predominant P2X receptor isoform in the cochlea and has expression in the synaptic area underlying outer hair cells. We found that P2X7 knockout (KO) mice had high gain in active cochlear amplification as measured by the gain of DPOAE. In wild-type (WT) mice, the gain of DPOAE was reduced as sound stimulation levels increased, especially, in high-intensities and high-frequencies. The gain reduction in active cochlear amplification is a physiological requirement for normal hearing to avoid over-exciting (tinnitus) and damage at high sound intensity stimulation. However, in the P2X7 KO mice, the gain of DPOAE was less changes as sound stimulation intensities increased. Corresponding to less gain changes in DPOAE, ABR thresholds in P2X7 KO mice had no significant difference in comparison with WT mice. However, after white-noise exposure (~ 100 dB SPL, 1 hr), P2X7 KO mice showed less recovery than WT mice, even both of WT and P2X7 KO mice had similar initial temporary threshold shift (TTS). In high frequencies, the P2X7 KO mice almost had no recovery. These data indicate that ATP-gated P2X7 receptors play a critical role in the gain regulation of active cochlear amplification. Dysfunction of this regulation or gain controlling can increase susceptibility to noise stress.

PS 113

G6PDH - a Crucial Enzyme in Protection Against Aminoglycoside Ototoxicity

Thomas Schrepfer[1]; Linghui Luo[2]; Jochen Schacht[1]

[1]University of Michigan; [2]Huazhong University of Science and Technology

The generation of reactive oxygen species (ROS) has been linked to the promotion of hair cell death by aminoglycoside antibiotics. Both endogenous and exogenous antioxidants can mitigate drug-induced oxidative stress and ototoxicity. For endogenous ROS removal systems, NADPH serves as the ultimate reductant supporting, for example, the activities of glutathione reductase and thioredoxin reductase by restoring their reduced state. The major cellular provider of NADPH is glucose 6-phosphate dehydrogenase (G6PDH), the rate-limiting enzyme catalyzing the first steps in the pentose phosphate pathway. We hypothesized that a decreased activity of G6PDH will lead to a compromised ability to counter oxidative stress and aggravate the adverse effects of the aminoglycosides.

In explants of the organ of Corti from CBA/J mice (postnatal day 2 – 3) gentamicin led to the formation of ROS (detected with CellROX) and progressive outer hair cell loss with a base-to-apex gradient and a half-maximal effective concentration of 4.7 µM for a 72-h incubation. To mimic a G6PDH deficiency, we inhibited G6PDH with 6-aminonicotinamide (6-AN), an NADP analogue. Decreased G6PDH activity caused an increase of ROS production and hair cell loss by gentamicin. In order to ascertain that the greater toxicity was indeed due to an NADPH deficiency, we stimulated a secondary pathway of NADPH synthesis via *$NADP^+$-linked malate enzyme*. In the presence of 6-AN, the simultaneous addition of malate and inhibition of fatty acid synthesis (to prevent competition for NADPH) protected hair cells against gentamicin toxicity.

These results strongly support the involvement of ROS in aminoglycoside-induced ototoxicity and the crucial role of NADPH and G6PDH as endogenous protectants. Interestingly, G6PDH deficiency is the most common human enzymopathy rendering carriers sensitive to oxidative agents including common foods (e.g., fava beans; “Favism”) and, by extension of our results, possibly to aminoglycoside antibiotics.

Funding

The study was supported by R01 DC-03685 from the National Institute on Deafness and Other Communication Disorders, NIH.

PS 114

Activation of the antigen presentation function of the mononuclear phagocyte population in the cochlea after acoustic overstimulation

Bohua Hu; Weiping Yang; R. Robert Vethanayagam; Youyi Dong; Qunfeng Cai
the University at Buffalo

Background

Acoustic overstimulation provokes the infiltration of monocytes into the cochlea. These immune cells differentiate into macrophages and play important roles in the inflammatory response and dead cell clearance. However, it is not clear whether these cells participate in antigen presenting function, an essential immune event for activation of adaptive immune reaction. Here, we report the activation of the antigen presentation function of mononuclear phagocyte populations in the cochlea after acoustic overstimulation.

Methods

C57BL/6J mice were exposed to a broadband noise at 120 dB (SPL) for 1 hour. The cochleae were collected at 1, 4 and 10 days after noise exposure for the transcriptional and protein analyses of the expression of antigen presenting-related genes and for the analysis of the antigen processing function of macrophages. The cochleae were also examined for the recruitment of $CD4^+$ T cells, an antigen presenting partner, into the cochlea.

Results

Tissue macrophages are present beneath the basilar membrane under steady-state conditions. Notably, these cells in the apical and the basal sections of the basilar membrane display distinct morphologies and immune protein expression patterns. Following acoustic trauma, monocytes infiltrate into the region of the basilar membrane, and these cells transform into macrophages. While monocyte infiltration and transformation occurs in both the apical and the basal sections of the basilar membrane, only the basal monocytes and macrophages display a marked increase in the expression of MHC II and CIITA, a MHC II production cofactor, suggesting the site-dependent activation of antigen-presenting function. Consistent with the increased expression of the antigen-presenting proteins, macrophage antigen processing function increases. Moreover, $CD4^+$ T cells infiltrate into the region of the basilar membrane where antigen-presenting proteins are upregulated. Further pathological analyses revealed that the basal section of the cochlea displays a greater level of sensory cell damage, which is spatially correlated with the region of antigen-presenting activity.

Conclusion

The antigen-presenting function of the mononuclear phagocyte population is activated in response to acoustic trauma, which could bridge the innate immune response to adaptive immunity.

Funding

NIDCD 1R01DC010154

PS 115

Wnt activation Protects against Neomycin-induced Hair Cell Damage in the mouse cochlea.

Renjie Chai[1]; Liman Liu[2]; Yan Chen[2]; Yanping Zhang[2]; Yingzi He[2]; Wenli Ni[2]; Shan Sun[2]; Makoto M Taketo[3]; Huawei Li[2]
[1]Southeast University; [2]Fudan University; [3]Kyoto University

Background

Recent studies have reported the role of Wnt/β-catenin signaling in hair cell (HC) development, regeneration, and differentiation in the mouse cochlea; however the role of Wnt/β-catenin signaling in HC protection remains unknown.

Methods

In this study, we took advantage of transgenic mice to specifically knock out or over-activate the canonical Wnt signaling mediator β-catenin in HCs, which allowed us to investigate the role of Wnt/β-catenin signaling in protecting HCs against neomycin-induced damage.

Results

We first showed that loss of β-catenin in HCs made them more vulnerable to neomycin-induced injury, while constitutive activation of β-catenin in HCs reduced HC loss both *in vivo* and *in vitro*. We then showed that loss of β-catenin in HCs increased caspase-mediated apoptosis induced by neomycin injury, while β-catenin overexpression inhibited caspase-mediated apoptosis. Finally, we demonstrated that loss of β-catenin in HCs led to increased expression of Foxo3 and Bim, and decreased expression of antioxidant enzyme, thus increased reactive oxygen species (ROS) levels after neomycin treatment, which could be responsible for the increased aminoglycoside sensitivity of HCs. In contrast, β-catenin overexpression reduced Foxo3, Bim expression and ROS levels, suggesting that β-catenin is protective against neomycin-induced HC loss.

Conclusion

Our findings demonstrate that Wnt/β-catenin signaling plays an important role in protecting HCs against neomycin-induced HC loss and thus might be a new therapeutic target for the prevention of HC death.

Funding

This work was supported by grants from the 973 Program of China (2011CB504500, 2015CB965000), the National Natural Science Foundation of China (Nos. 81470692, 81371094, 81230019, 81100826 and 31500852), the Jiangsu Province Natural Science Foundation (BK20150022, BK20140620, BK20131290), and the Program of Leading Medical Personnel in Shanghai.

PS 116

Noise-induced Hearing Loss Is Mediated by the Activation of AMPK Signaling

Kayla Hill; Huigun Yuan; Xianren Wang; Suhua Sha
Medical University of South Carolina

Background

Cell survival depends upon maintenance of energy homeostasis, largely by AMPK. In response to stress, AMPK is activated by changes in intracellular ATP or calcium levels, consequently mediating cellular stress or defense mechanisms that ultimately determine cell fate. We have previously reported that noise exposure induces ATP depletion in cochlear tissues and activates AMPKα in outer hair cells (OHCs). Here we investigated traumatic noise-induced activation of AMPK in cochlear cell types and suggest a novel target pathway for intervention.

Methods

CBA/J mice at the age of 12 weeks were exposed to one of two noise exposure conditions: broadband noise (BBN) from 2–20 kHz for 2 hours at 98 dB SPL to induce permanent threshold shifts with loss of OHCs, while inner hair cells (IHCs) remain intact, or 106 dB SPL to induce severe permanent threshold shifts with losses of both OHCs and IHCs. An anti-AMPKα1 and anti-phospho-AMPKα (T172) antibody was used on cochlear surface preparations, cryosections, and Western blots to determine the activation of AMPK in the organ of Corti, spiral ganglion neurons (SGNs), and the stria vascularis. Auditory thresholds were determined by auditory brainstem responses (ABRs). OHC losses were quantified from surface preparations labeled with myosin VII and then stained with DAB. In order to examine the role of AMPK in NIHL, inhibition of AMPK via either molecular silencing or pharmacological inhibition was utilized.

Results

Noise exposure resulted in an increase in the phosphorylation of AMPK in hair cells in a noise-dose-dependent manner. Pretreatment with AMPKα1 siRNA attenuated losses of OHCs and IHC synaptic ribbons, and consequently noise-induced hearing loss (NIHL). Consistent with these results, treatment with the pharmacological AMPK inhibitor also reduced the level of NIHL and losses of OHCs and IHC synaptic ribbons.

Conclusions

These findings suggest that AMPK signaling is involved in the pathogenesis of noise-induced OHC death and IHC synaptic ribbon loss. Pharmacological targeting of AMPK signaling may provide a novel route to prevent NIHL.

The research project described was supported by the grant R01 DC009222 from the National Institute on Deafness and Other Communication Disorders, National Institutes of Health.

Funding

The research project described was supported by the grant R01 DC009222 from the National Institute on Deafness and Other Communication Disorders, National Institutes of Health.

PS 117

Astaxanthin nano emulsion can protect hair cells against aminoglycosides.

Kazuma Sugahara; Yoshinobu Hirose; Yousuke Takemoto; Yoshihiro Okazaki; Makoto Hashimoto; Hiroshi Yamashita
Yamaguchi University Graduate School of Medicine

Introduction

It was known that aminoglycoside induced hair cell death was related with the free radical generation. Many kinds of molecules can protect hair cells against aminoglycoside ototoxicity. Astaxanthin is a kind of carotenoid and provides the red color of **salmon** meat and the red color of cooked **shellfish**. Astaxanthin has the strong antioxidant activity. Therefore, the dietary supplement and cosmetics which contain astaxanthin were manufactured in many countries. However, Astaxanthin was difficult to transit to the living tissue, because the molecule is a lipophilic material. Nano emulsion of astaxanthin was developed in Fuji film company (Japan). The nano emulsion can diffuse into water and transit to the living tissue.

In the present study, we evaluated the protective effect of nano emulsion of astaxanthin on the inner ear sensory cells against neomycin ototoxicity.

Materials and Methods

Cultured utricles of CBA/N mice were used. Cultured utricles were divided to three groups (Control group, Neomycin group, Neomycin + Astaxanthin Nanoemulsion group, Neomycin + Astaxantin group). In the Neomycin group, utricles were cultured with neomycin (2 mM) to induce hair cell death. In Neomycin + Astaxanthin group, utricles were cultured with neomycin and Astaxanthin (100 – 1 μM). Twenty-four hours after exposure to neomycin, the cultured tissues were fixed with 4% paraformaldehyde. To label hair cells, immunohistochemistry were performed using anti-calmodulin antibody. The rate of survival vestibular hair cells was evaluated with the fluorescence microscope. In addition, immunohistochemistry against 4-hydroxy-2-nonenal was performed to evaluate the product of hydroxy radical.

Results

The survival rate of hair cells in Neomycin + Astaxanthin group was significantly more than that in Neomycin group. The signals of 4-hydroxy-2-nonenal were inhibited in neomycin + Astaxanthin group.

Discussion

As the clinical effects of astaxanthin, the inhibition of diabetic complications, eye diseases, cancer prevention, and anti-fatigue action has been reported. In this study we showed that nano emulsion of astaxanthin protects sensory hair cells against neomycin-induced death in mammalian vestibular epithelium. The nano emulsion of astaxanthin can be used as the protective drug in the inner ear.

PS 118

The magnitude of acoustic injury to the ear is inversely correlated with α9α10 nAChR activity.

Luis Ezequiel Boero[1,2], Juan Diego Goutman[2], Ana Belén Elgoyhen[1,2] and **Maria Eugenia Gómez-Casati**[1,2].
[1]*Tercera Cátedra de Farmacología. Facultad de Medicina, UBA.* [2]*Instituto de Investigaciones en Ingeniería Genética y Biología Molecular, Dr. Héctor N. Torres (INGEBI).*

Noise induced hearing loss (NIHL) has become a major public health problem. The protective role of the medial olivocochlear system (MOC) in NIHL has been well documented (Kujawa and Liberman, 1997; Taranda et al., 2009). Here, we explore the effects of acoustic overstimulation on the efferent innervation to the cochlea and analyze these changes in mice with different degrees of efferent feedback. For this purpose, we made use of a mouse model in which the α9 nicotinic receptor subunit bears a mutation and leads to enhanced MOC activity (*Chrna9L9'T* knock-in (KI)) in addition to one lacking the α9 subunit of the nicotinic receptor (*Chrna9* knockout (KO)).

We exposed WT, KI and KO mice to loud sounds (1-16 kHz noise at 100 dB, for 1 h.) at 3 weeks of age and tested at 1 and 7 days after the exposure. Auditory brainstem responses (ABR) and distortion product otoacoustic emissions (DPOAEs) were used to verify cochlear function. Olivocochlear terminals to outer hair cells (OHC) were quantified by whole mount immunostaining for synaptophysin, an integral protein of the synaptic vesicle membrane to reveal the overall efferent innervation.

We found large auditory threshold shifts one day after exposure in WT and KO mice (10-30 dB SPL). However, one week later, thresholds returned to normal in WT, whereas the KO ears did not recover. Synaptophysin immunostaining revealed abnormalities in efferent terminal number after acoustic trauma in WT mice. The number of terminals per OHC before exposure ranged from 1 to 5, with most OHC contacted by 2 and 3 terminals (40 and 42%, respectively). After acoustic trauma, most OHC were contacted by only 1 or 2 terminals (38 and 44%, respectively) and very few by more than two. Notably, the innervation pattern of KO mice before acoustic trauma is similar to the one observed in WT mice post-trauma, and it does not change after exposure to loud sounds. In contrast, auditory thresholds of KI displayed no changes after noise exposure. Additionally, *Chrna9L9'T* point mutation showed an increase in the number of terminals per OHC and as many as 7 terminals on some OHC. Interestingly, this innervation pattern was not altered by exposure to loud noise.

Results obtained suggest that the degree of protection from acoustic injury depends on the level of MOC activity. Most importantly, despite complete recovery of cochlear thresholds, exposure to loud noise can cause irreversible changes on the efferent innervation pattern to the inner ear.

Funding
Agencia Nacional de Promoción Científica y Tecnológica (Argentina); National Organization for Hearing Research and PEW Charitable Trust.

PS 119

Age-related macrophage fusion and functional transition in mouse cochleae

Bohua Hu; Weiping Yang; Binbin Xiong; Robert Vethanayagam; Wei Sun; **Bo Hua Hu**
University at Buffalo

Background
Tissue macrophages are present in the cochlea. These immune cells participate in cochlear stress responses in pathological conditions. At present, it is not clear how cochlear macrophages change their function with the increase of age when sensory cell degeneration takes place. Here, we report the occurrence of macrophage fusion and the shift of the M1/M2 functional status of macrophages in mouse cochlea with the increase in age.

Methods
C57BL/6J mice at the age of 4 weeks, 3 and 5 months were used. Macrophages beneath the basilar membrane were examined using immunolabeling of CD45 and F4/80. The expression levels of M1/M2 signature genes were examined using qRT-PCR. The antigen presenting function of macrophages was assessed by examining the expression of MHC II, an antigen presenting protein. The numbers of sensory cells and the thresholds of the auditory brainstem response were examined to determine the level of age-related cochlear degeneration.

Results
CD45-positive cells were identified in the scala tympani side of the basilar membrane. These cells displayed the immunoreactivity of F4/80, a marker protein of macrophages. The CD45-positive cells displayed a site-dependent diversity in their morphologies with apical cells being dendritic and basal cells being amoeboid. At 3 months, the ABR threshold measurement revealed high frequency hearing loss. Sensory cell quantification revealed hair cell loss in the basal end of the cochlea. CD45-positive cells in the basal end of the cochlea formed giant cells with multiple nuclei. These cells displayed reduced CD45 immunoreactivity and had the vacuoles of various sizes within their cytoplasm. At 5 months, the giant cells became more evidenced in the middle section of the cochlea. This shift of the site of macrophage fusion was related to the expansion of sensory cell lesions from the basal to the middle section of the cochlea. We did not detect the change in antigen presenting function of macrophages. However, we found an increase in the expression of M1-related genes and a decrease in the expression of M2-related genes. Because M1 and M2 functional activations of macrophages are associated with the inflammatory and the anti-inflammatory response, respectively, the shift of M1 and M2 function suggests that the enhancement of the pro-inflammatory function of macrophages as the age increases.

Conclusion
Cochlear macrophages undergo functional transition in response to age-related sensory cell degeneration.

Funding
NIDCD 1R01DC010154

PS 120

Protective Role of Sodium Selenite against Neomycin-Induced Hair Cell Damage: An Experimental Animal Study Using Zebra fish

Yoon Chan Rah[1,2]; Myung Hoon Yoo[3]; Sung Kyun Kim[4]; Jae-Jun Song[4]; Gi Jung Im[4]; Sung Won Chae[4]; Hak Hyun Jung[4]; June Choi[4]
[1]Korea University Medical Center, Ansan; [2]Seoul National University Hospital; [3]Korea University Ansan Hospital; [4]Korea University College of Medicine

Background
Aminoglycoside is a widely used bactericidal therapeutic agent, however, occasionally combined ototoxicity restricts their clinical application. The mechanisms of ototoxicity includes hair-cell loss caused by reactive oxygen species and intracellular mitochondrial damages. Sodium selenite is a trace element essential for many physiological functions in the body. It principally act as a cofactor for antioxidant enabling the reduction of oxidative DNA damage, which were clinically applied for gastric ulcer or gastritis. So, it could be possibly applied for protecting ototoxic drug-induced hair cell damages. In the present study, we investigated the protective role of sodium selenite against neomycin ototoxicity using zebra fish experimental animal model.

Methods
Five and six days post-fertilization, zebra fish larvae were co-exposed to 125 μM neomycin and various concentrations (10 μM, 100 μM, 250 μM, and 500 μM) of sodium selenite for 1 h. Hair cells within neuromasts of the supraorbital (SO1 and SO2), otic (O1), and occipital (OC1) lateral lines were analyzed by fluorescence microscopy (n = 10 for each group). The changes in the average viable hair cell counts in each neuromast were compared among groups. Apoptosis and mitochondrial damage of neuromasts were evaluated using the terminal deoxynucleotidyl transferase (TdT)-mediated dUTP-biotin nick end labeling (TUNEL) assay and 2-[4-(dimethylamino) styryl]-N-ethylpyridinium iodide (DASPEI) assay, respectively. Ultrastructural changes were evaluated using scanning electron microscopy and transmission electron microscopy.

Results
Sodium selenite reduced neomycin-induced hair cell loss in the neuromasts as a dose-dependent manner (control: 10.50 ± 1.23 cells, neomycin-only treatment group: 5.20 ± 0.86 cells, 500 μM sodium selenite co-treatment group: 9.80 ± 1.08 cells; $p<0.01$). Significantly less apoptosis (high TUNEL score) was observed in 500 μM sodium selenite co-treatment group (negative control: 1.75 ± 0.42, neomycin-only treatment group: 0.43 ± 0.48, sodium selenite co-treatment group: 1.10 ± 0.77; $p<0.01$). The co-treatment of sodium selenite (500 μM) significantly restored DASPEI reactivity (implying viable mitochondria) than neomycin-only treatment group (negative control: 1.98 ± 0.16, neomycin-only treatment group: 0.16 ± 0.46, sodium selenite co-treatment group: 1.19 ± 0.68; $p < 0.01$). Sodium selenite (500 μM) achieved almost complete protection against neomycin-induced ultra-structural damages of the kinocilium, the stereocilia and the mitochondria on electron-microscopic findings.

Conclusion
The sodium selenite seemed to protect against neomycin-induced hair cell damages. Suggested mechanisms includes the reduction of apoptosis, mitochondrial degradation.

PS 122

Comparison of the effect of lipoic acid and glutathione against cisplatin-induced ototoxicity in auditory cells

Gi Jung Im; Doo Yup Koo; Se Hee Lee; Sung Kyun Kim; Myung Hun Yoo; Yoon Chan Rah; Hak Hyun Jung
Korea University College of Medicine

Background
Lipoic acid is famous for recent use of anti-aging effects, which are induced by modulation of signal transduction improving the antioxidant status of the cell. Glutathione (GSH) is an important antioxidant to scavenge reactive oxygen species (ROS) or oxidative stress such as free radicals and peroxides. To examine lipoic acid or GSH-mediated protection against cytotoxicity following cisplatin exposure in HEI-OC1 auditory cell, and to measure the potential to scavenge ROS by lipoic acid and GSH. This study also compare the protective effect of lipoic acid and GSH, and discuss the determination of preventive doses or therapeutic doses.

Methods
HEI-OC1 cells were pretreated with lipoic acid or GSH for 24 h and then exposed to 15 μM cisplatin for 48 h. Resulting cytotoxicity was measured by the cell counting kit-8, and intracellular ROS was measured using flow cytometry. Protective effect or anti-ROS effect of lipoic acid and GSH were compared each other.

Results
Pretreatment with lipoic acid 100 μM and GSH 1 mM protected HEI-OC1 auditory cells against cisplatin-induced cytotoxicity and significantly reduced a cisplatin-induced increase in ROS. Lipoic acid showed a significantly more effective protection to cisplatin-induced ototoxicity compared with GSH (85.4% vs. 73.1% cell viability). Both lipoic acid and GSH showed different concentrations of maximal protective effect on normal condition and cisplatin-induced cytotoxic condition. It may suggest that preventive doses or therapeutic doses for harmful conditions are quite different in two drugs, and need careful drug dose adjustment.

Conclusion
This is a challenging study for comparison of the protective effects of the protective effect of lipoic acid and GSH against cisplatin-induced ototoxicity in an auditory cell line. Lipoic

acid and GSH showed a significant protective effect against cisplatin, and lipoic acid seems to be superior to GSH. Lipoic acid and GSH showed different concentrations of maximal protective effect on normal condition and harmful condition, which suggest the need of drug dose adjustment according to therapeutic purposes.

Funding
Funding This work was supported by a National Research Foundation of Korea grant funded by the Korean Government Ministry of Education, Science and Technology Research Promotion Fund (R1429731). These funding sources only provided financial support and played no specific scientific role in this study.

PS 123

Effective Protection Against Severe Noise-Induced Hearing Loss by an Inner Ear Penetrating, Small Molecule Clinical Drug Candidate Following Daily, Post-Trauma Systemic Administration

Jonas Dyhrfjeld-Johnsen; Mathieu Petremann; Veronique Brieuc; Audrey Broussy
Sensorion

Sensorineural hearing loss is caused by damage to the sensory hair cells and neurons of the cochlea and is the most common type of permanent hearing loss (American Speech-Language-Hearing Association; ASHA). Among adults, the 2 main causes of sensorineural hearing loss are excessive noise exposure and aging (Hearing Loss Association of America; HLAA). Currently no approved pharmaceutical treatment exists and recent meta-analysis of the standard-of-care, off-label use of corticosteroid therapy have concluded that neither systemic nor intratympanic administration has any significant treatment effect (Crane et al. 2015, Laryngoscope 125(1):209-17). We here demonstrate that the small molecule, clinical drug candidate SENS-218 significantly reduces permanent hearing loss and loss of outer sensory hair cells in a rat model of severe noise induced hearing loss after daily, post-trauma, systemic administration.

Following baseline audiometry, 7 week old awake and behaving male Wistar rats were exposed to 120 dB octave band noise (8-16 kHz) for 2 hours on a slowly rotating platform in a sound-attenuating cubicle. SENS-218 (n=7) or placebo (n=7) treatment was initiated after the end of acoustic trauma exposure using intraperitoneal administration and continued daily until day 13.

Both SENS-218 and placebo treated animals displayed up to ~60 dB temporary ABR threshold shifts at 24h (8/16/24 kHz) accompanied by strong or complete suppression of DPOAE amplitudes (4/8/16/24/32 kHz). However, on day 14, SENS-218 treated animals displayed up to ~60% lower permanent ABR threshold shifts and up to ~60% higher DPOAE amplitudes. Taking into account potential variability of individual acoustic trauma, both recovery of ABR thresholds and DPOAE amplitudes from 24h to day 14 were also determined to be significantly improved after SENS-218 treatment. The functional audiometry data were supported by significantly reduced mean outer hair cell loss after drug treatment determined from cochleograms constructed from cell counts in fixed cochlea at day 14.

In an additional cohort of animals, significant nanomolar exposure-levels of SENS-218 were quantified in samples of both perilymph and inner ear tissue after single intraperitoneal administration for at least 4 hours, with a time-course following that of blood plasma samples from the tail-vein.

Altogether, these results demonstrate that daily, systemic administration of the small molecule clinical candidate drug SENS-218 with demonstrated inner ear penetration strongly and significantly protects against permanent hearing loss and cochlear cell loss when treatment is initiated after severe acoustic overexposure.

PS 124

Role of Autophagy in Cisplatin-induced Ototoxicity

Sung Il Cho; Cha Kyung Youn; Juhwan Sim
Chosun University

Background
Hearing loss is a major side effect of cisplatin chemotherapy. Although cell death in cisplatin-induced ototoxicity is primarily caused by apoptosis, the exact mechanism behind the ototoxic effects of cisplatin is not fully understood. Autophagy is generally known as a pro-survival mechanism that protects cells under starvation or stress conditions. However, recent research has reported that autophagy plays a functional role in cell death also. This study aimed to investigate the role of autophagy in cisplatin-induced ototoxicity in an auditory cell line.

Methods
Cultured HEI-OC1 cells were exposed to 30 μM cisplatin for 48 h, and cell viability was tested using MTT assays. To evaluate whether autophagy serves to cell death after cisplatin exposure, western blotting and immunofluorescence staining for LC3-II were performed. Markers of two autophagy-related pathways, mTOR and class III PI3K, were also investigated.

Results
The formation of the autophagic protein LC3-II in response to 30 μM cisplatin increased with time. The early upregulation of autophagy exerted cytoprotective activity via the class III PI3K pathway. But later increase in autophagy induced cell death by suppressing the mTOR pathway.

Conclusion
Our results prove that autophagy could induce cell death during cisplatin-induced ototoxicity, and modulating the autophagic pathway might be another strategy against cisplatin-induced ototoxicity.

Funding
This study was supported by a research fund from Chosun University, 2014.

PS 125

The Effect of Endotoxemia on the Paracellular Permeability of the Blood-Labyrinth Barrier

Zachary Urdang[1]; Anastasiya Johnson[1]; William Meier[1,2]; Allan Kachelmeier[1]; Peter Steyger[1]
[1]Oregon Health and Science University; [2]Oregon State University

Background

Systemic inflammation increases molecular trafficking across the blood-labyrinth barrier (BLB). Experimental endotoxemia is a model for bacterial sepsis that is often treated with aminoglycoside antibiotics. During endotoxemia, greater concentrations of aminoglycosides enter the cochlea, enhancing the risk of ototoxicity and permanent hearing loss. We tested the hypothesis that endotoxemia enhances aminoglycoside trafficking across the BLB primarily through paracellular routes, using two vascular tracers, NHS-biotin and La^{3+}.

Methods

We injected mice with 1mg/kg lipopolysaccharide (LPS) or saline, and 24 hours later, intravenously injected NHS-biotin or $LaCl_3$ for 15 minutes, prior to systemic fixation and processing for confocal or transmission electron microscopy.

Results

Endotoxemic mice exhibited negligible increases in parenchymal uptake of NHS-biotin in the cochlear lateral wall compared to healthy mice. Capillaries of endotoxemic mice were vasodilated and displayed more intense GTTR fluorescence than non-endotoxemic mice. The distribution of $LaCl_3$ was confined to the intra-vascular space and glycocalyx of non-endotoxemic mice. However, $LaCl_3$ was observed between tight junctions of lateral wall capillaries and in the adjacent parenchyma of endotoxemic mice. Furthermore, the lumenal glycocalyx of endothelial cells in the lateral wall of endotoxemic mice appeared greatly diminished.

Conclusion

This acute study complemented prior work using hydrolyzed NHS-Texas Red (hTR), a ligand for multi-drug-resistant efflux transporters. NHS-biotin is a substrate for the biotin (vitamin H) transporter, while La^{3+} is impermeable to cation channels. All three tracers can potentially be trafficked via nonspecific transcytosis.

Trafficking of NHS-biotin was similar in both healthy and endotoxemic animals, corroborating prior hTR data, suggesting that paracellular trafficking of these small organic compounds is minimal. However, the presence of $LaCl_3$ in the lateral wall parenchyma adjacent to capillaries in endotoxemic mice suggests a degree of paracellular flux for cations below a specific size (La^{3+}, ionic radius <0.130 nanometers). Furthermore, $LaCl_3$ is a marker for glycocalyx that appears greatly diminished in endotoxemic mice, potentially facilitating trafficking of tracers across the BLB. We tentatively conclude that cations may more readily cross the BLB during low-dose endotoxemia, while trafficking of the larger organic molecules (>341 MW, NHS-biotin) is constrained by other factors including charge, hydrophobicity, and substrate specificity for transmembrane transporters and receptors. Further tracer studies are needed to parse the subtleties in trafficking mechanisms across the BLB during endotoxemia.

Funding

Funded by R01 DC012588 (PSS), an American Otological Society Fellowship, NRSA F30 DC014229-01, and Tartar Foundation (ZDU)

PS 126

Cisplatin-induced hair cell loss in vestibular organotypic cultures: Nonlinear dose-response

Haiyan Jiang; Dalian Ding; Kun Yang; Richard Salvi
University at Buffalo

Ototoxicity is one of the major dose limiting side-effects of cisplatin. Cisplatin-induced ototoxicity is initiated by cisplatin uptake into the sensory hair cells. The copper transporter, Ctr1 has been identified as a major influx transporter for platinum-based drugs, while copper transporters, ATP7A and ATP7B are involved in sequestration and efflux of cisplatin. Our previous studies in cochlear organotypic cultures indicated that cochlear hair cell loss initially increased with cisplatin dose; however, hair cell loss declined at higher levels. This unusual phenomenon may be due to intrinsic feedback mechanisms, such as the copper transporters, that regulate the influx and efflux of cisplatin into cochlear hair cells. To determine if vestibular sensory hair cells show a similar, nonlinear dose-response to cisplatin, we treated rat neonatal vestibular organotypic cultures with cisplatin doses ranging from 10 μM to 1 mM for 48 h. Initially, vestibular hair cell loss increased with cisplatin dose from 10 to 100 μM, but paradoxically hair cell loss declined at higher concentrations (400 and 1000 μM). The mechanism underlying this nonlinear cisplatin dose-response is currently being explored.

PS 127

Characterization of Cisplatin Ototoxicity and Clearance in Mice

Aaron Rusheen[1]; Lauren Amable[2]; Matthew Hall[3]; Lisa Cunningham[1]
[1]National Institute on Deafness and Other Communication Disorders; [2]National Institute on Minority Health and Health Disparities; [3]NCATS Chemical Genomics Center

Background

Cisplatin is a chemotherapeutic drug used to treat a variety of solid tumors. A major side effect of cisplatin is ototoxicity, resulting in hearing loss in large numbers of patients. Cisplatin is toxic to several cell types in the inner ear, including sensory hair cells and supporting cells. Much remains to be characterized on cisplatin uptake and clearance from the inner ear. We have recently developed a mouse model of cisplatin ototoxicity that is reminiscent of clinical cisplatin administration in that it utilizes repeated cycles of cisplatin administration followed by intervals of recovery. This protocol reliably results in moderate to severe cisplatin-induced hearing loss. In order to fully characterize this model system,

we have here examined cisplatin localization and clearance from the cochleas of cisplatin-treated mice.

Methods
We pre-tested four-month old CBA/CaJ mice for hearing by auditory brain stem responses (ABR) and distortion-product otoacoustic emissions (DPOAE). They were then treated with 3.5mg/kg cisplatin for four days, followed by a ten day recovery period. This was repeated three times. We examined hearing sensitivity by ABR and DPOAE after each cycle of cisplatin administration. We utilized two approaches to examine cisplatin localization and clearance from the cochleas of these mice: inductively coupled plasma mass spectrometry (ICP-MS) and immunohistochemical analysis of cisplatin-DNA adducts in cells of the sensory epithelium.

Results
Significant hearing loss required 3 cycles of cisplatin administration. Preliminary data indicate high levels of cisplatin are retained in the cochlea for extended periods (>10 days) after the final cisplatin administration. Further experiments at different timepoints are being conducted.

Conclusions
Our data indicate that cisplatin-induced hearing loss is robust in this model after three cycles of cisplatin administration. ICP-MS data suggest that cisplatin clearance from the inner ear may be prolonged and inefficient.

Funding
This work was supported by the NIH/NIDCD Division of Intramural Research (ZIA DC 000079).

PS 128

Antioxidants Reduce Neural Degeneration and Accumulation of Pathologic Tau Proteins in the Auditory System after Blast Exposure

Xiaoping Du[1]; Matthew West[1]; Weihua Cheng[1]; Donald Ewert[1]; Wei Li[1]; Robert Floyd[2]; Richard Kopke[1]
[1]Hough Ear Institute; [2]Oklahoma Medical Research Foundation

Background
Spiral ganglion degeneration is commonly observed in the cochlea after hair cell loss due to aging, ototoxicity, noise or blast exposure. Our laboratory previously demonstrated that rats exposed to three successive blast overpressures exhibited marked somatic accumulation of both normal and neurotoxic variants of the microtubule-associated protein Tau in the hippocampus and that antioxidant treatment (NAC plus HPN-07) significantly decreased this pathophysiological response pattern. In the present study, we examined neural degeneration and pathologic Tau protein accumulation in the cochlea after blast exposure and evaluated the potential therapeutic efficacy of antioxidants on short-circuiting these pathological processes.

Methods
Cochlear neural biomarkers (neurofilament-68 and neurofilament-200) and Tau proteins (Tau1, Tau 46, PHF-Tau and T22) were immunohistochemically examined in the cochleae of non-transgenic rats at sequential time points (24 hours, 7 days and 21 days) after three successive blast exposures in animals that were either left untreated or were subsequently treated with a regimen of antioxidants. The therapeutic antioxidants evaluated in the present study were a combinatorial regimen of 2,4-disulfonyl α-phenyl tertiary butyl nitrone (HPN-07) and *N*-acetylcysteine (NAC).

Results
The blast exposure employed in the present study induced neural degeneration in the cochlea as indicated by aberrant patterns of neurofilament staining. Moreover, pathologicTau accumulation was observed in the auditory system, spanning from the spiral ganglion to the auditory cortex, at all time points examined (24 hours, 7 days, and 21 days after blast exposure). Therapeutic intervention with the combinatorial antioxidant regimen significantly reduced pathologic Tau accumulation and neural degeneration, particularly in the spiral ganglion and the auditory cortex.

Conclusions
The combination of HPN-07 and NAC administrated shortly after a blast exposure can reduce neural degeneration and accumulation of pathologic Tau in the auditory system. Due to its coinciding accumulation patterns, atypical somatodendritic manifestations of Tau may actively contribute to pathologic destabilization of axonal microtubule structural dynamics in blast-induced cochlear neural degeneration.

Funding
This research was supported by grant N00014-09-1-0999 from the U.S. Department of the Navy, the Office of Naval Research.

PS 129

Effects of Noise Exposures Causing Small Permanent Threshold Shifts and Loss of Outer Hair Cells on Synaptic Ribbons and Auditory Brain Stem Responses

David Dolan; Diane Prieskorn; Karin Halsey; Cathy Martin; Ariane Kanicki; Susan DeRemer; Sanford Bledsoe; Josef Miller; Richard Altschuler
University of Michigan

Studies of noise-induced hair cell afferent synapse loss have generally used low levels that do not cause loss of hair cells or permanent threshold shifts (PTS). It stands to reason that comparable loss of afferent synapses and associated changes in dynamic range of function will also occur with noise of different characteristics and at levels that do cause some sensory pathology. In the rat model we assessed continuous and impulse noises, both at levels that cause a small PTS and loss of outer hair cells, and compared the efficacy of the same anti-excitotoxic intervention in both. One noise was a 90min,117dB 4k OBN; the other noise was a military relevant small arms fire (SAF) – like noise, 2.5 min, 50 biphasic impulses at 152 dB SPL. Auditory brain stem response (ABR) threshold and Input/Output (I/O) functions were assessed at 4, 8 and either 20 or 24kHz and CTBP2 immunolabeled ribbons were assessed at similar cochlear sites: 3.5, 5.5 and

6.5 mm from the apex. For the OBN and SAF exposures a 25 and 15dB PTS in ABRs was seen across the frequencies tested, respectively. A clear and significant reduction was also seen in the maximum output of the I/O functions for both exposures. Both exposures caused a similar significant loss of synaptic ribbons in the region 6.5 mm from apex, dropping from a mean of 21.2 ribbons per Inner Hair Cell (IHC) in normal cochleae to 13.2 ribbons per IHC at 21 days following the continuous OBN exposure and to 13.5 ribbons per IHC at 5 weeks following the SAF-like noise. Interestingly, anti-excitotoxic agents and antioxidants, Piribedil + Memantine + ACEMg that reduced loss of IHC synaptic ribbons not only reduced changes in suprathreshold I/O response, as expected, but also reduced the PTS. This suggests that there may not only be sparing of lost Low Spontaneous Rate (SR) fibers (sparing suprathreshold responses) but also Medium SR and High SR fibers that affect thresholds.

Funding
NIH Grants R01 DC011294 & P30 DC05188; DOD Grant W81XWH-11-1-0414

PS 130

Noise in the Vibration Spectrum of the Inner Hair Cell Stereocilia

Aritra Sasmal; Karl Grosh
University of Michigan

Background
The acoustical excitation of the organ of Corti (OoC) produces transverse fluid flow in the sub-tectorial space. The flow over the inner hair cell stereocilia bundle (IHB) gives rise to forces that are transduced into neural impulses through chemical and neural pathways at the base of the cell. The IHB is bathed in the viscous scala media fluid. According to the fluctuation dissipation theorem, such viscous elements also induce mechanical fluctuations which are transduced into current noise by the inner hair cell. We used a model of the fluid flow in the gap to analyze the response and noise spectrum dependence on the mode of fluid-structure interaction in the sub-tectorial space.

Methods
We used analytic expressions to model the fluid-structure interactions in the sub-tectorial space (STS). Asymptotic approximations were used to calculate the pressure field in the STS and the fluid equation coupled to the tectorial membrane (TM) degrees of freedom to yield the complete solution. The tectorial membrane was modelled as a beam possessing both extensional and transverse motion. The analytics were validated through a COMSOL model. The dispersion relation of the system was calculated along with their corresponding fluid and structural modes. The effective resistance on the IHB was calculated and the noise spectrum's dependence on the geometry and channel properties established.

Results
We found that the response as well as the input referred noise on the inner hair cell current spectrum is sensitive to the geometry and the type of forcing experienced. For a TM with high flexural rigidity, the IHB acts like a high pass filter when the TM is forced with constant transverse displacement. On the other hand, the IHB response to the sulcus pressure is highest at low frequency and rolls off at higher frequencies. The noise spectrum was found to decrease monotonically with frequency. Hence to maintain a reasonable signal to noise ratio, the sub-tectorial excitation should be shear driven at high frequencies and pressure driven at low frequencies. Similar results have been derived for low flexural rigidity as well.

Conclusions
The STS fluid dynamics has been coupled to the IHB dynamics within the framework of an analytic model. The response as well as the noise spectrum of the inner hair bundle to external excitation was analyzed and the regimes of different types of forcing established.

Funding
This work was supported by NIH-RO1-04084.

PS 131

Micromechanical Interactions between the Inner Hair Cells and the Organ of Corti

Srdjan Prodanovic; Yanju Liu; Sheryl Gracewski; Jong-Hoon Nam
University of Rochester

Background
The stereocilia bundle is the mechano-transduction apparatus of the inner ear. In the mammalian cochlea, the stereocilia bundles are situated in the subtectorial space (STS) – a micrometer-thick fluid-filled space between two flat surfaces vibrating relative to each other. Because microstructures vibrating in fluid are subject to high viscous friction, previous studies considered the STS as the primary place of energy dissipation in the cochlea. While there have been extensive studies on how metabolic energy is used to compensate the dissipation, much less attention has been paid to the mechanism of energy dissipation. Using a computational model, we quantified the power dissipation in the STS and investigated how/if the STS power dissipation affects the organ of Corti mechanics.

Methods
Two layers of computation model were used. A single inner hair cell (IHC) bundle in the STS was simulated using finite difference method (Prodanovic et al., 2015). After simulating IHCs at several different locations along the cochlea, the dissipating force of the STS was reduced to an analytic equation. The reduced STS response was combined with an existing finite element model of the organ of Corti (Liu et al., 2015). The organ of Corti micromechanics were solved together with the macro-fluid dynamics of the entire cochlea.

Results
Along the axis of the stimulating frequency, there were two asymptotic values of STS power dissipation. At high frequencies, the power dissipation was determined by the shear friction between the two flat surfaces of the STS. At low frequencies, the power dissipation was dominated by

the viscous friction around the IHC stereocilia bundle—the IHC stereocilia increased the STS power dissipation by 100 times. There exists a characteristic frequency for STS power dissipation, CF_{STS}, defined as the frequency where power dissipation drops to one half of the low frequency value. The IHC stereocilia stiffness and the gap size between the IHC stereocilia and the tectorial membrane determine the characteristic frequency. From the simulations of the whole cochlear model, the power dissipation in the cochlea was quantified. The phase relations between the organ of Corti micromechanics and the IHC mechano-transduction were analyzed.

Conclusions
The STS is a significant power sink in the cochlea and that effect of STS power dissipation is greater in the apex (low frequency locations). Because of STS fluid dynamics and organ of Corti micro-mechanics, the phase between basilar membrane vibration and IHC mechano-transduction is qualitatively different along the cochlear length.

Funding
Supported by NSF CMMI 1233595 and NIH R01 DC014685 to JN

PS 132

Mechanics of the chicken basilar papilla

Anping Xia[1]; Patrick Raphael[1]; Xiaofang Liu[1]; Brian Applegate[2]; John Oghalai[1]
[1]Stanford University; [2]Texas A&M University

The basilar papilla of the bird is unique in that it has similarities to both the mammalian cochlea as well as the auditory papillae of other non-mammalian species. Like mammals, it has two types of hair cells; like frogs, turtles, and lizards, its hair cells have electrical tuning. Like all of them, its hair cell stereociliary bundles have non-linear processes that can produce force. However in contrast to the mammalian cochlea, its hair cells do not also produce force through somatic electromotility. To understand how these similarities and differences impact the physiology of the bird cochlea, we used volumetric optical coherence tomography vibrometry (VOCTV) to measure sound-induced vibrations within the P5-10 chick cochlea *in vivo*. Traveling waves propagated from base to apex. The basilar membrane vibrated with a low-pass filter response, with a corner frequency that was tuned tonotopically. The displacement of the basilar membrane and the short hair cells that sit above it varied linearly with stimulus intensity and did not change post-mortem. The fibrocartilaginous plate under the tall hair cells vibrated in phase with the basilar membrane, although with a reduced magnitude. In response to the presentation of two tones of different frequencies, low-level distortion products were detected within basilar membrane vibrations and as sounds emanating from the ear canal, confirming the presence of active force generation. Together, these findings indicate that the chicken cochlea does not function like the mammalian cochlea, where frequency tuning within the auditory nerve derives from the vibratory characteristics of the organ of Corti which is shaped by active force generation. Instead, these data are consistent with the long-postulated concept that frequency tuning in birds derives from the electrical characteristics of their hair cells. Furthermore, while active force generation is present and measurable within the chicken cochlea, it does not amplify or sharpen the traveling wave.

Funding
This project was funded by NIH-NIDCD DC014450, DC013774, and DC010363

PS 133

Coupled scala media and scala tympani pressure measurements constrain dual-partition models

Sushrut Kale; Elizabeth Olson
Columbia University

In early cochlear models intracochlear pressure was decomposed into two modes, the compression pressure (fast-mode) and the traveling wave pressure (slow-mode). This fast mode is symmetric and the slow mode antisymmetric. When it comes to intracochlear motion, the compression mode is not significant due to the nearly incompressible nature of the cochlear fluids and tissues. Therefore, in most modern cochlear models, which are mainly concerned with intracochlear motion and its relationship to hair cell excitation, the symmetric compression mode is excluded. We measured intracochlear pressure in response to tones in scala media (SM) in gerbil cochleae. The measurements were made either in-vivo or within a few hours post-mortem with custom-built pressure sensors with ~ 80 μm outer diameter. Scala tympani (ST) pressure was measured in the same cochleae at the same longitudinal location. The combined findings from the two scalae supported predictions from early cochlear models that include relatively complete intracochlear pressure. The findings also constrain recent dual-partition models, in which the tectorial and basilar membranes (TM and BM) move somewhat independently.

Measurements of intracochlear pressure in ST made both close to and far from the BM had confirmed the presence of the predicted pressure modes. ST pressure close to the BM was tuned and nonlinear and the nonlinearity enhanced the tuning. However, even in passive cochleae the ST pressure was tuned in frequency. This passive tuning was at odds with cochlear models, which predict the pressure to be low-pass in the absence of activity. However, these models did not include the compressive pressure mode. Our measurements of intracochlear pressure in both ST and SM helped to clear up this discrepancy between model and measurement. After decomposing the measured SM and ST pressure into symmetric and antisymmetric modes, the antisymmetric (slow) mode was found to be ~ low-pass, as predicted by classical cochlear theories. In addition, in the frequency region of slow-mode dominance, SM and ST pressures at the sensory tissue were nearly anti-symmetric, as predicted by single-partition cochlear models. While this finding seems to be at odds with dual-partition models, more accurately our findings indicate that there is relatively tight coupling between the two partitions (TM and BM). These pressure results

inform the development of dual-partition models, which have been conveyed in the literature with partition coupling as a parameter.

Funding
NIH-NIDCD RO1 003130

PS 134

Longitudinal Coupling of the Tectorial Membrane Counteracts Viscous Loss in the Subtectorial Gap

Jonathan Sellon[1]; Roozbeh Ghaffari[2]; Dennis Freeman[3]
[1]Massachusetts Institute of Technology; [2]MIT Research Laboratory of Electronics; [3]MIT Department of Electrical Engineering and Computer Science

Background
Conventional cochlear models suggest that the sensitivity and frequency selectivity of hearing are both limited by viscous losses in the subtectorial space. On this basis, active processes, driven by electromotility of outer hair cells, are thought to be necessary for sharp tuning and sensitivity. However, these models do not account for longitudinal coupling through the tectorial membrane (TM).

Methods
We compare the relative contributions of TM mass, viscosity and stiffness on TM longitudinal coupling by developing a distributed impedance model of the TM. To determine the effects of cochlear loads on TM wave propagation, we represent the TM as a finite longitudinally distributed series of masses (M) coupled by viscous (b) and elastic (k) elements. We then characterize the effects of hair bundle stiffness (khb), an elastic limbal attachment (ksl), and viscous damping in the subtectorial space (bsts) for waves stimulated locally on the TM or via shear motions of the basilar membrane (modeled as a displacement source, XBM).

Results
Increasing the TM thickness parameter did not significantly affect TM wave decay constants at 7 kHz and 20 kHz. However, decreasing TM thickness in the model does have an effect on the spatial extent of TM waves. At 20 kHz, a reduction in TM thickness by half results in an approximately 20% decrease in TM wave decay constant. These results demonstrate that the natural thickness of the TM is sufficiently large so that the internal material properties of the TM overcome cochlear loads, and thereby determine spread of mechanical excitation in the cochlea.

Conclusions
Our results suggest that the TM is just thick enough to act as a conduit of energy that overcomes loss mechanisms in the subtectorial fluid, which would otherwise reduce both the sensitivity and frequency selectivity of hearing.

PS 135

Gain Control Dynamics in the Mechanics of the Mammalian Cochlea

Nigel Cooper; Marcel van der Heijden
Erasmus MC

Dynamic aspects of cochlear mechanical compression were studied by recording basilar membrane (BM) vibrations evoked by "beating" tone pairs ("beat stimuli") in the 11-19 kHz region of healthy gerbil cochleae. The frequencies of the stimulus components were varied to produce a range of beat rates at or near the characteristic frequency (CF) of the BM site under study, and the amplitudes of the components were balanced to produce near perfect periodic cancellations, visible as sharp notches in the envelope of the BM response. Stimulus levels were limited to minimise the spread of excitation along the cochlear partition, and evoked peak response magnitudes on the order of 1-10 nm (near the midline of the BM). Within this range, we found a compressive relation between instantaneous stimulus intensity and BM response magnitude that varied systematically with beat rate. Compression was strongest at low beat rates (e.g. 10-100 Hz), and reduced progressively (i.e. the responses became linearized) at higher beat rates. The rising and falling flanks of the response envelope became increasingly asymmetric with increasing beat rate; the falling flank becoming shallower than the rising flank. This hysteresis indicates that cochlear mechanical compression is not instantaneous, and is suggestive of a gain control mechanism having finite attack and release times. We suggest that the response linearization that occurs at higher beat rates does so because the instantaneous gain becomes smoothened, or low-pass filtered (with respect to the magnitude fluctuations in the stimulus) by a gain control system. The gain control is associated with a finite delay, which we find to be on the order of one cycle of the beating CF tones.

Funding
Supported the Netherlands Organization for Scientific Research, ALW 823.02.018

PS 136

Basilar membrane phase response in nonlinear transmission line models

Renata Sisto[1]; Arturo Moleti[2]; Christopher Shera[3]
[1]Italian National Institute for Workers Compensation; [2]University of Rome Tor Vergata; [3]Harvard University

Background
In experimental measurements of the basilar membrane response to tones (reviewed in Robles and Ruggero, 2001), while peak gain depends sharply on the stimulus level (30-50 dB variation in a 70-90 dB level range), the phase slope in the peak region shows a relatively weaker level dependence (30-50% in the same level range), with a typical phase behavior around the characteristic frequency/place. This fact may be counterintuitive as in linear resonant models both phase slope and gain are strongly dependent on the tuning factor of the resonance. In a recent paper (Sisto et al., 2015) it was demonstrated that, overall, nonlinearity helps decoupling

phase slope from gain, and that a straightforward nonlinear generalization of a linear passive model (anti-damping model, Moleti et al., 2009) still predicts a phase slope that is too sensitive to gain variations. A nonlinear version of the Zweig model, and (particularly) a nonlinear FF model showed intrinsically higher decoupling of the phase slope from gain, particularly in their fully nonlinear versions.

Method
The phase behavior of linear and nonlinear transmission line models is compared to data from animal experiments. In the linear model the gain is changed by explicitly changing the tuning factor, whereas in the nonlinear model, gain and phase are dynamically dependent on the stimulus level through the nonlinear dependence of the OHC active force on the instantaneous BM vibration level. The model is discretized using 2000 partitions, and tuned to represent the guinea pig and chinchilla cochlea, by suitably setting the tonotopic map parameters and the nonlinear gain variability range.

Results
Comparison with experimental data shows to what extent transmission line cochlear models are able to mimic the slow dependence of phase on stimulus level, as well as the typical phase behavior near the characteristic frequency/place. Depending on the choice of the model free parameters, the particularly weak dependence on stimulus level of the maximum phase slope of the nonlinear models may help fitting the data. This last behavior may be traced back to a property of some nonlinear resonant oscillators, which, in the perturbative limit, tend to share the phase behavior of their asymptotic linear counterparts.

Conclusion
The experimental behavior of the basilar membrane phase response in the resonant region is not incompatible with the predictions of classical nonlinear transmission line cochlear models, within the uncertainty associated with the choice of a few parameters of the models.

PS 137

Resolving the Discrepancies between Basilar Membrane, Reticular Lamina and Inner Hair Cell Tuning.

Alessandro Altoe'[1]; Sarah Verhulst[2]; Ville Pulkki[1]
[1]Aalto University; [2]Oldenburg University

Classical recordings from the basal region of the chinchilla cochlea (~8 kHz) show that neural tuning curves lie about halfway between basilar-membrane (BM) constant-velocity and constant-displacement tuning curves. This suggests that inner-hair cells (IHCs) respond to a combination of BM velocity and displacement; a statement that finds support in classical guinea-pig IHC recordings.

In this study, we offer an explanation for the well-documented relationship between neural and mechanical tuning that relies on a proportionality between IHCs stereocilia deflection amplitude and BM velocity up to the units' best frequency. By assuming well-established features of IHC processing, i.e. a Boltzmann type transduction nonlinearity followed by the low-pass filtering action of the IHC basolateral membrane, we derive the theoretical background for this work. We then validate our hypothesis using numerical simulations in a computational model of the inner hair cell/auditory nerve complex.

Unfortunately, the demonstrated proportionality between BM velocity and stereocilia deflection seems in contrast with recent in-vivo recordings from the ~18 kHz region of the guinea-pig cochlea that show a level-dependent sharper tuning of the reticular lamina (RL) compared to BM tuning. To resolve this discrepancy, we propose the existence of a mode of RL vibration that reflects the motion of the BM in a more basal cochlear region at a fixed distance. This mode of vibration can account for sharper RL than BM tuning in the 18 kHz region through a phase cancellation mechanism and we show this numerically using a linear nonlocal model that relates RL and BM vibrations. The suggested phase cancellation mechanism results in a mode that enhances RL vibrations at high-frequencies (above 10 kHz), but that leaves lower-frequency responses unaffected in agreement with the differences observed in the high (~18 kHz; guinea pig) vs lower (~8 kHz; chinchilla) frequency cochlear mechanics. Additionally, the proposed linear model is capable of capturing the apparent nonlinear relationship between RL and BM motion.

We propose a description of BM-RL-IHC transduction that is based on previous BM and IHC models, combined with (i) frequency dependent stereocilia low-pass filtering and (ii) a feedforward model of RL motion, and demonstrate that it can account for well-documented relationships between mechanical and neural tuning. We lastly point out that established functional models of the IHC/auditory-nerve complex tend to overestimate the neural response to low-frequency stimuli, resulting from an excessive low-pass filtering in the IHC stage.

Funding
Work supported by Aalto ELEC doctoral school and DFG Cluster of Excellence EXC 1077/1 â€œHearing4allâ€ .

PS 138

Sound-induced motion of the mouse organ of Corti measured in vivo by imaging through the ear canal using volumetric optical coherence tomography vibrometry (VOCTV)

Wenqing Yan[1]; Anping Xia[1]; Patrick Raphael[1]; Brian Applegate[2]; John Oghalai[1]
[1]Stanford University; [2]Texas A&M University

Vibratory measurements to study cochlear traveling waves *in vivo* have historically been made using invasive approaches, such as laser Doppler vibrometry, in which the otic capsule bone needs to be opened. These studies have provided critical information regarding the active and passive mechanical properties of the living cochlea, however the experiments are terminal because of the invasive nature of the surgical procedure to access the cochlea. The recent

development of VOCTV has permitted the measurement of intracochlear vibrations without needing to open the otic capsule. While this has improved measurement reliability and permitted study of all of the tissue structures within the organ of Corti, the middle ear bulla has still needed to be opened. Thus, experiments have remained terminal. We have now developed an approach to image the mouse cochlea through the ear canal, by directing the light so that it traverses both the tympanic membrane. The light passed through the side of the otic capsule bone so that the anatomic structure of the cochlea and organ of Corti could be visualized from the side. We then presented sound stimuli and measured sound-induced vibrations in the radial direction. The TM and RL demonstrated the sharp tuning and gain of cochlear amplification with a characteristic frequency of 13-15 kHz in live mice. Repeated measurements could be performed on the same mouse for several days in a row. Therefore, it is now feasible to perform long-term sequential studies of cochlear mechanics in mice using this minimally-invasive technique.

Funding
This project was funded by NIH-NIDCD DC014450, DC013774, and DC010363

PS 139

Computational Model for the Complex, Active Deformation of the Organ of Corti near the Cochlear Apex

Nikola Ciganovic[1]; Rebecca Warren[2]; Anders Fridberger[2]; Tobias Reichenbach[1]
[1]Imperial College London; [2]Linköping University

Background
The organ of Corti translates the sound-induced vibrations of the basilar membrane into deflections of the mechanosensitive hair bundles. It also mechanically amplifies weak vibration which boosts the inner ear's sensitivity to low-intensity sound. However, the details of the organ of Corti's micromechanics and how it implements mechanical amplification remain debated. In particular, the micromechanics near the cochlear apex differs from that near the base. Experiments on electrically-induced motion have, for instance, found unexpected multiphasic displacement patterns of the reticular lamina that were most pronounced at the cochlea's low-frequency end (Nowotny and Gummer, 2006, 2011; Jacob et al. 2011). The precise deformation pattern and how it arises through the active process remain debated.

Methods
We used detailed morphometric data and micrographs (Kelly 1989, Lenoir 2013) from the cochlear apex of guinea pig to create an idealised geometrical representation of a transverse section of the organ of Corti. To model its deformation, we assumed that the cross-sectional area of the organ of Corti remains constant, that is, there is no net longitudinal fluid flow within the organ. The resulting geometric equations then yield the displacements of anatomical elements in the organ of Corti with respect to the initial configuration when the outer hair cells (OHCs) change length. We also performed laser-interferometric measurements on electrically-evoked motion at the cochlear apex in *in vitro* preparations of the guinea-pig cochlea.

Results
The laser-interferometric measurements show that electrically-induced vibrations are large at the Hensen cells but negligible at the basilar membrane. Moreover, the Hensen cells move towards the scala vestibuli when the OHCs contract. Our geometric model reveals that this counter-intuitive behavior can be explained by the area conservation of a transverse section of the organ of Corti: contracting OHCs lead to a rotation of the junction between the OHCs and the Deiter's cells, and to a motion of the Hensen cells near the third row of OHCs away from the basilar membrane.

Conclusions
We provide a computational model for the active deformation of the organ of Corti near the cochlear apex. Our model makes quantitative predictions on the direction and amplitude of motion at various internal structures that are in excellent agreement with previous and newly acquired experimental data. Our model can be used for further investigating the implementation of the active process at low frequencies, as well as for studying the fluid flow around the deforming, active organ of Corti.

PS 140

Time-Domain Measurements of Pure-Tone Evoked Mechanical and Neuronal Response in an Insect Ear

Jan Scherberich; Manuela Nowotny
Goethe University Frankfurt am Main

To attract each other using acoustic stimuli is a common feature practiced by vertebrates but also in insects like bushcrickets (katydids). Sensory cells of the hearing organ *crista acustica* positioned above an acoustic trachea, inside the tibiae of the forelegs, are sensitive to sound-induced waves with frequencies above 3 kHz. A tonotopic arrangement of the sensory cells allows a frequency discrimination of sounds up to at least 80 kHz. In a recent ongoing project we combine mechanical (Laser-Doppler-Vibrometer) and neuronal response (intracellular recordings) measurements to compare the timing between mechanical vibrations evoked through airborne sound and cell spiking.

At the beginning of each in-vivo experiment, tuning curves with pure-tone stimuli were used to determine the characteristic frequency (CF) at the certain position along the *crista acustica*. Sound stimuli presented by a loudspeaker (R2904/700000, ScanSpeak, Videbæk, Denmark) had a duration of 40 ms (r/f 4 ms) and were randomly presented at a repetition rate of 250 ms. Subsequently, sensory cells were stimulated with pure-tone sounds at the CF and quarter and half octaves below and above it. These stimuli had a duration of 20 ms (r/f 0.5 ms) and were presented with a level of 60 to 80 dB SPL. Additionally, click response measurements were performed at 80 dB SPL and a duration of 3 ms. Simultaneous to the intracellular recordings the sound-induced mechanical response pattern were measured by a laser Doppler

vibrometer (MSV-300 with a sensor head OFV-534, Polytec, Waldbronn, Germany), allowing to measure the mechanical oscillation (250 averages, 0.4 µs resolution).

Short pure-tones near the CF evoke a response with 4 to 8 spikes during 20 ms stimulus duration. The first spike is timed very precisely at about 2 ms after the acoustical stimulation, followed by spikes with a rising variance in timing. Usually 0.5 - 4 ms after stimuli entrance through the spiracle sound-induced vibration of the *crista acustica* reached its maximum amplitude. Preliminary evaluation of the Q-values (determines the qualitative behavior of simple damped oscillators) of the mechanical ring-down after the stimulus at the certain CF exhibits higher Q-values of high-frequency distal sensory cells (Q-value: ~200) in comparison to low-frequency proximal sensory cells (Q-value: ~40). This points to the fact that damping is higher in the low-frequency region of the *crista acustica*.

We like to thank Manfred Kössl for technical support and fruitful discussions.

Funding
This work is supported by the DFG (NO 841/1-2).

PS 141

Gentamicin Distribution in the Ear Following Local Applications

Alec Salt[1]; Jared Hartsock[1]; Ruth Gill[1]; F. Kraus[2]; Elisha King[3]; Stefan Plontke[4]
[1]Washington University; [2]Universitätsklinikum Halle (Saale); [3]Bionics Institute, Melbourne, Australia; [4]University of Halle-Wittenberg, Halle (Saale)

Background
Although it has been widely assumed that intratympanically-applied gentamicin enters perilymph through the round window (RW) membrane, recent functional studies suggest that entry at the stapes can also occur. We have therefore quantified perilymph kinetics following local gentamicin applications to the ear.

Methods
Elimination kinetics of gentamicin in the guinea pig ear was first established by loading perilymph by injecting a 500 µg/ml solution at 1 µL/min for 60 min from a pipette sealed into the lateral semi-circular canal (LSCC). Perilymph was sampled from the LSCC site at a single time point 0 to 4 hours after injection. Sequential sampling was used to take 10 x 2 µL samples of perilymph in rapid succession which were each analyzed independently. In subsequent experiments, perilymph gentamicin levels were measured with the same sampling technique performed 1 – 4 hours after 40 mg/ml gentamicin application to the RW niche. In both cases, samples were analyzed by a particle enhanced turbidimetric inhibition immunoassay (Beckman Coulter) to quantify gentamicin distribution in the ear.

Results
Following perilymph loading by LSCC injection, gentamicin concentration declined slowly with time. The decline was dominated by concentration decrease in the basal part of scala tympani (ST), consistent with CSF-perilymph interactions (dilution by slow entry of CSF into ST and by respiratory pressure-induced oscillations across the cochlear aqueduct). Concentration decline of perilymph in the vestibule occurred more slowly than from ST.

Following applications of gentamicin to the RW niche, perilymph concentration was typically higher in the initial samples (originating in the vestibule and scala vestibuli (SV)) and lower in later samples originating from ST. The experiments were simulated with a computer model incorporating the perilymph kinetics dominated by interactions with CSF. The analysis revealed that more gentamicin typically entered at the RW, although the amount varied between animals. The lower perilymph concentrations found in ST were due to the higher rate of elimination there.

Conclusions
These data confirm that gentamicin enters perilymph of the vestibule directly in the vicinity of the stapes as well as through the RW. Gentamicin levels in the vestibule were substantially higher than those in ST following RW niche applications, probably contributing to the preferential vestibulotoxicity of the drug. Nevertheless, differences in perilymph kinetics between the vestibule, SV and ST need to be considered to account for the measured distribution.

Funding
Study supported by NIDCD R01 DC001368 and by the Foundation for Barnes-Jewish Hospital.

PS 143

Sensitivity and Amplitude of ABRs and LFPs in Different Species of FM Echolocating Bats

Hiroshi Riquimaroux[1]; Hidetaka Yashiro[2]; Andrea Simmons[3]; James Simmons[3]
[1]Shandong University; [2]Doshisha University; [3]Brown University

Many species of echolocating bats emit wideband FM biosonar sounds that cover 2-3 octaves in the 10 to 150 kHz frequency band. Sound pressure levels broadcasted by insectivorous bats hunting in the open can exceed 120 dB SPL, with maximum levels of about 135 dB SPL. Frugivorous bats, which forage in vegetation, emit generally lower levels of 75-80 dB SPL, with maximum levels up to 110 dB SPL. Many of these species live in colonies that range from a few individuals to thousands of bats in the same cave. When flying inside roosts or within emerging streams, they are regularly exposed to the intense sound emissions of multiple bats, at aggregate sound pressure levels exceeding 100-110 dB SPL for up to an hour or more. The focus of this research program is to uncover the mechanisms by which bats are able to echolocate and communicate in these intense, noisy soundscapes. We recorded auditory responses (ABRs, LFPs) from electrodes in the inferior colliculus evoked by FM sounds in biologically-relevant frequency bands in three species of bats, *Pipistrellus abramus* (Japanese house bat) and *Eptesicus fuscus* (big brown bat)—both insectivorous,

and *Carollia perspicillata* (short-tailed fruit bat), a frugivorous species. As expected, hearing sensitivity is optimal at biosonar frequencies and also at frequencies used for communication; sensitivity is also good at lower frequencies that may be used for passive listening for prey. After exposure to ultrasonic broadband noise (levels of 90-120 dB SPL for 30 min), ABR and LFP amplitudes exhibited little reduction of response strength, as would be expected if the noise exposure induced temporary threshold shifts. These physiological data are consistent with psychophysical data that show little or no impairment of hearing sensitivity post-exposure.

Funding
Japan Society for the Promotion of Science, Capita Foundation, Office of Naval Research

PS 144

Frequency Tuning of Synaptic Inhibition in Duration-Tuned Neurons of the Mammalian Inferior Colliculus

Roberto Valdizón-Rodríguez; Paul Faure
McMaster University

Duration tuning in the mammalian auditory midbrain is created by the interaction of excitatory and inhibitory synaptic inputs that are offset in time. We used paired-tone stimulation in combination with single-unit extracellular recording to measure the spectral tuning of the synaptic inhibition underlying duration-tuned neurons (DTNs) recorded from the inferior colliculus of the big brown bat (*Eptesicus fuscus*). We stimulated DTNs with a short duration, excitatory probe tone set to the cell's best duration (BD) and best excitatory frequency (BEF) and a longer duration, non-excitatory (NE) tone that was varied in frequency. The onset time of the BD tone was varied relative to the NE tone. Spikes evoked by the BD tone were suppressed when the NE tone frequency was near or within the cell's excitatory bandwidth (eBW). The effective duration of spike suppression decreased as the NE tone frequency moved away from the cell's BEF. This occurred because the offset of the inhibition evoked by the NE tone systematically decreased as the stimulus frequency moved away from the BEF. In contrast, the onset of the NE tone inhibition, which preceded the evoked excitation, did not change as a function of the NE tone frequency. We used the effective duration of the NE tone evoked inhibition to generate an inhibitory frequency response area from which the best inhibitory frequency (BIF) and inhibitory bandwidth (iBW) of each cell was measured. The BIFs of DTNs closely matched their BEFs; however, iBWs were significantly wider than eBWs in the same cell. We conclude that the synaptic inhibition responsible for creating duration-tuned circuits in the IC is broadly tuned in frequency and time-locked to stimulus onset, and these feature help to preserve the temporal selectivity of DTNs.

Funding
Research supported by an operating grant from the Canadian Institutes of Health Research (Institute of Neurosciences, Mental Health and Addiction), and infrastructure grants from the Canada Foundation for Innovation and the Ontario Innovation Trust.

PS 145

Tuning for the Rate or Duration of Frequency Modulated Sweeps in the Mammalian Inferior Colliculus

James Morrison; Roberto Valdizón-Rodríguez; Daniel Goldreich; **Paul Faure**
McMaster University

We investigated how the auditory midbrain encodes the temporal properties of frequency modulated (FM) sweeps by recording responses from so-called "FM duration-tuned neurons (DTNs)" in the inferior colliculus (IC) of the big brown bat (*Eptesicus fuscus*). The spiking responses of DTNs are selective for stimulus duration. This study examined how the responses of "FM DTNs" encoded two temporal properties of FM sweeps: signal duration, and the rate of frequency modulation. Based on previous studies, it was unclear whether "FM DTNs" were tuned to signal duration, like classic pure-tone DTNs, or the FM sweep rate. We addressed this question using single-unit extracellular recording in a population of IC neurons with responses selective for the duration of FM sweeps. First, we measured the best FM tuning of each cell by presenting it with linear FM sweeps that were randomly varied in center frequency and FM bandwidth. We used these parameters to stimulate each neuron with FM sweeps that were randomly varied in duration to measure the best duration and temporal bandwidth of FM duration tuning (all signals broadcast at +10 dB re: threshold). To separate FM rate tuning from FM duration tuning, we doubled (and then halved) the bandwidth of the best FM stimulus (while keeping the center frequency constant), and then re-measured the temporal bandwidth of duration tuning by presenting each cell with the bandwidth manipulated signals randomly varied in duration. If the neuron was "FM duration-tuned", then the range of excitatory signal durations should remain constant despite changes in FM bandwidth; however, if the cell was FM rate-tuned and not duration-tuned, then the range of excitatory signal durations should vary but correspond to similar sweep rates when stimulating with FM bandwidth manipulated signals. A Bayesian model comparison showed that the overwhelming majority of IC cells we tested were not FM duration-tuned, but were FM rate-tuned. We conclude that the dominant temporal response parameter for FM tuning in the mammalian IC is the FM sweep rate and not the FM signal duration.

Funding
Research supported by an operating grant from the Canadian Institutes of Health Research (Institute of Neurosciences, Mental Health and Addiction), and infrastructure grants from the Canada Foundation for Innovation and the Ontario Innovation Trust.

PS 146

Binaural Responses in the Auditory Midbrain of the Chicken

Roberta Aralla; Christine Köppl
Carl von Ossietzky University Oldenburg

Background

The representation of auditory space in the inferior colliculus and optic tectum of the barn owl has become a classic example of a derived sensory map. It is, however, not known whether the principles underlying its formation generalize to other, less specialized animals. We have begun to characterize responses in the inferior colliculus of the chicken, with the ultimate aim of testing for a topographic representation of auditory space and any intermediate steps in its synthesis.

Methods

Spike responses (mostly multi-unit) were recorded from the inferior colliculus (IC) of anesthetized chickens aged P27 to P34 using glass-insulated tungsten micro-electrodes. Stimulation was through closed sound systems inserted into both ears. We probed for responses to monaural and binaural stimulation and tested selectivity for frequency, interaural level differences (ILD) and interaural time differences (ITD). Small electrolytic lesions confirmed the locations of selected recording sites.

Results

Analysis of 85 recording sites (11 electrode tracks) from 5 chickens showed a variety of response types. A minority of sites (13 of 85) responded not to tones but only to broadband noise. Preliminary reconstruction of associated lesions suggested a location in the shell region and/or the external nucleus of the IC. Most recordings showed frequency selectivity, with best frequencies from 200 to 4000 Hz. All sites appeared to be binaural, i.e. responded to stimulation from either ear, with different combinations of excitation and inhibition. All sites showed response variation with ILD; half-maximal spike rates fell mostly within the physiological range of the chicken (up to 18 dB; Schnyder et al., 2014, PlosONE 9(11):e112178). About half of all tested sites, and preferentially those with BFs <1kHz, showed significant selectivity for ITD, with best ITDs distributed broadly up to 1000µs, contralaterally leading.

Conclusions

Previous work on chicken and pigeon IC had mainly used free-field stimulation (Coles and Aitkin, 1979, J Comp Physiol 134,241-251; Lewald, 1990, Exp Brain Res 82:423-436). Here, we used closed systems to dissociate the relative selectivities to ITD and ILD, and also made a first attempt to correlate response types with IC subdivisions. Our preliminary analysis suggests a similar principal organization of IC as in the barn owl (Singheiser et al., 2012, Front Neur Circ 6:45) and as shown histologically for the chicken (Puelles et al., 1994, J Comp Neurol 340:98-125). However, it remains to be explored whether there is any systematic representation of auditory space.

Funding

Deutsche Forschungsgemeinschaft (CRC Active Hearing, project A14)

PS 147

Neural correlates of behavioral frequency discrimination of single-formant stimuli in the budgerigar midbrain

Kenneth Henry[1]; Kristina Abrams[1]; Mathew Mender[1]; Erikson Neilans[2]; Fabio Idrobo[3]; Laurel Carney[1]
[1]University of Rochester; [2]University at Buffalo; [3]Boston University

Vowels make a crucial contribution to the intelligibility of running speech, but the neural mechanisms underlying vowel discrimination are poorly understood. Vowels are periodic, harmonic sounds with energy concentrated predominantly below a few kHz. Whereas fundamental frequency (F0; voice pitch) provides prosodic information (e.g., speaker gender and intonation), the basic vowel contrasts are established by differences in the frequencies of vowel formants. Formants are peaks in the spectral envelope of the acoustic signal produced by resonances of the vocal tract. The first two to three formants uniquely identify each vowel.

Here, we examine the neural mechanisms underlying behavioral frequency discrimination of single-formant stimuli in the budgerigar, an avian vocal specialist with the capacity to mimic human speech. Stimuli were synthesized with peak frequencies near 2 kHz, a triangular spectral envelope (200 dB/octave roll off), and a fundamental frequency of 200 Hz. Just noticeable differences (JNDs) for behavioral formant discrimination were estimated using operant conditioning. JNDs were investigated with the formant peak located either near a harmonic (~2 kHz) or between two harmonics (~2.1 kHz), and with or without masking noise. Neural JNDs were estimated for the same stimulus conditions in different, unanaesthetized birds using ROC analyses of multi-unit responses from the inferior colliculus (IC).

Budgerigars showed human-like behavioral sensitivity to changes in formant frequency under all stimulus conditions. Behavioral JNDs were more sensitive when the formant was located between two harmonics than when the formant was located near a single harmonic, as in humans, and more sensitive in quiet than in noise. Neural recording sites in the budgerigar IC typically showed increases in average discharge rate, envelope synchrony to F0, and synchronized rate to F0 as formant frequency shifted from being aligned with a harmonic to being between two harmonics. These patterns can be attributed to an increase in the modulation depth of the stimulus temporal envelope. Neural JNDs based on average rate were sufficient to explain behavioral formant discrimination under quiet conditions but not in noise. In contrast, JNDs based on both envelope synchrony and synchronized rate could explain behavioral JNDs for formant discrimination under all stimulus conditions.

These results suggest that, at the level of the midbrain, budgerigars may detect changes in the frequency of formants

based primarily on differences in neural envelope synchrony to F0. Humans might rely on envelope synchrony as well to achieve similar behavioral sensitivity to changes in formant frequency.

Funding
This work was supported by grants R01-001641 and K99-DC013792 from NIDCD.

PS 148

Neural Coding of Pinna Cues in the Auditory Midbrain

Thomas Varner; Laurel Carney
University of Rochester

Spectral cues introduced by the pinna contribute to the ability to externalize and localize a sound's source, yet relatively little is known about the neural encoding of these cues. Reflections in the pinna introduce high-frequency spectral notches to incoming sound with directional-dependence. These spectral slopes are relatively narrow with respect to the tuning of auditory nerve (AN) fibers, therefore changes in average discharge rates of AN fibers do not provide an accurate representation of the notch frequency. Furthermore, AN phase-locking to fine structure is relatively weak at the high frequencies of the spectral notches, precluding a fine-structure-based temporal code. Here, spectral notches were hypothesized to be encoded in the low-frequency temporal fluctuations caused by the interaction of steep spectral slopes in the stimuli and the sloping skirts of peripheral filters. Modulation-tuned midbrain neurons transform these neural fluctuations into rate profiles. Extracellular responses of inferior colliculus (IC) neurons to wideband sounds with spectral notches were recorded in awake rabbit. Neural responses were interpreted using each cell's response map and modulation transfer function. The spectral notches were represented in the rate profiles of modulation sensitive cells in the IC, consistent with responses of computational models of IC cells. Model IC cell parameters, including best frequency and best modulation frequency were chosen to correspond to those of physiologically characterized neurons. Mechanisms for how sound localization cues may be encoded in populations of IC cells with diverse modulation transfer functions were explored. These results are important for understanding how spectral sound localization and externalization cues are encoded in the auditory midbrain.

Funding
(Supported by NIDCD R01 DC01081)

PS 149

Coding of Sound Level in the Auditory Midbrain of Mammals with Different Hearing Ranges: a Comparative Study

Warren Bakay; Jose Garcia-Lazaro; David McAlpine; Roland Schaette
University College London

Introduction
A remarkable feature of the mammalian auditory system is the ability to accurately encode sounds even though the range of sound intensities greatly exceeds the dynamic range of neurons. Recent studies in guinea pigs have shown that neurons in the inferior colliculus (IC), a major relay nucleus in the auditory midbrain, adapt their firing rates to match the statistics of the ongoing distribution of sound intensities, thus improving coding of the most-commonly occurring sound intensities. (Dean et al 2005). It remains unclear whether this "adaptive coding" is a conserved feature of the mammalian auditory system or specific for the guinea pig. In this study, we therefore assess adaptive coding in three model species with differing hearing ranges.

Methods
We recorded in vivo extracellular responses to acoustic stimuli from neurons in the IC of animals under ketamine-based (mice, gerbils) or urethane-based anaesthesia (guinea pigs). Adaptive coding was assessed with a white noise stimulus where sound level was changed every 50 ms. Sound levels were drawn randomly from a distribution comprising sound levels from 24-96 dB SPL, in to one or more regions of sound levels that were chosen with a probability of 0.8 (high-probability regions, HPRs); the remaining levels were selected with an overall probability of 0.2.

Results
We estimated rate-level functions from the responses to the dynamic stimuli. Preliminary analysis of our data suggests that neurons in the mouse and gerbil IC shift the dynamic range of their responses to match the statistics of the ongoing sound level distribution in a manner that is analogous to that described by Dean et al, (2005 & 2008). However, the extent of adaptation might differ across species. In mice, adaptive coding shifts the threshold of the rate-level functions to higher levels than in gerbils or guinea pigs for similar HPRs. For a more detailed comparison, coding accuracy metrics, e.g. Fisher Information, will be employed.

Summary
In this study we assessed IC responses in rodent species with different hearing ranges to explore whether adaptive coding of sound level might be a conserved mechanism of the mammalian auditory system. Our preliminary results suggest that while adaptive coding occurs in all investigated species, there may be significant differences between animals specialised for low-and high-frequency hearing.

Acknowledgements
This work was supported by an Action on Hearing Loss PhD Studentship (WB) and MRC Grant MR/L022311/1 (RS and JAGL).

PS 150

Dopaminergic Projections of the Subparafascicular Thalamic Nucleus to the Auditory Brainstem, Midbrain, and Thalamus

Alexander Nevue; Cameron Elde; Christine Portfors
Washington State University Vancouver

Background
Sensory processing can be modulated by neurotransmitters, including dopamine. Dopamine, although commonly studied for its role in pleasure and reward, also modulates neuronal responses to sound. It is not entirely clear however, where the dopaminergic inputs to auditory nuclei arise. We previously found that the subparafascicular thalamic nucleus (SPF), part of the A11 dopaminergic cell group, sends dopaminergic projections to the inferior colliculus. The SPF also sends descending projections to the auditory brainstem but it is unknown whether these projections are dopaminergic. The purpose of this study was to determine where in the auditory pathway the SPF projects dopamine. The results from this study will ultimately help elucidate the functional role of the SPF in auditory processing.

Methods
We deposited an anterograde tracer (10K MW BDA) into the SPF of CBA/CaJ adult mice. After seven days survival time, we sectioned the brain from the dorsal cochlear nucleus through the SPF. We stained alternate sections for tyrosine hydroxylase, the rate-limiting enzyme in the dopamine conversion process to identify which anterogradely labeled fibers were dopaminergic. We also stained for dopamine beta hydroxylase (DBH) to differentiate dopamine from noradrenaline. Labeled fibers that were TH positive and DBH negative were identified and imaged using a Leica TCS SP8 confocal microscope.

Results
Anterogradely labeled fibers from the SPF that were TH-positive were seen bilaterally in the medial nucleus of the trapezoid body and the superior periolivary nucleus. Additionally, we observed colocalized fibers in the nuclei of the lateral lemniscus and the medial geniculate body. We did not find any anterogradely labeled TH-positive fibers in the dorsal cochlear nucleus, ventral cochlear nucleus, or auditory cortex.

Conclusions
The SPF sends dopaminergic projections to the auditory brainstem, midbrain, and thalamus. While the function of these dopaminergic neurons is not yet known, these results show that the SPF plays a role in modulating responses properties at multiple levels of the auditory pathway. Future directions include confirming these projections using retrograde tracing, and determining if single SPF neurons are projecting to multiple auditory nuclei.

Funding
This project was funded by NIDCD R01DC013102 to CVP

PS 151

Dopaminergic Modulation of Auditory Responses in the Inferior Colliculus acts via D2-like Receptors

Jeffrey Hoyt[1]; Richard Felix[1]; Christine Portfors[2]
[1]Washington State University Vancouver; [2]Washington State University

Background
The ability to understand speech relies on accurate processing of these sounds by the auditory system. A variety of factors may impede accurate representation, including disorders associated with neuromodulatory systems. For example, individuals with Parkinson's disease suffer from deficits in speech perception, suggesting that dopamine may be involved in the normal encoding of behaviorally-relevant sounds. The inferior colliculus (IC) receives inputs from multiple auditory and non-auditory sources and is rich in both dopaminergic fibers and D2-like receptors. Recent studies in our lab demonstrated that dopamine heterogeneously modulates responses of individual neurons to tones and noise in the IC of mice. However, it is currently unknown which type(s) of dopamine receptors is/are involved in such alteration of neuronal response to auditory stimuli, and whether dopamine affects neuronal response to communication sounds. In this study, we test the following hypotheses: dopamine acts via D2-like receptors to alter auditory-evoked neuronal response in the IC; dopamine alters neuronal response to conspecific vocalizations in the IC.

Methods
We recorded extracellular responses of single neurons in the IC of awake, normal hearing mice. We compared neuronal response to tones, noise, and mouse vocalizations before and after iontophoretic application of dopamine and D1- or D2-like agonists or antagonists. We quantified how activating or blocking dopamine receptors changed the rate and timing of action potential spikes

Results
We found that the effects of both dopamine and a D2-like agonist on spiking rate in IC neurons were heterogeneous as both similarly increased or decreased auditory-evoked responses to pure tones and broadband noise, and in some cases the spike timing was similarly altered. Additionally, both dopamine and a D2-like agonist similarly affected IC neuronal repsonses to vocalizations in the same relative direction as response to tones and noise. Finally, we found that a D2-like antagonist reversed the effect of dopamine.

Conclusions
Our study increases the understanding of neurophysiological mechanisms underlying hearing and auditory-based communication. We found that dopaminergic neuromodulation in the IC acts on responses to behaviorally-relevant sounds and that such modulation occurs via D2-like receptors. Understanding how dopamine modulates auditory processing

will ultimately provide insight into mechanisms underlying specific communication- and auditory-based neurological disorders.

Funding
Supported by NIH NIDCD R01DC013102

PS 152

Dopaminergic Modulation of Auditory Responses in the Bullfrog Inferior Colliculus

Jim Hall; Lilian Carter
University of Tennessee, Knoxville

Background
Anuran (frogs and toads) sexual behavior is mediated almost exclusively by acoustic cues embedded in the species mating call. The mating call, produced only by males, is highly stereotyped, species specific and utilized by females to locate and identify conspecific males for mating. Dopamine is an important neurotransmitter regulating sexual behavior in numerous vertebrate species, including anurans. Dopamine has been shown to modulate auditory processing in the central nervous system of several species. Thus, dopamine may function to enhance neuronal selectivity for behaviorally relevant signals, particularly those involved in mating. However, few studies of dopamine function have utilized socially relevant acoustic signals. Thus, the role of dopaminergic modulation on neural selectivity in the auditory system is poorly understood. The purpose of this study was to examine the effects of dopamine on neural responses in the inferior colliculus (IC) of the bullfrog to both conspecific and heterospecific mating calls. Typical of most vertebrates, the frog IC is a critical nexus for auditory processing, receiving convergent input from most brainstem auditory nuclei. Moreover, dopamine receptors and nerve terminals immunoreactive for tyrosine hydroxylase have been identified in the frog IC. Thus, dopamine modulation in the IC may play a critical role in the processing of the species mating call and guiding sexual behavior.

Methods
We recorded single unit responses in the IC of awake, paralyzed, bullfrogs to a repertoire of conspecific and heterospecific mating calls before, during and after the iontophoretic application of dopamine using piggy-back, multi-barrel electrodes. Changes in firing rate were used as the primary metric when evaluating the effects of dopamine application.

Results
The response of neurons in the IC varied – some responded to most species' mating calls while others showed selectivity for a subset of the calls presented. During dopamine application, the majority of neurons (67%) showed a decrease in firing rate while the firing rate increased for 8% of the cells sampled. In both cases, the magnitude of change was dependent upon the identity of the mating call used. Dopamine application had no effect on firing rate for 25% of the neurons tested.

Conclusion
Dopamine modulates the response of neurons in the IC to behaviorally relevant signals in a stimulus-dependent manner. The mechanisms underlying the observed effects of dopamine are currently under investigation.

Funding
Neuroscience Network of East Tennessee (NeuroNET)

PS 153

Endocannabinoid Modulation of Stimulus-Specific Adaptation in the Inferior Colliculus of the Rat

Catalina Valdés-Baizabal; Gloria Gutiérrez-Parra; Yaneri Ayala; Manuel Malmierca
University of Salamanca

Background
The endocannabinoid system modulates the synaptic transmission by regulating the strength of synaptic inputs in an activity-dependent manner. In the central nervous system, the metabotropic CB1-type receptor is located presynaptically while its ligand, the endocannabinoids (ECBs), is released from the somatodendritic domain of the postsynaptic neuron. Activation of CB1 receptors exerts a transient suppression of glutamate and/or GABA release from presynaptic neurons. Endocannabinoid modulation occurs at distinct auditory centers such as the dorsal and ventral cochlear nuclei, superior olivary complex and cochlear spiral ganglion. However, it is unknown whether ECBs participate on the inferior colliculus (IC) activity. IC neurons exhibit stimulus-specific adaptation (SSA) which is a specific response decrease to repetitive sounds. Since, depletion of neurotransmitter release occurring in repetitively activated inputs is a plausible mechanism for shaping SSA, we study the role of ECBs on SSA in the anesthetized rat.

Methods
We recorded *in vivo* extracellular single-unit responses (n=51) in the IC of ketamine/xylazine anesthetized young- adult Long Evans rats. Neural responses were recorded before and after the systemic application (*i.v.*) of a CB1 antagonist (AM251, 0.5 mg/Kg) or agonist (anandamine, 0.5 mg/Kg). A second agonist (O-2545, 25 mM) was locally applied by iontophoresis using multi-barreled pipettes. Typical retention and injection currents were -15 and 20 nA, respectively. Polarity of the drug application and retention current was selected on basis of the chemical structure of the drug. Acoustic stimulation consisted in two pure tones presented under the so-called oddball paradigm, in which, a high probable tone (standard, 90%) is randomly replaced by a second tone with a low-probability of occurrence (deviant, 10%).

Results
Our results show that ECBs exert a complex modulation on SSA affecting the spike count and firs spike latency for deviant and standard stimulus. AM251 application affects the SSA level in both directions, decreasing (10/29 neurons) or increasing SSA (18/29 neurons, Bootstrapping, 95% C.I). The same occurs with anandamide application which decreases

SSAin 11/22 neurons while exerts an SSA augmentation in 11/22 neurons. We found that O-2545 decrease SSA in most of the cells (5/7). All the drugs also affected the frequency response areaof IC neurons.

Conclusions
Our preliminary conclusion is that ECBs play an active role on shaping SSA responses of IC neurons. Likewise, it is likely that the observed effects on SSA, *i.e*., augmentation or decrease, depend on the strength of ECB modulation on presynaptic GABAergic, and/or glutamatergic neurons or terminals.

Funding
This project was funded by the MINECO grant BFU201343608-P and the JCYL grant SA343U14 to MSM.

PS 154

Genuine Deviance Detection Occurs in the Inferior Colliculus of the Anesthetized Rat

Guillermo Carbajal; Javier Nieto-Diego; Gloria Parras; Manuel Malmierca
University of Salamanca

Background
A class of neurons in the inferior colliculus (IC) show stronger responses to tones when presented as deviants than when presented as standards in the context of the "oddball" paradigm. This difference can be accounted for by stimulus-specific adaptation (SSA), an attenuation of the response to the repetitive standard tone that does not affect, or affects very little, the response to the less frequent deviant tone. On the other hand, the response to the deviant tone could also be enhanced by the fact that it breaks the regularity imposed by the standard, thus containing a component of "deviance detection". Yet, the contribution of deviance-related effects to single-neuron responses remains to be tested in subcortical stations of the auditory pathway.

Methods
We performed extracellular recordings of well isolated single neurons from all subdivisions of the IC in anesthetized adult Long-Evans rats. All stimuli were pure tones of 75 ms duration. One or more target sounds were selected from within each neuron's frequency response area, at different frequencies and intensities.

Each target sound was presented in the context of the "oddball" paradigm and the "many standards control" (Jacobsen and Schröger, 2001), in which the test sound retains its rarity without being a deviant any more. We also used the more conservative "deviant-alone" control, in which the deviant sound is presented whith no intervening standards, thus preventing any effect of cross-frequency adaptation.

Results
To dissociate the relative contribution of SSA and deviance-detection for each neuron, we normalized individual responses to the MSC response.

Individual responses to the deviant sound tended to be equal to or larger than responses to both the MSC and the deviant-alone control. This trend was significant at the population level, and the deviance-detection component was more prominent for low than for high intensity stimuli. Importantly, some individual neurons showed a highly specific sensitivity to deviant stimuli.

Conclusions
Our results provide compelling evidence for the existence of deviance-detector units in the auditory system as early as the level of the midbrain.

Funding
This project was funded by the MINECO grant BFU201343608-P and the JCYL grant SA343U14 to M.S.M. J.N.D. held a JCYL fellowship (ERIDI2007-2013)

PS 155

Neurons in the Auditory Thalamus exhibit Genuine Deviant Detection.

Gloria Gutiérrez-Parras; Javier Nieto-Diego; Guillermo Carbajal; Manuel Malmierca
University of Salamanca

Background
The ability to detect new events or changes in the environment is critical for survival. Hence, some neurons in sensory systems show Stimulus-Specific Adaptation (SSA), the ability to adapt their responses to frequent or "standard" stimuli, whereas responses to infrequent or "deviant" stimuli remain unaffected. Furthermore, responses to deviants could be even enhanced by the fact that they break the regularity imposed by standard stimuli, thus showing genuine deviance detection.

In the auditory system, some neurons of the medial geniculate body (MGB) show SSA. However, whether or not these MGB neurons also show genuine deviance detection remains to be tested. Jacobsen and Schröger (2001) originally designed the so-called "many standards" control (MSC) to assess the response to the deviant tone while controlling for its mere rarity. The comparison between the responses to the deviant stimulus presented in the context of the oddball paradigm and the MSC will thus provide us with a real estimation of a deviance detection component.

Methods
We recorded well isolated single units within different subdivisions of the MGB in anesthetized adult Long-Evans rats. One or more target sounds were selected from within each neuron's frequency response area, at different frequencies and intensities. Then we stimulated the animal using an oddball paradigm and the MSC. We also presented a "deviant alone" control which is supposed to produce the highest possible unadapted response to a given tone.

Results
Our results show that some MGB neurons show enhanced responses to the deviant tone with respect to the same tone when presented in the context of the MSC. We also found

that responses to low intensity tones contain a relatively larger component of deviance detection than responses to high intensity tones.

Conclusions
Therefore, our results allow us to conclude that a population of neurons in the auditory thalamus show clear signs of deviance detection in their responses to the oddball paradigm.

Funding
This project was funded by the MINECO grant BFU201343608-P and the JCYL grant SA343U14 to M.S.M., G.G.P., J.N.D

PS 156

Responses of Neurons in the Rat's Inferior Colliculus to Both Standard and Deviant Sounds in an Oddball Paradigm Are Dependent on the Spatial Relationship between the Sounds

Huiming Zhang; Chirag Patel
University of Windsor

Previous studies on neural sensitivity to novel sounds were conducted using oddball paradigms presented to one single ear. Using such paradigms, people have found that neurons in the rat's midbrain auditory structure the inferior colliculus (IC) generate stronger responses to a tone burst presented to the contralateral ear as a deviant (Dev) than as a standard (Std) sound. As a major integration center in the auditory system, the IC receives monaural and binaural inputs from structures on both sides of the brain. Integration among these inputs makes responses of IC neurons sensitive to binaural cues. In the present study, we wanted to examine whether responses of IC neurons to Dev and Std in an oddball paradigm were dependent on the spatial relationship between the sounds.

Action potential discharges in response to oddball paradigms were recorded from single neurons in the IC of anaesthetized rats. For a neuron with the best frequency at BF, the tone bursts for creating an oddball paradigm had frequencies at 0.951BF and 1.051BF (named as T_L or T_H) and intensity at 10 dB above the threshold at BF. Each oddball paradigm had a total of 200 sound presentations delivered at a constant rate of 4 /s. Each tone burst (T_L or T_H) was presented at a 90% probability (Std) in one oddball paradigm and at a 10% probability (Dev) in a complementary paradigm. T_L and T_H were presented from one single speaker or two spatially separated speakers.

Results indicated that IC neurons had various degrees of sensitivity to Dev when Std and Dev were both presented from a single speaker (i.e., co-localized) at the frontal midline (0°). The degrees were comparable with those shown by previous studies in which oddball paradigms were presented monaurally at the contralateral ear. When one sound in an oddball paradigm was relocated from 0° to an off-0° azimuth (either as Std or Dev), responses to this sound was changed. For most neurons, a reduction was observed when the sound was relocated to an ipsilateral azimuth. For many neurons, relocating one sound from 0° to an off-0° azimuth also changed the response to the sound remained at 0°. Most notably, the majority of neurons reduced their responses to an Std at 0° when the Dev was relocated to a contralateral azimuth.

Our results indicate that spatial separation changes responses to both Std and Dev in an oddball paradigm.

Funding
Natural Science and Engineering Research Council of Canada to HZ.

PS 157

Round Window Stimulation via a Conforming Coupler

Darcy Frear[1]; Hideko Nakajima[2]; Christof Stieger[3]
[1]Harvard University; [2]Harvard Medical School, Massachusetts Eye and Ear; [3]University Hospital Basel

Background
Instead of introducing sound to the inner ear by mechanically stimulating the oval window (as in normal air conduction), the cochlea can be driven in "reverse" by mechanically stimulating the round window (RW). Commercially available devices like the Vibrant Soundbridge floating mass transducer (FMT) are used for RW stimulation and other actuators have been proposed to reverse stimulate the cochlea. Hearing results with RW stimulation are sometimes good, but have been shown to be inconsistent across ears. To account for the variability among ears and to ensure the safety of the delicate RW membrane, we have developed a conformable coupler – a device that conforms to the shape of the RW niche and couples the volume velocity of an actuator to the RW membrane.

Methods
The coupler interfaces the delicate round-window membrane with a fluid-filled flexible balloon that is driven on one side by the motion of an actuator. Comparisons were made on fresh cadaveric human specimens with the different devices: RW coupler, direct rod tip driven by a piezoelectric device, and the FMT coupled and secured in an optimal configuration. In each ear, the stapes velocity was recorded using laser Doppler vibrometry in response to RW stimulation by the different devices.

Results
Preliminary data indicate improvement of sound transmission when using the coupler compared to direct rod stimulation. The coupler also has an improvement of sound transduction below 1 kHz as compared to the FMT. Overall, preliminary measurements suggest that the conformable coupler provides an improved method to stimulate the RW membrane. This coupler conforms to largely differing anatomy at the RW niche with no (or minimal) drilling of the bony overhang, which decreases the chances of cochlear trauma. The compliant interface more safely couples vibration to the delicate RW membrane, and the overall actuation method can be made to be more mechanically stable and consistent across ears.

Conclusion
The conforming RW coupler provides an alternative and effective way to stimulate the RW membrane and is less affected by anatomical variations in the middle and inner ear.

Funding
This project was supported by NIDCD/NIH R01DC013303 and the Speech and Hearing Bioscience and Technology NIH Training Grant.

PS 158

The Effect of Conical Shape on Sound Induced Motion Patterns of Human and 3D Printed Tympanic Membranes

Aaron Remenschneider[1,2]; Elliott Kozin[1,2]; Nicole Black[3]; Jeffrey Cheng[2]; Jennifer Lewis[3]; John Rosowski[2]
[1]Eaton Peabody Laboratory; [2]Massachusetts Eye and Ear Infirmary; [3]Harvard University

Background
The tympanic membrane (TM) is a complex structure that captures and transmits sound from the environment to the ossicles of the middle ear. Contemporary tympanoplasty techniques utilize tissues, such as temporalis fascia, to re-establish a barrier between the ear canal and middle ear, thereby improving sound transmission. Unfortunately, fascia does not possess the fibrous scaffold architecture or conical shape of the human TM. The lack of these features may, in part, explain why up to 30% of TM grafts fail following surgery and many patients experience post-operative conductive hearing loss. Recent advances in 3-dimensional (3D) printing allow the fabrication of biologic scaffolds on a micron scale. We hypothesize that biomimetic 3D printed TM grafts experience varied sound induced motion patterns dependent upon the graft's conical depth.

Methods
Scanning electron microscopic images of the human TM were used to design 3D TM scaffold architecture. Using filamentary extrusion 3D printing on a custom Aerotech printer, TM graft scaffolds were created using polydimethylsiloxane with fixed circular and radial fiber arrangements but varying conical depths: 0 (flat), 1, 2 and 3mm. Each TM scaffold was infilled with a bovine fibrin hydrogel. Human cadaveric TMs supported by the bony annulus but uncoupled from the middle ear load served as controls. Digital optical electronic holography (DOEH) and laser Doppler vibrometry (LDV) were used to compare acoustic responses of 3D printed TM composite grafts to cadaveric human specimens.

Results
TM composite grafts of varying conical depths all showed frequency dependent surface motion patterns that are similar to the cadaveric TM, ranging from simple (<1000Hz) through complex (3000Hz) to ordered (6000Hz). However, the absolute displacement of grafts relative to sound pressure level is affected by the depth of conical shape. Flat composite grafts generally move less than the conical shaped grafts above 1000 Hz. Cones with a depth of 1mm have relatively larger surface motion and point velocity than others. LDV demonstrated consistent velocity patterns across frequency sweeps (0.1~10,kHz) for composite grafts and cadaveric TMs. Maximal displacement and point velocity as measured by DOEH and LDV varied between cones of different depths.

Conclusion
3D printers can fabricate biomimetic TM scaffolds with a conical shape that approximate motion of human TM. These data have implications for 1) the clinical application of 3D printed biomimetic TMs and 2) the ability to isolate specific TM structural features for direct measurement or validation through finite element models.

Funding
American Otological Society Research Grant

PS 159

Middle Ear Responses to Low Frequencies and the Effect of Semicircular Canal Dehiscence

Stefan Raufer; Hideko Nakajima
Harvard Medical School, Massachusetts Eye & Ear

Background
Detection of low-frequency sounds (including frequencies below the sensitive human hearing range) and the relation to possible health effects such as vestibular and auditory ailments is of great interest, yet is poorly understood. Most of the studies conducted on infrasound-related health complaints are inconclusive, especially because symptoms reported by patients are subjective (such as being annoyed or fatigued by the sensation of these sounds). The behavior of middle ear structures or the inner ear in this frequency range has not been characterized in detail. Current research does not indicate how these sounds reach the peripheral auditory or vestibular system. Our goal is to better understand human low-frequency hearing with objective measurements conducted on fresh cadaveric human temporal bones.

Methods
Fresh human temporal bones were prepared to study umbo, stapes, and round-window membrane (RW) velocities at low frequencies between 0.6—500Hz and sound-pressure levels of 80—120dB SPL. Low-noise laser-Doppler vibrometry (LDV) was used to measure responses of middle-ear bones and RW to these sounds.

Results
Our measurements of stapes and umbo velocities suggest that the middle ear operates linearly in the measured frequency and intensity range, where the admittance decreases by approximately 20dB per decade below 500Hz and plateaus out below 2Hz. To determine the effect of an inner-ear low-impedance path, a semicircular canal dehiscence (SCD) was made and the stapes and RW velocities at low frequencies were measured. As expected, the stapes and round-window membrane move in opposite directions (1/2-cycle difference) at frequencies below 300—500Hz in normal ears. After opening the lateral aspect of the superior semicircular canal, the ½-cycle difference broke down, leaving an imperfect

phase difference between the two measures. The frequency at which the phase transition happened could be manipulated by the SCD size. The frequency-dependent magnitude of the ratio between RW and stapes velocities at low frequencies was also affected and monotonically changed with SCD size. However, across ears, the absolute value of effect on velocities varied for similar SCD sizes.

Conclusion
Our preliminary findings suggest that at frequencies below 300—500Hz, leaks in the inner ear result in considerable alterations of RW velocities, while stapes movements are hardly affected. Future research will show how intra-cochlear pressures, i.e. a correlate of hearing sensitivity, are affected by low-impedance paths in the cochlea at low frequencies.

Funding
German National Academic Foundation, Harvard Medical School Study Grant

PS 160

Middle Ear Sound Transmission under Repair and Reconstructed Conditions

Wei Dong[1,2]; Ying Tian[1]; Xin Gao[1]; **Timothy Jung**[2]
[1]VA Loma Linda Healthcare System; [2]Loma Linda University Healthcare

Background
Sound-evoked vibrations of the tympanic membrane and ossicular chain are complex and highly frequency-dependent. At low frequencies, the three ossicles move together as one 'rigid' body, in a rather simple rotational mode. However, with increasing frequency, the motion of ossicles becomes more complicated. Damaging the middle ear structure results in conductive hearing loss of up to 60–70 dB. Significant efforts have been made to restore hearing clinically by repairing or reconstructing middle ears using partial/total replacement of the ossicular chain prosthesis (PORP/TORP). However, the outcome of post-operative hearing varies and some are still far from ideal. The current study seeks to advance our understanding of the underlying mechanisms of conductive hearing loss resulting from ossicular chain damage, along with the effectiveness of repair/reconstruction strategies

Methods
This study was approved by the Institutional Review Board of Loma Linda VA Healthcare System. Temporal bones were used and the middle ear and the cochlea were approached using clinical facial access. Pure tone stimuli, 20–20,000 Hz, were generated digitally using TDT system III and delivered via a closed-sound system with a Fostex speaker. Under normal and abnormal conditions (damaged/repaired/reconstructed), velocity responses along the ossicular chain were measured using Laser Doppler Vibrometer (OFV 5000). Simultaneously, intracochlar pressure responses next to the stapes' footplate were measured via introducing a micro-pressure-sensor in scala vestibule through a hand-drilled hole.

Results
Middle ear transmission was characterized by (1) local transfer function (LTF), defined as the ratio of velocity of ossicle to ear canal pressure at the umbo ($V_{ossicle}/P_{EC}$); and (2) pressure gain (MPG), the ratio of sound pressure in scala vestibule to that of the ear canal at the umbo (P_{SV}/P_{EC}). Under normal condition, the LTFs along the ossicular chain and MPG were consistent with previous studies and formed the basis for comparison with those under abnormal conditions. Disarticulation of the incus and stapes caused more than 40 dB loss. Fixing the incus and stapes with medical glue restored responses at the stapes almost perfectly at frequencies below 5 kHz. As frequencies increased, more loss was found. Replacing the incus with PORP gave similar results as that of the fixation.

Conclusions
Combining velocity and pressure measurements advances our understanding of the structure-function relationships under pathological conditions. Vibration of ossicles in three-dimensional space is important to hearing especially at frequencies above 5 kHz, which suggests that flexible middle ear prosthesis may needed for ideal restoration.

Funding
NIDCD R01DC011506

PS 161

Optimization of Zwislocki's Human Middle-ear Circuit Model to Fit Modern Data

Peter Bowers; John Rosowski
Harvard University

The parameters of the classic Zwislocki model for the input impedance of the human ear were optimized to fit more modern impedance and transfer-function data. Unspecified values of the original model were estimated from published model predictions to provide a complete model for comparison; the two undefined values of the original model—the resistances of the aditus to mastoid antrum and of the tympanic cavity walls and Eustachian tube—were defined using a least-squares fit procedure. Other model parameters were then optimized using subjective and objective methods to fit experimental data of human middle-ear input impedance, stapes velocity transfer function, cochlear input impedance, and middle-ear cavity impedance. The sensitivity of model outcomes to different parameters was assessed using a normalized root-mean-square of the percent change in model predictions produced by +/- 10% changes in model parameters.

Funding
Speech and Hearing Bioscience and Technology, NIH Training Grants: 5 T32 DC000038-23 5 T32 DC000038-24

PS 162

Experimental modal analysis of tympanic-membrane vibration

Nima Maftoon[1]; Payam Razavi[2]; Ivo Dobrev[2]; Michael Ravicz[1]; Jeffrey Cheng[1]; Cosme Furlong[2]; John Rosowski[1]
[1]Harvard Medical School; [2]Worcester Polytechnic Institute

Our new high-speed digital holography system with a temporal resolution of less than 24 μs (Dobrev et al., J. Biomed. Opt. 2014; 19(9): 096001) enables us to measure responses of the tympanic membrane to transient stimuli. This gives us

an unprecedented opportunity to perform structural system identification of the motion of the tympanic membrane to determine its natural frequencies, damping and mode shapes using experimental modal analysis techniques. The transient displacement of the tympanic-membrane in response to an acoustic click measured using high-speed holography and the phase-locked transient pressure profile measured near the superior tympanic membrane rim were converted to the frequency domain using the Fourier transform. Frequency-response functions were calculated for all the measured tympanic membrane points by dividing the displacement by the pressure in the frequency domain. The impulse response functions, for each tympanic membrane point, were calculated by converting the frequency response functions back to the time domain. The complex exponential time-domain method was then applied to the impulse response functions to find the structure poles. The identification was done with a varying over-specified modal order to avoid identification bias and the unphysical poles (poles without a complex conjugate pair and poles with non-negative real components) were rejected. Mode shapes were calculated using the least-square frequency domain method based on the identified poles. Natural frequencies and modal damping were also derived from the identified poles. Damping, obtained in this study, is the least known material property of the tympanic membrane. The natural frequencies and mode shapes can be used to estimate material properties of the tympanic membrane in an inverse problem using finite-element model updating methods (e.g., Mottershead & Friswell, J Sound Vib 1993; 167(2): 347-375). This study also increases our understanding of wave motion on the tympanic membrane.

Funding
This work was supported by a funding from NIH/NIDCD (R01-DC008642).

PS 163

Wideband Acoustic Reflex Thresholds: A Preliminary Study in Adult Ears with Self-Induced Middle Ear Pressure

Xiao-Ming Sun[1]; Bailey McCoy[1]; Mitchell Frye[2]
[1]Wichita State University; [2]University at Buffalo The State University of New York

Background
Wideband acoustic immittance measurements assess middle ear function using wideband probe sounds (e.g. clicks). The procedure has been applied to measuring middle ear muscle reflexes, referred to as wideband acoustic reflex (WAR) test. This study aimed to examine the effect of middle ear pressure (MEP) on WAR thresholds, validity of a pressure compensation procedure, and test-retest variability.

Methods
WAR measurements were conducted in 21 young adults using a wideband tympanometry system (Interacoustics) with clicks as the probe and broadband noise as the reflex-activating stimulus. The activator was presented in 5-dB steps from 45 to 90 dB SPL in the same ear as the probe, i.e., ipsilateral test (ipsi-WAR), or in the other ear, i.e., contralateral test (contra-WAR). The WAR threshold was determined in two spectral bandwidths, low-frequency (0.38–2.8 kHz, θ_L) and high-frequency (2.8–8 kHz, θ_H). Both WAR tests were performed in two modes: at ambient pressure and at tympanogram peak pressure (TPP), which presumably counterbalances any non-zero MEP. Each test was duplicated. All tests were run before and after an MEP was induced. Subjects produced a positive MEP (pMEP) by performing the Valsalva maneuver and/or negative MEP (nMEP) by the Toynbee maneuver.

Results
For ipsi-WAR tests under nMEP (−108.5±70.2 daPa, n=10), the mean θ_L and θ_H were elevated by 11.0 (±5.7) and 11.5 (±12.5) dB, respectively (p<0.05, pared t-test), compared to the baseline. When tested at TPP, the changes of θ_L and θ_H were −5.5 (±6.4) dB (p<0.05) and 5.5 (±9.6) dB (p>0.05). For ipsi-WAR tests under pMEP (95.0±53.9 daPa, n=6), mean θ_L and θ_H were increased by 8.3 (±8.2) and 4.2 (±10.2) dB (p>0.05). For contra-WAR tests under nMEP (−108.2±38.8 daPa, n=11), mean θ_L and θ_H were increased by 15.0 (±15.3) and 11.0 (±14.1) dB (p<0.05). When tested at TPP, the changes of θ_L and θ_H were −2.7 (±4.7) and 2.5 (±17.0) dB (p>0.05). With data pooled for all ears (n=27) tested under MEP, the test-retest difference in θ_L and θ_H were 3.3 (±7.3) and 3.0 (±7.5) dB (p>0.05).

Conclusions
nMEP significantly increases both θ_L and θ_H by 10 dB or more for both ipsi-WAR and contra-WAR tests. The WAR test at TPP mode effectively rectifies the elevated thresholds, but it tends to cause a slight reduction of θ_L. pMEP tends to result in similar effects while not statistically significant due to a small sample size. The test-retest reliability of WAR tested in ears with MEP is good.

PS 164

Wave propagation on the surface of the skull in bone conduction stimulation

Christof Röösli[1]; Ivo Dobrev[1]; Jae Hoon Sim[1]; Rahel Gerig[1]; Adrian Dalbert[1]; Stefan Stenfelt[2]; Alex Huber[1]
[1]University Hospital Zürich; [2]Linköping University

Background
Bone conduction (BC) is an alternative to air conduction to stimulate the inner ear. In general, the stimulation for BC occurs on a specific location directly on the skull bone or through the skin covering the skull bone. The stimulation propagates to the ipsilateral and contralateral cochlea, mainly via the skull bone and possibly via other skull contents. This study aims to investigate on wave propagation on the surface of the skull bone during BC stimulation for stimulation on the mastoid.

Methods
Measurements were performed in three human cadaveric whole heads. A bone anchored hearing aid (BAHA) was attached to a percutaneously implanted screw or positioned with a 5-N steel headband at the mastoid. The BAHA was directly driven with stepped-sine signals in the frequency range of 0.1 – 10 kHz for measurement in frequency domain,

and two-cycle sine signals in the frequency range of 0.5 – 8 kHz for measurements in time domain. Simultaneously, skull bone vibrations were measured at multiple points on the skull using a Scanning Laser Doppler Vibrometer (LDV) system and a 3D LDV system. The 3D velocity components, defined by 3D LDV coordinate system, have been transformed into tangent (in-plane) and normal (out-of-plane) components in a local intrinsic coordinate system at each measurement point, which is based on the cadaver head's shape estimated by the spatial locations of all measurement points.

Results

Rigid body motion were dominant at low frequencies below 1 kHz, and clear transverse traveling waves were observed at high frequencies above 2 kHz for both measurement systems. The wave speed was about 450 m/s, and the corresponding trans-cranial time interval was 0.4 ms. The 3D velocity measurements confirmed the complex spatial and frequency dependence of the response of the cadaver heads indicated by the 1D data from the scanning LDV system. The tangent and normal components of the 3D velocity data, defined in a local intrinsic coordinate system at each measurement point, indicate higher magnitudes of the normal component with spatially varying phase at higher frequencies (i.e. > 2 kHz), being consistent with local bending vibration modes and traveling surface waves.

Conclusion

Both scanning LDV and 3D LDV data indicate that in propagation of sound waves along the skull bone, standing waves were dominant at low frequencies, whereas transverse (i.e. out-of-plane) travelling waves with a speed of 450 m/s were observed above 2 kHz.

PS 165

Sound transmission via the malleus-incus complex – dependence on physiological condition

Ivo Dobrev[1]; Rahel Gerig[1]; Sebastian Ihrle[2]; Christof Röösli[1]; Albrecht Eiber[2]; Alexander Huber[1]; Jae Hoon Sim[1]
[1]University Hospital Zurich; [2]University of Stuttgart

Background

The malleus-incus complex (MIC) plays a crucial role in the hearing process as it transforms and transmits acoustically-induced motion of the tympanic membrane, through the stapes, towards the inner-ear. However, the transfer function of the MIC under physiologically-relevant acoustic stimulation is still not fully elucidated. Further, measurements of the transfer function of the MIC are typically done on frozen temporal bones. While generally frozen temporal bones are accepted to be mechanically equivalent to fresh samples and living humans, there may still be significant physiological changes in the MIC transfer function with freezing. This study investigates three-dimensional motions of the malleus and incus with a full six degrees of freedom (6 DOF) in frozen and fresh temporal bones.

Methods

The motion of the MIC was measured in sets of frozen and fresh cadaveric human temporal bones with intact middle-ear structures excited via a loud speaker, embedded in an artificial ear canal. Three-dimensional (3D) shapes of the middle-ear ossicles were obtained by sequent micro-CT imaging, and an intrinsic frame based on the middle-ear anatomy was defined. All data were registered into the intrinsic frame, and rigid body motions of the malleus and incus were calculated with full six degrees of freedom.

Results

The preliminary results indicate that the hinged rotational motion is dominant at frequencies below 1.5 kHz , but the motion of the malleus and incus becomes complex with clear relative motion between the malleus and the incus at higher frequencies, for both fresh and frozen temporal bones. While the hinged rotational motion is larger at lower frequencies for the fresh temporal bones, the frozen temporal bones show similar magnitudes of the hinged rotational motion along the entire frequency range..

Conclusion

Effects of the MIC physiological conditions on the sound transmission have been analyzed based on the measurement of the full three-dimensional motions of the MIC.

Keywords

Malleus-Incus complex, 3D Laser Doppler Vibrometer, rigid-body motion, human middle-ear, 3D transfer function, incudo-malleolar joint; micro-CT, fresh and frozen temporal bones

Funding

This work has been funded by the Swiss national science foundation grant 138426 and German Reseach Council project number EI 236/6-1.

PS 166

Objective measurement in single side deafness and conductive hearing loss patients using a transcutaneous bone conduction Implant (Bonebridge)

Mohammad Ghoncheh; Thomas Lenarz; Hannes Maier
Medical University Hannover

Background

The intraoperative objective functional assessment of transcutaneous bone conduction implants is still a challenge because the physical access to the implant and the transducer is limited after implantation. This study primarily aims to show that Laser-Doppler-vibrometry and Outer Ear Canal Sound Pressure Level (OEC-SPL) can equivalently be used to determine the functionality of the implants. Second goal was to determine the dominant origin of the measured sound pressure in the outer ear canal.

Method

Here we compared vibration of the bone close to the implant measured intraoperatively by Laser-Doppler-vibrometer (LDV, Polytec Inc.) to OEC-SPL measurements in eleven single sided deafness (SSD) patients with contralateral intact

ossicular chains and eight conductive hearing loss (CHL) patients. All patients were implanted with a transcutaneous bone conduction implants (Bonebridge, MED-EL, Austria). SSD patients with a normal transmission between cochlea and the tympanic membrane on the contralateral side had a minor air-bone-gap (ABG) of 0.2 ± 0.4 dB (0.5, 1, 2, 4 kHz mean value (MV) ± standard deviation (SD)). However, in CHL patients an impaired middle ear existed with mean ABG of 47.5 ± 6.6 dB. The signal to noise ratio was higher than 12 dB in all measurements.

Results

Average displacement and OEC-SPL were strongly correlated in SSD (r^2=0.76) and CHL (r^2=0.86) patients. However, the correlation across individual results was weaker. When comparing results from Outer Ear Canal Sound Pressure Level in SSD and CHL patients no significant differences (t-test, $p<0.05$) were found. In addition, the transcranial attenuation (contralateral outer ear canal sound pressure vs ipsilateral) was calculated and compared to previous studies measuring vibration by LDV and accelerometer. The trend in the average data in patients was similar to previous studies measuring the OEC-SPL with less than 5 dB difference.

Conclusion

High correlation among the LDV and OEC-SPL shows that these measurements can be reliably used for intraoperative testing with sufficient signal-to-noise ratio. Further, OEC-SPL provides an easy, affordable and quantitative measurement tool to monitor the functionality of the implants, also postoperatively where the LDV measurement is not applicable. The comparison of OEC-SPL between CHL and SSD patients implies that the part of the measured sound pressure in the ear canal originating from the cochlea and emitted by the tympanic is not dominant and OEC-SPL is mainly due to emissions by the external ear-canal walls.

Funding

This work is supported by the DFG Cluster of Excellence EXC 1077/1 “Hearing4all”. The authors received travel support to conferences by MED-El.

PS 167

Vibration Patterns of the Bullfrog Tympanic Membrane

Sebastiaan Meenderink[1]; Christopher Bergevin[2]; Marcel van der Heijden[3]; Peter Narins[1]

[1]University of California, Los Angeles; [2]York University; [3]Erasmus MC

Introduction

Frogs are amazing. For example, they may turn into a prince when thrown against a wall (or kissed, depending on the story’s version). Also amazing, and unique among tetrapods, is the relatively long delay associated with forward transmission of sounds through the tympanic middle ear (~30x longer than in gerbil). The largest fraction of this delay is between the external sound pressure and the induced motion at the center of the tympanic membrane (TyM), where the single, middle-ear ossicle is attached. The present study sought to investigate the basis for this lag by mapping the velocity profile of the TyM using laser Doppler vibrometry.

Methods

Recordings were obtained from the tympani of adult American bullfrogs (*R. catesbeiana*) under free-field conditions. After the induction of anesthesia, the frog was placed inside a double-walled sound-attenuating chamber. A scanning laser Doppler vibrometer that allows the acquisition of vibration velocity across a user-defined grid, was used to map responses over the entire TyM surface. Stimuli were presented from a speaker which was in line with the incident laser beam, and positioned ~20 cm from the TyM. A microphone was placed in close proximity of the ipsilateral TyM, and its signal served as a reference to vibrometric recordings. Stimulus waveforms were tailored to study energy propagation along the tympanum, and consisted either of frequency sweeps or tone complexes with multiple inharmonic frequency components.

Results & Discussion

In our data, both the phase lags and group delays increase from the edge of the tympanum toward the membrane’s center (where the single ossicle is attached). These observations strongly suggest the presence of (radially symmetric) traveling waves on the surface of the TyM. This pattern occurs over a range of stimulus frequencies that corresponds to the range of bullfrog hearing (500 – 1700 Hz). For higher frequencies, the TyM vibrations are more complex. To capture the essential features, we propose a relatively simple model in which the TyM is a transmission line that couples the surrounding ear to the center of the TyM (i.e. the middle ear ossicle and inner ear). At those frequencies for which the characteristic impedances of the transitions are well matched, the response is dominated by a (slow) traveling wave. Mismatches between these impedances cause (partial) reflection of the propagating energy, resulting in multiple waves that propagate in opposite directions. Their interference causes standing waves or a response that is more complex.

PS 168

Preliminary Studies of the Design and Manufacture of Custom Middle Ear Prostheses

Brandon Kamrava[1]; Jonathan Gerstenhaber[2]; Yah-el Har-el[2]; Pamela Roehm[1]

[1]Temple University School of Medicine; [2]Temple University

Background

Ossicular discontinuity or fixation occurs in 55% of cases of conductive hearing loss. The majority of ossicular chain disorders affect the incus. Reconstruction has been achieved by a variety of methods including use of autograft incudes modified at the time of surgery, allograft incudes with similar intraoperative modification, iontomeric bone cement, and manufactured ossicular prostheses. Overall, there has been little improvement in hearing outcomes after ossiculoplasty in the past 50 years. We hypothesize that custom prostheses could be used to recreate the intact ossicular chain and improve hearing outcomes. We used a variety of 3-dimensional (3D) synthetic techniques to make custom artificial incus prostheses.

Methods
Precise measurement of the length, weight, major anatomical features, articular surface, and center of gravity were made on 38 cadaveric incudes. These measurements were combined with measurements published in the literature and micro-computed tomography (microCT) of cadaveric temporal bones at 25 microns resolution to generate a rasterizable idealized incus model. Using the model, a series of custom artificial incudes were synthesized and compared with the incudal measurements. Synthetic methods utilized included direct 3D printing, 3D printing with burnout to create a hollow model, printing of a mold for injection casting, milling from zirconia, and milling from titanium.

Results
Our cadaveric measurements corresponded well with those compiled from the medical literature. Using these measurements plus anatomical information from temporal bone microCT, the critical features of the incus, including the center of gravity and articular surfaces, remained in incudal model. As synthesis trials proceeded, incudal model features were modified to increase stability and facilitate synthesis, including broadening and thickening of the incudo-malleolar articulation surface and thickening of the lenticular process. Milling from titanium yielded artificial incudes that were too heavy, while milling from zirconia resulted in fragile incudes. Small features of the incudes were lost during casting from molds. Current 3D technology for direct printing of incudes in hydroxyapatite is limited at the lower bound of resolution, and cannot be utilized at the present time for incudal replacement synthesis. However, incudes printed from polylactic acid (PLA) at highest resolution are the size and shape required for custom incudes.

Conclusion
We have generated a rasterizable model for custom 3D synthesis of incudal prostheses. While current 3D printing in biocompatible materials at the size required is limited, the technology available is rapidly advancing, and 3D printing of incudal replacements with PLA is of the correct size and shape.

PS 169

The Sheep as a Large Animal Model: Transfer Function of the Middle Ear and Intracochlear Pressure

Dominik Péus[1]; Flurin Pfiffner[1]; Ivo Dobrev[1]; Lukas Prochazka[2]; Konrad Thoele[1]; Jae Hoon Sim[1]; Rahel Gerig[1]; Adrian Dalbert[1]; Francesca Harris[3]; Joris Walraevens[3]; Christof Röösli[1]; Alexander Huber[1]
[1]University Hospital Zurich; [2]Swiss Federal Institute of Technology (ETHZ) and Streamwise GmbH; [3]Cochlear Technology Centre

Background
Animal models are frequently used for the development, testing and establishment of new hearing devices. The middle ear and cochlea of many extensively examined animals such as rodents and cats differ significantly in dimension from that of humans. The sheep cochlea has been shown to be similar in its anatomical dimensions to the human cochlea. It has been used as a surgical training model for cochlear implants (CIs), but little is known about its function. The current study investigates the middle ear transfer function and intracochlear pressure in sheep temporal bones, with the aim of characterising the usefulness of sheep as a future experimental model for implantable hearing devices.

Method
In this experimental study, fresh sheep temporal bones were used. Firstly, velocities of the ossicles were measured with a laser Doppler vibrometer (LDV) in response to acoustic stimuli while sound pressure in the external auditory canal was recorded. Secondly, intracochlear pressure was recorded in the same temporal bones with the same stimuli using a newly-developed MEMS condenser hydrophone at different locations within the inner ear. Subsequently, micro-computed tomography and 3D reconstructions of the temporal bones were used to confirm the measurement sites.

Results
The measured umbo velocity, normalized for the ear canal pressure, was similar to previously reported data in humans at low frequencies (i.e. < 2 kHz); however, it was larger at higher frequencies. Middle ear pressure gains, derived from measurements in the scala tympani and in the external ear canal, were in agreement with our measurements of the middle ear ossicles, indicating larger gains at higher frequencies.

Conclusion
This work provides quantitative data regarding the middle ear transfer function and intracochlear pressure in sheep temporal bones. The results are compared to measurements in human temporal bones and published data in other species. Despite the anatomical differences with humans, particularly regarding the middle ear, we conclude that sheep are a comparative large animal model which is applicable to the research and development of implantable hearing devices.

Funding
This work is supported by a project “New receiver technology for totally implantable cochlear implants” funded by Cochlear Ltd.

PS 170

Stapes Velocities and Intracochlear Pressures for Differing Modes of Stimulation with an Implantable Middle Ear Hearing Device

James Easter[1]; Nathaniel Greene[2]; Daniel Tollin[2]; Stephen Cass[2]
[1]Cochlear Boulder LLC; [2]University of Colorado School of Medicine

Introduction
Middle ear transducers stimulate the cochlea by directly vibrating the ossicular chain. This stimulation is highly dependent upon coupling method, and a previous study from our laboratory suggested that stapes velocity is greater for attachments nearer the oval window. Here, stapes velocity

and intracochlear pressure were measured in human temporal bones using a middle ear actuator (Cochlear Boulder MET-7500). Configurations tested were a piston in contact with the incus body, a clip attached to the incus long process, and a bell attachment to the stapes capitulum.

Methods
An extended mastoidectomy was performed, exposing malleus handle, incus body and long process, posterior crus of the stapes and stapes tendon, a portion of the stapes footplate and the RWM. Pressure probes were placed ~100 µm inside the scala vestibuli (SV) and scala tympani (ST) by use of a fine pick to drill holes ~300 µm in diameter through the blue–lined scalae. Velocities at the stapes posterior crus were measured by laser Doppler vibrometry concurrently with intracochlear pressure measurement by a fiber optic pressure probe. After experiments were complete, the specimens were dissected to confirm correct probe placement.

Results
For incus body stimulation, velocities measured at the stapes posterior crus varied with frequency between 0.5 and 12 mm/sec/V, or 100 to 120 dBSPL equivalent at 1V input. The SV and ST electromechanical transfer functions varied with frequency from 20 to 300 Pa and 15 to 140 Pa re/ 1V input, respectively. For stimulation using either the clip or the bell, stapes velocities were greater on average by 6 dB than for the actuator in contact with the incus body. However, scala vestibuli and differential intracochlear pressures were not correspondingly higher for the clip and the bell than for incus body contact.

Conclusions
These results suggest that for middle ear devices the geometry of stimulation plays an important role. For similar configurations, differential intracochlear pressure and cochlear volume velocity are related through a fairly constant cochlear impedance; however, for different configurations of electromechanical stimulation, apparent cochlear impedance can vary. Measured in this way, cochlear impedance appears to be a property of the system, including the stimulator's line of action, rather than of the auditory anatomy alone. Thus, single-point stapes velocity measurement may not adequately characterize cochlear volume velocity for the purpose of estimating cochlear impedance.

Funding
NIDCD: 1T32-DC012280 (NTG)

PS 171

The Acoustic and Mechanical Properties of Silk Films for the Repair of Chronic Perforations of the Tympanic Membrane

Benjamin Allardyce[1]; Rangam Rajkhowa[1]; **Rodney Dilley**[2]; Zhigang Xie[1]; Luke Campbell[3]; Adrian Keating[4]; Marcus D. Atlas[2]; Magnus von Unge[5]; Xungai Wang[1]
[1]Deakin University; [2]Ear Science Institute Australia; [3]University of Melbourne; [4]University of Western Australia; [5]University of Oslo

Background
Repairing chronic tympanic membrane perforations using existing materials such as temporalis fascia, perichondrium or cartilage involves a trade-off between achieving the desired hearing outcome and providing sufficient mechanical stability to resist post-operative retraction. The performance of these grafts depend primarily on the mass density and elastic modulus of the material. Since the modulus of autologous materials is set, only the graft thickness can be modified to balance acoustic and mechanical properties. By contrast, synthetic or naturally derived grafts can be engineered with a higher stiffness to achieve the same levels of mechanical support as thick cartilage but with a thinner graft with acoustic properties that match or exceed fascia. Silk films have shown promise in this application since they are biocompatible and have good tensile mechanical properties. This study therefore assessed the acoustic properties of silk films and tested their ability to withstand pressure-induced displacement.

Methods
Silk films ranging from 5 µm to 100 µm thick were tested alongside 30 µm thick paper, 400 to 700 µm thick animal derived cartilage and fascia (approx. 100 µm) in a custom built model designed to match the volume of the external ear canal. Acoustic properties were determined using Laser Doppler Vibrometry over the frequency range of 12.5 Hz to 8 kHz using a periodic chirp signal. The mechanical properties of the materials were then tested by a combination of uniaxial tensile testing and by applying air pressure to the ear canal tube. Subsequently the physical displacement of the centre of the film was measured at pressures from 0 kPa to 6 kPa.

Results
All silk membranes showed excellent acoustic properties, with a peak amplitude of at least 10 dB higher than that of cartilage. The resonance freq uency of the silk films was within audible frequencies, ranging from 2.5 kHz to 7.9 kHz as the film thickness increased from 5 µm to 100 µm. The paper sample showed similar properties to silk membranes of a similar thickness. Silk films of 30 µm and thicker showed high resistance to displacement, deforming less than 720 µm thick cartilage over the entire pressure range tested. Wetting the films improved the mechanical properties (lowering resonance frequency) while still providing adequate resistance to pressure loads.

Conclusions
Silk films represent an opportunity to engineer a thin, transparent, biocompatible graft material with excellent

acoustic properties and adequate mechanical stability for myringoplasty or tympanoplasty.

Funding
This work was supported by an Australian Research Council (ARC) Linkage Grant (LP110200547).

PS 172

Using 3D Vibrometry to Test a Novel Adjustable Ossicular Replacement Prosthesis

Peter Gottlieb[1]; Xiping Li[2]; Ashkan Monfared[3]; Nikolas Blevins[1]; Sunil Puria[1]
[1]Stanford University; [2]Capital Medical University; [3]George Washington University

Background
The goal of an ossicular reconstruction prosthesis (ORP) is to effectively transfer sound-induced vibrations from the tympanic membrane cochlea, usually through a mobile stapes footplate. The efficacy of an implanted ORP is influenced by its alignment and appropriate tension between the tympanic membrane and the stapes footplate. A novel ORP with a flexible element that potentially allows for length adjustment in situ is presented. The flexible element may increase the ease of achieving optimal ORP placement, especially through a facial recess approach. 3D vibrometry was used to test the hypotheses that including this flexible element does not degrade acoustic performance relative to standard prostheses used for ossiculoplasty, and that using 3D vibrometry to measure sound-driven stapes velocity provides a more comprehensive understanding of the input to the cochlea than a simple single-axis measurement.

Methods
The 3D velocity of two to three points on the posterior crus of the stapes in six cadaveric human temporal bones was measured using a Polytec CLV-3D laser Doppler vibrometer. The middle ear cavity was accessed through a facial recess approach. The SyncAv measurement system was used to generate pure tones spaced logarithmically from 200Hz to 20kHz, while the sound pressure inside the closed ear canal was simultaneously recorded using an Etymotic ER-7C probe tube microphone. After measuring the intact response, the incus was removed and stapes velocity was measured in the disarticulated case, then after insertion of the new prosthesis, a conventional prosthesis (Kurz BELL Dusseldorf type), and a sculpted autologous incus prosthesis in each temporal bone. The resultant stapes velocity, defined as maximum magnitude of the 3D velocity vector over one time period, was calculated for each point. Finally, the 3D stapes velocity transfer function, or the resultant stapes velocity divided by the ear canal pressure, was calculated for each case and compared.

Results
While there was variability in the performance of each ORP between specimens, no significant differences in 3D stapes velocity transfer function were found between the new, conventional, or autologous ORPs. The 3D stapes velocity transfer function was smoother than the single-axis transfer functions of each individual velocity component, which often displayed sharp resonances and anti-resonances over narrow frequency bands.

Conclusion
The inclusion of an in situ adjustable element into the ORP design did not adversely affect its acoustic performance, and the 3D velocity measurement yielded additional information about stapes vibration modes.

Funding
This work is supported in part by Grants No. DC005960 (to SP) and FDC013943A (to PG) from the National Institute on Deafness and Other Communication Disorders of the NIH.

PS 173

Fabrication and Acoustic Testing of Electrospun Scaffolds for TM Repair

Jian Liu[1]; Ying Li[1]; Seyed Rohani[1]; Sumit Agrawal[2]; Hanif Ladak[1]; Wankei Wan[1]
[1]Western University; [2]London Health Sciences Centre

Background
In the pars tensa of the human tympanic membrane (TM), the organized fibrous layers, which are responsible for the acoustic properties of the TM, are composed of mainly radial and circular fibers. The average fiber diameter is approximately 60 nm. Studies have shown that the radial fibers are crucial for hearing at frequencies above 4 kHz. However, none of the current grafts used in myringoplasty can duplicate similar fiber organization as the native TM. The hearing outcomes for patients with TM perforation after surgical treatments could therefore potentially be compromised. As a versatile fiber fabrication technique, electrospinning is able to produce fibers with diameters in nanometer range. With appropriate experimental setup, fiber alignment can also be achieved. We hypothesize that scaffolds with fiber organization similar to that of the local structure of the human TM can be prepared using electrospinning. With scaffolds mimicking the microstructure of the native TM, acoustic properties similar to the TM can be achieved.

Materials and Methods
Polyvinyl alcohol (PVA) fibers were electrospun and collected as non-woven mats. Random fibers were collected on a stationary electrode. A rotating mandrel was used to collect parallel aligned fibers. To mimic the local structure of the native TM, two layers of orthogonally oriented fibers were collected. This was achieved by rotating the substrate 90° after collecting the first layer of aligned fibers. The acoustic properties of the scaffolds with random and organized fibers were measured using scanning laser Doppler vibrometry for frequencies up to 10 kHz.

Results
Scaffolds composed of random and organized PVA fibers were successfully fabricated using electrospinning. Scanning electron microscopy images show that the fiber diameters vary from 100 to 300 nm. However, diameters as low as 60 nm could be achieved. The frequency response function (FRF) of scaffolds with random and organized fibers showed

frequency dependent variations in motion patterns. The motion patterns were similar at frequencies below 1 kHz but differed at frequencies above 1 kHz. It was found that FRF of scaffolds with organized fibers can be tuned to mimic the vibration pattern of the human TM by adjusting fiber diameter and mechanics.

Conclusions
Preliminary studies show that scaffolds that mimic the local structure of the human TM can be fabricated by electrospinning. The acoustic properties of these scaffolds can be tuned by adjusting the materials and experimental parameters. These results demonstrated the viability of a biomimetic scaffold for TM repair.

Funding
Ontario Research Fund: Research Excellence; MITACS Elevate Postdoctoral Fellowship

PS 174

In Pursuit of the Ideal Human DP-gram: Isolating f2, Reflection and Basal Components

Barden Stagner[1]; Glen Martin[2]; Brenda Lonsbury-Martin[2]
[1]VA Loma Linda Healthcare System; [2]Loma Linda University Health

Background
Noninvasively measured distortion product otoacoustic emissions (DPOAEs) have advanced our scientific knowledge about cochlear function. However, their great promise as a rapid test of cochlear dysfunction in patients with significant sensorineural hearing loss is severely limited due mainly to poor signal-to-noise ratios (SNRs) particularly when measured at the recommended primary-tone levels of 65/55 dB SPL. DPOAEs elicited by higher primary levels have greater SNRs, but are both less sensitive and less frequency-specific in part due to the associated basal spread of both excitation and the resulting DPOAE components. Overcoming these limitations would enhance the clinical utility of DPOAEs.

Methods
Martin et al. (2010) described an 'augmented' DP-gram (ADP-gram) technique in rabbits whereby basal DPOAE components were eliminated by an interference tone (IT) placed 1/3 octave above f2 (1/3 oct IT). The resulting ADP-grams were more sensitive and frequency-specific than standard DPOAEs. In the present study, this technique was combined with an IT placed 44 Hz below the DPOAE (DP IT) to eliminate the reflection component often found in humans. DP-grams were obtained with no IT and by interleaving a DP IT with a 1/3 oct IT. Vector differences were computed to reveal both reflection and basal components as separate residuals, which were then subtracted to create an 'ideal' DP-gram composed of only f2 components. Human subjects with either normal hearing or with sensorineural hearing loss were tested at primary levels of 55, 65, 75, 80 and 65/55 dB SPL in 10th octave steps of f2 from 0.5–15 kHz for f2/f1=1.21. Routine and Bekesy audiograms were obtained for comparison.

Results
The 'ideal' DP-gram in general showed more linear growth as a function of primary-tone level at low frequencies, had reduced fine structure, and seemed more sensitive and frequency-specific in certain individuals with hearing loss. DP-grams elicited by 75- and 80-dB SPL primaries exhibited greater SNRs than the 65/55 dB SPL condition thus allowing for the evaluation of more severe hearing-loss patterns. Basal components were often as large or larger than their corresponding reflection components, and both evidenced compressive growth as a function of primary levels. DP-grams elicited by 65/55 dB SPL primary tones were often dominated by basal components at f2<3 kHz, and were consistent with the hypothesis that lowering L2 maximizes basal components.

Conclusion
The 'ideal' DP-gram represents a promising new technique that allows for the evaluation of the reflection, basal generation, and f2 nonlinear mechanisms in isolation.

Funding
National Institute on Deafness and Other Communication Disorders (US) (DC000613), U.S. Department of Veterans Affairs (US) (VA-RD-C449R), U.S. Department of Veterans Affairs (US) (VA-RD-C6212L)

PS 175

A DPOAE assessment of outer hair cell integrity in ears with age-related hearing loss

Robert Withnell[1]; Margarete Ueberfuhr[2]; Hannah Fehlberg[3]; Shawn Goodman[4]
[1]Indiana University; [2]Ludwig-Maximilians University; [3]University of Minnesota Medical Center; [4]University of Iowa

Background
Otoacoustic emissions are typically assessed at stimulus levels that probe outer hair cell function. At high stimulus levels, where the cochlear mechanical response is passive, integrity rather than function can be assessed. Cochlear nonlinearity generates mechanical distortion that can be measured in the ear canal. In this study, distortion product otoacoustic emissions (DPOAEs) were used to assess outer hair cell integrity in human ears with age-related hearing loss. Method: Sound pressure measurements were made in the ear canal over the stimulus range 40 to 90 dB SPL (L_2), with L_1 = 0.45∗L_2 +44 with F_2 = 2 and 3 or 4 kHz. Model-generated DPOAE I/O functions were fit to DPOAE data to quantify the contribution of loss of nonlinearity (OHC loss) to the hearing loss. In the model, a feedback parameter controlled gain and a factor in the exponent of the nonlinearity controlled the contribution of the nonlinearity. Results: DPOAEs were measured on 13 ears with age-related hearing loss. DPOAEs were absent concomitant with hearing loss in four ears. DPOAE I/O functions concomitant with hearing loss were fit with the model in nine ears. Reduction in the model feedback parameter and nonlinearity exponent was found from model fits to data for 8 of the 9 ears. Conclusion: Results suggest OHC loss as the primary cause of age-related hearing loss. This does not exclude a metabolic component.

PS 176

Similarities between Stimulus Frequency Otoacoustic Emissions, Distortion Product Otoacoustic Emission Components, and Audiograms

Joshua Hajicek[1]; Maryam Naghibolhosseini[2]; Simon Henin[1]; Glenis Long[1]
[1]Graduate Center of the City University of New York; [2]Michigan State University

Background

There are two major types of otoacoustic emissions (OAEs). Reflection OAEs, such as stimulus frequency OAEs (SFOAEs) arise from coherent reflection in the region near the best frequency place. Distortion product OAEs (DPOAEs) consist of at least two components. One of the components depends on cochlear nonlinearity and is generated from the overlap of the two primaries. Distortion product energy generated in the overlap region travels basally to the ear canal (generator component) and apically to its best frequency place where it is coherently reflected giving a second component with the same frequency (DPOAE reflection component). The major difference between the SFOAE and the DPOAE reflection component is the energy source reaching the best frequency region. Consequently it is expected that there would be a close relationship between the quasiperodicity of SFOAE and the DPOAE reflection component. The amount of nonlinear-generated energy reaching the best frequency region will depend on the health of the cochlea in the overlap region and how much it is amplified as it travels to the best frequency region. The difference in amplitude of the two DPOAE components is thus predicted to depend on cochlear health in different regions and will reflect the hearing status reflected in an audiogram.

Methods

Narrowband noise audiograms were measured at standard inter-octave intervals from 0.25-8 kHz from 19 ears. Stimuli were continuously swept to generate SFOAEs and DPOAEs between 1000-8000 Hz. DPOAEs were measured with L2 = 60 and 65 dB SPL, and f2/f1 = 1.22. SFOAE were measured at 35 dB SPL with and without suppression. Analysis was performed using a least squares fit (LSF) analysis. The LSF analysis used for SFOAE was optimized to minimize interference between the probe and SFOAE.

Results

The quasiperiodic pattern between SFOAEs and the DPOAE reflection component were similar in most ears. SFOAEs were frequently larger in amplitude than the DPOAE reflection component, but the relationship between individual audiograms and DPOAE components was complex. In a subset of participants, threshold sensitivity appeared to depend on DPOAE reflection component level while in other participants, or at other frequencies, it depended on the generator component.

Conclusions

As predicted from the similar origins, the DPOAE reflection component and SFOAE have similar quasiperodicity within individual ears. The relationship of the DPOAE components to the audiogram depends on the relative levels of each DPOAE component and hearing status.

Funding

This research was supported in part by the Office of Naval Research work unit number WU50904 through the Naval Submarine Medical Research Laboratory, and the CUNY Graduate Center Provost's Digital Innovation Grant, 2014-2015

PS 177

DPOAE Mapping as a Measure of Cochlear Sensitivity to Postural Changes

Allison Anderson[1,2]; Abigail Fellows[2]; Jay Buckey[1,2]
[1]Dartmouth College; [2]Geisel School of Medicine

Background

Distortion product otoacoustic emissions (DPOAEs) have been shown to be sensitive to changes in ICP and posture (Buki, Avan et al. 1996, Buki, Chomicki et al. 2000, Voss, Adegoke et al. 2010, Bershad, Urfy et al. 2014). Traditional DPOAE measurement techniques, however, evaluate a narrow band of frequencies and ratios. DPOAE level/phase mapping provides a comprehensive view of outer hair cell function across the cochlea by measuring at multiple f2 frequencies and ratios and plotting the results as a "map." This approach may be useful for assessing which cochlear regions are most affected by postural changes.

Methods

We used DPOAE level/phase maps to full characterize the cochlea over a broad range of frequencies and ratios in the seated, supine, and prone positions in 8 subjects (4 male, 4 female). The order of posture was randomized. A map with two primary tones emitted at 65 dB was taken after 30 minutes, and a map with 75 dB primary tones was collected at 45 minutes.

Results

The greatest differences between seated baseline and supine or prone maps occurred at 6-8 kHz, within the 2f1 – f2 spectrum. Half of the subjects showed an increase over baseline, while the other subjects showed a decrease over baseline within that region. Across postures, however, the individual subjects were consistent i.e. an "increaser" increased in both supine and prone. The absolute value of the difference averaged to show sensitivity is shown in Figure 1. In the prone position, an additional

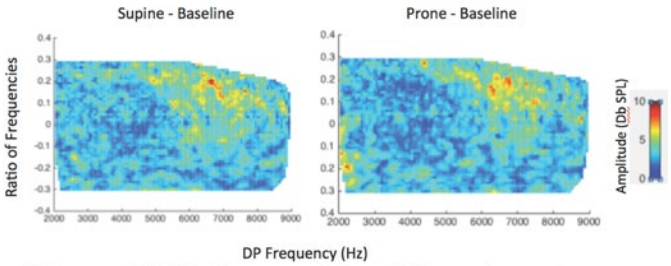

Figure 1: Sensitivity of DPOAE level maps to postural changes. Differences of supine and prone posture from baseline. Differences are absolute values of difference since some subjects increase in amplitude while others decrease in amplitude.

Conclusion

Previous studies have shown that peak stapes velocities and basilar membrane displacement occur at between 6 and 8 kHz and the basilar membrane dramatically increases in sensitivity beyond 6 kHz (Robles and Ruggero 2001). Therefore, it is feasible that changes in stapes placement and stiffness would be most easily detected in this range. DPOAE level maps have the potential to provide greater insight into the sensitivity of the cochlea to changes in posture. This has implications for noninvasive measure of ICP since a change in posture implies a change in intracranial pressure. A noninvasive measure of ICP has many important applications for patients with idiopathic intracranial hypertension, traumatic brain injury, or for astronauts in long-duration spaceflight.

PS 178

Auditory-Threshold Estimation Using Short-Pulse Distortion Product Otoacoustic Emissions in Normal and Hearing-Impaired Ears

Dennis Zelle; Lisa Lorenz; John Thiericke; Ernst Dalhoff; Anthony Gummer
University of Tübingen

Introduction

Distortion product otoacoustic emissions (DPOAEs) emerge in the healthy cochlea as a response of two simultaneously presented stimulus tones of frequencies f_1 and f_2 and mainly consist of two components, a nonlinear-distortion and a coherent-reflection component. Recently, it was shown that estimated distortion product thresholds (EDPTs) extrapolated from semi-logarithmic input-output (I/O) functions (Boege & Janssen, 2002) predict behavioral thresholds with high accuracy, if solely the nonlinear-distortion component is utilized (Dalhoff *et al.*, 2013). Here, a short-pulse stimulus paradigm is used (Zelle *et al.*, 2014) to extract the nonlinear-distortion component in the time domain and to estimate auditory thresholds for normal-hearing and hearing-impaired subjects in a clinically relevant frequency range.

Methods

DPOAE I/O-functions were recorded from 19 normal-hearing and 15 hearing-impaired subjects with sensorineural hearing loss. Stimulus levels were selected according to a frequency-specific paradigm $L_1 = a(f_2)L_2+b(f_2)$, with L_2 ranging from 25 to 75 dB SPL in 5-dB steps. Stimulus pairs comprising a 30-ms long f_1 pulse and a f_2 pulse with frequency-dependent half width were interlaced in the time domain to form pulse trains of 120-ms length. To acquire I/O-functions for eight frequencies f_2 = 1 – 8 kHz (f_2/f_1 = 1.2), two consecutive measurements were performed, each of them with pulse trains containing four f_1,f_2 pairs. The nonlinear distortion component was extracted from the averaged time-domain responses after band-pass filtering using onset decomposition (Vetešník *et al.*, 2009). I/O-functions with a correlation of $r^2 \geq 0.8$ and a standard deviation of the EDPT of $\sigma_{EDPT} \leq 10$ dB were accepted for auditory-threshold estimation. For sake of comparison, behavioral thresholds (BTHs) were obtained by Békésy audiometry.

Results

For Békésy thresholds lower than 20 dB SPL, 96% (99/103) of the corresponding I/O-functions were accepted. However, the acceptance rate decreases consistently with increasing amount of hearing loss, leading to an acceptance of only 13% in case of Békésy thresholds higher than 60 dB SPL. In total, 82% (223/272) of the I/O-functions provided reliable threshold estimates with a standard deviation of the estimation error of 6.0 dB. The overall data exhibit a significant correlation between EDPTs and BTHs ($r^2 = 0.7$; $p < 0.001$).

Conclusion

Short-pulse DPOAEs enable the separation of the two DPOAE source components. I/O-functions based on the nonlinear-distortion component yield accurate auditory-threshold estimates for both normal-hearing and hearing-impaired subjects. The results suggest short-pulse DPOAEs as a promising tool for quantifying hearing loss induced by an impaired cochlear amplifier.

Funding

Supported by the German Research Council DFG DA 487/3-2.

PS 179

Influence of spontaneous otoacoustic emissions on tone burst evoked otoacoustic emissions

W. Jedrzejczak[1]; Krzysztof Kochanek[1,2]; Edyta Pilka[1,2]; Henryk Skarzynski[1,2]
[1]Institute of Physiology and Pathology of Hearing; [2]World Hearing Center

Background

It has been reported that both click evoked otoacoustic emissions (CEOAEs) and distortion product otoacoustic emissions (DPOAEs) have higher amplitudes in ears that exhibit spontaneous otoacoustic emissions (SOAEs). The purpose of the present study was to investigate how presence of SOAEs influences another type of otoacoustic emissions – those evoked by tone bursts.

Method

Otoacoustic emissions (OAEs) were recorded from group of young adults. In each ear, a set of measurements were made: click evoked OAEs (CEOAEs), tone burst evoked OAEs (TBOAEs) at frequencies of 0.5, 1, 2, and 4 kHz, and a recording of spontaneous OAEs (SOAEs). For each stimulus

type input/output functions were measured for levels from 40 to 90 dB SPL, with 10 dB steps. Global and half-octave-band values of OAE response level were assessed. Additionally, time–frequency (TF) analysis of signals was performed using the matching pursuit method.

Results
In ears with recordable SOAEs, TBOAEs had higher levels than in ears without SOAEs. The differences were more prominent for global values, however they were also present for octave-band values. The slopes of input/output functions was similar for ears with and without SOAEs. The latencies tended to be longer for lower stimulus levels. However there were no significant differences in latencies between TBOAEs from ears with and without SOAEs. When comparing TBOAEs to CEOAEs the differences between recordings from ears with and without SOAEs seem to be more pronounced in CEOAEs.

Conclusion
Despite the fact that TBOAEs reflect activity from narrower cochlear region than CEOAEs they are still significantly influenced by presence of SOAEs. Therefore, whenever TBOAEs are used it should be done with knowledge about SOAEs coinciding in frequency.

Funding
This research was funded by the Institute of Physiology and Pathology of Hearing and by Polish Ministry of Science and Higher Education.

PS 180

After-effects of Intense Low-frequency Sound on Spontaneous Otoacoustic Emission Generation: Influence of Frequency and Level

Markus Drexl; Lena Jeanson; Lutz Wiegrebe
Ludwig-Maximilians-University, Munich

Background
The presentation of intense, low-frequency (LF) sound to the human ear can cause very slow, sinusoidal oscillations of cochlear sensitivity after LF sound offset, for which the term 'Bounce' phenomenon has been coined. Spontaneous otoacoustic emissions (SOAEs) are a sensitive measure of the phenomenon and undergo large, oscillating level changes after LF sounds offset. This can also lead to increased SOAE numbers, as SOAEs buried in the noise floor can become detectable after LF sound offset. In this study, we investigated the influence of LF sound level and frequency on SOAE level changes after LF sound offset.

Methods
Data were collected from 25 ears of 25 normal hearing subjects. The level of SOAEs was tracked as a function of time for one minute before LF sound exposure (duration 1.5 minutes) and for seven minutes after LF sound exposure. The whole 9.5 minutes lasting sequence formed one trial. Trials were carried out with several LF sound levels (93 to 108 dB SPL in 3 dB steps at a fixed frequency of 30 Hz) and different LF sound frequencies (30, 60, 120, 240 and 480 Hz at a fixed loudness of 80 phones). A bootstrapping procedure was employed to detect significant SOAE changes after LF offset.

Results
We recorded a total of 131 SOAEs. Measurements with different LF sound levels and a fixed LF sound frequency (30 Hz) revealed a median level of 102 dB SPL necessary to elicit the Bounce phenomenon to a significant extent. In some individuals, a LF sound level of 93 dB SPL (the lowest employed level) was sufficient to induce significant bouncing. Measurements with different LF sound frequencies showed that the intensity of the SOAE bounce also depended on the SOAE and LF sound frequencies: SOAEs with lower frequencies were equally affected at all LF sound frequencies whereas SOAEs with higher frequencies showed a decrease in Bounce strength with increasing LF sound frequency.

Conclusions
The Bounce Phenomenon can be induced with LF sounds at levels as low as 93 dB SPL, which indicates that environmental sounds with comparable levels and frequencies might be suited to induce the Bounce phenomenon. Our results also show that the strength of the Bounce phenomenon is not a simple function of SOAE and LF sound tonotopic proximity.

Funding
Funding: This work was funded by a grant (01EO1401) from the German Ministry of Science and Education to the German Center for Vertigo and Balance Disorders (IFB), project TRF6-II to M.D. and L.W.

PS 181

Musical experience sharpens human cochlear tuning

Gavin Bidelman; Caitlin Nelms; Shaum Bhagat
University of Memphis

The mammalian cochlea functions as a filter bank that performs a spectral, Fourier-like decomposition on the acoustic signal. Although cochlear filtering is initiated at the peripheral input, it establishes the tonotopic organization (i.e., frequency-place map) at all subsequent levels of the auditory system and ultimately limits the remarkable time-frequency acuity of human hearing. Human cochlear tuning is sharper compared to other mammals but is mature at birth and thus widely considered immune to the neuroplasticity apparent at all higher stages of the auditory brain. While tuning can be compromised (e.g., broadened with hearing impairment), whether or not human cochlear frequency resolution can be sharpened through experiential factors (e.g., training or learning) has not yet been established. Here, by directly mapping physiological tuning curves from otoacoustic emissions (cochlear emitted sounds), we show that human cochlear tuning is further sharpened (by a factor of 1.5x) in musicians and improves with the number of years of their auditory training. Our findings demonstrate an experience-dependent enhancement in the resolving power of the cochlear sensory epithelium and the spectral resolution of human hearing. These results establish a peripheral origin

to account for the pervasive perceptual benefits observed from music experience and open the possibility for improving broadened cochlear tuning and auditory perceptual acuity (e.g., in cases of hearing loss) through protracted auditory training.

Funding
GRAMMY Foundation

PS 182

Level Dependence of Stimulus-Frequency Otoacoustic Emissions at High Frequencies

James Dewey[1]; Sumitrajit Dhar[2]
[1]Stanford University; [2]Northwestern University

Cochlear hearing loss often progresses from high to low frequencies. In spite of this, the characteristics and potential utility of otoacoustic emissions (OAEs) have not been thoroughly explored above 8 kHz. Here, we describe the level dependence of stimulus-frequency OAEs (SFOAEs), i.e., OAEs evoked by single tones and measured at the frequency of stimulation, over a wide frequency range in young adults with clinically-normal hearing thresholds. SFOAE input-output functions were obtained from ~7.4-17.28 kHz in 1/9th-octave steps, as well as at the three 1/9th-octave-separated frequencies centered at 1, 2, and 4 kHz. At each probe frequency, responses were evoked by discrete tones presented in 6 dB steps from 0 to 66 dB forward pressure level (FPL) and extracted from the total ear canal pressure via the "suppression" method, with a 72 dB FPL suppressor tone presented 47 Hz below the probe frequency. While SFOAE responses with sufficient signal-to-noise ratios were often obtained for low-to-moderate probe levels up to 13.7 kHz, and for higher probe levels up to at least 14.8 kHz, SFOAEs generally declined in amplitude above 8 kHz. The amplitude difference between low and high frequency responses was slightly reduced with increasing probe level, due to a tendency toward less compressive response growth with increasing frequency. To examine the level dependence of SFOAE fine structure and phase, additional measurements were obtained from ~7-18 kHz in 1/100th-octave steps for a more limited range of probe levels. At higher probe levels (48 or 60 dB FPL), the slopes of the SFOAE phase-versus-frequency curves sometimes became shallower (indicating shorter group delays) than those at lower levels (24 or 36 dB FPL). The amplitude fine structure was also largely preserved with increases in probe level, though peaks and valleys often shifted in frequency and became slightly less pronounced. Overall, the data suggest that SFOAEs are measurable up to the highest frequencies of sensitive human hearing and that high-frequency SFOAEs can exhibit qualitatively similar behavior to those obtained at lower frequencies. However, the low amplitude of high-frequency SFOAEs may indicate that subtle age- or exposure-related declines in basal cochlear function have already occurred in the young individuals tested here. The use of higher probe levels (i.e., > 48 dB FPL) may therefore be beneficial for further examining SFOAE characteristics at high frequencies in a larger and/or more diverse test population.

Funding
Work supported by NIH/NIDCD F31 DC013710.

PS 183

Spontaneous Otoacoustic Emissions Throughout the Human Lifespan

Carolina Abdala[1]; Ping Luo[1]; Christopher Shera[2]; Amanda Ortmann[1]; Megan Moreh[3]; Agnes Youn[1]
[1]University of Southern California; [2]Massachusetts Eye and Ear Infirmary; [3]Beverly Hills High School

Spontaneous otoacoustic emissions are thought to be amplitude-stabilized cochlear standing waves arising though a process of multiple internal reflection (Shera, 2003). Our lab has accumulated hundreds of SOAE records spanning all decades of life: from prematurely born neonates tested as young as 31 post-conceptional weeks to geriatric subjects in their seventh and eighth decades. Some of these subjects were tracked longitudinally. To more reliably quantify SOAE features, we have adapted and extended existing methods (Talmadge et al., 1993; Pasanen & McFadden, 2000) to automatically detect and model spontaneous emissions. This poster describes the automated-detection algorithm as well as changes in SOAEs across the human lifespan as a gauge of age-related changes in cochlear mechanics.

SOAEs were recorded in normal hearing pre-term and term-born neonates, six- month-old infants, teens, young adults, middle-aged adults, and elderly adults tested over a 20-year period in the Abdala Laboratory. For most of these recordings, only the averaged spectra are available (11.7 Hz frequency resolution). However, for ~200 records, the raw sound file from a 3-minute recording is available for reanalysis. A peak-picking algorithm was implemented with averaged spectra to detect SOAEs with criterion SNR and bandwidth. Electro-magnetic artifacts were eliminated by identifying spikes at repeated frequencies among ears; also, harmonic distortion and distortion products created from proximal SOAEs were eliminated. For sound files, an artifact-rejection was also applied (based on time waveform rms amplitude and/or peak excursions) to enhance SOAE detection, after which peak-picking was implemented with criterion SNR and bandwidth. The detected emissions were fitted to a Lorentzian plus polynomial additive noise model to more accurately assess emission power, frequency and bandwidth SOAE prevalence, number per ear, magnitude, SNR, spectral distribution, and spacing will be analyzed across the human lifespan. Other OAE-based indices of maturation and aging have shown age effects suggestive of changes in cochlear mechanics throughout life (Abdala and Dhar, 2012). This comprehensive SOAE database will shed light on the shifting nature of human cochlear mechanics during maturation and aging and inform theories of SOAE generation.

Funding
NIH NIDCD R01 DC003552 (CA) and R01 DC003687 (CAS).

PS 184

Susceptibility of Stimulus-Frequency Otoacoustic Emissions and Cochlear Microphonics to Acoustic Trauma

Karolina Charaziak[1]; Christopher Shera[2]; Jonathan Siegel[3]
[1]Eaton-Peabody Laboratories; [2]Massachusetts Eye and Ear Infirmary; [3]Northwestern University

Otoacoustic emissions (OAEs) and cochlear microphonics (CMs) both depend on outer-hair-cell (OHC) function and may therefore be useful for locating cochlear regions with impaired OHCs noninvasively. CM and OAE evoked with low-level pure tones (stimulus-frequency, SFOAE) appear to be best suited for this application. However, both measures are contaminated by sources local to the recording site: The SFOAE is mixed with the stimulus pressure in the ear canal and cannot be directly separated, while the CM is dominated by voltage sources located close to the recording electrode, which limits its place-specificity. The goal was to see whether these limitations of both SFOAEs and CMs might be overcome using two-tone suppression measurements. Ideally, the suppressor saturates receptor currents near the peak of its excitation pattern, removing probe-frequency contributions from nearby OAE/CM sources. By varying the suppressor frequency, one may therefore hope to gauge the spatial locations of the sources excited by the probe. To test this idea, we simultaneously measured round-window CM and ear-canal pressure in response to 30-dB SPL probe tones (f_p = 0.3–10 kHz) in deeply anesthetized chinchillas, both before and after inducing acoustic trauma (~40 dB elevation in compound-action-potential, CAP, thresholds at ~4 kHz). A 55-dB SPL suppressor at either a nearby (f_p –43 Hz) or a higher frequency (f_s/f_p = 1.2, 1.4, 2.1, or 2.6) was presented with the probe on alternate runs. SFOAE and CM probe-frequency residuals were calculated as vector differences between the responses to probe-alone and probe+suppressor conditions.

The total CM obtained in the probe-alone condition was only moderately affected by acoustic trauma, supporting the view that far-field CMs are dominated by basal sources. As predicted, CM residuals extracted using a suppressor show greater sensitivity to acoustic trauma. They also closely track changes in the corresponding SFOAE residuals. In particular, both CM and SFOAE residual levels decrease by ~20 dB after trauma, but the range of affected frequencies depends on f_s/f_p : The higher the suppressor frequency, the lower the probe frequencies of largest change . However, when shifts in CM and SFOAE residual levels are plotted versus f_s, they correspond well to the frequency range of CAP threshold elevation. At least in chinchilla, these results suggest that both SFOAE and CM residuals originate predominantly near the cochlear place tuned to the suppressor rather than to the probe and can assess OHC function in that region.

Funding
Supported by R01 DC00419 (to M. Ruggero), R01 DC003687 (to C. Shera), and Northwestern University.

PS 185

On the Localization of the SFOAE Sources

Arturo Moleti[1]; Renata Sisto[2]; Giuseppe Parente[1]
[1]University of Roma Tor Vergata; [2]INAIL Research

Stimulus-frequency otoacoustic emissions (SFOAEs) are usually separated from the stimulus tone (at the probe frequency f_p), using a suppressor tone of nearby frequency f_s. The assumed role of the suppressor is to strongly decrease the gain of the outer hair cell nonlinear active amplifier in the cochlear region around the tonotopic place of frequency f_s, which is close to that of f_p, where generation of backward traveling waves is predicted by the coherent reflection filtering (CRF) mechanism. The CRF mechanism is sensitive to the local BM displacement, therefore it is commonly assumed that the SFOAE sources are localized in that tonotopic region. Recently, it has been demonstrated that significant SFOAE generation may occur slightly basally to the resonant region, within 1 mm in humans, corresponding to a relative frequency shift of order 10-20% (e.g., Moleti et al., JASA 2013). Such near-basal sources should correspond to the short-latency OAE components observed in humans (e.g., Sisto et al., JASA 2013). SFOAE suppression by high-frequency tones has been experimentally observed in chinchillas (Charaziak and Siegel, JARO 2015), and interpreted as the evidence for correspondingly far-basal otoacoustic sources. The CRF mechanism is not in contradiction with basal otoacoustic generation (as shown by Sisto et al., JASA 2015), if the quality factor is sufficiently low, as typically happens in animals at high stimulus levels. On the other hand, the relation between the localization of the “residual” source and a high-frequency suppressor needs further study, to understand whether suppression residuals have to be negligible in a “fully passive” cochlear region, and whether a residual obtained with a high-frequency suppressor really represents otoacoustic emissions generated near (and only near) the f_s characteristic place.

In this study, a nonlinear version of the Zweig model is used to show how high-frequency suppressors affect the vibration pattern along the basilar membrane, showing that the generation place of the observed otoacoustic residuals may not coincide with the characteristic place of the suppressor tone. From the experimental point of view, to clarify the same issue, a SFAOE acquisition method has been developed, which is not based on suppression or compression mechanisms, using time-frequency filtering only to separate the OAE response from the stimulus. Comparison between these spectra and those of conventional “suppression” SFOAEs may help clarifying the relation between true SFOAEs and the SFOAE residual.

Funding
Research Grant “Uncovering Excellence”, University of Roma Tor Vergata

PS 186

Acoustic Startle Reflex Audiometry Following Non-traumatic Noise Exposure in CBA/CaJ Mice

Martin Pienkowski
Salus University

Previous studies on mature rodents and cats have shown that auditory cortical function can be altered by persistent exposure to moderately loud background noise, even in the absence of any damage to the cochlea. For example, after continuous or even intermittent exposure to a sharply band-limited, moderately loud noise, auditory cortical responses to sound frequencies within the noise band can be strongly suppressed for weeks, whereas responses to frequencies just above and below the noise band can be enhanced. The effects of such cortical changes on auditory perception remain unclear, in spite of the great interest and substantial recent progress in understanding the neural underpinnings of loudness disorders such as hyperacusis and tinnitus.

In the present study, mature, normal-hearing CBA/CaJ mice were exposed to an 8–16 kHz octave-band noise at 70 dB SPL for 6 weeks, 24 h/day. Acoustic startle reflex-based (ASR) audiometry was performed before and after noise exposure, and in a group of unexposed, littermate controls. The goal was to determine whether the previously documented cortical changes correlate with frequency-specific changes in loudness perception. Specifically, the hypothesis was that exposure-induced cortical hypoactivity (at frequencies within the noise band) would correlate with perceptual hypoacusis, whereas cortical hyperactivity (above and below the noise band) would correlate with perceptual hyperacusis. Such an association would have important implications for the role of auditory cortex in loudness perception, and in pathological hyperacusis and tinnitus.

ASR audiometry is being conducted at 4, 6, 8, 11, 16, 23 and 32 kHz (i.e., within, at the edges of, and above and below the 8–16 kHz noise exposure band). To test the upper end of the intensity dynamic range, ASR input-output functions are recorded over 80–120 dB SPL. To test the lower end of the dynamic range, pre-pulse inhibition (PPI) of the broadband noise-evoked ASR is measured at pre-pulse intensities of 40–80 dB SPL.

PS 187

Acoustic Stimuli-induced CREB Phosphorylation via Sustained MAPK Signaling under Somatosensory Interference in Auditory Cortex

Nobuhiro Yamamoto; Makoto Nakanishi; Masaaki Nomura; Hideki Kawai
Soka University

Sensory stimuli-induced cortical activity leads to activation of cAMP-response element binding protein (CREB) in primary visual and somatosensory cortex. However, whether sound stimulation leads to CREB activation in auditory cortex is unclear. We observed previously that white noise exposure (WN) did not enhance CREB activation or Ser133-phosphorylation (P-CREB) using immunofluorescence imaging technique in primary auditory cortex (A1). However, when WN was followed by pin stab (PS) on the palm of forehands, P-CREB remained elevated compared to no WN control. The elevated P-CREB was due to the lack of reduction of P-CREB intensity by PS in WN-stimulated mice. These data suggested that prior WN exposure activates intracellular signaling that persists under the P-CREB reducing stimuli. Here, we investigated which kinase(s) involves in sustaining the P-CREB level. We examined this in entire P-CREB-positive and GAD67-coimmunopositive GABAergic neurons of A1.

Using C57BL/J mice (postnatal days 25-26), we observed that the fluorescence intensity of P-CREB immunopositive cells in response to WN and PS stimuli was about 1.6-fold more than PS control. The intensity of non-phosphorylated CREB was not different between these conditions. To investigate if the P-CREB elevation is mediated by the mitogen-activated protein kinase (MAPK) pathway, we injected a MAPK kinase (MEK) inhibitor, U0126, locally into one side of A1, while injecting U0124, an inactive analog of U0126, on the other side. U0126 inhibited the P-CREB elevation by WN and PS, while U0124 did not prevent it. We also examined the calmodulin-dependent kinase IV (CaMKIV) pathway by locally injecting a CaMK kinase inhibitor, STO-609, and found that STO-609 had little effects on the P-CREB elevation. Thus, WN activates the MAPK pathway to sustain an elevated level of P-CREB. Similar effects of inhibitors were seen in a subset of P-CREB positive GABAergic neurons.

We also examined the duration of the persistent signaling by varying the time between the end of WN and the start of PS. Up to 5 min separation between the stimuli was still capable of elevating the WN-induced P-CREB, while 30 min or more temporal separation reduced the P-CREB level to that of PS control, suggesting that WN-induced signaling lasted for at least 5 min.

In summary, while CREB activity elevated in A1 can be reduced by PS, auditory-induced MAPK pathway activation makes the elevated P-CREB resistant for several minutes to the PS-induced P-CREB reduction in A1.

Funding
Japan Society for the Promotion of Science (No. 23500402)

PS 188

Long-term, low-level noise exposure: Unexpected effects on ear and brain

Adam Sheppard; Guang-Di Chen; Senthilvelan Manohar; Dalian Ding; Kira Sullivan; Andrew Beak; Wei Sun; Bohua Hu; Richard Salvi
University at Buffalo

Background
Many individuals live or work in environments in which they are continuously exposed to low-level noise. Previous studies have shown long-term, low-level noise exposure that cause

little or no hearing loss can nevertheless disrupt intensity coding, temporal processing and tonotopy in the auditory cortex; however, it is unclear if these functional changes originate in the auditory cortex or more peripheral locations in the ascending auditory pathway. To address this issue, we made electrophysiological recordings from the inferior colliculus and cochlea of rats after long-term, low-level noise exposures.

Methods
Rats, all housed in their home cage in the vivarium, were divided into two groups: (1) Control group and (2) Long-term, low-level noise (10-20 kHz, ~70 dB SPL, 24 h/d for 6 weeks). Cochlear function was assessed by measuring the compound action potential (CAP) I/O functions. Local field potentials (LFP) and multiunit firing rates were recorded from the central nucleus of the inferior colliculus (CIC) using 16-channel microelectrodes. Cochleae were evaluated for histological damage.

Results
The long-term, low-level exposure caused: (1) a very mild (~8-10 dB) shift in CAP threshold between 10-20 kHz, but had no effect on thresholds below or above the exposure., (2) Surprisingly, CAP suprathreshold amplitudes were reduced roughly 50% at frequencies within and above the exposure band. These results indicate that low-level noise exposure can greatly reduce the neural output of the cochlea in a frequency specific manner. (3) Paradoxically, sound evoked neural activity (multi-unit local field potentials and spike discharge rates) in the CIC was enhanced at test frequencies from 10 to 20 kHz. These results suggest that the central auditory system increases its gain in the 10-20 kHz region to compensate for the reduced cochlear output at these frequencies and (4) there was no evidence of hair cell loss and no detectable changes in Ctbp2 ribeye immunolabeling for ribbon synapses in the inner hair cell region.

Conclusion
Our results indicate that low-level, long-term noise exposures, that would normally be considered “safe”, cause very mild CAP threshold shifts, but greatly reduce the neural output of the cochlea at frequencies within and above the exposure band. Despite a large reduction in cochlear output, sound evoked responses in the CIC are greatly enhanced within the exposure band. These results are consistent with models of Enhanced Central Gain in which the central nervous system compensates for a reduced cochlear output.

PS 189

Neurofilament heavy chain expression and neuroplasticity in rat auditory cortex after unilateral and bilateral deafness

Min-Hyun Park[1]; Jeong Hun Jang[2]; Jae-Jin Song[3]; Ho Sun Lee[1]; Seung Ha Oh[4]
[1]Boramae Medical Center, SMG-Seoul National University; [2]Kyongpook national university hospital; [3]Seoul National University Bundang Hospital; [4]College of Medicine, Seoul National University

Backgrounds
Deafness induces many plastic changes in the neural auditory system. Synaptic changes were happened and it was caused by dendritic changes in neural cells. SMI-32, a monoclonal antibody reveal auditory areas and recognize non-phosphorylated epitopes on medium- and high- molecular weight subunits of neurofilament proteins in dendrites of cortical pyramidal cells. We investigated the SMI-32-immunoreactive (-ir) protein levels after induced unilateral and bilateral deafness in the rat auditory cortex.

Methods
Three groups of adult male Sprague-Dawley rats were prepared for control, unilateral deafness and bilateral deafness. Deafness induced using cochlear ablation method. After deafening, 2, 4, 6 and 12 weeks later, auditory cortices were harvested for RT-qPCR and western blot. Immunohistologic staining was performed to evaluate the location of SMI-32-ir neurons.

Results
In the bilateral deafened group, mRNA expression and western blot showed increasing level of SMI-32-ir and it was increased significantly at 6 and 12 weeks after deafening. However, in the unilaterally deafened group, there were no significant changes in right and left auditory cortex in whole period.

Conclusion
This study showed that unilateral deafness did not affect so much to change the level of neurofilament and suggested that less plastic changes were happened in the auditory cortex of unilaterally deafened rats.

Funding
This study was supported by the Seoul National University Boramae Medical Center research fund 03-2014-2 (to Min-Hyun Park). The funding bodies had no role in study design, data collection and analysis, decision to publish, or preparation of the manuscript

PS 190

Effects of Presynaptic and Postsynaptic nAChR Activation in the Medial Geniculate Body

Sarah Sottile; Lynne Ling; Donald Caspary
Southern Illinois University School of Medicine

Background

The medial geniculate body (MGB) receives ascending excitatory and inhibitory input from inferior colliculus (IC), as well as descending excitatory projections from auditory cortex (AC), and descending inhibitory projections from the thalamic reticular nucleus. The relative strength of these MGB inputs can be modified by a significant cholinergic projection from the pontomesencephalic tegmentum (PMT) which is activated by attentional demands. Acetylcholine from PMT acts at pre- and postsynaptic nicotinic receptors (nAChRs) altering the response properties of MGB thalamocortical projection neurons. The present studies examined the effects of activating nicotinic receptors postsynaptically on MGB neurons and presynaptically on presynaptic terminals in contact with MGB neurons, while differentiating response properties and pharmacology between the MGB subdivisions and cell types.

Methods

Whole cell patch clamp recordings were performed in thalamocortical slices from 4-6 months old Fisher Brown Norway rats. Acetylcholine (1 mM) was pressure ejected adjacent to the patched cells or nicotine (1 μM) was bath applied in order to examine the effects of nAChR activation on the intrinsic membrane properties and action potentials of MGB neurons evoked by current injection or synaptic stimulation. Presynaptic spontaneous excitatory synaptic currents (EPSCs) or spontaneous inhibitory synaptic currents (IPSCs) were isolated using selective AMPA/NMDA or GABA blockade. Muscarinic receptors were blocked for all conditions. Neurobiotin-Alexa-488 was used in the patch pipette to establish the MGB location and morphology of recorded cell.

Results

Activation of postsynaptic nAChRs results in a significant depolarization reaching action potential threshold for most postsynaptic MGB neurons examined. Activation of presynaptic nAChRs significantly increased the frequency of IPSC's with larger significant increases in the frequency of EPSC's. Both of these increases in frequency of release were blocked by the nicotinic receptor antagonist mecamylamine.

Conclusions

Acetylcholine plays a critical role in modulating the responses of MGB neurons. Understanding the dynamics of nAChR requires further investigation. Upcoming studies will attempt to describe the location, subunit composition, and physiology of nAChR's, as well as how these properties are impacted with age.

PS 191

Behavioral Assessment of Temporal Processing in the Guinea Pig

James Fallon; Maartje Hendrikse; Emma Johnson; Cara Lo; Andrew Wise
Bionics Institute

Introduction

Guinea pigs have long been a model of choice for auditory neuroscience and cochlear implant research as their cochleae are surgically accessible and their central auditory pathway has been well characterized. Unfortunately, guinea pigs have been notoriously difficult to use in standard behavioral paradigms. However, recent modifications to the pre-pulse inhibition of the acoustic startle reflex paradigm, including the use of a gap in an ongoing background noise as the pre-pulse stimulus for tinnitus testing, have seen an increase in the behavioral assessment of auditory function in guinea pigs. Here, we further extend the startle reflex paradigm to the assessment of temporal processing.

Methods

All procedures were based on the standard pre-pulse inhibition of the acoustic startle reflex paradigm, but we extended the startle reflex paradigm to include monitoring of force, pinna movement and respiration to overcome the 'freezing' reflex that is observed in some animals. We also replaced the traditional pre-pulse stimulus with amplitude modulation of- or gaps in- ongoing background noise to enable the assessment of temporal processing.

Results

A 50ms gap produced a reduction in startle response of 78 ± 5 %, 60 ± 8 % and 48 ± 8 % for force, pinna movement and respiration respectively (n = 7). While the reduction in startle amplitude was larger for force (one-Way RM ANOVA, $p = 0.015$); there was greater intra-animal variability with this metric. Using a combination of the above metrics, we measured the gap detection threshold, defined as the half maximal reduction in startle, to be 7.9 ± 1.0 ms (n = 4) and the average detection threshold for 100Hz sinusoidal modulation, defined as the half maximal reduction in startle, to be 41 ± 4 % (n = 4).

Conclusions

Extension of the startle reflex paradigm to include the monitoring of force, pinna movement and respiration can provide a more accurate determination of the reduction in startle reflex. The extended paradigm has allowed us to provide normative gap and modulation detection thresholds for the guinea pig, in preparation for assessing the effects of various experimental interventions on temporal processing.

We thank Sam Irving, Nicole Critch and Amy Morley for technical assistance.

Funding

This work was funded by the NH&MRC and The Bionics Institute acknowledges the support it receives from the Victorian Government through its Operational Infrastructure Support Program.

PS 192

Changes in Temporal Pattern of AI Activity After Interval Discrimination of Repetitive Sounds in Guinea Pigs

Koki Hayashi[1]; Hisayuki Ojima[2]; Junsei Horikawa[1]
[1]Graduate School of Engineering, Toyohashi University of Technology; [2]Graduate School of Medical and Dental Sciences, Tokyo Medical and Dental University

Background

Studies on plasticity of auditory cortex have largely focused on spectral domain. In this study, we investigated plasticity of timing representation in primary auditory cortex (AI) after conditioning animals to a repetitive sound with a given intersegment interval (ISI). Specifically, neuronal activation of the AI was compared between trained and naive animals for possible effects of training periods on discrete representation of individual segments of the stimulus sounds.

Methods

Fifteen, 4 naïve and 11 trained, guinea pigs (Hartley, male, 350-400g) were used. All sounds used were generated by duplicating one short sound segments. A few environmental sounds were also used as distractors. Animals were first subjected to recognition training for 2 weeks during which they were conditioned, with food reinforcement, to a target sound of ten 80-ms noise-like footstep sound segments with a 680-ms (100%) ISI, and then to discrimination training for another 1 or 2 weeks during which animals were trained to discriminate between target and target-like sounds that had ISI reduced to 10% or 20% of the target. While the target was continuously reinforced, these target-like sounds were not.After the recognition or discrimination training, cortical activation was recorded using a voltage-sensitive dye from the AI of animals anesthetized with Ketamine and Xylazine and treated with a muscle relaxant (approved).

Results

Figure shows sets of optical signals (upper traces) in response to the repetitive stimulus segments of different ISIs (lower traces) for animals trained to discriminate between sounds with target (100%) and test (10% and 20%) ISIs. In naive animals, discrete AI activities were evoked only at the first several segments of the 10%-ISI sound, but attenuated greatly at the later segments. This was contrasted by secured generation of large response signals at each stimulus segment of longer ISI sound (20% and 100%). For trained animals, as training period was elongated from 2 to 4 weeks (i.e., vertical axis of Figure), there was a tendency that later segments of repetitive sounds became more effective in evoking discrete responses (see 10 and 20% ISIs).

Conclusion

These results suggest that, like unit recording, AI optical signals reflecting activation of populations of neurons are reduced for later sounds of a sound train with short ISIs. Such a reduction in responses to highly repetitive sounds can be improved by discrimination training of sounds with different repetitive rates.

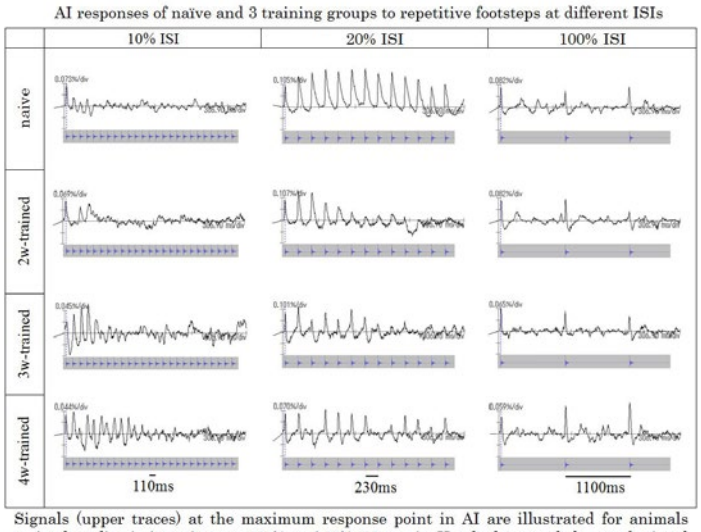

Signals (upper traces) at the maximum response point in AI are illustrated for animals trained to discriminate between 100%- and 20%-ISI sounds. Hatched traces below each signal record show stimulus sound waveforms used in optical imaging.

Funding

Supported by Grant-in-Aid for Scientific Research (C), no. 22500368 and no. 26430034 from JSPS.

PS 193

Altered Sequential Sound Coding within the Amygdala of a Mouse Model of PTSD

Jasmine Grimsley; Emily Hazlett
NEOMED

In healthy human subjects, cortical EEG responses to pairs of sounds reveal that neural activity to the second sound is attenuated, or gated. Reduced gating is one of several auditory deficits associated with Posttraumatic Stress Disorder (PTSD). The basolateral amygdala (BLA) is highly responsive to sound in healthy individuals and becomes hyperactive in patents with PTSD. We hypothesized that BLA dysfunction contributes to the auditory symptoms of PTSD and that the neural representation of sound pairs would be less gated within the BLA of a mouse model of PTSD.

To assess the effects of PTSD on the representation of sequential sounds in the BLA, we recorded spiking activity and local field potentials (LFP) to sound pairs using an acute, restraint-stress model of PTSD. Using wireless technology, we recorded from 13 awake, free-moving, adult CBA/CaJ mice with custom multi-electrode implants. Stimuli were 40 repetitions of sound pairs composed of repeated broadband noise bursts (BBN) or mouse vocalizations, separated by 500 ms and presented at a rate of 0.1 Hz. Gating was measured by the ratio of the response to the second sound relative to the first. For LFPs, gating of the p20 wave was compared. Wilcoxon signed ranks tests were used to examine if, as a population, BLA neurons and LFPs show altered gating under restraint.

Examination of restraint-dependent changes in gating levels support our major finding that, as a population, BLA units (n=41) and LFP's (7 animals) show diminished gating under restraint. Single units, multi-units and LFPs all exhibited similar gating levels and similar patterns of change with

restraint. Restrained mice showed poorer auditory gating as evidenced by higher gating ratios in response to BBN compared to free-moving mice, both for units (-0.35 vs. -0.52, p=0.024) and for LFPs (-0.22 vs. -0.50, p=0.035). Reduced gating occurred in 68% of units and in 6/7 animals LFP's. Units (58%) also showed reduced gating in response to pairs of vocalizations (-0.09 vs. -0.30, p=0.031).

These patterns of change in the mouse amygdala correspond to those measured via cortical EEG recordings in human. Human patients with PTSD show less gating of the p50 wave response. Here we show that the mouse analogue of the p50, the p20, is less gated in the BLA of a mouse model of PTSD. Further, we show that single and multi-unit activity is also less gated. These data implicate abnormal BLA function in auditory abnormalities in PTSD.

PS 194

Functional Segregation in Ascending Projections from the Gerbil Inferior Colliculus to the Auditory Cortex

Gilberto Graña; Kenneth Hutson; Andrew Pappa; William Scott; Harrison Lancaster; Yasr Assisou; Douglas Fitzpatrick
University of North Carolina at Chapel Hill

The ascending central auditory pathway from cochlear nucleus through cortex is characterized by multiple, anatomically distinct, processing stations. We are interested in the arrangement of pathways originating from the inferior colliculus (IC), projecting to the medial geniculate (MG) and from MG onto auditory cortex (AC). We are particularly interested in the distribution of functional properties among these pathways, that is, the degree to which functional properties might converge/diverge along the pathway. We investigated these pathways in the Mongolian gerbil using a combination of anatomical and physiological methods. We use the gerbil for our experimental model as their hearing range reasonably approximates that of humans.

Biotinylated dextran amine injections were placed into different locations within the MG. Such injections result in anterograde labeling of MG projections to layers of AC, as well as retrogradely labeled cells in both the IC and AC, The location and distribution of retrogradely labeled cells in the IC and patches of anterograde labelling in the AC from each injection were examined in 40 µm thick sections. A magnetic resonance image (MRI) of a gerbil brain served as a digital framework to localize and aggregate anatomical data from case to case and to overlay results from the physiological studies into a single composite image

The location of retrogradely labeled cells in the IC varied with the location of the injection in the MG. The plotted cells and results from electrophysiological recordings of binaural sensitivity in the IC were overlaid upon the same MRI framework, and allowed us to examine functional patterns within the IC in comparison to the location of labeled neurons. For example, depending on the location of the injection site in MG, the pattern of retrograde label in the IC correlated with electrophysiological measurements indicative of ITD sensitivity. In the cortex, when aligned using the MRI framework, "patches" of labeling appeared as stripes running dorsorostral to ventrocaudal, and different injections produced stripes at different locations within the areas. Thus our results indicate the presence of functional segregation among ascending pathways from the IC through the MG and the AC.

Funding
NIH NIDCD Grant No. R01 DC011347; NIH/NIBIB National Biomedical Technology Resource Center Grant No. P41 EB015897

PS 195

Plasticity in the auditory behavior of fruit flies

Nao Morimoto; Azusa Kamikouchi
Nagoya University

Animals utilize acoustic signals to communicate with each other. During courtship, male flies sing a courtship song by vibrating their wings to attract female flies. Then female flies gradually become receptive to mating. For male flies, the artificial courtship songs also lead to the chaining behavior, a display of homosexual courtship behavior in male flies. This behavior has long been used as an excellent model for analyzing auditory behavior responses, outcomes of acoustic perception and higher-order brain functions. Recently we found that continuous exposure of the song, which lasts for several tens of minutes, led to a decrease in the chaining behavior and that the shift of the sound pattern immediately released this behavioral suppression. These results indicate that such continuous acoustic stimuli are temporally stored in the brain to affect its physiological condition, under which flies display behavioral suppression and desuppression. However it remains unclear how the fly brain processes and stores continuous auditory information to evoke behavioral changes.

To address the mechanism of this, we first examined 1) how decrease ratio of chaining behavior is modulated by the accumulation of sound stimuli. We found that the behavioral decreases are explained by a combination of two types of decay functions, each of which has distinct kinetics: an initial fast decrease and a following slower one. This result predicts that the way to process information is different between these two decays, i.e. the early phase and the late phase. To explore the neural mechanism for these decays, we are now investigating 2) the neuronal substrates for a temporal storage of acoustic information that modify the chaining behavior and 3) molecular mechanisms that control the suppression of chaining behaviors, especially the mechanisms that contribute to the transition between these two decays. We will discuss our recent progress in this meeting.

Funding
KAKENHI (25115007, 25640010, 25710001), PREST from JST, the Human Frontier Science Program

PS 196

Comparison of Properties of Perceptual Switching in Auditory Streaming Based on Spectral and Temporal Cues

Shimpei Yamagishi[1]; Sho Otsuka[2]; Shigeto Furukawa[2]; Makio Kashino[1,2]
[1]Tokyo Institute of Technology; [2]NTT Communication Science Laboratories

Background

The ABA- streaming paradigm, comprised of sequentially presented two sounds (A and B), has been widely used to study how the auditory system organizes auditory components into perceptual streams. When we listen to the ABA- sequence, perception often switches between one stream and two streams. Here, we examine whether the properties of perceptual switching depends on domain of feature separation. We tested two types of stimuli. One consisted of tone bursts as the A and B sounds that differed in frequency, to examine feature separation in spectral domain. The other consisted of amplitude-modulated tone bursts with identical carrier frequency, but differing in modulation frequency. Here, the A and B tones differed in the time domain.

Methods

Thirteen listeners were presented with 400 repetitions of ABA- patterns. They pressed corresponding buttons whenever they experienced perceptual switching (one stream to/from two streams). The experiments consisted of TONE and AM conditions, in which A and B tones differed in spectral and time domains, respectively. In both conditions, the duration of each signal was 50 ms. The stimulus-onset asynchrony was 110 ms. In the TONE condition, the A-frequency was fixed at 315 Hz and frequency difference between A and B tones (ΔF) was varied in two-semitone steps from two to ten semitones. In the AM condition, modulation depth and carrier frequency of the signal were fixed at 100% and 4000 Hz, respectively. The modulation frequency of the A signal was fixed at 60 Hz. The modulation frequency difference between A and B signals (ΔFm) was varied in 0.5 octave steps from 0.5 to 2.5 octave.

Results

In the both conditions, the probabilities of two-stream percept increased with ΔF and ΔFm. At a comparative two-stream probability, however, the perceptual switching occurred more frequently in the TONE than the AM condition.

Conclusion

The results indicated the mechanism that is responsible for perceptual switching depends on the difference of cues. An interpretation is that a switching-related mechanism is specific to a feature domain. Another is that a property of feature representation at relatively early stage of auditory processing influences the higher-level, switching-related mechanism.

Funding

This work was supported by JSPS KAKENHI (Grant-in-Aid for JSPS Fellows) Grant Number 10886.

PS 197

The Effect of Harmonic Rank on Subjective Stream Segregation of Complex Tones

Sara Madsen[1]; Torsten Dau[1]; Brian Moore[2]
[1]Technical University of Denmark; [2]University of Cambridge

Pitch is an important perceptual attribute for segregation of sequences of sounds. Earlier studies have shown that the tendency to hear two streams in a sequence of A and B tones with different fundamental frequency (f_0) increases with increasing f_0 difference between the A and B tones (Vliegen *et al.*, 1999; Vliegen and Oxenham, 1999). Pitch salience, as assessed by f_0 difference limens (f_0DLs), is stronger for complex tones with low harmonics (low harmonic rank) than for complex tones with only high harmonics (Houtsma and Smurzynski, 1990). It was therefore hypothesized that complex tones with only high harmonics (weak pitch salience) would be less likely to be perceived as segregated on the basis of f_0 differences than tones that also contain low harmonics. However, Vliegen and Oxenham (1999) reported that subjective stream segregation judgements were similar for pure tones and for complex tones with and without low harmonics.

This study investigated the effect of harmonic rank on subjective stream segregation of complex tones for normal-hearing participants and compared the streaming judgements to f_0DLs. The complex tones used in both experiments were bandpass filtered between 2 and 4 kHz and harmonic rank was varied by changing f_0. The participants were asked to try to hear out one stream as separate from the other stream and to indicate when their perception changed between one and two streams. The amount of stream segregation was estimated as the percentage of time that the sequence was indicated to be segregated.

There was a significant effect of harmonic rank on stream segregation. Stream segregation tended to decrease with increasing harmonic rank. This is consistent with the proposed hypothesis but in contrast to what was reported by Vliegen and Oxenham (1999). The discrepancy might be explained by the large variability across participants. A negative correlation between the amount of stream segregation and f_0DLs was observed, indicating that better f_0 discrimination is associated with greater stream segregation.

Houtsma, A. J. M., and Smurzynski, J. (**1990**). "Pitch identification and discrimination for complex tones with many harmonics," J. Acoust. Soc. Am. **87**, 304-310.

Vliegen, J., Moore, B. C. J., and Oxenham, A. J. (**1999**). "The role of spectral and periodicity cues in auditory stream segregation, measured using a temporal discrimination task," J. Acoust. Soc. Am. **106**, 938-945.

Vliegen, J., and Oxenham, A. J. (**1999**). "Sequential stream segregation in the absence of spectral cues," J. Acoust. Soc. Am. **105**, 339-346.

Funding
This research was supported by the Oticon Centre of Excellence for Hearing and Speech Sciences (CHeSS). BCJM was supported by the Rosetrees Trust.

PS 198

Promotion of Stream Segregation by Deviants and Distractors

James Rankin; Pamela Popp; John Rinzel
New York University

Background
Sequences of repeating, interleaved high and low tones are perceived to separate into distinct streams in a process known as build up of stream segregation (van Noorden 1975, Bregman 1978). Sudden changes in the sound sequence can cause a re-setting of build up; see Moore & Gockel (2012) for a review. This resetting of build up can occur with changes in location or loudness of the streams (Rogers & Bregman 1998), with the introduction of deviant tones in timing, frequency or loudness (Haywood and Roberts 2010) or with gaps in the tone sequences (Beauvois & Meddis 1997, Denham et al 2010).

Methods
Eight subjects listened to short presentations of a repeating ABA-triplet stimulus and subsequently reported their percept as either integrated or segregated. In control conditions the stimulus had three or six test triplets. During test presentations the stimulus had six triplets, either with a frequency deviant replacing the third triplet's B tone, or with a distractor tone inserted during the silence following the third triplet (Fig 1A). Base frequencies were roved between trials and the inter-trial interval chosen to avoid carry-over and adaptation effects between trials.

Results
In control conditions the proportion segregated increased for longer presentations and increased for larger DF (Bregman 1978, Anstis & Saida 1985). In deviant and distractor conditions, there was no reset to integrated, but rather a significant increase in the proportion of segregation (Fig 1B). The deviant and distractor showed equivalent effects in promoting stream segregation. The demonstrated effect is opposite to the reset reported in Haywood and Roberts (2010) for a frequency difference deviant. Our paradigm differs in that the deviant (or distractor) tone occurs during an ongoing triplet sequence rather following an induction sequence (e.g. preceding A tones that induce segregation in the test sequence of triplets). We found further that the demonstrated promotion of segregation occurs only when the distractor's frequency is suffciently close to that of the B tone (<5st away).

Conclusion
We found, distinguished from previous reports, that sudden stimulus changes can promote segregation during build up. Further work should be directed at teasing apart the classes of stimulus manipulations that disrupt build up through reset to integration (Moore and Gockel 2012) or promote stream segregation as demonstrated here.

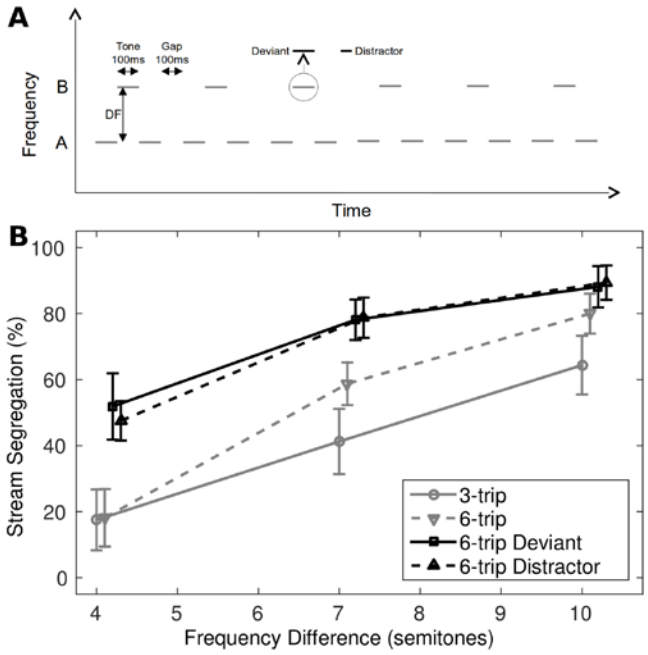

Figure 1: **A**: Stimulus paradigm. Repeating ABA- triplet stimulus with 100 ms tones (with 10 ms cosine on and off ramps) followed by 100 ms gap (total length of triplet unit with gap is 400 s). Low A and high B tones are separated by a DF of 4, 7 or 10 st. Control conditions consist of 3 or 6 triplets. In the deviant condition the third B tone is shifted up by 2st. In the distractor condition an additional 50 ms tone is inserted in the silent gap after the third triplet. **B**: Psychoacoustic results. Each condition was repeated 20 times per subject. Percentage stream segregation is mean across $N = 8$ subjects with SEM shown. Stream segregation (SS) increases with DF in all conditions. SS increases with longer presentation (compare dashed grey with solid grey). SS increases in Deviant condition (compare solid black with dashed grey) and in Distractor conditions (compare dashed black with dashed grey).

Funding
J Rankin is supported on a postdoc fellowship from the SwartzFoundation. POP acknowledges support from the NYU Dean's Undergraduate Research Fund. Partial support for JRinzel comes from an NIH K-18 award, K18 DC011602.

PS 199

Maximum likelihood estimation and entropy-based adaptive tracking for categorical loudness measurements

Andrea Trevino; Walt Jesteadt; Stephen Neely
Boys Town National Research Hospital

Loudness is a measure of suprathreshold perception that provides insight into the status of the auditory pathway. Categorical loudness scaling (CLS) is commonly used for studying loudness perception, due to both its ease of testing and ecological validity. Despite this, there remain concerns about CLS accuracy, and the nature of suprathreshold variability across listeners is not yet fully understood. We have developed a *multi-category psychometric function* (MCPF) that represents the probabilistic relationship between stimulus level and categorical loudness perception. The MCPF adds a new dimension to CLS data and facilitates parameterization of suprathreshold variability across listeners.

By generalizing the individual results for a group of listeners, we have developed a "catalog" of individual-listener MCPF

models. This catalog of statistical models may be used to incorporate optimal techniques from estimation and information theory into the methodologies of standard CLS testing. We present two such techniques: (1) maximum likelihood estimation (MLE) to compute both a listener's CLS function and their multi-category psychometric function from a relatively small number of data points, and (2) an entropy-based adaptive tracking (EBAT) approach that maximizes the expected information of each stimulus presentation. The MLE targets the *accuracy* of CLS measurements, while the EBAT is designed to improve the *efficiency* of CLS testing.

We present results for both of these techniques, for 16 normal-hearing and 33 hearing-impaired adults. We compare the MLE approach to existing techniques and the EBAT to the current ISO methods. In general, the MLE approach results in a more accurate CLS estimate than a conventional approach, while also generating a statistical model of the listener's categorical perception. We show how the EBAT selects stimulus levels that correspond to levels of maximum variability across previous populations of listeners.

These techniques can be combined with existing methods in order to improve the quality of measurements, and the resulting MCPFs can be used to extend the characterizations and analyses of individual-listener suprathreshold perception.

Funding
This research was supported by grants from the NIH: T32 DC000013, R01 DC011806 (WJ), R01 DC008318 (STN), and P30 DC004662.

PS 200

Effects of Harmonic Resolvability on the Perception of Multiple Complex Pitches

Jackson Graves; Andrew Oxenham
University of Minnesota

A potential mechanism for pitch perception is the rate-place code, which arises from the tonotopic organization of the auditory system. This code is usable only where harmonic peaks are spaced far enough apart relative to auditory filter bandwidths that they are resolved. Most studies of resolvability in pitch perception have concentrated on the pitch of single sounds, some have investigated the pitch of two simultaneously presented sounds, but few if any have investigated pitch perception with three or more simultaneous pitches. In contrast, presentation of multiple pitches is common in many natural listening contexts, especially music. We investigated the effects of resolvability using three simultaneously presented harmonic complexes, filtered into a single bandpass region to control the extent to which harmonic peaks in the resulting mixture were resolved. In one experiment, the three tones comprised the three possible inversions of a major or minor triad, and the listener's task was to discriminate between major and minor (a difference of one semitone). In another experiment, listeners were asked to compare the middle tone of the three-tone combination to a single reference pitch presented in isolation. Preliminary data suggest that in bandpass regions where individual tone complexes would be resolved in isolation, listeners were capable of discriminating at or below a semitone, even when tone complexes were filtered such that the combination of harmonic components should have been unresolved. This finding suggests resolved harmonics may not be necessary to extract the pitch from multiple complex tones. Predictions from various spectral and temporal models of pitch were compared with the results.

Funding
This work was supported by NIH grant R01 DC 05216.

PS 201

Infants' and Adults' Detection of Vowels and Two-Syllable Words in Speech Maskers

Monika-Maria Oster; Lynne Werner
University of Washington

Auditory skills and auditory development are increasingly studied with natural speech stimuli and multi-talker maskers. Although natural speech provides ecological validity, masking of speech created by competing speech is a complex function of energetic and informational masking, made more complex by the fact that listeners are often able to use spectral and temporal glimpsing to gain release from masking. How infants and children understand speech in a speech background is a topic of current interest. However, it is difficult to compare results from different laboratories, because a variety of speech stimuli and maskers are currently used. Differences in maskers and target speech may account for discrepancies in performance between studies.

An initial study of adults investigated how differences in the type and intonation of maskers and targets influenced detection thresholds. Results showed that detection thresholds depended on an interaction of masker type, masker intonation, target type and target intonation. To determine whether 7-month-old infants' detection of speech was similarly affected by those variables, four conditions were chosen based on the results from adults: The targets were either /a/ or 'baby' in a two-talker masker or matched spectrum noise. Both targets and the speech masker were produced using an adult-directed intonation. The targets were matched for duration and RMS amplitude. The stimuli were presented to infants' right ear using an ER2 insert phone. Maskers were presented continuously at 55 dB SPL, and targets were presented at 75 dB SPL. Infants were tested in one of the four conditions, using an observer-based procedure. Following training, infants completed 32 trials, half of which contained the target. The measure of performance was *d'*. Preliminary results indicate that infants are more sensitive to 'baby' than to /a/ in both speech-spectrum noise and the two-talker masker. In contrast, adults' detection thresholds were significantly lower for /a/ than for 'baby' in the two-talker masker and did not differ in the speech-spectrum noise'.

Although it is not clear what acoustic characteristics or listening strategies lead to the amount of masking observed, it is clear that infants are not affected by those variables as

adults are. Thus, characterization and standardization of speech stimuli used in developmental studies should be a priority for investigators in this field.

Funding
R01 DC000396, P30 DC004661, T32 DC000033

PS 202

Implications of Positive-Real Physical Quantities for Psychophysical Measures of Performance

Björn Friedrich; Peter Heil
Leibniz Institute for Neurobiology

In stimulus matching tasks, psychophysical measures of performance, such as the point of subjective equality (PSE), constant error (CE), difference limen (DL), and Weber fraction (WF), are conventionally defined by arithmetic statistics in conjunction with the Euclidean distance function $d_R(x, y) = |x - y|$ defined on the set of real numbers, R, with usual addition and scalar multiplication, $(R, +, \cdot)$. However, most fundamental and many derived physical quantities (with dimensions such as length, mass, duration, frequency, pressure, and velocity) can attain only positive real magnitudes, i.e., are elements of the set of positive-real numbers, $R_{>0}$. It is often assumed that the vector-space operations of R and the Euclidean distance function also apply to $R_{>0}$, because $R_{>0}$ is a subset of R. This is a misconception, however. The actual vector-space structure of $R_{>0}$ is the one with usual multiplication and exponentiation, $(R_{>0}, \cdot, \hat{})$, rather than usual addition and multiplication. Moreover, the log-ratio distance function $d_{R>0}(x, y) = \ln|\frac{x}{y}|$ is the analog to d_R.

We emphasize that arithmetic statistics, which are consistent on R, possess convexity biases when applied to random variables sampled from $R_{>0}$. The more dispersed the probability distribution, the larger the convexity biases. We demonstrate that rigorous regard for the allowed operations yields geometric statistics. Furthermore, we derive mathematically consistent, unbiased psychophysical measures based on these statistics in conjunction with the log-ratio distance function. We also demonstrate that the conventional CE may exaggerate the size of perceptual illusions or suggest illusions when none exist. Positive values of the CE may result from convexity biases rather than from brain-related effects.

Funding
Supported by the Deutsche Forschungsgemeinschaft (SFB/TRR 31)

PS 203

Manipulating the spatial relationship of visual and competing auditory stimuli in the sound-induced flash illusion.

Lindsey Kishline; Adrian KC Lee; Ross Maddox
University of Washington

Background
The human brain makes sense of incoming sensory information by combining auditory and visual stimuli that plausibly come from the same source into a single perceptual object. This process is trivial with a single stimulus in each sensory modality, but factors such as audio-visual spatial congruence have important perceptual effects once there is competition between stimuli. The sound-induced flash illusion (SIFI), in which the number of rapid auditory beeps affects the number of visual flashes reported, provides a way of testing for cross-sensory integration through perceptual illusion. However, previous work has led to inconsistent findings of the influence of auditory-visual spatial (in)congruence on the probability of illusory trials. To better assess this possible influence of spatial proximity, we used a parametric manipulation of the spatial separation of two competing auditory streams and a single visual stimulus using the SIFI.

Methods
In each trial, the subject was presented with two timbrally distinct auditory stimuli at different locations and one visual stimulus comprised of either one or two rapid flashes. They were asked to report whether they saw one visual flash or two. The visual flash(es) occurred either centrally or on the left or right side, for three possible locations. One of the auditory stimuli always occurred at the same location as the visual stimulus, and the other occurred at one of the other two remaining locations. One auditory stimulus always matched the number of visual flashes and one did not. We manipulated whether the auditory stimulus that matched the number of visual flashes was spatially congruent with the visual stimulus.

Results and Conclusions
In this study we tested whether the proximities of the matching and nonmatching auditory stimuli affected the likelihood of reporting a visual illusion. Previous studies have found little effect of the proximity of an auditory stimulus on the likelihood of a visual illusion, however most have used a non-competing auditory stimulus or have employed less fine-grained spatial arrangements of competing auditory stimuli. The present study thus tells us more about how the spatial congruence of auditory and visual stimuli affects their integration, an important element of multisensory processing.

Funding
T32-DC005361 (LRK), R01DC013260 (AKCL), K99DC014288 (RKM)

PS 204

Modeling the Integration of Audio-Visual Distance Information

Lubos Hladek[1]; Norbert Kopco[1]; Aaron Seitz[2]
[1]P. J. Safarik University in Kosice; [2]University of California, Riverside

Auditory and visual stimuli can fuse into a single percept even if each of them is presented from a different location. We recently examined this illusion, called the ventriloquism effect (VE), in the distance dimension [Hladek et al., (2014), Visual Calibration of Auditory Distance Perception, ARO San Diego Volume 37, PS-614, p. 384]. Typically, the fused object's perceived location is near the visual signal location,

even if the subject is instructed to localize the sound, and the visually induced shift persists even after the visual component is removed. This persistent shift, called the ventriloquism aftereffect (VA), reflects a rapid plasticity in the auditory space representation. Here, a quantitative model of audio-visual (AV) integration is proposed and evaluated on the Hladek et al. data.

In the previous study, two experiments were performed in a small reverberant room. Listeners localized a 300-ms broadband noise (A-only trials) coming from one of 8 loudspeakers placed at different distances in front of the listener. On interleaved audio-visual (AV) trials, sounds were paired with visual signals that were aligned with the sounds (V-Aligned) or displaced closer (V-Closer condition) or farther (V-Farther) from the sounds by 30%. The tested model is a simple model of optimal combination of visual and auditory information [Alais and Burr (2004)]. Several extensions of the model are considered, examining various sub-optimal information integration schemes. To model the VA data, the model is extended by adding memory noise to the representation of the visual component.

In the experiment, the AV responses shifted towards the visual component and the shift magnitudes varied with the distance and direction of the V-displacement. The persistence of the shift was observed on various timescales. In addition to the response bias, visual component also decreased the response variance. However, the direction of the shift had only negligible effect. The decrease in response variance also persists on the interleaved A-only trials when compared to sessions with no visual stimulus.

The simple optimal AV integration model cannot explain the observed data as the measured response variance in AV trials is much higher than the predicted response variance, determined mostly by the measured variance of the visual component. This mismatch also causes errors in the bias predictions. These result suggests that humans do not integrate the multisensory information optimally in this task, most likely because they put a higher-than-optimal weight on the auditory component of the stimulus.

Funding
Work supported by TECHNICOM (ITMS: 26220220182, EU R&D OP funded by ERDF) and APVV-0452-12.

PS 205

Perception of Auditory and Visual Disruptions to the Beat and Meter in Music

Jessica Nave-Blodgett; Erin Hannon; Joel Snyder
University of Nevada, Las Vegas

Humans can perceive an isochronous beat in rhythmic auditory patterns such as music and use this information to make perceptual judgments, tap to the beat, and dance. Beyond the beat level, beats can be grouped into repeating patterns of strong and weak beats, with some beats perceived as stronger (measure downbeats) and others heard as weaker (upbeats). Yet we do not know if people regularly perceive these so-called metrical hierarchies in music or in visual patterns like dancing. We wanted to determine if listeners could identify not only the beat but also the higher metrical levels like the measure-level downbeat in music. Adult musicians and non-musicians listened to excerpts of ballroom dance music paired with either auditory or visual metronome-like click tracks, and rated how well the metronome fit the music they heard. The metronomes could be synchronous with the music at the level of the beat, the measure (the strongest beat in the repeating strong-weak patterns), both the beat and measure, or neither. This yielded four metronome conditions: beat and measure asynchronous, beat asynchronous and measure synchronous, beat synchronous and measure asynchronous, and beat and measure synchronous. Auditory metronomes consisted of simple sine-wave beeps at the beat and measure level, while visual metronomes appeared as ticking clocks that marked the beat and measure. All participants experienced auditory and visual metronomes in separate experimental sessions. For auditory and visual metronomes alike, all participants rated beat synchronous metronomes as fitting the music better than beat-asynchronous metronomes. However, only musicians showed evidence of hierarchical perception, rating measure and beat synchronous visual and auditory metronomes as fitting the music than metronomes synchronous at the beat level alone. Non-musicians did not rate beat and measure synchronous metronomes as fitting the music better than metronomes that were synchronous at the beat level alone, regardless of metronome modality. In summary, adult musicians and non-musicians successfully extracted beat-level information from musical excerpts and matched it to the fit of auditory and visual metronomes. Only musicians were sensitive to the measure level information in the auditory and visual metronomes and their fit to the music. Because perceiving multiple hierarchical beat levels could be useful for musical performance and synchronization, formal training in music may enhance sensitivity to these additional levels. Without a need to use these hierarchical beat levels in their daily lives, non-musicians may not perceive or use these levels in judgments of fit.

PS 206

Sequential Streaming Under Reverberation: When Rooms Collide

Eugene Brandewie; Andrew Oxenham
University of Minnesota

Background
A physical difference between two stimuli has been known to elicit perceptual segregation when the segregation cue (such as F0) is perceptually salient. Previous work has shown that differences in the spectral qualities of reverberant tails facilitate perceptual segregation. Here we study the effect of differences in reverberant temporal envelopes with matching spectra using both a 3IFC detection task and a rhythmic masking segregation task.

Methods
For the discrimination task, two interleaved sequences of Gaussian noise bursts (target and interferer) were presented on each trial and listeners attempted to identify which of

two rhythms was presented in the target sequence. The difference in reverberation between the target and interferer was parametrically varied in an adaptive procedure to measure reverberation time thresholds. Listeners were tested in both monaural and binaural conditions at both 0 degree and 90 virtual azimuth for sources set 2 m away in a virtual room environment. For the detection task, the difference in reverberation time was also parametrically varied in an adaptive procedure, where listeners reported which of the three intervals contained more reverberation. In all tasks, level was roved by +/- 6 dB, ensuring listener responses relied on perceived differences in direct-to-reverberant (DRR) energy ratios, rather than overall level.

Results

The results suggest that streaming based solely on differences in reverberation time may be difficult, despite no difficulty in detecting these differences. These difficulties may relate to an inability of listeners to maintain two internal room models simultaneously.

Funding

Supported by NIH grant R01DC07657.

PS 207

Temporal Differences of Ear Lateralization in Dichotic Sample Discrimination Task

Alison Tan; Bruce Berg

University of California, Irvine

Background

Tan and Berg (2015) used a dichotic sample discrimination task to determinethat listeners have an unexpectedly wide range in ability to lateralize as shown by collected decision weights, efficiency measures and performancelevel (d'). Estimates of d' range from 0.7 – 2.4. In this follow-up study,intertone interval (ITI) was manipulated to examine changes in individualweighting strategies. Two subjects (AT and AL) were further examined dueto their inability to attend to the target ear from the initial experiment. Weexamine whether increased inter-tone interval (ITI) benefits listener performance and decision weighting strategy.

Methods

On each trial, seven 60-ms tones are drawn from a normal distribution withmeans of 1000 or 1100 Hz. Even numbered tones are the most informative (d'=2) and presented to one ear and the less informative, odd numberedtones (d'=0.5) are presented to the other ear, alternating sequentially. Participants indicate from which distribution the tones are sampled. Task difficulty is manipulated by presenting odd-and even-numbered tones atdifferent intensities. In easy conditions Right Loud and Left Loud (RL, LL),informative and less informative tones are presented at 70 dB, 50 dB, respectively. In hard conditions Right Quiet and Left Quiet (RQ, LQ), informative and less informative tones are presented at 50 dB, 70 dB,respectively.

In the initial study, there was an ITI of 0ms meaning that tones alternatingfrom each ear are without pause. In the follow-up, tones are presented with an ITI of 300ms for listeners who demonstrated reverse weighting for oddtones rather than even tones in the right quiet (RQ) condition will have anITI of 300ms.

Results and Discussion

Turner and Berg (2007) showed that observers altered their listening strategywhen ITI increased to 500ms. Our findings, however, suggest that dichoticlistening requires less time.

Initial findings in the RQ condition showed AL and AT both gave greater weight to the odd tones instead of the even tones at 0ms ITI. However, whenITI was extended to 300ms, the weights for AL and AT shifted into optimal weighting with greater weight for the even tones. Extending the temporalgap between tones increased performance (d') by a factor of 2 for both listeners. In future studies, we want to further investigate the temporalprocessing differences between diotic and dichotic listening.

PS 208

A New Approach to Model Pitch Perception Using Sparse Coding

Oded Barzelay[1]; Miriam Furst[1]; Omri Barak[2]

[1]Tel Aviv University; [2]Technion - Israel Institute of Technology

Our acoustical environment is abound with sounds that repeat to some extent over time, a repetition that is related to the perception of pitch. It is still unknown how the auditory system relates a physical stimulus and its percept. In mammals, all auditory stimuli are conveyed into the nervous system through the auditory nerve fibers (ANFs), and a model should explain the perception of pitch as a function of this particular input. Pitch perception is invariant to certain features of the physical stimulus. For example, a missing fundamental stimulus with resolved or unresolved partials, or a low and high level amplitude stimulus with the same spectral content – these all give rise to the same percept of pitch. In contrast, the ANFs' representations for these different stimuli are not invariant to these effects. In fact, due to saturation and non-linearity of both cochlear and inner hair cells responses, these differences are enhanced by the ANFs. Thus there is a difficulty to explain how the pitch percept arises from the activity of the ANFs.

We introduce a novel approach to extract pitch cues out of the ANFs' activities for a given arbitrary stimulus. The method is based on a technique known as sparse coding (SC). It is the representation of pitch cues by a few atoms (templates) out of a large set of possible ones (a dictionary). The amount of activity of each atom is represented by an active coefficient, analogous to an active neuron. Such a technique was successfully applied to other modalities, especially vision. The model is composed of a cochlear model, an SC processing unit, and a simple implementation of a harmonic sieve. We show that the model can cope with different pitch phenomena. In particular, it enables the extraction of resolved and non-resolved harmonics, missing fundamental pitches, pitch of iterative ripple noise, and stimuli with both high and low amplitudes.

Funding
ISF 563/12 (M. Furst), ERC FP7 CIG 2013-618543 (o. Barak), Adelis Fondation (O. Barak)

PS 209

Sound Texture Synthesis Based on Hierarchical Processing of Amplitude Modulations

Richard McWalter; Torsten Dau
Technical University of Denmark

Background
Sound textures, such as a campfire or swarm of insects, are characterized by their temporal homogeneity and their perception may depend on time-averaged statistics measured from a standard model of the auditory system. However, the perception of more advanced modulation structures, such as rhythmic patterns, are relatively unstudied for sound textures. Thus, we extended the sound texture synthesis system of McDermott and Simoncelli (2011) to include cascaded modulation filterbanks, accounting for the sensitivity of the auditory system to beating in the envelope-frequency domain. Such beating may be captured by an auditory mechanism sensitive to second-order amplitude modulations. We generated synthetic textures with various model parameters to investigate the significance of amplitude modulations in sound texture perception.

Method
An auditory model was developed to account for second-order modulation masking data (Ewert et al. 2002) that consisted of three linear filter stages – frequency selective peripheral filtering, first- and second-order modulation filtering – with inter-stage envelope extraction. Texture statistics, including marginal moments and pair-wise correlations, were measured at the output of the peripheral, first- and second-order filtering stages. Synthetic sound textures were generated with graduated texture statistic groups at each stage of the model. Listeners performed an identification task to evaluate the contribution of different statistic groups in texture perception. In each trial, listeners were presented with synthetic sound textures and selected a corresponding text descriptor from a list of five choices.

Results
Realistic synthetic textures could be generated from the statistics measured from a broad range of original sound textures using the extended texture synthesis system. Increased identification performance was observed for each stage of the model, and the inclusion of the second-order modulation processing yielded the highest identification performance, approaching that of the original textures. In addition, the statistics measured at the output of the second-order modulation filterbank varied across textures, indicating that this analysis stage may contribute to texture perception.

Conclusion
The results suggest the sensitivity of the auditory system to second-order modulations may contribute to sound texture perception. This mechanism could also mediate the time-averaged depth of first-order amplitude modulations. The inclusion of higher-order modulation processing may also play a roll in the perception of more complex sounds, such as speech.

Funding
Technical University of Denmark

PS 210

Effect of Voice Duration on Numerosity Judgments of Simultaneous Talkers

Takayuki Kawashima
Teikyo-Heisei University

Effect of stimulus duration on numerosity judgments of simultaneous talkers was examined to estimate time required for listeners' internal counting of multiple voices. After listening to multiple voices that were presented simultaneously, listeners (N = 12) were required to report the number of talkers by choosing one of the ten alternatives in each trial (from 0 to 9 talkers). Actual number of talkers was randomly selected from 4 conditions (from 1 to 4 talkers). The duration of voices was manipulated in 4 conditions: 0.2, 0.4, 0.6, and 0.8 s. Overall level of stimulus presentation was randomized within 20 dB range across trials.

When the duration of voices was more than 0.2 s, the average proportion of correct numerosity judgments was high (more than .9) both in 1 and 2 talker conditions and the difference between the two conditions was not statistically significant. When the duration of voices was shortened to 0.2 s, the proportion of correct judgments in the 1 talker condition was as high as before, however, it decreased from around unity in the 2 talker condition and the proportion was lower compared to that in the 1 talker condition. The average proportion of correct responses was relatively lower (less than .5) in 3 and 4 talker conditions, although the performance tended to be better as the duration became longer.

In another experiment block, white noise (1.0 s) was presented immediately after the simultaneous voices in each trial to disturb listeners' auditory memory use. The almost same tendencies were observed as in the previous experiment, excepting that the performance in 2 and 3 talker conditions was worse compared to that in no-noise conditions.

The results indicate that the duration of voices must be longer than 0.2 s for listeners to count multiple or two simultaneous talkers correctly. Because numerosity judgments for multiple voices would require listeners switching a target of selective listening during counting, the results suggest that a target shift of selective listening in a multiple talker condition is not accomplished within approximately 0.2 s or requires more than a few hundred milliseconds interval.

PS 211

A situation in which the ipsilateral ear does not contribute to the amount of perceived reverberation

Gregory Ellis; Pavel Zahorik
University of Louisville

Background

Binaural squelch is the perceptual reduction of reverberation when listening with two ears relative to one. Although it is often discussed in the hearing aid and cochlear implant literature, relatively little is known about the magnitude of the effect or the precise stimulus properties that underlie it. This study examines an auditory phenomenon that may help to better understand binaural squelch.

Methods

Stimuli were generated using virtual auditory space techniques. Binaural room impulse responses (BRIRs) were generated for sounds to the right of the listener (+90 degrees) in a moderately reverberant room. BRIRs were manipulated to scale the amount of reverberation in either the channel ipsilateral to the source or in both channels (3 dB steps from 0 to -21 dB re: unaltered BRIRs). The direct-path signal was unaltered. Sixteen BRIRs (seven scaled plus one anechoic in each of the 2 scaling conditions) were convolved with speech (single CRM sentence, female talker) to generate the stimuli used in the experiment.

Subjects performed a magnitude estimation task with a standard stimulus (the unaltered stimulus). Subjects were instructed to report the amount of perceived reverberation in the test stimulus relative to the standard using a ratio scale. Subjects could repeat the standard as many times as they wished. Subjects made at least five ratings per stimulus. Stimuli were presented in a random order.

Results

Power functions of the form $y = kx^a$ were fit to the data. Data show that subjects generally rate the stimuli in which the ipsilateral channel is altered to have the same amount of reverberation as the unaltered stimulus. Subjects also rate the binaurally altered stimuli to have progressively less reverbation as the physical amount of reverberation is reduced. These trends are strong and consistent across subjects.

Conclusions

Subjects are able to scale perceived reverberation consistently when reverberation is reduced in both ears.

Reducing the amount of reverberation in the ear nearest the source has little to no effect on ratings of perceived reverberation in the conditions tested (source at +90 degrees). This is therefore a demonstration of complete or near-complete binaural squelch.

PS 212

Undirected head movements when listening to speech in noise and competing speech

Yi Shen[1]; Monica Folkerts[2]; Virginia Richards[2]
[1]Indiana University; [2]University of California, Irvine

Background

Listeners are often free to move their head when listening to a target message in multi-source sound environments. However, the role of movements on the recognition of the target speech is not well understood. Among other things, the introduction of head movements may change the local signal-to-noise ratio and may reflect efforts to orient the head so that the target is forward. Past work suggests that a peripheral masker (e.g., noise) can better mask a speech stream than a central masker (e.g., competing speech). Therefore, we hypothesized that a noise masker would generate more reliable, and more rapid, head movements to reduce the amount of energetic masking.

Method

Undirected head movements were recorded during a task in which a target speech stream, two concatenated sentences produced by the same talker drawn from the Coordinate Response Measure (CRM) corpus, and a competing masker were presented through two loudspeakers located ±165˚ from the frontal center and 1.5 m away from the listener. The target stream was randomly assigned to one of the loudspeakers on each trial. The listener was instructed to keep track of the target speech, identified by the call sign “Baron” at the beginning of the first sentence, and to repeat back two keywords (a color and a number) contained in the second sentence of the stream. The masker was either a speech-shaped noise or a unique two-sentence stream from the CRM corpus. Ten listeners with normal hearing participated.

Results

Half of the listeners did not exhibit significant head movement during the presentation of the stimulus, and no significant difference in performance was found between the group of listeners who turned their head and the group who did not. The listeners who turned their heads oriented toward the target. There was no significant evidence that the speech-shaped-noise masker led to earlier head turns than the competing-speech masker, even when the speech recognition was significantly poorer for the noise than for the speech maskers. Interestingly, the source of intrusion errors was due to the portions of the masker temporally overlapping the target keywords to be detected.

Conclusion

For normal-hearing listeners, undirected head movements did not depend on whether the masker was speech or noise. Moreover, speech recognition was the same regardless of whether the subjects turned their head or not.

Funding

This research was supported by the NIH Grant R21DC013406 (MPIs: V.M.R. and Y.S.).

PS 213

Sound Recognition Depends on Real-World Sound Level

Sam Norman-Haignere; Josh McDermott
MIT

Instances of the same sound class (e.g. different dog barks) vary in their acoustics. How does the auditory system recognize sounds across such variation? As a simple case study, we investigated the effect of level on environmental sound recognition. In principle, level-invariant recognition could be achieved by a simple transformation that separates level from listeners' internal representation of sound identity (e.g. by a mechanism akin to RMS normalization). Alternatively, listeners could take advantage of the fact that different sound classes are typically heard at different levels. Thus, by internalizing the unique distribution of levels that characterize a sound, listeners could use level as a cue to aid recognition. A key prediction of this latter hypothesis is that sounds presented at atypical levels (those rarely encountered in daily life) should be more difficult to recognize. We tested this prediction by asking human listeners to identify 300 real-world sounds presented at one of 7 different sound levels between 30 and 90 dB SPL. We grouped these 300 sounds into those typically heard at low (e.g. salt-shaker) and high sound levels (e.g. jackhammer) using ratings collected via Mechanical Turk. For typically loud sounds, we found that recognition accuracy improved monotonically with increasing experiment level. But for typically quiet sounds, recognition accuracy declined when experiment levels exceed 60 dB SPL. This pattern demonstrates that listeners' ability to recognize a sound depends on the level at which that sound is typically heard. More generally, these results suggest that listeners may internalize the unique distribution of acoustic features that characterize individual sounds, and use this distribution to recognize them.

Funding
National Science Foundation Research Fellowship to Sam Norman-Haignere McDonnell Foundation Scholar Award to Josh McDermott NEC Research Support Award to Josh McDermott

PS 214

Tracking auditory thresholds

Dorothée Arzounian[1,2]; Mathilde de Kerangal[2]; Alain de Cheveigné[2]
[1]CNRS; [2]Ecole Normale Supérieure

Perceptual performance is thought to depend on ongoing brain state. In order to relate fluctuations of performance to measures of ongoing brain activity, it is necessary to accurately track these behavioral variations over time. We investigate here the benefit of interleaving multiple, independent tracks within an adaptive staircase procedure in order to track fluctuations of auditory thresholds. Numerical simulations demonstrate that the comparison of within- and inter-track correlations provides a sensitive index for the presence of temporal threshold variations. Besides, we show that multiple-track procedures improve threshold tracking over single-track procedures by providing more accurate local threshold estimates in case of slow, small-amplitude variations. Finally, experiments involving human participants validate the ability of a procedure with 4 interleaved tracks to accurately detect and track threshold changes induced by stimulus and attention manipulation.

Funding
EU H2020-ICT grant 644732 (COCOHA); Région Ile-de-France (DIM Cerveau & Pensée); Ecole Doctorale Frontières du Vivant (FdV) – Programme Bettencourt

PS 215

Determining the Energetic and Informational Components of Speech-on-Speech Masking using a Time-Frequency Glimpsing Model

Gerald Kidd Jr.[1]; Christine Mason[1]; Virginia Best[1]; Jayaganesh Swaminathan[1]; Elin Roverud[1]; Kameron Clayton[2]
[1]Boston University; [2]Harvard Medical School

Background
This study addressed some of the reasons for the large variation in findings across speech-on-speech masking studies. A reference condition was tested in which a high degree of informational masking (IM) was present. Three stimulus variables were tested in comparison conditions that were expected to provide a large release from masking. The same listeners participated under each of these conditions so that the effectiveness of each masking release variable could be examined and comparisons made. A means for estimating the intelligibility of the target speech after accounting for the energetic masking (EM) under each condition was implemented using an ideal binary mask procedure to produce "glimpsed" speech.

Methods
Identification of target speech was studied under masked conditions consisting of two or four speech maskers. Targets and maskers were 5-word sentences from a closed-set corpus. Identification was measured at six target-to-masker ratios in each condition. In the reference conditions, the maskers were colocated with the target, the masker talkers were the same sex as the target talker, and the masker speech was intelligible. The comparison conditions included spatial separation of the maskers from the target, different-sex masker talkers, and masker time-reversal. To account for EM, a binary mask was applied in which only the time-frequency units where the target energy exceeded the masker energy were retained and then the stimulus was resynthesized. Speech identification was then measured using these processed stimuli.

Results
Significant release from masking (re. the reference) was found for all test conditions and both numbers of masker talkers. The performance-level functions for all glimpsed cases were the same for a given number of maskers indicating that the differences observed in the natural speech conditions were not due to differences in EM. Furthermore, the release from

masking for the three comparison variables was generally correlated across individual subjects. The functions for the 4-talker glimpsed masker were shifted about 10 dB higher than for the 2-talker glimpsed masker, an effect that was related to the proportion of energy retained in the glimpsed stimuli.

Conclusions
The results were interpreted as indicating that the large release from masking found under all test conditions was due primarily to a reduction in IM and not to a reduction in EM caused by the masker manipulations. Furthermore, based on this analysis, the amount of EM across conditions was approximately the same and was governed by the number of masker talkers.

Funding
Work supported by NIH/NIDCD.

PS 216

Investigations into Effects of Basilar Membrane Nonlinearity on Interaural Cues Using the Novel Modular Software Framework of the Two!Ears Project

Chungeun Kim; Armin Kohlrausch
Eindhoven University of Technology

Nonlinearity of the basilar membrane operation in response to changing input sound levels is a well-known finding in peripheral auditory processing. However, its consequences in terms of variations in binaural cues related to spatial perception have not been systematically evaluated. This study investigates, by means of computational simulations, some binaural cues known to be dependent upon the basilar membrane responses, with a view to revealing the effects of input level caused by the nonlinear basilar membrane operation. A novel software framework was developed which enabled the simulation, in an on-going European project named TWO!EARS (http://www.twoears.eu/). This framework allows for computational modelling of various known stages of auditory processing and feedback, including signal-driven (bottom-up) peripheral processing and hypothesis-driven (top-down) cognitive processing. It is also designed in an object-based modular manner such that each processing stage can be modeled as an individual module and be interconnected with one another, which ensures flexibility in simulation and extension with new findings. Using the peripheral part of the software, simulations were conducted with modules that mimic the processing at the outer/middle ear, the basilar membrane, the inner hair cells, and the adaptation properties of the auditory nerve. In particular, the basilar membrane processing was simulated with a Dual-Resonance Non-Linear (DRNL) filterbank model (Meddis *et al*., 2001, J. Acoust. Soc. of Am., 109(6), 2852–61). Internal representations such as Interaural Level Differences (ILDs) and Interaural Coherence (IC) were examined in response to binaural sinusoidal, narrowband-noise, and speech signals with varying overall reference levels and stimulus ILDs. As expected, the ILDs derived from the internal representation were in general smaller than the stimulus ILDs. The amount of ILD reduction from the stimuli to the internal representation depended on the reference level and the stimulus ILD, which finally determine the amount of compression by the basilar membrane in either ear. It was also observed that the IC is affected by the stimulus ILDs alone, which is not observed with linear peripheral models. The findings suggest that the aspects of spatial perception which depend upon these binaural cues need to incorporate this signal-level dependence. These simulation results thus motivate further perceptual investigations to reveal how the human auditory system copes with these level-dependent variations in binaural cues; one such example in the literature is the level dependence of time-intensity trading ratios found with short pulses (Deatherage and Hirsch, 1959, J. Acoust. Soc. of Am., 31(4), 486-492).

Funding
This research was funded by the European Union's Seventh Framework Programme for research, technological development and demonstration under grant agreement no. 618075.

PS 217

The Influence of Visual Cues on Sound Externalization

Juan Camilo Gil Carvajal; **Sébastien Santurette**; Jens Cubick; Torsten Dau
Technical University of Denmark

Background
The externalization of virtual sounds reproduced via binaural headphone-based auralization systems has been reported to be less robust when the listening environment differs from the room in which binaural room impulse responses (BRIRs) were recorded. It has been debated whether this is due to incongruent auditory cues between the recording and playback room during sound reproduction or to an expectation effect from the visual impression of the room. This study investigated the influence of a priori acoustic and visual knowledge of the playback room on sound externalization.

Methods
Eighteen naïve listeners rated the externalization of virtual stimuli in terms of perceived distance, azimuthal localization, and compactness in three rooms: 1) a standard IEC listening room, 2) a small reverberant room, and 3) a large dry room. Before testing, individual BRIRs were recorded in room 1 while listeners wore both earplugs and blindfolds. Half of the listeners were then blindfolded during testing but were provided auditory awareness of the room via a controlled noise source (condition A). The other half could see the room but were shielded from room-related acoustic input and tested without the controlled noise source (condition V). All listeners were also tested with all cues available (condition AV). Seven azimuthal source positions were reproduced, with loudspeakers visible at four azimuthal positions.

Results
In condition AV, the auditory images were perceived closer to the listener in rooms 2 and 3 than in room 1, with a larger effect in the reverberant than in the dry environment. In room 2, the

perceived distance of the virtual sounds was more accurate in condition V than in conditions A and AV, where it was reduced. In room 3, differences in distance judgments between A, V, and AV conditions were much less pronounced. In contrast to distance, localization and compactness judgments were largely room independent, although localization judgments were less accurate and compactness ratings less consistent in conditions V and A than in condition VA.

Conclusion
A mismatch between recording and playback room was found to be detrimental to virtual sound externalization. The auditory modality governed externalization in terms of perceived distance when cues from the recording and playback room were incongruent, whereby the auditory impression of the room was more critical the more reverberant the listening environment was. While the visual impression of the playback room did not affect perceived distance, visual cues helped resolve localization ambiguities and improved compactness perception.

Funding
This study was supported by the Technical University of Denmark and a research consortium between GN ReSound A/S, Oticon A/S, and Widex A/S.

PS 218

Sensitivity to Binaural Cues Beyond Threshold as Revealed by Eye Movements

Matthew Winn[1]; Alan Kan[2]; Ruth Litovsky[2]
[1]University of Washington; [2]University of Wisconsin-Madison

Background
Binaural cues are paramount for sound localization along the azimuth. Studies on the perception of the critical binaural cues, interaural differences in timing and level (ITDs and ILDs, respectively) have been typically concerned with measuring sensitivity at threshold using N-interval, forced choice paradigms. This approach gives little or no information regarding perceptual abilities beyond threshold. In this study, an eye-tracking paradigm was used as a novel measure to study binaural cue sensitivity throughout the perceptual range. This novel paradigm is sensitive to gradient (rather than all-or-none) perception of auditory cues.

Methods
An anticipatory eye movement (AEM) paradigm (c.f., McMurray, 2004) was used. Normal-hearing adults fixed their gaze on a moving ball displayed on a computer screen while listening to sounds under headphones. As the ball moved upwards it was occluded by a Y-shaped pipe. During this animation, a sound with ITD or ILD of zero was presented. While the ball was still occluded, the sound transitioned into a left- or right-leaning sound via an ITD or ILD cue, indicating the exit arm of the ball 1 second later. Participants anticipated the motion of the ball via eye gaze toward the correct end of the pipe.

Auditory stimuli were interaurally correlated and uncorrelated 1/3-octave narrowband noises for ITD and ILD conditions, respectively. Noisebands were centered at 500, 1500, or 4000 Hz. One second post stimulus onset, the sound contained an ITD change of 0, 63, 125, 250, 500 or 750 microseconds, or an ILD change of 0, 2, 4, 8, 16, 24 dB.

Results
All participants showed reliable AEMs that reflected gradient perception of binaural cues. Anticipatory looks to the correct side were absent for cues below threshold, at chance near threshold, and robust above threshold, with systematic shorter latencies and fewer gaze direction changes observed for greater cue levels. For ITDs, AEMs were consistent with known limitations in neural phase locking; reliable and early AEMs were measured for 500-Hz noises, with less reliable AEMs for 1500-Hz noises and virtually absent AEMs for 4000-Hz noises. For ILD cues, AEMs were elicited for all noise center frequencies, with shorter latencies for higher frequency noises.

Conclusion
Eye movements are able to reflect the reliability and speed of perceiving ITDs and ILDs within known frequency and threshold limitations, and shows that the perception of binaural cues for sound lateralization is gradient rather than all-or-none.

Funding
NIH-NIDCD (R01 DC003083 to RYL), and NIH-NICHD (P30 HD03352 to Waisman Center)

PS 219

Metacognition in a speeded localization task: real vs. artificial head

Guillaume Andeol; Bouy Jean Christophe; Suied Clara
Institut de recherche biomédicale des armées

Background
In a sound localization task, listeners can point towards the target position in the wrong front-back hemisphere; this is called a “front/back reversal”. In a previous study (Andéol et al, ARO Midwinter Meeting, 2015), using a circular array of loudspeakers, we showed that listeners responded with slower Reaction Times (RT) for positions where front/back reversals were more frequent. Because RTs are often positively correlated with confidence, we hypothesized that confidence was lower for those positions. Therefore, our results were in favor of a metacognition of the listeners in their front/back discrimination ability. Front/back reversals are considerably larger when listening with non-individual localization cues (e.g. listening through an artificial head). That raises the question whether the effect observed with a real-head situation still persists with an artificial-head situation. In the present study, we investigate the metacognition of the listeners in a front/back discrimination task by using a RT paradigm, with an artificial head.

Methods
An artificial head was positioned at the center of a 12-loudspeakers ring (Azimuth: 0 to 360 by 30°step), inside an anechoic chamber. A wideband noise target was presented at 70 dB SPL with a 10 dB roving range. Listeners sat in the control room of the anechoic chamber. They had

to indicate whether the target was in front of or behind them by pushing a switch. They were asked to respond as quickly and as accurately as possible. For half of the participants, a confidence rating between 0 and 9 was asked after each trial, in order to check the relationship between RT and confidence. This measure was done both with real and artificial head.

Results
While a strong positive correlation between RT and performance was found in the previous study with real head, (Andeol et al, ARO, 2015), a very different pattern was revealed here, with artificial head. The correlation between RT and confidence was very weak, and significantly lower than the one with real head. It suggests that with artificial head, participants were not conscious of their errors.

Conclusion
These results suggest that the listeners' metacognition is reduced when they use non individual localization cues.

Funding
Délégation générale pour l'armement (French Procurment Agency)

PS 220

The Equivalent Arc for Auditory Motion and the Non-Uniformity of Acoustic Space

W. Owen Brimijoin[1,2]; Michael Akeroyd[1]; Tom Freeman[3]
[1]MRC; [2]CSO; [3]University of Cardiff

It has been well established that both the minimum audible angle (MAA) and the minimum audible movement angle (MAMA) change as a function of source azimuth: the MAMA is roughly 1-2° in front of the listener and increases to about 4° at the side. Previous work on an apparently incomplete subtraction of self motion led us to hypothesize that neither the MAA nor the MAMA are simply measures of acuity, rather they reflect an underlying azimuth-dependent expansion of auditory space. This postulate -- which we term the 'equivalent arc' for auditory motion -- gives rise to the prediction that judgments of relative amounts of acoustic motion would depend on the angles with respect to the head from which the signals originated.

We therefore measured the point of subjective similarity for amount of acoustic motion between test and reference signals (amplitude modulated pink noise) that were both panned smoothly around our 3.5 m diameter ring of 24 loudspeakers. The reference signal moved 20° in a random direction and the test signal moved either less, the same, or more. Both the reference and the test signals could be centered at either 0°, 45°, or 90°. Test/reference order was randomized as was duration between 0.5 and 2 seconds, eliminating velocity and duration as cues for amount of motion and leaving only total excursion as the variable that listeners were asked to judge.

Across all conditions we found that the azimuth of two signals strongly affects their point of subjective similarity for motion. When compared to reference signals at 45°, test signals at 0° had to be moved significantly less to be perceived as moving the same amount, and test signals at 90° had to be moved significantly more. Signal motion at 90° had to be two to three times as large to be judged as equivalent to motion at 0°, which we take as strong evidence for an azimuth-dependent expansion of acoustic space. This finding has implications for the apparent stability of the acoustic world as we move, as well as for virtual acoustics and the creation of "hyper-stable" auditory environments.

Funding
Work supported by the Medical Research Council (UK) and the Chief Scientist Office (Scotland)

PS 221

Differential Maturation of Auditory and Auditory-visual Horizontal Localization Accuracy in Children

Filip Asp; Åke Olofsson; Erik Berninger
Karolinska Institutet

Background
Infant auditory and visual localization are both immature at birth. Improvements are related to increasing age, with a systematic increase of auditory localization accuracy from 6 months of age (Asp et al., in press). We studied the accuracy and development of auditory (A) and auditory-visual (AV) horizontal localization in a group of young children.

Subjects and Methods
Twelve children (29–157 weeks of age) who passed the universal newborn hearing screening participated. A corneal reflection eye tracking technique allowed detailed analysis of the spatial distribution of gaze toward randomly presented auditory (A) and auditory-visual (AV) targets in the frontal horizontal plane (± 55 degrees azimuth), at a temporal resolution of 20 Hz. The perceived azimuth was defined as the median of the intersections between gaze and spatial targets. Overall SLA was quantified by an Error Index (EI), where EI=0 corresponded to perfect match between perceived and presented azimuths, while EI=1 corresponded to chance.

Results
The medians of the perceived A-azimuths either coincided with the presenting A-azimuths, or were offset by a maximum of 20 degrees. The offset was towards the median plane in all subjects, except for frontal incidence (±5 degrees) where a lateral offset was found. By contrast, all the median perceived AV-azimuths coincided with the presenting AV-azimuths with quartile ranges = 0 at 6/12 azimuths, demonstrating high AV-localization accuracy across the entire spatial range tested.

While A-localization improved 16 percentage points per year, as demonstrated by linear regression analysis (EI = 0.62 – 0.003 × Age (weeks), r = -0.68, p = 0.015, n = 12), no effect of age on AV-localization accuracy was found (auditory-visual EI = 0.16 – 0.0003 x Age (weeks), r = -0.093, p = 0.77, n = 12) (Asp et al., in press).

Conclusions
Auditory and auditory-visual horizontal localization follow different developmental patterns in children from 6 months of age. Further research including larger samples need to be

conducted to determine by what age localization in these two modalities converge.

References
Asp. F., Olofsson Å., Berninger. E. (2015). Corneal Reflection Eye Tracking Technique for the Assessment of Horizontal Sound Localization Accuracy from 6 months of Age. *Ear Hear*. In Press.

Funding
Tysta Skolan Foundation The regional agreement on medical training and clinical research (ALF) between Stockholm County Council and Karolinska Institutet, and Karolinska University Hospital

PS 222

Horizontal Sound Localization Performance by a Gleaning Bat, Antrozous pallidus

Dustin Brewton; Khaleel Razak
University of California, Riverside

The auditory cortex is necessary for normal sound localization. Our understanding of how the cortex represents auditory space remains rudimentary. Recent studies in the pallid bat have generated testable hypotheses about bi-coordinate spatial representation in a mammalian auditory cortex. The pallid bat is a species that listens passively to prey-generated noise while reserving echolocation for obstacle avoidance. The noise-selective region of the pallid bat auditory cortex, putatively involved in localizing prey-generated noise, is organized into two binaural clusters, based on ILD selectivity. Cells within the peaked cluster respond weakly to monaural stimulation of either ear, and best to stimuli coming from the midline with ILD ~ 0 dB. Cells within the EI cluster respond best to contralateral stimuli. The first step to study the relative contributions of these two binaural clusters to sound localization is to determine horizontal localization accuracy in a behavior task. This was the primary goal of this study. Four bats were trained to localize noise stimuli for a food reward on an approach to stimulus task. The effect of sound duration and speaker location on the localization accuracy of each bat was measured. Performance was calculated by a scoring system in which a correct response generated a score of 1, approach to one speaker off of the target generated a score of 0.8, missing by 2 speakers generated a score of 0.6, and so on. Mean scores of the 4 bats for each duration were 0.832 (50 ms), 0.867 (100 ms), and 0.879 (200 ms). Performance for 50 ms duration stimuli differs significantly from performance for 100 ms stimuli ($p=0.000221$) and for 200 ms stimuli ($p=0.000000560$) (Two-way ANOVA, Holm-Sidak test). Performance is equal at all stimulus locations for durations of 200 ms. These results demonstrate that performance in localizing noise is not affected by stimulus location when the duration of the stimulus is above a certain threshold, in this case approximately 200 ms. Subsequent studies of the effect of spectral content on the same task will be performed. Because the neurons within the peaked cluster adjust their selectivity patterns when elicited with tone stimuli, we hypothesize that broadband signals are necessary for normal accuracy on the horizontal localization task for midline locations.

PS 223

Comparison of Sensitivity in Prepulse Inhibition and Operant Conditioning Procedures measuring Sound Localization Acuity in the Mouse

Derik Behrens; Georg Klump
Cluster of Excellence Hearing4all, Oldenburg

Background
In an intensity difference limen paradigm in C57BL/6 mice, the sensitivity observed in an operant conditioning procedure was much larger than the sensitivity observed with a prepulse inhibition (PPI) procedure (Behrens & Klump 2015). Here, we compare the sensitivity of both procedures in a sound localization paradigm investigating, whether the sensitivity difference observed in an intensity difference limen paradigm may also be found in other paradigms.

Methods
The mice were presented with an acoustic background of repeated 100 ms noise stimuli broadcast from a reference speaker. At random times, one of the stimuli in the sequence was replaced by a stimulus that was broadcast from a test speaker located 12.5° to 180° apart from the reference speaker. Broadband (20 kHz bandwidth, 20 kHz center frequency) and narrowband (500 Hz bandwidth, 25 kHz center frequency) noise stimuli were presented in separate sessions. In the operant procedure, a Go/No-Go paradigm with food rewards was used and hit- and false-alarm rates served to calculate the sensitivity measure d'. In the PPI procedure, the movement of the mouse elicited by a 110 dB SPL startle stimulus (35 ms, 2-50 kHz) was measured using a piezo-electric pressure transducer. We applied an ROC analysis by comparing the distribution of startle amplitudes with a change in speaker location to that without such a change and calculated d(a) values, a sensitivity measure that corresponds to d'.

Results
For both procedures, the mean sensitivity measure increased with an increase of the angle between test and reference speaker. In the operant conditioning procedure, the sensitivity for large speaker separations reached d'-values of around 3.0 (broadband noise) and 2.0 (narrowband noise). The results obtained by the PPI procedure showed a much lower sensitivity, reaching d_a-values of 1.0 (broadband noise) and only 0.3 (narrowband noise).

Conclusions
The higher sensitivity observed in the operant procedure results in lower thresholds for localizing broadband noise than in the PPI procedure in which the subjects showed a lower sensitivity. The operant procedure also revealed a large sensitivity of C57BL/6 mice to localize narrowband noise stimuli, whereas in the PPI procedure the sensitivity was so low that no threshold could be determined. Thus, the operant procedure will allow obtaining measures of localization acuity

when the PPI procedure fails. The observation of a higher sensitivity in operant conditioning procedures compared to PPI procedures appears to be a more general effect.

Funding
This study was funded by the DFG (TRR 31 and Cluster of Excellence "Hearing4all")

PS 224

Behavioral Sensitivity to Interaural Level and Time Differences in the Mongolian Gerbil tested using Virtual Headphones

Sandra Tolnai; Rainer Beutelmann; Maike Lammers; Jacqueline Hillenbrand; Georg Klump
University of Oldenburg

Gerbils' sound localization ability has extensively been tested under free-field stimulation (e.g., Heffner & Heffner, 1988; Maier & Klump, 2006; Carney et al., 2011; Lingner et al., 2012). While many neurophysiological studies use closed-field or near-field stimulation to present signals with interaural time and level differences (ITD and ILD, respectively), the gerbil's behavioral sensitivity to ITD and ILD has so far only been derived from acoustic measurements (Maki & Furukawa, 2005) and free-field stimuli that favor the use of one or the other interaural cue (Lesica et al., 2012). Here we investigate the behavioral sensitivity of gerbils to ITD and ILD using free-field loudspeakers to mimic stimulation via headphones.

Six Mongolian gerbils were trained in a left/right discrimination task using broadband noise stimuli presented from a loudspeaker array (-90° to +90°, minimum angle between loudspeakers 12°). Data collection under the so-called virtual-headphone stimulation started when animals reliably reached >95% correct responses for the outermost loudspeaker positions. Two loudspeakers in the array presented virtual-headphone stimuli using cross-talk cancellation in order to eliminate the undesired signal paths between the speakers and their respective contralateral ears. The cross-talk cancellation filters were based on head-related transfer functions measured prior to the experiments from a gerbil carcass.

Stimuli were narrow-band noise bursts (bandwidth: 200 Hz, centre frequency: 0.75, 1, 2, 4, or 6 kHz, 60 dB SPL) to which either ITD (up to ±500 µs) or ILD (up to ±20 dB) were applied. Psychometric functions were derived from the animals' responses and thresholds calculated at a sensitivity level corresponding to a d' of 1.

We found that all gerbils tested were able to lateralize sounds depending on the applied ITD or ILD. For stimuli with an ILD, reliable responses could be obtained for narrow-band noises with center frequencies ≥2 kHz. For stimuli with an ITD, reliable responses could be collected for center frequencies up to 2 kHz. Responses to stimuli with an ITD were cyclic indicating the use of phase information by the animals.

The data will be discussed in terms of its applicability by comparing thresholds collected under virtual-headphone stimulation with data from free-field stimulation.

Funding
This study was funded by the DFG (TRR 31 and Cluster of Excellence "Hearing4all").

PS 225

The contribution of acoustic onsets and offsets to the temporal modulation spectrum of vocalization sequences and speech

Fatemeh Khatami; Heather Read; Monty Escabi
University of Connecticut

In vision, natural scenes exhibit 1/f power spectrum where visual edges are main contributors and cortical neurons are tuned to effectively extract edge related information (Field, 1987). Similarly, in audition, temporal modulations in vocalized sounds exhibit 1/f modulation power spectrum (Voss and Clark, 1975) and central auditory neurons can respond efficiently to such statistics (see discussions, Escabi et al., 2003; Rodriguez et al., 2010). Numerous factors contribute to temporal fluctuations in vocalized sounds including articulatory gestures, vocal tract filtering, and vocal fold vibration. Yet how such factors contribute to 1/f structure is unclear. Vocalized sounds contain a variety of temporal cues, including rhythmic fluctuations (< 20 Hz), onsets and offsets at the beginning and end of vocalizations (e.g., isolated words, species specific calls), and periodic structure such as from vocal fold vibrations (e.g., periodicity pitch) and these vary extensively over several orders of magnitude (from a few Hz for rhythmic information to ~800 Hz for pitch). It is plausible that 1/f structure arises from the combined contribution of such physical cues.

We used vocalization sequences from a variety of animals, including nonhuman primates, mice, birds, infant cries, and speech to evaluate the role of vocalization transients, duration and amplitude variation in the sound temporal envelope. First, the modulation spectrum from isolated vocalization and vocalization sequences was compared. Synthetic vocalization sequences were generated based on statistics of the vocalization duration, timing, and amplitude variation of natural sequences and artificially perturbed to investigate contributing factors. Furthermore, a statistical model containing the three forms of variability was also evaluated in close form. In all instances, the presence of onsets and offsets at the beginning and end of isolated vocalizations predicted the observed 1/f modulation spectrum observed in vocalization sequences. Though timing, duration, and amplitude variation shaped the modulation power spectrum these only accounted for small amount of residual variation around the observed 1/f trend.

The results demonstrate that acoustic "edges" are largely responsible for 1/f modulation structure found in vocalization sequences including speech. This is similar in principle to visual edges being main contributors to 1/f spectrum of visual images. Since central auditory neurons are particularly sensitive to temporal onsets and are adapted for 1/f structure, the findings imply that temporal edge detection is a major determinant for neural coding of vocalizations sequences.

Funding
NSF IOS 1355065 NIH R01DC015138

PS 226

Normal Hearing Listener Vowel and Consonant Confusion Patterns from Spectrally-manipulated Vocoder Stimuli

Mishaela DiNino; Richard Wright; Julie Bierer
University of Washington

The ability to resolve the frequency components of an auditory signal is essential for accurate identification of speech sounds. This study was designed to simulate hearing through a cochlear implant and the distortion and loss of spectral resolution that might occur for these listeners. The patterns of phoneme identification errors resulting from specific spectral degradation have not yet been systematically examined using these methods. Spectral information was degraded in two ways after stimuli were processed through 15-channel noiseband vocoder: 1) low, middle and high frequency regions of information were removed or set to zero output, and 2) the same regions were smeared by sending filter outputs to neighboring filters. Twelve normal hearing adults were tested on naturally spoken male- and female-talker vowels in \hVd\ context and male-talker consonants in \aCa\ context. Each spectral manipulation ("Set to Zero" or "Split") was randomly presented through channels corresponding to either apical, middle, or basal cochlear locations, which were chosen to cover the first, second, and third formants of the vowel sounds, respectively. A condition in which no spectral manipulation occurred was included as a control.

All combinations of vocoder manipulation and location resulted in significantly decreased performance relative to the control condition ($p < .05$) for both male- and female-talker vowels, but only the zero output condition significantly lowered performance for consonants. Repeated measures analysis of variance (ANOVA) for each phoneme list revealed an interaction between type of manipulation and location of target regions for the male- ($p < .001$) and female- ($p = .001$) talker vowels. For consonants, a main effect of manipulation type ($p < .001$) was found. Analysis of vowel error patterns revealed that removing or degrading vowels' second formant frequencies resulted in confusions of vowels with the most similar first formants, and manipulating third formant frequencies elicited confusion of vowels closest in vowel space. However, manipulating first formant frequencies resulted in some vowels being confused with those most comparable in duration rather than second formant frequency, demonstrating the significance of the first formant for vowel recognition. Consonant error patterns were found to be much less affected by vocoder manipulation type or location, as confusions occurred between consonants most similar in manner of articulation for all vocoder conditions. These results provide an improved understanding of the effects of diminished spectral information on phoneme identification performance and error patterns.

Funding
This research was supported by NIDCD DC012142 and NIH T32DC005361.

PS 227

Effects of Periodicity and Vocoding in Modelling the Intelligibility of Speech in Background Noise

Kurt Steinmetzger; Stuart Rosen
UCL

Auditory models concerned with predicting the intelligibility of speech presented in background noise are usually evaluated with maskers that vary widely regarding both their envelope fluctuations and spectral properties, for example speech-shaped noise and interfering talkers. Here we took the opposite route and investigated how model predictions are affected by a single acoustic factor, the presence or absence of periodicity in both masker and target speech. Secondly, little is known about how acoustic degradations of the target speech itself affect the performance of common auditory models. We thus additionally lowered the spectral resolution of the target speech using a channel vocoder. Harmonic complexes based on the F0-contours of real speech were used as periodic maskers, while speech-shaped noise was used as aperiodic masker. Periodicity in the target speech was either discarded using a noise-vocoder or synthesised with a pulse train following the natural F0-contour. A number of existing models – extended speech intelligibility index (ESII), speech-based speech transmission index (sSTI), multi-resolution speech-based envelope power spectrum model (mr-sEPSM), and short-time objective intelligibility measure (STOI) – were used to predict previously obtained behavioural data. In line with the data, all four models predicted that listeners would benefit from periodicity in the masker, but the size of this effect was consistently underestimated. Secondly, although all models correctly predicted that preserving periodicity information in the target speech did not have an effect on intelligibility rates, only the STOI was able to account for the substantially lower intelligibility of vocoded speech. These results suggest that spectral information is not sufficiently represented in current auditory models and that additional processing steps may be needed. Additionally, a correlation-based back-end, as used in the STOI, appears to be a promising technique that seems to account for a wider range of conditions than traditional SNR-based measures.

Funding
This work was supported by the Medical Research Council (Grant Number G1001255) and the European Commission under Contract FP7-PEOPLE-2011-290000.

PS 228

The Roles of Periodicity and Modulation Spectrum in Determining How Well a Dynamic Harmonic Complex Masks Speech

Stuart Rosen; Kurt Steinmetzger
UCL

Harmonic complexes mask speech much less effectively than a noise with the same overall spectral envelope, but the reasons for this are far from clear. Explanations tend to focus on three major factors. Firstly, harmonic complexes consist of discrete spectral components so that, at least at low frequencies where harmonics are resolved, there may be 'glimpsing' into frequency regions between harmonics where there is little masker energy. Secondly, there is increasing evidence that masking may be determined more by interference between modulations in the masker and those in the target speech than by the energy in the masker *per se*. Therefore, the substantial differences between the modulation spectra of noise and harmonic complexes may be important. Finally, the periodicity of a harmonic complex may allow it to be more effectively segregated or 'cancelled out'. We have investigated the roles of periodicity and modulation spectrum by comparing the relative masking effectiveness of complex tones in which the discrete spectral components form either a harmonic or inharmonic series. The harmonic dynamic complexes have fundamental frequency (F0) contours modelled on connected speech (with interpolation through silence and voicelessness), but no other spectral or temporal modulations. Inharmonic complexes are created either by: 1) spectrally rotating the harmonic complexes around a centre frequency near 2 kHz, or 2) shifting all the harmonics up or down by a constant amount. Both manipulations preserve harmonic spacing but create series that are inharmonic, except fleetingly, when the original F0 has particular values. In this way we create maskers that differ in periodicity, but provide similar opportunities for inter-harmonic glimpsing, since they are composed of equivalently spaced discrete spectral components. Importantly, the modulation spectra of the rotated maskers differ considerably from those of the shifted and unprocessed maskers, which are quite similar. Speech Reception Thresholds (SRTs) will be determined adaptively for sentences in the presence of the three kinds of maskers, which will have the same long-term average spectrum. Comparing the SRTs for the three conditions will allow a quantitative assessment of the importance of periodicity and modulation spectrum in making a harmonic masker less effective than a noisy one. An attempt will be made to explain the results through auditory models that either include a modulation filter bank or not, and make different assumptions about the metric to use in predicting performance (i.e., based on correlation or the signal-to-noise ratio in the envelope domain).

Funding
This work was supported by the Medical Research Council (Grant Number G1001255) and the European Commission under Contract FP7-PEOPLE-2011-290000.

PS 229

Recognition Performance for Hebrew Monosyllabic Words Presented in Noise: The Effects of Acoustic, Phonetic, and Lexical Variables

Nitza Horev; Tal Bronner; Avigail Chason; Hanna Putter-Katz
Ono Academic College

Background
In order to develop hierarchical intervention programs for improving listening in noisy environments, it is necessary to characterize the factors that affect recognition performance. The purpose of the present study was therefor to examine the acoustic (duration and amplitude), phonetic (vowel, place, manner and voicing,) and lexical variables (word frequency and familiarity) that may predict recognition performance for Hebrew CVC words presented in babble noise.

Methods
Following the work of McArdle and Wilson (2008), 275 CVC real words in Hebrew were recorded and combined with eight talkers babble noise at four Signal-to-Noise Ratios (-7, -2, +3, +8dB SNR). Words were presented for open-set identification, to 30 young, normal hearing Hebrew speakers. The 50% point in dBSNR was calculated for each word, using the Spearman-Karber equation (Finney, 1952). Regression and variance analysis examined which lexical, phonetic and acoustic factors affected the 50% point. In addition, for each SNR and for each phoneme, error analysis was conducted.

Results
The selected variables explained 50.6% of the variance in the 50% point [predicting variables ($p<0.05$) by order: final consonant voicing, word familiarity, initial consonant sonority, word duration, initial consonant voicing, initial consonant manner]. Significant negative correlations were found between 50% point and word duration and word familiarity, indicating that longer and more familiar words were easier to recognize. Significant main effects were found for vowel identity, consonant voicing and for consonant sonority. Initial and final phonemes were affected differently by these last phonetic factors: in final position, voiceless consonants were easier to identify compared with voiced consonants, whereas in initial position sonorants were easier to identify compared with obstruents. Error analysis also enabled to scale Hebrew phonemes according to the ease of identification in noise.

Conclusion
When building intervention materials for improving speech-in-noise understanding, it is important to take into account the phonemic distribution separately for initial and final consonants and to take into account the familiarity of the words. In addition, error analysis results may aid in organizing the intervention program hierarchically. Such intervention programs can be beneficial for improving listening in challenging environments among listeners with hearing loss and/ or with difficulties in understanding speech in background noise (e.g. APD, bilinguals).

PS 230

The Effect of Elevated Intensity on Consonant Recognition in Noise by Normal Hearing, Aged Subjects

Robert Shepard; Christopher Boven; Jont Allen; Fatima Husain; Robert Wickesberg
University of Illinois at Urbana-Champaign

Years of psychoacoustic experiments have demonstrated that the intelligibility of most consonants begins to decrease when presented above a certain intensity. This effect was first described by French and Steinberg (1947), replicated by several researchers in following years (e.g. Fletcher and Galt, 1950; Jerger and Jerger, 1971; Studebaker et al., 1999; Hornsby et al., 2005), and has been called the "roll-over" effect (Molis and Summers, 2003). These studies have tested young normal hearing listeners and sometimes those with significantly raised thresholds to characterize the phenomenon; neglecting the portion of the aging population that have trouble deciphering speech in loud, noisy environments but who have normal hearing. The purpose of this experiment was to examine the roll-over effect in this group.

We recruited 18 subjects between 45 and 70 years of age with normal hearing based on a standard audiometric evaluation. All subjects complained of developing difficulty understanding speech in noisy environments. Subjects were presented 6 plosive and 2 nasal CV pairings, spoken by 2 males and 2 females, across two signal-to-noise ratios (0 and -6 dB SNR) and three intensity conditions (45, 65, and 85 dBA).

At 0 dB SNR, the recognition scores for /d/, /g/, /k/, /b/, /m/, /n/ from these older, normal hearing adults displayed the roll-over effect with the highest scores for the consonants presented at 65 dBA, and lower scores for the 45 and 85 dBA conditions. The consonants /t/ and /p/ were notable exceptions to this effect, which is consistent with previous reports. Interestingly, some subjects displayed dramatic decreases in response accuracy at 85 dBA despite being considered normal hearing and being able to recognize the consonants at 65 dBA. At -6 dB SNR, the roll-over effect was more pronounced for some consonants, but less pronounced for others because of an overall decline in recognition scores.

Although the physiological basis for this nonlinear effect of level remains unknown, only the low and medium spontaneous, higher threshold auditory nerve fibers are able to encode speech cues in the presence of loud noise (Silkes and Geisler, 1991; Boven and Wickesberg. 2013, 2014). The loss of these fibers, either with age or through noise damage (Kujawa and Liberman, 2013), could explain a diminished ability of subjects to recognize speech particularly at higher intensities, despite subjects having normal hearing thresholds.

Funding
Department of Psychology, University of Illinois at Urbana-Champaign

PS 231

The Role of Better-ear Glimpses and Interaural Phase Differences in Binaural Speech Intelligibility

Stephan Ewert; Wiebke Schubotz; Thomas Brand; Birger Kollmeier
Universität Oldenburg

Background
In binaural listening situations with a frontal target and two maskers symmetrically placed at each side of the head, long-term interaural level differences (ILD) and phase differences (IPD) are absent. Still, speech-reception thresholds (SRT) decrease as the target and maskers are spatially separated, referred to as spatial release from masking (SRM). In this case, speech intelligibility (SI) cannot be explained by an improved long-term signal-to-noise ratio (SNR) caused by ILD (head shadow effect) at one (better) ear. Nevertheless, short-term spectro-temporal segments ("glimpses") in each ear can still provide favorable SNRs and IPDs. It has been suggested that depending on the target and masker material, an optimal binaural glimpsing strategy can explain the SRM completely or to a large degree. The current study attempts to clarify the role of better-ear glimpsing and IPD processing for different types of maskers.

Methods
SRTs for a frontal target in two statistically independent, symmetrically placed maskers were assessed in normal-hearing listeners using the OlSa matrix sentence test. The spectro-temporal properties of the two maskers were systematically varied, ranging from stationary speech-shaped noise (SSN) and different modulated SNNs, to single talkers. Head-related transfer functions were used for headphone presentation and were manipulated to either provide natural ILDs or IPDs in isolation, both, or an "infinite" ILD. Additionally, a monaural signal was generated, based on better ear glimpses. Observed SRTs were compared to predictions of a binaural SI model.

Results
SRTs suggest that binaural SI is influenced by the spectral and temporal coherence of the amplitude modulations and the semantic content of the masker. Model predictions demonstrate the importance of a short-term analysis and suggest that better-ear glimpsing (based on ILD), IPD cues, as well as spectral changes in the masker spectrum occurring for the spatially separated maskers affect SRM.

Conclusions
Better ear-glimpsing alone cannot fully account for observed SRM with natural (partly correlated) maskers in both ears. For independent maskers in both ears, listeners cannot optimally derive better-ear glimpses. The suggested maskers and binaural conditions in combination with the observed data may provide a valuable benchmark to challenge SI models and computational auditory scene analysis approaches.

Funding
This work was supported by the Deutsche Forschungsgemeinschaft (DFG) SFB TRR 31 (B1).

PS 232

Modeling Binaural Unmasking of Speech in Noise with Time-Varying Interaural Phase Differences

Christopher Hauth; Thomas Brand
Carl von Ossietzky Universität Oldenburg

Background
Binaural speech intelligibility models have successfully been used to predict speech reception thresholds in scenarios, where the envelope of an interferer changed over time, but the binaural cues were stationary. In this study, the effect of an interfering noise with stationary frequency spectrum and time-varying interaural phase difference (IPD) on speech intelligibility is investigated.

Methods
Speech reception thresholds (SRT) of 50% correctly understood words are determined for 10 listeners with normal hearing using a sentence test. The speech is presented diotically via headphones together with a noise with the same long-term frequency spectrum. The IPD of the noise is sinusoidally modulated with frequencies of 0.25, 0.5, 1, 2, 4, 8, 16, 32, and 64 Hz. The outcome of the experiment is predicted using a binaural speech intelligibility model (BSIM) (Beutelmann et al., 2010), which combines an Equalization-Cancellation (EC) front-end with a speech intelligibility index (SII) back-end. Based on this model, a modified model approach is introduced that estimates the EC parameters blindly from the mixed speech and noise signals. Both versions differ in their underlying assumptions: The original model has access to speech and noise separately and the EC stage is assumed as a top-down mechanism that maximizes the SNR in each frequency band. Instead the blind model minimizes the overall level in each frequency band, which is equivalent to minimizing the dominant source. This assumption of a signal driven bottom-up processing achieves a binaural unmasking if the SNR is negative.

Results
In the perceptual data, the largest binaural unmasking is observed for the slowest IPD modulation frequency, where SRTs are decreased by 3 dB compared to the diotic presentation of speech and noise. This unmasking gradually decreases with increasing modulation frequency. The short-time BSIM is not able to predict this increase. Therefore, a second time constant is introduced in the short-time model: Additionally to the time-constant used to account for amplitude modulated signals, an EC time constant simulating binaural “sluggishness” is introduced in order to estimate the EC parameters on a different time scale. By using a binaural window in the order of 100 ms, the decreasing binaural unmasking with increasing modulation frequency can be predicted by both the top-down and bottom-up approach.

Conclusion
Our results indicate that a separate time constant of binaural processing is required to account for effects related to dynamically changing binaural cues on speech intelligibility.

Funding
Grant “The active auditory system” DFG SFB/TRR 31

PS 233

Improving Speech Intelligibility in Fluctuating Background Interference

Laura D’Aquila; Joseph Desloge; Charlotte Reed; Louis Braida
Massachusetts Institute of Technology

The goal of this research is to improve speech intelligibility for hearing-impaired (HI) listeners in fluctuating background interference. Masking release (MR; i.e., better performance in a fluctuating compared to a continuous noise background) evident for normal-hearing listeners is generally reduced or absent in hearing-impaired (HI) listeners for aided unprocessed speech materials. Recently, we have observed increased MR for HI listeners using various signal processing techniques including (i) preserving only the cosine of the Hilbert instantaneous phase of the signal, (ii) re-processing of the 40-band Hilbert envelope to extract the cosine of the Hilbert phase, and (iii) peak clipping. All three of these techniques reduced or removed amplitude variations in output energy, which appears to have led to greater audibility during the gaps in fluctuating interference and to greater MR. However, these techniques also introduced distortions, and the increased MR arose from a performance drop in continuous noise as opposed to a performance increase in interrupted noise.

The work reported here is concerned with achieving similar reductions in signal amplitude variation (thus leading to improved speech intelligibility in fluctuating interference) without suffering a loss in intelligibility in continuous background noise. A method was developed and evaluated, which operates blindly on a speech-plus-noise signal without the need for segmentation, uses relative levels of the speech and interference, and does not require a reference signal.

Consonant-identification tests were conducted on HI listeners to measure performance in backgrounds of continuous and fluctuating noises (including square-wave and sinusoidally modulated noises as well as those derived from speech envelopes). Similar scores were obtained for processed and unprocessed speech materials in quiet and continuous-noise backgrounds, while superior performance was obtained for the processed speech in fluctuating background noises. These results support the conclusion that greater MR is related to decreased amplitude variation and increased audibility of the speech during gaps in the noise for the processed signals.

Funding
This research was supported by the National Institute on Deafness and Other Communication Diseases of the National Institutes of Health under Award Number R01DC000117.

PS 234

A Pilot Study of AUT00063, an Oral Modulator of Voltage-gated Potassium Channels, in Adult Post-lingual Unilateral Cochlear Implant Recipients: the QuicK+fire-Pilot

Peter Harris[1]; Shakeel Saeed[2]; Robert Carlyon[3]; Susan Waltzman[4]; Daniel Polley[5]; Charles Large[1]
[1]Autifony Therapeutics Ltd; [2]The Royal National Throat, Nose & Ear Hospital and National Hospital for Neurology and Neurosurgery, London; [3]MRC Cognition & Brain Sciences Unit; [4]New York University School of Medicine; [5]Massachusetts Eye and Ear Infirmary, Harvard Medical School

Cochlear implants define *the* major success story in subjects with profound hearing loss, and represent a unique synthesis of surgical expertise, electronic advancement and psychoacoustics. They have transformed thousands of lives, but not all outcomes are optimal. We are conducting a pilot evaluation of the benefits of AUT00063 on some aspects of central auditory processing for CI users. Recognizing that device programming and interventions occur over the 9-12 months post-implantation, this study recruits subject 9-24 months post CI.

AUT00063 positively modulates Kv3 potassium channels, found at all levels of the auditory system, and which are important in central auditory neurons that must fire rapidly and with precise timing such as in circuits involved in decoding speech and animal vocalisations. For example, in a model of auditory neuropathy in mice, AUT00063 improved the timing of firing and synchronisation of neurons in the inferior colliculus in response to auditory stimuli (Polley et al. 2014, Soc. Neurosci.).

This pilot study is evaluating AUT00063 versus a matching placebo in a balanced randomised crossover design of 28 days daily dosing with a washout period between the two. Inclusion will be based upon the BKB sentence score in quiet. The Minimum Speech Test Battery (AzBio sentences, CNC word test, BKB) form the main speech perception outcome measures, along with a standard audiogram, Speech Detection Threshold, Spondee Reception Threshold, Impedance (tympanometry and reflexes), and OAEs. Subjects also complete the Nijmegen Cochlear Implant Questionnaire.

Uniquely in this drug study, the psychophysics of temporal processing is evaluated using a direct stimulation method that bypasses the cochlear implant speech processor. The tasks will include rate discrimination at low and high rates, and gap detection with a high-rate pulse train, for stimulation of individual electrodes. On the basis of the Kv3 mechanism of AUT00063 it can be hypothesized that the rate discrimination at high rates will be better with drug than with placebo and at baseline; this difference will be larger than at low rates; Similarly, it is hypothesized that gap detection will be improved with drug compared to placebo and/or baseline conditions.

Here we present the CT design and some of the issues.

Funding
Funded by Autifony Therapeutics Ltd, a development stage biopharmaceutical company funded by leading venture capital investors. The company works closely with hearing research experts at University College Londonâ€™s Ear Institute, Yale University, Massachussetts Eye and Ear Infirmary, the University of South Florida and other academic collaborators around the world.

PS 235

The Effect of Occluding the Ear on Variations in Voice Level and Fundamental Frequency with Changing Background Noise Level and Talker-to-Listener Distance: A Pilot Study

Rachel Bouserhal[1]; Ewen MacDonald[2]; Tiago Falk[3]; Jeremie Voix[1]
[1]University of Quebec in Montreal; [2]Technical University of Denmark; [3]Institut national de la recherche scientifique

Speech production in noise and varying talker-to-listener distance has been well studied for the open ear condition. However, occluding the ear canal can affect the auditory feedback and cause deviations from the models presented for the open-ear condition. Considering that communication is still the main concern for people wearing Hearing Protection Devices (HPD), a smarter radio communication protocol must be developed. To achieve this, it is necessary to understand and model speech production in noise while wearing HPDs. The results of a pilot study aimed to investigate the effects of occluding the ear on changes in voice level and pitch (F0) in noise and with varying talker-to-listener distance are presented. Results show a general trend similar to the open ear condition with the exception of the occluded quiet condition. As noise level and distance increase both voice level and F0 significantly increased. This implies that a model can be developed to better understand speech production for the occluded ear.

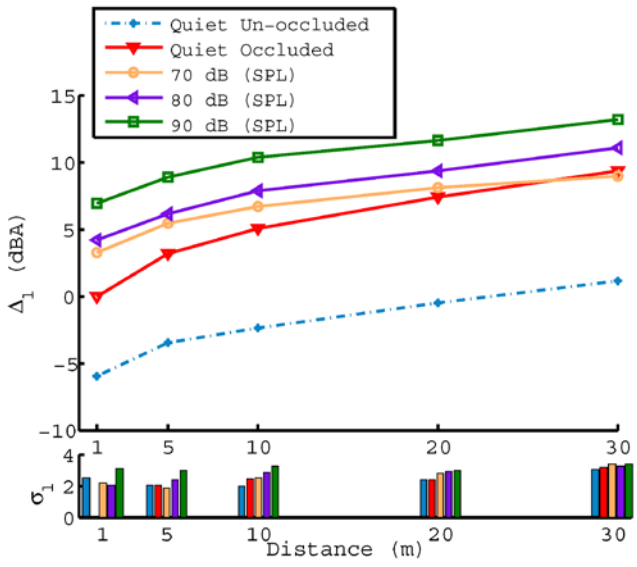

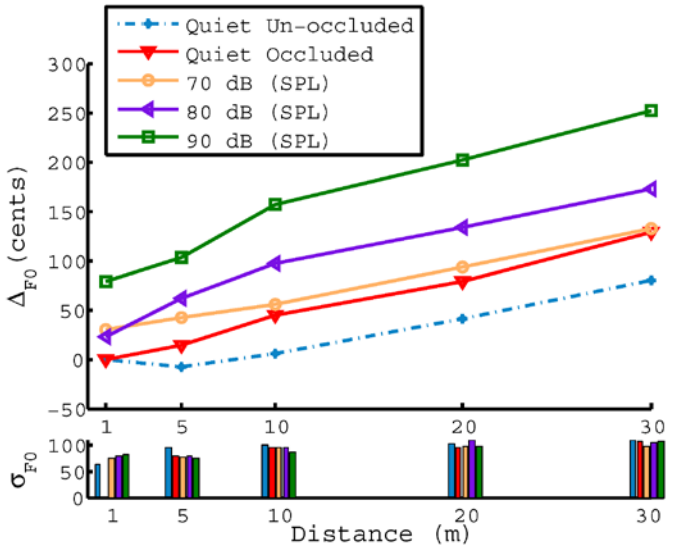

Funding

This work was made possible via funding from the Centre for Interdisciplinary Research in Music Media and Technology, the Natural Sciences and Engineering Research Council of Canada, the Erasmus Mundus student exchange program in Auditory Cognitive Neuroscience and the Sonomax-ETS Industrial Research Chair in In-Ear Technologies.

PS 236

A Model for Sub-lexical Processing of Chinese Speech

Yu-Xuan Zhang; Tingting Yan; Xiang Gao

Beijing Normal University

Background

While 60% of world languages are tonal, relatively little is known about tone processing, as reflected in the scarcity of speech perception models for tonal languages. Compared to segmental information (consonant and vowel), tone is generally observed to be slower and harder to access, though this disadvantage has been reported to diminish or even be reversed with a constraining context.

Methods

Native Mandarin speakers (N=48) made speeded same/different judgments on two sequentially presented spoken tokens of monosyllable Chinese characters (e.g., ma1 and da4) based on the entire token (Word task), the syllable regardless of tone (Syllable task), only the consonant (Consonant task), only the vowel (Vowel task), or only the tone (Tone task). A block of 48 trials was collected for each task. Non-target dimensions (e.g., consonant and vowel for Tone task) were independently manipulated.

Results

Both error rate and reaction time (RT) varied significantly across tasks (Fig. 1 a,b). Error rate divided the tasks into two groups, with Word and Syllable being less erroneous than Consonant, Vowel, and Tone. In terms of RT, Tone was the slowest, followed by Vowel, while Consonant, Word, and Syllable were equally fast.

Model

Extending the influential TRACE model for non-tonal languages, we proposed a Syllable Access Model (SAM) for sub-lexical processing of Chinese (Fig. 1c). SAM consists of multiple processing layers with mutual excitatory connections, among which feature, phoneme, and word layers are after TRACE, while syllable and tone layers are added specially for Chinese. SAM has two critical features. First, segmental information is integrated at a syllable layer before tone is added. Second, information is readily accessible only from the syllable level and up, while lower levels can only be accessed by top-down reactivation.

Conclusions

SAM provides a simple and congruent account for the current results as well as major observations in the literature. For the current results, Word and Syllable tasks can be performed at readily accessible levels, while the remaining tasks requires reactivation, making them slower and more erroneous. Acoustic properties render Consonant the fastest in the reactivation group. The generally observed tone disadvantage arises because segmental information can be readily accessed from the syllable level while tone requires reactivation. However, if a constraining context activates the word level in advance, this preparation would pass down to the tone level earlier than to the phoneme level due to one fewer step of connections.

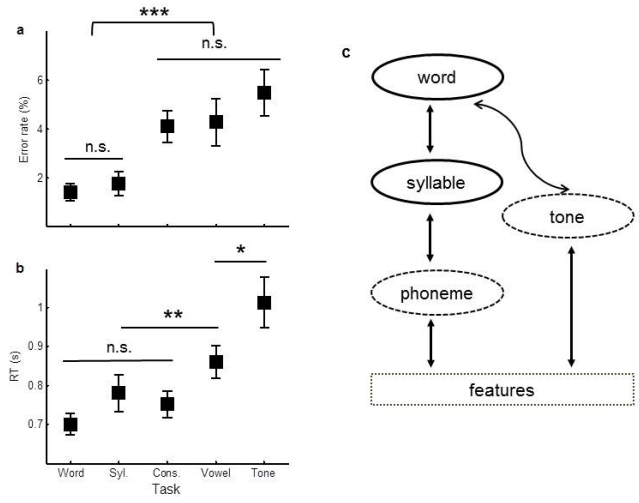

Funding

The work is funded by National Natural Science Foundation of China, grant # 31300935.

PS 237

Computational auditory model of intensity effects on amplified speech perception

Evelyn Davies-Venn[1]; Nursadul Mamun[2]; Muhammad Zilany[2]

[1]University of Minnesota; [2]University of Malaya

Introduction

Some listeners with hearing loss show poor speech recognition scores in spite of using hearing aid amplification that optimizes

audibility. Beyond audibility, studies have suggested that differences in recognition scores for amplified speech may be explained by listeners' suprathreshold abilities such as spectral resolution. Physiological and behavioral measures have shown that as presentation level increases, frequency tuning broadens. In an effort to assess factors that govern individual variance in speech recognition scores for listeners with hearing loss, this study used acoustic, behavioral measures, and computational modeling to evaluate the effect of audibility, spectral resolution, and high intensities in explaining variances in amplification outcomes for listeners with mild-to-moderate and severe hearing loss. The main motivation was to examine the underlying mechanical and physiological processes that correlate well with behavioral measures of presentation level effects on amplified speech.

Methods

A within-subjects repeated measures design was used to obtain consonant recognition scores at three different intensities for amplified speech. Listeners wore a commercially available BTE hearing aid coupled with custom-made earmolds. All sound stimuli were presented in soundfield, and concurrent acoustic recordings were made using a probe microphone that was positioned in the ear canal, at the output of the hearing aid. A physiological model of the auditory periphery (Zilany et al., 2014) was used to assess stimulus and level-dependent changes in basilar-membrane and auditory-nerve (AN) fiber responses due to hearing loss, hearing aid signal processing and high intensities. Model AN fiber responses were simulated for a wide range of characteristic frequencies to construct neurograms. Behavioral scores were estimated using two predictors of speech intelligibility, correlation coefficient of neural responses (ρ) between normal and impaired conditions, and neurogram orthogonal polynomial measure (NOPM). Both metrics make use of either an "all-information" neurogram with small time bins (temporal fine structure, TFS) or a "mean-rate" neurogram with large time bins (envelope, ENV).

Results and conclusions

The model-estimated scores were correlated with measured speech recognition scores to assess the predictive accuracy of the model simulations. Results to date suggest level-dependent changes in specific components of basilar-membrane responses and auditory-nerve spike-time coding predicts intensity effects on amplified speech perception scores. Specifically, evaluation of individual phonemes revealed differential susceptibility to intensity level effects across different consonant categories. The sensitivity of ρ_{TFS} to intensity effects was modulated by the amount of hearing loss. ρ_{ENV} best accounts for individual variance. The implications of these findings for amplification will be discussed.

Funding

This work supported by the University of Minnesota research funds awarded to EDV, and by grants UM.C/625/1/HIR/152 and RG157-12AET awarded to MZ.

PD 17

Representation of Bi-coordinate Space in the Auditory Cortex

Khaleel Razak; Stuart Yarrow; Dustin Brewton
University of California, Riverside

The auditory cortex is necessary for sound localization. The mechanisms that shape bi-coordinate spatial representation in the auditory cortex remain unclear. Here we propose a novel mechanism of 2D spatial representation in the auditory cortex of the pallid bat. The pallid bat localizes prey by listening passively to prey-generated noise while reserving echolocation for obstacle avoidance. A part of the primary auditory cortex is selective for prey-generated noise (noise selective region, NSR). The NSR is subdivided into two clusters based on ILD selectivity. The peaked cluster responds best to sounds from the midline. The EI cluster responds best to sounds from contralateral space. We previously showed that the extent of active cortex changes systematically with azimuth in the EI cluster of the NSR (Razak, 2011).

Here we studied how source elevation influences this azimuth map in the EI cluster. Responses were measured for broadband noise presented from up to 55 speaker locations (11 horizontal, 15° resolution and 5 vertical, 30° resolution) in the frontal space of the bat to determine 2D spatial receptive field (SRF). In 81/104 neurons, SRFs were recorded at two different sound levels. The SRF centroid azimuth and elevation (~best position) and gyradius (~SRF size) were quantified. Data indicate: (1) The SRF centroid and gyradius show relatively little change with change in sound level indicating strong level tolerance. (2) The SRFs of NSR neurons occupy a single contiguous range of locations in frontal space with no fragmentation even at the highest sound levels tested. (3) The SRF size was larger in elevation than in azimuth. (4) Interestingly, there were significant relationships between characteristic frequency (CF) and SRF properties. Neurons with low CF exhibited larger SRFs and lower elevation centroid elevation. With increasing CF, the SRFs became smaller and restricted to upper elevation.

These relationships indicate that the tonotopic map and source elevation will restrict the azimuth dependent spread of activity within the EI cluster. Because of the azimuth map, the cortical activity will increase in a rostrolateral to caudomedial direction as source moves from ipsilateral to contralateral space. As the source moves from low to high elevations, activity will recruited along the tonotopic map with high frequency neurons contributing only when sound source is in higher elevations. Thus the overlapping ILD-tonotopic maps will predictably restrict extent of cortical activity in a 2D location dependent manner suggesting a novel model for 2D spatial representation in auditory cortex.

Funding

National Science Foundation CAREER Award - IOS1252769

PD 18

Fine-scale Spatial Representation of Interaural Level Differences in mouse A1 revealed through In Vivo Two-Photon Calcium Imaging.

Mariangela Panniello; Andrew King; Johannes Dahmen; Kerry Walker
University of Oxford

The spatial arrangement of neuronal responses to sound level differences between the two ears (Interaural Level Differences; ILDs) in primary auditory cortex (A1) has been extensively studied across several animal species using microelectrode recording techniques. These experiments have yielded controversial results that are still under discussion. Bands or clusters of neurons with similar binaural preferences have been described throughout the cortical depth and across isofrequency contours in some studies, while others reported a more heterogeneous organization. A topographic, point-to-point cortical map of the auditory space has never been reported in mammalian auditory cortex.

The above studies sparsely sampled neurons to examine the organization of binaural responses on a large spatial scale, but microelectrode recordings do not allow us to densely sample neighbouring neurons within a local patch of cortex. In this study, we used *in vivo* two-photon (2p) calcium imaging in the anesthetized mouse to study ILD sensitivity and binaural properties of A1 neurons (layers II-III) at a much higher spatial resolution than possible with microelectrode recordings. We imaged the individual responses of over 2000 neurons in 16 mice who underwent stereotaxic A1 injections of an AAV vector carrying GCaMP6m and 3 mice from a reporter line expressing GCaMP6f under a CamK2 promoter. During imaging, we presented binaural noise bursts over a 0-30 dB ILD range (average binaural levels 40-60-80 dB SPL), monaural noise bursts (at 40-60-80 dB SPL), and pure tones (2 - 50 kHz, 40-100 dB SPL).

Among the ILD sensitive neurons, the majority was found to prefer contralateral positions at all three average binaural levels. We found a relatively high heterogeneity of ILD tuning for neurons within the same imaging field (250 µm x 250 µm), with pair-wise noise correlations only weakly decreasing with distance over this range. This result is consistent with the locally heterogeneous tuning model proposed in previous 2p imaging studies analysing frequency tuning in mouse A1. At the larger scale across imaging fields (~1 mm), we observed a smooth gradient of frequency preferences, but no systematic changes in ILD preferences, nor in binaural properties.

These results shed a light on the long-held question of how sound location is represented on a local scale in A1 and demonstrate more generally that even neighbouring neurons in mammalian sensory cortex can have very different tuning properties.

Funding
Wellcome Trust Newton Abraham Trust

PD 19

Auditory Attention Networks in the Frontal Lobe Show Strong Sensory Modality Preferences

Abigail Noyce; David Somers; Barbara Shinn-Cunningham
Boston University

Human lateral frontal cortex (LFC) has long been considered domain-general or multiple-demand, as LFC recruitment, especially along the precentral sulcus and inferior frontal sulcus/gyrus, is observed in a wide range of cognitive tasks. Using fMRI, we have previously documented an exception to this principle, discrete interdigitated structures within LFC that reliably participate in either auditory or visual cortical networks. Here, we replicated that finding, and further investigated the sensory-biased versusmultiple-demand nature of these regions. Subjects (n=16) performed auditory and visual working memory tasks using non-verbal stimuli (animal calls and faces) while undergoing fMRI brain scanning (3T field, TR = 2 s, TE = 30 ms, 2mm isotropic resolution). Performance was equivalent on both tasks. In a direct contrast of auditory to visual working memory activation, we identified four bilateral sensory-biased regions (2 auditory and 2 visual) in a majority of subjects, replicating our earlier finding. Further, when each working memory task was contrasted with its sensorimotor control condition, we observed additional activity in areas biased towards the other sensory modality (i.e., auditory working memory recruits some visual-biased areas, and vice versa), as well as in adjacent LFC regions. We compared the magnitude of each region's activity in both working memory tasks, and measured the proportion of vertices that demonstrated visual-only, auditory-only, or multiple demand patterns of activity. While a majority of vertices were multiple-demand, many were also strongly biased toward one or the other sensory modality. Visual-biased areas were more multiple-demand, while auditory-biased areas were more strictly selective. This asymmetry in the degree of crossmodal recruitment suggests striking differences between the roles of auditory-biased and visual-biased regions in high-level cognitive tasks. Our results confirm sensory specialization in LFC, and begin to reconcile conflicting accounts of LFC's organization and importance in human cognition.

Funding
Supported by CELEST, an NSF Science of Learning Center (SMA-0835976) and by NIH R01-EY022229.

PD 20

Modulation of Cortical Responses by Spatial and Non-spatial Auditory Selective Attention.

Yuqi Deng[1]; Inyong Choi[2]; Hari Bharadwaj[3]; Hannah Goldberg[4]; Barbara Shinn-Cunningham[1]
[1]Boston University; [2]University of Iowa; [3]MGH/HST Martinos Center for Biomedical Imaging, Harvard Medical School; [4]Harvard University

Auditory selective attention suppresses the processing of task-irrelevant stimuli, which is crucial for effective communication in social settings. Previous studies show that

space-based and pitch-based auditory attention engages different neural networks. However, the cortical dynamics underlying spatial and non-spatial auditory attention are unclear. To understand these effects, we used behavioral and magneto-/electroencephalography (M/EEG) measures and explored both space-based and pitch-based attention. Based on growing evidence that selective suppression is related to alpha band oscillation (8-14 Hz), we explored how attention modulates M/EEG alpha oscillation power, as well as cortical N1 responses, under different conditions. We compared effects during ***focused*** attention (where listeners maintain focus on one "target" stream among multiple competing streams) and ***broad*** attention (where listeners are prepared to switch attention to a "super-target" stream that may or may not appear after the "target" stream). Both space-based attention and pitch-based attention trial blocks included some trials that were physically identical and that required the same subject response. This allowed us to directly compare neural activity and performance for the two forms of selective attention. We find that compared to pitch-based attention, space-based attention shows overall stronger alpha power modulation in M/EEG responses, with a different spatial distribution across the central-parietal cortex. Behaviorally, we find that monitoring multiple streams (***broad*** attention) is more costly than focusing on one stream (***focused*** attention); this difference is further reflected in differences in how event-related potential responses in temporal cortex are modulated during a trial. This behavioral-neural monitoring cost is more prominent in space-based attention than in pitch-based attention. Our findings suggest that the cortical processes involved when engaging spatial auditory selective attention differ from those engaged during non-spatial attention.

Funding
NIH, NSSEFF/DoD, NSF SMA-0835976

PD 21

The effect of Auditory Visual temporal coherence on the representation of one of two competing sound streams in ferret auditory cortex

Huriye Atilgan; Stephen Town; Katherine Wood; Gareth Jones; Jennifer Bizley
University College London

We have previously observed that when the size of a visual stimulus was coherently modulated with amplitude of a target auditory stream, human listeners were better able to report brief deviants in the target stream than when the visual stream was coherent with an non-target auditory stream (Maddox et al., *2015*). Here, we used modified versions of the same stimuli to explore how the coherence between temporally modulated auditory and visual stimuli can influence neuronal activity in auditory cortex. The auditory stimuli were continuous artificial vowel sounds which were amplitude modulated with a <7 Hz noisy carrier envelope. Two such vowels (/u/ and /a/) were generated, with different fundamental frequencies, and modulated with independent envelopes. These were then presented either individually ('single stream') or concurrently ('dual stream'). In both cases the auditory stimuli were accompanied by a luminance-modulated visual stimulus, whose envelope matched one of the auditory streams. Therefore in the single stream case, the auditory and visual stimuli either had identical temporal envelopes or independent ones, and in the dual stream case the visual stimulus was coherent with one of the two auditory streams. Recordings were made in anesthetised ferret auditory and visual cortex and in the auditory cortex of awake, passively listening ferrets.

Single unit and local field potential data were analysed. In the single stream case, we determined that the across-trial reliability of the phase of the local field potential was enhanced when the visual and auditory stimuli were temporally coherent. In the dual stream case the visual stimulus modulated the phase of oscillatory activity such that the coherent auditory stream was enhanced. Analysis of spiking activity in response to the dual stream stimuli showed that neurons in auditory cortex were more likely to represent the auditory stream which was temporally coherent with the visual stimulus. These data suggest that a visual stimulus can enhance the ability of auditory cortex to separate sound sources by enhancing the representation of a temporally coherent sound. As similar results were observed in passively listening animals as well as under anesthesia it seems unlikely that attentional mechanisms contribute to these effects. We therefore suggest that one role for early-cross sensory integration in auditory cortex is to provide a bottom-up mechanism through which auditory scene analysis is enhanced.

PD 22

Incorporating Midbrain Adaptation to Mean Sound Level Improves Models of Cortical Auditory Processing

Benjamin Willmore[1]; Oliver Schoppe[2]; Andrew King[1]; Nicol Harper[1]; **Jan Schnupp**[1]
[1]University of Oxford; [2]Technische Universität München

Adaptation to stimulus statistics, such as the mean level and contrast of recentlyheard sounds, has been demonstrated at various levels of the auditory pathway. It allows the nervous system to operate over the wide range of intensities and contrasts found in the natural world. Yet, current standard models of the response properties of auditory neurons do not incorporate such adaptation. Here, we present a model of neural responses in the ferret auditory cortex (the IC Adaptation model), which takes into account adaptation to mean sound level at a lower level of processing – the inferior colliculus (IC).

The model performs highpass filtering with frequency-dependent time constants on the sound spectrogram, followed by halfwave rectification, and passes the output to a standard linearnonlinear (LN) spectrotemporal receptive field model. We find that the IC Adaptation model consistently predicts cortical responses better than the standard LN model, for a wide range of synthetic and natural stimuli. Our IC Adaptation model is based on published IC adaptation time constants,

and thus introduces no extra free parameters. It therefore improves predictions without sacrificing parsimony. In order to understand why neurons in IC exhibit these useful adaptation parameters, we analysed a corpus of natural sounds. We assumed that each neuron responds to sound in a limited frequency band, and that adaptation to mean sound level has an exponential time course. We asked what time constants are required to optimally predict the mean sound level in the near future. We found that the time constants were frequency dependent, and similar to the adaptation time constants reported for the IC. This suggests that neurons in the auditory midbrain predict the mean level of future sounds, and adapt their responses appropriately.

Funding
Supported by the Wellcome Trust (082692 and WT076508AIA) the BBSRC (BB/H008608/1) and Action on Hearing Loss (PA07)

PD 23

Synaptic and Neuromodulatory Signature of (sub)Optimal States for Detecting Sounds in Noise

Matthew McGinley[1]; Jacob Reimer[2]; Stephen David[3]; Andreas Tolias[2]; David McCormick[1]
[1]Yale University; [2]Baylor College of Medicine; [3]Oregon Health Sciences University

The cortical membrane potential, synaptic, and neuromodulatory dynamics underlying optimal detection of sounds in noisy environments are not well known. Human and animal studies have reported that performance on signal detection tasks is highly state-dependent, exhibiting an inverted-U dependence on arousal and the activity of neuromodulatory pathways. This relationship, known as the Yerkes-Dodson curve, predicts that optimal performance occurs at intermediate levels of arousal (Yerkes and Dodson, 1908). But what are the synaptic, circuit, and neuromodulatory mechanisms of this inverted-U dependence of optimal states for behavior and neural responses?

To address this question, we recorded membrane potentials of auditory cortical neurons in mice trained on a challenging tone-in-noise detection task while assessing arousal with simultaneous pupillometry and hippocampal recordings. We find that the mouse's internal state fluctuates continuously and rapidly (in seconds or less), and arousal can be quantified simply as the diameter of the pupil. The pupil diameter closely tracks the rate of occurrence of hippocampal sharp waves. In addition, auditory cortical membrane potentials of layer 4/5 excitatory neurons exhibit: slowly fluctuating (1-10 Hz) rhythmic activity with low arousal; hyperpolarization and low variability at intermediate arousal; depolarization and variability with sustained hyper-arousal (with or without walking); and transient depolarization in synchrony with micro-arousal events.

Optimal signal detection behavior and sound-evoked responses, at both sub-threshold and spiking levels, occurred at intermediate arousal when pre-decision membrane potentials were stably hyperpolarized. These results reveal a cortical physiological signature of the classically-observed inverted-U relationship between task performance and arousal, and that optimal detection of sounds in noise exhibits enhanced sensory-evoked responses and reduced background synaptic activity. In addition, these results provide a framework with which to resolve apparent discrepancies between species and sensory systems in cortical membrane potential dynamics.

In ongoing experiments, we are determining the temporal relationship between noradrenergic and cholinergic release and pupil-indexed state changes. Revealing the neural and neuromodulatory mechanisms by which the state of the auditory cortex is controlled on a moment-to-moment basis promises to clarify many interesting aspects of neural network function, including the neural basis of optimal performance, and may reveal a nervous system that is considerably more accurate and less variable than previously thought.

Yerkes RM & Dodson DJ (1908). The relation of strength of stimulus to rapidity of habit formation. Journal of Comparative Neurology and Psychology 18, 459-82.

Funding
5R01N2026143 (DAM) F32 DC012449 (MJM)

PD 24

Invariance to Frequency and Time Dilation Along the Ascending Ferret Auditory System

Alexander Dimitrov[1]; Zachary Schwartz[2]; Stephen David[2]
[1]Washington State University Vancouver; [2]Oregon Health Sciences University

The sense of hearing requires a balance between competing processes of perceiving and ignoring. Behavioral meaning depends on the combined values of some sound features but remains invariant to others. The invariance of perception to physical transformations of sound can be attributed in some cases to local, hard-wired circuits in peripheral brain areas. However, at a higher level this process is dynamic and continuously adapting to new contexts throughout life. Thus the rules defining invariant features can change.

In this project, we test the idea that high-level, coherent auditory processing is achieved through hierarchical bottom-up combinations of neural elements that are locally invariant, i.e., invariant to small perturbations of the stimulus. The main questions we address in the context of an auditory system are: 1. What kinds of changes in sound do not affect initial stages of auditory processing? 2. How does the brain process these small effects to achieve a coherent percept of sounds?

Local probabilistic invariances, defined by the distribution of transformations that can be applied to a sensory stimulus without affecting the corresponding neural response, are largely unstudied in auditory cortex. We assess these invariances at two stages of the auditory hierarchy using single neuron responses to narrowband noise and ferret vocalizations, from primary auditory cortex (A1) and secondary auditory cortex (dPEG) of awake, passively listening ferrets

(methods in [1,2]). The same stimuli were presented in their undistorted original form and after dilation in frequency and/or time.

Our results show that stimulus invariance to frequency and time dilations are present at every tested stage and increase along the hierarchical auditory processing pathway (Figure 1). Standard STRF-based parametric models, while explaining a portion of response variance, fail to reproduce the transformation invariances observed on Figure 1. In A1, parametric models having invariance properties by design (competitive softmax hierarchical models) are better-suited to describing observed biological function.

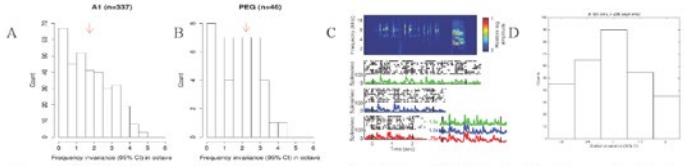

Figure 1: 95% CI in frequency for the highest responses in A1 (**A**) and PEG (**B**) as tested with narrowband noise stimuli. The higher values found in PEG compared to A1 demonstrate higher invariance to frequency shifts in PEG than in A1for both stimuli. (**C**) A ferret vocalization (top) and three responses to different time dilations (bottom). The inset shows the aligned firing rates, indicating similarities and differences in the responses. (**D**) 95% CI in time dilation for equivalent response epochs in A1 relative to unperturbed vocalization.

1. S. Atiani, S.V. David, D. Elgueda, M. Locastro, S. Radtke-Schuller, S.A. Shamma, J.B. Fritz. Emergent selectivity for task-relevant stimuli in higher order auditory cortex. Neuron (2014), 82(2): 486-99.

2. S. V. David, N. Mesgarani, and S. A. Shamma. Estimating sparse spectro-temporal receptive fields with natural stimuli. Network 2007, 18(3):191–212.

Funding

Funded in part by NIH grant R00DC010439 to SVD and WSU internal grant to AGD.

SYMP 5

Blood-brain barrier (BBB) and Neurodegeneration: How the BBB informs inner ear research

Berislav Zlokovic

University of Southern California

Blood vessels in the brain are organized with surprising precision, patterned in parallel with the major brain circuits tasked with sensation, memory and motion. This tight interrelationship may reflect key functional roles in neuronal normal function, disease and brain aging. I will discuss i) the molecular and cellular pathways in the central nervous system (CNS) capillaries, particularly during astrocyte-pericyte-endothelial signal transduction mechanisms that when turn awry can cause neuronal injury and neurodegenerative changes; ii) the effects of Alzheimer's-associated genes (*APOE4, PICALM, CLU*) on small blood vessels and blood-brain barrier (BBB) integrity; and iii) the effects of rare monogenic human disorders affecting primarily brain endothelial cells and pericytes that lead to BBB breakdown and development of a neurological disorder (*GLUT1, MSFD2A, PDGFB/PDGFRb*). I will also discuss microstructural and connectivity changes through various diffusivity, anisotropy and fiber tracking maps derived from the diffusion weighted MR images, and how we can quantify small vessel disease and BBB breakdown in rodent models of neurological disorders and the aging human population using imaging and molecular biomarkers. Finally, I will discuss whether repairing small blood vessels can retard neuronal dysfunction and degeneration, and how BBB research can inform inner ear research.

SYMP 6

Structure and Function of the Strial BLB and Noise-Induced Hearing Loss

Xiaorui Shi

Oregon Health & Science University

A functional blood-labyrinth-barrier (BLB) is critical for maintaining solute and ion homeostasis in the inner ear and preventing the influx of toxic substances. Disruption of the BLB is associated with many clinical hearing disorders, including autoimmune inner ear disease, Meniere's disease, drug-induced hearing loss, noise-induced hearing loss, sudden deafness, and genetically-linked hearing dysfunction. Despite its importance, the physiology of the BLB remains poorly understood. Recent progress in understanding the blood-brain barrier (BBB) and blood-retinal barrier (BRB) has led to significant improvements in ameliorating stroke, traumatic brain injury, and Alzheimer's disease. Better characterization of the BLB will likewise lead to more effective medical interventions. Recent studies have revealed that the strial BLB is more complex than previously understood. The BLB consists of microvascular endothelium closely associated with a substantial population of accessory cells (pericytes and perivascular resident macrophages) and extracellular basement membrane proteins that, together, constitute a unique "cochlear vascular unit." Dysfunction in any of the BLB components can lead to a specific inner ear disorder. This presentation will review structure and function of the strial BLB in the cochlea, and, in particular, will review of recent findings on the pathophysiological role of cochlear pericytes and perivascular resident macrophages in controlling blood labyrinth barrier integrity in noise-induced hearing loss.

SYMP 7

The BLB in disease- and age-related hearing loss

Michael Anne Gratton

Saint Louis University

The structures of the inner ear are replete with both structural extracellular matrix as well as intricate networks of basement membranes. The dynamic transitions in basement membrane composition during development suggest cochlear basement membranes may function to direct differentiation and/or terminal cytodifferentiation of the complex cellular compartments of the cochlear epithelium. The role of basement membranes in the adult cochlea remains to be fully identified. However, one role of basement membranes that impacts the cochlear vasculature and thereby the blood-labyrinth barrier is as a selective barrier for macromolecules moving from the vasculature to strial tissue

and vice versa. The diffusion capacity of macromolecules through the basement membrane is determined in part by the molecular components of the basement membrane as well as by its width or thickness. The thickened basement membrane results from dysequilibrium between the constant synthesis and obligatory degradation of basement membrane proteins. This can be due to increased synthesis of basement membrane proteins or decreased enzymatic activity of the matrix metalloproteinases responsible for basement membrane degradation.

In various pathological conditions associated with hearing loss, such as Alport syndrome, diabetes mellitus, and presbyacusis, thickened strial capillary basement membranes have been observed. The altered strial capillary basement membranes noted in animal models of these pathological conditions are thought to contribute to diminished auditory function. Strial capillaries and their basement membranes were studied in a mouse model of Alport syndrome, gerbil and mouse models of presbycusis, mouse models of Type 2 diabetes mellitus using histological, immunohistochemical, biochemical, molecular and imaging techniques. Changes in the molecular composition of the thickened strial capillary basement membranes and measures of diffusion capabilities are discussed. Mechanisms by which the altered strial capillary basement membranes can affect cochlear homeostasis and auditory function are presented

SYMP 8

Inflammation Alters Blood-labyrinth Barrier Function and Potentiates the Risk of Ototoxicity

Peter Steyger
Oregon Health & Science University

The functional blood-labyrinth barrier (BLB) selectively restricts access of blood-borne nutrients and toxins to inner ear tissues, fluids and hair cells. Nonetheless, ototoxic drugs are able to cross the BLB and exploit the unique electrophysiological environment of the inner ear to exert their cytotoxic effects in both the cochlea and vestibular system. Furthermore, systemic inflammation, induced via several mechanisms, enhances inner ear uptake of ototoxic drugs and exacerbates their cochleotoxic effect. It is crucial to identify the molecular mechanisms by which ototoxic drugs cross the BLB into the inner ear tissues and fluids, particularly endolymph, and to develop novel strategies that modulate drug trafficking across the BLB. This presentation will discuss the trafficking routes and the potential mechanisms by which ototoxic drugs can enter inner ear tissues and fluids.

SYMP 9

Cochlear inflammation and the dynamic blood-perilymph barrier

Keiko Hirose; Jared Hartsock; Alec Salt
Washington University School of Medicine

Background
The blood-perilymph barrier (BPB) serves a critical role by separating the components of blood from inner ear fluids, and limiting traffic of inflammatory cells, proteins and other solutes into the labyrinth, and allowing gas (O_2-CO_2) exchange. Local infection and inflammation produce changes in these barriers, resulting in increased permeability of blood vessels. In the inner ear, it is thought that compromise of the blood-perilymph barrier leads to hearing impairment through loss of the endocochlear potential (EP). In fact, the effect of increasing cochlear vascular permeability on hearing function and EP is poorly understood. We have developed a method to measure the integrity of the blood-perilymph barrier (BPB) and demonstrate the effects of barrier compromise on hearing threshold and EP. We also investigate the contribution of cochlear macrophages to barrier function after systemic exposure to lipopolysaccharide (LPS).

Methods
Blood perilymph barrier integrity was intentionally disrupted by treatment with systemic lipopolysaccharide (LPS). Adult mice were injected with saline or LPS, and ABR thresholds and EP were measured. A separate cohort of mice was treated with saline or LPS for barrier permeability studies through blood and perilymph sampling. Perilymph was collected from a fenestra in the posterior semicircular canal 30-35 minutes after systemic injection of fluorescein. Fluorescein content in the perilymph was normalized to fluorescein content in the serum. In a separate experiment, cochlear macrophages were depleted using diphtheria toxin in CX3CR1-DTR mice, and the macrophage-depleted mice were treated with saline or LPS. Barrier function was assessed in these mice to determine the effect of macrophages on barrier integrity at baseline and in mice depleted of macrophages.

Results and Conclusions
Systemic LPS treatment induced a profound change in vascular permeability, which correlated with only minor change in ABR threshold and EP. Macrophage depletion did not alter the baseline permeability of cochlear vessels, but did result in partial preservation of barrier function in LPS-treated mice. We conclude that LPS-induced sepsis results in compromise of the BPB. Despite the increased permeability of the BPB, ABR thresholds and EP were minimally altered. In addition, cochlear macrophages were not required to maintain the BPB at baseline, and cochlear macrophages may be an important factor in breakdown of the barrier after LPS treatment. Whether vascular leakiness measured by perilymph sampling would be similar to vascular leakiness in the intrastrial space is unknown.

Funding
Study supported by NIH R01 DC001315 (KH)

PD 25

Next generation sequencing and animal studies: a multistep approach for the discovery of new Hereditary Hearing Loss genes.

Giorgia Girotto[1,2]; Anna Morgan[1]; Dragana Vuckovic[3]; Elisa Rubinato[1]; Mariateresa Di Stazio[1]; Ramin Badii[4]; Moza Al-Kowari[2]; Diego Vozzi[3]; Paolo Gasparini[1,2]
[1]University of Trieste; [2]Sidra Medical Research Hospital; [3]IRCCS Burlo Garofolo; [4]Molecular Genetics Laboratory, Hamad Medical Corporation (HMC)

Introduction

Hereditary Hearing Loss (HHL) is characterised by the presence of a large genetic heterogeneity. In order to overcome this problem, a multistep strategy has been designed: STEP1) screening of 113 HHL genes by targeted re-sequencing (TS). In negative cases: STEP2) whole exome sequencing (WES) to detect causative mutation in new genes, STEP3) validation by functional studies and development of animal models (i.e. Zebra fish).

Methods

TS of 113 different HHL genes was based on Ion Torrent PGM™ (LifeTechnologies) (4.356 amplicons ensuring ~92,6 % coverage of 744,38Kb of the target region). After genome variants annotation, data were filtered according to quality value, allele frequency (i.e. ExAC, 1000 Genomes, ESP6500 and NCBI dbSNP databases), pathogenicity prediction (e.g.Polyphen2, SIFT) and conservation score (PhyloP, GERP++). As regards to WES protocol (Ion Proton™-LifeTechnologies), after exome enrichment step, data analysis was performed as above described.

Results

Our algorithm has been applied to 40 families negative for GJB2 (25 coming from Italy and 15 from Qatar). In particular, STEP1 (TS) allowed us to characterize 18 families out of 40 (45%) with mutations in known genes (TECTA, TMPRSS3, TMC1, MYO15A, LOXHD1, WFS1, P2RX2, POU4F3, STRC, OTOA). As regards to STEP2, so far, 16 families entered the WES pipeline and the following new HHL genes were identified: a) BDP1 (Girotto G. Plos One-2014) b)TBL1Y, a candidate gene for Y-linked hearing loss for which functional studies are at the end stage, c)PSIP1 gene, a transcriptional co-activator regulated by miR-135b in vestibular hair cells of the mouse inner ear. More recently, we found mutations in the following genes: d)PLS1, the most abundant actin-bundling proteins of stereocilia in mouse, e)LAMC1, a member of the laminin family whose members play an important role in the hearing system, f)KTNM, an actin-binding protein described as expressed in the tip links of stereocilia and proposed as a candidate gene for HL (Bearer EL et al. 2000). Overall, 24 families have been positively characterised leading to the identification of new HHL alleles/genes (60%). In the remaining families, data are under the final step of analysis. Finally, in STEP3, functional studies on the identified new genes will be performed using Zebra fish models followed by an accurate phenotypic characterization.

Conclusions

These findings clearly highlight the importance of NGS technologies followed by animal model validation as well as the usefulness of this strategy to better understand the genetic basis of HHL. Updated data will be presented and discussed.

Funding

The study was supported by funds from Italian Ministry of Health (RC16/06 and RF2010) (to PG)

PD 26

The International Mouse Phenotyping Consortium: New insights into the genetics of deafness

Steve Brown[1]; The International Mouse Phenotyping Consortium (IMPC)
[1]MRC Harwell; 0

Background

A major challenge facing mammalian genetics over the next decade is the systematic and comprehensive annotation of mammalian gene function. As part of the International Knockout Mouse Consortium, several programmes are ongoing to generate conditional mutants for all mouse genes. An even greater challenge will be the determination of phenotypic outcomes for each mutation and the identification of disease models. The International Mouse Phenotyping Consortium (IMPC, www.impc.org) is undertaking the development of a comprehensive Catalogue of Mammalian Gene Function.

Method and Results

The IMPC incorporates 18 major mouse centres around the world that undertake mouse production and phenotyping. The IMPC programme has two phases: Phase 1, 2011-2016, is approaching completion and will deliver the phenotypes of around 5000 mouse mutant lines; Phase 2 from 2016-2021 will undertake the analysis of the remaining genome. IMPC centres operate a core, standardised, broad-based adult phenotyping pipeline encompassing the major biological and disease systems, including gross pathology and tissue collection as a mandatory requirement. Importantly, each mouse mutant line undergoes an ABR test to assess hearing. In addition, lacZ expression data is being collected for adult organs and E12.5 embryos. All data from each production and phenotyping centre is uploaded to a central Data Coordination Centre (DCC), and following QC and analysis is archived and disseminated to the wider biomedical sciences community along with appropriate annotation tools. In the first 4 years of the programme, nearly 8000 ES cell lines have been injected, over 4800 mouse mutant lines generated and phenotype data from nearly 2500 mutants collected at the DCC. To date, 1727 genes have been analysed by ABR, and we find that 5.7% (99 genes) have significant threshold shifts and impaired auditory function. Many of these genes are novel and have not been previously implicated in auditory function, and we will describe a number of the new mutants demonstrating hearing loss. Moreover, IMPC plans an ageing

component to the phenotyping pipeline, with the opportunity to identify genes underlying presbycusis.

Conclusion
IMPC is providing many new insights into the genetic and molecular bases of disease, and generating numerous novel disease models. The data from auditory testing to date suggests that there are around 1000 genes in the mammalian genome that are important for auditory function. IMPC is identifying a plethora of new genes that will be important for understanding the genetic pathways involved with auditory function.

Funding
IMPC is funded by a number of national funding agencies, including the NIH, MRC, Wellcome Trust, Helmholtz, Genome Canada, INSERM.

PD 27

New Genes Involved in Deafness from a Large-scale Mouse Mutant Screen

Karen Steel[1]; Selina Pearson[2]; Elisa Martelletti[1]; Jing Chen[1]; Annalisa Buniello[1]; Morag Lewis[1]; Jacqueline White[2]; Neil Ingham[1]
[1]King's College London; [2]Wellcome Trust Sanger Institute

Hearing impairment is highly heterogeneous with many genes involved as well as environmental factors. Mutations causing hearing impairment give us access to the molecules required for normal auditory development and function. A more complete knowledge of the genes involved will facilitate diagnosis in affected people by sequence analysis and give us insight into the molecular pathways underlying normal hearing and the pathological processes leading to deafness.

We used a public resource (KOMP/EUCOMM) of targeted ES cells to generate new mouse mutants and screened them for multiple phenotypic features including hearing using Auditory Brainstem Response (ABR) recording at 14 weeks old. Responses were recorded to clicks and tonebursts at 6-30 kHz with 5dB stimulus intensity increments in ketamine/xylazine-anaesthetised mice. Thresholds and waveform features were analysed offline. Heterozygotes were screened if homozygotes were sub-viable, and the majority of lines were on a C57BL/6N genetic background.

Over 1000 genes have been screened so far using ABR. A total of 30 new genes associated with raised thresholds have been found with varied patterns including 7 mild, 7 moderate and 5 severely affected lines plus 10 with high frequency and 1 with low frequency impairment. A wide range of pathology was found, such as middle ear inflammation (eg *Mcph1*), reduced endocochlear potentials (eg *Spns2*), and synaptic defects (eg *Wbp2*).

These genes had no previous indication that they might be required for normal hearing and all represent good candidates for involvement in human deafness. Assuming the first 1000 genes tested are a random sample of the 22,000 protein-coding genes in mice and humans, these findings suggest that a further 600 genes will be found to be essential for hearing, adding to the 300 that we currently know to be involved in deafness from mouse and human studies.

Funding
Wellcome Trust EUMODIC MRC

PD 28

Suceptibility to noise-induced hearing loss: A genome-wide association study in mice.

Joel Lavinsky[1]; Marshal Ge[2]; Amanda Crow[2]; Calvin Pan[3]; Pezhman Salehide[2]; Eleazar Eskin[3]; Hooman Allayee[2]; Aldons Lusis[3]; **Rick Friedman**[2]
[1]Federal University of Rio Grande do Sul; [2]University of Southern California; [3]University of California, Los Angeles

Background
In the United States, roughly 10% of the population is exposed daily to hazardous levels of noise in the workplace. Twin studies estimate heritability for noise-induced hearing loss (NIHL) of approximately 36% and strain specific variation in sensitivity has been demonstrated in mice. Based upon the difficulties inherent to the study of NIHL in humans we have turned to the study of this complex trait in mice. In this study we present, for the first time, a completed genome-wide association analysis of NIHL in mice with correction for population structure.

Methods
We exposed 5 week-old mice from the Hybrid Mouse Diversity Panel (HMDP) to a 10 kHz octave band noise at 108 dB for 2 hours and assessed the permanent threshold shift 2 weeks-post exposure using frequency specific stimuli (ABR, DPOAE). These data were then used in a genome-wide association study (GWAS) using the Efficient Mixed Model Analysis (EMMA) to control for population structure.

Results
In addition to our recent description of the role of Nox3 in susceptibility to NIHL we have identified eight additional novel loci throughout the genome with a genome-wide significance of greater than 4.61X10-6.Similar to our recent publication of the genetic landscape of baseline strain variation in hearing we see a frequency specific genetics to NIHL susceptibility.

Discussion
We have completed the first genome-wide association study in mice for susceptibility to NIHL with correction for population structure. Several new candidate genes are identified and the implications for future study and the potentials for translating into humans will be discussed.

Funding
NIH/NIDCD R01 DC010856-01 (RAF)

PD 29

Genome Wide Association Studies (GWAS), Targeted Re-Sequencing (TRS) and Animal Studies: a combined approach aimed to investigate the genetic causes of Age-related Hearing Loss (ARHL)

Anna Morgan[1]; Diego Vozzi[2]; Dragana Vuckovic[2]; Martina La Bianca[2]; Maria Pina Concas[3]; Mario Pirastu[3]; Paolo Gasparini[1,4]; Giorgia Girotto[1,4]

[1]University of Trieste; [2]IRCCS Burlo Garofolo; [3]Institute of Population Genetics, National Research Council of Italy; [4]Sidra Medical Research Hospital

Background

ARHL is the main sensory impairment in the elderly. It results from age-related degeneration of the cochlea due to genetic and environmental components. To date little is known about the genetics of ARHL. In order to overcome this lack of knowledge, we developed a TRS panel of 46 ARHL candidate genes and sequenced ~500 ARHL Italian patients coming from both inbred and outbred populations.

Methods

Genes were selected based on GWAS (Girotto et al. 2014, Wolber et al. 2014, Vuckovic et al. 2015), literature updates and animal studies (in collaboration with M.Bowl-MRC, S.Dawson-UCL). TRS was performed using Ion Torrent PGM(LifeTechnologies). 1942 amplicons ensuring 96,55% coverage of the target region (392,89 Kb) were analysed. Data were filtered according to quality value, pathogenicity prediction (e.g. Polyphen2, SIFT) and conservation score. Frequency values were checked using ExAC, 1000 Genomes, ESP6500 and NCBI dbSNP. All mutations were confirmed by Sanger sequencing and tested in controls coming from the same population.

Results

56 mutations of interest were identified: 5 frameshift indels, 2 nonsense and 49 missense mutations. All are predicted as pathogenic by at least 1 in silico predictor tool and are absent in any public database or present with a MAF<0.01. Three scenarios are present: 1) different mutations in the same gene, 2) the same mutation in different patients and 3) different mutations in the same patient (Figure1). As regards to 1)three frameshift deletions in XIRP2 were found. Genotype-phenotype correlation revealed that all patients showed high-frequency HL strongly resembling the phenotype described in animal models(Francis et al. 2015). In the second scenario (2) a nonsense mutation in SLC28A3 was detected in 19 patients belonging to a large Sardinian pedigree from an isolated village. Sequencing of 112 matched controls revealed a significant difference in allele frequency. Finally, in agreement with the complex genetic structure of ARHL, (3) up to 3 mutations in different genes were detected in some patients. Most of them are missense mutations affecting conserved residues and predicted to be pathogenic(Figure 1c). In this light, pathway analysis can highlight key interactions.

In order to validate the pathogenicity of these variants, functional studies are now in progress using K/I, K/O Zebra fish models followed by an accurate phenotypic characterisation.

Conclusions

These findings demonstrate the potential role of these genes in causing ARHL showing that a multistep approach is needed to understand the molecular basis of this disease. Complete and updated results will be presented.

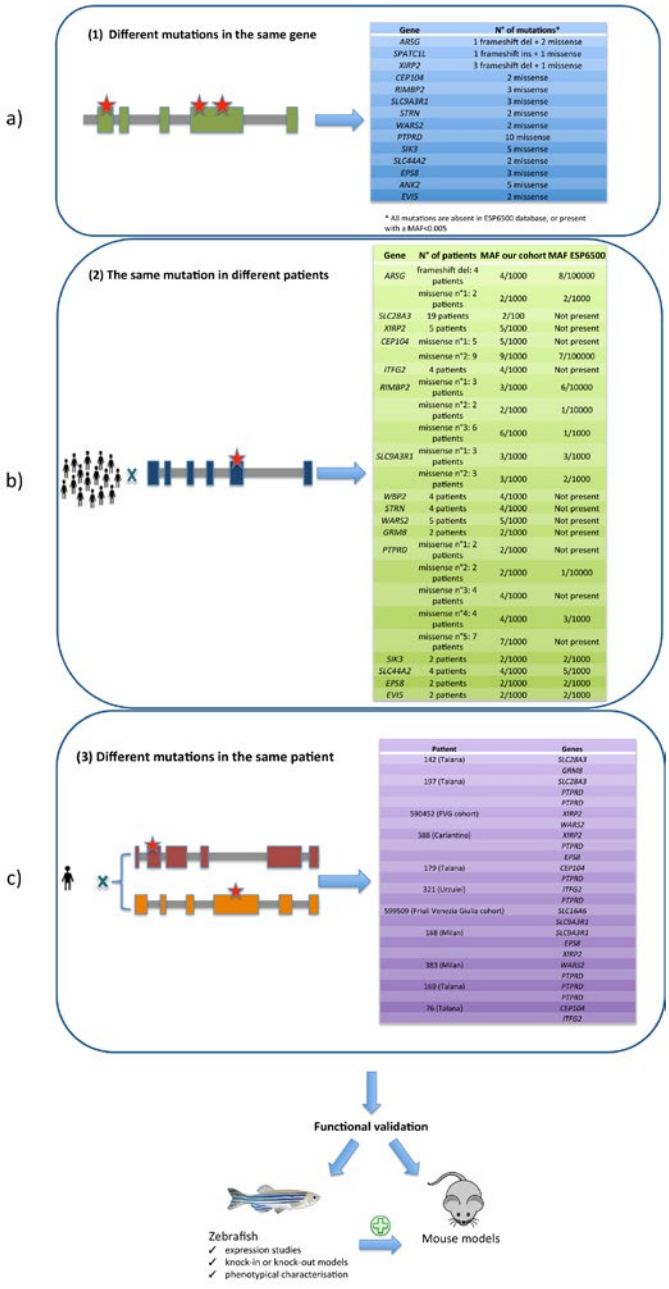

Funding

The study was supported by funds from Italian Ministry of Health (RC16/06 and RF2010) (to PG)

PD 30

Correction of the Cdh23-ahl Allele and Auditory Phenotype in C57BL/6N Mice Via CRISPR/Cas9-Mediated Homology Directed Repair

Michael Bowl; Joffrey Mianné; Lauren Chessum; Saumya Kumar; Carlos Aguilar; Gemma Codner; Marie Hutchison; Andrew Parker; Ann-Marie Mallon; Sara Wells; Michelle Simon; Lydia Teboul; Steve Brown
MRC Harwell

Background

Nuclease-based technologies have been developed that enable targeting of specific DNA sequences directly in the zygote. These approaches provide an opportunity to modify the genomes of inbred mice, and allow the removal of strain-specific mutations that confound phenotypic assessment. One such mutation is the *Cdh23^{ahl}* allele, present in several commonly used inbred mouse strains, which predisposes to age-related progressive hearing loss.

Results

We have used targeted CRISPR/Cas9-mediated Homology Directed Repair (HDR) to correct the *Cdh23^{ahl}* allele directly in C57BL/6NTac zygotes. Employing offset-nicking Cas9 (D10A) nickase with paired RNA guides and a single-stranded oligonucleotide donor template we show that allele repair was successfully achieved. To investigate potential Cas9-mediated 'off-target' mutations in our corrected mouse, we undertook whole-genome sequencing and assessed the 'off-target' sites predicted for the guide RNAs (≤4 nucleotide mis-matches). No induced sequence changes were identified at any of these sites.

Correction of the progressive hearing loss phenotype was demonstrated using auditory-evoked brainstem response testing of mice at 24- and 36-weeks of age, and rescue of the progressive sensory hair cell loss was confirmed using scanning electron microscopy of dissected cochleae from 36-week old mice.

Conclusions

CRISPR/Cas9-mediated HDR has been successfully utilised to efficiently correct the *Cdh23^{ahl}* allele in C57BL/6NTac mice, and rescue the associated auditory phenotype. Going forward, this experimental design can be employed to repair the *Cdh23^{ahl}* allele in other mouse strains e.g. C57BL/6J. Importantly, the corrected mice described in this report will allow age-related auditory phenotyping studies to be undertaken using C57BL/6NTac-derived models, such as those generated by the International Mouse Phenotyping Consortium (IMPC) programme. In addition, models aged on the repaired background can also be employed for age-related behavioural studies that utilize acoustic stimuli as part of the test paradigm, such as acoustic startle and pre-pulse inhibition.

Funding

This work was supported by the Medical Research Council (MC_A390_5RX80 to SDMB) and Action on Hearing Loss (PA05 to MRB).

PD 31

Restoration of hearing by CRISPR/Cas9-medated genome editing in the Pmca2 deafness mouse model by protein delivery

Zheng-Yi Chen[1]; Yong Tao[1]; Xue Gao[2]; Yujuan Hu[1]; Pu Dai[3]; Weijia Kong[4]; David Liu[2]
[1]Harvard Medical School, Massachusetts Eye & Ear Infirmary; [2]Harvard University; [3]Chinese PLA General Hospital; [4]Union Hospital, Tongji Medical College, Huazhong University of Science and Technology

Introduction

1 in 500 newborns suffer from genetic hearing loss, and hundreds of genes are likely to be responsible for genetic hearing loss when mutated. Approaches including AAV-mediated gene delivery, anti-sense oligos and shRNA have been developed as potential treatment. Due to the limitations of each method, new approach is needed for the treatment of different forms of genetic hearing loss. CRSIPR/Cas9-mediated genome editing emerged as potential new treatment due to the permanent editing results. However most CRISPR/Cas9 has been performed in germline or *in vitro* by viral vectors or DNA vectors, which raise long-term safety concerns. Further *in vivo* efficiency has been generally low. We report here hearing restoration in a PMCA2 deaf mouse model (Obl-*Oblivion)* by direct protein delivery and CRISPR/Cas9 mediated genome editing.

Methods

gRNAs against the Pmca2 mutation were screened by *in vitro* endonuclease assay and by using Obl fibroblasts. Potent gRNAs were complexed with Cas9 protein by lipid formulation, which were then injected to neonatal mouse *Obl* inner ear. Control gRNAs were similarly injected. Hearing studies were performed at one, two and three months after injection, with tissues harvested for characterization.

Results

ABR (auditory brainstem response) and DPOAE (distortion product otoacoustic emissions) demonstrated dramatic hearing recovery across most frequencies at the ages studied. Hearing recovery of 10-45dB were observed, with the middle frequencies recovered the most. Hearing recovery is specific to gRNAs against the mutation, whereas in control inner ear no recovery was detected. Further hearing recovery is dose-dependent. In the experimental inner ears, genome editing led to significant improvement in outer hair cell survival, demonstrating recovery of Pmca2 function in the outer hair cells. Preservation of neurites of auditory ganglion neurons was detected by genome editing.

Conclusion

PMCA2 mutations have been associated with human deafness. Our study demonstrates high-efficiency genome editing and hearing restoration in the *Obl* deaf mouse model

by transient *in vivo* inner ear delivery of Cas9 and gRNA complex. The study further uncovers the dominant effect of the *Oblivion* mutation, which was previously shown to be the result of haploinsufficiency. This is the first time that CRISPR/Cas9 mediated genome editing has been successfully applied to disrupt mutation and restore function in a genetic disease model by direct protein delivery in vivo. Our strategy is applicable to restoration of hearing in a wide range of genetic hearing loss models with potential for the application in human.

Funding
NIH DC-006908 Frederick and Ines Yeatts Hair Cell Regeneration Grant

PD 32

Early Replacement of Slc26a4 Expression Prevents Hearing Fluctuation in a Mouse Model of EVA

Ayako Nishio[1]; Taku Ito[1]; Tracy Fitzgerald[1]; Philine Wangemann[2]; Andrew Griffith[1]
[1]National Institute on Deafness and Other Communication Disorders; [2]Kansas State University

Background
Patients with enlargement of the vestibular aqueduct (EVA) can have fluctuating or progressive hearing loss. The most common cause of EVA is mutations of SLC26A4. SLC26A4 encodes pendrin, which is expressed in non-sensory epithelial cells of the endolymphatic sac and lateral wall of the cochlea. Recently, we generated a doxycycline (dox)-inducible Slc26a4-insufficient mouse model of EVA. Administration of dox from conception to E17.5 ("DE17.5") resulted in mice with hearing fluctuation between 1 and 3 months of age (Ito et al., Neurobiol. Dis., 2014). In this study, we hypothesized that Slc26a4 is required to maintain stable hearing in DE17.5 ears. Our hypothesis predicts that re-initiation of Slc26a4 expression in mature DE17.5 mice will prevent fluctuation of hearing.

Methods
DE17.5 mice were each divided into three groups: (1) no re-administration of dox (no-readmin); (2) dox readministered at 1 month of age (readmin-1M); and (3) dox readministered at postnatal day 6 (readmin-P6). We also included a control group that received dox continuously from conception (IE0). Click ABR thresholds were measured at 1, 2 and 3 months of age. Fluctuations were defined as a >10 dB difference in click threshold between monthly measurements. After 3 months of age, cochleae were processed for analysis of pendrin expression with anti-pendrin antibodies and immunofluorescence microscopy.

Results
In DE17.5 ears, readmin-P6 resulted in significantly less fluctuation in comparison to no-readmin or readmin-1M (Table 1). In spindle-shaped cells of the stria vascularis, readmin-P6 resulted in significantly higher pendrin expression than in no-readmin or readmin-1M ears. There was no significant correlation of click ABR thresholds with pendrin expression in spindle-shaped cells, root cells or sac cells. There was no significant correlation of cumulative threshold shifts and pendrin expression in the lateral wall of the cochlea or the endolymphatic sac.

Conclusions
Readministration of doxycycline at P6 prevented fluctuation of hearing in DE17.5 ears between 1 and 3 months of age. The effect of doxycyline readministration at P6 may have been due to increased pendrin expression in spindle-shaped cells. Pendrin appears to be necessary to maintain stable hearing in ears that experience Slc26a4 insufficiency during development.

Table 1. Numbers of ears with fluctuating or stable hearing.

	Fluctuating	Stable	Total
DE17.5: no-readmin	13	25	38
DE17.5: readmin-1M	10	16	26
DE17.5: readmin-P6	1	25	26
IE0	1	11	12
Total	25	77	102

Funding
This work was supported by NIH intramural research funds Z01-DC000060 and Z01-DC000080. A.N. was supported in part by a JSPS Research Fellowship for Japanese Biomedical and Behavioral Researchers at NIH. P.W. was supported by NIH grant R01-DC012151.

PD 33

NIDCD Research and Training Workshops

NIDCD will offer two concurrent workshops targeted to specific audiences. Both are training workshops for those with limited experience submitting grant applications to NIH.

Workshop #1: Applying for NIDCD Training and Career Development Awards
This workshop will include an overview of research training and career development opportunities appropriate for graduate students, postdoctoral fellows and new clinician investigators. The presentation will include essential information on the submission and review of individual NRSA fellowship awards (F30, F31 & F32), as well as selected mentored career development (K-) awards. Drs. Alberto Rivera-Rentas and Melissa Stick will lead the discussion and provide updates on these funding mechanisms.

Workshop #2: Early Stage Investigators (ESI) and New Investigators (NI)
This workshop will provide essential information for junior scientists seeking to obtain their first research project grant. The goal is to provide a better understanding of the process of application, review, and award for the NIDCD Small Grant (R03) and NIDCD New-Investigator R01 award. This workshop is targeted to postdoctoral trainees ready to transition to independence as well as individuals who have recently transitioned to independence, e.g. accepted a new faculty position, and are in the early stages of establishing their own independent laboratory/research program. The presentation will include an overview of the NIDCD R03 Small Grant Program, provide information to facilitate the most expeditious route to funding for New-Investigator R01s,

and clarify the roles of NIH program, review, and grants management staff. Drs. Janet Cyr and Shiguang Yang will lead the discussion and provide updates on these funding mechanisms.

Investigators of all stages are welcome to attend. The emphasis however will be on information most useful to those in early career stages seeking NIH/NIDCD funding for research or training and career development.

Funding
NIDCD

SYMP 10

White Matter Plasticity in Response to Functional Activity

Douglas Fields
National Institutes of Health, NICHD

Nervous system function requires the proper impulse transmission speed through all axons, and this is highly dependent on myelin and node of Ranvier structure. A wide range of studies from a number of laboratories suggest that white matter can change in response to functional activity, environmental experience, learning, and in the auditory system, accommodate for changes in interaural latency. Molecular mechanisms that have been identified for activity-dependent effects on myelin will be reviewed and new results presented showing that the node of Ranvier and myelin thickness are dynamically regulated by paranodal astrocytes. Exocytosis of ATP from astrocytes acts in an autocrine manner on purinergic receptors to reorganize glial intermediate filaments and alter cell shape. The nodal gap increases as astrocytes withdraw from the node, allowing detachment of the paranodal loops of myelin by thrombin-dependent cleavage of Neurofascin 155 in axo-glial septate junctions, and thinning the myelin sheath. This process is reversed by restoring ATP release from astrocytes, but also requires functional activity in axons. Activity-dependent effects on myelin could contribute to information processing and plasticity by optimizing the timing of spike time arrival at relay points in neural networks.

SYMP 12

Microglia Promote Synaptic Maturation in the Auditory Brainstem

Karina Cramer; Minhan Dinh; Sarah Rotschafer
University of California, Irvine

Introduction
Microglia originate in the yolk sac and infiltrate the nervous system early in development. They function as macrophages in immune responses in the mature brain. Recent studies have demonstrated that microglia also participate in synaptic pruning and elimination, in part by linking neuronal activity with engulfment of cell components tagged for degradation. Our previous study showed that microglia populate the auditory brainstem nuclei at early postnatal ages when auditory circuits mature. Projections from the ventral cochlear nucleus (VCN) to the medial nucleus of the trapezoid body (MNTB) undergo refinement and growth at these early ages. MNTB cells initially receive multiple inputs, and synapses are eliminated until exactly one input remains and expands to become a mature calyx of Held. Here we examined the role of microglia in the refinement of the projection from VCN to MNTB.

Methods
We investigated the maturation of these synapses in mice lacking Cx3cr1, a receptor for a cytokine released from neurons that mediates neuron-microglia communication. We used immunofluorescence for the vesicular glutamate transporter (VGluT1), sparse axonal tracing to label individual calyces, and histological analysis. We examined cell size, calyx size, and cell coverage in MNTB. Additionally, auditory brainstem responses were studied in mice at two months of age.

Results
At postnatal day 8, MNTB cells were significantly smaller in *Cx3cr1* KO mice than in wild type animals; this difference remained when measured at two months. We found that at P8 calyx size was significantly smaller in *Cx3cr1* KO mice than in wild type mice. The difference in calyx size exceeded that seen in MNTB cell size. Thus, calyces in P8 *Cx3cr1* KO mice covered a significantly smaller proportion of their target neuron than calyces in wild type mice. Immunofluorescence for VGluT1 confirmed the presence of additional unlabeled inputs in *Cx3cr1* KO mice. ABR measurements showed similar amplitudes between genotypes. *Cx3cr1* KO mice displayed significantly longer latency responses for peaks 1-3 than control mice.

Conclusions
Our anatomical findings in MNTB suggest a deficit in synaptic pruning in *Cx3cr1* KO mice. ABR analysis demonstrates lasting defects in auditory brainstem function. These findings suggest that microglia contribute to auditory maturation and that this role requires communication with neurons through Cx3cr1.

SYMP 13

Oligodendroglial Excitability in the Auditory Brainstem

Jun Hee Kim; Emmanuelle Berret
University of Texas Health Science Center, San Antonio

Oligodendrocyte maturation and axon-glial communication are required for proper myelination in the auditory nervous system in the developing brain. Oligodendroglia excitability may be a potentially important mechanism for promoting axon myelination and neuron-glia interaction. However, the ability of oligodendrocyte lineage cells to fire action potentials is still controversial. Furthermore, the necessity of Na^+ channel and electrical excitability of oligodendroglia in relation to their maturation to myelinating stage in the auditory nervous system remains unknown. Here, we investigated the physiological characteristics and spiking properties of oligodendrocyte lineage cells in the medial nucleus of the trapezoid body (MNTB) in the auditory brainstem. We found that immature

oligodendrocytes in their pre-myelinating stage (pre-OLs; CNPase- and DM20-positive, but NG2-negative) displayed action potential firing. There were two distinct classes of pre-OLs: one had typical passive membrane properties, while the other expressed substantial voltage-activated Na^+ currents and generated action potentials. Electrophysiological, pharmacological, and immunostaining data demonstrate that spiking in excitable pre-OLs was driven by $Na_v1.2$ channels. Pre-OLs received glutamatergic inputs from neighboring neurons through axon-glia synaptic interaction, and $Na_v1.2$–driven spiking was dependent on AMPAR-mediated synaptic currents, indicating that glutamatergic inputs trigger oligodendrocyte spiking. Furthermore, excitable pre-OLs were detected throughout postnatal development up to postnatal day 62, suggesting that $Na_v1.2$-driven spiking of pre-OLs is not limited to a transient stage of early development. Rather, spiking behavior of immature oligodendrocytes persists into the young adult brain. Together these data indicate that the axo-glia interaction leading to AP firing in pre-OLs is required for their normal functioning and maturation in myelinated areas in the auditory nervous system.

SYMP 11

Glycine and GABA Transporters in LSO Astrocytes

Eckhard Friauf; Jonathan Stephan
University of Kaiserslautern

Neurotransmitter clearance from the synaptic cleft is a major function of astrocytes and requires neurotransmitter transporters. In the rodent lateral superior olive (LSO), a conspicuous auditory brainstem center, both glycine and GABA mediate synaptic inhibition. However, the main inhibitory input from the medial nucleus of the trapezoid body (MNTB) appears to be glycinergic by postnatal day (P)14, when circuit maturation is almost accomplished (Kotak *et al*., 1998; Nabekura *et al*., 2004).

Using whole-cell patch-clamp recordings in acute brainstem slices at P3-20, we analyzed glycine transporters (GlyT1) and GABA transporters (GAT-1, GAT-3) in mouse LSO astrocytes, emphasizing on their developmental regulation. Astrocytes were identified using sulforhodamine 101-labeling, by which classical astrocytes can be unambiguously identified in acute tissue slices (Kafitz *et al*., 2008). Application of glycine or GABA induced a dose- and age-dependent inward current and a respective depolarization. The GlyT1-specific inhibitor sarcosine (2 mM) reduced the maximal glycine-induced current ($I_{Gly\ (max)}$) by about 60%. The GAT-1 and GAT-3 antagonists NO711 (10 µM) and SNAP5114 (40 µM), respectively, reduced the maximal GABA-induced current ($I_{GABA\ (max)}$) by about 35%. Furthermore, $[Cl^-]_o$ reduction decreased $I_{Gly\ (max)}$ and $I_{GABA\ (max)}$ by about 85-95%, showing the Cl^- dependence of GlyT and GAT. $I_{GABA\ (max)}$ was stronger than $I_{Gly\ (max)}$, and the ratio increased developmentally from 1.6-fold to 3.7-fold. Furthermore, I_{Gly} and I_{GABA} interfered with each other, resulting in a sub-additive summation of the single currents.

Together, our results demonstrate the functional presence of the three inhibitory neurotransmitter transporters GlyT1, GAT-1, and GAT-3 in LSO astrocytes (Stephan and Friauf, 2014). Furthermore, the uptake capability for GABA was higher than for glycine in LSO astrocytes from neonatal and juvenile mice, pointing toward eminent GABAergic signaling in the mature LSO, although the source of GABA is of speculation. GABA may originate from another source than the MNTB-LSO synapses - namely from another projection -, from vesicular dendritic release from LSO neurons, or directly from reversal of astrocytic GATs. Altogether, neuronal signaling in the LSO appears to be more versatile than previously thought.

SYMP 14

Postnatal refinement of axonal conduction speed in the mammalian brainstem

Conny Kopp-Scheinpflug; James Sinclair
Ludwig-Maximilians-University, Munich

Trapezoid body (TB) axons are of large diameter, with each fiber giving rise to a single giant calyx of Held synapse. In myelinated axons fiber diameter positively correlates to an increase in conduction velocity. However, conduction velocity also depends on neuron-glia interactions which are developmentally and activity-dependently regulated. Postsynaptic to the calyx of Held are the principal cells of the medial nucleus of the trapezoid body (MNTB) which are well known for their fast and temporally precise firing behavior facilitated by distinct set of voltage and ligand gated ion channels. Here we ask whether conduction velocity in the afferent fibers and intrinsic properties in MNTB neurons are co-regulated during development and whether there are species specific differences between mouse and gerbil in the maturation of this pathway.

We performed patch-clamp recordings of the MNTB in mouse and gerbil to assess developmental changes in the intrinsic properties. Conduction velocity of single TB fibers was measured by whole-cell recordings of MNTB neurons while electrically stimulating the TB fibers in two locations. Comparison of intrinsic properties of mouse MNTB principal cells showed a developmental decrease in input resistance from pre-hearing onset (P8-P11: 192.9±65.8 MΩ, n=43) to post-hearing onset (P13-P16: 143.7±51.4 MΩ, n=38). No further decrease in input resistance was observed between up to 4 weeks of age. This change in input resistance was accompanied by a decrease in membrane time constant between pre-hearing onset (6.2±2.9ms, n=43) and post-hearing onset (4.9 ±2.4ms, n=38). Capacitance remained around 30pF for all age groups. When comparing MNTB intrinsic properties between mouse and gerbil, both, input resistance (g: 107.9±55.0 MΩ, n=38; m=144.3±64.4 MΩ, n=52) and membrane time constant (g: 3.3±2.2ms, m: 4.7±2.1ms) were lower in gerbil than mouse. These concurrent changes resulted in no difference in the calculated membrane capacitance (g: 31.1±14.7pF, n=38; m: 33.6±7.4pF). Preliminary data suggest that conduction velocity increases post hearing onset in the mouse between P8 and P33 (P9: 4.2±1.7m/s (n=13); P17-P33: 7.8±3.5m/s (n=10). In gerbil,

conduction speed at post-hearing ages is similar to that of age-matched mice (P17-P27, 9.7±6.0m/s, n=23).

Our data suggest a parallel refinement of intrinsic properties and axonal conduction characteristics with hearing onset. In addition to increasing our knowledge of the development of the auditory system these results provide a starting point to investigate determining factors of axonal conduction speed in the mammalian CNS, using the trapezoid body calyx of Held-MNTB synapse as a model system.

SYMP 15

Synaptic Communication Between Neurons and Oligodendrocyte Progenitors in the Developing Nervous System

Dwight Bergles; Amit Agarwal
The Johns Hopkins University School of Medicine

The mammalian CNS contains an abundant, widely distributed population of glial cells that expresses the chondroitin sulfate proteoglycan NG2 (CSPG4) and the alpha receptor for PDGF (PDGFaR). Although initially defined as a class of astrocytes, studies completed over the past two decades indicate that these cells are morphologically and physiologically distinct from astrocytes: They do not express GFAP, do not contact capillaries and do not express glutamate transporters at high densities. Genetic analyses indicate that these $NG2^+$ cells are part of the oligodendrocyte lineage and serve as progenitors for oligodendrocytes (OLs) during early development, and thus are often referred to as oligodendrocyte precursor cells (OPCs). Physiological studies in acute brain slices indicate that they express ionotropic receptors for various neurotransmitters and form direct synapses with glutamatergic and GABAergic axons in all brain regions that have been examined, including the medial nucleus of the trapezoid body. This remains the only known example of direct neuron – glial cell synapses in the nervous system. The AMPA and NMDA receptors expressed by these cells may provide a means to link neuronal activity to calcium-dependent processes in NG2+ cells to regulate their growth and development. However, the physiological significance of this rapid neuron-glial cell communication has not been established, as pharmacological manipulations cannot distinguish between neuron:neuron and neuron:glial synapses. To overcome this difficulty, we developed transgenic knock-in mice in which a dominant negative AMPA receptor subunit (dnGluA2) containing a single point mutation in the pore region can be expressed in a cell specific manner. Conditional expression of this subunit renders AMPA receptors non-functional and blocks excitatory postsynaptic currents. *In vivo* studies indicate that blocking AMPA receptor function in $NG2^+$ cells maintains these cells in a proliferative state and prevents their differentiation into oligodendrocytes, suggesting that neuron-glial cell synaptic communication in the developing nervous system promotes oligodendrogenesis and myelination. We have also developed new lines of transgenic mice that have allowed us to manipulate gene expression within these progenitors, track their fate, monitor their dynamics on timescales of minutes to months *in vivo*, and selectively ablate these cells from the adult CNS. These studies are providing new insight into the ability of these cells to maintain their density in the adult CNS, regenerate oligodendrocytes in the context of disease, and participate in tissue repair following acute CNS injury.

PD 34

Long-Term Effects of Transient Cochlear Nerve Demyelination on Auditory Function

Guoqiang Wan; Gabriel Corfas
The University of Michigan

Introduction

The cochlear axons that innervate inner hair cells (IHCs) are myelinated by Schwann cells. This myelination is important for normal conduction velocity of action potentials and synchronized impulse transmission of the cochlear nerve. Damage to peripheral axons and their myelin sheaths are known to cause many forms of peripheral neuropathy. However, the effects of Schwann cells loss and demyelination on auditory function is poorly understood. Here, we specifically ablated Schwann cells in mature cochlea in mice *in vivo* and examined how this affected cochlear neuron survival, innervation, myelination and auditory functions.

Methods

We used mice carrying a Plp/CreERT transgene and a Cre-inducible diphtheria toxin (DTA) allele to ablate cochlear Schwann cells by injecting tamoxifen at P21-P23. At different times after induction, auditory brainstem responses (ABR) were measured to assess hearing function. Then, cochleae were isolated and cochlear histopathology analyzed by immunostaining followed by confocal imaging or by transmission electron microscopy (TEM).

Results

DTA expression resulted in ablation of cochlear Schwann cells and acute demyelination of the cochlear nerve within 1 week post-induction. However, within 16 weeks post-induction, Schwann cells had completely regenerated and the cochlear nerves had recovered normal myelin thickness and node of Ranvier density. Remarkably, physiological recordings performed at different times after tamoxifen induction (1 week to 1 year) showed that the Schwann cell ablation resulted in long-lasting reduction in ABR wave 1 amplitudes and increase in ABR wave 1 latencies, without affecting the ABR threshold, suggestive of persistent auditory neuropathy after transient demyelination. Immunostaining for node of Ranvier proteins showed that while nodal density along the nerve was lost and then recovered after transient demyelination, the first heminodes proximal to the auditory nerve terminals were permanently disrupted. Specific and permanent disruption of these heminodes may be the underlying cause of nerve conduction dyssynchrony and auditory pathophysiology.

Conclusions

Our findings indicate that transient cochlear nerve demyelination results in permanent auditory neuropathy that may be characterized as a form of “hidden hearing loss”, i.e. alterations in ABR amplitudes and latencies but not

thresholds. We also show that although the mature cochlea has remarkable capability for Schwann cell regeneration and remyelination of cochlear axons, the first Schwann cells at the habenula perforata fail to reform normal hemi-nodal structures. These findings are suggestive of potential long-lasting hearing deficits in patients with acute demyelinating neuropathies, such as Guillain-Barre Syndrome and leprosy.

Funding
R01 DC04820

PD 35

Activation of PI3K Signaling Prevents Aminoglycoside-Induced Hair Cell Death in the Murine Cochlea

Azadeh Jadali; **Kelvin Kwan**
Rutgers University

The loss of sensory hair cells of the inner ear due to aminoglycoside exposure is a major cause of hearing loss. Identification of therapeutically targetable pathways that prevent loss of hair cells is of clinical significance. We used an immortalized multipotent otic progenitor (iMOP) cell line to identify specific signaling pathways that promote otic cell survival. Validation of these pathways was done using a heuristic selection of inhibitory small molecules. Of the signaling pathways identified, the PI3K pathway emerged as a strong candidate for promoting hair cell survival. To determine whether activation of PI3K signaling can be repurposed for promoting hair cell survival, PI3K was upregulated in hair cells using a small molecule, bpV(HOpic) or by genetic ablation of PTEN. Hair cell ototoxicity was initiated by addition of gentamicin to cochlear cultures. Both paradigms showed that hyper-activation of PI3K signaling prevented aminoglycoside-induced hair cell death. Identifying PI3K signaling in the cochlea as a target for preventing aminoglycoside-induced hearing loss provides a new avenue for therapeutic intervention.

PD 36

Hair cell stereociliary bundle regeneration by espin gene transduction after aminoglycoside damage and hair cell induction by Notch inhibition

Akiko Taura[1]; Kojiro Taura[1]; Yukinori Koyama[1]; Norio Yamamoto[1]; Takayuki Nakagawa[1]; Juichi Ito[1]; **Allen Ryan**[2]
[1]Kyoto University; [2]University of California, San Diego

Introduction
Once inner ear hair cells (HCs) are damaged by drugs, noise or aging, their apical structures including the stereociliary arrays are frequently the first cellular feature to be lost. While this can be followed by progressive loss of HC somata, a significant number of HC bodies often remain even after stereociliary loss. However, in the absence of stereocilia they are nonfunctional. HCs can sometimes be regenerated by Atoh1 transduction or Notch inhibition, but they also may lack stereociliary bundles. It is therefore important to develop methods for the regeneration of stereocilia, in order to achieve HC functional recovery.

Methods
Espin is an actin bundling protein known to participate in sterociliary elongation during development. We evaluated stereociliary array regeneration in damaged vestibular sensory epithelia in tissue culture, using viral vector transduction of two espin isoforms. Utricular HCs were damaged with aminoglycosides. The utricles were then treated with a γ-secretase inhibitor, followed by espin or control transduction and histochemistry.

Results
While γ-secretase inhibition increased the number of HCs, few had stereociliary arrays. In contrast, 46 hours after espin1 transduction, a significant increase in hair-bundle-like structures was observed. These were confirmed to be immature stereociliary arrays by scanning electron microscopy. Increased uptake of FM1-43 uptake provided evidence of stereociliary function. Espin4 transduction had no effect.

Discussion
The results demonstrate that espin1 gene therapy can restore stereocilia on damaged or regenerated HCs.

Funding
(Supported by grants from the NIH/NIDCD and VA Research Service, USA; Ministry of Health, Labor and Welfare & Ministry of Education, Science, Sports, Culture and Technology, Japan. James Bartles kindly provided plasmids encoding espin1 and espin4 conjugated to EGFP.)

PD 37

Stress granules and mechanisms of RNA triage during cochlear stress

Ana Claudia Goncalves; Naila Haq; Emily Towers; Lisa Nolan; Sally Dawson; Jonathan Gale
University College London

Stress granules (SGs) are cytoplasmic aggregates of proteins and mRNA formed as a consequence of cellular stress. RNAs sequestered by SGs are effectively silenced, allowing the translation of essential proteins to continue. Dysregulation of SG-formation has recently been linked to age-related disease and neurodegeneration, supporting the hypothesis that SGs play a critical role in cell survival during cellular stress.

In the present study we have characterised the SG profile in the auditory system of C57BL/6 mice during ageing, identifying SG formation in both the organ of Corti and in spiral ganglion neurons. We detected changes in the expression of known SG-marker proteins including the RNA-binding proteins Caprin-1 and TIA-1 and we used immuno-RNA-Fluorescence *In Situ* Hybridisation (FISH) to localise polyA+ RNA to Caprin-1/TIA-1 labelled-SGs. We are currently using similar approaches to determine the effect of aminoglycoside treatment on SG formation *in vivo*.

We have used inner ear-derived UB/OC-2 cells and cochlear explants from C57BL/6 mice to investigate the formation and regulation of SGs. Immunofluorescence images of TIA-1 and Caprin-1 were used to quantify SG formation. Heat shock

and arsenite stress promoted SG formation in both OC-2 cells and *ex-vivo* cochlear explants. In addition, we are able to manipulate the SG pathway using specific drugs in order to assess their effects on cell survival/death. To reveal the molecular nature of the RNA triage that occurs as a result of SG formation we performed an RNA-immunoprecipitation (RIP-seq) study and identified RNAs bound to both TIA-1 and Caprin-1 during either heat shock or arsenite stress in OC-2 cells. We are currently using sequence specific RNA FISH probes to determine the cellular localisation of RIP-seq-identified RNAs during stress.

In summary, we have demonstrated the formation of SGs in OC-2 cells, cochlear explants and in the cochlea *in vivo*. We aim to profile the RNAs sequestered by SGs, determine those that are preferentially translated during cochlear stress and investigate how such SG profiles change as a function of age.

Funding
ACG funded by an Action on Hearing Loss PhD Studentship.

PD 38

Increased Susceptibility to Noise Induced Hearing Loss in Stresscopin (UCN3) Knockout Mice

Matthew Fischl[1]; James Sinclair[1]; Jan Deussing[2]; Conny Kopp-Scheinpflug[1]
[1]Ludwig-Maximilians University; [2]Max Planck Institute of Psychiatry

Introduction
Stresscopin, or urocortin 3 (UCN3) is a small neurotransmitter involved in stress signaling. Stress response signaling is important for both protection from damaging stimuli and recovery of homeostasis after stress. Recent studies suggest that stress signaling molecules and their receptors are localized in the cochlea and may modulate activity during audiogenic stress and play a role in protection from noise induced hearing loss (Graham & Vetter 2011, Graham et al. 2011, Basappa et al. 2012; Graham et al. 2010). There is unexpected evidence for UCN3 expression in neurons in the auditory brainstem including the superior paraolivary nucleus (Li et al. 2002, Deussing et al. 2010). Here we use various techniques to explore the role of UCN3 in stress response and hearing protection.

Methods
We use immunocytochemistry to examine the expression patterns of the CRHR2 and UCN3 in the auditory brainstem. Intrinsic properties and response patterns to auditory stimuli are examined with *in vitro* patch clamp and *in vivo* single unit recordings. Auditory brainstem response (ABR) recordings were performed on wild type mice and UCN3 knockout mice to determine hearing thresholds before and after noise exposure (84 or 94dB, 8-16kHz bandwitdth, 2hr).

Results
Our immunocytochemical results indicate that CRHR2 and UCN3 are localized in the auditory brainstem. UCN3 showed specific expression in some cells of the cochlear nucleus and in the SPN. Electrophysiology results indicate that response properties in naïve UCN3 knockout mice are similar to wild type counterparts. However, our ABR recordings show that UCN3 knockout animals have significantly larger threshold shifts and recover more slowly from a single bout of noise exposure.

Conclusions
Our results reveal that the CRHR2/UCN3 system is available to modulate activity in the auditory brainstem. Mice lacking the UCN3 gene are more susceptible to noise induced hearing loss and recovery more slowly from audiogenic stress. Determining the locus of this deficit is a goal of future experimentation.

Funding
DFG KO2207/3-1 DFG SFB 870/2-A10

PD 39

A High-throughput Screen identifies Small Molecules that Protect against Cisplatin- and Noise-induced Hearing Loss

Tal Teitz; Jie Fang; Asli Goktug; Justine Bonga; Shiyong Diao; Yinmei Zhou; Cheng Cheng; Taosheng Chen; Jian Zuo
St. Jude Children's Research Hospital

There are currently no FDA approved drugs to treat cisplatin- and noise- induced ototoxicity. Here we present the results of high-throughput drug screens employing a cell line, HEI-OC1, derived from the organ of Corti of the immortomouse. We screened libraries of >4,375 unique FDA approved and biologically-active compounds for those that confer protection from cisplatin-induced cell death. The biological assay measured the ability of the tested compounds to inhibit caspase-3 activity induced by cisplatin treatment. The top 157 compound hits of the primary screen were validated in the HEI-OC1 cell line by dose response analysis and viability assays. The best 13 compounds with IC50 of 0.04-7.6 μM were tested ex-vivo in neonatal (P3) mouse cochlear explant cultures. Ten of the top 13 compounds exhibited protection in the cochlear explants as measured by hair cell viability after 24 hours cisplatin co-treatment. The top hit compound, SJZuo-4, had an excellent therapeutic index >200 in the cochlear explants with IC50 of 150 nM and LD50 of >30 μM. In vivo, SJZuo-4 showed protection against cisplatin-induced hair cell loss in the zebra fish lateral line after 24 hour co-treatment. In addition, SJZuo-4 was effective in protecting against cisplatin and noise in vivo in adult FVB mouse ears via local transtympanic injection (5 μL at 250 μM) to the ear. When the mouse was administered intraperitoneally with cisplatin (30 mg/kg) 2 hours after SJZuo-4 or DMSO control (0.5% in PBS) injection to either ear, the SJZuo-4 injected ear exhibited ~10 dB reduction of ABR threshold shift 14 days post-treatment. SJZuo-4 also reduced outer hair cell loss at the basal cochlear turn induced by cisplatin 24 hours and 14 days after injection. When the mouse was exposed to 100 dB SPL, 8-16 kHz octave band of noise for 2 hours before SJZuo-4 or DMSO control was injected to either ear, the SJZuo-4 injected ear displayed ~12

dB reduction of ABR threshold elevation and less reduction of pre-synaptic ribbons 14 days post acoustic damage. We will next optimize SJZuo-4 as a lead compound by enhancing local delivery methods, identifying better SJZuo-4 analogs via structure-activity relationship (SAR) and structure-property relationship (SPR) studies, and further developing in vivo biomarkers. Our studies will provide lead compounds for pre-clinical and clinical trials for protection against cisplatin- and noise-induced hearing loss.

Funding
This work was supported in part by grants from the NIH (DC006471, DC013879, CA21765), the Office of Naval Research (1N000140911014, N000141210191, and N000141210775) and the American Lebanese Syrian-Associated Charities of St. Jude Children's Research Hospital.

PD 40

Cochlear Inflammation is Modulated by IL-10/CO-mediated Negative Regulation of CCL2 Expression

Sung Moon; Sung-Hee Kil; David Phak; David Lim
University of California, Los Angeles

Background
Cochlear inflammation is associated with a variety of acquired sensorineural hearing loss such as cisplatin ototoxicity and tympanogenic labyrinthitis. Previously, we have demonstrated a pivotal role of spiral ligament fibrocytes (SLFs) in cochlear inflammation through up-regulation of chemokines such as CCL2 and CXCL2. Induction and resolution of inflammation are tightly controlled to avoid massive tissue injury, but modulation of cochlear inflammation remains unclear. In this study, we aim to determine the molecular mechanism involved in cochlear protection from inflammation-mediated tissue damage, focusing on IL-10 and hemoxygenase-1 (HMOX1) signaling.

Method
The rat spiral ligament cell line (RSL) was used as a model of spiral ligament fibrocytes, and nontypeable *Haemophilus influenzae* (NTHi), as a pro-inflammatory stimulant. We used cobalt protoporphyrin IX (CoPP) as an endogenous source of carbon monoxide (CO), and CO-releasing molecule [CORM]-2 as an exogenous source of CO. To determine expression of IL-10 receptors, immunolabeling and RT-PCR analysis were performed. To determine CCL2 regulation, quantitative RT-PCR analysis, luciferase assays, and ELISA were conducted. To determine binding of NF-κB, chromatin immunoprecipitation was performed. To develop tympanogenic labyrinthitis, live NTHi was intratympanically injected into C57BL/6 and IL-10-deficient mice.

Results
We demonstrated that IL-10Rs are expressed in the cochlear lateral wall, particularly in SLFs. The RSL cells were found to inhibit NTHi-induced up-regulation of monocyte chemotactic protein-1 (MCP-1; CCL2) in response to IL-10. This inhibition was suppressed by silencing IL-10R1 and was mimicked by CoPP and CORM-2. In addition, IL-10 appeared to suppress monocyte recruitment through reduction of NTHi-induced RSL-derived chemoattractants. Silencing of HMOX1 was found to attenuate the inhibitory effect of IL-10 on NTHi-induced MCP-1/CCL2 up-regulation. Chromatin immunoprecipitation assays showed that IL-10 inhibits NTHi-induced binding of p65 NF-κB to the distal motif in the promoter region of MCP-1/CCL2, resulting in suppression of NTHi-induced NF-κB activation. Furthermore, IL-10 deficiency appeared to significantly affect cochlear inflammation induced by intratympanic injections of NTHi.

Conclusion
Taken together, our results suggest that IL-10/HMOX1 signaling is involved in modulation of cochlear inflammation through inhibition of MCP-1/CCL2 regulation in SLFs, implying a therapeutic potential for a CO-based approach for inflammation-associated cochlear diseases.

Funding
[Supported by NIH grant DC011862]

PD 41

Intracochlear Sound Pressure Levels During Acoustic Shock Wave Exposure

Nathaniel Greene[1]; Mohamed Al Hussaini[1]; Timothy Walilko[2]; Theodore Argo IV[2]; James Easter[1]; Daniel Tollin[1]
[1]University of Colorado Anschutz Medical Campus; [2]Applied Research Associates, Inc.

Introduction
Injuries to the peripheral auditory system are among the most common results of high intensity impulsive acoustic exposure. Prior studies of high intensity sound transmission by the ossicular chain have relied upon either measurements in animal models or measurements at more moderate sound intensities. Here, we directly measure intracochlear pressure via fiber optic pressure sensors placed in both scala vestibuli (SV) and tympani (ST), in human cadaveric temporal bones, during exposure to shock waves with peak positive pressures between 1 and 12 psi.

Methods
Eight full-cephalic human cadaver heads were exposed to acoustic shock waves in an 18" diameter shock tube with a 18' long expansion cone. Specimens were exposed to impulses with nominal peak overpressures of 1, 4, 8 & 12 psi (171, 183, 189, & 192 dB SPL) measured in the free field adjacent to the forehead. Specimens were prepared bilaterally by mastoidectomy and extended facial recess to expose the ossicular chain. Ear canal (EAC), middle ear, and intracochlear sound pressure levels were measured with fiber-optic pressure sensors (FISO Inc.), securely mounted and protected from the blast wave in narrow stainless-steel tubing, rigidly attached to the skull. Additional sensors measured SPL and skull strain near the opening of each EAC and at the forehead.

Results
Peak pressures incident at the forehead showed pressure twice that measured by adjacent free-field and EAC entrance sensors, as expected based on the sensor orientation

(normal vs tangential to the shock wave propagation. At 1 psi, EAC pressure showed gain consistent with the ear canal resonance, and intracochlear pressure (normalized to the EAC) was consistent with previously reported middle ear transfer functions (Nakajima et al. 2009, Greene et al. 2015). Responses to higher intensity impulses tended to show lower intracochlear gain relative to EAC, suggesting reduced transmission along the ossicular chain at high intensities, but continued to increase linearly with the free-field sound pressure level. Tympanic membrane rupture was consistently observed following exposures greater than 4 psi.

Conclusions
Intracochlear pressures reveal reduced gain relative to the ear canal that effectively cancels the ear canal resonance for extremely high sound pressure levels, thus reduces cochlear exposure compared to more moderate sound intensities. These results are consistent with lowered transmissivity of the ossicular chain at high intensities, and are consistent with our prior report measuring middle ear transfer functions in human cadaveric temporal bones with more moderate intensity tone pips (Greene et al. 2014).

Funding
DOD: W81XWH-13-MOMJPC5

PD 42

Distinct Time Constraints on When Different Types of Stimulus Exposure Can Enhance Auditory Learning Following Task Performance

David Little; Beverly Wright
Northwestern University

Introduction
Human auditory skills can improve with practice, providing a means to remediate perceptual disorders and enhance perceptual abilities. This learning does not arise from mere stimulus exposure, but rather requires task performance, limiting its practical application. Easing this practice burden, periods of stimulus exposure alone can contribute to learning on a target task so long as they are paired with periods of target-task performance, even when the task performance on its own does not generate learning. The combination of such extra-task exposures and task performance is also effective when the exposures occur as part of a non-target auditory task. However, current evidence indicates that the periods of extra-task exposure and target-task performance must be within 15 minutes of each other for maximum benefit. Here we report that this time constraint depends on the nature of the extra-task exposures.

Method
We trained three groups of normal-hearing adult listeners (n=8 per group) on a frequency-discrimination task (standard stimulus: two 1-kHz 15-ms tones separated by 50 ms). All groups practiced frequency discrimination for 45 trials/day on 3 consecutive days. A control group received only these trials. The two experimental groups received these trials followed 30 minutes later by a period of 360 trials of extra-task exposure. These extra-task exposures were presented either (1) as part of performance of a non-target temporal-interval discrimination task that used the same standard stimulus as the frequency task (as was the case for the exposures previously shown to be ineffective 15-minutes after target-task performance) or, (2) in the background as an exact replay of target-task stimuli while listeners performed a written symbol-to-number matching task.

Results
Two of the regimens yielded no learning: practice on the target-task alone and target-task practice followed 30 minutes later by interval-task practice. However, learning did occur when target-task practice was followed 30 minutes later by an exact replay of the task stimuli presented in the background.

Conclusions
The present results demonstrate that the viability of extra-task exposures 30 minutes after target-task performance depends on the nature of those exposures: exposures during a non-target task did not contribute to learning (replicating prior outcomes) while an exact replay of task stimuli with no auditory-task performance did. One interpretation of these data is that the extra-task exposures enhance learning by contributing to memory consolidation. If so, the distinct effects of the different kinds of extra-task exposure at a given time point would indicate distinct states of consolidation.

PD 43

Mature Auditory Skill-Learning Ability in Young School-Age Children

Yael Zaltz[1]; Daphne Ari-Even Roth[1]; Avi Karni[2]; Liat Kishon-Rabin[1]
[1]Tel Aviv University; [2]University of Haifa

Rationale & Purpose
The purpose of the present study was to explore the characteristics of auditory skill learning (i.e., time course of learning, generalization of learning-gains and retention) in young school-age children compared to that of adults following single- and multi-session training. Evidence from language and motor learning exploiting sensitive periods of increased brain plasticity early in life is in keeping with the notion of a well-developed skill learning in young children. In contrast, the prolonged development of learning-related cognitive abilities such as attention and memory, as well as the extended development of the central auditory system, may support the notion of immature auditory learning in young children. Studies on auditory skill learning in children have been so far limited and equivocal, with some studies showing significant improvements following training whereas others showing limited improvements if any.

Method
40 children (7-9y) and 45 adults (18-30y) took part in a single training session and a follow-up testing session. Of them, 20 children and 24 adults continued training for eight additional sessions. All training sessions comprised of six measurements of difference limen for frequency (DLF) at 1000 Hz. Generalization of the learning gains to the opposite

ear and to a different reference frequency (2000Hz) was assessed following single- and multi-session training. Retention of learning was estimated 6-8 months later.

Results
50% of the children attained mature learning, reaching 'adult-like' performance after a single session of training. These children "maintained" their 'adult-like' performance until the end of the multi-session training, with most of them also showing mature generalization of the learning-gains. The other 50% showed poorer learning (in terms of their rate of improvement and variance reduction) and poorer generalization, although their performance improved significantly 6-8 months post-training. Naive DLF performance (first three measurements) together with non-verbal intelligence explained 72% of the variance in the training outcomes. The best-predicting factor for the results was, however, the children's DLF performance following the first training session.

Conclusions
The time course of learning, the ability to generalize the learning-gains to untrained conditions, and the ability to retain these gains show different trajectories of maturation, with some children reaching mature performance in all these learning characteristics by 7-9y. A short exposure to the trained task may be sufficient to reflect the maturation of these learning characteristics, thus providing important clinical information as to which child can benefit the most from training at his/her specific developmental stage.

PD 44

Cortical and subcortical plasticity following short-term perceptual learning on auditory and visual tasks

Bonnie Lau; Dorea Ruggles; Sucharit Katyal; Stephen Engel; Andrew Oxenham
University of Minnesota

Background
Short-term training can lead to improvements in the behavioral discrimination of both auditory and visual stimuli. In the auditory domain, fluency with tonal languages and musical training have been associated with long-term cortical and subcortical plasticity, but less is known about the effect of short-term exposure and training. This study combines behavioral measures with simultaneous subcortical and cortical steady-state EEG responses to investigate short-term learning and neural plasticity in both auditory and visual domains.

Methods
Naïve subjects with less than 5 years of musical training were trained for about 40 min/day for 6 days on one of three discrimination tasks: fundamental frequency (F0), amplitude modulation rate, or visual orientation. The auditory stimuli consisted of unresolved harmonic complexes with a 137 Hz F0 that were sinusoidally amplitude modulated at 13 Hz with 100% depth, embedded in a threshold-equalizing noise. The visual stimuli consisted of flickering Gabor patterns (spatial frequency: 1 cycle/deg; flicker frequency: 13 Hz) embedded in noise. Steady-state visually evoked potentials (SSVEP) to the flicker frequency of the visual stimuli as well as simultaneous subcortical envelope-following responses (EFR) to the F0 and cortical auditory steady-state responses (ASSR) to the modulation rate of the auditory stimuli were measured in addition to behavioral thresholds pre- and post-training. All EEG and behavioral measures were repeated again 30 days post-training to investigate whether training effects were maintained. A fourth, no-training control group was also included where subjects received behavioral and EEG pre-, post-, and maintenance tests at comparable time intervals to subjects in the other groups but were not trained on any discrimination task.

Results
Perceptual learning was seen across all training groups with behavioral thresholds significantly lower at post-test than pre-test but no evidence of task-specific differences was observed. Preliminary analysis of EEG results revealed a tendency for the cortical ASSR but not the subcortical EFR to increase following training. Further analysis of changes in EEG measures will allow for comparison with behavioral results.

Conclusions
Short-term training led to improvements in the discrimination of the F0 and amplitude modulation rate of harmonic complex tones as well as the visual orientation of Gabor patterns. Preliminary EEG results suggest plasticity of cortical but not subcortical responses to auditory stimuli following training. Comparison of changes in the SSVEP, EFR, and ASSR to changes in behavioral thresholds across groups will provide a method of investigating cortical and subcortical plasticity following short-term auditory and visual perceptual learning.

Funding
This work has been supported by NIH grant R01DC05216.

PD 45

Acute Deafness in Young, But Not in Aged, Adult Rats Results in Loss of Tonotopic Order in the Central Auditory System

Nicole Rosskothen-Kuhl; Sarah Green; Robert-Benjamin Illing
University of Freiburg

Background
During ontogeny, tonotopic order develops in most central auditory brain regions, depending on sensory input during early sensitive periods. We raised the question of how robust this tonotopic order is when hearing fails in adulthood. To answer this question, we investigated the expression pattern of the activity and plasticity marker Fos after cochlear implant (CI) stimulation in adult rats deafened at different ages. Apart from being an initial marker for neural sensory activation, Fos participates in regulating the expression of genes associated with neural plasticity and extracellular matrix remodeling by combining with Jun to activator protein-1 transcription factor.

Methods
Bilateral hearing loss was induced at 3 or 12 months after birth by injecting a loop diuretic in combination with an aminoglycoside. As a result, a rapid and permanent rise of hearing threshold by ~90 dB was measured in both groups. One month after hearing loss, anesthetized rats received electrical intracochlear stimulation (EIS) for 2 h after inserting a CI into the medial turn of the left cochlea. Immunoreactivity of neurons containing Fos provided quantitative results for anteroventral cochlear nucleus (AVCN), lateral superior olive (LSO), and central inferior colliculus (CIC).

Results
Following EIS of adult-deafened rats, the pattern of Fos expressing neurons significantly differed between the two groups. Fos expression of 13 months old rats was limited to a region tonotopically corresponding to the intracochlear stimulation position in ipsilateral AVCN and LSO, and contralateral CIC, indicating tonotopic order. By sharp contrast, Fos expression in 4 months old rats was found to be expanded over the middle to low frequency range on the side of EIS in all of these regions, indicating loss of tonotopic order. Comparing these Fos expression patterns with our previous results acquired in normal hearing and neonatally deafened rats, Fos distribution in old adult-deafened rats was similar to the tonotopic activation pattern seen in normal hearing rats, but young adult-deafened rats showed a non-tonotopic Fos response pattern similar to that of neonatally deafened rats.

Conclusion
Our data indicate that the central auditory system of young and old rats differentially adapt to sudden and complete deafness. One month of deafness has far-reaching consequences for the interneuronal communication underlying tonotopic processing in young adult rats, but no such consequence emerged in aged rats. We conclude that neuronal plasticity prevails in the central auditory system of young adult rats, whereas neuronal stability prevails in the brains of aged adult rats.

Funding
Cochlear Research and Development Limited; Faculty of Medicine of the Albert-Ludwigs University of Freiburg

PD 46

Viewing the location of BDNF transcripts at their site of translation following sound induced activity-dependent promoter usage

Marlies Knipper[1]; Hyun-Soon Geisler[1]; Jing Hu[1]; Carlos Duarte[2]; Gabriele Baj[3]; Enrico Tongiorgi[3]; Dario Campanelli[1]; Lewis Sze Chim Lee[1]; Karin Rohbock[1]; Lukas Rüttiger[1]; Thomas Schimmang[4]; Ulrike Zimmermann[1]; Thomas Ott[1]; Rama Panford-Walsh[5]; Wibke Singer[1]
[1]University of Tübingen; [2]University of Coimbra; [3]University of Trieste; [4]Universidad de Valladolid y Consejo Superior de Investigaciones Científicas; [5]University of Ottawa

Brain-derived neurotrophic factor (BDNF) is a predicted key player within potentiating and depressive hippocampal trisynaptic circuits (Waterhouse and Xu, 2009; Cohen-Cory et al., 2010, Cowansage et al., 2010; Yoshii and Constantine-Paton, 2010uccato and Cattaneo, 2009; Castren and Rantamaki, 2010).. To what extent the differential usage of distinct BDNF promoters is related to hippocampal circuit deteriorations as it can occur e.g. following acoustic trauma (Singer et al., 2013) is an intriguing question. It is currently technically not feasible to simultaneously visualize activity-dependent synapse and circuit changes within potentiating or depressive networks. We generated a new transgenic mouse line *B*DNF *live exon v*iewing (BLEV) that allows to locate the untranslated BDNF exons IV and VI through CFP or YFP fluorescence at their site of translation following activity-dependent promoter usage. When CFP and YFP are monitored in the trisynaptic hippocampal path, following enriched or traumatic acoustic stimuli, a striking dynamic differential BDNF transcript usage was observed which that the BLEV mice can be a novel tool to extract the role the limbic system plays for hearing disorders.

Supported by a grant from the Marie Curie Research Training Network CavNET MRTN-CT-2006-035367, Deutsche Forschungsgemeinschaft, grant DFG-Kni316-8-1.

Funding
Supported by a grant from the Marie Curie Research Training Network CavNET MRTN-CT-2006-035367, Deutsche Forschungsgemeinschaft, grant DFG-Kni316-8-1.

PD 47

Perceptual Training in Post-lingually Deafened Users of Cochlear Implants and Adults with Normal Hearing: Does One Paradigm Fit All?

Matthew Fitzgerald[1]; Susan Waltzman[2]; Mario Svirsky[2]; Beverly Wright[3]
[1]Stanford University; [2]New York University School of Medicine; [3]Northwestern University

Post-lingually deafened recipients of cochlear implants (CIs) undergo a learning process that can last for months, even with active practice on listening tasks. In young adults with normal hearing (NH), combining periods of active practice with periods of stimulus-exposure alone can result in learning that is more rapid and of greater magnitude than learning resulting solely from active practice. Here we asked whether this combined paradigm also promotes learning in users of CIs . If so, it would provide a means to enhance patient performance with a reduced amount of practice. If not, it could indicate that there are differences in the mechanisms that underlie perceptual learning between NH and CI populations. Such differences would be relevant for developing optimal training regimens for the hearing impaired.

In a pilot investigation, we trained five monolingual-English-speaking users of CIs aged 21 to 33 years on a phonetic-categorization task using a combination of practice and stimulus-exposure alone. Participants were asked to categorize speech syllables that varied in voice-onset-time (VOT) as belonging to one of three phonetic categories: negative VOT (<-25 ms) vs. near-zero VOT (-25 ms to +25 ms) vs. positive VOT (>+25 ms). This three-way phonetic contrast

in VOT is present in many languages, but English has only a two-way contrast between near-zero and positive VOTs. In each of two 60-75 minute sessions, participants completed a pre-test, a training phase, and a post-test. The pre- and post-tests consisted of the phonetic-categorization task without feedback. The training phase consisted of alternating periods of task performance with feedback and periods of exposure to the same stimuli during performance of a written task.

Using this training paradigm, young adults with NH show a steepening of the non-native category boundary between the negative and near-zero VOT. In contrast, none of the five CI users showed any improvement. Analysis of the electrical stimulation patterns elicited by the stimuli suggested that the voicing information needed to make the non-native VOT contrast was confined to a single apical electrode. While preliminary, these results suggest the same perceptual training paradigm can have different effects on CI users compared to NH listeners. These differences may stem from a reduction in the available cues to categorize this contrast due to the CI speech processor. An alternative possibility is that deprivation from hearing loss alters perceptual-learning mechanisms.

Funding
NIH / NIDCD

PD 48

Binaural Pitch Fusion in Children and Adults with Bilateral Cochlear Implants

Lina Reiss; Curtis Hartling; Jennifer Fowler; Gemaine Stark; Yonghee Oh
Oregon Health & Science University

Background
Previously, we showed that bimodal cochlear implant (CI) users experience abnormally broad pitch fusion between ears, i.e. fuse sounds that differ by as much as 3-4 octaves in pitch between ears (Reiss et al., JARO 2014). The goal of this study was to determine whether bilateral CI users who use CIs in both ears also experience broad binaural pitch fusion.

Methods
Seventeen bilateral CI users were recruited, including 13 adults (8 Cochlear, 5 Med-El) and 4 children (all Cochlear) between 6-8 years of age. Dichotic fusion ranges were measured by presenting a reference electrode in one CI ear simultaneously with a comparison electrode in the contralateral CI ear. Subjects were asked to indicate if one or two sounds were heard, and if two sounds were heard, to indicate which ear had the higher pitch. The comparison electrode was varied across trials to find the range of electrodes in the contralateral CI ear that fused with one electrode in the reference CI ear. Within-ear and across-ear electrode pitch ranking measurements were also obtained in adult subjects.

Results
Adult bilateral CI listeners had binaural pitch fusion ranges that varied in size from 0-11 mm (average 4.9 ± 3.3 mm), equivalent to 0-18.7 electrodes for Cochlear (average 8.6 ± 6.0 electrodes or 5.2 ± 3.6 mm) and 0.5-5 electrodes for Med-El (average 2.3 ± 1.7 electrodes or 4.4 ± 3.2 mm). These fusion ranges are roughly equivalent to 1.2 octaves in the cochlear place frequency domain at 1000 Hz, and broader than the 0.01-0.03 octaves typically seen in normal-hearing listeners. Preliminary findings in children with bilateral CIs indicate wide variability, with fusion ranges varying from 0-20 electrodes (average 6.6 ± 6.3 mm), i.e. either no fusion or fusion across nearly all electrodes in the contralateral ear. No correlations were observed between fusion ranges and within- or across-ear pitch discrimination abilities.

Conclusions
Bilateral CI users can exhibit broader binaural pitch fusion ranges than those seen in normal-hearing listeners, but fusion ranges are highly variable across individuals. The lack of association of pitch discrimination abilities with fusion ranges suggests that broad fusion is more likely due to central auditory processing differences in how information is combined binaurally, rather than peripheral factors such as poor electrode discrimination. As in bimodal cochlear implant users, broad fusion may explain the variability of binaural benefits in bilateral CI users.

Funding
Funding: Supported by NIH-NIDCD grant R01 DC013307.

PD 49

Stimulus constraints of memory reactivation following training on an interaural-level-discrimination task

Robert Baudo; David Little; Beverly Wright
Northwestern University

Introduction
During learning, memories are transformed from a fragile to a stable state through a process of consolidation. There is increasing evidence that when consolidated memories are accessed they re-enter a state of instability, during which they can be modified, and then must be consolidated again. This cycle of reactivation and reconsolidation is revealed by reports that consolidated memories are susceptible to retrograde interference following a reminder of the memory, even when the reminder occurs weeks to months after the initial training. We recently obtained behavioral evidence in auditory perceptual learning of a mechanism similar to reconsolidation, but in which reactivated memories are susceptible to anterograde interference only within 24 hours of the initial training. Here we asked what stimulus components must be consistent between the initial training and the reminder for memory reactivation to occur.

Method
We examined the influence of three different two-day training regimens on performance on a target interaural-level-difference (ILD) discrimination task, using a two-interval forced-choice procedure. In all regimens, listeners first practiced the target task in isolation (L_1) and then 30 minutes later practiced two tasks in immediate succession: a non-target interaural-time-difference discrimination task (T)

followed by a second bout of the target task (L_2) (L_1-30min-TL_2). The standard stimulus during L_1 was always a 4-kHz tone with a 0-dB ILD. Across regimens, the standard stimulus during L_2 matched the stimulus in L_1 (n=14), had a different frequency (6 kHz vs. 4 kHz; n=8), or a different ILD value (6 dB vs. 0 dB; n=8). Performance on the non-target (T) and target (L_1) tasks was tested the next day.

Results

Neither the matched-stimulus (previous data) nor the different-frequency regimens yielded improvement on the target task. However, there was learning with the different-ILD regimen.

Conclusion

Memory reactivation on the present ILD-discrimination task did not require that the standard stimulus in the reminder bout (L_2) be the same as in the initial bout (L_1). Rather, the reminder stimulus could differ from the initial stimulus in frequency, though not in ILD value, and still reactivate the memory. One interpretation of this outcome is that 30 minutes after training the location but not the frequency of the trained stimulus is represented in the memory trace. Thus, it appears that the memory of different aspects of a trained auditory stimulus can consolidate at different rates.

Funding

Funding from NIH.

PD 50

Layer-specific effects of congenital deafness in secondary auditory cortex

Christoph Berger; Daniela Kühne; **Andrej Kral**
Medical University Hannover

Layer-specific effects of congenital deafness on the development of primary auditory cortex have been described functionally in primary auditory cortex (Kral et al., 2005, Cereb Cortex). We analyzed the secondary auditory cortex in four adult congenitally deaf white cats (CDCs) and compared the results to four adult normal hearing control cats (HCs). All animals were under deep anaesthesia transcardially perfused with phosphate buffer, 4% formaldehyde and 10% sucrose solution in succession. The brain was immersed in 30% succrose for few days and was crysectioned (frontal) to 50 µm sections. Sections were stained with Nissl and SMI-32 antibody staining. The sections in the middle of the distance between anterior and posterior ectosylvian sulcus (rostro-caudal dimension) together with sections 0.5 mm rostral and caudal to it were used to safely avoid nearby sulci. Auditory primary field A1, secondary fields A2 and DZ and, as a control, the visual region in the middle of the middle suprasylvian gyrus (SSG) in the same section were analyzed. Field borders were determined by the SMI-32 staining pattern (Mellott et al., 2010, Hear Res). In each section, five different regularly-spaced positions in each field and section were used for measurements. Two-tailed Wilcoxon-Mann-Whitney test was used for statistical testing (with Bonferroni correction where applicable).

The Nissl-stained cortex in A1 and A2 was significantly thinner in CDCs. The regions DZ and SSG were not different between the two groups of animals. To determine which layers contributed to this result, SMI-32 stained sections were analyzed in detail. The borders of layer II and III, III and IV, IV and V and also the superficial part of layer V could be precisely determined, thus the thickness of layers I+II, III, IV and upper layer V (Va) could be quantified. These were analyzed in absolute values as well as normalized to the same layers in the visual cortex of the same sections. The thickness of LI + LII and LIII were not significantly different between the animal groups in both absolute and normalized measures. However, LIV and LVa was significantly thinner in all auditory regions in CDCs, both in absolute and relative measures. The data support our previous functional results from A1 and demonstrate that developmental effects of deafness are layer-specific also in higher-order auditory areas.

Funding

Supported by Deutsche Forschungsgemeinschaft (Cluster of Excellence Hearing4all)

PD 51

Leveraging Bilateral Implants to Improve Cochlear Implant Patients' Spectral Resolution

Justin Aronoff[1]; Amulya Gampa[2]; Julia Stelmach[1]; Monica Padilla[3]; David Landsberger[3]
[1]University of Illinois at Urbana-Champaign; [2]University of Illinois at Chicago; [3]New York University

Background

Bilateral cochlear implantation has resulted in considerable benefit to patients compared to unilateral implantation. However, bilateral cochlear implant (CI) patients are still typically provided with two unilateral maps with very little coordination between the two ears. Coordinating the two processors can allow stimulation in the two ears to be perceptually aligned, potentially improving performance. Additionally, with bilateral CIs, different frequency ranges can be used in each ear. This allows for a smaller frequency range to be used in each ear, effectively increasing the spatial separation of the spectral components of the signal along the cochlea. Similarly, stimulation can be divided between the arrays to increase the spacing between stimulation locations. This can improve spectral resolution by reducing channel interaction while still providing the same spectral information when the signal from the two ears is combined centrally. Two methods were investigated to leverage bilateral implants to improve spectral resolution.

Methods

Seven bilateral CI users participated in Experiment 1. After completing a pitch matching task, the frequency allocation for the left and right processor were either modified so that electrode pairs that were pitch matched were allocated the same frequency region (pitch-matched) or the frequency allocation was based only on electrode number (numerically-matched). Because electrodes at one edge of an array often do not have a pitch-matched pair in the opposite ear, for the pitch-matched condition the two ears received frequency ranges which only partially overlapped. This meant that a smaller frequency range could be presented to each ear,

effectively spacing out the spectral information, while still delivering the full frequency range when the two ears are combined centrally.

Eight bilateral CI users participated in Experiment 2. After completing a pitch matching task, either pitch-matched maps were used where both ears received the entire signal, or the frequency range was divided into multiple frequency regions with every other region delivered to pitch-matched locations in opposite ears (interleaved). In both experiments, spectral resolution was evaluated with the Spectral-temporally Modulated Ripple Test (SMRT).

Results and conclusions
In Experiment 1, using pitch-matched electrode pairs resulted in better spectral resolution than using numerically-matched pairs for all seven participants. In Experiment 2, dividing the signal between the ears yielded improved spectral resolution for seven out of eight participants. These results demonstrate that creating bilateral maps can yield improved spectral resolution for bilateral CI users.

Funding
Funding provided by National Organization for Hearing Research, NIH/NIDCD R03-DC-013380, T32DC009975, R01-DC12152 R01-DC001526, R01-DC004993, R03-DC010064. Equipment provided by Advanced Bionics.

PD 52

Loudness and Pitch Perception using Dynamically Compensated Virtual Channels

Waldo Nogueira[1]; Leonid Litvak[2]; Amy Stein[2]; Chen Chen[2]; David Landsberger[3]; Andreas Büchner[1]
[1]Medical University Hannover and Cluster of Excellence "Hearing4all"; [2]Advanced Bionics LLC; [3]New York University School of Medicine

Power consumption is important for the development of smaller cochlear implant (CI) speech processors. Simultaneous electrode stimulation may improve power efficiency by minizing the required current applied to a given electrode. To create a more power efficient virtual channel, we developed the Dynamically Compensated Virtual Channel (DCVC) using four adjacent electrodes. The two central electrodes are current steered using the coefficient whereas the two flanking electrodes are used to focus/unfocus the stimulation with the coefficient . Specifically the electrodes (ordered from apical to basal) provide the following currents: . With increasing values of power can be saved at the potential expense of generating broader electric fields. Additionally, by reshaping the electric fields, it might also alter place pitch coding.

The goal of the present experiment is to investigate the tradeoff between place pitch encoding and power savings using simultaneous electrode stimulation in the DCVC configuration. We developed three experiments to investigate:

1. Equal loudness contours at most comfortable levels (M) for different values of .
2. Discrimination of virtual channels (jnd of) for different values of .
3. The ranges of , defined as the difference between maximum and minimum value of producing the same pitch height for different values of .

Preliminary results from 7 adult Advanced Bionics CI users have been collected. Results from experiment 1 show that the required current to produce M levels is significantly reduced with increasing as predicted by the model of Litvak et. al. (2007). This suggests that increasing improves power efficency. Experiment 2 demonstrates that the jnd of becomes poorer when focusing the field (i.e. decreasing). Experiment 3 shows that focusing the field increases the ranges of . Dividing the range's by the jnd of the corresponding can give an estimation of the number of discriminable steps in a fixed range. No significant differences in the estimated number of discriminable steps were detected for the different values of .

DCVCs can reduce power consumption without decreasing the number of discriminable steps.

Funding
Support provided by the DFG Cluster of Excellence "Hearing4all", Advanced Bionics and the NIH/NIDCD (R01 DC012152, PI: Landsberger).

PD 53

Spectral Resolution with Cochlear Implants in Adults and Children: A Pilot Study

Monica Padilla[1]; Amy Martinez[2]; Laurie Eisenberg[2]; David Landsberger[1]
[1]New York University; [2]University of Southern California

A study by Eisenberg et al. (2000) showed developmental effects in speech perception with reduced spectral information. Specifically, younger children required a greater number of spectral channels than older children and adults to achieve equivalent scores on speech materials by subjects with normal hearing listening through vocoded cochlear implant simulations. It is unknown whether the age differences were caused by poorer spectral resolution abilities and/or linguistic/cognitive factors.

In the current pilot study, we explore the effects of age and hearing status on a test of spectral resolution that is independent of linguistic knowledge. We hypothesize that children who are implanted with a cochlear implant (CI) from a very early age will make better use of the spectral information than post-lingually implanted adults due to plasticity during a sensitive period for auditory development. To our knowledge this prediction has never been tested and has important implications for designing advanced speech processing strategies for children.

A psychophysical test of spectral processing, the SMRT Test (Aronoff and Landsberger, 2013) was administered to four groups of listeners (adults and children with normal hearing; adults and children with CIs). The stimuli were presented through a loudspeaker in a sound-treated booth at 65 dB A.

Within the pediatric group, two age groups were assessed (5-8 years old and 9-12 years old). Subjects listened to three sounds and were asked which one was perceived to be different. The higher scores indicated better spectral resolution. Normal-hearing listeners were also tested with stimuli processed by an eight-channel vocoder for comparison to the CI groups.

Preliminary data show larger variability in spectral discrimination by normal-hearing children than normal-hearing adults. The children tended to perform lower than adults with the vocoded stimuli, although some children reached adult-like performance. CI users performed better than the normal listeners with the vocoded stimuli, and CI older children users performed as well as CI adult users. Lastly, the younger children (normal hearing and CI) tended to perform lower than adults and older children. Early trends suggest that children with CIs can achieve adult-like performance but require experience with the CI. Preliminary data also suggest that children with normal hearing also require experience to improve their processing of spectral information, implying that spectral resolution is influenced by development. The data suggest that normal-hearing children demonstrate better spectral resolution than children with CIs, indicating the potential need for better access to spectral information.

PD 54

Light Driven Hearing System: A Multi-center Clinical Study

Bruce Gantz[1]; Rodney Perkins[2]; Michael Murray[4]; **Suzanne Levy**[2]; Sunil Puria[2,3]
[1]University of Iowa; [2]Earlens Corporation; [3]Stanford University; [4]Camino Ear Nose and Throat Clinic

Background

The Earlens Light Driven Hearing System (Earlens) is a non-surgical device consisting of two components: a Tympanic Lens (Lens), which is a light-activated balanced-armature transducer that drives the middle ear through direct umbo contact; and a Sound Processor that encodes amplified sound into pulses of light emitted via a Light Tip in the ear canal to wirelessly power and drive the Lens. In comparison to air conduction hearing aids, the Earlens provides higher levels of output and functional gain over a broad frequency range, extending to 10 kHz.

Study Design and Methods

A single arm, open-label investigational device clinical trial was conducted with the objective to assess the safety and efficacy of the Earlens. Forty-eight subjects with mild to severe sensorineural hearing loss were bilaterally treated across three clinical sites (MP, SJ, and IC). The study physician placed a custom Lens onto each ear, where it stayed in contact with the umbo and the ear canal medial wall. The Sound Processors were programmed to provide appropriate wide-bandwidth amplification after fitting. The primary safety endpoint was the determination of 'no change' (defined as < 10 dB change in PTA4) in residual hearing. The primary efficacy endpoint was word recognition using NU-6 at 45 dB HL with sound field presentation. Secondary efficacy endpoints included 1) functional gain from 2 to 10 kHz (the difference between unaided to aided sound field thresholds) and 2) speech in noise metric (Reception Threshold for Sentences (RTS), using the HINT left/right paradigm) with the Sound Processor in omnidirectional and directional microphone modes. Efficacy endpoints were assessed at the 30-day interval and measurements were repeated at the 120 day interval.

Results

The results on the 82 ears (41 subjects) determined a mean change of -0.37 dB in PTA4 indicating no change in residual hearing ($p<0.0001$) after the 120-day safety endpoint interval. There were no serious device- or procedure-related adverse events or unanticipated adverse events. Word recognition with the Earlens improved significantly ($p<0.0001$) over the unaided baseline performance and increased by 35% on average. Mean improvement in functional gain was 31 dB in 2-10 kHz range with the Earlens. Average RTS improvement was 0.75 dB ($p=0.028$) and 3.14 dB ($p<0.0001$) for the omni and directional microphone modes, respectively.

Conclusions

The Earlens was shown to be safe over the 4 months period tested, effective in providing amplification to 10 kHz, and improving speech understanding in quiet and in noise.

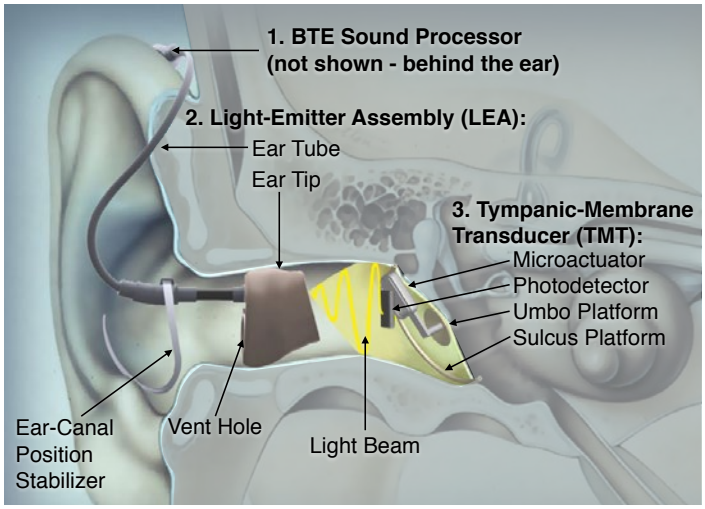

Funding

Work supported in part by SBIR Phase IIB grant R44 DC 08499 from the NIDCD of NIH.

PD 55

Development of Light-Sensitive Human Neural Progenitor Cells for Use in an Optogenetic-Based Cochlear Implant

Alyson Kaplan; Xiankai Meng; Elliott Kozin; Sumi Sinha; Ariel Hight; Albert Edge; Daniel Lee
Massachusetts Eye and Ear Infirmary

Background

Optogenetics offers the promise of precise control of neuronal activity with hundreds of independent channels using narrow band light stimulation. Our group has demonstrated the feasibility of optogenetic activation of the

central auditory pathways *in vivo* using a viral-based gene transfer techniques. However, this approach has not been associated with efficient and robust opsin expression in the auditory periphery. We hypothesize that optogenetic control of spiral ganglion neurons can be achieved with non-virally mediated gene transfer of opsins into stem cells. Herein, we aim to photosensitize human neural progenitor cells (NPC) with Channelrhodospin-2 using a lipofectamine approach.

Methods
Human NPC's were exposed to a plasmid vector containing Channelrhodpsin-2 (ChR2) in a Tol2 transposase system with YFP as reporter gene using Lipofectamine 2000. Three different ratios of DNA to Lipofectamine reagent were trialed. Successfully transfected YFP positive cells were isolated using fluorescence-activated cell sorting (FACS). Transfection efficiency was measured via percentage of YFP positive cells and cell viability over time.

Results
Using Lipofectamine as a gene transfer reagent, NPC's were successfully transfected with ChR2. Initial percentage of YFP positive cells was less than 1%, however increased to up to 25% and 98% following one and two cycles of FACS, respectively. Cells maintained YFP expression 40 days and 8 passages post-initial transfection. Cells remained YFP positive following freezing and subsequent thawing. Highest transfection efficiency was seen using 1:2 DNA (ug):Lipofectamine reagent (uL).

Conclusion
Stable expression of NPCs with ChR2 was achieved using the Lipofectamine 2000 reagent. Proliferation and continued expression of YFP positive NPC suggests stability of opsin gene transfer. A homogenous culture of ChR2 containing NPCs will require additional rounds of FACS. Future studies will determine whether neuronal stem cells expressing opsins will be associated with narrowband light-evoked near and far field electrical responses. Successful delivery of these light-sensitive human NPCs will allow for the development of a clinically translatable cochlear implant based on optogenetics.

PD 56

BiCI users' sensitivity to interaural phase differences for single- and multi-channel stimulation

Stefan Zirn[1]; Susan Arndt[2]; Antje Aschendorff[2]; Roland Laszig[2]; Thomas Wesarg[2]
[1]University of Applied Science Offenburg; [2]Medical Center - University of Freiburg

The detection of a signal masked by noise is improved when interaural phase differences (IPD) either in the masker or the signal are present relative to a condition without IPD. This phenomenon called binaural unmasking is known in normal-hearing (NH) listeners.

Some bilaterally implanted cochlear implant (BiCI) users are able to perceive IPD implemented as interaural pulse timing differences at low pulse rates on pitch-matched electrode pairs. IPD thresholds as low as 200 µs have been shown by Laback et al. (2007). The speech coding strategy FS4, clinically available in MED-EL CI systems, processes fine-structure information in terms of adjusted pulse timing on four apical electrodes. Therewith, FS4 enables binaural acoustic coupling of bilateral CI stimulation with limited temporal precision.

However, the perception of IPD in psychophysic experiments has typically been shown in BiCI users on single pitch matched electrode pairs. We determined the sensitivity to IPD in BiCI users in single-channel and multi-channel experiments. The single-channel experiments were conducted on interaural electrode pairs with stimulation patterns derived from acoustic stimuli (phase modulated tones) with either constant rate stimulation or with fine-structure coding. The same BiCI users were also tested in a multi-electrode condition. For this purpose, binaural unmasking of speech in noise was investigated using either constant rate stimulation or fine-structure coding.

The results revealed large differences in IPD thresholds on single interaural electrode pairs between the two coding strategies favoring fine-structure coding. In contrast, the multi-channel experiment revealed no significant difference in binaural unmasking between the two coding strategies. These outcomes indicate that the single-channel IPD performance does not predict the multi-channel performance in binaural unmasking in BiCI users.

Funding
This study has been supported by MED-EL

PD 57

Using the Panoramic ECAP Method to Measure Excitation Patterns and to Identify Dead Regions and Cross-Turn Stimulation in Cochlear Implant Users

Stefano Cosentino[1]; John Deeks[2]; Etienne Gaudrain[3]; **Robert Carlyon**[2]
[1]Medical Research Council; [2]Cognition and Brain Sciences Unit; [3]CNRS

Electrically evoked compound action potentials (ECAPs) have been employed as measures of neural excitation evoked by cochlear implant (CI) stimulation. A forward-masking procedure is commonly used to reduce stimulus artefacts. This method estimates the joint neural excitation produced by two electrodes – one acting as probe and the other as masker; as such, the measured ECAPs depend on the excitation patterns produced by both. Therefore attempts to measure excitation patterns by varying only the masker or the probe electrode may be misleading. We describe an approach - termed Panoramic ECAP ("PECAP") - that allows reconstruction of the underlying neural activation pattern of individual channels from ECAP amplitudes, obtained from all combinations of masker and probe electrode. The proposed approach combines a constrained and an unconstrained nonlinear optimization stage. PECAP was validated against simulated and physiological data from CI users. The

physiological data consisted of ECAPs measured from four users of Cochlear® devices. For each subject, an 18x18 ECAP amplitude matrix was measured using a forward-masking method.

The results from computer simulations indicate that our approach can reliably estimate the underlying excitation pattern from ECAP amplitudes even for instances of neural "dead regions" or cross-turn stimulation. The operating signal-to-noise ratio (SNR) for the proposed algorithm was 5 dB or higher, which matched well the SNR measured from human physiological data. Human ECAPs were fitted with our procedure to determine neural activation patterns. Our approach may have clinical application as an objective measure to identify undesirable features of the neural activation pattern of individual CI users and to devise ad hoc stimulation strategies. At present the method is limited to identifying a single instance of a dead region or cross-turn stimulation. Future developments aim to relax this limitation and to improve the robustness of the algorithm.

Funding
This work was supported by the MRC (MC-A060-5PQ70) and by Action on Hearing Loss (MC-A060-5PQ75).

SYMP 22

Introduction to Pharmaceutical Interventions for Hearing Loss (PIHL) and the Need for Standardization in Research Design

Tanisha Hammill; Mark Packer
Defense Hearing Center of Excellence

Hearing loss and tinnitus are the two most prevalent Veteran disabilities affecting millions worldwide. Hearing Protective Devices (HPDs) fail to prevent hearing loss from noise when not used, used improperly, or when exposure to high-energy noise or blasts exceeds HPD's protective capability. Protective or rescue pharmaceutical agents to safeguard those exposed from imminent or extreme noise hazards is needed. Research to develop pharmacologic agents to prevent, reduce, or reverse acute noise- or drug-induced hearing loss has been ongoing for over four decades yet the research methodologies in such research are disparate and incomparable. Current issues facing scientists in this field include: 1) poor translation from animal to human model; 2) study population access and other logistical concerns; 3) targeted translational funding; 4) undeveloped commercialization pathways; and 5) no comparable study outcomes to guide research, due to a lack of unified study design guidance for investigations and investigators.

The Department of Defense (DOD) Hearing Center of Excellence (HCE) Pharmaceutical Interventions in Hearing Loss (PIHL) collaborative research working group is working to address these issues. HCE has produced a series of streamlined guidances, through subject matter expert and stakeholder consensus, for research investigators, program sponsors, professional societies, publishers, and pharmaceutical developers. To accomplish this goal, the PIHL group - comprised of DOD, VA, US Public Health Service, National Institutes of Health, academic and industrial experts in Otology, Audiology, Pharmacology, Public Health, Occupational Health, Industrial Hygiene, Statistics, Genomics and other related fields - has met regularly since 2011, growing to over 175 members, to discuss and create these documents through volunteered peer-reviewed and consensus. The resulting eight clinical study guidance documents will be explored in this workshop session with the overall aim to gain acceptance by the Academies, Associations and their professional constituents to consider and utilize these documents as criterion standards or recommended guidance, as appropriate.

SYMP 23

Temporary and Permanent Noise-Induced Threshold Shifts

Jonathan Kil[1]; Allen Ryan[2]; Sharon Kujawa[3]; Tanisha Hammill[4]; Colleen Le Prell[5]
[1]Sound Pharmaceuticals; [2]University of California, San Diego; [3]Massachusetts Eye & Ear Infirmary; [4]Dept. of Defense; [5]University of Texas, Dallas

Exposure to intense sound or noise can result in temporary increases in hearing thresholds or in permanent hearing loss. In the latter case, a loss that is apparent immediately after noise exposure does not recover to pre-exposure hearing levels. Acute changes in hearing sensitivity are known as temporary threshold shift (TTS), while chronic deficits in hearing sensitivity are termed permanent threshold shift (PTS). As in many forms of hearing loss, the high-frequency, basal regions of the cochlea are more sensitive to noise damage than the apex. In addition, resonance of the ear canal results in a frequency region of high sensitivity to noise at 4-6 kHz. A primary target of intense noise is the cochlear hair cell. While the mechanisms that underlie noise-induced hair cell damage remain unclear, there is evidence to support a role for reactive oxygen species, stress pathway signaling and apoptosis. Another target of noise is the synapse between the hair cell and the primary auditory neurons of the spiral ganglion. Large numbers of these synapses and their neurons can be lost after noise, even though hearing thresholds may return to normal. This in turn affects auditory processing and the detection of signals in noise. The consequences of TTS and PTS include significant deficits in communication that can impact performance of military duties or obtaining/retaining civilian employment. Tinnitus and exacerbation of post-traumatic stress disorder are also potential sequelae.

SYMP 24

Guidelines for Auditory Threshold Measurement for Significant Threshold Shift (STS)

Kathleen Campbell[1]; Colleen Le Prell[2]; Michael Hoffer[3]; Tanisha Hammill[4]; Jonathan Kil[5]
[1]Southern Illinois University; [2]University of Dallas; [3]University of Miami; [4]Defense Hearing Center of Excellence; [5]Sound Pharmaceuticals

This presentation's purpose is to a) provide guidelines for determining Significant Noise-Induced Hearing Threshold Shifts in clinical trials involving human populations, and b) to highlight logistics factors for study deign consideration. The session will review recommendations for the standards to be referenced for human subjects testing, equipment and test environments, as well as additional guidelines to be applied in military population research. The importance of appropriate personnel selection, time allocation, and licensure and certification standards will be discussed. For military settings, special considerations for personnel justifications, impact statements, and factors impacting time availability are reviewed. Guidelines for the calibration of audiometers, sound booth allowable noise levels, and immitance equipment are provided. In addition, the guidance provides specific suggestions for the subjects' history prior to study onset, and otoscopy.

Test frequencies for threshold determination and methods of threshold determination are reviewed for air conduction and bone conduction for both baseline testing and later determination of either a temporary (TTS) or permanent threshold shift (PTS). If a

Significant Noise-Induced Threshold Shift is determined, subjects should be counseled or referred for additional medical evaluation. Guidance for reporting procedures and the data capture into a computerized study database are described. Finally, experimental designs suggested for noise-induced otoprotection clinical trials are described. Participants will gain practical knowledge immediately applicable to any future auditory human trial study design.

SYMP 25

Potential Effects of Noise on Hearing: Supra-Threshold Testing using Speech-in-Noise and Auditory Evoked Potentials

Colleen Le Prell[1]; Douglas Brungart[2]
[1]University of Texas at Dallas; [2]Walter Reed National Military Center

In human listeners, the accepted clinical standard for detecting and measuring hearing loss is the behavioral audiogram, which is based on the absolute detection threshold of pure-tone stimuli. Recent results from noise-exposed animals demonstrate that some noise exposures can result in temporary threshold shifts where the pure tone auditory threshold returns to its pre-exposure level, but post-exposure dissection reveals that there is substantial damage to the synaptic ribbon population in the cochlea. This damage is not apparent in the threshold auditory brainstem response (ABR), which is based on the lowest stimulus level where the sound-evoked neural responses generated at the level of the eighth cranial nerve (wave I) and in the auditory brainstem (waves II- IV) can be detected above the noise floor. Instead, this damage is accompanied by decreases in the amplitude of the supra-threshold ABR. These noise-exposed animals have a reduced neural response as the auditory stimulus level increases above threshold.

On the basis of these animal model results, it has been suggested that clinical measures of auditory performance that are conducted with stimuli presented above the detection threshold may reveal unknown "hidden" functional changes related to inner hair cell loss or synaptic pathology in listeners who have a history of noise exposure but clinically normal auditory thresholds. Two possible methods that could be used for exploring these hidden hearing loss effects in human listeners are supra-threshold ABR responses and speech-in-noise testing. Both are theoretically sound, but, to this point, neither has been convincingly shown to correlate with noise exposure in across-subject studies of listeners with clinically normal thresholds. However, there is some possibility that these measures could be more sensitive to small changes in hearing in within-subject studies, including those designed to assess the effectiveness of interventions designed to prevent NIHL. Here we review possible strategies for using supra-threshold speech-in-noise testing and supra-threshold ABR responses as supplements to the behavioral audiogram for assessment of possible neurodegeneration in noise-exposed listeners.

SYMP 26

Measurements of Noise-Induced Tinnitus

Dawn Konrad-Martin
National Institutes of Health, NICHD

Chronic tinnitus is the persistent sensation of hearing a sound that exists only inside the head. Anything that can cause hearing loss can also cause tinnitus, with noise exposure being the most common cause of both. The prevalence of chronic tinnitus in adults in the U.S. is estimated at 10-15%. For about 20% of these individuals the tinnitus is significantly bothersome. Although myriad therapies for tinnitus are offered (often at significant cost), most are not evidence-based. Difficulty in the assessment and further development of interventions for tinnitus stems from the limitations of techniques used to evaluate these interventions. Questionnaires are widely available to "measure" (tinnitus can only be *indirectly* measured) functional effects of tinnitus, such as difficulty sleeping and concentrating, and negative emotions such as anxiety, depression, and annoyance. Questionnaires have recently been documented for sensitivity to change in response to intervention (i.e., "responsiveness"). All of these questionnaires function well to assess the overall impact of tinnitus. The limitations mentioned pertain primarily to (a) the common misconception by patients that hearing problems are caused by tinnitus; and (b) interpreting measures of tinnitus *perception*. The first limitation (confusing tinnitus and hearing loss) can be addressed by administering the 10-item

Tinnitus and Hearing Survey. The second limitation involves measures of tinnitus perception, which typically include the psychoacoustic measures of tinnitus loudness and pitch matches, tinnitus spectral content, minimum masking levels, and residual inhibition. These measures, which are obtained routinely in many clinics and as part of research studies, have not been validated for being diagnostic, prognostic, discriminative, or responsive. In order for these measures to become clinically meaningful, normative standards are needed, both for baseline measures and for repeated measures of tinnitus perception. Evidence-based intervention for tinnitus requires accurately measuring both the perception of, and reactions to, tinnitus. This presentation focuses on each of the above issues. In addition, the new Tinnitus Screener will be described along with data supporting its efficacy for identifying the presence/absence of tinnitus. If the Tinnitus Screener reveals the presence of tinnitus, then it is also capable of differentiating between temporary, intermittent, or constant tinnitus.

SYMP 27

Use of Otoacoustic Emissions in Clinical Trials

Dawn Konrad-Martin[1]; Gayla Poling[2]; Laura Dreisbach[3]; Kelly Reavis[1]; Garnett McMillan[1]; Judi Lapsley Miller[4]; Lynne Marshall[4]

[1]VA Portland Health Care System; [2]Mayo Clinic; [3]San Diego State University; [4]U.S. Navy

Otoacoustic emissions (OAEs) provide a rapid, noninvasive measure of outer hair cell system function and are used to screen for hearing loss and damage related to noise or ototoxic drug exposure. OAEs therefore represent a potentially powerful way to assess the efficacy with which otoprotectants mitigate such damage. This presentation describes benefits and limitations of OAEs for use as a clinical trial outcome. Questions remain concerning the most appropriate OAE protocols to use for this purpose although they must be theoretically sound based on known patterns of damage, involve minimal time, generate valid results in the majority of individuals tested, and be accurate and repeatable. Developing a standardized OAE protocol may not be an appropriate goal because damage patterns and patient factors will differ across trials, which is presumably in part why various protocols are in clinical use. Instead, literature is synthesized to guide protocol choices. Active areas of OAE research are described including emerging protocols and analyses, and improvements in measurement system capabilities. Methods for determining "significant" OAE changes are discussed, which may differ for a clinical trial as compared with the criteria used clinically to determine OAE changes. Critical to the effective use of OAEs is the ability to minimize measurement variability in order to improve test precision; therefore, sources of variability are described and methods for determining test-retest reliability for individual testers and test sites are discussed. Finally, recommendations are provided for standardized reporting of results so that useful comparisons can be made across trials.

SYMP 28

Oxidative Damage and Inflammation Biomarkers: Strategy in Hearing Disorders

Gerald Haase[1]; Kedar Prasad[2]

[1]University of Colorado; [2]Premier Micronutrient Corporation

Excess free radical-induced oxidative stress and inflammatory processes are increasingly recognized as causative factors in hearing and balance disorders. Antioxidant micronutrients neutralize free radicals and, at adequate doses, reduce inflammation and demonstrate benefits in animal models and human trials. Therefore, it is reasonable to expect that biomarkers of oxidative damage and inflammation are appropriate correlative biological outcome parameters in clinical hearing intervention studies.

The tenets of antioxidant science dictate that there are a great variety of free radicals and that they attack different cellular targets. They also demonstrate varying functions in different cellular environments. In addition, oxidative stress and inflammation may cause direct injury to tissues, cell membrane lipids, proteins and nuclear DNA.

To accommodate these many pathways, the useful categories of potential biomarkers become extensive. The degree of injury is also reflected by separate markers of inflammation and measures of antioxidant levels. Therefore, in order to provide a reliable indication of oxidative damage, inflammation and antioxidant level, it is necessary to determine a broad spectrum of lipid peroxidation markers, adducts of DNA, oxidation levels of proteins and pro-inflammatory cytokines.

This report aims to highlight some of the most clinically relevant and well-studied biomarkers in each category of tissue damage. It also includes those markers with which the authors have had direct positive clinical experience. The outcome from these studies is intended to provide a list of adjunctive measures that can be recommended as a relevant biomarker panel in hearing disorder clinical trials.

SYMP 29

Genetics of Noise-Induced Hearing Loss - a Link to Pharmaceutical Intervention

Royce Clifford

Harvard School of Public Health

Several types of studies have elucidated genes and miRNAs that may be associated with noise-induced hearing loss, and there are a few clinical trials of pharmaceuticals in progress, however targeting of specific genes leading to therapeutic interventions has yet to be accomplished. **Methods**: Researchers have used means of identifying genes, including: 1. Candidate genes to identify single nucleotide polymorphisms, 2. Studies of knockout animals to pinpointed genetic response to acoustic trauma, 3. GWAS studies of noise-exposed populations, and 4. Micro-RNA studies using microarrays. The genetic findings have focused on pathways of cellular response to stress, signal transduction, metabolism, and the immune system. A review of these findings in these areas will be discussed in relationship to cellular pathways

that may be targeted for pharmaceutical intervention. Future studies may include RNA-sequencing in animals after acoustic trauma, discovery of plasma biomarkers including miRNAs, and long non-coding RNAs.

SYMP 16

Hearing Loss and Human Genetics: Science, Policy and Beyond Overview

Avril Holt[1]; Lina Reiss; Deniz Başkent; Evelyn Davis-Venn; Michael Hoa; Mirna Mustapha; Diana Peterson; Tilak Ratnanather; Shurud Rajguru; Astin Ross; Chang Liu; Howard Francis

[1]Wayne State University School of Medicine

In recent years there has been a rapid increase in identification of heritable genes underlying hearing loss. Like other clinical areas, the auditory field is now focused on targeted treatments, or designer therapeutics based upon a person's genetics. This genetics-based approach to preventing or curing hearing related conditions leads to questions of who will have access to this next generation of treatment, as well as when and how treatment will be applied across various segments of our society. To address this pressing concern there is a need for increased awareness and research regarding how scientific discovery intersects with specific social constructs and governmental policy. The goals of this symposium are two-fold: first, to highlight recent advances in research on the genetics underlying hearing loss/communication disorders and new designer treatments for hearing loss; second, to encourage dialogue about the implications of these new genetics-based therapies for policy and society. The speakers will provide an overview of personalized medicine for individuals with hearing loss. There will also be discussion about disparities in outcomes across socioeconomic groups with those using hearing aids and cochlear implants. The speakers will also present some of the latest data on the impact of genetic counseling and testing for deaf genes on hearing parents of deaf children, and on deaf adults, including those who use American Sign Language. Finally, insight will be provided into the present and future status of policy governing access to treatments (hearing aids, cochlear implants, genetics-based designer therapeutics) especially given that baby boomers are coming to an age where hearing-related pathologies are evident, with the demand for effective treatment high and crossing socioeconomic strata.

SYMP 17

The Genetics of Hearing Loss: So Much Achieved and So Much More to be Achieved

Karen Avraham

Tel Aviv University

A significant proportion of hearing loss in individuals of all ages has a genetic basis. Identifying the genetic cause in a patient aids in determining the prognosis of hearing loss and other potential abnormalities, as well as assessing the recurrence rate in family members. Aiming at discovery, clinical and research laboratories worldwide have worked towards determining the spectrum of pathogenic variants contributing to non-syndromic and syndromic hearing loss. Since the discovery of the first gene for non-syndromic hearing loss, connexin 26, in 1997, more than 100 genes have been attributed to deafness and in some cases, the intervening mechanisms leading to reduced hearing have been elucidated.

The recent advances in high throughput sequencing have facilitated the discovery of many more deafness genes worldwide. A combination of targeted deafness gene capture and deep sequencing, as well as exome sequencing alone, has been used since 2010. We have applied these techniques to determine the cause of deafness in the Middle Eastern hearing impaired population. However, the cause of hearing loss in many families is still unknown. The underlying cause of hearing loss may be in regulatory regions that will require whole genome sequencing. The inability to study regulatory variants using RNA from patients makes determining the mechanism challenging, requiring appropriate animal models. The recent use of retroviruses and oligonucleotides to attempt rescue of hearing in mouse models has been encouraging. The challenge ahead of us is how the transition from animal models to human patients will be implemented. Moreover, the costs for research – both for gene discovery and 'personalized' gene and cell therapy – are very high.

Included in these considerations is respect and care for the very patients the clinical and basic research is intended to help. Do deaf individuals want to know the cause of their hearing loss? Should incidental findings be reported to the patient? Will the therapies being developed improve the quality of life of these people? These are some of the questions to be addressed by our scientific and medical community.

SYMP 18

Genetic Basis of Age- and Noise-Induced Degeneration of Auditory Nerve Fibers.

Srividya Sundaresan; Suganthalakshmi Balasubbu; **Mirna Mustapha**

Stanford University

Background

In both noise- and age-related hearing impairment, there is considerable degeneration of peripheral auditory nerve fibers. This cochlear nerve degeneration, or auditory neuropathy, is invisible, not expected to affect audiometric thresholds, and therefore, undetectable in conventional hearing tests offered in the clinic. This degeneration, however, is key to problems with hearing and speech discrimination in noisy environments, characteristic of impaired hearing ability in aging ears or presbycusis. Understanding the molecular and physiological changes that underlie synaptic degeneration will be critical for a better understanding of the causes and consequences of auditory neuropathy.

Methods

Cell adhesion molecule thrombopsondin (TSP) family, knockout mice TSP1 and TSP2 on the FVB background were used. Hearing thresholds were assessed using Auditory Brainstem Responses (ABRs) and Distortion Product

Otoacoustic Emissions (DPOAEs) at several time points before and after noise exposure. Cochlear morphology was assessed using immunohistochemisty. RNA level was verified by quantitative RT-PCR.

Results

Hearing tests revealed elevated ABR thresholds but not DPOAEs in TSP2 mutants at an early age. Results of TSP1 mutant hearing tests were normal until one-year of age at which time the mutant TSP1 mice exhibited increased ABR thresholds at higher frequencies and decreased wave 1 amplitudes compared to wild type controls.

Accelerated hearing loss was observed in mice lacking both TSP1 and TSP2 following noise exposure. Interestingly, threshold shift was observed in the low and mid but not high frequencies in TSP1 mutants. In TSP2 mutants, however, only the mid and high frequency regions were affected. Our physiology data is in agreement with the roles predicted for these genes based on our expression studies. Our morphological data demonstrated loss of afferent synapses at a higher rate in these mutants when compared to WT controls.

Conclusion

Together, these data suggest an important role for TSP cell adhesion molecules in the maintenance of auditory nerve connections and fibers in noise-exposed and aging ears. Future studies are designed to correlate cell morphology with physiology, allowing study of changes in the auditory system after noise-induced loss of specific auditory neurons. These steps are important towards understanding the etiology of human noise-induced and age-related hearing impairment.

SYMP 19

Childhood Development after Cochlear Implantation: The Role of Social Determinants as Modifiers of Outcome

John Niparko[1]; Emily Tobey[2]; Donna Thal[3]; Laurie Eisenberg[1]; Nae-Yuh Wang[4]; Alexandra Quittner[5]; Ann Geers[2]; Christine Carson[4]

[1]University of Southern California; [2]University of Texas; [3]San Diego State University; [4]Johns Hopkins University; [5]University of Miami

The goal of this prospective, longitudinal study is to determine the predictive value of clinical and social variables as they relate to communication, behavior, and economic outcomes of cochlear implantation in young children with profound sensorineural hearing loss. The CDaCI Study Team involves 62 investigators from six university-based clinical sites and two data coordination centers. The study attempts to address the complexity of language development under conditions of restored audition in the very young child when a variety of operational skills develop rapidly. A major aim is to determine the impact of conventional clinical indicators and parent-child interactions on levels of oral language, speech recognition, selective attention, and quality-of-life attained with cochlear implantation. CDaCI methods are based on novel approaches to outcome assessment, including video analysis of parent-child interactions. The goal of this presentation will be to assess the impact of social determinants, including familial socioeconomic status, on long range outcomes after early cochlear implantation.

SYMP 20

Interplay between Genetic Information and Cultural and Linguistic Diversity

Christina Palmer

University of California, Los Angeles

Cultural and linguistic diversity arises from differences in perception of sound. Just as humans who perceive sound within a certain range have formed communities with a spoken language and cultural behaviors, humans who do not perceive those sounds have formed communities with a signed language and cultural behaviors. The Deaf community has particular values, traditions, as well as rules for behavior, and language (e.g., American Sign Language, ASL) that are actively transmitted across generations. Deaf communities are often close-knit and comprised of individuals who embrace being deaf as a valued personal characteristic, not a disability or medical condition. In this cultural and linguistic minority group, individuals cherish their signed language. For the Deaf community genetic testing highlights the different perspectives on cultural and linguistic diversity that society at large holds, particularly with respect to the value of being Deaf and the importance of sign language, the native language of Deaf individuals. For the Deaf community, the past eugenics history and concomitant view of deafness as a pathology has raised concerns surrounding current genetic technology. For example, genetic information could have a negative impact on deaf individuals that may also extend into the culture of the Deaf community eliminating the Deaf community and sign language. Though there are concerns, there is also interest in genetic testing in the Deaf community. Unfortunately, because genetic information is predominantly available in print or spoken language, Deaf individuals have unequal access. Unequal access to any medically relevant genetic health information, e.g., cancer genetics, can increase health disparities for the Deaf community. Therefore, scientists and physicians should be aware of how access to, motivations for, and the impact of, genetic information is, in part, a function of culture and language.

SYMP 21

One Woman's View of Deafness and the Impact of Science, Policy and Culture on Achieving her Career Goals

Claudia Gordon

U.S. Department of Labor

Overview

Claudia Gordon will provide an overview of her journey that has led her to where she is today, not only as the Chief of Staff for the Department of Labor's Office of Federal Contract Compliance Programs (OFCCP), but also as an independent deaf woman of color on a mission to promote inclusion and access for individuals with disabilities in our society. Ms.

Gordon suddenly lost her ability to hear at the age of eight. Placed in isolation and stigmatized, two years would pass before she emigrated to the U.S. and was enrolled at a school for the deaf. A whole new world opened up for her once she learned to communicate in American Sign Language. When Ms. Gordon expressed an interest in furthering her education and becoming a lawyer, she was advised that she might not do as well in a hearing environment. Undeterred, she attended Howard University and subsequently American University Washington College of Law (WCL). During her time at Howard University and WCL, she had access to sign language interpreters for her classes, and this is still her preferred mode of communication.

Ms. Gordon has served as a senior policy advisor with the U.S. Department of Homeland Security's Office for Civil Rights and Civil Liberties, staff attorney for the National Association of the Deaf Law and Advocacy Center and Vice-President of National Black Deaf Advocates, Inc. Ms. Gordon is also a member of the Gallaudet University Board of Trustees. As a member of the Obama Administration since 2009, she initially served as Special Assistant to the Director of OFCCP and is now OFCCP's Chief of Staff. OFCCP enforces the civil rights of applicants and employees of companies benefitting from government contracts. Notably, in 2013 – 2014 she conducted a temporary assignment with the White House Office of Public Engagement as an Associate Director where she served as liaison to the disability community, advising on disability policies. She was awarded the Department of Homeland Security Secretary's Gold Medal, and the Paul G. Hearne Leadership Award, both for her work with the disabled community.

Ms. Gordon will speak about the numerous challenges faced along her journey, her resiliency and deep commitment to advancing equality of opportunity for people with disabilities. "People with disabilities are defined not by our limits but by our potential. With the right tools and support from the scientific community as well as our policymakers, anything is possible."

SYMP 35

Theoretical, Technical and Practical Aspects of Local Magnetic Resonance Spectroscopy in a Super High Magnetic Field

Boris Odintsov
University of Illinois, Urbana-Champaign

Local magnetic resonance spectroscopy (MRS) provides a powerful non-invasive window on local tissue biochemistry by quantifying the tissue levels of key metabolites. The purpose of this presentation is to highlight the features of *in vivo* local MRS at super high magnetic field combined with some basic requirements for reliable metabolic profiling. Localized MRS has seen substantial developments over the past two decades. It has been able to take advantage of the great improvements in hardware, including the shift to higher magnetic fields, faster and stronger magnetic field gradients, parallel RF receive/transmit technology etc. Acquisition methods have benefited from more flexible RF and gradient pulse shapes, more rapid sampling of *k*-space and efficient automated shimming algorithms. Spectral processing and quantification have seen the development of fitting packages. Chemical shift and J-coupling are the basis for the key role of MRS in structural and analytical chemistry. The main benefits of high magnetic fields application are an increased intrinsic signal-to-noise ratio (SNR), chemical shift dispersion and decreased strong coupling effects which improve quantification precision. In animal models, super high field ^{1}H MRS allows detection up to 20 metabolites with μL spatial resolution. The maximal gradient strength is important aspect of the MRS hardware. RF coils for signal transmission and receiving on high-field magnets should be optimized in shape and size to enhance RF field (B_1) homogeneity and SNR. MRS is prone to artifacts such as motion, poor water or lipid suppressions, field inhomogeneity, eddy currents, and chemical shift displacement (CHD). High field MRS is more sensitive to magnetic field inhomogeneity and some artifacts are more pronounced with it particularly susceptibility and eddy currents ones. With increased B_0 field strength, spectral dispersion and CHD artifacts become larger and cause problems achieving sufficient pulse bandwidth without exceeding SAR limits. Resonance linewidths and relaxation times depend on B_0 strength. Longitudinal relaxation times (T_1) increase with B_0, which leads to increased signal saturation at shorter repetition times. However, no further increase in T_1 relaxation times has been observed beyond 9.4 T. In contrast, T_2 and T_2* decrease considerably with increasing B_0, which leads to line broadening, overlapping and decreased peak height. Acquisition performed at a short TE and long TR minimizes the effects of relaxation thus improving the absolute metabolite quantification. A variety of substances containing MR-detectable nuclei other than ^{1}H can be detected at super high magnetic fields thereby allowing complementary insights in pathoneurochemistry.

SYMP 36

A direct determination of GABA, glutamate and choline in the auditory pathway of animals with tinnitus, using high resolution point-resolved proton magnetic resonance spectroscopy (1H-MRS).

Tom Brozoski[1]; Carol Bauer[1]; Donald Caspary[1]; Boris Odintsov[2]
[1]Southern Illinois University School of Medicine; [2]University of Illinois, Urbana Champaign

Following high-level sound exposure, central auditory changes are evident long afterward. Homeostatic mechanisms appear to compensate and in some instances overcompensate for peripheral insult. Overcompensation may produce the sensation of sound without an objective physical correlate, i.e., tinnitus. However not everyone exposed to auditory trauma develops tinnitus. Similarly, in a controlled laboratory environment, not every animal exposed to high-level sound develops tinnitus. The mechanisms responsible for tinnitus and its physiological signature are incompletely understood. Compensatory neural actions, such as increased spontaneous activity, have been identified, but underlying mechanisms are

poorly understood. The underlying mechanisms may involve down-regulation of inhibitory neurotransmission mediated by γ-amino butyric acid (GABA), and/or up-regulation of excitatory neurotransmission, mediated by glutamic acid (Glu). Neuromodulation by other systems, such as acetylcholine, is also possible. Because neural systems are integrated and well-regulated, neurochemical interactions can be complex. Compensatory changes in one system may produce reactive changes in others. Some or all may be relevant to tinnitus. To examine the roles of GABA, Glu and acetylcholine (indirectly indicated via choline, Cho), high-resolution point-resolved proton magnetic resonance spectroscopy (1H-MRS) was used to quantify their levels in the central auditory pathway of rats with and without tinnitus. Included in the survey were the dorsal cochlear nucleus (DCN), inferior colliculus (IC), medial geniculate body (MGB), and primary auditory cortex (A1). Chronic tinnitus was produced by a single high-level unilateral noise exposure, and was measured using an operant psychophysical procedure sensitive to tinnitus. Contrary to expectation, dramatic decreases in GABA were not evident in tinnitus animals. In tinnitus animals, GABA levels were slightly decreased in the IC contralateral to the exposed ear, while Glu levels were elevated both in the ipsilateral DCN, and contralateral A1. Also contrary to expectation, GABA levels were moderately elevated in the contralateral DCN and A1 of tinnitus animals. In exposed animals without tinnitus, GABA levels were elevated in the ventral MGB, suggesting that inhibitory compensation at that level might counter overcompensation elsewhere. Choline levels were elevated only in the contralateral A1 of tinnitus animals. These region-specific alterations in GABA and Glu may reflect a distributed alteration of inhibitory- excitatory equilibrium. The choline elevation seen in tinnitus animals could indicate an added attention factor. The present results suggest that targeting multiple neurotransmitter systems may be necessary when developing more generally effective therapeutics.

SYMP 37

Neurochemical Phenotypes in Animal Models of Neurotrauma: Studies with High Resolution Magic Angle Spinning ^{1}H Magnetic Resonance Spectroscopy (HRMAS ^{1}H-MRS)

Matthew Galloway; Farhad Ghoddoussi; VS. Sujit Saja; Anthony Cacace; A. Genene Holt; Pamela VandeVord
Wayne State University; Virginia Polytechnic and State University

Technical advances over the past 2 decades in proton magnetic resonance imaging represent a pinnacle of translational medicine, catapulting the basic science of nuclear physics into a panoply of clinical neuroimaging modalities. In particular, the use of ^{1}H magnetic resonance (^{1}H-MRS) to extract a neurochemical profile from the living brain in a non-invasive, relatively rapid fashion is exponentially accelerating our knowledge of human neurobiology. Despite the remarkable technical ability to assess the neurochemical phenotype of the normal and diseased human brain, interpretation of changes in the MR-visible neurometabolome lags far behind the plethora of clinical observations based on ^{1}H-MRS. Reasons for this disconnect include the unique neurobiology (relative to conventional neurochemical assessments) of MR-visible neurochemicals: ^{1}H-MRS cannot differentiate intracellular from extracellular compartments, several neurochemicals serve dual roles as neurotransmitter and metabolic intermediate, and others participate in previously understudied neuronal or glial functions. Moreover, clinical ^{1}H-MRS *in vivo* is hampered by issues related to resolution and elevated baseline.

To further our understanding of the MR-visible neurometabolome, we use high resolution, magic angle spinning (HR-MAS) ^{1}H-MRS *ex vivo* in intact, anatomically-discrete tissue specimens to interrogate neurochemical phenotypes in defined animal models of aberrant human neuroplasticity. Keeping in mind the limitations of animal models, we will discuss applications of HR-MAS ^{1}H-MRS to study blast overpressure induced neurotrauma (BINT) as well as noise-induced tinnitus (Holt *et al.* this meeting). For the BINT studies, HR-MAS ^{1}H-MRS data, immunohistochemistry, and behavioral observations support temporal patterns of neuroplasticity and neurodegeneration. In the tinnitus model, unbiased HR-MAS ^{1}H-MRS assessment of the auditory cortex supports further studies of disrupted pyruvate metabolism, oxidative stress, and membrane phospholipid turnover.

Neurometabolome-wide, unbiased, association studies using HR-MAS ^{1}H-MRS in animal models that recapitulate specific domains of human hearing disorders provide a valuable platform to understand and interpret clinical ^{1}H-MRS observations, discovery of novel drug targets, and generation of testable hypotheses in humans.

SYMP 38

Single Voxel Proton Magnetic Resonance Spectroscopy (1HMRS) in Noise and Blast Induced Tinnitus and Vestibular-Related Dysfunctions

Anthony Cacace
Wayne State University

This presentation will focus primarily on adult human testing using *in vivo* single voxel proton magnetic resonance spectroscopy (^{1}HMRS) in left and right auditory cortex in relation to noise and blast-induced tinnitus and in left and right posterior/inferior parietal and inferior insular cortices in relation to blast-induced vestibular system involvement.

Data on noise and blast induced tinnitus were collected at the MR Research Facility, Harper Hospital, Wayne State University, Detroit, MI on a 3.0 Tesla MRI scanner; vestibular related data were collected on a 1.5 Tesla scanner at the Mountain Home VA Medical Center MRI facility, Mountain Home, TN.

In one experiment on 25 adults, low frequency (1-Hz) repetitive transcranial magnetic stimulation (*r*TMS) was applied over auditory cortex of the left temporal lobe as a treatment modality for *noise-induced tinnitus* using a prospective randomized single-blinded sham-controlled

cross-over design. Pre-post outcome measures for sham versus active *r*TMS conditions included differential changes in tinnitus loudness; self perceived changes in response to the Tinnitus Handicap Questionnaire (THQ), and neurochemical changes of brain metabolite concentrations. In this context, the most notable effect showed that active but *not* sham *r*TMS produced a down regulation in the excitatory neurotransmitter glutamate that was highly correlated ($r = 0.77$, $p < 0.05$) with a reduction in the tinnitus loudness levels measured with a magnitude estimation procedure. Active *r*TMS also showed self-perceived improvements in several content areas of the THQ dealing with social, emotional, behavioral, tinnitus and hearing-related issues.

In another experiment on 22 adults, we evaluated neurochemical, neuropsychological, audiological, and questionnaire data to better understand the sequlae of *blast-induced tinnitus*. Multiple regression analyses revealed that glutamate levels in left auditory cortex, pure-tone measures of hearing sensitivity, and monosyllabic word recognition performance in quiet for the left ear were significantly related to processing speed and delayed recall memory performance. Left auditory cortex glutamate levels were also positively related to speeded mathematical processing. Choice reaction time performance was negatively related to myo-Inositol levels in left and right auditory cortex. Our findings provide evidence for tinnitus-related abnormalities at the neural level in auditory cortex that may contribute to neuropsychological deficits on speeded/cognitively demanding tasks. While tinnitus was the primary focus area herein, vestibular, balance, and gait relationships will also be addressed in relation to blast exposures.

Overall, our schemata emphasize the emerging fields of perceptual and cognitive MRS and provide a perspective on a new frontier in auditory, tinnitus, and vestibular-related research.

SYMP 30

Lessons Learned: From Academia to Start-Up to Corporation

Andrew Sabin
Bose Corporation

In this talk I will share experiences from my recent journey transitioning from academia to start-up. My company, Ear Machine, developed and researched novel methods for users to adjust audio signal processing parameters. We were a three-person company all with backgrounds in auditory research but differing specialties in terms of programming, business, and audiology. I intend to discuss some of the realities we encountered associated with university-owned intellectual property, Small Business Innovation Research (SBIR) grants, and, more generally, business formation and management. I will also share some insights about our recent transition from start-up to working at a large consumer electronics company. Our experience with Ear Machine presents an alternative to the well-known model in which a start-up raises large amounts of venture funding and seeks exponential growth. Instead, with a very small team, we identified a critical gap in the marketplace, raised modest amounts of money (primarily an SBIR from NIDCD), focused intensely on a solution for that gap, and sought out a large partner to bring it to market.

SYMP 31

Making a Business from a Lizard's Ear.

Jakob Christensen-Dalsgaard; John Hallam
University of Southern Denmark

Our foray into the business world started as a basic science venture: We wanted to understand how the lizard ear works.

As it turned out, the lizard ear not only exhibited a remarkable directionality, but this directionality was also easy to capture in a simple model of the ear. The lizard eardrums are coupled through the mouth cavity, and sound in a relatively broad frequency band(>1 kHz) can reach both sides of the eardrums with equal amplitudes. The interaction of sound components on both sides of the eardrum amplify or cancel eardrum movement depending on the phase differences .The directionality is strongly asymmetrical across the midline, so a bilateral neural comparison (EI cells) leads to a strongly lateralized response. From this study it was natural to make a simple robot incorporating this neural comparison and a motor output, almost like a Braitenberg vehicle. We mostly thought of the robot as the simplest possible model of a directional hearing system. We tested this robot and were surprised how well such a simple model worked, and that gave us the idea that a design based on our lizard model might be useful also in technological applications.

We patented the lizard robot and pursued the business case through an innovation grant that allowed a small company, Lizard Technology, to be founded and to develop marketable prototypes.

There are other sound localizing systems out there, but the advantage of the lizard ear model is that it is very compact; in fact, the model will fit in a plastic brick used by a popular toy company. We are certain that the model has many other uses, but the real limiting factor is to secure startup funds to keep a business running. I think there is a lesson in that: inventing and patenting is relatively easy, compared to the chance of obtaining the necessary high-risk investments for a budding company.

SYMP 32

From the International Space Station to Tanzania to a Brewery: the Makings of Innovative Audiology Tools

Odile Clavier; James Norris
Creare

What do the International Space Station (ISS), Tanzania and a noisy brewery have in common? They require comprehensive, noise-tolerant, portable devices for hearing testing. Early on in the ISS program, the National Aeronautics and Space Administration (NASA) noted that astronauts were coming back from ISS missions with hearing loss. NASA funded Dartmouth and Creare to build a lightweight, portable hearing-testing system that would leverage the existing

equipment on the space station to allow the astronauts to self-administer hearing tests. Consider this field testing at its most challenging, especially considering the relatively high noise environment on board. Although the system never flew to the Space Station, we leveraged the technology to support a new NIDCD-funded study into the effects of HIV/AIDS, treatments for HIV/AIDS, and HIV/AIDS comorbidities on patients' hearing. The study took place on a large clinical cohort located in Tanzania, where no sound booth was available, and study administrators had limited training in hearing assessment. At the same time, the Office of Naval Research funded our team to develop a field system to monitor noise-induced hearing loss using new, advanced DPOAE protocols that required fast signal processing.

Over a period of ten years, these projects and others, funded by the Department of Defense, the National Institutes of Health, and NASA, through a variety of mechanisms (SBIR, BAA, RO1, others) allowed Creare and its many clinical partners to mature our technology and expertise to the point where we could focus on innovative products that reduce the reliance on local infrastructure and improve access to hearing healthcare. One such device is a wireless headset that performs automated audiometry and is controlled through a mobile tablet or smartphone. Highly-attenuating ear cups integrate with the testing system to shield the user from background noise. The resulting device allowed ANSI-compliant threshold audiometry to take place in "quiet rooms" on the campus of a noisy brewery, without need for a sound booth. This system is currently in the early stages of production (first 100 headsets to be sold in Winter 2016), and transition to a manufacturer of other hearing diagnostic and screening equipment is ongoing. Creare, as a Research and Development company, leverages its many areas of technical expertise to incubate innovative technology which can then transition to new ventures or existing established businesses to reach the market place.

SYMP 33

Development of a hearing in noise test for children

Ruth Litovsky
University of Wisconsin Madison

The development of a hearing in noise test for children will be discussed. This test was intended to measure how well children with normal hearing and hearing loss can hear speech in the presence of different types of maskers and how well they can benefit from spatial separation of the speech and maskers. Research in Ruth Litovsky's lab led to publications in children with normal hearing and hearing impairment. The test was patented by the University of Wisconsin-Madison's entrepreneur partners. MBA students worked on this project to develop a business plan. A small company Binaural Solutions, LLC was formed for the purpose for sales and distribution but was eventually terminated. The lessons learned for this effort will be discussed.

SYMP 34

Growing an Idea and a Company: How the Light-Driven Hearing System Came to Exist

Sunil Puria
EarLens Corporation and Stanford University

While the idea of directly driving the eardrum to treat hearing loss was first proposed in the 1960s, it was not until 2003 that temporal-bone experiments demonstrated that it could deliver lower feedback pressure and wider bandwidth than conventional acoustic hearing aids, without requiring surgery, thus potentially leading to improvements in gain margins, sound quality, and one's ability to hear in noisy environments. This discovery led to the formation of EarLens Corporation, which has since grown from 2 to 80 employees and is now within 1-2 years of releasing its first commercial product.

With about $25M of initial capital from angel investors and NIH SBIR funding, EarLens had fewer than 10 key employees during its first 6-7 years. During this time, a major inflection point in the course of the company was the switch from a magnetic transducer to a light-driven transducer. Three to four years of research and development efforts led to the conclusion that a magnetic transducer was incapable of producing adequate output, but fortunately an efficiency revolution had been taking place in the photonics industry at the same time that made it possible to switch from magnetic to photonic physics. The prototype and well protected patent portfolio developed during this period allowed the hiring of a successful CEO who raised $30M of additional funding, and at this point the company grew exponentially to nearly 30 employees one year later and 80 employees the following year.

Thus, a small group with relatively little capital developed and implemented the key technology behind the wide-bandwidth light-driven hearing system. Getting to the next stage, with an FDA-approved, manufacturable, and commercially viable product, required the raising of additional capital and nearly 10 times the manpower of the original team.

What can be learned from the story of Earlens that could help you take your own ideas to the next level? As researchers, we don't always have the contacts and trust of the investment community to attain funding for our ideas. On the other hand, entrepreneurs that know how to raise funds often don't have the scientific and engineering knowledge to convey to investors that a concept has a chance of success and that technical challenges can be tackled. A successful business-growth strategy requires allegiances between these groups, as well as a top-notch leadership team that will create an appropriate culture, which is a key component to hiring and retaining talent.

PS 238

Mapping the auditory corticostriatal pathway in humans using diffusion tensor imaging

Han-Gyol Yi; Seth Koslov; W. Maddox; Bharath Chandrasekaran
The University of Texas at Austin

The basal ganglia receive extensive sensory input from the cerebral cortex. Tracing studies in non-human animals have shown that the different regions of the superior temporal cortex project to multiple targets within the striatum. Cortical projections onto the striatum have been posited to underlie category learning wherein the perceptual regions are implicitly mapped onto discrete representations. Functional neuroimaging studies in humans have demonstrated that the striatum is co-active during category learning. Response patterns that imply implicit mapping between perceptual input and category representations are associated with increased recruitment of the striatum. These findings strongly support the role of striatum in category learning. Currently, it is not clear whether the striatal co-activation with auditory signals is related to its connectivity with the auditory cortex. This is primarily due to the fact that the functional role of auditory corticostriatal pathways have not been explored in humans. We hypothesized that auditory-perceptual category learning in humans is based on the properties of the corticostriatal pathways. To test this hypothesis, we asked young adult native speakers of English (N = 30; ages 18 to 35) to learn nonnative speech sound categories, using trial-by-trial corrective feedback. Following the training session, diffusion-weighted images were acquired. Probabilistic tracking was conducted to identify the most representative pathway between the primary auditory cortex and the striatum. The identified pathway included the anterior part of the internal capsule, which connects the cerebral cortex with the striatum. The external capsule was also identified in the pathway, which has been implicated in cholinergic transmission from the nucleus accumbens. The average fractional anisotropy (FA) value for each participant was calculated in the aforementioned pathway. We predicted that, if auditory category learning is based on the pathway extending from the primary auditory cortex to the striatum, the average FA value within the corticostriatal pathway will be associated with individual variability in performance in the non-native speech category learning task. Mixed effects modeling analysis revealed that the participants with higher FA values were also more likely to be able to correctly categorize a given nonnative speech sound. This result suggests that the integrity of the auditory corticostriatal pathway is related to auditory category learning performance. This study represents the first systematic approach to identify the structural properties of the auditory corticostriatal pathways in humans, as well as highlighting its possible functional relevance.

Funding
This work was supported by the National Institutes of Health (NIH) – National Institute on Deafness and Other Communication Disorders grant (NIDCD; DC013315) to BC.

PS 239

Imaging Brain Structures in Children with Auditory Neuropathy Spectrum Disorder

Hannah Cooper; Doris-Eva Bamiou; Lorna Halliday; Chris Clark
University College London

Background
Auditory neuropathy spectrum disorder (ANSD) is a complex condition affecting around 10% of children with hearing loss. Individuals with ANSD show a vast range of functional hearing abilities from normal hearing detection thresholds with minor difficulties hearing speech in noise, to no functional hearing or access to spoken language. ANSD often results in fluctuating hearing loss and auditory temporal processing abnormalities leading to degraded and inconsistent auditory input. The abnormal subcortical transmission of sound experienced by children with ANSD may therefore result in the disruption of normal cortical development. Here, we investigate the effects of the disordered auditory input common in ANSD on neural development and brain structure.

Method
Eleven children aged 7 to 15 years with a diagnosis of ANSD participated in the study. All children had spoken English as their primary language. Most children had a history of neonatal jaundice. Structural MR images were acquired and behavioural testing, including tests of auditory processing, was carried out. Eleven normally hearing children matched for age and gender also took part in the imaging study.

Results
T1-weighted volumetric images were analysed. Children with ANSD showed significant thinning of the cortex in the left transverse temporal gyrus (typically considered to be the site of the primary auditory cortex) compared to controls. Mean cortical thickness was significantly reduced in children with ANSD in both hemispheres. There were significant reductions in volume of the brainstem, globus pallidus, and thalamus, all known to be vulnerable to unconjugated bilirubin. Behavioural results showed that children with ANSD had varying levels of difficulty hearing speech in quiet and in noise. Tests of auditory processing showed impairment of temporal processing as well as of binaural hearing.

Conclusion
To our knowledge this is the first study to demonstrate differences in brain structure in children with ANSD compared to normally hearing controls. Abnormal transmission of sound due to ANSD is associated with changes in subcortical structures and thickness of the primary auditory cortex. A future study will investigate white matter connectivity giving insight into auditory information transfer in children with ANSD.

Funding
This project is funded by the National Institute for Health Research NIHR/CSO Healthcare Science Doctoral Research Fellowship Programme. Conference attendance is funded by the Action on Hearing Loss Conference Bursary Scheme.

PS 240

Acute Effects of Nicotine on Human Central Auditory Processing

Carol Pham; Sahara George; Thomas Lu; Raju Metherate; Fan-Gang Zeng
University of California, Irvine

Introduction

In our studies of rodent A1 systemic nicotine narrows frequency receptive fields, and for tone-evoked responses, increases peak amplitudes and decreases onset latency and variance. Thus, we postulate that nicotine in humans may enhance related aspects of central auditory processing, findings that would align with studies showing improvements in diverse cognitive functions. Experiment I measured tone-in-noise detection at two sound levels to test the hypothesis that nicotine increases central gain. Experiment II involved detecting a temporal gap between two tone bursts of the same frequency (within-channel, WC) or different frequencies (between-channel, BC) to test the hypothesis that nicotine improves temporal acuity. Experiment III used spectral ripples to test the hypothesis that nicotine increases frequency selectivity.

Methods

Normal hearing, adult nonsmokers and occasional smokers abstaining from nicotine served as participants. In a single-blind, placebo-controlled paradigm, participants randomly received nicotine (Nicorette 6 mg) or placebo (Eclipse) gum in the first session and the opposite in the subsequent session. On each session (separated by ≥1-3 days) subjects performed tests before and after treatment. All experiments used a 3-interval forced choice, adaptive procedure. Experiment I measured thresholds for detecting a 2 or 4 kHz tone in noise. Experiment II measured a detectable gap between a pair of 2 kHz-tone bursts (WC) or with a 4 kHz-leading tone burst and a 2 kHz-lagging tone burst (BC). Both Experiment I and II presented tones at 45 and 70 dB SPL in pink noise at 50 dB SPL designed to minimize spectral splatter. Experiment III measured dynamic spectral resolution in terms of ripples per octave with stimuli presented at 45 dB SPL (Aronoff and Landsberger 2013).

Results

Early results (≤5 subjects per experiment) show that tone-in-noise detection remained constant per frequency and level with both treatments. BC gap thresholds exceeded WC gap thresholds independent of level and treatment. With increasing level, WC gap thresholds decreased by an order of magnitude whereas, surprisingly, BC gap thresholds failed to change. Nicotine had a slight tendency to decrease BC gap thresholds but failed to change tone-in-noise detection thresholds, WC gap thresholds, or ripple discrimination.

Summary

Preliminary data suggest that nicotine may slightly improve BC gap detection but fail to improve tone-in-noise detection, WC gap detection, or spectral ripple discrimination.

Funding

This work was funded by NIH grants RO1-DC008858, P30-DC008369, R21-DC013406, R01 DC013200, & UL1-TR000153.

PS 241

Acoustic change complex (ACC): an objective tool to assess auditory training effects

Chun Liang[1]; Ivy Thompson[1]; Kayla Whitaker[1]; Jing Xiang[2]; Fawen Zhang[1]
[1]University of Cincinnati; [2]Cincinnati Children's Hospital

The ability to discriminate pitch changes in sounds is critical for music and speech perception. It is well known that musicians, who experience long-term auditory training with music stimuli, perform better than non-musicians in pitch perception and these musician benefits have been reported to positively affect speech perception (Schön et al., 2004; Fuller et al., 2014). Understanding the underlying neural mechanisms of pitch perception in musicians will have important implications in designing auditory rehabilitation strategies for individuals with hearing impairments. In addition, if there is a relationship between neural responses and behavioral performance, the neural responses can be used as objective measures to assess training effects. The aims of this study were: 1) to examine the cortically generated acoustic change complex (ACC) elicited by pitch changes in musicians and non-musicians; 2) to determine the relationships between ACC measures and behavioral performance of pitch change detection.

Twenty-four young normal hearing listeners including 12 musicians and 12 non-musicians participated. All subjects underwent a psychoacoustic test to determine the threshold for pitch change detection and electroencephalographic (EEG) recordings. For the psychoacoustic test, the stimuli were a series of tones of approximately 1 sec duration containing upward pitch changes at 0.5 sec after the tone onset. The base frequency examined was 160 Hz (similar to the F0 of woman voice). A two-interval, two-alternative forced-choice paradigm was used to measure the minimum pitch change that could be detected by the subjects. For EEG recording, the stimuli similar to those used for behavioral tests were used, with the base frequencies at 160 Hz and 1200 Hz. The magnitude of pitch changes were 0% (no change), 5%, and 50% for each base frequency. Subjects were asked to ignore the stimuli during EEG recordings.

For both subject groups, the N1 and P2 amplitudes of the ACC increased and latencies decreased as the magnitude of pitch change increased. Musicians showed significantly shorter N1 latencies compared with non-musicians for the base frequency of 160 Hz. ACC measures (P2 latency, amplitude) for 120 Hz 5% pitch change were significantly correlated to the pitch change detection thresholds.

The ACC can reflect the effects of music training on pitch change detection. Both ACC amplitude and latency are good indicators for behavioral performance in pitch change detection. Because the ACC is recorded without subject's

voluntary response, it provides an objective biomarker of pitch change detection at the cortical level to document training effects.

PS 242

Development of an infant-friendly flat-panel earphone for non-invasive functional brain imaging on awake babies using cartilage conduction

Seiji Nakagawa[1]; Toshiaki Imada[2]; Hiroshi Hosoi[3]; Andrew Meltzoff[2]; Patricia Kuhl[2]
[1]National Institute of Advanced Industrial Science and Technology (AIST); [2]University of Washington; [3]Nara Medical University

To see the baby's auditory developmental stage, non-invasive functional brain imaging on awake babies have been conducted recently. One of the problems in such hearing experiments on awake babies is that many babies take away their insert earphones during measurements. Auditory stimulation with a loudspeaker also has problems, such as unbalanced time-varying acoustic characteristics between two ears brought by baby's head motion during measurements. To solve these problems, a new earphone for MEG measurement on awake babies should be developed. The requirements for the earphone are: (1) No insertion into ear canals or no pressing strongly against heads or ear; (2) Excellent and stable acoustic characteristics; (3) Small magnetic disturbances to sensors.

We started developing an infant-friendly earphone using the cartilage conduction. The cartilage conduction is a novel kind of bone conduction. In the ordinary bone conduction, vibrators are attached to bony sites, e.g., the mastoid process of the temporal bone. On the other hand, in the cartilage conduction, vibrators are attached to softer and more elastic sites, e.g., the pinna or concha. Sounds are conveyed via both air- and bone-conduction pathways in the cartilage conduction.

The new earphone is composed of a piezoelectric vibrator that is firmly glued to a flat round brass panel, with a diameter of 35 mm, to amplify the vibration. The earphone can be attached to the baby head cap, and just mildly touched to baby's pinna. By the earphone, sounds are conveyed via both air- and bone-conduction (mainly osseotympanic emission) pathways. The enhancement of low frequency component is expected by the occlusion of the ear canal.

Clear auditory evoked MEG responses were obtained from awake babies (6-month-old and 8-month-old) as well as adults, using our first prototype flat-panel earphone. Also, the babies did not dislike to wear the developed earphone at all. The earphone enables an experiment of dichotic listening that was quite difficult for awake babies.

Funding
A part of this research was supported by the Funding Program for Next-Generation World-Leading Researchers provided by the Cabinet Office, Government of Japan, and Grants-in-Aid for Scientific Research (26282130, 26560320 & 25280063) from the Japan Society for the Promotion of Science (JSPS) for SN.

PS 243

Late Auditory Evoked Potentials in Blast-Exposed Veterans

Melissa Papesh; Curtis Billings; Robert Folmer; Frederick Gallun
United States Department of Veterans Affairs

Background
A common auditory complaint of Veterans who have been exposed to high-intensity blast waves is increased difficulty understanding speech in noise. The objective of this study is to use late auditory evoked potentials (AEPs) to assess cortical auditory processing abilities of blast-exposed Veterans.

Methods
Participant groups included Veterans exposed to high-intensity blast waves during recent military conflicts and age-matched non-blast-exposed controls. Using a P300 oddball paradigm, AEPs were measured in response to a tonal contrast (500 and 1000 Hz tones) and a speech contrast (/ba/ and /da/ syllables) presented in both quiet and multitalker babble conditions. Behavioral measures included the Color-Word Stroop test, the Trail Making test, and multiple tests of speech in noise perception. Self-report measures were also used to gauge self-perceived difficulty with auditory tasks as well as general neurobehavioral functioning.

Results
Preliminary results based upon 16 blast-exposed Veterans and 12 controls clearly indicate that P300 AEP responses to oddball stimuli are decreased in amplitude and increased in latency in injured Veterans compared to control participants in nearly every condition. Though the inclusion of background noise degraded P300 responses in all participants, these effects were generally more severe in blast-exposed participants. Earlier cortical responses including the N100 and P200 components were similar between groups, indicating relatively normal function of early cortical pathways.

Conclusions
P300 data clearly indicate that blast exposure has the capacity to degrade and delay the cortical encoding of changes in sound. The presence of background noise further exacerbates this condition. These data are some of the first to objectively demonstrate that blast exposure can yield long term alterations in higher-order auditory function, even when only "mild" traumatic brain injury was incurred. These changes likely underlie chronic difficulty with higher order auditory functions such as speech perception in noise. Further analysis will focus on differences between stimulus parameters in blast-exposed and control groups as well as correlations with behavioral and self-report measures of hearing and neurobehavioral status.

Funding
This work was supported by an Advanced Research Fellowship in Polytrauma / Traumatic Brain Injury Rehabilitation from the United States Department of Veterans Affairs Office

of Academic Affiliations (OAA) as well as career development award #1IK1RX001820-01A1 from the Department of Veterans Affairs Rehabilitation Research and Development Service (PI: Papesh).

PS 244

Automated detection of auditory discrimination responses in the EEG of infants during sleep staging

Kristin Uhler[1]; Christine Yoshinaga-Itano[2]; Kaylee Watson[3]; Phillip Gilley[4]

[1]University of Colorado, Denver; [2]SLHS; [3]University of Colorado, Boulder; [4]Marion Downs Center

Background

The validation of appropriately fit amplification in babies within the first few months of life after hearing aids are fit is currently not possible to assess clinically. Recent studies suggest that amplification is commonly fit inadequately in more than half of all hard-of-hearing children, which has negative implications for language outcomes. In the present study, we sought to develop an objective, electrophysiological measure of auditory discrimination with the goal of obtaining a "Go/No-Go" response to indicate the detection of a deviant sound in an oddball paradigm. While studies of evoked potentials in infants report stability in peak parameters (latency, amplitude, etc.) across various stages of alertness, including sleep, none have attempted to control attention during testing. Testing during sleep not only reduces the potential of attentional effects on the evoked responses, it has the added benefit of reducing data loss associated with movement.

Methods

Test stimuli included three auditory frequent-deviant pairs (500 Hz pure tone vs. White Noise, /a/ vs. /i/, and /ba/ vs. /da/) presented in the sound field at 70 dB SPLA. Continuous electroencephograph (EEG) was recorded from 11 scalp electrodes in 30 normal hearing infants aged 1 to 4 months during sleep staging. The EEG from each channel was expanded to the time-frequency domain using a continuous wavelet transform, and then subjected to a PCA-based wavelet lifting scheme with bootstrap statistical testing of the frequent versus deviant responses, including a non-deviant control test.

Results

This study indicates that 1.) the continuous wavelet transform is sufficient for separating exogenous auditory responses from oscillatory activity during sleep staging, 2.) the wavelet lifting scheme is a viable tool for identifying a discrimination response, and 3.) the statistical testing procedure provides a reliable probability estimate of the discrimination response.

Conclusion

These results suggest that an automated EEG procedure may be an ideal approach for assessing auditory discrimination in infants even during sleep. A physiological marker of speech discrimination in infants would provide a means to assess adequate amplification in children with hearing loss during the crucial early months of development.

Funding

This research was supported by the National Institute on Deafness and Other Communication Disorders to author KU (NIDCD K23DC013583). National Institute on Disability, Independent Living, and Rehabilitation Research to authors PMG and CYI (NIDILRR grant number 90RE5020-01-00).

PS 245

Matrix metalloproteinase-9 deletion rescues auditory evoked potential habituation deficit in a mouse model of Fragile X Syndrome

Jonathan Lovelace[1]; Teresa Wen[1]; Sarah Reinhard[1]; Mike Hsu[1]; Harpreet Sidhu[2]; Iryna Ethell[1]; Devin Binder[1]; Khaleel Razak[1]

[1]University of California Riverside; [2]Scripps Research Institute

Fragile X Syndrome (FXS) is a leading genetic cause of intellectual disability and autism. Auditory processing deficits are common in autism spectrum disorders, but the underlying mechanisms are unclear. Electrophysiological responses in humans with FXS show reduced habituation with sound repetition and this deficit may underlie auditory hypersensitivity in FXS. Our previous study in *Fmr1* knockout (KO) mice revealed an unusually long state of increased sound-driven excitability in auditory cortical neurons suggesting that cortical responses to repeated sounds may exhibit abnormal habituation as in humans with FXS. Here, we tested this prediction by comparing cortical event related potentials (ERP) recorded from anesthetized wildtype (WT) and *Fmr1* KO mice. We report a repetition-rate dependent reduction in habituation of N1 amplitude in *Fmr1* KO mice. Recent clinical trials show that minocycline reverses ERP habituation deficits in humans with FXS, possibly by inhibiting matrix metalloproteinase-9 (MMP-9) activity. Our studies demonstrate a significant up-regulation of MMP-9 levels in the auditory cortex of adult *Fmr1* KO mice, suggesting that MMP-9 may contribute to reduced ERP habituation. We tested this hypothesis by examining ERPs in *Mmp-9/Fmr1* double knockout (DKO) mice and report that deletion of *Mmp-9* reverses ERP habituation deficits in *Fmr1* KO mice. Despite an increase in average N1 amplitude, the ERPs habituated in *Mmp-9*/*Fmr1* DKO mice similar to WT mice. We also compared habituation in awake and freely moving mice using screw electrode implants in the auditory cortex. This data set allows us to quantify power spectral density in WT and KO mice and investigate differences during repeated sound presentation and during rest when no stimulation was present. Together these data establish ERP habituation as a pre-clinical measure of auditory processing deficits in humans with FXS and suggest that abnormal MMP-9 regulation is a possible mechanism underlying auditory hypersensitivity in FXS.

Funding

The work is supported by U54HD082008 grant from NICHD (KR, DB, IE) and an NSF graduate research fellowship (SR).

PS 246

The Angular Gyrus: New Views on its Anatomy and Location

Alyssa Everett; Barrett St. George; Nicole Denny; Frank Musiek
University of Arizona

Introduction:
The Angular Gyrus (AG) is an association area of the human cerebral cortex that plays a role in several processes, including auditory function. A focused literature review was conducted regarding the anatomy and function of the AG. The parallel and count-back methods (as termed by the present authors) have been traditionally used to locate the anatomical location of the AG. However, in our experience, due to the gyral and sulcal variability of the cortex, it appears these methods may be imprecise and possibly misleading. Therefore, we qualitatively compared these two methods for locating the AG and assessed their co-reliability and overall accuracy to gain a better understanding of the locational variability of the AG.

Methods
Twenty high-resolution MRI images of normal, right-handed human brains, sequentially chosen from the OASIS online database were analyzed using two different techniques: 1) skull-stripped 3-dimensional surface renderings providing an external view of the cortex; and 2) serial sagittal slices (inspected orthogonally), allowing for medial (5 – 10 mm) inspection of the cortex.

Results
Examination of both methods for locating the AG showed better agreement for the right (80%) than left (55%) hemisphere for both surface and more medial sites. Several factors were identified that may compromise the co-reliability of these two methods: 1) There is a greater degree of fissuration in the left temporal lobe compared to the right, distorting the anterior-to-posterior course of the superior temporal sulcus (STS); 2) The sulcal depth of the STS varies across brains. A shallower STS was more likely to have one or more transverse gyri interrupting its path. In these instances, the posterior extension of the STS was ambiguous. In 43% of brains, breaks were found along the STS, with most occurring in the left hemisphere; and 3) The presence of a posterior ascending ramus of the Sylvian fissure sometimes creates a marked separation between the supramarginal gyrus (SMG) and the posterior extension of the STS. Furthermore, when the parallel method was employed, the anterior portion of the AG overlapped with the SMG's posterior portion 30% of the time in both hemispheres.

Our finding of poor co-reliability between the parallel and count-back methods suggests that the AG is sometimes difficult to identify in MRI scans, particularly in the left hemisphere. This places the traditional methods for locating the AG in question and opens the door for the development of new techniques to define this area of human neuroanatomy.

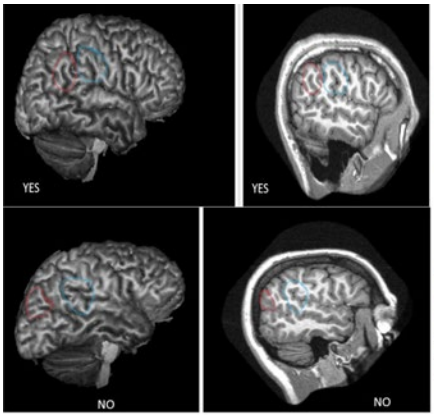

Figure 1 shows the location of the angular gyrus (red) and its relation to the supramarginal gyrus (blue) in the right hemisphere of an adult male. The parallel and count-back methods are in agreement in this case. Images generated from the OASIS database (Marcus et al., 2007).

Figure 2 shows a clear disagreement of the parallel and count-back methods for locating the AG in the right hemisphere of an adult female. In this example, there is a prominent gyrus that intervenes between the SMG (blue) and AG (red). Images generated from the OASIS database (Marcus et al., 2007).

PS 247

Unusual Morphology of the Sylvian Fissure: Trifurcations and False Ascending Rami

Barrett St. George; Andrew DeMarco; Frank Musiek
University of Arizona

Introduction
The Sylvian fissure (SF) and perisylvian cortex have been associated with areas of audition and the overlaid functions of speech and language. Yet, the detailed anatomy of the cortex surrounding the planum temporale continues to be debated. One challenge to identification of structures in this region relates to natural morphological variability of the cortical anatomy.

Classically, the SF is described as frequently having a posterior ascending ramus and less often, a posterior descending ramus. However, individuals accustomed to reading brain images or examining cadaver brains have noticed variability in the posterior Sylvian anatomy.

Although some studies have parenthetically mentioned atypical branching patterns within the posterior SF, there have been no systematic attempts to explore how regularly they occur in healthy adults. Hence the goal of this study was to investigate the prevalence and define these atypical morphological patterns in the branches of the posterior SF.

We focus on two atypical branching patterns, including (a) a false ascending ramus (FAR), defined as a ventral, discontinuous extension of the post-central sulcus joining the SF and (b) a trifurcation in the posterior SF, characterized by an ascending ramus, descending ramus, and FAR, all branching from the same location on the SF.

Methods
High-resolution structural MRI brain scans of fifty-eight healthy, right-handed adults were sequentially drawn from the cross-sectional OASIS database. The presence of a FAR and trifurcation were noted in each hemisphere during a larger study of posterior SF asymmetries. SFs were assessed via visual inspection and detailed measurements of the cortical surface of skull-stripped brains rendered in three-dimensions were made.

Results and Discussion

Of the 58 brains examined, 25 (43%) exhibited an FAR in at least one hemisphere. Of the 36 total FARs observed, 64% occurred in a left and 34% in a right hemisphere. Trifurcations were observed in 8 (14%) of brains examined. Of the 8 trifurcations observed, 63% occurred in a left and 37% in a right hemisphere. These results suggest that atypical branching patterns of the posterior SF are not rare and should therefore be considered when identifying structures of posterior perisylvian cortex. Misidentification of structures in this critical region may impact the interpretation of studies of audition and auditory processing, which rely on precise anatomical knowledge, including lesion studies, studies using functional MRI and MRI, and studies using evoked potentials.

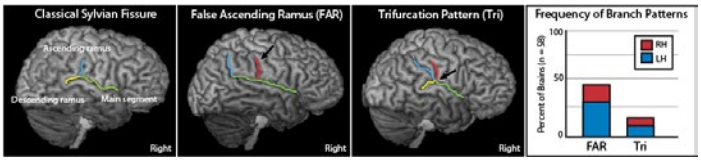

PS 248

Axo-Axonic Cartridges of Chandelier Neurons in the Auditory Cortex of C57BL/6J Wild Type and Parvalbumin-Deficient Mice

Ladislav Ouda[1]; Beat Schwaller[2]; Josef Syka[1]

[1]Institute of Experimental Medicine, Academy of Sciences of the Czech Republic; [2]University of Fribourg

Background

Parvalbumin-deficient mice (PV-/-) backcrossed to a C57BL/6J background were compared to wild type (WT) C57BL/6J mice in order to investigate putative changes caused by the absence of PV. Although the expression of calcium-binding proteins, including parvalbumin (PV), is assumed to play an important role in the maintenance of intracellular calcium (Ca^{2+}) homeostasis, PV-/-mice do not show an obvious phenotype when maintained under standard housing conditions. The morphological and functional changes are rather subtle, manifested in specific behavioral experiments or detectable at cellular levels. The chandelier cells represent a subset of GABAergic fast-spiking neurons prevalently expressing PV. The axons of these cells form arrays of terminals (cartridges), which have synaptic contacts exclusively on the axon initial segment of pyramidal neurons. In the present study, we aimed to quantitatively determine the presence of chandelier cell cartridges in the brain of PV-/- mice in comparison to WT mice. Moreover, we were interested to detect age-related changes in the number of the axo-axonic cartridges in either WT or PV-/- mice.

Methods

Brain sections containing the auditory cortex (AC) of WT and PV-/- mice were stained for the glutamate transporter 1 (GAT-1), which allows to visualize the axo-axonic cartridges of chandelier GABAergic neurons. The unbiased stereological method, the optical fractionator (Stereo Investigator software, MicroBrightField, Inc.), was used for determining the number of chandelier cell cartridges in the AC.

Results

In contrast to non-neocortical areas (such as the piriform and entorhinal cortices), in the sensory cortical fields including the AC, the numerical density of chandelier axo-axonic cartridges was relatively low. However, such cartridges were observed in all auditory cortical areas with a significant prevalence in the infragranular layers and the secondary ACs in comparison with the primary AC. Interestingly, no significant differences in the cartridge densities were found between WT and PV-/- mice. Only a slight decrease in the number of the axo-axonic cartridges was observed with aging and the decrease was similar in both genotypes.

Conclusions

The absence of PV does not significantly affect the presence of chandelier cell cartridges in the mouse AC, although in WT mice these cells are prevalently PV-expressing neurons. The possible effects caused by the absence of PV in PV-/- mice on the function of these axo-axonic neurons require future investigations. In addition, our preliminary results also suggest that these axo-axonic cartridges are relatively well preserved with aging, irrespective of the presence of PV.

Funding

This study was supported by the Grant Agency of the Czech Republic P303/12/1342 and P303/12/1347.

PS 249

Bimodal Stimulation Leads to Long-Term Changes in Neural Firing Rates in Primary and Anterior Auditory Cortex After Noise Exposure

Gregory Basura[1]; Joe Takacs[2]; Mohamad Issa[1]; Susan Shore[1]

[1]University of Michigan; [2]Hendrix University

Background

We recently demonstrated that bimodal stimulation (spinal trigeminal nucleus (Sp5) paired with tone at best frequency), resulted in changes in tone-evoked and spontaneous firing rates (SFRs) in primary auditory cortex (A1) 15 minutes after pairing (0 and 10ms bimodal interval; BI) in animals with and without evidence of noise-induced tinnitus. Neural responses were influenced by the interval and order of the bimodal stimuli, reflecting spike-timing-dependent plasticity (STDP).

Objective

Here we investigated whether the effects of bimodal stimulation following noise exposure leads to long-term changes in neural firing rates (tone evoked and SFRs) in A1 and in the adjacent anterior auditory field (AAF).

Methods

Three months after adult guinea pigs were subjected to unilateral (left ear) noise leading to a temporary threshold shift, extracellular neural recording electrodes were placed in the contralateral (right) A1 and AAF. Tone at best frequency and SP5 stimulation (both ipsilateral to noise exposed ear) were then paired at 0ms (simultaneous stimulation) or at +10ms where Sp5 stimulation preceded tone.

Results
Sixty and 120 minutes after bimodal stimulation, tone-evoked and SFRs were significantly decreased in sham-controls when tone and Sp5 where presented simultaneously (0ms); an effect that was preserved only at 120 minutes following noise exposure. Stimulation at 10ms, a BI that led to robust enhancement 15 minutes after pairing in shams, did not lead to long-term changes in shams, yet resulted in significant increases in SFRs and tone-evoked activity 60 minutes after pairing in noise-exposed animals and only in SFRs 120 minutes after pairing in the same animals. Interestingly, bimodal stimulation (both 0 and 10ms) led to significant suppression of SFRs and tone-evoked activity in AAF 60 and 120 minutes after pairing in sham-controls. Following noise-exposure, only simultaneous (0ms) stimulation robustly enhanced SFRs and tone-evoked firing rates 60 and 120 minutes after pairing in AAF while pairing at 10ms led to a significant suppression of firing only at 120 minutes after stimulation.

Conclusions
Together, these findings suggest that bimodal plasticity has long-lasting effects in A1 following noise damage that also has effects that extend to AAF that may have implications for tinnitus generation and therapeutic intervention across the central auditory circuit.

Funding
This work was supported by Clinician Scientist Developmental Award Sponsored by the American Otological Society (GJB).

PS 250

The Effects of Noise-induced and Age-related Hearing Loss on Parvalbumin and Perineuronal Net Expression in the Mouse Auditory Cortex

Anna Nguyen; Dustin Brewton; Shafika Khaleel; Oliva Jiminez; Eloy Rosales Pena; Khaleel Razak
University of California, Riverside

48 million Americans are affected by hearing loss. Consequences of this condition include presbycusis, tinnitus, poor speech discrimination, social isolation and cognitive decline. The dysfunction at the level of the auditory cortex following noise-induced or age-related hearing loss is not well characterized. Here, we quantified the expression of parvalbumin (PV) and perineuronal nets (PNN) in the auditory cortex of permanent noise-induced (PNIHL) and age-related hearing loss (ARHL) mouse models. PNIHL mice were exposed to 6-12 kHz noise at ~103 dB for 8 hours. Two strains of mice (C57, CBA) were compared for ARHL, the C57 mice line develop accelerated hearing loss while the CBA line is more resistant to ARHL.

Cortical PV+ cells are inhibitory interneurons and are known to decrease with age in C57 mice model of accelerated hearing loss. Perineuronal nets (PNN) are extracellular structures that form near the end of the critical period during development and primarily surround the soma of PV+ interneurons, implicating these components in the maturation of cortical circuits. In addition, PNNs are known to protect PV cells against oxidative stress.

PNIHL mice did not present a difference in the number of PV+, PNN+ and colocalization of PV+/PNN+ at 1, 10, or 30 days following hearing loss compared to controls. Moreover, the overall cell count did not change as a result of PNIHL. Thus, hearing loss caused by noise did not induce morphological and parvalbumin cell death nor degradation of the specialized extracellular matrix, the PNNs, at least in the short term (≤ 30 days).

PV+, PNN+, and PV+/PNN+ cell populations decrease with age in the C57 mouse strain, but not in the CBA mouse strain. Moreover, PV negative/PNN+ cell populations do not decrease with age, indicating that the decrease of PNN is restricted to PV+ cells. Alternatively, PV+/PNN negative cells decrease with age, indicating that the loss of PV+ cells is more general. Due to PV's contribution to auditory temporal processing, the decline of PV+ cells in the auditory cortex with age may indicate a functional role of PV in presbycusis. The PNN loss that occurs selectively around PV+ cells suggests the loss of PNN may make PV+ cells susceptible perhaps through oxidative stress. Future studies will examine the impact of permanent and temporary hearing loss on auditory cortical aging and PV/PNN expression.

PS 251

Circuit level effects of sound trauma in the auditory cortex

Marcus Jeschke[1]; **Max Happel**[2]; Konstantin Tziridis[3]; Holger Schulze[3]; Frank Ohl[2]
[1]University Medical Center Goettingen; [2]Leibniz-Institute for Neurobiology; [3]University Erlangen-Nuremberg

Environmental exposure to intense sounds is a major risk factor for developing hearing deficits and hearing loss. Further, such traumata are one key reason for the development of chronic tinnitus with increasing prevalence in society. While peripheral damage is considered to be the initial driving force of many pathophysiological phenomena in the entire auditory pathway, long-term reorganizations of central brain activity are increasingly recognized as a fundamental etiological factor. Along this line, many studies indicate that tinnitus is related to maladaptive changes in cortical circuits of audition following partial functional deafferentiation of defined cochlear frequency channels. However, we still lack a sufficient circuit understanding of sound trauma consequences on auditory cortical physiology.

Here, we investigated pathophysiological changes in circuits of auditory cortex (AC) at several time points after sound trauma. Sound trauma was induced in anesthetized Mongolian gerbils by presenting a 2 kHz pure tone at 115 dB SPL for 75 min. Pure tone-evoked laminar current source density (CSD) profiles in AC were recorded before, immediately after the sound trauma and after 4 weeks of recovery. We characterized respective changes of CSD-derived frequency-response-functions and rate-level-functions at specific locations within

the tonotopic gradient of AC. At the trauma frequency, sound trauma led to an increase in threshold of up to 60 dB. Increase in threshold was extending the trauma frequency region strongly biased towards higher frequencies (up to 2.5 octaves away), not readily explained by the spectrum of the delivered sound trauma. By utilizing the analysis of the relative residual CSD as a quantitative measure of horizontally routed corticocortical activity, we dissociated effects on cortical activity inherited by subcortical input structures and those emerging from altered corticocortical processing. Such changes in lateral cortical processing were only seen acutely after the sound trauma induction, particularly in the high-frequency neighborhood. After 4 weeks of recovery, this imbalance of local vs. lateral processing was compensated at all cortical sites of measurement. We further observed corresponding qualitative changes of the laminar synaptic activation pattern immediately after the trauma which were characterized by a stronger recruitment of synaptic inputs in infragranular layers and altered supragranular inputs.

In summary, our findings suggest that sound-trauma-induced plastic rearrangements in auditory cortex are not limited to the thalamocortical input projections corresponding to the deafferented regions but strongly involve lateral projections from corticocortical circuits. Moreover, the relative contributions of thalamocortical and intracortical inputs to trauma-induced reorganizations show marked temporal dynamics

Funding
This work was supported by a grant from the Deutsche Forschungsgemeinschaft (DFG; SFB-TRR 31) to F.W.O. and a grant from the Interdisciplinary Center for Clinical Research (IZKF, Project E7) at the University Hospital of the University of Erlangen-Nuremberg to H.S.

PS 252

Optoacoustic effects explain cochlear laser responses

Peter Baumhoff[1]; Nicole Kallweit[2]; Andrej Kral[1]
[1]Hannover Medical School; [2]Laser Zentrum Hannover e.V.

Intracochlear stimulation with pulsed laser emissions has been shown to evoke neuronal responses. The mechanism of excitation is still obscure. While intact cochleae can easily be stimulated by pulsed lasers, no convincing results of laser stimulation in profoundly deaf ears exist. In this study we characterize laser induced intra-cochlear responses through a combination of neuronal- and pressure recordings in-vivo and a comparison to ex-vivo results.

We recorded cochlear compound action potentials (CAPs) and multi unit activity (MUA) along the tonotopic axis of the inferior colliculus (IC) in 23 anaesthetized adult guinea pigs. Hearing condition was quantified by acoustic stimuli and CAP recordings. Two laser systems were used for stimulation: A tunable optical parametric oscillator (Ekspla NT342A; nanosecond pulses; 420 nm to 2200 nm) and an infrared neural stimulator (Capella R-1850; pulses at 10 µs to 20 ms; 1800 nm to 2000 nm). Optical pulses were delivered to the cochlea through an optical fiber inserted through a basal cochleostomy.

We additionally recorded pressure changes at the cartilaginous external meatus in-vivo, at the bony external meatus in a bone preparation and perpendicular to the beam-paths in air. A Fourier frequency analysis was performed on the recorded pressure signals.

In hearing condition, responses were observed in IC units with best frequencies (BFs) between 5 kHz and 10 kHz. The frequency range did not depend on laser wavelengths, but the response rates were highest for pulses in the near-infrared range (NIR). As a rule, frequency regions with the lowest acoustic response thresholds also had the lowest response thresholds for laser pulses.Pressure measurements in air demonstrated optoacoustic effects of up to 60 mPa (peak sound-pressure levels of up to 70 dB SPL p.e.). Maximum levels and spectral frequencies corresponded with the response characteristics of CAPs and MUA laser responses. We did not observe laser induced responses after pharmacological deafening. Electric stimulation after deafening resulted in normal response thresholds and rates, confirming normal auditory nerve function and absence of neuronal laser stimulation.

Pulsed laser emissions in the cochlea result in acoustic pressure changes. The frequency spectrum of laser-evoked sounds had high power in low frequencies (below 10 kHz). All aspects of neuronal responses could be explained by optoacoustic stimulation. Deafening completely eliminated laser responses. None of our results was consistent with any direct neuronal stimulation by pulsed lasers.

Supported by DFG (Cluster of Excellence Hearing4All), EU ACTION (FP7/ICT project 611230) and MedEl Company, Innsbruck, Austria.

Funding
DFG (Cluster of Excellence Hearing4All) EU ACTION (FP7/ICT project 611230) MedEl Company, Innsbruck, Austria

PS 253

Optogenetic Stimulation of Mouse Cochlear Nucleus in an Auditory Brainstem Implant Model using Transgenic Lines for Cell-specific Expression of Opsins

Ariel Hight[1]; **Shreya Narasimhan**[2]; Xiankai Meng[3]; Albert Edge[3]; M. Christian Brown[3]; Daniel Lee[3]
[1]Harvard University Medical School; [2]École polytechnique fédérale de Lausanne; [3]Massachusetts Eye and Ear Infirmary, Harvard Medical School

Introduction
The auditory brainstem implant (ABI) restores hearing sensations to individuals who are deaf and cannot benefit from a cochlear implant due to a damaged or abnormal auditory nerve or cochlea. ABI outcomes are variable and lag behind those of the cochlear implant (CI). The limiting factor of the ABI is likely due to electrical current spread, reducing the number of effective channels and increasing side effects

due to activation of nonauditory neurons. Optogenetics provides the promise of enhanced spatial resolution but targeted expression of opsins in the cochlear nucleus (CN) is needed to reduce non-specific activation of neighboring photo-sensitized neurons. In this study, we explore the implications of delivering visible blue light using a laser collimator and targeting stimulation to specific cell types in the CN by employing 7 unique transgenic mouse lines.

Methods

Cell specific expression of opsins were generated by breeding either floxed-ChR2 or floxed-ChETA mice with one of the following: Bhlhb5-cre (Meng et al. 2014), Atoh1-cre, Parvalbumin-cre, Nestin-cre, and CaMKII-cre (jax.mice.org). Moreover, we also tested VGlut2-ChR2, and Serotonin-ChR2. Evoked neural activity were measured using standard auditory brainstem response (ABR) electrode configurations, and multi-unit activity in the inferior colliculus was quantified using a single-shank 16-site recording probe (Neuronexus) placed along the tonotopic axis. The focused beam of light (32 µm diameter) was shifted between a 3x7 matrix along the rostro-caudal and medio-lateral axis, respectively. Post-experiment histology demonstrated opsin expression among many cell types of the cochlear nucleus.

Results

Optically evoked ABRs (oABR) were measured in 3 out of 7 transgenic lines- Bhlhb5-ChR2, Atoh1-ChETA, and VGlut2-ChR2. Of these 3 lines, neural activity in IC was observed during light stimulation of the CN of Bhlhb5-ChETA and Atoh1-ChETA mice. Shifts in evoked activity along the IC tonotopic axis spanned the entire frequency range of the IC stimulation shifted along the medio-lateral axis of the CN. No shifts were measured in the rostral-caudal axis. Histological analysis of all transgenic lines reveals expression of opsins in the cochlear nucleus. Opsin expression is consistent with previously published results on expression patterns of promoters and transcription factors.

Conclusion

Histological evaluation of 7 transgenic lines show expression of opsins in the CN, but only a limited number of these lines can be used for optical stimulation in an auditory brainstem implant model. These results suggest that the selection of promoter or transcription factor for targeting cell-specific opsin expression is essential for an optically-based ABI.

Funding

Fondation Bertarelli and NIH F31 DC014871-01

PS 254

Optogenetic Stimulation in a Mouse ABI Model Reveals Superior Access to the Tonotopic Axis Compared to Electrical Stimulation

Shreya Narasimhan[1,2]; **Ariel Hight**[3]; Amelie Guex[4]; Stephanie Lacour[4]; M.Christian Brown[2]; Daniel Lee[2]

[1]EPFL; [2]Massachusetts Eye and Ear Infirmary, Harvard Medical School; [3]Harvard Medical School; [4]Federal Institute of Engineering, Lausanne, EPFL

Introduction

The auditory brainstem implant (ABI) provides hearing sensations to patients not eligible for cochlear implants because of a damaged or missing auditory nerve. Clinical outcomes among ABI users are variable and lag behind those with cochlear implants (CI). A possible explanation for this may be the spread of electrical stimulation activating large regions of the cochlear nucleus (CN), compromising the delivery of frequency cues. This may explain the limited performance of ABI subjects (Colletti and Shannon 2005). Our study aims to evaluate how well frequency cues are provided by comparing the clinical approach using symmetrical biphasic electrical pulses with: 1) electrical stimulation using novel pulse waveforms and 2) optogenetic stimulation using focused beams of light in an acute mouse ABI model. Optogenetics uses blue light to activate neurons expressing light-sensitive proteins, called opsins.

Methods

Surgical exposure of the CN is performed acutely in CBA/CaJ or Transgenic mice [Kozin et al 2014, JoVe]. Electrical stimulation is delivered via an 8–channel microelectrode array [Guex et al. 2015]. Electrodes are evenly spaced across the entire CN. Four different charge-balanced waveforms are tested in monopolar stimulation conditions at 28 pulses/s: symmetric and asymmetric biphasic, and asymmetric triphasic. Waveforms are designed to target cell bodies or fibers or deeper layers of tissue [Macintyre and Grill 2002]. Light stimulation is delivered by a diode laser at 28 pulses/s. Light beams are focused using an adjustable laser collimator [Hight et al. 2015]. To compare with electrical stimulation, the beam of light is shifted along the rostral-caudal and medio-lateral axes. The transgenic line used is Bhlhb5-ChR2 [Meng et al 2014]. For both types of stimulation, evoked neural activity is measured in the inferior colliculus using a single shank, 16-site recording probe inserted across the tonotopic axis of the IC. Access to the tonotopic axis is evaluated by measuring the center of evoked-activity along the recording sites in the IC as a function of stimulation site on the CN.

Results and Conclusions

With optical stimulation, movement of the stimulus along tonotopic axis of the CN resulted in shifts in the response areas in the IC (n=4 mice). With electrical stimulation, shifts were difficult to observe mainly because the response areas in the IC were so large (n=5 mice). These experiments suggest that optogenetic stimulation may provide better frequency cues than electrical stimulation in mouse models of the ABI.

Funding
This work is funded by the fondation Bertarelli

PS 255

Direct Intracochlear Acoustic Stimulation using a PZT Microactuator

Clifford Hume; Chuan Luo; Irina Omelchenko; Robert Manson; Guozhong Cao; Elizabeth Oesterle; I-Yeu Shen
University of Washington

Combined electric and acoustic stimulation has proven to be an effective strategy to improve hearing in some cochlear implant users. We describe our continued work to develop an intra-cochlear acoustic actuator. The actuator takes the form of a silicon membrane driven by a piezoelectric thin film (PZT) that is 800 microns by 800 microns wide, with a diaphragm thickness of 1 μm in silicon and 1 μm in PZT. In the current study, we established an acute guinea pig model to test the actuator for its ability to deliver auditory stimulation to the cochlea in vivo.

A series of PZT microactuator probes was fabricated and tested in vitro using laser Doppler vibrometry to measure the velocity of the diaphragm when driven by a swept-sine voltage from 0-100 kHz. A spectrum analyzer was used to obtain a frequency response function (FRF) and determine the natural frequency and gain of the FRF. The impedance and phase angle of each probe was also measured to assess current leakage.

Nine guinea pigs were used for a series of in vivo tests. ABR measurements at 4, 8, 16 and 24 kHz were obtained prior to surgery and after each subsequent manipulation. Using a dorsal approach, the PZT probes were placed through the round window into the scala tympani. An oscilloscope was used to determine calibrated voltage values and acoustic stimuli were delivered via the actuator. A mechanically non-functional probe was used to assess current leakage. In some animals, an ear level ABR was obtained after removal of the probe to assess loss of hearing related to the procedure. Wave I peak latencies, interpeak latencies and wave I amplitude growth were calculated for both auditory and microactuator stimulation to compare stimulation via an ear canal microphone vs the intracochlear PZT probe. In some animals, the temporal bone was harvested for histologic analysis of cochlear damage.

We show that the microactuator has the desired response characteristics in vitro and is capable of stimulating auditory brainstem responses in vivo in an acute guinea pig model with latencies and growth functions comparable to stimulation in the ear canal. Our results suggest that this approach is promising to be effective and minimally traumatic. Further experiments will be necessary to evaluate the efficiency and safety of this modality in long-term auditory stimulation and its ability to be integrated with conventional cochlear implant arrays.

Funding
NSF CBET-1159623, NIDCD P30 DC-04661, NICHD P30 HD-02774, U54 HD083091

PS 256

Micro-Goldwire Electrode for Neural Activity Recording

Yingyue Xu[1]; Xiaodong Tan[1]; Nan Xia[2]; Claus-Peter Richter[1]
[1]Northwestern University; [2]Chongqing University

Background
The electrode that can chronically record neural activity from individual neurons in awake animals has developed into the ideal tool for neurophysiological and neuroprosthetic research. These electrodes, being able to record neural activities from awake animals, can facilitate the investigation of neurophysiological studies since anesthesia is a confounding factor for neural activities. Such electrodes can also serve brain-interfacing neuroprosthetic devices: chronic implantation in the neural tissue and send information to artificial devices. The purpose of this study is to investigate the mechanical and biological properties needed for chronic neural recording electrodes, and design such electrodes and test their performances.

Method
To chronically record neural activities from awake animals, the core material of the electrode should firstly be compliant. Thus it can follow the movement of brain tissue and reduce tissue injuries and local inflammations which may be the main reason behind the deteriorating recording capability of existing electrodes over time. Micro-goldwire (diameter 25 μm with 5 μm insulation) featuring ultra-flexibility was selected as core materials. Multiple wires were soldered to a multi-channel flexible printed circuit board using conductive silver epoxy. In addition, the surface materials of the electrode should feature stiffness for insertion and also biocompatibility for the longevity of recording capabilities. The previously described gelatin coating is known to have the mechanical stiffness to penetrate neural tissue and biological degradability, leaving minimum chronic effects in the surrounding neural tissue. Here, gelatin (40% slution) was used to coat the goldwires. Currently, these designed micro-goldwire electrodes has been successfully tested for acute recording in the inferior colliculus (ICC) of cats and guinea pigs. Chronic implantation and recording will also be tested in the near future.

Results
Gelatin coating of the electrode was dissolved in the tissue within minutes after insertion, which was estimated by the gradually detectable neural activity. Electrode movements were observed following the movement of the brain induced by breathing. Stable neural activities in the ICC were recorded largely independent of such brain motion, which leads to modulation of the neural responses when recorded with a stiff electrode.

Conclusion
We successfully fabricated implantable multi-channel micro-goldwire electrodes for neural activity recordings in ICC. Tentative results showed that stable recordings were achievable even in the presence of brain movements. Future studies will be carried out aiming at chronic implantation using this electrode and recording from awake animals.

Funding
Funded in parts with federal funds from the NIDCD, R01 DC011855

PS 257

Multichannel Cochlear Implant Systems for Chronic Unilateral and Bilateral Stimulation in the Free-Moving Mongolian Gerbil

Armin Wiegner[1]; Charles Wright[2]; **Maike Vollmer**[1]
[1]University Hospital Wuerzburg; [2]University of Texas, Dallas

The Mongolian gerbil is an established rodent model in auditory science for studying the effects of hearing loss and deafness. Its hearing sensitivity is similar to that of humans, and its inner ear is readily accessible for physiological and morphological studies. Gerbils are born deaf and have a lifespan of only 3 to 4 years that allows to fully control the gerbil's auditory environment throughout life.

Auditory deprivation can induce profound changes in both temporal and spectral neural processing of auditory signals. To explore whether normal function can be recovered by restoring auditory input during certain epochs, we have developed multichannel cochlear implant (CI) systems that allow chronic unilateral and bilateral stimulation in the free-moving gerbil**.**

For unilateral implantation, the flexible intracochlear electrode array consisted of five platinum sheet contacts embedded in a 350-µm diameter silastic carrier. For bilateral stimulation, each array consisted of two broadly spaced ball electrodes. A platinum-iridium ball contact under the neck muscle served as reference electrode. Electrodes were connected via submuscular lead-wires to a common head-mounted low insertion-force connector. For chronic stimulation, a multichannel commutator on top of the cage allowed low resistance cable rotation and stable electrical connectivity to the current source. Chronic stimulation was applied for 4-6 weeks. Impedances and electrically evoked auditory brainstem responses (eABR) were measured regularly. In final electrophysiological experiments, temporal and spectral/spatial response properties were recorded in the inferior colliculus (IC) and primary auditory cortex (AI).

During unilateral and bilateral chronic stimulations no device failure was observed, and animals showed no signs of distress. Median insertion depth of the most apical electrode was 4.7 mm, corresponding to 7.1 kHz. Large inter-individual differences in impedance were due to intrinsic electrode properties rather than differences in cochlear pathology. During chronic stimulation, impedances slightly increased across all electrode pairs by 2.8 kOhm (9%). EABR thresholds were stable for all electrodes. Typically, thresholds were lowest on apical contacts. Final electrophysiological mapping experiments revealed selective tonotopic electrode representation in IC and AI. Stimulation-induced changes in temporal coding of electric interaural time differences were evaluated in IC and auditory brainstem.

Cochlear implantation and chronic electric stimulation were stable and effective. The described CI systems are successfully used to study experience-dependent temporal and spectral plasticity in the deaf gerbil. This will provide a useful tool to determine the effects of psychophysical performance on functional plasticity and long-term structural changes in the deaf central auditory system.

Funding
Supported by DFG VO 640/2-1

PS 258

Cochlear Implant Use in Rodents

Julia King; Ina Shehu; Mario Svirsky; Robert Froemke
New York University, New York NY

Cochlear implants (CIs) are neuroprosthetic devices that can restore meaningful hearing to the profoundly deaf. However, asymptotic speech recognition and time to reach asymptotic levels are variable, ranging from 0 to 100% speech recognition and from <6 months to >2 years, respectively (Tyler et al., 2000; Chang et al., 2010). The causes of individual differences in adaptation and outcome are poorly understood; elucidating their underlying mechanisms can provide direction in development of additional post-implantation therapies to improve patient outcomes.

To investigate the neural mechanisms of CI adaptation, we developed a rat model of CI use. We first modified an existing surgical approach for rat CI insertion (Lu, Wu and Shepherd, 2005) to minimize surgical time and post-surgical side effects. Our basal turn cochleostomy approach increases insertion depth and allows for an 8-channel array to be inserted a full cochlear turn, comparable to typical insertion depths in humans. We then trained animals on a self-initiated auditory go/no-go sound detection and recognition task (Froemke et al., 2013; Martins and Froemke, 2015). We bilaterally deafened animals with a combination of cochlear trauma and intrascalar ototoxic drugs, and assessed the degree of both physiological (ABR) and functional (behavioral) hearing loss. In deafened animals, behavioral responses (d') dropped from 2.34±0.15 to 0.07±0.07 ($p<0.01$), while click ABR thresholds rose >50 dB SPL ($p<0.01$), with ABRs undetectable up to 90 dB SPL. These data indicate that animals were profoundly deaf. However, with training, animals fitted with a unilateral 2-channel CI regained hearing perception and improved in behavioral performance, with d' returning to 2.11±0.38 over a period of approximately two weeks. During sessions when the CI was inactivated, behavioral performance fell back to chance (d'=0.02±0.04, $p<0.01$), indicating that perceptual gains were directly due to CI use.

We are exploring neural responses that underlie changes in auditory perception with CI use. We performed multi-unit

mapping of auditory cortex in a naïve rat acutely bilaterally deafened and unilaterally implanted. We found that CI stimulation broadly activated auditory cortex and that evoked spiking in response to stimulation of separate CI channels was highly correlated (r=0.9), indicating that in the acute post-implantation phase the auditory cortex responds non-specifically to CI stimulation. This demonstrates that auditory cortex is activated by the CI, and suggests that refinement of cortical CI responses might be a promising mechanism for improving hearing with CI training.

Funding
NIDCD, NYU Grand Challenge

PS 259

Inferior colliculus responses to intra-cochlear electro-stimulation using Oticon Medical Animal Stimulation Platform in-vivo.

Lucy Anderson; Matthieu Recugnat; David McAlpine
University College London

Cochlear implants (CIs) are one of the most successful sensory implantable devices when judged by their ability to restore sensory function. However, compared to normal-hearing listeners, CI users are considerably disadvantaged in even a moderately challenging listening environment. Cochlear implant user performance has been improved by advances in CI insertion techniques and the number of electrode-channels on the array, but the uncontrolled current spread within the cochlea remains a major factor limiting CI efficiency.

In recent years, advances in CI performance have been led by improvements in signal processing technologies, in particular the development of strategies to limit the area of stimulation. Further advances in CI performance could be made through enhancement of the electrode-neuron interface. To achieve this, we need to better understand how the CI stimulation strategy relates to the biological properties of auditory neurons, and how this information is transformed along the auditory pathway. Our recent research has shown that by adding a rising slope to the electrical pulse shape it is possible to alter the response threshold of cultured SG neurons. To assess the potential for ramped pulses to limit the spread of neural excitation *in-vivo*, we generated a similar stimulation strategy using the Animal Stimulation Platform (ASP) developed by Oticon Medical on the basis of the new generation stimulation chip. This ASP allows the generation of complex electrical stimuli in various combinations of temporal and spatial configurations.

Here, we present extracellularly recorded data from the central nucleus of the inferior colliculus (ICc) of the urethane-anaesthetized, CI-implanted, guinea pig stimulated using the ASP. Stimulation via the CI evoked neural activity within selected regions of the ICc. Changing the spatial configuration of the stimulus waveform from a mono-polar biphasic square wave to one with a rising slope had no effect on the response threshold of ICc neurons. However, neural activity at supra-threshold levels was reduced as the rising slope of the stimulation waveform increased. This decrease in the spatial spread of excitation throughout the ICc in response to CI stimulation suggests that stimulation via ramped pulses may lead to greater frequency resolution and increased temporal fine structure, all of which could help improve the performance of CIs.

Funding
EU grant - Advancing Binaural Cochlea Implant Technology. Funding Program 7-Health. Ref #: 304912

PS 260

Relationship between ECAP Measures and Cochlear Health in Awake Guinea Pigs Using Measures Applicable to Human Subjects

Deborah Colesa[1]; Kara Schvartz-Leyzac[1]; Aaron Hughes[1]; Stefan Strahl[2]; Ning Zhou[3]; Yehoash Raphael[1]; Bryan Pfingst[1]
[1]University of Michigan; [2]Med-El GmbH; [3]East Carolina University

Introduction
Many studies using cochlear implants in animals have shown relationships between auditory-nerve survival and electrophysiological responses to electrical stimulation of the cochlea. These electrophysiological measures can potentially be useful in human subjects for non-invasive assessment of the condition of the cochlea near the cochlear implant electrodes. However, to be clinically useful, it is important that the measures be easily assessable in awake human subjects at various times during the long-term use of the implant. In the study reported here we measured electrically-evoked compound action potential (ECAP) amplitude-growth functions in guinea pigs using neural response telemetry and assessed the relationship between these measures and cochlear health. To assure that these measures were applicable in human subjects we conducted all measures in awake guinea pigs which had long-term, stable responses to electrical stimulation.

Methods
Electrophysiological measures included slopes of ECAP amplitude-growth functions in response to stimuli with 2.1 µs to 30 µs interphase gaps (IPGs), slope differences as a function of IPG, and area under the amplitude-growth functions. Stimulus amplitudes were below those eliciting any sign of facial-nerve stimulation. All current levels were in the range for which the guinea pigs would work routinely in self-initiated positive-reinforcement detection tasks. The ECAP amplitude growth functions were followed over time until stable and only the long-term stable measures (≥150 days post implantation) were used for comparison to anatomical measures of cochlear health. Measures of cochlear health included spiral ganglion neuron (SGN) density and inner hair cell (IHC) survival.

Results
The long-term stable electrophysiological measures were correlated with SGN survival to various degrees depending on both the electrophysiological metric and the presence of

IHCs. In the best cases, more than 50% of the variance in the electrophysiological measures could be accounted for by SGN survival.

Conclusions
Based on the results in guinea pigs, we conclude that clinically applicable ECAP measures can be used to assess conditions in the cochlea near the cochlear implant electrodes in human subjects. In a companion poster (Schvartz-Leyzac and Pfingst, 2016 ARO MWM) we assess the relationship in human subjects between these measures and speech recognition.

Funding
NIH/NIDCD R01 DC010412 and P30 DC05188 and an Organogensis Research Team grant from the U. of M. Center for Organogenesis.

PS 261

A Mouse Model of Hybrid Cochlear Implantation

Alexander Claussen[1]; Jonathon Kirk[2]; Brian Mostaert[1]; Viral Tejani[1]; Franklin Canady[1]; Murat Salihoglu[3]; Paul Abbas[4]; Kristien Verhoeven[5]; Marlan Hansen[1]
[1]University of Iowa Hospitals and Clinics; [2]Cochlear Americas; [3]GATA Haydarpasa Training Hospital; [4]University of Iowa; [5]Cochlear Technology Centre

Background
Improvements in cochlear implant (CI) design and surgical techniques now allow for preservation of functional acoustic hearing following implantation. However, some patients lose their residual acoustic hearing at extended time periods after implant activation (Kopelovich et al., 2014); the cause of this loss is not well understood. Here, we describe the development of a mouse model for residual hearing loss in hybrid cochlear implants. The model will be coupled with a tethered stimulator system developed for chronic electrical stimulation.

Methods
CBA/CaJ mice (n=7) aged 10-12 weeks underwent unilateral, left ear implantation with a 3-contact 0.15mm diameter electrode array. The electrode array was designed by Cochlear™ specifically for use in the mouse and other small rodents. Right ears served as non-operative controls. Hearing status was assessed via auditory brainstem response (ABR) and distortion product otoacoustic emissions (DPOAE) pre-operatively and at post-operative weeks 2, 4 and 6. Criteria for hearing preservation included post-operative ABR threshold shifts ≤15 dB at 8 and 16 kHz and a present DPOAE signal. X-ray imaging was performed at 6 weeks to evaluate intra-cochlear positioning of the electrode array.

Results
6/7 mice met our criteria for hearing preservation. 1 mouse was excluded secondary to absent DPOAE signal and ABR threshold shifts > 30 dB at all frequencies tested on all post-operative days. Operative ear ABR threshold shifts ≤15 dB were seen in the 8 and 16 kHz frequencies for all mice with slightly higher threshold shifts seen at 32 kHz. No significant difference ($p < 0.05$) in ABR threshold shift occurred between post-operative weeks 2 to 6. Preservation of DPOAE signal in the implanted ear was seen at all frequencies tested except at the 4 and 5.657 kHz f_2 frequencies. No significant difference ($p < 0.05$) in DPOAE signal between testing days was seen. X-ray imaging at post-operative week 6 revealed that all 6 electrode arrays maintained intra-cochlear positioning.

Conclusion
We show the feasibility of cochlear implantation with hearing preservation surgery in a mouse model. The device can be coupled to a Cochlear Nucleus Freedom implant emulator and CP910 sound processor via a free moving tether mounted within an animal housing. This allows programming using Custom Sound (Cochlear™), enabling chronic electric stimulation with clinically relevant programming strategies. This mouse model may be used to study exposure to both acoustic and electrical stimulation and the resulting pathophysiology.

Funding
Cochlear Americas contract, NIH/NIDCD Grant T32 DC000040, NIH/NIDCD Grant 5P30DC010362

PS 262

Comparison between two Strategies for Sound Intensity Coding in Cochlear Implants: Results based on eCAP and eABR on Chronically Implanted Guinea Pigs

Victor Adenis[1]; Boris Gourévitch[1]; Dan Gnansia[2]; Matthieu Recugnat[2]; Elisabeth Mammelle[3]; Yann Nguyen[3]; Jean-Marc Edeline[1]
[1]University Paris-Sud, Orsay; [2]Oticon Medical; [3]Pitié Salpêtrière, Paris

Background
Coding strategies to improve speech understanding in cochlear implanted patients have been improved over the last decades. Current processor technology allows new possibilities and the optimal coding strategy has not been necessarily tested yet. Many parameters can be manipulated to improve cochlear nerve fibers recruitment and to obtain a more focused activation at sound presentation. Among the different strategies which can be used for coding sound intensity, two have been already implemented in clinical devices: a louder sound can be coded, either by an increase in pulse amplitude, or by an increase in pulse duration. We compared these 2 strategies with the electrically evoked CAP (eCAP) and electrically evoked ABR (eABR) collected in chronically implanted guinea pigs. These physiological measurements were collected from 1 week to 4 months post-implantation.

Methods
Six guinea pigs were chronically implanted with cochlear implants (6 electrodes). After a week of recovery, the eCAP and eABR were tested once a week under isoflurane anesthesia. During each session, we tested the responses to 20 increments in pulse amplitude and 20 increments in pulse duration which largely overlapped in terms of total amount of delivered current. Each value of pulse amplitude/duration was repeat-

ed 128 times at 23Hz. The different waves of the eCAP and eABR were automatically detected by an in-house MatLab code, which quantified the amplitude and latency values of these waves.

Results
For the eCAP, we found that the amplitude and the duration strategy generated similar values of threshold, latency and maximum amplitudes. On average, this was also the case for the quantification of the different eABR waves. However, in two animals, we observed that despite similar threshold, the maximal values of the eABR were lower with the pulse duration strategy. Both for the eCAP and for the eABR, the slope of the growth function was steeper for the pulse duration strategy suggesting a potentially better recruitment with this strategy.

Conclusions
Our data suggest that the pulse duration strategy is a valuable strategy to mimic a growing sound level. In addition, some aspects of these results indicate either that spread of excitation might be more limited with this strategy or that it could be a better strategy for recruiting nerve fibers.

Funding
Supported by Oticon Medical

PS 263

Neural coding of ITD with bilateral cochlear implants using short inter-pulse intervals and amplitude modulation

Brian Buechel[1]; Kenneth Hancock[2]; Yoojin Chung[2]; Bertrand Delgutte[2]
[1]Harvard Medical School; [2]Massachusetts Eye & Ear Infirmary

Background
Coding strategies to improve speech understanding in cochlear implanted patients have been improved over the last decades. Current processor technology allows new possibilities and the optimal coding strategy has not been necessarily tested yet. Many parameters can be manipulated to improve cochlear nerve fibers recruitment and to obtain a more focused activation at sound presentation. Among the different strategies which can be used for coding sound intensity, two have been already implemented in clinical devices: a louder sound can be coded, either by an increase in pulse amplitude, or by an increase in pulse duration. We compared these 2 strategies with the electrically evoked CAP (eCAP) and electrically evoked ABR (eABR) collected in chronically implanted guinea pigs. These physiological measurements were collected from 1 week to 4 months post-implantation.

Methods
Six guinea pigs were chronically implanted with cochlear implants (6 electrodes). After a week of recovery, the eCAP and eABR were tested once a week under isoflurane anesthesia. During each session, we tested the responses to 20 increments in pulse amplitude and 20 increments in pulse duration which largely overlapped in terms of total amount of delivered current. Each value of pulse amplitude/duration was repeated 128 times at 23Hz. The different waves of the eCAP and eABR were automatically detected by an in-house MatLab code, which quantified the amplitude and latency values of these waves.

Results
For the eCAP, we found that the amplitude and the duration strategy generated similar values of threshold, latency and maximum amplitudes. On average, this was also the case for the quantification of the different eABR waves. However, in two animals, we observed that despite similar threshold, the maximal values of the eABR were lower with the pulse duration strategy. Both for the eCAP and for the eABR, the slope of the growth function was steeper for the pulse duration strategy suggesting a potentially better recruitment with this strategy.

Conclusions
Our data suggest that the pulse duration strategy is a valuable strategy to mimic a growing sound level. In addition, some aspects of these results indicate either that spread of excitation might be more limited with this strategy or that it could be a better strategy for recruiting nerve fibers.

Funding
Supported by Oticon Medical

PS 264

Extending a Leaky Integrate and Fire Model of the Electrically Stimulated Auditory Nerve Fiber for Pulse Train Stimulation

Marko Takanen; Bernhard Seeber
Technische Universität München

Cochlear implants provide hearing for people suffering from sensorineural deafness by directly stimulating auditory nerve fibers (ANFs). Ideally, the electrical stimulation should evoke a percept that contains the essential information about the auditory scene. However, current stimulation schemes cannot yet achieve this. Computational models of the electrically stimulated ANF could provide a useful tool for the developers, giving them estimates of the peripheral responses that different stimulations evoke.

Here, we present a functional model for the ANF response to biphasic electric pulse sequences able to consider pulse rate and parameters of the biphasic pulse. It is adapted from stochastic leaky integrate-and-fire model by Horne et al. (in review). In that model, the ANF is thought to integrate incoming electrical current and to release an action potential (i.e., to spike) if the cumulative membrane voltage exceeds a stochastic threshold. The latency and jitter of the ANF neuron depend on how greatly the threshold is exceeded. Another underlying assumption is that exceeding the threshold triggers an action potential initiation process and that spiking may only occur after that process has been completed. The spike may still be cancelled if the neuron is hyperpolarized before the initiation process finishes.

We have now extended the model by Horne et al. to simulate the refractory and recovery behavior of the ANF neuron following the approach by Hamacher (PhD thesis, 2003) which dynamically changes the threshold. After a spike, the next action potential may be released only when an absolute refractory period has passed. Further, the gradual recovery of the neuron is simulated with a relative refractory period, during which the threshold is first increased and then gradually restored to the original level.

We show that the model is capable of reproducing ANF response statistics from previous studies. The extended model can account for various pulse train stimulations while preserving the ability of the original model to reproduce physiological data from single pulse stimulations. For instance, the model output reflects the relationship between the pulse rate and the neuron's firing pattern and efficiency. The model output is also in accordance with psychoacoustical data on how polarity orders of two consecutive biphasic pulses and their inter-pulse interval affect the threshold for the latter pulse. Limitations of the model are also identified and discussed.

Funding
Supported by BMBF 01 GQ 1004B (Bernstein Center for Computational Neuroscience, Munich).

PS 265

Heterogeneity of HCN Half-Maximal Activation Potentials Explains Variability in Intrinsic Adaptation of Spiral Ganglion Neurons

Jason Boulet; **Ian Bruce**
McMaster University

Background
It remains unclear as to why high-rate stimulation leads to variable outcomes of speech perception performance for people with cochlear implants (CIs). Although many factors might contribute to this perceptual variability, temporal interactions in the responses of spiral ganglion neurons (SGNs) likely contribute to variable constraints on acoustic information coding by CIs. Specifically, in response to high-rate electrical pulse train stimulation, electrical recordings of Type I SGNs have shown a large range in the degree to which they exhibit both subthreshold and spike-dependent adaptation of their excitability. A computational model by Negm & Bruce (IEEE TBME 2014) demonstrated that hyperpolarization-activated cyclic nucleotide-gated cation (HCN) channels may play an important role in regulating the degree of adaptation in response to pulse train stimulation. We hypothesize that experimentally observed heterogeneity in HCN half-maximal activation potentials could contribute to variability in adaptation.

Methods
We developed a stochastic computational membrane model of cat Type I SGN based on the Hodgkin–Huxley model plus HCN and low-threshold potassium (KLT) conductances. We compared the simulation results obtained with the older HCN channel model taken from VCN cells (Rothman & Manis, J Neurophysiol 2003) to those produced by a newer HCN model from SGNs (Liu et al., JARO 2014). HCN half-activation potentials were explored over a physiologically-plausible range of values. Various stimulus paradigms were implemented to provide predictions of published *in vivo* CI stimulation data, including build-up and recovery of adaptation (Zhang et al., JARO 2007; Miller et al., JARO 2011) and refractory functions (Miller et al., JARO 2001).

Results
The simulation results showed that changing the half-activation potential of either type of HCN model could greatly influence the strength of adaptation that a model SGN exhibited to pulse-train stimuli, from strongly-adapting to non-adapting. Overall, the published data was best explained by the newer HCN channel model combined with the KLT channel model. Model absolute refractory periods were also observed to be within the known physiological range, in contrast to the alternative adaptation model proposed by Miller et al. (JARO 2011).

Conclusions
Our results suggest that physiologically-realistic variation of HCN half-maximal activation potentials could determine the range of adaptation and recovery from adaptation seen in the physiological data while maintaining refractoriness within physiological bounds.

Funding
[The authors would like to thank Dr. Paul Manis for supplying his HCN(q,s) channel model code. Supported by NSERC Discovery Grant 261736.]

PS 266

Phase Processing in the Auditory System

Maxin Chen; Yingyue Xu; Xiaodong Tan; Claus-Peter Richter
Northwestern University

Background
Complex sounds are the combination of pure tones of different frequencies with varying amplitudes and phases. The speech processing algorithms of contemporary cochlear implants (CI) pick representing frequencies of sounds, and incorporate mostly the amplitude information, but neglect the phase. It is our interest to learn whether the phase is essential for CI users in speech perception, and how phase is processed. Two approaches were taken. Firstly, we investigate whether the disruption of phase information will influence speech perception of normal hearing individuals with reduced frequency components, mimicking inputs to CI users. Secondly, since auditory neurons preferentially fire at a certain phase in response to low frequency (<5 kHz) pure tone, i.e., phase locking, we examined whether phase locking can be identified in the auditory system in response to speech.

Method
10 sentences were selected as speech stimuli, and short-time Fourier transform was applied to extract the amplitude and phase information for different frequencies. Then, we picked

6 frequencies out of 65 bands following m-of-n selection rules in CIs, reconstructed speech signals with (1) original phase, (2) original phase shifted to a certain amount, and (3) randomized phase. Then these reconstructed sentences were played to normal hearing individuals to test intelligibility.

To further examine the phase locking in the auditory system to complex acoustic signals, responses to speech were recorded from isolated single units in the inferior colliculus of guinea pigs. The temporal patterns of the neural activity were examined.

Results
Our results showed that speech signals reconstructed using original phase shifted to a certain amount, and randomized phase of 6 out of 65 frequency components disrupted the intelligibilities to a great extent for normal hearing individuals. Histograms of the time differences between the neighboring two spikes showed neurons with low characteristic frequency (CF) preferentially fire with a certain repetition rate that is close to their corresponding CF.

Conclusion
Phase information is essential for speech perception of normal hearing individuals when reducing frequency components. Thus, CI users, with limited access of frequency information, may benefit from adding phase information. Further supporting evidence for the importance of phase locked firing of neurons was seen in low CF ICC neurons in response to speech signals. Future studies will focus on phase locking in the auditory neurons, and investigate how phase information is processed in response to running speech and music.

Funding
Funded in parts with federal funds from the NIDCD, R01 DC011855

PS 267

High Frequency Electrical Stimulation May Completely Block Firing after a Single Spike in Most Auditory Nerve Fibers

David O'Gorman
Boston University

An electrode of a cochlear implant is typically used to deliver current, but can also be used to record a neural response. Such recordings show that, when the rate of a uniform pulse train exceeds about 2 kHz, the response elicited by the second and all subsequent pulses is greatly reduced in amplitude relative to the first (Wilson et al., 1997). The aim of this poster is to use a biophysical model to fit these data and then to use this model to infer the mechanism that suppresses the response after the first pulse.

Methods
In this work, it was assumed that the response is determined by the voltage-sensitive channels that underlie spike generation and that the properties of these channels are similar to those measured in the primary-like cells of the guinea pig cochlear nucleus by Rothman and Manis (2003). The *Mathematica* software was used to numerically solve the differential equations that summarize their measurements.

Results
Above 2 kHz, the model predicts firing to only the first pulse, with smaller, non-spiking responses generated subsequently. The amplitude of these non-spiking responses decreases with decreasing inter-pulse time, with the rate of decrease determined by the concentration of the low-threshold potassium channels (gLT). Adjusting gLT to a value of 0.46 (relative to the sodium channel concentration) allows this model to predict, to within a few percent, the corresponding reduction present in the data. This best-fitting value of gLT is within the range observed by Rothman and Manis in their study (0.1-0.6).

Conclusion
These results suggest that *steady*, *unmodulated* high rate stimulation (>2 kHz) prevents the de-activation of low-threshold potassium channels after an initial action potential, thereby blocking subsequent firing; the diminished responses apparent in intracochlear measurements likely reflect synchronous non-firing events.

Implication for Cochlear Implants
Speech, especially its higher frequency components, is sparse, meaning that the acoustic energy is localized in short, discrete "packets" that are separated in time. By properly accounting for the influence of low-threshold potassium channels, it should be possible to optimize the neural representation of these "packets." This optimization would likely improve the ability of an implantee to separate a talker of interest from competing ones (Mi and Colburn, 2015).

PS 268

AMPA Receptor Modulation by Synaptically Released Zinc.

Bopanna Kalappa[1]; Charles Anderson[1]; Jacob Goldberg[2]; Stephen Lippard[2]; Thanos Tzounopoulos[1]
[1]University of Pittsburgh; [2]Massachusetts Institute of Technology

AMPA receptors (AMPARs) mediate the vast amount of fast excitatory neurotransmission in the mammalian nervous system. As a result, AMPAR mediated synaptic transmission is implicated in nearly all aspects of neural function, plasticity and development. Despite the central role of AMPARs in excitatory synaptic transmission, the fine tuning of synaptic AMPAR responses by endogenous modulators is poorly understood. Here we show that synaptic zinc, co-released with glutamate by single pre-synaptic action potentials, inhibits AMPAR currents in dorsal cochlear nucleus (DCN) and hippocampal excitatory synapses. Exposure to loud sound reduces presynaptic zinc levels in the DCN synapses and abolishes zinc inhibition, implicating zinc in experience–dependent AMPAR synaptic plasticity. These results establish zinc as an activity-dependent, endogenous modulator of AMPARs that tunes fast excitatory neurotransmission and plasticity at glutamatergic synapses.

Funding
This work was supported by funding from the NIH: SJL:RO1-GM065519; TT: RO1-DC007905

PS 269

Control of Action Potentials in Cartwheel Cells by Ca2+-Induced Ca2+ Release

Tomohiko Irie; Laurence Trussell
Oregon Health Science University

Background
Intracellular Ca^{2+} stores in the endoplasmic reticulum (ER) play crucial roles in cytosolic Ca^{2+} regulation and cellular activity in muscle and neurons. In many cases, the release of ER Ca2+ is controlled by ryanodine receptors, which are opened by Ca^{2+} from the cytosolic side and contribute to amplification of Ca^{2+} signaling. This Ca^{2+}-induced Ca^{2+} release (CICR) can be triggered by activation of voltage-gated Ca^{2+}channels and enhances the activity of Ca^{2+}-activated K+ channels. However, quantitative relationships among these channels and intracellular Ca^{2+} dynamics in neurons are poorly understood.

The dorsal cochlear nucleus (DCN) of mammals integrates auditory and non-auditory information, and is thought to contribute to monaural sound localization. The glycinergic cartwheel interneurons of the DCN, have long been known to possess abundant subsurface cisterns of ER in their somata, as well as prominent Ca^{2+}-dependent signaling. Therefore, cartwheel cells may therefore be a good model for quantitative study of CICR.

Methods
We investigated CICR-induced changes in cartwheel cell firing in current clamp, and associated outward currents in voltage clamp, using patch-clamp recordings in brainstem slice preparations of P18-26 mice.

Results
Blockade of CICR by ryanodine dramatically changed the spontaneous spike output of cartwheel cells, transforming predominantly spontaneous simple spikes into burst firing, and lengthening the duration of spontaneous complex spikes. In voltage clamp recordings in the presence of synaptic blockers, mild depolarizations from rest led to appearance of spontaneous miniature outward currents (SMOCs), which were inhibited by iberiotoxin (a blocker of BK Ca^{2+}-activated K channels) or by a Ca^{2+}-free extracellular solution. Ryanodine also eliminated SMOCs, indicating that they are mediated by spontaneous CICR events triggered BK activation. Larger voltage steps activated transient outward current that was also Ca^{2+} sensitive and was reduced by ryanodine.

Conclusion
We propose that action potentials rapidly trigger BK channel currents through CICR, and that this process tunes the size and duration of complex spikes in cartwheel cells.

Funding
R01DC004450

PS 270

5-HT Differentially Modulates the Output of Auditory and Multisensory Inputs onto Fusiform Cells in the Dorsal Cochlear Nucleus

Zheng-Quan Tang; Laurence Trussell
Oregon Health and Science University

Background
Although the physiological function of serotonin (5-HT) has been intensively investigated in the CNS, it remains unclear how 5-HT regulates the integration of signals in sensory systems. The dorsal cochlear nucleus (DCN), which is involved in sound source localization, integrates auditory and multisensory signals and receives a dense serotonergic input. We have previously reported that 5-HT directly excites the fusiform principal cells. However, it is unclear how circuit-level information-processing properties in the DCN are modulated by 5-HT.

Methods
To address how 5-HT influences the neural circuit activity of the DCN, we used a combined electrophysiological, pharmacological and transgenic approaches in acute brain slices from P16-24 mice.

Results
After blocking inhibitory inputs with antagonists of glycinergic and GABAergic transmission, bath application of 5-HT reduced excitatory postsynaptic currents (EPSCs) evoked by stimulation of auditory nerve (AN), but not those evoked by stimulation of parallel fiber (PF) that carries multisensory signals. 5-HT decreased the inward component (EPSC), but increased the outward component (IPSC) of disynaptic currents evoked by AN stimulation, without changing disynaptic currents evoked by PF stimulation, suggesting that 5-HT selectively enhances AN-, but not PF-driven feed-forward inhibition onto fusiform cells. Therefore, 5-HT shifted the balance towards inhibition in auditory input processing, without changing the balance of excitation and inhibition in multisensory input processing. Strikingly, paired-recordings in inhibitory microcircuits demonstrated that the enhancement of feed-forward inhibition onto fusiform cells results from increasing excitability of inhibitory vertical cells by 5-HT, but not through a conventional presynaptic mechanism. Finally, under current-clamp conditions, due to interplay between an increase in neuronal excitability and a shift in the balance towards synaptic inhibition, 5-HT had little effect on spike firing probability evoked by AN stimulation. In contrast with 5-HT's effects on AN evoked spikes, 5-HT significantly increased firing probability of spikes evoked by PF-stimulation by directly increasing the excitability of fusiform cells.

Conclusion
Our findings demonstrate that 5-HT selectively reduces excitatory synaptic transmission of AN, but not PF inputs, and enhances AN-input- but not PF-input-driven feed-forward inhibition onto fusiform cells. These results suggest that modulation of sensory inputs in the DCN is input- and circuit-dependent, and provide a novel circuit mechanism by which 5-HT could shift the integration of sensory signals towards

enhanced responses to multisensory signals. Thus, we propose that 5-HT might facilitate the orientation to sounds of interest through “multisensory enhancement”.

Funding
NIH grants R01DC004450 and R01NS028901 (L.O.T.), Hearing Health Foundation (Z.Q.T.).

PS 271

Effect of the Modulation of Kv3 Potassium Channels on Neuronal Excitability of Dorsal Cochlear Nucleus Fusiform Cells, in Young and Adult Rats

Nadia Pilati[1]; Marcelo Rosato-Siri[1]; Giuseppe Alvaro[1]; Charles Large[2]
[1]Autifony s.r.l.; [2]Autifony Therapeutics

Kv3 potassium channels play a major role in determining the pattern and frequency of neuronal firing in several systems. In particular, Kv3 potassium channels are highly expressed in the auditory brainstem where they permit temporal fidelity and high-frequency firing of auditory neurons. The dorsal cochlear nucleus (DCN) is the first relay of the central auditory pathway. This nucleus is involved in the localization of sound in the vertical plane and is also the site of integration between multimodal sensory inputs and auditory information. The physiological role of fusiform cells (Fcs), the principal cells of DCN which display high level expression of Kv3 protein, has been extensively studied. Nevertheless the functional role of Kv3 conductance in this cell type remains to be clarified. The present study extends our understanding of the role of Kv3 channels in Fc cellular excitability and firing. We took advantage of the action of a novel series of proprietary small molecules (Autifony) that can modulate human and rat Kv3 channels (Rosato-Siri et al., 2015). We examined the effects of these compounds on Fc neuron firing, comparing their action with the effects of tetraethylammonium (TEA) at 1mM, which is a reasonably selective blocker of these channels at this concentration. In adult rat slices (3-5months), TEA significantly reduced the maximal firing frequency and altered the firing pattern by switching evoked firing from regular to irregular. This was accompanied by an increase in the action potential (AP) half width and a reduction in the after-hyperpolarization (AHP) amplitude. In contrast, bath perfusion of AUT3 enhanced the maximal FC firing frequency and regularity, reduced AP half-width and increased the AHP amplitude, consistent with positive modulation of Kv3-mediated currents.

Previous studies have shown that acoustic over-exposure (AOE) rapidly alters the excitability of DCN Fcs, which is associated with a reduction in Kv3-like potassium currents (Pilati et al., 2012). Selective action on FCs by pharmacological manipulation of Kv3 channels, could therefore have considerable potential for the treatment of hearing disorders such as noise-induced hearing loss and tinnitus.

References:
Pilati N, Large C, Forsythe ID, Hamann M (2012) Acoustic over-exposure triggers burst firing in dorsal cochlear nucleus fusiform cells. Hear Res. 283(1-2):98-106

Rosato-Siri MD, Zambello E, Mutinelli C, Garbati N, Benedetti R, Aldegheri L, Graziani F, Virginio C, Alvaro G, Large CH. (2015) A Novel Modulator of Kv3 Potassium Channels Regulates the Firing of Parvalbumin-Positive Cortical Interneurons. J Pharmacol Exp Ther. 354(3):251-60.

PS 272

Neural Selectivity to Behaviorally Relevant Sounds Emerges in the Auditory Brainstem

Patrick Roberts; Christine Portfors
Washington State University Vancouver

Background
Identifying sounds is critical for an animal to make appropriate behavioral responses to environmental stimuli, including vocalizations from conspecifics. Identification of vocalizations may be supported by neuronal selectivity in the auditory pathway. The first place in the ascending auditory pathway where neuronal selectivity to vocalizations has been found is in the inferior colliculus, but very few brainstem nuclei have been evaluated. Here, we tested whether selectivity to vocalizations is present in the dorsal cochlear nucleus (DCN).

Methods
We recorded extracellular neural responses to ultrasonic vocalizations in the DCN of awake, restrained CBA/CaJ mice. We focused our study on responses of fusiform cells because these are the output neurons of the DCN that project to the inferior colliculus.

Results
We found that fusiform cells responded selectively to mouse ultrasonic vocalizations. Most fusiform cells responded to vocalizations that contained spectral energy at much higher frequencies than the characteristic frequencies of the cells. To understand this mismatch of stimulus properties and frequency tuning of the cells, we developed a dynamic, nonlinear model of the cochlea that simulates cochlear distortion products on the basilar membrane. We preprocessed the vocalization stimuli through this model and compared responses to these distorted vocalizations with responses to the original vocalizations. We found that neuronal responses were driven by the cochlear distortions created by the vocalizations. In addition, the selective neuronal responses were dependent on the presence of inhibitory sidebands that modulated the response depending on the temporal structure of the distortion product.

Conclusion
We conclude that neural selectivity to vocalizations emerges in the dorsal cochlear nucleus. This suggests that selectivity among behaviorally relevant sounds begins at one of the lowest levels of auditory processing.

Funding
This work was supported in part by the National Institute of Deafness and Communication Disorders under Grant No. DC13414 to CVP

PS 273

The Temporal Precision of Vocalization Responses Increases from the Dorsal Cochlear Nucleus to the Inferior Colliculus

Richard Felix; Christine Portfors
Washington State University Vancouver

Background
A critical function of the auditory system is to extract meaning from complex acoustic signals, including animal vocalizations and human speech. This feat is accomplished in large part by accurately detecting and encoding temporal sound features. Although deficits in temporal processing accompany several prominent hearing disorders, the extraction of temporal information from vocalizations in the normal hearing brain remains poorly understood. The purpose of this study was to examine how coding of temporal information in vocalizations may change from the auditory brainstem to the midbrain.

Methods
Neuronal responses to tones and conspecific vocalizations were recorded in the dorsal cochlear nucleus (DCN) and inferior colliculus (IC) of normal hearing mice expressing channelrhodopsin under control of the VGlut2 promoter. Separate electrodes in the DCN and IC were controlled independently and pairs of neurons were chosen based on matching frequency tuning. The functional connectivity of cell pairs was examined by stimulating DCN neurons with pulses of light emitted focally at the recording site while concurrently recording responses in the IC. Additional dual DCN-IC recordings were conducted using a representative suite of vocalization syllables as stimuli. In cases where pairs of neurons responded to at least three common syllables, these syllables were presented repeatedly in succession, separated by silent periods of variable duration. This was done to provide a more natural stimulus, as syllables are typically emitted in bouts.

Results
Light-evoked activity of DCN neurons exhibited sustained spiking to square pulses of stimulation. Spiking was robust near threshold and quickly saturated with increasing light intensity. In cases where light stimulation of the DCN evoked spiking of single units in the IC, the IC spiking closely resembled that of the DCN. In contrast to direct light stimulation, sound evoked IC responses differed from those in the DCN. When vocalization bouts were presented, both neurons in the recorded pair responded selectively, however, IC responses had greater precision of spike-timing to individual syllables and segmented the elements contained in bouts more clearly compared to DCN responses.

Conclusion
Light stimulation of the DCN evokes similar spiking patterns in the IC, suggesting the DCN provides substantial excitatory input in these cases. The observation that responses to vocalizations are refined at the level of the IC argues for additional inputs that mediate these changes. Knowledge of how temporal features are extracted by the ascending auditory system has implications for a variety of hearing disorders associated with timing deficits.

Funding
Supported by NIDCD R01DC013102 to CVP

PS 274

Serotonin Affects Auditory Processing in the Dorsal Cochlear Nucleus

Cameron Elde[1]; Richard Felix[1]; Patrick Roberts[1]; Christine Portfors[2]
[1]Washington State University Vancouver; [2]Washington State University

Background
Deficits in neuromodulator circuits are implicated in a variety of disorders, many of which include auditory components. For example, serotonin (Hydroxytryptamine; 5-HT) has been implicated in tinnitus, a disorder in which the dorsal cochlear nucleus (DCN) is thought to play an integral role. Despite growing interest in this topic few studies have examined the effects of serotonin in the DCN *in vivo* and none (that we are aware of) have examined this effect in awake animals. Understanding the impact that exogenously applied 5-HT has on the behavior of neurons in the DCN of awake mice is an important step to better understanding the role of serotonin in the auditory system.

Methods
We recorded responses of neurons in the DCN of awake restrained CBA/CaJ mice before and after iontophoretic application of serotonin. Piggyback electrodes were used to iontophoretically apply serotonin. We evaluated how 5-HT affected responses to pure tones and broadband noise in well-isolated single neurons. We focused our recordings specifically on fusiform cells.

Results
We found that serotonin affected response properties of fusiform cells in a diverse manner. Application of serotonin increased spiking in some neurons and decreased spiking in others. Additionally, the application of 5-HT heterogeneously altered the sensitivity of DCN neurons to sound stimuli. Neurons with increased excitability tended to have increased spiking evoked by tones and broadband noise as well as a decrease in threshold. Neurons with decreased excitability tended to have decreases in evoked spiking and increased thresholds.

Conclusions
The main effect of serotonin on fusiform cells in the DCN was to modify excitability. This modification to excitability may affect responses to salient stimuli, however it is still unknown under what conditions serotonin is released in a behaving animal. In addition, it is possible that changes in both spiking behavior and sensitivity in the DCN due to changes in the

serotoninergic system could contribute to the physiological underpinnings of tinnitus.

Funding
Supported by NIDCD R15DC13414 to CVP

PS 275

Long-Term Effects of Bimodal Auditory-Somatosensory Stimulation on Ventral Cochlear Nucleus Units

Amarins Heeringa; Susan Shore
University of Michigan

Somatic tinnitus is defined as the condition in which a tinnitus patient can modulate his or her tinnitus with somatic maneuvers of the head and neck and is prevalent in up to 80% of tinnitus patients. Cross-modal auditory-somatosensory plasticity in the cochlear nucleus (CN) is of potential importance for somatic tinnitus. Previous studies showed alterations in auditory-somatosensory plasticity in the dorsal CN (DCN) in a noise-induced tinnitus model (Koehler and Shore, J Neurosci, 2012). The ventral CN (VCN) is also innervated by somatosensory ganglia and brainstem nuclei: VGLUT2-positive small boutons from the spinal trigeminal nucleus (Sp5) terminate in the VCN magnocellular region (Zhou et al., 2007, J Comp Neurol) and the dendrites of bushy cells are innervated by VGLUT2-positive terminals (Gómez-Nieto and Rubio, Neuroscience, 2011). Furthermore, hyperactivity, a widely accepted correlate of tinnitus, is shown in VCN neurons after cochlear damage (Bledsoe et al., J Neurophysiol 2009; Vogler et al., J Neurosci 2011). Therefore, we hypothesized that the VCN may also be involved in somatic tinnitus. As a starting point, this study explores the long-term effects of bimodal auditory-somatosensory stimulation on the VCN.

Single units of the VCN of normal-hearing guinea pigs were classified by assessing their response type to a pure tone at the best frequency. Somatosensory stimulation was introduced as a short burst of electrical deep-brain stimulation (100 μA) of the spinal trigeminal nucleus (Sp5). Tone rate-level functions were evaluated before, immediately after, 15 minutes after, and 30 minutes after bimodal stimulation, in which somatosensory stimulation preceded a 50 ms pure tone by 10 ms.

Pilot experiments revealed that tone-evoked firing rates, as measured by rate-level functions, were enhanced in onset units 30 minutes after bimodal stimulation. In contrast, rate-level functions of primary-like and primary-like with notch units showed suppression of evoked firing rates 30 minutes after bimodal stimulation. The effect was independent of whether the tones were presented at the best frequency.

The results demonstrate that cross-modal plasticity is evident in the VCN as well as the DCN, and has an enhancing effect for onset units, likely derived from D-multipolar or octopus cells. The suppressing effect for primary-like and primary-with-notch units is likely derived from spherical and globular bushy cells, respectively. These findings encourage investigating the effects of tinnitus-inducing noise exposure on bimodal plasticity in different cell types of the VCN.

Funding
Supported by NIH RO1-DC004825 (SES) and NIH P30-DC05188 (SES)

PS 276

NMDA and mACh receptors selectively mediate baseline activity and stimulus-timing dependent plasticity in the dorsal cochlear nucleus

Roxana Stefanescu; **Susan Shore**
University of Michigan

Fusiform cells (FC) in the dorsal cochlear nucleus (DCN) integrate auditory information relayed by the auditory nerve fibers synapsing on their basal dendrites and somatosensory information relayed by the axons of the granule cells, the parallel fibers (PFs) which synapse on their apical dendrites. Previous *in vitro* studies demonstrated spike-timing dependent plasticity (SpTDP) at PF-FC synapses characterized by a Hebbian “learning rule” (LR) mediated primarily by NMDA and endocannabinoid receptor CB1 receptors (Tzounopoulos et al. Nat Neurosci., 7(7):719-25, 2004). Furthermore, physiological activation of the M1/M3 muscarinic acetylcholine receptor (mAChR) converted Hebbian long term potentiation to anti-Hebbian long term depression (Zhao et al. J Neurosci., 31(9):3158-3168, 2011).

Stimulus-timing plasticity (StTDP) of FC responses, is an *in vivo* equivalent of SpTDP, which can be be produced by bimodal auditory-somatosensory stimulation: when sound and electrical stimulation of the trigeminal or dorsal column somatosensory pathways are presented in close temporal proximity (Koehler et al., PLoS One, 8(3):e59828, 2013, Wu et al., Front Syst Neurosci., 9:116, 2015). StTDP LRs are primarily Hebbian in the normal DCN but anti-Hebbian in animals with behaviorally confirmed tinnitus (Koehler et al. J Neurosci, 33(50):19647-56, 2013). However, little is known about the contribution of various receptors to FC StTDP.

In this study we attempt to clarify the contribution of the NMDA and mACh receptors to baseline FC activity and StTDP- induced LRs.

In vivo, baseline activity and StTDP induced LRs were evaluated after recordings from single FC in the healthy guinea pig DCN before and after infusion of the NMDA receptor antagonist (2μl CPP, 100μM) or the mAch receptor antagonist (2μl atropine 80 μM) to the FC layer of DCN.

Blocking NMDA receptors decreased the synchronization of FC spontaneous activity and induced three patterns of alternations of mean LR profiles including transitions from Hebbian to anti-Hebbian and suppressive profiles and from anti-Hebbian to Hebbian profiles. Blocking mACh receptors altered the initial Hebbian LRs inducing a dominant pattern of transition towards an anti-Hebbian profile.

We conclude that NMDA and mAch receptors contribute significantly to bimodal plasticity in the DCN by differentially modulating various features of FC activity and plasticity. These results may provide insight in the mechanisms of maladaptive plasticity associate with tinnitus pathology.

Funding
This study was supported by grant NIH R01-DC 004825(SES) and P30DC05188

PS 277

Targets of Descending Input from the Ipsilateral Inferior Colliculus in the Dorsal Cochlear Nucleus in the Mouse

Giedre Milinkeviciute[1,2]; Michael Muniak[1]; Katanyu (Tan) Pongstaporn[1]; Annie Cho[1]; David Ryugo[1,2]
[1]Garvan Institute of Medical Research; [2]University of New South Wales

Background
The dorsal cochlear nucleus (DCN) and inferior colliculus (IC) are two major central auditory system structures that are interconnected by ascending and descending projections. The main target of DCN projections is the contralateral IC with sparse terminations in the ipsilateral IC. In turn, the IC sends bilateral descending projections back to the DCN. The DCN has a complex internal circuitry consisting of inhibitory interneurons (stellate, cartwheel, Golgi, and vertical cells) and excitatory cells (granule, pyramidal, giant, and unipolar brush cells) that are contained in the molecular (I), pyramidal (II), and deep (III) layers of the DCN. This project is focused on identifying cells in the DCN that receive synaptic connections from descending axons originating from the ipsilateral IC. These data will help infer circuit mechanisms involved in signal processing at the cellular level.

Methods
Different cells types in the DCN are identifiable using published descriptions in conjunction with transgenic GlyT2EGFP and GAD67EGFP mouse models and neuronal tracer dye data. An anterograde tracer, biotinylated dextran amine (BDA), was injected into the left IC of unanesthetised CBA/Ca mice after recording electrophysiological multiunit frequency data. Brains were processed using standard histologic methods for visualization and examination of neuronal tracer dye using bright field microscopy (LM) and electron microscopy (EM). Cells contacted by BDA-filled synaptic terminals were identified.

Results
Ipsilateral descending projections from the central nucleus of the IC are topographic, frequency-specific, and excitatory in nature. Prominent BDA labelling was observed in layers II and III, where pyramidal and giant neurons—projection neurons of the DCN—reside, respectively. Sparsely distributed BDA-filled terminals were also observed in layer I. Granule, pyramidal, giant, and cartwheel cells are amongst the target cells that receive descending input from the IC.

Conclusions
Descending projections to pyramidal and giant cells of the DCN suggest a mechanism for frequency-specific enhancement of acoustic signals. Conversely, synapses on inhibitory cartwheel neurons might regulate the firing of pyramidal cells through feedback or lateral inhibition, facilitating the sharpening of acoustic signals. Input from the ipsilateral IC to granule cells is suggestive of signal modulation through parallel fibre synapses onto pyramidal and cartwheel neurons, respectively, and is likely influenced by somatosensory information that granule cells receive through mossy fibres. Controlled auditory signal amplification together with regulated inhibitory and multimodal non-auditory influences prompt speculation for involvement of the ipsilateral IC-DCN circuit in signal discrimination in noisy backgrounds.

Funding
Australian Postgraduate Awards (APA), NHMRC grant #1009482, #1087334, Fairfax Foundation, Alan and Lynne Rydge, Walker Family Foundation

PS 278

Cells Responding to Auditory Stimulus in the Paraflocculus of the Cerebellum

Courtney Voelker; Gabriella Sekerková; Marco Martina; Claus-Peter Richter
Northwestern University Feinberg School of Medicine

Background
Recent studies suggest that Unipolar Brush Cells (UBCs) are important in establishing the timing of synaptic transmission and are thought to be an important integrator cell in the cerebellum. This unique integrator role of UBCs may play an important role in auditory and vestibular function and pathologic processes such as ataxia, chronic imbalance, and tinnitus. However, UBCs are one of the least known neuronal cell types within the central nervous system, and more specifically, the cerebellum. We do know that UBCs are glutamatergic interneurons found in the dorsal cochlear nucleus (DCN) and the cerebellum, particularly in the paraflocculus and flocculus.

Purpose
The purpose of this study was to characterize the electrophysiological properties of cells responding to auditory stimulus in the paraflocculus of the cerebellum.

Methods
Adult gerbils were used because their paraflocculus is easy to access by opening the bulla. After anesthesia was induced, the gerbil's skull was fixed in a stereotactic head holder. The paraflocculus of the cerebellum was accessed through a postauricular incision followed by a bullectomy. The bone over the paraflocculus was carefully removed. To confirm the animals had normal hearing, an auditory brainstem response was conducted. Auditory tone input was given. Conventional glass micropipettes were used for single unit recordings. Spontaneous and pure tone evoked neural activity were recorded from cells located in a parafloccular area rich in UBCs. From the neural responses, basic characteristics

including best frequency, threshold, and Q10dB were determined from each tuning curve.

Results
Single unit recordings were made from seven neurons in the UBC-rich area of the paraflocculus. Tuning curves were generated. The characteristic frequency ranged from 881.18-1947.4 Hz (mean = 1314.2 Hz). The thresholds ranged from 23.98-64.6 dB (mean = 38.2 dB). The Q10dB ranged from 1.30-2.11 (mean = 1.59).

Outlook
The collected data will be used to further analyze the intensity-response contours, post stimulus time histograms (PSTHs), interspike time histograms (INTHs), firing efficiency (FE), and vector strength (VS).

Conclusions
Cells responding to auditory stimulus were successfully recorded in the UBC-rich area of the paraflocculus. The electrophysiologic characteristics closely match those of primary auditory nerve fibers in the gerbil. Data from more neurons need to be collected to confirm these results. Histology from filled neurons needs to be performed to confirm that the cells responding to auditory stimuli are UBCs.

PS 279

Hyper-Synchrony of Dorsal Cochlear Nucleus Fusiform Cells Correlates with Behavioral Evidence of Tinnitus

Calvin Wu; David Martel; Susan Shore
University of Michigan

Tinnitus, the perception of phantom sounds, is correlated with increased neural activity throughout the central auditory system. While hyperactivity resulting from homeostatic plasticity after deafferentation is observed in both the ventral and dorsal divisions of the cochlear nucleus, to date, hyperactivity as a tinnitus correlate has only been behaviorally verified in fusiform cells of the dorsal cochlear nucleus (DCN) (Brozoski, Bauer, & Caspary, J Neurosci 2002; Kaltenbach et al., Neurosci Lett 2004; Dehmel et al., J Neurosci 2012). In more central regions – the auditory cortex (AC) and inferior colliculus (IC) – hyperactivity, or increased spontaneous activity is accompanied by increased neural synchrony (Norena & Eggermont, Hear Res 2003; Bauer et al., J Neurosci Res 2008; Engineer et al., Nat Commun 2012). Neural synchrony in the DCN and its relationship to tinnitus has not yet been explored. In this study, we exposed guinea pigs to narrow band noise (1/2 octave, centered at 7 kHz, 97 dB SPL) for two hours to induce temporary threshold shifts. Tinnitus was assessed using gap/prepulse-inhibition of acoustic startle (GPIAS; Turner et al., Behav Neurosci 2006; Dehmel et al., Front Sys Neurosci 2012), and quantified using z-distribution differences between pre- and post-exposure GPIAS values. Once chronic tinnitus was established (z-score>95%; 8 weeks after noise-exposure), the animals were anesthetized with ketamine/xylazine and 16-channel probes were inserted stereotaxically into the DCN. Spontaneous activity was recorded from fusiform single units. Neural synchrony was computed using pairwise cross-correlations across recording sites. Unit spontaneous rate as well as pairwise correlation coefficients (synchrony) positively correlated with tinnitus z-scores. Spontaneous activity, however, did not correlate with neural synchrony, suggesting that while hyperactivity and hyper-synchrony in DCN are both physiological correlates of tinnitus they are generated by different mechanisms. The two correlates may also reflect different aspects of tinnitus perception. It has been suggested that synchrony may consolidate the phantom sound as an auditory object (Eggermont, Front Neural Circuit 2015), while spontaneous activity alters signal-noise gating mechanisms that decrease the ability for the auditory system to isolate external stimuli (Buran et al., J Neurosci 2014).

Funding
R01-DC004825 (SES), T32-DC00011 (CW), Tinnitus Research Consortium, Wallace H. Coulter Translational Research Partnership

PS 280

Endolymphatic Duct and Sac Development in Chick and Quail Embryos

Claire Schenkel; Sean Megason
Harvard Medical School

Previous studies in the Megason Lab have noted pulsing behavior and unique lamellar cell junctions in the developing endolymphatic duct and sac of the zebra fish. The goal of this study is to determine the generality of these features in other species with more complex otic anatomy. We chose to begin this investigation with avian embryos for several reasons: relative ease of setting up suitable incubation, culture, and imaging facilities; availability of fertilized eggs from commercial sources; and ease of access to the ear in the developing embryo, for both imaging and manipulations such as dye injections. Using a combination of *in ovo*, intact *ex ovo*, and explanted embryonic culture techniques in order to optimize embryonic health and longevity as well as imaging clarity, we have gained a sense of the three-dimensional anatomy of the live, developing endolymphatic duct and sac beyond the previously published body of literature from fixed paint-fill and slice preparations. By incorporating fluorescent protein transgenics that have not been previously used to study the ear, we have gained new perspectives on ear development without the necessity of potentially disruptive injection procedures. Additionally, parallel experiments performed in both chick and quail have illuminated differences in both anatomy and timing of otic development between species. Our preliminary timelapse imaging data suggest that the avian endolymphatic duct and sac may undergo inflations and deflations during development, though at a slower rate than in zebra fish. Using what we have learned about optimal culture and imaging techniques, we hope to replicate this finding in future work. Additional upcoming experiments will utilize electroporated fluorescent protein constructs to mosaically label the developing endolymphatic duct and sac epithelium, enabling investigation of the morphology of individual cells and possible lamellar junctions.

Funding
NIH, Harvard Speech and Hearing Bioscience and Technology Program

PS 281

Tempo-Spatial Requirements of Hedgehog and BMP Signaling During Middle Ear Development

Harinarayana Ankamreddy[1]; Xiao Yang[2]; Eui-Sic Cho[3]; Jinwoong Bok[1]
[1]Yonsei University College of Medicine, Seoul; [2]Beijing Institute of Biotechnology, Beijing, China; [3]Chonbuk National University School of Densitry

Background
The mammalian middle ear (ME), responsible for transmitting mechanical vibrations from the outer ear to the inner ear, is comprised of a chain of three ossicles: malleus, incus, and stapes. Any failure of ME function can lead to conductive hearing loss. ME ossicles are derived from neural crest cells (NCCs); malleus and incus are derived from NCCs that migrated into the first branchial arch (BA1), whereas the stapes is originated from NCCs that migrated into the BA2. The molecular mechanisms involved in NCC migration in forming ME ossicles remain unclear. Here, we investigated the role of Bmp4 and Hedgehog (Hh) in mediating ossicle formation.

Methods
To elucidate the mechanisms by which NCCs migrate and differentiate into specific ME ossicles, we generated mouse mutants to specifically manipulate Hh (*Wnt1-Cre;Smo$^{lox/lox}$*, *Wnt1-Cre;Smo$^{M2/+}$*) and TGF-β (*Wnt1-Cre;Smad4$^{lox/lox}$*) signaling in NCCs. Additionally, we generated *Foxg1-Cre;Bmp4$^{lox/lox}$* mouse mutants to knockdown Bmp4 signaling in the pharyngeal endoderm (PE).

Results
Previously, Hh signaling has been implicated in the NCC differentiation into ME ossicles. In our *Wnt1-Cre;Smo$^{lox/lox}$* mutants, in which NCCs failed to respond to Hh signaling, the initial condensation of the three ossicle anlages based on *Sox9* expression is observed at E10.5, but this expression disappeared by E11.5. These results suggest that Hh signaling is not required for initial condensation but for subsequent development of ME ossicles. Constitutive activation of Hh signaling in NCCs in *Wnt1-Cre;Smo$^{M2/+}$* mutants resulted in enlarged condensation in both BA1 and BA2 at E10.5 and in fused ME ossicles displaced from the inner ear at E15.5. Notably, we observed that initial condensation of stapes in BA2, but not in BA1, is closely associated with *Bmp4* expression domain in PE. Upon inactivation of TGF-β signaling in NCCs using *Wnt1-Cre;Smad4$^{lox/lox}$* mutants, NCCs failed to migrate to the prospective stapes region in BA2, but not in BA1. Similar phenotypes were observed in *Foxg1-Cre;Bmp4$^{lox/lox}$* mutants, in which endodermal *Bmp4* expression was abolished, suggesting that Bmp4 signaling emanating from PE dictates migration and initial condensation of NCCs to form stapes in BA2.

Conclusion
Our results suggest that Bmp and Hh signaling regulate migration and differentiation of NCCs into ME ossicles in a tempo-spatial-dependent manner, such that endodermal Bmp4 signaling guides NCCs to migrate to the prospective stapes region in BA2, and Hh signaling subsequently plays roles in maintenance and further development of ME ossicles.

Funding
Supported by the BK21 PLUS Project for Medical Science, Yonsei University

PS 282

Development of Biomarkers to Study Strial Development

Martín Basch[1]; Tiantian Cai[2]; Andrew Groves[2]
[1]Case Western Reserve University; [2]Baylor College of Medicine

The stria vascularis is an epithelial structure responsible for maintaining homeostasis in the mammalian cochlea. It is a highly vascularized tissue localized in the lateral wall of the cochlea, composed of three main cell types of distinct embryonic origin: the marginal cells, which line the scala media and are derived from the otic epithelium, the intermediate cells which are melanocyte-like cells derived from the neural crest, and basal cells which are adjacent to the fibrocytes of the spiral ligament and are of mesenchymal origin. Intersperesed between these cell layers there are numerous blood vessels that make the stria one of the most highly vascularized tissues in the human body. The function of the stria vascularis is essential for normal hearing and many human syndromes involving profound hearing loss are associated with defects in this structure. Over the past decade, a great effort has been made to understand the development of the sensory cells in the mammalian cochlea with the aim of applying their developmental principles to regenerative therapies. By contrast, very little is known about the development of the stria and the molecular identity of the cell types that form it. Our long term goal is to understand how the stria vascularis develops and apply this knowledge towards the regeneration and repair of the damaged stria. To accomplish this goal, we need to develop biomarkers that can be used to analyze the normal development of the stria as well as changes that may occur due to developmental or age related defects. We have recently completed a transcriptome profiling of the intermediate cells of the stria. In this study, we have identified over 2000 transcripts that are highly enriched in intermediate cells of the stria. In addition to serve as useful stria molecular markers, many of these genes will allow us to address developmental questions regarding the specification and differentiation of the stria vascularis.

Funding
Hearing Health Foundation

PS 283

FGFR2b Ligands in Cochlear Non-Sensory Specification and Inner Ear Morphogenesis

Suzanne Mansour[1]; Lisa Urness[1]; Xiaofen Wang[1]; Shumei Shibata[2]; Takahiro Ohyama[3]
[1]University of Utah; [2]Graduate School of Medical Sciences, Kyushu University; [3]Keck School of Medicine, University of Southern California

Signaling by FGFR2b ligands is required for many aspects of inner ear development. *Fgf3* and *Fgf10* are required for the earliest stage of otic placode induction and hindbrain-expressed *Fgf3* is required to initiate endolymphatic duct outgrowth from the otocyst, but continued expression of both genes within the otocyst suggests additional roles during morphogenesis of the labyrinth. Loss of *Fgf10* alone was implicated previously in semicircular canal agenesis. We showed that *Fgf10*$^{-/+}$ embryos also exhibit a reduction or absence of the posterior semicircular canal, revealing a dosage-sensitive requirement for FGF10 in vestibular morphogenesis. In addition, we found that *Fgf10*$^{-/-}$ embryos have previously unappreciated defects of cochlear morphogenesis, including a somewhat shortened duct, and, surprisingly, a substantially narrower duct. The mutant cochlear epithelium lacked Reissner's membrane and a large portion of the outer sulcus--two non-sensory domains. Marker data indicated a dual role for *Fgf10* in cochlear development: to regulate outgrowth of the duct and subsequently as a bidirectional signal that sequentially specifies Reissner's membrane and outer sulcus non-sensory domains (Dev Biol (2015) 400:59).

To address post-induction roles for FGFR2b ligands in otic development, we conditionally inactivated both *Fgf3* and *Fgf10* using Tg-*Pax2-Cre* and also induced a soluble (dominant-negative) form of FGFR2b at various times. We are evaluating otic epithelial morphogenesis, proliferation and patterns of gene expression. Our data show that *Fgf3* and *Fgf10* are required together to initiate both cochlear and vestibular outgrowth from the otocyst and that FGFR2b ligands are required continuously between E8.5 and E13.5 for otic morphogenesis. Progress in identifying the specific targets of FGFR2b signaling via RNA-seq analysis will be presented.

Funding
NIH/NIDCD R01DC011819

PS 284

SoxC transcription factors are essential for the development of the inner ear

Ksenia Gnedeva; A. James Hudspeth
The Rockefeller University

Background
Hair cells, the mechanosensory receptors of the inner ear, underlie the senses of hearing and balance. Unlike non-mammalian vertebrates, adult mammals cannot adequately replenish lost hair cells, which often results in deafness or balance disorders (1). In the present work we attempt to understand *why* the sensory organs of mammalian inner ear loose the capacity for hair cell regeneration.

Methods
In the sensory epithelia of the mammalian inner ear, the ability to produce hair cells declines late in development, largely as a result of a diminished proliferative capacity in supporting cells (2). Using high throughput RNA sequencing, we assessed gene expression during the critical stage and identified several transcription factors that are sharply downregulated contemporaneously with the cessation of hair cell production. Two of these—Sox4 and Sox11—were intriguing owing to their known roles in cell proliferation and neurogenesis (3-5). By creating inner ear-specific conditional knockouts for *Sox4* and *Sox11* in mice and by overexpressing these genes with adenoviral vectors we were able to study their role in the developing inner ear.

Results
We determined that *SoxC* genes are expressed in actively dividing supporting cells at the growing periphery of the utricle and in newly differentiated hair cells. The expression of both genes disappears in the mature sensory epithelium. We also found that conditional knockout of only a single allele of each of the *SoxC* genes in the inner ears of mice results in vestibular ataxia and partial deafness. The loss of both copies of *Sox4* and *Sox11* in the developing inner ear yields severely stunted vestibular and cochlear sensory organs that completely lack hair cells (Fig. 1 *A* and *B*). Finally, we demonstrated that *Sox4* and *Sox11* can reactivate supporting cell proliferation and hair cell production when overexpressed *in vitro* in mature, normally quiescent utricles (Fig. 1 *C* and *D*).

Conclusions
These results suggest that Sox4 and Sox11 are necessary for the production of hair cells and that their downregulation with age results in the loss of regenerative capacity in the sensory epithelia of the inner ear. Further characterization of the roles of SoxC in the developing ear might therefore lead to the discovery of ways to overcome hearing and balance impairment.

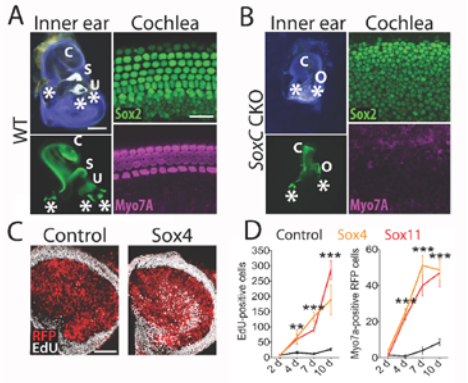

Fig. 1 The role of SoxC genes in the inner ear. (*A*) A wholemount preparation of the inner ear (top left) from a wild-type (WT) mouse shows the cochlea (C), saccule (S), utricle (U), and ampullae of semicircular canals (white asterisks). The scale bar represents 500 µm. Immunolabeling for Sox2 reveals the size and position of the sensory epithelia within these organs (bottom left, green). In the organ of Corti of a wild-type E17.5 embryo, supporting cells are immunolabeled for Sox2 (top, green) and the four rows of hair cells are immunolabeled for Myo7A (bottom, magenta). The scale bar represents 50 µm. (*B*) Identical preparations of the inner ear of a *Sox4 Sox11* doubly conditional-knockout mouse highlight the underdevelopment of the inner ear's sensory organs and the absence of hair cells. (*C*) In representative images of cultured utricles transfected 7 d previously with control or *Ad-Sox4-RFP* virus, transfected cells are marked by RFP (red) and proliferating cells are labeled for EdU (white). The scale bar represents 100 µm. (*D*) The numbers of EdU-positive cells and newly formed hair cells rise significantly in *SoxC*-transfected utricles between 2 d and 10 d in culture. The significances of the differences from control values are indicated by two asterisks ($p < 0.01$) or three asterisks ($p < 0.001$).

References:

1. Warchol, M. E. Sensory regeneration in the vertebrate inner ear: differences at the levels of cells and species. Hear Res 273, 72-79 (2011).
2. Burns, J. C., On, D., Baker, W., Collado, M. S. & Corwin, J. T. Over half the hair cells in the mouse utricle first appear after birth, with significant numbers originating from early postnatal mitotic production in peripheral and striolar growth zones. J Assoc Res Otolaryngol 13, 609-627 (2012).
3. Mu, L. et al. SoxC transcription factors are required for neuronal differentiation in adult hippocampal neurogenesis. J Neurosci 32, 3067-3080 (2012).
4. Jiang, Y. et al. Transcription factors SOX4 and SOX11 function redundantly to regulate the development of mouse retinal ganglion cells. J Biol Chem 288, 18429-18438 (2013).
5. Dy, P. et al. The three SoxC proteins – Sox4, Sox11 and Sox12 – exhibit overlapping expression patterns and molecular properties. Nuc Acids Res 36, 3101-3117 (2008).

PS 285

Sox2 in Inner Ear Neurosensory Specification

Martina Dvorakova[1]; Romana Bohuslavova[1]; Bernd Fritzsch[2]; Tetyana Chumak[3]; Josef Syka[3]; **Gabriela Pavlinkova**[1]

[1]Institute of Biotechnology CAS; [2]University of Iowa; [3]Institute of Experimental Medicine CAS

Introduction

Sox2 is a transcription factor expressed in the embryonic stem cells and neural stem cells and is necessary for maintaining pluripotency. During inner ear development, Sox2 is expressed in neurosensory precursors. The expression pattern of Sox2 indicates its possible role in the specification of neurosensory cells and in the regulation of differentiating transcription factors, such as *Neurog1* and *Atoh1*. Later in the development of the inner ear, Sox2 is downregulated in differentiated hair cells and neurons. Our aim is to determine the function of Sox2 in the development of the inner ear using the tissue specific deletion of *Sox2*.

Methods

We used the Cre-loxP system for *Sox2* gene deletion (*Islet1-cre; Sox2* $^{flox/flox}$). We used immunohistochemistry to analyze inner ear development: Sox2 and Prox1 for supporting sensory cells, Myosin7A (Myo7a) for hair cells, Tubulin for nerve fibers, Islet1 for ganglion cells and Pax2 for the early otic placode. The mutant inner ear morphology was reconstructed as a 3D structure and the organ of Corti was further examined by electron microscopy. Cranial nerves were visualized by the dye tracing method.

Results

The conditional *Sox2* homozygous mutants (*Sox2* CKO) died shortly after birth. The morphology of the mutant inner ear was severely affected. The vestibular system had disconnected semicircular canals. The size of sensory epithelia of the vestibular organs was significantly reduced, missing cristae and reduced utricle and sacculus. The length of the cochlea was not altered in *Sox2* CKO compared to their littermate controls. A few isolated Myo7 positive hair cells were detected only in the base of the cochlea but none in the middle or apex. A severe reduction of radial neuronal fibers in the cochlea was visualized by tubulin staining at E18.5 mutant embryos. Additionally, the development of cranial neurons was altered by *Sox2* deletion, as shown by the dye tracing method.

Conclusion

The conditional deletion of *Sox2* within the inner ear alters the development of hair cells in all sensory organs. Specifically, semicircular canal cristae were nearly lost, the utricle and saccule were smaller, and the cochlea had isolated hair cells only near the base. In addition, the innervation of the cochlea was severely altered. Taken together, these results demonstrate that Sox2 is necessary for the formation and differentiation of sensory cells and neurons in the inner ear.

Funding

This work was supported by the Czech Science Foundation (Grant Agreement No. 13-07996S); by BIOCEV CZ.1.05/1.1.00/02.0109 from the ERDF; and by the Czech Ministry of Education, Youth and Sports (Grant Agreement No. AVOZ50520701).

PS 286

How does Lmx1a regulate tissue boundary formation in the inner ear?

Zoe Mann; Vincent Plagnol; Nicolas Daudet

University College London

The inner ear contains distinct sensory epithelia, which appear to derive from a common 'prosensory domain' during its early embryonic morphogenesis. The LIM Homeodomain transcription factor alpha (Lmx1a), expressed in non-sensory cells, has been shown to be necessary for the correct segregation of the sensory patches: Lmx1a mutations induce

severe defects in inner ear morphology, including enlarged cristae and some fusion between the vestibular and auditory patches. Furthermore, our ongoing work suggests that Lmx1a may act in part by antagonizing Notch activity, which is required for and promotes early sensory patch formation. In this study, we used gain-of-function approaches in the chick inner ear and an Lmx1a-GFP knock-in mouse line to test this idea further and to investigate how Lmx1a regulates tissue boundary formation in the inner ear. In Lmx1a-GFP heterozygous mice, GFP fluorescence is progressively excluded from the Sox2 and Jagged1-positive prosensory domains, which suggests a repositioning of sensory patch boundaries as cells commit to a sensory or non-sensory fate. In the embryonic chick inner ear, overexpression of cLmx1b (the functional homologue of Lmx1a) disrupts sensory patch boundaries by preventing commitment to a sensory cell fate. Furthermore the cells overexpressing cLmx1b tend to segregate from sensory cells and to form clusters of cells with constricted apical surfaces, suggesting a modification of their adhesive and cytoskeletal properties. Altogether these data indicate that Lmx1a/cLmx1b could regulate sensory patch segregation by i) antagonizing acquisition of a sensory fate and ii) preventing cell mixing at sensory patch borders. We will be presenting preliminary data from transcriptome profiling experiments aimed at identifying the molecular targets regulated by Lmx1a and potentially implicated in tissue boundary formation in the inner ear.

Funding
BBSRC

PS 287

The Tunnel of Corti is not an Anatomical Boundary of Lineage Restriction in the Developing Mouse Inner Ear

Han Jiang[1]; Kevin Beier[2]; Lingyan Wang[1]; Constance Cepko[2]; Donna Fekete[3]; **John Brigande**[1]
[1]Oregon Health & Science University; [2]Harvard University; [3]Purdue University

Background
Retrovirus-mediated lineage analysis identifies which cell types arise from a common progenitor cell. Assignment of lineally related cells to known domains of gene expression can provide insight into the genetic regulation of patterning and cell fate. We showed previously by injecting a virus encoding human placental alkaline phosphatase (AP) and a 24-bp oligonucleotide tag into the embryonic day 11.5 (E11.5) mouse otocyst that clone frequency (5/ear) and the number of cells/clone (3.2/ear) were likely related to the proximity of otic progenitor cells to their terminal mitoses at the time of viral integration. The paucity of clones, particularly in the organ of Corti, made comprehensive clonal analysis of the E11.5 otocyst problematic. To address this limitation, we deploy a virus with a 10-fold higher titer to enhance the frequency of infection. Additionally, the virus encodes cytoplasmic GFP, rather than AP, to provide improved cell-type identification using confocal microscopy.

Methods
The GFP lineage virus ($1X10^8$ infectious units/mL) was introduced into the E11.5 mouse otocyst by transuterine microinjection. GFP+ inner ear cell types were identified by confocal microscopy in serial, 14 µm cryostat sections at postnatal day 6. GFP+ cells were microdissected and subjected to nested PCR to amplify the 24-bp tag, and cells sharing the same sequence tag were identified as likely arising from a common precursor.

Results
800 GFP+ cells were picked from 17 inner ears and 484 sequences were identified, of which, 344 were unique. 282 of the sequences were from unrelated cells and 62 sequences were shared by cells lineally related. On average, there were 3.6 clones/ear (range: 2-6) and 3.3 cells/clone (range: 2-6). Deiters' cells could be related to outer hair cells, inner hair cells, border cells or inner phalangeal cells. Vestibular hair cells in the crista were related to one another, their supporting cells, and the nonsensory epithelium lining the ampulla. Saccular and utricular macula hair cells were related to their supporting cells.

Conclusion
While the GFP lineage virus did not enhance the frequency of clones, it did show similar clone sizes to the AP virus used previously. Furthermore, chance infections of individual cycling progenitor cells within the organ of Corti allowed us to rule out the presence of a lineage boundary in the middle of the organ of Corti at ~E12.5 (after accounting for the time required for virus infection, integration and marker gene expression).

PS 288

The Evaluation of Nestin in the Developing Inner Ear

Cynthia Chow[1]; Parul Trivedi[1]; Madeline Pyle[1]; Jacob Matulle[1]; Samuel Gubbels[1,2]
[1]University of Wisconsin-Madison; [2]University of Colorado Denver

Background
Nestin is an intermediate filament protein expressed in multi-potent and neural stem cells in the adult central nervous system (CNS). Nestin is universally expressed during CNS development and is later down-regulated and restricted to cells with progenitor cell characteristics in adulthood. Recent studies have demonstrated that nestin is expressed in the adult inner ear in a restricted cell population in the organ of Corti. We sought to characterize the expression of nestin in the developing mouse inner ear and to evaluate the relationship of nestin expression to hair and supporting cell differentiation.

Methods
Nestin GFP-transgenic mice were used to characterize the expression pattern of nestin in hair cells and supporting cells of the developing mouse inner ear. Cochlear tissue was harvested at a series of embryonic and postnatal time points and analyzed using immunohistochemistry for hair cell and sup-

porting cell marker co-localization amongst the GFP-expressing cell population.

Results
Initial data suggests nestin is expressed as early as E13.5 in the developing inner ear and is later expressed in hair cells and supporting cells. Immunohistochemisty for otic progenitor and mature cell markers suggest nestin-expressing cells give rise to both hair cells and supporting cells.

Conclusions
Nestin-expressing cells are observed in the embryonic inner ear and give rise to hair cells and supporting cell types. Further studies are ongoing to better characterize the expression pattern and proliferative capacity of nestin-expressing cells in the inner ear.

Funding
NIH/NIDCD: 1 R03 DC012432-01, 1 R01 DC013912-01, NIH/NIMH R01MH080434, and NIH P30 HD003352. UW-Madison; KL2 award and Type I pilot from the CTSA program, previously through the NCRR grant 1UL1RR025011, and now by NCATS grant TL1 UL1TR000427.

PS 289

Neuroblast-specific Bias for CHD7 with Potential Roles in Regulation of Long Genes in the Inner Ear

Donna Martin[1]; Robert Durruthy-Durruthy[2]; Daniel Fuentes[2]; Margot Bowen[2]; Adrienne Niederriter[1]; Ethan Sperry[1]; Jennifer Skidmore[1]; Anshika Srivastava[1]; Laura Attardi[2]; Tomek Swigut[2]; Joanna Wysocka[2]; Stefan Heller[2]; Peter Scacheri[3]
[1]The University of Michigan; [2]Stanford University; [3]Case Western Reserve University

Background
CHD7 is a chromatin remodeling protein critical for proper formation of the mammalian inner ear. Humans with CHARGE syndrome and heterozygous pathogenic variants in CHD7 exhibit sensorineural/conductive hearing loss and inner ear dysplasia, including abnormalities of the semicircular canals and Mondini malformations. Chd7Gt/+ mice also exhibit dysplastic semicircular canals and mild mixed conductive-sensorineural hearing loss. Prior studies have demonstrated that reduced Chd7 dosage in the ear disrupts expression of genes involved in morphogenesis and neurogenesis, yet the specific underlying mechanisms are not well understood. Here we sought to define roles for CHD7 in global regulation of mammalian gene expression and histone modifications.

Methods
Single cell multiplex qRT-PCR (FLUIDIGM) analysis was performed on 192 genes from E10.5 Pax2cre;Chd7Gt/+;mT/mG and Pax2cre;Chd7+/+;mT/mG mouse otocysts. RNAseq was performed on 7 Chd7+/+ and 7 Chd7Gt/+ pairs of microdissected E10.5 otocysts. ChIPseq using antibodies against H3K27ac and H3K4me3 was performed on pooled pairs of microdissected inner ears from 20 wild type and 20 Chd7Gt/+ E12.5 embryos.

Results
Single cell analysis of 215 cells from wild type and 251 cells from Chd7Gt/+ E10.5 otocysts indicated a relative enrichment of neuroblasts in Chd7Gt/+ compared to wild type. RNAseq analysis demonstrated a transcript length-dependent gene misregulation in E12.5 Chd7Gt/+ ears ($p<0.001$) compared to wild type, with long genes being preferentially sensitive to Chd7 loss. Similarly, dosage sensitive effects on long genes were observed in mouse embryonic stem (ES) cells and in E10.5 Chd7Gt/Gt otocysts, with more pronounced changes in null vs. heterozygous null states. ChIP-seq analyses showed that CHD7 is enriched in the bodies of transcriptionally active genes (compared to nearby flanking regions), while H3K27ac or H3K4me3 marks in E12.5 Chd7Gt/+ and wild type ears were unchanged.

Conclusions
Loss of one functional copy of CHD7 is associated with an increase in the prevalence of otic derived cells with neuroblast identity (vs otic vesicle identity), and with preferential disruption in transcription of long genes versus short genes. Combined with the ChIP-seq results, our observations suggest that CHD7 may function in transcriptional elongation, with long genes being more susceptible than short genes to Chd7 haploinsufficiency. Length-dependent gene misregulation has recently been described in Rett syndrome, Autism Spectrum Disorder, and Fragile X syndrome, suggesting possible links between the molecular etiologies of these disorders and CHARGE syndrome.

Funding
Supported by NIH-DC009410 and an NIH OMIC supplemental award

PS 290

MicroRNA-124 regulates cell specification in the cochlea through modulation of Sfrp4/5

Brigitte Malgrange; Aurelia Huyghe; Priscilla Vandenackerveken; Rosalie Sacheli; Pierre-Paul Prevot; Nicolas Thelen; Justine Renauld; Marc Thiry; Laurence Delacroix; Laurent Nguyen
University of Liege

Proper development of the mammalian cochlea is prerequisite for normal hearing. One of the major aspects is to obtain the correct types and numbers of cells at appropriate locations and proper timing. Among the molecules involved in the patterning of the cochlea, miRNAs – a class of short non-coding RNAs – emerge as crucial regulators. Indeed, it has been shown that miRNAs are involved in the early patterning of the otic vesicle and in hair cell maintenance. However, nothing is known about their role in modulating critical events during cell fate determination and specification in the cochlea. In this study, we uncover for the first time novel and essential functions of miRNAs in the cochlear development. Indeed, analysis of mice mutant for Dicer, an enzyme essential for miRNA biogenesis, showed that miRNAs control proliferation and differentiation in the organ of Corti. We also show that miRNAs are necessary for a normal cochlear planar cell polarity. To go deeper into the identification of which specific

miRNA is involved in those developmental processes, we made used of microarrays for miRNAs and for their potential targets by comparing mRNAs expression in WT and Dicer-cKO mice. We discover that miR-124 is highly expressed in the developing cochlea and present a pattern of expression compatible with a role during cell fate specification. We also provide evidence that Wnt signalling pathway is an essential target for miR124 during cochlea development.

Funding
This work has been funded by grants from the F.R.S.-F.N.R.S., the Fonds Le?on Fredericq, the Fondation Me?dicale Reine Elisabeth, the university of Liege and the Belgian Science Policy (IAP-VII network P7/07).

PS 291

Identification of Progenitor Cells in the Cochlea: Lgr5-positive Supporting Cells

Albert Edge
Harvard Medical School

Wnt signaling is required for the differentiation of hair cells during embryogenesis. Wnt stimulates otic progenitors to express transcription factor, Atoh1, which is required for hair cell development. Lgr5, a downstream target of the Wnt pathway and a protein that marks intestinal epithelial stem cells, is expressed in Lgr5-positive cells that gave rise to hair cells based on lineage tracing. Lgr5 continued to be expressed in the postnatal cochlea in a specific subset of supporting cells. In vitro analysis showed that Lgr5-positive cells had distinct phenotypes from the other (Sox2-positive) supporting cells and differentiated to hair cells at a higher rate, consistent with these cells playing a role as hair cell progenitors. The in vitro studies also showed that hair cells did not differentiate from Lgr5-negative cells. Hair cell replacement seen following ototoxic damage in neonatal ears was due to supporting cell transdifferentiation to hair cells, directly, or after cell division in a spontaneous response to damage, without pharmacological intervention. The response to damage was accompanied by Wnt release and was blocked by inhibition of Wnt signaling. Both cell division and hair cell differentiation were increased by treatment with an inhibitor of gamma-secretase. Based on lineage tracing, upregulation of Wnt signaling in the newborn inner ear, even in the absence of damage, specifically targeted the Lgr5-expressing cells, leading to proliferation, and the cells transdifferentiated to hair cells after increasing expression of Atoh1, which was downstream of Wnt. These data suggest that manipulation of signaling pathways increases regeneration of hair cells and that Lgr5-positive cells act as hair cell progenitors in the cochlea.

PS 292

RFX Transcription Factors are Essential for Survival of the Terminally Differentiating Outer Hair Cells in Mice

Ran Elkon[1]; Beatrice Milon[2]; Laura Morrison[2]; Manan Shah[2]; Sarath Vijayakumar[3]; Manoj Racherla[2]; Carmen Leitch[2]; Lorna Silipino[2]; Shadan Hadi[4]; Christoph Schmid[5]; Ashley Barnes[2]; Yang Song[2]; David Eisenman[2]; Efrat Eliyahu[6]; Gregory Frolenkov[4]; Scott Strome[2]; Bénédicte Durand[7]; Norann Zaghloul[2]; Sherri Jones[8]; Walter Reith[9]; **Ronna Hertzano**[2]
[1]Tel Aviv University; [2]University of Maryland Baltimore; [3]University of Nebraska Lincoln; [4]University of Kentucky; [5]University of Basel; [6]Icahn School of Medicine at Mount Sinai; [7]Université Claude Bernard Lyon-1; [8]University of Nebraska Lincoln; [9]University of Geneva

Cellular differentiation and survival is a multi-step process largely regulated by transcription factors. In the mammalian inner ear hair cell (HC), differentiation is initiated by the ATOH1 transcription factor, downstream of which function POU4f3 and GFI1. Forced expression of *Atoh1*, *Pou4f3* and *Gfi1* in a variety of combinations only leads to production of HC-like cells. To search for regulators of HC differentiation and survival in the postnatal mouse inner ear, we undertook a cell-type specific transcriptomic approach. HC, epithelial non-hair cells (ENHCs) and non-epithelial cells (NECs) were isolated from inner ears of newborn *Atoh1-nGFP* mice by flow cytometry. Gene expression was recoded from RNA extracted from the sorted populations. We identified in this dataset hundreds of genes with significantly elevated expression in HCs. Computational analysis of *cis*-regulatory DNA elements identified in the promoters of these genes a single, highly enriched motif. This motif corresponded to the binding motif of RFX family of transcription factors. Comparative genomics analysis demonstrated that the motif is conserved in the promoters of HC genes across human, mouse and zebra fish. Expression analysis revealed that five of the eight mammalian RFX transcription factors are expressed in HCs, of which the ciliogenic transcription factor RFX3 had the highest expression level. We further show that while conditional deletion of *Rfx1* or *Rfx3*, alone, did not result in a defect in early post-natal HC differentiation, the *Rfx1/3* conditional knockout mice suffered from severe hearing loss already at the onset of hearing. Morphological and functional analyses indicated that the early postnatal HCs form properly polarized kinocilia and stereociliary bundles, uptake FM1-43 and express HC markers. However, while the HCs are present throughout the length of the cochlear duct at P12, by P15 we observed a near complete loss of outer HC (OHC) from the basal and middle turn of the cochlear duct. These data indicate that RFX1/3 deficiency results in a rapid loss of OHC at the onset of hearing and are consistent with a novel role for the RFX transcription factors in the survival of the terminally differentiating HCs.

Funding
Triologic Society Career Development grant NIDCD/NIH R01DC013817 NIDCD/NIH R01DC03544 DOD CDM-

RP MR130240 Swiss National Science Foundation grant 310030B-144085 Swiss National Science Foundation grant 3100-06489 Fondation pour la Recherche MÃ©dicale FRM DEQ20131029168 ANR Ciliopath-X Nebraska Tobacco Settlement Biomedical Research Development Funds NIDCD/NIH R01DC014658 NIDDK/NIH K01DK092402 NIDDK/NIH R01DK102001

PS 293

A conserved role of Emx2 in establishing hair bundle polarity pattern in the neuromasts of the zebra fish

Tao Jiang[1,2]; Katie Kindt[1]; Wu Doris[1]
[1]NIDCD/NIH; [2]University of Maryland, College Park

Background

Sensory hair cells are responsible for transducing mechanical signals from the environment to the central nervous system. This process is mediated by depolarizing and hyperpolarizing a given hair cell in order to produce an excitatory or inhibitory signal, respectively. Deflections of the stereocilia towards the kinocilium open mechanotransduction channels on the tip of the cilia, which lead to hair cell depolarization, whereas deflections in the opposite direction lead to hyperpolarization. Thus, the alignment of hair bundle orientation within a given sensory organ is intimately related to its function. Our preliminary studies in mice indicate that Emx2, a homeodomain transcription factor, is both necessary and sufficient to establish the line of polarity reversal (LPR) that is unique to the two maculae within the inner ear. However, a similar LPR is also present in the neuromasts of the zebra fish lateral line system, which is responsible for detecting pressure change of the surrounding water. Neuromasts of zebra fish are aligned in either the anterior-posterior (A-P) or dorsal-ventral (D-V) direction relative to the body axis. Within each neuromast, ten to twenty sensory hair cells are separated into two groups with opposing polarity. Given the similarity in the stereocilia arrangement between the mouse maculae and neuromasts, we investigated whether Emx2 has a similar role in establishing the LPR in the neuromasts.

Methods

Zebra fish larvae of 3-5 days post fertilization (dpf) were processed for anti-Emx2, anti-parvalbumin (labels hair cells) and phalloidin staining. To ectopically express *Emx2* only in the sensory hair cell, we generated a *Myosin6b:Emx2-p2A-nls-mCherry* plasmid, which was co-injected with *tol2* transposase mRNA into one-cell stage *Myosin6b:β-actin-GFP* zebra fish embryo. Then, hair cell polarity in the neuromasts were imaged live using confocal microscopy.

Results

Similar to the mouse utricle and saccule, *Emx2* expression in a given neuromast is restricted to only half of the hair cells that share the same stereocilia orientation. In the A-P oriented neuromasts, *Emx2* is only expressed in hair cells that are pointing towards the posterior, whereas it is only expressed in hair cells that are facing ventrally in D-V oriented neuromasts. Overexpression of *Emx2* in nascent sensory hair cells was sufficient to orient all stereocilia to point towards the posterior in the A-P neuromasts and towards the ventral in the D-V neuromasts.

Conclusion

Our results suggest that *Emx2* has a conserved role in establishing stereocilia polarity pattern in mechanosensory organs of vertebrates.

Funding

Government

PS 294

Single-cell Transciriptome Protocol of the Cochlear Development

Norio Yamamoto[1]; Yosuke Tona[1]; Takayuki Nakagawa[1]; Juichi Ito[2]
[1]Kyoto University; [2]Shiga Medical Center Research Institute

Since the cochlear development takes a complex process and it is composed of various types of cells with different characteristics, comprehensive analysis of gene expression on a single-cell basis is important. For this purpose, most of studies use transgenic mice of fluorescent protein and a cell sorter to obtain a single target cell. Although this method is quite efficient, this can change the gene expression patterns from physiological patterns. There are two factors that cause this kind of change. One is the usage of transgenic system. Insertion of transgene of fluorescent protein in the genome can affect the enhancer or promoter of some genes. Even knock-in of fluorescent protein gene may cause the haploinsufficiency of the targeted gene. The other factor is the cell sorter. When a single cell runs through the sorting tube, the quite fast run-through and narrow diameter of the tube distort the form of the single cell. The cell form distortion can change the gene expression pattern of the cell.

In addition to the method to pick up a single cell, the amplification of cDNA also raises a problem. In a usual amplification protocol, the amplification is not linear. In other words, genes whose expression level is low is not amplified sufficiently.

To overcome these weak points of a conventional single cell analysis protocol, we established a technique to pick up a single cell from dissociated cochlear and to amplify all genes linearly. As a first step we dissect out the embryonic cochlea and divide the epithelia and mesenchyme using thermolysin. After dissociation of the cochlear epithelia, we pick up a single cell using glass pipette with diameter of 40 μm. The picked-up cells are subject to the extraction of mRNA and the established cDNA amplification protocol (Kurimoto et al. 2006). The method directionally amplifies cDNAs highly representatively from single cells using relatively few PCR cycles and achieves the linear amplification of cDNA. We confirmed that the amplified cDNA is suitable for quantitative RT-PCR and microarray analysis.

Funding

JSPS KAKENHI Grant Numbers 24592545 and 15K10749 to NY and 23229009 to JI

PS 295

The Lin-41 (Trim71)/let-7 axis controls sensory progenitor cell proliferation and auditory hair cell differentiation in the developing auditory organ

Lale Evsen; Angelika Doetzlhofer
Johns Hopkins School of Medicine

Lin-41, as well as its negative regulator *let-7* (*lethal-7* miRNA family), was initially identified in a screen for heterochronic genes in *C. elegans.* Lin-41, an ubiquitin ligase and RNA-binding protein, plays a critical role in stem cell maintenance and proliferation. Lin-41 has been recently shown to negatively control differentiation events through inhibition of mature *let-7* miRNAs biogenesis. We recently discovered that *Lin-41* (official name *Trim71*) is highly expressed in neural-sensory progenitors in the murine and avian auditory organs. *Lin-41* is expressed early, within the otic vesicle neural-sensory competent domain and later in auditory progenitors, but rapidly declines in expression with increasing hair cell (HC) differentiation in both the murine and avian inner ear. This is in contrast to mature *let-7* levels, which increase in expression with increasing HC differentiation. To address the role of *Lin-41* and *let-7* miRNAs in auditory sensory development we manipulated their levels in the developing chicken auditory organ using *in ovo* micro-electroporation together with *in ovo* cell proliferation assays. We found that over-expression of *Lin-41* in the chick auditory organ lead to excess progenitor cell proliferation and an inhibition of HC differentiation. Over-expression of a *let-7* sponge, which inhibits the activity of all let-7 miRNAs, lead to an increase in *Lin-41* mRNA expression and resulted in an increase in progenitor proliferation and inhibition of HC differentiation similar to the *Lin-41* over-expression phenotype. Over-expression of *let-7b* resulted in a decrease of *Lin-41* mRNA level and in a decrease in progenitor proliferation; however, surprisingly we did not observe premature HC differentiation, instead we observed a loss/or reduction of *Atoh1 and Sox2* mRNA expression. These findings suggest that Lin-41 is critical for maintaining auditory sensory progenitors in a proliferative and undifferentiated state. Moreover, our data suggest that let-7b negatively regulates *Atoh1* and *Sox2* mRNA expression in the developing auditory organ and too high *let-7b* levels block auditory HC differentiation.

Funding
NIDCD Grant T32 DC000023 to L.E.

PS 296

Combinatorial Effects of Atoh1 and Neurod1 Deletion on Inner Ear Development

Iva Macova[1]; Romana Bohuslavova[1]; Tetyana Chumak[2]; Josef Syka[2]; Bernd Fritzsch[3]; **Gabriela Pavlinkova**[1]
[1]Institute of Biotechnology CAS; [2]Institute of Experimental Medicine CAS; [3]University of Iowa

Background
Inner ear development is governed by temporal and spatial regulated expression of transcription factors that form a gene regulatory network. Expression of ISLET1 (Isl1), a LIM-homeodomain transcription factor, suggests a role in cell lineage specification and differentiation of prosensory progenitors of the inner ear. We describe the effects of the conditional deletions of *Atoh1* and *Neurod1* with *Tg*(*Isl1-cre)* on ear development.

Methods
We crossed mice with the targeted *Cre* recombinase gene in the *Isl1* locus in one allele and *Atoh1* or/and *Neurod1* flanked by loxP sites to obtain the conditional knock out (CKO) of *Atoh1*, *Neurod1,* or double CKO of *Atoh1/Neurod1*. Inner ear morphology and hearing functions (ABR and DPOAE recording) were compared between CKO mutants and controls.

Results
Neither hair cells nor supporting cells were identifiable in the *Atoh1* CKO inner ear at postnatal day 0 (P0). The innervation of the vestibular organs and the cochlea was significantly decreased comparable to Atoh1 null mice. In contrast, development of hair cells of *Neurod1* CKO was not affected with the exception of four rows of outer hair cells in the apex of the cochlea. However, spiral ganglion neurons were altered, as shown by the profound changes in ABR thresholds at 1-month of age. Similarly to the *Atoh1* CKO, *Atoh1/Neurod1* CKO mice carrying the double mutation had no Myosin 7a positive hair cells and no Sox2 positive supporting cells in the inner ear at P0. The innervation pattern differed from that of *Atoh1* CKO at P0. Innervation was condensed in the place of the missing organ of Corti with loops expanded over the lost cochlear epithelia.

Conclusion
The deletion of *Atoh1 $^{f/f}$* with *Tg*(*Isl1-cre)* results in an epithelium without any hair and supporting cells. *Isl1-cre; Neurod1$^{f/f}$* mice reach adulthood without any gross phenotype beyond deafness as demonstrated by altered ABR thresholds. Although the double CKO mutants, *Isl1-cre; Atoh1 $^{f/f}$; Neurod1 $^{f/f}$,* have a flat epithelium as *Atoh1* CKO, the innervation pattern is different with more axons forming an irregular network in the area of the epithelium of the organ of Corti. We confirm and extent previous CKO studies and show that *Isl1-cre* is as effective as *Pax2-cre* and *Foxg1-cre* to delete conditionally *Atoh1* and *Neurod1.*

Funding
The study was supported by the Charles University in Prague (project GA UK No 324615), the Czech Science Foundation (#13-07996S); by BIOCEV CZ.1.05/1.1.00/02.0109 from the ERDF; and by the Czech Ministry of Education, Youth and Sports (Grant Agreement No. AVOZ50520701).

PS 297

The Role of Par3 in cochlear morphogenesis and hair cell polarity

André Landin Malt; Xiaowei Lu
University of Virginia, Charlottesville

In the mammalian cochlea, planar cell polarity (PCP) signaling regulates elongation of the cochlear duct and the uniform

orientation of V-shaped hair bundles atop sensory hair cells. Recent advances demonstrate that multiple intercellular PCP signaling pathways impinge on a hair cell-intrinsic polarity machinery to orient hair bundles in the organ of Corti (OC). This hair cell-intrinsic machinery consists of Rac-PAK and Cdc42-aPKC signaling modules and an evolutionarily conserved complex for asymmetric cell division, which coordinately regulate positioning of the kinocilium/basal body during hair bundle morphogenesis. To further understand how intercellular PCP signaling regulates cochlear morphogenesis and hair cell PCP, we hypothesize that Par3 (or Pard3, par-3 family cell polarity regulator) is a critical PCP effector in the OC. Par3 plays an evolutionarily conserved role in regulating cell polarity in invertebrates and vertebrates, including asymmetric cell divisions and epithelial polarity. However, its role in the cochlear epithelium is unknown. We found that Par3 is asymmetrically localized at intercellular junctions in the OC during hair bundle morphogenesis, suggesting a function in mediating interactions between centriolar microtubules and lateral hair cell cortex. Using a Par3 conditional allele, we have generated inner-ear specific conditional knockout (cKO) mutants. A preliminary analysis of Par3 cKO cochleae revealed defects in elongation of the cochlear duct and hair bundle morphogenesis, consistent with a role in PCP regulation. Ongoing experiments are aimed to understand functional interactions of Par3 with other components of the cell-intrinsic machinery as well as intercellular PCP signaling pathways. Details of our analysis will be presented.

PS 298

Transcriptome-wide Comparison of the Impact of Atoh1/miR-183 Family on Pluripotent Stem Cells and Multipotent Otic Progenitors

Michael Ebeid; Prashanth Sripal; Jason Pecka; Kirk Beisel; Garrett Soukup
Creighton University

Introduction

A barrier to hearing restoration after hair cell (HC) loss is the inability of mammalian auditory HCs to spontaneously regenerate. Multiple factors are shown to be crucial for HC development and represent good candidates for regenerative studies. Atoh1 is widely accepted to be necessary and contextually sufficient for driving HC fate. Furthermore, the miRNA-183 family is known to be expressed at the time of HC differentiation, and mutations in miR-96 (one member of the family) can cause deafness both in mouse and human. Our goal is to identify and compare the impact of Atoh1/miR-183 family alone and in combination on the transcriptome of two different developmental models; mouse pluripotent stem cells (mPSCs) and immortalized mouse otic progenitors (iMOPs).

Methods

We have developed an array of plasmid vectors (pVs) expressing miR-183 family alone or in combination with Atoh1, along with red fluorescent protein (RFP) from a single transcript. HEK293 cells were used to validate protein expression by western blot analysis, RFP expression by flow cytometry, and miRNA expression by quantitative RTPCR. mPSCs & iMOPs were transfected with pVs, and RFP-positive cells were sorted 48 hours post-transfection using fluorescence activated cell sorting. Gene expression profiling was assessed using Affymetrix Mouse Gene ST Arrays. Taqman RTPCR was used to validate a subset of differentially expressed genes.

Results

In HEK293 cells, vectors functioned as expected by yielding Atoh1, RFP and miRNA expression. Gene expression profiling of mPSCs expressing Atoh1 showed 353 differentially expressed genes, of which 214 were upregulated (linear fold change ≥ 1.5 and p value < 0.05). Functional annotation clustering of upregulated genes revealed enrichment in transcriptional regulators, notch signaling pathway, epithelial development, and neuronal development genes. Using qRTPCR, we were able to validate 24 differentially expressed genes including Dll3, Dll1, Snai2, Lbh, Id2, Pou3f1, smad3, lama1, & Ndnf. Pluripotency markers (Nanog, Nr5a2, Prdm14, Sox15 and Klf4) were found to be downregulated. Mir-183 expression in conjunction with Atoh1 further downregulated 43 transcripts (linear fold change ≥ 1.2 and p value < 0.05), five of which are predicted target genes (Slc6a9, Sh3bp4, Greb1, Eif5, Sh3pxd2b). Expression profiling of iMOPs is in process.

Conclusion

Our analysis indicated numerous targets for Atoh1 in mPSCs, some of which can be associated with HC development. Comparing the impact of Atoh1/miR-183 on the transcriptome of mPSCs & iMOPs will provide better insight into the roles of these factors in HC development.

Funding

Nebraska LB606 and LB69, and NIH P20GM103471

PS 299

Derivation of Inner Ear Organoids from Pax2EGFP/+ Mouse Embryonic Stem Cells via Optimized FGF Signaling

Stacy Schaefer; R. Keith Duncan
University of Michigan

The practical use of stem cell-derived hair cells will rely upon production in large quantities. Recently, a reliable method of producing inner ear organoids from mouse embryonic stem (ES) cells was described (Koehler et al., 2013). This method replicates major signaling events of auditory development in vitro, including fibroblast growth factor (FGF) receptor activation at the key otic induction stage. Subsequently, a small fraction of cells upregulate Pax2 and become pre-otic. FGF signaling is mediated by ERK, AKT, and PLCγ pathways; ERK has been implicated in inner ear development in zebra fish and chickens, while AKT is thought to drive auditory neurogenesis (Yang et al., 2013; Wang et al., 2015). Manipulating specific pathways downstream of FGF2 with pharmacological inhibitors may allow tighter control over the intended outcome: enriched Pax2+ otic progenitors that progress toward hair cell fate. Elucidating mechanisms in hair cell derivation from mouse ES cells may precede regenerative therapies

and drug discovery studies and provide insight into normal otic development.

The role of FGF signaling in otic induction was examined with mouse Pax2+/EGFP ES cells, using the published method of inner ear organoid production (Koehler et al., 2013). FGF2 was applied at 0, 5, 25, and 100 ng/mL, and activation of downstream pathways was measured by Western blotting. During the maturation stage, EGFP+ vesicles became visible within the aggregates. As expected, many vesicles migrated to the outer surfaces of the aggregates, where they protruded and expanded. EGFP+ cells in the organoid regions—located at vesicle-aggregate junctions—tended to become hair cell-like. At day 20, organoids were fixed in 4% paraformaldehyde, dissected from the aggregates, and prepared for immunofluorescence.

FGF2 resulted in a robust increase in ERK phosphorylation within 1 hour and was necessary for vesicle formation. Higher concentrations tended to promote vesicle formation, although the benefit from 25 to 100 ng/mL varied. Immunofluorescence staining revealed Myo7a+, F-actin bundle+ cells in both 25 and 100 ng/mL conditions. Uptake of the styryl dye FM4-64 suggested functional mechanotransduction channels.

In this system, EGFP provides a useful report on Pax2 upregulation. Otic induction can therefore be measured by fluorescence microscopy and fluorescence-assisted cell sorting. Despite being heterozygous for Pax2, the cells are capable of being driven toward hair cell fate by FGF2. We conclude that FGF signaling is necessary for otic induction, which may be mediated by ERK. In future studies, preferential activation of ERK over parallel pathways may further promote otic lineage.

Funding
T32 training grant NIH T32-DC00011 DoD USAMRMC W81XWH-12-1-0492

PS 300

Comparing the Influence of Noise Duration on the Development of Hearing Loss in Mice, Rats, and Gerbils

Lenneke Kiefer[1]; Bernhard H. Gaese[2]; Manuela Nowotny[2]
[1]Goethe University Frankfurt/Main; [2]Institute of Cell Biology and Neuroscience

Background
Tinnitus and hyperacusis are among the serious health impacts of acoustic overstimulation on the population of industrialized countries. Therefore it is important to investigate the influence of noise sound pressure on the time course of hearing loss following acoustic overstimulation. Trying to determine the underlying mechanisms we compared noise-induced hearing loss in three rodent species mainly used in auditory research by applying acoustic stimuli with identical parameters (duration, frequency, SPL and anesthesia).

Methods
Experiments were performed on 10 adult Mongolian gerbils (*Meriones unguiculatus*), 10 adult rats (*Rattus norvegicus*) and 4 adult mice (*Mus musculus*). Hearing ability was investigated by means of auditory brainstem responses (ABRs) measured at 2, 8 and 14 kHz. This was repeated before, during, and after intense noise stimulation as well as 8 weeks after the trauma (center frequency 8 kHz, +/- 0.5 oct., 105 and 115 dB SPL). Changes (i.e. increases) in ABR threshold values were measured at different time points during the stimulation procedure of up to 2 h noise duration.

Results
Rats and gerbils exhibit comparable changes in ABR threshold values for a noise level of 105 dB SPL at the center frequency of the traumatizing noise (8 kHz). Rats are slightly more sensitive, since they show about 26 dB threshold shift after 30 min, whereby gerbils need 60 min to develop a threshold shift of only about 19 dB. In contrast to that, ABR thresholds of mice are not influenced at a noise level of 105 dB SPL applied for a duration of up to 90 min. At a frequency above the traumatizing noise (14 kHz) threshold changes were highest in rats (shift after 30 min: rats = 36 dB, gerbils = 20 dB, mice = 2 dB). Only an increase of the noise SPL by 10 dB (to 115 dB SPL) induces an ABR threshold elevation in mice by about 12 dB (at 8 kHz) and about 25 dB (at 14 kHz). This additional increase in trauma SPL also induces a threshold shift in gerbils and rats.

Conclusion
We found strong differences in sensitivity to acoustic noise between mice, gerbils and rats. Rats are most sensitive as indicated by the noise-induced threshold shift.

Funding
We like to thank Manfred KÃ¶ssl and Steven Abendroth for technical support. This work was supported by the DFG (NO 841/4-1).

PS 301

Sox2 is Required for Inner Ear Neurogenesis

Aleta Steevens; Amy Kiernan
University of Rochester

Background
Neurons of the cochleovestibular ganglion are critical for processing hearing and balance information. While they are known to be the first inner ear cellular lineage to differentiate, the mechanisms through which they are specified are not completely understood. The basic helix-loop-helix transcription factor NGN1 is critical for the development of inner ear neurons. Overexpression studies have also implicated an involvement of the high mobility group transcription factor SOX2 in otic neurogenesis. However, detailed *Sox2* loss-of-function experiments have not been performed to test its necessity in this process. In the present study we used an inducible genetic system in the mouse to investigate the role of SOX2 during inner ear neurogenesis

Methods
Sox2 was deleted and fate-mapped by crossing conditional *Sox2-CreER*^{T2} knock-in mice and *Ngn1-Cre* transgenic mice with a *Sox2*$^{+/Flox}$/Rosa26$^{CAG\text{-}tdTomato}$ line. Embryos were

collected and processed for histology. Imaging and cell counts were performed using Axiovision (Carl Zeiss, Germany).

Results

Cre induction and subsequent deletion of *Sox2* throughout the period of neurogenesis (E8.5-E11.5) resulted in the near absence of NGN1-expressing neuroblasts, an effect that translated into a drastically reduced cochleovestibular ganglion volume. Interestingly, an effect of haploinsufficiency was found, as the number of NGN1-positive neuroblasts and ganglion was significantly reduced in *Sox2*$^{+/CreERT2}$/Rosa26$^{CAG\text{-}tdTomato}$ controls that only have one copy of *Sox2*. These observations suggest that the level of *Sox2* directly influences neuronal specification. A significant increase in the number of Caspase3-positive cells was observed in the *Sox2* deleted mutants, suggesting that neuronal precursors die in the absence of *Sox2*. We confirmed that SOX2 is required upstream of NGN1, as deleting *Sox2* under the *Ngn1* promoter did not produce a similar phenotype. Interestingly, SOX2 fate mapping did not match the previously reported sequence of NGN1 expression, where early NGN1 expression initially labels the vestibular ganglia and subsequently labels the spiral ganglion. Rather, early (E8.5) SOX2 reporting labeled both ganglia.

Conclusions

SOX2 has previously been shown to be necessary and sufficient for inner ear sensory specification. To our knowledge, this study is the first to show through a detailed loss-of-function approach that SOX2 is necessary for otic neurogenesis. We found that SOX2 is required for inner ear neurogenesis, acts in a dose dependent manner, and is needed upstream of NGN1. However, fate mapping SOX2's expression during inner ear neurogenesis does not parallel that of NGN1, suggesting that SOX2 plays a more complex role in the otocyst than simply activating a proneural pathway.

Funding

Neuroscience Graduate Program Institutional Training grant: 5T32NS007489-14 Olschowka, J (PI) Center for Navigation and Communication Disorders Institutional Training Grant:5T32DC009974-05 Newlands, S (PI) NIH/NIDCD 1R01 DC009250 Kiernan, AE (PI)

PS 302

Deciphering Transcriptional Principles of Tonotopy in the Mature Cochlea

Joerg Waldhaus[1]; Eun Jin Son[2]; Robert Durruthy-Durruthy[1]; Stefan Heller[1]

[1]Stanford University; [2]Yonsei University College of Medicine

The mouse cochlea is organized tonotopically, with higher frequencies being represented at the base while lower frequencies are detected at the apex of the organ. This tonotopic arrangement correlates with anatomical features like basilar membrane width, hair cell size and hair bundle morphology. Likewise, based on work in non-mammalian species one might expect physiological differences in hair cells along the tonotopic axis including changing mechanoelectrical transduction channel properties and concentration differences of Ca2+-buffering proteins. Ultimately, anatomical and physiological parameters are expected to complement each other in order to enable for the excellent frequency discrimination properties of the auditory system.

The aim of this study is to identify and characterize molecular gene expression profiles of individual inner and outer hair cells and relate them to their anatomical position along the cochlear duct. We used Myo15Cre/Ai14-tdTomato reporter mice to label inner and outer hair cells. Cochleae were dissected at postnatal day 28, when hearing is fully mature. Fluorescence-activated cell sorting was used to isolate viable, single tdTomato-expressing hair cells and deposited individual cells into single wells of 96-well plates. Single cell multiplex quantitative RT-PCR was conducted for 192 preselected hair cell-associated transcripts. We hypothesized that the expression of some markers is asymmetrically distributed along the tonotopic axis. Computational analysis allowed us to identify inner and outer hair cells using expression distribution of well-characterized landmark genes that discriminate between both populations. Furthermore, we were able to reconstruct the cells' spatial tonotopic organization *in silico*, and detect tonotopic expression of several physiologically relevant genes at location-specific resolution.

The results of this study will add to our understanding of how organ of Corti hair cell function is correlated with spatially encrypted expression of genes encoding for example ion channels, Usher genes, ion-transporters, Ca2+ binding proteins, synaptic components, and other metabolically relevant genes.

Funding

This work was supported by NIH grants R01 DC04563 to S.H. and by P30 core support (DC010363). J.W. is supported in part by a fellowship (Wa 3420/1-1) from the Deutsche Forschungsgemeinschaft.

PS 303

Speech Detection in the Presence Of Background Noise Is Effected by both Spiral Ganglion and Outer Hair Cell Function.

Mark Parker[1]; Efoe Nyatepe-Coo[2]; Gifty Easow[3]

[1]Tufts University School of Medicine; [2]Northwestern University; [3]Indiana University

The overall aim of this research is to describe the functional roles played by hair cells and spiral ganglion neurons in audition. Several recent lines of research have highlighted the critical functional role of the spiral ganglion in complex listening situations, such as speech recognition in the presence of background noise. This study extends this work to determine whether the outer hair cells also play a role in speech processing during complex listening situations. To test this, normal and hearing impaired subjects (N=25) were subjected to speech recognition testing in quite (NU-6) and in the presence of competing background noise (Quick SIN), and then outer hair cell function (DPOAE amplitude) and spiral ganglion (ABR wave I amplitude) function was measured.

Statistical differences between normal and impaired groups was measured by students t-test and ANOVA, and a linear mixed regression model was used to identify correlations between subject age, pure tone average, NU-6 scores, DPAOE amplitudes, and wave I amplitudes. The preliminary results indicate that poorer Quick SIN scores (<5 SNR loss; p=0.00), but not NU-6 scores (p=0.23), are associated with both reduced DPOAE amplitudes (mean 4KHz DPOAE=>-7. 7 +/- 2.2 s.e.m.) and reduced wave I amplitudes (mean peak-trough > 0.12 μV+/- 0.05 s.e.m.). Furthermore, there is a stronger correlation between speech recognition in noise and hair cell and spiral ganglion function as the patient ages. These preliminary results suggest that both outer hair cells and the spiral ganglion play a functional role in speech discrimination in the presence of background noise, but not in quiet.

PS 304

Contralateral Inhibition of Click- and Chirp-Evoked Human Compound Action Potentials

Spencer Smith[1]; Jeffery Lichtenhan[2]; Barbara Cone[1]
[1]University of Arizona; [2]Washington University School of Medicine

Background

The medial olivocochlear (MOC) reflex inhibits the gain of the cochlear amplifier by reducing outer hair cell (OHC) electromotility. Traditionally, contralateral inhibition of otoacoustic emissions paradigms have been used as *pre-neural* assays of the human MOC reflex. However, if the putative function of the human MOC reflex is to unmask *neural* encoding of signals in noise, it is imperative to study the effect of MOC activation on the auditory nerve. The purpose of the present study was to quantify the effect of MOC reflex on click- and chirp-evoked, auditory-nerve compound action potentials (CAPs). Click-evoked CAPs were recently used to study human MOC inhibition (Lichtenhan et al. Hearing Research, In Press). However, chirp stimuli, which synchronize excitation along the entire length of the basilar membrane, evoke CAP measurements that are more robust and have practical benefits over click stimuli, such as fewer response averages.

Method

Normal hearing young adults participated in this study. 100-ms clicks and 10-ms chirps were used to evoke CAPs, which were recorded with tymptrodes placed on the tympanic membrane. The chirp characteristics were based on human derived-band CAP latencies (Chertoff et al., 2010). The spectra of both stimuli were indistinguishable when recorded with an ear-canal probe microphone positioned to avoid standing waves. Level-series measurements using 50-80 dB ppeSPL stimuli in 10 dB steps were obtained with a chained stimulus paradigm. Measurements made in quiet and with 60 dB SPL contralateral broadband (0-10,000 Hz) noise were interleaved for each stimulus type. Average response waveforms for each subject were made from approximately 18,000-20,000 stimulus presentations at each stimulus level. The MOC reflex was quantified with standard measures of "effective attenuation" and "dB Change".

Results

MOC effects were greatest at lower stimulus levels (50 and 60 dB) for both click and chirp evoked CAPs. Low level chirp-evoked CAPs were inhibited to a greater extent than click-evoked CAPs.

Conclusions

Inhibition of CAP amplitude at lower stimulus levels with contralateral broadband noise is consistent with the MOC-induced attenuation of cochlear amplifier gain. The larger effect of MOC inhibition on chirp-evoked CAPs suggests a possible solution to using auditory-nerve based measures of MOC inhibition, as fewer response averages are needed for chirp-evoked CAPs.

Funding

The first author is supported by the following awards: RUTH L. KIRSCHSTEIN NATIONAL RESEARCH SERVICE AWARD(NRSA) INDIVIDUAL PREDOCTORAL MD/PHD OR OTHER DUAL-DOCTORALDEGREE FELLOWSHIP (#1 F30 DC014180-01A1) Student Investigator Grant from the American Academy of Audiology

PS 305

Evidence for Auditory-Nerve Contribution to Individual Differences in Suprathreshold Brainstem Temporal Coding

Hari Bharadwaj[1]; Leonard Varghese[2]; Golbarg Mehraei[3]; Christopher Shera[4]; Barbara Shinn-Cunningham[2]
[1]Massachusetts General Hospital; [2]Boston University; [3]Massachusetts Institute of Technology; [4]Massachusetts Eye and Ear Infirmary

Animal models of acoustic overexposure and early aging demonstrate that it is possible to sustain considerable auditory-nerve (AN) damage, e.g., losing up to 50% of afferent synapses ("cochlear synaptopathy") without elevated audiometric thresholds. In the lab, listeners with normal audiograms exhibit large individual differences in performance on perceptual tasks requiring the use of subtle temporal cues. We previously argued (Bharadwaj et al., Front Syst Neurosci 2014) that differences in AN coding fidelity caused by cochlear synaptopathy could contribute to these differences. Indeed, brainstem envelope-following responses (EFRs) to stimuli designed to reveal the effects of synaptopathy correlate with individual differences in perceptual temporal sensitivity (Bharadwaj et al., J Neurosci 2015). Here, we examine whether individual differences in suprathreshold temporal coding, as measured by EFRs, are inherited in part from differences present at the level of the AN.

Auditory brainstem responses (ABRs) were measured to 100 microsecond clicks using an ipsilateral ear-canal electrode referenced to a distributed set of 15 fronto-central and parietal scalp electrodes. Clicks (12,000 total; 6,000 per polarity) were presented at each of two sound levels (80 and 100 dB peSPL) and responses averaged across polarities.

EFRs were measured in response to a modulated (223 Hz, 63% modulation depth) 3--10 kHz band noise at 75 dB SPL.

We measured acoustic middle-ear muscle reflex (MEMR) responses as an additional assay of AN health. Both anatomical tracing studies and physiological studies of acoustic tuning of stapedius motor neurons suggest that the MEMR is triggered by the integrated activity of AN fibers with low-spontaneous discharge rates (low-SR). These low-SR fibers are particularly vulnerable in animal models of cochlear synaptopathy. We obtained MEMR responses elicited by a 25 ms, 100 dB SPL, high-frequency noise burst by measuring MEMR-induced pressure changes in the contralateral ear using probe tones at different frequencies.

Preliminary results suggest that ABR wave-I amplitudes at both 80 and 100 dB peSPL correlate with EFR phase locking. Further, the latency of the peak MEMR-induced pressure change correlated with wave-I amplitude and EFR phase locking (i.e., shorter latencies correspond to larger wave-I and greater phase locking). This suggests that differences in AN survival contribute to individual differences in suprathreshold temporal coding at the level of the brainstem, consistent with the notion that cochlear synaptopathy may be common among listeners with normal hearing thresholds.

Funding
This work was supported by the National Institute on Deafness and Other Communication Disorders (NIDCD) of the National Institutes of Health under award number R01 DC013825.

PS 306

p43 deletion increases susceptibility to age-related hearing loss in mice

Sabine Ladrech [1,2], Marc Lenoir[1,2], François Casas[3] , Chloë Richard[1,2], Carolanne Coyat[1,2], Nesrine Benkafadar[1,2], Jean-Luc Puel[1,2] and Jing Wang[1,2]
[1]INSERM - UMR 1051, Institut des Neurosciences de Montpellier, 34295 Montpellier, France, [2]Université Montpellier 1&2, 34295 Montpellier, France, [3]CNRS - UPR1142, Institut de Génétique Humaine, Montpellier, France

Background
Age-related hearing loss (ARHL), known as presbycusis, is a degenerative disorder and a major public health problem**.** The onset and severity of ARHL is determined by a combination of genetic and environmental factors. Recently, a N-terminally truncated form of the thyroid hormone receptor TRα1 with molecular weight of 43 kDa (p43) has been identified in mitochondria. p43 invalided mice displayed a decreased activity of the mitochondrial respiratory chain, a major defect in insulin secretion leading to glucose intolerance during aging together with a moderate reduction of life expectancy. These results suggested that p43 may be a candidate gene for age-related disorders.

Aim
The present study was designed to elucidate the role of p43 on the hearing function and to investigate the effects of its deletion on the susceptibility of the cochlear hair cells and ganglion neurons to aging.

Results
ABR and DPOAE recordings showed that mice with the deletion of p43 have accelerated age-related hearing loss. SEM investigations revealed outer hair cell losses. TEM examinations demonstrated myelin degradation around the soma of the ganglion neurons, and losses of spiral ganglion neurons. Finally, we found increased mitophagy, mitochondrial supercomplex instability and reduced pro-survival protein expression preceding cochlear cell degeneration.

Conclusion
These results support an important role of p43 in contributing to the maintenance of auditory sensory-neural structures and opens new perspectives for the exploration and the treatment of age-related mitochondrial neurosensory hearing loss.

PS 307

Effect of Contralateral Stimulation on Low Frequency Hearing in Human

Eric Verschooten[1]; Elizabeth Strickland[2]; Nicolas Verhaert[1]; Philip Joris[1]
[1]Univ. of Leuven; [2]Purdue University

Background
Based on physiological measurements in anesthetized animals (Guinan, 2011; Kawase and Liberman, 1993; Buñ̲o, 1978; Liberman, 1989; Warren and Liberman, 1989; Dolan and Nuttal, 1988) the medial olivocochlear reflex (MOCR) has been hypothesized to enhance the response to signals in noise. Several lines of evidence support such a role for the MOCR in humans. Psychophysical studies have shown effects on behavioral responses that are consistent with MOCR involvement. In our previous study in humans we did not observe a significant effect of contralateral simulation on cochlear mass potentials (compound action potentials (CAP) and cochlear microphonic (CM) at 4 kHz, but a preliminary measurement at 800 Hz indicated some effect on the neurophonic (NP). In this study we focus on low frequencies and assess electrophysiological and psychophysical effects in the same subjects.

Methods
Psychophysical experiments were conducted to measure the effects of contralateral noise on threshold for short, low- (800 Hz) and high- (4 kHz) frequency tones. Electrophysiological experiments were performed on the same subjects using a minimally invasive transtympanic procedure to extract averaged mass-potentials of short tones from the cochlear promontory or the niche of the round window. This involved a custom made ear mold to control acoustic stimulation (ER-2 earphone, calibrated in-situ with ER-7 microphone). Averaged mass responses (CAP, CM, NP) to tones with and without contralateral noise (below stapedius reflex) were extracted using paradigms based on polarity alternation and forward masking. All subjects were audiometrically normal (audiogram, tympanogram, reflex threshold).

Results
Psychophysics: All subjects (n=9) showed an increase in behavioral threshold at 800 Hz with contralateral noise. The average threshold increase with contralateral level for the population was ~0.14 dB/dB (50-80 dB SPL). At 65 dB SPL, the increase at 800 Hz was 3.2 dB, which was much larger than at 4 kHz (1 dB; n=6; one outlier excluded). Electrophysiology: Most of the effects of contralateral noiseon CAP and NP (1st harmonic) at low frequencies were rather small and variable due to a limited signal-to-noise ratio. We analyzed the 2nd harmonic of the sustained response in two subjects. We found a clear decreasing trend with contralateral level, with an average trend similar to that of the psychophysics.

Conclusion
In humans, we observed a progressive reduction with contralateral noise level for behavioral threshold and low frequency neurophonic (2nd harmonic). This preliminary result may indicate efferent activation at low frequencies.

Funding
Supported by FWO (G.0961.11) and BOF (OT-09-50 and OT-14-118)

PS 308

Estimating Neural Synchrony and Spectral Power from the Auditory Nerve Compound Action Potential in Humans

Kelly Harris; Judy Dubno
Medical University of South Carolina

The long-term goal of this research is to describe and distinguish the underlying neural pathology of human presbyacusis. Animal models of age-related hearing loss demonstrate a loss of afferent auditory nerve fibers (ANF) prior to elevated neural thresholds. This loss may affect perception of complex sounds, which requires precise phase locking of ANFs to efficiently and accurately encode temporal information.Traditionally, AN activity is estimated by acquiring the averaged compound action potential (CAP) and estimating the amplitude and latency of the N1 response. Acquiring single-trial data provides the means to assess differences in neural synchrony and power not necessarily evident in the averaged response. Thus, the purpose of this experiment was to develop and test new recording and analysis methods for the CAP to examine the extent to which neural synchrony and power propagate along the auditory nerve.

Methods
CAPs were recorded from a group of normal-hearing adults with an electrode placed on the tympanic membrane. CAPs were elicited by a100-µs broadband click train, and input-output functions were generated (70-110 dB pSPL). N1 amplitude and latency values were estimated from averaged CAP responses and modified Matlab functions were used to perform time-frequency analyses. To assess neural synchrony, phase locking value (PLV), or the consistency of phase across trials at a given frequency, were measured. We also estimated power in the CAP by measuring the event-related spectral perturbation (ERSP), or dynamic changes in the EEG spectrum that are stimulus-locked, but not necessarily phase locked. PLV and ERSP were averaged across time windows roughly corresponding to the CAP wave I, and Waves III and V of the ABR.

Results
Increases in ERSP and PLV were observed at time points surrounding the peaks of the CAP and ABR. ERSP was positively correlated with ABR peak amplitudes. Measures of PLV were propagated along the AN, such that greater PLVs at Wave I were associated with greater values at Wave V. These results provide new information about auditory nerve function in humans and demonstrate how neural synchrony and spectral dynamics propagate through the auditory system.

Conclusions
Determining the contribution of neural synchrony and spectral dynamics to AN responses may provide an improved understanding of how ANF loss with increasing age and/or hearing loss affects structure and function in the peripheral auditory system.

Funding
Work supported in part by NIH grants R01 DC014467 and P50 DC000422

PS 309

"Excuse me, I'm with the Band": Neural Activation Patterns Reveal Robust Auditory Nerve Synchrony Evoked with Octave-Band Chirps

Ivy Thompson; Brian Earl
University of Cincinnati

Background
Recent research has suggested that the amplitude of high-level compound action potentials (CAPs) can detect auditory nerve degeneration that is missed by traditional threshold measurements. Octave-band chirp stimuli evoke larger CAP responses than tonebursts at corresponding frequencies. Therefore, the use of octave-band chirps may enhance neural synchrony and provide clinicians and researchers a precise tool for identifying changes in auditory nerve integrity. The purpose of this study is to compare the neural activation patterns generated by octave-band chirps to those generated by tonebursts using a high-pass masking paradigm. The central hypothesis for this study is that neural activation patterns for octave band chirps will show increased neural firing density but narrower bandwidth than those for traditional toneburst stimuli.

Methods
CAP-derived amplitude-intensity functions were acquired from normal-hearing Mongolian gerbils (N=9) with octave-band chirps and short-duration tonebursts at 2, 4, 8, and 16 kHz. Cumulative amplitude functions were constructed for both stimulus types at 80, 60, and 40 dB SPL by tracking CAP amplitude during simultaneous masking noise high-passed in 1/3 octave intervals between 0.4 and 62 kHz.

Derivatives of these amplitude growth functions yield neural activation patterns from which the density, peak location, and the bandwidth of neural firing were inferred.

Results
Amplitude-intensity functions for octave-band chirps revealed significantly larger CAP amplitudes than those for toneburst stimuli across all intensities. Consistent with the first component of the central hypothesis, neural activation patterns indicated greater neural firing density at the peak location for octave-band chirps than for tonebursts across all frequencies. However, neural activation patterns showed a broader bandwidth of activation for the octave-band chirp stimuli than for tonebursts, opposite of what was hypothesized.

Conclusions
These preliminary data indicate that octave-band chirps evoke robust neural firing density, which is a marker of synchronous firing among auditory nerve fibers. This suggests that octave-band chirps could be more optimal than tonebursts for assessing regional auditory nerve integrity. The masking paradigm provides a method to assess supra-threshold auditory nerve function which may differ for individuals with history of noise exposure or other neurodegenerative conditions but who do not show elevated hearing thresholds. Future experiments will be conducted to determine how the neural activation patterns for octave-band chirps differ in animals experiencing auditory nerve degeneration.

Funding
University of Cincinnati's Office of Research

PS 310

Peri-stimulus time response of the auditory nerve recorded at the round window

Charlène Batrel[2]; Antoine Huet[2]; Gilles Desmadryl[2]; Jean-Luc Puel[2]; **Jérôme Bourien**[2]
[1]Inserm U1051; [2]Institute for Neurosciences of Montpellier - Inserm U1051

In animal models, temporal encoding of sounds can be probed by single-fiber recordings from the auditory nerve. Here, we investigate the possibility to extract temporal properties of the auditory nerve fibers using the electrical neural noise from the round window. Electrical round window noise was recorded using an electrode placed onto the round window niche in adult gerbils. The signal was filtered (300-1200 Hz), rectified and averaged (x100) in response to bursts of third octave band noise centered to a probe frequency (2 to 32 kHz). Interestingly, the round window response mimics the peri-stimulus time histogram obtained using single-fiber recordings (i.e. onset peak followed by adaptation, steady state and offset responses). Concomitant recordings of single-fiber and round window responses show comparable kinetics of adaptation, which can be fitted using two decaying exponential models (*i.e.* t_{fast} and t_{slow}) plus a constant term (*i.e.* steady state). Time constant of the fast adaptation (t_{fast}) decreases with the level of stimulation from 10 to 1 ms, while the slow adaptation (t_{slow}) was level-independent (~60 ms). The peak to steady state ratio decreases with the probe frequency from low- to high-frequency stimulation. When compared with the spontaneous rate of the fibers, the peak to steady state ratio reflects the heterogeneity of auditory nerve fibers in gerbils (*i.e*. a majority of high spontaneous rate fibers in the apex, and a more balanced distribution at the base). In conclusion, the peri-stimulus time response may provide a useful tool to probe the temporal properties of the auditory nerve in various animal models and in human.

Funding
This work was funded by Cochlear (CB) and ANR (AH).

PS 311

Using Auditory Steady-State Responses to Evaluate Compression and Auditory Nerve Integrity in Normal-Hearing and Hearing-Impaired listeners

Gerard Encina-Llamas[1]; Torsten Dau[1]; James Harte[2]; Bastian Epp[1]
[1]Technical University of Denmark; [2]Interacoustics Research Unit

Background
The healthy auditory system has the ability to enable communication in challenging acoustical environments with high levels of background noise. Hearing impairment often leads to a deterioration of this ability, however the degree of which varies widely. It is believed that the specific underlying pathology plays an important part in determining this variability. It has been shown that loss of outer hair cells leads to a reduction in peripheral compression. It has also recently been shown in animal studies that noise over-exposure, producing temporary threshold shifts, can cause auditory nerve fiber (ANF) deafferentation in predominantly low-spontaneous rate (SR) fibers. In this study, auditory steady-state response (ASSR) level growth functions were measured both in normal-hearing (NH) and mildly hearing-impaired (HI) listeners to evaluate the applicability of ASSR to assess peripheral compression and the capacity to code intensity fluctuations at high stimulus levels.

Methods
ASSRs were measured using a 64-channel EEG recording amplifier with active electrodes. ASSR level growth functions were measured in adults at stimulus levels between 20 and 90 dB SPL. Subjects were NH, or mildly HI listeners towards higher frequencies. To evaluate compression, sinusoidally amplitude modulated (SAM) tones at carrier frequencies of 0.5, 1.0, 2.0 and 4.0 kHz were presented simultaneously with a modulation depth of 85%. To evaluate intensity coding at high intensities, a single SAM tone with 2 kHz carrier frequency and modulation depths of 25% and 85% was presented.

Results
For all listeners at frequencies with normal audiometric thresholds, ASSR level growth functions exhibited consistently compression of about 0.25 dB/dB up to 60 dB SPL. At frequencies with impaired audiometric thresholds, an increased slope of the level growth function, i.e. a reduced compression, was found. For the shallow modulation depth of

25% and levels above 60 dB SPL, the growth function slope showed higher variability across NH subjects than for levels below 60 dB SPL. The same effect was found in HI listeners at the non-impaired frequencies.

Conclusions
The results show that compression estimates derived from the slope of ASSR level growth functions are similar to other estimates of peripheral compression. Peripheral compression can be estimated simultaneously at four frequencies for levels up to 60 dB SPL, both for NH and HI listeners. Above 60 dB SPL, the results indicate that the slope of the ASSR level growth function obtained using shallow modulation depths provides information about the capacity to code intensity fluctuations.

Funding
This work was funded by the Oticon Center of Excellence for Hearing and Speech Sciences (CHeSS) at the Technical University of Denmark (DTU).

PS 312

Comparison of Effectiveness of ABR-Based Methods in Diagnosis of Retrocochlear Pathologies

Krzysztof Kochanek[1]; Lech Sliwa[1]; Marek Golebiewski[2]; Adam Pilka[1]; **Henryk Skarzynski**[1]
[1]World Hearing Center, Institute of Physiology and Pathology of Hearing; [2]Medical University of Warsaw, Poland

Background
The purpose of this study was to compare effectiveness of three different ABR-based methods in screening for retrocochlear pathologies. The study was aimed at evaluating sensitivity, specificity and effectiveness of these methods, and finding most effective screening procedures.

Method
The considered methods were: (i) standard ABR utilizing click-evoked responses, (ii) Stacked-ABR (SABR) based on derived-band responses, (iii) method based on ABRs evoked by tone-pips (TABR). The examined group included patients with retrocochlear pathologies (acoustic neuroma, neuro-vascular conflicts, etc.) confirmed by GaT1W MRI examination, and normal-hearing subjects without otologic impairments. The system and software Nav-Pro AEP Nav-Pro v. 6.2.0 (BioLogic – Natus) was used in the tests. Standard procedures, recommended by the producer, were applied. Prior to the tests, all subjects were subjected to comprehensive audiologic and otologic examinations, including MR imaging. Effectiveness of the methods was assessed based on sensitivity and specificity functions, predictive values and ROC analysis. Cost effectiveness was also evaluated.

Results
The SABR method realized in the applied Nav-Pro system exhibits high sensitivity in detecting retrocochlear pathologies. However, specificity of these tests is very low, which is due to high variability of Stacked-ABR amplitudes and interaural amplitude differences. The standard ABR method has good specificity, but low sensitivity in cases of small tumors (below 1 cm in diameter). Much better sensitivity and specificity was obtained by using the TABR method.

Conclusion
Application of SABR method allows for detecting small acoustic tumors, however, its usefulness is limited because of excessive percentage of false positive results. One can slightly improve performance of this method by modifying normative values of Stacked-ABR amplitudes. The TABR method offers good sensitivity and specificity, and relatively high predictive value. For optimal cost effectiveness (minimal unit cost of detecting a retrocochlear pathology in high-risk population), the best possibility would be application of a two-stage screening test, consisting of standard ABR in the first stage, and the TABR test in the second stage, and eventual GaT1W MRI examination.

Funding
The research was supported by the Grant NN403 136439 from the Ministry of Science and Higher Education in Poland.

PS 313

Temporary effect of short-duration acoustic exposure on human frequency following responses

Sho Otsuka[1]; Minoru Tsuzaki[2]; Satomi Tanaka[2]; Junko Sonoda[2]; Shigeto Furukawa[1]
[1]NTT Communication Science Laboratories, NTT Corporation; [2]Kyoto City University of Arts

Background
Recent animal and modeling studies have revealed that acoustic overexposures cause non-reversible neuronal degeneration of auditory nerve fibers as well as damage to the outer hair cells, thereby causing temporal processing deficits. However, there is limited evidence that acoustic exposure degrades temporal coding in humans.

This study aimed to examine whether short-duration exposures, which would not induce permanent hearing loss, affect temporal coding. We measured the frequency-following response (FFR), which reflects the temporal coding precision of supra-threshold sound at early stages of the auditory pathway.

The subjects were violin players, who, during their regular instrument practice, were exposed to violin sounds loud enough (ranging from 85 to 100 dB A) to induce temporary hearing loss. The FFRs before and after a short-duration practice session were compared.

Methods
Nine audiometrically normal undergraduates and graduate course students who are majoring in the violin participated in the experiment. FFRs were recorded to transposed stimuli, which were generated by multiplying a half-wave rectified 100-Hz pure tone with a 4-kHz pure tone. The duration of stimuli was 2.5 s, including 10-ms rise/fall times. The original

and inverted-polarity stimuli were presented 200 times alternatively before and after a one-hour practice session. To see the recovery process, phase locking values (PLVs) were estimated for the responses measured 0-5, 5-10, 10-15, and 15-20 min after the end of the practice session. These PLVs were compared with PLVs before the practice. The stimuli were delivered to the left ears at 80 dB SPL.

Results
PLVs at 100 Hz decreased significantly 0-5 min after the violin practice compared with those before the practice. On the contrary, PLVs 5-10, 10-15, 15-20 min after the practice did not show significant decreases. The FFR amplitude at 100 Hz also showed a similar tendency, although its effect was not statistically significant.

Conclusion
This study observed that the fidelity of the FFR decreased temporarily after acoustic exposure. This result implies that even a short-duration exposure can induce temporary degradation of temporal coding at early stages of the auditory pathway.

Funding
The study was supported by internal NTT research funding and Grant-in-Aid for Scientific Research (A) Grant No. 24243070.

PS 314

Longitudinal assessment of auditory function in a mouse model of mild traumatic brain injury

Reza Amanipour; Robert Frisina; Cesario Borlongan; Samantha Crescoe; Joseph Walton
University of South Florida

We hypothesize that traumatic brain injury negatively impacts auditory processing including difficulty hearing in background noise. Life altering physical, behavioral, and cognitive symptoms occur in individuals following mild traumatic brain injury (mTBI). In this study we examined behavioral and electrophysiological outcomes to answer the following questions: 1) are perceptual auditory disorders observed following mTBI and do the behavioral responses change overtime following injury, 2) is there evidence of electrophysiological deficits in auditory brainstem response measures following mTBI in a mouse model?

Subjects were 16 (equal gender), 6 month old CBA/CaJ mice obtained from our in-house colony. All experimental protocols were approved by the University of South Florida Institutional Animal Care and Use committee (IACUC). Mice were exposed to either sham or to mTBI administered using a controlled cortical impactor, placed at the frontoparietal cortex. Mild TBI was produced using a velocity of 6.0 m/s reaching a depth of 0.5 mm below the dura. Sham surgery consisted of animals subjected to scalp surgery and craniotomy only.

Auditory behavioral responses were measured using the acoustic startle response (ASR). The ASR input-output function was generated from wideband noise startle elicitors (SESs). Noise pre-pulse inhibition (NPPI) and gap prepulse inhibition stimuli (70 dB narrowband noise, with either a 0 or 50 ms gap prior to a 110 dB SES). Auditory brainstem response (ABR) audiograms from 8 to 32 kHz were used to measure hearing function and peak 1, 2, and peak 4 amplitudes were measured. A gap-in-noise paradigm (70 dB SPL markers with gap durations of 2 to 64 ms) was also used to assess temporal processing.

All TBI animals showed symptoms immediately following TBI: motor lethargy, poor appetite and mild weight loss, with recovery seen within 3 days. Behavioral and electrophysiological assessments were completed at 3, 7, 14, 28, 35, and 45 days post-TBI. Three days post-TBI startle amplitude functions were comparable between TBI and sham groups. At 7 days NPPI was *reduced* compared to baseline for both groups and there were no significant differences for gap detection. For ABRs, there was a significant decrease in the amplitudes of P1 (22%) and P4 (30%), and an increase in P4 latency in the mTBI mice.

These findings indicate that mTBI can result in significant deficits of auditory processing and the mouse model may prove to be a translational model for understanding the pathology and treatment of mTBI-induced auditory dysfunction

Funding
Work supported by: The University of South Florida - Tampa, FL

PS 315

Human frequency following responses to vocoded speech with amplitude modulation, and amplitude modulation plus frequency modulation.

Chandan Suresh; Ananthanarayan Krishnan
Purdue University

The speech processing strategy in most cochlear implants only extracts and encodes amplitude modulation (AM) in a limited number of frequency bands. Zeng et al (2005) proposed a novel speech processing strategy (FAME) that encodes both AM and frequency modulations (FM) to improve cochlear implant performance. Using behavioral assessment they reported better speech, speaker and tone recognition with this novel strategy. In this study, we recorded electrophysiological responses, specifically human FFR's, a non-invasive neural index of representation of speech sounds at the level of upper brainstem, to evaluate the contribution of AM and AM+FM (FAME) for speech encoding at 2, 4, 8 and 16 channels using a diphthong /au/. The results of the study indicate that the encoding of speech information is superior with FAME than AM alone when compared at 2, 4, 8 and 16 channels. The spectral slice data of vowels (/a/, /u/) and transition (a-u) also revealed better representation of speech cues with FAME than AM alone at 2, 4,8 and 16 channels. Interestingly, the recorded responses of 16 Channel FAME were equivalent to control stimulus and 2 channel FAME responses were comparable to 8 channel AM alone responses. The stimulus to response spectral correlation analysis revealed a correlation

coefficient of three times greater for FAME compared to AM alone at 8 and 16 channel responses. This indicates better encoding of complete harmonic structure for FAME strategy compared to AM alone. The results also reveal that FAME encoding provide better cues for pitch perception than AM alone by clear representation of fundamental frequency and equally spaced harmonics. Taken together, these results suggest that neural information preserved in the FFR may be used to evaluate signal processing strategies considered for cochlear implants.

Funding
Research supported by NIH 5R01DC008549 (A.K.).

PS 316

An Investigation of Hidden Hearing Loss in Young Adults with Normal Hearing

Garreth Prendergast[1]; Hannah Guest[1]; Deborah Hall[2]; Karolina Kluk-de Kort[1]; Agnès Léger[1]; Ann Hickox[3]; Michael Heinz[4]; Kevin Munro[1]; Christopher Plack[1]
[1]University of Manchester; [2]Nottingham Hearing Biomedical Research Unit; [3]Northwestern University; [4]Purdue University

Hidden hearing loss is a popular term describing a deficit in auditory function due to loss of synapses between inner hair cells and auditory nerve fibers (cochlear synaptopathy). Cochlear synaptopathy has been shown to occur in numerous rodent models as a result of both noise exposure and ageing, and is thought to affect primarily low-spontaneous-rate fibers that encode moderate to high intensity sounds. In humans, cochlear synaptopathy is not thought to be detectable by pure tone audiometry, as thresholds to quiet sounds in the rodent models are not permanently elevated.

To date there are three studies which provide some evidence for synaptopathy in young adult humans. Schaette & McAlpine (2011) showed a reduced wave I amplitude in the auditory brainstem response (ABR) for a group of tinnitus sufferers relative to controls. Reduced wave I amplitude has been demonstrated in the rodent model, and is a consequence of a loss of synapses. Therefore, cochlear synaptopathy is a candidate for an underlying cause of the tinnitus. Similar results were reported by Gu et al (2012). More recently, Stamper & Johnson (2015) reported wave I amplitude is negatively correlated with degree of noise exposure over the previous year.

The current study is a large-scale investigation of the relations between noise exposure, cochlear synaptopathy and perceptual performance in young adults with normal hearing. To provide a measure of neural function, we use the ABR and the frequency-following response. Behavioral measures include a number of basic psychophysical tasks as well as two speech-in-noise tasks. We compare results to those of a noise-exposure questionnaire which attempts to characterise the total amount of exposure to high level (>90 dBA) sounds over the course of an individual's lifetime.

Preliminary analysis of the first 100 individuals reveals no systematic reduction in ABR wave I as a function of estimated noise exposure. None of the electrophysiological or behavioral measures currently show a strong relation with noise exposure. In addition, wave I amplitude does not relate strongly to any of the behavioral measures. This initial analysis suggests that cochlear synaptopathy due to noise exposure may not be a major contributor to the variability between individuals on these measures of auditory function.

Funding
This work was supported by the Medical Research Council (MR/L003589/1).

PS 317

The Auditory-Brainstem Response to Continuous Speech is Modulated by the Speech Envelope and Can Inform on Speech Comprehension

Tobias Reichenbach[1]; Chananel Braiman[2]; Chagit Reichenbach[2]; Nicholas Schiff[2]; A. Hudspeth[3]
[1]Imperial College London; [2]Weill Cornell Medical College; [3]The Rockefeller University

Background
Speech evokes a complex auditory brainstem response (ABR) that encodes many aspects of the acoustic stimulus. In particular, the brainstem's response can track the fundamental frequency of speech that typically varies between 100 Hz and 300 Hz. Because the brainstem also receives extensive efferent feedback from the auditory cortex, the brainstem may engage in the processing of speech as well as in attention to one of multiple speakers. Recent research on the potential modulation of the ABR to short speech signals such as vowels by attention or speech intelligibility has, however, yielded inconclusive results. This may be partly due to the small signal-to-noise ratio of the brainstem's response, which necessitates many repetitions of short speech signals to which the brain may then adapt.

Methods
We sought to measure the ABR to continuous non-repetitive speech. We thus employed the computer-linguistic program Praat to convert natural continuous speech, in which the fundamental frequency varies, to monotone speech in which the spectral structure remains constant. We then recorded ABRs from healthy volunteers presented with a monotone speech stream. To assess whether the ABR is modulated by speech comprehension, we measured the response of the auditory brainstem both when presenting intelligible, forward speech as well as unintelligible speech played in reverse.

Results
We found that the brainstem exhibited a reliable response at the constant fundamental frequency and at higher harmonics of the monotone speech. We further found that this response is modulated by the envelope of the voiced parts of speech, and has a characteristic delay of about 10 ms. We accordingly introduced a novel measure that assesses the ABR as modulated by the speech envelope, at the fundamental frequency of speech and at the characteristic latency of the response. This measure has a high signal-to-noise ratio and can hence be aptly employed to measure the ABR to

continuous speech. We then used this novel measure to show that the auditory brainstem response is weaker to intelligible speech than to unintelligible, time-reversed speech.

Conclusions
We show that the ABR to the fundamental frequency of monotone, continuous speech can be reliably detected, and we demonstrate that this signal is modulated by speech comprehension. The methods that we develop here can be employed for further research on speech processing in the auditory brainstem, as well as for future clinical diagnosis of the functionality of the brainstem and higher cognitive processes.

Funding
This research was supported by a National Science Foundation Graduate Research Fellowship to C.S.R., by a National Institutes of Health T32 pre-doctoral training grant to C.B, and by EPSRC grant EP/M026728/1 to T.R.. A.J.H. is an Investigator of Howard Hughes Medical Institute.

PS 318

Frequency Following Response Elicited by Mandarin Lexical Tones in Mandarin Speaking Elderly Adults

Shuo Wang[1]; **Jiong Hu**[2]; Gabriella Musacchia[2]
[1]Beijing Tongren Hospital; [2]University of the Pacific

Background
Perceptual studies have shown that elderly adults may have difficulty in speech discrimination, especially in the presence of background noise. It has been proposed that speech discrimination difficulties suffered by elderly adults even with normal hearing may be attributed to a decrease in temporal processing ability. Supporting this notion, electrophysiological studies have found delayed neural timing, decreased neural synchrony, and decreased temporal processing ability with aging. Recent studies, however, have also demonstrated that language experience and auditory training enhances the temporal dynamics of sound encoding in the auditory brainstem response. The purpose of this study was to explore the age effect in pitch processing ability in population with a tonal language background.

Method
Mandarin speaking elderly (n=12) young (n=12) adults were recruited. They all had normal audiometric test results as well as normal suprathreshold click-evoked ABR timing. Four Mandarin Chinese syllables with different fundamental frequency pitch contours were used to elicit brainstem responses. All stimulus tokens were controlled by NeuroScan Stim2 system and presented monaurally at 70 dB SPL. EEG signals were collected using standard ABR procedures. Fundamental frequencies (f0) of both the stimulus and the responses were digitally extracted and compared to individual brainstem responses. Three indices were used to examine different aspects of pitch processing ability at the brainstem level: Pitch Strength, Pitch Correlation and Response Robustness. Responses elicited by different tones were also compared across and within the elderly and young adult groups.

Results
Pitch contours elicited overall weaker brainstem responses in the elderly group. However, significant group differences were only found when the tone with a falling f0 were used as the stimulus, where all three test indices were measured. The other three tones, on the other hand, provided variable group comparison results.

Conclusion
Results of this study demonstrated that in tonal language speaking population, the pitch processing ability at the brainstem level in elderly adults are not as strong and robust as their younger counterparts. This is not surprising given that their temporal processing capacity have decreased with aging. However, Mandarin tone elicited FFR have been shown to correlate with the length of language exposure. Mandarin speaking elderlies' degraded but not drastically declined FFR responses supported the hypothesis that although age does affect pitch processing ability at the brainstem level in Mandarin speaking elderly adults, their long-term language exposure somewhat counteract such change and help reducing the degradation rate in their temporal processing capacity.

PS 319

Comparison of ASSRs and TEOAEs for Measuring MOC Function in Humans

Ian Mertes; Marjorie Leek
VA Loma Linda Healthcare System

Background
The medial olivocochlear (MOC) branch of the auditory efferent system modulates cochlear function, which appears to benefit speech perception in noise. Measurement of MOC function may therefore be clinically useful in the assessment of speech-in-noise problems. In normal-hearing humans, MOC function is quantified as the amount of change in otoacoustic emission (OAE) amplitude with versus without MOC activation. However, OAEs are often weak or absent in ears with hearing loss, so little is known about MOC function in the presence of hearing impairment. A potentially useful alternative method to assess MOC function is the auditory steady-state response (ASSR), a measure of neural function which can be elicited in hearing-impaired ears using suprathreshold stimulus levels (Vander Werff & Brown, ***Ear Hear***, 2005). Animal work has shown that MOC activation can cause larger changes in the amplitudes of neural responses relative to OAEs (Puria et al., ***J Acoust Soc Am,*** 1996). Therefore, the ASSR may allow for more robust measurements of MOC function than OAEs, especially in hearing-impaired ears. This study served as an initial investigation into the feasibility of using the ASSR to assess MOC function in humans.

Method
Adults with normal hearing or mild sensorineural hearing loss participated. To directly compare results between ASSRs and TEOAEs, the measurements were obtained concurrently

using 60 dB pSPL clicks presented at 39.06/s. Contralateral acoustic stimulation (CAS) for activating the MOC consisted of broadband Gaussian noise presented at 60 dB SPL. Three sets of recordings were obtained, with CAS interleaved on and off during the recordings. Methods were implemented to control for middle-ear muscle reflex activation. MOC effects were quantified as the change in response amplitude in dB, measured with versus without CAS, where a larger change suggested stronger MOC function.

Results

Adequate signal-to-noise ratios were obtained for both measurements, demonstrating the feasibility of concurrent measurements of ASSRs and TEOAEs. Preliminary results indicated considerable inter-subject variability in the size and stability of MOC effects. However, some subjects showed MOC effects on ASSRs that were 4–6 dB larger than those of TEOAEs.

Conclusion

ASSRs appear to be a feasible assay of MOC function in adults with normal and near-normal hearing, and can demonstrate larger MOC effects than TEOAEs. Further work will determine if the results extend to individuals with more severe hearing losses and will also examine the correspondence between ASSR-based measures of MOC effects and speech-in-noise abilities.

Funding

Work supported by NIDCD.

PS 320

Transcriptome of hearing loss in mice segregating the highly prevalent human GJB2 p.V37I variant

Ying-Chang Lu[1]; **Chung-Wei Yu**[1]; Yen-Hui Chan[1]; Chen-Chi Wu[1]; Chuan-Jen Hsu[1]; Xi Lin[2]

[1]National Taiwan University Hospital; [2]Emory Univ School of Medicine

The recessive p.V37I allele of the *GJB2* gene is a variant with debatable pathogenicity. The allele frequency of *GJB2* p.V37I is as high as ~10% in certain East Asian populations, and it is estimated that > 5 millions people are homozygous for *GJB2* p.V37I. Despite its contribution to sensorineural hearing impairment (SNHI), the pathogenic mechanisms of p.V37I remain elusive, and clinically the audiological phenotypes vary significantly among homozygous individuals. Recently, we generated knock-in mice homozygous for *Gjb2* p.V37I (the V37I mice) which demonstrated progressive hearing loss with age. At 30 weeks, a significant difference in hearing thresholds were observed between V37I mice and wild-type mice (ABR clicks: 52.6 ± 7.3 dB SPL vs. 39.2 ± 3.3 dBSPL, $p < 0.05$). Because of the variation in hearing levels, we further divided V37I mice into two groups: mice with better hearing (V37I-BH; 45.9 ± 3.2 dBSPL, n=16) and those with poorer hearing (V37I-PH; 59.3 ± 2.7 dBSPL, n=7) in the present study. We then performed RNA-seq analyses on the inner ear extracts obtained from these two groups and the wild-type (WT) mice (n=10). The RNA-seq data were subjected to Ingenuity Pathways Analysis (IPA) and Kyoto Encyclopedia of Genes and Genomes (KEGG), and the differentially expressed genes were validated by quantitative polymerase chain reaction (qPCR) and immunohistochemistry (IHC) staining. We identified 137 genes differentially expressed between the WT and V37I-PH groups, 64 genes differentially expressed between the WT and V37I-BH groups, and 49 genes differentially expressed between the V37I-BH and V37I-PH groups. Genes considered highly correlated to hearing loss included: *Celf3*, *Cxcl10*, *Cyp2f2*, *Cyp4a12a*, *H2-Q6*, *Ltf*, *Mmp9*, and *Saa1*. By using qPCR and IHC assays, we have validated the expression of these genes in the inner ear. Canonical pathways identified by IPA included communication between innate and adaptive immune cells and LXR/RXR activation, indicating that immune system and reactive oxygen species might play a pivotal role in the development of hearing phenotypes associated with *GJB2* p.V37I. Our results provide insights into the molecular pathology of hearing loss related to the *GJB2* p.V37I variant, and may inform future studies on the potential therapeutic implications of modulating the associated genes or pathways.

PS 321

The gEAR portal – gene Expression for Auditory Research

Joshua Orvis[1]; Amiel Dror[2]; Beatrice Milon[1]; Ran Elkon[2]; Anup Mahurkar[1]; Ronna Hertzano[1]

[1]University of Maryland Baltimore; [2]Tel Aviv University

Next generation sequencing as a tool for recording gene expression has increased in popularity over the past decade. If 2001-2010 were marked by the use of microarray technology as the primary tool for global analysis of gene expression, 2011 marked a general transition to next generation sequencing as the primary tool. In parallel, new approaches have been developed for cell type-specific analysis of the inner ear. These range from flow cytometry to single cell isolation and translatome analysis in a variety of animal models. Together, these developments make next generation sequencing a commonly used tool in most molecular research laboratories. While each experiment is designed to answer a unique investigator-initiated question, the datasets that are generated form a wealth of data that could be used by the research community at large. However, query, cross-comparison and even presentation of two datasets side by side is a complicated and time-consuming task for most biologists.

The gEAR portal (http://gear.igs.umaryland.edu/) is a website for dissemination, presentation and cross-comparison of cell type-specific gene expression from the auditory and vestibular systems in the public domain. The gEAR is focused on accurate quantitative representation of complex gene expression data in a simple and intuitive graphical format, simplifying access to gene expression data for all researchers in the inner ear community. New features since ARO 2014 include numerous additional datasets, personal accounts for flexible viewing of datasets, self-upload of datasets for personal and/or public viewing, inner ear single-

cell RNA-seq data and much more. The gEAR portal is a free online resource. We invite you to use the site, and provide us feedback so we can improve the portal. In addition we urge you to share your data with the larger research community through the gEAR portal.

Funding
NIDCD/NIH RO1DC013817

PS 322

Unraveling Spiral Ganglion Neuron Heterogeneity by Single-neuron RNAseq

Brikha Shrestha; Lisa Goodrich
Harvard Medical School

An important aspect of auditory perception is the faithful representation and transmission of sound stimuli by spiral ganglion neurons (SGNs), the primary sensory neurons of the auditory pathway. Functional and anatomical investigations of these neurons, some dating almost half a century ago, have revealed intriguing details about their heterogeneity; yet, the molecular underpinnings of this SGN property remain largely unknown. This has been a major roadblock for comprehensive circuit-level inquiry of how SGNs contribute to our sense of hearing beyond relaying information from hair cells to the cochlear nucleus. Elucidating SGN heterogeneity at a molecular level may also provide crucial new insights into their varying vulnerabilities to noise-inflicted and age-associated damage, both of which carry significant health implications for the general public. Here we sought to gain insight into the molecular basis of SGN heterogeneity by conducting single-neuron transcriptional profiling by the RNAseq method. cDNA libraries representing individual post-hearing SGN transcriptomes were made and sequenced using the Illumina Hiseq 2500 platform. Results of comparative gene expression analyses of SGNs are presented and their direct implications for SGN heterogeneity as well as broader significance for SGN vulnerabilities are discussed.

Funding
Lefler Foundation, Harvard Medical School; Harvard Brain Science Initiative, Harvard University

PS 323

Transcriptome Profiling of Spiral and Vestibular Ganglion Neurons

Anastasia Levichev-Connolly[1]; Robert Durruthy-Durruthy[1]; Rose Leu[1]; Cuiping Zhong[1,2]; Danielle Gochez[1]; Stefan Heller[1]; Mirna Mustapha[1]
[1]Stanford University; [2]Lanzhou General Hospital of People's Liberation Army

Background
Spiral and vestibular ganglion neurons (SGNs and VGNs) relay information from sensory hair cells to the central nervous system. Two types of SGNs exist: myelinated type I neurons that innervate inner hair cells and unmyelinated type II neurons that innervate outer hair cells. In the vestibule, VGNs are categorized as calyx, dimorph, or bouton, which are all structurally and functionally distinct. However, the genes and pathways that regulate neuronal development and provide transcriptional identity and functional diversity to SGN and VGN subtypes are poorly understood. A recent study (Lu et al., 2011) elucidated gene expression patterns in the spiral and vestibular ganglia throughout development. In our study, we extend this analysis by making use of transgenic reporters, which allow for separate transcriptome analyses of selected afferent neuron subtypes.

Methods
We used postnatal day (P)8 Prph1-GFP;Bhlhb5-Cre;Rosa26-tdTomato mice and fluorescence-activated cell sorting to collect four cell populations: type I SGNs, type II SGNs, calyx/dimorph VGNs, and bouton VGNs. Following RNA extraction and transcriptome-wide microarray analysis, we compared gene expression levels in a pairwise manner to identify genes that are differentially enriched. Gene ontology and Ingenuity Pathway analyses were employed to assess biological processes and signaling pathways that differ between the populations.

Results
Type I and type II SGNs both expressed genes involved in development, which were often different members of the same family, such as Foxd1 in type I and Foxd3 in type II. Gene ontology analysis revealed that type I SGNs expressed genes known to play crucial roles in inner ear development, such as Neurod1 and Zic2, while type II SGNs expressed many transcripts associated with guidance and adhesion.

In the vestibule, calyx/dimorph neurons expressed various members of the Fgf, Neurod, and Zic families, which are involved in cell differentiation, while bouton neurons expressed many metabolism-related genes.

Interestingly, pairwise analysis revealed that calyx/dimorph VGNs and type I SGNs are strikingly similar, as indicated by the small number of differentially expressed genes between the populations. Transcriptional profiles of type II SGNs and bouton VGNs were not as similar. Type IIs expressed many physiology-related genes, such as Nrxn I and II, and Syn I and II, while bouton VGNs expressed many transcripts involved in adhesion and cell matrix organization.

Conclusions
Our study identified differentially expressed genes that could serve as markers for novel mouse models to distinctively label SGN and VGN subtypes and permit further study of these neurons.

Funding
NIH DC009590 (MM)

PS 324

Identification of genetic factors contributing to age-related hearing loss in humans

Hui Li[1]; Megan Kobel[1]; Zhenyu Jia[1]; Brent Spehar[2]; Nancy Tye-Murray[2]; Robert Frisina[3]; Jianxin Bao[1]
[1]Northeast Ohio Medical University; [2]Washington University in St. Louis; [3]University of South Florida

Background

Age-related hearing loss (ARHL), also known as presbycusis, is a universal feature of mammalian aging and is characterized by a decline of auditory function, such as increased hearing thresholds, poor frequency resolution, starting at high frequency regions, and difficulty processing complex sounds in background noise. Clinically, ARHL is comprised of a combination of genetic and environmental factors. Previous genome-wide association studies (GWAS) failed to identify genetic variations that account for hearing abilities with age, suggesting that ARHL is caused by many causative genetic elements, each with small influences. To identify these multiple genetic elements, more stringent sampling, more powerful technology to detect rare genetic variants and more robust statistical methods are required.

Methods

We obtained a dataset including 636 subjects over 55 years old from the Rochester, NY greater metropolitan area. The hearing ability of each subject was measured by a battery of auditory tests: pure-tone audiogram, supra-threshold gap detection, speech recognition threshold and Hearing-in-Noise-Test (HINT). The subjects were classified into five groups based on pure-tone audiograms: golden ear (GE), flat, high-frequency steep slope (HFSS), high-frequency gentle slope (HFGS), and mixed; each of which represents a unique audiogram configuration. The representative members from each group were selected for whole exome sequencing (WES), which is a powerful technology to detect both common and rare variants in the protein-coding regions of human genes.

Results

WES data from 118 subjects were collected with an average of 39,769 single-nucleotide polymorphisms (SNPs) and 3,531 insertion/deletion (indels) per subject. The attempt to identify SNPs associated with ARHL defined by pure-tone thresholds did not yield any genome-wide significant association, consistent with previous findings.

Conclusion

Our results confirmed that ARHL is a complex trait and contributed collectively by SNPs that fail to reach genome-wide significance. New statistical methods to identify ARHL-associated genetic patterns which represent a collection of genetic elements need to be developed, along with ongoing analyses of relations of more complex hearing test with candidate genes for presbycusis.

Funding

Work supported by NIH-NIA grant P01 AG009524.

PS 325

Simultaneous Multigene Mutation Detection in a Multi-Ethnic Cohort of Patients with Sensorineural Hearing Loss Through MiamiOtoGenes Panel

Denise Yan
University of Miami

Background

Genetic causes of hearing loss are very heterogeneous. Thus far, more than 66 genes have been characterized for nonsyndromic hearing loss. In addition approximately 150 genetic loci have been mapped, and it is estimated that the number of genes could reach 300, equivalent to 1% of all human genes. Extreme genetic heterogeneity of deafness combined with striking variations in the distribution of causative variants in different ethnic groups has made genetic diagnosis expensive and time consuming using traditional methods.

Methods

We took advantage of the SureSelect target capture system (Agilent; https://earray. chem.agilent.com/suredesign/) to develop a custom capture panel (MiamiOtoGenes) to contain all exons, 5' UTRs and 3' UTRs of 180 known and candidate deafness causing genes. A target size of approximately 1.158 MB comprising 3494 regions was designed to include genes associated with both syndromic and nonsyndromic hereditary hearing loss. We undertook a targeted sequencing of the 180 genes in a multi-ethnic cohort (South American consisting of Brazilian, Guatamalan, Tunisian, Nigerian, indigenous South African, Turkish, Iranian, Indian, South Florida multi-ethnic patients) of 360 GJB2 mutation–negative probands. Hearing loss (HL) was congenital or prelingual-onset with a severity variant from mild to profound. The Genomes Management Application (GEMapp; https://secureforms.med.miami.edu/hihg/gem-app) was used for data filtering. Single-nucleotide variants (SNVs), insertion/deletions (INDELS) and copy-number variations (CNVs) were determined. Computational functional prediction algorithms [ClinVar; American College of Medical Genetics and Genomics (ACMG) guidelines] and conservation scores (PHASTCONS, GERP) were also applied.

Results

Overall, the mutation detection rates for a likely pathogenic variant are high, at 55% to 75%, for South American, Indian, Tunisian, Turkish, Iranian, Indian, South Florida groups. In contrast, the pickup rates for Nigerian, indigenous South African are currently low, with only approximately 14% to 50% of probands have sequence changes identified as a probable cause of deafness. There are no predominant recurring mutations in the selected genes within ethnic groups. The lower rate of mutations found amongst sub-Saharan African patients may be indicative of the link of infectious disease to deafness.

Conclusion

Our study highlights the utility of next generation sequencing techniques combined with functional studies analysis tools

to provide insight into the etiology of a genetically heterogeneous human disorder such as deafness. Furthermore our data indicate that a deafness gene based panel may be a more cost effective way of assessing genetics of hearing loss in a particular population.

Funding
The work is supported by NIH R01DC012115, R01DC005575, R01DC009645 and the University of Ibadan TETFund Grant.

PS 326

A Sequential Screening Strategy for Efficient Rare Gene Discovery in Small Families

XueZhong Liu[1]; Mhamed Grati[1]; Rahul Mittal[1]; Zhongmin Lu[2]; Susan Blanton[1]; Mustafa Tekin[1]; Denise Yan[1]
[1]University of Miami Miller School of Medicine; [2]University of Miami

Background
The extreme heterogeneity of nonsyndromic sensorineural hearing loss (NSHL) makes serial sequencing approaches unfavorable in terms of efficiency and cost. However, the discovery that genes at only 2-3 loci account for a major component of human deafness suggested that the sequential screening of DNA samples from probands in multiplex sibships for mutations would be a cost effective strategy. Although next-generation sequencing has expedited the discovery of genetic variants, the large number of variants naturally present in each individual makes it challenging to pinpoint the causative mutations. We aim to identify the genetic cause of NSHL through an integrated paradigm combining microarray, copy number variations (CNVs) analysis, whole genome sequencing (WES), and a hearing-centric database.

Methods
We are using a DNA microarray panel (Miami-CapitalBio) as the initial screening to simultaneously detect the most common deafness-causative mutations from four genes (GJB2, GJB6, SLC26A4 and 12S rRNA). We then perform a custom capture/next-generation sequencing gene panel (MiamiOtoGenes) composed of 180 known deafness genes (Agilent SureSelect DNA Design). Patients for whom the two panels do not provide a meaningful result, WES is performed to achieve a comprehensive interrogation of the full spectrum of variants to detect single-nucleotide variants (SNVs), insertion/deletions (Indels) and CNVs. The Genomes Management Application (GEMapp; https://genomics.med.miami.edu/) is applied for data analysis. Computational functional prediction algorithms (PolyPhen, SIFT, MutationTaster) and conservation scores (PHASTCO, GERP, PHYLOP) are also applied. Causative mutations for the enrolled individuals are stored in the HL Genotype Database, a web-based resource GeneHeal.

Results
In this study we perform WES on five families that are not amendable to conventional approaches. Approximately, 92,000 SNVs and 9,206 INDELS per sample were obtained before variant filtering. Coverage of targeted exons for >10 reads were ranged from 90.3% to 93.5% and >20 reads from 80% to 83.5%. By our filtering strategy, we have rapidly identified homozygous and heterozygous variations in the five families presenting autosomal recessive and dominant NSHL, respectively. Sanger sequencing confirmed co-segregation of the variants in five new genes with the disease phenotype in each family.

Conclusion
We have identified several novel new genes for NSHL. Their functional studies will be presented and discussed. Our study shows that the integrated screening strategy is an efficient approach to rare hearing-loss gene discovery in small families not suitable for linkage analysis. If variants are not found in the genes included on Miami-CapitalBio and MiamiOtoGenes, WES should be considered in small multiplex families.

Funding
The work is supported by R01DC012546, R01DC121125, and R01DC005575 to XZL

PS 327

SEQaBOO – Sequencing a Baby for Optimal Outcome: A Clinical Genomic Application of Newborn Hearing Screening

Anne Giersch[1]; Jun Shen[1]; Margaret Kenna[2]; Michael Cohen[3]; Jennifer Hochschild[4]; Shamil Sunyaev[1]; Michael Talkowski[5]; Margaret Toro[6]; Cynthia Morton[1]
[1]Brigham and Women's Hospital, Harvard Medical School; [2]Children's Hospital Boston, Harvard Medical School; [3]Massachusetts Eye and Ear Infirmary, Harvard Medical School; [4]Harvard University; [5]Massachusetts General Hospital, Harvard Medical School; [6]Brigham and Women's Hospital

SEQaBOO (SEQuencing a Baby for an Optimal Outcome) will integrate high-throughput genomic approaches into routine newborn screening for hearing loss. The project will enroll approximately 500 newborns who do not pass their initial newborn hearing screening and their parents for genomic sequence analysis. Today, congenital hearing loss and other subtle birth defects are recognized in newborns through newborn screening, allowing early interventions that limit life-long disabilities. Development of next generation DNA sequencing technologies provides a new opportunity as well as challenge for researchers and clinicians dedicated to improving the lives of newborns with birth defects to investigate whether genetic etiologies of congenital defects can be more accurately and efficiently defined and whether improved genetic diagnosis translates into superior clinical care. In this project we aim to address this challenge by assessing the clinical impact of genomic data in newborns with congenital hearing loss. Analytic pipelines are being developed to provide automated variant prioritization and to support accurate clinical interpretation of genomic variants. When appropriate, genetic information will be returned to parents and physicians for early intervention purposes. Although not life threatening, hearing loss requires a number of adjustments by the family and patient to optimize quality of life. In some instances, cochlear implants can restore hearing to near normal levels.

Other therapeutic interventions for congenital hearing loss are under development. As there are many different etiologies of congenital hearing loss that range from genetic variation to viral infection, we surmise that appropriate therapies may vary depending on the precise etiology. Genetic causes of hearing loss are highly heterogeneous and pathogenic variants in >115 genes have already been identified. In this project, we will test the hypothesis that rapid discovery of the exact cause of a newborn's hearing loss will benefit management and therapeutic interventions. Annually we will survey the cohort of children to ascertain general health, including speech and language development in addition to hearing status, and parental attitudes on genomic sequencing. In sum, we will analyze and assemble genomic datasets, perform clinical genomic research of hearing loss identifiable through newborn screening and explore implications of integration of genomic sequencing into newborn screening. All of this will inform the impact of genomic sequencing on the care and management of newborns with congenital hearing loss and allow us to investigate factors associated with our society's acceptance of this new technology for "optimal outcome" of a newborn baby.

Funding
NIDCD

PS 328

A Multi-Ethnic Genome-Wide Association Study of Age-Related Hearing Impairment

Thomas Hoffmann[1]; Catherine Schaefer[2]; Neil Risch[1]; Lawrence Lustig[3]
[1]University of California, San Francisco; [2]Kaiser Permanente; [3]Columbia University

Age-related hearing impairment (ARHI) is a complex disease that makes understanding speech and communication difficult, reducing overall quality of life. Research has shown that ARHI is heritable, but it has proven difficult to implicate specific loci in humans, with no replicated locus yet found. We conducted a genome-wide association study of time-to-onset of age-related hearing impairment on 8,180 individuals who had progressed to ARHI (average age 75.1, sd 9.2) and 86,015 individuals who had not yet developed ARHI (average age 67.5, sd 13.6) in the racially/ethnically diverse Kaiser Permanente Research Program on Genes, Environment, and Health (RPGEH) Genetic Epidemiology Resource on Aging (GERA) cohort (80.8% non-Hispanic white, 8.5% Latino, 7.5% East Asian, and 3.5% African American). These individuals have genome-wide genotype data on over 650,000 SNPs, which have been imputed to millions more from the 1000 Genomes Project, as well as comprehensive electronic health records (EHR) (average 23 years of follow-up), from which we defined the onset of the ARHI phenotype and other time-varying covariates. We required two ICD-9 codes for the phenotype and each covariate. Using a cox proportional hazards model in non-Hispanic Whites, we found that being male (HR=1.4, p<2e-16), hypertensive (HR=1.6, p<2e-16), having osteoporosis (HR=1.5, p<2e-16), and having chronic pain (HR=1.9, p<2e-16) all increased the hazards ratio of ARHI, as expected based on previous literature; having diabetes was suggestive (HR=1.05, p=0.13). These effects may be biased downward due to misclassification of individuals who did not seek treatment. Although the phenotype definition is different in our cohort (several other studies have used hearing frequency thresholds), no evidence for any previously reported significant or suggestive loci was found. However, our GWAS scan implicated a potential novel loci in ARHI (p<5e-8), which we are working to confirm.

Funding
This work was supported by grant K01 DC013300 to TJH from the National Institutes of Health.

PS 329

Multivariate Genome-Wide Association Studies (GWAS) boost in power to detect new hearing loci: the example of hearing and BMI, Blood pressure and Coffee Intake

Dragana Vuckovic[1]; Maria Pina Concas[2]; Erik Fransen[3]; Umberto Ambrosetti[4]; Martina La Bianca[5]; Abdulhadi Khalid[6]; Guy Van Camp[3]; Mario Pirastu[2]; Paolo Gasparini[1,7]; Giorgia Girotto[1,7]
[1]University of Trieste, Italy; [2]Institute of Population Genetics, National Research Council of Italy; [3]University of Antwerp; [4]Università degli Studi di Milano and Fondazione IRCCS Cà Granda Ospedale Maggiore Policlinico; [5]Institute for Maternal and Child Health IRCCS "Burlo Garofolo", Trieste, Italy; [6]Hamad Medical Corporation; [7]Sidra, Doha, Qatar

Background
The genetic bases of complex traits such as Normal Hearing Function (NHF) and Age-Related Hearing Loss (ARHL) are largely unknown. Recently, we identified two new genes (*PCDH20* and *SLC28A3*) in a single-trait GWAS meta-analysis on NHF (Vuckovic et al. HMG 2015), whose mice models are now in progress. However, many biological features are better described by a combination of several variables, e.g. hearing, which is measured on different frequencies. In order to investigate the audiometric curve we applied a multi-trait GWAS to analyse 4 hearing thresholds (HT) simultaneously. Furthermore, we tested the association between HT and other phenotypes that might play a role with the auditory function such as Body Mass Index (BMI), Blood Pressure (BP) and coffee consumption in 2059 subjects coming from isolated populations in Italy and Central Asia (discovery set) and in ~2000 subjects from independent cohorts (replication set-Figure1).

Methods
A multivariate linear mixed model regression was performed using GEMMA (Zhou&Stephens, Nat.Met. 2014). After adjusting for sex, age and relatedness, the following traits were tested: (a) 4 hearing thresholds (HT) (0.5, 2, 4, 8 kHz); (b) HT and BMI; (c) HT and BP; (d) HT and coffee consumption. Results were combined in a multivariate meta-analysis based on inverse-variance weights using the R-package MultiMeta (Vuckovic et al. Bioinformatics 2015).

Results

Preliminary results for HT (a) identified the following top SNPs: rs181948008 (p=4e-09) within *CYP4B1* gene, rs1523730 (p=3.04E-07) close to *CNTNAP2,* a gene located within the deafness locus DFNB13 and rs72984055 (p=2.27E-07) within *MMP20* (metalloproteinases were already involved in hearing loss). In order to investigate previous epidemiological data in which higher BMI was associated with poorer hearing (Curhan et al. 2013), analysis (b) was performed revealing suggestive association with rs62418085 (p=2.47E-07) located within *PRIM2,* a gene already associated with fatty acid levels. Interestingly, analysis (c) highlighted rs17176633 (p=2.07E-07) close to *STK39* gene involved in phosphorylation of Na(+)-dependent chloride co-transporters, which play a critical role in both renal salt balance and hearing (Ponce-Coria et al. 2014). Finally, (d) identified a region close to a transcription factor (*TCF4*). The replication step is in progress to confirm present findings in ~2000 samples from independent and genetically diverse populations in Belgium, Qatar and Italy.

Conclusions

Results show that multivariate testing gives significant boost in power to detect new loci affecting NHF and ARHL, while also allowing the genetic detection of both interactions (between HT and other phenotypes) and pleiotropic loci.

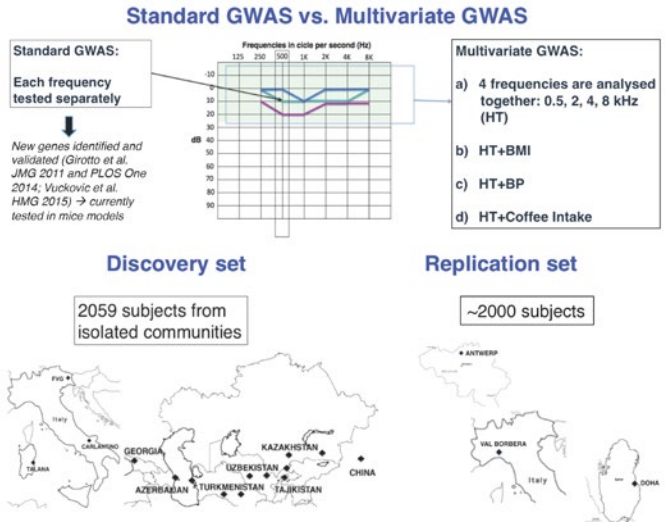

Funding

The study was supported by funds from Italian Ministry of Health (RC16/06 and RF2010) (to PG).

PS 330

OtoScript: a Novel Genetic Testing Platform to Improve the Accuracy and Efficiency of Clinical Molecular Genetic Diagnosis of Hearing Loss

Jun Shen[1,2]; Dong-Young Lee[1]

[1]Brigham and Women's Hospital; [2]Harvard Medical School

Each year, more than 12,000 babies are born with hearing loss in the United States alone, and about half of them are due to genetic causes. Knowing the exact genetic lesions allows early diagnosis even before the onset of noticeable symptoms, informs the choice of optimal management plans, and predicts risks for relatives including future babies. Recent advances in gene therapy are very promising to enable personalized medicine, but its realization requires the identification of the precise causative genetic lesion, so that gene therapy can specifically target the culprit lesion to maximize efficacy and minimize side effects. Targeted high-throughput sequencing of genomic DNA has become state of the art in clinical molecular genetic diagnostics, resulting in the identification of a large number of DNA variants. However, the diagnostic yield remains unsatisfactory due to the lack of functional and statistical evidence to determine their clinical significance. Here we report the development of OtoScript, a novel targeted RNA-seq-based genetic testing approach. It combines advantages of both targeted next-generation sequencing of genomic DNA and RNA-Seq of the transcriptome to enable improved variant identification and interpretation, which is fundamentally different from current genomic-sequencing-based clinical genetic testing platforms. We evaluated all known hearing loss genes and updated the information at the Shared Harvard Inner Ear Laboratory Database (https://shield.hms.harvard.edu), and shared the information in this useful resource with the research community. We developed a bioinformatics tool that automatically designs RNA-seq capture libraries with even tiling depths, complete coverage, and reduced cost. Using this tool, we developed a custom-designed OtoScript capture kit of 115 known hearing loss genes and control probes. We performed the OtoScript test on three cell lines derived from a hearing loss patient with the *USH1C* (NM_005709.3): c.216G>A variant and both heterozygous parents. Our results demonstrated that OtoScript has highly enriched transcripts of hearing loss genes from lymphocytes, including genes with expression levels barely detectable in this type of tissue, such as *GJB2*. It has successfully detected the USH1C variant in the samples and revealed the splicing defect. In summary, OtoScript not only detects genetic variation that may be missed by conventional genomic sequencing, but also reveals functional consequences at the transcriptional level, allowing accurate assessment of the clinical significance of genetic variants. This novel approach holds the potential to improve the accuracy and efficiency of clinical molecular genetic diagnosis of hearing loss.

Funding

NIH R03DC013866

PS 331

Newborn genetic screening for hearing impairment: a population-based longitudinal study

Yingchang Lu[1]; **Chen-Chi Wu**[2]; Ching-Hui Tsai[2]; Chia-Cheng Hung[2]; Yin-Hung Lin[2]; Chuan-Jen Hsu[2]; Yungling Leo Lee[2]
[1]National Taiwan University; [2]National Taiwan University Hospital

Background
The feasibility of genetic screening for common deafness mutations in newborns has been reported in several recent studies. However, there is still a paucity regarding the long-term results in those screened positive for deafness mutations, which are crucial to determine the cost-effectiveness for justifying population genetic screening.

Methods
We performed simultaneous newborn hearing screening and newborn genetic screening targeting four common deafness mutations (namely p.V37I and c.235delC of *GJB2*, c.919-2A>G of *SLC26A4*, and the mitochondrial m.1555A>G) in 5173 newborns, and analyzed serial audiometric results up to 6 y in those with conclusive genotypes.

Results
Newborn genetic screening identified a total of 82 (1.59%) babies with conclusive genotypes, including 62 (1.20%) with *GJB2* p.V37I/p.V37I, 16 (0.31%) with *GJB2* p.V37I/c.235delC, and 4 (0.08%) with m.1555A>G. Among them, 56% passed hearing screening at birth. Long-term follow-up demonstrated progressive hearing loss in children with the *GJB2* p.V37I/p.V37I and p.V37I/c.235delC genotypes which deteriorated approximately 1 dBHL per year.

Conclusions
Our results delineated the longitudinal auditory phenotypes of the highly prevalent *GJB2* p.V37I mutation on the general population basis, and confirmed the utility of newborn genetic screening in identifying infants with late-onset or progressive hearing impairment undetectable by newborn hearing screening.

PS 332

Deafness Mutation Screening Results Obtained from Sporadic Adult and Newborn Subjects Support the Clinical Utility of the Next Generation Sequencing (NGS) Approach

Jingqiao Lu; **Xi Lin**
Emory University School of Medicine

Background
Targeted capture and sequencing of all reported human genes linked to deafness by the NGS approach may provide a powerful screening tool for finding genetic mutations in patients who suffer deafness caused by genetic mutations. However, the basic parameters of clinical utilities in using such a NGS technology for mutation screening among deafness genes are unknown.

Methods
In order to answer this question we have tested three groups of patients: (1) sporadic adult patients (N=583) who are diagnosed of sensorineural hearing loss suspected of genetic reasons; (2) newborns who failed the newborn hearing screening (N=205) due to reasons that are highly suspected of genetic origin; (3) adults (average age about 30) confirmed to be normal hearing by pure-tone audiogram (N=481). The genetic variations and mutations among these subjects were sequenced using an Illumina HiSeq platform and processed by a bioinformatic pipeline developed in the lab.

Results
The number of false positives was greatly reduced by using the genetic variants found in adult normal hearing controls as filters. Among the sporadic adult patients the test sensitivity and specificity was 0.66±0.03 and 0.7±0.04, respectively. For newborn samples, the sensitivity was significantly increased to 0.91±0.02, while specificity was unchanged at 0.69±0.03. Youden's index improved from 0.36 to 0.61. Negative predicative value increased from 0.46 to 0.91. Preliminary data showed a spectrum of mutations in following genes (prevalence among our samples are given in parentheses): GJB2 (54.2%), SLC26A4 (17.8%), MYO7A (4.7%), WFS1 (3.7%), OTOF (1.9%), MT-TM (1.9%), CDH23 (1.9%), USH2A (1%), USH1C (1%). Among the likely pathogenic mutations (new mutations not reported in literature) we found: MYO7A (43.5%), TMPRESS3 (42%), TMPRESS5 (2.7%), SPINK5 (1.2%), MYH14 (1.2%), PCDH15 (0.8%), MYO3A (0.8%), MYO1A (0.8%), MYO15A (0.8%), KCNQ1 (0.8%).

Conclusions
Newborns who failed the hearing screening may represent a more homogenous population than the sporadic adult patient population. The NGS data we collected by screening 130 deafness genes support the benefits and the clinical utility of applying a NGS approach, especially in the newborn population, in genetic screening of mutations responsible for causing hearing loss.

Funding
Supported by NIH grants RO1 DC006483 and R33 DC010476

PS 333

Targeted Gene Capture and Exome Sequencing Identifies New Variants Leading to Deafness

Zippora Brownstein[1]; Amal Abu-Rayyan[2]; Maria Birkan[1]; Ofer Isakov[1]; Fabio Martins[1]; **Nada Danial-Farran**[3]; Asher Peretz[1]; Suleyman Gulsuner[4]; Ming Lee[4]; Silvia Casadei[4]; Noam Shomron[1]; Bela Davidov[5]; Tzippora Falik-Zaccai[6]; Lina Basel[5]; Stavit Shalev[7]; Michal Sagi[7]; Moshe Frydman[8]; Bernard Attali[1]; Reuven Sharony[9]; Moein Kanaan[2]; Karen Avraham[1]

[1]Tel Aviv University; [2]Bethlehem University, Bethlehem, Palestine; [3]Technion - Israel Institute of Technology; [4]University of Washington, Seattle; [5]Rabin Medical Center; [6]Western Galilee Hotel, Nahariya, Israel; [7]Ha'Emek Medical Center, Afula, Israel; [8]Sheba Medical Center; [9]Meir Medical Center

Next Generation Sequencing has become the optimal method to identify heterogeneous Mendelian disease genes, in particular for deafness. Determining the etiology of hearing loss is crucial for clinical management, determining the prognosis of hearing loss and other abnormalities and assessing the recurrence rate in family members. Moreover, gene discovery can lead to the determination of the mechanism of hearing loss, facilitating future gene and cell therapy. The use of isolated populations, such as those of the Middle East, has had a strong influence on finding deafness genes worldwide, due to consanguinity and founder effects. We applied Targeted Gene Capture (TGC), along with exome sequencing, of 284 human genes and human orthologues of mouse deafness genes on unrelated families of Israeli Jewish and Palestinian Arab origin.

Overall, over 150 families were evaluated using this approach, allowing us to identify new variants, including splice mutations and copy number variants (CNVs), in almost 30 genes, as well as variants previously associated with deafness. We also found variants in mouse genes not previously associated with human deafness. Among the latter was a splice variant in the *SLC12A6* gene. The family with dominantly inherited hearing loss exhibited severe to profound hearing loss with late teen onset. The effect of the variant on splicing was tested on cDNA derived from patient lymphoblasts, revealing skipping of a single exon. SLC12A6, also known as KCC3, encodes a potassium-chloride co-transporter that plays a crucial role in regulating ion concentrations in the cell. *SLC12A6* variants lead to Anderman syndrome, with agenesis of the corpus callosum and peripheral neuropathy (OMIM #218000). A mouse knock-out of the *Slc12a6* gene led to deafness, in addition to neurodegeneration of the peripheral and central nervous systems (Boettger et al., *EMBO J*. 2003). Our localization experiments of the wild-type and mutant proteins in transfected COS7 cells demonstrated that the mutant is retained in the endoplasmic reticulum, whereas the wild-type targets the plasma membrane, suggesting this variant is indeed pathogenic. This experiment demonstrates the importance of conducting functional assays in order to reveal the mechanism of pathogenic variants in causing deafness.

Funding

NIH/NIDCD grant R01-DC011835, I-CORE Gene Regulation in Complex Human Disease

PS 334

Application of Gene Therapy to a Mouse Model of Vestibular Dysfunction

Jack Shteamer[1]; Kevin Isgrig[1]; Meghan Drummond[1]; Inna Belyantseva[1]; Thomas Friedman[1]; Tracy Fitzgerald[1]; Sherri Jones[2]; Andrew Griffith[1]; Lisa Cunningham[1]; Wade Chien[1]

[1]NIH; [2]UNIVERSITY OF NEBRASKA–LINCOLN

Background

Vestibular dysfunction is a common and debilitating medical condition. As many as 35% of US adults >40 years of age have evidence of a balance dysfunction. The whirler mouse, a model of vestibular dysfunction, has a recessive mutation in *Whrn*, the gene encoding whirlin, a PDZ-containing scaffold protein. Whirlin is necessary for the development and elongation of stereocilia on the apical surface of hair cells in the inner ear. Homozygous mutant whirler mice ($Whrn^{wi/wi}$) have short stereocilia that lack whirlin expression, are deaf, and display circling behavior associated with vestibular dysfunction. In contrast, heterozygous littermates have functional whirlin protein that localizes to the tips of stereocilia and normal auditory and vestibular function. In this study, we assess the efficacy of replacement therapy with wild type whirlin cDNA for vestibular dysfunction in the whirler mouse.

Methods

In neonatal homozygous $Whrn^{wi/wi}$ mice (P0-P5), adeno-associated virus serotype 8 containing whirlin cDNA (AAV8-whirlin) was delivered in vivo to the left vestibular system via a posterior semicircular canal approach. Treated animals were evaluated for vestibular function and whirlin localization one month after surgery. Motor vestibular behavior was measured using an Any-Maze video tracking system. Stereocilia morphology and whirlin expression in control and experimental mice were examined using phalloidin staining, immunohistochemistry, and confocal microscopy.

Results

One month after AAV8-whirlin gene therapy, 40% of utricle hair cells of homozygous $Whrn^{wi/wi}$ mice expressed whirlin at the stereocilia tips. There was a significant difference in utricle hair cell stereocilia lengths between AAV-8-treated (6.77±2.33 μm) and untreated (4.10±0.93μm) utricles (one-tail t-test, $p = 0.03$). After AAV8-whirlin gene therapy, 9 of 30 mice (30%) had AnyMaze tracking results (rotations per meter traveled) that were comparable to those of wild type and heterozygous littermates.

Conclusion

Injection of AAV8-whirlin into the posterior semicircular canal successfully restored expression of whirlin in hair cells of the utricle. Additionally, gene therapy resulted in a statistically significant increase in the length of hair cell stereocilia in the utricle. This lead to recovery of normal motor vestibular behavior in 9 of 30 whirler mice (30%). These results indicate that AAV8-based gene therapy administered via the posterior

semicircular canal may be a promising treatment for inherited vestibular dysfunction. Further study and optimization of the therapy is needed to increase success rates.

PS 335

Microtubule Meshwork Remodeling Accounts for the Auditory Neuropathy AUNA1

Régis Nouvian[1]; Clément Surel[1]; Marie Guillet[1]; Marc Lenoir[1]; Jérôme Bourien[1]; Gaston Sendin[1]; Benjamin Delprat[1]; Marci Lesperance[2]; Jean-Luc Puel[1]
[1]Inserm; [2]University of Michigan, Ann Arbor

The auditory neuropathy 1 is a form of human deafness, which results from a point mutation in the 5'untranslated region of the *Diaphanous homolog 3* (*DIAPH3*) gene. Strikingly, the *DIAPH3* mutation leads to the overexpression of the DIAPH3 protein, a formin family member involved in the cytoskeleton nucleation and stabilization. Here, we examined in further details the anatomical, functional and molecular mechanisms, which account for AUNA1. We found out that the diaph3-overexpressing transgenic mice (TG) show a progressive threshold shift associated to a defect in the inner hair cells (IHCs). While synaptic function was not affected, diaph3-overexpression results into a selective and early-onset alteration of the inner hair cells (IHCs) cuticular plate, a dense plateform anchoring the stereocilia bundle. Molecular dissection of the apical components revealed that the microtubule meshwork undergoes an aberrant targeting into the cuticular plate of the TG IHCs at early onset, leading to the inabilities of these sensory cells to transduce incoming sound stimulation at later stages.

Funding
Inserm, ANR, Labex EpiGenMed

PS 336

Hunting for Mechanotransduction Components in Hair Cells

Bo Zhao[1]; Zizhen Wu[1]; Nicolas Grillet[2]; Wei Xiong[1]; Ulrich Mueller[1]
[1]The Scripps Research Institute; [2]Stanford University

Hair cells are the mechanosensory cells of the inner ear. Mechanotransduction channels in hair cells are gated by tip links. The molecules that connect tip links to transduction channels are not known. Here we show that the transmembrane protein TMIE forms a ternary complex with the tip-link component PCDH15 and its binding partner TMHS/LHFPL5. Alternative splicing of the PCDH15 cytoplasmic domain regulates formation of this ternary complex. Transducer currents are abolished by *Tmie*-null mutations. Functional studies indicate that subtle *Tmie* mutations that disrupt interactions between TMIE and tip links also affect transduction, suggesting that TMIE is an essential component of the hair cell's mechanotransduction machinery that functionally couples the tip link to the transduction channel. The multi-subunit composition of the transduction complex and the regulation of complex assembly by alternative splicing is likely critical for regulating channel properties in different hair cells and along the cochlea's tonotopic axis.

Funding
This work was funded with support from the NIH (U.M. DC005965, DC007704), the Dorris Neuroscience Center, the Skaggs Institute for Chemical Biology, and the Bundy Foundation (U.M.)

PS 337

Laser-capture micro dissection combined with next-generation sequencing analysis of cell type-specific deafness gene expression in the mouse cochlea

Shin-ya Nishio; Yutaka Takumi; Shin-ichi Usami
Shinshu University School of Medicine

Background
Hereditary hearing loss is one of the most common congenital sensory disorders worldwide, with approximately one hundred genes estimated to be involved. Recent advances in molecular genetic analysis technology using next-generation sequencing have accelerated the exploration of novel genes involved in genetic deafness, and also allowed the identification of mutations in each patient in a relatively short period. Cochlear implantation (CI), which directly stimulates the cochlear nerves, is the most effective and widely used medical intervention for patients with severe to profound sensorineural hearing loss. The outcomes of CI, however, vary among patients. The etiology of the hearing loss is speculated to have a major influence of CI outcomes, particularly in cases resulting from mutations in genes preferentially expressed in the neurons of the spiral ganglion.

Methods
To elucidate more precise gene expression levels in each part of the cochlea, we performed laser-capture micro dissection in combination with next generation-sequencing (LMD-NGS) analysis and determined the expression levels of all known deafness-associated genes in the organ of Corti, spiral ganglion, lateral wall, and spiral limbs of mice. We also compared our LMD-NGS data to cDNA microarray data and quantitative PCR results.

Results
Gene expression profiles of these cochlear parts analyzed by LMD-NGS were mainly consistent with those of previous reports. Among the 119 genes examined, *Sall1*, *Col4A5*, *Clic5*, *Lhfpl5*, *Hars2*, *Gpsm2*, *Diap1*, and *Myo15a* showed high levels of organ of Corti-specific gene expression. In the lateral wall, *Pou3f4* and *Gjb6* were highly expressed at five-fold or more the levels observed in the other parts. *Ildr1*, *P2rx2*, *Six5*, *Myh9*, *Ids*, *Ccdc50*, *Cemip*, *Serpinb6*, *Elmod3*, *Hsd17b4*, and *Nf2* were highly expressed in the spiral limbus, and *Clrn1 and Lrrc51* were predominantly expressed in the spiral ganglion neurons.

Conclusion
We demonstrated the deafness gene expression profiles in the organ of Corti, lateral wall, spiral limbus, and spiral ganglions in the mouse cochlea using LMD-NGS analysis. The expression profiles of these cochlear parts were mainly consistent with those of previous reports based on

immunocytochemistry or *in situ* hybridization. However, our results provided quantitative data and were more accurate than previous imaging results. We believe that this will be useful for further investigation of gene expression in the cochlea and the analysis of gene functions as well as prediction of CI outcomes from each patient's specific etiology.

PS 338

Transcription Analyses of Sensory Epithelia in the Inner Ear of Zebra fish

Rahul Mittal
University of Miami Miller School of Medicine

Background

The transcriptome is the set of all RNA molecules, including mRNA, rRNA, tRNA, and other non-coding RNA transcribed in one cell or a population of cells. (In our study, we primarily focus on the mRNA.) Transcriptome analysis can provide crucial information that will help in understanding the genetic mechanisms that control differentiation, proliferation, senescence, metabolism, morphology, and function of a cell or tissue under normal and pathological conditions. Recently, zebra fish model is gaining increasing attention for the study of the development and function of the vertebrate inner ear. The aim of this study is to examine the differential gene expression in saccular, utricular, and lagenar maculae of zebra fish, which helps us to understand the molecular basis underlying functional differences among three otolith organs.

Methods

Sensory epithelia were carefully dissected out from the saccule, utricle and lagena of adult transgenic zebra fish (Et(krt4:GFP)sqet4). Total RNA per sample was prepared using the Ovation Pico WTA System V2 and yielded cDNA product that was fragmented and labeled using the Encore Biotin Module according to the manufacturer's protocol. Affymetrix Zebra fish Gene 1.0 ST Array were scanned using GeneChip Scanner 3000 7G system. Following quality control, the signal estimates were uploaded for differential expression analysis to the Affymetrix Transcriptome Analysis Console (TAC). The results were statistically analyzed using ANOVA and p values <0.05 were considered significant.

Results

We observed that there was differential expression of genes in the saccule, utricle and lagena. We uncovered hundreds of differentially expressed genes in the three otolith organs. Some of these differentially expressed genes are related to the otolith development and balance in zebra fish, or related to the deafness in human. However, some of the genes were conserved among all three otolith organs. Uniquely expressed genes accounted for <10% of all genes in either otolith organ. Gene ontology and pathway enrichment analyses also provided insights into the gene expression signatures of each otolith organ.

Conclusions

The present study provides a dataset that will help in identifying and exploring the role of deafness and balance related genes. It will help in validating the utilization of zebra fish as a model to study human auditory and vestibular disorders. Morphants and mutants would help in deciphering the physiological effects of these genes in hearing and balance functions.

Funding

This work was supported by NIH/NIDCD grants R01DC012546, R01DC121125, and R01DC005575.

PS 339

Probing Protein Complexes In Vivo Using a Myosin-Based Filopodia Interaction Assay, FilopodIA

Melanie Barzik; Meghan Drummond; Stacey Cole; Eva Morozko; Spencer Goodman; Daniel Sutton; Erich Boger; Inna Belyantseva; Thomas Friedman; Jonathan Bird
National Institutes of Health

Background

The assembly and regulation of multi-protein machines is central to the function of all cellular systems, including many delicate structures in the inner ear that are indispensable for proper auditory function. Numerous methodologies exist to experimentally validate novel protein-protein interactions, however only a few approaches operate within the native environment of an intact, living cell. To address this, we developed the Filopodia Interaction Assay (FilopodIA) that exploits spatial correlation between fluorescently tagged proteins to quantitatively validate interactions *in vivo*.

Methods

Our assay uses an expressed bait protein fused to fluorescently tagged myosin 10, a processive molecular motor that accumulates at the distal tips of filopodia, antennae-like actin-based membrane protrusions that extend beyond the cell's edge. In the presence of a stable interaction *in vivo*, the myosin 10-bait chimera co-transports a prey protein tagged with a spectrally distinct fluorophore along the filopodia shaft. In contrast to existing techniques that analyze fluorescence co-localization in the cytoplasm, bait and prey interactions are assessed within filopodia where there is negligible background fluorescence. A robust quantitative framework and corresponding software tool are presented to allow for statistical analysis of the correlation between bait and prey fluorescence along filopodia.

Results

As a proof of principle, we used time-lapse total internal reflection microscopy (TIRFM) to show that fusions of myosin 10 with bait proteins are still functional as molecular motors, and that these chimeric molecules actively co-transport prey proteins along filopodia. The FilopodIA technique was validated against a panel of known protein interactions, including binary and ternary protein complexes, expressed in both mammalian and insect cell lines. FilopodIA was further applied to explore the interactome of taperin (*TPRN*), the protein mutated in human hereditary hearing loss, DFNB79. Protein phosphatase 1 (PP1) alpha, chloride intracellular channel 4 (CLIC4) and 5 (CLIC5), and chromodomain helicase DNA binding protein 7 (CHD7) were identified as potential taperin binding partners using either yeast two-

hybrid or co-immunoprecipitation screens. FilopodIA was then employed to independently verify these interactions, in addition to performing domain mapping and alanine scanning mutagenesis. Our results identify previously unknown protein binding motifs within taperin and its interaction partners.

Conclusion

FilopodIA is a powerful new tool to identify and dissect the composition of multiprotein complexes *in vivo*. We propose modifications that would allow the FilopodIA platform to be further expanded for high-content screening.

Funding

This work was supported by National Institutes of Health intramural funds from the National Institute on Deafness and Other Communication Disorders (NIDCD) 1 Z01 DC000039-17 to TBF

PS 340

Characterization of Transcriptomes of Pillar and Deiters' Cells from Adult Mouse Cochleae

Huizhan Liu[1]; Cody Barta[1]; Paul Judge[2]; Yi Li[3]; Kirk Beisel[1]; **David He**[1]

[1]Creighton University; [2]University of Nebraska; [3]Beijing Tongren Hospital

Pillar and Deiters' cells are two types of functionally important and morphologically distinct cells in the mammalian cochlea. Recent evidence suggests that pillar and Deiters' cells retain some capacity to transdifferentiate into immature hair cells using a gene therapy. The molecular mechanisms that define their morphological and functional specializations are largely unknown. The transcriptome reflects the genes that are being actively expressed in a cell and holds the key to understanding the molecular mechanisms of the biological properties of the cell. We examined the transcriptomes of these two types of supporting cells isolated from adult mouse cochleae to gain a better understanding of the molecular mechanisms of their biological properties. Two thousand pillar cells and 2,000 Deiters' cells were individually collected from adult mouse cochleae using the suction pipette technique. We then used RNA-seq technique to determine what genes are commonly expressed in both populations and what genes are uniquely expressed in each population. The availability of the transcriptomes of inner and outer hair cells also allows us to compare the gene expression profiles of hair cells and supporting cells. Our dataset will hold an extraordinary trove of information about the molecular mechanisms underlying morphology, function, and cell cycle control of these two types of supporting cells.

Funding

NIH R01 DC 004696 from the NIDCD.

PS 341

Transcriptome Characterization of Adult Zebra fish Inner-Ear Hair Cells

Cody Barta[1]; Huizhan Liu[1]; Paul Judge[2]; Kenneth Kramer[1]; Kirk Beisel[1]; **David He**[1]

[1]Creighton University; [2]University of Nebraska

Hair cells are the vital mechanotransducer cells found in the mammalian auditory and vestibular systems of both mammals and non-mammals. Mammalian hair cells are non-regenerative, and thus their death leads to irreversible losses in hearing. Hair cells in zebra fish and other non-mammalian organisms such as chickens have regenerative properties, which makes them important to study. In zebra fish, hair cells exist in inner ear sensory epithelia as well as on the exterior in lateral-line neuromasts. Our study focuses on the transcriptomes of the inner-ear hair cells in the adult zebra fish. Using a *pou4f3*-GFP line of transgenic zebra fish, hair cells from the three inner sensory epithelia, the utricle, saccule, and lagena were isolated. Two thousand GFP+ cells (hair cells) and 2,000 GFP- cells (surrounding cells in the inner ear) were individually collected by suction pipetting. RNA-seq was performed and the transcriptomes of the GFP+ and GFP- cells were analyzed and compared. Using a 1 FPKM threshold, 12,423 total genes were found to be expressed in GFP+ hair cells, with 1,978 genes being uniquely expressed when being compared to the GFP- cells. A total of 13,105 total genes were found in the GFP- cells, with 2,151 being uniquely expressed genes. The top ten differentially expressed genes in GFP+ cells include *anxa5a*, *s100s*, *cd164l2*, *pvalb9*, *s100t*, *pvalb8*, *si:ch73-199k24.2, atp1b2b, cabp2b,* and *atp1a3b.* In addition, 102 zebra fish orthologs of human deafness-related genes were examined; 73 genes are present in the GFP+ hair cells while 41 genes are present in GFP- cells. Our RNA-seq data provides a valuable resource to the study of hair cell regeneration and evolution.

Funding

NIH grant R01 DC 004696

PS 342

Expression and Role of Rac GTPases in Cochlear Hair Cells During Postnatal Development

Takadhi Nakamura[1]; Shigefumi Morioka[1]; Yuzuru Ninoyu[1]; Takehiko Ueyama[2]; Noaki Saito[2]; Hirofumi Sakaguchi[1]

[1]Kyoto Prefectural University of Medicine; [2]Kobe University

Background

Rho family small GTPases, including Rac and Cdc42, are known as regulators of cytoskeletal remodeling and numerous other cellular processes. However, the function of Rho family GTPases in cochlea hair cells is not well clarified. We previously showed that Cdc42 influence the maintenance of stereocilia and apical junctional complexes in cochlear hair cells. In this study, we elucidated the function of Rac GTPases in cochlear hair cells.

Method
The expression of *Rac1* and *3* mRNA in hair cells was evaluated using *in situ* hybridization. We next used the transgenic mice expressing a Rac1 fluorescence resonance energy transfer (FRET) biosensor to evaluate the activation of Rac1 in cochlear hair cells. Furthermore we generated Rac1 and Rac3 double knockout (Rac1/3-DKO) mice, which is a progeny of hair-cell-specific conditional Rac1-KO mice and conventional Rac3-KO mice. We assessed the hearing function and the morphology of hair cells in Rac1-KO mice and Rac1/3-DKO mice.

Results
We confirmed the expression of both *Rac1* and *Rac3* mRNA in wild type cochlear hair cells. Furthermore, we revealed that Rac1 is activated in hair cell, particularly at stereocilia using cochlear explants dissected from Rac1-FRET biosensor mice. However, the hearing function and the morphology of cochlear hair cells are normal in both Rac1-KO mice and Rac1/3-DKO mice.

Conclusions
In this study, we found that Rac1 and 3 are present in hair cells but not necessary for their postnatal development or maintenance, which suggests possible redundancy in the function of Rho GTPases. Moreover, the role of Rac1 and Rac3 in the development of hair cells during embryonic stage should be elucidated in future.

PS 343

Identity of VGLUTs in OHCs and Cochlear Nucleus Neurons Activated by Type-II Afferents in Response to Sound.

Catherine Weisz; Chad Eckard; Kristen Fantetti; Shenin Dettwyler; Christopher Divito; Maria Rubio; Karl Kandler; Rebecca Seal
University of Pittsburgh

Outer hair cells (OHCs) are critical for normal hearing and work through an electromotile mechanism, which amplifies sound and sharpens the frequency tuning curve. However the cells also form synapses with centrally projecting type II afferents and release vesicular glutamate, the role of which is still unclear. Unlike inner hair cells (IHCs), which clearly show the presence of VGLUT3 by immunostaining, the VGLUT(s) used by OHCs have been more difficult to discern. Here we used a number of approaches including RT-PCR, distribution of floxed reporter proteins in VGLUT-Cre expressing mice and patch clamp recordings of OHC-type II afferent synapses in VGLUT knockout mice to demonstrate that VGLUT3 is the predominate isoform in the OHCs, but that VGLUT2 is also expressed at least at early postnatal ages. In addition, we examined the distribution of cochlear nucleus neurons activated as a consequence of specifically inducing OHCs to signal centrally in response to sound. For this study, we took advantage of a Cre mouse line that expresses the recombinase in only IHCs and not OHCs and crossed it to our conditional VGLUT3 knockout mice to eliminate VGLUT3 from inner and not outer hair cells. After exposure of the mice to a 115 dB SPL broadband noise, we assessed the distribution of c-Fos, a marker of neuronal activity, in the cochlear nucleus. Post-hoc analyses of the cochleae demonstrate no loss of hair cells or stereocilia. The study shows the functional recruitment of neurons specifically within the granule cell layer of the cochlear nucleus. Data presented here provide important new information about OHC-type II afferent glutamate signaling that will aid in determining the role of this pathway in auditory function.

Funding
T32 DC011499 and F32 DC013207 (CJW), NIDCD 013048 (MER), NIDCD 04199 (KK), Hearing for Health Foundation, Pennsylvania Lions Hearing Research Foundation, Department of Neurobiology Startup Funds (RPS)

PS 344

Characterizing Afferent and Efferent Activity at the Zebra fish Hair Cell Ribbon Synapse

Xinyi He; Katie Kindt
National Institutes of Health

Background
The ribbon synapse is a specialized presynaptic structure found in hair cells and other sensory receptors. It is composed of an electron-dense ribbon body with filaments tethered to glutamate vesicles and is responsible for rapid and sustained vesicle release. In the zebra fish lateral line system, hair cells are arranged in neuromasts that have afferent and/or efferent projections, forming a microcircuit. Calcium influx through L-type Ca^{2+} channels triggers exocytosis from the ribbon synapses. However, little is known about the relationship between the synaptic ribbons of the hair cell and the downstream or upstream processes. Our research uses zebra fish to investigate how the afferents and efferents encode sensory stimuli and potentially even alter synaptic transmission.

Methods
To look at activity within the hair cells and neurites, we do *in vivo* confocal microscopy of zebra fish larvae. We use a variety of zebra fish transgenics that express genetically encoded fluorescent indicators including indicators for vesicle release (SypHy) and calcium indicators in the hair cell and in the afferent and efferent neurites. Using two-color calcium imaging, we can simultaneously look at activity in the hair cell and neurite during a fluid jet stimulus. The calcium indicators provide spatial information allowing us to localize influx to specific cells and regions within the neuromast and neurites. Further downstream signals in the afferents are examined by performing electrophysiological recordings of spontaneous and evoked activity on the cell bodies in the posterior lateral line ganglion. We also use CRISPR/Cas9 technology to create mutants to disrupt this signaling pathway and observe how this changes normal activity.

Results
Using double transgenic zebra fish larvae, we were able to correlate Ca^{2+} activity at the hair cell and afferent and efferent fibers. Preliminary results show a positive relationship between activity at the hair cell and activity in the afferents. However,

the correlation with efferent activity is not as straightforward. We have created a mutant that disrupts efferent activity and aim to use that to study the role of efferents in signal transduction.

Conclusion
Our data show that there is a complex relationship in the microcircuitry of zebra fish hair cells and their afferents and efferents. More work will be done to study the function of the efferents in the circuit and how they may affect activity at the hair cell level.

Funding
National Institute on Deafness and Other Communication Disorders

PS 345

Effects of Conditional Deletion of Neurotrophins only in Hair Cells on Innervation and Hair Cell Viability

Jennifer Kersigo[1]; Hui Li[2]; Jianxin Bao[2]; **Bernd Fritzsch**[1]
[1]University of Iowa; [2]Northeast Ohio Medical University

Background
The innervation of mammalian ear during early development critically depends on two neurotrophins (BDNF, NT-3) and their receptors (Ntrk2, Ntrk3). In contrast to this defined embryonic function, adult function of neurotrophins is less clear. Recent advances using conditional deletion in supporting cells (SCs) or hair cells (HCs) have provided some surprising results of unusual dependency of long term innervation maintenance on NT-3 in cochlear SCs but not HCs, and on BDNF in vestibular SCs but not HCs. Data on the importance of *Ntf3* in cochlear SCs is consistent with expression patterns in embryos and neonates; data on innervation loss in vestibular organs with a SC-cre line is surprising given the expression of *Bdnf* nearly exclusively in embryonic HCs. We report here on conditional deletion mutants using Tg*Atoh1-cre*.

Methods and Results:
We used Tg*Atoh1-cre* to eliminate floxed *Ntf3* and *Bdnf* exclusively in HCs of all sensory epithelia starting at the time Atoh1 is upregulated in differentiating HCs. This approach keeps earlier function of BDNF and NT-3 (starting at E10.5) in neurosensory precursors while eliminating both of them after HCs differentiate. This TgAtoh1-cre; $Ntf3^{f/f}$; $Bdnf^{f/f}$ mouse model shows normal density of afferent and efferent fibers near IHCs. However, the mice show no afferent synapses on basal IHCs and only outgrowth of efferent fibers to OHCs. Even a single allele of Bdnf suffices to rescue some innervation to HCs but in a longitudinal gradient: middle turn is near normal whereas the basal turn shows reduction. Consistent with previous reports of embryonic expression of *Bdnf* nearly exclusively in vestibular HCs, conditional deletion of *Bdnf* only in HCs suffices to eliminate the innervation almost as effectively as in *Bdnf* null mutants. Additional deletion of *Ntf3* causes no further effect.

Conclusions:
Our data using Tg*Atoh1-cre* are only partially compatible with previous suggestions on the postnatal role of neurotrophin expression in SCs and HCs. While we confirm that afferents remain when both *Ntf3* and *Bdnf* are eliminated from cochlear HCs, the presence of at least one allele of Bdnf (or Ntf3) in HCs is required to retain at least some afferent innervation. In contrast to recent claims of dependency of vestibular epithelia innervation on *Bdnf* expressed in SCs, we find that elimination of *Bdnf* only in HCs suffices to eliminate nearly all innervation almost as effectively as complete Bdnf deletion. This leaves little room for BDNF function in SCs, consistent with most data on *Bdnf* expression.

PS 346

Unilateral Cochlear Delivery of Virally Mediated Gene Therapy Demonstrates Bilateral Expression in VGLUT3 Knockout Mice

Omar Akil[1]; Ruwan Kiringoda[1]; Rebecca Seal[2]; Lawrence Lustig[3]
[1]University of California San Francisco; [2]University of Pittsburgh School of Medicine; [3]Columbia University Medical Center

Background
VGLUT3 is known to be expressed centrally in the dorsal and medial raphe nuclei, as well as peripherally in muscle. VGLUT3KO mice are congenitally deaf due to loss of glutamate release at the inner hair cell (IHC) afferent synapse. Previously we demonstrated that delivery of AAV1 carrying VGLUT3 gene to neonatal mice via RWM restored hearing in VGLUT3KO mice. Communication between cochlear perilymph and cerebrospinal fluid, as demonstrated by Kawai 2010 suggests that successful delivery of AAV1-VGLUT3 of a single cochlea may lead to VGLUT3 expression in the contralateral cochlea and extracochlea spread. The aim of this study is to examine the degree to which virally-mediated gene therapy results in extracochlear transfection.

Methods
1µl of AAV1-VGLUT3 virus (1.8E13vg/ml) was injected to P1-3 VGLUT3 KO mice, through the RWM. The ABR was collected from both ears of the WT, VGLUT3KO and rescued KO mice at P25. Gropu1: WT and rescued VGLUT3KO left (injected) and right (contralateral) cochleae were harvested for whole mount VGLUT3 immunofluorescence (IF) labeling and counts of IHC that stained positive for VGLUT3 expression. Group2: WT and rescued KO left and right cochlea, brain and neck muscle were harvest and tested for quantitative PCR analysis of relative levels of VGLUT3 mRNA expression in each tissue compared to the WT. Group3: WT, VGLUT3KO and rescued KO brain was harvested for VGLUT3 IF and Toluidine blue staining.

Results
As expected, all KO mice were completely deaf with no expression of VGLUT3 in the IHC or cochlea nucleus. In contrast, all rescued KO mice had average ABR thresholds

on the injected ear (left) similar to WT, while non-injected ears also demonstrated ABR threshold recovery, albeit to a lesser extent than the injected side. In the injected ear, ~86% of IHCs were expressing VGLUT3, while only ~30% on the contralateral, non-injected ear. RT-PCR and qPCR data demonstrate that the expression of VGLUT3mRNA is much higher in both the injected and the contralateral cochlea. VGLUT3mRNA was also detected in the brain and the neck muscle. Lastly, VGLUT3 protein was detected in the cochlear nucleus using IF labeling.

Conclusions
Hearing restoration and IHC transfection occurs bilaterally after unilateral injection. Further expression of VGLUT3 can be detected in brain cells and neck muscle. Overall, our results support a model of extracochlear viral spread via cerebrospinal fluid and perilymph when delivered at this age, and have important potential implications for future implementation of cochlear gene therapy.

Funding
Hearing Research Inc.

PS 347

Are SK2 Calcium-Dependent Potassium Channels Necessary for Cochlear Efferent Synapse Formation and/or Maintenance?

Isabelle Roux[1]; J. Michael McIntosh[2]; Haya Al-Grain[1]; Elisabeth Glowatzki[1]
[1]The Johns Hopkins University School of Medicine; [2]University of Utah, Salt Lake City

Background
In the developing mammalian cochlea, inner hair cell (IHC) activity is modulated by cholinergic efferent inputs from the brain. This synaptic activity is mediated by activation of calcium-permeable α9α10 nicotinic acetylcholine receptors (nAChRs) and subsequent activation of calcium-dependent potassium channels (SK2), resulting in IHC inhibition. Interestingly, IHCs of SK2 knockout ($SK2^{-/-}$) mice recorded one to two weeks after birth, completely lacked ACh responses and efferent synaptic activity (Kong et al., 2008). These results led to the hypothesis that SK2 channels may be necessary for nAChR assembly/functionality in IHC membranes, and subsequent efferent function. In the study here, this hypothesis was tested further.

Methods
Whole-cell recordings of IHCs of $SK2^{-/-}$ mice (Bond et al. 2004) were performed to test for ACh responses (Glowatzki and Fuchs, 2000). To co-label SK2 channels and nAChRs in acutely excised cochlear preparations, a fluorescently labeled apamin was developed that specifically binds to SK2 channels. Fluorescently labeled α-bungarotoxin was used to label nAChRs (Roux et al., 2011).

Results
First, IHCs of $SK2^{-/-}$ mice were tested for ACh responses at the time around the onset of efferent function (P0 to P2, base of the cochlea) (Roux et al., *in preparation*). Surprisingly, most $SK2^{-/-}$ IHCs (P2, n = 17/18) responded to 1 mM ACh, indicating that initially nAChRs can assemble and be functional at the IHC membrane in absence of SK2. These responses were completely and reversibly blocked by 10 μM (+)-tubocurarine (n = 2) or strychnine (n = 4), suggesting that they were mediated by α9-containing nAChRs.

Second, the presence of SK2 channels at each IHC cholinergic synapse was investigated. In apical IHCs at P8, a fluorescently labeled apamin cluster was found to be associated with each fluorescently labeled α-bungarotoxin cluster, suggesting that SK2 channels are associated with each nAChRs cluster. On average, 21 SK2/nAChRs clusters representing cholinergic efferent post-synapses, were identified per IHC (n = 61).

Conclusions
SK2 channels expression in IHCs is not necessary for the initial expression of functional nAChRs. However, it seems necessary for its maintenance as ACh responses were not found after one week in $SK2^{-/-}$ IHCs (Kong et al., 2008). As SK2 was found at each efferent synapse, further experiments are under way to determine whether SK2 is necessary for synapse formation and/or maintenance.

Funding
Supported by NOHR Foundation 2010, Hearing Health Foundation 2012 and NIDCD R03DC013374 to IR and NIDCD R01DC006476 to EG.

PS 348

SorCS2 as a Master Regulator of Hair Cell Planar Asymmetry

Dan Jagger[1]; Ruth Taylor[1]; Mike Lovett[2]; Sally Dawson[1]; Andy Forge[1]
[1]University College London; [2]Imperial College London

Background
A mouse line was identified in which inner ear hair cells displayed developmental abnormalities, characterized by mis-shapen and mis-oriented stereociliary bundles (Forge et al, this meeting). Genetic analysis revealed disruption of *SorCS2,* coding for a Vps10p-domain family pro-neurotrophin receptor. Here, the molecular aetiology of the bundle abnormalities was further characterized.

Methods
Cochleae from wild-type mice, and from those heterozygous or homozygous for the *SorCS2* disruption, were paraformaldehyde-fixed and prepared as surface whole-mounts or vibratome sections. Key proteins were localized by confocal immunofluorescence (IF) using previously characterized antibodies.

Results
SorCS2 was detected using antibodies targeting distinct regions the molecule (Glerup et al, Neuron 2014). In early postnatal wild-type mice SorCS2 IF was localized primarily to the membrane of supporting cells, but also to the membrane of inner hair cells and sub-apical cytoplasmic densities in both inner and outer hair cells. In individual heterozygous and homozygous littermates, detection of SorCS2 protein

could be correlated with *SorCS2* gene expression measured by quantitative PCR. The G-protein-dependent signalling pathway that controls intrinsic hair cell apical asymmetry (Ezan et al, Nature Cell Biol 2014; Tarchini et al, Dev Cell 2014) was disrupted in homozygous mice. Gαi3 and its binding partner LGN were largely absent from the lateral "bare zone" behind the hair bundle, and the normally asymmetrically-localized atypical protein kinase C (aPKC) was distributed evenly around the hair cell periphery. However, the core PCP protein Vangl2 was localized normally. The basal bodies of outer hair cells in homozygous mice appeared to be arranged eccentrically, as determined by IF for the Alstrom Syndrome protein Alms1 (Jagger et al, Hum Mol Gen 2011).

Conclusion.
The transmembrane receptor SorCS2 appears to play important roles in the development of inner ear sensory epithelia, and may act upstream of the G-protein-dependent pathway that controls hair cell apical asymmetry. Further work will be required to dissect the signal transduction mechanisms involved, and to determine how SorCS2 regulates the molecular events leading to the formation and orientation of the stereociliary hair bundle.

Funding
This work was supported by funding from Action on Hearing Loss (#P35021)

PS 350

Usherin is responsible for late onset progressive hearing loss

Ménélik Labbé[1]; Vincent Michel[1]; Jacques Boutet de Monvel[1]; Inga Ebermann[1]; Paul Avan[2]; **Nicolas Michalski**[1]; Christine Petit[3]
[1]Institut Pasteur; [2]Université d'Auvergne, UMR Inserm 1107; [3]Collège de France, Institut Pasteur, INSERM UMRS 1120, UPMC

Usher syndrome (USH) is an autosomal recessive disease characterized by a dual sensory impairment affecting both hearing and vision. Three clinical subtypes, Usher I, II and III, are classified according to the severity of hearing and visual impairment, as well as the presence or absence of a vestibular dysfunction. Usher II (USH2) is the most common form, characterized by moderate to severe congenital hearing impairment and post-pubertal vision loss. USH2 is genetically heterogeneous, and three different causal genes have been identified, of which *USH2A* is the most frequently implicated. *USH2A* encodes a large transmembrane protein called usherin and forms part of the ankle link complex with two other USH2 proteins, VLGR1 and whirlin. Ankle links are transient lateral links connecting adjacent stereocilia in the growing hair bundles of auditory sensory cells. Little is known about the function of usherin in the ankle link complex, and mutant mice defective for the protein have failed to faithfully reproduce the human phenotype. To address the role of Usherin in the ankle links, we generated a new mouse model of USH2A, in which the transmembrane domain of usherin has been deleted (*Ush*$^{TM/TM}$ mice). *Ush*$^{TM/TM}$ mice did not display any early hearing defect, but they had abnormal ankle links. Later in life (from 3 months old onward), the mutant mice underwent progressive hearing loss and showed frequency selectivity defects consistent with the auditory phenotype of some USH2A patients. Therefore, unlike VLGR1 defects that cause severe hearing loss and absence of the ankle links, usherin defects do not result in the loss of ankle links and are associated with a delayed auditory phenotype.

Funding
European Union Seventh Framework Programme, under grant agreement HEALTH-F2-2010-242013 (TREATRUSH), LHW-Stiftung, Fondation Raymonde & Guy Strittmatter, Fighting Blindness, FAUN Stiftung, Conny Maeva Charitable Foundation, Fondation Orange, ERC grant 294570-hair bundle, LABEX Lifesenses [ANR-10-LABX-65], "the Foundation Fighting Blindness Paris Center Grant" and the Fondation Voir et Entendre

PS 351

Taperin, Encoded by Deafness Gene TPRN, Has Three Motifs that Interact with Chloride Intracellular Channel (CLIC) Proteins

Daniel Sutton[1]; Eva Morozko[1]; Alexandra Boukhvalova[1]; Tracy Fitzgerald[1]; Elizabeth Wilson[1]; Erich Boger[1]; Velayuthan. Padmakumar[2]; Stuart Yuspa[3]; Atteeq Rehman[1]; Meghan Drummond[1]; Jonathan Bird; Thomas Friedman[1]; Inna Belyantseva[1]
[1]NIDCD/NIH; [2]NCI/NIH; [3]Center for Cancer Research, NCI/NIH;

Background
Mutations of *TPRN*, encoding taperin, cause non-syndromic deafness DFNB79 (Rehman *et al*., 2010). Taperin has been reported to interact with chloride intracellular channel proteins (CLIC1, CLIC4, and CLIC5) in yeast two-hybrid screens (Lehner *et al*., 2004; Salles *et al*., 2014; our unpublished data). Mutations in human and mouse *Clic5* cause hearing loss and balance impairment (Gagnon *et al*., 2006; Seco *et al*., 2015). Taperin and CLIC5 both localize to the base of hair cell stereocilia (Rehman *et al*., 2010; Gagnon *et al*., 2006). CLIC4 is expressed in inner ear cells of zebra fish, rat, mouse, and human (Gabashvili *et al*., 2007). We sought to determine: (i) which CLIC family members interact with taperin *in vivo*; (ii) if the absence of functional CLIC4 causes deafness in mice; and (iii) the CLIC interaction motif of taperin.

Methods
A filopodial transport based protein-protein interaction assay (FilopodIA) was used to study the interaction between taperin and the CLIC family of proteins. Taperin deletion constructs and site-directed mutagenesis were used to reveal the motif(s) within taperin that interact with CLIC proteins. Targeting of EGFP-CLIC4 to hair cell stereocilia was evaluated by gene gun transfection. Auditory function of CLIC4-deficient mice was tested by auditory brainstem response (ABR) at 4, 7, 10, and 12 week time points. Localization of endogenous taperin in postnatal day 7 wild-type and CLIC4 mutant mice was determined by immunolabeling of cochlear sensory epithelia with antisera against taperin.

Results
Data from FilopodIA assays revealed three interaction domains (denoted "CLIC boxes") containing a conserved motif within exon 1 of taperin. These CLIC boxes mediate the interaction between taperin and all tested CLIC family members (CLIC1, CLIC3-CLIC5). Similar to CLIC5, overexpressed EGFP-CLIC4 was targeted to the taper region of hair cell stereocilia. However, taperin localized normally at the base of hair cell stereocilia and in supporting cells of the organ of Corti in CLIC4-deficient mice. No significant differences in ABR responses were observed between CLIC4-deficient mutants and wild-type littermates at any of the ages tested.

Conclusions
Three CLIC-box domains within exon 1 of taperin mediate the interaction with CLIC1, CLIC3-CLIC5 proteins. Similar to CLIC5, CLIC4 is not necessary for normal localization of taperin. However, auditory function in CLIC4-deficient mice, indistinguishable from wild-type littermates, argues against CLIC4 as a protein necessary for hearing. The loss of CLIC4 function may be compensated by CLIC5, but not vice versa.

Funding
Supported by funds from the NIDCD Intramural Program (1ZIADC000039 and 1ZIADC000048) to Thomas B. Friedman.

PS 352

Intratympanic delivery of oligoarginine-conjugated nanoparticles as a gene(or drug) carrier to inner ear

Keum-Jin Yang[1]; **Ji Young Yoon**[2]; Da Eun Kim[2]; Kyu-Yup Lee[3]; Jong-Duk Kim[2]; Dong-Kee Kim[4]
[1]St. Mary's Hospital, Daejeon, Republic of Korea; [2]KAIST; [3]Kyungpook National University; [4]The Catholic University of Korea

A drug delivery system to inner ear using nanoparticles consisting of oligoarginine peptide (Arg8) conjugated to poly(amino acid)(poly(2-hydroxyethyl l-aspartamide; PHEA) was investigated whether the limitations of low drug transport levels across the round window membrane (RWM) and poor transport into inner ear target cells including hair cells and spiral ganglion, could be overcome. Three types of carrier materials, *i.e.*, PHEA-g-C18, PHEA-g-Arg8, and PHEA-g-C18-Arg8, were synthesized to examine the effects of oligoarginine and morphology of the synthesized carriers. Nile red (NR) was incorporated as a fluorescent indicator as well as a model drug of hydrophobic drug. Compared with PHEA-g-C18-NR nanoparticles, oligoarginine-conjugated nanoparticles of PHEA-g-C18-Arg8-NR and PHEA-g-Arg8-NR entered into HEI-OC1 cells with a significantly high level. Further, we observed the strongest fluorescence intensity at nuclei when nanoparticles of PHEA-g-C18-Arg8 tested *in vitro.* The high uptake rates of PHEA-g-C18 and PHEA-g-C18-Arg8 nanoparticles were observed at *ex vivo* experiments of hair cells. PHEA-g-C18-Arg8 nanoparticle showed comparable or better transfection capabilities than the commercially available Lipofectamine reagent. After the delivery of PHEA-g-C18-Arg8 nanoparticle with reporter gene transfer, the EGFP (Enhanced Green Fluorescent Protein) expression was monitored as an indication of a gene delivery. The inner ear cells with PHEA-g-C18-Arg8 penetrated *in vivo* across the RWM of C57/BL6 mice exhibited the nile red image and GFP expression in various inner ear tissues. In fact, PHEA-g-C18-Arg8 nanoparticles were successfully transported into inner ear through the intratympanic route, and proposed as promising candidates as delivery carriers for addressing inner ear diseases.

Funding
The ??Brain Korea 21(BK21) Program and Clinical Research Institute, The Catholic University of Korea Daejeon St. Maryâ€™s Hospital (CMCDJ-P-2014-006). The Basic Science Research Program through the National Research Foundation of Korea (NRF) funded by the Ministry of Science, ICT and Future Planning (2014R1A1A1002911).

PS 353

Immunological Responses to Adeno-Associated Virus-Mediated Gene Delivery in Inner Ear

Jasmine Saleh[1]; Will Shteamer[2]; Lisa Cunningham[1]; Wade Chien[1]
[1]National Institute of Health; [2]Emory School of Medicine

Introduction
Adeno-associated virus (AAV) vectors are among the most frequently used viral vectors for gene therapy. Recent data suggest that host immune responses triggered by AAV infection may limit transduction efficiency. The effects of immunity against AAV on the outcomes of inner ear gene delivery are poorly understood. In this study, we investigated the effects of innate and adaptive immune responses against AAV serotype 2 (AAV-2) on transduction efficiency following gene delivery to the cochlea.

Methods
CBA/J mice aged 1-2 months were included in the study. They were divided into four groups: no exposure to AAV-2, intraperitoneal AAV-2 injection, AAV-2 round window surgery, and AAV-2 cochleostomy. Innate immunity was examined 48 hours after surgery by assessing CD45 immunofluorescence, which stains for leukocytes. Neutralizing antibodies directed against AAV-2 were examined one month after surgery by luciferase assays to characterize the adaptive response. Auditory brainstem responses (ABRs) were measured pre-operatively and post-operatively to assess auditory function. Whole-mount immunostaining of cochleae was performed to measure AAV-mediated GFP expression.

Results
At 48 hours after surgery, animals that underwent cochleostomy had higher levels of CD45 immunofluorescence compared to animals that underwent round window surgery, suggesting a stronger innate immune response with the cochleostomy group. At one month after surgery, mice with AAV injection demonstrated a significant increase in neutralizing antibodies against AAV-2 compared to those without any exposure to AAV. Mice with higher neutralizing antibody titers exhibited a

decrease in the number of GFP-expressing inner hair cells. No association was observed between hearing outcomes and neutralizing antibodies.

Conclusion
Injection of AAV-2 into the cochlea induces production of AAV-2 neutralizing antibodies. Increase in neutralizing antibody production decreases transduction efficiency in inner hair cells, suggesting that the adaptive immune response may play an important role in transduction efficiency following cochlear gene delivery.

PS 354

Reciprocating Micropump for Acute and Chronic Intracochlear Drug Delivery with Electronically Controlled Dosing

Vishal Tandon[1]; Wooseok Kang[2]; Tremaan Robbins[1]; Abigail Spencer[1]; Ernest Kim[1]; **Erin Pararas**[1]; Michael McKenna[2]; Sharon Kujawa[2]; Mark Mescher[1]; Jason Fiering[1]; William Sewell[2]; Jeffrey Borenstein[1]
[1]Draper Laboratory; [2]Massachusetts Eye and Ear Infirmary

Introduction
Localized drug delivery methods will be critical in treatment of inner-ear disorders, as many potential therapeutic agents have undesirable side effects when delivered systemically. Direct intracochlear delivery is preferable to other local delivery methods (e.g. round window membrane delivery) owing to its potential for highly controlled doses and compatibility with large and/or unstable molecules. Furthermore, treatment of sensorineural hearing loss by stimulating hair-cell regeneration may require local delivery of a series of agents on a time scale of months to years.

To address these challenges, we have developed a micropump to deliver timed, controlled doses of drug directly into the cochlear fluids over extended durations. The micropump is designed to be integrated into a head-mounted enclosure and run from a portable controller and battery. We optimized the—microfluidics and operating conditions to minimize power consumption and reduce flow rates for safety. Our pump employs reciprocating delivery, whereby drug is first infused into the cochlea and allowed to diffuse. Then fluid is withdrawn at a later time, leading to delivery of drug with zero net volume infused. Integrated electromagnetic actuators and drug storage reduce the overall system size, making this type of system adaptable for clinical use.

Methods
We fabricated the microfluidics by laminating sheets of laser-cut polymers together, then mounting electromagnetic actuators and control circuitry to the fluidics to form the micropump. Valves isolate an integrated drug reservoir from the infusion line, so drug is only delivered when first loaded into the infusion line. We demonstrated electronically-controlled dosing by using fluorescein as a test drug on the bench, and a glutamate receptor antagonist (DNQX) as a test drug for acute delivery in guinea pigs. For the animal experiments, we monitored CAPs and DPOAEs during delivery, as DNQX was expected to affect CAPs but not DPOAEs.

Results
Bench-top experiments with fluorescein confirmed that fluid from the drug reservoir was dispensed by the pump only when we intentionally (i.e. electronically) initiated drug loading. For acute delivery in guinea pigs, infusion/withdrawal of AP produced minimal changes in CAP and DPOAE thresholds. After we electronically initiated DNQX delivery, CAPs were reduced immediately for frequencies near the infusion site (16 kHz), and later for other frequencies with continued infusion. No systematic changes in DPOAEs were observed during the same period of monitoring. We reproduced our results with 4 biological replicates.

Funding
This work was supported by NIH NIDCD Grant 5 R01 DC006848-08.

PS 355

Computational Model for Reciprocating Intracochlear Delivery with Convection, Diffusion and Drug Binding

Marc Weinberg[1]; **Erin Pararas**[1]; Mark Mescher[1]; William Sewell[2]; Jeffrey Borenstein[1]
[1]Draper Laboratory; [2]Massachusetts Eye and Ear Infirmary

Introduction
Intracochlear drug delivery is emerging as a clinical therapy for treatment of sensorineural hearing loss and drug ototoxicity. Recent advances in reciprocating microfluidic drug delivery present an opportunity for safe and efficacious treatments with emerging therapeutic compounds. The balance between efficacy and safety requires optimization of the rate of drug infusion and the total drug delivered. Toward this end, we are developing a computational model that accounts for micropump-induced convection, drug diffusion and clearance, and drug binding to proteins in the perilymph. These factors govern the pharmacokinetic profile, and device optimization requires a parametric analysis of the design space. In previous studies, we investigated the influence of drug diffusion and protein binding on the drug distribution profile over time. Here we expand the model to incorporate drug convection due to micropump reciprocation during extended, pulsed delivery.

Methods
The computational model presented here extends the earlier reported model, coded in *Mathematica* (Wolfram Research), a computational environment capable of solving coupled differential equations, which describe multiphysics associated with drug distribution. The principal new advance is the incorporation of a method for recapitulating the reciprocating motion of the micropump, accomplished by introducing rapid bolus injections for each infusion and withdrawal cycle. This approach is combined with the already-established means for accounting for drug diffusion and binding to immobile protein binding sites in the perilymph. Additional features of the new model include a structure representing the cochlear aqueduct and a varying radius for the scala tympani along its length. This model has been applied across a range of pump cycling conditions, pulse durations and binding site concentrations.

Results
The primary computational challenges remain the handling of boundary conditions and the high Peclet number for typical drug delivery conditions. These challenges are addressed by accurate replication of experimental delivery profiles across a range of experimental conditions. Drug binding occurs rapidly relative to diffusive time scales, and diffusion along the scala tympani using a small tracer molecule typically takes tens of hours to reach apical regions. Frequent replenishment of drug rapidly reaches diminishing returns, as the diffusion times predominate other physical processes.

Conclusions
An expanded computational model that accounts for repetitively cycled reciprocating delivery as well as drug diffusion and protein binding in a scala tympani model with varying radius has been developed and applied to therapeutically relevant conditions for applications in extended intracochlear drug delivery.

Funding
This work was supported by NIH NIDCD Grant 5 R01 DC006848-08.

PS 356

Development of a Poly(lactic-co-glycolic acid) (PLGA) Microneedles for the Sustained Delivery of Drugs in Cochlea

Stefania Goncalves[1]; Chunhui Chen[2]; Esperanza Bas[1]; Emre Dikici[3]; Chunlei Wang[2]; Sapna Deo[3]; Sylvia Daunert[3]; Fred Telischi[3]
[1]University of Miami Ear Institute; [2]Florida International University; [3]University of Miami

Background
The development of drug delivery techniques into the inner ear is a challenging field that has been hindered by the cochlear anatomy that limits molecular transportation. Biodegradable polymers allow continuous release of bioactive molecules and are promising in this field; however, some authors have reported ototoxicity. The present study is aimed to determine non-ototoxic blending techniques for future otologic applications.

Methods
Biopolymer microneedles were prepared using two different methodologies and their drug release and ototoxicity profiles were determined. In the first method, different compositions of PLGA polymer were melted on a glass substrate. After cooling to allow the PLGA to solidify, 1.0 mm thick pieces of the polymeric film were cut. In the second method, 50% solutions of different compositions of PLGA were dissolved in acetone. The solution was degassed using an ultrasonic bath and cast into an aluminium mold shaped as the desired microneedles. In order to study the drug release profile a fluorescent drug surrogate, rhodamine B, was dissolved in molten PLGA prior to casting. The prepared microneedles were then placed in a quartz cuvette containing an artificial perilymph solution. The absorbance of the perilymph solution was checked every 30 min until the absorbance of the solution at 552 nm was constant. Ototoxicity assessment was performed using whole organ of Corti (OC) explants dissected from 3-day-old rat cochleae and exposed to the needles with and without dexamethasone, and then cultured for 72 hours. Fluorescent microscopy for viable hair cell (HC) counts (FITC-phalloidin) was performed. ANOVA and Tukey post hoc testing were used for statistical analysis.

Results
The needles' drug release profile determined by measuring the absorbance of the rhodamine B dye at 552 nm showed a total release of the dye within 6 hours from the time of immersion into the artificial perilymph solution. The ototoxicity assessment of the microneedles showed that those needles prepared using the melt casting technique presented inner and outer HCs losses predominantly in the basal turns of the OC explants that was prevented when combining dexamethasone. Microneedles prepared using acetone as an organic solvent showed no HCs losses regardless of the PLGA composition ratio (65:35; 25:75) when compared with the first technique ($p<0.001$). The release profile of the steroid is currently being studied.

Conclusions
Blending techniques can impact biopolymers' toxicity profile when targeting sensitive organs such as the OC. The use of an organic solvent is suitable when considering otologic applications.

PS 357

Verifying the Therapeutic and Adverse Effect of Intra-tympanic Drug Delivery Vehicles for Noise Induced Hearing Loss

Yujung Hwang[1]; Mina Park[1]; Shinwook Woo[1]; Taesoo Noh[1]; Jeongsug Kyong[1]; Junho Lee[1]; Seungha Oh[1]; Mookyun Park[1]; Jihoon Park[2]; Moonsuk Kim[2]; Myungwhan Suh[1]
[1]Seoul National University Hospital; [2]Ajou University

Background
Intratympanic (IT) drug delivery is one of the mainstream treatment for acute hearing loss(HL). But since the drug is usually injected in a fluid form, it is easily drained through the Eustachian tube. If the drugs can be delivered through a vehicle that lasts longer in the middle ear, more drug may be delivered into the inner ear. In this study we tested the treatment efficiency of several vehicles. We verified the hearing outcome in noise induced hearing loss animals and compared the incidence of adverse inflammatory reaction due to the vehicles.

Method
A total of 28 male (55 ears) SD rats with normal hearing and tympanic membranes (TM) were used. IT dexamethasone (10mg/ml) was delivered via three different vehicles: normal saline (saline-dexa, n=14), MPEG-PCL (PCL-dexa, n=15), and hyaluronic acid (HA-dexa, n=15). Another 11 ears served as a control. Rats were exposed to white noise (110-120 dB C) for 3 hours. After confirming the HL, rats were treated with dexamethasone/vehicle injection. ABR threshold was

measured before and after treatment for 2 months (0, 4, 8, 12, 30, 45 and 60 days). Middle ear histology and inner ear surface preparation was performed after sacrifice. Also, serial micro CT and endoscopy of the TM was performed to evaluate the adverse reaction.

Results

PCL-dexa and HA-dexa groups resulted in significantly better hearing as compared to baseline at 30days. But no improvement was found in the saline-dexa group. Hearing threshold was 53.5±5.7 dB SPL before treatment. Thirty days after treatment the hearing threshold was 39.0±7.4 dB SPL in the control group, 39.2±9.3 dB SPL in the saline-dexa group, 34.3±10.3 dB SPL in the PCL-dexa group, and 30.9±7.6 dB SPL in the HA-dexa group. Drug/vehicle was visible in CT up to 0.0±0.0 days in the saline-dexa group, 34.7±25.9 days in the PCL-dexa group. 2.8±7.8 days in the HA-dexa group. Adverse inflammatory response was found in 0.0% of the saline-dexa group, 56.3% of the PCL-dexa group, and 0.0% of the HA-dexa group. TM perforation healed within 20.7±9.8 days in the saline-dexa group, 14.6±11.1 days in the PCL-dexa group, and 23.3±9.4 days in the HA-dexa group.

Conclusion

We found a beneficial effect IT dexamethasone delivery via PCL and HA vehicle. It seems that the treatment outcome was better with these vehicles, because the drug lasted a longer time in the middle ear. Delivering IT drug via HA may be a safe and efficient method.

Funding

NRF National Research Foundation of Korea

PS 358

Direct Administration of 2-Hydroxypropyl-Beta-Cyclodextrin into Intact Cochleae: Effects on Objective Auditory Measurements

Jeffery Lichtenhan[1]; R Duncan[2]; Alec Salt[1]

[1]Washington University in St. Louis; [2]University of Michigan

Background

2-Hydroxypropyl-Beta-Cyclodextrin (HPβCD) is a commonly used excipient to stabilize and solubilize pharmaceuticals. HPβCD binds cholesterol and is used to treat Niemann-Pick type C disease – a progressive neurological disorder caused by cholesterol and glycolipid accumulation in the lysosomes. HPβCD has been shown to be toxic to outer hair cells in laboratory animals (Cronin et al. 2015 JARO), and the mechanism(s) remains unknown. Previous studies on the effects of HPβCD on the cochlea administered it systemically or intracerebroventricularly to guinea pigs, cats, or mice, or to excised preparations. In the present study we have studied the effects of HPβCD by administering directly into perilymph of intact guinea pig cochleae.

Methods

HPβCD was administered with a pipette sealed into the cochlear apex. Previously we have shown that apical injection drives solutions toward the cochlear aqueduct at the base of scala tympani, allowing the entire scala to be filled uniformly with solution (Lichtenhan et al. 2014 JARO). In this study, a number of objective measurements of cochlear physiology were made during, and following, administration of up to 15 mM concentrations of HPβCD: 1) compound action potential (CAP) thresholds at multiple frequencies; 2) endocochlear potential (EP); 3) distortion products (DPs) measured simultaneously from the endolymphatic space and ear canal (i.e., distortion product otoacoustic emissions, DPOAE); 4) cochlear microphonic (CM) responses from the endolymphatic and perilymphatic spaces, including the round window; 5) auditory nerve overlapped waveform (ANOW), a measure of low-frequency auditory-nerve function.

Results

The amplitude of ANOW was reduced and CAP thresholds were raised by approximately 40 dB, consistent with attenuation of cochlear amplifier gain. Odd-order DPOAEs (e.g., $2f_1$-f_2) amplitudes rapidly declined, while the even order DPOAEs (e.g., f_2-f_1) amplitudes transiently increased before declining. These changes were consistent with measured changes of estimates of the *in vivo* operating point and harmonic distortions ($2f_1$, $3f_1$) in CM measured from the endolymphatic space. Interestingly, EP transiently increased and the endolymphatic CM, while only slightly reduced in amplitude, showed phase changes.

Conclusions

HPβCD may be a useful manipulation to study the origins of objective measures of cochlear function, as it suppresses outer hair cell function leaving the EP intact. To reconcile the interesting decline of DP measurements while CM and EP were maintained, alternative origins of post-treatment responses are being considered, such as CM from inner hair cells or alterations in *in vivo* transducer function operating point underlying DP changes.

Funding

R03 DC012844, R01 DC001368

PS 359

Gene Transfer in the Neonatal Mouse Inner Ear by Adeno-associated Virus Serotype 8

Guo-Peng Wang; Jing-Ying Guo; Yu-Ying Liu; Zhe Peng; Teng-Fei Qu; Shu-Sheng Gong

Capital Medical University, Beijing

Background

Impairments of the inner ear result in sensorineural hearing loss and vestibular dysfunction in humans. A large portion of them are congenital and involves both auditory and vestibular systems. Therefore, genetic interference to correct the deficit must be administered in the early developmental stage for them. In the present study, we aimed to evaluate adeno-associated virus serotype 8 (AAV8)-mediated gene transfer in the neonatal mouse inner ear.

Methods

AAV8 harboring green fluorescence protein (GFP) gene was inoculated into the inner ear of mice, born within 24 hours, through the posterior semicircular canal. In the control group, normal saline was used instead of AAV8. At

thirty days following surgery, all animals underwent auditory brainstem response (ABR) measurements and swim tests. Then they were sacrificed and otocysts were harvested for either whole mounts or frozen sections. GFP expression and morphological changes of the inner ear were assessed by immunohistochemistry.

Results

No significant difference was found between the AAV8-inoculated group and the control group when comparing results of either ABR thresholds or swim test scores. In the AAV8-inoculated group, extensive GFP expression and no morphological lesions were detected in the inner ear tissues, including the organ of Corti, the lateral wall, the spiral ganglion, the utricle, the saccule and the ampulla. Robust GFP expression was found in inner hair cells, marginal cells, spiral ganglion neurons, and vestibular hair cells and supporting cells. In contrast, no GFP expression was observed in the control group.

Conclusions

AAV8 inoculation through the posterior semicircular canal of neonatal mouse achieved extensive over-expression of exogenous gene in the inner ear without lesions of hearing and vestibular function. Thus, it serves as a promising approach for gene transfer in congenital inner ear diseases affecting both the cochlea and the vestibule.

Funding

National Natural Science Foundation of China (81100717 and 81570912)

PS 360

Application of Genome Editing to the Mouse Inner Ear

Joan Guitart[1]; Kevin Isgrig[1]; Justin Siegel[2]; Matthew Porteus[3]; Jizhong Zou[1]; Lisa Cunningham[1]; Meghan Drummond[1]; Wade Chien[1]

[1]National Institutes of Health; [2]New York Medical College; [3]Stanford

Background

Designer nucleases (zinc-finger nucleases, TALENs, CRISPR/Cas9) have gained widespread attention for their ability to modify genomic DNA in a programmable manner. These genome-editing nucleases have the ability to make double-stranded breaks at specified loci in the genome, and desired changes can be made when a homologous donor template is provided (homology-directed repair, HDR). In this study, we examine whether HDR can be applied to the mouse inner ear.

Methods

Homology-directed repair was tested using a HEK293-GFP^{STOP} cell line and a transgenic mouse line containing a mutated GFP gene with a premature stop codon (GFP^{STOP}), in which GFP cannot be produced unless the stop codon is removed by genome editing. A plasmid (pZFN-37GFP) containing ZFNs that target near the stop codon and a homologous donor template encoding a partial wild-type GFP cDNA was used to repair the GFP^{STOP} allele in HEK293-GFP^{STOP} cells. Additionally, adeno-associated virus serotype 2 (AAV2) encoding the above ZFNs and homologous donor template (AAV2-ZFN-37GFP) was generated to test HDR in neonatal GFP^{STOP} mouse cochlear explant cultures. Furthermore, AAV2-ZFN-37GFP was delivered to the cochleae in neonatal GFP^{STOP} mice via a round window approach in vivo. Mice were examined for HDR one month after surgery. HDR was examined using immunohistochemistry with and anti-GFP antibody.

Results

HEK293-GFP^{STOP} cells transfected with pZFN-37GFP resulted in 3.8% GFP-positive cells, indicating that these cells had undergone genome editing via homology-directed repair (HDR). Control HEK293-GFP^{STOP} cells without ZFN plasmid resulted in 0% GFP positive cells ($p=0.005$) indicating that expression of GFP does not occur in the absence of genome editing. HEK293-GFP^{STOP} cells infected with AAV2-ZFN-37GFP resulted in lower levels of HDR (0.3%). In addition, HDR was not detected in GFP^{STOP} mouse cochlear explant cultures treated with AAV2-ZFN-37GFP. Preliminary data suggest a low level of HDR-mediated genome editing in hair cells after in vivo surgical delivery of AAV2-ZFN-37GFP.

Conclusions

pZFN-37GFP was effective at restoring GFP expression in the HEK293-GFP^{STOP} cell line via genome editing and HDR. AAV2-ZFN-37GFP was capable of inducing HDR but at much lower efficiency in the HEK293-GFP^{STOP} cell line. AAV2-ZFN-37GFP was not effective at inducing HDR in neonatal GFP^{STOP} mouse cochlear explant cultures. Finally, results from surgical delivery of AAV2-ZFN-37GFP to mouse cochlea demonstrate genome editing via HDR. However, our data demonstrate this is a very low frequency event indicating genome editing in post-mitotic hair cells is not ideal for gene therapy applications.

PS 361

Pharmacokinetics of Drugs Delivered by a Cochlear Implant with Cannula in Guinea Pigs.

Alec Salt[1]; Jared Hartsock[1]; Daniel Smyth[2]; Kristien Verhoeven[2]

[1]Washington University, St Louis; [2]Cochlear Technology Centre

Background

Application of drugs to the ear during and following cochlear implantation has the potential to help preserve residual low frequency hearing, reduce inflammation and bone growth, and to maintain neural function. One approach is to apply drugs through a cannula incorporated into the cochlear implant. To date there have been no pharmacokinetic studies of drug levels achieved in perilymph with different application protocols.

Methods

Cochlear implants appropriately-sized for the guinea pig and incorporating a polyimide cannula were inserted through a cochleostomy into the basal turn of scala tympani (ST). Artificial perilymph containing FITC-dextran marker was

injected using a syringe pump or implantable micropump (iPrecio SMP-200). After two hours application, ST perilymph was sampled from the cochlear apex using a sequential sampling technique, allowing drug gradients along the ear to be quantified. Sample data were interpreted with our inner ear fluids simulator, incorporating the dead space of the cochlear implant, drug delivery, and fluid flows associated with perilymph sampling. Based on prior studies with FITC-dextran we predicted that perilymph levels in the basal turn of ST following two hour injections at 100 nl/min would reach 80% of the applied concentration.

Results
In 12 animals some fluid leakage from the cochleostomy continued after implantation, even when sealed with fascia, as evidenced by fluid accumulation in the auditory bulla during the two hour injection period. In 4 animals a complete seal was achieved, with no fluid accumulation in the bulla. In those animals where a seal was achieved, dextran levels near the base of ST approached (mean 60%), but did not reach, the predicted concentration. In animals where a seal was not achieved, dextran levels were substantially lower (mean 30% of the applied concentration). The inclusion in simulations of a fluid leak from the cochleostomy driven by CSF entering the cochlear aqueduct was insufficient to account for the low measured dextran concentrations. We also needed to include a degree of stirring of perilymph in the basal turn of the cochlea.

Conclusions
Knowledge of perilymph pharmacokinetics is largely based on studies performed with the inner ear in the normal, sealed state. Cochlear perforation, even when "almost sealed" with a cochlear implant and fascia has a dramatic influence on drug levels achieved in ST. Washout of drug was much larger than expected from fluid leakage. Understanding drug levels under practical conditions is essential to advance the field.

Funding
This study was supported by Cochlear Corp.

PS 363

Fluvastatin attenuates acoustic injury

Hunter Young; Virginia Smith-Bronstein; Claus-Peter Richter; Donna Whitlon
Northwestern University

Background
We reported that fluvastatin administered to guinea pigs at the time of high level noise exposure protects against noise induced hearing loss (Whitlon et. al. ARO 2015). Here we determined the effect of fluvastatin on hearing loss when administered before or after noise exposure.

Methods
We delivered fluvastatin (50mM in saline solution containing 0.5% DMSO) to adult albino guinea pigs (300-800g) by means of a cannula in the left cochlea attached to a mini osmotic pump. The Fluvastatin cannula and pump were implanted either 7 days before (Δt=-7) or 7 days after (Δt=+7) noise exposure (4-8kHz, 4 hours, 120dB SPL). As reported earlier, the right cochlea responds to fluvastatin and was used for analysis. Animal hearing thresholds, tested using auditory brainstem responses (ABRs), were acquired up to a month after pump implantation. As noise exposed controls, we exposed animals to noise and either a) implanted a pump filled with saline, b) inserted a cannula filled with saline and tied off, or c) preformed no surgical implantation. Classical histology was preformed to assess the damage of cochlear structures.

Results
The Δt=-7 treatment group protected against noise induced hearing loss, showing threshold elevations similar to experiments in which implantation and noise exposure occurred simultaneously. Fluvastatin given 7 days after noise exposure was not as effective, but did show a mild protection when compared to the untreated, noise exposed animals. Histological data is pending.

Conclusion
Our experiments indicate that fluvastatin, delivered directly to the cochlea, works as a prophylaxis against noise induced hearing loss. While there was some reduction in threshold elevation in the Δt=+7 group when compared to the noise damaged control animals, it was not as dramatic as the Δt=-7 group. The results are consistent with the idea that fluvastatin reduces damage and possibly halts ongoing cell degradation, but it does not repair damage that has already occurred.

Funding
ONR grant# N000141210173 ONR grant# N00014-15-1-2130

PS 364

Development of a Controlled Release Round Window Implant for Meniere's Disease

John Brewer[1]; **Matthew Ku**[1]; Yen-Jung Angel Chen[2]; Federico Kalinec[2]; William Slattery[1]; Erik Pierstorff[1]
[1]O-Ray Pharma; [2]David Geffen School of Medicine at UCLA

Background
Meniere's Disease (MD) is a disorder of inner ear in which patients experience episodes of spinning vertigo, hearing loss and tinnitus. The National Institutes of Deafness and Other Communicative Disorders (NIDCD) estimates that approximately 615,000 Americans are currently diagnosed with MD, with 45,500 new cases diagnosed every year. Intratympanic injection of gentamicin is one popular option to treat severe episodic vertigo caused by MD. The mechanism whereby gentamicin achieves its therapeutic effect is thought to be via vestibular ablation. Gentamicin doses vary from 20-40 mg/day and up to a total of 600 mg of total drug administered. While these high dose injections are effective, they can be accompanied by major side effects, such as substantial hearing loss, prolonged periods of dizziness and vertigo. Advances in the field have shown that continuous low dose administration of gentamicin can relieve symptoms of Meniere's with much less drug given and without leading to hearing loss. Thus, a sustained release of gentamicin may be more effective and safer than bolus intratympanic injections.

Methods
A prototype gentamicin delivery system for guinea pigs was developed to test the proof of concept of a slow release gentamicin implant in an animal model. This utilized an impermeable polymer tube containing ~300 µg gentamicin. One end of the tube is coated with a layer of semi-permeable polymer allowing for the slow dissolution of the packaged drug. Dissolution experiments were performed *in vitro* to monitor the release of drug. Additionally, drug delivery implants were placed into the middle ear of guinea pigs against the round window (n=20) and hearing was monitored via ABR recordings (days 4, 7, and 10) and drug levels in the perilymph were determined (days 1, 4, 7, and 10).

Results
In vitro dissolution study showed a continuous release over 5-7 days. Gentamicin levels measured in the perilymph ranged between 1 and 10 µg/ml and were relatively constant through the 10 day conclusion of the study. Post implantation ABR levels showed slight elevation in thresholds, consistent with a gentamicin effect.

Conclusion
Prototype gentamicin round window implants were developed and tested *in vitro* and in an animal model. These studies demonstrate excellent, reproducible drug release and lay the foundation for further preclinical and clinical work. The ultimate goal of this project is to develop the delivery system to achieve ablation of vestibular function, thus treating the symptoms of Meniere's Disease, while preserving normal hearing.

PS 365

3-D Subject-Atlas Image Registration for Micro-Computed Tomography Based Characterization of Drug Delivery in the Murine Cochlea

Zhenlin Xu[1]; Nathan Cahill[1]; Gary Martinez[2]; Mikalai Budzevich[2]; Robert Frisina[3]; Joseph Walton[3]; David Borkholder[1]
[1]Rochester Institute of Technology; [2]Moffitt Cancer Center and Research Inst.; [3]University of South Florida

Dynamic contrast enhanced (DCE) Micro-computed tomography (µCT) imagery of the rodent inner ear has been successfully used to noninvasively characterize drug delivery inside the cochlea (Haghpanahi *et al.*, Annals of Biomedical Engineering, 41(10):2130-2142, 2013). Using a series of manually segmented and labeled histological sections of a mouse inner ear as an atlas, Haghpanahi *et al.* registered selected 2-D atlas images to slices of the mCT image, allowing the atlas labels to be propagated to identify and segment the intracochlear structures in the subject mouse. With this technique, drug concentration profiles can be quantified in each segmented structure. In this work, we present two improvements in the atlas-based registration step; i) full automation, which improves analysis by removing the need for an expert user to select specific slices from the µCT image for registration, and ii) full three-dimensional registration, which improves segmentation accuracy by incorporating *all* atlas images instead of a user-selected subset. To enable full automation, we carry out the following steps: (i) threshold the µCT image to identify bone regions (+700 to +3000 HU), (ii) identify the sagittal plane by maximizing the Jaccard index (a measure of symmetry) between the left and right bone regions, and (iii) localize the region containing the inner ear by searching for geometric features matching those of the atlas that are preserved when reflected through the sagittal plane. Once the inner ear region has been automatically localized, we perform 3-D atlas-based registration by first identifying the 3-D affine transformation that optimally aligns the atlas with the inner ear, and then refining the registration result by performing 3-D deformable registration. Using the 3-D deformation aligning atlas to subject, we propagate the manually identified region labels from the atlas to yield estimates of the locations of the scala media, scala tympani, and scala vestibule. Finally, we refine the predicted boundaries of the different scalae via a level-set energy minimization approach. Using multiple µCT subject images, we illustrate that our fully automated approach that uses the full three dimensions of data from the atlas and subject images enables more accurately segmented scalae regions than are attainable using the previous approach of estimating a collection of 2-D transformations between atlas and subject slices and interpolating the results.

Funding
Supported by the National Institute On Deafness and Other Communication Disorders of the National Institutes of Health under Award Number R01DC014568.

PS 366

A Scalable Peristaltic Micropump with 3D-printed Features and Phase Change Actuation for Inner Ear Applications

Farzad Forouzandeh[1]; Chaitanya Mahajan[1]; Jing Ouyang[1]; Robert Carter[1]; Xiaoxia Zhu[2]; Bo Ding[2]; Lauren Mannix[2]; Joseph Walton[2]; Denis Cormier[1]; Robert Frisina[2]; David Borkholder[1]
[1]Rochester Institute of Technology; [2]University of South Florida

Controllable drug delivery systems will become increasingly important as protective and restorative biotherapies for noise induced-, sensorineural-, and age-related hearing loss; deafness, and vestibular disorders are developed. Miniaturized pumps create opportunities for therapy development in animal models, and will be essential for fully implanted or behind the ear systems for human translation. In particular, since mice have become such a successful biomedical, genetic and bioengineering lab animal of choice, development of micropumps that can be implanted subcutaneously in mice is quite important. This will allow *in vivo* testing of novel drug treatments in transgenic, knock-in, knockout and various strains of mice that model different human diseases. Here we present progress on a scalable micropump platform based on direct, phase change actuation of either microtubing or micro-fabricated diaphragms for

peristalsis. The first approach integrates commercially available 250 µm outer diameter/125 µm inner diameter polyurethane catheter tubing that serves as the micropump flow channel, reservoir interconnect, and cannula connection to the drug delivery site. Direct-write, 3D print technologies are used for definition of micropump features, heaters, and accurate delivery of paraffin wax for phase change actuation. In the latter case, the fluid pumping chambers are formed by a spin-coated PDMS (polydimethyl siloxane) layer peeled off from a 3D printed mold. Then the chambers are bonded with directly-written heaters/paraffin wax actuators embedded in the PDMS diaphragm to integrate a micropump. Results with a proof-of principal device are presented showing an ability to deliver volumes at less than 10 nL per actuation event. This can be scaled readily to higher flow rates by increasing the tubing/paraffin reservoir size and frequency of peristalsis. To test for biocompatibility, procedures consistent with the ISO 10993 standard for implantable medical devices were used. An epithelial cell line was cultured under standard conditions. The micropump components were sterilized with ethylene oxide and then inserted into the center of the cell culture wells. Biocompatibility data analyses are ongoing, but assays of cell cytotoxicity so far reveal no toxicity. Future work will integrate the micropump with a drug reservoir and control electronics for wireless communication and *in vivo* testing in the mouse model system.

Funding
Supported by the National Institute On Deafness and Other Communication Disorders of the National Institutes of Health under Award Number R01DC014568.

PS 367

Towards Direct-Write Integrated Electronics on 3D Substrates – Comparison of Low Temperature Isotropic Silver and Anisotropic Conductive Adhesives for Assembly of Micropump Control Electronics

Kyle Smith[1]; Taylor Swanson[1]; S. Ramkumar[1]; Denis Cormier[1]; Robert Frisina[2]; David Borkholder[1]
[1]Rochester Institute of Technology; [2]University of South Florida

Advanced micropumps that enable chronic delivery of therapeutic agents with controlled delivery profiles require integrated electronics and wireless communication capabilities. Traditional assembly approaches require high temperature soldering processes that preclude direct integration with micropumps designed with temperature sensitive polymer components. Here we present *low temperature* assembly of commercial, off-the-shelf surface mount electronic components electrically connected to the substrate interconnects through a conductive adhesive. The anisotropic conductive adhesive process uses a magnetic field to align conductive particles from 0.5 to 3 µm within the adhesive in the z-direction during curing, providing electrical bridges between the electronic components and the substrate, and insulating between pads in the x-y directions. The isotropic silver adhesive has uniform high conductivity, but must be placed precisely to prevent horizontal bridging. Micropump electronics are demonstrated including embedded microprocessor, power regulation, feedback control of thermal actuators, and Bluetooth low-energy wireless communications. The overall dimensions of the complete assembly are 8.2mm x 8.8mm x 1.8mm. The controller is assembled using the smallest commercially available parts, wafer-level chip-scale packages at 0.4mm contact pitch and 0.15mm contact spacing. Assembly is carried out by applying the adhesive to the substrate, placing the components, and then curing at a maximum temperature of 70 °C. Integrated micropump electronics assembled using isotropic and anisotropic conductive adhesive processes are demonstrated for feasibility and performance. The approach enables use of power-efficient, commercial off-the-shelf electronics and integration over low-temperature substrates. Future work will leverage this approach to integrate these electronics directly on a micropump with interconnects defined using direct-write technologies.

Funding
Supported by the National Institute On Deafness and Other Communication Disorders of the National Institutes of Health under Award Number R01DC014568.

PS 368

Use of an Osmotic Pump Device for Intracochlear Drug Delivery in a Rat Model

Amar Gupta[1]; Hao Luo[1]; Syed Ahsan[2]; Jinsheng Zhang[1]
[1]Wayne State University; [2]Henry Ford Health System

Background
The objective of this research project is to describe a model that may be used for localized and controlled delivery of a test substance into the cochlea. Intracochlear drug delivery is a valuable tool that has previously been used in various studies, including those relating to meningitis, hearing loss, and tinnitus. The range of agents delivered via an intracochlear route has also been varied in the literature and ranges from monoclonal antibodies and neurotrophic factors to viral vectors. Our model will provide future investigators a well described surgical procedure and methodology to conduct such research.

Methods
Test animals (adult male Sprague-Dawley rats) were anesthetized with isoflurane and using sterile technique, the middle ear bulla was exposed via a post-auricular incision. A drill was used to fenestrate the bulla and the middle ear cavity, exposing the round window region and taking care to avoid injury to the stapedial artery. A mouse intrathecal catheter (Alza Corp., Palo Alto, CA, USA) of outer diameter 0.36mm was inserted into the cochlea via the round window membrane and secured in place with dental cement. This catheter was connected to an osmotic pump (Alza Corp., Palo Alto, CA, USA) that was filled with 100 microliters of test agent. The agent was eluted at a predictable rate of 0.5 microliters per hour directly into the scala tympani of the cochlea over 7 days. The pump was placed in a subcutaneous pocket in the dorsal scapular region by undermining skin from the post-au-

ricular incision site. The skin was sutured closed over the pump. Auditory brainstem responses (ABRs) were measured before and after the chronic implantation.

Results
The results show that our surgical technique allowed us to locate the round window niche and place the osmotic pump device. This technique also allowed preservation of the stapedial artery and did not require cauterization. In addition, no significant change in hearing threshold was noted postoperatively by ABR testing following surgical recovery from implant placement.

Conclusions
The model described by our laboratory can be used for reliable, precise, and localized delivery of a test agent into the rat cochlea. Round window catheter placement does not appear to be deleterious to hearing thresholds based on our preliminary data and research is ongoing to assess effects on animal behavior. Future directions involve testing agents in the management of tinnitus but eventually, the development of one device that allows electrical, chemical, and optogenetic neuromodulation from a cochlear level.

Sources
Li X, Mao XB, Hei RY, et al. Protective role of hydrogen sulfide against noise-induced cochlear damage: a chronic intracochlear infusion model. PLoS ONE. 2011;6(10):e26728.

Song BN, Li YX, Han DM. Effects of delayed brain-derived neurotrophic factor application on cochlear pathology and auditory physiology in rats. Chin Med J. 2008;121(13):1189-96.

Kuntz AL, Oesterle EC. Transforming growth factor-alpha with insulin induces proliferation in rat utricular extrasensory epithelia. Otolaryngol Head Neck Surg. 1998;118(6):816-24.

Prieskorn DM, Miller JM. Technical report: chronic and acute intracochlear infusion in rodents. Hear Res. 2000;140(1-2):212-5.

Ma C, Billings P, Harris JP, et al. Characterization of an experimentally induced inner ear immune response.Laryngoscope 2000; 110: 451–56.

El kechai N, Agnely F, Mamelle E, Nguyen Y, Ferrary E, Bochot A. Recent advances in local drug delivery to the inner ear. Int J Pharm. 2015;494(1):83-101.

Stathopoulos D, Chambers S, Adams L, et al. Meningitis and a safe dexamethasone-eluting intracochlear electrode array. Cochlear Implants Int. 2015;16(4):201-7.

Nair TS, Prieskorn DM, Miller JM, Mori A, Gray J, Carey TE. In vivo binding and hearing loss after intracochlear infusion of KHRI-3 antibody. Hear Res. 1997;107(1-2):93-101.

Schindler RA, Gladstone HB, Scott N, Hradek GT, Williams H, Shah SB. Enhanced preservation of the auditory nerve following cochlear perfusion with nerve growth factors. Am J Otol. 1995;16(3):304-9.

Lalwani AK, Walsh BJ, Reilly PG, Muzyczka N, Mhatre AN. Development of in vivo gene therapy for hearing disorders: introduction of adeno-associated virus into the cochlea of the guinea pig. Gene Ther. 1996;3(7):588-92.

Funding
Lions Club International Foundation Research Grant

PS 369

Potentiation of Excitotoxicity in Spiral Ganglion Neurons (SGNs) by cAMP

Sriram Hemachandran
The University of Iowa

Introduction
Cochlear inner hair cells (IHCs) transmit auditory stimuli by releasing the neurotransmitter glutamate onto the afferent nerve fibers (type 1 spiral ganglion neurons (SGNs). Noise causes excessive glutamate release leading to excitotoxic destruction of the synapse (synaptopathy.) Excitotoxicity involves Ca^{2+} entry into the bouton, apparently via Ca^{2+}-permeable AMPA-type glutamate receptors (CP-AMPARs) -- AMPA receptors lacking GluA2 subunits.

The SGN “dendrite” is innervated by axons of the lateral olivocochlear (LOC) efferent projection. Among the neurotransmitters and neuromodulators used by the LOC efferents is the neuropeptide CGRP. In vitro experiments indicate that CGRP exacerbates synaptopathy caused by the excitotoxic glutamate receptor agonist kainic acid (KA). This effect of CGRP is due to recruitment of the second messenger cyclic AMP (cAMP) by CGRP receptors. We ask here how does cAMP exacerbate synaptopathy?.

Hypothesis
1) cAMP triggers increased surface expression of CP-AMPARs, thereby increasing the Ca^{2+} influx during exposure to glutamate agonists. This could be evident as reduced levels of surface GluA2.

2) cAMP permits Ca^{2+} entry through additional channels other than glutamate receptors, e.g., voltage-gated Ca^{2+} channels.

Method
1) The dissociated SGNs were cultured on an 8 well plate with wells exposed to a cell membrane-permeable cAMP analog (cpt-cAMP) for 30, 60 or 120 min**.** The cells were then fixed and the ratio of surface to total GluA2 determined, for each cell, by binding of antibody before and after permeabilzation and calculation of the ratio of resulting immunofluorescence.

2) Ca^{2+} influx was measured by loading SGNs with the fluorescent Ca^{2+} reporter Oregon Green-BAPTA. KA-induced Ca^{2+} influx was compared between SGNs pretreated with cpt-cAMP for 15 min prior to KA exposure and control SGNs.

Result and Summary
1) cAMP pretreatment for up to 120 min did not significantly alter surface expression of GluA2.

2) Ca^{2+} influx in response to KA exposure was significantly increased by pretreatment with cAMP. Without cpt-cAMP

pretreatment, KA-induced Ca^{2+} influx was entirely prevented by IEM-1460, a selective blocker of CP-AMPARs. In contrast, in cpt-cAMP-pretreated cells, a Ca^{2+} influx component not blocked by IEM-1460 was observed. This suggests that cpt-cAMP recruits a novel channel for Ca^{2+} entry.

Funding
DoD - W81XWH-14-1-0494; R01DC009405(SHG); P30DC010362

PS 370

A Platform-based Microphysiological Model for Cochlear Drug Screening and Ototoxicity

Brett Isenberg[1]; Else Frohlich[1]; Abigail Spencer[1]; Will McLean[2]; Danielle Lenz-Kasher[2]; Jonathan Coppeta[1]; Mark Mescher[1]; Albert Edge[2]; Jeffrey Borenstein[1]; **Erin Pararas**[1]
[1]Draper Laboratory; [2]Massachusetts Eye and Ear Infirmary

Current *in vitro* cell/tissue cultures models fail to capture the dynamic nature of *in vivo* drug distribution nor are they capable of elucidating potential interactions between multiple organ systems. To this end, we have developed a reconfigurable platform that precisely recapitulates *in vivo* pharmacokinetics in a collection of multiple interacting *in vitro* microphysiological tissue/organ models for use in drug discovery and toxicity studies. Our approach connects these individual tissue/organ models through a common fluidic network using a series of electromagnetic actuators, enabling tissue interactions and pharmacokinetics in an environment that more closely mimics *in vivo* studies. As a pilot study to demonstrate the value of the platform for early-stage toxicity testing, we exposed inner ear tissue models to an aminoglycoside aiming to recapitulate the well-known problems of the ototoxicity of these compounds when given to treat life-threatening bacterial infections. We cultured either a cochlear cell line (HEI-OC1) or a differentiated primary inner ear hair cells in “inner ear” modules and dosed them with gentamicin from a “plasma” module at concentrations and time scales that mimic *in vivo* pharmacokinetics. Additionally, we varied the concentration to demonstrate dose-response profiles. Cellular responses including cell number, morphology, and phenotype were assessed. We further validated ototoxicity response on platform with the primary inner ear sensory epithelium by monitoring the expression of Atoh1, a marker of hair cell differentiation, over time. Cochlear cell line and primary sensory cells showed significant responses to gentamicin dosing on platform. HE1-OC1 metabolic activity decreased ~30% when exposed to a peak concentration of 50uM gentamicin, as measured by the WST-1 assay. Furthermore, HE1-OC1 apoptotic activity increased over 24 hours of exposure to gentamicin. In the primary hair cells, Atoh1 expression decreased after 24 hours of gentamicin exposure indicating an adverse effect of this drug on differentiation/survival. In conclusion, this pilot study demonstrates that this biomimetic platform is a powerful instrument for toxicity testing, which, along with the tissue models, will likely be a useful tool for investigating the cellular and molecular mechanisms involved in aminoglycoside and other toxicities. Furthermore, the reconfigurable nature of the platform will enable integrated studies with additional tissues/organs models that participate in drug metabolism (e.g., the liver) as well as other tissue/organ models that may also be affected by the drug of interest (e.g., aminoglycosides are also nephrotoxic).

Funding
This work was supported by NIH NIDCD Grant 5 R01 DC13909-2.

PS 371

The Immunohistological Study of Eosinophil Infiltration to the Inner Ear in the Model Animal of Eosinophilic Otitis Media

Naomi Kudo; Hisanori Nishizawa; Atsushi Matsubara
Hirosaki University Graduate School of Medicine

Background
Eosinophilic Otitis Media (EOM), which is known as an intractable otitis media with eosinophil-enriched middle ear effusion. It is reported that EOM is a high risk disease often involving severe sensory hearing loss. We have succeeded in constructing the model animal of EOM, and reported that the number of eosinophils infiltrating to the intratympanic space and middle ear mucosa increases as the period of inflammation prolongs (Nishizawa 2012, Matsubara 2014).

The purpose of the present study was to elucidate the mechanism of eosinophil infiltration to the inner ear through histological and immunohistological analysis for the chemokines which were considered to play a key role in eosinophilic inflammation.

Methods
We constructed the model animals of EOM by systemic and topical sensitization using Ovalbumin (OVA): after intraperitoneal injection of OVA, daily intratympanic injection was continued for 7days, 14days, and 28days. We examined the infiltrating cells in the inner ear and the extent of inner ear damage by histological study. In addition, the sections were immunohistologically stained for Eotaxin 3 and RANTES.

Results
In the inner ear of 7-day stimulation side, a few eosinophils were seen in the scala tympani, although no structural damage was observed. In the 14-day stimulation side, the number of eosinophils infiltrating to the scala tympani increased. In the 28-day stimulation side, we observed more inflammatory cells infiltrating to the perilymph than 14-day stimulation side, accompanied with severe morphological damage of the organ of Corti. As for immunohistological examination, Eotaxin 3 positive cells were observed in the middle ear mucosa of both 7-day and 14-day stimulation side. The number of the immunoreactive cells increased in the latter. We observed similar tendency for the RANTES positive cells in the middle ear mucosa.

Conclusions
From the results of the present study, it is indicated that the eosinophilic inflammation of the inner ear becomes more serious as the duration of OVA stimulation become longer.

Moreover, the number of Eotaxin3 positive cells and RANTES positive cells in the middle ear mucosa also increase as the duration of OVA stimulation. These chemokines are thought to induce eosinophil infiltration to the middle ear mucosa, and they might transfer into the inner ear, possibly through the round window membrane, to elicit eosinophil infiltration to the inner ear.

PS 372

Ion Channel Modulation Limits Cyclodextrin-Induced Ototoxicity

Ian Patterson; Karin Halsey; Liqian Liu; Thomas Schrepfer; **Robert Duncan**
University of Michigan

Hydroxypropyl-β-cyclodextrin (HPBCD) is a powerful excipient that is also capable of extracting lipids from cell membranes. Recently, HPBCD gained Orphan Drug status as a potential treatment for the lipid storage disorder Niemann Pick Disease Type C (NPC). However, HPBCD has emerged as a new ototoxin when given in high doses, resulting in widespread loss of outer hair cells (OHCs) (Cronin et al., 2015). NPC patients receiving HPBCD in a recent clinical trial have also exhibited high-frequency hearing loss (Maarup et al., 2015). The mechanisms remain unknown. In this study, we sought to examine the impact of cyclodextrin on hair cell function and evaluate a number of potential otoprotectants.

Cyclodextrin modulates ion channel activity in chick hair cells (Purcell et al., 2011), raising the possibility that HPBCD negatively impacts OHC excitability. Whole-cell electrophysiology was conducted on OHCs from FVB/NJ mice (P13-17) treated for 30-60 min with 1 mM methyl-β-cyclodextrin (MBCD). Current-voltage curves revealed a reduction in outward current, primarily due to the inhibition of the negatively activated potassium conductance associated with KCNQ-type potassium channels. Since the loss of KCNQ4 in mutant mice leads to OHC death, we assessed whether the KCNQ-activator Retigabine could prevent cyclodextrin-induced hearing loss. Retigabine was examined alongside other otoprotectants targeting mitochondrial dysfunction and oxidative stress: MitoTEMPO, cyclosporin A, D-methionine, vitamin-enriched chow, and N-acetylcysteine. Auditory brainstem response (ABR) thresholds were obtained for FVB/NJ mice (4-6 weeks old) at 4, 16, and 32 kHz 7-10 days after HPBCD injection. A dose-response curve for single, subcutaneous injections of HPBCD was constructed to identify the minimum dose that induces a robust, near maximal response. A steep-dose response curve was obtained, ranging over only a 3-fold change in drug concentration. A dose of 6,000 mg/kg was selected for the otoprotection study. Candidate otoprotectants were delivered by IP injection for 4-5 days with HPBCD co-injected on the first or second day of this regimen. Retigabine (10 mg/kg) limited HPBCD-induced ABR threshold elevation at all test frequencies by 15-20 dB ($P < 0.05$). D-methionine (300 mg/kg) was modestly effective at 4 kHz only. No other otoprotectant significantly limited cyclodextrin ototoxicity. While Retigabine dose, timing, and delivery route must be optimized and examined in NPC model systems, our findings provide mechanistic insight into hearing loss by HPBCD and offer a potential avenue for the prevention of HPBCD-induced hearing loss in NPC patients.

Funding
Support Of Accelerated Research for Niemann Pick type C (SOAR-NPC)

PS 373

Connexin 43 acts as a pro-apoptotic modulator in cisplatin-induced auditory cell death

Yeon Ju Kim; Young Sun Kim; Beomyong Shin; Jong Joo Lee; Oak-Sung Choo; Yun-Hoon Choung
Ajou University

Background
Gap junction (GJ) coupling may play a role for intercellular communication by the “Good Samaritan effect” or “bystander effect” under pathological conditions. Non-junctional connexins (Cxs) also may play some gap junction-independent roles in cell death or survival. The purposes of this study were to investigate the role of non-junctional Cxs in ototoxic drug-induced apoptosis of auditory cells and to evaluate the effect of GJ inhibitors on cisplatin-induced hearing loss using *in vivo* animal models.

Methods
Non-junctional Cx43 proteins in HEI-OC1 cells were prepared with three techniques. 1) Low confluence culture (5X103/cm2). 2) Construction of short lengthened Cx43 - Cx43-NT (amino acid 1-256, membrane domain) and Cx43-CT (amino acid 257-382, cytoplasmic domain). 3) Brefeldin A (BFA), an ER-Golgi trafficking inhibitor. A live/dead cell viability assay and western blotting were done under knock-down conditions (siRNA-Cx43). Additionally, For *in vivo* animal studies, carbenoxolone (CBX, 50 mg/kg) and 18- alpha glycyrrhetinic acid (18α-GA, 100 mg/kg) was intraperitoneally injected to rats treated with cisplatin (16 mg/kg). Auditory brainstem response and morphologic analysis were done with immunihistochemistry.

Results
Knock down of non-channel Cx43 (siRNAalone treated rats. In SEM findings, loss of stereocilia in outer hair cells was much more in the cisplatin-treated rats than in the CBX+cisplatin-treated rats.) inhibited cisplatin-induced cell death in MTT assay and Western blot. This finding was not changed by disruption of Cx43 trafficking with BFA. HeLa cells expressing the Cx43-FL (full length), Cx43-NT or Cx43-CT showed enhanced sensitivity to cisplatin compared to Mock cells. In animal studies, hearing thresholds of ABR in CBX+cisplatin-treated rats were significantly better than those in the cisplatin-

Conclusion
Cx43 plays a pro-apoptotic role in cisplatin-induced auditory cell death, which is either dependent or independent on GJ intercellular communications. The control of Cx-mediated

signaling may be necessary for designing new therapeutic strategies for drug-induced ototoxicity.

Funding
This work was supported by the Basic Science Research Program through the National Research Foundation of Korea (NRF) funded by the Ministry of Education Science and Technology (NRF-2013R1A2A2A01008325).

PS 374

Measurement of cochlear function after acoustic overexposure during in embryo and neonatal mice

Kazuya Arakawa; **Ryoukichi Ikeda**; Yohei Honkura; Kazuhiro Nomura; Tetsuaki Kawase; Yukio Katori
Tohoku university

Backgrounds
There are a lot of studies about exposure to acoustic noise in adult human or the other animals, however, little has been reported on exposure to acoustic noise during in embryo and neonatal stage. In clinical, exposure of the fetus to 1.5-T Magnetic resonance imaging (MRI) during the second and third trimesters of pregnancy is not associated with an increased risk of substantial neonatal hearing impairment (Reeves MJ, et al. Radiology 2010). The aim of this study was to establish whether acoustic overexposure is associated with cochlear function in embryo and neonatal mice.

Methods
C57/BL6 mice (Embryo: E12, 14, 16, 18, Postnatal: P1, 3 and 5 days) were exposed to octave band noise (4-8kHz) for 2h at 116 dB SPL (group A) and 8-16kHz for 2 h at 110 and 116 dB SPL (Group B). All mice underwent auditory brainstem responses (ABR) and inner ear hair cell count at P28 days.

Results
Group A showed better result in ABR threshold shift as compared with Group B when tested P28 days.

Conclusions
These results showed that acoustic overexposure during in embryo and neonatal mice effected on various extent of cochlear function at postnatal 28 days. Additional studies are needed to determine precise mechanism of acoustic effect to embryo and neonatal mice.

Funding
This study was supported by a grant from the Ministry of Education, Culture, Sports, Science and Technology-Japan

PS 375

Cognitive dysfunction in mice with noise-induced hearing loss

Shi Nae Park; Min Jung Kim; Hu Erxidan Sikandaner; So Young Park
College of Medicine, The Catholic University of Korea

Background and Objectives
The relationship between auditory and cognitive functioning in the elderly has been the subject of many investigations yielding conflicting results. Hearing impairment have been reported to be a potential risk factor for cognitive decline although the role of sensory functions in cognition still remains to be clarified. It is challenging to determine cognition in non-verbal laboratory animals and various cognitive behavioral tests have been developed to estimate their cognition. We performed this study to investigate the association between hearing and cognition using radial arm maze (RAM) and novel object recognition (NOR) tasks in an inbred mouse strain.

Subjects and Method
Twenty-four male C57BL/6 mice aged 1 month with ABR thresholds for 8/16/32 kHz tones ≤ 20 dB were used. Twelve mice in the hearing loss group were exposed to daily 110 dB SPL white noise for 60 min for 20 days. At post-noise 6 months, all mice underwent RAM and one-trial NOR test. (1) Total trial time (TT) to accomplish the task, (2) WM error (WME, re-entry), (3) RM error (RME, incorrect entry), and (4) correct entry ratio (CER, correct entry/total entry) were the indicators of the radial maze performances. In NOR test, novel object (NO) contact time and familiar object (FO) contact time were measured.

Results
All experimental mice showed permanent threshold shifts of approximately 30 dB at the test stimuli after noise exposure. In RAM task, WME, RME and CER showed significant improvement within each group across 5 trials probably due to learning effect: p = 0.029, 0.004, and 0.004 for WME, RME, and CER, respectively. Significant interaction was not found between group and trial, which implies that the tendency for task learning, more or less, is similar between the normal and hearing-impaired mice. However, the hearing loss group exhibited significantly poorer performances than the control group with respect to TT in trials 1 (p = 0.048) and 5 (p = 0.028), WME in trials 1 (p = 0.018) and 5 (p = 0.035), and CER in trial 5 (p = 0.035). NOR discrimination index of the hearing loss group (1.5%) was significantly lower than that of the control group (19.8%) (p = 0.024), while the total contact times representing the baseline motor activity were not different between the groups.

Conclusion
Moderate hearing loss induced by noise in younger mice resulted in cognitive dysfunction associated with spatial working and recognition memories at post-noise 6 months.

Funding
The National Research Foundation of Korea(2013- ***)

PS 376

Hearing Sensitivity and Susceptibility to Hearing Loss in CHOP Knockout Mice

Eric Bielefeld; Ryan Harrison; J. DeBacker; Izabela Jamsek
The Ohio State University

The condition of endoplasmic reticulum (ER) stress occurs when there is an accumulation of unfolded proteins in the rough ER. It occurs most commonly in conditions of intense metabolic demand or alterations in cellular calcium

homeostasis, which in turn can occur as the result of oxidative stress. In response to ER stress, the cell engages the unfolded protein response (UPR). In situations of acute ER stress, the UPR works to protect the cell and restore ER function. For prolonged or severe ER stress, the UPR enters the cell into an apoptosis cycle, resulting in cell death. Apoptosis is a prominent pathway for organ of Corti cell death underlying noise-induced and cisplatin-induced hearing losses. Therefore, the current study explored knock out of a prominent molecule of the UPR's apoptosis cascade, CAAT/enhancer-binding protein homologous protein (CHOP), for possible effects on noise- and cisplatin-induced hearing losses. Knockout of CHOP has been shown to reduce ER stress-induced apoptosis in several cell types and organ systems in the body. CHOP -/- knockout mice and control C57Bl/6J mice were obtained from Jackson Labs. The initial phase of the study tested auditory brainstem response thresholds and P1 wave input-output functions in the CHOP -/- mice. CHOP -/- mice were tested at four, eight, twelve, and sixteen weeks of age. Fifty percent of the initial group of CHOP-/- mice had severely elevated thresholds by eight weeks-old. Breeding of the mice demonstrated that offspring of the mice with poor hearing had elevated thresholds by eight weeks of age. Offspring of CHOP -/- mice with better hearing had higher thresholds than C57Bl/6J controls in the high frequencies, but low-frequency thresholds and P1 amplitudes were not significantly different. Sub-sets of mice four to eight weeks old were then exposed to cisplatin (8, 12, or 16 mg/kg by intra-peritoneal injection) or high-level noise. There was no evident difference in susceptibility to noise-induced hearing loss in CHOP -/- mice exposed to a one-hour, 110 dB SPL continuous noise. The knockout mice did show differences in susceptibility to cisplatin-induced threshold shift and cochlear injury. The results indicate that ER stress and the UPR may be involved in the maintenance of normal of organ of Corti homeostasis and in determining the magnitude of cell death from cisplatin.

Funding
Research was supported by a seed grant from the American Cancer Society Institutional Research Grant # IRG-67-003-47 to The Ohio State University. Additional support was provided by The Ohio State University's College of Arts and Sciences, division of Social and Behavioral Sciences, and Undergraduate Research Office.

PS 377

The Role of the Master Clock and the Light-Dark Cycle in the Regulation of Noise Injury

Jung-sub Park; Christopher Cederroth; Barbara Canlon
Karolinska Institutet

Background
The mammalian circadian timing system regulates many bodily functions with a 24-hour period. We have shown previously that cochlea has a circadian clock machinery and that day noise and night noise differentially affect the mouse cochlea. However, detailed mechanisms of synchronization and circadian regulation of the peripheral auditory system by the master clock of the body, the suprachiasmatic nucleus (SCN) have not been investigated. In addition, the role of the SCN in the generation of noise-induced hearing loss also needs to be determined for the development of effective chronopharmacological treatment. Here, we unequivocally showed that the peripheral auditory organ is regulated not only by the SCN, but also by external light-dark signals.

Methods
The role of the SCN in auditory function was determined by making bilateral electrolytic lesions in this structure. Moreover, the effect of the light-dark cycle (LD) on the auditory system was also studied. We compared the physiological condition in 12-h LD cycle and constant darkness (DD, dark-dark). Young male CBA mice were exposed to 105 dB SPL with a 6-12 kHz narrow band white noise for 1 h. To assess the compound threshold shift (CTS) and permanent threshold shift (PTS), auditory brain stem response (ABR) was performed at 24-h and 2-week after noise exposure. After ABR measurements, cochleae were sampled to assess the circadian expression of core clock genes, as well as other clock-related genes.

Results
SCN lesioned animals with LD cycle showed a significant PTS of 20 dB after night noise exposure while sham animals with LD cycle showed a small PTS of 9 dB after night noise exposure. Furthermore, SCN lesioned animals with abolishment of light cues (DD) incurred significant CTS and exacerbated PTS after both day noise and night noise exposure, especially in the high frequency area (30 kHz). Circadian gene expressions with around the clock qPCR data will also be presented.

Conclusion
These data demonstrate that noise sensitivity of peripheral auditory system is regulated from not only SCN but also external cues such as LD cycles.

Funding
Funding: This work was supported in part by National Institute on Deafness and other Communication Disorders of the National Institutes of Health, National Research Foundation of Korea grant (2014R1A6A3A03058661) funded by the Korea government and Tysta skolan.

PS 378

The oral administration of teprenone can protect the ribbon synapses of inner hair cells against noise trauma.

Yoshihiro Okazaki; Kazuma Sugahara; Yoshinobu Hirose; Hiroaki Shimogori; Hiroshi Yamashita
Yamaguchi University Graduate School of Medicine

Introduction
In the previous research, we reported that heat shock proteins are expressed in the inner ear after intense noise exposure and the expression of heat shock proteins can protect the hearing function in the Noise trauma model of guinea pigs. It is known that teprenone can induce the heat shock response in many kinds of organ. In the previous meeting, we reported

that teprenone might protect the ribbon synapses of inner hair cells morphologically 3 days after intense noise exposure but not protect functionally. In the present study, we evaluate the effect of oral administration of teprenone on the recovery of ribbon synapses of inner hair cells 7 days after intense noise exposure.

Materials and Methods
Hartley male guinea pigs (500 - 900 g) with the normal tympanic membranes and the normal Preyer's reflexes were used in this study. Animals were divided into 2 groups (Noise group, Teprenon+Noise group).

In Teprenone+Noise group, animals were fed with the food containing 0.5% of teprenone before intense noise exposure. In Noise group, animals were fed with normal food. To evaluate the expression of heat shock proteins, the western blot analysis was performed using the extract from the cochleae of the animals.

The animals in both groups were exposed to the intense band noise (130 dBSPL for 3 hours). 7 days later, the temporal bone was removed to evaluate the ribbon synapse count. To ravel the ribbon synapses, the immunohistochemistry was performed using the anti-CtBP2 antibody. These samples were observed with the fluorescence microscope. ABR examination was performed 7 days after the noise exposure and ABR thresholds were compared between those groups.

Results
The density of signals of CtBP2 was lower in both groups than that in control animals. In the Teprenon+Noise group, the significantly higher density of signals of CtBP2 and the significantly lower ABR thresholds was observed than those in Noise group.

Discussion
We have reported the effect of the heat shock inducer, teprenone in the hearing functional recovery after the intense noise exposure. However, the mechanism of the protective effect of teprenone is unclear. Bechtold has reported that heat shock proteins were expressed in synapse of the rat brain after heat stress. In addition, Karunanithi has reported that heat shock proteins protect synapse in Drosophila models. Combined with our results, it was suggested that teprenone might protect the synapses of inner hair cells 7 days after the noise trauma.

PS 379

Attenuation of Noise Induced Hearing Loss by Near-Infrared-Light pre-Treatment

Dietmar Basta[1]; Moritz Gröschel[1]; Ira Strübing[1]; Dan Jiang[2]; Patrick Boyle[3]; Arne Ernst[1]
[1]University of Berlin; [2]Guys' and St Thomas' NHS Foundation Trust London; [3]Advanced Bionics European Research Center

Background
Beside changes of central auditory structures, noise induced hearing loss (NIHL) is accompanied by a reduction of cochlear hair cells. Different approaches are investigated for the prevention of noise induced apoptosis/necrosis. Physical intervention is one approach currently under study. It has been shown recently that near-infrared light (NIR) can decrease the cochlear hair cell loss significantly if applied daily after a noise exposure.

The present study aimed at investigating the effect of a single NIR-pre-treatment to prevent or limit NIHL.

Method
The cochleae of adult mice were pre-treated with NIR-light (808 nm, 120 mW) for 10 or 30 minutes via the external ear canal. All animals were noise exposed immediately after the pre-treatment by broad band noise (5 - 20 kHz) at 115 dB SPL. Frequency specific ABR-recordings were carried out before all treatments and 2 weeks after the noise exposure. Spiral ganglion cell density and cochlear hair cell loss were determined. One group was noise exposed only and served as control.

Results
ABR-tresholds were significantly less elevated ($p<0.05$) two weeks after the noise exposure if the animals were pre-treated by NIR-light for 30 min. They showed 35.2 dB lower thresholds on average than controls. A NIR pre-treatment for 10 min had no effect on ABR-thresholds.

Conclusions
The results suggest that a very effective protection of cochlear hair cells is possible by a single NIR pre-treatment. However, the optimal dosage and time frame for the application should determined in future studies.

The results could be of high relevance for the protection of residual hearing in otoneurosurgery such as cochlear implantation.

Funding
This study was supported by Advanced Bionics GmbH, Hanover, Germany.

PS 380

Protective effect in herbal medicine "Shimotsuto" on noise-induced hearing loss in the guinea pig

Yoshinobu Hirose; Kazuma Sugahara; Makoto Hashimoto; Hiroshi Yamashita
Yamaguchi University

Background
The zebra fish lateral line is a powerful system for studying hair cells and hair cell death. Hair cells can be easily labeled and imaged in vivo with fluorescence microscopy. We reported in 2014 ARO meeting that eight herbal medicines were screened for protective effects against aminoglycoside. All of them showed protective effect, especially in Shimotsuto. In 2015 ARO meeting, we show Shimotsuto protects sensory hair cells against neomycin-induced death in CBA/N mice vestibular epithelium. Now we investigate whether Shimotsuto can protect hair cells in guinea pig against acoustic trauma for oral administration.

Methods
We investigated the effect of Shimotsuto on acoustic trauma in guinea pigs. Animals were divided into two groups. All animals were exposed to intense band noise centered at 4 kHz for 3 h (130 dB sound pressure level). In the Shimotsuto group (n=3), Shimotsuto (500 mg/kg/day) was dissolved in water, administrated for oral 3 days before noise exposure. In the control group (n=3), water was given for oral. Seven days after noise exposure, we assessed auditory brainstem response (ABR) threshold. In addition we observed the cochlear hair cell damages.

Results
The ABR threshold shift was significantly less in Shimotsuto group than in control group. But there was no significant difference between in Shimotsuto group and in control group in the proportion of defective outer hair cells.

Conclusion
The results indicated that Shimotsuto protect inner ear against acoustic trauma. Shimotsuto can be a powerful protective drug against inner ear damage.

Funding
This research was supported by grants from Grant-in-Aid for Young Scientists (B), Japan Society for the Promotion of Science, Grant Number 25861564.

PS 381

Protective effect of JHX-4, a multi-functional antioxidant, against gentamicin-induced ototoxicity in cochlear and vestibular organotypic cultures

Kun Yang[1]; Dalian Ding[2]; Peter Kador[3]; Richard Salvi[2]
[1]Hubei General Hospital, Wuhan University; [2]University at Buffalo; [3]University of Nebraska Medical Center

Gentamicin is a highly effective antibiotic used to treat bacterial infections, mostly Gram-negative and some Gram-positive; however, significant ototoxic and nephrotoxic side effects limit is use. Since gentamicin ototoxicity may arise from the generation of free radicals and reactive oxygen species (ROS), compounds that scavenge ROS molecules may protect against gentamicin ototoxicity. JHX-4, a multifunctional antioxidant, is a highly effective free radical scavenger and has been shown to protect against a rat model of age-related macular degeneration. Therefore, we speculated that JHX-4 might protect against aminoglycoside-induced hair cell loss in the inner ear. To test this hypothesis, we prepared cochlear and vestibular organotypic cultures from postnatal day 3 rats and treated the cultures with gentamicin alone (0.1 or 0.2 mM) or the combination of JHX-4 (100 to 1000 μM). Gentamicin induced hair cell loss in both cochlear and vestibular system in a dose-dependent manner. The 0.1 mM dose of gentamicin caused extensive hair cell loss in both cochlear and vestibular cultures. Cochlear hair cell loss was greatest near the base of the cochlea and progressively decreased towards the apex. In vestibular cultures, the most severe vestibular hair cell loss occurred in the macula of utricle. The addition of JHX-4 at low concentrations of 100 μM and 500 μM suppressed gentamicin-induced hair cell loss in both cochlear and vestibular cultures. However, higher doses of JHX-4 damaged both cochlear and vestibular hair cells. These results indicate that low concentration of JHX-4 can protect against gentamicin ototoxicity. However, high levels of JHX-4 can exacerbate hair cell damage presumably by disrupting endogenous antioxidant defense systems in the inner ear.

PS 382

A c-Jun-N-Terminal Kinase Inhibitor (SP600125) Blocks Pro-death Signaling in TNFα-induced Auditory Hair Cell Loss In Vitro

Christine Dinh; Esperanza Bas; Seo Moon; John Dinh; Ly Vu; Gia Hoosien; Adrien Eshraghi; Thomas Van De Water; Xue Liu
University of Miami

Background
Tumor necrosis factor-alpha (TNFα) is a pro-inflammatory cytokine that is expressed in the cochlea in various disorders of or following a trauma to the inner ear. TNFα can bind to its receptor on the cell membrane of auditory hair cells (HC) and activate c-Jun N-terminal kinase (JNK), an enzyme that promotes apoptosis-related signaling. SP600125 is an inhibitor of JNK that can potentially block downstream phosphorylation of c-Jun (p-c-Jun) and Bax-mediated mitochondrial death signaling and production of reactive oxygen species (ROS) in TNFα-challenged organ of Corti explants.

Methods
Organ of Corti (OC) explants were dissected from 3-day old rats and cultured in: (1) no treatment (control); (2) TNFα; (3) TNFα + SP600125; (4) SP600125; and/or (5) TNFα + pan-caspase-inhibitor for 0, 24, 48 or 96 hrs in vitro. Fluorescence imaging studies for viable HC counts, oxidative stress and mitochondrial membrane potential, immunolabeling imaging studies for p-c-Jun, EndoG, AIF, and caspase-3, ELISA for p-c-Jun and Smac expression, real-time PCR for Bax, Bcl-2, TNFR1, and Smac, and assays for catalase and superoxide dismutase (SOD) activity were performed at different in vitro time points. Data analysis was performed with ANOVA and with Tukey HSD post-hoc testing with significance set at $p<0.05$.

Results
TNFα-injured OC explants demonstrated more HC loss and were associated with higher levels of p-c-Jun, EndoG, AIF, Smac, and caspase-3 protein expression, up regulation of Bax, Smac, and TNFR1 mRNA transcription, depolarization of the mitochondrial membrane potential, increased oxidative stress, and reductions in catalase and SOD activities. Treatment of TNFα-injured OC explants with SP600125 resulted in reversals of the pro-apoptotic molecular trends observed within the TNFα-only explants; SP600125 also increased activities of pro-survival SOD and catalase proteins that are important for protection of cells against damage by oxidative stress, i.e. ROS.

Conclusion
These findings suggest that TNFα initiated significant losses of auditory HCs in OC explants in vitro, in part by JNK phosphorylation of c-Jun and downstream transcription of pro-death Bax and Smac and pro-inflammatory TNFR1 genes. TNFα ototoxicity also promoted HC death through JNK-mediated shifts in the mitochondrial membrane potential, release of pro-apoptotic mitochondrial proteins, generation of ROS, and caspase-3 activation. SP600125, a small molecule inhibitor of JNK, is capable of reversing several of the intrinsic and extrinsic mechanisms of TNFα-initiated apoptosis and has great potential as a treatment to prevent or limit the level of inflammatory cytokine-associated HC loss.

Funding
This study was supported by grants from MED-EL to VDW and R01DC012546 and R01DC005575 to XZL.

PS 383

Aging influences wound healing, hearing preservation, and response to corticosteroids in cochlear implantation.

Esperanza Bas; Christine Dinh; Jorge Bohorquez; Adrien Eshraghi; Thomas Van De Water
University of Miami

Background
A robust inflammatory response occurs in the cochlea immediately after cochlear implant insertion trauma. This wound healing process can become chronic and promote fibrosis in the inner ear, which can lead to increases in electrode impedance, electrode array extrusion, and device malfunction. Older patients and children may demonstrate different wound healing responses in the cochlea, which can play a major role in hearing outcomes after cochlear implantation.

Material and methods
Young (i.e. 3 months of age) and old (i.e. 12-15 months of age) Norway Brown rats received cochlear implants (CI) with either 0% Dexamethasone base (DXMb) or 10% DXMb. The pre-implantation hearing threshold response and the contralateral ears were used as controls. Auditory Brainstem Responses (ABR), Cochlear Action Potentials and impedances were recorded at different time points up to 3 months post-implantation. Gene expression studies of the endothelial cell biology of the cochlea were carried out at 7 days post implantation.

Results
Young animals with electrode insertion trauma (EIT) demonstrated greater ABR threshold shifts in the high frequencies and higher impedances when compared to older animals. Incorporation of 10% DXMb into the silicone of the cochlear implant electrode arrays resulted in a higher level of otoprotection in young animals for up to 3 months, when compared to old rats. 10% DXMb eluting electrode arrays significantly delayed changes in impedance in young animals, while no effect was seen with older animals. Higher levels of *Calca* (responsible for vasodilation and transmission of pain) and chemokines *Ccl2, Ccl5* and *Cxcl1,* were observed in implanted ears of aged rats, Several cell-extracellular matrix interaction molecules such as *Fn1,* integrins, *Sele, Selp, Thbs1*, and the proliferative and pro-fibrotic factors *Fgf1* and *Tgfb1* were overexpressed in cochleae of young implanted animals compared to older rats. These genes were suppressed in 10% DXM electrode array implanted cochleae.

Conclusions
EIT triggers a wound healing response, characterized by increased gene expression of several inflammatory cytokines, inducible enzymes, cell adhesion molecules and chemokines. Differences in expression of these genes are demonstrated between young and older implanted cochleae, and can be reversed with 10% DXMb. Age of implantation also influenced the severity of ABR threshold shifts and cochlear implant impedances and response to corticosteroid treatment. Our results demonstrate the protective effects of DXMb-eluting cochlear implant electrode arrays against post-implantation hearing threshold shifts and the inflammatory, fibrosis, and wound healing responses.

Funding
This study was supported by grants from MED-EL to VDW and EB.

PS 384

Kanamycin-induced hearing loss in a transgenic TFB1M mouse model of mitochondrial stress

Lei Song[1]; Sharen McKay[1,2]; Jianwen Xu[3]; Gerald Shadel[1]; Joseph Santos-Sacchi[1]; Jie Song[3]
[1]Yale University School of Medicine; [2]University of Bridgeport; [3]University of Massachusetts Medical School

Our recently described transgenic mouse model TFB1M (Tg-TFB1M) displays non-syndromic hearing loss with properties similar to human maternally-inherited deafness caused by the mtDNA mutation A1555G. The hearing loss, measured by auditory brainstem response (ABR) in 9-12 month old mice, is accompanied by cochlear pathology that includes reduction of endocochlear potential (EP) and loss of cells in the spiral ganglion. Notably, there is no loss of either inner or outer hair cells at a point in the disease process where ABR thresholds are substantially increased. This suggests the hearing loss may be reversible.

To further explore the relationship of the mouse model to the human disease, we asked whether TFB1M mice are also susceptible to aminoglycoside insult (similar to A1555G carriers) by locally applying the antibiotic kanamycin to the inner ear. To deliver kanamycin over time we have introduced a newly developed 'click' hydrogel (Xu et al 2014) as a drug carrier. Kanamycin embedded in the gel is released as the gel degrades. Kanamycin-containing hydrogel stock solutions (hydrogel formulation engineered to ensure gel degradation over 2 weeks) were injected intra-tympanically and ABRs were measured immediately prior to and after the injection and then after a 2 week treatment period. Controls injected with a blank gel showed healed tympanic membranes

and complete post-injection recovery of ABR thresholds. Kanamycin containing gels elevated ABR threshold in tested animals and studies are underway to determine the level of susceptibility to kanamycin in wildtype vs. TFB1M mice. The hydrogel system enables us to confirm the validity of our model and may, in the future, provide a therapeutic platform for preventing or reversing early hearing loss in A1555G carriers.

Funding
Supported by Ohse Research Grant to L.S., NIH R01 AG047632 and a pilot grant from The Yale Claude D. Pepper Older American Independence Center to G.S.S., and NIH NIDCD R01 DC000273 and R01DC 007894 to J.S.S.

PS 385

Larval Zebra fish Lateral Line as a Model for Acoustic Trauma

Phillip Uribe[1]; Beija Villalpando[1]; Zecong Fang[1]; Jie Xu[2]; Allison Coffin[1]
[1]Washington State University, Vancouver; [2]University of Illinois at Chicago

Excessive noise exposure leads to permanent hearing loss and there are no effective pharmacological therapies to ameliorate noise damage. To increase the rate of drug discovery, we need an efficient pipeline for the identification of compounds that protect hair cells from acoustic trauma. Larval zebra fish are a tractable model for ototoxicity and otoprotection research, including large-scale drug discovery. Zebra fish posses an externally located lateral line system containing clusters of hair cells which can be rapidly assessed and are homologous to those found in the mammalian inner ear. This project demonstrates the utility of the lateral line system as a model to study hair cell loss associated with acoustic trauma. Larval zebra fish were placed in a 24-well plate that was suspended in a water bath above four ultrasonic transducers resulting in underwater cavitation to acoustically stimulate lateral line hair cells. The ultrasonic field interacts with microbubbles in the aquatic environment, resulting in fluctuations in bubble volume that lead to bubble implosion. Bubble implosion generates intense broadband noise that emits frequencies between 20 Hz and 10,000 Hz, which includes low frequencies within the range of lateral line sensitivity. Following acoustic trauma, vital dye staining conducted 0 - 24 hours post noise exposure indicated that hair cell loss was time- and intensity-dependent and maximal loss was observed 24 hours post cessation of exposure. After as little as fifty minutes of exposure, we observed significant hair cell loss when assessed 24 hours post-exposure, whereas no hair cell loss was observed immediately following stimulus cessation. The delayed onset of cell death led us to investigate if protein synthesis is required for loss of hair cells following acoustic trauma. Administration of the protein synthesis inhibitor, cyclohexamide, for three hours immediately post-exposure conferred robust hair cell protection from noise, indicating hair cell death is protein synthesis dependent. TUNEL labeling demonstrated that damage caused by underwater cavitation first occurred 6 hours post-exposure and was specific to hair cells. Additionally, surviving hair cells exhibited kinocilial blebbing, a sign of sub-lethal damage. These results demonstrate that lateral line hair cells respond to acoustic trauma similarly to mammalian hair cells, making zebra fish a tractable model for the study of acoustic trauma. We are now utilizing this model in a large-scale drug discovery effort to identify compounds that protect hair cells from acoustic damage.

PS 386

AAV-Mediated Neurotrophin Gene Therapy Promotes Improved Spiral Ganglion Survival in the Deafened Cochlea

Patricia Leake[1]; Stephen Rebscher[1]; Chantale Dore'[1]; Lawrence Lustig[2]; Bas Blits[3]; Omar Akil[1]
[1]University of California, San Francisco; [2]Columbia University; [3]uniQure bipharma B.V.

Background
The efficacy of cochlear implants (CI) depends partly upon survival of the cochlear spiral ganglion (SG) neurons that progressively degenerate following deafness. In early-deafened cats, electrical stimulation from a CI partly prevents SG degeneration, and intracochlear infusion of Brain Derived Neurotrophic Factor (BDNF) further improves neural survival. However, BDNF also elicits disorganized, ectopic sprouting of radial nerve fibers, which would be detrimental to optimum CI function due to loss of tonotopicity. Also, in many prior studies, BDNF was delivered by osmotic pumps, which is not practical for clinical application. The current study explores using adeno-associated viral vectors (AAV) to elicit targeted neurotrophic factor (NT) expression by cells within the cochlea.

Methods
AAV2-GFP (green fluorescent protein), AAV5-GFP, AAV2-BDNF, or AAV5-GDNF (glial-derived neurotrophic factor) was injected (1ul) into the scala tympani of FVB mice (1-2 days postnatal) through the round window. Mice were studied 7-21 days later. Additional studies assessed AAV efficacy in transducing cells in the cochlea of normal and deafened cats. Kittens were deafened prior to hearing onset by systemic injections of neomycin sulfate. ABRs showed profound hearing loss by 16-18 days postnatal. AAV (10uλ) was injected at 3-4 weeks of age. Animals were studied 4 weeks later for GFP immunocytochemistry or 14 weeks post-injection to evaluate SG survival.

Results
Following AAV2-GFP injections in mice, immunohistochemistry showed strong expression of the GFP reporter gene in inner (IHCs), outer hair cells (OHCs), inner pillar cells, and some SG neurons. With AAV5-GFP, transduction of IHCs and many SG neurons was robust, but few OHCs and supporting cells expressed GFP. Patterns of GFP expression for the 2 viruses were similar in the cat cochlea. Initial data in deafened cats examined 14 weeks after AAV2-BDNF injections showed significant neurotrophic effects, with ~12% higher SG density vs. contralateral and higher density of radial nerve fibers.

Importantly, no ectopic sprouting of radial nerve fibers was observed.

Conclusions
AAV-GFP (both serotypes) elicited GFP expression in IHC and SG neurons in both mice and cats; AAV2-GFP additionally transduced OHCs and some inner pillar cells. A single injection of AAV2-BDNF apparently elicits sufficient expression of BDNF in the deafened cat cochlea over >3 months to promote improved SG neuron and radial nerve fiber survival, which likely would be beneficial for CI performance. Given the strong transduction of SG neurons by AAV5-GFP, further studies are now underway to evaluate and compare potential neurotrophic effects of AAV5-GDNF in deafened cats.

Funding
The authors thank K. Bankiewicz and uniQure biopharma B.V. for donating the AAV vectors for these studies. This research was supported by NIDCD Grant R01DC013067, the Epstein Fund, and uniQure biopharma B.V.

PS 387

Supplementation of three antioxidants ameliorates cochlear damage induced by chronic application of germanium dioxide

Akinori Kashio; Kazuo Yasuhara; Teru Kamogashira; Akinobu Kakigi; Shinichi Iwasaki; Tatsuya Yamasoba
University of Tokyo

Germanium dioxide (GeO_2) is widely available for the manufacture of integrated circuits, nanoelectronic devices, and solar cells. Germanium is also ingested to enhance health as it is believed to have an anti-tumor effect and immunomodulative activity. However, long-term ingestion of GeO_2 has been shown to cause kidney, muscle, and nervous system disorders. Chronic administration of GeO_2 to rats also can induce ragged-red fibers and cytochrome *c* oxidase (COX)-deficient fibers in the skeletal muscles, which resemble pathological changes observed in patients with mitochondrial encephalomyopathy associated mitochondrial DNA abnormalities. We previously demonstrated that CBA mice administered 0.15% GeO_2 exhibited degeneration of the stria vascularis (SV) and spiral ganglion cells (SGC) and significant auditory brainstem response (ABR) threshold shifts. Further, analysis of the gene expression in the cochlea revealed down-regulation of genes associated with hearing function, energy metabolism, etc. and up-regulation of genes related to apoptosis and inflammation. These findings suggest that GeO_2 induces inflammation and decline of energy metabolism due to mitochondrial dysfunction, which then trigger apoptotic cell death in the cochlea, causing deafness. It is well known that mitochondrial dysfunction is closely related to the generation of reactive oxygen spices. In the current study, therefore, we examined whether supplementation of antioxidants, taurine, hydrogen, and CoQ10, can prevent/ameliorate hearing loss and degeneration of cochlear tissue caused by chronic application of GeO_2.

Two-month-old normal hearing CBA mice were used. They were assigned to one of the five groups and fed normal chow and water or chow containing 0.15% GeO_2, and normal water or water containing 0.3% taurine, 150 μM water-soluble CoQ10, or hydrogen (0.4mM). Three months later, ABR was measured and the cochlea was dissected and examined under a microscope.

Animals given normal chow and water did not show hearing loss or obvious histological changes, whereas those given chow containing GeO_2 exhibited moderate hearing loss associated with marked vacuolar degeneration in the SV and reduction of SGC. All three supplements significantly attenuated the ABR threshold shifts and the cochlear degeneration when compared to animals given only GeO_2. Of the three antioxidants, taurine showed the most significant effect both on ABR threshold shifts and histopathological changes, followed by CoQ10. These findings indicate that supplementation of these antioxidants can ameliorate cochlear damage caused by GeO_2. Because pathological findings in patients with mitochondrial encephalomyopathy resemble those induced by chronic application of GeO_2, these three antioxidants may be promising therapeutic agents for mitochondrial encephalomyopathy.

Funding
This work was supported by MEXT KAKENHI Grant Number

PS 388

Catastrophic Hearing Loss After Noise Exposure in Foxo3 Knock-Out Mice

Felicia Gilels; Stephen Paquette; Patricia White
University of Rochester

Foxo3 is a forkhead box O transcription factor that mediates oxidative stress responses, apoptosis, and cell cycle withdrawal in many systems. In other systems, Foxo3 can be activated by excitotoxicity or mechanical stress. Previously, we had shown that mutation of Foxo3 causes adult onset auditory neuropathy and altered synaptic architecture. Additionally, we had previously shown that noise exposure promotes Foxo3 nuclear localization in spiral ganglion neurons. Here we have characterized the phenotype of the Foxo3-KO mouse after noise exposure.

All experiments were conducted on Foxo3 wild-type and knock-out littermates, on the FVB/n strain. Two month old mice were exposed to a noise limited to the 8-16kHz octave band at 105dB for 30 minutes. Auditory function was assessed with Auditory Brainstem Responses (ABR) and Distortion Product Otoacoustic Emissions (DPOAE) at baseline (7-8 weeks old), one day and fourteen days post noise exposure. Immunohistochemistry was used to analyze cochlear cells, including neurons and hair cells, fourteen days post noise exposure. Synaptic analyses were performed using Amira 3-D reconstructions and algorithmically assessed with custom scripts written in Mathematica.

Foxo3-KO mice demonstrate catastrophic permanent hearing loss, compared to their wild-type littermates fourteen days post noise exposure. Significant outer hair cell loss is evident

in the basal region of the Foxo3-KO cochlea at this time. Interestingly, no significant synapse or spiral ganglion losses were observed, leading to the idea that loss of Foxo3 function may not create a propensity for synaptic or neuronal loss. Preliminary data indicate that there may be abnormalities present in the noise exposed Foxo3-KO inner hair cells. Taken together, these data indicate that Foxo3 may promote hair cell survival and/or function after noise exposure.

Funding
Hearing Health Foundation NIH R01 DC014261

PS 389

Vibrant Soundbridge: Comparison of Alternative Coupling Methods of the Floating Mass Transducer

Susan Busch; Thomas Lenarz; Hannes Maier
Medical University Hannover

Research background
The active middle ear implant Vibrant Soundbridge provides a variety of coupling modalities of the floating mass transducer (FMT) to various structures of the ossicular chain and the round window. The aim of this study was to (1) determine the efficacy of different FMT coupling modalities for increasing degrees of hearing loss (2) compare the speech performance outcome and the effective gain between the coupling types and (3) evaluate the risk of additional hearing loss for each coupling modality.

Methods
In a retrospective study, 137 cases were analyzed with the FMT coupled to the incus (N = 59; bone conduction (BC) $PTA_{(0.5 - 4\ kHz)}$ = 42.2 dB HL), round window without coupler (RW; N = 22; BC PTA = 32.8 HL), round window with coupler (RWC; N = 23; BC PTA = 37.2 HL) or the oval window with coupler (OWC; N = 33; BC PTA = 37.0 dB HL). Pre- and post-operative thresholds and the word recognition scores (WRS, in % correct) in the Freiburg monosyllable test (at 65 dB SPL) were compared between coupling modalities. A logistic regression function was used to describe the relationship between WRS and the mean BC hearing loss.

Results
The surgical procedure had no effect on the bone conduction thresholds of patients with RWC and OWC. For patients with Incus coupling, BC thresholds improved at 0.5 kHz ($p = 0.01$, Wilcoxon), but worsened significantly at 3, 4 and 6 kHz ($p < 0.009$, Wilcoxon). For RW patients, the BC significantly increased at 0.5 kHz ($p = 0.015$, Wilcoxon).The predicted BC PTA at which WRS decreases below 50% was similar for Incus (48.2 dB HL), RW (47.8 dB HL) and OWC (49.0 dB HL), but higher for the RWC (67.9 dB HL). However, the median WRS was 80% or better with no significant differences in speech perception between coupling types (Kruskal-Wallis $p = 0.229$).The effective gain showed an advantage for incus coupling in the mid-frequencies (1-3 kHz). The other couplings provided more amplification at low frequencies (0.5 kHz). At higher frequencies (4-6 kHz), a similar performance was observed across all coupling types.

Conclusion
The performance of the FMT coupling modalities was equally good for patients with a mild-to-moderate hearing loss but the efficacy of coupling types differed for patients with hearing loss > 50 dB BC HL.

Funding
Cluster of Excellence Hearing4all, Medical University Hannover, Hannover, Germany

PS 390

Output Level of the MET® T2 Transducer under Controlled-Force Coupling Conditions

Hannes Maier; Rolf Salcher; Thomas Lenarz; Martin Grossöhmichen
Hannover Medical School

Background
For the treatment of sensorineural or mixed hearing losses the actuator of the Active Middle Ear Implant (AMEI) MET® (Cochlear™ Ltd.), the electromagnetic transducer MET® T2, is attached to the incus body, the stapes or the round window. During implantation the transducer is advanced toward the point of attachment by an integrated adjustment to maximize transmission to the inner ear and to minimize a possible attenuation of the movement of the ossicular chain. This is usually done intraoperatively by the transducer loading assistant (TLA, Cochlear™ Ltd.). Here we investigated the transducer output level and implantation related “air bone gap” (ABG) of the MET® T2 as a function of displacement and static force preload. Transducer output was characterized via intracochlear differential pressure, where possible, stapes footplate vibration.

Methods
Experiments were performed in human cadaveric temporal bones (TBs) compliant to the modified acceptance criteria (Rosowski et al. 2007) of ASTM F2504-05. The MET® T2 transducer was coupled to the middle ear at controlled static preload forces recorded by a force sensor. For this purpose the transducer was advanced to the incus body in increments smaller than commonly used with the MET® adjustment. At each step the transducer was electrically driven and the vibration of the stapes was measured by Laser Doppler vibrometry. Simultaneously, the sound pressure level at the tympanic membrane was recorded with a probe microphone and the intracochlear sound pressure difference between scala vestibuli and scala tympani were measured with off-the-shelf pressure sensors.

Results
The relationship between the static force preload on coupling efficiency of the vibration transmission to the ossicles and normal sound transmission from the tympanic membrane to the stapes footplate could be determined. An optimal range of static preload force was identified providing high output levels in combination with minimized ABG and low distortions.

Conclusions
When loading the MET® T2 transducer, controlled coupling conditions such as static preload forces are good indicators

for optimal coupling in terms of achieved maximized output level, minimized ABG and low variability in coupling efficiency across patients.

Funding
This project was funded by the Cluster of Excellence Hearing4all and Cochlearâ„¢ Ltd.

PS 391

Development of an Electroacoustic Chinchilla Ear Model for Validation of the Auditory Hazard Assessment Algorithm for the Human (AHAAH)

David Chhan; Paul Fedele; Joel Kalb
Army Research Laboratory

The Auditory Hazard Assessment Algorithm for the Human (AHAAH) has now become an integral part of the new military design standard (MIL-STD-1474E). AHAAH (available at www.arl.army.mil) incorporates a mathematical model of the ear using electroacoustic elements to predict auditory hazard from high-level impulsive noise. While AHAAH is a useful tool in providing estimates of hearing damage and hazard assessment, additional research may provide further validation. AHAAH was theoretically and mathematically developed based on physiological values of the cat ear (cat was the choice for animal auditory research at the time) and adapted to the human ear. Since AHAAH's inception, there is a large body of experimental work on the effects of impulsive noise on chinchilla (Patterson et al., 1985; Hamernik et al., 1987). Therefore to further validate the AHAAH and continue to build a consensus on damage risk criterion (DRC) for calculating risks and assessing hazard, a chinchilla model would be helpful. In this work, we present an integrated electroacoustic model of the chinchilla ear that includes the outer ear, the middle ear, and the cochlea. The model predicts frequency characteristics of the middle ear transfer function (ear canal sound pressure, ***Pec*****,** to stapes velocity, ***Vs***), cochlear input impedance, ***Zc*** and middle-ear pressure gain (ear canal sound pressure, ***Pec*****,** to scala vestibuli sound pressure, ***Pv***) in general agreement with experimental measurements (Ravicz and Rosowski 2012, 2013). More importantly, the model provides a calculation of the basilar membrane displacement, ***Xbm*****,** from free field sound pressure, ***Pff***. This allows us to apply the model in the time domain at high intensities (above 140 dB) with non-linear behavior of the stapes, calculate the risks, and validate against available experimental data.

Funding
Army Research Laboratory, Oak Ridge Associated Universities fellowship

PS 392

In-Line Phase-Contrast Micro-CT Imaging of the Middle Ear: Improving Soft-Tissue Visualization

Hanif Ladak[1]; S. Alireza Rohani[1]; Sumit Agrawal[2]; Ning Zhu[3]
[1]Western University; [2]London Health Sciences Centre; [3]Canadian Light Source

Background
Micro-computed tomography (micro-CT) is commonly used to image the middle ear. Although micro-CT provides excellent visualization of the ossicles, soft tissues are difficult to discern because of poor contrast. Staining agents such as phosphotungstic acid and iodine potassium iodide have been applied to the middle ear to enhance soft-tissue contrast; however, the staining process is time-consuming and may cause tissue shrinkage. In this study, we consider in-line phase-contrast imaging (PCI) combined with micro-CT for visualizing soft tissues without the use of staining agents. Regular micro-CT is based on attenuation of X-rays as they traverse the sample, whereas with in-line PCI, the phase shift caused by the sample is transformed into detectable variations in X-ray intensity.

Objective
To visualize the middle-ear soft tissues using in-line PCI with micro-CT.

Methods
Since micro-CT requires a small sample size, the middle ear was dissected from a fixed human cadaveric temporal bone, keeping the cochlea intact. No exogenous stains were used. The dissected specimen was imaged using in-line PCI with micro-CT at the BioMedical Imaging & Therapy facility at the Canadian Light Source (CLS). The third generation synchrotron radiation source at CLS was used because it provides high brilliance, monochromaticity, high collimation, tunability, pulsed occurrence and superb spatial resolution. For this specific scan, the detector used has an isotropic pixel size of 8.9 μm. The acquired 3D image volume was visualized using 3D Slicer (www.slicer.org).

Results
All soft tissues (e.g., tympanic membrane, all ligaments, both muscles, facial nerve and chorda tympani) were visible in the 3D image. As an example, Figure 1 shows 2D image slices extracted at a variety of angles to show some of these structures.

Conclusions
Using in-line PCI with micro-CT, it is possible to simultaneously visualize both the bony and soft-tissue structures of the middle ear without using exogenous staining agents.

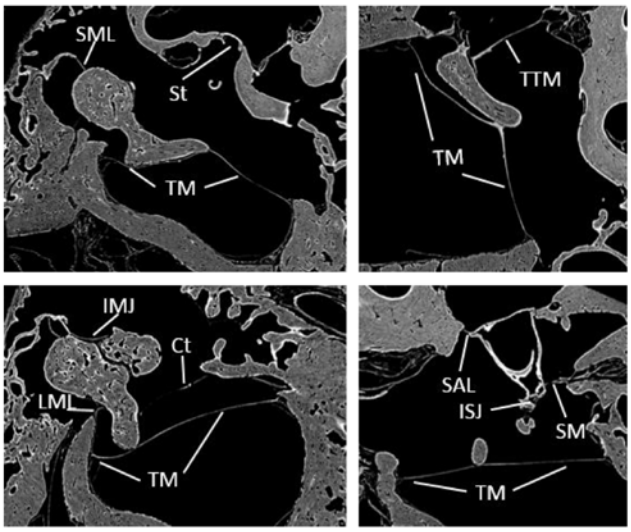

Figure 1: Sample 2D image slices showing tympanic membrane (TM), stapes (St), chorda tympani (Ct), incudomallear joint (IMJ), incudostapedial joint (ISJ), superior mallear ligament (SML), lateral mallear ligament (LML), tensor tympani muscle (TTM), stapes annular ligament (SAL) and stapedius muscle (SM).

Funding
Research was performed at the Canadian Light Source, which is supported by the Canada Foundation for Innovation, Natural Sciences and Engineering Research Council of Canada, the University of Saskatchewan, the Government of Saskatchewan, Western Economic Diversification Canada, the National Research Council Canada, and the Canadian Institutes of Health Research.

PS 393

Arrangement of Collagen Fibers in the Tympanic Membrane of Guinea Pigs

Lin Yang[1]; Jieying Li[1]; Youzhou Xie[1]; Caiqin Wu[2]; Keqiang Wang[1]; Tianyu Zhang[1]
[1]Fudan University; [2]Shanghai University of Traditional Chinese Medicine

Background
The guinea pig is the main hearing experimental animal thanks to the considerable size of tympanic bulla and easy access to the tympanic cavity for mechanical motions of the ossicles. The acousto-mechanical transformer behavior of the TM in Guinea Pig (GPTM) is mainly determined by its structure properties. The main components responsible for the mechanical behavior of the GPTM are collagens. The microstructures of the GPTM have not been fully described. The collagen fibers of TM are key to high-frequency sound conduction. The radial collagen fibers in the human TM play an important role in the conduction of sound above 4 kHz (O'Connor, 2008). Different collagen types have specific properties regarding resistance to forces. The data presented in publishes of hearing medicine complement those descriptions only to a small extent. In order to better understand high-frequency characteristic of GP, we examined the arrangement of collagen fibers of the GPTM using polarizing light microscope (PLM) and scanning electron microscopy (SEM). In this study, we firstly analyzed the collagen types by PLM.

Methods
The TMs were collected from 10 adult GP, with average weight of 300g. The TMs were taken from the bullae under the dissecting microscope. The special Sirius-Red staining was applied to the TMs for PLM examination.

Results
From the ear canal view, the radial collagen bundles at the lateral side of the GPTM were strong and yellow on PLM, which belongs to type I collagens. These radial collagen bundles were thick (Ø40nm-100nm) and dense. The fibers originated from the umbo and spread uniformly toward the tympanic annulus. From the tympanic cavity view, circular fibers at the medial side of the GPTMs were loose and thin (Ø<1 nm), nevertheless, they crossed over and went underneath the radial fibers, running parallel to the annulus. The circular fibers in the medial side of the TM were poorly developed so as to thread the radial fiber bundles, forming a fabric-like arrangement near the tympanic annulus and the manubrium border.

Conclusions
The radial fibers and fabric-like structures of the tympanic membrane could be an important factor in maintenance of the tensile force and therefore in high-frequency sound conduction related to the GPTM.

Funding
National Natural Science Foundation of China (NSFC, No.81570934). Shanghai Committee of Science and Technology, China (No. 13DZ1940902 and 13DZ1940903)

PS 394

A Method to estimate the Effect of Mastoid Cavity Obliteration on the Displacement Output of Electromagnetical Transducers in vitro

Martin Grossöhmichen; Burkard Schwab; Rolf Salcher; Thomas Lenarz; Hannes Maier
Hannover Medical School

Background
Electromagnetical transducers of Active Middle Ear Implants or Direct Acoustic Cochlear Implants are usually intended for implantation in the air-filled middle ear cavity. In patients who underwent a subtotal petrosectomy, the transducers are surrounded by obliterated fat tissue of unknown elastic properties potentially affecting the mechanical transducer output. Here the elastic properties of this tissue were characterized and its impact on the displacement output of common transducers was investigated experimentally in vitro using a new developed method.

Methods
The Young's moduli of human fatty tissue samples (3 mm diameter) taken fresh from the abdomen and from the radical mastoid cavity during revision surgeries were determined

by indentation tests. Two phantom materials were identified as having Young's moduli suitable for realistic and worst case simulation of obliterated tissue. Three commonly used electromagnetical transducers (Codacs™, MET® (both Cochlear Ltd); FMT (Med-EL)) were embedded in the phantom materials in a model radical cavity. When they were electrically driven at 0.1 – 10 kHz, their displacement output was measured with Laser Doppler Velocimetry and compared to the output of the non-embedded devices.

Results
The Young's moduli of fresh human abdominal fatty tissue determined here were comparable to moduli of human breast fat tissue from literature. In both phantom materials the displacement output amplitudes of the Codacs™ and MET® at 0.1 – 10 kHz were slightly reduced by ≤ 5 dB. The output amplitude of the FMT was also minorly affected (max 4 dB reduction) at 0.5 – 10 kHz, but significantly reduced by up to 35.0 dB at lower frequencies. The resonance frequencies of all transducers were shifted by 50 Hz or less.

Conclusions
The effect of obliteration on the displacement output of electromagnetical transducers can be estimated *in vitro* using the method developed here. Based on our results, the decrease in displacement output amplitude of the transducers Codacs™ and MET® in obliterated mastoid cavities is expected to be minor having no major effect on clinical indication. For the decision to implant an FMT into a radical mastoid cavity obliterated with fat, the attenuation of its displacement output amplitude at <0.5 kHz has to be taken into account.

Funding
This project was funded by Cochlear Ltd. and the DFG Cluster of Excellence EXC 1077/1 "Hearing4all".

PS 395

A Finite Element Study of the effects of the ossicular ligaments on middle ear transfer function

Nikolaos Tachos[1]; Antonis Sakellarios[1]; George Rigas[1]; Ioannis Spyridon[1]; Frank Böhnke[2]; Dimitrios Fotiadis[1]; **Thanos Bibas**[3]
[1]University of Ioannina; [2]Technische Universität München; [3]University of Athens, Greece; UCL Ear Institute

Background
There are only a limited number of studies on the role of the ossicular ligaments on the physiology of the middle ear. The aim of this study is to investigate the effect of mallear and incudal ligaments to the tympanic membrane and the stapes footplate transfer functions in a finite element model of the middle ear.

Method
A finite element model of the middle ear was developed in ANSYS using a realistic geometry of the middle ear which is reconstructed utilizing micro-CT images. The acoustic pressure from the ear canal, was modeled with a 90 dB SPL uniform pressure load on the surface of the tympanic membrane. The cochlea load and its effect to the dynamic response of the middle ear is simulated using a Kelvin-Voigt component, which is represented as a dashpot and spring element connected in parallel. Three cases were simulated: (A) without the ligaments, (B) including the posterior incudal and the anterior mallear ligaments and (C) including in addition the superior mallear and incudal ligaments.

Results
For case A, the maximum stapes footplate displacement was 0.033 μm, at a frequency 820 Hz. For case B, a maximum displacement 0.030 μm occurred at a frequency of 830 Hz. Finally, for case C, a maximum displacement 0.023 μm occurred at the frequency 1024 Hz. the phase angle change of the stapes footplate displacement for the three cases and the comparison with experimental and computational results. Regarding stapes footplate phase angle data, case C has the best fit with the experimental findings, while cases A and B present a positive phase angle around 400 Hz frequency, probably caused by the weak "holding" of the middle ear. Similarly, regarding umbo frequency response and phase angle data, the best fit is observed in case C.

Conclusion
Inclusion of the superior ligaments are most necessary for an accurate representation of the middle ear frequency response and excellent agreement is observed between our results and human temporal bone experimental data and other finite element studies. This suggests that the most important role of these ligaments is to stabilize the middle ear rotation axis.

Funding
Funded by the European Union FP7-ICT grant No 600933

PS 396

Analytical and finite-element modelling of the incudostapedial joint

Majid Soleimani[1]; W. Robert J. Funnell[1]; Willem F. Decraemer[2]
[1]McGill University; [2]University of Antwerp

The joints of the ossicular chain significantly affect sound transmission through the middle ear, but the mechanical behaviour of these joints is not well understood. We previously analyzed the incudostapedial joint using a finite-element (FE) model with a simplified geometrical description of the pedicle of the lenticular process, based on histological serial sections and X-ray micro-CT, and using *a priori* estimates for material-property parameters, but we neglected the presence of synovial fluid (SF) in the joint. We later included SF in a FE model and made preliminary comparisons with experimental tension and compression measurements.

In the present work, we use the theory of large deformations of elastic membranes to analytically model the incudostapedial joint. By assuming a uniform circular cross section for the joint, we find an exact solution for the joint-capsule deformations when the joint is subjected to tensile or compressive loads. Assuming that the capsule strain-energy function has the Mooney form, and that SF is incompressible, several force-

displacement curves are calculated for various material properties and geometrical configurations. The results can be used to validate FE solutions when the bending stress is negligible compared with tensile stress in the joint capsule.

In addition, our existing FE model is modified to have a more realistic geometry, and the analytical and FE results are compared with experimental data. The results provide insight into the mechanical behaviour of the incudostapedial joint and are useful for studying the middle ear under static and dynamic pressures. For example, this investigation helps to understand the asymmetry that is observed experimentally and in our FE simulations of joint tensile and compression tests.

Funding
Canadian Institutes of Health Research, the Natural Sciences and Engineering Research Council of Canada, and Fund for Scientific Research (Flanders, Belgium)

PS 397

Characterization of Ear-Canal Feedback Pressure due to Umbo-Drive Forces: Finite-Element vs. Circuit Models

Morteza Khaleghi; Kevin O'Connor; Sunil Puria
Earlens Corporation

Background
Hearing-aid users often complain of poor sound quality and difficulty understanding speech in noisy situations. One of the main reasons for this is that the microphone in a hearing aid is typically located above the pinna, rather than inside the ear canal, in order to minimize feedback. This, in turn, reduces the subject's ability to perceive the acoustic pinna cues above about 4 kHz that are needed for sound localization. Various strategies for minimizing the feedback pressure (thereby increasing the Maximum Stable Gain, MSG) of a wide-bandwidth non-surgical Tympanic Lens are investigated numerically to facilitate placement of a microphone in the ear canal.

Methods
The ear-canal feedback pressure due to mechanical stimulation of the tympanic membrane (TM) was calculated using a 1D circuit model representing the TM as a distributed-parameter transmission line and the ossicular chain and cochlea as a network of lumped elements (O'Connor and Puria, 2008), and using a 3D finite-element model (FEM) representing the human middle ear (Puria et al., 2014). In both cases, the ear canal was terminated with an impedance boundary condition of rho*c for air. Circuit-model and FEM responses to umbo-force stimulation are compared with experimental data from four human cadaveric temporal bones (Puria et al., 2015).

Results
The MSG calculated from the two models and TB measurements decreases from about 40 dB at 0.1 kHz to about 15 dB at 1 kHz. Between 1.5 and 4 kHz the MSG is about 10 dB. As the frequency increases above 4 kHz, the MSG of the FEM, in agreement with experimental data, increases to 40 dB at 8 kHz. However, the MSG of the circuit model only reaches a maximum of 10 dB at 6 kHz. Furthermore, the direction of the force vector at the umbo can be optimized to increase the MSG by up to 10 dB in the 1–4 kHz range.

Conclusions
While the feedback pressure in devices that mechanically stimulate the umbo is significantly lower than in acoustic hearing aids, it is still not zero, and this limits the placement of a microphone in the ear canal for patients with significant hearing loss. Attempts at reducing the feedback pressure by altering the umbo-force vector have been studied using two computational models. While both of the models predicted the feedback pressure precisely below about 4 kHz, only the FEM results come close to the measurements at higher frequencies.

PS 398

Fractional-Order Modeling of the Human Ear

Maryam Naghibolhosseini[1]; Glenis Long[2]
[1]Michigan State University; [2]Graduate Center of the City University of New York

Middle ear function depends on how different parts of the middle ear work together during sound transmission. One way to model middle ear structures is to employ lumped element modeling, which has the benefit of quantitatively specifying the function of different parts of the middle ear. To increase the accuracy of a lumped element model, more elements could be incorporated into the model, which increases the number of unknown parameters requiring excessive data and parameter fitting in higher dimensional space. Hence, adding more elements may not be an efficient strategy for improving lumped element models. An alternative approach is to incorporate more realistic lumped elements (i.e., fractional-order elements), which are better adapted to the physical nature of the biological materials. In the proposed research, a physical/mathematical model of the human ear was developed, which employed fractional-order lumped elements to include the viscoelastic characteristics of biological tissues in the human ear. Impedance estimates from wideband reflectance measurements from seven normal hearing adults were used for parameter fitting of the proposed model. The performance of the model was evaluated using outer-middle ear transmission estimates from distortion product otoacoustic emissions (DPOAEs). The outer-middle ear transmission of the model was defined as the sum of forward and reverse outer-middle ear transmissions. To estimate the reverse transmission of the model, the probe-microphone impedance was calculated by solving its Thevenin-equivalent circuit using acoustic measurements obtained in a number of test cavities with known impedances. The model was successfully fit to the magnitude and phase impedance estimates from power reflectance measurements from seven individuals; the performance of the model was also satisfactory for each individual. The normalized RMS errors of impedance magnitudes and phases were smaller than 20% and 27%, respectively. The RMS errors between

outer-middle ear transmission estimates from the model and using DPOAE did not exceed 16% for any of the individuals. The outer-middle ear transmission estimates from the model range from −48 to −17 dB between 0.2 − 6 kHz and have one or two minima attenuations between 0.8 − 1.4 and/or 3.2 − 5.1 kHz in all individuals. Incorporating fractional-order elements into the traditional lumped element models yields new possibilities for fine tuning models of complex biological systems to fully capture the viscoelastic response of the biomaterials in human ear. Such modeling enhances our understanding of the roles of different parts of the ear and how they work together to determine their function

PS 399

Fluid-structure finite-element modelling of the wideband acoustic input admittance of the newborn ear canal and middle ear

Hamid Motallebzadeh; Jacob Pitaro; W. Robert J. Funnell; Sam Daniel
McGill University

The anatomical differences between the newborn ear and the adult one result in different input-admittance responses in newborns than in adults. Taking fluid-structure interactions into account, we have developed a finite-element model to investigate the wideband admittance responses of the ear canal and middle ear in newborns for frequencies up to 10 kHz. Four sets of sensitivity analyses were performed, to investigate the contributions of the ear canal and middle ear to the overall admittance responses as well as the effects of the material parameters, measurement location and geometrical variability. The model was validated by comparison with two sets of clinical data. Because of the interactions between the incident and reflected acoustic waves, at 2 kHz the pressure at the entrance of the canal and the pressure at the tympanic membrane already differ by more than 30%; the assumption of a uniform pressure distribution along the canal at low frequencies is found to be rather inaccurate above about 1 kHz. The model provides a quantitative understanding of the canal and middle-ear resonances around 500 and 1800 kHz, respectively. The results show that at frequencies around the middle-ear resonance the admittance of the newborn ear is mainly dominated by that of the middle ear. In addition, the model predicts the effects of the first resonance mode of the middle-ear cavity (around 6 kHz) as well as the first and second standing-wave modes in the ear canal (around 7.2 and 9.6 kHz, respectively).

Funding
Canadian Institutes of Health Research; Natural Sciences and Engineering Research Council of Canada.

PS 400

Testing the effects of tympanic-membrane material properties on human middle-ear sound transmission using a 3D finite-element model

Kevin O'Connor; Hongxue Cai; Peter Gottlieb; Charles Steele; Sunil Puria
Stanford University

Background

The human tympanic membrane (TM) is an approximately cone-shaped composite material containing radially and circumferentially oriented collagen-fiber layers sandwiched between layers of softer material. As such, one could argue that the TM should be treated as an orthotropic material with different Young's modulus (E_{TM}) and/or shear modulus (G_{TM}) values defined for the radial (R), circumferential (Φ), and surface-normal (θ) directions. Still, considerable room for interpretation remains when choosing E_{TM} and G_{TM} for a given TM, and the practical consequences of an orthotropic rather than isotropic TM remain unclear.

Methods

This study uses a micro-CT-based 3D finite-element model of a human middle ear to test the effects of variations to the material properties of the TM and annulus on the middle-ear gain (MEG), which is the cochlear-vestibule pressure divided by the ear-canal pressure: MEG=Pcoch/Pec. The orthotropic directions of a given point on the TM in the model were approximated using a spherical coordinate system centered at the umbo.

Based on estimates of collagen-fiber-layer thicknesses and Young's modulus values from Fay et al. (2005), E_{TM} for the three spherical directions (R,θ,Φ) ranged from (51,20,26) to (503,20,318) MPa, with a baseline value of (140,20,75) MPa. The R and Φ values are only affected by the fibers oriented in the corresponding direction, with the rest of the thickness fraction treated as 3 MPa "ground substance". The 20 MPa θ value was selected to achieve smooth animations of the TM surface for the baseline case. G_{TM} was defined based on an isotropic ground substance only: G_{TM}=3 MPa/(2*(1+v)), where v is the Poisson's ratio (0.4).

In addition to testing the range of orthotropic E_{TM} values, E_{TM} for R and Φ were also in turn assigned low values (3 MPa). The TM was next treated as purely isotropic with E_{TM} varying from 0.1 to 1000 MPa and as "quasi-isotropic" with a fixed ground-substance-based G_{TM} value. Additional variations to G_{TM}, the density and loss factor of the TM and annulus, and the Young's modulus of the annulus were also tested.

Results

When the isotropic TM annulus is set to 3 MPa, varying E_{TM} from (51,20,26) to (503,20,318) MPa generally kept MEG within 5–10 dB of the baseline, while a purely isotropic TM most resembles the baseline between 20 and 51 MPa, with further increases causing low-frequency attenuation and an unrealistic boost at higher frequencies.

Orthogonal Directions (R,θ,Φ) of a Point on the TM Surface, Based on a Spherical Coordinate System Centered at the Umbo

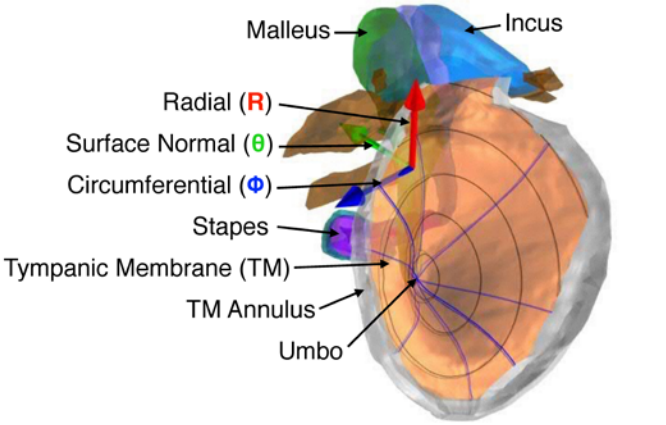

Funding
[Work supported by R01 DC05960 from the NIDCD of the NIH.]

PS 401

3-dimensional geometric shape analysis: a new tool for investigating mechanisms of conductive hearing loss

Donald Swiderski[1]; David Barton[1]; Michelle Caird[1]; Joan Marini[2]; Kenneth Kozloff[1]; Yehoash Raphael[1]
[1]University of Michigan; [2]NIH

Introduction

Middle ear ossicles transmit sound to the inner ear; their loss or fusion causes a substantial loss of hearing ability. Large qualitative shape differences have been reported between species with vastly different hearing abilities. Small scale shape variations among non-pathological individuals within species have not been rigorously and quantitatively described; consequently, the effects of these variations on hearing remain unknown. Several studies have quantified specific mensural features such as mass or lever arm lengths to construct models of sound energy transfer, but geometric analyses of shape variation have not been performed. As a step toward addressing this lack, we have performed 3D shape analyses of the Brtl mouse, a model of osteogenesis imperfecta, a congenital bone disorder frequently associated with conductive hearing loss. These mice have an elevated frequency of hearing loss compared to their wild-type litter mates, but not all Brtl mice with hearing loss have gross anatomical anomalies like stapedial fusion.

Methods

We constructed surface models of stapes from high resolution CT scans, obtained coordinates for a series of discrete anatomical loci (landmarks) and captured the curvature of the crural arches using points that correspond in their relative positions along the crura (semilandmarks). Using the geomorph package in R, we performed principal components analysis to describe the major axes of shape variation and performed statistical tests of specific hypotheses posed to explain that variation.

Results

We found variation in the height of the stapes relative to its width and depth, robustness of crura and curvature of the ventral crus. We did not find significant differences between Brtl mice and wild-types or a correlation with ABR thresholds. There also was no difference between males and females, but there was a difference between right and left sides.

Conclusions

These results demonstrate the value of combining high resolution imaging with quantitative shape analysis to investigate morphological variation that was previously inaccessible to study. We described variation in stapes shape that would be expected to have mechanical implications, but hearing loss in Brtl mice cannot be attributed to a specific pattern of variation, leaving open the possibility that ossicular chain defects may not account for all hearing loss in these mice. Further studies are needed to address the relationship of ossicular shape variations to hearing ability, using more sensitive tools than ABR thresholds, and to determine whether there is correlated variation in the shapes of other ossicles.

PS 402

High-speed holographic methods to study tympanic membrane motions in-vivo

Payam Razavi[1]; Jeffery Cheng[2]; Nima Maftoon[2]; Michael Ravicz[2]; Ivo Dobrev[1,3]; Cosme Furlong[1]; John Rosowski[2]
[1]Worcester Polytechnic Institute; [2]Harvard Medical School; [3]Universitätsspital Zürich

Background

Our research is focused on the study of the Tympanic Membrane (TM) and its role in transforming sound energy in the ear canal into mechanical vibration of the ossicles. Our work has concentrated on studying the mechanics of post-mortem TM's of different mammalian species subjected to continuous single-tones, transient acoustic and mechanical stimuli by various holographic methods. There is interest in studying the TM in-vivo in order to advance our knowledge of TM mechanics. However, in the live subject the confined anatomical location of the TM together with its nanometer-scale displacements affected by micrometer scale motion artifact (caused by head motion, heartbeat, breathing, etc.) make in-vivo measurements challenging. We are developing novel High-speed Digital Holographic Methods (HDHM) to overcome such challenges by increasing the temporal resolution of holographic acquisition in combination with recently developed image and data processing algorithms.

Methods

Our developments, unlike other similar approaches, utilize the full capabilities of a high-speed camera without sacrificing spatial and temporal resolutions (>147,000 points at 42,000 fps) to measure nanometer-scale high-frequency TM motions (0.2-20 kHz) without interference from low frequency (1-100 Hz) body motions. A novel Local-phase Correlation (LC) algorithm was implemented to accurately quantify the complex motion of the TM during the extent of a transient acoustical excitation. In addition, the experimental setup was

redesigned to include a standard otoscope head with high-speed holographic measuring capabilities.

Results
We present preliminary measurements on an anesthetized chinchilla with outer ear canal partially removed for better view in a controlled anechoic chamber in both in-vivo and in-vitro conditions. Transient displacements in response to an acoustic click (50 μs square wave excitation) and random white noise (1μs resolution - 140 ms long) were measured**.** Each of the measurements was repeated thrice consecutively (with ~100 ms interval) in order to study the repeatability of the motion with steady environmental conditions. These measurements are suitable for estimating the spatial distribution of mechanical properties across the TM, including Q factors, Eigen-frequencies, mode shapes, and response time.

Conclusions
We successfully measured, to the best of our knowledge for the first time, acoustically induced full-field motions of chinchilla TM in-vivo. These measurement results will be compared with postmortem TM motions to improve our knowledge of the structure and function of the TM. These techniques establish the potential of HDHM as a clinical tool to quantify TM motions in live human ears.

Funding
We thank the NIH/NIDCD (R01-DC008642), Massachusetts Eye and Ear Infirmary, Worcester Polytechnic Institute, and the Mittal Fund.

PS 403

An experimental study of vibrations in the gerbil middle ear under static pressure

Orhun Kose; Richard Shapiro; W. Robert J. Funnell; Sam Daniel
McGill University

Knowing the vibration response of the eardrum is essential to understanding the mechanics of the middle-ear, and knowing its response to static pressures is essential to understanding tympanometry. The Mongolian gerbil has become widely used in middle-ear research, because it is low in cost and its middle-ear structures are relatively accessible. This study presents the effects of static pressurization on the vibration response of the gerbil eardrum. A single-point laser Doppler vibrometer was used to acquire frequency responses in *post mortem* gerbil ears using multiple pressurization protocols. Magnitudes of vibration were normalized with respect to sound pressure level measured near the eardrum and are presented over the range of 0.2 to 10 or 11 kHz. In each gerbil, measurements on the manubrium and on the pars tensa are presented. For the unpressurized measurements the inter-specimen variability was small and measurements were more or less repeatable from cycle to cycle. Pressurized responses exhibited magnitude reductions at lower frequencies, then rose to a peak and exhibited sharp features at higher frequencies. As pressure increased, magnitudes decreased and the peak was shifted to higher frequencies. The eardrum break-up frequency was shifted beyond the frequency range of our measurements. The pars tensa exhibited significant magnitude changes from cycle to cycle. Our results are compared with previous data in the literature. Understanding the vibration response of the eardrum in the presence of pressurization, as well as the roles of viscoelastic and temporal effects, will lead to a better understanding of clinical tympanometry, which is particularly important in infants where the response to tympanometry is not well understood

Funding
Canadian Institutes of Health Research, the Fonds de recherche en santÃ© du QuÃ©bec, the Natural Sciences and Engineering Research Council of Canada, the MontrÃ©al Childrenâ€™s Hospital Research Institute, the McGill University Health Centre Research Institute

PS 404

Expression of Apoptotic versus Anti-apoptotic proteins in Middle Ear Cholesteatoma

Jae Ho Chung; Seung Hwan Lee; Chul Won Park; Han Seok Yoo
Hanyang University

Background and Objectives
To explore the role of anti-apoptotic and apoptotic processes in the development of cholesteatoma by investigating the expression of an anti-apoptotic (c-FLIP) and apoptotic (p53) protein relative to the expression of a proliferation marker (Ki-67).

Subjects and Methods
An immunohistochemical investigation was performed on 35 cholesteatoma specimens (21 acquired, 14 congenital) and 10 normal retroauricular skins to evaluate the expression of c-FLIP, p53 and Ki-67. The expression rate of each marker was measured to assess the difference between retroauricular skin and cholesteatoma, as well as between congenital and acquired cholesteatoma.

Results
c-FLIP expression was significantly higher in the cholesteatoma specimens than in retroauricular skin ($p<0.05$), while the expression of p53 did not significantly differ between the two. Ki-67 expression in cholesteatoma was significantly higher than in retroauricular skin ($p<0.001$). The c-FLIP expression rate was positively correlated with that of Ki-67 ($r=0.47$ $p=0.001$), and there was no significant correlation between the expression level of p53 and that of Ki-67 ($r= 0.152$, $p=0.319$). In addition, no differences in c-FLIP, p53 and Ki-67 expression rates were evident between congenital and acquired cholesteatoma.

Conclusions
The up-regulation of c-FLIP together with unchanged p53 suggests an altered equilibrium between apoptosis and anti-apoptosis, favoring anti-apoptosis, may play a role in the pathogenesis of cholesteatoma.

Figure 1. Immunohistochemical analysis of c-FLIP (A), p53 (B) and Ki-69 (C) expression and localization in retroauricular skin (1), acquired cholesteatoma (2) and congenital cholesteatoma (3). (*: extracellular matrix, **: stratum corneum, Magnification x400)

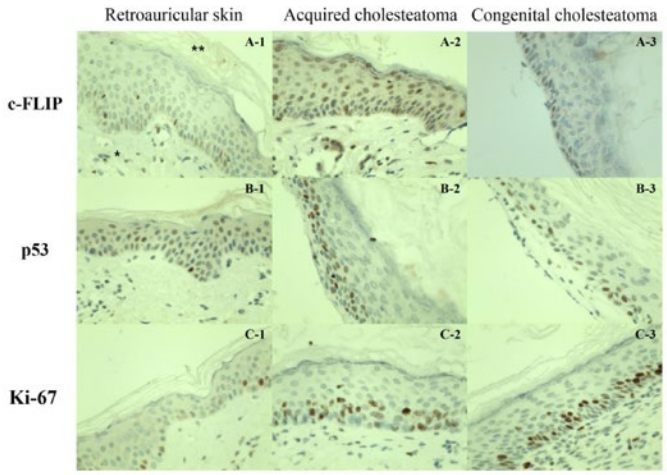

Figure 2. The correlations between the expression rate of Ki-67 and those of c-FLIP and p53 in the suprabasal layer of cholesteatoma epithelium (35 cases). A: Ki-67 versus c-FLIP , B:Ki-67 versus p53.

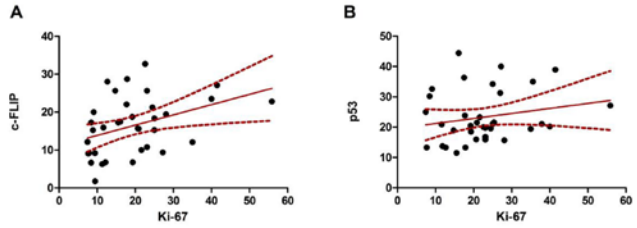

Table 1. . Demographic and clinical characteristics of the subjects

	Cholesteatoma		
	Acquired	**Congenital**	**Total**
Number	21	14	35
Age (mean ± SD)	47.2 ± 17.6	6.0 ± 5.9	30.7 ± 24.7
Sex (Male : Female)	14 : 7	10 :4	24 : 11
Disease extent (CT)			
Middle ear	1	6	7
Middle ear + attic	14	5	19
Middle ear + attic + mastoid	6	3	9
Pre-operative status			
History of otorrhea	15 (71.4%)	-	15 (42.9%)
Presence of granulation tissue	6 (28.6%)	0 (0 %)	6 (17.1%)
Prior use of antibiotics	15 (71.4%)	-	15 (42.9%)
Prior use of steroid	None	None	None

Table 2. Comparison of the expression rates of c-FLIP, p53 and Ki-67 in retroauricular skin (n=10) and cholesteatoma (n=35)

	Expression rate (mean ± SD , %)	**Basal layer**	**Suprabasal layer**	**Total**
C-FLIP	Retroauricular skin	32.5 ± 9.0	8.0 ± 3.6	15.1 ± 4.5 (6.8~28.9)
	Cholesteatoma	33.2 ± 11.9	18.8 ± 6.6	23.5 ± 6.4 (9.4~32.3)
	p value *	0.946	< 0.001	**< 0.05**
p53	Retroauricular skin	15.9 ± 3.0	11.1 ± 2.4	12.9 ± 1.3 (11.3~15.9)
	Cholesteatoma	16.2 ± 4.4	12.4 ± 3.3	13.4 ± 2.1 (8.2~18.4)
	p value *	0.946	0.228	0.396
Ki-67	Retroauricular skin	20.5 ± 8.5	8.2 ± 2.9	12.1 ± 3.2 (7.3~18.2)
	Cholesteatoma	20.3 ± 13.0	22.6 ± 10.6	21.5 ± 8.3 (11.5~53.2)
	p value *	0.799	< 0.001	**< 0.001**

* Mann-Whitney test

Table 3. Comparison of the expression rate of c-FLIP, p53 and Ki-67 in acquired cholesteatoma and matched retroauricular skins (n=10)

	Expression rate (mean ± SD , %)	**Basal layer**	**Suprabasal layer**	**Total**
C-FLIP	Retroauricular skin†	32.5 ± 9.0	8.0 ± 3.6	15.1 ± 4.5 (6.8~28.9)
	Cholesteatoma	34.7 ± 11.3	20.3 ±7.5	23.0 ± 6.3 (10.2~32.3)
	p value *	0.235	**0.007**	**0.013**
p53	Retroauricular skin	15.9 ± 3.0	11.1 ± 2.4	12.9 ± 1.3 (11.3~15.9)
	Cholesteatoma	17.3 ±4.3	11.6 ± 2.1	13.1 ± 2.1(8.2~16.3)
	p value *	0.508	0.314	0.799
Ki-67	Retroauricular skin	20.5 ± 8.5	8.2 ± 2.9	12.1 ± 3.2 (7.3~18.2)
	Cholesteatoma	23.5 ±14.4	25.2 ±13.5	24.2 ± 12.1(13.5~53.2)
	p value *	0.508	**0.005**	**0.005**

†The matched control of retroauricualr skin in acquired cholesteatoma
* Wilcoxon signed rank test

Table 4. Comparison of the expression rates of c-FLIP, p53 and Ki-6 in acquired (n=21) and congenital cholesteatomas (n=14).

	Expression rate (mean ± SD , %)	**Basal layer**	**Suprabasal layer**	**Total**
C-FLIP	Acquired	31.3 ± 11.8	18.9 ± 6.2	20.2 ± 5.4 (12.0~32.2)
	Congenital	36.2 ± 11.9	18.5 ± 7.3	23.3 ± 6.4 (9.36~32.3)
	p value *	0.296	0.775	0.654
p53	Acquired	16.1 ± 4.7	12.2 ± 3.3	13.0 ± 2.0 (8.2-16.5)
	Congenital	16.1 ± 4.1	12.7 ± 3.4	13.1 ± 2.1 (9.3-18.4)
	p value *	0.325	0.175	0.145
Ki-67	Acquired	19.7 ± 15.1	26.2 ± 11.3‡	23.5 ± 10.1 (16.7-53.2)
	Congenital	20.9 ± 10.9	18.7 ± 8.6	19.3 ± 5.8 (11.5- 43.2)
	p value *	0.568	0.049	0.351

* Mann-Whitney test

PS 405

Role of BPIFA1 in Otitis media

Apoorva Mulay[1]; Michael Cheeseman[2]; Steve Brown[3]; Lynne Bingle[1]; Colin Bingle[1]
[1]University of Sheffield; [2]University of Edinburgh; [3]Medical Research Council

Background

Secretory innate immunity molecules play an important role in middle ear (ME) protection and epithelial abnormalities are commonly implicated in the pathogenesis of middle ear inflammation or *Otitis media* (*OM*). SNPs in *BPIFA1,* a member of BPI fold containing family of putative innate defence proteins, have been associated OM. We have

previously shown that Bpifa1 is expressed in the middle ear (ME) of *Wt* mice and its expression decreases with *OM* development in the *Junbo (Jbo$^{+/-}$)* model of chronic *OM*.

Objective
We aim to characterize a role for *BPIFA1* in the ME and study the effect of infection by the human otopathogen, Non-Typeable *Haemophilus influenza (NTHi) in vivo,* using mouse models and *in vitro,* using a novel system for culture of primary middle ear epithelial cells.

Methodology
ABR and histological analysis were used to determine spontaneous development of *OM*. Intranasal *NTHi* challenge experiments were used to study ascending infection from the nasopharynx into the ME of mice. We used RT PCR, Immunofluorescence confocal microscopy, Western Blotting and Mass spectometry to determine the differential expression of various epithelial markers in an *in vitro* model for culture of primary ME epithelial cells at an Air Liquid Interface (ALI). We infected *Wt* and *Bpifa1$^{-/-}$*cultures with *NTHi*. qPCR was used to study expression of inflammatory markers in isolated ME cells from compound *Bpifa1$^{-/-}$Jbo$^{+/-}$* mutants in comparison to *Jbo$^{+/-}$* mice.

Results
Bpifa1$^{-/-}$ mice do not develop OM spontaneously and intranasal *NTHi* challenge of *Bpifa1$^{-/-}$* mice does not result in increased ascending bacterial infection. However, in the *Bpifa1$^{-/-}$Jbo$^{+/-}$* compound mutants, *OM* severity and ME mucosal thickness is significantly higher than in *Jbo$^{+/-}$* mice. Our *in vitro* model demonstrates that ME epithelial cells differentiate within 14 days at ALI. Transcriptional and proteomic analysis suggests that they express markers of specific epithelial cell types, such as ciliated cells, goblet cells and secretory cells. We show that *Bpifa1* loss increases susceptibility to *NTHi* infection in culture.

Conclusions
Current data indicates that BPIFA1 plays an immunomodulatory role in the ME and alteration in its levels is associated with *OM* development and an exaggerated phenotype in existing models of OM. Furthermore our novel *in vitro* culture system can be widely applied as an effective model to study interaction between the ME epithelium and otopathogens.

Funding
This work was jointly funded by: University of Sheffield (United Kingdom) and Mammalian Genetics Unit, Medical Research Council, Harwell (United Kingdom)

PS 406

HB-EGF Plays a Pivotal Role in Mucosal Hyperplasia in Poly(I:C)-Induced Otitis Media

Takashi Sakamoto; Kwang Pak; Arwa Kurabi; Allen Ryan
University of California, San Diego

Background
Otitis media (OM) is one of the most common childhood infections and can be caused by bacterial and/or viral infection. Hyperplasia of the middle ear (ME) mucosa is an important component of OM that can contribute to the deleterious sequelae of OM. Our previous research revealed that hyperplasia of ME mucosa in bacterially induced OM was mediated by heparin-binding epidermal growth factor (HB-EGF). In contrast, mechanisms of hyperplasia in virally induced OM remains to be elucidated. The current study was designed to test the hypothesis that hyperplasia in viral OM is also mediated by HB-EGF.

Methods
We examined the ME response to polyinosinic-polycytidylic acid [Poly(I:C)], a synthetic analog of viral double-stranded RNA in rats. [Poly(I:C)] was introduced into the ME, with and without the specific HB-EGF inhibitor, CRM197. Control MEs were untreated. Thickness of the ME mucosa was evaluated over time and dose. Immunostaining was used to assess the expression of HB-EGF.

Results
Poly(I:C) induced prominent ME mucosal hyperplasia two days after ME inoculation in a dose-dependent manner. Immunostaining using anti-HB-EGF antibody revealed that HB-EGF was highly expressed in response to Poly(I:C). HB-EGF inhibition strongly reduced the hyperplastic response of the mucosa.

Conclusions
The results suggest that viral double-stranded RNA can induce a strong proliferative response of the ME mucosa. They also indicate that HB-EGF is the dominant growth factor responsible for this mucosal hyperplasia.

Funding
Supported by grants from the NIH/NIDCD (DC012595; DC000129; DC006279) and the Research Services of the Veteran Administration (BX001205).

PS 407

The candidate tumor suppressor ECRG4 mediates the innate immune inflammatory response to acute Otitis Media

Arwa Kurabi[1]; Kwang Pak[2]; Allen Ryan[2]
[1]University of California, San Diego; [2]UCSD

Introduction
Otitis media (OM) is a common pediatric disease where innate immune responses are generally implicated in the disease pathogenesis. We have previously shown that esophageal cancer related gene 4 (ECRG4) is normally expressed in the middle ear (ME) of wild-type (WT) mice and that its expression decreases with OM development. Furthermore, its constitutive expression appears to play a role in regulating mucosal hyperplasia. Herein, we evaluated OM in mice deficient in ECRG4 gene to better elucidate its role in the innate immune mechanism.

Methods
OM was induced in ECRG4 knock-out (KO) and matched control C57BL/6 wild-type (WT) mice by infecting the ME with nontypeable Haemophilus influenza (NTHi). OM

pathogenesis and changes in ME were characterized by histology, qPCR, immunoprecipitation, Western blotting and quantifying the inflammatory cell infiltration. The extent of macrophage microbicidal activity was assessed with a phagocytic and intracellular killing assay.

Results

Within the normal WT mouse ME, a 14 kDa ECRG4 isoform is localized to the mucosal cell membranes. However, during OM, an 8 kDa isoform dominates, consistent with thrombin-cleavage at an extracellular serine site. Co-immunoprecipiation identified that the shorter isoform of ECRG4 associate with TLR4 and its co-receptor CD14/MD2 binding partners, suggesting a role in innate immunity. Histopathological analysis revealed that ECRG4 KO mice strain exhibited inflammatory abnormalities when compared to WT mice: greater mucosal hyperplasia at day 2 post-infection; reduced ME infection period and increased bacterial clearance from the ME. ECRG4-deficient peritoneal macrophages also had higher phagocytic activity *in vitro*.

Conclusions

While higher expression levels of ECRG4 correlate with improved survival in cancers indicating a role as a candidate tumor suppressor gene, our results are the first to demonstrate its multifunctional role in regulating the innate immune response in an *in vivo* bacterial infection model. ECRG4 appears to interact with the innate immune receptor TLR4 and to regulate downstream NF-kB and IFNg signaling cascades, hence modulating the balance between pro-inflammatory cytokines and anti-inflammatory regulators.

Funding

[Supported by NIH/NIDCD grants DC000129/DC012595/DC006279 and grants from the Veteran Affairs Administration Research Service]

PS 408

Microbiomes in the normal middle ear and chronic otitis media

Shujiro Minami[1]; Hideki Mutai[1]; Arata Horii[2]; Koichiro Wasano[3]; Motoyasu Katsura[4]; Fujinobu Tanaka[5]; Tetsuya Takiguchi[6]; Naoki Oishi[7]; Masato Fujii[1]; Kimitaka Kaga[1]

[1]National Tokyo Medical Center; [2]Niigata University; [3]Japanese Red Cross Shizuoka Hospital; [4]National Ureshino Medical Center; [5]National Nagasaki Medical Center; [6]National Kanazawa Medical Center; [7]Keio University

Background

The human body is colonized by a wide variety of microorganisms. Recent advances in Next Generation Sequencing technologies have now enabled us to characterize these highly complex microbial communities on various sites of the human body by analysis of prokaryotic 16Sribosomal RNA gene (16SrRNA). However, the middle ear microbiome has not been clarified so far. The aim of this study was first, to reveal the normal middle ear microbiome, and, second, to compare the microbiome from the normal middle ear with those from chronic otitis media (COM).

Medthod

In order to study the composition of the microbiome in the normal middle ear, 14 patients undergoing ear surgery for conditions other than otitis media, cochlear implantation for deafness, stapes surgery for otosclerosis, tympanoplasty for middle ear malformation, and facial nerve decompression for Bell's palsy, were recruited. Thirty-six patients with COM undergoing tympanoplasty surgery were also recruited to this study. Sterile swab samples were collected from the middle ear mucosa during surgery. After genomic DNA was extracted from the swabs, the V4 region of the 16SrRNA in each sample was amplified with region-specific primers adapted for Illumina MiSeq sequencer. Amplicons of fifty samples were subjected to sequencing, then quality-filtered and assigned to Operational Taxonomic Units (OTUs) defined as bacterial sequences with at least 97% sequence identification using MetaGenome@KIN toolkit.

Results

The most abundant phylum identified in normal middle ear mucosal surfaces was *Proteobacteria* (70.0%), followed by *Actinobacteria* (21.8%), *Firmicutes* (6.0%), *Bacteroidetes* (1.7%). In the samples from COM with non-active inflammation (dry ear), similar to the samples from the control group, the middle ear was predominantly colonized by *Proteobacteria* (69.9%), followed by *Actinobacteria* (20.4%), *Firmicutes* (5.8%), *Bacteroidetes* (3.3%). In the samples from COM with active inflammation (otorrhea +), *Proteobacteria* decreased to 42.5%, whereas *Firmicutes* increased to 33.5%.

Conclusion

In comparison with conventional culture-based methods, a large number of rarely isolated microbes were identified in the human middle ear mucosa in this study, demonstrating that the human middle ear is inhabited by much more rich and diverse microbial communities than was previously thought. The study also showed that the *Proteobacteria* phylum was the most predominant in the normal middle ear mucosa. However, the *Proteobacteria* phylum decreased and *Firmicutes* phylum increased in COM patients with active inflammation. Thus, we suggest that this alteration of the middle ear microbiome may contribute to the pathogenesis of COM active inflammation.

Funding

This research was supported by grant in aid from National Hospital Organization, Japan.

PS 409

The role of group 3 innate lymphoid cells during experimental otitis media in rat

Chang Gun Cho[1]; Sung Ho Gong[1]; Joo Hyun Park[1]; Hwan-Ho Lee[2]

[1]Dongguk University Hospital; [2]Kosin University, College of Medicine

Background

The objective of this study is to evaluate the role of group 3 innate lymphoid cells (ILC3) in the middle ear mucosal response to bacterial infection in rat. To confirm the role of ILC3

in bacterially induced otitis media, the serum concentrations of IL-17 and IL-22 and the expression levels of IL-17 and IL-22 in infected ME mucosa by immunohistochemical staining were assessed.

Method
20 Sprague-Dawley rats were used as a surgically induced animal model of otitis media. Otitis media was induced by inoculation of non-typeable H. influenza (NTHi) into the middle ear cavity of rats. 20 rats were divided into 4 experimental groups: 3 NTHi infected groups and 1 control group. Infected groups were subdivided into sets of 5 rats, 1 for each of 3 time points (1 day, 4 days and 7 days after inoculation of NTHi). For determination of rat IL-17 and IL-22 expressions in NTHi infected rats and control rats, serum concentration of IL-17 and IL-22 were analyzed by ELISA. Also, infected or control middle ear mucosae were analyzed by immunohistochemistry with specific antibodies directed against IL-17 and IL-22.

Results
The results of ELSA showed that the levels of IL-17 and IL-22 were significantly increased in bacterially induced otitis media. IL-17 and IL-22 serum concentrations were not significantly changed 1 day after inoculation of NTHi. However, significantly higher serum concentrations of both IL-17 and IL-22 were observed in infected rats sacrificed 4 days and 7 days after inoculation compared with control rats. Also, IL-17 and IL-22 protein expression was observed in all infected middle ear mucosa of rats sacrificed after 1 day, 4 days and 7 days after inoculation of NTHi.

Conclusion
ILC3 releasing IL-17 and IL-22 are associated with the bacterially induced proliferative and hyperplastic responses of middle ear mucosa which are characteristic features in pathogenesis of otitis media. The results of this study suggest that ILC3 may promote immune responses against bacterial infection and contribute to the pathogenesis of bacterially induced otitis media.

PS 410

Efficacy of Topographically Controlled Horse Bone powder for Bone Regeneration in Cranial Bone Defects of Rabbits

***Beomyong Shin**[1]; Kyoung-Je Jang[2]; Hoon Seonwoo[2]; Yeon Ju Kim[1]; Young Sun Kim[1]; Jong Joo Lee[1]; Oak-sung Choo[1]; Jong Hoon Chung[2]; Yun-Hoon Choung[1]
[1]Department of Otolaryngology, Ajou University School of Medicine, Suwon, Republic of Korea [2]Department of Biosystems & Biomaterials Science and Engineering, Seoul National University, Seoul, Republic of Korea

Background
Injured bones have limited capacity for self-repair requiring reconstruction with bone substitutes. For reconstruction, autogenous bone graft is the gold standard however, limitations of donor site morbidity and additional surgical procedures bring our attention to allograft or xenograft or combination of both. Thus, the aim of the present study was to explore the bone regeneration effect of horse bone powder in *in vivo*. Both 5 and 100 μm sized-horse bone powders were used for comparison of their efficiency with bovine powder (Bio-oss®).

Methods
Ten New Zealand white rabbits were used and four standardized defects were created in the parietal bones using an 8 mm diameter trephine bur. Three experimental defects were filled with Bio-oss®, 5 μm horse bone powder, and 100 μm horse bone powder with one remaining defect used as control. Specimens were collected after 8 and 16 weeks, and were prepared for qualitative and histological analysis.

Results
Qualitative analysis evaluated by Micro-CT showed significant difference of bone formation between the experimental and control groups. At 8 weeks, all bone volumes of the experimental groups were greater than that of the control. In addition, the two horse bone powder groups showed higher hyper-density of new bone formation compared with the Bio-oss® group. Through histologic evaluation using hematoxylin and eosin (H&E) staining, much more densely formed new bone was observed in the 100 μm size horse bone powder group rather than other groups at 8 weeks.

Conclusion
Horse bone powder is a compatible biomaterial for bone injury and bone defect significantly inducing bone regeneration.

Funding
This research was supported byTechnology Development Program for Korea Institute of Planning and Evaluation for Technology in Food, Agriculture, Forestryand Fisheries (IPET), Republic of Korea (312031-3).

PS 411

Stable Isotope Labeled by Amino acid in Culture (SILAC) strategy to analyze Human middle ear epithelial cells (HMEEC) secretome in response to NTHi lysates: evidence of the implication of exosomes in Otitis Media

Stéphanie Val; Stephanie Jeong; Marian Poley; Anna Krueger; Gustavo Nino; Kristy Brown; Diego Preciado
Children's National Medical Center

Background
Otitis Media (OM) is characterized by middle ear infection that leads to persistent effusions in the middle ear. Non-typeable Hemophilus influenza (NTHi) is implicated in the progression of the disease But little is known about the biological mechanisms that lead to chronic OM.

This study aimed at characterizing the secretome of HMEEC-1 and to evaluate its regulation in response to NTHi lysates and better understand the pathogenesis of OM.

Method
HMEEC-1 were labeled with heavy isotopes of arginine and lysine to obtain a spike-in standard. The spike-in standard was mixed with the conditions of interest (control or treated

24hrs, secretions recovered 24hrs or 48hrs) and separated by SDS-PAGE. Peptides generated by in-gel digestion were analyzed by LC-MS/MS. Middle ear effusions (MEEs) from patients having chronic OM were analyzed to validate the results obtained with HMEEC.

Results

767 proteins were detected by MS in HMEEC secretions at both 24hrs and 48hrs. The more abundant proteins detected were components of the extracellular matrix, proteins implicated in the innate immune response, and surprisingly proteins implicated in the processing and packaging of RNA. These proteins were heterogenous nuclear ribonucleoproteins A2/B1 (hnRNPA2B1) and K (hnRNPK) enriched at the 24hrs time point (1.99 and 1.78 fold change respectively) and Q at 48hrs (hnRNPQ, fold change 4.76) in response to NTHi lysates. We then hypothesized that these proteins were implicated in the packaging of miRNAs in exosomes in response to NTHi lysates. An exosome marker assay showed the presence of exosomes in both the cell secretions and MEEs. A western blot analysis of MEE exosome proteins showed the presence of hnRNPs as in cell secretions. Finally, a Nanostring chip assay demonstrated the presence of 29 miRNA in MEEs, mostly reported to be produced by epithelial cells and neutrophils.

Conclusion

We characterized the secretome of HMEEC in response to NTHi lysates treatment that show a remodeling of the extracellular matrix of the epithelium and a potential implication of exosomes in the pathogenesis of OM. We demonstrated the presence of exosomes in HMEEC secretions and MEEs, transporting miRNAs packaged by hnRNP proteins. These findings underline the importance of exosomes in cell communication in OM, a new field of research that needs to be further investigated.

Funding

This project is funded by the National Institute of Health.

PS 412

Ectopic Mineralization and Conductive Hearing Loss in Enpp1asj mutant mice

Cong Tian[1]; Kenneth Johnson[2]; Belinda Harris[2]

[1]The Jackson Laboratory, University of Maine; [2]The Jackson Laboratory

Background

Otitis media (OM), inflammation of the middle ear, is a common cause of hearing loss in children and in patients with many different syndromic diseases. Studies of the human population and mouse models have revealed that OM is a multifactorial disease with many environmental and genetic contributing factors. Mouse models for otitis media need to be developed to explore the mechanisms underlying the development of middle ear infection, and develop and test new therapeutic strategies for otitis media treatment.

Methods

We report on otitis media-related hearing loss in *Enpp1*$^{asj/asj}$ (asj, ages with stiffened joints) mice, which bear a point mutation in the *Enpp1* gene. We applied electrophysiological and histological techniques to characterize the new model for otitis media.

Results

Auditory-evoked brainstem response (ABR) measurements revealed that around 90% of the mutant mice (*Enpp1*$^{asj/asj}$) tested had moderate to severe hearing impairment in at least one ear. The ABR thresholds were variable and generally elevated with age. We found otitis media with effusion (OME) in all of the hearing-impaired *Enpp1*$^{asj/asj}$ mice by anatomic and histological examinations. The volume and inflammatory cell content of the effusion varied among the *Enpp1*$^{asj/asj}$ mice, but all mutants exhibited a thickened middle ear epithelium with fibrous polyps and more mucin-secreting goblet cells than controls. Otorrhea was detected in older *Enpp1*$^{asj/asj}$ mice, with 100% penetrance by 5 months of age, and contributes to the progressive nature of the hearing loss.

Conclusion

This is the first report of hearing loss and ear pathology associated with an Enpp1 mutation in mice. The *Enpp1*$^{asj/asj}$ mouse provides a new animal model for studying otitis media and also provides a specific model for the hearing loss recently reported to be associated with human ENPP1 mutations causing generalized arterial calcification of infancy and hypophosphatemic rickets.

Funding

This research is supported by NIDCD R01DC004301 to Dr. Kenneth R. Johnson.

PS 413

Multi-Voxel Pattern Representation of Interaural Time and Level Difference Cues in Human Auditory Cortex

Nathan Higgins; G. Christopher Stecker

Vanderbilt University

The auditory cortex (AC) plays a pivotal role in sound localization, and exhibits sensitivity to both major localization cues: interaural time (ITD) and level differences (ILD). Functional magnetic resonance imaging (fMRI) studies measuring cortical sensitivity to these cues reveal a dominant contralateral response to ILD, and contralateral (though relatively weaker) responses to ITD cues. These results, along with MEG studies of cross-cue adaptation, suggest that AC representations of ITD and ILD partially overlap. However, it is not clear whether the same patterns of cortical activity are elicited by ITD and ILD. Because fMRI offers the capability to simultaneously image responses throughout the brain, direct comparisons of ILD and ITD activation patterns can be made.

Here, continuous event-related fMRI was used to measure cortical responses to trials of amplitude-modulated noises varying parametrically in ITD or ILD in two runs each (total of 4 runs). Following preprocessing, functional data were subjected to a standardized hemodynamic regression analysis to extract an activation measure for each trial. Next, a linear classifier (LIBSVM) was trained using trial-to-trial

variation in AC voxel response patterns from each single run, and used to classify trials from the same voxels in each other run (i.e. manipulating the same or different cue type). Trials presented one of five values of each cue, corresponding to center (0dB ILD, 0μs ITD), moderate (±10dB, ±400μs), or large (±20dB, ±800μs) lateralization to either side.

Better than average classification was observed for both ILD and ITD classification when classifiers were trained on the same cue, with the highest classification probabilities at extreme contralateral and ipsilateral cues (ILD: $F(4,8)=25.9$, $p<0.001$; ITD: $F(4,9)=5.0$, $p<0.01$). Better than chance classification was also observed when ITD trials were classified by ILD classifiers ($F(4,9)=2.67$, $p<0.05$) and when ILD trials were classified by ITD classifiers ($F(4,9)=5.47$, $p<0.01$). Once again, the highest probabilities were observed at extreme contralateral and ipsilateral cues in both cross-classification conditions.

Successful cross-classification of ITD and ILD provides strong evidence that spatial cues are represented by similar, overlapping activity patterns in human AC, rather than by discrete populations or distinct coding strategies. ILD classifiers performed better when classifying ILD than ITD trials, suggesting widespread intensity-dependent (non-spatial) responses not observable in the ITD trials. In contrast, ITD-trained classifiers performed similarly for ILD and ITD trials, suggesting that learned patterns were not cue-dependent. That is, ITD classifiers utilized patterns of activity across AC subregions that specifically encode auditory location.

Funding
[Supported by NIH R01-DC011548]

PS 414

Perceptual Weighting of Modulation Depth during Monaural Distance Judgments

Paul Anderson[1]; Pavel Zahorik[2]
[1]Murray State University; [2]University of Louisville

Background
The direct-to-reverberant energy ratio (D/R) has been established as a primary auditory distance perception (ADP) cue; however, it is unlikely that D/R is directly encoded in the auditory system because it is difficult to extract from ongoing signals. It has been proposed that D/R is indirectly encoded in the auditory system, through sensitivity to other acoustic parameters correlated with D/R. A proposed D/R correlate relies on attenuation of amplitude modulation (AM) as a function of distance (Kim et al., 2015). A perceptual weighting paradigm was used to measure the relative perceptual weights assigned to intensity and modulation depth during distance judgments. The goal was to characterize the extent to which AM attenuation contributes to ADP relative to other cues.

Methods
Distance judgments were measured in two conditions where AM was either modulated at a high (32 Hz) or low (4 Hz) rate. Modulation rates were determined based on an analysis of the modulation transfer function (MTF) of the room where it was found that high rates were in general more attenuated than low rates. Virtual auditory space techniques were used for stimulus presentation. The simulated sound source was located 90° to the listener's right at 9 distances logarithmically spaced between .35 and 5.6 m. All stimuli were presented to the ipsilateral ear. The carrier signal was a 1-octave wide band of noise with a center frequency of 4 kHz (2000 ms duration). To determine weights, modulation depth was randomly roved over a +/- 2dB range and intensity was independently roved +/- 6. Distance judgments were measured using direct estimates from listeners in both conditions. Nine normal-hearing participants completed judgments in both conditions.

Results
Results from the weighting analysis suggest that modulation depth was a perceptually weighted, salient distance cue. Its weighting was approximately half that of intensity in both modulation conditions. When only the physical distance region where modulation depth was most attenuated by the room (> 2 m) was analyzed, distance judgments were more compressed/less accurate in the 4 Hz modulation condition. Judgments were most accurate when modulation was more attenuated by the room (32 Hz condition at physical distances > 2 m).

Conclusions
For monaural stimuli, modulation depth attenuation by the room improves the accuracy of distance judgments for physical distances where modulation depth is most attenuated by the room. The amount of benefit from the modulation depth attenuation cue may be predicted by the MTF of the room.

PS 415

Decoding Speech Sound Source Direction from Electroencephalography Data

Daniel Wong[1]; Ulrich Pomper[2]; Emina Alickovic[3]; Jens Hjortkjær[4]; Carina Graversen[5]; Sahar Akram[6]; Malcolm Slaney[7]; Daniel Pressnitzer[1]; Shihab Shamma[1]; Alain de Cheveigné[1]
[1]Ecole Normale Supérieure; [2]University College London; [3]Linköping University; [4]Technical University of Denmark; [5]Eriksholm Research Centre; [6]University of Maryland; [7]Stanford University

Background
We have developed a method capable of decoding the direction of incoming speech presented to a subject from single trial electroencephalography data. Previous studies have demonstrated that in the average response, sound location can affect both evoked response amplitudes in the auditory cortex, as well as event-related superior-parietal alpha activity.

Methods
Using 5 subjects, speech from an audio story from was broken into 3 minute segments and presented from speakers at -45 and +45 degrees azimuth, at 0 degrees elevation. The subjects kept their eyes fixated straight ahead while 64-channel EEG was recorded. A 3-level wavelet decomposition was then performed to split the data into 0-4, 4-8 Hz, 8-16 Hz and 16-

32 Hz bands. For each band, the 4 independent components that had the largest power were taken. Over data segments of 5 s, the power within each component was then computed for each band. A deep neural network was trained on these features, using stochastic backpropagation. The output of the network was the angle of the incoming sound source.

Results
The neural network was able to distinguish between the two azimuths. Analysis of the first-layer neural network weights indicates that features in the 0-4 and 4-8 Hz band contribute most dominantly to the decoder (73% together), whereas 8-16 Hz features contribute less (16%). An analysis of the sensor-space topography of the independent component with the strongest input weights, for each band, showed that the 0-4 Hz and 4-8 Hz components had a topography consistent with activation in temporal areas, whereas 8-16 Hz component was consistent with activation in superior-parietal areas.

Conclusion
The features that primarily drove the decoder have independent component topographies consistent with earlier reports of auditory attention modulated activity in the auditory cortex and superior-parietal areas. The ability to discern the direction of an incoming sound using short single-trial data segments is a step toward developing “smart” hearing prostheses that can amplify a specific attended sound source.

Funding
Funded by the European Commission H2020 COCOHA Research and Innovation Action

PS 416

Coherent Noise Binaural Beats: Single and Continuous Beat Construction Percept Characteristics and Basic Electrophysiology

Jorge Bohorquez; Ozcan Ozdamar
University of Miami

Background
Conventional binaural beats (BB) are generated by sinusoidal stimuli with slightly different frequencies presented binaurally to separate ears. These two stimuli generate the percept of continuous BB whose rate is determined with the frequency difference of the dichotic tones.

Methods
In this study we develop a new method for single or continuous BB percept formation from noise stimuli. Noise stimuli are designed to be perceived as stationary (no beating) when presented monaurally and non-stationary (beating) when they presented dichotically. The Coherent Noise Binaural Beat (CNBB) stimuli are designed to have specific bandwidth, beat duration and onset intervals.

The left and right components of CNBB are band-pass filtered white noise signals with the same RMS and spectral characteristics. The CNBB generation is controlled by a “modulating” Correlation Probabilistic Function (CPF) that represents the probability that the stimulus reaching right and left ears have a correlation coefficient ranging from -1 (CPF=0) to 1 (CPF=1). The manipulation of the CPF as function of time allows the generation of the CNBB events of specific onset, rise/fall time and duration. For a single perception CNBB, the CPF is zero until the BB onset at which CPF transitions to a positive value followed by a return to zero. The duration of the whole cycle determines the CNBB duration. For continuous beat construction, the CPF function is generated as a periodic sequence of similar CPF cycles.

CNBB stimuli having different rates (0.33-10Hz), durations (90ms - 300ms) and bandwidths (0.25-1KHz, 1-2KHz and 2-4KHz), were applied to adult normal hearing subjects to assess beat detectability. Auditory evoked responses (AEP) were recorded using 200ms, 250Hz-1KHz bandwidth CNBBs at rates of 0.33Hz and 1Hz to test the feasibility of electrophysiological detection of CNBBs

Results
Low-frequency bandwidth CNBBs had the highest detectability (100%) followed by the medium frequency. The low stimulation rate CNBBs had the highest detectability (100%) while the 10Hz were detected as beats by lower number of subjects. Low rate and bandwidth CNBBs elicited reliable AEPs with P1-N1-P2-N2 peaks and all subjects hearing them as centrally generated beats.

Conclusion
Dichotically presented pulsating coherent noise generated with low frequency noise presented at low rates are perceived as pulsating beats similar to conventional BBs. When monaurally presented, no pulsating beats are perceived. Since stimulus parameters are easily controlled, CNBBs offer great advantages investigating central auditory phenomena such as BBs and sound localization by psychophysical and electrophysiological methods.

Funding
Institutional

PS 417

Steady-state evoked responses and psychophysical detection of periodic changes in carrier IPD – effects of carrier frequency and IPD size

Nicholas Haywood; Jaime Undurraga; David McAlpine
Macquarie University

A steady-state response can be evoked from salient periodic changes in interaural phase difference (IPD). Stimuli comprised a five-minute sinusoidally amplitude modulated (AM) tone (70 dB SPL, modulation frequency = 41 Hz). The AM envelope was held diotic, and the carrier tone was presented with one of six possible IPDs: 22.5º, 45º, 90º, 112.5º, 135º, or 157.5º. Every six successive modulation cycles, at a rate corresponding to 6.8 Hz, the carrier IPD was modulated so that carrier phase led in the opposite ear than previously. This resulted in a stimulus which alternated periodically between right- and left-leading, but where the overall size of the IPD was constant. Monaural phase-shift cues were minimised by presenting each phase modulation at a minimum in the AM

cycle. The carrier frequency was varied experimentally (250 Hz – 1000 Hz).

Electroencephalographic responses from fifteen normally-hearing subjects will be recorded. The stimuli were not attended during the recording session. Our previous experiments have shown that salient periodic IPD switches evoke a robust 6.8 Hz steady-state following response which can be detected reliably. This response has been termed the interaural phase modulation following response (IPM-FR). Preliminary data from the current experiment (n = 5) suggest that for each carrier frequency tested, IPM-FR magnitude was largest typically when the IPD was set to 90º. Response magnitude decreases at both larger and smaller IPD condtions. This may be attributable to the fact that the ±90º modulation corresponded to an overall (maximal) IPD change of 180º. Response magnitude also varies with carrier frequency, with lower-frequency carriers evoking overall larger magnitude responses. Preliminary data also indicate that response magnitude across all different conditions is partially predicted by the size of the change in interaural time difference (ITD) – more specifically, for IPD conditions of 90º or less, response magnitude increases linearly with the size of the ITD change, across differing carrier frequencies and IPDs. Only when IPD values exceeded 90º, did response magnitude decrease progressively for each carrier frequency.

In a 2I-2AFC psychophysical task, subjects identified a target tone with a modulated IPD from a reference tone with an equivalent but static IPD. Tones were presented for one second. The stimuli were presented with an interaurally uncorrelated pink noise, the level of which was varied adaptively to estimate threshold signal-to-noise ratio (SNR). Performance in this task will be correlated with IPM-FR magnitude. Correlation between behavioural and EEG measures will be explored.

PS 418

Cross-Species Comparison of Binaural Characteristics of the Binaural Interaction Component of the Auditory Brainstem Response

Alexander Ferber; Daniel Tollin
University of Colorado Anschutz Medical Campus

The binaural interaction component (BIC) is the residual auditory brainstem response (ABR) after subtracting summed monaurally-evoked from binaurally-evoked ABRs. The β peak is the first negative peak of BIC, and it may have diagnostic value: altered β amplitudes and latencies correlate with and predict behavioral binaural processing deficits. β amplitude depends upon binaural cues to location, exhibiting maximal amplitude for interaural time differences (ITDs) of zero and systematically smaller amplitudes for larger ITDs. However, in most species, β continues to be modulated for ITDs well outside the physiological range of ITDs, suggesting that the mechanism producing the BIC is not constrained by ITD magnitudes available to particular species; it is rather produced by basic synaptic mechanisms of binaural processing shared by most mammals. Indeed, previous studies have demonstrated similar functions relating ITD and β amplitude across species that have dramatically different physiological ranges of ITD. However, while the overall trend is consistent, some apparent differences persist between studies. We hypothesize inter-study variability is due to parametric differences between studies, variable calibration of sound delivery systems, and experimental factors affecting signal-to-noise ratio.

Investigating the relationship between ITD and β amplitude, we compare ABR/BIC recordings in guinea pig, chinchilla, rat and other species. Recordings were made under ketamine/xylazine anesthesia using the same experimental apparatus, featuring a sound delivery system calibrated at each recording. Recordings were made with needle electrodes at apex, nape and hind leg using click stimuli. 1000 repetitions (excluding EKG artifact-rejections) per monaural and binaural condition were recorded across an ITD range spanning ±2000μs, bandpass-filtered (0.1-3kHz) and averaged. Normalization of β amplitude by average RMS amplitude of monaural ABRs was applied to account for signal-to-noise variability in individual recordings. To facilitate cross-species comparisons, a Gaussian curve was fitted to β amplitude versus ITD functions, and fit parameters were compared.

Gaussian curves fit the data well (R^2=0.92-0.98). No significant differences were found between the center of the curve for guinea pig, chinchilla or rat; all centered around zero ITD. Similarly, curve widths did not vary significantly between guinea pigs (672±45μs, SE), chinchillas (685±47μs), and rats (672±83μs) despite physiological ITD ranges between species varying by a factor of 2.

Previously reported cross-species differences in the relationship between BIC β amplitude and ITD were insignificant when measured using identical experimental methods. These results support the hypothesis that BIC is produced by brainstem mechanisms that are not constrained by species-specific physiological ranges of ITDs.

Funding
Support: NIDCD R01-DC011555, 1F30-DC013932

PS 419

Characterization of the Binaural Interaction Component in Barn Owl (Tyto alba)

Nicolas Palanca-Castan[1]; Geneviève Laumen[2]; Darrin Reed[3]; Christine Köppl[1]
[1]Cluster of Excellence Hearing4all, School of Medicine and Health Sciences, Carl von Ossietzky University, Oldenburg; [2]Cluster of Excellence Hearing4all, Animal Physiology and Behavior Group, Department for Neuroscience, School of Medicine and Health Sciences, Oldenburg University; [3]Center for Computational Neuroscience and Neural Technology, Boston University

Background
The auditory brainstem response (ABR) is an evoked potential that reflects the responses to sound by the brainstem neural centers. The binaural interaction component (BIC) is obtained

by subtracting the sum of the monaural ABR responses from the binaural response. It is assumed to represent the activity of binaural nuclei (Jewett, 1970, *Electroencephalogr. Clin. Neurophysiol.* 28: 609–618). The amplitude and latency of the BIC are dependent on the binaural cues presented (Furst et al., 1990, *Hear. Res*. 187: 63–72). The BIC can be used to non-invasively test binaural processing. However, any conclusions are limited by the lack of knowledge of the relevant processes at the level of individual neurons. The aim of this study is to characterize the ABR and BIC in the barn owl, an animal where the ITD-processing neural circuits have been extensively studied.

Methods
ABRs were measured in 9 adult barn owls. Responses to chirps at different levels and ITDs were recorded, and the BIC was derived as a function of ITD. To determine the extent of the crosstalk caused by the presence of the interaural canal, compound action potential (CAP) recordings were collected for two other adult barn owls. All BIC measurements were taken below the level of crosstalk.

Results
The ABR in barn owl showed 2-3 waves in the first 10 ms of recording. Wave I only appeared consistently at high levels. Wave II and III increased in amplitude and decreased in latency with increasing stimulus level. The most salient component of the BIC was a negative deflection (DN1) that corresponded to wave III. The latency of DN1 closely corresponded to the latency of local neurophonic potentials recorded in nucleus laminaris (Carr et al. 2015, J. *Neurophysiol.*, in press). Both the amplitude and latency of DN1 varied with changing ITD.

Conclusion
The most visible component of the BIC (DN1) was associated with nucleus laminaris and is thus likely to reflect the known processes of ITD computation in this nucleus. DN1 was a negative deflection, which indicates a smaller response to binaural stimulation than predicted by the sum of monaural responses. This negative polarity is not consistent with previous predictions (Wada and Starr, 1989, *Electroencephalogr. Clin. Neurophysiol*. 56, 340–351) for an excitatory-excitatory system such as the one present in barn owl, and alternative models like the one by Gaumond and Psaltikidou (1991, *J. Acoust. Soc. Am.* 89: 454:456) need to be considered.

Funding
NPC, GL, CK funded by the DFG (TRR31) and the cluster of excellent “Hearing4all”. DK supported by the program “Function and pathophysiology of the auditory system” funded by the state of Lower Saxony, Germany.

PS 420

Detailed Analysis of High Frequency Auditory Brainstem Response in Tinnitus Patients: A Preliminary Study

Raymundo Munguia-Vazquez[1]; **Joseph Pinkl**[2]; Matthew Wilson[2]; Danica Billingsly[2]
[1]Purdue University; [2]Northern Illinois University

Background and Aim
Spontaneous firing rates and increased neural synchrony is believed to be the underlying cause for tinnitus. The perceived pitch of tinnitus may be dictated by neural activity localized to frequency specific neural fibers of the subcortical pathway, or it can be the projection of altered cortical activity as a result of tonotopic reorganization. Subcortical neural activity in relation to tinnitus can be characterized using auditory brainstem response (ABR) measurements of frequency specific stimuli parameters reflecting the perceived frequency of the tinnitus.

Methods
11 patients (21 ears) with constant tonal tinnitus were included in the study. They were divided into two groups: tinnitus with normal hearing (**GI**) and tinnitus with hearing loss (**GII**). A control group (**GIII)** of ten (monaurally tested = ten ears) normal hearing subjects within the frequency range of 250-20000 Hz, with no tinnitus, ear surgeries or ototoxic medication were tested. Due to the presence of unilateral tinnitus and asymmetric hearing loss, testing addressed each ear individually.

All participants underwent puretone audiometry in the frequency range of 250-20000 Hz. The experimental group underwent pitchmatching testing. Click ABRs and toneburst ABRs matching the perceived pitch of the tinnitus were performed on the experimental group. All ABR norms were established using the control group GIII.

Independent t tests were used to analyze components of the ABR including wave I, III and V absolute latencies, I-III, III-V, and I-V interpeak latencies and V amplitudes of the three groups.

Results
Concerning click ABRs, interpeak III-V latencies was significantly prolonged ($p<.05$) for GI and GII.

Statistically significant absolute and interpeak latencies with toneburst ABR were noted at three (total of six ears) of the seven frequencies tested for GII.

Conclusions
Click ABRs results are suggestive of upper brainstem abnormalities for both GI and GII. While GI demonstrated significantly prolonged III-V interpeak latencies, no significant differences for the ABR analysis were found during toneburst ABR testing for GI. This suggests that there is no frequency specific characteristic associated with subcortical spontaneous activity within the normal hearing with tinnitus population. There were varying results found within GII when comparing click to toneburst ABR waveforms; frequency

specific properties for subcortical spontaneous neural activity cannot be identified.

The current research design should be continued on a larger scale for statistically significant findings.

Figure 1 & 2: Click ABR

Click ABR measurements were averaged in GI and GII. Table 1 compares GI measurements to the established norm (GIII). Table 2 compares GII measurements to the established norm. Statistical significant findings ($p<.05$) are labeled with an asterisk.

ABR Measurement	Group I	Group III	t-Test	Sig. (2 tailed)
I Latency	1.723 ± .10233	1.556 ± .10233	-1.931	.069
III Latency	3.699 ± .40534	3.761 ± .14746	.455	.655
V Latency	5.604 ± .32756	5.509 ± .14403	-.84	.412
V Amplitude	.538 ± .368841	.511 ± .15509	-.214	.833
IPL I-III	2.066 ± .50608	2.0206 ± .16628	.831	.417
IPL III-V	1.906 ± .44144	1.751 ± .19886	-1.012	.0331*
IPL I-V	3.836 ± .17411	3.954 ± .18307	1.477	.157

ABR Measurement	Group II	Group III	t-Test	Sig. (2 tailed)
I Latency	1.5809 ± .32164	1.556 ± .10233	-.244	.812
III Latency	3.6245 ± .3638	3.761 ± .14746	1.145	.272
V Latency	5.8109 ± .38316	5.509 ± .14403	-2.431	.03*
V Amplitude	.4109 ± .14039	.511 ± .15509	1.553	.137
IPL I-III	2.0464 ± .25839	2.0206 ± .16628	1.664	.113
IPL III-V	2.1864 ± .56197	1.751 ± .19886	-2.409	.032*
IPL I-V	4.23 ± .48512	3.954 ± .18307	-1.755	.103

Figure 3, 4, & 5: Toneburst ABR

Toneburst ABR measurements were averaged in GI and GII and compared to the established norm. Three (total of six ears) of the seven frequencies tested for GII yielded significant differences ($p<.05$) for several of the ABR measurements. Statistically significant findings are labeled with an asterisk.

GII: 6000 Hz Toneburst

ABR Measurement	Group I	Group III	t-Test	Sig. (2 tailed)
I Latency	2.175 ± .2129	1.9 ± .43765	-.829	.434
III Latency	3.75 ± .35355	4.1643 ± .68266	-.8	.45
V Latency	5.585 ± .54447	6.5571 ± .33979	-3.225	.015*
V Amplitude	.19 ± .24042	.3329 ± .12539	-1.209	.266
IPL I-III	1.575 ± .57276	2.2657 ± .84668	-1.059	.325
IPL III-V	1.835 ± .19092	2.3929 ± .74748	-1	.351
IPL I-V	3.415 ± .7566	4.6586 ± .73814	-2.094	.075

GII: 12500 Hz Toneburst

ABR Measurement	Group I	Group III	t-Test	Sig. (2 tailed)
I Latency	2.475 ± .45962	1.3857 ± .14909	3.302	.176
III Latency	4.58 ± .42426	3.1243 ± .48675	3.769	.007*
V Latency	6.78 ± .14142	4.7914 ± .66702	4.001	.005*
V Amplitude	.24 ± .07071	.21 ± .13128	.301	.772
IPL I-III	2.105 ± .03536	1.7 ± .52243	1.044	.331
IPL III-V	2.2 ± .56569	1.6643 ± .53935	1.23	.258
IPL I-V	4.3 ± .59397	3.4057 ± .77724	1.48	.182

GII: 14000 Hz Toneburst

ABR Measurement	Group I	Group III	t-Test	Sig. (2 tailed)
I Latency	1.485 ± .30406	1.0757 ± .173	2.59	.036*
III Latency	3.165 ± .12012	2.66 ± .39328	1.172	.13
V Latency	6.6065 ± .33234	4.71 ± .6509	2.745	.024*
V Amplitude	.55 ± .18385	.2686 ± .2098	1.702	1.33
IPL I-III	1.68 ± .42426	1.5843 ± .3774	.311	.765
IPL III-V	2.9 ± .45255	1.9257 ± .42634	2.825	.026*
IPL I-V	4.575 ± .03536	3.5114 ± .65096	4.301	.005*

PS 421

Longitudinal MRI Analysis of Volumetric Differences in Brainstem Neurons Following Noise Induced Temporary Threshold Shift

Antonela Muca[1]; Jaymin Patel[2]; Susumu Mori[2]; Tilak Ratnanather[3]; Avril Holt[1]

[1]Wayne State University School of Medicine; [2]Johns Hopkins University School of Medicine; [3]Johns Hopkins University

Background

Even exposure to loud noise resulting in temporary deafness often leads to conditions such as tinnitus. Noise over-exposure has been a major risk factor for chronic tinnitus for those in occupations associated with noisy environments. Currently there is no effective treatment for tinnitus. This emphasizes the need to determine metrics that will allow for longitudinal studies of tinnitus progression. Noise induced tinnitus has been associated with changes in neuronal activity. Magnetic resonance imaging (MRI) has been used to track longitudinal changes in tinnitus related neuronal activity using manganese enhanced MRI (MEMRI). In addition to activity, neuronal volume has also been suggested to change in people with chronic tinnitus. Temporal and spatial changes in brain volume were examined longitudinally in several brain regions, including the inferior colliculus (IC), following a single noise exposure.

Methods

Hearing thresholds were determined (ABRs) in two groups (noise and no noise) of male Sprague Dawley rats. Noise animals were exposed to a 16 kHz, 106 dB SPL tone for 1 hour. For each group, T_1-weighted MRI images were obtained (7T Clinscan) before (baseline) and after noise exposure (1, 28, and 84 day(s)). Deficits in Gap detection were used as a measure of tinnitus. Morphology for regions of interest (ROIs) was identified on a single subject brain atlas using MRIStudio software. The atlas was registered to the subjects using Automated Image Registration (AIR) and Large Deformation Diffeomorphic Metric Mapping (LDDMM) in order to map the ROIs onto each subject. ROI volumes from the two groups were compared at each time point.

Results

Differences in the volume of the IC occurred as early as 1 day after noise exposure, with significant decreases in the central nucleus of the IC (CIC) of noise exposed animals compared to control. Although hearing thresholds had returned to

normal, significant volumetric decreases were seen 84 days after noise exposure in the CIC of noise exposed animals. With the exception of the first week, Gap detection deficits were present at all time points (20 kHz, 60dB).

Conclusions
An outcome of our study is the production of a rat volumetric atlas with brain region coordinates that can be used as a template by others. Volumetric information may provide another crucial metric for understanding the effects of noise over-exposure on the progression of tinnitus.

Funding
Grant 1I01RX001095-01 U.S. Dept. of Veterans Affairs Grant T42 OH008455 from the National Institute for Occupational Safety and Health, Centers for Disease Control and Prevention

PS 422

Transdermal Stimulus-Timing Dependent Plasticity in Dorsal Cochlear Nucleus Reduces Tinnitus in Guinea Pigs

David Martel; Calvin Wu; Susan Shore
University of Michigan, Ann Arbor

Introduction
Nearly two-thirds of tinnitus patients can modulate their tinnitus with somatic maneuvers of the face and/or neck (Levine et al, 2007), which is likely mediated by somatosensory connections to the cochlear nucleus (CN). The dorsal cochlear nucleus (DCN) integrates auditory inputs with somatosensory inputs from trigeminal and dorsal column systems. Fusiform cells, the principle output neurons of the DCN, exhibit stimulus-timing dependent plasticity (STDP) in response to bimodal auditory-somatosensory stimulation: Hebbian-like plasticity occurs when neurons increase their activity responding to somatosensory-preceding auditory stimulation, but anti-Hebbian rules occur when auditory- precedes somatosensory stimulation (Koehler and Shore, 2013a). In tinnitus animals, Hebbian-like rules invert to anti-Hebbian-like rules with broadened temporal windows (Koehler and Shore, 2013b). Our recent work demonstrated that fusiform cell STDP can be induced non-invasively using transdermal stimulation (Wu et al., 2015). To test whether STDP can be harnessed to treat tinnitus, we applied paired auditory-somatosensory stimulation, via transdermal neck stimulation, to noise-damaged guinea pigs with behavioral and neural evidence of tinnitus. Preliminary data shows decrements in both behavioral and neural correlates of tinnitus after one month of 30 min bimodal stimulation.

Methods
Guinea pigs were noise-exposed with a 7 kHz-centered, half-octave band at 97 dB SPL for 2 hours to induce a temporary threshold shift. Gap-Prepulse Inhibition of Acoustic Startle (GPIAS) was used to assess tinnitus. Somatosensory stimulation was provided via transdermal stimulating electrodes placed near the C2 cervical vertebrae. Short electrical stimuli were presented within 20 ms of 40 dB SL sounds matching the tinnitus spectra. Tinnitus animals were treated for four weeks concurrently with biweekly tinnitus assessments. Following cessation of treatment, single unit recordings from DCN were obtained with recording electrodes placed stereotaxically into the DCN fusiform cell layer after ketamine/xylazine anesthesia. Unit responses to tones and noise were assessed for units with best frequencies ranging from 4 kHz to 32 kHz.

Results
Animals with tinnitus showed elevated spontaneous activity and neural synchrony at the measured tinnitus frequencies. In contrast, exposed animals without tinnitus animals did not show elevated spontaneous rates or synchrony compared to unexposed animals. Animals receiving bimodal STDP induction showed decreases in spontaneous rates and neural synchrony, which correlated with a reduction in behavioral evidence of tinnitus.

Conclusions
Our results demonstrate that non-invasive, long-term alteration of DCN neural activity through bimodal STDP can be used to alleviate behavioral and neural correlates of tinnitus. This treatment strategy may provide relief in human tinnitus sufferers.

Funding
R01-DC004825 (SES) P30-DC05188 T32-DC00011 (CW) Wallace H. Coulter Translational Research Partnership

PS 423

Analysis of Auditory and Non-Auditory Input in the Dorsal Cochlear Nucleus in a Rat Model of Tinnitus & Noise-Induced Hearing Loss

Christopher Neal; Andrea Freemyer; Jennifer Nelson-Brantley; Hinrich Staecker; Dianne Durham
University of Kansas Medical Center

Background
Hair cell damage resulting from acoustic trauma not only alters hearing thresholds but may also initiate a cascade of maladaptive plastic changes in central auditory nuclei. Increasing evidence has implicated such plastic changes in the dorsal cochlear nucleus (DCN) in the induction of chronic tinnitus. The DCN consists of 3 layers (molecular, fusiform, and deep), which create a circuit. Fusiform cells in the DCN are the main output cells of the DCN circuit, and they are also the first site of multi-sensory integration in the auditory system. Input to fusiform cells can be identified as auditory or non-auditory by the distribution of vesicular glutamate transporters (VGlut). Fusiform cell basal dendritic fields receive auditory input via the auditory nerve (molecular and fusiform layers) and their apical dendritic field receives non-auditory input via parallel fiber projections (molecular and fusiform layers) from granule cells. We sought to quantify changes in auditory and non-auditory input to the DCN following acoustic trauma.

Methods
Adult male, Long-Evans rats were unilaterally exposed to a 118 dB, 16 kHz pure-tone for 4 hours (n=8) while anesthetized using isoflurane, and allowed to recover for 2 weeks. Pre-

exposure and post-exposure auditory brainstem response (ABR) and gap detection data (12, 16, and 20 kHz background) were collected. Rats were sacrificed, perfused and the brains were collected. Sectioned brain tissue containing the DCN was processed for fluorescent immunohistochemistry using antibodies against VGlut1 (auditory input), VGlut2 (non-auditory input) and imaged using confocal microscopy. The Otsu method of automated local thresholding was applied to images, and puncta density was determined for each label.

Results & Conclusions
Rats exhibited statistically significant post-exposure elevations in hearing thresholds at 11.3, 16, 22.6, and 32 kHz. Six of 8 rats were positive for tinnitus for at least one background tone frequency, and 5 of 8 are positive for tinnitus at a 20 kHz background tone. An in progress analysis of immunohistochemical data shows a small (~10%) decrease in the density of VGlut1 puncta (deep + fusiform layers), and a concomitant increase (~20%) in the density of VGlut2 puncta (fusiform + molecular layers) in DCN ipsilateral to the acoustic trauma. These results suggest that non-auditory inputs to the DCN increase following cochlear injury. Further studies will determine the relationship of these CNS changes to hearing loss and tinnitus.

Funding
Kansas Intellectual and Development Disabilities Research Center (NICHD HD02528) The Madison and Lila Self Graduate Fellowship at the University of Kansas

PS 424

Hyperactivity in the inferior colliculus following sound exposure is not well correlated to behavioral evidence of tinnitus in CBA/CaJ mice

Ryan Longenecker; Alexander Galazyuk
Northeast Ohio Medical University

Background
A substantial body of evidence suggests that spontaneous firing rates increase in neurons of most auditory nuclei following sound exposure. This hyperactivity has commonly been suggested as an underlying neural correlate of tinnitus. Recent studies on rats and guinea pigs have challenged this idea with data that suggests that hyperactivity is simply a result of sound exposure without a direct link to behavioral evidence of tinnitus. Increased bursting activity, a prevalent temporal change of spontaneous firing patterns, has also been associated with the behavioral evidence of tinnitus. However, neither of these neural correlates has been linked to individual animals with specific behavioral evidence of tinnitus/ hearing loss. Our goal was to test for a possible link between tinnitus, hearing loss, hyperactivity, bursting activity in the auditory system in individual animals after sound exposure.

Methods
Mice were unilaterally exposed to 116dB SPL narrowband noise (centered at 12.5 kHz) for 1 hour under general anesthesia. Gap-induced prepulse inhibition of the startle reflex was used to assess behavioral evidence of tinnitus in individual mice. PPI audiometry was used to assess behavioral hearing thresholds. Following behavioral assessments, single unit firing activity were recorded from ipsi- and contra-lateral inferior colliculi.

Results
Following sound exposure all mice demonstrated increased spontaneous activity independently of tinnitus behavior or severity of hearing loss. Bursting activity did not increase in animals identified as tinnitus positive, but did so only in animals with severe hearing loss.

Conclusion
Hyperactivity does not appear to be a reliable biomarker of tinnitus. Increased bursting activity might be used as a biomarker of severe hearing loss.

Funding
This research was supported by grant R01 DC011330 and 1F31DC013498-01A1 from the National Institute on Deafness and Other Communication Disorders of the U.S. Public Health Service.

PS 425

Changes in neural activity in the inferior colliculus following acute electrical stimulation of the round window in an animal model of tinnitus

Emma Johnson; James Fallon; **Andrew Wise**
The Bionics Institute

Background
Tinnitus is the perception of sound in the absence of external acoustic stimuli. It often occurs as a result of damage to the cochlea, which causes a change in the afferent input, leading to maladaptive plastic changes in central auditory neurons. Cochlear implant use can suppress tinnitus in people with severe tinnitus. It is thought that re-establishment of neural activity reverses the plastic changes responsible for tinnitus. However, the extent of suppression remains variable and the mechanism(s) responsible are unknown. Consequently, there has been only limited clinical use of bionic devices to treat tinnitus. The current study examined the acute effects of electrical stimulation from a round window electrode on neural firing in the central nucleus of the inferior colliculus (ICC).

Methods
Adult guinea pigs were used (n=11). Auditory brainstem responses (ABRs) were measured before and following acoustic deafening. Eight animals were unilaterally deafened (10 kHz, 124 dB SPL, two hours). The acoustic startle reflex was used to obtain behavioural evidence of a tinnitus percept. Data was obtained before deafening, and in the two week period following deafening, after which an acute electrophysiological experiment was carried out. Animals were anaesthetised and a platinum ball electrode was placed on the round window membrane. A 32 channel probe was inserted along the tonotopic gradient of the ICC.

Spontaneous neural activity and responses to acoustic input was measured before and immediately following a one hour period of electrical stimulation (bipolar pulses delivered in 100 ms bursts (100 pps), at 5 Hz). The cochleae were then collected for histology.

Results
A significant shift in hearing thresholds was observed following noise deafening and inner and outer hair cell lesions were observed in the basal turn. Behavioural evidence of tinnitus was observed in half the noise deafened animals via the startle reflex. There was evidence of hyperactivity in the spontaneous firing rates of ICC neurons with characteristic firing frequencies >10 kHz exhibiting significantly higher firing rates than neurons with characteristic frequencies of <10 kHz (ANOVA $p<0.001$). There was a significant reduction in spontaneous firing rates following the acute bout of electrical stimulation (ANOVA $p<0.001$).

Conclusions
Electrical stimulation from a bionic device can be used to alter neural firing properties associated with tinnitus and therefore help in determining the neural correlates of tinnitus. The potential use of a round window implant may provide a therapeutic option for people with intractable tinnitus.

Funding
This work was funded by the NHMRC and supported by the Victorian Government through its Operational Infrastructure Support Program.

PS 426

Salicylate-Induced Changes of Auditory Responses of the Caudal Pontine Reticular Nucleus – The Sensorimotor Interface of the Acoustic Startle Reflex

Guang-Di Chen; Vijaya Prakash Krishnan Muthaiah; Benjamin Auerbach; Kelly Radziwon; Senthilvelan Manohar; Stewart Clark; Richard Salvi
University at Buffalo

Background
The amplitude of acoustic startle reflex (ASR) and pre-pulse inhibition of the ASR are now widely used as behavioral readouts of tinnitus and hyperacusis. The ASR is triggered by moderate to high intensity sounds and adapts with a short inter-stimulus interval. It is mediated by a simple neural circuit composed of the cochlear nucleus, caudal pontine reticular nucleus (PnC) and spinal motoneurons. The ASR amplitude is greatly enhanced by high-doses of sodium salicylate (SS). Moreover, our functional magnetic resonance imaging study revealed significant hyperactivity in the pontine reticular nucleus during salicylate-induced tinnitus and hyperacusis. These results suggest that high-dose SS might enhance ASR amplitudes by altering sound-evoked neural activity in the PnC. To test this hypothesis we made electrophysiological recordings from the PnC before and after SS treatment.

Methods
A 16-channel microelectrode array (NeuroNexus) was inserted into the PnC to record sound-evoked neuronal discharges and local field potentials (LFP). Neural responses were recorded before and after treatment with 250 mg/kg SS, a dose known to reliably induce tinnitus and hyperacusis in rats.

Results
Neurons in the PnC responded to acoustic stimulation with very short first-spike latencies (~3-4 ms) and response thresholds varying by frequency with the lowest threshold at the characteristic frequency (CF). The lowest CF-thresholds were on the order of 30-40 dB SPL; however, in most cases the CF-thresholds were 50-60 dB SPL or higher. Sound-evoked discharge rates increased with inter-stimulus interval (ISI) saturating after 1000 ms, similar to that observed in the inferior colliculus (IC). Response thresholds of the PnC neurons increased 20-30 dB post-SS-injection, but paradoxically, responses at high intensities were enhanced whereas first-spike latencies were prolonged ~1-2 ms. The SS-effect was frequency dependent with the greatest enhancement occurring at the mid-frequencies similar to the frequency-specific enhancement previously observed in the auditory cortex and the lateral amygdala.

Summary
SS reduces the neural output of the cochlea, but paradoxically enhanced sound-evoked PnC responses at high stimulation levels, consistent with the increase in ASR amplitude after SS treatment. The SS-induced enhancement of PnC responses could be due to a reduction of GABA-mediated inhibition in the PnC or alternatively, indirect effects of SS on the amygdala which in turn enhances activity in the PnC.

Funding
Research supported in part by grants from NIH (R01DC011808), and NIOSH (R01OH01023501)

PS 427

Neural Correlates of Noise-induced Tinnitus in Rats: Intra- and Inter-auditory and Non-auditory Structures

Hao Luo; Edward Pace; Anika Meggo; Winston Zhang; Jinsheng Zhang
Wayne State University

Subjective tinnitus is a sound sensation that cannot be attributed to an external sound source, and is a prevalent health problem. It is often accompanied with limbic associated disorders such as anxiety, depression, distress and fear. To investigate the underlying neural mechanisms in auditory and non-auditory structures, in this study, we used 10 adult rats and implanted chronically with the microelectrode arrays in the right auditory cortex and basolateral region of the right amygdala of each rat. The left ear was exposed to 115 dB white noise for 3 hours. A gap detection acoustic startle reflex paradigm was used to assess the rat's behavioral evidence of tinnitus after noise exposure. Based on presence of tinnitus and noise exposure, rats were re-grouped as tinnitus positive,

tinnitus negative and control groups. Spontaneous activities were recorded simultaneously from the auditory cortex and amygdala at before, two and six weeks after noise exposure. The results showed that rats with tinnitus developed increased the spontaneous firing rates in the auditory cortex and amygdala, as well as intra- and inter- auditory cortex and amygdala neurosynchrony. Data indicate that the hyperactivity found in the auditory cortex and amygdala of tinnitus positive rats directly represents the neural substrate underlying tinnitus, and the correlation between auditory and non-auditory structures and inter-neural synchrony also play important role to tinnitus induced by acoustic trauma.

Funding
Tinnitus Research Consortium

PS 428

Neural Correlates of Residual Inhibition in a Mouse Model of Tinnitus

Derek Gavin; Andrea Lowe; **Joseph Walton**
University of South Florida

Tinnitus is a disorder characterized by the perception of sound in the absence of an external stimulus. It is often perceived as a ringing or buzzing sound, and can be transient or chronic in nature. Nearly 50 million Americans reportedly experience bouts of tinnitus, however there is currently a lack of an objective and efficient measure of this disorder. Residual inhibition (RI) is the temporary suppression of tinnitus which occurs after the presentation of stimuli with a pitch near the tinnitus percept, and typically lasts in the order of several seconds to minutes. Recent studies have suggested utilizing a forward masking paradigm that can produce RI as a potential assay for tinnitus. The objective of this study was to measure the effects of various stimulus parameters (masker frequency, duration, intensity, and probe delay interval) on neural correlates of residual inhibition, and their efficacy as a measure of tinnitus.

An auditory brainstem responses (ABR) forward masking (FM) paradigm was used to assess the presence of RI young adult CBA/CaJ mice. Tinnitus was induced via intraperitoneal injections of 250 mg/kg sodium salicylate, and compared to baseline measures in the same animals. Following verification of normal hearing levels, ABRs were collected for stimuli consisting of narrow-band FMs centered at 8, 12, 16, and 24 kHz, followed by a 70dB 5 ms probe tone of the same frequency. Masker signals were presented at 55 and 70dB for durations of 100 or 450ms, and followed by silent masker-probe intervals of 0, 10, 20, 40, or 80 ms, with a no-masker condition run for each paradigm.

Our previous work established that salicylate induced a consistent increase in the peak 2/peak 1 amplitude ratio for frequency stimuli near the tinnitus percept, which was also significantly correlated with behavioral measures of tinnitus. This study confirmed these findings in the no-masker condition, and found that the long duration masker eliminated this measure of central hyperactivity, indicative of residual inhibition. These effects were evident for the shorter masker-probe intervals when the masker was at 55dB, and for all time intervals when the masker was set to 70dB, suggesting a duration and intensity dependency. However, while other studies have found that residual inhibition could be measured using the overall root-mean-square measure of waveform variance, this could not be replicated in our study, indicating that this may not be a more efficient neural assay than those already in use.

Funding
Supported by NIH-NIA Grant P01 AG009524

PS 429

Neuroplasticity and Depression in an Animal Model of Tinnitus

Andrea Freemyer; Christopher Neal; Jennifer Nelson-Brantley; Hinrich Staecker; Dianne Durham
University of Kansas Medical Center

Background
Tinnitus is the perception of sound with no corresponding external stimulus. There are approximately 50 million individuals with tinnitus in the United States with roughly 2 million debilitated by the disorder. The etiology of tinnitus is not clear and there is no effective treatment. Tinnitus induced by hearing loss is common and often the result of exposure to loud noises. However, not all individuals with hearing loss present with tinnitus. Thus it is important to distinguish between hearing loss and hearing loss that corresponds with the onset of tinnitus. Mood disorders such as depression occur concomitantly with tinnitus. Noise damage has been shown to affect both auditory brain regions as well as limbic brain regions such as the hippocampus. We evaluated whether neuroplasticity and depression behavior play a role in the onset of tinnitus in the rat.

Methods:
We exposed male, Long-Evans rats to a 114 dB, 16 kHz pure tone for 1 hour. Auditory brainstem response was used to measure hearing loss. We utilized gap detection to determine if animals displayed tinnitus behavior. Depression behavior was measured using the sucrose preference test in rats before and after sound damage. We evaluated Doublecortin (DCX) labeling in the hippocampus of damaged and control rats as a measure of neuroplasticity.

Results and Conclusions
All sound exposed animals showed mild to moderate hearing loss across most frequencies. 30% of animals displayed behavioral evidence of tinnitus at one or more background frequencies, 30% displayed a trend toward tinnitus behavior, and 40% of animals showed no evidence of tinnitus behavior. Only 2 out of 10 animals showed behavioral evidence of anhedonia (decreased sucrose preference), while a surprising 50% showed an increase in sucrose consumed. In the remaining animals, there was no difference in baseline sucrose preference relative to post damage preference. Qualitative assessment of DCX labeling shows a bilateral decrease in DCX labeled cells in the dentate gyrus of the

hippocampus in sound damaged (n=7) animals relative to controls (n=4).

Our results for hearing loss and tinnitus behavior are in line with other published reports in both clinical and animal studies. This mild sound damage paradigm does not lead to anhedonia, a hallmark characteristic of depression in humans, but does negatively impact neuroplasticity in a limbic brain region.

Funding
Kansas Intellectual and Development Disabilities Research Center (NICHD HD02528) The Madison and Lila Self Graduate Fellowship at the University of Kansas

PS 430

Sensitivity and Specificity of Automatic Hearing Screening in a Swedish cohort

Åsa Sksjönsberg[1]; Catrine Heggen[1]; Meisere Jamil[1]; Ann-Christin Johnson[1]; Per Muhr[1]; Ulf Rosenhall[2]
[1]Karolinska Institutet; [2]Division of audiology

One-hundred participants (51 females and 49 males) were recruited to participate in this study at the same day that they had an appointment at the hearing clinic for undergoing clinical audiometry.

The age varied between 18 and 84 years with a mean age of 45.9 for females and 52.3 for males.

All participants underwent both clinical standardized audiometry performed by a skilled audiologist and automatized screening audiometry at the same day.

The participants were divided into four groups, dependent of type of hearing. Twenty-three had normal hearing thresholds, 40 had sensorineural hearing loss, and 19 had conductive hearing loss and 18 showed side discrepancy or deafness at one ear.

The Sensitivity for the automatized hearing screening test was between 86%-100%, while the specificity was between 56%-100%.

The group that were showing the poorest sensitivity (86 %) and specificity (56 %) was the group that consisted of persons with conductive hearing loss. The group consisting of subjects with sensorineural hearing loss showed the smallest variation in difference between the two methods.

The results from the present study shows that the automatized hearing screening test serve as an test method well suitable to screen for hearing loss but screening levels need to be selected with respect to the cause of screening and environmental factors. For patients with a large side discrepancy it is also necessary to consider the effect of over hearing.

Funding
This research was supported by grants from the Swedish Council for Working Life and Social Research, Contract number 2006-1526, AFA insurance.

PS 431

A Selective Averaging Process Underlies Sound Texture Perception

Richard McWalter[1]; Josh McDermott[2]
[1]DTU; [2]MIT

Background
The perception of sound textures – relatively stationary signals resulting from large numbers of acoustic events, as in rain, fire, or swarms of insects – present a largely unstudied example of temporal integration. Prior research suggests that textures are represented with statistics that capture their average acoustic properties (McDermott et al., 2013), raising the question of the means by which the averaging occurs. We characterized the averaging mechanism using synthetic signals whose statistical properties changed over time. We measured how far back in time the stimulus history exerted biasing effects on texture judgments, and tested whether discontinuities in the signal would alter the integration of the stimulus history.

Methods
Texture "gradients" – signals whose statistical properties change at some point during their history – were generated from an extended McDermott and Simoncelli (2011) synthesis system. Listeners were presented with two intervals: a texture gradient and a probe texture with constant statistical properties that varied across trials. Listeners were asked to compare the endpoint of the texture gradient to the probe and identify which interval was most similar to a previously heard reference texture. We compared performance for gradients that underwent a step at either 1 or 2.5 seconds from the end of the stimulus. In addition, some conditions included a 200 ms silent gap at the step location, to test whether the stimulus history would be discounted when demarcated by a salient change to the texture.

Results
Performance was biased by the presence of a step in the texture gradient, suggesting that stimulus history is incorporated into texture representations via an averaging process. The biasing effects were pronounced when the step occurred 1 second prior to the stimulus endpoint, but were substantially reduced when the step was pushed back to 2.5 seconds from the endpoint. An ideal observer model operating on statistics measured from the stimuli mirrored the psychophysical results when window durations of several seconds were used to compute statistics. However, the biasing effects of the step were also substantially reduced in conditions with a silent gap.

Conclusion
The results suggest that texture perception is mediated by an obligatory averaging window of several seconds, but that the averaging process is partially reset when there is evidence that a change occurred in a texture.

Funding
Technical University of Denmark to RM, McDonnell Scholar Award to JHM

PS 432

Predicting the Abilities of Normal Hearing and Hearing Impaired Subjects to Detect Tones in The Presence of White Noise

Miriam Furst; Naama Bartal; Chava Muchnik; Yael Henkin
Tel Aviv University

Hearing impairment is manifested by elevated pure tone thresholds and by reduced speech understanding especially in a presence of background noise. Existing models suggest that the possible underlying sources of hearing impairment are outer hair cells and inner hair cells dysfunction. These models, however, have not quantitatively estimated thus far, the ability of the hearing impaired to detect sounds in the presence of background noise.

We present a model that predicts subjects' ability to detect threshold of pure tones in quiet and in presence of background noise. The model includes a nonlinear one-dimensional time domain cochlear model followed by a synaptic model that simulates the instantaneous rate of the auditory nerve. In order to simulate the result of a threshold experiment, we assume that the brain behaves as an optimal processor, and its task is to estimate the sound's level on basis of the neural activity. Since, the auditory nerve response is considered as Non-Homogeneous-Poisson-Process, its probability density function depends only on the instantaneous rate. Thus, the information provided by the model is sufficient to derive the pure tones' threshold by calculating the Cramer Rao lower bound.

Hearing impairment is modeled by combination of outer and inner hair cells loss. Each type of cell is modeled by a single parameter along the cochlear partition. The model predicts that outer hair cell loss causes reduction in the basilar membrane displacement as a response to acoustic stimulus in comparison to normal performance. Inner hair cell loss exhibits reduction in the rate of the auditory nerve response followed by normal basilar membrane motion.

Pure tone thresholds were measured in quiet and in the presence of white noise at different low levels (below 55 dB HL) in normal hearing and hearing-impaired listeners. The effect of the white noise was different in the low frequency range (below 1 kHz) and high frequency range (above 2 kHz) in both groups. In normal hearing listeners, detectability of high frequencies in the presence of noise was enhanced compared to that of low frequencies. In hearing-impaired listeners, on the other hand, high-frequency thresholds in quiet were elevated and the low intensity noise did not affect thresholds. Detectability at the low frequency range was poorer in hearing-impaired compared to normal hearing listeners.

The model successfully predicted the performance of both groups of subjects by adjusting both outer and inner hair cells parameters.

Funding
ISF 563/12

PS 433

Interaction between AM and FM processing: Effects of age and hearing loss

Nihaad Paraouty[1]; Stephan D. Ewert[2]; Nicolas Wallaert[1]; Christian Lorenzi[1]
[1]Ecole Normale Supérieure; [2]Medizinische Physik and Cluster of Excellence Hearing4All, Universität Oldenburg

Background
Many psychophysical studies have attempted to disentangle the roles of temporal-envelope (ENV) and temporal fine-structure (TFS) cues in frequency modulation (FM) detection. Interference effects between amplitude modulation (AM) and FM have been used to assess the relative strengths of these cues in FM detection. These studies measured FM detection thresholds with and without an interfering AM intended to disrupt ENV cues resulting from cochlear filtering. The current study extends this interference paradigm by systematically assessing the effects of interfering AM on FM detection and conversely, interfering FM on AM detection.

Methods
FM and AM detection thresholds were measured at 40 dB sensation level for 3 groups of listeners: young normal-hearing (<30 years), older normal-hearing (40-65 years) and older hearing-impaired listeners (40-65 years; mild-moderate hearing loss at 500 Hz) for a carrier frequency of 500 Hz and a modulation rate of 5 Hz. In the AM detection task, FM at the same rate as the AM (5 Hz) was superimposed at varying FM depths. In the FM detection task, a 5 Hz-AM was superimposed at varying AM depths.

Frequency selectivity was also assessed for each listener using the notched-noise masking method. The thresholds for detecting a 500-Hz pure tone in a 600-Hz wide notched-noise centered at 500 Hz were measured using three spectral notch widths: 0, 150 and 300 Hz.

A simple model which used the output of an ENV-processing pathway was developed in order to support the behavioural data.

Results
The data shows clear perceptual interference effects between AM and FM. AM detection was degraded by interfering FM similarly across the 3 groups of listeners. Hence, the interference effect measured this way seems to be independent of age and hearing loss. FM detection was deteriorated by interfering AM for all groups of listeners and was also globally degraded by age and hearing loss. This interference effect was stronger in the hearing-impaired group.

Conclusion
The relative roles of ENV and TFS cues in modulation detection, as well as the effects of age and hearing loss on FM detection will be discussed in light of behavioural and modelled data.

Acknowledgements
Work supported by ANR-Heart, ANR-11-0001-02 PSL, ANR-10-LABX-0087 & Entendre-SAS.

Funding
Work supported by ANR-Heart, ANR-11-0001-02 PSL, ANR-10-LABX-0087 & Entendre-SAS.

PS 434

Effects of age on AM and FM detection

Nicolas Wallaert[1]; Brian C. J. Moore[2]; Christian Lorenzi[1]
[1]Ecole Normale Supérieure; [2]University of Cambridge

Amplitude-modulation (AM) and frequency-modulation (FM) detection thresholds were measured for a carrier frequency of 500 Hz and modulation rates of 2 and 20 Hz for young and older listeners with normal absolute thresholds below 3 kHz. FM detection thresholds were measured in the presence of uninformative AM in both intervals of a forced-choice trial, to disrupt the use of excitation-pattern cues. The number of modulation cycles ranged from 2 to 9. The results show that for both groups and for each number of modulation cycles, AM and FM detection thresholds were lower for the 2-Hz than for the 20-Hz rate. For both groups, AM and FM detection thresholds decreased with increasing number of modulation cycles, this effect being greater for AM than FM. Thresholds were higher for older than for younger listeners, especially for FM detection at 2 Hz. This result is interpreted as reflecting a detrimental effect of age on the use of temporal-fine-structure cues for low-rate FM detection. The effect of increasing number of modulation cycles was similar across groups for both AM and FM for the 2-Hz rate. For the 20-Hz rate, the older listeners showed a slightly greater effect of increasing number of modulation cycles than the younger listeners for both AM and FM. These findings suggest that ageing spares temporal integration of the cues used to detect AM and FM.

Funding
N. Wallaert was supported by a grant from Neurelec Oticon Medical. C. Lorenzi was supported by two grants from ANR (HEARFIN and HEART projects). This work was also supported by ANR-11-0001-02 PSL* and ANR-10-LABX-0087.

PS 435

Auditory Learning of Temporal Information for Normal-Hearing Listeners and Cochlear Implant Users

HiJee Kang[1]; Olivier Macherey[2]; Daniel Pressnitzer[1]
[1]Laboratoire des Systèmes Perceptifs, CNRS UMR 8248, École Normale Supérieure; [2]LMA-CNRS UPR 7501, Aix-Marseille Univ.

The ability to understand complex acoustic scenes depends partly on recognizing the sound sources comprising the acoustic mixture. The problem is especially acute for cochlear implant users, who have to learn or re-learn about sound sources with only limited acoustic cues. Here, we investigate one mechanism of perceptual learning that has been demonstrated for adult, normal-hearing listeners (Agus et al., 2010; Andrillon et al., in press). In these studies, repeated exposure to random sensory patterns led to rapid improvements in behavioral performance and associated neural coding. However, normal-hearing listeners can use both spectral and temporal cues to learn acoustic patterns, whereas cochlear implant patients must rely mostly on temporal cues.

We adapted the test design from previous study (Kang et al., 2015). A random time-interval sequence was generated by means of a train of high-pass clicks, here with Poisson-distributed random inter-click intervals. The average click rate was 10 Hz. Click trains had either random time intervals for a 2-s duration (Random click trains, C), or random time intervals for 1s with the same intervals immediately repeated for another 1s (Repeated click trains, RC). Finally, one specific RC (Reference repeated click trains, RefRC) re-occurred identically several times within a test block. Listeners were not informed about the across-trial re-occurrence of RefRC and simply asked to report within-trial repetitions. We observed that the RefRC led to higher behavioral performance, signaling perceptual learning of purely timing cues. Moreover, performance was higher for Poisson-distributed clicks than for uniformly-distributed clicks, for the same average rate. A similar paradigm will be run for cochlear implant users. First, the same click sequence will be transmitted through a subset of electrodes quasi-simultaneously, to restrict the cues to within-electrode temporal information. Second, different click sequences will be transmitted to different electrodes, to allow for cross-electrodes timing information.

The comparison between normal-hearing and cochlear-implant listeners has both practical and fundamental relevance. In particular, the neural mechanisms underlying plasticity may be very different for a purely temporal code compared to a full spectro-temporal code. If across-channel cues appear to facilitate perceptual learning, they would need to be better preserved by cochlear implants stimulation algorithms.

References

Agus, T.R., Thorpe, S.J., & Pressnitzer, D. (2010). Rapid formation of auditory memories: Insights from noise. Neuron, 66, 610-618.

Andrillon, T., Kouider, S., Agus, T., & Pressnitzer, D. (2015). Perceptual learning of acoustic noise generates memory-evoked potentials. Current Biology, in press.

Kang, HJ., Agus, T.R., & Pressnitzer, D. (2015). Auditory Memory for Time-Domain Information. 38th MidWinter Meeting of the Association for Research in Otolaryngology, p. 536, Baltimore, USA.

Funding
Korean government scholarship, ERG grant ADAM #295603

PS 436

Perceptual Learning of Feature Trajectories

Kevin Woods[1]; Josh McDermott[2]
[1]Harvard University; [2]Massachusetts Institute of Technology

Introduction

Auditory scenes often contain multiple sound sources, but typically one is of particular interest and must be selected for further processing. This 'cocktail party problem' is especially difficult when sources are similar and change over time (e.g., speakers of the same gender), since the sources may not

have features that consistently distinguish them from each other. Our recent work has shown that human listeners meet this challenge with a movable focus of attention that can track a source of interest as it changes over time (Woods and McDermott, 2015). While the sources used in this prior work took random trajectories through feature space, natural sound sources (such as speech) often exhibit statistical regularities which, if learned, might be expected to aid source separation and selection.

Methods
Simulated voices were synthesized that varied randomly in several feature dimensions (e.g. f0, f1, and f2). Listeners were presented with mixtures of two such time-varying sources, and were cued beforehand (with the starting portion of one voice) to attend to one of them. We measured listeners' ability to attentively track this cued voice by subsequently presenting them with the tail end of one voice. Their task was to judge whether this 'probe' segment belonged to the cued voice. Success at this task is intended to reflect tracking of the cued voice as it varied throughout the mixture. Critically, some trajectory shapes occurred repeatedly over the course of the experiment, with repeated versions of a trajectory related by transformation (time-dilation and transposition), as might occur in natural sound sources.

Results
Listeners exhibited rapid learning of feature trajectories, evident in better task performance for repeated compared to non-repeated trajectories. Learning occurred even though the learned trajectories were never exact repetitions and were never heard in isolation. The learning effect began within the first few presentations of the 'repeated' trajectory. A control experiment confirmed that this performance benefit was not due to memorization of a particular cue-probe relationship (indeed, the transformations imposed between 'repeated' versions of a trajectory were intended to destroy any such relationship).

Conclusion
Listeners learn the abstract 'shape' of an attentively tracked trajectory through a speech-relevant feature space, with improved tracking performance for trajectories that recur under transformation. Knowledge of trajectory regularities appears to benefit the tracking of target sources, and demonstrates one way in which familiarity aids the separation and selection of sound sources under challenging listening conditions.

Funding
This work was supported by a McDonnell Scholar award and NSF CAREER award to J.H.M.

PS 437

Evaluating the Efficacy of a Visually Guided Hearing Aid Using a Dynamic Question-Answer Task

Virginia Best; Timothy Streeter; Elin Roverud; Jayaganesh Swaminathan; Christine Mason; Gerald Kidd, Jr.
Boston University

The goal of this work is to evaluate the performance of a visually guided hearing aid (VGHA) using a realistic conversation-style task. The VGHA uses eye-gaze to steer a highly directional beamforming microphone array. Previous evaluations of the device have used static sound sources and trial-based sentence recall tasks that have limited ecological validity. Measuring the performance of the VGHA in situations that are dynamic and require comprehension of ongoing speech is crucial for a full characterization of its efficacy.

For this purpose, a corpus of 227 simple questions, and their answers, was recorded from 12 male and 12 female talkers. The questions cover five broad categories: days (e.g., "What day comes before Monday?"), months (e.g., "What month comes after April?"), arithmetic (e.g., "What is 2 plus 2?"), colors (e.g., "What color is the sky?"), and comparisons (e.g., "Which is bigger, an elephant or a mouse?"). Each question is associated with a single-word answer (e.g., "Tuesday", "May", "4", "Blue", "Elephant"). The materials can be used flexibly for different experimental purposes. In this first implementation, sequences of question-answer pairs are presented and listeners must determine whether the answer is correct or not. Responses are given as simple key presses, which are quick, easy to score, and do not require verbal responses or eye movements (which would interfere with ongoing listening and visual steering, respectively).

Here we present normative data collected on young listeners with normal hearing, who listened to each of the questions in speech-shaped noise at different signal-to-noise ratios. We also present an experiment designed to evaluate the VGHA under realistic conditions. The experiment uses sequences of 12 question-answer pairs that are spatialized and presented in a mixture of competing everyday conversations. Performance will be compared for a "dynamic" condition, in which the location of the questions and answers is varied randomly, to performance for a "fixed" condition in which the pairs are all presented from one location. This comparison will be made for both natural binaural listening conditions and for listening through the VGHA.

Funding
Work supported by NIDCD and AFOSR.

PS 438

Evaluating the Efficacy of a Visually-guided Hearing Aid Using a Dynamic Audio-visual Congruence Task

Elin Roverud; Virginia Best; Christine Mason; Timothy Streeter; Jayaganesh Swaminathan; Gerald Kidd, Jr.
Boston University

Listeners with hearing loss experience difficulty with understanding a particular talker in the presence of multiple competing talkers. The visually-guided hearing aid (VGHA) is a device being developed in our laboratory to aid these individuals with dynamic listening in multi-talker environments. This device uses highly directional amplification (a beamforming microphone array) directed by eye gaze. Currently, the efficacy of this device is being assessed in the laboratory using an audio-visual paradigm where the location of a target talker changes dynamically and unpredictably in the presence of masker talkers. The present study is an extension of a previous study [Kidd et al., 2015, ARO abstract], with methodological modifications to increase the reliability of the data.

Subjects are seated in a sound-proof booth in front of a computer screen, with auditory stimuli delivered through headphones. On each trial, a word is printed at one of three locations on the computer screen, which indicates the (virtual) location of the simultaneously-presented auditory target word. Auditory masker words are also presented at the other spatial locations. The subject's task is to follow the location of the printed word with their eyes, and press one of two buttons to indicate whether or not the auditory target matches the printed word on the screen. The subject's look direction is measured with an eye tracker, which controls the beamforming array (stimuli processed using impulse responses measured from a KEMAR manikin wearing the beamforming microphone array in a sound field). In a second condition, the beamforming information is high-pass filtered at 800 Hz and combined with natural binaural information (using impulse responses recorded through KEMAR's ears) low-pass filtered at 800 Hz – a "hybrid" condition. In a third condition, stimuli are presented with natural binaural cues only at all frequencies. The stimuli are either natural speech or speech processed with 6-channel vocoding to increase the overall difficulty. Accuracy as well as response times will be compared for stimuli processed with the beamformer, beamformer+binaural cues, and with only binaural cues, for natural and vocoded speech conditions.

Funding
NIH NIDCD and AFOSR

PS 439

Evaluating Cochlear Implants Using the STRIPES Test

Robert Carlyon[1]; Rosy Southwell[1]; John Deeks[1]; **Alan Archer-Boyd**[1]; Matt Davis[1]; Richard Turner[2]
[1]Medical Research Council; [2]University of Cambridge

A number of methods, e.g. novel speech-processing algorithms, for improving performance by cochlear implant (CI) users have been proposed. However, it has not always proved possible to demonstrate the benefits of these approaches. This may be due to the absence of a genuine benefit, or test limitations. Listeners have learnt the relationship between their regular speech processing strategy and speech segments, making it difficult to know if a new strategy is effective on the basis of a speech test, which could result in an underestimation of the benefits of a new method. This obstacle can be overcome by using psychophysical tests; however these typically require either spectral or temporal processing, but not both.

The STRIPES (Spectro-Temporal Ripple for Investigating Processor Effectiveness) test requires, like speech, both spectral and temporal processing to perform well. It is robust to learning effects and contains no recognisable phonemes, overcoming the problems associated with learned speech segments.

The test requires listeners to discriminate between stimuli whose spectrograms contain diagonal stripes that go up or down in frequency over time. The task is to detect which of three consecutive stimuli contains stripes of the opposite direction to the other two. The starting time is varied in successive presentations, requiring the listener to use the global, multi-channel perception of the stripe direction, not simply cues from a single spectro-temporal segment. The task difficulty is increased by increasing the thickness of the spectro-temporal stripes. As stripe thickness increases, the stimulus approaches a broadband noise and the stripe direction becomes more difficult to determine.

Results from normal-hearing listeners using a vocoder simulation show that performance decreases markedly as the number of channels decreases from 16 to 4, with a modest deterioration as the envelope cut-off is decreased from 300 to 4 Hz (16-channel vocoder). Pilot results from three Advanced Bionics CI users and with non-vocoded stimuli showed good performance with a 16-channel map and chance performance with a 4-channel map. However, a further three CI users performed at around chance using both 4- and 16- channel maps. Subsequent changes to the stimuli and the testing paradigm have identified possible reasons for this poor performance, and we will present results from a modified version of the test obtained with a larger number of CI patients.

We conclude that the STRIPES test has the potential to enable fast, reliable verification and optimization of new speech-processing and fitting algorithms for CIs.

Funding
Work supported by the Baroness de Turckheim fund, MRC programme number MC-A060-5PQ70, and Advanced Bionics. Author AAB is also funded by an Action on Hearing Loss travel grant

PS 440

Auditory attention and source segregation in children with cochlear implants or normal hearing

Sara Misurelli[1]; Alan Kan[1]; Matthew Goupell[2]; Ruth Litovsky[1]
[1]University of Wisconsin-Madison; [2]University of Maryland-College Park

The ability to attend to target speech while simultaneously ignoring irrelevant information is an important skill, particularly for children who spend the majority of their day in noisy educational environments. Intelligibility of target speech improves as a result of spatial unmasking in the free field for normal hearing (NH) children. Conversely, children who use bilateral cochlear implants (BiCIs) demonstrate little to no benefit in similar situations, although these children have reduced access to spatial cues, which may not account for the poor spatial unmasking observed. The first goal of this study was therefore to examine the potential contribution of a non-spatial phenomenon: auditory attention. In addition, because very little is known about this phenomenon in NH children, the developmental trajectory of unmasking due to auditory attention was studied.

Children 7-17yrs with NH and BiCIs were tested. The task was to identify target speech in the presence of interfering speech (different-sex from target speech) at various signal-to-noise ratios. Stimuli were presented to NH children via headphones and to children with BiCIs via direct audio input to their speech processors. Instructions were to attend either to the right or left ear in four different conditions: (1) no interferer, (2) contralateral interferer, (3) ipsilateral interferer, and (4) ipsilateral+contralateral interferer.

Children with BiCIs demonstrated a large benefit from contralateral unmasking (conditions 2 vs. 3). The majority of children with BiCIs demonstrated only a small difference in threshold between conditions 1/2, indicating that they are able to attend to the target when the interferer is in the opposite ear. While NH children have the same ability to benefit from directed auditory attention in the above-mentioned conditions, they showed less variability than the children with BiCIs. Comparison of conditions 3/4 was aimed at determining whether children could fuse a bilaterally presented interferer so that its perception in the center of the head would result in perceived spatial separation from the unilateral target. However, neither group showed unmasking with this condition. Finally, regarding the developmental trajectory in NH children, results thus far suggest that adding an interferer in the ipsilateral or contralateral ear has more adverse effects for younger than older children. Together, results suggest that when children with BiCIs have weak or absent spatial unmasking, this may not be due to the inability to attend to target speech. Hence, findings in the free field may indicate reduced spatial unmasking due to poor encoding of spatial cues.

Funding
Funded by NIH-NIDCD (R01DC003083 and R01DC008365) and NIH-NICHD (P30HD03352)

PS 441

Musicians are better than non-musicians in overcoming the limitation of spectral resolution and noise masking

Fawen Zhang[1]; Chun Liang[1]; Brian Earl[1]; Qian-jie Fu[2]
[1]University of Cincinnati; [2]University of California, Los Angeles

Both speech and music contain rich changes in pitch cues, which convey melodic, prosodic and semantic information. Unfortunately, due to the limited spectral resolution transmitted by the cochlear implant (CI), CI users generally have poor pitch perception, thus making speech understanding in noise and music perception difficult (McDermott, 2004). It is well known that musicians, who experience long-term auditory training with music stimuli, perform better on pitch perception tasks than non-musicians and this musician benefit has been reported to positively affect speech perception in noise (Schön et al., 2004; Fuller et al., 2014). Therefore, the comparison between musicians and non-musicians provides a unique approach for studying music training effects, which may be informative of how CI subjects should be trained to improve their performance in pitch-based tasks. The goal of this study was to determine whether musicians still perform better in detecting pitch changes even with degraded spectral resolution (i.e., CI simulation), or even under more challenging conditions such as CI simulations with a noise background. Twenty-four young normal hearing listeners including 12 musicians and 12 non-musicians participated. The stimuli were a series of tones of approximately 1 sec duration containing upward pitch changes at 0.5 sec after the tone onset. The base frequency examined was 160 Hz (similar to the F0 of woman voice). A two-interval, two-alternative forced-choice paradigm was used to measure the minimum pitch change that could be detected by the subjects. All subjects underwent pitch detection threshold tests with 6 stimulus conditions: tones containing pitch changes (Stim 1), tones containing pitch changes masked by high-level noise (Stim 2), tones containing pitch changes masked by low-level noise (Stim 3), and corresponding 8-ch vocoded versions of these 3 stimuli (Stim 4, 5, and 6). Results showed that musicians significantly outperformed non-musicians in Stim 1, 2, 4, and 5. Results showed that musicians do have advantages over non-musicians in detecting pitch changes in various conditions from the easiest (Stim 1) to the most challenging listening conditions (Stim 5), this may indicate that musicians have better bottom-up and top-down processes than non-musicians for pitch processing. The results indicate the importance of auditory training for maximizing pitch perception through the CI.

PS 442

Toward a Systematic Analysis of Binaural Pitch Averaging Trends in Hearing Impaired Listeners

Yonghee Oh; Lina Reiss
Oregon Health & Science University

Background

Bimodal cochlear implant (CI) users exhibit broad dichotic pitch fusion ranges, in which binaural fusion occurs over a broad range of pitch differences between the ears (Reiss et al., JARO 2014). Further, this fusion often leads to averaging of the different pitches perceived in the two ears. The current study was designed to systematically measure these pitch averaging phenomena and give insight into how hearing-impaired listeners might generally integrate spectral information between ears. This study focused on pitch averaging trends in bilateral hearing aid (HA) users and bimodal CI users with broad fusion ranges.

Methods

Nine HA users and four bimodal CI users were tested on a set of experiments: interaural pitch matching, dichotic fusion range measurement, fusion pitch matching, and frequency discrimination. Prior to all experiments, loudness was sequentially balanced at comfortable levels within/across the ears. In the main experiment of fusion pitch matching, the reference fused stimulus pair consisted of a constant pure tone (HA users) or electrode (CI users) in a designated "reference" ear presented simultaneously with a pure tone (selected within subject's fusion range) in the contralateral ear. The comparison stimulus consisted of a pure tone presented sequentially to the contralateral ear, with frequency varied pseudo-randomly across trials. Subjects were asked to choose the stimulus with the higher pitch.

Results

All HA users showed the following trends in their fusion pitch matching results: 1) Dominance of the lower pitch, in which the perceived binaural pitch of the fused tone was determined by the component with the lower pitch. 2) Pitch averaging, in which the fusion pitch was a weighted average of the pitches of the two components. The pitch averaging occurred when the paired tone was in a range of 0.5 - 1 octaves around the reference tone. Switching references between the ears showed similar fusion pitch averaging trends. Preliminary findings from four bimodal CI users also suggest the presence of both dominance and averaging regions in this group.

Conclusions

In hearing impaired listeners with broad fusion ranges, weighting of each component in a fused pair varies with the pitch difference between components. These findings suggest that binaural spectral integration of broadband sounds such as speech in hearing-impaired listeners is more complex than previously thought.

Funding

This work was supported by NIH-NIDCD grant R01 DC013307.

PS 443

Binaural Pitch Fusion in Normal-Hearing Listeners Varies as a Function of Sound Level

Sean Anderson[1]; Yonghee Oh[2]; Lina Reiss[2]
[1]University of Wisconsin-Madison; [2]Oregon Health and Science University

Unlike normal-hearing (NH) listeners, hearing-impaired listeners who use cochlear implants and/or hearing aids exhibit broad pitch fusion, i.e. they fuse together two tones over a broad range of interaural frequency differences when presented simultaneously and independently to each ear (Reiss et al., 2014). The reason for this abnormally broad binaural pitch fusion in hearing-impaired listeners is unclear. The purpose of the present study was to investigate whether overall sound level affects binaural pitch fusion in NH listeners. We hypothesized that increasing level would result in broader fusion, which may explain the broader fusion seen in hearing-impaired listeners. It was further hypothesized that changes in pitch mismatches between the ears with level would account for changes in fusion with level.

Six NH listeners were tested on binaural pitch fusion using a one-interval, two-alternative forced-choice (1I-2AFC) discrimination task. In this task, a constant 3 kHz frequency pure tone was presented to one (reference) ear simultaneously with a variable frequency pure tone in the other (comparison) ear using a method of constants procedure. Subjects reported whether they heard one or two distinct pitches. The pitch-match frequency for the comparison ear relative to the reference ear was also estimated using a 2I-2AFC discrimination task. The constant (3 kHz) reference ear and variable frequency comparison ear stimulus were presented sequentially, and listeners chose the tone of higher pitch. Stimuli were presented at 5 sensation levels (55, 61, 68, 75, and 81 phon), and experimental runs were blocked by level and counterbalanced.

Results from the binaural pitch fusion task indicated variable trends with sound level. Changes in fusion range across levels were on average 573 Hz or 0.27 octaves. Pitch matches were also variable with level, but not such that they were consistent with the binaural pitch fusion task.

The results suggest that the binaural pitch fusion ranges in NH listeners can change as a function of level, but the changes are neither consistent across subjects nor large enough to explain the broad fusion ranges of 3-4 octaves observed in hearing-impaired listeners. Further, changes in interaural pitch mismatches were not predictive of changes in binaural pitch fusion ranges as a function of level, implying that monaural pitch perception and binaural pitch fusion are mediated by different mechanisms.

Funding

This work was supported by NIH-NIDCD grant R01 DC013307.

PS 444

'Hidden Hearing Loss' and Intense Music Exposure in Humans

John Grose; Emily Buss; Joseph Hall IV; Joseph Hall III
University of North Carolina at Chapel Hill

Background

Recent animal work has shown that noise exposure sufficient to cause temporary, but not permanent, shifts in absolute threshold can result in permanent damage to the peripheral auditory system [cf., Kujawa & Liberman (2015), Hearing Research, Epub ahead of print]. The noise-induced pathophysiology renders the neural substrate depleted or dysfunctional but spares sufficient elements to support normal audiometric sensitivity. Evidence of such neurodegeneration is therefore more likely to be found for suprathreshold processing of complex stimuli. The purpose of this project is to test this hypothesis by measuring effects of long-term exposure to intense music on suprathreshold auditory processing in humans with normal audiograms.

Method

Subjects comprise audiometrically normal young adult listeners who regularly attend loud music venues/events. Sound levels at these events can cause temporary threshold shifts in typical listeners. The experimental subjects, and their age-matched controls, are tested on a battery of psychophysical, electrophysiological, and speech tests, including (1) spectral modulation detection as a function of level and frequency region; (2) temporal modulation detection as a function of level and signal-to-noise ratio (SNR); (3) frequency dependence of interaural phase discrimination (IPD); (4) auditory brainstem response (ABR) Wave I input/output function; (5) envelope following response (EFR) as a function of modulation depth; (6) acoustic change complex (ACC) elicited by interaural phase inversions; (7) performance-intensity function for filtered monosyllabic words; and (8) SNR for threshold sentence recognition as a function of overall level.

Results

Results to date have focused primarily on the psychophysical testing. Spectral modulation detection remains relatively stable across level (40, 60, 80 dB SPL) and frequency (one-octave bands centered at 1.4, 3.0, 4.2 kHz), although there appears to be some separation at the higher level. In terms of temporal modulation detection, sensitivity to an 80-Hz modulation carried by a 4243-Hz tone is markedly worse in background noise (+10 dB SNR) than in quiet, but shows some level dependence (70 vs. 85 dB SPL). For IPD, the highest frequency at which a diotic signal can be distinguished from an interaurally out-of-phase signal is in the 1200-Hz region. (Results from speech and electrophysiological testing will also be reported.)

Conclusions

Findings to date suggest considerable overlap between the experimental and control groups. One emerging factor that requires additional control is that many of the subjects in the experimental group are themselves musicians. It is possible that these listeners have an inherently more 'practiced ear' in complex listening tasks.

Funding

Work funded by the Hearing Industry Research Consortium

PS 445

Notch signaling acts as a negative regulator for the proliferation of progenitors in mammalian cochleae

Wenyan Li[1]; Hui Jiang[2]; Wenli Ni[1]; Jingfang Wu[1]; Huawei Li[1]
[1]Affiliated Eye and Ear, Nose, Throat Hospital of Fudan University; [2]Jinshan Hospital of Fudan University

Inner ear sensory epithelium consists of a mosaic of hair cells and supporting cells, generated from the same progenitors in the prosensory domain during development. It has been reported that the formation of the mosaic HC and SC pattern is mediated by lateral inhibition through the Notch signaling pathway, and Wnt-responsive leucine-rich repeat-containing G protein-coupled receptor 5 (Lgr5+) cells are the progenitors with the capacity to regenerate HCs under certain condition. As two fundamental pathways that regulate the cell-fate determination and the proliferation in the inner ear, the relationship between Wnt and Notch is largely unknown. We show that Notch1 inhibition initiates proliferation of supporting cells (SCs) and mitotic regeneration of HCs in E14.5, as well as in neonatal mouse cochlea. Through lineage tracing, we identify that a majority of the proliferating SCs and mitotic-generated HCs induced by Notch inhibition are derived from the Wnt-responsive leucine-rich repeat-containing G protein-coupled receptor 5 (Lgr5+) progenitor cells. We conclude that Notch signaling acts as a negative regulator for the proliferation of progenitors in mammalian cochleae and plays an important role on maintaining the homeostasis of cochlear sensory epithelium on cell number and structures, which may provide a new route for the hair cell regeneration process in mammalian cochleae through manipulating Notch and Wnt signaling.

PS 446

Single-cell mRNA-Seq of Supporting Cells in the Adult Mammalian Cochlea: Establishing a Basis for Targeting the Adult Inner Ear Supporting Cell

Michael Hoa; Robert Morell; Matthew Kelley
NIDCD/NIH

Introduction

Previous work in animal models has demonstrated the potential for immature supporting cells to serve as progenitors for new hair cells. This work has spurred interest in transdifferentiating surviving supporting cells into hair cells in the human cochlea. There has been some limited success with this approach in perinatal and juvenile mammalian organ of Corti supporting cells. In contrast, attempts at transdifferentiating adult mammalian supporting cells have been unsuccessful. Current strategies target

supporting cells in a non-specific manner. Understanding the transcriptome profile of adult cochlear supporting cells will aid in developing more specific targeting strategies. Recent work has demonstrated the utility of single-cell mRNA-Seq to characterize cellular heterogeneity in the neonatal organ of Corti. Utilizing this technique, we sought to characterize the transcriptome profile of subpopulations of adult cochlear supporting cells.

Method
Cochleae were dissected from Tg(Lfng-EGFP) adult mice (where most cochlear supporting cells express EGFP), dissociated to a single cell suspension, and FACS-purified to enrich the samples for EGFP-positive cochlear supporting cells. Isolated supporting cells were then captured using a Fluidigm C1 microfluidics platform. Isolated supporting cells were lysed, reverse-transcribed and amplified within each capture chamber. The amplified cDNA from each cell was converted to a barcoded Nextera DNA library and sequenced on an Illumina HiSeq. Following mapping and quality assessment, relative expression profiles of individual cells were examined by principal component analysis and hierarchical clustering using the Singular Analysis package within R software. Potential supporting cell subpopulations were validated based on expression of both known and newly-identified cell-specific markers.

Results
Analysis of single adult cochlear supporting cells demonstrates a distinct transcriptome profile from neonatal cochlear supporting cells. Correlation with limited known adult cochlear supporting cell markers and newly identified adult cochlear supporting cell markers reveals potential genes to use for specific targeting of adult supporting cell subpopulations.

Conclusions
Adult cochlear supporting cell transcriptome profiles will serve as a resource for future attempts at targeting adult mammalian cochlear supporting cells for hair cell regeneration.

Funding
Funding provided by the NIDCD Intramural Research Program to M.H. (DC000088-01)

PS 447

Capacity of a New Gamma-Secretase Inhibitor for Hair Cell Induction from Supporting Cells in Mouse Cochleae

Takayuki Nakagawa; Takushi Miyoshi; Norio Yamamoto; Juichi Ito
Kyoto University

Background
Sensorineural hearing loss (SNHL) is the most common disability in the world, and the loss of sensory hair cells in the cochlea is one of the major causes for SNHL. Therefore, regeneration of cochlear hair cells has been a main topic in the field of inner ear biology. Recently, pharmacological manipulation of Notch signalling has gained considerable attention as a strategy for induction of hair cells from supporting cells. Yamamoto et al. (2006) demonstrated hair cell generation from supporting cells in neonatal cochleae by inhibition of Notch signalling genetically or pharmacologically. Mizutari et al. (reported that LY411575, a gamma secretase inhibitor, induced robust generation of hair cells from supporting cells (2013). In addition, they demonstrated hearing recovery by local application of LY411575 in damaged cochleae due to noise exposure (Mizutari, 2013).

Methods
In the current study, aiming future clinical application, we examined the capacity of a new gamma secretase inhibitor for hair cell induction from supporting cells in embryonic and neonatal cochlear explants.

Results
In E13.5 cochlear explants, a new compound exhibited the capacity for hair cell induction from supporting cells in a similar level to LY411575. A new compound showed a dose-dependent increase of hair cell numbers in E13.5 cochleae. These findings indicated that a new compound had a similar activity of transdifferentiation of supporting cells into hair cells. Based on this, the potential of a new compound for hair cell induction was examined using P1 cochlear explants. As results, no significant increase of hair cell numbers was observed in cochlear explants by treatment of either a new compound or LY411575. We also investigated the potential of a new compound using P1 cochlear explants damaged by gentamicin. In cochlear specimens damaged by gentamicin, no significant increase of hair cell numbers was found in either new compound- or LY411575-treated cochleae, although ectopic hair cells were found in both conditions.

Conclusion
These findings suggest that treatment with a gamma secretase inhibitor may not be sufficient for hair cell induction in cochleae after birth.

Funding
This work was supported by a Grant-in-Aid for Scientific Research (S) from the Ministry of Education, Culture, Sports, Science and Technology in Japan, a Grant-in Aid for Scientific Research (C) from the Japan Society for the Promotion of Science.

PS 448

Differential Ability of Supporting Cell Subtypes to Regenerate Hair Cells in the Neonatal Mouse Cochlea

Melissa McGovern; Michelle Randle; Kaley Graves-Ramsey; Brandon Cox
Southern Illinois University, School of Medicine

In the mammalian cochlea, five major groups of supporting cell (SC) subtypes reside in close proximity to hair cells (HCs) and may have the potential to regenerate HC after damage. These subtypes include the greater epithelial ridge, inner phalangeal/border cells, pillar cells, Deiters' cells, and Hensen/Claudius cells. During embryonic development,

progenitor cells differentiate into HCs or one of the SC subtypes by Notch-mediated lateral inhibition. In the neonatal mouse cochlea, many studies have shown that inhibition of Notch signaling allows SCs to convert into HCs in both normal undamaged cochleae, as well as in drug-damaged cochlear explants. This mechanism is also implicated during spontaneous HC regeneration that occurs in non-mammalian vertebrates. We and others have recently observed that spontaneous HC regeneration can also occur in the neonatal mouse cochlea. However, little is known about the molecular mechanism or the SC subtypes which act as the source of regenerated HCs. In the neonatal mouse cochlea, HCs were killed *in vivo* by Cre-mediated expression of diphtheria toxin fragment A (DTA) using Atoh1-CreER+::Rosa26-loxP-Stop-loxP-DTA$^{+/f}$ mice (Atoh1-DTA) and tamoxifen administration at birth. Subsequently, SCs formed new HCs by either direct transdifferentiation or mitotic regeneration. To investigate whether the Notch signaling pathway was involved in HC regeneration in the neonatal mouse cochlea, we measured the expression of the Notch target gene, Hes5, using a knock-in Hes5^{nlsLacZ} reporter mouse. When analyzing the total SC population, there was no significant difference in the number of Hes5-LacZ+ cells after HC damage. However, when only Deiters' cells (DCs) and pillar cells (PCs) were quantified, the number of Hes5-LacZ+ cells was significantly reduced in Atoh1-DTA:: Hes5^{nlsLacZ} cochleae compared to controls without HC damage. In addition the number of Sox2+ cells in the DC/PC population increased in Atoh1-DTA::Hes5^{nlsLacZ} cochleae. Therefore, we hypothesize that SC subtypes have differential abilities to regenerate HC after damage. To investigate which subtypes are capable of regenerating HCs, we are currently fate-mapping SC subtypes by combining Pou4f3^{DTR} mice, where injection of diphtheria toxin will induce HC-specific damage, with several CreER lines that target different SC subtypes. Based on our Hes5 results, we predict that DC and PCs will be the main progenitor cells for HC regeneration.

Funding
Supported by the Office of Naval Research (N000141310569), Office of the Assistant Secretary of Defense for Health Affairs (W81XWH-15-1-0475), and the National Center for Research Resources-Health (S10RR027716).

PS 449

The Mature Cochlea Does Not Proliferate or Regenerate in Response to Wnt/Beta-Catenin Activation

Patrick Atkinson; Juleh Eide; Alan Cheng
Stanford University

Background
Canonical Wnt signaling plays diverse roles in the developing inner ear including otic induction, proliferation, prosensory cell specification, and hair cell differentiation. Stabilization of

β-catenin, the central mediator of canonical Wnt signaling, induces proliferation of prosensory cells and overproduction of hair cells during development. In the neonatal cochlea, stabilization of β-catenin also leads to proliferation of supporting cells and ectopic hair cell formation. Further, after hair cell loss in the neonatal mouse utricle, supporting cells modestly regenerate hair cells via proliferation and transdifferentiation. The current study aims to determine whether the stabilization of β-catenin can similarly induce proliferation and regeneration in the damaged mature cochlea.

Methods
To assess the effects of activating the Wnt pathway in the mature cochlea, the transgenic mice lines *Fgfr3-icre*; *Rosa26R-tdTomato; Pou4f3-DTR* and *Catnnb-flox(exon3)* were used. Postnatal-day-21 (P21) mice were deafened either with a combination of the aminoglycoside sisomicin and the loop-diuretic furosemide or using transgenic Pou4f3-DTR mice, where hair cells were selectively ablated with diphtheria toxin. Cre induction was also performed at P21 via a single tamoxifen injection. To assess proliferation EdU was injected at P23, 24 and 25. Animals underwent hearing testing at P28 after which they were sacrificed and cochleae collected for histologic examination.

Results
Both the sisomicin and furosemide treatment or diphtheria toxin (in mice expressing the Pou4f3-DTR allele) at P21 resulted in profound hearing loss across all frequencies at P28 as compared to littermate controls (one-way ANOVA, $p<0.05$). Histological examination demonstrated a significant loss of hair cells across all turns of the cochlea. In comparison to saline controls, sisomicin and furosemide treatment resulted in a significant loss of outer hair cells (36.8 ± 2.4 vs. 0.3 ± 0.7 hair cells/100 µm, t-test, $p<0.05$). Diphtheria toxin treatment primarily affected the inner hair cells (11.8 ± 0.8 vs. 3.5 ± 1.4 hair cells/100 µm, t-test $p<0.05$). Tamoxifen injection led to tdTomato-labeling in 72% ± 10.6 of supporting cells in all cochlear turns. Using this regimen to stabilize β-catenin in supporting cells, we failed to detect any EdU uptake or increase in hair cell number in the mature cochlea one week after damage (P28).

Conclusions
Increasing canonical Wnt signaling through the stabilization of β-catenin does not promote supporting cell proliferation or hair cell formation in the mature mouse cochlea after damage.

Funding
Department of Defense W81XWH-14-1-0517 NICDC/NIH RO1DC013910 Akiko Yamazaki and Jerry Yang Faculty Scholarship

PS 450

Canonical Wnt Signaling Regulates Auditory Hair Cell Regeneration in Birds

Jennifer Stone[1]; Sophie Seo[1]; David Karera[1]; JiaLin Shang[1]; Michael Lovett[2]; Mark Warchol[3]
[1]University of Washington; [2]Imperial College London; [3]Washington University

Ototoxic injury to the auditory epithelium of birds (basilar papilla; BP) leads to hair cell (HC) death. In response, supporting cells (SCs) divide or phenotypically convert into replacement HCs,

resulting in functional recovery. Although we understand the basic cellular processes involved in HC regeneration, we know little about its molecular regulation. Canonical Wnt signaling controls cell proliferation, differentiation, and survival in the developing inner ear and during HC regeneration in zebra fish neuromasts. We have examined the roles of canonical Wnt signaling in HC regeneration in the chicken BP after aminoglycoside ototoxicity in vitro.

Cochlear ducts were explanted from post-hatch White Leghorn chickens, cultured in streptomycin for 1-2 days to kill HCs, and maintained in culture for various periods after streptomycin treatment. Additional cochlear ducts (controls) were maintained without streptomycin for corresponding periods. We used RNAseq and in situ hybridization to assess expression of transcripts for canonical Wnt pathway genes in control and streptomycin-treated BPs. We also transfected SCs in streptomycin-treated cochlear ducts with a fluorescent TCF/LEF reporter in order to assess activation of canonical Wnt signaling. We also activated canonical Wnt signaling by blocking GSK-3b using two agents – BIO and CHIR – and assessed effects on transcripts for Atoh1 (an early marker of HC differentiation), SC division, and HC differentiation.

Several Wnt pathway receptors (Fzd2,3,7,9,10), ligands (Wnt5A,5b,7b, 9a), target genes (Lgr5, axin2, Vefga, Bmp4), and extracellular antagonists (Sfrp1, 2, Dkk3, Fzdb) were transcribed in undamaged BPs, and their transcription varied during the course of HC damage and regeneration. SCs showed TCF/Lef activity during early stages of regeneration, and regenerated HCs showed activity during later stages of regeneration. Short treatments (2-3 days)with BIO or CHIR (1-5 μM) caused elevated TCF/Lef activity, reduced expression of Atoh1, and increased SC division. We are currently examining effects of BIO and CHIR on the numbers of regenerated HCs in later cultures.

In summary, we found that canonical Wnt signaling is activated in the auditory epithelium of chickens after HC damage. Augmentation of Wnt signaling by GSK-3b inhibition increases SC division and may antagonize HC differentiation.

Funding
Hearing Health Foundation (Hearing Regeneration Project) to JS, MW, and ML.

PS 451

Supporting Cells Generate Type II Hair Cells in Undamaged and Damaged Adult Mouse Utricles

Stephanie Bucks[1]; Brandon Cox[2]; Brittany Vlosich[1]; James Manning[1]; Tot Nguyen[1]; Jennifer Stone[1]
[1]University of Washington; [2]Southern Illinois University School of Medicine

In utricles of adult Pou4f3^{DTR} mice, approximately one half of the type II hair cell (HC) population is regenerated after diphtheria toxin-mediated HC ablation. Here, we assessed if type II HCs are added to utricles under normal conditions (without HC damage) and if the rate of HC addition increases after HC ablation. We also tested if utricular type II HCs convert into type I HCs under normal conditions.

In undamaged adult mice, we assessed HC addition in two ways. First, we examined utricles for immature HC bundles using antibodies to protocadherin15-CD2. Second, we fate-mapped supporting cells (SCs) to determine if they convert into HCs under normal conditions. We used a SC-specific inducible Cre mouse line (Plp-CreER^{T2}) bred to ROSA26$^{CAG\text{-}tdTomato}$ mice and injected tamoxifen to induce tdTomato expression in SCs. Utricles were analyzed at 1, 4, 10, and 15 weeks post-tamoxifen, to determine if any HCs were tdTomato-positive. We used a similar approach to fate-map SCs in adult mice after HC damage, using Plp-CreER^{T2}::ROSA26$^{CAG\text{-}tdTomato}$::Pou4f3^{DTR} mice. Finally, in undamaged adult mice, we fate-mapped a subset of type II HCs over 14 weeks to determine if type II HCs transdifferentiate into type I HCs during that time. We used Atoh1-CreER^{TM} mice bred to ROSA26$^{CAG\text{-}tdTomato}$ mice, which selectively labels half the type II HC population after tamoxifen at 6 weeks.

In three strains of undamaged adult mice, we detected 3-32 immature stereociliary bundles per utricle. Using SC fate-mapping in undamaged mice, we found the average number of SC-derived HCs per utricle increased from 17 to 48 over 14 weeks, and new HCs were predominantly type II. Following HC damage to Plp-CreER^{T2}::ROSA26$^{CAG\text{-}tdTomato}$::Pou4f3^{DTR} mice, the rate of SC to type II HC transdifferentiation was increased 3-fold during the first 3 weeks after damage compared to the rate of conversion without damage. Using HC fate-mapping in undamaged mice, we found that 92% of the labeled HCs were type II at 7 weeks of age. Neither this proportion nor the position of type II HCs changed between 7 and 21 weeks of age, suggesting this subpopulation of type II HCs is stable during early adulthood.

We demonstrated that a slow rate of type II HC addition occurs in the undamaged utricles of adult mice, and type II HCs with Atoh1 enhancer activity do not convert into type I HCs during the period we examined. We also found that the rate of HC addition increases after HC ablation.

Funding
This research was funded by the NIH (F32 DC013695 to SAB, R01 DC013771 to JSS, and P30 DC04661 to the UW Research Core Center) and the Office of Naval Research (N000141310569 to BCC).

PS 452

p53 and Regenerative Potential of Auditory Supporting Cells

Maarja Laos; Anni Herranen; Tommi Anttonen; Ulla Pirvola
University of Helsinki

The capacity of the mammalian inner ear supporting cells (SCs) to respond to cell cycle manipulations, a step often included in the development of regenerative approaches to replace lost hair cells (HCs), declines with age. We have previously demonstrated that upon forced cell cycle re-entry, SCs of the juvenile cochlea upregulate the tumour suppressor p53, fail to complete the cell cycle and often show a death-

prone phenotype. In contrast, cell cycle reactivated SCs of the juvenile utricle do not upregulate p53 and are able to mitose (Laos et al., Aging 2014). These results suggested that p53 might be a negative regulator of regenerative plasticity, particularly in the cochlea. Currently only little is known about the restrictions hindering regenerative interventions in the inner ear. Data in other tissues point to the importance of p53 in antagonizing regeneration, e.g. in the case of natural regeneration of the amputated salamander limb. To investigate the function of p53 in the postnatal organ of Corti, we employed a loss-of-function mouse model where p53 was ablated from the embryonic stages onward in the otic epithelium and a gain-of-function model where a negative regulator of p53 was inactivated in auditory SCs in a conditional and inducible manner. p53 inactivation did not cause detectable alterations in the inner ear morphology. Also the cell cycle and survival status of the cells of the organ of Corti were unaltered. Furthermore, SCs in p53-inactivated explants were refractory to proliferation-promoting conditions. When ototoxic lesion was applied to these explants, no proliferative response was seen. We continued to study the impact of p53 upregulation on SCs, induced by genetic interventions. Interestingly, p53 upregulation caused a distinct defect in SC differentiation. The failure of proper differentiation led to apoptotic death of SCs and, importantly, to a secondary loss of adjacent HCs. Our data suggest that p53 inactivation does not increase regenerative plasticity in the organ of Corti. However, our results show that preventing the increase in p53 levels is critical for normal development and survival of SCs and, secondarily, for HC survival. These results are consistent with prior data showing devastating effects of pharmacological p53 upregulation on auditory HC survival (Sulg et al., J. Neurochem. 2010). Cell cycle manipulations are often accompanied by an increase in p53 levels. Our data suggest that keeping p53 in check is important for the success in regenerative attempts and for homeostatic functions in the auditory organ.

Funding
Funded by Sohlberg and Paulo Foundations

PS 453

Co-manipulation of p27Kip1 and Atoh1 Reveals Roles for Gata3 and Pou4f3 in Auditory Hair Cell Regeneration in the Mature Mouse Cochlea

Bradley Walters; Emily Coak; Grace Bailey; Bryan Kuo; Jian Zuo
St. Jude Children's Research Hospital

Ectopic expression of Atoh1 has been shown to convert cochlear supporting cells into hair-cell-like cells. However, the ability to induce this regenerative phenotype in genetic mouse models declines abruptly after postnatal maturation. Here we ectopically expressed Atoh1 while, simultaneously, we conditionally deleted p27Kip1 from pillar and Deiters cells (PCs and DCs) in mature mouse cochleae (≥ P28), *in vivo*. An HA tag on the Atoh1 transgene (Atoh1-HA) allowed us to fate map the supporting cells that were manipulated, and check for the upregulation of hair cell specific markers (Pou4f3, myosinVI, myosinVIIa, parvalbumin, calbindin) in these cells. Consistent with our previously published results, ectopic expression of Atoh1 alone in the p27Kip1$^{+/+}$ littermates resulted in little to no upregulation of hair cell specific markers in HA positive supporting cells. Co-manipulation of p27Kip1 and Atoh1, however, yielded significantly greater numbers of HA positive supporting cells that co-expressed known hair cell markers (e.g. ~2500 PCs and DCs per cochlea that upregulated Pou4f3). Furthermore, following continuous treatment of the mice with 5-bromo-2'-deoxyuridine (BrdU) for a two week period after induction, we were unable to detect any BrdU positive supporting cells or hair cells suggesting that this enhanced conversion occurs independently of cell proliferation. Rather we found that as the mice age, PCs and DCs lose the expression of Gata3, which is a known co-factor for Atoh1. Immunostaining for Gata3 also revealed that the deletion of p27Kip1 restores Gata3 expression in mature PCs and DCs. To test whether the loss of Gata3 is responsible for the relative inability of mature PCs and DCs to respond to ectopic Atoh1-HA, we simultaneously overexpressed both Gata3 and Atoh1-HA and found that this phenocopied the p27Kip1/Atoh1-HA compound mutant and caused a significant number of PCs and DCs to upregulate Pou4f3 and other hair cell specific markers. To determine whether Pou4f3 is an integral downstream target of Atoh1 in this process, we also ectopically expressed Pou4f3 in conjunction with Atoh1-HA and observed the upregulation of hair cell specific genes in a significant number of PCs and DCs as compared to the ectopic expression of either Atoh1-HA or Pou4f3 alone. Combined, these data illuminate the roles for several factors in a gene regulatory network that controls the initial steps of auditory hair cell regeneration and suggests p27Kip1, Gata3, or Pou4f3 as therapeutic targets that may be useful to bolster current Atoh1 based gene therapies for the rehabilitation of sensorineural hearing loss.

Funding
National Institutes of Health (DC006471, DC013879, CA21765) the Office of Naval Research (N000140911014, N000141210775, and N000141210191), the National Organization for Hearing Research, the Hearing Health Foundation, and the American Lebanese Syrian Associated Charities of St. Jude Children's Research Hospital.

PS 454

Long-term Analysis of the Function and Composition of the Damaged, Adult Mouse Utricle

Zahra Sayyid[1]; Tian Wang[1]; Sherri Jones[2]; Alan Cheng[1]
[1]Stanford University; [2]University of Nebraska-Lincoln

Background
The utricle requires sensory hair cells to detect linear acceleration such as gravity. Unlike the mature cochlea, the utricle exhibits limited capacity to regenerate lost hair cells. Previous studies have demonstrated the formation of immature hair cells following aminoglycoside insults both in vitro and in vivo, suggesting that the postnatal mouse utricle contains

cells with the innate ability to regenerate new hair cells after damage. The origin of these regenerated hair cells are likely supporting cells, a phenomenon observed in non-mammalian vertebrates, yet lineage tracing has not been performed to support this notion. Using a previously established hair cell damage model with 3,3'-iminodipropionitrile (IDPN) as a synthetic vestibulotoxic nitrile compound, we have compared and correlated the histological changes of the mouse utricle to recovery of vestibular function as measured by vestibular evoked potentials (VsEPs) 1 week to 6 months post damage.

Methods

Mice (wild-type CD1 strain and Plp1CreERT/+;R26RtdTomato/+) received IDPN on postnatal day 30 and tamoxifen on day 32. VsEPs were measured at 1 week, 1 month, 3 months, and 6 months post-injection (n=6-48 for controls, 10-26 for IDPN-treated). Utricles were immunostained for hair cell and supporting cell markers (Myo7a and Sox2). Densities of hair cells, supporting cells, and Plp1-traced hair and supporting cells were determined in both the striola and extrastriola.

Results

One week after IDPN injection, >95% of IDPN-treated mice showed elevated VsEP thresholds in comparison to saline-treated controls. One and three months after damage, 88.2% and 60.0% of treated mice showed elevated thresholds, respectively. However, by six months after damage, 66.7% of treated mice showed elevated thresholds. Treated mice had significantly higher thresholds at 1 week ($p<0.01$) but not at later time points examined. As a group, IDPN-treated mice had significantly longer P1 latencies and lower P1-N1 amplitudes than those of saline-treated controls at time points examined. Plp1CreERT/+;R26RtdTomato/+ mice injected with IDPN had significant hair cell loss in the utricular sensory epithelium in both the striola and extrastriola (28.6% and 27.5% remaining, respectively). Six months after injection, hair cell numbers increased to 51.4% and 56.2% relative to controls in the striola and extrastriola, respectively. The number of traced hair cells also increased from 1 week to 6 month post damage.

Conclusions

After IDPN-induced loss of hair cells and utricular function, a partial recovery of both is observed. Ongoing studies aim to better characterize the source and functionality of the newly generated hair cells.

Funding

California Institute for Regenerative Medicine RN3-06529; Akiko Yamazaki and Jerry Yang Faculty Scholarship; Nebraska Tobacco Settlement Biomedical Research Development Funds; Stanford Medical Scholars Research Program; Howard Hughes Medical Institute.

PS 455

Manipulation of the Human Vestibular Environment to Generate Hair Cells

Ruth Taylor[1]; Jeffrey Holt[2]; Michael Lovett[3]; Anastasia Filia[3]; Andrew Forge[1]

[1]University College London; [2]Harvard Medical School; [3]Imperial College London

Background

In the vestibular system, loss of hair cells leads to balance dysfunction, dizziness and vertigo. Whilst loss of hair cells in the mammalian cochlea does not result in regeneration there is a limited capacity for spontaneous hair cell regeneration in the mammalian vestibular system. Previous studies suggest that the new hair cells arise by direct phenotypic conversion of the supporting cells into hair cells without an intervening mitotic event. Recent evidence suggests that phenotypic conversion can be induced by the transfection of supporting cells with the gene encoding Atoh1, a transcription factor shown to be necessary and sufficient to commit inner ear sensory precursors to a hair cell fate. There is also evidence that the components of the Notch-Delta lateral inhibition system, which regulates hair and supporting cell differentiation during development, are re-expressed following hair cell loss in the mammalian inner ear. Manipulation of this pathway has been suggested. These methods offer possibilities for replacing lost hair cells in the vestibular system.

Methods

A model system was developed using human sensory epithelia from the vestibular system, obtained from patients undergoing surgery for acoustic neuromas. Tissue was exposed to TAPI-1, a TACE inhibitor, following hair cell ablation with gentamicin and or transfected with Ad2- *ATOH1-GFP* and maintained in culture for up to 21 days post-treatment. Control tissue was exposed to gentamicin alone. Cultures were examined by immunohistochemistry and electron microscopy to determine the presence of hair cells. Additionally, downstream targets of *ATOH1* were determined by RNA seq in transfected tissue.

Results

Many supporting cells but not all cells were GFP labelled in tissue transfected with Ad2- *ATOH1-GFP* following hair cell ablation with gentamicin. The number of myosin VIIa positive cells in samples exposed to TAPI-1 and/or transfected with Ad2- *ATOH1-GFP* was greater in the experimental groups than utricles cultured for the same time period. Electron microscopy revealed cells with 'hairy' projections, some of these cells extended from the basement membrane to the luminal surface of the tissue. RNA seq revealed changes in the expression pattern of several genes consistent with hair cell generation.

Conclusions

Explant human vestibular cultures are the only means to perform experimental studies upon human inner ear tissue. Here we demonstrate that in our system, after hair cell ablation, both transfection with the gene encoding Atoh1 and manipulation of the Notch-Delta system results in an increase in the population of myosin VIIa labelled cells.

Funding
Medical Research Council UK (MRC) Action on Hearing Loss
The Dunhill Medical Trust

PS 456

Molecular and morphologic phenotypes during supporting cell-hair cell transition in the regenerating mouse utricle

Tian Wang[1]; Nicole Pham[1]; Jiayi Luo[1]; Lindsey May[2]; Lisa Cunningham[2]; Alan Cheng[1]
[1]Stanford University School of Medicine; [2]National Institutes of Health

Funding
California Institute for Regenerative Medicine RN3-06529 Akiko Yamazaki and Jerry Yang Faculty Scholarship

PS 457

Profiling the Transcriptional Program of Cellular Differentiation in the Utricle Provides a Roadmap for Regeneration

Joseph Burns; Michael Kelly; Stephen McInturff; Robert Morell; Matthew Kelley
NIDCD/NIH

Background
Utricular supporting cells (SCs) and hair cells (HCs) display characteristics that vary within distinct regions of the sensory epithelium. Furthermore, utricular HCs throughout the epithelium can be subdivided into two sub-types. This regional and sub-type heterogeneity is essential for proper sensation of acceleration. When the epithelium is damaged in adult mammals, spontaneous repair occurs at very low levels and appears insufficient for recovering vestibular function. Therefore, stimulating regeneration in a manner that restores both regional and sub-type heterogeneity will be essential to fully regain function. However, a better understanding of how heterogeneity is established during development is necessary to guide efforts to recapitulate this process in adults.

Methods
RNA-Seq was performed on >500 single cells isolated from utricular sensory epithelia of E16.5, P1, P12, and P100 mice. For each time point, dimensionality reduction and clustering algorithms were used to group the single-cell transcriptomes by cell type and region of origin. Groups that shared common lineages were temporally ordered across ages using trajectory analysis. Genes that varied significantly along the trajectories were identified and validated. These profiles were then used to determine the differentiation status of HC-like cells that were induced through forced expression of Atoh1 in SCs *in vivo*.

Results
Because cells within the developing utricle are heterochronic, we were able to profile temporal changes in gene expression that occur as progenitors become determined and then differentiate into mature SCs and HCs. The resolution was sufficient to distinguish trajectories that initiate at the level of immature HCs and then branch into distinct striolar, Type I, and Type II identities. Moreover, the trajectories suggest that differentiation of both SCs and Type I HCs is essentially complete by P12, but Type II HCs are comparatively delayed and retain expression of many immature HC genes. A variety of new markers for adult HC sub-types were also identified. Using these markers, we examined utricles following forced expression of Atoh1 in adult SCs *in vivo*. Results indicate that Atoh1 expression reprograms adult SCs into immature HCs, but these cells fail to develop the characteristics of differentiated Type I's and Type II's.

Conclusions
Single-cell RNA-Seq resolves the transcriptional programs of progenitors as they differentiate into discreet cell types. This data can be used to accurately gauge the effectiveness of strategies that seek to reprogram SCs into replacement HCs. Finally, the results suggest that Atoh1 alone is insufficient to induce mature HCs in adult utricles.

Funding
This project was supported by funds from the Intramural Program at NIDCD to M.W.K. (DC000059).

PS 458

Pre- and Postsynaptic Roles for α7 Nicotinic Acetylcholine Receptors in the Gerbil Superior Olivary Complex.

Sonia Weimann; R. Burger
Lehigh University

The ionotropic α7 nicotinic acetylcholine receptor (nAChR) has broad distribution throughout the mammalian brain (Dominguez et al. 1942; Marks et al. 1996; Morley et al. 1977). The function of this receptor can vary based on it cellular location and developmental expression. Presynaptic expression of α7 nAChRs is known to facilitate neurotransmitter release due to it's high calcium permeability (Albuquerque et al. 1997; McGehee et al 1995) while postsynaptic expression can have broad effects including the regulation of gene expression, neuron survival, and the mediation of excitatory currents. Happe and Morley (2004) showed that, the α7 nAChR is richly expressed in the superior olivary complex (SOC), in neurons specialized to compute sound location. However, physiological relevance within these nuclei has not been investigated.

The synaptic function of α7 nAChRs was examined using in vitro whole-cell patch clamp on brain stem slices obtained from gerbils age P9-15. Measurements of sEPSC amplitude and frequency were taken during application of agonist, acetylcholine (ACh) and antagonist, methyllycaconitine (MLA). Additionally, carbachol, a cholinergic agonist, was applied using a 250 mS puff while other drugs were bath applied. The impact of α7 nAChRs on excitatory synaptic transmission was measured by evoking presynaptic currents and pairing them with a pre-puff of nicotine. Lastly, effects of α7 nAChRs on cell excitability were measured in current clamp sing 50 pA steps paired with bath application of nicotine.

Our results demonstrate that α7 nAChRs have a role in enhancing excitatory transmission in the SOC. Bath application of ACh caused an increase in both the frequency and amplitude of sEPSCs indicating both pre and postsynaptic α7 nAChRs. Furthermore, puff application of carbachol evoked inward currents that were blocked by the α7 specific antagonist MLA. Lastly, evoked EPSCs were enhanced when paired with a nicotine pre-puff and cell excitability was increased when current steps were paired with bath application of nicotine. These data combined demonstrate the presence of functional α7 nAChRs on pre and postsynaptic sites within the SOC and that cholinergic signaling via α7 nAChRs influences broad multi-modal physiological mechanisms in the mammalian sound localization pathway. This suggests that cholinergic signaling may contribute to the development of the sound localization circuitry or mediate excitatory currents involved in the precision of temporal coding.

PS 459

Inter-aural Time Sensitivity of Superior-olivary-complex Neurons is Shaped by Systematic Cochlear Disparities

Mark Sayles[1]; Philip Smith[2]; Philip Joris[1]
[1]University of Leuven; [2]University of Wisconsin - Madison

Background

Sensitivity to micro-second inter-aural timing differences is critical for spatial hearing. Medial superior olive (MSO) neurons are tuned to a particular inter-aural time difference (ITD) in response to broadband noise; their "best delay" (BD). At the population level, BDs are biased to ITDs with the contra-lateral ear leading and tend to decrease with CF: the origin of these features is much debated. One possible source, cochlear-tuning disparities (Schroeder, 1977), has received little experimental attention. Previous work in this laboratory on auditory-nerve-fiber spike-train coincidence patterns, indicated that small cochlear disparities could account for the distribution of BDs observed experimentally, but requires systematically biased higher-frequency tuning ipsi-laterally. Here, we directly tested the existence of cochlear disparities in the inputs to MSO neurons and their ability to account for ITD tuning.

Methods

We recorded spike trains from presumed MSO axons in the anesthetized-chinchilla lateral lemniscus (LL) at an anatomical level below the dorsal nucleus of the LL. We presented inter-aurally correlated (+1) and anti-correlated (-1) broadband noise at a range of ITDs to construct noise-delay functions. We then presented inter-aurally uncorrelated (0) noise, and used spike-triggered reverse correlation to estimate the impulse responses of ipsi- and contra-lateral inputs independently.

Results

Noise-delay functions showed a damped oscillatory pattern. From the difference between the +1 and -1 noise-delay functions, the "difcor", we determined BD. Most BDs were within the π limit, with a bias to positive ITDs. We cross-correlated the ipsi- and contra-lateral impulse responses to predict the difcor: for most units, the prediction was excellent (correlation >0.9), indicating that these neurons act as ideal cross correlators and that our characterization of monaural inputs successfully captures the features needed for binaural tuning. We found significant inter-aural frequency-tuning differences (up to 0.5 octaves) in many units. As hypothesized, these differences were biased toward higher-frequency tuning ipsi-laterally. Furthermore, although some units had a BD of opposite polarity to that predicted by the observed tuning disparity, for the majority of units tuning disparity and BD were positively correlated. Various response features suggest that the bulk of recordings originated from MSO axons and, tentatively, a minority from the lateral superior olive.

Conclusions

Frequency-tuning disparities are commonly observed in the inputs to ITD-sensitive neurons in the superior olivary complex, and show a bias towards higher-frequency tuning ipsi-laterally. However, some units' responses appear to indicate some additional source(s) of delay.

Funding

Supported by a postdoctoral fellowship of the Research Foundation - Flanders (FWO) to M.S., NIH R01 DC012782 to P.H.S. and P.X.J., and grants to P.X.J. from FWO (FWO G.091214N and G.0961.11) and the University of Leuven Research Fund (OT/14/118).

PS 460

Non-primary excitatory inputs shape MSO principal neuron responses

Brian Bondy[1]; Tom Franken[2]; Philip Joris[2]; Nace Golding[1]
[1]University of Texas at Austin; [2]KU-Leuven, Belgium

Background

The MSO is highly specialized to detect differences in arrival time of a sound to each ear (intraural time difference, ITD) for the purposes of spatial hearing. MSO neurons are tuned to ITD, but the mechanisms of this tuning have been debated. In vivo patch clamp recordings have shown that ITD tuning of many MSO neurons is strongly dependent on immediately preceding patterns of synaptic activity; out-of-phase EPSPs can substantially shift the neuron's ITD curve. Here we investigate the characteristics and origins of these synaptic potentials.

Methods

We performed whole cell current clamp recordings from MSO neurons both in vivo and in horizontal slices from P14-P29 Mongolian gerbils. In slices at 35°C, ipsi- or contralateral cochlear nucleus (CN) axons were electrically activated with glass stimulating electrodes placed lateral or medial to the MSO, respectively. In slices, whole-cell patch recordings from MSO principal neurons were made in presence of 1 μM strychnine to block glycinergic inhibition.

Results

During in vivo whole-cell patch recordings from MSO principal neurons, responses to binaural beat stimuli evoked not only strong summating bilateral EPSPs but also smaller (<3 mV) EPSPs out of phase with peak depolarizations. In

recordings from MSO principal neurons in slices, strong electrical stimulation of pharmacologically isolated excitatory inputs evoked not only direct monosynaptic EPSPs, but also 1-3 additional EPSPs with longer and more variable latencies (observed in 74% of MSO neurons with either ipsi- or contralateral stimulation). Late EPSPs had many characteristics of polysynaptic inputs: high stimulus thresholds, long latencies, a high degree of temporal jitter and low reliability. They could be seen in response to trains of stimuli as well. Late EPSPs were eliminated in the presence of high divalent ACSF or partial block of AMPA receptors (80 nM NBQX), consistent with these events arising from a polysynaptic input. Blockade of NMDA (50 µM APV), and GABA (50 µM Gabazine) receptors had no effect on the presence of late EPSPs. Interestingly, non-principal cells could be activated with both ipsi- and contralateral excitation, and spike latency and jitter from synaptic stimulation matched the characteristics of polysynaptic EPSPs in MSO principal neurons.

Conclusions

MSO principal neurons receive polysynaptic inputs that arise from the superior olivary complex itself, possibly from MSO non-principal neurons, with timing that differs from primary inputs. Because “mis-timed” EPSPs affect ITD-sensitivity in vivo, these inputs are likely important for shaping the ITD sensitivity of MSO principal neurons.

PS 461

Dynamic Range Adaptation of Monaural Inputs for Efficient Encoding of Sound Source Locations under Naturalistic Conditions

Helge Gleiss[1]; Todd Jennings[1]; Joerg Encke[2]; Werner Hemmert[2]; Benedikt Grothe[1]; **Michael Pecka**[1]
[1]Ludwig Maximilians University Munich; [2]Technische Universitaet Muenchen

Faithful separation of sound sources is a prerequisite for navigation and communication under dynamic natural conditions. Information about the location of azimuthal sound sources is computed by neurons of the lateral superior olive (LSO) by detecting direction-specific differences in the intensity level at the two ears (ILDs). Specifically, LSO neurons integrate excitatory inputs from the ipsilateral side with inhibitory inputs from the contralateral side to gauge the relative sound levels at the two ears. However, using naturalistic acoustic stimuli, the auditory nerve fibers upstream to the LSO continually adapt the dynamic range of their spiking output to match the intensity distribution of the current stimulus. This universal mechanism for the stimulus-statistic-dependent adjustment of sensory processing has been termed Dynamic Range Adaptation (DRA) and is thought to optimize the efficiency of neural coding, as the metabolic costs of information transfer are minimized. However, for large ILDs, the inputs to the LSO from the left and right ear will consequently be adapted to drastically different intensity levels as a direct result of DRA of auditory nerve fibers. Yet, the effect this divergent DRA of ipsi- and contralateral LSO inputs has on the binaural computation and the coding of ILDs in LSO neurons is unknown. We performed *in vivo* extracellular single-cell recordings in anesthetized Gerbils and used computer modeling of auditory nerve fibers to investigate the neuronal encoding of ILDs in the LSO for different monaural adaptation levels. Broadband stimuli with similar bimodal intensity statistics but different absolute sound level distributions on the two ears were presented to mimic natural binaural acoustic conditions. We find that the divergent intensity distributions between ipsi- and contralateral inputs account for drastic dynamic range shifts in LSO neurons. Remarkably, these shifts resulted in near-optimal separability of nearby ILD in the range of those ILDs that were most likely to occur. The extent (several dB), direction and rapidity (tens of milliseconds) of dynamic range shifts in LSO neurons were accountable for by divergent DRA of the upstream auditory nerve fibers. Nonetheless, detailed analysis of the time course of LSO rate adaptation suggested the involvement of additional adaptational mechanisms that acted on the time scale of seconds. We conclude that sound intensity-dependent DRA of auditory nerve fibers allow for the efficient coding and optimal separation of sound source locations by the LSO under naturalistic acoustic conditions and contributes to dynamic gain control in LSO on multiple time scales.

Funding

German Research Council (DFG) German Center for Vertigo and Balance Disorders (IFG) Bavarian Academy of Sciences

PS 462

Coding Amplitude-Modulated Sounds by Coincidence Detection in the Lateral Superior Olive

Go Ashida[1]; Jutta Kretzberg[1]; Daniel Tollin[2]
[1]University of Oldenburg; [2]University of Colorado School of Medicine

Background

Neurons in the mammalian lateral superior olive (LSO) detect interaural level differences by comparing excitatory inputs from the ipsilateral cochlear nucleus with inhibitory inputs driven by contralateral sounds. LSO neurons also show sensitivity to binaural phase-differences of amplitude-modulated (AM) sounds. Although binaural coding by LSO has been extensively studied both theoretically and experimentally, monaural response characteristics of LSO to AM sounds are only marginally understood. Previous *in vivo* recordings in cat LSO showed that spiking rates of LSO neurons generally decrease with increasing modulation frequency, but that variations of modulation-frequency dependence across neurons were considerably large (Joris and Yin, 1998, J. Neurophysiol.). In this study, we aim to reveal the underlying mechanisms for this monaural AM coding using a simple computational model of LSO.

Methods

Phase-locked excitatory inputs to LSO were modeled as an inhomogeneous Poisson process with a periodic intensity function, while spontaneous inhibition was modeled as homogeneous Poisson process. Similar to a previous modeling study (Franken et al., 2014, Front. Neural Circuits),

the LSO neuron was modeled as a counter of coincident inputs. Namely, if the number of excitatory inputs within a pre-set coincidence window reached or exceeded the threshold, an output spike was generated. Then the model is in the refractory period, in which no more spikes are generated. Effects of inhibition were modeled as a transient increase in threshold. We systematically varied parameters of the model and examined how they affect AM-tuning of the model neuron.

Results

By changing the model parameters, most variations of AM-tuning curves observed *in vivo* were reproduced. Frequency-dependence of input parameters (spike rates, degrees of phase-locking, and spontaneous inhibition) had only minor effects on LSO output spike rates. In contrast, increasing coincidence threshold or shortening the coincidence window resulted in lower output spike rates. Moreover, lower coincidence thresholds led to higher half-peak positions of AM-tuning curves. The duration of the refractory period affected the AM-tuning curve only below 300 Hz.

Conclusion

Our modeling results suggest that coincidence detection is one of the most fundamental operations in LSO and that variations of coincidence parameters may explain the empirical neuron-to-neuron variations in AM coding. Investigating the relations between the abstract parameters of our coincidence counting model and underlying biophysical factors (such as membrane and synaptic properties) would be an important subject of future study.

Funding

Supported by the Cluster of Excellence "Hearing4all" (GA, JK), by the NIH Grant DC011555 (DJT), and by a Hanse-Wissenschaftskolleg (HWK) Fellowship (DJT).

PS 463

Temporary Unilateral Conductive Hearing Loss During Development Impairs Auditory Spatial Discrimination Ability and Information Processing in Neurons of the Inferior Colliculus

Kelsey Anbuhl; Nathaniel Greene; Alexander Ferber; Victor Benichoux; Andrew Brown; Daniel Tollin
University of Colorado Anschutz Medical Campus

Children experiencing persistent conductive hearing loss (CHL) early in life often display binaural hearing impairments that persist long after the CHL is resolved, suggesting abnormal central auditory development. It is not clear what neurophysiological correlates underlie these deficits. Here, we examined the effects of unilateral CHL on both spatial hearing and neural information processing in developing guinea pigs. Custom silicone earplugs were used to induce CHL in animals (n=7) from birth (P0) through adulthood (P56). After earplug removal, animals were tested on behavioral spatial acuity using the speaker-swap paradigm based on the pre-pulse inhibition (PPI) of the acoustic startle reflex. We determined the smallest angle that adults could discriminate across the midline by presenting continuous broadband or high-pass noise from one speaker and swapping to a second speaker for a short interval preceding a loud startle-eliciting stimulus. The response was quantified as PPI of the startle, defined as 1 minus the ratio of RMS amplitude of response to control; positive PPI indicates stimulus discrimination. Following behavior, extracellular recordings from neurons in the central nucleus of the inferior colliculus (ICc) were collected with a focus on neural coding of ILD cues. We used the mathematical framework of Mutual (MI) and Fisher (FI) information to test the hypothesis that spatial hearing deficits arise from a reduction in neural information processing of ICc neurons. Earplugs produced a mild-moderate, frequency-dependent CHL of ~15-40 dB. ABR thresholds were normal for all animals, indicating normal periphery. Animals raised with a unilateral earplug could discriminate changes in source location across the midline of $\geq$30° for broadband, and 30-45° for high-pass (>4 kHz) noise compared to 7.5° and 15°, respectively, for age-matched controls. Using acoustic directional transfer function measurements and behavioral discrimination thresholds for high-pass noise, we estimate that a developmental unilateral earplug impairs ILD sensitivity by ~3-6 dB. Extracellular ICc recordings contralateral to the earplug showed modest reductions in MI in ILD sensitive neurons, with the mean MI of 0.9 ± 0.4 (SD) bits vs 1.1 ± 0.2 bits for control animals. Using FI to determine the neurons' abilities to discriminate changes in ILD (ΔILD), we found the mean ΔILD in the population of neurons from earplugged animals was 7.1 ± 5.5 dB vs 5.7 ± 2.5 dB from controls, suggesting a ~2dB ILD deficit. This information-processing reduction in ICc neurons may in part explain the spatial discrimination deficits observed in animals and children with developmental CHL.

Funding

R01-DC011555, T32-DC012280, F31-DC014219

PS 464

Effects of Masker Bandwidth, Mistuning and Binaural Cues on the Representation of Components in a Harmonic Tone Complex in the Gerbil Inferior Colliculus

Yoko Kato; Georg Klump
Cluster of Excellence Hearing4all

Harmonicity is an important cue to group components of sounds from a specific source in the acoustic environment. If a component of a harmonic sound is slightly shifted in frequency, that tone becomes distinct from other harmonics components in a complex with a specific fundamental frequency. In a human psychophysical study, Klein-Hennig and colleagues (2012) determined masked thresholds for detecting a single component of a tone complex in relation to its mistuning and binaural phase by asking the subjects to report the presence of the target component presented at different sound levels. Unexpectedly, when adding masker harmonics outside the auditory filter tuned to the target frequency the masked threshold increased. This is in contrast to the expectation, that a higher number of components would make it easier to separate the complex from the target.

To investigate the mechanisms underlying this observation, we recorded single- and multi-unit responses from inferior colliculus neurons of anesthetized gerbils that have been demonstrated to have a high sensitivity for detecting mistuning of components in a harmonic complex (e.g., Klinge-Strahl et al. 2013). Complex tone maskers were centered at the target frequency and either had 8 or 32 harmonic components equally distributed to both sides of the target. Maskers with two different phase relation between components were applied: random phase and sine phase maskers. Target tones were either tuned or mistuned with respect to the masker fundamental. Maskers were always played with the same phase to both ears. Targets of different levels were played either with the same phase or with a phase difference of 180 degrees between the two ears. Spike rate and temporal patterns of spike sequences (analysis with van Rossum [2001] metrics) were used to determine neuronal response thresholds. Neuronal sensitivity (da) was determined by subjecting the response measures to an ROC analysis comparing responses to masker plus target and masker alone.

In general, an increased target level resulted in a higher da for both the rate response and the temporal spike pattern. Similar to the human psychophysical data (Klein-Hennig et al. 2012), the sensitivity for both response measures was considerably reduced in a fraction of the neurons if the bandwidth of the harmonic complex masker was increased. Also the phase relation of the masker components affected the response. However, the impact of mistuning and target phase was only small. The relation between the neurophysiological and the psychophysical data will be discussed.

Funding
This study was funded by the DFG (TRR 31 and Cluster of Excellence “Hearing4all”)

PS 465

Spike-Frequency Adaptation in the Barn Owl’s Auditory Space Map

Roland Ferger; Lina Kenzler; Hermann Wagner
RWTH Aachen University

Adaptation has been observed in many nuclei of the auditory pathway. One aspect of adaptation is that a neuron’s response may decrease during an ongoing stimulus. This kind of adaptation is called spike-frequency adaptation (SFA). We investigated SFA as a function of the interaural time difference (ITD) of a stimulus in the external nucleus of the inferior colliculus (ICX) in the barn owl. This bird is a specialist in sound localization. For localizing sound sources in the horizontal plane it relies primarily on the ITD. An auditory space map is formed in ICX by combining binaural cues for azimuth and elevation and integrating across frequency channels.

Extracellular recordings were obtained from neurons in ICX. The stimuli (each 300ms duration, 5ms onset/offset ramps) were presented via earphones. The stimulus level was chosen to elicit 50% of the saturating response. De-novo broadband noise served as stimulus. Five to seven ITDs separated by 30 µs were chosen around the best ITD to cover the main peak entirely and investigate the influence of ITD on SFA. Peri-stimulus time histograms (PSTH) were assembled from responses to 200 repetitions for each ITD.

We observed different response types in ICX: Most neurons responded “phasic-tonic” (or primary like) at the best ITD (89%), i.e. with a strong onset peak followed by a sustained response over the whole stimulus length. The other most prominent types were “pure phasic” (only an onset peak and no sustained response), “pure tonic” (no onset peak but a constant response) and “inhibited” (spike rate below the spontaneous activity, possibly with an initial onset peak). The tonic component was strongest for responses to the unit’s best ITD and became weaker for less favorable ITDs (24% phasic responses and 34% inhibited). By fitting a double exponential function to the decay slope of the response rate, we quantified several response characteristics. The parameters in the time dimension (time of maximal response and both time constants) as well as response latency showed very little variation with ITD. Response rate related parameters (maximal rate or the steady state rate towards the end of the stimulus), however, strongly varied with ITD. We could also show that units with inhibition at unfavorable ITDs have a significantly narrower tuning to ITD than units without inhibition.

Neurons in the barn owl’s ICX exhibit SFA. Since it is higher at unfavorable ITDs than at the best ITD, this also improves the representation of ITD.

Funding
Deutsche Forschungsgemeinschaft (DFG); Grant WA606/23-1

PS 466

Time Varying Side-Peak Suppression in ICx Neurons in the Barn Owl and Its Possible Contribution to Sound-Localization Behavior

Lutz Kettler; Patrick Schillberg; Hermann Wagner
RWTH Aachen University

Barn owls use interaural time differences (ITD) to detect the azimuthal position of a sound source. ITDs are represented in the external nucleus of the inferior colliculus (ICx) where neurons with distinct receptive fields form a map of auditory space. With broadband stimuli the response of ICx neurons is unambiguous, i.e. the neuron responds maximally to a preferred ITD. Response to non-preferred ITDs is suppressed (side-peak suppression). Under certain circumstances ICx neurons may respond equally or almost equally strong to different ITDs, though. One such case is the response to narrowband stimuli. Side-peak suppression is also not constant during ongoing stimulus presentation. Furthermore, ambiguous neural responses correlate with phantom source localizations in behavior. Phantom sources can be predicted from the ITD and the period of the narrowband signal.

We quantified the time course of side peak suppression during ongoing stimulus presentation and performed behavioral experiments to demonstrate the influence of varying side-peak suppression in the ICx on sound localization behavior. Therefore, we collected ITD tuning curves from 27 ICx units and calculated the response ratio between the main peak and the average of the two neighboring side peaks (side speak suppression). We recorded from multi units to obtain a reliable number of spikes within 2 ms bins and because multi units reflect spatial tuning in the ICx. Side-peak suppression was calculated for each bin from stimulus onset to offset.

The electrophysiological recordings showed that the average side-peak suppression increased from 0%, i.e. equal response at main and side peak, at the stimulus onset to 55% at steady state response. The data was well fitted with an exponential function with a time constant of 7 ms indicating that short stimuli lead to localization errors due to lack of side peak suppression.

We also performed behavioral experiments with two barn owls. We tested whether the ability to precisely localize sound sources depended on stimulus durations. The owls' task was to localize broadband and narrowband noise with different durations.

Our preliminary behavioral experiments revealed that even very short stimuli were precisely localized by the owls, if the sounds were broadband. Only if narrowband stimuli were presented, the owls tended to localize phantom sound sources. However, behavioral performance did not depend on stimulus duration with both narrowband and broadband stimuli.

From this we concluded that additional mechanisms other than side-peak suppression in the ICx might be involved in the disambiguation of the sound source.

Funding
Deutsche Forschungsgemeinschaft (grant WA 606/20-2)

PS 467

Encoding of Large Interaural Level Differences: Implications for Sound Localization

Andrew Brown[1]; Victor Benichoux[1]; Heath Jones[2]; Daniel Tollin[1]
[1]University of Colorado School of Medicine; [2]University of Wisconsin - Madison

Background
Sound source localization is a basic function of the auditory system. In humans and a variety of studied animal species, localization acuity is highest for sources near the frontal midline and lower for more eccentric locations. Lower acuity at eccentric locations can be partially accounted for by compression of physical cues for sound localization (interaural time and level differences [ITD and ILD]) at extreme left and right source angles. However, neural and behavioral sensitivity to the cues, particularly ILD, may also change across azimuth. Here we consider interactions between acoustical constraints, precision of neural encoding, and psychophysical use of ILD cues for sound localization.

Methods
Neural rate-ILD tuning curves were obtained from well-isolated single neurons of the inferior colliculus of anesthetized chinchillas (*Chinchilla lanigera*), a species that is audiometrically comparable to humans. Neuronal ILD thresholds were then estimated for single neurons and bootstrapped populations of neurons and compared to human behavioral ILD thresholds. Behavioral ILD thresholds were estimated using both discrimination and lateralization tasks.

Results
A majority of ILD-sensitive neurons were maximally modulated by ILDs near 0 (i.e., half-maximal ILDs tended to cluster near the interaural midline, with a slight contralateral bias in the population mean). Nonetheless, neurons with half-maximal ILDs as large as 15-25 dB and predicted neuronal ILD thresholds as small as 1-2 dB were also observed. In humans, behavioral ILD discrimination thresholds generally increased when the "reference" ILD was increased, but the magnitude of increase depended on the task considered (discrimination versus lateralization).

Conclusions
Behavioral localization acuity is generally reduced for eccentric source locations. Part of this reduction may arise from poorer encoding of large ILDs. However, behavioral ILD thresholds across "reference" ILDs depend upon the task considered, and estimates of neural population ILD thresholds depend highly upon (1) the number of neurons considered and (2) the nature of the code assumed, i.e., lower-envelope (use of the best neurons in the population) versus compulsory pooling across the population.

Funding
[Funding provided by NIH Grant Nos. F32-DC013927 (ADB) and R01-DC011555 (DJT, HGJ, VLB)]

PS 468

Unification of Somatosensory And Auditory Localization in the Oculomotor Cerebellum With the Mechanism For Visual Saccades

Mark Riggle
Causal Aspects, LLC

Modeling multisensory integration -- where visual, auditory and tactile stimuli can be correctly located in 3D-space -- is greatly complicated by the current model of auditory localization [assumed to occur only via the ascending auditory pathway]. The difficulty is that auditory localization, as does tactile localization, recovers with Superior Colliculus (SC) ablation, and this lead to the conclusion that localization for both must also occur in the forebrain for both mammals and birds. This is troublesome complexity.

This contrasts with the Vestibular Origin of Hearing theory (VOH) where spatial hearing originated with vestibular processing for localization calculation and then piggybacked

on tactile localization. In VOH, auditory localization is through cerebellar connections and is processed similarly to the head-in-world vestibular orientation. Then, because that head orientation is used in tactile localization, auditory localization follows along as tactile localization. The problem becomes; if not the forebrain, then where and how is tactile localization performed.

We show that tactile localization to the SC and forebrain can derive from the visual saccade system [controlled by the oculomotor cerebellum]: particularly from predictive saccades. Predictive saccades occur if the visual target is moving because then a static saccade (requiring 100ms) will not be correct (the target has moved). The oculomotor cerebellum (OMC), just as in static target saccades, uses the target position (passed from the optic part of SC to the deeper SC then to the OMC) plus all relevant inputs (e.g. eye-position and the target velocity supplied by retinal direction cells) to look-up the predicted saccade target position. This means that, based on other input to the OMC, an initial saccade target in the deep SC can be remapped (by learning) to an arbitrary location. This OMC remapping provides the mechanism for tactile localization. Because the sensory nuclei have fixed projections to the deep SC, a tactile stimulus causes stimulation at a particular SC location; then, just like the visual target passed from the optic SC, it can be remapped based on multiple cerebellar inputs (e.g. head-to-body orientation and the sensory nuclei). For all saccades (visual, predictive, tactile, and auditory), the calculations must be learned by trial-and-error with feedback. Our model unifies tactile and auditory localization with the vestibular and the saccade systems including how the OMC indicates targets in multiple reference frames – world, head, and retinal. No localization by forebrain required.

PS 469

Vertical Alignment Nulling and Torsional Alignment Nulling as Measures of Ocular Misalignment

Elizabeth Liu; Michael Schubert
The Johns Hopkins University School of Medicine

Background
Asymmetries in oculomotor behavior provide evidence of physiological otolith asymmetries. Among other roles, the otolith organs control vertical and torsional eye movements related to gravito-inertial accelerations (GIA). Yet in light, the brain can fuse any ocular misalignment using binocular cues.

Methods
Vertical Alignment Nulling (VAN) and Torsional Alignment Nulling (TAN) are perceptual tasks of monocular position. In darkness, the VAN and TAN tests use a tablet computer that displays one horizontal red line and one horizontal blue line while viewing through color-matched red and blue filters; this provides separate visual information to each eye. One of these horizontal lines, designated as the stationary line, remains fixed on the screen, while the subject 'swipes' the screen to adjust the moving line vertically during VAN or rotationally during TAN. VAN, TAN. In patient subjects cervical and ocular VEMPS were measured.

Results
To date, we have collected data in n=12 subjects in altered gravitational level (parabolic flight), n=3 patients with vestibular hypofunction, and n=8 healthy controls. Our data suggest both VAN and TAN can identify ocular misalignment in situations of altered gravity and severe vestibular hypofunction.

Conclusions
These data suggest that VAN and TAN are valid, novel measures of ocular misalignment, presumably from otolith end organ dysfunction. Ocular misalignment appears to be more common than previously thought, probably due to the binocular cues typically uncontrolled for.

Funding
Department of Defense Congressionally Directed Medical Research Program

PS 470

Head Stability During Gait can be Affected by Otolith Function – A Study in Cases with Unilateral Acoustic Neuroma

Kazuo Ishikawa; Yoshiaki Itasaka; Eigo Omi; Ko Koizumi
Akita University

Background
Peripheral vestibular end organ play an important role for postural and gait stability. However it has not yet been fully elucidated on how each organ can affect gait control system, especially toward head stability during gait. Now newly introduced tests to examine the function of otolith organ such as cVEMP and oVEMP have made it possible to examine their function (utriculus function and sacculus function) separately. Our aim for the present study is to elucidate how the otolith organ could affect the head stability during gait in cases with acoustic neuroma which cause various functional abnormality of otolith organs.

Method
Twenty unilateral acoustic tumor patients and nine age and height matched healthy control subjects were enrolled in this study. Subjects were asked to walk freely with comfortable pace with eyes open and eyes closed at a distance of about four meters, and 3-D movement analysis was performed. In this study, the analysis was mainly focused on head movements and peripheral vestibular function. Functional status of the peripheral vestibular nerve was examined by cVEMP & oVEMP.

Results
In AT cases, three cases had normal cVEMP and oVEMP, five cases had abnormal cVEMP with normal oVEMP, three cases had normal cVEMP with abnormal oVEMP, and nine cases had abnormal abnormal in both cVEMP and oVEMP. Regarding the relation between those abnormalities and head instability, AT cases had greater horizontal sway movement, especially in cases with oVEMP abnormality. AT cases with cVEMP abnormality had greater pitch and roll movement than

that of the control, especially under gait with eyes closed. AT cases with both VEMPs abnormality had the greatest head instability. However, no significant change was found in yaw plane head movement during gait.

Conclusion
Thus peripheral otolith function plays an important role for stabilizing head during gait, and could have somewhat different contribution between utriclar system and saccular system.

PS 471

The Influence of Time a Day on Vestibular Test Performance

Ariel Grobman[1]; Mikhaylo Szczupak[1]; Carey Balaban[2]; Alex Kiderman[3]; Michael Hoffer[1]
[1]University of Miami Miller School of Medicine; [2]University of Pittsburgh; [3]Neuro Kinetics, Inc.

Background
The differential diagnosis of most balance disorders can be narrowed down based on history and physical exam alone. However, to narrow this differential diagnosis still further or to provide some indication of the nature of a balance disorder in those where history and physical do not provide a diagnosis, vestibular testing is often ordered. Unlike many other tests in medicine, which provide clear objective ordinal values, the results of vestibular tests are not always clear-cut. A variety of factors account for this and include such issues as the true definition of normal function, the meaning of borderline abnormalities, and confusion when two tests point to different etiologies. These issues are compounded on the more complex tests that can provide the most detailed information about a particular balance disorder. Moreover, it appears that these more complex tests may be affected by the attentiveness and overall level of arousal of the subject. Because of these factors many investigators believe that these tests may give different values at different times of the day. The goal of this presentation is to examine performance on a short set of oculomotor, vestibular, and reaction time (OVRT) tests as a function of time of day.

Methods
Twenty balance normal subjects participated in this pilot project. The testing paradigm was composed of a 12-minute battery of OVRT tests. All subjects underwent a baseline test between 10 am and 12 pm. Ten subjects were assigned to the early group and their other test was between 7 am and 8 am and ten subjects were assigned to the late group and their other test was between 330 pm and 430 pm. The order of the tests was randomized to negate any order effect and the two tests were conducted on different days.

Results
We compare the outcomes of each subject's baseline balance test to the values obtained early or late. Comparisons included test results on horizontal and vertical smooth pursuit and saccades, predictive saccades, saccade reaction time, subjective visual vertical, and vergence.

Conclusions
The findings of this work will help influence how vestibular testing is performed and interpreted. Understanding the tests that can be influenced by time of day will allow for more accurate diagnosis and better understanding of recovery data. This work provides the basis for studying the underlying complex extra vestibular influences that might affect the both test outcomes and overall balance function.

Funding
The University of Miami Ear Institute and Head Health Challenge II (sponsered by the National Football League, Underarmour, and General Electric)

PS 472

Subjective Visual Vertical in Bilateral Vestibular Loss: Role of Proprioception

Michel Toupet[1]; Chritian Van Nechel[2]; Ulla Duquesne[3]; Charlotte Hautefort[4]; Sylvie Heuschen[5]; Alexis Bozorg Grayeli[6]
[1]Centre d'Exploration Fonctionnelle Otoneurologique, Paris and Dijon University Hospital; [2]Brugmann University Hospital and Clinique des Vertiges; [3]Clinique des Vertiges; [4]Lariboisiere University Hospital, Paris 7 University; [5]Centre d'Exploration Otoneurologique; [6]Dijon University Hospital and UMR-6306 CNRS, Burgundy University

Introduction
Subjective Visual Vertical (SVV) is a routine test assessing the otolithic function. The participation of proprioceptive input in SVV is probably significant but unclear. In order to evaluate this participation, we aimed to study SVV in patients with bilateral vestibular loss and different body and neck tilts.

Materials and Methods
This prospective study included 22 patients with idiopathic bilateral vestibular loss (mean age : 58, sex ratio : 1.2) and 30 adult controls (mean age : 51, sex ratio: 1.3). SVV was measured by asking the patient to place vertically a red line on a screen using a remote control. Deviation from vertical was measured in degrees (negative values to the left and positive to the right). The patient was seated on a tiltable seat (TRV seat, Apt, France). SVV was measured in 7 body positions: vertical, head and body tilted 12° to right, then 24°, and then body tilted at 24° with the head upright, subsequently same positions were tested on the left. In each position, SVV was measured 6 times.

Results
At vertical position, no difference in SVV was observed between vestibular loss and controls (-0.2° ± 1.05 versus -0.1° ± 1.98 respectively, unpaired t-test). However, patients with vestibular loss were more sensitive to body tilt (-8.5° ± 4.64 for vestibular loss versus 0 ± 3.26 for control at 24° body and head tilt to the left, $p<0.01$, unpaired t-test). Placing the head upright while the body was still tilted significantly reduced this difference suggesting that cervical proprioceptive inputs participate in SVV. Similar results were observed on the right.

Conclusion
Not only otolithic function but also proprioceptive entries, especially cervical sensors, participate in SVV.

Funding
Institue de Recherche en Otoneurologie (IRON) and Société ORL de Bourgogne

PS 473

How Much Error in Superior Semicircular Canal Dehiscence Diagnosis? A Comparison Between FPCT and MSCT.

Carolina Trevino Guajardo; Monica Pearl; John Carey
Johns Hopkins University

Background and Rationale
Superior semicircular canal dehiscence syndrome (SCDS) is caused by a defect in the bony labyrinth that allows the abnormal transmission of pressure or sound. Patients afflicted by this condition can experience sound-induced vertigo, hearing loss, and autophony. The diagnosis of SCDS relies in the symptomatology presented in addition to the identification of the dehiscent bone in a high resolution multi slice computed tomography (MSCT). MSCT has been shown to overestimate the defect size when comparing radiologic measurements versus those taken intraoperatively. In 191 patients undergoing MSCT, a dehiscence was identified in 5.8% of the ears scanned, however only 0.5% showed signs, symptoms and audiometric findings suggestive of SCDS.

Some SCDS patients undergoing repair surgery have been found to have thinning of the bone rather than a true dehiscence. Near dehiscence SCDS patients have been reported to be at a greater risk for complications than those with frank dehiscence with 45% reporting a recurrence of at least one symptom after surgical repair.

Flat-panel computed tomography has reported to yield higher resolution scans for cadaveric temporal bones compared to MSCT. This newer technique may help identify in a more graded scale the status of semicircular canal bone, especially in those cases with small or near dehiscence. The purpose of this cross-sectional study is to determine how intraoperative measurements correlate with FPCT and MSCT and if there is difference between imaging techniques.

Study Design
This is a cross sectional study retrospective study.

Study population
Inclusion Criteria: all patients that have been diagnosed with superior semicircular canal dehiscence clinically and/or with the aid of audiometry and electrophysiologic findings and undergone surgery its treatment and had a MSCT (n=30) or FPCT (n=13) done prior repair surgery. Exclusion Criteria: None.

Analytical Plan
Dehiscence size in millimeters was used as outcome measurements. We calculated the residual errors (RE) and did a 2 sample t-test where null hypothesis is that there is no difference between scans.

Results and Conclusions
We found that FPCT had significantly smaller measured residual errors with a mean residual error of -0.03 mm (95% CI -0.30, 0.22) compared to MSCT which had a mean of -1.68 mm (95% CI –1.64, -1.11), p= 0.004. The gold standard for radiologic diagnosis of SCD has been MSCT, but FPCT may offer improved images given its better spatial resolution.

PS 474

Vestibulotoxic effects of Platinum-based Chemotherapy in Patients with Head and Neck Cancer

Angela Wenzel[1]; Boris Stuck[2]; Dorotheea Cazan[1]; Richard Birk[1]; Karl Hörmann[1]; Claudia Umbreit[3]; Roland Hülse[1]
[1]University Hospital Mannheim; [2]University Hospital Essen; [3]University Hospital Jena

Background
Cochleotoxicity is a well-known side effect of pharmacotherapy such as platinum-based chemotherapy or antibiotic therapy with e.g. gentamicin. Little is known whether platinum-based chemotherapeutics additionally affect vestibular function. Consecutively, the aim of this study was to assess potential vestibulotoxic effects of platinum-based chemotherapy in patients treated for head and neck cancer.

Methods
Vestibular function was assessed in patients undergoing adjuvant or primary chemotherapy for head and neck squamous cell carcinoma using video-head impulse test (vHIT) to quantify semicircular canal function and ocular and cervical vestibular evoked myogenic potentials (o/c VEMPs) to evaluate otolith function. The tests were performed prior to treatment and 3 months after completion of chemotherapy. Statistical analysis was performed using nonparametric Wilcoxon rank-sum test and t-test.

Results
16 patients (2 female, 14 male) were enrolled in this prospective study (median age 61.9ys), 7 of 16 (44%) patients were treated with adjuvant, 9 (56%) with primary chemoradiation. Median gain was 1.01 (+/-0.4) for horizontal head impulses to the right and 1.03 (+/- 0.51) to the left before treatment. After chemoradiation, median gain was statistically significantly reduced to 0.86 (+/- 0.35) when the right and to 0.79 (+/- 0.41) when the left horizontal semicircular canal was tested (both $p<0.05$). Cervical VEMPs with reproducible test results could be obtained in 14 patients (87.5%; p13= 14.6msec, n23= 22.5msec) prior to treatment. Reproducible oVEMPs results were accomplished in 13 patients (81.25%; n1=10.4msec, p1=15.6)).Three months after platinum-based chemotherapy, cVEMPs were absent in 7 patients (57.9%, p13=16.5msec; n23=24.6msec) and oVEMPs in 8 patients (57.1%, n1=11.8msec; p1=16.8msec) and latencies appeared to be prolonged.

Conclusions
Patients treated with platinum-based chemotherapeutics seem to develop a significant loss in vestibular function. Future studies are needed to further differentiate vestibulotoxicity in this patient cohort.

PS 475

Developing Personalized Sensorimotor Adaptability Countermeasures for Spaceflight

Ajitkumar Mulavara[1]; Rachael Seidler[2]; Brian Peters[3]; Helen Cohen[4]; Scott Wood[5]; Jacob Bloomberg[6]
[1]Universities Space Research Association; [2]University of Michigan; [3]Wyle Science Technology and Engineering Group; [4]Baylor College of Medicine; [5]Azusa Pacific University; [6]NASA

Astronauts experience sensorimotor disturbances during their initial exposure to microgravity and during the re-adaptation phase following a return to an Earth-gravitational environment. Interestingly, astronauts who return from spaceflight show substantial differences in their abilities to readapt to a gravitational environment. The ability to predict the manner and degree to which individual astronauts would be affected would improve the effectiveness of countermeasure training programs designed to enhance sensorimotor adaptability. In this paper we will be presenting results from our ground-based study that show how behavioral, brain imaging and genomic data may be used to predict individual differences in sensorimotor adaptability to novel sensorimotor environments. This approach will allow us to better design and implement sensorimotor adaptability training countermeasures against decrements in post-mission adaptive capability that are customized for each crewmember's sensory biases, adaptive capacity, brain structure, functional capacities, and genetic predispositions. The ability to customize adaptability training will allow more efficient use of crew time during training and will optimize training prescriptions for astronauts to ensure expected outcomes.

Funding
This work is supported by the National Space Biomedical Research Institute through NASA NCC 9-58 and by NASA

PS 476

Compensatory Saccade Metrics Are Associated with Physical Performance in Older Adults: Data from the Baltimore Longitudinal Study of Aging

Yanjun Xie[1]; Eric Anson[1]; Eleanor Simonsick[2]; Stephanie Studenski[2]; Yuri Agrawal[1]
[1]Johns Hopkins University School of Medicine; [2]National Institute on Aging, National Institute of Health

Background
Head impulse testing (HIT) assesses the function of the angular vestibulo-ocular reflex (VOR). Individuals with a deficient VOR can be identified by HIT based on the compensatory saccades they generate to maintain a stable gaze. These saccades can be measured and quantified using the new video head impulse testing (vHIT) techniques. In this study, we investigate whether compensatory saccade metrics such as saccade amplitude and latency predict physical performance in a cohort of healthy older adults. We also examine the association between VOR gain and physical performance for comparison.

Method
We used cross-sectional data on a sample of healthy older adults in the Baltimore Longitudinal Study of Aging seen between 2013 and 2014 who underwent vHIT. Using custom software, we computed mean VOR gain, mean compensatory saccade amplitude (degrees), and mean compensatory saccade latency (milliseconds) for each individual who made compensatory saccades. Physical performance was assessed using the tests that comprise the Short Physical Performance Battery (SPPB): standing balance tests (feet side-by-side, semi-tandem, and tandem stand), repeated chair stands, and a 6-meter timed walk. Multivariable logistic regression evaluated the association between saccade amplitude and latency and SPPB performance, adjusting for age, sex, race, education, cardiovascular risk factors (smoking status, hypertension, and diabetes), and VOR gain.

Results
183 adults (mean age 71.8±13.2 years) who had compensatory saccades and underwent SPPB testing were included in this study. Mean saccade amplitude was 2.22 degrees (standard deviation [SD] 1.78) and mean latency was 276 milliseconds (SD 71.1). Higher mean saccade amplitude was associated with a higher odds of failure on the tandem stand task (odds ratio [OR] =1.39, p=0.029). Further, higher mean saccade latency was associated with lower odds of failing the tandem stand (OR=0.99, p=0.020). We did not observe a significant association between saccade amplitude or latency and performance on the repeated chair stands or usual gait speed. VOR gain was not associated with any of the physical performance measures.

Conclusion
We observed in a cohort of older adults that compensatory saccade amplitude and latency significantly predict the ability to hold the tandem stance, a challenging postural task for 10 seconds. In contrast, VOR gain was not associated with any physical performance measure. These data suggest the importance of quantifying compensatory saccade metrics to capture the impact of vestibular impairment on physical function in older adults.

Funding
This work was supported by the National Institute of Health grant NIDCD K23-DC013056.

PS 477

Functional Measure of Gaze Shifting in Normal Individuals

Chung-Lan Kao[1]; Po-Yin Chen[2]; Michael Schubert[3]
[1]National Yang-Ming University, Taipei Veterans General Hospital; [2]Institute of Physical Therapy and Assisted Technology, School of Biomedical Science and Engineering, National Yang-Ming University; [3]Johns Hopkins University School of Medicine

Background

A gaze shift involves an initial eye rotation to the target of interest, followed by a head rotation towards the same target. Gaze shifts are thus combined eye and head rotations that bring the fovea of the retina to a visual target of interest, commonly used in daily activities such as walking on the street and avoiding oncoming traffic. We have incorporated a dynamic visual acuity test with a gaze shift strategy and developed a functional measure of gaze shifting (gaze shift DVA test (gsDVA)) and compared the differences between the young and old populations.

Method

One monitor was placed 2m in front of subjects. Two additional monitors were placed 60d to the right and left of the centered monitor. Once the subject's head rotated to 60 degrees, an optotype flashed on the eccentric monitor and the subject was asked to identify its orientation. An examiner entered the subject's response, and the optotype disappeared. When the subjects' head was within 15d of neck neutral for > 2 seconds, an arrow flashed on the centered monitor directing the subject to gaze shift again to either the right or left. Gaze shift DVA (gsDVA) was measured both in quiet stance and during walking at a self-selected task specific speed.

Results

We have collected data on 50 healthy adults (n=36 < 65 y/o, mean age: 39.785±13.19 years; and n=14≧65 y/o, mean age: 73.5±5.003 years). In quiet stance, left gsDVA was 0.003LogMAR±0.034 in young vs 0.063 LogMAR ±0.097 in old, p = 0.041; right gsDVA was-0.004v±0.03 in young vs 0.037 LogMAR ±0.095 in old, p = 0.138. During walking, left gsDVA was 0.0009 LogMAR ±0.04 in young vs 0.062 LogMAR ±0.09 in old, p = 0.025; right gsDVA was-0.008 LogMAR ±0.04 in young vs 0.058 LogMAR ±0.10 in old, p = 0.029.

Conclusion

Our data suggests age affects gsDVA score and that in healthy controls, visual acuity degrades during gaze with age. We believe this measure will be a useful metric in evaluating dynamic visual acuity while walking in different age groups.

Funding

Ministry of Science and Technology, Taiwan Grant number: 102-2314-B-075-004-MY3

PS 478

Endolymphatic Sac Decompression, a New Old Therapy for Meniere´s Disease

Ioana Herisanu[1]; Mark Praetorius[1]; Peter Plinkert[1]; Bodo Schiffmann[2]
[1]University of Heidelberg; [2]Vertigo Center Sinsheim

Introduction

The operative approach of Meniere´s disease is in many practises not infocus despite decades of invasive vestibular neurotomy, labyrinthectomy and endolymphatic sac drainage. This may be because of the high rate of quality of life impairing complications as deaf ear, facial pulsy, poor compensation of vestibular function. The endolymphatic sac decompression however prooved, from our point of view, to be a safe procedure for the hearing, with good chances of vertigo episodes remission.

Matherial and methods

We report here 16 patients who underwent a endolympahtic sac decompression procedure in our department between 2013-2014, having over one year follow-up. According to the guidelines of the AAOHNS 1985, nine patients had defined Meniere´s disease, 6 possible and 1 probable. We discuss the preoperative diagostic panel and postoperative quality of life outcome.

Results

All but one patient showed recent typical fluctuating hearing or hearing loss in the low frequencies. Six patients had normal subjective visual vertical (SVV), 8 pathologic and 2 were not tested for SVV. Ten patients had pathologic caloric test results in the affected ear, three of them with horizontal eye movements in the videonystamography. Five had pathologic saccades in head impulse testing. Especialy cVEMPS but also oVEMPS were partial absent or diminished, showing 58,33% oVEMPS correlation to the SVV. The posturography is also varying from normal to cervial syndrom or M. Meniere specific.

Interviewing the patients one year or later after the intervention all but one reported benefit from the procedure. Thirteen patients are free of vertigo attack mostly even without medication. In one patients the hearing worsend, so she considers to undergo a cochlear implantation. Two people report an interaural constant pressure, an no tinnitus. The hearing fluctuation also stopped in all patients. One patient had a revision surgery because of new attacks 4 month after the first intervention and is free of vertigo now. Three patients were lost to follow up.

Conclusions

The diagnosis of the endolymphatic hydrops requires a panel of investigations showing no specific pattern. When oral betahistin therapy fails, the endolymphatic sac decompression seams to be, in well selected patients, a good choice with high rates of vertigo attack remission, hearing improvement and preservation of the organ of equilibrium. It should be taken into consideration before organ of hearing and equilibrium deactivating methods as gentamicin application. Revision

surgery can also be a good choice if the attacks reoccur months after the first intervention.

PS 479

Quantitative analysis of nystagmus by original real-time video-oculography and image filing system.

Makoto Hashimoto[1]; Takuo Ikeda[2]; Hironori Fuji[1]; Kazuma Sugahara[1]; Yoshinobu Hirose[1]; Hiroshi Yamashita[1]
[1]Yamaguchi University Graduate School of Medicine;
[2]Tsudumigaura medical center for children with disabilities

Background
It is essential to use an infrared CCD camera in clinical examination of the vestibular system. Devices are currently available that can quite accurately record human eye movements, based on the principle of video-oculography (VOG). We have devised an original VOG (HI-VOG) system using a commercialized infrared CCD camera, a personal computer and public domain software program (ImageJ) for data analysis. We revised the VOG and image filing system for real-time quantitative analysis of nystagmus.

Methods
The video image from the infrared CCD camera was captured at 30 frames per second at a resolution of 640*480 pl.. For analysis of the horizontal and vertical components, the X-Y center of the pupil was calculated using the original macro. For analysis of torsional components, the whole iris pattern, which was rotated by 0.1 degree, was overlaid with the same area of the next iris pattern, and the angle at which both iris patterns showed the greatest match was calculated.

Results
For quantitative analysis, the slow phase velocity of each occurrence of nystagmus, the average value of the slow phase velocity and the visual suppression value, were analyzed automatically.

Conclusion
Using the revised VOG system, it was possible to perform real-time quantitative analysis of nystagmus parameters from video images recorded with an infrared CCD camera.

Funding
R & D Promotion Subsidy System (Yamaguchi Prefecture Government)

PS 480

SHIMPs - A Simple New Variant of the Video Head Impulse Test (vHIT) Enhances Semicircular Canal Testing.

Ian Curthoys[1]; Hamish MacDougall[1]; Leigh McGarvie[2]; Konrad Weber[3]; Leonardo Manzari[4]; Michael Halmagyi[2]
[1]University of Sydney; [2]Royal Prince Alfred Hospital;
[3]University Hospital, Zurich; [4]MSA ENT Academy Center

In the usual vHIT test the subject is instructed to maintain fixation on an earth-fixed target during small, abrupt, passive, unpredictable head turns (head impulses) in the plane of the canal under test. In healthy subjects the vestibulo-ocular reflex (VOR) acts to drive the eyes to correct for the head turn and so maintain fixation on the target, without any corrective saccades. For a patient with a loss of canal function, the VOR gain is low, so during a head turn to the affected side, the eyes do not correct for head movement but are dragged, with head, so that at the end of the head turn a corrective saccade (a “HIMPs” saccade) is necessary to regain fixation on the target.

A simple variation (which we term SHIMPs) of this procedure is that during the same head impulse stimulus the subject is required to maintain fixation on a head-fixed target (a spot of light from a cyclist’s headlamp worn by the subject and projected on the wall in front of the subject).

The results are complementary; now ***healthy*** subjects make a corrective saccade (a “SHIMPs” saccade), whereas patients with complete canal loss do not. For healthy subjects the VOR is activated at the onset of the head turn and acts to drive the eyes opposite to head turn, so that their eyes are driven off the moving target and at the end of the head turn the healthy subject must make a corrective (SHIMPs) saccade to regain the target. For a patient with loss of canal function, the eyes will be dragged with head - the VOR will not drive the eyes off the target - and at the end, the eyes will remain on target and so no corrective saccade will be necessary

Discussion
Healthy subjects can suppress their VOR but such suppression takes time (around 80ms for abrupt unpredictable stimuli) and during that time the VOR will be driving the eyes to compensate for head turn and so be driving the eyes off the head-fixed target, requiring a corrective saccade at the end of the head turn to regain the target. Patients with complete canal loss do not have a VOR to suppress, so their eyes move with head during the head turn and remain on target, so no saccade is necessary. SHIMPs is especially useful for detecting any residual function.

Funding
Garnett Passe and Rodney William Memorial Foundation National Health and Medical Research Council No 1046826

PS 481

Normalizing Methods For Cervical Vestibular Evoked Myogenic Potentials

Toru Seo; Katsumi Doi
Kinki University Faculty of Medicine

Background
As cervical vestibular evoked myogenic potentials (cVEMP) can detect otolith dysfunction, it has been one of the fundamental examinations for neurotological clinic. The amplitude of cVEMP depends on the constriction of sternoclaidmastoid muscle (SCM). To neglect this, normalization is required. We know two normalizing ways for cVEMP. One; normalized results are obtained after averaging with each raw wave. The other; normalized results is from average with each normalized wave.

Methods
VEMP were recorded in 8 healthy volunteers without neither ontological nor neurotological disorders. Method A: Averaged raw wave were obtained by 100 times sound stimuli. The normalized amplitude was determined from amplitude of averaged raw wave divided by the integral value of 20 msec before stimulus of rectified raw wave. Method B: A hundred raw waves were obtained by sound stimuli. Root mean square (RMS) values of 20 msec before stimulus were obtained in each stimulus. The normalized waveform demanded it from the average of the wave which divided each raw wave by RMS value.

Results
The mean asymmetry ratio of subjects was 13.6 ± 12.2 on method A and 10.8 ± 10.1 on method B. The former was slightly smaller than the later, however there was not significant difference.

Conclusion
The accurate normalization for cVEMP may be obtained from method B. Method B requires specific signal processing devices but method A dose not. Method A provides us enough accurate value in clinical use.

PS 482

Balance and Dizziness Problems and Associated Risk Factors among Older Adults: the AGES-Reykjavik Population-Based Cohort Study, 2002–2011

Chuan-Ming Li[1]; Howard Hoffman[1]; Hannes Petersen[2]; Charles Della Santina[3]; Gudny Eiriksdottir[4]; May Chiu[1]; Christa Themann[6]; Diana Fisher[7]; Mary Frances Cotch[7]; Lenore Launer[5]; Tamara Harris[5]; Palmi Jonsson[2]; Vilmundur Gudnason[4]
[1]National Institute on Deafness and Other Communication Disorders, NIH; [2]University of Iceland; [3]Johns Hopkins University; [4]Icelandic Heart Association; [5]National Institute of Aging, NIH; [6]National Institute for Occupational Safety and Health, Centers for Disease Control and Prevention; [7]National Eye Institute, NIH

Introduction
Balance and Dizziness problems (BDP) are among the most common reasons for a visit to a physician's office for adults of all ages.

Objective
Estimate prevalence of BDP and falling among older adults and identify risk factors associated with BDP and falling in older adults.

Methods
The Age, Gene/Environment Susceptibility–Reykjavik Study (AGES-RS I) 2002–2006, interviewed and examined a population-based cohort of 5,764 adults aged 66–96 years. Five years later, 3,411 surviving subjects were followed-up in AGES-RS II. Participants were asked about problems during the last 12 months with spinning or vertigo sensations (vertigo); floating, spacey, or tilting sensations (floating); light-headedness without a sense of motion (light-headedness); feeling that one will pass out or faint (fainting); blurring of vision when moving head (blurred vision); or feeling off-balance or unsteady (unsteadiness). BDP was positive if respondents said 'yes' to any of the above symptoms. Complete information for BDP was obtained from 2,844 participants. We used logistic regression to calculate odds ratios (OR) and 95% confidence intervals (CI).

Results
In the AGES-RS II cohort, 72 or more years of age, BDP prevalence was 39.9% (35.3% in males, 43.6% in females). The prevalence of each symptom was: vertigo 16.5%, floating 3.1%, light-headedness 10.4%, fainting 7.7%, blurred vision during head movement 3.6%, and unsteadiness 28.6%. BDP symptoms that were most bothersome were unsteadiness 54.8% and vertigo 28.8%. After multivariable adjustment, risk factors independently associated with increased BDP included: memory loss last 12 months (OR=1.94; CI:1.49–2.54); diabetes (OR=1.43; CI:1.00–2.04); hypertension (OR=1.24; CI:1.02–1.52); coughing-up phlegm in the morning during winter (OR=1.64; CI:1.13–2.37); numbness/sensory loss of complete body side or limb (OR=2.54; CI:1.72–3.76); hip pain, aching or stiffness (OR=1.40; CI: 1.09–1.79); joint pain, aching or stiffness on most days (OR=1.53; CI:1.24–1.88); having fallen and landed on the floor (OR=1.78; CI:1.42–2.24); tinnitus (OR=1.31; CI:1.04–1.66); and self-reported hearing loss (OR=1.31; CI:1.07–1.60). Prevalence of falling during the last 12 months was 23.0% (31.4% in males, 17.4% in females). Of those who fell more than once in the last year, 70.2% reported BDP. After adjusting for confounders, BDP was significantly associated with risk of falling (OR=1.51; CI:1.14–2.00).

Conclusions
Dizziness is a broad term used to describe a variety of sensations. This study is based on specific characterization of BDP symptoms. In older adults, BDP is common, disabling, costly, and it confers greatly increased risk of falling.

PS 483

The Association Between Vestibular Function and Visuospatial Ability in Individuals with Dementia

Aisha Harun; Robin Bigelow; Esther Oh; Yuri Agrawal
Johns Hopkins University

Background
There is growing evidence of an association between vestibular dysfunction and cognitive impairment, particularly with respect to the cognitive domain of visuospatial ability. Visuospatial impairment is one of the most common deficits in dementia. We sought to assess the association between vestibular function and visuospatial function among patients with cognitive impairment (including dementia) to further explore this potential link. This represents one of the first studies of vestibular function in patients with dementia, a critical public health problem.

Methods
Individuals with a diagnosis of cognitive impairment (either mild cognitive impairment or dementia) were recruited from the Memory and Alzheimer's Treatment Center. Thirty-five patients underwent vestibular and visuospatial testing out of a planned enrollment of 50 patients. Vestibular testing consisted of assessments of cervical and ocular vestibular-evoked potentials (cVEMP and oVEMP) indicative of saccular and utricular function respectively, and of the vestibular ocular reflex (VOR) with video head impulse testing. Visuospatial testing included the Money Road Map Test (MRMT) and the Trail-Making Tests Part A and B (TMT-A and TMT-B). Linear regression models adjusted for age, gender, and education were developed to explore the association between vestibular function and performance (i.e. time for completion) of the visuospatial tests.

Results
In regression analyses, we observed that higher oVEMP amplitude was associated with a shorter time to complete the TMT-B (β= -16.3 seconds, p= 0.031). Similarly, higher oVEMP amplitude was associated with a shorter time to complete the MRMT (β= -8.9 seconds, p=0.081). There was no statistically significant difference in the time to complete the visuospatial testing with cVEMP amplitude or VOR gain in the data collected so far.

Conclusion
Among patients with cognitive impairment, we observed that individuals with better utricular function had better performance specifically on visuospatial cognitive function tests. Further data collection and analysis are ongoing. The long-term goal of this research will be to establish whether loss of vestibular function is a cause of cognitive decline.

PS 484

Hormonal change during salt reduced diet in Meniere's disease

Takenori Miyashita; Ryuhei Inamoto; Shinjiro Fukuda; Hiroshi Hoshikawa; Nozomu Mori
Kagawa University

Background
A low salt diet has been the mainstay of therapy for Meniere's disease (MD) since the 1930s. Although, the mechanisms of a low salt diet has not been elucidated. This salt reduction associated with a physiological increase in plasma aldosterone. In the inner ear, especially in the endolymphatic sac, several experimental reports suggest that aldosterone may increase endolymph absorption. Aldosterone increase by a low salt diet may be able to increase endolymph absorption in the endolymphatic sac. In this study, urinary sodium excretion, serum aldosterone, and other hormones were measured during salt reduced diet treatment in MD.

Method
We included 13 patients (7 men and 9 women) with unilateral definite MD, who were diagnosed at the Kagawa University Hospital with MD. A national registered dietitian provided nutritional guidance for 14 enrolled patients with MD to consume a low-salt diet (2 g Na per day). Twenty-four hour urine was before and 2, 4, 6, 8 weeks, 6 months, 12 months, 18 months, 24 months after consuming the low-salt diet. Osmotic pressure, Na, K, Cl were measure form this urine and 24-hour urinary Na, K and Cl excretion was estimated. Aldosterone, cortisol, renin activity, ADH, Na, K, Cl, and plasma osmotic pressure, and other hormones were measured from the blood. All candidates underwent salt reduced therapy for more than 2 years. Fourteen patients with MD were provided salt reduced therapy, and one patient was dropped out during 2 years.

Results
Group 1 included patients whose urinary sodium excretion average was less than 3 g/day urinary sodium excretion, and Group 2 included patients whose urinary sodium excretion average was greater than or equal to 3 g sodium per day. Vertiginous states of all Group 1 patients are complete control (Class A), and Group 2 patients are Class A (4 patients, 66%), Class C (1 patients, 17%) and Class D (1 patients, 17%), respectively. Plasma aldosterone was significantly increased during a low salt diet for 2 years. Plasma aldosterone of Group 1 was tend to be higher than that of Group 2. Hearing improvement after 2 years of Group 1 was significantly better than that of Group 2.

Conclusion
A low salt diet was effective as one of the treatment of Meniere`s disease. The mechanisms of a low salt diet may induced by increase of plasma aldosterone. The plasma aldosterone increase might activate ion transport and absorbing endolymph in the endolymphatic sac.

Funding
This study was financially supportsed in part by Grants-in-Aid for Scientific Research (#19791208) from the Ministry of Education, Culture, Sports, Science and Technology of Japan.

PS 485

Vertical and Torsional Alignment Nulling as Measures of Ocular Misalignment

Michael Schubert[1]; **Elizabeth Liu**[2]; Kara Beaton[3]
[1]Johns Hopkins University; [2]School of Medicine, Department of Otolaryngology Head and Neck Surgery; [3]Wyle Science Technology and Engineering

Background
The otolith organs contribute to vertical and torsional eye position relative to gravito-inertial accelerations (GIA). Recently, we validated a handheld behavioral measure of ocular alignment in the parabolic flight environment, when the GIA fluctuate. We are interested to investigate asymmetries in oculomotor position in patients with vestibular hypofunction as evidence of otolith pathophysiology. However, in light the brain can fuse even large ocular misalignments using binocular cues. Thus, we have developed a monocular eye position test to be measured in darkness.

Methods
In darkness, n=4 patients with vestibular hypofunction and n=8 healthy controls performed the Vertical Alignment Nulling

(VAN) and Torsional Alignment Nulling (TAN) tests. VAN/TAN are perceptual tasks of monocular position tests using a tablet computer that displays one horizontal red line and one horizontal blue line while viewing through color-matched red and blue filters. The red/blue filters provide separate visual information to each eye thereby eliminating binocular cues. One of these horizontal lines, designated as the stationary line, remains fixed on the screen, while the subject 'swipes' the screen to adjust the moving line vertically during VAN or torsionally during TAN. The final amount by which the lines are separated from one another vertically or torsionally (relative to one another) provides a perceptual measure of vertical and torsional ocular misalignment, respectively.

Results
Healthy controls and patients alike set the moving line either above or below the stationary line. The healthy controls set the lines within 0.6 degrees of each other for both VAN and TAN. The patient subjects set the line more than 1.5 degrees from each other for both VAN and TAN.

Conclusions
Our pilot data suggest both VAN and TAN are able to distinguish ocular misalignment in vestibular hypofunction, presumably from otolith end organ dysfunction. Ocular misalignment due to otolith pathology may be more common than previously thought perhaps due to the fact that most testing involves the use of binocular cues, which may in fact be obscuring the pathological finding.

PS 487

Low frequency tone burst evokes a new positive peak (P2) in cervical VEMPs between the traditional P1-N1

Chunming Zhang[1]; Jun Huang[2]; Youguo Xu[2]; William Mustain[2]; Hong Zhu[2]; **Wu Zhou**[2]
[1]First Affiliated Hospital, Shanxi Medical University;
[2]University of Mississippi Medical Center

Background
Tone burst-evoked myogenic potentials recorded from tonically contracted sternocleidomastoid (SCM) muscles (cervical VEMP or cVEMP) are widely used to assess the vestibular function. It is well known that cVEMPs are characterized by a positive peak (P1) followed by a negative peak (N1). However, we recently found that some cVEMP responses exhibited a second positive peak (P2) between P1 and N1. Although similar P2 responses are noticed in published cVEMP waveforms, to the best of our knowledge, the P2s have not been reported and analyzed. The goal of this study was to document and characterize the new P2 response, which may provide new insights into understanding neural mechanisms that mediate cVEMP responses.

Method
Tone-evoked cVEMP responses were measured in 11 normal subjects. Subjects were seated upright, with head turned to one side and instructed to maintain upright head position while pushing against varying levels of resistance. Single channel EMG was recorded from electrodes placed over the midpoint of the SCM muscle (noninverting electrode) and the sternoclavicular junction (inverting electrode), with ground electrode on the forehead. Tone burst stimuli (100 dB nHL, 10ms duration, 1ms rise/fall) of 125 Hz, 250 Hz, 300 Hz, 500Hz, 700 Hz, 1000 Hz, 1500 Hz, 2000 Hz and 4000 Hz were delivered monaurally, via an insert earphone, at 5/second, to the ear ipsilateral to the activated SCM muscle. The EMG was amplified (2,500), bandpass filtered (5 Hz- 1K Hz), sampled at 10K Hz and averaged over 100 stimulus repetitions. Tuning curves for each subject were recorded at either three or four different levels of tonic SCM muscle contraction, ranging from 50-300 uV.

Results
All subjects exhibited tone-frequency dependent cVEMP responses characterized by P1 and N1. In 8 subjects, however, some cVEMP responses exhibited a positive response (P2) between P1 and N1. By assuming that the cVEMP waveforms follow an exponential decay from P1 to N1, the new P2 responses were quantified to compute its latency and frequency tuning. We found that the new P2 responses were sharply tuned to 125Hz with a latency of 27.1$\pm$0.4ms, which was between P1 (18.4$\pm$0.3ms) and N1 (32.7$\pm$0.5ms).

Conclusions
These preliminary results show a new P2 response in cVEMPs in normal human subjects. However, little is known about its underlying neural mechanisms. Future studies are needed to understand this new component and its implications for assessing the vestibular function.

PS 488

Subjective visual vertical testing in a pediatric population: the bucket test vs the Chronos system

M. Geraldine Zuniga; Robert Labadie; Devin McCaslin
Vanderbilt University Medical Center

Background
The utricle is used to sense horizontal linear motion and when the head moves horizontally, the fluid in the inner ear displaces sensory hair cells embedded in the utricle. These cells send information to the vestibular cranial nerve and then to the central nervous system, indicating where the body is positioned in space. Damage to the utricle is detrimental to overall vestibular function and can lead to potentially harmful side effects such as imbalance, which can be permanent. Its function can be measured using ocular vestibular evoked myogenic potentials or the subjective visual vertical (SVV), a perceptual measure of one's upright horizon. By measuring a patient's SVV as compared to true gravitational vertical, it is possible to determine if utricular function is impaired. People with normal utricular function estimate their perceived vertical to be within 2 degrees of true vertical (Akin & Murnane, 2009; Halmagyi & Curthoys, 1999). The purpose of this study was to measure SVV estimation using the Chronos (SVV) system in a pediatric cohort and to compare it to the SVV measurement using the bucket test.

Methods
The study aimed to include a total of 10 pediatric patients from ages 5-10. Subjects completed both tests of SVV: the Chronos system and the bucket test. Exclusion criteria included prior history of repeated falls or complaints of dizziness.

Results and conclusions
All participants were able to complete the testing session. There were no immediate complications. Results indicate that SVV testing is feasible in a pediatric cohort and comparable to normative adult data (2 degrees of true vertical, as stated above). There were no significant differences between the Chronos system and the bucket test in this pediatric cohort. The bucket test may be a useful resource to test for utricular function in a pediatric population.

PS 489

Vestibulo-Ocular Responses to Vertical Translation using a Hand-operated Chair as a Field Measure of Otolith Function

Scott Wood[1]; David Campbell[2]; Millard Rschke[3]; Liesl Prather[1]; Gilles Clément[4]
[1]Azusa Pacific University; [2]Wyle; [3]NASA Johnson Space Center; [4]Lyon Neuroscience Research Center

The translational Vestibulo-Ocular Reflex (tVOR) is an important otolith-mediated response to stabilize gaze during natural locomotion. One goal of this study was to develop a measure of the tVOR using a simple hand-operated chair that provided passive vertical motion. Binocular eye movements were recorded with a tight-fitting video mask in ten healthy subjects. Vertical motion was provided by a modified spring-powered chair (swopper.com) at ~2 Hz (± 2 cm displacement) to approximate the head motion during walking. Linear acceleration was measured with wireless inertial sensors (Xsense) mounted on the head and torso. Eye movements were recorded while subjects viewed near (0.5m) and far (~4m) targets, and then imagined these targets in darkness. Subjects also provided perceptual estimates of target distances. Consistent with the kinematic properties shown in previous studies, the tVOR gain was greater with near targets, and greater with vision than in darkness. We conclude that this portable chair system can provide a field measure of otolith-ocular function at frequencies sufficient to elicit a robust tVOR.

Funding
NASA Human Research Program

SYMP 39

Canonical Wnt Signaling Regulates Progenitor Cell Identity in the Zebra fish Lateral Line

Hillary McGraw[1]; Austin Forbes[1]; Yuanyuan Xie[2]; Richard Dorsky[2]; Alex Nechiporuk[1]
[1]Oregon Health & Science University; [2]University of Utah

The mechanosensory lateral line system of aquatic vertebrates is composed of hair cells, arrayed on the surface of the animal, that display remarkable cellular and molecular similarities to hair cells of the auditory and vestibular systems. Development of the zebra fish lateral line has proven to be an elegant model for studying hair cell formation, because superficial hair cells are easily amenable to live imaging and genetic manipulation. The posterior lateral line (pLL) forms from the posterior lateral line primordium (pLLP), a cohort of ~100 cells which collectively migrate along the trunk of the developing zebra fish embryo. The pLLP is comprised of proliferative progenitor cells and organized epithelial cells that will form the hair cell-containing mechanosensory organs of the pLL. Wnt signaling is active in the leading progenitor zone of the pLLP and regulates cellular proliferation, survival and maintenance. Here we examine the downstream targets of canonical Wnt signaling and their role in mediating pLLP progenitor cell behavior. We used an RNA-sequencing approach to identify genes that are altered in zebra fish embryos carrying mutations in members of the canonical Wnt pathway that are known to regulate pLL formation, i.e. *lef1* and *kremen1*, as compared to wild-type controls. We then selected a subset of genes that are expressed in the migrating pLLP and generated targeted mutations using a CRISPR-Cas9 mediated genome-editing approach. One of the genes we selected for further analysis is the protocadherin Fat1b, which is strongly expressed in the wild-type pLLP and is downregulated following loss of Wnt signaling. Preliminary experiments suggest that knockdown of Fat1b function results in failed pLLP migration in a manner that is striking similar to previously described canonical Wnt signaling mutants. We are in the process of defining the cellular and molecular bases of this phenotype. These data suggest that our approach should reveal how molecular targets of the canonical Wnt signaling pathway regulate various cellular behaviors.

SYMP 40

Dynamic Studies of ER-Mitochondrial Communication During Aminoglycoside-Induced Hair Cell Death in the Zebra fish Lateral Line

Robert Esterberg; Edwin Rubel; David Raible
University of Washington, Seattle

The regulation of Ca^{2+} transfer between endoplasmic reticulum (ER) and mitochondria is increasingly recognized for its role in regulation of multiple cellular processes, ranging from bioenergetics to cellular dysfunction and death. For these types of studies we employ the zebra fish lateral line system, as it provides an opportunity to directly monitor intracellular Ca^{2+} changes during ototoxin-induced cell death *in vivo*. We generated a number of transgenic zebra fish expressing genetically encoded Ca^{2+} indicators specifically within hair cells. These include ER and mitochondria, the largest Ca^{2+} stores within the cell. We then exposed anesthetized larvae to concentrations of aminoglycoside that induce hair cell death within a subset of lateral line hair cells, allowing us to compare the time course of intracellular Ca^{2+} dynamics between living and dying cells exposed to the same concentration of aminoglycoside. We recently demonstrated that disruption of intracellular Ca^{2+} homeostasis within mechanosensory hair cells is an essential signal and a reliable predictor of hair cell death following ototoxic aminoglycoside antibiotic exposure.

We have now employed additional genetic and chemical tools to determine the impact of disruptions in the ER-mitochondrial Ca^{2+} transfer due to aminoglycoside exposure on reactive oxygen species (ROS) generation in the cytoplasm and in the mitochondria. Mitochondria and cytoplasm become increasingly oxidized in hair cells destined to die, and do so in a manner that is tightly correlated with mitochondrial Ca^{2+} uptake. Inhibition of mitochondrial Ca^{2+} uptake reduces both mitochondrial and cytoplasmic oxidation, suggesting that mitochondrial Ca^{2+} drives ROS generation in dying hair cells exposed to aminoglycosides. Our data places Ca^{2+} disruption as an event upstream of ROS generation during aminoglycoside -induced hair cell death.

Our current studies are aimed at identifying changes in organellar microenvironments that precipitate these events. We have identified several characteristics of hair cells that are first to succumb to the toxicity induced by aminoglycosides, and will discuss how we are applying recent DNA editing and imaging techniques to the zebra fish in an effort to extend these findings.

SYMP 41

Understanding Hair Cell Death and Protection in the Zebra fish Lateral Line

Allison Coffin
Washington State University Vancouver

The larval zebra fish lateral line system contains externally located sensory organs called neuromasts, each composed of ~8-20 hair cells. Lateral line hair cells are homologous to vertebrate inner ear hair cells and share similar susceptibility to ototoxic damage. In the last decade, the lateral line has emerged as a powerful model system for understanding hair cell death mechanisms and for identifying novel protective compounds. Current work in our lab examines the effect of natural compounds, such as herbal extracts, on lateral line hair cells. Natural product use is often through self-medication, so mild hearing loss would likely go undetected clinically and not be linked to the potential causative agent. Conversely, some natural products may have otoprotective properties, yielding a wealth of new compounds for drug development efforts. We have conducted parallel screens of a natural products library for compounds that modulate hair cell survival; one screen was designed to uncover potential occult ototoxins, while the other targeted compounds that protected hair cells from aminoglycoside damage. We discovered that the plant flavonols quercetin, kaempferol, and isorhamnetin all significantly damage hair cells. Interestingly, all three flavonols co-occur in ginkgo biloba, a popular herbal supplement. Our protection screen also yielded compounds of interest, in this case multiple bisbenzylisoquinoline derivatives that confer protection from aminoglycoside ototoxicity. In addition to chemical ototoxins, our lab has recently used the zebra fish lateral line to study noise-induced hearing loss, which impacts a much greater proportion of the human population. Our unique acoustic trauma model demonstrates that lateral line hair cells exposed to intense noise die in a time- and intensity-dependent manner, similar to hair cells in the mammalian cochlea. This model will facilitate rapid drug discovery efforts, similar to prior research on aminoglycoside otoprotectants. Collectively, this work demonstrates the power of the lateral line for mechanistic studies of hair cell death and protection and offers new therapeutic compounds for future translational research.

SYMP 42

Excessive Activation of Hair-Cell Localized Ionotropic Glutamate Receptors Induces Hair-Cell Damage and Death

Lavinia Sheets
Harvard Medical School

A hallmark of exposure to excessive noise is the release of high levels of the neurotransmitter glutamate from cochlear hair cells. The excitotoxic effect of excess glutamate signaling on afferent nerve fibers innervating hair cells has been well characterized. Yet whether excess glutamate directly damages hair cells has remained unclear because isolating hair-cell specific effects of glutamate toxicity in mammalian cochlea *in situ* is not practicable. I therefore investigated whether glutamate toxicity directly damages hair cells in 5-day-old zebra fish larvae exposed to drugs that mimic glutamate-induced excitotoxic trauma. Exposure to high levels of the AMPA/kainate glutamate receptor (GluR) agonist kainic acid (KA) contributed to significant, progressive hair cell loss in zebra fish lateral-line organs. This result was surprising—the presence of functional KA or AMPA receptors in sensory hair cells had not been definitively established, so GluR overactivation has not been considered as a direct effector of noise-induced hair-cell death. Because NMDA-type GluRs are also known play a major role in excitotoxic cell death, I exposed larvae to NMDA and observed that NMDA exposure led to significant hair-cell loss. These data support that overactivation of GluRs, possibly on the hair cells themselves, contributes to noise-induced hair-cell damage and death.

To exclude the possibility of hair-cell damage being solely a result of over-stimulating innervating afferent neurons, I exposed *neurogenin1a* morphants—fish that have morphologically mature and electrically active hair cells devoid of afferent and efferent innervation —to KA or NMDA. Significant hair-cell loss occurred in KA and NMDA exposed morphants, and the loss was comparable to that observed in wild-type siblings. Cumulatively, these data suggest that excessive glutamate signaling mediates damage to hair cells independent of damage to postsynaptic terminals, and implies the presence of functional GluRs on hair cells.

Consequently, I performed a survey of GluR gene expression in hair cells and have identified two candidate hair-cell localized GluR subunits: *grik4* and *grin1a*. My future aim is to modulate hair-cell expression of each identified receptor subtype and determine their specific contributions to hair-cell function and noise-induced hair-cell damage. Uncovering the physiological roles of each hair-cell GluR subtypes will provide information toward clinical therapies that can protect or repair damaged hair cells and restore hearing acuity.

SYMP 43

Hair-cell encoding of stimulus intensity in zebra fish

Josef Trapani; Eileen Troconis; Alexander Ordoobadi; Thomas Sommers; Razina Aziz-Bose; Ashley Carter
Amherst College

As the sensory receptors of the auditory, vestibular, and lateral line systems, hair cells must quickly and precisely transform mechanical stimuli into trains of action potentials (spikes) in afferent neurons. In addition to neuronal identity, stimulus features including intensity are encoded within the temporal patterns of evoked spike trains that are then transmitted to the brain for both perception and initiation of reflexes. We examined hair cell encoding of stimulus intensity in wild type and transgenic zebra fish with hair-cell expression of Channelrhodopsin-2 (ChR2). Specifically, we performed in vivo recordings from single afferent neurons in the lateral line while delivering to innervated hair cells both mechanical stimuli using a fluid jet and optical stimuli using controlled flashes of ~470 nm light. Our experiments tested the hypothesis that intensity would be correlated with the latency of the first evoked spike (FSL) and the number of spikes evoked during each stimulus. Furthermore, by using optogenetic activation of hair cells delivered to whole animals, we could examine the intensity dependence of behavioral startle responses evoked with stimuli similar to those used for afferent neuron recordings. Together, our whole-animal in vivo results indicate that intensity-dependent changes in startle response properties can be attributed to intensity-dependent changes in the temporal patterns of afferent spike trains.

SYMP 44

Using localized indicators in zebra fish to investigate how sensory information is encoded in vivo

Katie Kindt; Qiuxiang Zhang; Suna Li
National Institutes of Health, NIDCD

Introduction
Auditory and vestibular systems require sensory hair cells of the inner ear to sense sound and process vestibular stimuli. In order to reliably transmit auditory and vestibular information, hair cells use specialized pre-synaptic structures called ribbon synapses. We combine genetic, molecular, and imaging-based approaches to understand ribbon synapse function and development in vivo using the zebra fish lateral-line system. This system provides excellent access to sensory hair cells for pharmacology, in vivo imaging, and stimulation. In addition to the ease of access, powerful genetics make this an excellent system to explore ribbon synapse function and sensory encoding in vivo.

Methods
To examine ribbon synapse function we have created an extensive collection of transgenic zebra fish. These transgenic fish express genetically encoded fluorescent proteins that are subcelluarly localized to specific synaptic structures, allowing assessment of both synaptic morphology and function. For example, we have generated transgenic lines for measuring mechanotransduction, calcium influx at the ribbon synapse, synaptic vesicle release and postsynaptic activity. Imaging of localized indicators enables spatial resolution not possible using electrophysiological approaches. Where possible, we use two-color imaging to simultaneously measure multiple features. More recently, we have combined imaging of transgenic fish with the use of CRISPR technology in order to dissect the molecular components involved in ribbon synapse function.

Results and Conclusions
Using these methods we aim to understand how sensory input is converted to electrical activity in the postsynaptic neuron. For example, we aim to understand how all the hair cells and synapses within an organ such as a lateral line neuromast coordinate to encode sensory stimuli. This work is leading to new insights on ribbon synapse function and revealing the complex nature of how sensory information is encoded in vivo.

SYMP 45

Sensory-evoked synaptic currents in vestibulospinal neurons in vivo

Martha Bagnall
Washington University in St. Louis

Vestibulospinal neurons are responsible for transforming information about head orientation and movement into compensatory postural reflexes. While the sensory-evoked spiking activity of these neurons has been well characterized in mammalian single-unit studies, there has been no corresponding analysis of their recruitment at the synaptic level. Using larval zebra fish, we first show that anatomically, the vestibulospinal population is anatomically highly homologous to the Deiters' or lateral vestibular nucleus population in mammals, with innervation from both the vestibular (stato-acoustic) ganglion and cerebellar Purkinje cells. Second, we demonstrate that ablation of vestibulospinal neurons disrupts the animal's ability to orient with respect to gravity. Third, we take advantage of the transparency and accessibility of the preparation to make in vivo whole-cell physiological recordings from vestibulospinal neurons, and find that they receive barrages of excitatory synaptic currents in response to head translation. We discuss these data in the context of vestibular-evoked righting reflexes in fish and mammals, with emphasis on the recruitment of axial musculature.

SYMP 46

A New Model System To Understand the Development of Postural Kinematics

David Schoppik; David Ehrlich
New York University Langone School of Medicine

Tight regulation of posture is vital and must be acquired early in life. Reflexive corrective movements continuously correct sway by differential contraction of dorsal and ventral musculature. Early in development, the gain of these corrective movements can be inappropriately high, resulting

in overcompensation and falls. Later, refinement of these reflexes permits stable posture and anticipates changes that accompany voluntary locomotion. Reflex development relies on proper integration of information from multiple modalities including the vestibular, visual, and somatosensory systems. Human postural development occurs over the course of years under largely unconstrained conditions, making it difficult to study dynamic changes and their sensory underpinnings.

Here, we present the first report of a new model system to understand the ontogeny of posture. Because of their small size, genetic tractability, and external development, larval zebra fish have proven their utility as a vertebrate model system for understanding the development and neural underpinnings of a variety of sensory-driven reflexive behaviors. We constructed an apparatus to record the orientation of the long axis of freely swimming fish relative to the horizon (pitch), as well as their position in the water column. Recordings were made over the first month of life, approximately 1/3 of the way to sexual maturity. During this time, larvae must swim properly to find food, avoid predators, and interact with conspecifics.

Larvae at all ages propel in discrete, rhythmic swimming bouts. Surprisingly, these bouts are preferentially accompanied by fast upward rotations in the pitch axis. These propulsive rotations compensate for slow, downward pitch rotations that accrue slowly between bouts. Younger larvae spend less time than older larvae level with the horizon, due in part to exaggerated rotations between propulsive bouts. In addition, older larvae more reliably generate corrective propulsions when at eccentric postures or experiencing fast pitch rotations. At all ages, the fastest propulsions corresponded with the greatest angular accelerations in the pitch axis. Immature larvae tended to generate such angular accelerations using complex rotations with both head-up and head-down components, while older larvae produced fast, monophasic rotations.

Together, these data describe the developmental refinement of postural reflexes that enable proper control of pitch. We aim to leverage these data to generate specific predictions about underlying nervous system development improving vestibular and visual acuity as well as spinal motor control.

PD 58

Potential Mechanisms of Afferent Terminal Damage Following Sustained AMPA Release

Joy Sebe; Edwin Rubel; David Raible
University of Washington, Seattle

Exposure to loud noise can cause temporary hearing loss, measured as an increase in the threshold required to elicit an electrical response from the brain or a behavioral response to auditory stimuli. Studies of TTS have demonstrated that while the hair cells remain intact, the postsynaptic terminals of spiral ganglion cells are damaged. Noise induced damage of spiral ganglion cell terminals and a transient elevation of hearing thresholds can be mimicked by perilymphatic perfusion of the glutamate receptor agonist, AMPA. The inaccessibility of afferent neurons in the cochlea has made it difficult to examine afferent terminal damage and recovery in real-time. To visualize and record changes in afferent neuron morphology and function following AMPA application we are utilizing the zebra fish lateral line system. We first demonstrated that AMPA causes both afferent terminal damage and lack of terminal responsiveness to hair cell activation. Further, both the morphological and functional damage have at least partially recovered within an hour after AMPA washout. The *objectives* of the current work are to determine the physiological conditions and cellular mechanisms that cause terminal damage. We used *in vivo* time lapse imaging of afferent terminals of transgenic zebra fish larvae (6-7 days post fertilization) expressing the fluorescent calcium indicator GCaMP5. We found that AMPA mediated increases in GCaMP5 fluorescence intensity, a measure of neuronal depolarization, required Ca^{2+} permeable AMPA receptors, not NMDA receptors. Further, we examined whether hair cell death alone following treatment with the aminoglycoside antibiotic neomycin caused terminal damage and increases in GCaMP5 fluorescence intensity. An array of additional imaging and pharmacological studies were also conducted to determine the pumps and channels that contribute to calcium accumulation in the afferent terminal. Together, these data provide insight into the factors that mediate glutamatergic transmission and calcium homeostasis at the hair cell to afferent neuron synapse.

Funding
NIDCD

PD 59

Endothelin-1 Mediated Induction of Extracellular Matrix Genes in Strial Marginal Cells Underlies Strial Capillary Basement Membrane Thickening in Alport Mice.

Dominic Cosgrove[1]; Michael Anne Gratton[2]; Daniel Meehan[1]; Duane Delimont[1]; Brianna Dufek[1]; Grady Phillips[2]
[1]Boys Town National Research Hospital; [2]Saint Louis University

Introduction

Alport syndrome, a type IV collagen disorder, manifests as delayed onset and progressive glomerular disease associated with sensorineural hearing loss. Progressive thickening and lamination of the glomerular basement membranes and the strial capillary basement membranes (SCBMs) results, in part, from dysregulation of extracellular matrix (ECM) and metalloproteinase genes. We have identified a critical role for endothelin-1 (ET-1) activation of endothelin A receptors (ET_ARs) in driving pathogenesis in both tissues. In this study we explore the mechanism of ET-1 mediated pathology in the stria using both *in vitro* and *in vivo* approaches.

Methods

Wild type (WT) and autosomal Alport mice on the 129 Sv background were treated with the ET_AR antagonist, sitaxentan, from 2 to 7 weeks of age. The stria vascularis of these mice and untreated mice was analyzed by TEM for SCBM thickness

and by immunofluorescence for ECM proteins. Another set of WT and Alport mice were exposed to hypoxia or normoxia and the isolated stria analyzed for hypoxia-related and ECM genes by qRT-PCR. A conditionally immortalized strial marginal cell line was analyzed for expression of hypoxia-related genes and/or ECM transcripts after being cultured under normoxic and hypoxic conditions, or stimulated with ET-1 in the presence or absence of MAPkinase inhibitors.

Results

Alport mice showed thickened SCBMs and markedly elevated expression of collagen α1(IV), laminin α2, and laminin α5 proteins relative to WT mice. The SCBM thickening and the elevated ECM expression was ameliorated by ET_AR blockade with Sitaxentan. Remarkably, in stria isolated from untreated normoxic Alport mice and hypoxic WT mice there was a significant upregulation of hypoxia- related transcripts, ECM transcripts, and ET-1 transcripts. Both ET-1 stimulation and hypoxic culture conditions up-regulated ECM transcripts in cultured marginal cells. Blocking MAPkinase signaling with herbimycin prevented ET-1 mediated ECM gene induction in these same cultured cells.

Summary

ET-1 mediated activation of ET_ARs on strial marginal cells results in elevated expression of ECM genes, likely through ET_AR-mediated activation of the MAPkinase signaling pathway. This elevated ECM expression underlies the observed thickening of the SCBMs in Alport mice. SCBM thickening results in hypoxic stress further elevating ECM and ET-1 gene expression, exacerbating the strial pathology and predisposing the mice to hearing loss.

Funding

Supported by NIH R01 DK055000 and R01 DC006442

PD 60

Hypervulnerability to sound-exposure through impaired adaptive proliferation of peroxisomes

Sedigheh Delmaghani[1]; Jean Defourny[1]; Saaid Safieddine[1]; Paul Avan[2]; **Christine Petit**[1]

[1]Institut Pasteur; [2]Laboratoire de Biophysique Sensorielle, Université d'Auvergne

Adeficiency of pejvakin, a protein of unknown function, causes a strikingly heterogeneous form of deafness. Pejvakin-deficient (*Pjvk*$^{-/-}$) mice also exhibited variable auditory phenotypes. Correlation between their hearing thresholds and the number of pups per cage suggested a possible harmful effect of pup vocalizations. Direct sound or electrical stimulation showed that the cochlear sensory hair cells and auditory pathway neurons of *Pjvk*$^{-/-}$ mice and patients were exceptionally vulnerable to sound. *Pjvk*$^{-/-}$ cochleas displayed features of marked oxidative stress and impaired anti-oxidant defenses. We showed that pejvakin is associated with peroxisomes, and is required for the oxidative stress-induced proliferation of these organelles. In *Pjvk*$^{-/-}$ hair cells, peroxisomes displayed structural abnormalities after the onset of hearing. Noise-exposure of wild-type mice rapidly upregulated *Pjvk* cochlear transcription, and triggered peroxisome proliferation in hair cells and primary auditory neurons. Our results reveal that the anti-oxidant activity of peroxisomes protects the auditory system against noise-induced damage. *Pjvk* gene transfer can rescue auditory dysfunction in *Pjvk*$^{-/-}$ mice.

Funding

This study was supported by grants from Louis-Jeantet Foundation, ANR – NKTH "HearDeafTreat" 2010-INTB-1402-01, Humanis Novalis-Taitbout, Réunica-Prévoyance, BNP Paribas, and French state program ''Investissements d'Avenir'' (ANR-10-LABX-65).

PD 61

Type II Spiral Ganglion Afferent Drive of the Medial Olivocochlear Reflex Reduces Hearing Loss from Acoustic Overstimulation

Gary Housley[1]; Kristina Froud[1]; Jennie Cederholm[1]; Matthias Klugmann[1]; Jean-Pierre Julien[2]; Allen Ryan[3]

[1]UNSW Australia; [2]Laval University; [3]University of California, San Diego and the VA Medical Center

Background

Peripherin is a type III intermediate filament that is expressed by the type II spiral ganglion neurons (SGN) and has a role in establishing the sensory innervation of the outer hair cells (Froud et al., 2015; Nature Comm 6:7115 (ref.1)). The distributed type II SGN innervation of the outer hair cells is absent in the peripherin knockout (*Prph*$^{-/-}$) mouse and this results in loss of contralateral and ipsilateral suppression mediated by the medial olivocochlear (MOC) reflex (ref.1). Thus the type II SGN afferent innervation drives the MOC reflex and the *Prph*$^{-/-}$ mouse therefore provides an elegant model for studying the role of the MOC reflex in oto-protection.

Methods

Prph$^{-/-}$ and wildtype (WT) littermates underwent baseline ABR hearing function analysis under ketamine, xylazine, acepromazine anaesthesia (ref. 1), and were then treated with one of a range of open-field noise exposures (4 – 32 kHz white noise, 93 dB SPL – 108 dB SPL, 1 hour). Hearing function was re-analysed immediately afterwards, and then two weeks later.

Results

Both the WT and *Prph*$^{-/-}$ mice (6 - 8 per group) exhibited significant elevation in ABR thresholds immediately after noise, at all tested sound levels. There was no significant difference based on genotype (two way ANOVA, $P > 0.05$; combined mean ABR threshold shift at 24 kHz for 108 dB SPL noise = 66.6 ± 1.1 dB). Two weeks later thresholds in the WT mice had returned to pre-noise levels, however the *Prph*$^{-/-}$ mice exhibited a sustained elevation in thresholds at frequencies above 16 kHz (difference in mean thresholds between WT and *Prph*$^{-/-}$ mice at 24 kHz = 7.7 dB; difference in residual threshold shift at 14 days at 24kHz = 10.8 dB; $P = 0.013$, unpaired t-test). These data indicate that the *Prph*$^{-/-}$ mice had cochlear damage (waves P1 – N1 – P2).

Conclusion
These findings indicate that type II SGN afferent drive of the MOC reflex confers protection from acoustic overstimulation. Hence efferent feedback to the cochlear amplifier extends the safe upper limit of hearing.

Funding
NHMRC grant APP1052463

PD 62

Noise-induced Startle Hypersensitivity in Larval Zebra fish is Mediated by AMPA in Auditory Pathways

Ashwin Bhandiwad; David Raible; Joseph Sisneros
University of Washington

Background
Acoustic overexposure can result in perceptual auditory deficits, including temporary threshold shift (TTS), tinnitus, and hyperacusis. In rodents, these deficits have been linked to postsynaptic changes at the hair cell ribbon synapse and mediated by AMPA receptors. The larval zebra fish has emerged as a powerful model of understanding hair cell death, but has not been extensively studied in terms of behavioral changes due to noise exposure. The zebra fish acoustic startle response is a reliable, quantifiable behavioral readout mediated by a simple circuit of auditory neurons, Mauthner neuron and motor neurons.

Methods
Groups of 24 larval (5 days post-fertilization) wild-type AB zebra fish were exposed to a 10 dB (re. 1 m/s^2) flat-spectrum noise stimulus for 18 hours. Behavioral sensitivity was measured using a startle response assay in which pure tone stimuli (30-310 Hz) were presented at intensities of 14 to -16 dB (re. 1 m/s^2) and response probabilities were measured. Cohorts of fish were retested at 4 hr, 8 hr, or 12 hr post-exposure. To investigate potential neurotransmitters involved in hypersensitization, fish were noise exposed with either 20 uM APV (NMDA receptor antagonist), 20 uM DNQX (AMPA-receptor antagonist), or 100 uM bicuculline (GABAa-receptor antagonist) added to solution. To test for changes in Mauthner cell excitability, fish were noise exposed and startle responses were induced using an electrical field potential (EFP) designed to bypass the auditory input and directly activate the escape response.

Results
After 18 hours of noise exposure, startle thresholds decreased by up to 10 dB (re. 1 m/s^2) at all frequencies tested. Threshold shifts were temporary, returning to unexposed control levels after 12 hours of recovery. Changes in threshold in APV and bicuculline treated fish were similar to noise-exposed fish with no added drugs. However, DNQX treated fish showed no change in threshold after noise exposure. EFP experiments showed no significant changes in Mauthner cell excitability in noise-exposed fish compared to no-noise controls.

Conclusion
We find that acoustic overexposure results in hypersensitization of the acoustic startle response in larval zebra fish. Furthermore, we show that this effect is temporary, presynaptic to the Mauthner cell, and mediated through AMPA receptors. These results suggest conserved mechanisms of sensitivity changes due to acoustic overexposure in zebra fish and in other examined vertebrates and thus provide a new paradigm to use larval zebra fish as a model for understanding sub-lethal auditory damage and perceptual changes (such as hyperacusis) after moderate noise.

Funding
NIH DC5987 to DWR; UW Bridge Funding to JAS; UW auditory neuroscience training grant (NIH 2T32DC005361-11) to AAB

PD 63

Cochlear Pendrin Contributes to Recovery of Hearing after Noise Exposure

Laura Constance; Leah Freilich; Joel Sanneman; Tracy Miesner; Philine Wangemann
Kansas State University

Background
Mutations of *SLC26A4* are a common cause for progressive hearing loss. *SLC26A4* codes for pendrin, which is expressed in the endolymphatic sac, the vestibular labyrinth and the cochlea. During development cochlear pendrin expression was found unnecessary for the acquisition of hearing, whereas pendrin expression in the endolymphatic sac was found to be required (Choi et al., 2011; Li et al., 2013). It is not known whether pendrin expression in the cochlea has a function.

Objectives
The goal of our study is to determine whether cochlear pendrin expression confers protection against noise induced hearing loss.

Methods
We used a transgenic mouse model consisting of Tg(-);*Slc26a4*$^{\Delta/+}$ mice that express pendrin in the cochlea and Tg(+);*Slc26a4*$^{\Delta/\Delta}$ mice lack cochlear pendrin expression. The model was generated in a mixed background and was backcrossed into the 129S6 strain for four generations. Tg(-);*Slc26a4*$^{\Delta/+}$ and Tg(+);*Slc26a4*$^{\Delta/\Delta}$ mice differ not only in cochlear pendrin expression but also in renal and adrenal pendrin expression. Hearing thresholds were determined from auditory brain stem recordings (ABR) before and after noise exposure. Cochlear nerve conduction was evaluated by analysis of wave I. The vestibular aqueduct and pigmentation of stria vascularis were evaluated by histology. Blood pressure was measured with a tail-cuff.

Results
Tg(-);*Slc26a4*$^{\Delta/+}$ and Tg(+);*Slc26a4*$^{\Delta/\Delta}$ mice had similar hearing thresholds before noise exposure, however, noise-induced permanent threshold shifts were elevated in Tg(+);*Slc26a4*$^{\Delta/\Delta}$ mice. Tg(-);*Slc26a4*$^{\Delta/+}$ and Tg(+);*Slc26a4*$^{\Delta/\Delta}$ mice did not differ in blood pressure. No difference was found

in the cross-sectional area of the vestibular aqueduct and no hyperpigmentation of stria vascularis was seen after noise exposure in either type of mouse.

Conclusion
Pendrin appears to protect the cochlea from noise-induced hearing loss by supporting the recovery after noise exposure. Thresholds before noise exposure were similar whereas permanent threshold shifts after noise exposure were larger in Tg(+);*Slc26a4*$^{\Delta/\Delta}$ compared to Tg(-);*Slc26a4*$^{\Delta/+}$ mice. The absence of an enlarged vestibular aqueduct in Tg(+);*Slc26a4*$^{\Delta/\Delta}$ mice argues against a developmental difference related to the transgenic expression of pendrin in the endolymphatic sac. The lack of differences in wave I before noise exposure argues against a hidden compromise in cochlear nerve conduction in Tg(+);*Slc26a4*$^{\Delta/\Delta}$ mice. The absence of differences in blood pressure argues against a greater susceptibility to ischemia as a cause for larger threshold shifts in Tg(+);*Slc26a4*$^{\Delta/\Delta}$ mice. In conclusion, the data suggest that restoration of cochlear pendrin expression may be beneficial to slow progression of hearing loss in humans carrying mutations of *SLC26A4*.

Funding
NIH-R01-DC012151 and KSU-CVM

PD 64

Overexpression of LMO4 Mitigates Cisplatin-induced Cytotoxicity in UBOC1 cells

Samson Jamesdaniel; Rajamani Rathinam
Wayne State University

Background
Ototoxicity is one among the major side-effects of cisplatin, a highly effective anti-neoplastic drug used in the treatment of solid tumors. Cytotoxic effects of cisplatin occur primarily through apoptosis. Several reports have defined the regulation of cellular apoptosis by LIM domain only 4 (LMO4), a transcriptional regulator. However, the role of LMO4 in cisplatin-induced cytotoxicity is yet to be fully characterized. We reported that cisplatin treatment leads to nitration and downregulation of LMO4 and hypothesized that downregulation of LMO4 facilitates cochlear apoptosis in cisplatin-induced ototoxicity. This study investigates whether overexpression of LMO4 can prevent the cytotoxic effects of cisplatin.

Methods
UBOC1 cells, which are immortalized auditory sensory epithelial cells derived from C57 BL6 mice, were cultured in MEM supplemented with GlutaMAX, 10% fetal calf serum, and 50 U/ml gamma-intereferon, to facilitate proliferation and then cultured without gamma-intereferon for a week to facilitate differentiation. In order to induce transient overexpression of LMO4, HA-LMO4 plasmids were generated/isolated using mammalian expression vector pRK5 and fully differentiated UBOC1 cells at 50-60% confluence were transfected with HA-tagged LMO4 using lipofectamine reagent. After 48 h, the transfected cells were treated with or without cisplatin and cultured for another 24 h. LMO4 expression was determined by immunoblotting and RT-qPCR, while cytotoxicity was determined by a count of viable cells after trypan blue staining.

Results
Consistent with our previous reports, immunoblotting with anti-LMO4 indicated that cisplatin treatment induced a decrease in LMO4 protein levels in UBOC1 cells, while a corresponding decrease in LMO4 gene levels was not observed. The dose-dependent decrease in LMO4 protein strongly correlated with cell viability (r = -0.964). However, transient overexpression of LMO4 not only prevented the cytotoxic effects induced by 5 μM cisplatin treatment, but significantly increased the number of viable cells ($p<0.0001$), 24 h post-treatment. The increase in cell viability observed after overexpression of LMO4 suggested a potential anti-apoptotic role of LMO4. Transfection efficiency was verified by immunoblotting the HA tag attached to exogenous LMO4 in transfected UBOC1 cells.

Conclusion
The results of this study indicated that overexpression of LMO4 mitigates cisplatin-induced cytotoxicity while downregulation of LMO4 strongly correlates with the cytotoxic effects of cisplatin in UBOC1 cells. Collectively, these findings suggest a critical role of LMO4 in facilitating the ototoxic effects of cisplatin.

Funding
This research was supported by start-up funds to SJ from Wayne State University and P30 grant (P30 ES020957) to Center for Urban Responses to Environmental Stressors (CURES) from NIEHS.

PD 65

Secreted Factors from Human Vestibular Schwannomas Can Cause Cochlear Damage

Lukas Landegger; Sonam Dilwali; Vitor Soares; Daniel Deschler; Konstantina Stankovic
Massachusetts Eye and Ear Infirmary, Harvard Medical School

Background
Vestibular schwannomas (VSs) are the most common tumors of the cerebellopontine angle. Ninety-five percent of people with VS present with sensorineural hearing loss (SNHL), but the mechanism of this SNHL is currently unknown.

Method
To establish the first model to study the role of VS-secreted factors in causing SNHL, murine cochlear explant cultures were treated with human tumor secretions from thirteen different unilateral, sporadic VSs of subjects demonstrating varied degrees of ipsilateral SNHL.

Results
The extent of cochlear explant damage due to secretion application roughly correlated with the subjects' degree of SNHL. Secretions from tumors associated with most substantial SNHL resulted in most significant hair cell loss and neuronal fiber disorganization. Secretions from VSs associated with good hearing or from healthy human nerves

led to either no effect or solely fiber disorganization. Our results are the first to demonstrate that secreted factors from VSs can lead to cochlear damage. Further, we identified tumor necrosis factor alpha (TNFα) as an ototoxic molecule that correlates with degree of SNHL due to VS, and fibroblast growth factor 2 (FGF2) as an otoprotective molecule that correlates with level of hearing in VS patients. Antibody-mediated TNFα neutralization in VS secretions partially prevented hair cell loss due to the secretions.

Conclusion

Taken together, we have identified a new mechanism responsible for SNHL due to VSs.

Funding

This work was supported by the National Institute of Deafness and Other Communication Disorders grant T32DC00038 (S.D., K.M.S.), Department of Defense grant W81X-WH-14-1-0091 (K.M.S.), the Bertarelli Foundation (K.M.S.), Nancy Sayles Day Foundation (K.M.S.) and the Lauer Tinnitus Research Center (K.M.S.).

PD 66

A Tale of Non-Coding RNAs in the Mouse Inner Ear: Micro-, Linc- and Ce-RNAs

Kathy Ushakov[1]; Kobi Perl[1]; Tal Koffler[1]; Maya Enoch[1]; Yoni Bhonker[1]; Shaked Shivatzki[1]; Carmit Levy[1]; Ran Elkon[1]; Igor Ulitsky[2]; **Karen Avraham**[1]

[1]Tel Aviv University; [2]Weizmann Institute of Science

Much of the damage leading to hearing loss occurs in the sensory epithelium of the cochlea and vestibule, two of the organs that reside in the inner ear sensing sound and balance, respectively. These tissues are extremely complex and harbor intricate programs that must orchestrate perfectly. Gene expression and regulation play a crucial role in the function of both the auditory and vestibular systems of the inner ear. Non-coding RNA (ncRNA) species have been discovered with diverse regulatory roles attributed to them and their importance has been exemplified in sensorineural systems. microRNAs (miRNAs) are small non-coding RNAs that regulate gene expression post-transcriptionally. Long intervening noncoding RNAs (lincRNAs) are an ncRNA species with an expansive role in gene regulation. Finally, RNAs communicate with one another to form a large-scale regulatory network across the transcriptome via Competing Endogenous RNAs (ceRNAs), which can be coding or ncRNA transcripts, including mRNAs, lincRNAs, pseudogenes and circular RNAs. Changes in ceRNA regulation may lead to disease due to changes in expression levels of ceRNA transcripts that regulate key genes.

To identify ncRNAs in the sensory epithelium, RNA was harvested from vestibular and cochlear sensory epithelia of C57Bl/6 mice at two developmental stages, E16.5 and P0. RNA-Seq analysis revealed almost 500 microRNAs and thousands of lincRNAs expressed in the inner ear, with a portion differentially expressed between cochlea and vestibule. Gene targets were identified for a portion of these miRNAs, including the second most abundant miRNA, miR-181 (after miR-182). Reconstruction and filtering of the transcriptome of the inner ear using these libraries allowed us to identify known and novel lincRNAs active in the cochlea and vestibule. Finally, our analysis has revealed a ceRNA network in the inner ear. We crossed a list of human deafness genes and the Hermes ceRNA network, a multivariate analysis method created for glioblastoma (Sumazin et al. *Cell* 2011) that systematically infers candidate modulators of miRNA activity from genome-wide expression profiles of genes and miRNAs. Fifty-one of the deafness genes were found in the Hermes network. As our working hypothesis is that these genes represent a spectrum of the functional roles of ceRNAs in the ear that are involved in deafness, a variety of filtering rules and thresholds were applied to these genes, using mRNA and miRNA deep sequencing data from our laboratory. Our work is leading to the identification of novel non-coding regulators with roles in the mechanisms of hearing and deafness.

Funding

ISF grant 1320/11, BSF grant 2013027 and I-CORE Gene Regulation in Complex Human Disease Center No. 41/11

PD 67

A transcription factor involved in maintenance of hearing function in the mouse.

Neil Ingham; Jing Chen; Karim Boustani; Karen Steel

King's College London

Mice carrying a targeted mutation in the zinc-finger transcription factor-719 (*Zfp719*$^{tm1a(EUCOMM)Wtsi}$) have a hearing defect. We are defining the pathologies caused by the mutant allele in this mouse as a potential model of human hearing impairment.

Auditory Brainstem Responses (ABRs) were used to assess hearing sensitivity. Distortion Product Otoacoustic Emissions (DPOAEs) were used to assess Outer Hair Cell (OHC) function. Measurements of endocochlear potential (EP) reflected function of the stria vascularis. X-Gal staining was used to visualise structures expressing the *Zfp719* gene. Scanning Electron Microscopy (SEM) was used to examine the ultrastructural morphology of the organ of Corti.

Zfp719 was expressed in the lower part of the spiral ligament, the organ of Corti and in cells within the spiral ganglion of the mouse cochlea. ABRs indicated normal hearing sensitivity in mice that were heterozygous or homozygous for the targeted allele at post-natal day (P)14. By P21-P28, heterozygotes developed threshold elevations at 30kHz and above, which were relatively stable with further aging. Homozygotes showed progressive ABR threshold deterioration, to a profound impairment at all tested frequencies by 6 months old. DPOAEs (2f1-f2) at P14 were comparable in all genotypes but at P28 a similar pattern of threshold elevation to that seen in the ABRs was found, suggesting that outer hair cells do not function normally in the *Zfp719* mutant mice. Whilst the positive EP was comparable in all genotypes of mice tested at P21, the negative (anoxia) EP, indicative of current flow from the endolymph, was reduced from -30mV in wildtypes

to -18mV in homozygotes. This suggests that hair cells may have reduced permeability to positive ions in the mutants. Examination of the organ of Corti at P21 using SEM indicated some loss or fusion of individual stereocilia of OHCs while IHCs appeared normal. More severe changes were observed at P56, including stereocilia fusion and patchy degeneration of both OHCs and inner hair cells.

We are developing an understanding of the pathologies underlying this interesting progressive hearing loss phenotype. The mutation appears to primarily affect OHCs. However, the subtle anatomical abnormalities do not account for the severity of the hearing loss seen in mice.

Funding
Supported by The Wellcome Trust and the BBSRC

PD 68

Transcriptional Regulation of the Highly Abundant Otic-Specific Gene Fbxo2

Byron Hartman; Stefan Heller
Stanford University School of Medicine

Fbxo2 is arguably the most abundant gene in the mammalian inner ear. It encodes the ubiquitin ligase F-box protein, Fbx2, which is essential for cochlear protein quality control, homeostasis, and hair cell survival. Fbx2 was first identified as the most abundant protein in the adult guinea pig cochlea. Recently, Fbxo2 was categorized as the highest ranked otic sensory lineage-specific transcript in a transcriptome-wide comparison of developing mouse otic versus non-otic tissues. We generated Fbxo2-H2BVenus knock-in reporter mice to define expression of Fbxo2, which is present throughout the early otic vesicle and then becomes concentrated in the floor of the developing cochlear duct at around E13.5. In the neonatal cochlea, Fbxo2 is expressed throughout the organ of Corti as well as the lesser epithelial ridge. Ultimately, in the adult, Fbxo2 is expressed strongly in auditory hair cells and supporting cells, is exceptionally high in Boettcher and Claudius cells, and is found at lower levels in some cells of the lateral wall and spiral ganglia as well as a subset of vestibular hair cells.

Here we aim to decipher how the robust and specific expression of Fbxo2 is regulated. Phylogenetic comparison of Fbxo2 across vertebrate species reveals several conserved noncoding regions, including a ~2kb promoter and nine highly evolutionarily conserved regions (ECRs) downstream. Several potential binding sites were identified in silico, including sites for Pax2/5/8, Gata3, and Sox10. Conservation and clustering of binding sites within the promoter and ECRs is suggestive of combinatorial transcription factor binding. We hypothesize that Fbxo2 is regulated through multiple cis-regulatory modules located within the promoter and ECRs.

Thus, we produced a reporter mouse (Fbox2*tdTomato) with a transgene that mimics the native 100kb Fbox2 locus while condensing it to about 10kb by excluding non-conserved regions and replacing the Fbxo2 coding region with tdTomato. All nine of the ECRs were individually positioned similar to their native orientation and loxP and FRT sites were strategically included to allow subsequent excision of ECRs in two groups. The proximal ECRs 1-5 can be removed with Cre recombination while the distal ECRs 6-9 can be removed with Flip recombination. Crossing to the Fbxo2-H2BVenus enables direct comparison of the Fbxo2*tdTomato expression pattern with that of nuclear Venus driven by the native locus. The full-length transgene will test whether all of the conserved elements are sufficient to confer the normal pattern of Fbxo2 expression, while Cre/Flip excision will test for necessity within the ECR clusters.

Funding
Funding was provided by NIH grants R01 DC04563 (SH) and P30DC010363. BH is supported by Individual NRSA F32DC013210 and LRP awards through NIH/NIDCD.

PD 69

RNA-Seq Analysis of Regenerated Hair Cells in the Postnatal Mouse Cochlea

Tetsuji Yamashita[1]; **Fei Zheng**[1]; Ken Sugino[2]; David Finkelstein[1]; Bradley Walters[1]; Jian Zuo[1]
[1]St. Jude Children's Research Hospital; [2]Janelia Farm, HHMI

Background
Recent studies demonstrated that cochlear hair cells can be generated by ectopic Atoh1 expression at neonatal and juvenile ages, in mice, in vivo. However, these newly regenerated hair cells (or converted hair cells, cHCs) are immature. The aim of this study is to identify genes and pathways that are important for HC regeneration and maturation in the postnatal mammalian cochlea.

Methods
We used mouse models where induced ectopic expression of Atoh1 in neonatal cochlear supporting cells (SCs) led to new, immature HC (cHC) formation at adult ages. From cochleae of mice aged between postnatal day 21 (P21) and P33, we manually isolated ~20-40 fluorescently labelled cells of cHCs, endogenous mature SCs, and endogenous mature outer hair cells (OHCs). We then performed RNA Seq on amplified samples, analysed the comparative transcriptome profiles, and confirmed the expression patterns of several previously uncharacterized genes by other methods including immunostaining, quantitative in situ hybridization or Fluidigm single cell RT-PCR. We also overexpressed candidate transcription factors (TFs) in cochlear explant cultures by electroporation and looked for the upregulation of early and terminal HC markers in non-HCs.

Results
Independent replicates of each cell source were nearly identical; cHCs expressed >12 HC and SC markers that have been previously confirmed by immunostaining; hierarchical clustering suggests cHCs were hybrids between SCs and OHCs, supporting our previous characterization by immunostaining.

Among 1425 genes encoding TFs analyzed, we found 52 genes that were differentially expressed in these cHCs vs. endogenous mature SCs and OHCs. Interestingly, most of these TFs did show significant change in gene expression

profiling studies of chicken, zebra fish, or mammalian utricle regeneration.

Conclusion
We have identified ~50 candidate TFs that likely play key roles in HC conversion and maturation in postnatal mouse cochleae, several of which are being further characterized.

Funding
National Institutes of Health (DC006471, DC013879, CA21765the Office of Naval Research (N000140911014, N000141210775, and N000141210191), and the American Lebanese Syrian Associated Charities of St. Jude Children's Research Hospital.

PD 70

Distinct Function of Two MYO15 Isoforms in the Auditory and Vestibular Hair Cells

Qing Fang[1]; Sherri Jones[2]; Artur Indzhykulian[3]; Jonathan Bird[4]; Ashley Godin[1]; Anastasia Nelina[3]; Stephanie Edelmann[3]; Michael King[1]; Mirna Mustapha[5]; David Dolan[1]; Thomas Friedman[4]; Gregory Frolenkov[3]; Sally Camper[1]
[1]University of Michigan; [2]University of Nebraska-Lincoln; [3]University of Kentucky; [4]National Institute on Deafness and Communication Disorders; [5]Stanford University

Hearing impairment and equilibrium dysfunction are often comorbid conditions; estimates of vestibular dysfunction in individuals with congenital deafness vary widely, ranging from 16-50%, or more. Mutations in several unconventional myosins cause deafness and balance disorders in mouse and human: MYO1C, MYO7A, MYO6, and MYO15. These proteins are necessary for normal establishment of stereocilia on the surface of neurosensory cells of both the vestibular and auditory organs, processes which occur in late gestation and early postnatal mouse development, respectively. Mutations in either the motor or tail domains of MYO15 cause profound congenital deafness and vestibular dysfunction. In these mutants stereocilia are initiated in a normal pattern in response to planar cell polarity signals, but they fail to elongate further, consistent with the failure to transport the cargo proteins whirlin and Eps8 to the stereocilia tips. Two isoforms of MYO15 are generated from alternatively spliced transcripts, and the longer isoform has an unusual, highly conserved, 133 kDa proline-rich domain located N-terminal to the motor domain. Both isoforms are expressed in the auditory and vestibular systems, and the shorter isoform is sufficient to promote stereocilia elongation. To understand the function of the long isoform we generated *Myo15*$^{E1068X/E1068X}$ mice, which express only the short isoform, and tested their vestibular and auditory function and examined the structure of the hair cell stereocilia bundles. These mutant mice are deaf, but they have no obvious balance disorder. They lack circling behavior and swim normally. Preliminary data suggest slight differences in vestibulo-collic reflexes. The vestibular evoked responses from both 6-week and 6-month old mutants had slightly increased prolonged P1 latency and reduced P1-N1 amplitude, but the magnitude of the changes are consistent with normal behavior. In early postnatal ages, the mutant mice develop cochlear and vestibular hair cells with normal stereocilia bundles. However, 6-week old mutants exhibit degeneration of the mechanotransducing shorter row stereocilia in the cochlea, but vestibular stereocilia are intact. In conclusion, we discovered that the 133kDa domain unique to the long isoform of MYO15 is essential for maintenance of cochlear stereocilia and auditory function, but it appears to be dispensable for normal balance. Perhaps the evolution of myosin genes has involved incorporation of unique domains to regulate function in diverse neurosensory organs.

Funding
DC000039-18 DC000048-18 R01 704 DC05053 R01 DC008861 P30 DC05188 Hearing Health Foundation

PD 71

A Mutation in SLC22A4 Encoding an Organic Cation Transporter Expressed in the Cochlear Strial Endothelium Causes Human Recessive Non-Syndromic Hearing Loss DFNB60

M'hamed Grati
University of Miami Miller School of Medicine

Introduction
The high prevalence/incidence of hearing loss (HL) in humans makes it the most common sensory defect. The majority of the cases are of genetic origin. Non-syndromic hereditary HL is extremely heterogeneous. Genetic approaches have been instrumental in deciphering genes that are crucial for auditory function.

Goal
Mapping and identification of the gene causing ARNSHL in a large consanguineous Tunisian family (FT13), and characterization of the function of the encoded protein.

Methods
We used NADf chip to screen for common North African HL-causing mutation in FT13. We performed genome-wide linkage analysis to map the causative gene. We performed whole-exome sequencing on patient DNA to identify homozygous variants in genes within the determined locus that would cause the disease. We screened a cohort of small Tunisian HL families searching for additional patients carrying the same variants. We studied the targeting properties of candidate proteins in cell lines and performed immunofluorescence on rat inner ear preparations to study their tissue and cellular localization. We used morpholino-based gene knockdown, live imaging, immunofluorescence, and electrophysiological recordings to study auditory function of the orthologous genes in zebra fish.

Results
We first excluded the implication of known North-African mutations in deafness in family FT13. We then assigned the deafness gene locus to a 12.8 Mb critical region on ch:5q23.2-31.1, corresponding to DFNB60 locus. Moreover, we uncovered aminoacid substitution p.Cys113Tyr in a novel protein SLC22A4 (OMIM#604190), as the cause of ARNSHL DFNB60. Besides, screening a cohort of 71 Tunisian HL families led to uncover a deaf proband of consanguineous

parents that is homozygous for p.Cys113Tyr. This patient carried a homozygous microsatellite marker haplotype bordering SLC22A4 gene locus that was identical to that transmitted within FT13, indicating that this mutation is ancestral. SLC22A4 transports various compounds including organic cations, such as physiological carnitine, and naturally occurring potent antioxidant ergothioneine. Within tissues, carnitine facilitates fatty-acid transport into mitochondria to enter ß-oxidation for energy production. Using immunofluorescence, we demonstrate that Slc22a4 is expressed in the stria vascularis (SV) endothelial cells of adult rat and mouse cochlea and targets their apical plasma membrane. These observations were corroborated by finding Slc22a4 transcripts in our RNA-seq library from purified primary culture of mouse strial endothelial cells. Finally, slc22a4 disruption in zebra fish causes sensorineural HL.

Conclusions
We present SLC22A4 as an organic cation transporter of the SV that is essential for hearing, and its mutation causes DFNB60 form of HL.

Research Funding
The National Institutes of Health: R01DC005575, 2P50DC000422-Sub-Project 6432 and R01DC012115 to X.Z.L.; R21DC009879 and the University of Miami Provost Research Award to Z.L.; R21DC012398 and R01DC010844 to X.R.S.; R01DC009645 to M.T.; the International Centre for Genetic Engineering and Biotechnology and Ministry of Higher Education and Research of Tunisia to S.M.

PD 72

Carriage of an A2ML1 Duplication Variant that Confers Susceptibility to Otitis Media Influences the Middle Ear Microbiome

Regie Lyn Santos-Cortez[1]; Nadim Jose Ajami[1]; Ma. Rina Reyes-Quintos[2]; Ma. Leah Tantoco[2]; Patrick John Labra[3]; Sheryl Mae Lagrana[2]; Melquiadesa Pedro[2]; John Belmont[1]; Tasnee Chonmaitree[4]; Generoso Abes[2]; Joseph Petrosino[1]; Suzanne Leal[1]; Charlotte Chiong[2]
[1]Baylor College of Medicine; [2]University of the Philippines Manila – National Institutes of Health; [3]University of the Philippines College of Medicine – Philippine General Hospital; [4]University of Texas Medical Branch

Otitis media is an important public health problem worldwide and is a major cause of hearing loss across all age groups. Strong evidence exists for genetic susceptibility to otitis media, but no rare variants were previously associated with otitis media. We recently identified an *A2ML1* duplication variant that confers susceptibility to otitis media within an indigenous Filipino community and 3 European-/Hispanic-American children who had tympanostomy tubes at age 6 months. The variant is included in a short founder haplotype that is estimated to be 1,800 years old, and was not identified in >62,000 alleles from non-otitis samples, thus resulting in genome-wide significant association. A2ML1 protein is expressed in middle ear mucosal epithelium. To further determine the effect of the A2ML1 duplication variant on the middle ear, ear swabs were obtained from 16 indigenous individuals with chronic otitis media, of whom 11 carried the *A2ML1* variant. 16S rRNA sequencing revealed rarely reported bacteria in the middle ear including *Oligella.* At phylum level *Proteobacteria* and *Bacteroidetes* were more abundant in wildtype individuals and variant carriers, respectively. At genus level, *Haemophilus* had higher abundance in wildtype individuals, while *Porphyromonas* and *Fusobacterium* were increased in variant carriers. Carriage of the *A2ML1* variant influences middle ear microbial profiles, which can be used to guide antibiotic use and vaccination.

Funding
National Organization for Hearing Research Foundation, Hearing Health Foundation, and Action On Hearing Loss (to R.L.P.S.C.); University of the Philippines Manila-NIH (to G.T.A.); Albert and Margaret Alkek Foundation (to J.F.P.); NIH-National Institute on Deafness and Other Communication Disorders R01 DC011651 and R01 DC003594 (to S.M.L.).

PD 73

Application of Next Generation Sequencing for Gene Discovery in Otosclerosis

Sally Dawson[1]; Joanna Ziff[1]; Michael Crompton[1]; Jeremy Lavy[2]; Aldren Christopher[3]; Karen Steel[4]; Shakeel Saeed[2]
[1]University College London; [2]Royal National Throat Nose and Ear Hospital; [3]The Princess Margaret Hospital, Windsor; [4]King's College London

Otosclerosis is a common form of conductive hearing loss characterised by abnormal bone remodeling within the otic capsule, leading to fixation of the stapes bone in the middle ear. Approximately 30% of cases are familial with an apparent autosomal dominant inheritance pattern that exhibits variable penetrance. A number of investigative strategies have been utilised to identify genes involved in the disease process, including linkage analysis. However, to date no definitive causative genes have been identified. Consequently, development of a drug based therapy is hindered by lack of an understanding of the pathological mechanism.

In this study we performed whole exome sequencing in 4 families, each exhibiting monogenic inheritance of otosclerosis. After target enrichment using Agilent SureSelect Human All Exon V3 kit the whole exome DNA library from each participant was sequenced using Illumina HiSeq 2000 with 100bp paired-end reads and mapped to the reference human genome (GRCh37_hs37d5) based on the sequence alignment. Both single-nucleotide polymorphism (SNPs) and insertions-deletions (indels) were identified using SAMtools, GATK and Dindel. Variants were filtered within families so that only variants common to all affected individuals were retained. We focused on non-synonymous variants, those affecting splice sites and indels in coding genes. Known variants with a frequency greater than 0.02 were filtered out based on the 1000 Genomes Project and 500 Exomes Project. At this stage 2 parallel filtering pipelines were applied. These were (i) a robust "naive pipeline" based on retaining variants predicted to be deleterious by either Polyphen or SIFT and absent from dbSNP134 and (ii) a "candidate-gene pipeline"

where only variants in an otosclerosis candidate gene list of 494 genes were retained. After filtering the remaining variants were annotated and prioritised for follow-up firstly in segregation analysis and subsequently in a cohort of 57 unrelated cases of familial otosclerosis. Sanger sequencing identified six further individuals with additional rare variants in the same gene implicating this gene in the pathogenesis of otosclerosis. Functional analysis of the effect of the mutations on the protein is currently underway.

Funding
Action on Hearing Loss; Deafness Research UK; British Society of Audiology; Centers for Mendelian Genomics; Wellcome Trust Sanger Institute

PD 74

Whole-cell recordings from type II vestibular hair cells with basolateral processes in the mature mouse utricular macula

Antonia Gonzalez-Garrido[1]; Jennifer Stone[2]; Ruth Eatock[1]
[1]University of Chicago; [2]University of Washington

In the vestibular epithelia of mammals, hair cells classified as type I or type II have different shapes, afferent innervation, and voltage-dependent conductances. Recent reports (Golub et al., 2012, J Neurosci 32:15093; Pujol et al., 2014, J Comp Neurol) indicate that some mature type II hair cells in the utricles of mice and some other rodents have basolateral processes that contact supporting cells and other hair cells. To assess if these branched type II hair cells have distinctive electrophysiological properties, we are recording whole-cell voltage-gated currents and current-evoked voltages from utricular type II hair cells from mice, 3-13 weeks old.

Utricles were excised and pinned out in L-15 medium at room temperature; recording locations were documented. Recording pipettes were filled with a KCl-based internal solution and a fluorescent dye (sulforhodamine 101 or Lucifer Yellow). Results have been compared for cells with and without basolateral processes and across epithelial zones: the striola (S) and lateral and medial extrastriola (LES, MES). From images of dye-filled type II cells, 16 of 24 cells had obvious basolateral processes: 9 of 12 LES cells, 5 of 7 S cells, and only 2 of 15 MES cells. There was no indication of dye-coupling with adjacent cells, consistent with the lack of morphological evidence for gap junctions (Pujol et al., 2014).

Average resting properties did not differ between branched and unbranched cells or across zones: cell capacitances were ~4 pF, resting potentials were ~-60 mV, and input resistances were 0.8-1 GΩ. The steady-state voltage dependence of outwardly rectifying K^+ currents also did not differ across zones or with basolateral processes. Activation curves resembled those reported for utricular type II hair cells of younger rodents. Voltage responses to current steps in current clamp were also consistent with previous reports from less mature cells: positive steps evoked a sharp initial peak, negative steps evoked a slower transient hyperpolarization ("nose") attributable to activation of HCN current, and steady-state responses were strongly rectified. These results do not rule out subtle differences but suggest that cells with large basolateral processes do not have unusual electrophysiological properties. Moreover, the lack of strong zonal differences in the voltage-gated conductances of these mature type II hair cells suggests that reported differences in more immature rodent utricles may reflect zonal differences in developmental state.

Funding
NIDCD R21 DC013358

PD 75

Characterization of EPSCs at the Vestibular Type I Hair Cell Calyx Synapse

Matthew Kirk; Francis Meredith; Dylan Ray; Katherine Rennie
University of Colorado, Anschutz Medical Campus

Background
Mammalian vestibular neuroepithelia contains two sensory hair cell types. Type I hair cells (HCI) are engulfed by afferent calyx nerve endings, whereas type II hair cells (HCII) have smaller afferent bouton synapses. These afferent fibers fire spontaneously with stimulus modulation driving firing frequency (Goldberg 2000). Synaptic transmission is mediated via highly specialized ribbon synapses and previous recordings of excitatory post-synaptic currents (EPSCs) from calyx terminals support quantal release of neurotransmitter. However it remains unclear how EPSCs impact action potential firing and how responses vary with ribbon numbers across vestibular epithelia.

Methods
Whole cell patch clamp recordings were made from calyx afferent terminals isolated with their HCI from gerbil crista (postnatal days 19-28). This technique removes input from efferent fibers and afferents from HCII. Neurotransmitter release from HCI was measured as EPSCs in voltage clamp (between -70 and -100 mV). Sodium and potassium currents in the calyx were blocked with intracellular QX314 and cesium. Transverse crista slices allowed comparison of EPSCs from central and peripheral regions.

Results
Spontaneous EPSCs exhibiting a rapid rise-time (<0.15 ms) and monoexponential decay were classified as simple monophasic events. Remaining events (about 40% of EPSCs) showed complex characteristics. EPSC peak amplitude ranged from 15.5 pA to 885 pA (mean: 51.58 pA). Application of extracellular strontium (8 mM) increased median EPSC frequency from a control value of 0.59 Hz to 3.72 Hz (P=<0.001, N=10), with no effect on median amplitude.

In strontium stimulated cells, median frequency decreased from 3.72 Hz to 0.91 Hz (N= 9, P<0.001) in the presence of NBQX (40 μM; AMPA receptor blocker), and from 3.807 Hz to 1.124 Hz (N=7, P=<0.001) in Nifedipine (20 μM; L-type calcium channel blocker).

BayK-4866 (25 μM;, calcium channel agonist), increased mean EPSC frequency from a control value of 0.96 Hz to 2.88 Hz (N=4, P=0.032). γ-DGG (2 mM; low-affinity AMPA receptor antagonist) reduced simple events from 53.2% to 34.6% subsequently increasing complex events (N=5, P=<0.001) with no significant change to amplitude or frequency.

In crista slices, median EPSC frequency was similar in central and peripheral cells: 2.04 Hz (N=12) and 2.05 Hz (N=18) respectively.

Conclusion
Quantal transmission at the HCI/calyx synapse is largely mediated by AMPA receptors. Presynaptic L-type calcium channels regulate transmitter release. γ-DGG impacted simple events more suggesting glutamate accumulation in the HCI/calyx cleft contributes to complex events. Spontaneous EPSC frequency was similar in central and peripheral calyces.

Funding
Supported by American Hearing Research Foundation and Hearing Health Foundation

PD 76

Spontaneous And Driven Activity Of Vestibular Afferent Calyces In The Extrastriolar Zone Of The Mouse Utricle

Omar Lopez Ramirez; Ruth Eatock
University of Chicago

Vestibular primary afferents in the utricle form calyceal endings surrounding type I hair cells, bouton endings contacting type II hair cells, or both. Functional differences between afferents are correlated with zones (striola and extrastriola) in the sensory epithelia: chinchilla extrastriolar (ES) primary afferents have more regular spike timing and adapting responses than striolar afferents (Goldberg, Exp Brain Res 130:277, 2000). In whole-cell recordings from ex vivo saccules of immature rats (postnatal days, P, 1-9), extrastriolar calyces were more regular than striolar calyces (Songer & Eatock J Neurosci 33:3706, 2013). Recordings from the immature rat striola also provided evidence for both quantal and non-quantal transmission from type I hair cells to calyces. Here we report findings from calyces in the lateral extrastriola of utricles from CD-1 mice that were more mature (P10-30; mean 18 ± 1.7, SE, n=23).

Utricles were excised and pinned out at 25-28°C in L-15 medium. Recordings were made with a KCl-based pipette solution, with fluorescent dye to fill the terminal arbors. Recordings were made from calyces of LES afferents that formed complex or simple calyces around 2-4 type I hair cells plus 3-10 boutons on type II hair cells. Sinusoidal stimulation (2-100 Hz) of individual hair bundles with a coupled probe evoked postsynaptic potentials that were quantal (epsps, 6), non-quantal (3), or both (1). Thus, non-quantal transmission from type I cells to calyces is not restricted to the striola. The evoked spiking was more broadly tuned and less precisely phase-locked than in striolar rat calyces, consistent with *in vivo* zonal differences in afferent response dynamics.

In contrast to the regular firing of ES afferents in vivo (chinchilla utricle) or ex vivo (rat saccule), spontaneous spike timing in mouse utricular LES afferents was irregular: CV = 1.2 ± 0.1, Fano factor = 0.4 ± 0.1, average rate 17 ± 2.6 spikes/s (n=11). Possible factors in this difference include species, organ, development stage, extrastriolar sub-zone, and recording method. The underlying mechanism could be variation in the expression of low-voltage activated K (K_{LV}) channels (Kalluri et al., J Neurophysiol 104:2034, 2010). Consistent with this proposal, pharmacological block of K_{LV} channels produced regular spiking in mouse LES calyces (CV 0.05 ± 0.01, Fano factor 0.0008, rate 25 ± 4 spikes/s, n=4).

Funding
NIDCD R01DC012347

PD 77

Vestibular nucleus neuron activity is modulated by hindlimb movement in the conscious cat

Andrew McCall; Derek Miller; William DeMayo; George Bourdages
University of Pittsburgh

The central nervous system (CNS) controls posture by adjusting efferent outflow in response to afferent inputs from multiple modalities. While the CNS processing of certain balance-related inputs has undergone considerable scientific inquiry (e.g. the processing of somatosensory inputs from the neck), little consideration has been given to the role of somatosensory inputs from the limbs in balance control. We recently demonstrated in decerebrate cats that the activity of vestibular nucleus (VN) neurons is modulated in accordance with hindlimb movement and position. The principal goal of the present study was to determine if VN neuronal activity is similarly modulated by hindlimb movement and position in conscious cats. Single unit recordings were obtained from VN neurons in conscious cats during ramp-and-hold movements of the hindlimb in the rostral-caudal plane and during vertical plane whole body rotations. We identified 40 VN neurons whose activity was modulated by both hindlimb movements and vertical plane rotations. The activity of only one of these neurons was modulated in accordance with hindlimb movement and position; all other neurons solely encoded dynamic limb movement without encoding limb position. These findings confirm that VN neuronal activity is modulated by both hindlimb somatosensory inputs and vestibular inputs in conscious animals. However, the response properties to hindlimb movement among conscious animals differ from those seen in decerebrates suggesting that supratentorial inputs influence the processing of hindlimb somatosensory inputs within the vestibular nuclei.

Funding
Support for this project was provided by NIDCD (K08 DC-013571 to AAM)

PD 78

Human Perception of Concurrent Translation and Rotation in the Horizontal Plane

Benjamin Crane
University of Rochester

During common activities such as ambulation concurrent translation and rotation are experienced. How these movements are perceived has important implications for problems such as fall prevention, but previous work in this area has largely focused on single isolated movements. The current project investigated perception of concurrent rotation (yaw) and translation (sway and surge) in the horizontal plane. The study included 11 normal controls age 20-33 (mean 25). In all the investigators the subjects were fixed to a 6-degree-of-freedom motion platform. After each 1s stimulus presentation, subjects reported their direction of travel as one of two choices – left/right or forward/backward. Subsequent stimuli were adjusted based on these responses so that curve fitting could be used to measure any bias and perceptual threshold. The control experiments were done with isolated movements in the surge, sway, or yaw direction. Combined movements included surge-yaw, sway-yaw, yaw-surge, and yaw-sway. During each of these conditions, subjects were instructed to report only one type of movement, the first listed in each series. In addition in two additional experiments subjects reported the direction of translation while the axis of yaw rotation was varied. Perceptual thresholds were significant higher during combined movements. The threshold for surge alone was 1.1 ± 0.28 cm/s (mean±SE) and 2.3 ± 0.5 cm/s when combined with ±14°/s yaw. The threshold for sway was 0.75 ± 0.14 cm/s and 3.9 ± 0.8 cm/s when combined with yaw. The threshold for yaw alone was 0.96 ± 0.16°/s and 1.28 ± 0.27°/s when combined with ±14 cm/s surge and 1.55 ± 0.25°/s when combined with sway. Significant biases occurred with perception of sway during a 14°/s yaw, in which the point of subjective equality occurred with a sway of 3.7 ± 0.4 cm/s opposite the direction of rotation. However perception of yaw was not biased by a simultaneous sway. When the rotation axis was varied and subjects were asked the judge the direction of translation, the axis had to be located 13 ± 4 cm anterior to the inter-aural axis for sway to be equally likely to be identified rightward or leftward motion. These findings demonstrate that yaw rotation significant increases the threshold of translation perception as well as biases this perception in the direction of rotation. This may help tune perception so that the nature pattern of head motion during ambulation are filtered out and movements outside this pattern are more like to be perceived.

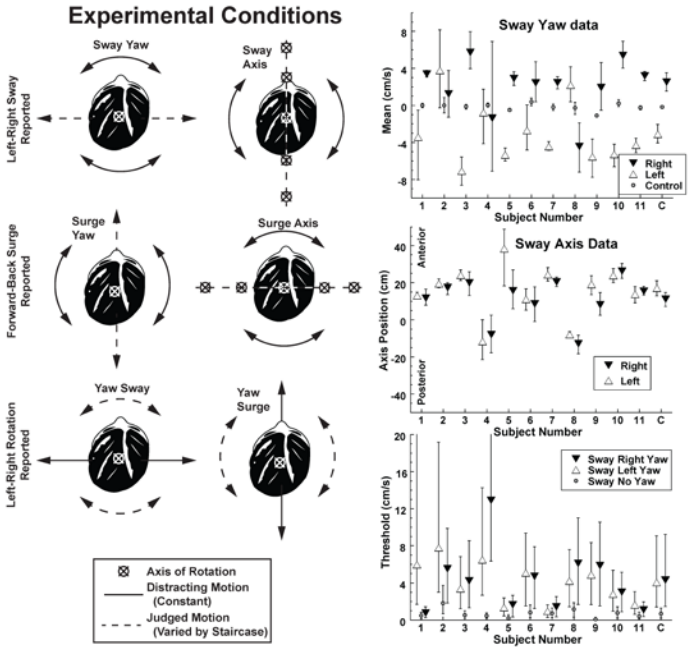

Funding
NIDCD R01 DC013580; NIDCD K23 DC011298; Triolocal Society Career Scientist Award

PD 79

Safe Direct Current Stimulation Increases the Dynamic Range of Head Velocities Encoded by the Vestibular Prosthesis

Gene Fridman; Charles Della Santina; Yu (Erin) Zheng
Johns Hopkins University

Vestibular labyrinths located in each inner ear, detect head motion about three spatial axes and deliver the input to stabilize balance and visual gaze. There are currently no therapies for bilateral vestibular dysfunction (BVD) beyond rehabilitation exercises.

A multichannel vestibular prosthesis (MVP) containing gyroscopes that sense head rotational velocity has shown considerable promise of delivering the sensation of head motion in animal and more recently, human studies. To encode head velocity, the MVP modulates the frequency of electrical current pulses delivered to each of the three branches of the vestibular nerve.

The vestibular afferents maintain a spontaneous discharge rate at rest (~100 spikes/s). In a normal individual when the head is turning toward one side, the afferents' firing rate will increase above the spontaneous rate and when the head is turning away their firing rate drops below the spontaneous activity. For someone suffering from BVD, the MVP can encode head movements toward the implanted side by increasing pulse rate. However, encoding head movements away from the implant presents a problem because pulse presentation from the prosthesis cannot inhibit the afferents, which persistently maintain their spontaneous activity.

Safe Direct Current Stimulation (SDCS) technology that we developed in our laboratory can inhibit neural firing. Conceptually, the SDCS we developed converts alternating charge balanced-pulses delivered to two metal electrodes submerged in an electrolyte within an implantable device to direct ionic current delivered to the tissue at the output of the device via electrolyte-gel-filled tubes, we refer to as SDCtubes.

We tested the hypothesis that the range of head rotation velocities that could be encoded by the MVP would be greater if the spontaneous activity of the neurons were suppressed with SDCS while the MVP artificially emulated the spontaneous activity and modulated spike activity to encode head rotation. We compared the effect of predetermined sinusoidal pulse-frequency modulation on the evoked VOR eye movements with and then without SDCS simultaneously presented to the vestibular labyrinth via the SDCtubes. In confirmation of the hypothesis, the range of head velocities that could be encoded across six canals in two implanted chinchillas was a factor of 4.5±2.5 greater for the head movements toward the prosthesis and a factor of 3.3±1.6 greater for the head movements away from the prosthesis when the SDCS current was used to suppress spontaneous activity.

Funding
NIH R21NS081425 NIH R01DC009255 MedEl Corporate Contract

PD 80

Ocular Torsion and Skew Deviation Findings During Electrical Stimulation in Human Subjects with a Chronically Implanted Vestibular Prosthesis.

James Phillips; Leo Ling; Christopher Phillips; Kaibao Nie; Jay Rubinstein
University of Washington

Background
We have developed a fully implantable vestibular stimulator to replace or augment vestibular function lost to disease or injury. This device has been implanted in human subjects and studied with intermittent stimulation over several years. During these initial studies, some subjects experienced subjective perception tilt and lateral postural sway with electrical stimulation of the lateral canal. This result suggests that such stimulation may also produce unilateral activation of utricular afferents. To evaluate this quantitatively, we recorded 3 dimensional eye movements binocularly and performed subjective visual vertical testing, during electrical stimulation with a vestibular prosthesis.

Methods
A vestibular prosthesis was implanted in the right ear of 4 subjects with Meniere's disease. The device had three leads that were implanted into the perilymphatic space of 3 semicircular canals. Each lead had 3 stimulation sites, capable of producing biphasic pulse electrical stimulation of the vestibular nerve. During testing, electrically elicited eye movements were recorded binocularly in the dark with a 3D video-oculography system (NKI). Subjective visual vertical testing was performed by asking the subjects to align a laser projected line with subjective vertical in otherwise complete darkness. Electrical stimulation was performed with constant pulse frequency and constant current amplitude pulse trains.

Results
Electrical stimulation of the right ear in complete darkness produced largely conjugate nystagmus over the duration of stimulation. Fast phases were synchronous in both eyes, and the direction of the eye movements was largely consistent. Large amplitude skew deviation was not observed. The velocity of the nystagmus increased with increasing current amplitude, but the direction of the eye movements was not consistent across current amplitudes. The eye movements often had torsional components. During subjective visual vertical testing, electrical stimulation produced deviation of the line away from the stimulated ear, which scaled with current amplitude.

Conclusions
Electrical stimulation with a vestibular prosthesis produces largely conjugate eye movements. The direction varies with current amplitude. Only subtle differences are present between the two eyes. Electrical stimulation also produces consistent changes in the perception of visual vertical. These findings suggest that some activation of the utricular afferents is likely during intended semicircular canal stimulation.

Funding
This work funded by 1 R01 DC014002-01,Wallace H. Coulter Foundation, and a gift from Sarah Kranwinkle. The technology under study was developed under HHS-N-260-2006-00005-C.

PD 81

Vergence testing in Mild Traumatic Brain Injury

Mikhaylo Szczupak[1]; Michael Hoffer[1]; Alexander Kiderman[2]; Robin Ashmore[2]; Carey Balaban[3]
[1]University of Miami; [2]Neuro-kinetics, Inc.; [3]University of Pittsburgh

Overview
Mild traumatic brain injury (mTBI) is an increasingly common public health issue that is seen in athletes, service members and the general population. One of the most critical issues in the study of mTBI involves making an accurate diagnosis. Unfortunately many diagnostic paradigms rely on patient history and physical examination, and a number of the most common deficits rely heavily on self-report. Our group has been examining a set of neurosensory sequelae that can be objectively tested using oculomotor, vestibular, and reaction time (OVRT) tests. Among the critical components of this testing series are four primary eye movement measurements 1) Saccadic movements, 2) smooth pursuit, 3) vestibulo-ocular movements, and 4) vergence movements. Most investigators are well acquainted with all of these eye movements except vergence. This may be because vergence is difficult to test in a clinical setting or because vergence is

the one eye movement that does not involve conjugate gaze. Nevertheless there is mounting evidence to support the hypothesis that vergence dysfunction contributes to disability after mTBI and vergence recovery is an important aspect in mTBI recovery. The goal of this presentation is to examine a novel test of vergence function and study the relationship of vergence abnormalities to other objective findings in both normal controls and subjects with mTBI

Methods
Fifteen individuals with new onset mTBI along with a group of 50 controls were included in this study. All individuals underwent an assessment of oculomotor, vestibular, and reaction time tests in the IPAS portable assessment system (Neuro Kinetics, Inc., Pittsburgh, PA). Two vergence stimuli were run: disparity fusion and smooth pursuit at 0.1Hz frequency. Output parameters included divergence and convergence time. These were measured as a decay time constant and eye displacement for the disparity fusion test and the time course and amplitude of vergence tracking in the smooth pursuit test.

Results
Vergence calculations utilizing both near and far horizontal responses were compared with OVRT time tests in both groups of individuals as well as between the control and mTBI subgroups.

Conclusions
Vergence deficiencies can be accurately measured and characterized using this portable eye-tracking device. Characterizing normal function and pathological dysfunction in mTBI patients will likely be a valuable tool in the management and study of mTBI. Vergence information may be used as a tool in the diagnosis of this disorder and an even more important tool in assessing progress for return to activity determination.

Funding
Head Health Challenge II (NFL, UA, and GE) and DoD

PD 82

The effect of visual rotation on perception of roll in normal humans and migraineurs

Mark Miller; Benjamin Crane
University of Rochester

Background
Vection is an illusory perception of motion that can occur when a visual motion is presented in the majority of the visual field. We used both certainty estimate (CE) and inertial nulling (IN) techniques to study the effect of visual stimuli on roll perception in humans with and without migraine.

Method
Nineteen human subjects were recruited, ten with typical migraine and nine controls. A visual star-field stimulus consistent with clockwise or counterclockwise roll motion was presented for 1 or 8s. For the IN method, an inertial nulling stimulus was delivered during the final 1s of the visual star-field stimulus. Subjects reported the overall perceived direction of motion during the final 1s of the stimulus. The magnitude of inertial motion was varied based on previous responses to find the point of subjective equality (PSE) at which clockwise (CW) and counter-clockwise (CCW) responses were equally likely to be perceived. For the CE trials, the same durations of visual motion were used but without inertial motion and subjects rated their certainty of motion on a scale of 0-100.

Results
For IN trials, the overall difference in PSE between 1s and 8s subjects is significant ($p=0.03$). Additionally, migraineurs had a greater deviation in IN studies in the 8s than 1s ($p=0.01$), but controls did not ($p=0.72$) (see **Figure 1)**. The variance among migraine subjects at the 8s ($\sigma^2=2.32$) was much greater than controls ($\sigma^2=0.35$) in IN trials. Two-way ANOVA by population and duration was significant for duration and subjects matching for both CE and IN trials, and the interaction between the two approached significance in the IN trials ($p=0.06$). The correlation between CE and IN was small across all trials. Interestingly, the correlation between clockwise and counterclockwise studies was modest in the IN trials ($r=0.44$), whereas the correlation for CE was unusually high ($r=0.97$).

Conclusion
IN is a useful tool in measuring vection in the roll plane. The marked difference in correlation between clockwise and counterclockwise studies between IN and CE studies highlights the fact that CE studies may be less sensitive to variations in observed motion due to the nature of the reporting tool. Perception of roll rotation in migraine subjects was more influenced by visual roll relative to controls. However, this had a lot of variation between subjects.

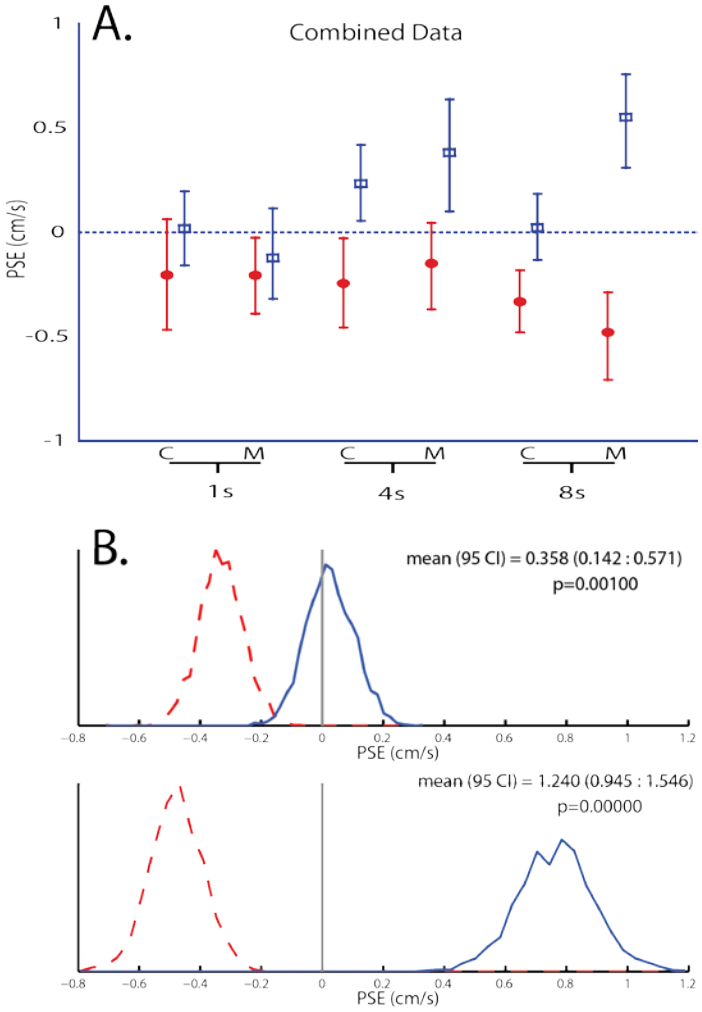

Figure 1: Panel A: Combined subject data by population and trial. Counterclockwise visual stimuli are represented with filled red circles, clockwise visual stimuli are represented by blue open squares. A positive PSE indicates that neutral motion would be perceived as clockwise self-motion. Error bars represent 95% CI. Panel B: 8s histogram comparing combined controls and migrainers response using a random resampling of responses. Responses from all subjects were included. Responses collected with counterclockwise visual stimuli are represented with a dashed red line, clockwise visual stimuli responses are represented with a solid blue line.

Funding
NIDCD K23 DC011298, R01 DC011298, Tribological Society Career Scientist Award

SYMP 47

The Mechanism of Auditory Scene Analysis in the European Starling Forebrain.

Naoya Itatani; Georg Klump
University of Oldenburg

In the natural environment, integrating or segregating multiple sounds according to their acoustic features is crucial for auditory scene analysis. Relevant features are frequency spectra, temporal fine structure, signal envelope and binaural features such as ITD or ILD and these will interact in forming the auditory streaming percept. Human psychophysical studies have identified a range of features that allow stream segregation (e.g., Moore and Gockel, 2012). Many of these features have now been tested in the European starling (*Sturnus vulgaris*) to evaluate the neuronal correlate of stream segregation. Starlings are known to produce complex acoustic communication calls and have a basic auditory perception comparable to that of humans. Hence, this species is an ideal animal model for auditory scene analysis research.

Separate populations of neurons being activated at different times appear to be a prerequisite of auditory stream segregation (e.g., Fishman et al. 2001). Presenting stimuli in the ABA– paradigm (van Noorden 1975) that allows studying stream segregation in humans and starlings, we could demonstrate a separate representation of A and B sounds processed in separate auditory streams by different populations of neurons. Amplitude modulated tones were segregated by the separation of their modulation frequencies, similar to the segregation by pure tone frequency difference. Harmonic complexes with different temporal structure also elicited segregation although their frequency spectrum was identical. All these features that provide for stream segregation in humans have a representation in the starling forebrain by separate populations of neurons.

The starling allows even to record the forebrain neurons' response while the bird perceives the stimuli and makes a decision. In the starling, we used the onset time shift detection paradigm to obtain an objective measure of the streaming percept. The birds were trained to detect an onset time shift of the middle B tone of an ABA– triplet which is more difficult if A and B tones are processed in separate streams. Comparisons between behavioral and neuronal sensitivities used a similar metric of sensitivity derived from signal-detection theory. Both the behavioral and neuronal discrimination performance deteriorated with increasing feature differences between A and B tones. Hence the results obtained in the objective time shift paradigm showed an excellent correspondence between the neuronal representation and the perception reflected in the bird's behavior. This approach also allows studying the interaction of multiple cues in auditory stream segregation such as spatial v.s. non-spatial features of sounds.

Funding
Funded by the DFG (TRR31).

SYMP 48

Neural Correlates of Relative Sound Localisation

Katherine Wood; Stephen Town; Huriye Atilgan; Gareth Jones; Jennifer Bizley
University College London

Two major models of the encoding of auditory space have been proposed; the two-channel model where the location of a sound in space is given by the relative activity of two broadly tuned channels and the topographic model where the location of a sound in space is represented by the firing rates of individual or small populations of neurons. Few studies

have attempted to determine whether neural responses in the cortex of behaving animals are consistent with these models. In this study we recorded from the primary auditory cortex of ferrets performing a novel localisation task and used the subsequent responses to test models of the cortical representation of auditory space. Ferrets were trained in a two-alternative forced choice task that required subjects to report whether a target sound occurred to the left or right of a preceding reference stimulus. Reference and target stimuli were separated by 30 degrees in the azimuthal plane and the task therefore required that the subject must actively discriminate the location in azimuth of the two stimuli and then compare their relative positions. Like humans (Wood & Bizley, 2015), trained ferrets perform well in the task, with performance best around the midline and decreasing towards the periphery. Around 50% of individual units recorded from were found to contain information about the location of the reference or the target location. To test the models, maximum likelihood decoders were used to decode cortical responses using either a two-channel or topographic model. Sound location was better decoded using a topographic model than a two-channel model. While both decoders perform above chance levels, only the topographic encoding can account for localisation ability of ferrets. Individual units were also found to contain information about the direction the sound moved in conjunction with the target location, suggesting that the firing patterns of units in auditory cortex represent not only the current stimulus location but the stimulation history, consistent with findings from non-human primates (Malone et al. 2002).

SYMP 49

Electrophysiological Markers of Auditory Perceptual Awareness and Release from Informational Masking

Andrew Dykstra; Alexander Gutschalk
Ruprecht-Karls-Universität Heidelberg

How acoustic stimuli transcend subconscious processing and enter awareness is not well understood, particularly in the sort of complex acoustic environments where audibility is limited not only by resolution of the auditory periphery but by the information-processing capacity of the brain. This talk will give a brief overview of studies we have been conducting using multimodal neuroimaging to examine the neural correlates of auditory perceptual awareness and release from informational masking. All studies utilized jittered versions of the so-called multi-tone masking paradigm, in which a stream of spectrally isolated, suprathreshold target tones is embedded in a 'cloud' of random maskers. Due target uncertainty and/or target-masker perceptual similarity (i.e., informational masking), the targets in such paradigms often remain subliminal, permitting isolation of neural activity associated with conscious perception. Early work using such paradigms identified a broad, long-latency response arising from auditory cortex that strongly covaried with listeners' perception of the target tones. However, our recent studies indicate that the processes underlying auditory perceptual awareness and release from informational making are much more diverse and widespread, incorporating multiple brain areas and distinct neuronal markers. Which of these reflect "true" correlates of conscious perception vs. merely its prerequisites or consequences remains a topic of intense debate.

SYMP 50

Real-time decoding of auditory selective attention and neurofeedback training using EEG

Inyong Choi[1]; Camille Dunn[1]; Bruce Gantz[1]; Barbara Shinn-Cunningham[2]
[1]University of Iowa; [2]Boston University

Selective attention modulates the neural representation of the auditory scene, enhancing the representation of a target sound and suppressing the background. Previous studies showed that the attentional modulation of electroencephalographic (EEG) signals measured non-invasively on scalp is sufficiently robust that it could be used to control brain-computer interfaces (BCIs). Most state-of-the-art BCI mechanisms are powerful because they allow "learning" of their classifier parameters, having users engage in long-term use of the system while receiving feedback. We envision that attention-operated BCI could be also used for post-implant training of cochlear implant (CI) recipients who have communication difficulty in multi-talker environments. However, excessive, long learning periods are impractical in our patient-use scenarios. Here, we propose a learning-free BCI mechanism whose operation leverages prior results describing how attention modulates spectrotemporal and topographic patterns in EEG signals. We presented two concurrent streams of consonant-vowel (CV) combinations; listeners were asked to attend and transcribe one of the streams. Which of the two streams they attended was randomly selected from trial to trial. We found that the cortical responses could be fit as weighted sum of event-related potentials (ERPs), each of which was modeled by the ERP evoked by a single CV. We then used a template-matching classification scheme to classify single-trial EEG signals after we converted them into the equivalent-current dipole time courses for left and right auditory cortices. We found that in our normal-hearing subjects, we could determine which stream the subject was attending significantly better than by chance, even without subject-specific training. Moreover, classification accuracy was comparable to that of learning-based classifiers. A computer game that is controlled by the proposed decoding mechanism will be tested on CI recipients who participate in post-implant training.

SYMP 52

Computational auditory scene analysis in complex multi-talker scenarios

Angela Josupeit; Volker Hohmann
Universitaet Oldenburg

In complex listening situations involving competing talkers normal-hearing human listeners are still able to understand their speaker of interest. This task involves the identification,

localization, tracking and finally understanding of the target talker. This study presents an auditory model for solving this task. The model is evaluated using a call-sign based experimental procedure in which multiple spatially separated talkers are presented simultaneously [Brungart and Simpson, Perception & Psychophysics, 2007, 69 (1), 79-91]. The task was to identify the target talker via a call-sign ("Baron") and to recognize the color and number word uttered by this target talker. The model consists of three steps: (1) The target talker is identified using a target template-matching procedure of primarily periodicity features. (2) The target talker is localized using interaural time difference information; target-related binaural features are selected with binary masks that were calculated based on the template-matching procedure in stage (1). (3) Color and number words are recognized using the combination of binary masks based on the identified location in stage (2) and a template-matching procedure using primarily temporal periodicity based features. An earlier study [Josupeit and Hohmann, ARO, 2015] showed the general feasibility of this approach and found good target identification and localization performance (stages 1 and 2). This contribution focuses on stage (3). Pilot tests show that the energy of periodic signal components ("periodic-component energy") in target-dominated regions of the multi-talker signal is mostly consistent with the periodic-component energy of the unmasked target talker. Furthermore, periodic-component energy seems to show word-specific characteristics. It is thus investigated how periodic-component energy, as well as the interaural parameters (Interaural Time Difference, ITD, and Interaural Level Difference, ILD) derived from the periodic components can contribute to template-based word recognition.

SYMP 51

Relating Measured and Self-Assessed Selective Listening Abilities to Behavioral and Electrophysiological Assays of Spatial Coding

Ross Maddox; Adrian Lee
University of Washington

Under realistic listening conditions, one often attempts to focus on one sound in a mixture of many coming from distinct spatial locations. While humans are adept at performing this feat, it is a fragile ability that depends on a healthy auditory system capable of coding and interpreting fine temporal cues. Listeners with elevated audiometric thresholds are understandably less able to listen selectively, but they are not the only ones who struggle—even some listeners with normal hearing as measured by clinical tests report significant difficulty. Recent work has related impoverished brainstem frequency-following responses with poor performance understanding masked speech. These results suggest that poor monaural temporal coding may drive some listeners' difficulties, but they do not account for subsequent processing issues, particularly in midbrain nuclei that are critical to binaural spatial processing. We sought to improve our understanding of the role of spatial processing integrity in listening ability in noise. We recruited subjects with normal hearing thresholds with and without self-identified difficulty listening in noise or locating sounds. In four sessions, we collected self-report data from the SSQ Questionnaire, behavioral data from a number of established psychoacoustical tasks of masked speech understanding as well as more basic binaural and monaural thresholds, and electrophysiological measurements from EEG recordings using stimuli designed to test binaural and monaural coding fidelity. We related the results across individuals to determine how different levels of auditory processing affect listening ability and perceived listening difficulty.

Behavioral performance on basic monaural and binaural tasks was correlated with performance variations in a speech-on-speech selective listening task. The EEG measurements had some predictive power of performance in the speech-on-speech task. Responses to the SSQ Questionnaire, however, seemed to have little predictive value for behavioral performance or physiological measurements.

Actively listening to speech in noisy conditions is a complex process that depends on accurate coding of stimuli, binaural processing, and higher order attentional and cognitive mechanisms. The present study sheds some light on the variation of these processing stages across the population and how each contributes to individuals' listening abilities.

SYMP 54

Influence of supra-threshold deficits associated with hearing loss and age on speech intelligibility

Agnes Leger[1]; Christian Lorenzi[2]; Brian Moore[3]; Christine Petit[4]
[1]University of Manchester; [2]École Normale Supérieure; [3]University of Cambridge; [4]Institut Pasteur

Sensorineural hearing loss and age are associated with poor speech intelligibility, especially in the presence of background sounds. The extent to which this is due to reduced audibility or to supra-threshold deficits is still debated.

The influence of supra-threshold deficits on intelligibility was investigated for normal-hearing (NH) and hearing-impaired (HI) listeners with high-frequency losses by limiting the effect of audibility. The HI listeners were generally older than the NH listeners. Speech identification was measured using nonsense speech signals filtered into low- and mid-frequency regions, where pure-tone sensitivity was near normal for both groups. The older HI listeners showed mild to severe intelligibility deficits for speech presented in quiet and in various backgrounds (noise or speech).

The intelligibility of speech in quiet and in noise was also measured for a large cohort of older NH and HI listeners, using linear amplification for listeners with mild to severe hearing losses. A measure was developed that quantified the influence of noise on intelligibility while limiting the contribution of linguistic/cognitive factors. The pure-tone average hearing loss accounted for only a third of the variability in this measure.

Overall, these results suggest that speech intelligibility can be strongly influenced by supra-threshold auditory deficits.

SYMP 55

Timing of the Speech-Evoked Auditory Brainstem Response Is Dependent on Cochlear Spectral Processing

Helen Nuttall[1]; David Moore[2]; Johanna Barry[3]; Jessica de Boer[3]

[1]University College London (UCL); [2]Cincinnati Children's Hospital Medical Center; [3]MRC Institute of Hearing Research

It has been suggested that deficits in certain speech and language skills, such as speech perception and phonological awareness, are related to reduced neural timing precision at the brainstem, particularly in noise (Anderson et al., 2010; White-Schwoch & Kraus, 2013). A neurophysiological correlate of this timing deficit has been proposed in the speech-evoked auditory brainstem response (speech-ABR), the latency of which is considered to reflect neural timing. Consequently, the speech-ABR has been suggested as a potential 'biomarker' for temporal processing deficits in the central auditory system. To date, however, little is known about the neural mechanisms underlying the inter-individual differences in speech-ABR timing. On the other hand, the effect of cochlear spectral processing on the ABR evoked by simple stimuli such as clicks and tones is well-documented (Dau, 2003). Of particular importance for ABR timing is cochlear response time (CRT), which is dependent on cochlear spectral filtering. CRT increases from higher to lower cochlear frequency regions, and is preserved up to wave V of the ABR, which is thought to originate from the same approximate location as the speech-ABR. Here, using normally-hearing young adults (n=26, aged 18-39) we investigated whether speech-ABR timing is similarly affected by cochlear filtering. Using high-pass noise masking, we recorded speech-ABRs to a synthetic [da] syllable from four octave-wide cochlear frequency regions centred around 0.7, 1.4, 2.8 and 5.7 kHz. The results showed that the speech-ABR integrates cochlear activity over at least four octaves, and that the response latency decreases significantly with increasing centre frequency in a manner compatible with changes in CRT. A second experiment investigated the effect of noise on speech-ABR latency. Noise increased the latency of the overall speech-ABR but had no significant effect on the timing of speech-ABRs recorded from delimited cochlear frequency regions. Amplitude, however, was significantly reduced, most substantially in the higher frequency regions rather than the low. This suggests that the noise-induced latency shift of the speech-ABR results from a change in cochlear spectral weighting and therefore a cochlear place mechanism. A loss of higher frequency cochlear contributions in noise results in a more low frequency cochlear origin, which is associated with a longer CRT. This cochlear timing influence is then preserved in the latency of the overall speech-ABR. These data highlight the importance of considering the effect of cochlear processing on the formation of speech-ABRs, and caution against interpretations based purely on neural timing deficits.

SYMP 56

Functional changes in inter- and intra-hemispheric cortical processing underlying degraded speech perception

Gavin Bidelman; Megan Howell

University of Memphis

Previous studies suggest that at poorer signal-to-noise ratios (SNRs), auditory cortical event-related potentials are weakened, prolonged, and show a shift in the functional lateralization of cerebral processing from left to right hemisphere. Increased right hemisphere involvement during speech-in-noise (SIN) processing may reflect the recruitment of additional brain resources to aid speech recognition or alternatively, the progressive loss of involvement from left linguistic brain areas as speech becomes more impoverished (i.e., nonspeech-like). To better elucidate the brain basis of SIN perception, we recorded neuroelectric activity in normal hearing listeners to speech sounds presented at various SNRs. Behaviorally, listeners obtained superior SIN performance for speech presented to the right compared to left ear (i.e., right ear advantage). Source analysis of neural data assessed the relative contribution of region-specific neural generators (linguistic and auditory brain areas) to SIN processing. We found that left inferior frontal brain areas (e.g., Broca's areas) partially disengage at poorer SNRs but responses do not right lateralize with increasing noise. In contrast, auditory sources showed more resilience to noise in left compared to right primary auditory cortex but also a progressive shift in dominance from left to right hemisphere at lower SNRs. Region- and ear-specific correlations revealed that listeners' right ear SIN advantage was predicted by source activity emitted from inferior frontal gyrus (but not primary auditory cortex). Our findings demonstrate changes in the functional asymmetry of cortical speech processing during adverse acoustic conditions and suggest that "cocktail party" listening skills depend on the quality of speech representations in the left cerebral hemisphere rather than compensatory recruitment of right hemisphere mechanisms.

SYMP 57

Individual Differences in Brain Oscillations when Listening to Speech in Noise.

Andrew Dimitrijevic; Michael Smith; David Moore

Cincinnati Children's Hospital

Background

Hearing ability is not fully explained by the pure tone audiogram; some individuals with normal clinical pure tone thresholds (≤ 20 dB HL) have impaired speech perception at suprathreshold levels in noisy environments. An electrophysiological test using speech-in-noise stimuli may provide insight into the mechanisms of suprathreshold hearing. There is also increasing realization that individual differences in typically developing individuals can be reflected in correlations between auditory behavior and electrophysiology. In this

study we examined individual differences in digit perception in noise (the Digit Triplets Test, DTT), and in brain oscillatory power. In particular, we hypothesized that alpha (8-12 Hz) and gamma (40-60 Hz) power in typically developing children and adults would be related to speech perception during active listening. Alpha was chosen because previous work has suggested that increases in power are related to listening in noisy environments and gamma was chosen because increases in power have been associated with object recognition.

Methods
Thirteen normal hearing adults were tested. The DTT presents trials of three digits in speech-shaped noise. In an initial behavioral task, the signal to noise ratio (SNR) was varied adaptively until 50% of digits were identified correctly, the Speech Reception Threshold (SRT). Afterwards, 64 channel EEG recordings were made during DTT listening at individualized suprathreshold levels.

Results
Listening to speech in noise was associated with increased alpha power, averaged across individuals. However, some individuals had decreased alpha, localized to auditory cortex, while others had increased alpha localized to parietal cortex. Individual increased or decreased alpha did not depend on SRT or SNR. However, all individuals had both higher alpha and gamma power when the digits were correctly identified.

Conclusions
The power of an individual's alpha shows little relationship to the physical characteristics of the stimulus. Rather individual alpha appears to be consistently related to perceptual performance on a trial-by-trial basis.

SYMP 58

Does auditory brainstem response wave-V latency in forward masking reflect auditory nerve fiber survival?

Golbarg Mehraei[1]; Andreu Gallardo[2]; Hari Bharadwaj[3]; Torsten Dau[2]; Barbara Shinn-Cunningham[4]
[1]Massachusetts Institute of Technology; [2]Technical University of Denmark; [3]Martinos Center for Biomedical Imaging,Massachusetts General Hospital; [4]Boston University

Introduction
Growing evidence from animal and human studies suggests that acoustic exposure too modest to elevate hearing thresholds can nonetheless cause auditory nerve fiber (ANF) loss that interferes with the coding of supra-threshold sound. Low spontaneous rate fibers (low-SR), important for encoding of acoustic information at supra-threshold levels and in noise, are more susceptible to degeneration than high spontaneous rate fibers (high-SR). Although noise-induced ANF loss affects how auditory brainstem response (ABR) wave-I amplitude grows with level, ABR latencies have not been thoroughly investigated. Models suggest that ANF loss affects how ABR wave-V latency changes with increasing background noise, or due to a preceding masker. We have previously shown that ABR wave-IV latency changes in noise are affected by ANF loss in mice. Further, in normal hearing threshold (NHT) humans, wave-V latency changes in noise correlate with perceptual temporal sensitivity. Here, we investigate whether differences in recovery rate from forward masking in ANFs with different spontaneous rates may be reflected in ABR wave-V latency changes.

Methods
We measured ABR in a forward-masking paradigm and evaluated wave-V latency changes with increasing masker-to-probe intervals (MPI). The masker was a broadband noise presented at 35 and 70dB SPL. The probe was a broadband "synchronized" chirp at a fixed level of 90 dB peSPL presented at MPIs of 20, 40, 201ms. In the same listeners, we measured forward-masking detection thresholds using the same noise masker and chirp probe but at additional MPIs of 72, 132, 168ms. We hypothesized that 1) a loss of ANFs increases forward masking thresholds at short MPIs, and 2) a preferential loss of low-SR fibers results in a faster recovery time of wave-V latency as the slow contribution of these fibers is reduced.

Results
The results showed that young NHT listeners with a faster change in wave-V latency with MPI are affected more by a preceding masker, especially at short MPI. Furthermore, the amount of wave-V latency change with MPI was correlated with the rate of change in forward masking detection thresholds: listeners with a larger change in wave-V latency also had a greater change in forward masking detection thresholds at short MPIs.

Conclusion
The findings here are consistent with our hypothesis of a selective loss of low-SR fibers and may be predictive of how well individuals can hear in noisy environments.

SYMP 53

Cochlear Damage Related to Tinnitus

Brandon Paul; Larry Roberts; Ian Bruce; Daniel Bosnyak; David Thompson
McMaster University

Background
Evidence from human and animal studies suggests that chronic subjective tinnitus occurs when central auditory structures are deafferented by cochlear damage caused by noise exposure or the aging process. However, not all cases of tinnitus are associated with audiometric hearing loss. One explanation is that tinnitus may be associated with cochlear damage not expressed in the audiogram. Type I auditory nerve fibers (ANFs) with low firing thresholds and high spontaneous firing rates (LT-HS ANFs) may have been comparatively well preserved for these tinnitus subjects, resulting in a normal audiogram. However, high-threshold low-spontaneous rate (HT-LS) ANFs may have been damaged in the tinnitus subjects, which could be expected to affect the processing of suprathreshold sounds but would not be expected to express in threshold measures.

Methods
To test this hypothesis we measured the ability of tinnitus and control subjects with clinically normal hearing to detect the presence of 19 Hz amplitude modulation (AM) in a suprathreshold 5 kHz tone (75 dB SPL), which lies in the frequency region where tinnitus is typically experienced and where hidden hearing loss was expected to be present in tinnitus. All tones were presented against narrowband noise (40 dB spectrum level centered at 5 kHz) intended to saturate LT-HS ANFs such that their ability to contribute to encoding AM is greatly reduced. In a separate condition we recorded the 85 Hz auditory steady state response (generated in the midbrain), evoked by an 85 Hz AM, 5 kHz tone (75 dB SPL) at modulation depths of 100%, 75%, and 50% also against narrowband background noise. A no-noise control condition was also included.

Results and Conclusions
Preliminary results show that tinnitus subjects (N = 10) had higher AM detection thresholds in noise compared to controls (N = 25). Interestingly, tinnitus subjects had reduced midbrain responses in all conditions compared to controls, including the no-noise condition in which LT-HS ANFs were not saturated by noise. Simulations of ANF responses based on the auditory periphery model of Zilany, Bruce and Carney (2014) suggests that ~100% loss of HT-LS ANFs combined with additional ~30% loss of LT-HS fibers is sufficient to account for the reduced brain responses observed in the tinnitus subjects and the differing effects of the background noise for the tinnitus and non-tinnitus subjects. A loss of ~30% of LT-HS ANFs would not be expected to have a substantial effect on hearing thresholds.

Funding
Supported by NSERC of Canada

PD 83

A systems biology approach to understanding hearing regeneration in zebra fish

Shawn Burgess[1]; Wuhong Pei[1]; Lisha Xu[1]; Gaurav Varshney[1]; Sunny Huang[2]; Jennifer Idol[3]
[1]National Human Genome Research Institute; [2]University of Iowa; [3]Jackson Laboratory

Tissue regeneration is the result of a complex integration of injury signals, stem cell activation, inflammation responses, reactivation of developmental programs and regeneration-specific processes. We have developed a systematic approach to dissect and analyze the various pathways involved in hearing regeneration by using zebra fish as a model organism. By using a high-throughput "guided" genetics and chemical genomics screen to identify the key genes and pathways involved in hearing regeneration, we have significantly enriched our success rate for identifying regeneration-specific genes. From our previous work, we had collected 2000 candidate genes involved in hearing regeneration by transcriptionally profiling regenerating zebra fish adult inner ears after sound damage. We've built an efficient gene knockout pipeline, first using retroviral mutagenesis but now using CRISPR/*Cas9* targeting and we are systematically inactivating the 2000 candidate genes and testing their role in both normal hair cell development and hair cell regeneration. In addition, we have screened a broad number of well-characterized pharmacological inhibitors to identify genes that cannot be easily tested by KO because of their important roles in early development. From our first one hundred and fifty genes and twenty chemical inhibitors tested, we have identified four genes that reduce the number of hair cells in a normal embryo, and we have identified an additional seven genes and three chemical inhibitors that specifically disrupt regeneration of the hair cells without affecting normal development. We will present data on the genetic strategy used to generate and screen hundreds of zebra fish gene knockouts for hearing regeneration defects, the pathways emerging from our genetic and chemical genomic analysis, and the deeper phenotypic characterization of a sample regeneration-specific mutant we have identified

Funding
This work was supported by the Intramural Research Program of the National Human Genome Research Institute, National Institutes of Health.

PD 84

MicroRNA expression during in vitro hair cell regeneration in the avian inner ear

Anastasia Filia[1]; Mark Warchol[2]; Michael Lovett[1]
[1]Imperial College London; [2]Washington University, St Louis

Background
The avian inner ear is comprised of the vestibular and auditory organs. The sensory epithelia (SE) in both organs are formed of mechanoreceptors known as hair cells (HCs) and supporting cells (SCs) which surround the HCs. Unlike mammals, lower vertebrates have the capacity to restore hearing in response to damage. In avians, the SCs are the 'stem' cells of HC regeneration. We recently published an analysis of changes in the mRNA transcriptome of SE from the chick utricle (vestibular SE) after HC killing in organotypic cultures. We have also recently completed a similar analysis from the regenerating chick basilar papilla (auditory SE). The aim is to pinpoint key regenerative components that can be tested in mammalian HC restoration. The basic hypothesis of the current study is that an additional class of RNAs (microRNAs) are potent regulators of HC regeneration and may provide good therapeutic targets.

MicroRNAs are short, single-stranded, regulatory RNAs targeting multiple mRNAs for translational repression/degradation. MicroRNAs represent attractive candidates for therapeutic manipulation, since altered expression of just a few can change cell fate. The complete spectrum of microRNAs expression has not yet been investigated in HC regeneration.

Methods
We have explored the entire spectrum of microRNAs expression during chick utricle HC regeneration (by microRNA-Seq), using the same *in vitro* time-course as our mRNA-Seq study. We have also embarked upon a parallel

study in the basilar papilla. This allowed us to directly compare microRNAs with the presence/abundance of potential mRNA targets using various computational tools and specific knockdown or over-expression of microRNAs.

Results
The microRNAs expressed during avian SE regeneration and their abundance profiles, closely match those seen during mouse SE development. A set of ~70 microRNAs were differentially expressed during SE regeneration. Statistical clustering algorithms revealed microRNAs with expression patterns that parallel phenotypic changes as seen in our mRNA-Seq data. High-likelihood mRNA targets for five microRNAs were predicted by a combination of knockdowns, bioinformatics and mRNA-Seq approaches. Several of these predicted targets are components of Notch signaling.

Conclusions
By a combination of microRNA-Seq, computational clustering analysis and RNAi knockdowns we have identified the spectrum of microRNAs that are differentially expressed during avian SE regeneration and their most likely mRNA targets.

Funding
NIH, Hearing Health Foundation

PD 85

Complex Interplay of Notch, Wnt/β-catenin and Fgf Signaling During Zebra fish Lateral Line Hair Cell Regeneration

Dong Liu; Yuting Wu; Xiaoxiao Mi; Hong Guo; Guozhu Tang; Yuanhe Zhang
Peking University

Background
Zebra fish posterior lateral line (pLL) system has long been used to study mechanosensory hair cell (HC) damage/regeneration. Currently, pLL is likely a compensatory regeneration model, in which neuromast replaces its lost HCs through mitotic regeneration. Notch, Wnt, Fgf, RA and Tgfβ signaling are all involved in pLL development and some, if not all, signaling pathways are shown to be important for HC regeneration. HC regeneration process is generally considered to be a recurring process of HC development.

Methods and Results
In present study, a viable mutant (two alleles) is identified with normal pLL that fails to fully regenerate its lost HCs. The mutations are mapped to the locus of a bHLH-PAS family member encoding gene, in which a large insertion or nucleotide substitution results in a truncated protein containing only bHLH domain. Interestingly, mutant HC regeneration defect is apoptosis (cisplatin) and Wnt dependent, and the truncated protein negatively regulates a Dishevelled homolog gene expressed in neuromast. However, simply supplying Wnt/β-catenin (stabilizing β-catenin) fails to rescue the mutant. Instead, activating Wnt signaling and inhibiting Notch signaling together restore HCs in mutant neuromast, mainly through phenotypic conversion (transdifferentiation). Furthermore, inhibiting Fgf signaling during cisplatin treatment phenocopies the mutant defect.

Conclusion
The zebra fish mutant identified in this study is the first of kind that shows only pLL HC regeneration but not development defect. By characterizing the mutant, the roles of Notch, Wnt/β-catenin and Fgf signaling are found to be rather distinct, compared to their roles in pLL development. Moreover, phenotypic conversion can be a dominant mode of HC regeneration in zebra fish lateral line once mitotic regeneration is blocked, making zebra fish pLL an attractive model to study HC regeneration.(YW, XM and HG contributed equally)

Funding
National Basic Research Program of China (973 Program; 2012CB944503), MOST; State Key Laboratory of Membrane Biology

PD 86

Intensive supporting cell proliferation and mitotic hair cell generation by genetic reprogramming in neonatal mouse cochlea in vivo

Wenli Ni; Chen Lin; Wenyan Li; **Huawei Li**
Affiliated Eye and ENT Hospital of Fudan University

Hair cell (HC) loss is the predominant cause for hearing and balance disorder. In mammals, only limited HC regeneration has been identified in neonatal cochleae in vivo. The direct trans-differentiation of supporting cells (SCs) into new HCs exhausts the SC population, which may in turns against the stability of the hearing epithelium; Furthermore, the activation of progenitor cells were more obvious at the apical regions of cochlea, while majority of HC loss was at the basal region, which provided new challenges for the HC regeneration in cochlea by manipulating a single pathway. To address these challenges, we investigated the hair cell generation in neonatal mouse cochlea through genetic reprogramming approach, by which multiple signaling pathways were co-regulated in Sox2+ supporting cells, and followed with the investigation of the proliferation and transdifferentiation of SCs.

In this study, by activating Wnt signaling and inhibiting Notch signaling in transgenic mice in vivo, we genetically reprogrammed the Sox2+ SCs and observed intensive proliferation of SCs, both in sensory epithelium and in GER regions at neonatal mice cochleae. We found the proliferation of SCs extended into base part of auditory sensory epithelium along with the significantly increased SCs number. Further, upon the activation of Atoh1, more EdU+/Myo7a+ HCs were identified in auditory epithelium and GER region. The mechanism underneath intensive proliferation by manipulating Notch1 and Wnt signaling were investigated by RNA-seq and double knockout transgenic mouse.

In our current study, we concluded that more proliferative generated HCs could be reached, through stimulated SC proliferation by Wnt activation (via beta-catinen overexpression and Notch1 inhibition) and then introduced

prosensory signals, Notch inhibition (via lateral inhibition) and Atoh1 overexpression, to direct HC differentiation, which provided the first piece of evidence for the proliferative HC generation by genetic reprogramming process including multiple genes.

PD 87

Resistance to Mechanical Deformation May Limit Regeneration in Mammalian Hair Cell Epithelia

Mark Rudolf; Jeffrey Corwin
University of Virginia

Background

Sensory epithelia in the ears of fish, amphibians, and birds maintain a lifelong capacity to add and replace hair cells. In mammalian ears, however, hair cell addition and replacement decline sharply during early postnatal life. This loss of plasticity closely mirrors the development of robust E-cadherin junctions and exceptionally thick and stable circumferential F-actin "belts" in supporting cells; in contrast, supporting cells in fish, amphibians, and birds express little E-cadherin and possess thin F-actin belts from birth to adulthood. The massive apical F-actin belts may confer mechanical stability conducive to high frequency hearing in mammals, but also impede the transmission of intercellular signals produced during hair cell death. In other tissues, such mechanical signals have been shown to regulate stem cell turnover and differentiation, wound healing, and morphogenesis.

Methods

In order to investigate the role of mechanical stability in sensory and non-sensory epithelia, we applied a micropipette aspiration technique to quantify tissue-level resistance to deformation. By measuring the negative pressure required to produce a hemispherical deformation at the apical surface, we calculated tension values for sensory and non-sensory epithelia from chickens and mice at various ages. These comparisons allow us to determine whether the sensory epithelia of mature mice are more resistant to deformation than the highly proliferative non-sensory epithelium and the readily regenerative sensory epithelia from the ears of chickens.

Results

Preliminary results show that mouse utricles are twice as resistant to deformation as chick utricles during the first week of life (24 vs. 12 nN/μm). Tension values in mouse sensory epithelium then increase in an age-dependent manner, more than doubling between P6 and adulthood (24 vs. 63 nN/μm). In mature mouse utricles, whose F-actin belts fill 89% of the apical area in supporting cells, tension values from the sensory epithelium are approximately 4 times those of adjacent non-sensory epithelium (63 vs. 16 nN/μm), where belts remain relatively thin. Future studies will more definitively test the mechanical stability hypothesis using pharmacological inhibitors to modulate the F-actin belts and reduce the activity of non-muscle myosins, both of which may contribute to our measured tension values.

Conclusions

The preliminary measures of resistance to deformation are consistent with the hypothesis that the reinforced junctions and F-actin belts in mature mammalian supporting cells stiffen the sensory epithelium and may limit the ability of supporting cells to sense and respond to hair cell loss.

Funding

This research is generously supported through the National Institute on Deafness and Other Communication Disorders (NIDCD) Project No. 5R01DC000200-30.

PD 88

Chicken Utricle Hair Cell Regeneration at the Single Cell Level

Mirko Scheibinger[1]; Robert Durruthy-Durruthy[1]; C. Eduardo Corrales[2]; Michael Lovett[3]; Mark Warchol[4]; Stefan Heller[1]
[1]Stanford University School of Medicine; [2]Harvard Medical School, Boston; [3]Imperial College London; [4]Washington University School of Medicine, Saint Louis

Non-mammalian vertebrates regenerate sensory hair cells in response to ototoxic insults. Transcriptome-wide analyses of cultured regenerating utricular and cochlear sensory epithelia at various time points after streptomycin-induced hair cell loss have previously revealed candidate genes and signaling pathways that potentially play important roles in the regenerative process. However, the order of events that initiate, execute, sustain, and terminate the different modes of hair cell regeneration remain unknown.

Here, we established a reliable ototoxic insult model, using one application of streptomycin to the chicken inner ear *in vivo*. This results in reproducible 70-95% hair cell loss in the utricle when assessed 48h after surgery. We quantified cells entering S-phase at 24h, 48h, 72h and 120h after ototoxic insult using a 24h EdU pulse. In addition, we determined the identity of mitotically generated cells 10 days after insult. This allowed us to establish a timeline of symmetric and asymmetric cell divisions as well as to resolve occurrences of phenotypic conversion of supporting cells.

Bioinformatics cluster analyses of expression of 192 genes in individual cells of untreated chicken utricle sensory epithelia allowed us to classify transcriptionally distinct cell populations including hair cells and supporting cells. In treated utricles we identified discrete populations of 'responding' cells with transcriptional profiles displaying features of both, hair cell and supporting cell identity. These newly occurring groups may be classified by their gene expression profiles for example as i) early responding hair cells that are affected by the streptomycin-treatment, ii) supporting cells that respond to signals received from affected hair cells, iii) supporting cells that begin to phenotypically convert into new hair cells, iv) supporting cells that initiate asymmetric cell division, and finally v) as distinct groups of regenerated hair cells. Furthermore, we utilized dimension-reduction algorithms to resolve cellular heterogeneity on a temporally defined measure. This enabled an in-depth characterization of the

transcriptional changes that occur during regeneration as well as described a defined sequence of these events as the chicken utricle initiates and executes the regenerative responses. Our experiments revealed that the chicken utricle presents a powerful model to study the molecular events that control hair cell regeneration and the results may provide important insights into development of therapeutic strategies for mammalian hair cell regeneration.

Funding
Supported by the NIDCD (P30 DC010363), Hearing Health Foundation (HRP) and DFG (SCHM 2804/1-1)

PD 89

Sox2 in the differentiation of cochlear progenitor cells

Judith Kempfle[1,2]; Albert Edge[1]
[1]Massachusetts Eye and Ear Infirmary; [2]Harvard Medical School

Background
Sox2, a high mobility group (HMG) domain transcription factor, is part of a core transcriptional regulatory network that maintains stem cell pluripotency by blocking transcription of cell fate-determining genes. In the inner ear, Sox2 has previously been associated with expansion of sensory progenitors that develop into hair cells. Downregulation of Sox2 was thought to promote activation of Atoh1, a transcription factor required for hair cell differentiation. Here, we explore the importance of Sox2 levels for regulation of Atoh1.

Methods
Chromatin immunoprecipitation (ChIP) demonstrated that extent of Atoh1 activation correlated with different levels of Sox2. Atoh1 activation by Sox2 was required for embryonic hair cell development in vivo: deletion of Sox2 in an inducible mutant, even after progenitor cells were fully established, halted development of hair cells, and silencing with Sox2 siRNA inhibited postnatal differentiation of hair cells induced by inhibition of g-secretase in vitro.

Results
We show that Sox2 level is crucial for the development and regeneration of cochlear hair cells. Activation of the Atoh1 enhancer was dependent on the level of Sox2, and the extent of enhancer binding correlated to the extent of activation.

Conclusions
Sox2 levels are crucial in the cochlea to both expand sensory progenitor cells and initiate their differentiation to hair cells.

PD 90

Direct lineage conversion of mouse and human fibroblasts into hair cell-like cells

Suhasni Gopalakrishnan; Louise Menendez; Juan Llamas; Litao Tao; Welly Makmura; Justin Ichida; Neil Segil
Keck School of Medicine of the University of Southern California

Hearing impairment is the most common sensory deficit in humans. It affects individuals of all ages and is most commonly caused by loss of sensory hair cells and neurons of the inner ear. Extremely limited availability and accessibility of biological material is a critical roadblock to translational research for hearing loss. Cellular reprogramming methods to generate inner ear sensory cells will help overcome this problem by providing an in vitro system to study the inner ear development and cellular differentiation. Much of the current efforts to derive inner ear hair cells in vitro have focused on directed differentiation approaches with ES or iPS cells as starting material. This method uses precise timing and concentrations of signaling molecules to mimic in vivo development of the inner ear.. Direct lineage conversion of one cell type to another via over-expression of transcription factors, offers an efficient and faster route to generate target cell types, bypassing the intermediate step of creating a stem-cell like state. This technique has successfully generated highly specialized cell types such as hepatocytes, cardiomyocytes, and neurons from primary mouse and human fibroblasts.

We recently succeeded in generating inner ear sensory hair cell-like cells using direct lineage conversion methods. Transcriptome analysis of purified hair cells, allowed us to identify a set of transcription factors that are enriched in inner ear sensory hair cells, including factors known to be crucial for their development. Viral transduction of mouse and human fibroblasts with these transcription factors gave rise to induced hair cells (iHCs). The iHCs express a reporter GFP driven by the Atoh1 enhancer, are positive for hair cell markers such as parvalbumin and MyosinVI, and display polarized phalloidin staining. The iHCs rapidly take up FM4-64 dye, as well as the antibiotic gentamicin, similar to the primary inner ear hair cells from the organ of Corti. In addition, we have found that the reprogramming cocktail used is able to convert purified and in vitro cultured P6 supporting cells, which are normally resistant to transdifferentiation, into hair cell-like cells at increased efficiency relative to MEFs. Ths suggests that these factors could be used for in vivo reprogramming to stimulate hair cell regeneration. These observations establish our iHCs as a suitable mammalian cell-based platform for initiating disease modeling and therapeutic drug screening. Going forward, further functional assays will assess iHC's ability to achieve proper physiological status, synapse formation, and in vivo engraftment.

Funding
We thank the USC Stem Cell Regenerative Medicine Initiative, the Hearing Health Foundation, and the Sidgmore Family Foundation for their generous support.

SYMP 59

Central Gain Restores Auditory Processing Following Near-Complete Cochlear Denervation

Daniel Polley
Massachusetts Eye and Ear Infirmary, Harvard Medical School

Cochlear degeneration induces a host of cellular and physiological changes in the periphery as well as the brain.

At higher stages of the central auditory pathway, where physiological processing enables the perception of sound, this plasticity must contribute to the perceptual sequelae of cochlear hearing impairment. However, disambiguating the peripheral and central determinants of hearing loss has proven difficult. Here, we show that many aspects of auditory processing recover after profound cochlear denervation due to a progressive, compensatory plasticity at higher stages of the central auditory pathway. Lesioning >95% of cochlear nerve afferent synapses, while sparing hair cells, in adult mice virtually eliminated the auditory brainstem response and acoustic startle reflex, yet tone detection behavior was nearly normal. As sound-evoked responses from the auditory nerve grew progressively weaker following denervation, sound-evoked activity in the cortex – and to a lesser extent the midbrain – rebounded or even surpassed control levels. Increased central gain supported the recovery of rudimentary sound features encoded by firing rate, but not features encoded by precise spike timing such as modulated noise or speech tokens. What mechanisms might be employed by a cortical amplifier to change input gain? To address this question, we used a transgenic strategy to express channelrhodopsin in parvalbumin+ (PV) fast-spiking cortical interneurons. By implanting an optetrode assembly in the auditory cortex, we were able to track day-by-day changes in local inhibitory tone and sound-evoked single unit activity over an extended period surrounding cochlear afferent denervation. We found that PV-mediated inhibition and sound responsiveness were tightly coupled. Cortical inhibitory tone plummeted following cochlear denervation. Inhibition partially returned in mice that spontaneously recovered auditory sensitivity but remained at the noise floor in mice that never recovered. In all cases, changes in PV-mediated inhibitory tone lagged changes in sound responsiveness by 2-3 days, suggesting that disinhibition is an important feature of cortical gain changes but is not a determinant. Collectively, these findings highlight the default homeostatic response of higher auditory circuits deprived of bottom-up afferent drive. This plasticity enables the restoration of firing rate codes to support basic audibility and rudimentary feature selectivity. However, it does not support (and might even impede) recovery of fine temporal processing required for perception of complex signals such as speech or music.

SYMP 60

Using Optogenetics Combined with Electron Tomography to Unravel the Vesicle Release at Inner Hair Cell Ribbon Synapses

Carolin Wichmann; Rituparna Chakrabarti; Susann Michanski; Lina Jaime Tobón; Sangyong Jung; Tobias Moser

University of Goettingen

Cochlear inner hair cells (IHCs) employ specialized synapses for transmitting acoustic information at hundreds of Hz with submillisecond precision. They are characterized by a specific electron-dense structure, the synaptic ribbon. Even though great progress has been made identifying potential release mechanism(s) (Glowatzki and Fuchs, 2002; Neef et al., 2007; Chapochnikov et al., 2014), the sequence from vesicle recruitment to final fusion is still poorly understood. The molecular machinery mediating recruitment and fusion differs from conventional synapses. For example, neuronal SNARE proteins and conventional priming factors like CAPS and Munc13 seem not to play a functional role in exocytosis at IHC ribbon synapses (Nouvian et al., 2011; Vogl et al., 2015). Moreover, a large proportion of synaptic vesicles resides on filamentous tethers at the membrane of the active zone (AZ) membrane (Frank et al., 2010; Vogl et al., 2015) rather than being docked. Whether these vesicles represent the readily releasable pool is also still not understood.

Here we present our progress in investigating early phases of exocytosis on the ultrastructural level using optical stimulations of channelrhodopsin 2 expressing IHCs. We first performed patch-clamp experiments to characterize the IHC photo responses. We then used short (10 ms) stimulation by a 473 nm blue LED coupled to a high pressure freezing machine. This method allows us to freeze the samples within 10 milliseconds after stimulation, to preserve the structure to a near-native state and finally to relate morphology to function. Combined with electron tomography we analyzed parameters such as the number or position of vesicles at the AZ and tethering. Our data revealed that upon short 10 ms stimulation more vesicles are tethered to the AZ membrane than found after long stimulation. Moreover, we observed proper docking of vesicles to the plasma membrane (membrane-membrane contact), which is not or rarely found at AZs of IHCs that are immobilized after long stimulation. We propose that the sequence of exocytosis at IHC AZs proceeds from initial tethering, to docking and to fusion.

SYMP 61

Characterization of Activity along the Auditory Pathway evoked by Optogenetic Cochlear Stimulation

Marcus Jeschke[1]; Christian Wrobel[1,2]; Alexander Dieter[1]; Daniel Keppeler[1]; Gerhard Hoch[1]; Michael Schwaerzle[3]; Patrick Ruther[3]; Tobias Moser[1]

[1]University of Göttingen Medical Center; [2]Ruhr-Universität Bochum; [3]University of Freiburg

Cochlear implants are by far the most successful neuroprostheses - implanted in more than 300000 patients - and enable open speech comprehension in the majority of users. To ameliorate common drawbacks of cochlear implants which are related to the wide current spread from stimulation contacts we are pursuing the development of optogenetic cochlea implants. In a proof-of-concept study we demonstrated that blue light stimulation of channelrhodopsin-2 expressing spiral ganglion neurons was capable of driving auditory activity. In this presentation, we will highlight current experiments aimed at further optimizing and characterizing the optogenetically driven activity.

To test whether individual neurons in central parts of the auditory pathway were activated by optical cochlear stimulation, we employed transgenic mice and performed single and multi unit recordings in the inferior colliculus

and auditory cortex contralateral to the stimulated cochlea. In the inferior colliculus, only a small number of neurons responded to optogenetic cochlea stimulation while the response to best frequency (BF) tones was modulated by laser stimulation in a larger fraction of neurons. In contrast, the majority of neurons in the auditory cortex was driven by laser stimulation, independent of BF. In almost all neurons it was possible to modulate BF tone responses by optogenetic cochlear stimulation.

Towards clinical translation, we established virus mediated transfections of spiral ganglion neurons in adult Mongolian gerbils using CatCh, a modified channelrhodopsin-2 variant with increased light sensitivity. Immunohistochemical analysis revealed CatCh expression throughout the membrane of spiral ganglion neurons within the injected cochlea. Auditory brainstem responses were observed with brief (< 1 ms) light pulses of down to 0.8 mW intensity which is only 4 times as high as necessary for electrical stimulation. Similar to results from transgenic mice, a large number of neurons in the auditory cortex were driven by optogenetic cochlear stimulation. Further, the response to BF tones of almost all neurons tested was modulated by laser stimulation. The BFs of cortical neurons that could be activated by cochlear optogenetics were spread throughout the tonotopic gradient of the auditory cortex with a trend towards minimal thresholds corresponding to the site of stimulation – either a cochleostomy at the middle cochlear turn or round window.

Taken together, our data demonstrate that optogenetic cochlea stimulation activates the auditory pathway up to the auditory cortex and reveal a marked coding transformation between the midbrain and cortex. Implications for future applications in auditory research and prosthetics will be discussed.

SYMP 63

Developing the Cell-Penetrating JNK Inhibitor AM-111 for Acute Otoprotection

Thomas Meyer
Auris Medical AG, Basel

Despite extensive research into the pathophysiology of acute sensorineural hearing loss (ASNHL) and the devastating effect that it may have on a patient, there still exists no treatment that has shown unequivocal evidence of efficacy. Ideally, early treatment during a therapeutic time window could protect at-risk sensorineural structures within the cochlea and preserve functional hearing.

The c-Jun N-terminal kinase (JNK) is involved in apoptosis of stress-injured hair cells and spiral ganglia neurons. JNK signaling is implicated in various types of inner ear injuries such as acute noise trauma, drug ototoxicity, infections or vascular disturbances that may result in permanent hearing loss and other symptoms of cochlear dysfunction. Its inhibition can prevent upregulation of pro-apoptotic and pro-inflammatory proteins and downregulation of pro-survival proteins.

AM-111 is a cell-penetrating JNK inhibitor formulated in a biocompatible hyaluronic acid gel that is being developed for treatment of ASNHL by way of intratympanic injection. AM-111's effector domain has been derived from the scaffold protein islet-brain 1, which retains JNK in the cytoplasm; it is coupled to the trans-activator of transcription (TAT) protein transduction domain. Treatment with AM-111 was shown to be otoprotective in various animal models of cochlear insult: acute noise trauma, acute labyrinthitis, aminoglycoside ototoxicity, bacterial infection, cochlear ischemia, and cochlear implantation trauma.

Clinical development of AM-111 was initiated with a Phase I/II clinical trial in patients suffering from New Year's Eve firecracker trauma. This was followed by a placebo-controlled Phase II trial enrolling 210 patients within 48 hours from ASNHL onset. The study established proof of concept for AM-111 in the treatment of severe-to-profound ASNHL: single dose AM-111 0.4 mg/mL showed statistically significant, clinically relevant, and persistent improvements in hearing and speech discrimination and higher tinnitus remission compared with placebo. In addition, the drug was well tolerated. These outcomes together with exchanges with regulatory agencies informed the design of Phase III trials.

The talk aims to illustrate the conceptional and development work required to take a compound to clinical proof of concept in an orphan drug indication such as ASNHL as well as the various hurdles that had to be overcome. Specifically, the talk will discuss challenges such as the lack of reliable and comprehensive data on the natural history of ASNHL, the need to control for spontaneous recovery, the selection of an appropriate patient population and subject enrolment within a relatively short time window.

SYMP 64

Phase 2b Clinical Trial to Assess Safety and Efficacy of Extended-Release Dexamethasone Thermosensitive Gel for Intratympanic Administration in Patients with Ménière's Disease

Carl LeBel[1]; John Carey[2]; Paul Lambert[3]; Anthony Mikulec[4]
[1]Otonomy, Inc.; [2]Johns Hopkins Medical; [3]Medical University of South Carolina; [4]Saint Louis University

Background
Although not FDA-approved for intratympanic (IT) use, IT steroids are routinely used to treat Ménière's disease. However, limited inner ear exposure and rapid middle ear clearance are limitations to their use. This clinical trial investigated the safety and efficacy of a sustained-exposure steroid compound, OTO-104 (6% dexamethasone in thermosensitive gel) in unilateral Ménière's disease patients. A previous Phase 1b study showed OTO-104 reduced vertigo and tinnitus in 44 Ménière's patients.

Methods
This was a prospective, randomized, double-blind, placebo-controlled, multi-center Phase 2b clinical trial in 154 Ménière's patients, 18 to 80 years old. Patients entered a 1-month

baseline period, followed by randomization (1:1) to OTO-104 (12 mg) or placebo (gel only) IT injection and a 4-month follow-up period. The primary endpoint was the reduction in vertigo frequency during Month 3 following treatment compared with the 1-month baseline period. Tinnitus frequency and severity, and quality of life (SF-36) were exploratory endpoints. Safety was assessed with otoscopy, audiometry and tympanometry.

Results

The Phase 2b study had comparable patient populations and similar average baseline vertigo episodes counts (7-8 episodes) to the previous Phase 1b study. The primary endpoint analysis (mixed model repeated measures) showed that patients given OTO-104 had a 61% reduction from baseline in vertigo frequency in Month 3 compared with 43% for the placebo group (p=0.067). A similar positive trend was observed during Month 2 following treatment. Using a predefined Poisson regression analysis, a statistically significant reduction in the number of definitive vertigo days was observed for OTO-104 versus placebo in both Month 3 (p=0.030) and Month 2 (p=0.035). Secondary endpoints for change in vertigo severity score and average daily vertigo count showed statistically significant improvements for OTO-104 compared to placebo. Exploratory endpoints evaluated several scales of the SF-36, which showed statistically significant improvements with OTO-104 compared to placebo. There was no OTO-104 treatment effect observed for the tinnitus endpoints. OTO-104 showed no drug-related serious adverse events. At the end of Month 4, persistent perforations of the tympanic membrane were observed in two patients who received OTO-104.

Conclusions

In this Phase 2b trial, while narrowly missing the primary endpoint, secondary endpoint analyses demonstrated that single administration of OTO-104 provides a statistically significant improvement in vertigo frequency, as measured by a reduction in definitive vertigo days, and vertigo severity compared to placebo three months following treatment. These results provide a basis to advance OTO-104 into Phase 3 testing for Ménière's disease.

SYMP 65

Oral Glutathione Peroxidase mimic (SPI-1005) for the Prevention and Treatment of Acute Noise-Induced Hearing Loss

Jonathan Kil; Eric Lynch
Sound Pharmaceuticals

Trial Design

To determine the safety and efficacy of SPI-1005, a novel glutathione peroxidase (GPx1) mimic, in preventing noise induced hearing loss (NIHL). A randomized double blind placebo controlled Phase 2 clinical trial was conducted in young adults (18-31) at the University of Florida, NCT01444846. 160 subjects were screened and 83 subjects were enrolled between December 2012 and November 2013 and randomized to either placebo or SPI-1005 (200, 400 or 600 mg) delivered orally twice daily for four days, beginning two days prior to a single noise exposure or calibrated sound challenge (CSC).

Methods

The CSC consisted of pre-recorded music lasting 4 hrs delivered via insert earphones and induces a temporary threshold shift (TTS) that resolves in 24 hrs (Le Prell et al., 2012). Manual pure-tone audiometry was performed two times before and six times after the CSC over 4 clinic visits and the group averages were determined for several critical TTS parameters including severity at 4 kHz (dB), duration (return to baseline in hrs) and incidence of a significant threshold shift (STS $\geq$10 dB). Significance was based on pairwise comparisons of a SPI-1005 group to placebo using a mixed effect multiple repeated measures model.

Results

SPI-1005 reduced TTS severity at 4 kHz (4.1 vs 1.3 dB, p<0.01), duration (24 vs 1.3 hrs, p<0.01) and STS incidence (60% vs 25%, p<0.01). SPI-1005 was well tolerated with no drug-related adverse events.

Conclusions

These results indicate that SPI-1005 was safe and effective in preventing a noise-induced TTS and establishes the importance of GPx1 activity in acute NIHL.

SYMP 66

From Bench to Booth: An Oral Modulator of Voltage-gated Potassium Channels (AUT00063) for the Management of Age-related Hearing Loss (ARHL): the CLARITY-1 Study.

Peter Harris[1]; Victoria Sanchez-Williams[2]; Robert Frisina[2]; Theresa Chisolm[2]; Sandra Gordon-Salant[3]
[1]Autifony Therapeutics Ltd; [2]University of South Florida, Tampa; [3]University of Maryland, College Park

Kv potassium channels are expressed at all levels of the auditory system, and allow neurons to fire rapidly and with precise timing, such as in circuits involved in decoding speech and animal vocalizations. Knockout of the Kv3.1 channel impairs auditory function in mice, while age-related hearing decline is associated with reduced Kv3 channel expression in brainstem auditory centres in rodents. Reduced activity may account for aspects of hearing performance decline in humans; thus Kv3 channels represent a new target for treatment of ARHL.

AUT00063 is a novel small molecule that positively modulates Kv3 channel function. In a model of ARHL, AUT00063 improved auditory temporal processing in 20-month old F344 rats, as measured using a behavioural gap detection paradigm (Popelář et al., 2014, ARO Abstr.). In a model of auditory neuropathy in mice, AUT00063 improved the timing of action potential firing and synchronization of neurons in the inferior colliculus in response to auditory stimuli (Polley et al. 2014, Soc. Neurosci. Abstr.).

Clinical evaluation of AUT00063 in healthy young and elderly human volunteers confirmed an excellent safety and pharmacokinetic profile, and provided evidence for Kv3 target engagement measured using phEEG. In older subjects (60-75yrs) with normal hearing, AUT00063 did not impair the performance of audiological tests (middle ear immitance, tympanometry, acoustic reflex testing, PTA, HINT, DPOAE, binaural unmasking, and ABR). Similarly, the drug did not impair cognitive performance.

AUT00063 is now being evaluated in a Phase IIa clinical trial ("CLARITY-1") in subjects with ARHL across 12 sites in the US. Given the lack of precedent for clinical assessment of pharmaceutical treatments for ARHL, the CLARITY-1 trial was designed in part to translate the preclinical animal model measures into human subjects performance, but also to assess clinically relevant measures of central auditory processing, notably speech-in-noise processing.

CLARITY-1 is a double-blind, parallel group study of AUT00063 versus placebo in older subjects (60-89 yrs), with daily dosing for 28 days. Efficacy will be assessed comparing Day 28 findings with Day 1 baseline. A full pre-baseline test battery is conducted to reduce learning effects. Consistent with FDA feedback on efficacy measures via a pre-IND consultation, the primary outcome will be changes in QuickSIN speech-in-noise performance. Secondary measures include a time-compressed sentence recognition test, a speech-in-noise test with varying spatial cues, a psychoacoustic measure of temporal resolution, and questionnaires assessing self-perceived hearing abilities (e.g. SSQ, and global improvement). The study is due to complete by mid-2016.

PD 91

The Metabotropic Purinergic Receptor P2ry1 Mediates ATP-dependent Burst Firing in the Developing Cochlea.

Travis Babola; Han Chin Wang; Dwight Bergles
Johns Hopkins University

Spontaneous electrical activity is a prevalent feature of the developing nervous system, which has been shown to influence the maturation and survival of neurons, as well as the refinement of circuits in the brain. In the auditory system, bursts of activity are initiated in the cochlea when ATP is released by inner supporting cells (ISCs) within Kölliker's organ (greater epithelial ridge). This periodic release of ATP induces inward currents, crenations (cell shrinkage), and Ca^{2+} waves in ISCs, as well as depolarization of inner hair cells (IHCs). Our studies indicate that purinergic receptor activation on ISCs causes efflux of Cl^- and K^+ into the extracellular space. The elevation of extracellular K^+ depolarizes IHCs, triggering bursts of Ca^{2+} action potentials that induce burst firing in spiral ganglion neurons (SGNs). However, the receptors that mediate the effects of ATP remain undefined, limiting our ability to define functional consequences of this activity. Using whole cell patch clamp and DIC imaging, we found that spontaneous currents and crenations of ISCs were inhibited by chelation of intracellular Ca^{2+} or by inhibition of phospholipase C, suggesting that metabotropic receptors play an essential role in generating these events. We found that both forms of ISC activity were abolished by the P2ry1 antagonist MRS2500 and were absent in P2ry1$^{-/-}$ mice. Moreover, confocal imaging of cochleae from mice expressing GCaMP3 revealed that spontaneous Ca^{2+} waves in Kölliker's organ were eliminated by MRS2500, indicating that P2ry1 is responsible for initiating spontaneous activity in ISCs. Loose patch recordings from SGNs in cochlear whole mounts from P2ry1$^{-/-}$ mice revealed a marked reduction in SGN burst firing. A similar effect was observed by application of MRS2500 in cochleae from wild type mice, suggesting that inhibition of burst firing is due to loss of P2ry1. Simultaneous imaging of Ca^{2+} events in ISCs, IHCs, and SGNs confirmed that synchronized activity requires P2ry1. Together, these data suggest that P2ry1 is responsible for initiating spontaneous activity in ISCs and synchronizing the firing of groups of adjacent hair cells. However, both genetic and pharmacologic removal of P2ry1 led to an increase in the total number of action potentials in SGNs, suggesting that P2ry1 mediates both periodic excitation of ISCs and tonic inhibition of IHCs. The dual effect of ATP on P2ry1 in the developing cochlea may enhance the impact of burst firing by eliminating spurious action potential generation and promoting long intervals of quiescence between bursts.

Funding
T32 EY17203-15, T32 DC000023-31

PD 92

MEKK4 signaling regulates sensory cell development and function in the mouse inner ear

Daisy Haque[1]; Atul Pandey[1]; Hong Zheng[1]; Suhua Sha[1]; Saima Riazuddin[2]; **Chandrakala Puligilla**[1]
[1]Medical University of South Carolina; [2]University of Maryland

Mechanosensory hair cells (HCs) residing in the inner ear are critical for hearing and balance. Precise coordination of proliferation, fate-specification and differentiation during development is essential to ensure the correct patterning of HCs in the cochlear and vestibular epithelium. Recent studies have revealed that Fgf20 signaling is critical for proper HC differentiation. However, the mechanisms by which Fgf20 signaling promotes HC differentiation remain unknown. Here, we show that mitogen-activated protein 3 kinase 4 (MEKK4) expression is highly regulated during inner ear development and is critical to normal cytoarchitecture and function. Mice homozygous for a kinase-inactive MEKK4 mutation exhibit significant hearing loss. Lack of MEKK4 activity in vivo also leads to a significant reduction in the number of cochlear and vestibular HCs suggesting that MEKK4 activity is essential for overall development of HCs within the inner ear. Furthermore, we show that loss of Fgf20 signaling in vivo leads to inhibition of MEKK4 activity while gain of Fgf20 function stimulates MEKK4 expression which suggests that Fgf20 modulates MEKK4 activity to regulate cellular differentiation. Finally, to investigate the mechanisms of MEKK4 regulation, we examined the expression of JNK, a known target of MEKK4,

and found no alterations in JNK levels in MEKK4 mutants suggesting a novel JNK-independent function in regulation of cell-fate specification and differentiation. Collectively, this study provides compelling evidence of an essential role for MEKK4 in inner ear development, including normal HC differentiation and morphogenesis, and identifies Fgf20 signaling as a novel upstream regulator of MEKK4 function in the mammalian cochlea.

PD 93

Genome-wide profiling of cis-regulatory elements in the developing Organ of Corti: chromatin landscape of progenitors anticipates hair cell and supporting cell gene expression

Litao Tao; Yassan Abdolazimi; Zlatka Stojanova; Haoze Yu; Juan Llamas; Tymon Tai; Neil Segil
Keck School of Medicine of the University of Southern California

Sensory hair cells and supporting cells differentiate from a postmitotic, prosensory domain to form the highly specialized structures of the organ of Corti. Differentiation is an orchestrated process, conducted cooperatively by transcription factors and epigenetic regulatory mechanisms. To begin to decipher the signaling process by which differentiation is regulated, we FACS-purified cells from postnatal day 1 (P1) hair cells, supporting cells, and their E14.5 progenitors, and collected data of three kinds: RNAseq, to study cell type-specific expression, ATACseq to study the differential accessibility of chromatin between cell types, and ChIPseq, to study histone post-translational modifications indicative of active enhancers. Our initial goal is to identify and validate distal cis-acting elements in the DNA sequence (enhancers) that may be responsible for regulating expression of genes within these three cell types, and then to build these into a transcription factor network unique to each cell type.

We have found several interesting characteristics of the three cell types analyzed:

1) Typically, promoters of actively expressed genes are maintained in an open-chromatin configuration, and we found this to be true for hair cells. Interestingly, most of the genes in hair cells with open promoters are also found in a promoter-open configuration in Lfng-GFP$^+$ supporting cells (94%), suggesting that these genes are poised for expression. This is consistent with the ability of P1 supporting cells to rapidly transdifferentiate in response to Notch inactivation.

2) Many, but not all, of the genes differentially expressed in hair cells and supporting cells can be recognized in the prosensory, postmitotic progenitors by the presence of an open-chromatin structure at their promoter (96%). This suggests that the chromatin "landscape" of the progenitors is established prior to initiation of frank differentiation. In contrast, many genes with open promoters in progenitors, are not found in an open chromatin configuration in hair cells (51%) or supporting cells (20%), suggesting that there is a progressive "shutting-down" of chromatin during the early differentiation process.

3) As defined by our ATAC-seq data, only a portion of the distal elements identified in hair cells and supporting cells are shared (17,440), with 24,625 additional ATAC-seq peaks specific for hair cells, and an additional 46,827 specific for supporting cells. This suggests the extent of the regulatory needs attendant on inner ear cell type specification.

Using additional epigenetic markers, we will discuss our attempts to reconstruct the transcriptional networks governing hair cell and supporting cell differentiation.

Funding
We thank the Hearing Health Foundation, and the Sidgmore Family Foundation

PD 94

Analysis of Vangl1;Vangl2 Double Knockouts Reveal Conserved and Unique Polarity Mechanisms in the Developing Utricle

Michelle Stoller[1]; Orvelin Roman[1]; Andrew Francl[2]; Michael Deans[1]
[1]University of Utah; [2]Boston College

Planar polarity is critical for proper hair cell function and accurate stimulus detection in the peripheral vestibular system. The utricular macule exhibits striking examples of both Planar Cell Polarity (PCP); the coordinated orientation of stereociliary bundles between cells, and regional planar polarity. This latter organization is apparent in the two regions of hair cells with opposite stereociliary bundle orientation that are separated by the line of polarity reversal (LPR). Currently, little is known regarding the requirement of core PCP proteins for aligning hair cell orientation across the LPR though a general assumption is that PCP function is conserved between Drosophila and vertebrate hair cells. However, while the core PCP protein Vangl2 is essential for coordinating PCP in the specialized striola region, in Looptail mice with a dominant-negative Vangl2 mutation the orientation of hair cells in the lateral extrastriolar region (LES) is unaffected. Therefore, it remains possible that a second, independent signaling pathway regulates planar polarity in the LES and that this is also the basis of LPR formation. To ascertain the necessity of core PCP on opposite sides of the LPR, we removed vangl1 and vangl2 throughout the developing inner ear using the ear-specific Pax2-Cre driver. Stereociliary bundle orientation in utricles was assessed using immunofluorescence and Acrux polarity analysis software. Utricles devoid of vangl1 and vangl2 show widespread hair cell orientation defects throughout the utricle, including the LES region. To our surprise, we also found small groups of hair cells (3-5 cells) that retained coordinated orientation. The mechanism of this organization is unclear, however, based upon immunofluorescent labeling these cells also lose expression of the core PCP protein Celsr1. This finding suggests that the mechanism involves a second, PCP independent polarity pathway. Regardless, these results still indicate that Vangl proteins coordinate PCP throughout the utricle in a manner similar to Drosophila. In contrast, it

remains unclear if core PCP signaling in the mouse utricle functions in the same non-autonomous domineering manner as in Drosophila. To investigate conservation of function further, we capitalized on an unexpected recombination pattern of the Nestin-Cre line, which occurs specifically in the supporting cells and not hair cells of the striola. Ongoing experiments are using this line to further test whether Vangl2 relays polarity information across the utricle and between hair cells and supporting cells.

Funding
This research was supported by R01DC013066.

PD 95

Rack1 is Essential for Mouse Development and Planar Cell Polarity Regulation of the Inner Ear

Dehong Yu[1]; Erika Alexander[1]; Hao Wu[2]; Xi Lin[1]; Ping Chen[1]
[1]Emory University; [2]Shanghai Jiaotong University

Background
Planar cell polarity (PCP) refers to coordinated polarization of neighboring cells. PCP regulates many cellular processes, including convergent extension (CE) and the precise orientation of sensory hair cells. PCP pathway acts through membrane complexes containing Vang or Frizzled at cellular junctions to orient neighboring cells coordinately. The mechanisms underlying the action of membrane PCP protein complexes in PCP signaling, however, are yet to be delineated. Previously, we showed Rack1 interacts with the mammalian Vang homolog, Vangl2, and the requirement for Rack1 in PCP processes in zebra fish. This study aims to dissect the molecular and cellular role of Rack1 in PCP signaling using the inner ear as a model system.

Methods
We examined the localization of Rack1 in the cochlea, and generate a novel mouse model carrying a floxed allele of

Rack1 (*Rack1*$^{Loxp/loxp}$). To circumvent the embryonic day 14 (E14) lethality in Pax2-Cre or FoxG1-Cre Rack1 conditional knockout (CKO), we used an *Esr1-Cre* line to optimize temporal CKO of Rack1 that allows the analysis of the in vivo role of Rack1. We also included an mT/mG reporter allele to gauge the efficiency of CKO of floxed alleles. CKO was induced by two tamoxifen injections, and embryos were harvested at different developmental stages to determine the optimized experimental condition and to evaluate the requirement for Rack 1 in development.

Results
Embryos harvested at E17.5 achieve sufficient CKO of the floxed alleles and survived tamoxifen injections at E12 and E13. The *Rack1 CKO* animals have shortened limbs, a shortened snout and mandible, vascular abnormalities, and a shortened inner ear. In the cochlea, *Rack1 CKO* animals show distinct hair bundle misorientation, and a shortened cochlear duct with cellular patterning abnormalities similar to that observed in known PCP mutants. In addition, the localization of E-cadherin in the adherens junctions is greatly reduced and the cellular packing is abnormal. Infection of cultured cochleae with a viral vector directing the expression of tagged Rack1 protein showed that Rack1 is localized to the plasma membrane.

Conclusion
Together, our results suggested an essential role of Rack1 for mouse development and in multiple PCP processes, including a role in CE and hair cell orientation in the cochlea. At the molecular and cellular level, Rack1 may be involved in modulating activities at the adherens junctions to stabilize and/or recruit Vangl2, regulating adherens junction strength directly, and/or regulating surface tension of cells for CE and hair cell polarity during PCP signaling.

Funding
NIH RO1 DC005213

PD 96

A Unique Transcription Factor Signature Defines Hair Cells of Uniform Stereociliary Bundle Orientation

Jeremy Duncan; Michael Deans
University of Utah

Hair cells of the utricle and saccule are segregated into two distinct populations with oppositely oriented stereociliary bundles that are separated by a boundary called the line of polarity reversal (LPR). Planar cell polarity (PCP) proteins are asymmetrically localized in hair cells and supporting cells. While these proteins coordinate the orientation of stereociliary bundles between adjacent cells, they cannot contribute to LPR formation because the asymmetric localization of PCP proteins is not altered between cells with opposite bundle orientation. One possibility is that the maculae are patterned into two distinct regions with unique transcriptional profiles that guide bundle orientation. While hair cells on both sides of the LPR can be identified based on relative position and organization of stereocilia; candidate genes that could direct the development of one stereociliary bundle orientation over another have not been identified. Previous transcriptome profiling studies examining the developing macular epithelium utilized entire tissue preparations and cannot be used to glean regional differences.

To address this we have developed a unique genetic model that produces a utricle lacking mRNA expressed specifically by hair cells of one orientation while leaving the other unaffected. The advantage to this approach is that unlike FACS whole maculae could be easily dissociated from fresh tissue and RNA immediately preserved and extracted. This premise was validated because intense averaging of replicates and the data were not required. In order to accomplish this we have taken advantage of Emx2^{cre} which drives recombination on one side of the LPR in both maculae, corresponding to hair cells of a single orientation. We have combined this line with Atoh1$^{f/f}$ mice to prevent the differentiation of hair cells from one side of the LPR. The size of the mutant sensory epithelia was not significantly altered in the absence of the lateral hair

cells, and the striola formed normally including the expression of unique markers. We utilized RNA-seq and compared the mutant maculae with control maculae over a developmental time course. The transcriptional profiles of the mutant maculae were subtracted from control profiles to reveal lateral specific gene expression. We have for the first time identified molecular differences leading to hair cell heterogeneity in the vestibular maculae; specifically the molecular signature of vestibular hair cells with a single stereociliary bundle orientation. Candidate transcription factors with differences consistent over the developmental time course are being tested to determine their role in regional identity or bundle orientation.

Funding
This work was funded by F32DC014390 to JSD and R01DC013066 to MRD.

PD 97

Search for genes driving embryonic differentiation of OHCs vs IHCs

Ann Hogan[1]; Sarah Lorenzen[1]; Joege Cantú[1]; Freddie Márquez[1]; Anne Duggan[1]; Anna Osipovich[2]; Mark Magnuson[2]; Jaime García-Añoveros[1]
[1]Northwestern University; [2]Vanderbilt University Medical Center

Background
Cochlear hair cells arise during embryogenesis, but how they specifically differentiate into IHCs or OHCs remains unknown. We found a presumed transcription factor (INSM1) expressed in incipient OHCs, but not in IHCs, during mouse embryogenesis (E15.5 to P2). This is the only gene known to be uniquely expressed in nascent, early differentiating OHCs (but not IHCs). Mice lacking INSM1 die during late embryogenesis, limiting their study to E18.5. We hypothesize that INSM1 regulates specific OHC development by activating or repressing other genes early in OHC differentiation. We generated a mouse *Insm1*$^{GFP.Cre}$ reporter and KO allele that selectively labels OHCs from their onset to cell sort and identify genes regulated by INSM1 in nascent OHCs as well as genes uniquely or preferentially expressed in embryonic OHCs or IHCs.

Methods
We generated two types of null alleles: one (*Insm1*$^{-}$) that deleted the entire coding sequence and another (*Insm1*$^{GFP.Cre}$) that replaced the CDS with that of a GFP reporter fused to a Cre recombinase and hence labelled all OHCs embryonically. We FACS sorted OHCs from E18.5 embryos with (*Insm1*$^{GFP.Cre/+}$) and without (*Insm1*$^{GFP.Cre/-}$) INSM1, collected RNA from separate pools of 2000-5000 OHCs each (3 pools per genotype), converted to cDNA, amplified it (NuGEN Ovation) and performed RNAseq to obtain ~50 million reds per sample. We aligned the clean reads to the mouse genome (mm10) using STAR, and calculated read counts for each gene using htseq-count. Hence we obtained the transcriptomes of E18.5 OHCs with and without INSM1.

Results
As expected, most abundant transcripts are expressed at similar levels regardless of phenotype, while expression of less abundant transcripts is more subject to RNAseq variability. As further proof of data reliability, the coding sequence of *Insm1*, which is present in the wild type (+) but missing in both KO (- and GFP.Cre) alleles, was detected in all *Insm1*$^{GFP.Cre/+}$ OHC pools but none of the *Insm1*$^{GFP.Cre/-}$ OHC pools. We identified 331 genes that may be regulated by INSM1 in nascent, embryonic OHCs. In addition, by comparing our E18.5 OHC transcriptome with the transcriptomes of E16.5 and P0 cochlear hair cells (OHCs + IHCs) we identified 108 genes that may be uniquely or selectively expressed in embryonic IHCs. Among these are *fgf8* (previously known to be expressed in embryonic IHCs but not OHCs) and several transcription factors.

Conclusions
These studies are uncovering the molecular events accompanying the development of cochlear hair cells into distinct OHCs and IHCs.

Funding
Knowles Hearing Center (JGA) and F31 DC012483 (SML).

PD 98

Differentiation of human induced pluripotent stem cell-derived posterior otic placode progenitors into inner ear hair cell lineage

Hanae Lahlou[1]; Alejandra Lopez[1]; Arnaud Fontbonne[1]; Emmanuel Nivet[1]; Francçois Feron[1]; Azel Zine[1,2]
[1]University of Aix Marseille; [2]University of Montpellier

Background
Human induced pluripotent stem cells (hiPSCs) technology holds great expectations for drug discovery and clinical applications such as cell transplantation. Along this line, progresses have been made in applying hiPSC technology to a variety of organ systems such as the retina, the cardiovascular system as well as the peripheral and central nervous systems. Noteworthy, the inner ear represents another system of particular interest for translational studies relying on the use of hiPSCs. Up to date, only a few studies have reported the *in vitro* generation of hair cell (HC)-like cells from hiPSCs. However, the efficiencies associated to available protocols remain unsatisfactory and urge the search optimized protocols able to recapitulate *in vitro* the developmental steps leading to human otic/HC lineages. In this study, our main objective is to develop a hiPSC-based protocol allowing efficient derivation of otic progenitors and HC-like cells.

Methods
Using a two-step strategy, we first sought to induce the generation of otic progenitor cells prior to proceed to their further differentiation into HC-like cells. To this end, hiPSCs were cultured onto a laminin coated-matrix using a serum-free culture medium supplemented with FGF3 and FGF10 during 12 days. Then, newly generated otic progenitor cells were seeded onto laminin/poly-ornithine-coated plates and

maintained in a basal culture medium containing either retinoic acid (RA) and EGF or Notch pathway modulators for 2-4 weeks. At the end of each of the two steps, quantitative PCR and immunocytochemical analyses were performed to assess the expression of otic- and HC-associated markers, respectively.

Results

At the end of the initial 12-day culture period, which corresponds to the induction phase of our protocol, we observed the generation of cells upregulating comprehensive otic placode lineage markers such as PAX2 and EYA4. Interestingly, a fraction of these cells were found to express HC markers upon further differentiation. Our results revealed that otic progenitor cells differentiated under Notch inhibition were more prone to upregulate a subset of HC markers *i.e.*, Pou4F3 and MyosinVIIa when compared to RA/EGF-treated cultures.

Conclusion

Our data indicate that interference with Notch pathway as a potent mean to derive human HC-like cells from hiPSC-derived otic progenitors. This work could set the bases to a better understanding of the mechanisms controlling human HC differentiation and for the development of new protocols that could benefit to cell-based therapy for inner ear disorders.

Funding

Supported by the European Commission, under the FP7-HEALTH-2013 INNOVATION-OTOSTEM project.

PS 490

The Effect of HRT on IGF-1r and FOXO3 Expression in SVK-1 Cells

Tanika Williamson; Bo Ding; Xiaoxia Zhu; Robert Frisina
University of South Florida

Introduction

The purpose of the present investigation is to gain insight on the effects of hormone replacement therapy (HRT) on IGF-1r and FOXO3 levels in the cochlea, both of which have been linked to anti-apoptotic responses. The results could help explain why estrogen (E) and progesterone (P) can have a positive effect on the auditory system; however, note, that when these hormones are combined, hearing thresholds increase significantly (Price et al., *Hear. Res.* 252: 25-36, 2009).

Methods and Materials

SVK-1 epithelial cells derived from the stria vascularis (SV) of the P14 Immortomouse (obtained from Dr. Federico Kalinec, Univ. South. Cal.) were utilized. SVK-1 cells were proliferated in DMEM medium (Corning Manassas, VA) with 10% FBS and incubated at 33°C in a humidified 10% CO_2 atmosphere. Once the cells reached an ~80% confluence, treatment began in a humidified 5% CO_2 atmosphere at 37°C. Three types of hormone treatment were administered: E, P, E+P. Hormone therapy was administered to SVK-1 cells in a time dependent manner, which included treatment durations of 4 and 24 hours. Following treatment, the cells were washed and extracted using the protocol from the RNeasy Mini Kit (Qiagen). RT-PCR tests were then performed to compare the expressions of IGF-1r and FOXO3 in each of the HRT groups.

Results

After 4 hours of treatment, SVK-1 cells treated with E had a higher expression of FOXO3 than cells treated with E for 24 hours. We also found a higher FOXO3 expression occurred for SVK-1 cells treated with E compared to P. Additionally, IGF-1r levels increased in cells treated individually with E and P compared to untreated cells. Combination HRT (E+P) showed a significant *decline* in IGF-1r expression after 4 hours of treatment in comparison to control cells. Interestingly, IGF-1r levels did increase after 24 hours.

Conclusions

These findings suggest that both E and P are possible factors in the upstream signaling of IGF-1r and FOXO3. Previous studies have shown that declining FOXO3 levels have been linked to auditory neuropathy. Similarly, IGF-1 plays a key role in the maintenance and possibly the survival of cochlear supporting cells and hair cells. Therefore, increasing gene expression after E and P exposure could facilitate cellular preservation in the auditory system. Contrarily, the low expression of IGF-1r seen in E+P treated cells may be due to the inhibition of anti-apoptotic responses.

Funding

Work supported by the Nat. Inst. on Aging, NIH grant P01 AG009524.

PS 491

Female hormones modulate auditory temporal processing in young adult CBA/CaJ mice

Xiaoxia Zhu; Carlos Cruz; Alaa Taha; Tanika Williamson; Bo Ding; Robert Frisina; Joseph Walton
University of South Florida

Background

Hormone replacement therapy (HRT) has functional effects on auditory processing, as found by behavioral and physiological tests in both menopausal women and aging female CBA/CaJ mice (Guimaraes et al., Proc. Nat. Acad. Sci. 103: 14246-9, 2006. Price et al., Hear. Res. 252: 29-36, 2009. Zhu et al., ARO Abstract #507, 2015). In the present study, we hypothesized that female hormones modulate auditory pathway temporal processing even in young adult CBA/CaJ.

Methods

Young adult (2 months (mon)) CBA/CaJ served as the animal model and were formed into three groups: ovariectomized female (OVX, N=5), control female (CF, N=5) and male control (M, N=5). These mice received Auditory Brainstem Response (ABR) and ABR gap-in-noise (GIN) tests at baseline, before the ovariectomy. Post ovariectomy (PO) 1 mon, the mice underwent functional hearing testing (ABR audiogram, ABR GIN, acoustic startle response (ASR) and prepulse inhibition of ASR (PPI)). These hearing tests were repeated over a 6 mon period.

Results
ABRs thresholds showed slight and comparable increases in threshold across the 3 subject groups from 2-8 mon old, as the mice aged. However, there were significant declines in temporal processing, as measured by ABR GIN responses peak1 (P1) amplitude, for the OVX group for PO 2 mon and 4 mon, compared to baseline (2 to 32 msec gap durations). The ASR I/O functions were significantly lower for the OVX and CF groups, compared to the males, at PO1 and PO3 mon. Later the startle amplitudes of the OVX group increased to the level of the M group at PO6 mon. The CF group had greater noise PPI responses, suggesting increased salience for noise signals near threshold. There were significant differences between the CF and M groups at 55 dB SPL prepluse at PO1 mon, and for 20 and 40 dB SPL prepluses at PO3 mon. No differences were found between the three subject groups at PO 6 mon.

Conclusions:
The present study results suggest that even at young adult ages, female hormones can significantly influence auditory temporal resolution, and therefore, play a role in helping control the nervous system's sensory gating processes.

Acknowledgements
Work supported by the Nat. Inst. on Aging, NIH grant P01 AG009524

PS 492

Effects of envelope shape on phase-locking of inferior colliculus neurons in young and aged rats

Björn Herrmann[1]; Aravindakshan Parthasarathy[2]; Edward Bartlett[3]
[1]The University of Western Ontario; [2]Harvard Medical School; [3]Purdue University

Realistic temporal processing requires representations of varying stimulus periodicities as well as envelope shapes which are often asymmetric. Phase-locking of auditory evoked potentials to asymmetric sound envelopes indicate that the representation of both periodicity and envelope shapes degrade with age. The current study investigates whether those differences are present in inputs to the inferior colliculus (IC), a major integrating hub in the ascending auditory pathway, and explores the input-output transformations that occur in the IC in response to these stimuli.

We recorded extracellular local field potentials (LFPs) and spiking activity from IC neurons in young (3-6 months, N=93) and aged (22-26 months, N=90) anesthetized F344 rats. Animals were presented with broadband noises (300 ms) that were amplitude-modulated at 45 Hz, 128 Hz, or 256 Hz. We tested the ability of IC neurons to represent periodicity and envelope shape for five amplitude envelopes ranging from strongly damped to strongly ramped generated by varying parameters of a beta function.

LFPs to the noise onset were smaller in aged compared to young rats, while no age difference was found for onset spike rates. LFPs exhibited consistent phase-locking responses at all three modulation frequencies with significantly larger phase-locking responses for younger rats at 128 Hz and 256 Hz. Reliable phase-locking was also observed for spikes at 45 Hz and 128 Hz, while spike phase-locking was small for 256 Hz, in particular for aged rats. At 45 Hz, aged rats exhibited larger spike phase-locking compared to young rats, paralleling a relative increase from LFPs to spike rates for onset responses in aged rats. In addition, we observed that damped and ramped envelopes affected the phase lag (relative to the modulation cycle) of LFP and spike phase-locking. In particular, for 45 Hz stimuli, the phase lag for two damped conditions did not differ while the ramped conditions showed different phase lags. For modulation frequencies of 128 Hz and 256 Hz, phase lags were different for both damped and ramped envelopes.

In sum, we observed relative increases in the transformation from LFPs to spikes for aged rats, suggesting a relative increase in neural excitability or a relative decrease in neural inhibition at the output level of the IC that accompanies aging. Our data also suggest that both LFPs and spiking are able to represent periodicity and envelope shape up to 128 Hz, while only LFPs are able to represent them at 256 Hz.

PS 493

Expression of Group II Metabotropic Glutamate Receptors in the Aging Auditory Cortex of Mice

Blaise Clarke[1]; Yuchio Yanagawa[2]; George Strain[1]; Charles Lee[1]
[1]Louisiana State University; [2]Gunma University

Presbycusis, or age-related hearing loss, continues to be a major, global health issue; occurring gradually over time, it affects approximately one in three people over the age of 65, and one in two people over 85.. Among its neurobiological causes, changes to the balance of neuronal excitation and inhibition in the central auditory system plays an important role in the perceptual deficits arising from this condition. This balance has been studied with respect to alterations in the GABAergic and glycinergic pathways of the central auditory system. However, largely overlooked is the potential role of age-related changes to glutamatergic inhibition, mediated by Group II metabotropic glutamate receptors (mGluRs). In our study, we assessed whether expression of Group II mGluRs were altered with age in an aging mouse model. Therefore, we examined aging mice, using anatomical and physiological tests, to examine the expression of Group II mGluRs in the aging auditory cortex, to document expression over time and its potential contribution to age-related hearing impairments. Hearing was assessed in animals using auditory brainstem responses and behaviorally via evoked startle responses to pure tones at various frequencies. Our results indicate a difference in the magnitude of Group II mGluR expression in older animals in comparison to its expression in younger animals, which suggest that Group II mGluRs are a potential factor in the emergence of age-related hearing deficits and

an overlooked mechanism for regulating excessive neuronal activity in the auditory cortex.

Funding
NIH Grant R03 DC 11361; Action on Hearing Loss Grant F32; American Hearing Research Foundation Grant

PS 494

Altered ABR Waveforms and Ribbon Synapse Changes in the FBN Rat Model of Aging

Rui Cai; **Scott Montgomery**; Donald Caspary; Brandon Cox
Southern Illinois University School of Medicine

Background
The Fisher Brown Norway (FBN) rat, an aging model provided by the NIA has been used to demonstrate age-related changes related to inhibition and temporal processing of acoustic information. Previous studies found significant outer hair cell loss in the aged FBN rat, with minimal inner hair cell (IHC) loss. Loss of low frequency spiral ganglion cells has also been shown for Brown-Norway rats (Keithley et. al., 1992). Recent studies compared age-related changes in auditory brainstem evoked response (ABR) and synaptic changes at the IHC acoustic nerve fiber (ANF) synapse in mice (Sergeyenko et al., 2013). Here we performed similar studies in the FBN rat.

Methods
Young (5m), middle (20m), old (32m) FBN rats were used in the present study. Sounds for ABR testing were delivered at 30dB HL and 80dB SPL using an electrostatic speaker fitted to a tube in the left ear canal. Electrodes were placed under the skin of ketamine/xylazine anesthetized rats at the vertex and left mastoid with a toe ground. ABR signals were amplified and filtered from 300Hz to 10kHz. ABR thresholds, latencies and amplitudes were obtained between 2-40kHz + clicks. ANF synapses were examined in cochlear whole mounts immunostained for the presynaptic ribbon protein (Ctpb2) and post-synaptic glutamate receptor (mGluR2) and quantified at 4, 12, and 24kHz regions using a rat cochleogram (Viberg and Canlon, 2004).

Results
All groups had best threshold at 12kHz and showed an age-related 22dB parallel elevation between young and old rats. ABR wave I and V amplitudes progressively decreased with age with greatest changes seen for clicks, 4kHz and 24kHz. As predicted, the V-I ratio was increased with age with greatest increases seen for clicks at 80dB SPL. Preliminary data suggests preservation of ANF synapse numbers in young and middle aged rats, with loss of synapses from old samples that were most severe at the 4kHz region. Old rats showed an increased number of orphan synapses, where the presynaptic ribbon protein was present, but the post-synaptic glutamate receptor was not detected.

Conclusions
As predicted from previous studies in FBN and Brown-Norway rats, the greatest age-related ABR changes occurred at low frequencies reflecting apical synaptopathy. The relative age-related maintenance of wave V amplitude likely reflects previously observed down-regulation of central inhibition in auditory brainstem (Caspary et al., 2008).

Funding
Funding: Supported by the Office of Naval Research (N000141310569), National Center for Research Resources-Health (S10RR027716), NIDCD DC000151 and SIU-SM shared investigator award.

PS 495

Differences In Hearing Function And Cochlear Morphology Between Male And Female Fisher 344 Rats.

Tetyana Chumak[1]; Jiří Popelář[2]; Francesca Chiumenti[3]; Zuzana Balogová[4]; Josef Syka[2]
[1]Institute of Experimental Medicine; [2]Institute of Experimental Medicine, Academy of Sciences of the Czech Republic; [3]Faculty of Medicine, University of Padova; [4]1st Faculty of Medicine, Charles University in Prague, University Hospital Motol, Prague, Czech Republic

Background
The Fischer 344 (F344) strain of inbred albino rats is known to have accelerated age-related hearing loss. It is also known, that F344 males are more susceptible to ageing compared to females concerning peripheral retinal degeneration, dopaminergic functioning and renal pathology. In the present study we investigated whether young and old male F344 rats have deteriorated hearing function and cochlear morphology compared to female F344 rats.

Method
The hearing function of F344 rats of both sexes was assessed using recording of auditory brainstem responses (ABRs) and distortion products otoacoustic emissions (DPOAEs). Cochlear paraffin sections and surface preparations were analyzed to assess possible morphological differences between cochleas of male and female rats. Hair cells loss, efferent/afferent cochlear innervation and the state of the cochlear lateral wall were analyzed.

Results
Hearing thresholds and otoacoustic emissions did not differ between young (3 months old) male and female F344 rats. Though, young males had a significantly smaller volume of inner hair cell (IHC) ribbons than female rats, that persisted throughout their lifespan (up to 30 months old). Starting at about 8 months old, the hearing of male F344 rats began to deteriorate faster compared to hearing of females, manifested by higher ABR thresholds and lower DPOAE amplitudes in the males. Animals of both sexes underwent moderate age-related OHC loss, however this tended to be slightly higher in old males. In both, male and female rats, cochlear MOC terminals degenerated and the number of IHC ribbons decreased with age, although, to the same extent. The most pronounced morphological differences between male and female rats were found in the state of the cochlear lateral wall: in males the marginal cell layer in the stria vascularis

was profoundly damaged and the spiral ligament looked less dense compared to female rats (see Buckiová et al., 2007).

Conclusion

Our results showed that IHC ribbons in young male F344 rats were smaller compared to female rats, although this did not manifest physiologically. Ageing in F344 animals of both sexes was accompanied by similar degrees of outer hair cell loss and degeneration of efferent and afferent fibers. The cochlear lateral wall in old male rats, however, was more profoundly damaged compared to female rats, most likely being the cause of the faster decline in hearing function in ageing F344 male rats.

Funding

Supported by grants P304/12/G069 and P304/12/1342.

PS 496

Auditory Threshold Shift In Age-Related Hearing Loss Is Reduced By An Oral Combination Of Antioxidants And Mg++.

Jose Juiz[1]; Juan Alvarado[1]; Veronica Fuentes-Santamaría[1]; Pedro Melgar-Rojas[1]; Maria Gabaldon-Ull[1]; Josef Miller[2]

[1]University of Castilla-La Mancha; [2]University of Michigan

The increasing rate of age-related hearing loss (ARHL) in the population, with subsequent reduction in quality of life and increase in health care costs, makes it necessary to develop new intervention strategies to prevent or reduce this condition associated to aging. The goal of this study was to determine whether auditory threshold shifts in presbycusis could be reduced by administering a combination of free radical scavengers (vitamins A, E and C) plus the natural vasodilator magnesium (ACEMg) to adult animals. ACEMg has been shown to limit the consequences of noise-induced hearing loss, significantly improving auditory thresholds in ABRs.In this study, 3 month-old Wistar rats were distributed into two groups according to whether they were fed orally with a normal diet (ND) or an ACEMg enriched diet (ED). In order to accelerate and increase ARHL, ND and ED rats were exposed to a continuous white noise at 118 dB SPL for 1h during 5 days a week, causing temporary threshold shifts, until the animals reached the age of 12-14 months. The ED treatment began 10 days before the noise stimulation. ABR recordings were performed at 0.5, 1, 2, 4, 8, 16 and 32 kHz at 3 and 12-14 months of age. The results showed that in both ND and ED animals of 12-14 months there was a significant increase in auditory thresholds at all frequencies tested. However, the threshold shift observed in ED rats was significantly lower than that seen in ND rats at medium frequencies. These findings suggest that the synergistic effect of an oral combination of free radical scavengers and Mg++ seems to be a feasible approach to limit the consequences of ARHL.

Funding

Ministry of Economy and Competitiveness of the Government of Spain, BFU2012-39982-C02andBFU2012-39982-C01. European Commission 7th Framework Programme (PROHEARING 3592)

PS 497

Age and Sex Influence Ultrasonic Vocalization Detection by CBA/CaJ Mice

Anastasiya Kobrina; Micheal Dent

SUNY University at Buffalo

Age-related hearing loss (ARHL), or prysbycusis, is a universal feature of mammalian aging. This condition is characterized by the progressive decrease in hearing sensitivity from high to low frequencies, as well as a decrease in the perception of complex auditory signals, such as speech. Mice are frequently used as an animal model for human hearing research, yet their hearing capabilities have not been fully explored. Previous studies (Ehret, 1975; Radziwon et al. 2009) have established auditory threshold sensitivities for pure tone stimuli using behavioral methodologies. Further, pure tone thresholds have been measured in the CBA/CaJ strain using ABRs across the lifespan (Henry, 2004). This strain shows sex differences in hearing loss similar to humans, with males having high frequency hearing loss earlier than females. While it is clear that the CBA/CaJ mouse resembles human ARHL for pure tones, little is known about how this strain perceives their own ultrasonic vocalizations (USVs) or how aging and sex influence that perception. Our aim was to establish auditory threshold sensitivity for several USV types, as well as to track these thresholds across the mouse's lifespan. We hypothesized that thresholds would vary across USVs differing in spectrotemporal complexity. Further, we expected to see sex differences in USV thresholds, with males having higher thresholds than females. In order to determine how well mice detect these complex communication stimuli, several CBA/CaJ mice were trained and tested at various ages in a detection task using operant conditioning procedures. The detection of seven USV call types, as well as a 42 kHz pure tone stimulus, were measured. These stimuli were presented at various intensities according to the Method of Constant Stimuli. Thresholds for detection of these calls were calculated using d'=1.5. The mice were tested at various ages throughout their lifespan. Results showed that mice are sensitive to their complex vocalizations even into old age. Not surprisingly, thresholds differed for the different USV types. Mice were able to detect some USVs at a lower intensity than pure tones of the same frequency range. Overall, male and female mice exhibited hearing loss for USVs and the pure tone across the lifespan. Elderly male mice showed higher thresholds for some USVs compared to females. In conclusion, the results highlight the importance of USVs for survival and communication, and lay the groundwork for future studies on complex signal perception and aging in this species.

Funding

This work was supported by NIDCD grant R01-DC012302

PS 498

Effects of Meaningful vs. Meaningless Noise on Speech Representations in the Aging Midbrain and Cortex

Alessandro Presacco; Jonathan Simon; Samira Anderson
University of Maryland

Introduction

Humans have a remarkable ability to understand speech in the presence of competing speech. However, older adults often complain about their inability to hear in crowded situations, and their performance on speech-in-noise perceptual tasks is poorer than that of younger adults. Older adults may rely on cognitive resources to compensate for these perceptual deficits. For example, their speech-in-noise performance may be better in the presence of a nonmeaningful distractor (foreign language) compared to a meaningful distractor (native language), but this same difference is not seen in younger adults. In this study we used neuroimaging techniques (Electroencephalography (EEG) and Magnetoencephalography (MEG)) to investigate the interacting effects of aging and attention on neural processing of speech in noise.

Methods

Participants comprised 17 younger adults (18–27 years old) and 15 older adults (61–73 years old) with clinically normal audiometric thresholds. Midbrain activity was assessed by recording Frequency Following Responses (FFRs) to a 170-ms /da/ speech syllable presented binaurally in quiet and in single-talker competing speech, and cortical activity was assessed by recording MEG responses while listeners attended to one of two simultaneously presented speech streams. Responses were recorded in quiet and in the presence of competing speech at different signal-to-noise ratio levels (+3, 0, -3 and -6 dB). The competing speech signal was either meaningful (narrated story in English) or meaningless (narrated story in Dutch).

Results

In midbrain, the younger adults' speech envelope was more robust to noise than that of older adults, though no effect of noise type (meaningless vs. meaningful) was observed in either age group. Conversely, in the cortex only older adults' responses were affected by background type, such that reconstruction fidelity of the target speech envelope improved in the presence of Dutch vs. English background narrations.

Conclusions

Our findings suggest that competing speech degrades auditory temporal processing in midbrain and cortex in older adults to a greater extent than in younger adults. Furthermore, cortical responses in older adults are also affected by the background noise type (meaningful vs. meaningless), suggesting possible top-down cognitive processes that may affect the neural representation of the attended speech signal.

PS 499

Assessment of Age-related Middle-ear Function using Power Reflectance and Umbo Velocity

Salwa Masud[1]; Song Cheng[2]; John Rosowski[2]; Hideko Nakajima[2]
[1]Harvard University; [2]Harvard Medical School, Massachusetts Eye and Ear

Previous studies have investigated age effects in the human middle ear to further our understanding of the aging process of the auditory system. These effects have been examined using multifrequency tympanometry, admittance measures at 220 or 660 Hz, wideband acoustic immittance (WAI), and laser Doppler vibrometry (LDV). However, studies using different modalities have conflicting results, some suggesting that there is a conductive component to age-related hearing loss (presbycusis), and others finding no age-related conductive component. To clarify these discrepancies we utilized power reflectance (PR) obtained from the WAI measurement at the ear canal and umbo velocity (UV) obtained by laser Doppler vibrometry to compare young and old subjects.

The young group consisted of 21 normal hearing adults between 16 and 30 years old where 36 ears were measured. The older group had 16 adults over 55 years old, consisting of fourteen subjects that were diagnosed with presbycusis (26 ears tested) and two subjects with normal hearing (4 ears tested), resulting in total of 30 older ears. PR is derived from WAI measurements and is the square of the magnitude of the fraction of the forward acoustic sound that is reflected by the tympanic membrane back into the ear canal. UV is measured through the ear canal at the tympanic membrane in response to nine simultaneous sound frequencies. Standard audiograms were conducted by a trained audiologist.

All subjects in this study had no history of middle-ear disorders. Significant age-effects were found in PR measures. Specifically, in older adults there was a significant decrease in PR at 215 Hz, 315 Hz, 500 Hz to 1000 Hz and at 6000 Hz. At these frequencies, the average PR values for older adults were about 12% less than the younger adults. This result proposes a decrease in middle-ear stiffness with age. Moreover, there were significant age-related changes in UV at 700 Hz, 1000 Hz, 2000 Hz and 4000 Hz. The UV at 700 Hz, 1000 Hz, and 2000 Hz increased with age about 40% compared to the younger adults. Additionally, at 4000 Hz there was a significant decrease in UV for older adults of about 29%. Consistent with the PR data, the UV data also suggests that stiffness of the human middle-ear decreases with age. The findings of this study suggest that there may be a mechanical (possibly a middle-ear) factor to age-related hearing loss.

Acknowledgements: NIH/NIDCD R01 DC004798; NIH Speech and Hearing Bioscience and Technology Training grant

Funding

NIH/NIDCD R01 DC004798; NIH Speech and Hearing Bioscience and Technology Training grant

PS 500

Metabolic presbyacusis: Longitudinal changes in hearing for middle-aged and older adults

Kenneth Vaden; Mark Eckert; Lois Matthews; Judy Dubno
Medical University of South Carolina

Background

Age-related hearing loss can be characterized as distinct metabolic and sensory phenotypes, based on audiometric patterns established in animal models (Dubno et al., 2013; Schmiedt, 2010). As seen in quiet-aged animals, metabolic presbyacusis involves deterioration of the cochlear lateral wall and a reduced endocochlear potential, resulting in a mild, flat hearing loss at lower frequencies coupled with a gradually sloping hearing loss at higher frequencies. Following environmental exposures of excessive noise or ototoxic drugs, sensory presbyacusis involves damage to sensory and non-sensory cells and loss of the cochlear amplifier, which produces 50-70 dB threshold shifts at higher frequencies. The current study examined the stability of audiometric phenotypes in audiograms measured longitudinally in middle-aged and older adults, and tested the hypothesis that metabolic phenotypes are more common with increasing age.

Methods

Audiograms were collected longitudinally from adults 50-93 years old (n = 686 ears) and submitted to a Quadratic Discriminant Analysis (QDA) to classify audiograms from each ear as 1) older-normal, 2) metabolic, 3) sensory, or 4) metabolic + sensory phenotypes. The classifier was trained on fitted curve parameters for 338 initial audiograms that were previously selected as exemplar cases of each phenotype by human experts. In cross-validation tests performed with the training dataset of exemplars, the phenotype classifications were 94% accurate.

Results

Pure-tone thresholds increased with age, but audiometric phenotypes did not change for most ears (>60%). Most subjects with stable phenotypes demonstrated matching phenotypes for both ears across all time points (~90%). Consistent with hypothesized strial declines, most ears with changing phenotypes transitioned to metabolic phenotypes. Ears that transitioned to the combined metabolic + sensory phenotype exhibited distinct longitudinal patterns of change; cases that were initially sensory showed additive declines consistent with a metabolic phenotype, whereas cases that were initially metabolic showed additive declines primarily at higher frequencies.

Conclusion

Audiograms from middle-aged and older adults contained information that can distinguish audiometric phenotypes, consistent with animal models of sensory and strial pathologies. Although hearing loss increased with age, most ears exhibited stable phenotypes over time. Ears with changing phenotypes were consistent with metabolic phenotypes increasing with increasing age, consistent with hypothesized metabolic pathology. Together with differences in how sensory and metabolic cases transitioned to the combined metabolic + sensory phenotype, these findings are consistent with the view that age-related hearing loss is a metabolic/neural disorder rather than a sensory disorder.

Funding

This work was supported in part by grants from the NIH/NIDCD (P50 DC 00422), and NIH/NCRR (C06 RR14516).

PS 501

Influence of Age on Physiological Spread of Excitation

Katrien Vermeire[1]; Ingeborg Dhooge[2]; Andrea Vambutas[1]
[1]Long Island Jewish Medical Center; [2]Ghent University Hospital

Age-related changes in sensory sensitivity and acuity are amongst the most robust findings in audiology. Such declines will become more common as the world's population shifts towards a greater number of older adults.

In the case of acquired severe to profound hearing loss where there is no benefit from conventional amplification, cochlear implantation has proven to be beneficial. Cochlear implantation remains controversial in the geriatric population because it is sometimes assumed that elderly patients might perform poorly, especially with speech understanding. There are numerous factors specific to the elderly that can influence outcomes, including otologic factors as well as physical and cognitive capabilities. Otologic factors include age-related changes in both the peripheral and central auditory systems. Presumably these are caused by long durations of hearing loss and diminished communication needs. However, it is unclear to what extent the poorer outcomes with the elderly population are dependent on peripheral or central degradations.

In the present study, we will measure physiological spread of excitation which is a purely peripheral process. The spreads of excitation will be measured using a standard forward masked paradigm using electrically evoked compound action potentials (ECAP). The measures will be made for cochlear implant users of a wide range of ages. We will investigate if the elderly population has a greater spread of excitation than the younger population. If so, the data would suggest that performance deficits with the elderly are not exclusively caused by central deficits. If not, the data would suggest that processing deficits in the elderly are primarily central. Additionally, we will evaluate speech in noise scores with these subjects to verify that the elderly in our population do indeed have processing deficits.

PS 502

Age-Related Changes in Temporal Responsiveness of the Auditory Nerve

Shuman He; Tyler McFayden
Boys Town National Research Hospital

Background

Temporal cues, especially rapid spectral and amplitude changes or acoustic onsets, are prominently represented in the response of the auditory nerve (AN). This study aims to investigate age-related changes in temporal responsiveness of the AN in human listeners. It tests the hypothesis that aging decreases temporal responsiveness the AN, which can be evaluated using electrophysiological measures of the electrically evoked compound action potential (eCAP).

Methods

This study recruits three groups of subjects: young (25-45 years), middle-aged (46 to 60 years), and older (≥65 years) cochlear implant (CI) users. To date, three young (Y1-Y3), four middle-age (M1-M4) and three older (O1-O3) CI users have participated in the study. All subjects had a full insertion of Cochlear freedom contour advanced or System 5 electrode arrays in the test ear and use a pulse rate of 900 pps per channel in their programming MAPs. All subjects had normal cognitive functions. They were matched on duration of profound deafness, residual hearing prior to CI and listening experience with their devices. Two types of stimuli were used: a single biphasic pulse and a train of biphasic pulses. Stimuli were directly presented to one basal, two middle-array and one apical electrode in a monopolar-coupled stimulation mode. All measures were conducted for each of the four electrodes tested in this study. Each subject completed the following measures: behavioral dynamic range measured for each type of stimulus, the amplitude growth function of the eCAP, adaptation of the AN evaluated by measuring eCAP amplitude in response to individual pulses in pulse trains with pulse rates of 500, 900, 1800, and 2400 pulse per second (pps), and recovery from single-pulse and pulse-train forward masking assessed using eCAP responses. Results measured from the four electrodes were averaged together to obtain the mean dependent variables for each measures in each subject.

Results

Our preliminary data showed a negative correlation between the slope of the eCAP amplitude growth function and subject age, which may suggest reduced neural density with advanced age. Older subjects also exhibit more neural adaptation and slower recovery from the forward masking effect introduced by the pulse train at the level of the AN, especially at fast pulse rates.

Conclusions

These preliminary data suggest that temporal responsiveness of the AN reduces with advanced age. These age-related changes can be evaluated using eCAP measures in CI users.

PS 503

Why does spectral and temporal resolution degrade between the auditory nerve and cortex? Implications for noise robust coding of speech

Fatemeh Khatami; Monty Escabi
University of Connecticut

The mammalian auditory system is highly resilient to acoustic variability, such as background noise and multiple talkers, yet how the brain achieves a robust neural representation is unclear. Several processing mechanisms, such as spike timing dependent plasticity and gain control (Mesgarani et al 2014), have been recently shown to contribute to robustness. However, its unclear to what extent the organization of the auditory pathway and its sequential transformations contribute to a noise robust coding. Notably, spectral and temporal encoding resolution progressively degrades between the auditory nerve and cortex. Using a computational auditory network, we tested the possibility that this sequential organization is necessary for noise robust coding of speech. The network consists of a cochlear model, a spiking neural network with six neuron layers that model the principal structures between the auditory nerve and cortex, and a Bayesian classifier that is used to read out the neural spike trains. The network was trained and tested with a ten alternative forced choice word recognition task using speech from multiple talkers and in the presence of babble noise (SNR=-5 to 20 dB). Several basic properties of the ascending auditory pathway, such as the sequential loss of temporal and spectral resolution seen in neural receptive fields and increasing sparseness and selectivity, are predicted upon training the network to maximize speech recognition performance in noise. For comparison, we also considered a network in which temporal and spectral resolution remain constant across layers. We tested the performance of both networks in the presence of noise and measured spectrotemporal receptive fields (STRFs) and mutual information at each layer to characterize the sequential layer-to-layer transformations. For the high-resolution network, STRFs, mutual information rates (bits/sec) and spike information (bits/spike) remained relatively constant between layers indicating a minimal loss of acoustic information between the first and last layer. In contrast, STRFs became progressively slower and spectrally coarser, information rates decreased while spike information and word recognition accuracy increased systematically across layers for the optimal network. Thus despite a total loss of acoustic information between the first and last layer, individual action potentials become sequentially more informative about the sound identity, ultimately enhancing the recognition performance in noise. These findings suggest that the sequential transformations of the ascending auditory pathway, in which temporal and spectral resolution sequentially degrade, forms a near optimal strategy for feature extraction that maximizes sound recognition performance in the presence of noise.

PS 504

Olivocochlear Reflex Strength and Distractibility with Noise and Vocalizations during Selective Attention to Visual Stimuli.

Macarena Bowen; Gonzalo Terreros; Felipe Moreno-Gomez; Macarena Ipinza; **Luis Robles**; Paul Delano
Universidad de Chile

Background

In addition to the olivocochlear (OC) system, the auditory efferent network comprises descending projections from the auditory cortex to the superior olivary complex (SOC). The medial olivocochlear (MOC) bundle emerges from the SOC and makes synapses with outer hair cells of the cochlea. MOC function can be assessed by measuring the OC reflex strength through distortion product otoacoustic emissions (DPOAEs) amplitude changes induced by contralateral acoustic stimulation (CAS). The OC reflex strength is highly variable among subjects, producing suppressions and enhancements of DPOAEs. One of the possible functions of the efferent system is the modulation of cochlear sensitivity during selective attention to visual stimuli (Delano et al., 2007). Similarly to the OC reflex, behavioral performance in visual attention tasks is also variable in different individuals. Whether there is a relation between the variability of the OC reflex and that of visual attention performance is unknown. In this work, we hypothesize that the inter-subject variability of OC reflex magnitude is related to the capability of avoiding auditory distractors, which are irrelevant for the performance in the visual attention task.

Methods

Seven chinchillas were used to correlate OC reflex magnitude and behavioral performance. To measure OC reflex strength, CAS effects on DPOAE amplitudes were recorded before, during and after contralateral broad-band noise (BBN 60dB SPL, 0.2 – 10 kHz). Then all the chinchillas were trained in a two-choice visual discrimination task. The behavioral performance was evaluated in a 12 days protocol divided into three blocks of 4 days: without auditory distractors (base-line), with BBN and with male chinchilla vocalizations (fundamental frequency between 537 and 854 Hz), as auditory distractors.

Results

CAS-induced DPOAE amplitude reductions had an average of 1.5 ± 1.95 dB, with high intersubject variability. There was also variability in the behavioral performance with auditory distractors, being the first day of presentation the most affected, with significant differences in accuracy between base-line and BBN ($p=0.027$) and increases in response latencies between base-line and vocalizations ($p=0.037$) and BBN and vocalizations ($p=0.012$). There were correlations among OC reflex magnitudes and omitted responses ($r=-0.46$ for BBN and $r= -0.5$ for vocalizations) showing that weak OC reflex is associated with bad performance.

Conclusions

Our preliminary results show a tendency that suggests a relationship between OC reflex magnitude and behavioral performance during selective attention to visual stimuli in presence of auditory distractors.

Funding

Supported by FONDECYT 1120256 and 3130635.

PS 505

Vision influences the encoding of formant transition in the auditory cortex, facilitating phonemic restoration

Antoine Shahin
University of California, Davis

Background

Phonemic restoration (PR), also known as continuity illusion or illusory filling-in, is a phenomenon whereby listeners perceive interrupted speech as continuous, provided the interruption is replaced by another sound (i.e., noise). Previous research demonstrated that lip-reading convey information about the speech envelope and in turn can enhance PR by preserving the neural representations of the speech envelope despite the interruptions. However, the impact of other visually-mediated speech cues (e.g., formant transitions) on PR is not well understood. In this study, we hypothesized that vision, via lip-reading, further supports PR by encoding formant dynamics (filling-in of formant transition representations) at the auditory networks.

Methods

Individuals listened to /ba/ and /wa/ consonant vowel pairs (CVs) that had the consonant /b/ and /w/ replaced by white noise. The speech envelopes of both CVs were equalized. Consequently, the two CVs differed only in formant transition, with /ba/ exhibiting faster formant rise time than /wa/. The acoustics were either accompanied by a video of the person uttering /ba/ or /wa/ or a static (no lip movements) video of the talker. Listeners made judgments on what they heard (/ba/ or /wa/), not what they saw.

Results

In the audiovisual task, auditory perception was congruent with the CV conveyed by the lip movements over 95% of the time. In the static condition, listeners reported the interrupted CVs as /ba/ around 70% of the time and as /wa/ around 30% of the time.

Conclusions

Vision, through lip-reading, not only influences how the temporal representations of the speech (amplitude envelope) are neurophysiologically encoded, but also influences the encoding of the formant dynamics, resulting in enhanced PR.

Funding

This study was supported by a NIH/NIDCD award (R01-DC013543)

PS 506

Mating-Related Interactive Vocal Communication with Sub-centisecond Precision in Guinea Pigs

Masataka Nishimura; Yuta Shiromi; Wen-Jie Song
Kumamoto University

Introduction

Vocalization is widely considered to be used for communication in mammals, but evidence for vocal communication in animals is still scarce. Interactive vocalization can be taken as an indication of vocal communication, because it requires confirmation of successful transmission of message between individuals, as in human dialogue. Finding animals having interactive vocalization is the first step to establish an animal model for studying neural mechanism of human conversation (Neunuebel et al., 2015). Here we chose guinea pigs as a model, because of their variety of vocalizations (Rood, 1972; Berryman 1976), to investigate whether they vocalize in an interactive manner.

Methods

A brace of sexually-matured animals (< five-month-old) were put into a transparent arena and their behaviours and vocalizations were simultaneously recorded with one or two microphones and infra-red cameras. Vocalizing animal was identified with the two microphones based on the travelling time and relative intensity of the vocalization. Spectral pattern and timing of vocalization were analysed with short-time windowed Fourier transform by sliding window at steps of the sampling interval.

Results

Males vocalized purr during the courtship behaviour of rumba (Rood, 1972; Berryman 1976), i.e., circling around the female with vocalization intervals ~70 – 90 msec. In some bouts of purr, males vocalized another call consisting of sequential up and down frequency-modulated sweeps, named chirp here in accordance with a previous report in a different social situation (Rood, 1972). Each syllable of chirp during the courtship was strictly phase-locked to the syllable of purr. Syllable duration of a female vocalization, chut or chutter (Berryman 1976), was found to be shortened according to her receptiveness or arousal (Rood, 1972). More interestingly, when females showed receptiveness, they vocalized significantly more number of chuts having syllabic interval matched to that of male purr or chirp, within 0.5 sec after the offset of chirp sequence. The temporal error of female vocalization interval against the male one was < 10 msec in most cases, suggesting that females controlled the vocalization interval with sub-centisecond precision to respond to the male courting call.

Conclusion

Receptive female guinea pigs vocalized chut in response to male courting calls by controlling syllabic interval with sub-centisecond precision. This observation suggests interactive vocalization in guinea pigs. Guinea pigs can thus be a prospective model for examining neural mechanisms of human conversation.

Funding
JSPS KAKENHI #15K16566, Shibasaburo Program

PS 507

Spatiotemporal Response Properties Across Auditory Cortical Fields Under Widefield Imaging

John Issa; Benjamin Haeffele; Manning Zhang; Eric Young; David Yue
Johns Hopkins University

Auditory cortex is composed of several distinct auditory fields, but how these fields coordinate their activity to process sound is not well understood. This limitation reflects upon the tools typically used to record neural activity. At the single neuron level, microelectrodes are the gold standard as they offer high temporal resolution and signal quality, but lack spatial detail across larger regions. On the other hand, intrinsic imaging allows for characterization of neural responses across a large spatial extent but suffer from low temporal resolution and signal quality. Ideally, what is needed is an imaging approach capable of temporal resolution well-matched to the dynamics of cortical events with sufficient signal quality to allow for single-trial analysis.

Here we utilize widefield imaging of mice expressing the genetically encoded Ca2+ indicator GCaMP6f. This approach furnishes three key advantages: the ability to image large regions of cortex simultaneously, temporal resolution on the order of tens of milliseconds, and signal quality adequate for single-trial analyses. Imaging is performed in head-fixed awake mice using a low magnification objective, allowing for the entire mouse auditory cortex to be visualized. Pure tones and sinusoid amplitude modulated (SAM) tones are played to the contralateral ear.

Using this approach, several cortical fields and their respective tonotopic organization are readily identified, including the primary auditory cortex (AI), the anterior auditory field (AAF), and the secondary auditory cortex (AII). We then examined whether simultaneous activity taken from these different areas can be compared on a single-trial basis. The attached figure shows responses from these three regions (left panel, baseline fluorescence of imaging field) in response to a 3 kHz pure tone with a duration of 50 msec. While the baseline-corrected fluorescence signal fails to betray timing differences between these regions (traces in middle panel), deconvolution of signals reveals that the response seen in AAF occurs with the shortest latency (traces in right panel), consistent with the conclusions of past microelectrode studies in rodent auditory cortex. Further analysis will quantify the reliability of this approach across multiple trials and its ability to discern coordinated patterns of activity in response to more complex stimuli. These results establish the utility of widefield imaging in GCaMP6f-expressing transgenic mice for the study of spatiotemporal dynamics across large regions of cortex.

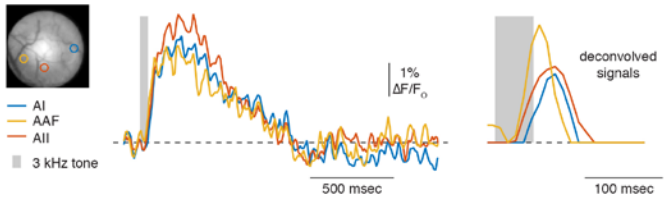

Funding
Kleberg Foundation, NINDS, NIDCD

PS 508

Top-down Attentional Modulation of Responses in Ferret Higher Order Auditory Cortex

Diego Elgueda[1]; Daniel Duque[1]; Stephen David[2]; Susanne Radtke-Schuller[1]; Shihab Shamma[1]; Jonathan Fritz[1]
[1]University of Maryland, College Park; [2]Oregon Health and Science University

Rapid spectrotemporal receptive field (STRF) plasticity enhances the ability of primary auditory cortex (A1) to encode task-relevant sounds during auditory discrimination by increasing representation contrast between stimuli belonging to different behavioral categories. We have recently shown (Atiani et al., 2014) that this contrast is further increased in non-primary auditory cortical areas in the dorsal Posterior Ectosylvian Gyrus (dPEG). Previous studies in ferret dorsolateral frontal cortex (dlFC) are consistent with a model in which plasticity in auditory cortex is modulated by feedback from dlFC. However, the pathways by which dlFC top-down signals reach auditory cortex are not fully known. In order to better understand how top-down attentional modulation affects auditory cortical processing, we studied responses in ventral-anterior PEG (vaPEG), including areas pro-PPF, PSSC and VPr, which have been shown in a previous tracer study to be connected with dlFC (Radtke-Schuller et al., 2011). Five ferrets were trained on go/no-go conditioned avoidance tone-detection and click-rate discrimination tasks, in which they learned to refrain from licking water upon being presented with target stimuli. We recorded local field potentials (LFPs) and >300 single-unit responses in awake head-fixed ferrets during passive sound presentation and performance of the auditory tasks. Compared to A1 and dPEG, vaPEG neurons were weakly responsive to tonal stimuli, more broadly tuned, and displayed longer response latencies and durations. Also, vaPEG neurons had weaker phase locking to the envelope of rippled noise, making it difficult in most cases to compute STRFs. During auditory task performance, we observed modulatory effects in both tasks, with a general tendency to selectively enhance responses to target sounds, suppress responses to non-target sounds, or enhance the difference between responses to target and reference stimuli. Similar to dlFC, some vaPEG neurons showed behaviorally gated, selective responses to target stimuli and no response during passive presentation of task stimuli. Although most behavioral effects rapidly recovered to baseline firing rates, there were also cases of post-behavioral persistent effects, consistent with previous observations in ferret A1 and dlFC. We measured functional connectivity with frontal areas by simultaneously recording vaPEG and dlFC LFPs. We found an increase in interareal coherence in theta and beta bands during task performance. Granger-causality analyses revealed top-down and bottom-up influences were differentially enhanced during behavior. The striking behavioral modulation observed in vaPEG suggests that it lies in a pivotal position in the processing hierarchy between purely sensory encoding and the encoding of sound meaning.

Funding
NIH/NIDCD-R01-DC00577, R00-DC010439, CONICYT/Becas-Chile and Fulbright.

PS 509

Selective increase of auditory cortico-striatal coherence during auditory-cued Go/NoGo discrimination learning

Andreas Schulz; Marie Woldeit; Katja Saldeitis; Ana Goncalves; Frank Ohl
Leibniz Institute for Neurobiology

Cortico-striatal connections have been identified as crucial circuits for transformation of sensory information into decisions and motor actions. A flexible mechanism is required allowing mapping of complex spectro-temporal stimuli to a wide variety of animal behaviors. In a previous study (Xiong et al., Nature, 2015) the main principle of this mapping has been shown. This method allowed the identification of neuronal potentiation in specific subsets of cortico-striatal connections, selectively in spatially non overlapping high- and low-frequency projections between auditory cortex and striatum.

This general mechanism needs also to be active when sensory stimuli carrying discernible behaviorally relevant information that is not mapped via topographically separated cortico-striatal projections. To test this hypothesis an experimental paradigm is required in which sensory stimuli evoke largely overlapping sensory cortical representations and must be associated with different behavioral actions. According to these requirements we have trained Mongolian gerbils (Meriones unguiculatus) in Go/NoGo auditory discrimination task in a shuttlebox using rising (CS+, 1-2 kHz) and falling (CS-, 2-1 kHz) frequency-modulated tones which traverse an identical frequency interval and produce activity on largely overlapping regions in the cortical tonotopic map. Local field potentials were measured in auditory cortex and ventral striatum during the behavioral task. To track changes of functional coupling between auditory cortex and ventral striatum we measured the stimulus-evoked coherency.

The results showed that during acquisition of an auditory Go/NoGo task, the coherence in the theta/alpha frequency range increased over training sessions at the onsets of the CS+, but neither at the onsets of the CS- stimuli, nor during time-periods without acoustical stimulation.

Using this approach we demonstrate that auditory stimuli activating tonotopically overlapping cortical areas begin to variably modulate cortico-striatal coupling when they

are associated with different goal-directed behaviors in an auditory discrimination task.

Funding
Deutsche Forschungsgemeinschaft (DFG) German Federal Ministry of Education and Research (BMBF)

PS 510

Macaque Parabelt Responses to Click Trains

Deborah Ross[1]; Yoshinao Kajikawa[1]; Troy Hackett[2]; Charles Schroeder[1]
[1]Nathan Kline Institute; [2]Vanderbilt University

Background
The parabelt (PB) region is composed of caudal and rostral PB areas (CPB and RPB). While those areas have been studied anatomically, their physiological properties remain relatively unknown. In this study, we examined the temporal following capacity of PB areas, using click train stimulation in an awake monkey. As PB areas are at the later stages of auditory processing, it was expected that they would not respond strongly to clicks, and similarly, that they would not synchronize well to rapid click repetitions.

Methods
Click trains of several repetition rates (duration: 640 ms, inter-click intervals (ICI): 640, 320, 160, 80, 40, 20 and 10 ms) were delivered through free-field speakers binaurally to a macaque monkey sitting quietly in a chair. Responses in CPB and RPB were recorded using linear-array multielectrodes that penetrated the left superior temporal gyrus perpendicularly through a recording chamber implanted on the lateral surface of the brain. Electrical signals were filtered to extract multiunit activity (MUA) and field potentials. MUA in the granular layer was analyzed for changes in the magnitude and periodicity of firing in local neurons.

Results
Of 35 sites, about one-quarter did not respond to clicks, and more than one-half did not exhibit periodic responses. Non-periodic responses generally appeared as MUA suppression with or without weak excitatory responses observable at low repetition rates (ICI: $\geq$160ms). Suppression became apparent at high repetition rates (ICI: $\leq$50 Hz) as small inhibitory responses to clicks accumulated. Periodic responses occurred only in CPB, and not in RPB. Some CPB sites could synchronize to 100 Hz click trains, with the strongest synchrony at 25 Hz.

Conclusions
PB areas largely did not respond well to click sounds, consistent with suggested roles of PB in more complex sound processing. A small fraction of CPB sites could follow click trains of 100 Hz in synchronized manner like upstream auditory areas, but none in RPB, consistent with an additional hierarchy step from CPB to RPB.

Funding
NIH R21 DC012918 NIH R01 DC011490

PS 511

Functional and Anatomical Organization of the Orbito-Frontal to Primary Auditory Cortex Synaptic Pathway is tonotopically dependent

David Vumbaco; Jason Middleton
LSU Health Sciences Center

The ability of the Primary Auditory Cortex (A1) to meaningfully encode acoustic stimuli is reliant upon its tonotopic organization. The tonotopy is influenced by top down pathways that can act to shift receptive field (RF) frequency preferences and thus the perception of auditory stimuli. Top-down modulatory signals may originate from the Nucleus Basalis, the Ventral Tegmental Area and the Prefrontal Cortex (PFC). A sub region of the PFC, the orbitofrontal cortex (OFC) can act to reshape A1 RF distributions. However, the functional and anatomical characteristics of the OFC-to-A1 pathway are not yet well described. To quantify the functional and spatial characteristics of OFC projections entering A1 we performed fluorescent tracing and whole cell electrophysiology *in vitro*. We show that the OFC axons entering A1 exhibit an organization that depends upon the rostrocaudal (RC) axis. In particular, the deep layers in caudal and rostral A1 (low frequency preferring and high frequency preferring respectively) show a higher density of labeled OFC projections than the intermediate region between them. Additionally, we observed fluorescence in the superficial layers of A1, which was restricted to the rostral regions. Our electrophysiological analysis shows that the OFC-to-A1 pathway is glutamatergic and also exhibits a dependence upon the RC axis with the caudal neurons in A1 receiving a stronger OFC input than the rostral neurons. Taken together, these findings suggest that the OFC-to-A1 pathway possesses a unique anatomical and physiological organization that is tonotopically dependent – and may underlie unique forms of frequency specific top-down modulation. As such, the OFC-to-A1 pathway likely plays an important role in auditory signal processing and in the progression of diseases that demonstrate anatomical and functional changes like chronic hyperacusis and tinnitus.

Funding
NIH/NIDCD R03DC012585 NIH/NIGMS P30GM103340

PS 512

Effects of Partial Auditory Forebrain Inactivation on Tempo and Pitch Discrimination in Songbirds

Gunsoo Kim
Sungkyunkwan University

Background
How different auditory percepts such as tempo and pitch of an auditory object emerge along the auditory pathways remains poorly understood. Songbirds, with their rich vocal communication behavior, offer an excellent model for understanding the neural processing of complex vocalizations. In a previous study, we discovered a topographic organization of spectral bandwidth within the primary cortical area field L, where bandwidth increases from 0.6 to 1.6 octaves

mediolaterally. This organization enables us to examine whether cortical subregions with different spectrotemporal tuning contribute differentially to auditory perception. Here we asked whether the lateral broadband subregion is specialized for temporal aspects of perception by inactivating the region during operant perceptual behavior.

Methods
Female adult zebra finches were trained to categorize song stimuli into two groups based on tempo or pitch in a two alternative forced choice paradigm. In the tempo task, birds were required to categorize temporally compressed or stretched renditions of a song as fast (-4, -8, -16% change in duration) or slow (+4, +8, +16%). In the pitch task, birds were required to categorize pitch-shifted renditions of a song as high (+20, +50, +100 cents) or low (-20, -50, -100 cents). After birds have learned a task, microdialysis probes were bilaterally implanted in lateral field L (~2 mm lateral). Then muscimol (1 mM) or saline was reverse-dialyzed during behavior.

Results
Most birds reached the performance levels of 85-90% correct trials after ~1000 trials (or about a week) of training. During bilateral infusion of muscimol, the performance dropped significantly in both tempo and pitch tasks (3 birds per task type). In the tempo task, overall performance (percentage of correct trials) decreased by 20% from 91±1% to 72±1% in muscimol blocks compared with saline control. In the pitch task, performance decreased by 14% from 87±2% to 75±2% in muscimol blocks. When data were analyzed at each magnitude of shift separately, while the performance drop was consistent across different tempo shifts, it was smaller and less consistent across pitch shifts.

Conclusions
Our data show partial inactivation of the cortical auditory forebrain significantly impairs performance on auditory tasks with vocalization stimuli. Moreover, although birds' performance decreased in both task types, the effect was greater and more consistent in the tempo task, raising the possibility that the lateral broadband subregions might be more specialized for extracting temporal information.

Funding
NIDCD R03 DC012428

PS 513

Coding of Sound Sequences in the Mouse Frontal Cortex

Hemant Kumar Srivastava; Madhur Parashar; Muneshwar Mehra; Sharba Bandyopadhyay
Indian Institute of Technology, Kharagpur

An important role of the orbitofrontal cortex (OFC) is to assign value to different sensory inputs based on their contextual or behavioral relevance. OFC is known to also direct attention to salient features of the sensory environment and is further also involved in inhibiting or allowing motor responses to sensory stimuli depending on needs in a dynamic environment. Our studies have shown encoding of rare stimuli (deviant, D) in the midst of other repeating (standard, S) stimuli. OFC single neurons signal presence of D stimulus in the midst of similar ongoing stimuli through strong responses to the deviant. Occurrence of a rare stimulus is one way to think of a stimulus that is of high value and such responses can play a role in directing other processes in the sensory or motor cortex.

We use an auditory stimulus paradigm where a deviant stimulus occurs in a train of similar/same stimuli and various other sound sequences in order to understand coding of sound sequences with such deviant stimuli in different sequential contexts. Local field potentials in the OFC and responses of single neurons in the OFC were collected from the anesthetized mouse frontal cortex. Responses clearly show OFC responding strongly to deviant stimuli with general adaptive increase in responses over repeated trials. We find presence of predictive response to onsets of sequences and to deviants and both responses vary over repeated trials. Randomization of location of D sound in a sequence and variation in length of sequences are used to test the mechanisms with which such adaptive and predictive coding occurs. We also compare encoding of different types of sounds in such sequences in order to correlate with the observed anatomical projections to OFC from auditory area. Further comparisons are made with response to same sequences in order understand sensory transformations between the auditory cortex and OFC. We find that responses in OFC are sensitive to extremely long time scales of stimulus history and hence hypothesize that it can play a profound role in auditory sensory encoding through its projections to the auditory cortex in different layers.

Funding
Wellcome Trust DBT India Alliance

PS 514

An Auditory Selective Listening Paradigm to Investigate Spatial Attention Networks in Nonhuman Primates

Corrie Camalier; Anna-Leigh Brown; Mortimer Mishkin; Bruno Averbeck
National Institute of Mental Health

Auditory spatial attention is critical for navigating everyday listening environments, yet its neural underpinning is poorly understood, in some part due to the historical difficulty of training nonhuman primates on auditory tasks. In this work, we describe the methods by which rhesus monkeys have been trained on a novel spatial selective listening paradigm adapted from human paradigms. We also describe psychophysical performance for these monkeys. To begin shaping behavior, we first trained monkeys to detect the presence of a tone by bar release and determined the behavioral detection thresholds. Next, we trained the monkeys to ignore a noise masker that was concurrently played with the target. Once detection thresholds were determined, the animals were trained to perform a spatial selective listening task in which they responded to the target from the cued side but ignored a target coming from the noncued side. In these "ignore" trials, monkeys withhold release until presentation of the

target from the cued side. Finally the animals were trained to maintain central fixation throughout the task. In this way, we have successfully shaped nonhuman primates to perform an attentionally demanding selective listening task. Future work will focus on the neural mechanisms underpinning the ability to selectively listen to a spatial location.

Funding
DIRP, NIMH/NIH

PS 515

fMRI Responses to Natural and Model-Matched Synthetic Sounds Reveals a Hierarchy of Auditory Cortical Computation

Sam Norman-Haignere; Josh McDermott
MIT

A central goal of auditory neuroscience is to understand the neural representation of natural sounds. One approach is to use "encoding models" to predict neural responses from stimulus features. However, there is no guarantee that features which predict neural responses are those that actually drive them, because distinct features are often correlated across natural stimuli. Here we introduce an alternative approach utilizing "model-matched stimuli" synthesized to evoke the same response as a natural sound in a model of neural computation. If the model provides a good description of the neural response, then the neural response to natural sounds and matched synthetic sounds should be similar even though the sounds may differ in many other respects. We used this approach to explore the sensitivity of different regions in human auditory cortex to standard acoustic features hypothesized to underlie their response. Using fMRI, we measured cortical responses to natural and synthetic sounds that were matched in average spectrotemporal modulation power, using a variant of existing texture synthesis methods. Crucially, the synthetic sounds were constrained only by their modulation power statistics, and as such were perceptually distinct from the natural sounds they were matched to (which exhibit additional higher-order statistical dependencies not made explicit by the spectrotemporal modulation model, and thus not replicated in the synthetic matches). Despite these perceptual differences, the natural and model-matched synthetic sounds produced nearly equivalent voxel responses in primary auditory cortex, suggesting that modulation power accounts for much of the neural response there. In contrast, voxel responses in non-primary regions differed markedly to the two sound sets, with many voxels producing little to no response for the synthetic sounds. This functional difference was much less pronounced using encoding models: modulation statistics were effective predictors of voxel responses in both primary and non-primary regions, presumably because they are correlated with higher-order features to which non-primary regions are tuned. Our approach reveals higher-order selectivity in non-primary regions of human auditory cortex and illustrates the use of model-matched stimuli in testing theories of cortical computation.

Funding
National Science Foundation Research Fellowship to Sam Norman-Haignere McDonnell Foundation Scholar Award to Josh McDermott NEC Research Support Award to Josh McDermott

PS 516

Neural Codes for Pitch Perception in the Actively- and Passively-Listening States

Kerry Walker[1]; Jennifer Bizley[2]; Jan Schnupp[1]; Fernando Nodal[1]; Andrew King[1]
[1]University of Oxford; [2]University College London

Previous studies in both anaesthetized and behaving ferrets, as well as in awake, passively listening macaques, have shown that neurons distributed widely throughout primary and secondary auditory cortex can represent the fundamental frequency (F0) of complex sounds. In ferrets, these distributed neural responses often represent the animals' behavioural decisions on a pitch discrimination task more accurately than the F0 of the sound presented. On the other hand, marmoset studies have demonstrated that only neurons in a small region of auditory cortex situated near the anterolateral primary-secondary border are specialized to represent the F0 of missing fundamental sounds and the temporal regularity of sounds. It is unknown how all of these neural representations of F0 may be altered during pitch decision making, and what roles they play in animals' pitch decisions. The present work addresses these questions by comparing how neurons in primary and secondary auditory cortex represent the F0 of a common set of sounds during both passive listening and when ferrets carry out a pitch discrimination task. On each trial in the task, ferrets are required to judge whether a variable "target" sound is higher or lower in pitch than a constant "reference" sound. We found that in the passive state, neurons tended to encode F0 in transient responses immediately following sound onset and offset, whereas F0 was represented more continuously during sound presentation when ferrets were behaving. Furthermore, neural responses to the reference, but not the target stimuli, were relatively suppressed during behaviour. Finally, we found that only a small subset of those neurons that were modulated by F0 were also sensitive to the temporal regularity (i.e. the "jitter") of a click train, in keeping with the findings of Bendor and Wang (2005). The jitter-sensitive neurons showed better F0 discriminability during the behavioural task than jitter-insensitive neurons, particularly in the secondary tonotopic fields of auditory cortex. When ferrets were presented with the same jittered click trains on our pitch discrimination task, their behavioural performance fell to chance. Together, these results suggest that auditory cortical neurons' representation of sound F0 may peak earlier and enhance target responses during active listening. While populations of cortical neurons across the primary and secondary fields can account for ferrets' discrimination of the F0 of a regular click train, only a small subset of these cortical neurons can account for ferrets' sensitivity to the temporal regularity of click trains.

Funding
BBSRC and Wellcome Trust

PS 517

Cortical pitch responses to a native pitch contour is more resistant to noise degradation in native speakers of Mandarin

Chandan Suresh; Ananthanarayan Krishnan; Jackson Gandour
Purdue University

The deleterious effects of noise and reverberation on the ability to identify and discriminate speech sounds are well documented. Long-term experience been shown to enhance brainstem and cortical representation of linguistic and musical pitch in favorable listening conditions. While there is evidence suggesting greater resilience of the brainstem response to reverberation we do not know whether cortical pitch extraction mechanisms in native speakers of tone languages are less susceptible to signal degradation in adverse listening conditions. Herein we recorded cortical pitch responses (CPR) from native speakers of Mandarin, and English in response to a monosyllabic speech sound /yi/ with a Mandarin lexical rising Tone 2 pitch contour presented diotically in quiet and in the presence of noise presented at SNRs of +5, 0, and -5 dB. In addition, CPRs were recorded in a dichotic condition in which the target stimulus was in phase, and noise out of phase at each ear. The aim was to determine if cortical representation of pitch-relevant information in native speakers of tone and non-tone languages show similar resilience in adverse listening conditions. Both groups showed decrease in CPR response amplitude and latency prolongation with increasing noise levels, with responses difficult to identify at -5 dB SNR. However, amplitude reduction of CPR components was greater for the English compared to the Chinese even at a relatively low noise level (+5 SNR). Also, only Chinese showed a rightward hemispheric asymmetry under all experimental conditions. Finally, the release from masking in the dichotic condition was more robust for the Chinese compared to the English. The greater resiliency of the cortical pitch responses in the presence of background noise and the more robust release from masking in the Chinese suggests that long-term tonal language experience strengthens neural mechanisms of pitch in the auditory cortex and brainstem, resulting in more robust and stable representation of behaviorally relevant acoustic features that would be more resilient to deleterious effects of noise.

Funding
Research supported by NIH 5R01DC008549 (A.K.).

PS 518

Cortical Pitch Representations of Complex Tones in Musicians and Non-musicians

Federica Bianchi[1]; Jens Hjortkjaer[1]; Sébastien Santurette[1]; Hartwig Siebner[2]; Robert Zatorre[3]; Torsten Dau[1]
[1]Technical University of Denmark; [2]Danish Research Center for Magnetic Resonance; [3]Montreal Neurological Institute, McGill University, and BRAMS

Background
Musicians have been shown to have an enhanced pitch-discrimination ability compared to non-musicians for complex tones with either resolved or unresolved harmonics. It is unclear whether this perceptual enhancement can be ascribed to an enhanced neural representation of pitch at central stages of the auditory system. The aim of this study was to clarify whether (i) cortical responses increase with harmonic resolvability, as suggested in previous studies, and whether musicians show (ii) differential neural activation in response to complex tones as compared to non-musicians and/or (iii) finer fundamental frequency (F0) representation in the auditory cortex. Assuming that the right auditory cortex is specialized in processing fine spectral changes, we hypothesized that an enhanced F0 representation in musicians would be associated with a stronger right-lateralized response to complex tones compared to non-musicians.

Method
Fundamental frequency (F0) discrimination thresholds were obtained for harmonic complex tones with F0s of 100 and 500 Hz, filtered in either a low or a high frequency region to vary the resolvability of audible harmonics. A sparse-sampling event-related functional magnetic resonance imaging (fMRI) paradigm was used to measure neural activation in all listeners while performing the same pitch-discrimination task for conditions of varying resolvability. The task difficulty was individually adjusted according to the previously obtained F0 discrimination thresholds.

Results
Preliminary results from 6 listeners (3 musicians and 3 non-musicians) showed that the behavioral discrimination thresholds of musicians were, on average, lower than the thresholds of non-musicians by about a factor of 2.3, independent of harmonic resolvability. A group analysis on the 6 listeners revealed no differential neural activation for resolved vs unresolved conditions, suggesting that cortical responses did not increase with increasing stimulus resolvability, when adjusting for the task difficulty across conditions and participants. A significant effect of processing demand, i.e., task demand estimated from both stimulus resolvability and task difficulty, was observed in both auditory cortices, with a larger neural activation in the right auditory region. Additionally, no differential activation was observed in the musicians vs. the non-musicians.

Conclusion
Overall, these preliminary findings suggest an involvement of a postero-lateral region in both auditory cortices during a

pitch-discrimination task with conditions of varying processing demand. Cortical responses were larger in the right than in the left auditory cortex, suggesting an increasing activation of the right-lateralized pitch-sensitive cortical areas with increasing task-processing demand.

Funding
This work was funded by the Technical University of Denmark.

PS 519

Differences in neural activity relevant to pitch salience at the brainstem and cortical levels

Ananthanarayan Krishnan; Jackson Gandour; Chandan Suresh
Purdue University

Neural representation of pitch-relevant information at both the brainstem and cortical levels of processing is influenced by language experience. Less is known about the interplay between brainstem and cortical neural mechanisms in hierarchical pitch processing. A well-known attribute of pitch is its *salience*. Brainstem frequency following responses and cortical pitch specific responses, recorded concurrently, were elicited by a pitch salience continuum spanning weak to strong pitch of a dynamic, iterated rippled noise pitch contour—a homolog of a lexical tone. The aims of this study were to assess how language experience (Chinese, English) affects i) enhancement of neural activity associated with pitch salience at brainstem and cortical levels, ii) the presence of asymmetry in cortical pitch representation, and iii) patterns of relative changes in magnitude along the pitch salience continuum. Peak latency (Fz: Na, Pb, Nb) was shorter in the Chinese than the English group across the continuum. Peak-to-peak amplitude (Fz: Na-Pb, Pb-Nb) of the Chinese group grew larger with increasing pitch salience, but an experience-dependent advantage was limited to the Na-Pb component. At temporal sites (T7/T8), the larger amplitude of the Chinese group across the continuum was both limited to the Na-Pb component and the right temporal site. At the brainstem level, F0 magnitude gets larger as you increase pitch salience, and it too reveals Chinese superiority. A direct comparison of cortical and brainstem responses for the Chinese group reveals different patterns of relative changes in magnitude along the pitch salience continuum. Such differences between the auditory brainstem and cortex may point to a transformation in pitch processing at the cortical level presumably mediated by local sensory and/or extrasensory influence overlaid on the brainstem output.

Funding
Research supported by NIH 5R01DC008549 (A.K.).

PS 520

Cortical pitch responses to a native pitch contour is more resistant to noise degradation in native speakers of Mandarin

Chandan Suresh; Ananthanarayan Krishnan; Jackson Gandour
Purdue University

The deleterious effects of noise and reverberation on the ability to identify and discriminate speech sounds are well documented. Long-term experience been shown to enhance brainstem and cortical representation of linguistic and musical pitch in favorable listening conditions. While there is evidence suggesting greater resilience of the brainstem response to reverberation we do not know whether cortical pitch extraction mechanisms in native speakers of tone languages are less susceptible to signal degradation in adverse listening conditions. Herein we recorded cortical pitch responses (CPR) from native speakers of Mandarin, and English in response to a monosyllabic speech sound /yi/ with a Mandarin lexical rising Tone 2 pitch contour presented diotically in quiet and in the presence of noise presented at SNRs of +5, 0, and -5 dB. In addition, CPRs were recorded in a dichotic condition in which the target stimulus was in phase, and noise out of phase at each ear. The aim was to determine if cortical representation of pitch-relevant information in native speakers of tone and non-tone languages show similar resilience in adverse listening conditions. Both groups showed decrease in CPR response amplitude and latency prolongation with increasing noise levels, with responses difficult to identify at -5 dB SNR. However, amplitude reduction of CPR components was greater for the English compared to the Chinese even at a relatively low noise level (+5 SNR). Also, only Chinese showed a rightward hemispheric asymmetry under all experimental conditions. Finally, the release from masking in the dichotic condition was more robust for the Chinese compared to the English. The greater resiliency of the cortical pitch responses in the presence of background noise and the more robust release from masking in the Chinese suggests that long-term tonal language experience strengthens neural mechanisms of pitch in the auditory cortex and brainstem, resulting in more robust and stable representation of behaviorally relevant acoustic features that would be more resilient to deleterious effects of noise.

Funding
Research supported by NIH 5R01DC008549 (A.K.).

PS 521

Experience-dependent enhancement of cortical pitch responses limited to turning point locations with acceleration rates that fall inside maximum speed of pitch change

Ananthanarayan Krishnan; Jackson Gandour; Chandan Suresh
Purdue University

Transient components of the CPR (cortical pitch-specific response) have been shown to be sensitive to multiple

attributes of dynamic pitch contours: salience, acceleration rates, location of peak acceleration, and overall pitch trajectory (curvilinear vs linear). The extant literature shows that the location of the turning point may serve as a perceptual cue to tonal recognition. Herein we recorded CPR responses from native speakers of Mandarin, and English listeners in response to iterated rippled noise stimuli representing a five-stimulus falling-rising pitch continuum (TP1-TP5) with turning points at 32,74, 116, 156, and 212 ms, respectively. TP3 and possibly TP4 fall within maximum limits of speed of pitch change. The aims of this study were to assess whether (i) language experience (Chinese, English) shows selective enhancement to stimuli in the continuum that fall within normal range of production and (ii) if the experience-dependent enhancement exhibits hemispheric asymmetry in cortical pitch representation. Peak latency of CPR components Na (pitch onset response) and Pb were generally shorter with increasing TP location for both groups. In contrast, Nb latency was the longest for TP4 with relatively shorter latencies for the other stimuli. Peak-to-peak amplitude of Na-Pb and Pb-Nb showed an experience-dependent enhancement for Chinese for TP3, TP4, and TP5 only. By temporal site (T7/T8), Chinese group showed larger responses than English over the right site ; by group, Chinese group showed larger responses over the right temporal site compared to the left. Experience-dependent enhancement of cortical pitch responses is restricted to pitch contours (TP3 and TP4) that have turning points and acceleration rates that fall within speech production limits. It is likely that both changes in the location of turning point, and its influence on pitch acceleration contribute in a complex manner to the effects observed here. These results suggest a “natural region of auditory sensitivity” that may be exploited for linguistic functions within the constraints of maximum speed of pitch change.

Funding
Research supported by NIH 5R01DC008549 (A.K.).

PS 522

Temporal Context Effects on Neural Response Adaptation in Oddball Paradigms

Björn Herrmann; Ingrid Johnsrude
The University of Western Ontario

Investigations of sensory memory function commonly make use of an oddball paradigm in which a regularly presented standard sound is occasionally interrupted by a deviant sound. In general, the more standards before a deviant, the larger the deviant response; this has been interpreted as resulting from greater contrast of the deviant with the preceding standard since the representation of the standard is thought to sharpen with repetition. However, an alternative explanation is that the response to the deviant depends on the degree to which that response is adapted – in general, the greater the interval between deviants, the less the adaptation due to a preceding deviant and the greater the response magnitude. Indeed, recent human electroencephalography (EEG) studies demonstrate long-lasting response adaptation by stimulus repetition (in non-oddball paradigms), making this alternative hypothesis a plausible one.

In the current EEG study, participants passively listened to pure tones in oddball sequences (standard = 1000 Hz; deviant = 1600 Hz). We manipulated the temporal pattern with which deviants occurred among standards (while keeping the overall deviant probability at 15.7%). Deviant intervals were either organized (i.e., the occurrence of deviants alternated between speeding up and slowing down) or random (i.e., the same deviant-to-deviant intervals as for the organized context occurred but in random order). We compared neural responses to deviants that were preceded by the identical number of standards within different temporal contexts. Any differences in deviant response magnitudes between contexts must be due to the extended temporal history of previous sounds. As a control, we recorded data from participants listening to the same deviant tones in isolation (i.e., without standards).

Neural responses to deviants increased with the number of preceding standard tones, but were not different between temporally organized versus random contexts. This contrasts to the response patterns we observed for deviant tones presented in isolation, for which response modulation was smaller in the random context. Critically, deviant responses within temporally organized sequences were larger in a speeding-up compared to a slowing-down context, similar to what we observed for deviant tones presented in isolation. The similar patterns suggest that the temporal history of deviants within oddball sequences has a strong influence on the magnitude of the deviant response. The data thus indicate that the sensory memory trace induced by the repetition of standards is not the only influence on deviant responses.

Funding
CIHR

PS 523

Integration of Statistical Information in complex acoustic environments

Yves Boubenec[1]; Jennifer Lawlor[1]; Urszula Górska[2]; Shihab Shamma[1]; Bernhard Englitz[3]
[1]Ecole Normale Supérieure; [2]Jagiellonian University; [3]Donders Institute, Nijmegen

Many natural sounds are best characterized by spectro-temporal regularities on a statistical level, *e.g.* wind, fire or rain. While their local structure is highly variable, the spectro-temporal statistics of these auditory *textures* can still be used for their recognition. To explore the neural representation of these statistics and how it might relate to the encoding of more structured complex stimuli such as speech and music, we measured the dynamics of detectability of changes in the spectral statistics of auditory textures. Specially designed tone cloud with precisely controlled statistical predictability were created for this purpose: At random times, the marginal probability of the tone cloud changed, and the listeners had to detect this change as rapidly as possible.

We find that the size of change as well as the time available to sample the original statistics correlate positively with performance and negatively with reaction time, suggesting the accumulation of evidence. Changes in statistics that occur nearby in the spectrum are more easily detected than equally large changes which are distributed along the frequency domain, compatible with a detection mechanism locally integrating sound statistics. Further, if the change occurred at a spectral location with high prior probability of occurrence, performance again increased and reaction time decreased, indicating an effect of the uncertainty in the initial statistics.

We demonstrate that one can account for the human performance and reaction times with a modified but minimal drift-diffusion model, which captures the integration of statistical evidence. A cortical spectro-temporal filterbank model naturally implements these computations and thus replicates human performance, including the dependence on the distribution of the spectral location. This match suggests that sensory cortical filters can represent 0-th order statistics and implement dynamical change detection.

A centroparietal positive potential (CPP), previously described as a "decision variable" signature in EEG recordings, was correlated with successful change detection. We found out that the latency of this signal was modulated by change times, consistent with the psychophysics observations. EEG profiles also showed close resemblance with the activations in the filterbank model, which suggests that this decision variable may already be precomputed by sensory integration filters.

Funding
Financial support was provided by the ERC ADAM E-138 senior grant.

PS 524

Hearing Statistical Regularities in Fractal Melodies: an EEG study

Benjamin Skerritt-Davis; Mounya Elhilali
Johns Hopkins University

The brain's ability to extract statistical regularities from sound is an important tool in auditory scene analysis, aiding in tasks such as stream segregation, structural learning (e.g., for speech or music), and detecting new events in one's sound environment. Characterization of these regularities and how and at what level of the auditory processing stream they are extracted is largely unknown. Using pure-tone melodies based on random fractal sequences, we use EEG to examine how the neural response changes according to the amount of structure in the melody. Random fractals (also known as power-law noise with $1/f^{ß}$ spectrum), while inherently random, contain regularities that scale with the spectral exponent, ß. Tone sequences are generated by mapping random fractals to pitch, providing a non-trivial stimulus to explore regularity extraction. When presented with stimuli that change between a random-but-structured fractal melody with ß>0 and a random-and-unstructured fractal melody with ß=0, humans are able to detect the change, indicating that there is some statistical regularity in the fractal melody accessible to the brain. We investigated correlates between the neural response and the statistical regularities in the fractal melodies recorded from EEG during a behavioral change-detection task.

Funding
NIH

PS 525

Attentive object tracking in busy dynamic scenes

Daniel Bates; Ulrich Pomper; Maria Chait
University College London

Recent physiological work has demonstrated that cortical activity accurately tracks the envelope of speech. Moreover, when a second speaker is introduced, humans are able to maintain a clear neural representation of the attended speaker as well as the speaker they had been instructed to actively ignore (Ding & Simon, 2012a; 2012b; Mesgarani & Chang 2012; O'Sullivan et al, 2015). [M1] In this high-density EEG experiment we aim to understand cortical tracking of multiple concurrent acoustic sources within busy artificial scenes, and how this tracking is modulated by selective attention. Human participants were required to listen to 30 second long auditory scenes composed of 1, 2 or 4 different regularly repeating tone-pip sequences. Each sequence within a scene had a unique carrier frequency (evenly spaced values between 400 and 5000Hz) and modulation rate (3, 5, 13 or 23Hz). A change detection task was utilised to ensure participants actively maintain attentional focus on a designated target sequences. This task required that participants respond to omission of tones within a target sequence, whilst inhibiting responses to any omissions appearing within the non-target distractor sequence(s). (ongoing) analysis of the EEG data demonstrates that all scene components are represented in the neural response and that this representation is modulated by whether the components are actively attended or ignored. You must actually list the references in the bottom of the abstract

Funding
This project has received funding from the European Union's H2020 ICT2014-1 programme under grant agreement No 644732

PS 526

Temporal Predictability in Crowded Acoustic Scenes Modulates Early Stages of Perceptual Organization: Evidence from MEG

Ediz Sohoglu; Maria Chait
University College London

Models of auditory scene analysis increasingly emphasize the role of predictable statistical structure for successful perceptual organization (Ellis, 1999; Winkler et al., 2009). In the current MEG study, we asked whether temporal predictability modulates early or late stages of cortical processing during perception of crowded acoustic scenes (see Bendixen, 2014).

Acoustic scenes contained seven concurrent sources, each formed of a sequence of tone pips with a unique carrier frequency and temporal modulation pattern (see Cervantes Constantino et al., 2012). The temporal modulation pattern of each source was either regular or random. Listeners (N=14) performed an incidental visual task so as to assess 'automatic' sound processing.

We demonstrate that the brain's response to changes in these acoustic scenes, manifested as the abrupt appearance of a new source, is enhanced when the temporal patterning of scene sources is regular versus random. Critically, this effect is already apparent in the earliest observable neural response deflection (with a peak at around 80 ms).

These findings suggest that temporal predictability modulates the earliest detectable stage of cortical processing during auditory scene analysis, consistent with predictive coding accounts that hypothesize a central and pervasive role for statistical structure in perceptually organizing the sensory input (Rao and Ballard, 1999; Friston, 2010).

Funding
BBSRC

PS 527

Low-frequency neural oscillations in auditory stream segregation

Jens Hjortkjær; Torsten Dau
Technical University of Denmark

Background
Slow cortical oscillations below 10 Hz have been shown to track envelope fluctuations in natural stimuli, like speech, even in the presence of competing sound sources. This suggests the possibility of using low-frequency oscillatory activity to investigate auditory streaming. Using pure tones with different repetition rates, we hypothesized that periodic tone repetitions would give rise to steady-state-like cortical responses only when they are perceived as belonging to a single periodic stream.

Methods
Our stimuli consisted of two alternating pure-tone sequences with a frequency spacing Δf . The tone sequences were presented at different repetition rates (corresponding to repetition periods of 0.33 sec and 0.22 sec, respectively), where the faster rate was not a multiple of the slower one. Δf was varied to create either a one-stream percept with a complex '3-by-2' rhythm for small Δfs, or a two-stream percept with two individual repetition rates for large Δfs. The encephalogram was recorded at 64 electrode positions (Biosemi Active Two), while normal-hearing listeners were presented with either the "one-stream" or the "two-stream" stimulus in continuous trials of 45 sec. Each EEG channel was referenced to the average of the two mastoid electrodes and bandpass filtered between 1-8 Hz. The continuous EEG data from both conditions was then Fourier-transformed.

Results
In the two-stream condition, peaks occurred at the spectral components corresponding to the repetition rates of the two sequences tones (3 Hz, 4.5 Hz) at frontocentral scalp electrodes. In contrast, the steady-state responses obtained at the same repetition rates were strongly diminished, or absent, during the one-stream percept.

Conclusion
The results suggest that our paradigm consitutes a feasible method for studying streaming phenomena with low-frequency steady-state responses.

Funding
Oticon Centre of Excellence for Hearing and Speech Sciences

PS 528

Neural Signatures of Speech-on-Speech Selective Attention

Vibha Viswanathan[1]; Hari Bharadwaj[2]; Barbara Shinn-Cunningham[1]
[1]Boston University; [2]Massachusetts General Hospital

The ability to understand speech in the presence of other talkers and background noise is critical for everyday communication. Yet the neural mechanisms supporting speech-on-speech selective attention are poorly understood.

Previous invasive (e.g., electrocorticography and using depth electrode arrays) and non-invasive (e.g., electro/magnetoencephalography; EEG/MEG) electrophysiological studies show that cortical responses to speech track the spectro-temporal speech features. Specifically, the low-frequency speech envelope elicits phase-locked EEG/MEG responses in both the corresponding frequencies (delta band: 1 -- 4 Hz and theta band: 4 -- 7 Hz) and in the slowly varying envelopes of high frequencies (low-gamma band: 30 -- 60 Hz and high-gamma band: > 70 Hz) of the neural response.

Here, using EEG, we studied the effect of selective attention on phase-locked cortical responses to speech in a mixture. In each trial block, two running speech streams (narrated stories), one spoken by a male and the other by a female, were presented simultaneously, but with different interaural time delays. Each subject performed four blocks; within each block, they were instructed to attend to one of the two talkers. EEG data was simultaneously recorded using a 32-channel system. At the end of each block, all subjects were able to recount details of the attended story accurately, and reported being largely unaware of the details of the unattended story.

The envelope of each of the speech streams was extracted using an eight-channel gammatone filterbank with center-frequencies uniformly spaced along the cochlea according to a place-frequency map. Envelopes of the gamma-band EEG were computed by band-pass filtering and applying a Hilbert transform. Preliminary results showed that the low-frequency (delta and theta) bands of the EEG were more phase-locked to the envelope of the attended stream than the unattended stream. Similarly, the envelope of the EEG high-gamma band

phase locked more strongly to the delta band of the attended speech envelope than that band of the unattended speech.

Our results are in line with the theory of the role of gamma oscillations in selective attention and previous findings of multi-scale entrainment of neural activity by speech. Our finding also suggests novel brain-computer interface applications using multi-scale EEG features.

Funding
This work was supported by the National Institute on Deafness and Other Communication Disorders (NIDCD) of the National Institutes of Health (NIH) under award number R01 DC013825.

PS 529

The Impact of Gaze Direction on Human Auditory Processing

Ulrich Pomper; Maria Chait
University College London

In everyday live, we constantly change the direction of our visual gaze, depending on our current tasks and goals. How this direction of gaze influences auditory processing in humans is not well understood. Animal research has suggested that changes of gaze modify the response properties of neurons in the inferior and superior colliculus, as well as in the auditory cortex. Responses are increased to sounds coming from the direction of gaze, as compared to another direction. The frontal eye field might act as a mediating structure between visual and auditory areas. In the present study, we set out to investigate how direction of gaze impacts the behavioural and neural responses to either attended or unattended sounds from different locations. We presented rapid (0.7 Hz) streams of pure tones independently from three speakers (left, right, central, with frequencies of 440 Hz, 660 Hz and 990 Hz, resp.). Participants (N=10) performed a speeded response to occasional targets in one of the streams. Targets were characterized by an amplitude modulation of the pure tones. In each condition, participants gazed at one of the three speakers, and independently responded to targets from the same or from another speaker, while ignoring the sounds from the other speakers. We found significantly higher signal detection rates (d prime) in conditions where gaze and attention where directed at the same location, as compared to conditions where there where directed to different locations. This suggests that gazing towards the source of a sound facilitates the processing of that sound, while suppressing distracting input from other sources. High-density EEG data, including evoked responses, alpha-band power and connectivity analysis, will be presented.

Funding
This project is supprted by COCOHA (Cognitive control of a hearing aid), which is part of the European Union's Horizon 2020 research and innovation programme (grant agreement 644732).

PS 530

Listeners can be biased to use object-level analysis during change detection

Christina VandenBosch derNederlanden; Joel Snyder; Erin Hannon
University of Nevada, Las Vegas

Background
When we listen to the sounds around us, we use both acoustic details (e.g., pitch or harmonicity) and our knowledge about object categories and meaning in order to process every day sounds. However, paying attention to object-level representations may sometimes interfere with the perception of the features that make up those objects. When attempting to discriminate two complex auditory scenes, a bias toward adopting an object level of analysis may lead listeners to overlook the physical magnitude of an acoustic change and instead rely solely on object category information.

Method
In two experiments, each with 16 adult participants, we employed a one-shot change deafness paradigm used previously by Gregg and Samuel (2009) to assess whether participants would be more likely to miss changes when a change relied on semantic category knowledge (within-category: small dog to big dog; between-category: dog to trumpet) or when the change relied on the magnitude of an acoustic change (small or large acoustic changes in pitch and harmonicity). In both experiments, participants heard two 1-second scenes comprised of 4 objects with simultaneous onsets and listeners reported whether the scenes were the same or different (i.e., an object from scene 1 was replaced by a new object in scene 2). In Experiment 2, we biased an object level of analysis with an object-encoding (OE) task followed the change detection task on each trial, in which a single sound was presented in isolation and participants reported whether or not the sound was present in either of the two scenes of the current trial or not.

Results
Participants from both experiments exhibited change deafness (Different: 25% error, Same: 1% error, $p<.001$), and there was no difference between experiments in the overall amount of error ($p=.77$). However, as shown in Figure 1, the weighting of acoustic change magnitude was altered when the OE task was present, with a larger effect for within vs. across category changes compared to small vs. large acoustic changes (Without OE: category effect=10%, acoustic effect=5%, $p=.141$; With OE: category effect= 25%, acoustic effect=0%, $p<.001$).

Conclusion
The data suggest that the addition of the object-encoding task likely biased participants to use object-level analysis. We thus provide evidence that a secondary task can bias the level of representation used to detect changes in complex auditory scenes.

Funding
Supported by Army Research Office grant W9IINF-I2-I-0256

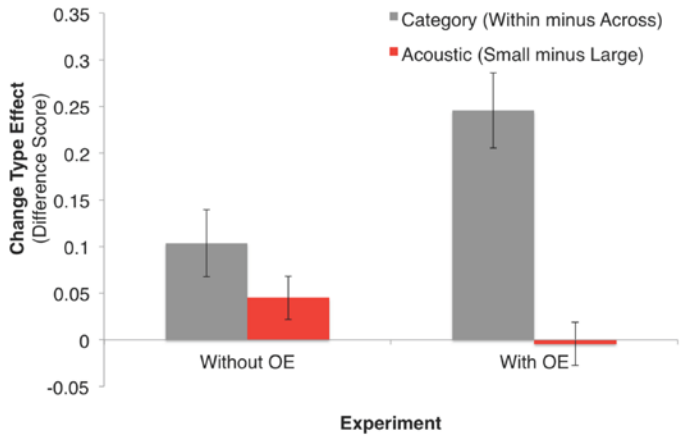

Figure 1. When there is no OE question present, participants weigh category changes and acoustic magnitude changes similarly. However, with the addition of an OE question, participants only rely on category knowledge.

Funding
Supported by Army Research Office grant W9IINF-I2-I-0256

PS 531

Direct Recordings of Oscillatory Activity in the Human Brain During Working Memory for Tones

Phillip Gander[1]; Sukhbinder Kumar[2]; Kirill Nourski[1]; Hiroyuki Oya[1]; Hiroto Kawasaki[1]; Matthew Howard III[1]; Timothy Griffiths[2]
[1]University of Iowa; [2]Newcastle University

Working memory is the capacity to hold and manipulate behaviourally relevant information in mind in the absence of ongoing sensory input. Here we explored the hypothesis that working memory for tones requires a network of oscillatory activity in auditory cortex, frontal cortex, and hippocampus, and examined the form of such activity in neuronal ensembles.

We recorded local field potentials from six human subjects undergoing invasive monitoring for pre-surgical localization of epileptic foci. The subjects were implanted with depth electrodes along the axis of Heschl's gyrus (HG) containing primary cortex in the medial part, and subdural electrodes over temporal and frontal cortex. Following a visual alert subjects were presented with a pair of tones (0.5 s duration, 750 ms ISI) belonging to two different categories ('Low': 300-570 Hz; 'High': 2000 -2800 Hz). A visual cue (750 ms) then informed the subjects which tone (first or second) to keep in mind. A 3 s retention period was followed by a tone which could be the same or different (frequency difference ±20%) from the tone held in mind. The subjects made a same/different judgement. A total of 160 trials (80 each of 'Low' and 'High' tone retention) were presented. We measured average ERPs and carried out single-trial time-frequency analysis using a wavelet transform.

During perception, both the magnitude of ERPs (~100 ms after stimulus onset) and gamma-band (60-120 Hz) power in electrodes located in HG and lateral superior temporal gyrus (STG) showed category-specific responses. High tones elicited stronger responses in medial HG and low tones in lateral HG.

During retention, sustained induced low frequency power in the delta/theta-band (2-8 Hz) was observed in HG, frontal cortex (inferior and superior gyri), and hippocampus. Sustained low frequency activity was observed in all contacts that showed gamma-band responses during perception. Low-frequency power during retention also showed a recency effect: a greater response in HG electrodes was observed for the most recently presented (second) tone. On the STG, however, the opposite effect was observed: a greater 2-8 Hz power for retention of the first compared to the second tone.

The data demonstrate: 1) a network of brain regions during auditory working memory that includes auditory, frontal, and hippocampal cortex 2) theta-band correlates of tone retention in auditory cortex in the same neural ensembles that are active in the gamma band during perception 3) neural bases in the auditory cortex for interference effects within tonal working memory.

Funding
NIH R01-DC04290 Wellcome Trust WT091681MA

PS 532

Brain Oscillations in Children when Listening to Speech in Noise.

Andrew Dimitrijevic; Michael Smith; David Moore
Cincinnati Children's Hospital

Background
Hearing ability is not fully explained by the pure tone audiogram; some individuals with normal clinical pure tone thresholds (≤ 20 dB HL) have impaired speech perception at suprathreshold levels in noisy environments. Various learning problems in children, including auditory neuropathy, auditory processing disorder, and attention deficit disorders, may be associated with similar audiograms, but have different etiologies. The development of an electrophysiological test for difficulties of speech perception in noise, the most common complaint made by people about their hearing, could differentiate sites of disorder in these children.

Methods
Children aged 6 to 12 years (mean 9 years) participated in the study. The task was identification of three digits within speech shaped noise, the Digits in Noise (DiN) test. In an initial behavioral task, the signal to noise ratio (SNR) was varied adaptively until 50% of digits were identified correctly, the Speech Reception Threshold (SRT). Afterwards, 64 channel EEG recordings were performed in two different listening conditions: (1) Attend: children repeated the digits they heard, and (2) Passive: Children were asked to ignore all sounds while they watched a closed captioned movie of their choice. In both conditions, the SNR was at the child's own SRT.

Results
Children's SRTs were slightly higher than previously tested control adults (-15 dB in children vs -16 dB in adults). Children

displayed an immature event-related potential waveform consisting of a large positivity near 100 ms post stimulus onset. However, the brain oscillations appeared to have the same features as adults. Both children and adults had alpha synchronization during attentive listening to the digits in noise that was maximal over parietal electrodes. When the same stimulus was delivered during Passive listening, no alpha synchronization was observed. No correlations in alpha synchronization were seen with the child's age.

Conclusions
Auditory attention to speech in noise can be studied in children as young as 6 years old using the Digits in Noise test. Brain oscillations and event-related potential (ERP) waveforms appear to mature at different rates; brain oscillations may have a closer correspondence to behavior than ERP waveforms.

PS 533

Evaluation of a Novel Continuous Stimulus for use in the Electrophysiological Analysis of the Human Auditory System

Denis Drennan; Edmund Lalor
Trinity College Dublin

Background
The event-related potential (ERP) has long been the canonical technique for conducting electrophysiological analyses of the human auditory system, and for good reason. As is apparent from both the auditory brainstem response (ABR) and auditory-evoked potential (AEP), ERPs can index processing along the auditory hierarchy with excellent temporal resolution. One shortcoming of the traditional ERP approach however is that the sound stimuli used are often quite simple in nature e.g. discrete, repeated, clicks or tone-bursts. Such stimuli may not be optimal in characterizing a system that is capable of processing such intricate stimuli as music and speech.

An alternative approach which seeks to circumvent these limitations focuses on deriving what is known as a Temporal Response Function (TRF; Theunissen et al., 2001; Lalor et al., 2009). Typically this is done by regressing neural data against some feature of a continuous stimulus. In the context of EEG this has been done, for example, by regressing the EEG on each electrode against the envelope of an amplitude modulated carrier signal (Lalor et al., 2009), or even speech (Lalor & Foxe, 2010). This has been shown to elicit ERP style responses and, due to the continuous nature of the stimuli being presented, has facilitated research which could not easily be conducted using a traditional ERP approach (Power et al., 2012). However, the SNR of these TRFs is typically not as high as those of a traditional ERP. Also it is unknown whether the approach can facilitate the resolution of ABR components.

Method
Here, we present a novel approach to deriving EEG TRFs using a stimulus that consists of a number of impulses which are pseudorandomly spaced, which we refer to as PULSETRAIN. This can be considered a combination of the two aforementioned techniques; it possess the discrete impulse nature of the ERP technique while still providing a continuous envelope to which the TRF technique can be applied.

Results
We show that this approach leads to TRFs with much higher SNR than those derived using fully continuous, amplitude modulated stimuli. We characterize the early and late components of these TRFs through comparison with ABRs and AEPs derived using standard approaches.

Conclusion
We have introduced a novel stimulus paradigm for rapidly deriving highly temporally resolved electrophysiological indices of processing across the human auditory processing hierarchy, something that could be useful in many subdomains of both clinical and cognitive auditory neuroscience research.

Funding
Irish Research Council Enterprise Partnership Scheme

PS 534

Intracochlear Micro-magnetic Stimulation: Finite Element Modeling

Sagarika Mukesh[1]; Pamela Bhatti[2]
[1]Georgia Institute of Technology; [2]Georgia Institute of Technology, Emory University

Background
Recent in-vivo studies have shown that electromagnetic stimulation at a micro scale successfully elicits neural activity. This is a potentially transforming technique for intracochlear stimulation as it completely bypasses the highly conductive cochlear fluid, thereby reducing current spread. The aim of our finite element modeling study was to determine how electromagnetically induced fields behave in a biological medium and to see how these fields scale with inductor size (0.5 mm x 0.5 mm, 0.25 mm x 0.25 mm) with the overall goal of assessing their feasibility for a cochlear prosthesis.

Methods
Coils used for the in-vivo study were modeled in COMSOL 5.1 (COMSOL Inc., Burlington, MA). Coil geometries were drawn using Solidworks CAD Solutions (Solidworks Corp., Waltham, MA) and imported to COMSOL for further analysis. The intracochlear environment was simulated by surrounding each inductor with a perilymph-like liquid (Permittivity 30, permeability 1, electrical conductivity 1.8 S/m). AC/DC (low-frequency) magnetic fields physics was applied and the resulting electric and magnetic fields were studied. First, a 0.5 mm x 0.5 mm inductor suitable for activation of the cochlear base was stimulation via a 0.1 A sinusoidal excitation current at 10 kHz. Next, an inductor with dimensions 0.25 mm x 0.25 mm was simulated in a similar manner; followed by an array of inductors to analyze the current spread. The array simulation used 2-D axis symmetry, for ease of visualization and calculation.

Results

The magnetic flux density norm produced by the inductor with dimensions 0.5 mm x 0.5 mm had a maximum value of 0.0342 T, whereas that produced by the inductor with dimensions 0.25 mm x 0.25 mm had a maximum value of 0.0319 T. Given that the larger inductor has been demonstrated to elicit neuronal activity in a feline model, the observed flux density norm suggests that the smaller inductor may also elicit neuronal activity. Additionally, both magnetic and electric fields were observed to be highly directional, showing minimal current spread, as compared to the electrically stimulated array.

Conclusion

Vector fields produced by the two inductors suggest that an array of inductors, varying in size from 0.5 mm x 0.5 mm to 0.25 mm x 0.25 mm, may potentially be used to stimulate the basal turn of the cochlea. In addition, the electromagnetically activated array demonstrated less current spread than the electrically activated array.

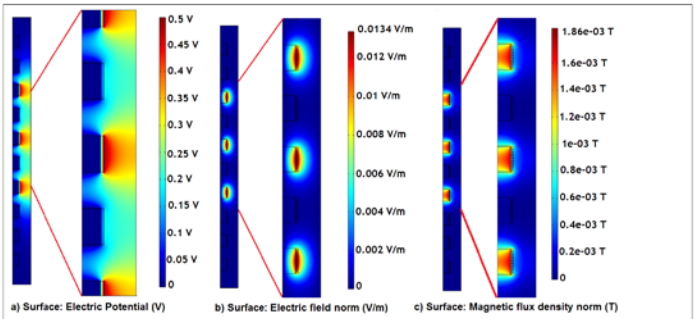

The figure compares an electrically stimulated electrode array (left most) to an electromagnetically stimulated electrode array (right). Electric potential has been plotted for the former array (a) whereas electric field and magnetic flux density norms (b-c) have been plotted for the latter array. The directionality of fields and limited current spread can be clearly observed in the latter array.

Funding

National Science Foundation Grant ECCS-0927103 and CAREER ECCS-1055801.

PS 535

Sensing Sound inside the Cochlea with a Completely Implantable Artificial Organ of Corti (CIAO)

Chuming Zhao[1]; Katherine Knisely[2]; Deborah Colesa[1]; Bryan Pfingst[1]; Yehoash Raphael[1]; Karl Grosh[1]

[1]University of Michigan, Ann Arbor; [2]University of Michigan

Background

Cochlear implants (CIs) are an effective therapeutic solution to treat sensorineural hearing loss. Most commercially available CIs have an external microphone/processing unit, an inductive link, and intra-cochlear electrodes. Although the performance of CIs is acceptable, such configuration has the limitation of high cost, high power consumption (20-40mW) and high latency (20ms). Besides, the external unit and inductive link are inconvenient and cannot be used in all environments. Fully implantable CIs are an attractive alternative which could potentially overcome, or at least reduce, these limitations.

Method

We used Micro-Electrical-Mechanical System (MEMS) techniques to build a Completely Implantable Artificial Organ of Corti (CIAO). The CIAO is a piezoelectric transducer comprised of variable length (200-350 m) aluminum nitride (AlN) bimorph cantilevers (400 m wide and 2.2 m thick). The CIAO was tested in air and underwater to determine its input-output characteristics. In vivo tests were performed by implanting a CIAO into an anesthetized guinea pig's cochlea. Probe impedance was measured with an Agilent E4980A LCR meter. 0.1V-5V input voltages were used to drive a Tucker-Davis Technologies speaker directed via a speculum to the ear canal. A SR830 lock-in amplifier was used to measure the electric response of the CIAO located inside the cochlea.

Results

The sensitivity of the CIAO to pressure differences around the cantilevers was 300-2000 V/Pa. In vitro voltage actuation tests found that in air resonances were 40-90 kHz and fluid loaded resonances were 10-40 kHz. In-vivo test signals were above the noise floor and immune to electrical interference. A linear phase backbone, consistent with the acoustic delay from the speaker to the cochlea, was measured along with additional rad phase shifts passing through resonance. Using the speaker's calibration to approximately normalize to an input pressure level of 110dB SPL, the response showed multiple peaks around resonances of the cantilevers. Based on the in vivo response, we estimated the pressure difference across the beams was 0.1-1Pa for 110dB SPL input.

Conclusion

The CIAO was successfully fabricated, characterized and tested in vitro and in vivo. The transducer worked like the organ of Corti, in that electric signals were generated when excited by acoustic signals. The electrical signals from the CIAO showed repeatability and linearity. The signals collected with the CIAO inside the cochlea indicated that we can sense the sound within the cochlea of a live guinea pig using our miniature piezoelectric sensors (CIAO).

Funding

Funding through the University of Michigan Center for Organogenesis and gift funds to the University of Michigan.

PS 536

Low Repetition Rate Coding Strategy for Cochlear Impants

Claus-Peter Richter[1]; Christopher Heddon[2]; Charlotte Garcia[2]; Reagan Roberts[2]

[1]Northwestern University; [2]Resonance Medical, LLC

Background

Despite the success of Cochlear implants (Cis), their performance declines in challenging listening environments and for music. More than 50 perceptual channels in a normal hearing subject are reduced to 4-7 channels in a Ci patient. The dynamic range of the acoustic signal in normal hearing subjects is 120 dB with 60-100 discernible steps, but it is represented by a mere 6-12 dB change in current level with about 20 discernible steps in Cis. Research shows that per-

formance of Cis can be improved by increasing the number of independent electrode contacts, by using both the envelop of the acoustic signal and the frequency fine structure, and by providing a greater dynamic range. To overcome current limitations, we propose a novel coding strategy where loudness is encoded by the number of pulses at each electrode contact and across electrode contacts in a given time frame. Because the amplitude of the pulses at each electrode contact is constant, higher loudness levels do not create areas of overlap in nerve stimulation due to adjacent contacts, but remain separate at louder levels. We expect that this approach will provide a greater dynamic range and more discernible steps, therefore providing Ci users with an increased number of independent perceptual channels.

Method
The purpose of this study is to validate the novel code and to optimize the coding strategy by testing it with Ci users. Ci users will perform standard speech and speech-in-noise tests with the novel coding strategy as well as music perception tests. The experiments also determine discernible loudness and frequency steps using a two-alternative forced choice (2AFC) method.

Results
Initial testing has shown word recognition in sentences at 30-40% immediately after switching to the novel coding strategy that improved to 60% with some training. The results are similar to Ci user performance immediately after activation with current coding strategies. We have also achieved a lower pulse repetition rate averaging under 200 Hz per channel, which is compared to 250-1000 Hz in current strategies. This also significantly lowers the processing power of the device.

Conclusion
The impact of this research will also have a broader reach, as this novel method can be applied to other neural interfaces such as spinal cord stimulators and retinal implants.

Funding
We have applied for and are waiting on an phase 1 SBIR NIH Grant

PS 537

Modelling the Vibration Output Function of the Tympanic Membrane in Response to Optical Stimulation

Patricia Stahn[1]; Marius Hinsberger[1]; Michaela Schürmann[2]; Cathleen Schreiter[1]; Benjamin Hoetzer[1]; Hecker Dietmar[3]; Hubert Lim[4]; Hans-Jochen Foth[2]; Langenbucher Achim[1]; Bernhard Schick[1]; Gentiana Wenzel[1]
[1]Saarland University, Homburg/Saar; [2]University of Kaiserslautern; [3]Saarland University Medical Center, Homburg/Saar; [4]University of Minnesota, Minneapolis

Background
Controlled activation of different frequency channels of the auditory system is necessary to code complex acoustic signals, such as speech. Laser light with specific parameters can be used to activate the peripheral hearing system at different levels (Wenzel et al, 2010). However, within the duration of a word, it is not possible to switch between different laser wavelengths with current laser systems. To investigate frequency-specific modulation of the audible frequency spectrum using monochrome laser pulses, we developed a mathematical model based on a convolution method. This model predicts the displacement of the tympanic membrane (TM) in response to optical pulse patterns.

Method
All calculations, the signal generation and modelling were performed with MATLAB® (R2014a, The MathWorks Inc., Natick, USA). We inserted ex vivo a 365 µm diameter optic fiber into the outer ear canal of guinea pigs and directed it towards the TM. Using a scanning laser Doppler vibrometer (LDV, PSV-500, Polytec GmbH, Waldbronn) we recorded the vibration velocity of the TM at the umbo after application of 10 ns laser pulses, with a maximum energy of 50 µJ/pulse (532 nm Q-switched, INCA-laser system, Xiton Photonics, Kaiserslautern). We calculated the displacement from the measured velocity data and convolved this impulse response with an input signal, simulating different laser pulse patterns. The results were compared to LDV recordings performed after stimulation of the TM with the same patterns with energies of 0-16 µJ/pulse.

Results
Increasing the number of laser pulses per stimulation burst, with pulse rates of 0.5 - 16 kHz and pulse trains of 1-1600 pulses, led to a definite peak of the spectrum in the model output, corresponding to the laser pulse rate. With more complex pulse patterns and pulse rates up to 100 kHz, a shift of the main peak could be predicted by the model for different input frequencies (0.5-16 kHz).

Conclusions
This study demonstrates that a convolution based model of the TM vibrations with different laser pulse patterns leads to an output function that is comparable to the experimental LDV measured data. Additionally, these results are consistent with the previously presented in vivo recordings of neurons in the central nucleus of the inferior colliculus (ICC) in response to optical stimulation (Stahn et al. 2015). Studies to further develop and use the applied model to find the optimal laser parameters for optical stimulation of the peripheral hearing organ are in progress.

Funding
The research leading to these results has received funding from the European Research Council under the European Union's Seventh Framework Programme (FP7/2007-2013) / ERC grant agreement n°[311469]*.

PS 538

Validation of an Intracochlear Piezoelectric Microphone

Francis Creighton[1]; Xiying Guan[1]; Steve Park[2]; Ioannis Kymissis[2]; Hideko Nakajima[1]; Lisa Olson[2]
[1]Massachusetts Eye and Ear, Harvard Medical School; [2]Columbia University

Background

Despite advances in cochlear implantation, all currently available devices require external hardware. A fully implantable cochlear implant will require an internalized microphone and currently available technologies for implantable microphones have significant drawbacks. Previously we demonstrated early feasibility of a piezoelectric sensor positioned just within the round window of a gerbil to measure input from the external auditory canal (EAC). Here we take the study further by inserting improved sensors into the scala tympani of fresh human temporal bones, and measuring its response to sound stimuli applied to the EAC.

Method

A polyvinylidene difluoride (PVDF) piezoelectric pressure sensor was embedded in a PDMS body with similar size and diameter to a cochlear implant electrode. This sensor was then inserted into the round window of a human fresh cadaveric temporal bone, via an extended facial recess approach to the round window. The sensor was inserted at varying depths and an external sound pressure stimulus over a broad frequency range was applied to the EAC. EAC pressure, stapes velocity, and piezoelectric sensor voltage output were recorded.

Results

The PVDF sensor was able to detect the intracochlear sound pressure response to acoustic input to the EAC. The frequency response of the pressure measured with the intracochlear sensor was similar to that of the pressure at the EAC, with an expected phase delay, indicating the sensor was detecting intracochlear pressure changes. The magnitude of the sensor response increased and became a smoother function of frequency as the sensor was inserted more deeply into the scala tympani.

Conclusion

This study shows a novel method to use intracochlear pressure as an input source for an otologic microphone composed of a piezoelectric polymer, and demonstrates a critical step towards feasibility. Our next goal is to improve device sensitivity and specificity of the area that is mechano-electrically sensitive. Our long-term objective is to develop a fully implantable cochlear implant that incorporates the piezoelectric intracochlear sound pressure microphone embedded in the electrode array that delivers electrical stimulus to the cochlea.

PS 539

Animal-to-Human Brain Interface for Cochlear Implants

Petrina LaFaire; Xiadong Tan; Nan Xia; Pamela Fiebig; Alan Micco; Claus-Peter Richter
Northwestern University

Introduction

By establishing a brain-to-brain interface, sensory information from animals can be transmitted to humans. For deaf individuals, this could mean restoring their hearing to levels far surpassing current cochlear implants. It could also provide the possibility to improve on current cochlear implant strategies by providing insight into the natural coding of the auditory information.

Method

To investigate the possibility of a brain-to-brain interface, the action potentials of the single units in the central nucleus of the inferior colliculus were recorded while a series of 53 words from a Speech-in-Noise (SIN) test were played to the anesthetized guinea pigs. The firing patterns from the single units with different characteristic frequencies were encoded and played to the cochlear implant of deaf adults via a system on loan from Advanced Bionics. The frequency map used for stimulation had 6-12 channels, limited by lack of random access memory. Patients were asked to complete a forced-choice test between 4 words, one being the word played to the patient. Patients were also asked to complete an identical retest. Throughout both tests, patients were not provided with the correct answer.

Results

Patient trails have shown the ability to discern the length of word and rhythm; loudness differences were evident despite stimulation with constant current. When patients completed a forced-choice test between four words, their scores were significantly higher than chance as shown through a binomial test that allowed for rejection of the null hypothesis at $p=0.00027$. The overall ability to identify the correct word sits at 34% amongst both tests. Recognition, defined by the ability to choose the same word twice, whether right or wrong, was also higher than chance, rejecting the null with $p=1.34e-14$. The overall recognition score is 56%, indicating that patients can recognize words well, though the lexical meaning may be misrepresented. Improvements in recognition were seen when the frequency map was adjusted to better match that of the cochlear implant. Additionally, all of the trials occurred with no training of the patient, which could be greatly beneficial in improving accuracy.

Conclusions

Initial results show promise that lexical information can be transmitted from an animal to a human auditory system. The approach would allow parallel stimulation at 16 electrode contacts and reduce the power by reducing the average repetition rate at each channel well below 100 Hz. Loudness is not encoded by current level, which can be held constant at stimulation threshold.

Support
This project has been funded in part by Northwestern University McCormick Undergraduate Research Grant, and in parts by the NIH, NIDCD grant R01-DC011855.

PS 540

Position of Auditory Brainstem Implant Electrode Array Correlates with Audiometric Outcomes

Samuel Barber[1]; Elliott Kozin[1]; Mary Cunnane[1]; Sid Puram[1]; Parth Shah[1]; Max Smith[2]; Aaron Remenschneider[1]; Barbara Herrmann[1]; Chris Brown[1]; Daniel Lee[1]
[1]Massachusetts Eye and Ear Infirmary; [2]Massachusetts General Hospital

Background
The auditory brainstem implant (ABI) provides hearing sensation to patients who are not eligible for cochlear implantation (CI) due to anatomic constraints. In contrast to the CI array that is inserted into the scala tympani of the cochlea, the ABI array is placed on or near the cochlear nucleus without bony anatomy to guide insertion. Although electrically evoked auditory brainstem responses (eABR) are used to guide ABI electrode implantation, audiometric outcomes vary widely among similar cohorts of ABI users. We hypothesize that specific ABI array orientation correlates with audiometric outcomes.

Methods
Subjects included pediatric (n=4) and adult (n=5) ABI patients. True-axial reformatted series of post-operative computed tomography were created using the McRae line. The basion and electrode tip coordinates were marked using multiplanar reconstructed views. Angles and linear distances between basion and electrode tip coordinates were measured. Angles included (V) vertical in sagittal plane, (H) horizontal in axial plane, and (T) medial tilt in coronal plane. Distances were (D1) vertical from basion and (D2) lateral from midline. Electrode positions were categorized into Classifications I-IV (using angle V) with subtypes A, B, and C (using angle T). Audiometric data included threshold and comfort levels, the number of active electrodes, pure tone audiometry (PTA), and pitch ranking. Data was analyzed for correlation between audiometric data and classification.

Results
Mean angles for V, H, and T were 39.97° ± standard deviation (SD) 33.8, 20.91° ± 30.5°, and 32.83° ± 57.52°. Average distances for D1 and D2 were 1.78cm ± 0.29 and 1.34 ± 0.47 cm for adults and 1.34 cm ± 0.025 and 0.99cm ± 0.20 cm. In adult type II and III arrays pointing posteriorly, pitch ranking values generally increased from low to high frequencies across the length of the electrode from proximal to distal end (4/5). Threshold levels were higher on the distal aspect of the array on most subtype A arrays (7/8). In contrast, higher threshold levels were identified proximally on both B subtype arrays (2/2). In one pediatric subject, electrodes inactivated due to non-auditory stimulation corresponded to a region on the array inferior and lateral, consistent with the relative location of the rostral medulla.

Conclusions
This study demonstrates that ABI placement varies widely among patients. Preliminary data suggest that ABI array position correlates with audiometric findings. Our findings may be useful in the refinement of intraoperative placement techniques, as well as prognostication of non-auditory electrodes and audiometric outcomes.

PS 541

Optoacoustic effect as the fundamental mechanism for intracochlear optical stimulation

Nicole Kallweit[1]; Peter Baumhoff[2]; Alexander Krueger[1]; Nadine Tinne[1]; Alexander Heisterkamp[1]; Andrej Kral[2]; Tammo Ripken[1]; Hannes Maier[2]
[1]Laser Zentrum Hannover e.V.; [2]Hannover Medical School, Institute of Audioneurotechnology

Laser stimulation of the cochlea has received researchers' attention as a potential treatment for sensorineural hearing loss in recent years. Laser stimulation would be a potential alternative to electrical cochlea implants as hearing animals show responses to intracochlear stimulation with pulsed laser light. However, in former experiments stimulation of acutely deafened animals has never resulted in auditory responses over a wide range of laser parameters. In this study, we hypothesized and investigated optoacoustic effects caused by laser pulses and found physical evidence that the underlying mechanism of optical cochlear stimulation in hearing animals is optoacoustic.

In order to cover different regimes of laser parameters two pulsed lasers (laser 1: 845 nm -1961 nm, 4 ns; laser 2: 1860 nm, 20 µs - 20 ms) were used to deliver light into an optical fiber of 105 µm core diameter. The fiber tip was either inserted into the cochlea of hearing guinea pigs (n=8) or placed in a water tank close to a sensitive hydrophone. *In vitro* recorded acoustic signals by the hydrophone were compared to *in vivo* measured compound action potentials (CAPs).

Results showed evident similarities between laser induced acoustic responses in water and evoked CAPs. The signal amplitude depended on the pulse peak power, the absorption coefficient and the temporal development of the laser pulses. The maximum of the first time derivative of the stimulating laser pulse power was the decisive factor for the amplitude level of both signals. Furthermore, both signals showed an on- and offset response only at the beginning and end of laser pulses. The rate of change in power was essentially for the amplitude of the resulting signals. A positive correlation between the absorption coefficient and the signal amplitude was observed below a wavelength limit where correlation became negative, reproducing former *in vivo* results where a higher absorption coefficient beyond this limit led to a reduction of the CAP amplitude.

In conclusion, the findings of *in vivo* and *in vitro* experiments strongly support the hypothesis that optoacoustic effect is the basic mechanism for optical cochlea stimulation. For sensing such optoacoustic signals, the presence and functional

integrity of hair cells are mandatory. Together with former negative results on acutely deafened animals with confirmed hair cell dysfunction direct optical stimulation of spiral ganglion cells of the cochlea becomes unlikely.

Funding
Supported by Cluster of Excellence Hearing4all and the German Research Foundation (DFG).

PS 542

Influence of Cochlear Array Design on Insertion Forces among 28 Surgeons of Various Experiences in a Synthetic Model of Scala Tympani.

Yann Nguyen[1,2,3]; Guillaume Kazmitcheff[1,2,3]; Renato Torres[1,2,3]; Daniele De Seta[1,2,3,4]; Elisabeth Mamelle[1,2,3]; Evelyne Ferrary[1,2,3]; Olivier Sterkers[1,2,3]; Daniele Bernardeschi[1,2,3]
[1]Hospital Pitié Salpêtrière; [2]Sorbonne University, UPMC Univ Paris 06, UMR S 1159; [3]INSERM, UMR S 1163; [4]Sapienza University of Rome

Research Background
It has been shown that array design could influence insertion forces of cochlear implants (CI) when array comparison is performed with reproducible motorized insertion tools. Manual insertion is subject to intra- and interindividual variations thus affecting the results of an improved array design. The goal of the study was to compare two array designs among a large group of surgeons with various experiences.

Material and methods
Twenty eight surgeons with various experiences (no experience in CI to 300 surgeries achieved) were enrolled in the study during two instructions course for CI. An artificial model of scala tympani was mounted on a 6-axis force sensor in order to measure insertion forces. After a training session, participants were asked to insert Hi-Focus 1J (lateral wall array, 1J) and Hi-Focus Mid-Scala (pre-curved array design with style, MS) arrays (Advanced Bionics, Valencia, USA). The following metrics were used to compare, (Student paired test p-value One side) the insertions force profiles: peak of force applied during the insertion (in N), the total change in momentum , number of occurrence where the applied forces were over 0.1 N, number of time where forces were increased by 50% during 0.1 s (sudden rise), and smoothness of the curve, studied as 'jerk' variation (in N.s-1).

Results
A better result has been observed for MS array compared to 1J array for 24/28 surgeons for the peak of force (0.30+/- 0.191N vs 0.15+/-0.181N ; 1J vs MS; p<0.001, mean gain 42%), for 24/28 surgeons for the total change in momentum (1.03+/- 0.802Ns vs 0.54+/-1.086Ns, 1J vs MS; p<0.001; mean gain 40%). The number of occurrence where the applied forces were over 0.1 N was reduced for 26/28 surgeons (3+/-2.7 vs 1+/-1.6 times; 1J vs MS; p<0.001; mean gain 61%) The number sudden rises was improved for 21/28 surgeons (21+/-14.7 vs 13+/-16.0 times, 1J vs MS; p<0.001 mean gain de 11%). The 'jerk' variation was improved for 22/28 surgeons (0.19+/- 0.134 vs 0.11+/-0.096 $N.s^{-1}$; 1J vs MS; p<0.01 mean gain 33%).

Conclusion
This study shows that a reduced diameter and the use of a guiding stylet with automated retraction in a pre-curved array can lead to an improvement of force profiles among a group of surgeons with various experiences.

Funding
Instruction courses were sponsored by Advanced Bionics (Valencia, USA). Arrays were provided by Advanced Bionics (Valencia, USA).

PS 543

Pressure in the cochlea during infrared irradiation

Nan Xia[1]; Xiaodong Tan[2]; Yingyue Xu[2]; Teresa Mao[2]; **Claus-Peter Richter**[2]
[1]Chongqing University; [2]Northwestern University

Background
Laser tissue interactions are defined by the laser parameters and the irradiated tissue properties. In the infrared, the absorption of the photons by water dominates the laser-tissue interaction. Following the absorption of the photon, its energy is converted into heat. Heating also results in a thermal expansion and the generation of a quasi steady state stress. We measured the laser-induced pressure in scala tympani directly with a micro-pressure-probe. The results were confirmed with measuring the ear canal pressure using a sensitive microphone. We addressed the question of whether laser stimulation of the cochlea produces a pressure wave, which is large enough to stimulate hair cells and evoke and acoustic response.

Methods
Optical fibers were inserted through either the round window or two cochleostomies in the bony wall of scala tympani and scala vestibuli to deliver the radiation. Micro-pressure-probes were used for intracochlear pressure measurement. A sensitive microphone (ER10C) was placed in the ear canal to measure the sound pressure level during laser stimulation. The laser-induced pressure was calculated using the middle ear transfer function in guinea pigs. In addition, a patch clamp electrode was used to determine the temperature changes in front of the optical fiber in vitro.

Results
3D representations of the temperature change in front of the optical fiber were constructed. Heating is confined to the irradiated volume with a cone-like profile along the optical axis. The profile remains robust over the time course of the heating. Direct intracochlear pressure measurements with the micro-pressure-probe and indirect ear canal pressure measurements gave similar results. The pressure in scala tympani was 68 dB (re 20 µPa) at radiant energies, sufficient to evoke an auditory response, and was 95 (dB re 20µPa) at maximum radiant energy for 100 µs laser pulses (164 µJ/pulse) generated by the Aculight diode laser. According to the literature, the reverse transfer function from the scala tympani

to the ear canal is 25 dB. Hence, at stimulation threshold for infrared neural stimulation, the ear canal pressure is about 43 dB (re 20 µPa).

Conclusion
For normal hearing animal, laser stimulation in the cochlea that can produce a pressure in the ear canal of 43 dB (re 20 µPa) is not negligible and the evoked CAPs are likely a combination from a direct interaction between the radiation and the spiral ganglion neurons and a photomechanical effect. For a deaf animal the pressure should not interfere with INS.

Funding
This work is supported by the NIH, R01-DC011855. We thank Drs. Elizabeth Olson and Michael Carapezza from Columbia University for their assistance in building the pressure probe.

PS 544

Nanopatterning of Cochlear Implant Electrode Contacts Results in a Delayed Increase in Impedance

Gerrit Paasche[1]; Ines Linke[1]; Elena Fadeeva[2]; Boris Chichkov[2]; Thomas Lenarz[1]
[1]Hannover Medical School; [2]Laser Zentrum Hannover e.V.

Background
Impedances at the electrical contacts increase during the first weeks after cochlear implantation. This increase is typically explained by the formation of fibrous tissue around the electrode array. Cell growth on surfaces can be influenced by certain surface structures. Nanopatterning of platinum surfaces by femtosecond laser irradiation was earlier shown to increase hydrophobicity of the surface and to reduce growth of fibroblasts on these patterned surfaces *in vitro.* These nanostructures were now transferred to surfaces of animal cochlear implant electrodes.

Methods
In order to selectively pattern either the cylindrically shaped electrode contacts or the silicone space between the contacts, a special handling system for the electrodes was developed including an autofocus and process observation system. Patterned electrodes were then implanted for 4 weeks in the inner ears of guinea pigs. Impedances were monitored daily from day 0 to 14 and later weekly with the fitting system as used for cochlear implant patients. Additionally the hearing status of the animals was assessed weekly by auditory brainstem response measurements after providing electrical stimuli. After explantation cochleae were prepared for histology and ground with the electrode in situ. As 2-4 contacts of the electrode array were inserted into the cochlea, group comparisons were performed for the contact at the tip of the array.

Results
The impedance was generally reduced compared to controls in all groups with nanostructured electrodes at all times. The overall increase was lowest in the group with nanostructured silicone surface whereas all groups with patterned contacts showed a similar increase as the controls. In two of the groups with nanoroughness on the contacts the impedance increase was significantly delayed compared to controls. Electrical hearing thresholds increased during the first week to different degrees followed later by a slight recovery. The pattern of the threshold development did not correlate with the impedance development in the groups. Histology showed less tissue growth in two groups with nanoroughness on the contacts after 4 weeks but this reduction was not significant.

Conclusion
Nanostructuring of cochlear implant electrode arrays was proven to influence also the impedance development in vivo, but this approach has to be further optimized to achieve a long lasting effect.

Funding
Supported by: German Research Foundation SFB 599 / T2

PS 545

Systemic Delivery of Opsins to Cochlear Nucleus Neurons Using AAV2/9

Sumi Sinha; Alyson Kaplan; Ariel Hight; Elliott Kozin; Shreya Narasimhan; Xiankai Meng; M Brown; Daniel Lee
Massachusetts Eye and Ear Infirmary

Background
Despite recent advances in auditory brainstem implant (ABI) technology, user experiences vary widely and have not reached the same potential as cochlear implants. An optogenetic-based ABI, using light instead of electrical stimulation, would reduce electrical spread and non-specific activation of the cochlear nucleus (CN) to potentially decrease undesired side effects and increase specificity of ABIs. Previous work from our group demonstrated that the CN neurons can be photosensitized by viral-mediated gene delivery of opsins, such as ChR2 or Chronos. This approach involves local introduction of viral vector with opsin. Local vector delivery, however, necessitates an invasive surgical craniotomy approach and in human direct access to the CN for local injection would be limited. Here we assess the effectiveness of systemic injection to deliver opsins to the CN in a murine model as an alternative to direct injection. CN photosensitization via injection into the superficial temporal vein or tail vein would move the model closer to a translatable optically based ABI.

Methods
CBA/CaJ mice at age P2 were injected with adeno-associated viral vector (AAV) serotype 2/9 carrying a CAG promoter for the GFP or Chronos-GFP coupled gene into the superficial temporal vein. Control mice were either injected with saline or received no injection. After 6-14 weeks of recovery, AAV2/9-CAG-GFP mice underwent transcardiac perfusion with 4% PFA and extracted brains were cryoprotected in 30% sucrose for two days. Samples were then frozen in Tissue-Tek OCT compound, sectioned, and mounted onto slides for histological evaluation. Slides were stained for GFP expression along with nuclear marker DAPI and neuronal marker NeuN. GFP expression was evaluated using confocal microscopy.

Results
Compared to no injection, AAV2/9-CAG-GFP showed GFP expression in the cerebellum, which confirmed effective transfection as demonstrated in previous studies. GFP expression was also found within the CN, demonstrating the ability to transfect the CN using viral delivery. Mice injected with AAV2/9-CAG-Chronos-GFP showed GFP expression co-localizing with NeuN staining, suggesting effective transfection of neurons within the CN.

Conclusions
The histological expression of GFP in the CN after injection of vector into the superficial temporal vein shows that it is possible to use a viral mediated systematic approach. This work will further be evaluated with physiological testing to determine whether gene transfer of Chronos into CN neurons will be associated with light-evoked responses as measured in upstream auditory centers.

Funding
Bertarelli Foundation, NIH, HHMI

PS 546

Evaluation of Preoperative Dexamethasone-Hydrogel Application for Otoprotective Effects in a Cochlear Implant Model

Clemens Honeder[1]; Chengjing Zhu[1]; Hanna Schöpper[2]; Julia Gausterer[3]; Elisabeth Engleder[3]; Lukas Landegger[1]; Manuel Walter[1]; Franz Gabor[3]; Christoph Arnoldner[1]
[1]Medical University of Vienna; [2]University of Veterinary Medicine Vienna; [3]University of Vienna

Background
Poloxamer407 hydrogels have been shown to deliver glucocorticoids to the inner ear for a long time after their intratympanic injection. Another line of research indicates, that the preoperative use of glucocorticoids reduces hearing threshold-shifts caused by cochlear implantation more effectively than their intraoperative application. As only limited data on very early application, and no data on the preoperative use of glucocorticoid-hydrogels was available, the aim of this study was to evaluate the application of a 6% dexamethasone/poloxamer407 hydrogel 1 day or 7 days prior to surgery for effects on postoperative hearing threshold-shifts.

Method
1 day or 7 days before the implantation of a cochlear implant electrode, 50 µl of the 20% poloxamer407 hydrogel with 6% w/v dexamethasone or the control-hydrogel were injected into the tympanic bullae of the experimental guinea pigs (n=10/group). Hearing was evaluated by the measurement of compound action potentials and auditory brainstem responses before the application, pre- and postoperatively, as well as after 3, 7, 14, 21 and 28 days. Stimuli used included clicks and tone-bursts from 1 to 32kHz. At the end of the study, temporal bones were harvested and histologically evaluated after the preparation of organ of Corti whole mounts or histological slides.

Results
The application of the 6% dexamethasone-hydrogel one day before cochlear implantation resulted in reduced compound action potential threshold-shifts as compared to the control group ($p<0.05$). In addition to the audiometric results, histological findings will be presented.

Conclusion
The application of the dexamethasone-hydrogel one day prior to cochlear implantation protected residual hearing in this guinea pig model. Such an application protocol could easily be translated into clinics and should therefore be evaluated in clinical trials.

Funding
Austrian Science Fund (FWF) MedEl Austria

PS 547

Objective and Subjective Evaluations of the Nurotron® Venus™ Cochlear Implant System via Animal Experiments and Clinical Trials

Na Gao[1]; Xin-Da Xu[1]; **Fang-Lu Chi**[1]; Fan-Gang Zeng[2]
[1]University Of Fudan; [2]University Of California

Background
A number of cochlear implant systems have been developed for people with profound hearing loss. Generally, it is believed that a greater number of intracochlear electrodes improve the user's resolution and provide greater sound detail. To restore hearing to people with severe to profound deafness, a 26-electrode auditory prosthesis- Nurotron® Venus™ cochlear implant system was specially designed. The study is to observe the performance of the Nurotron® Venus™ cochlear implant (CI) system via electrophysiological and psychophysical evaluations.

Methods
A 26-electrode CI system was specially designed. The performance of MRI in animal and cadaveric head experiments, EABR in cats experiment, the correlation between ESRT and C level, and psychophysics evaluations in clinical trials were observed.

Results
In the animal and cadaveric head experiments, magnet dislocation could not be prevented in the 1.5 T MRI without removal of the internal magnet. The EABR was clearly elicited in cat experiment. In the clinical trial, the ESRT was strongly correlated with C level ($P<0.001$). The human clinical trial involving 57 post-lingually deafened native Mandarin-speaking patients was performed. Residual hearing protection in the implanted ear at each audiometric frequency was observed in 27.5 - 46.3% patients postoperatively. A pitch ranking test revealed that place pitches were generally ordered from apical to basal electrodes. The recognitions of the perceptions of 301 disyllabic words, environment sounds, disyllabic words, and numerals were significantly better than the preoperative performance and reached plateaus.

Conclusion

This study described objective and subjective evaluations of the Nurotron® Venus™ Cochlear Implant System and indicated that this system produced a satisfactory performance.

Table 1. Summary of preoperative residual hearing in each frequency and unaided acoustic hearing thresholds in each frequency on the implanted side in the one month post-operative evaluation

Increase in HTL (dB)	Pure-tone test frequency (Hz)				
	250 Hz	500 Hz	1000 Hz	2000 Hz	4000 Hz
Preoperative (n)	41	54	49	40	25
0-10 dB (n)	13 (31.7%)	12 (22.22%)	11 (22.45%)	11 (27.5%)	6 (24%)
11-20 dB (n)	3 (7.31%)	4 (7.41%)	4 (8.16%)	0 (0%)	0 (0%)
21-40 dB (n)	3 (7.31%)	3 (5.56%)	0 (0%)	0 (0%)	1 (4%)
Not measurable (n)	22 (53.7%)	35 (64.81%)	34 (69.39%)	29 (72.5%)	18 (72%)

The percentage of patients for whom threshold changes fall into each decibel range is indicated for each frequency.

Table.2. Subjects information of CI users who participated electrode pitch ranking tests

Subjects	Gender	Age (years)	Etiology	Numbers of active electrode	Speech perception (close)
S1	Male	23	Sudden Deafen	24	92.9%
S2	Female	35	Ototoxic Deafen	24	100%
S3	Male	26	Ototoxic Deafen	23	100%
S4	Male	20	Ototoxic Deafen	22	97.1%
S5	Male	36	Noise Induced	24	100%
S6	Female	20	Ototoxic Deafen	19	92.9%

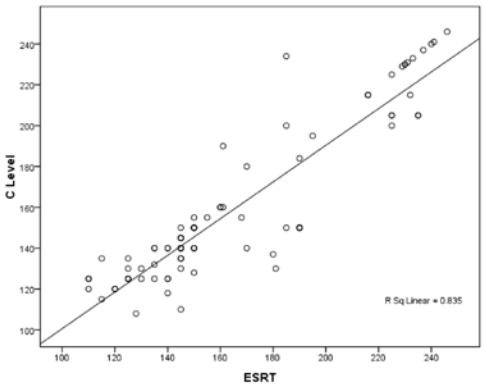

Fig. 1. The correlation between the ESRT and C level, with the R-Sq linear=0.835 (R=0.91, P<0.001), indicating that the ESRT is highly correlated with C level obtained through subjective judgments.

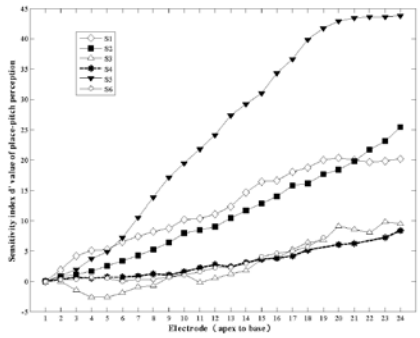

Fig.2. The electrode pitch ranking results of six CI subjects. The horizontal axis shows the 24 electrodes ordered from apical (bottom) to basal (top). Place pitch were generally ordered from apical to basal electrodes. The apical electrodes were judged lower in pitch than basal electrodes. Large individual difference was found, maybe due to the different conditions of nerve survival in cochlea.

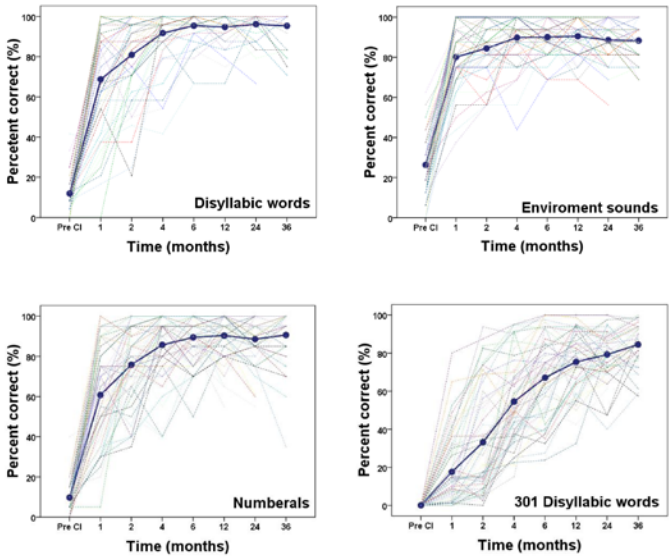

Fig.3. The data of open-set and close-set recognition in quiet. Individual (dotted lines) and average (circles connected by a solid line) recognition scores as a function of device usage time for environment sounds, numerals, disyllabic words and 301 disyllabic words.

Funding

This study was supported by grant from NSFC (No. 81271084, No. 81420108010, No.81500785.), and from Innovation Project of Shanghai Municipal Science and Technology Commission (No. 11411952300).

PS 548

Polyethylene glycol diacrylate (PEGDA) based hydrogels are capable of moving an electrode array perimodiolarly.

Elise Cheng[1]; Braden Leigh[2]; C. Allan Guymon[2]; Marlan Hansen[1]

[1]University of Iowa Hospitals and Clinics; [2]University of Iowa

Introduction

Despite advances in electrode design and sound processing strategies, cochlear implant (CI) performance has largely plateaued due, at least in part, to the inability to increase the effective number of stimulation channels. Free-fitting CIs typically rest laterally in the scala tympani, away from the target neural elements in the modiolus. Each channel's stimulation spreads to adjacent spiral ganglion neurons, reducing the number of effective channels of stimulation. Thus the CI is unable to replicate the inherent intimacy of afferent cochlear innervation. While a number of methods to move the array closer to the modiolus have been developed, many have proven potentially damaging to the modiolus.

Methods

Polyethylene glycol diacrylate (PEGDA) hydrogels were prepared by mixing high molecular weight PEGDA monomer (M_n 4600) with photoinitiator in aqueous solution, and were polymerized under ultraviolet light for ten minutes. Swelling forces of PEGDA hydrogels were measured directly using a force transducer. The forces needed to flex eight lateral wall model human cochlear implant arrays by 30 degrees were also measured using a force transducer. Electrode arrays

were then asymmetrically coated in PEGDA, dried, and inserted into a 3D printed model of the human scala tympani. Photos were taken prior to swelling and after swelling in artificial perilymph for 24 hours. 13 male and female Sprague Dawley rats were subjected to a baseline ABR, then a 10%, 15% or 20% segment of PEGDA either 1mm or 3mm long was inserted into the left cochlea via the round window. A 2-week postoperative ABR was performed, then the rats were sacrificed by transcardial perfusion and the cochleae were harvested. Basilar membrane morphology was assessed on histological sections.

Results

The swelling forces of PEGDA were less than published measurements of forces that are capable of disrupting the basilar membrane, but exceeded measurements of forces required to flex a lateral wall cochlear implant by 30 degrees. Hearing was preserved in most cochleae implanted with PEGDA hydrogels with a range of moderate 10-30 dB threshold shifts, though some animals did lose all hearing in the operated ear. Animals with significant hearing loss showed significant disruption of the basilar membrane. Interestingly, several animals that retained hearing with moderate threshold shifts had aberrant implantations (ie into the scala vestibuli).

Conclusions

PEGDA hydrogels represent a potential gentle, effective positioning agent compatible with hearing preservation.

Funding

NIH T32 DC000040, NIH R01 DC012578, NIH P30 DC010362

PS 549

Hearing preservation in cochlear implantation – Impact of electrode design, individual cochlear anatomy and preoperative residual hearing

Thomas Lenarz; Andreas Buechner; Anke Lesinski-Schiedat; Marie-Charlot Suhling; Waldemar Wuerfel

Hannover Medical University

Background

The percentage of patients with residual hearing undergoing cochlear implantation has increased over the last years. The preservation of residual hearing allows electroacoustic stimulation and the use of hybrid systems. The hearing preservation rate (PTA, speech perception) varies substantially.

Material Methods

Over all 560 patients were included in this retrospective study. The patients had post lingual onset of hearing loss and they all were implanted by using the round window approach through the posterior tympanotomy. Systemic corticosteroids were used intraoperativly. The mean PTA pre- and postoperatively, the unaided and aided speech perception were measured using monosyllabic word testing, HSM-sentence test in quiet and noise and OLSA sentence test in noise. The amount of hearing loss was classified into less than 15 dB PTA, 15-30 dB PTA and more than 30 dB PTA (total loss). Patients were followed over a time up to several years. The following types of the electrodes were used: Nucleus Hybrid-L, Nucleus SRA, MedEl Flex 20, Flex 24 and Flex 28, Advanced Bionics HiFocus 5 (Mid-Scala). Using pre- and postoperative Cone Beam CT scans the cochlear length was measured and the cochlear coverage (ratio between part of the cochlear covered by a used electrode vs. total length) was calculated in our cases.

Results

Hearing preservation is possible with all types of electrodes. However there are significant differences in hearing preservation rates. The most important factor is the electrode length with significantly higher preservation rates for electrodes shorter than 20 mm which cause a smaller increase in hearing loss over time compared to longer electrodes. Larger cochlear coverage resulted in poorer hearing preservation scores. There is a positive correlation between cochlear length and hearing preservation rate. Electro-acoustic hearing could be used in patients with PTA threshold in the low frequencies of better than 75 dB HL. The stimulation rate is important for the long duration preservation of residual hearing. Higher rates and short pulse stimulation show higher rates of hearing loss. Patients with sudden hearing loss developed cumulative higher losses of postoperative residual hearing (> 30 dB) in contrast to patients with a progressive hearing loss.

Conclusion

Hearing preservation in cochlear implantation can be achieved with different types of electrodes and surgical concepts. The relevant parameters for hearing preservation are electrode length, cochlear coverage, type of electrical stimulation, and history of hearing loss.

PS 550

Improvement of the Variability of the Insertion Axis to the Scala Tympani by a semi-automatic Robotic System in Cochlear Implantation

Renato Torres[1,2,3]; Guillaume Kazmitcheff[2,3,5]; Daniele De Seta[1,2,3,4]; Jean Loup Bensimon[2,3,6]; Evelyne Ferrary[1,2,3]; Dan Gnansia[7]; Olivier Sterkers[1,2,3]; Yann Nguyen[1,2,3]

[1]Pitié-Salpêtrière Hospital, AP-HP; [2]UPMC Univ. Paris 06, Sorbonne University; [3]UMR-S 1159, Paris 6 UMPC Univ, Inserm; [4]Policlinico Umberto I, Sapienza University of Rome; [5]Shacra Inria, Lille Nord-Europe, Université Lille-1; [6]Cabinet de Radiologie; [7]1. Neurelec/Oticon Medical

Background

The cochlear implant is a hearing aid that stimulates the ganglion cells to restore hearing in deaf people. The insertion of the electrode array along the scala tympani axis would improve the quality of the cochlear implantation. However, the cochlear anatomy and the mental representation of the insertion axis are highly variable. The aim of the study was to assess the improvement of the mental representation of the insertion axis by navigation and robotic devices, and to measure the semi-automatic robotic system accuracy in alignment with the insertion axis.

Methods
Three ENT surgeons were evaluated on four temporal cadaveric bones. The surgical approach was performed to show the round window region and a cone beam CT was obtained in all specimens. The optimal insertion axis was defined as follows: 1) the centerline of the scala tympani in the basal turn of the cochlea in the coronal view, 2) a tangent line between the entry point to the cochlea and the centerline of the scala tympani, and 3) rotation of this axis according to the facial canal position in axial view. A neuronavigation system (Digipointeur®, Collin, Bagneux, France), Robotol V3 (a prototype developed in our laboratory), and SmartOtol (a software allowing a semi-automatic alignment to the Robotol) were used as surgical devices for performing the alignment of the insertion axis. Four procedures were performed to assess reproducibility of the insertion axis: manual, manual navigation-assisted, robot navigation-assisted and robotic semi-automatized. The angle between the optimal insertion axis and the instrument axis was measured by ImageJ on first three procedures. The angle between the optimal axis in a 3D reconstruction model from the CT slices, and the position of the instrument in a 3D model obtained by photogrammetry was measured in the fourth procedure.

Results
The average error was 8.5+/-4.4° for the manual, 9.6+/-3.8° for the manual navigation-assisted, 3.3+/-2.5° for the robot navigation-assisted, and 0.9+/-0.5° for the robot semi-automatized procedures (n=20). A better accuracy was observed on semi-automatized procedure than manual ($p<0.01$), robot navigation-assisted ($p<0.01$), and robot navigation-procedure ($p<0.05$) (Kruskal Wallis post-test). There was no difference between manual, manual navigation-assisted, and robot navigation-assisted procedures.

Conclusions
The manual alignment is a complex gesture and cannot be improved by the navigation systems. A robotic device made easier, but not reproducible the alignment of the insertion axis. A semi-automatized procedure could improve the precision and reproducibility of a pre-planned insertion axis of temporal bone.

Funding
This work was funded in a Cifre convention (NÂ° 2015/0269) by Neurelec / Oticon Medical.

PS 551

Essential role of miRNA96 in the auditory hindbrain

Tina Schlüter[1]; Elena Rosengauer[1]; Karen Steel[2]; Hans Gerd Nothwang[1]
[1]Carl von Ossietzky University Oldenburg; [2]King's College London

MicroRNAs are small-noncoding RNAs that mainly function on the post-transcriptional level by binding to specific sites in the 3'UTR of target mRNAs. They participate in multiple processes in development, differentiation, and cellular homeostasis. MicroRNA96 (miR-96) is part of the miR-183 cluster, consisting of miR-183, -96 and -182 and is highly expressed in sensory cells. Point mutations in miR-96 cause deafness due to arrested cochlear hair cell development (Mencía et al., 2009, Lewis et al., 2009). We recently showed that miR-96 is expressed and postnatally upregulated in the mouse brainstem (Rosengauer et al., 2012). Here we report a prominent miR-96 expression in the auditory brainstem by using RNA *in-situ* hybridization. To investigate its retrocochlear function, we performed anatomical studies in young-adult homozygote *Dmdo* mice. These mice harbor a point mutation in miR-96, which causes peripheral deafness. A significant 25-35% volume reduction was observed in various auditory brainstem nuclei, due to both cell loss and reduced cell size. In contrast, neonatal *Dmdo* mice showed no significant volume reduction, while an intermediate reduction was observed at P4, demonstrating a postnatal maturation defect. We also determined the volume of a non-auditory brainstem structure, the nucleus of the 7th nerve. Only a slight volume decrease of 7.5% was found in young-adult *Dmdo* mice. On the back of this, deaf *Claudin14*$^{-/-}$ mice were investigated. These mice display a cochlear phenotype similar to *Dmdo* mice and were included in the study to examine the contribution of peripheral deafness to the volume reduction in the auditory brainstem of *Dmdo* mice. *Claudin14*$^{-/-}$ mice showed only minor changes in the volume of auditory brainstem nuclei. This indicates that the observed volume reductions in *Dmdo* mice are due to an on-site effect of the mutated miR-96 and do not merely reflect a general degeneration of auditory brainstem structures in deaf mice. All data together demonstrate that mutations in miR-96 affect postnatal development of the auditory brainstem of mouse, implying an important role of miR-96 throughout the auditory brainstem. This adds miR-96 to the list of deafness genes with a function in both, the cochlea and central auditory pathways.

Funding
This work was supported by the DFG (GRK 1885).

PS 552

Anisotropic Panglial Networks in the Lateral Superior Olive

Jonathan Stephan[1]; Vanessa Augustin[1]; Charlotte Bold[1]; Simon Wadle[1]; Julia Langer[2]; Ronald Jabs[3]; Camille Philippot[3]; Dennis Weingarten[1]; Christine Rose[2]; Christian Steinhäuser[3]; Eckhard Friauf[1]
[1]University of Kaiserslautern; [2]Heinrich Heine University; [3]University of Bonn

Astrocytes form connexin (Cx)-mediated gap junctional networks, which participate in homeostasis by redistribution of ions and neurotransmitters within the syncytium. In the auditory brainstem, astrocytes are heterogeneously distributed and strongly aggregate in its nuclei.

We immunohistochemically labeled Cx43 and Cx30 to investigate their developmental expression in the lateral superior olive (LSO). In order to analyze the degree of astrocyte coupling and the network shape in the LSO, we utilized acute brainstem slices from C57Bl6 mice at postnatal days (P)10-20. Astrocytes were identified *a priori*

by sulforhodamine 101-labeling before subjecting them to whole-cell patch-clamp recordings. The intracellular solution contained gap junction permeable neurobiotin and impermeable alexa fluor (AF) 568 to label the network and the patched cell, respectively. After tissue fixation, neurobiotin was tagged with avidin AF488 and the LSO was marked immunohistochemically against GlyT2 to define the network location. Additionally, we performed wide field sodium imaging in order to analyze the capability of ion redistribution within the LSO.

The expression of Cx43 was strong during early development and decreased with age. In comparison, Cx30 onset was delayed and started around P16. LSO astrocytes formed large networks, which were independent from development (P10-20). Networks showed great variation regarding their size and were predominantly restricted to the LSO. Unexpectedly, networks originating from astrocytes located in the internuclear space between the LSO and the neighboring superior paraolivary nucleus extended into both nuclei. While astrocytic networks are almost circular in many CNS regions, those in central parts of the LSO were often oriented orthogonally to the tonotopic axis. Electrical stimulation of individual astrocytes in the LSO caused sodium elevations in their somata. Additionally, sodium elevations were consecutively present also in neighboring cells, indicative of a spread of sodium through gap junctions. Surprisingly, not only neighboring SR101-labeled astrocytes, but also SR101-negative cells responded to the stimulus. In order to analyze the contribution of non-astrocytic cells to the networks we used PLP-GFP mice in which oligodendrocytes were labeled. Astrocyte-derived networks contained several GFP-positive oligodendrocytes showing the formation of panglial networks.

Taken together, our results demonstrate heterogeneous astrocyte networks in the LSO regarding their orientation. Moreover, these networks do not only include SR101-positive astrocytes, but apparently include oligodendrocytes, forming a panglial network. We assume that the morphological properties of the networks in the LSO lead to a spatially restricted homeostasis and therefore to a limited cross-talk towards neighboring isofrequency bands.

Funding
This study was supported by the DFG (Priority Program PP1608: Ste 2352/2?1; Ste 552/4; Ro 2327/8-1).

PS 553

Neuromodulation of Excitatory Transmission by Group I mGluRs in MNTB Neurons in a Mouse Model of Fragile X Syndrome

Yong Lu
Northeast Ohio Medical University

Background
Fragile X syndrome (FXS) is the leading single-gene cause for mental retardation. Among other deficits, FXS patients experience compromised sensory processing. Previous research has shown that in a fragile X mental retardation gene 1 (FMR1) knock out mouse model (Fmr1 KO), auditory cortical neurons exhibit abnormal auditory responses and impaired neural plasticity. In MNTB, calyces become larger, cell size decreases, and Kv channels change their distribution. The loss of FMR protein function also results in exaggerated activity of group I metabotropic glutamate receptors (mGluR I). Altered neuromodulation may contribute to the compromised auditory processing. Here, we investigated mGluR 1 neuromodulation of the glutamatergic transmission in MNTB neurons of both Fmr1 KO and wild type (WT) mice.

Methods
The KO and WT mice (with a background of C57/B6) were purchased from the Jackson Laboratory and bred at NEOMED. Brainstem slices (250-300 µm) were prepared from P14-P22 mice. Whole-cell voltage clamp was used to record spontaneous and electrically evoked EPSCs (sEPSC and eEPSC) in MNTB neurons at 35 °C.

Results
MNTB neurons of the WT showed primarily all-or-none eEPSC, while most KO neurons showed graded input-output functions. Proportionally more KO neurons exhibited synaptic facilitation in a paired-pulse paradigm. The sEPSC frequency in both WT and KO neurons varied widely, while the sEPSC amplitude and kinetics were similar between WT and KO neurons. In about half of the recorded neurons, activation of mGluR I by 3,5-DHPG (200 µM) inhibited eEPSC, and the inhibition in the KO was moderately stronger than in the WT. 3,5-DHPG also produced a small inward current at the holding potential of -60 mV. The sEPSC amplitude remained unchanged upon mGluR I activation. Surprisingly, 3,5-DHPG increased sEPSC frequency in both WT and KO neurons. In other words, mGluR I regulated both spontaneous and evoked release of glutamate, but in the opposite direction.

Summary
The basal level of excitatory transmission in MNTB neurons of the Fmr1 KO seems to be slightly compromised. Suppression of evoked glutamate release by mGluR I appears to be exaggerated in KO. The differential modulation of sEPSC and eEPSC suggests that the vesicle pools responsible for spontaneous and evoked glutamate release, as well as the mechanisms underlying mGluR modulation of the two release machineries, are different.

Funding
Supported by NEOMED Bridge Funding to YL.

PS 554

Synaptic Reliability and Temporal precision during ongoing stimulation: Auditory brainstem synapses outperform Hippocampal synapses

Elisa Krächan; Alexander Fischer; Eckhard Friauf
University of Kaiserslautern

Synapse performance is limited by physical, chemical, and biological factors. Elucidating such limitations is central to understanding the heterogeneity of synaptic systems. At early stations of the auditory pathway, information is encoded

in the precise signal timing and the signal rate. Auditory synapses must maintain the relative timing of events with high precision even during sustained high-frequency stimulation. In non-auditory brain regions, synapses are often activated at considerably lower frequencies. In order to assess whether non-auditory synapses are also capable of precise transmission along sustained high-frequency stimulation, we compared the performance of auditory and non-auditory synapses. We performed whole cell patch-clamp recordings in acute tissue slices of juvenile mice at three synapse types in the auditory brainstem and the hippocampus: synapses formed by neurons of the medial nucleus of the trapezoid body (MNTB) onto neurons of the lateral superior olive (LSO) as well as CA3-CA1 synapses and inhibitory synapses between the entorhinal cortex (EC) and granule cells of the dentate gyrus (DG), both located in the hippocampal formation. We detailed several aspects of synaptic plasticity upon challenging the synapses with frequencies ranging from 0.2-200 Hz in the milliseconds-to-seconds and the tens of seconds-to-minutes range. As continuous stimulation is virtually ubiquitous in natural environment, experiments employing prolonged stimulation (≥60 s) formed the center of our study. We found a multitude of performance differences between MNTB-LSO synapses and their hippocampal counterparts. First, short-term plasticity in the milliseconds-to-seconds range comprises facilitation at CA3-CA1 synapses, but not at the other two systems. Second, synaptic fatigue, as assessed in the tens of seconds-to-minute range, is least profound at MNTB-LSO synapses. Third, recovery from synaptic fatigue is efficient at both MNTB-LSO and EC-DG synapses, yet appears to be quite ineffective at CA3-CA1 synapses. MNTB-LSO synapses recover remarkably speedily, even after extreme challenge periods. Fourth, faithful transmission without failures is a hallmark of MNTB-LSO synapses compared to both hippocampal synapse types as half maximal fidelity is reached at a ~10-fold higher frequency. Fifth, vesicle replenishment mechanisms of MNTB-LSO synapses are most efficient, enabling them to release ~370 vesicles s^{-1}. Finally, the temporal precision of synaptic responses in the seconds-to-minute range is drastically higher at MNTB-LSO synapses. Their superior performance likely supports the functional demands and appears to be due to very efficient replenishment mechanisms that go along with a high quantal content, thus enabling robust, yet temporally precise release events during sustained activation.

Funding
This study was supported by the DFG (Priority Program PP1608: Fr 1784/17-1)

PS 555

A novel and exotic Inhibitory Synapse in the Auditory Brainstem

Dennis Weingarten; Nadine Patschull-Keiner; Alexander Fischer; Eckhard Friauf
University of Kaiserslautern

Principal neurons of the lateral superior olive (LSO) compute interaural level differences (ILD). They receive excitatory input from the ipsilateral ventral cochlear nucleus (VCN) via the ventral acoustic stria (VAS). In combination with inhibitory input from the ipsilateral medial nucleus of the trapezoid body (MNTB), which carries information from the contralateral VCN, the classical neuronal circuit for computing ILD is formed. In this study, we show an additional exotic inhibitory input from the VCN into the ipsilateral LSO (inhibVCN-LSO). Whole-cell patch-clamp recordings were performed in acute brainstem slices of C57BL/6 mice at P 10-12 at 37° C. Focal electrical stimulation of the VAS evoked inhibitory postsynaptic currents (eIPSCs), which were pharmacologically identified as glycinergic. The average number of inputs per neuron was 4 as determined by stepwise increases of the stimulation intensity. As reliable high-frequency transmission and precision are hallmarks of synapses in the auditory brainstem, we stimulated unitary inhibVCN-LSO inputs at 1-333 Hz for 60 s each. In comparison to MNTB-LSO synapses, inhibVCN-LSO synapses showed stronger depression of their eIPSC peak amplitudes at stimulation-frequencies >20 Hz resulting in a higher failure rate during high-frequency transmission. InhibVCN-LSO synapses displayed slower eIPSC kinetics than glycinergic MNTB-LSO synapses (Kramer *et al*., 2014). Furthermore, these exotic synapses exhibited less temporal precision during high frequency stimulation in comparison to MNTB-LSO, but increased precision compared to non-auditory synapses (see poster by Kraechan *et al.* at this meeting). To confirm that the VCN is the origin of these ipsilateral inputs into the LSO, the biotinylated dextran tracer was stereotactically injected into the VCN of adult mice. Fluorescence labeling against both biotin and the neuronal glycine transporter GlyT2 was subsequently performed, showing co-localization of the tracer and GlyT2 in the ipsilateral LSO. Therefore, we conclude that the exotic glycinergic inputs arise from neurons in the ipsilateral VCN.

In summary, inhibVCN-LSO synapses are suited for a lower frequency spectrum of synaptic transmission compared to other, conventional synapses in the auditory brainstem (MNTB-LSO synapses: Kramer *et al*., 2014; VCN-MNTB synapses: Taschenberger and von Gersdorff, 2000) but still more reliable and precise compared to non-auditory synapses (Kraechan *et al*.) Therefore, we suggest that inhibVCN-LSO synapses are in the position to participate in ILD detection, rather than having a purely modulatory effect.

Funding
This study was supported by the German Research Foundation DFG (Priority Program PP1608: Fr1784/17-1).

PS 556

Cholinergic Signaling Modulates Sound Evoked Responses in MSO and MNTB of the Adult Gerbil

Chao Zhang[1]; Michael Pecka[2]; Elise Esposito[1]; R. Michael Burger[1]
[1]Lehigh University; [2]Ludwig Maximilians University of Munich

The superior olive complex (SOC) is composed of brainstem auditory nuclei and functions as a major hub of ascending

and descending circuitry. Neurons of the medial superior olive (MSO) and medial nucleus of the trapezoid body (MNTB) are devoted to processing information related to computation of sound location within SOC. Neurons in both nuclei are specialized to preserve temporal information in their firing patterns. MSO computes interaural time disparities (ITDs), a localization cue, via both excitatory and inhibitory inputs derived from each ear. MNTB converts monaurally derived, phase-locked excitation to inhibition that is distributed to its many postsynaptic targets including the MSO. Within this circuitry, however, modulatory mechanisms underlying response features of these neurons have yet to be fully illuminated. One such modulatory system is the cholinergic system, which influences neural signaling throughout the brain. In the SOC, Happe and Morley (1998) showed intense labeling of nicotinic acetylcholine receptors (nAChRs), suggesting potentially strong cholinergic modulation of both MNTB and MSO neurons. Despite this evidence, no physiological investigation of this input has been reported for SOC neurons, and the putative cholinergic projections to these regions have not been described. In order to investigate the role of cholinergic input to the SOC, we made *in vivo* extracellular recordings from anesthetized gerbil SOC, using piggyback multibarrel electrodes. This configuration allowed us to pharmacologically manipulate cholinergic input with iontophoresis of agonist and antagonists of nAChRs. Application of the ACh agonist, nicotine (NIC), significantly increased sound driven spike rates of both MSO and MNTB. A complementary decrease in spike rates was observed in the presence of the nicotinic receptor antagonist, mecamylamine (MEC). The latter result suggests an endogenous cholinergic signal is present in these nuclei during acoustic stimulation. These data are the first, to our knowledge, confirming that ACh provides a strong modulatory input to MSO and MNTB, one that functions to powerfully shape responses to acoustic input.

PS 557

Perineuronal Nets Contribute to Fast-spiking of MNTB Principle Neurons

Timothy Balmer
Marine Biological Laboratory

Background

Perineuronal nets (PNNs) are a specialized condensation of extracellular matrix molecules that surround the somata of fast-spiking neurons. PNNs are prevalent throughout the auditory brainstem, which transmits signals with high speed and precision. It is unknown whether PNNs contribute to the fast-spiking ability of the neurons they surround. The majority of what we know about PNNs comes from studies in which PNNs are degraded enzymatically *in vivo*. Degradation of PNNs with chondroitinase (ChABC) has been reported to cause remarkable plasticity in adult brains, allowing recovery from amblyopia or from injury in the central nervous system. It is unclear how degradation of PNNs causes these changes and what PNNs contribute to normal neuronal function. All principal neurons of the medial nucleus of the trapezoid body (MNTB) fire action potentials at ~1000 Hz and develop PNNs around their somata by P21 in mice. This relatively homogenous population of PNN-surrounded neurons was used to test how PNNs contribute to fast-spiking *in vitro*.

Method

Whole-cell recordings were made from MNTB neurons in acute brain slices from P21-27 C57BL/6 mice. PNNs were degraded by incubating the slices in ChABC and compared to slices that were maintained in a control enzyme (Penicillinase). Action potentials were elicited by somatic current injection.

Results

ChABC treatment effectively degraded the PNNs, verified by lectin histochemistry. ChABC did not affect the passive properties of MNTB neurons, nor did it affect the shape of a single action potential triggered by somatic current step or pulse. During high-frequency trains of current pulses (100-1000 Hz) ChABC treated cells had more spike failures than penicillinase treated cells. The spike amplitudes of the ChABC treated cells decreased during the train more than penicillinase treated cells. Gaussian white noise current stimulation was used to create F/I curves, which showed that ChABC treated cells fired significantly less in response to the same current injection than control cells. Spike triggered averages showed that ChABC treated cells required a larger current injection to fire than penicillinase treated cells.

Conclusion

PNNs contribute to the fast-spiking activity of MNTB neurons by preventing spike failures, maintaining spike amplitude and affecting spike threshold. The development of PNNs around somata of fast-spiking neurons may be essential to the fast and precise sensory transmission in the auditory system.

Funding

Grass Foundation Fellowship

PS 558

The tonotopic distribution of Na+ channels at the nerve terminal in the auditory brainstem

Emmanuelle Berret; Jie Xu; Jun Hee Kim
UTHSCSA

A fundamental organizing principle of auditory brain circuits is tonotopy, the orderly representation of the sound frequency to which neurons are most sensitive. In the medial nucleus of the trapezoid body (MNTB), principal neurons are topographically organized along a medio-lateral axis with the most medially located cells responding best to high sound frequencies, progressively changing to lower characteristic frequencies in the most lateral cells. Previous studies have demonstrated that the high-threshold potassium channel expression along the tonotopic gradient is important for the firing properties in the MNTB principal neurons. However, there is little known about the relationship between presynaptic firing properties and ion channel expression at the nerve terminal along the tonotopic gradient in the MNTB. We studied the relationship between presynaptic firing properties and voltage gated sodium channel (Na_v) expression and location at the calyx of Held terminal across the medio-lateral axis. Our electrophysiological and immunostaining results demonstrated that Na_v channel

location at the axon heminode is medio-lateral dependent. There is no significant difference in the size of Na_v clusters, however, the length of the heminode, defined as the distance between the Na_v cluster and the calyx terminal, is much shorter in medial than in lateral MNTB. Consequently, the distance from the heminode to the next node is longer in medial than in lateral regions. This result indicates that the last two nodes, where action potential fires before the calyx terminal, are much closer in lateral than medial MNTB regions. At postnatal days 10-13, the calyx of Held terminal located in the medial region reliably fires action potentials following to 300 Hz in room temperature, whereas the calyx terminal in the lateral region showed a number of action potential failures in response to the same stimulation. Our results suggest that the location of the Na_v channels adjacent to the presynaptic terminal determines the frequency-dependent firing along the tonotopic gradient in the MNTB.

Funding
NIDCD (R01, DC013157)

PS 559

How Action Potential Duration Affects the Activation of Presynaptic Voltage-Gated Calcium Channels.

Matthew Scarnati; **Kenneth Paradiso**
Rutgers University

Background
The response of voltage-gated calcium channels to the presynaptic action potential is an essential component in processing auditory information. Presynaptic calcium channels are activated during the depolarizing phase of the action potential. During the falling phase of the action potential, calcium channels continue to open and the driving force for calcium entry increases as the membrane potential becomes more negative. The percentage of calcium channels that are activated by the action potential is highly important in determining the amount of neurotransmitter release. However, the change in driving force makes it difficult to determine the number of calcium channels that are active at different times during the action potential. To resolve this, we have used voltage jumps at different times during the action potential to determine calcium channel activation at different times during the action potential.

Methods
To study how presynaptic calcium channels respond to the action potential we performed presynaptic patch clamp recordings at calyx of Held nerve terminal in acute slices from the auditory brainstem. To optimize recording quality, recordings were made from the axonal heminode, and parasagittal slices were used to limit the size of the axon. Action potential-like stimuli were used to activate presynaptic voltage-gated calcium channels.

Conclusions
Our results indicate that approximately 70% of the total available calcium channels open during an action potential. The rising phase of the action potential only activates one quarter of the channels that will be activated, the remainder activate during the repolarization phase of the action potential. The peak number of calcium channels are activated when the membrane potential reaches approximately zero millivolts. By varying the duration of the repolarization phase, we find that as the duration of the repolarization phase increases, the peak activation of voltage-gated calcium channels occurs earlier and lasts for a longer portion of the action potential. This demonstrates that modulation that produces a longer presynaptic action potential repolarization causes larger postsynaptic responses by activating the peak number of calcium channels sooner and for a longer period of time.

Funding
NIH:NS051401-42.

PS 560

Strength of the efferent olivocochlear system modifies the activity of a central auditory nuclei.

Mariano Di Guilmi[1]; María Eugenia Gómez-Casati[1,2]; Luis Boero[1,2]; Ana Belén Elgoyhen[1,2]
[1]Instituto de Investigaciones en Ingeniería Genética y Biología Molecular, INGEBI-CONICET; [2]Tercera Cátedra de Farmacología. Facultad de Medicina, UBA.

The auditory system in many mammals is immature at birth but precisely organized in adults. Spontaneous activity in the inner ear comes into play to guide this process. This spontaneous activity is modulated by an efferent pathway that descends from the brain (Walsh et al., 1998). In the medial nucleus of the trapezoid body (MNTB), neurons are topographically organized along a medio-lateral axis with the most medially located cells responding to high frequencies, changing to lower characteristic frequencies in the most lateral cells. The specific aim of this work is to understand the role of the medial olivocochlear (MOC) system in the correct establishment of the MNTB tonotopy.

We used mice with enhanced MOC activity (*Chrna9L9'T*, knock-in, KI) in which the α9 nicotinic receptor subunit bears a point mutation that leads to a gain of function (Taranda et al., 2009). Auditory brainstem responses (ABR) at P21 and electrophysiological recordings between P12-14 (patch-clamp, whole-cell configuration) on brainstem slices containing the MNTB were evaluated. Both current and voltage-clamp configurations were performed in order to study the tonotopy of the MNTB.

Wave I amplitude of the ABR was the same for WT and KI mice at 8, 16 and 32 KHz. However, there was a reduction in the amplitude of wave III in KI mice that was larger at high frequencies (~ 23% reduction at 16 KHz and 35% at 32 KHz). These observations suggest a central dysfunction. In order to analyze in depth these functional observations and focus on tonotopy, we studied the MNTB nucleus. Under current-clamp mode, while medial MNTB neurons in WT showed a more depolarized membrane potential and a larger membrane resistance than lateral ones; both properties were not tonotopically distributed in KI mice. Additionally, medio-lateral

action potential firing differences after a depolarized current pulse injection observed in WT (medial: 201±11 Hz; lateral: 153±18 Hz; p=0.03) were absent in KI mice medial: 182±14 Hz; lateral: 155±10 Hz, p>0.05). Under voltage-clamp mode, I_h current was larger in medial compared to lateral cells in WT. However, this tonotopic difference was reduced in KI animals.

These results suggest that medial efferent activity before hearing onset is involved in the refinement of the tonotopic map of the MNTB.

Funding
Financial Source: Agencia Nacional de PromociÃ³n CientÃfica y TecnolÃ³gica (ABE)

PS 561

Functional Connectivity of Chick Cochlear Nucleus Neurons to an Inhibitory Circuit

David Brown; Richard Hyson
Florida State University

Background
Sound intensity processing in the avian central auditory system begins at the cochlear Nucleus Angularis (NA), which contains a heterogeneous population of neurons whose specific sensory roles are uncertain. Multiple neuronal subtypes exist as classified by morphology, current pulses in vitro, and tone stimulation. Furthermore, NA projects to at least four ascending auditory targets, yet specific cellular connectivity is unknown. To better understand the role of NA neurons in acoustic processing, we aimed to identify the electrophysiological subtype(s) that project to the inhibitory Superior Olivary Nucleus (SON). Additionally, acoustic stimuli in vivo lead to time-varying neural activity more complex than simple current steps, so we examined how intrinsic cellular properties affect NA firing patterns in response to simulated auditory nerve fiber (ANF) input.

Methods
Chicks (P0) were used for retrograde tracer injection into SON. Stereotaxic coordinates were determined via spontaneous or sound evoked neural activity with a low impedance electrode. After a 2 day survival period, chicks were anesthetized and sections of the auditory brainstem were prepared. In vitro whole-cell current clamp recordings of tracer-positive NA neurons were used to determine the electrophysiological phenotype of NA-SON projection neurons.

To investigate how NA heterogeneity might affect responses to input similar to that experienced in vivo, we developed a post-synaptic current model with which to stimulate NA neurons via dynamic clamp. Our model incorporates previously reported experimental measurements of excitatory post-synaptic conductance, decay time constant, number of inputs, ANF firing frequency, and ANF adaptation rate. Firing frequency and number of inputs were primary independent variables; temporal responses to simulated ANF input were evaluated with peri-stimulus time histograms (PSTH).

Results
Electrophysiological responses to current steps were consistent with previous reports of Single-Spiking and multiple subtypes of Tonic firing neurons. Preliminary recordings from tracer-positive neurons revealed that multiple physiological subtypes project to SON.

In vitro PSTH classification included primary-like and transient chopper, based on similar characteristics to previously reported acoustically driven responses. However, cells exhibited multiple response phenotypes depending on modeled presynaptic firing frequency and number of inputs.

Conclusion
Preliminary results suggest that multiple NA subtypes drive SON. ANF input simulation accurately reproduced a portion of temporal responses previously reported in vivo. Overall, these data suggest that physiological phenotypes in NA are not segregated according to their downstream targets, and that NA may signal multiple acoustic features to SON.

PS 562

Origin and Spatial Structure of two Distinct Frequency Components in the Extracellular Field Potential in the Avian Nucleus Laminaris

Thomas McColgan[1]; Paula Kuokkanen[1]; Ji Liu[2]; Hermann Wagner[3]; Catherine Carr[2]; Richard Kempter[1]
[1]Humboldt-Universität zu Berlin; [2]University of Maryland; [3]RWTH Aachen

Acoustic clicks evoke two distinct frequency components in the extracellular field potential (EFP) within the avian nucleus laminaris (NL). The high-frequency component corresponds roughly to the best frequency (BF) of the recording location. The low-frequency component (< 1.5 kHz) has a distinct dipolar spatial structure, and its origin is a matter of debate. We hypothesize that the EFP is generated by presynaptic population activity: the low-frequency component, in particular, is due to the refractory period of the neurons in nucleus magnocellularis (NM), and its dipolar structure is due to the spatial arrangement of NM axons projecting to NL.

Here we present three model constituents that account for the origin and the spatial distribution of both frequency components of the click-evoked EFP in the barn owl. The first constituent elucidates the relationship between the refractory period and the low-frequency component of the EFP by simulating a population of NM neurons and the input they receive from auditory nerve fibers. The other two constituents are concerned with the distinct spatial behavior of the EFP within NL. One is a multi-compartment model of NM axonal arbors from which the EFP can be calculated numerically, while the other is a more abstract mathematical model from which the EFP can be derived analytically. Together, this model of the NM population activity provides a simple explanation for the distinct spatio-temporal behavior of high- and low-frequency components in NL.

The model predicts that the low-frequency component and the distinct spatio-temporal structure of the EFP is generated not

only by clicks but also, in an intensity-dependent manner,by tonal and noise stimuli. To test this and further model predictions, we recorded the EFP in response to different classes of stimuli with a linear multi-electrode array, which allowed for simultaneous recording at different locations. These experiments confirmed all model predictions about the spatial and temporal structure of the EFP. Together, model and data are consistent with a low-frequency component of the neurophonic in NL generated by the axonal projections from NM.

Funding
NIH DCD 000436 to Catherine E Carr, NSF 1516357

PS 563

Synaptic Inhibition in the Avian Interaural Level Difference Circuit

Rebecca Curry[1,2]; Yong Lu[1]
[1]Northeast Ohio Medical University; [2]Kent State University

Introduction
Compared to the mammalian interaural level difference (ILD) circuitry, the cellular mechanisms underlying ILD coding in the avian system are less understood. In birds, the first central auditory nucleus encoding ILD is the posterior portion of the dorsal nucleus of the lateral lemniscus (LLDp; formerly VLVp, the nucleus ventralis lemnisci lateralis pars posterior), and is functionally equivalent to the lateral superior olive (LSO) in mammals. Previous *in vivo* and histological studies have indicated that LLDp neurons receive excitatory inputs from the contralateral cochlear nucleus angularis (NA), as well as inhibitory inputs primarily from the other LLDp. However, little is known about the cellular properties of LLDp neurons that enable them to encode ILD. More critically, direct physiological evidence for reciprocal inhibitory connections between the two LLDp is lacking.

Methods
In physiological experiments, coronal brainstem slices (300 µm) were prepared from late chick embryos (E17-19) and early hatchlings (P0-P3). Whole-cell current and voltage clamp experiments were used to measure intrinsic and synaptic properties of LLDp neurons at 35 °C. In histological experiments, $GAD_{65/67}$ was detected using fluorescent immunohistochemistry.

Results
Puff application of muscimol (agonist for $GABA_A$ receptors) and glycine revealed that all recorded LLDp neurons have functional $GABA_A$ and glycine receptors. Electrical stimulation of the contralateral LLDp, or areas immediately medial to the ipsilateral LLDp, resulted largely in GABAergic IPSCs. Occasionally a glycinergic component was also seen. On average, ipsilateral stimulation resulted in IPSCs three times larger than contralateral stimulation. The latency of the contralaterally evoked IPSC was on average 5 ms and significantly longer than ipsilateral stimulation. Puff application of glutamate to the contralateral LLDp resulted in GABAergic IPSCs in the recorded LLDp neurons. $GAD_{65/67}$ labeled both boutons and axons in the LLDp and highlighted the long projecting axons that cross the midline towards the contralateral LLDp. Additionally, LLDp was more strongly $GAD_{65/67}$ reactive than the anterior portion of the LLD (LLDa, a part of the interaural time difference circuit), clearly showing the delineation between the two areas, especially at rostral regions.

Summary
A large population of LLDp neurons receive direct inhibitory inputs from the contralateral LLDp. The majority of these inhibitory inputs are GABAergic. Therefore, along with the excitatory inputs from the NA, contralateral GABAergic inhibition is the major player in encoding ILD in LLDp. The glycinergic component may become more prominent under specific conditions, modulating ILD processing.

Funding
Supported by NEOMED Bridge Funding to YL.

PS 564

Subthreshold and Spike Resonance in Gerbil MSO Involves GKLT

Jason Mikiel-Hunter[1]; John Rinzel[2]
[1]NYU; [2]Center for Neural Sciences and Courant Institute

Background
Subthreshold resonance (STR) refers to a cell's response property to weak sinusoidal current inputs with a maximal voltage response for input at a non-zero frequency. The high-frequency (>80Hz) STR observed in the guinea pig Medial Superior Olive (MSO) has been linked to its principal neurons' express suitability for processing binaural cues in the temporal fine structure of low-frequency stimuli (Remme et al, 2014). The low-threshold potassium conductance, gKLT, has been implicated both as the 'resonant' conductance as well as the prominent conductance endowing principal neurons with both phasic and band-pass firing properties as well as slope-sensitivity. Indeed gKLT may also determine the firing frequency selectivity of MSO principal neurons at just superthreshold stimulus amplitudes, a phenomenon we call spike-threshold resonance (SpkTR). Since STR and SpkTR are probed using stimuli of vastly different amplitude, the relationship between these two resonances is poorly understood; as a result their relevance to larger, more ethologically relevant stimuli which are potentially spike-eliciting is poorly understood. We have therefore studied subthreshold resonance in the gerbil MSO using sinusoidal stimuli of varying amplitude and waveform and comparing this experimental data to results from an MSO model in order to better characterize the conductances involved in both STR and SpkTR with particular emphasis on the role of gKLT.

Methods
We injected sinusoidal current stimuli (whole-cell, current clamp) of varying waveforms into gerbil MSO neurons, in vitro at temperature 34C0. gKLT was blocked and replaced, using dynamic clamp, by a virtual gKLT to confirm the involvement of the conductance in STR. We used a Hodgkin-Huxley-like model and its linearized form to not only reproduce the exper-

imental data but also to make and confirm further predictions about STR and SpkTR in the gerbil MSO.

Results/Conclusion

Subthreshold resonance was observed in all patched gerbil MSO neurons (average peak resonant frequency of 266±11.9Hz, n = 23). gKLT and its activation gating were implicated in underlying this subthreshold resonance. Peak resonant frequency of STR increased with stimulus amplitude until, at perithreshold values, it closely matched the SpkTR frequency (Figure 1). Half-wave rectifying stimuli was also conducive to an increase in peak resonant frequency. Given that these sinusoidal current stimuli are not ideal representations of the brief excitatory synaptic currents in MSO, it remains unclear how extensively MSO principal neurons make use of STR to process synaptic input in vivo.

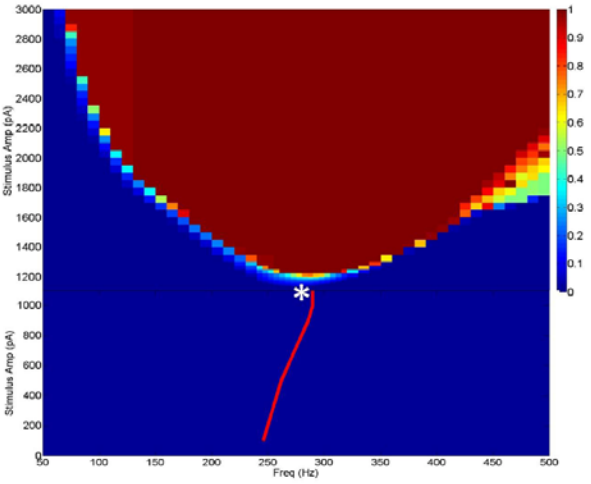

Figure 1. The peak resonant frequency of STR (Red line) at large, subthreshold stimulus amplitudes matches closely the SpkTR frequency of the superthreshold responses (*) in an MSO neuron model. The heat map for the superthreshold responses represents the number of spikes observed per cycle.

PS 565

Non-primary excitatory inputs shape MSO principal neuron responses

Brian Bondy[1]; Tom Franken[2]; Philip Joris[2]; Nace Golding[1]
[1]University of Texas at Austin; [2]KU-Leuven, Belgium

Background

The MSO is highly specialized to detect differences in arrival time of a sound to each ear (intraural time difference, ITD) for the purposes of spatial hearing. MSO neurons are tuned to ITD, but the mechanisms of this tuning have been debated. In vivo patch clamp recordings have shown that ITD tuning of many MSO neurons is strongly dependent on immediately preceding patterns of synaptic activity; out-of-phase EPSPs can substantially shift the neuron's ITD curve. Here we investigate the characteristics and origins of these synaptic potentials.

Methods

We performed whole cell current clamp recordings from MSO neurons both in vivo and in horizontal slices from P14-P29 Mongolian gerbils. In slices at 35°C, ipsi- or contralateral cochlear nucleus (CN) axons were electrically activated with glass stimulating electrodes placed lateral or medial to the MSO, respectively. In slices, whole-cell patch recordings from MSO principal neurons were made in the presence of 1 µM strychnine to block glycinergic inhibition.

Results

During in vivo whole-cell patch recordings from MSO principal neurons, responses to binaural beat stimuli evoked not only strong summating bilateral EPSPs but also smaller (<3 mV) EPSPs out of phase with peak depolarizations. In recordings from MSO principal neurons in slices, strong electrical stimulation of pharmacologically isolated excitatory inputs evoked not only direct monosynaptic EPSPs, but also 1-3 additional EPSPs with longer and more variable latencies (observed in 74% of MSO neurons with either ipsi- or contralateral stimulation). Late EPSPs had many characteristics of polysynaptic inputs: high stimulus thresholds, long latencies, a high degree of temporal jitter and low reliability. They could be seen in response to trains of stimuli as well. Late EPSPs were eliminated in the presence of high divalent ACSF or partial block of AMPA receptors (80 nM NBQX), consistent with these events arising from a polysynaptic input. Blockade of NMDA (50 µM APV) and GABA (50 µM Gabazine) receptors had no effect on the presence of late EPSPs. Interestingly, non-principal cells could be activated with both ipsi- and contralateral excitation and spike latency and jitter from synaptic stimulation matched the characteristics of polysynaptic EPSPs in MSO principal neurons.

Conclusions

MSO principal neurons receive polysynaptic inputs that arise from the superior olivary complex itself, possibly from MSO non-principal neurons, with timing that differs from primary inputs. Because "mis-timed" EPSPs affect ITD-sensitivity in vivo, these inputs are likely important for shaping the ITD sensitivity of MSO principal neurons.

Funding

This work was supported by a Harrington Doctoral Fellowship to BJB, a Ph. D. fellowship of the Research Foundation-Flanders (FWO) to TPF, project grants from FWO (G.0714.09, G.0961.11) and Research Fund KU Leuven (OT/09/50) to PXJ, and US National Institutes of Health grants DC011403 (NLG and PXJ) and DC006788 (NLG).

PS 566

Binaural Integration of Pitch in the Guinea-Pig Medial Superior Olive

Sami Alsindi[1]; Mark Sayles[2]; Ian Winter[1]
[1]University of Cambridge; [2]KU Leuven

Background

Harmonic tone complexes (HTCs) evoke a strong pitch percept corresponding to their fundamental frequency (F0), whether harmonics are presented to one ear or are alternately distributed across both ears (dichotic HTCs). This has led to theories of a 'central pitch processor' receiving inputs from neurons in which binaural information has already been

integrated; *i.e.*, binaural fusion occurs before pitch extraction. We hypothesized the necessary binaural integration occurs in the medial superior olive (MSO): MSO neurons cross-correlate their ipsi- and contra-lateral excitatory inputs from ventral cochlear nucleus spherical bushy cells. Here, we examined single-unit responses to dichotic HTCs in the guinea-pig (GP) MSO. We found the temporal properties of their spike trains corroborate the MSO's role in binaural fusion for pitch perception.

Methods
Extracellular single-unit recordings were made from low-best-frequency (<~1.5 kHz) temporal-fine-structure-(TFS)-sensitive principal cells of the left MSO of normal-hearing, anesthetized GPs. To characterize binaural-TFS sensitivity we presented 1-Hz binaural-beat stimuli with a range of carrier frequencies. We constructed composite curves to calculate a unit's best delay (BD), and phase-frequency functions to calculate characteristic delay (CD) and characteristic phase (CP). Recording sites were lesioned electrolytically, and brain tissue was processed histologically to confirm unit location in the MSO.

Binaural pitch responses were assessed using 250-ms duration cosine-phase HTCs. Stimuli were presented in three configurations: (1) *dichotic*, odd harmonics presented to one ear, even harmonics to the other; (2) *monaural*, odd harmonics alone or even harmonics alone; (3) *diotic*, odd and even harmonics to both ears. F0 was varied in octave steps between 31.25 and 500-Hz. Spike-train shuffled auto- and cross-correlograms were constructed to examine temporal representations of pitch.

Results
The interaural-phase sensitivity of GP MSO units is similar to other species: (1) BDs are distributed largely within the π-limit, and biased to positive (contra-leading) delays; (2) CD is negatively correlated with CP. For monaural-odd HTCs, correlograms indicated a pitch at F0, whereas monaural-even responses indicated a pitch at 2*F0. Importantly, for dichotic stimuli, spike-train correlograms showed a strong response at F0 of the binaurally-combined HTC stimulus. This was independent of the dichotic configuration (even-ipsi, odd-contra; odd-ipsi, even-contra).

Conclusions
Interaural-phase-sensitive MSO units combine inputs from both ears in a manner consistent with binaural pitch integration. This implies a fundamental role of the MSO as part of the neural machinery underlying pitch perception in mammals.

Funding
SA is supported by a PhD studentship from the Medical Research Council, UK and a travel award from Action on Hearing Loss; MS is a post-doctoral fellow of the Research Foundation â€“ Flanders, Belgium.

PS 567

A Novel Auditory Efferent Projection from the Ventral Nucleus of the Lateral Lemnicus to the Cochlea in the Mouse

Kirupa Suthakar; David Ryugo
Garvan Institute of Medical Research/University of New South Wales

Background
The olivocochlear (OC) efferent system has received considerable attention owing to the physiological significance of its capacity to modulate incoming sound. OC efferents are traditionally divided into medial (MOC) and lateral (LOC) groups, corresponding to differences in the location of cell bodies, differential projection patterns, and myelination. Whilst the exact organisation varies slightly between species, most reports place efferent cell bodies squarely in the superior olivary complex. In this study, we describe a previously unidentified group of auditory efferents located in the ventral nucleus of the lateral lemniscus (VNLL).

Method
Adult mice (CBA/Ca) received unilateral injections of retrograde neuronal tracer into the round window of the cochlea. To determine the neurochemical nature of these neurons, some sections were also double-labelled for choline acetyltransferase (ChAT), tyrosine hydroxylase (TH), glycine transporter 2 (GlyT2), or glutamate decarboxylase (GAD67). Light and electron microscopy were used to provide descriptions of these cells. Relative distributions of different populations of efferent cells were plotted throughout the brainstem and rendered in 3-dimensional reconstructions. To determine the peripheral projection pattern of VNLL efferents, injections of anterograde tracer dye were made in the VNLL and cochleae examined.

Results
In addition to previously described OC efferents, retrogradely labelled cells that double labelled for cholinergic markers were consistently observed in the ipsilateral VNLL. VNLL cells were negative for TH, GlyT2 and GAD67. Labelled VNLL efferents appear similar to LOC efferents by virtue of their size, ipsilateral projection pattern, ovoid somata, and large centrally located nucleus. Furthermore, we observed anterogradely labelled fibres and swellings under inner hair cells in the cochleae of animals that received unilateral dye injections directed into the VNLL.

Conclusion
Bidirectional transport of dye between the inner hair cell region of the cochlea and the VNLL has provided strong evidence for a novel efferent pathway. MOC efferents are implicated in signal extraction in noisy environments (Kawase et al., 1993) and protection from acoustic trauma (Liberman, 1991). Little is known about LOC efferents, however recent studies suggest they may be involved in interaural sensitivity to sound (Groff et al 2003; Darrow et al., 2006) and cochlea protection (Darrow et al., 2007). We have identified a novel group of cochlear efferents located in the VNLL and additional studies are required to determine their possible function.

Funding
Australian Postgraduate Award (APA), NHMRC Grant App#1080652, Fairfax Foundation, Alan & Lynne Rydge, The Walker Family Foundation

PS 568

High Frequency of GJB2 Splice-site Mutation c.-22-2A>C in a Large Cohort of Italian Age Related Hearing Loss Patients and Matched Controls

Elisa Rubinato[1,2]; Hela Azaiez[2]; Elizabeth Black-Ziegelbein[2]; Anna Morgan[1]; Kevin Booth[2]; Diego Vozzi[3]; Christina Sloan[2]; Kathy Frees[2]; Dragana Vuckovic[1]; Mariapina Concas[4]; Sean Ephraim[2]; Ginevra Biino[5]; Simona Vaccargiu[4]; Giorgia Girotto[1,6]; Mario Pirastu[4]; Paolo Gasparini[1,6]; Richard Smith[2]
[1]University of Trieste; [2]University of Iowa Hospitals and Clinics; [3]Institute for Maternal and Child Health IRCCS 'Burlo Garofolo', Trieste, Italy; [4]Institute of Population Genetics, National Research Council of Italy; [5]Institute of Molecular Genetics, National Research Council of Italy; [6]Sidra Medical Research Hospital

Background
Mutations in *GJB2* represent a major cause of pre-lingual, sensorineural non-syndromic hearing loss. The mutation spectrum and the carrier frequency vary among different populations. The splice-site variant c.-22-2A>C has been reported in compound heterozygosity with the 35delG mutation in patients with late onset progressive mild to moderate hearing loss. Similarities of the c.-22-2A>C associated phenotype and age related hearing loss suggest a hypothetical involvement in this latter. The aim of our study is to determine the possible association of *GJB2* c.-22-2A>C variant with ARHL.

Methods
We ascertained a total of 513 Italian samples, 278 affected by ARHL and 235 normal hearing controls, matched by age and ethnicity originating from three small villages in Sardinia. We used targeted genomic enrichment (TGE) and massively parallel sequencing (MPS) to screen 90 known NSHL genes. To replicate results obtained from TGE+MPS, we screened 3 additional Italian cohorts from Northern Italy; Friuli Venezia Giulia Genetic Park (72 patients and 60 controls), Milan (62 patients and 90 controls) and Trieste (18 patients) using RFLP and Sanger sequencing.

Results
The c.-22-2A>C variant in *GJB2* was detected either in heterozygote, compound heterozygote or homozygote state in 68 patients and 58 controls with an allele frequency of 12.95% and 12.77% respectively. Of the patients group, 4 were homozygous and 6 compound heterozygous with other known pathogenic variants in *GJB2* (p.Val37Ile, p.Met195Val, p.Asp159Val). There was no significant difference in allelic or genotypic frequencies between patient and control groups in the Sardinian cohort. Among the 3 other cohorts, the c. -22-2A>C variant was only detected in heterozygote state in 3 patients from Milan (MAF= 2.4%). It was absent form all other cohorts.

Conclusions
The similarity of genotypic and allelic frequencies of the c.-22-2A>C variant between ARHL patients and controls exclude its involvement in this disorder. Moreover, its high allele frequency in both patients and control groups in an Italian subpopulation is in contrast with its overall low MAF in several other populations including Italians (0.06% in ExAc database). These data indicate an ethnic-specific enrichment of this allele in the Sardinian population and strongly advocate for its reclassification as a non-pathogenic variant, although its disease-causing effect when in trans with a truncating mutation cannot be excluded.

PS 569

Missense Mutations of S1PR2 Cause DFNB68 deafness

Rabia Faridi[1]; Regie Lyn P. Cortez[2]; Atteeq Rehman[3]; Inna Belyantseva[3]; Robert Morell[3]; Elizabeth Wilson[4]; Richard Proia[5]; Rivka Isaacson[6]; Tanveer Qaiser[7]; Zil-e Bashir[7]; Muhammad Jawad Hassan[8]; Rana Amjad Ali[9]; Muhammad Ansar[2]; Sulaiman Shams[10]; Wasim Ahmad[11]; Sheikh Riazuddin[7]; Thomas Friedman1[4]; Suzanne M. Leal[2]
[1]National Institute of Health; [2]Baylor College of Medicine; [3]NIDCD, NIH; [4]Laboratory of Molecular Genetics, NIDCD, NIH; [5]Genetics of Development and Disease Branch, NIDDK, NIH; [6]King's College London; [7]Centre of Excellence in Molecular Biology, University of the Punjab; [8]Atta-ur-Rahman School of Applied Biosciences, National University of Science & Technology; [9]University of Lahore; [10]Abdul Wali Khan University; [11]Quaid-i-Azam University

Introduction

The human nonsyndromic deafness locus *DFNB68* maps to chromosome 19p13.2 and was reported in 2006. However, the causative gene was not identified until recently. The *DFNB68* locus spans 1.4 Mb and contains 40 genes. In this study, we used whole genome high density SNP genotyping and whole exome sequencing to identify an additional *DFNB68* family and discovered *S1PR2* as the underlying deafness gene.

Methods
Two consanguineous families segregating deafness were enrolled from Pakistan. Whole exome sequencing was performed using genomic DNA from two affected individuals from each of the two families. Sanger sequencing was used for DNA variant validation and segregation analyses.

Results
PKDF1400 presents with recessively inherited nonsyndromic hearing loss while family *DEM4154* segregates hearing impairment and a skeletal limb deformity. Audiograms of affected members of both families show profound hearing loss. Linkage analyses yielded a maximum multipoint LOD score of 4.6 for family *DEM4154* and two point LOD score of 3.3 for family *PKDF1400* on chromosome19p13.2-p13.12. Exome sequencing of two affected individual from each family revealed two missense mutations of S1PR2; c.323G>C

(Arg108Pro) (DEM4154) and c.419A>G (Tyr140Cys) (PKDF1400). These DNA variants co-segregate with profound hearing impairment in the respective families. Neither of these missense variants are present in 120,000 chromosomes from the Exome Aggregation Consortium database (ExAC), nor in 525 normal hearing individuals from Pakistan. The two DNA variants affect S1PR2 residues that are highly conserved among vertebrates. *S1PR2* is a G protein-coupled receptor that binds to sphingosine 1-phosphate, a sphingolipid thought to be involved in angiogenesis, inflammation, cytoskeletal organization and cell proliferation. In silico prediction tools (Mutation Taster, Mutation Assessor, Poly Phen-2, Provean, FATHMM) as well as protein modeling data predict these variants to be damaging affecting the structure of the ligand binding pocket of *S1PR2*.

Conclusions
We have identified two novel single nucleotide variants of *SIPR2* that cause *DFNB68* hearing loss. There are five related S1P receptors; each one is coupled to unique and overlapping signaling pathways. Our study reveals a necessary function of *SIPR2* in the human auditory system, which is consistent with the deaf phenotype of our reported knockout mouse model (Kono et al., 2007).

Funding
National Institute on Deafness and other Communication Disorders (NIDCD), National Institute of Health (NIH)

PS 570

Mutations of CLPP, encoding a mitochondrial ATP-dependent chambered protease, cause deafness in mouse and man

Alexis Oguh[1]; Ayako Nishio[1]; Shimon Francis[1]; Elizabeth Wilson[1]; Tracy Fitzgerald[1]; Andrew Griffith[1]; Georg Auburger[2]; Suzana Gispert[3]; Lisa Cunningham[1]; Thomas Friedman[1]; Meghan Drummond[1]
[1]NIH; [2]Goethe University Medical School; [3]Johann Wolfgang Goethe-Universität

Background
Perrault Syndrome is a clinically and genetically heterogeneous disorder characterized by hearing loss and ovarian dysgenesis (Newman et al., 2014). Previously, it was reported that mutations of four nuclear encoded mitochondrial genes, including missense mutations of Clpp, cause Perrault syndrome. CLPP is a mitochondrial protease that complexes with the ATP-dependent chaperone CLPX to degrade aggregated or misfolded proteins within mitochondria. In C. elegans, CLPP activity is required for activation of stress responsive genes as part of the mitochondrial unfolded protein response (UPRmt) (Haynes et al 2007, 2010). A null allele of mouse Clpp resulted in infertility in both male and female mice, and acoustic startle response testing suggested these mice had hearing loss. Here, we comprehensively evaluate the auditory phenotype of CLPP-null mice and a mouse model of Clpp with an orthologous recessive missense mutation (p.C143S) associated with Perrault Syndrome (Jenkinson et al., 2013).

Methods
TAL-effector nucleases (TALENs) were used to engineer a mouse model of the p.C143S Clpp missense mutation that causes Perrault Syndrome in humans. The auditory phenotype of Clpp mutant mice was evaluated by serial ABRs and measurements of endocochlear potentials. Additionally, immunohistochemistry and evaluation of hair cell architecture were performed on Clpp+/+, Clpp+/-, Clpp-/- and ClppC143S/C143S mutant mice. Noise exposure experiments designed to induce only temporary threshold shifts in Clpp+/+mice are underway to determine if susceptibility to noise-induced hearing loss is increased in Clpp-mutant mice.

Results
Serial ABR results indicate that Clpp-/- mice have a progressive high frequency hearing loss, first detected at 9 weeks of age. However, no difference in endocochlear potentials was observed between mutant and wild type mice. Preliminary results suggest that there are no obvious structural abnormalities of hair cells in Clpp-/- mice. The phenotype of TALEN-edited Clpp mutant mice and wild type sham control mice will also be reported.

Conclusions
Absence of CLPP leads to progressive hearing loss in mice. Endocochlear potential measurements and immunohistochemistry show that Clpp-/- mice have a functional stria vascularis and no loss of cochlear hair cells. Experiments are underway to determine the reasons for the hearing loss in CLPP deficient mice and by extension, humans.

PS 571

Copy Number Variants in the STRC Gene are a Common Cause of Genetic Hearing Loss in the Japanese Population

Hideaki Moteki[1]; A. Eliot Shearer[2]; Hela Azaiez[2]; Kevin Booth[2]; Christina Sloan[2]; Diana Kolbe[2]; Shin-ya Nishio[1]; Richard Smith[2]; Shin-ichi Usami[1]
[1]Shinshu University School of Medicine; [2]University of Iowa

Background
Sensorineural hearing loss (SNHL) affects at least 1 in 500 newborns, with genetic causes accounting for 50-70% of all childhood hearing loss. Hereditary hearing loss is a genetically heterogeneous disorder with 89 causative genes and more than 2,000 identified disease causing mutations. The majority of those mutations are single nucleotide variants (SNVs) or small indels. Recently, copy number variants (CNVs) have been recognized as a major cause of SNHL, identified in 18 deafness genes. CNVs in the gene *STRC*, involving large deletions or segmental duplication in chromosome 15 at the DFNB16 locus have been shown to be one of the most commonly occurring deafness-causing CNVs. *STRC* encodes the stereocillin protein which is expressed at the tip of stereocilia, and large deletion in *STRC* gene region leads to mild-moderate SNHL. In this study, we used targeted genomic enrichment with massively parallel sequencing (TGE-MPS) combined with CNV detection to identify the genetic cause of hearing loss in a group of Japanese patients with recessive SNHL.

Methods
We examined DNA from 40 probands with SNHL segregated as autosomal recessive inheritance. In all probands, mutations in *GJB2* were excluded by Sanger sequencing. We performed TGE-MPS on probands using post-capture multiplexing followed by OtoSCOPE® screening on the Illumina HiSeq. CNVs were determined using an R script based on a read-depth approach followed by expert curation of identified CNVs.

Results
We identified three probands with deafness-causing CNVs of the *STRC* genetic region. CNV analysis revealed that a deletion involving *STRC* and pseudogene with functionally null *STRC* in one proband, and also identified biallelic partial gene conversion involving *STRC* and pseudogene in the second proband. In the third proband, we identified large deletion of the entire region including *STRC*, the pseudogene and *CATSPER2* leading to deafness infertility syndrome. Their audiograms showed mild-moderate down-sloping hearing loss, and hearing loss phenotype was consistent with previously reported cases.

Conclusion
We identified, for the first time in the Japanese population, CNVs of the *STRC* genetic region as an important cause of hearing loss. We found three patients in our study subjects of 40 probands had a causative CNV in the *STRC* gene. At 7.5%, CNVs in *STRC* are a major cause of mild-moderate autosomal recessive SNHL in the Japanese population.

Funding
This research was supported in part by NIDCD RO1s DC003544, DC002842 and DC012049.

PS 572

Novel and de novo mutations extend association of POU3F4 with distinct clinical and radiological phenotype

Monika Oldak[1]; Agnieszka Pollak[1]; Urszula Lechowicz[1]; Anna Kędra[2]; Piotr Stawiński[1]; Małgorzata Rydzanicz[2]; Maciej Mrówka[3]; Piotr Skarżyński[1,4]; Mariusz Furmanek[5]; **Henryk Skarżyński**[3]; Rałał Płoski[2]
[1]Institute of Physiology and Pathology of Hearing; [2]Warsaw Medical University; [3]Oto-Rhino-Laryngology Surgery Clinic, Institute of Physiology and Pathology of Hearing; [4]Medical University of Warsaw; [5]Bioimaging Research Center, World Hearing Centre of the Institute of Physiology and Pathology of Hearing; Medical Centre for Postgraduate Education

Background
POU3F4 mutations (DFN3) are the most prevalent cause of hearing loss among all the X-linked loci identified to date. Clinical manifestation of DFN3 usually comprises of congenital hearing loss (HL) either sensorineural or mixed, a tendency to perilymphatic gusher during otologic surgery and temporal bone malformations. The aim of the present study was (i) to screen for *POU3F4* mutations in a large group of hearing loss patients, (ii) analyze audiological and radiological features in patients with HL caused by *POU3F4* defects and (iii) to present the authors' operating strategy and practical hints for cochlear implantation in these patients.

Method
Mutations in the *POU3F4* gene were first analyzed in a selected group of patients with gusher or gusher-like incidence (n= 26) through sequencing of the whole gene. Subsequently, the identified mutations were screened for in a large cohort of approx. two thousand males with HL The molecular techniques used to detect *POU3F4* mutations included whole exome sequencing, Sanger sequencing and real-time polymerase chain reaction. Hearing status was assessed with pure-tone audiometry and auditory brainstem response. Computer tomography scans were evaluated to define the pattern of structural changes in the temporal bones.

Results
Three novel (p.Glu187*, p.Leu217*, p.Gln275*) and one known p.Ala116fs141* *POU3F4* mutations were detected in the studied cohort. One of the novel mutations was revealed to be a *de novo* event. All probands with *POU3F4* defects suffered from bilateral prelingual severe to profound HL. Morphological changes of the temporal bone in these patients presented a similar pattern, including malformations of the internal auditory canal, vestibular aqueduct, modiolus and vestibule. Two of the patients with *POU3F4* mutations received cochlear implants with good outcome.

Conclusions
The study extends the association of *POU3F4* mutations with distinct clinical and radiological phenotype. Despite different localization all of the mutations severely affect the protein structure depriving POU3F4 of at least one functional domain. This strong impairment results in a similar and severe clinical manifestation. Sequencing of the entire *POU3F4* gene is recommended in patients with characteristic temporal bone malformations. In view of the many possible intra- and postoperative complications, the decision on cochlear implantation in *POU3F4* patients should be made with special caution and implementation of an appropriate operation technique and electrode array. Results of *POU3F4* mutation testing are important not only for a proper genetic counseling, but also for adequate preparation and conduction of the surgical procedure.

Funding
Founding was received by grants from NCN 2011/03/D/NZ5/05592 (to A.P.), 2012/05/N/NZ5/02629 (to U.L.) and 2013/09/D/NZ5/00251 (to M.R.) and from NCBiR project â€œIntegrated system of tools designed for diagnostics and telerehabilitation of the sense organs disorders (hearing, vision, speech, balance, taste, smell)â€ INNOSENSE, STRATEGMED Program (to H.S.).

PS 573

Impaired post-translational cleavage by novel COCH V123E mutation causes DFNA9-associated sensorineural hearing loss

Jinsei Jung; Mei Huang; Jeon Mi Lee; Jae Young Choi
Yonsei University, College of Medicine

Background

DFNA9 is an autosomal dominant disorder characterized by late-onset, non-syndromic hearing loss and vestibular dysfunction. Mutations in the *COCH* (coagulation factor C homology) gene encoding cochlin are etiologically linked to DFNA9. In previous study, cochlin is cleaved by aggrecanase during inflammation in the spleen and the cleaved LCCL domain functions as an anti-bacterial peptide. However, the physiological role of cochlin in the inner ear is not completely understood.

Method

We performed whole-exome sequencing on a family with a history of late-onset, slowly progressive inherited sensorineural hearing loss. Novel p.V123E *COCH* mutation was found in this family, which might be a DFNA9-causing mutation. To evaluate the molecular function of p.V123E mutated cochlin, we measured conchlin intracellular trafficking, dimer/multimer formation, and post-translational modification.

Results

p.V123E mutated cochlin had no defects in protein trafficking and did not make pathologic dimer/multimer formation. However, p.V123E had a significantly reduced post-translational cleavage by aggrecanase (about 20.5% compared to wild type cochlin). Notably, DFNA9-linked mutant cochlins including p.P51S, p.V66G, p.G88E, p.I109T, p.W117R, p.V123E, and p.C162Y also demonstrated reduced protein susceptibility to cleavage by aggrecanase; thereby, the LCCL domain remained uncleaved and was not secreted in sufficient amounts to extracellular compartment.

Conclusion

These results suggest that the impaired post-translational cleavage of cochlin mutants may be associated with pathological mechanisms underlying DFNA9-related sensorineural hearing loss. Given the role of cleaved LCCL domain in systemic innate immune fucntion, the cleavage deficiency of cochlin may contribute to progressive inner ear dysfunction probably due to recurrent infections and enriched endotoxins in the inner ear.

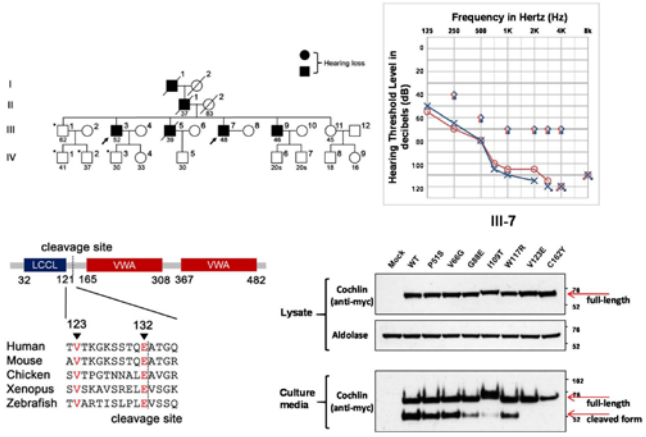

Novel *COCH* p.V123E mutation causes progressive sensorineural hearing loss with autosomal dominant pattern. *COCH* mutations causing sensorineural hearing loss show impaired cochlin post-translational cleavage and secretion.

Funding

the National Research Foundation of Korea (NRF) grant funded by the Ministry of Science, ICT & Future Planning, Korean government (No. 2013R1A1A2059696 and 2013M3A9D5072551 to C.J.Y)

PS 574

Diverse Auditory Phenotypes of KCNQ4 Mutations according to the Underlying Pathogenic Mechanisms

Mina Park[1]; Hyun Bin Cho[2]; Min-Young Kim[3]; Ah-Reum Kim[3]; Tong Mook Kang[2]; Byung-Yoon Choi[3]
[1]Seoul National University Hospital; [2]Sungkyunkwan University School of Medicine; [3]Seoul National University Bundang Hospital

Objective

The *KCNQ4* gene is one of the causative genes, which induce autosomal dominant non-syndromic hearing loss (ADNSH), especially high frequency loss. The KCNQ4 protein, mainly expressed in the outer hair cell of cochlea, plays a major role in recycling of potassium ion, and consists of 6 transmembrane domains (S1-S6) and a hydrophobic pore region between the S5 and S6. In this study, we describe two novel *KCNQ4* mutations, which were located in different domains and showed contrasting audiological configurations. We tried to elucidate the pathologic mechanisms underlying the different phenotype and extend the phenotypic spectrum of *KCNQ4* mutations.

Materials and Methods

Two ADNSH families (SB62-110, SB155-271), which show different audiologic configurations, were recruited. SB62-110 and SB155-271 showed ADNSH prominent in low- and high- frequency hearing loss, respectively. Targeted exome sequencing was performed to reveal a molecular etiology of ADNSH of the two families. The *KCNQ4* mutations detected from the families were cloned in expression vectors and expressed in mammalian cells. We compared the subcellular localization, K-current, and protein expression amounts of mutant KCNQ4 with those of the wild type. Additionally, we

performed protein modeling for the missense mutation of *KCNQ4* to pursue the pathogenic role.

Results
Molecular genetic testing revealed two novel mutations, p.R331Q and c.811_816del from SB62-110 and SB155-272, respectively. We could not identify any difference of subcellular localization of two mutant KCNQ4 protein compared with that of the wildtype. However, the 2 aa deletion mutant (c.811_816del) protein affecting p-loop showed significantly decreased expression compared with wildtype and p.R331Q mutant. Amounts of potassium currents were significantly lowered both in the p.R331Q and c.811_816del compared with wildtype, indicating the pathogenic potential of two variants. The pathogenic mechanism of p.R331Q was predicted to affect interaction of p.R331 residue in the proximal C-tail of KCNQ4 with phosphatidyl inositol 4,5-bisphosphate (PIP2) based on the 3D protein modeling.

Different pathogenic mechanism proposed for p.R331Q may account for the different audiologic configuration from that related to other KCNQ4 variants

Conclusion
Our study extends the audiologic phenotypic spectrum from high frequency SNHL to include low to mid frequency SNHL. The different pathologic mechanism seems to underlie the contrasting phenotypes of KCNQ4 mutations.

PS 575

The role of a new gap junction gene Panx1 in hearing and cell apoptotic process in the cochlea

Yan Zhu; Chun Liang; Jin Chen; Hong-Bo Zhao
University of Kentucky Medical Center

Gap junctions play a critical role in hearing. Pannexin (Panx) is a new-found gap junction gene family and also encodes gap junction proteins in vertebrates. We previously reported that Panx1 is a predominant pannexin isoform and has extensive expression in the cochlea (Wang et al., J, Comp. Neurol. 512: 336-346, 2009). Here, we report that deletion of Panx1 in the cochlea could produce a progressive hearing loss. The auditory brainstem response (ABR) recording showed that hearing loss was moderate to severe and severe at high-frequencies. Distortion product otoacoustic emission (DPOAE) was also reduced. We further found that Panx1 deletion reduced ATP release and endocochlear potential. On the other hand, it has been reported that Panx1-mediated ATP release plays a critical role in cell apoptosis. We found that Panx1 deficiency could also activate Caspase-3 cell apoptotic pathway to cause cell degeneration in the cochlea. Connexin gap junction gene mutations can induce a high incidence of hearing loss. Our study demonstrates that like connexins Panx1 deficiency can also cause hearing loss. Moreover, these new data suggest that pannexin may have an important role in the cell apoptotic process for cell degeneration in the cochlea.

Funding
This work was supported by NIDCD DC 05989

PS 576

Role of Acsl4 and Lipid Metabolism in Hearing Loss

Elisa Martelletti[1]; Annalisa Buniello[1]; Neil Ingham[1]; Jacqueline White[2]; Karen Steel[1]
[1]King's College London; [2]Sanger Institute

Introduction
Acsl4 (Acyl-CoA synthetase long-chain family member 4) is an enzyme which activates free fatty acids converting them to fatty acyl-CoA esters before further metabolic processing. It prefers arachidonic acid as substrate and it is a key enzyme in eicosanoid synthesis and steroid production. We are interested in exploring the effect of Acsl4 mutation and lipid metabolism on auditory function and identifying alternative targets for drug manipulation using small molecules.

Methods
The Acsl4tm1a(EUCOMM)Wtsi mutant mice were generated as part of the Sanger Institute Mouse Genetics Project and exhibited high frequency hearing loss. Auditory Brainstem Response (ABR) measurements were recorded from ketamine/xylazine anaesthetised mice at 4, 8 and 14 weeks old in response to click stimuli and tone pips ranging from 3-42kHz. Immunohistochemestry analysis was performed on sections of whole inner ear in P5 wildtype albino mice. The morphology of the nerve endings in the organ of Corti was studied in whole mount preparations labelled with anti-neurofilament and CtBP2 antibodies.

Results
We found that Acsl4 is expressed in both inner and outer hair cells in the organ of Corti, spiral ganglion and stria vascularis. Low transmission of the mutated allele was observed in the Acsl4tm1a mutant colony, suggesting an effect on viability. Therefore, we generated Acsl4 conditional knockout mice in order to delete this gene only in the inner ear. The Acsl4tm1a mutant mice were firstly crossed with FLPeR (Rosa26) mice producing the Acsl4tm1c allele. These Acsl4tm1c mutant mice were crossed with Sox10-Cre mice producing the Acsl4tm1d allele. We performed ABR measurements at 4, 8 and 14 weeks old. Acsl4tm1c mutant had normal thresholds, as Acsl4 gene function had been restored. On the other hand, Acsl4tm1d mutant mice showed an increase of ABR thresholds for all the frequencies, not only high frequency. Dissection of the middle ear show transparent tympanic membrane, air-filled middle ear cavity and normal morphology of ossicles in Acsl4tm1d mutant mice. Moreover, inner ear clearing revealed no major abnormalities in the overall structure of the inner ear. Preliminary results on the morphology of nerve terminals showed no innervation defect in Acsl4tm1d mutant mice when compared with littermate controls at 4 weeks.

Conclusions
The Acsl4 conditional knockout mice were successfully generated and showed a more severe auditory phenotype which suggests the Acsl4tm1a allele may not completely knockout

Acsl4 function. Moreover, it suggests that Acsl4 is important for normal hearing function locally within the inner ear.

Funding
Action on Hearing Loss and Wellcome Trust for funding. Sanger Institute for the Acsl4 mutant mouse.

PS 577

Hair Cell-Specific Analyses using the Gfi1-cre Mouse

Maggie Matern[1]; Beatrice Milon[1]; Zachary Margulies[1]; Yang Song[1]; Sarath Vijayakumar[1]; Rani Elkon[2]; Sherri Jones[3]; Ronna Hertzano[1]
[1]University of Maryland Baltimore; [2]Tel Aviv University; [3]University of Nebraska Lincoln

Cell type-specific analyses of the inner ear have proved to be extremely helpful in understanding the molecular basis of auditory and vestibular function. These studies range from cell type-specific inactivation of gene expression (i.e. cre-mediated deletion to generate conditional knockout mice) to cell type-specific analysis of gene expression. Within the auditory field, the *Gfi1-cre* knock-in mouse is commonly used for hair cell-specific recombination. GFI1 is a transcription factor that, in the late embryonic and postnatal inner ear, is expressed in all hair cells. *Gfi1-null* mice are profoundly deaf and suffer from severe vestibular dysfunction, while heterozygous littermates of the *Gfi1-null* mice are reported to have normal hair cell development. Based on these data, it has been assumed that replacement of a single copy of the *Gfi1* gene with Cre-recombinase results in hair cell-specific recombination with no subsequent effects on hearing or balance. In this study we performed a comprehensive analysis of the *Gfi1-cre* knock-in mouse to determine the specificity and utility of the *Gfi1-cre* driver in analyzing hair cell-specific gene expression. Using immunofluorescence and FAC sorting, we first show that *Gfi1-cre* mice produce a pattern of gene recombination that is not strictly limited to hair cells. We theorize that this is likely due to a more extensive pattern of *Gfi1* expression in the inner ear than what has been previously described. We also analyze inner ear transcriptomes of both wild type and heterozygous *Gfi1-cre* mice to determine whether the omission of one copy of *Gfi1* affects overall gene expression. We then compare the hair cell translatome as obtained using *Gfi1-cre*/RiboTag mice with transcriptomes of sorted hair cells. Finally, we performed a detailed auditory and vestibular physiologic analysis of the *Gfi1-cre* mice as compared with their wild type littermate controls using auditory brainstem response measurements (ABR) and vestibular evoked myogenic potentials (VsEP). This study is the first to critically evaluate the effects of loss of one copy of *Gfi1* in the *Gfi1-cre* mice both in relation to hearing and changes in gene expression. While our results indicate that *Gfi1*mediated recombination is not specific to hair cells as previously described, these mice are still a valuable model for inner ear research. Overall, a detailed knowledge of the effects that loss of one copy of *Gfi1* has on the inner ear is helpful for appropriate interpretation of conditional knockouts using the *Gfi1-cre* mice.

Funding
NIDCD/NIH R01DC013817 and R01DC03544, DOD CDMRP MR130240, and NIDCD/NIH training grant DC?00046.

PS 578

Methionine Sulfoxide Reducates A (MsrA) Knockout Mice Show Abnormal Expression of MsrB1, MsrB3, and Loss of Spiral Ganglion Neurons.

Safa Alqudah[1]; Marcello Peppi[1]; Jackob Moskovitz[2]
[1]University of Kansas Medical Center; [2]University of Kansas

Background
Methionine sulfoxide reductases A (MsrA) protects the biological activity of proteins from oxidative stress damage and fight onset of age-related hearing loss (Alquadh, ARO 2015). In the current study we characterized the age-related expression of Msrs in adults MsrA knockout mice and the role of MsrA in preventing loss of spiral ganglion neurons from aging.

Method
Real-time qRT-PCR was performed to measure transcript levels of Msr genes in the cochlea of one and six month old MsrA knockout mice and wild-type control. For each sample, the cochleae from both ears were pooled, the bony tissue removed, and the RNA extracted with Trizol reagent. Real-time quantification was accomplished with iTaqTM universal probe Supermix using the following probes (Life Techonologies, NY): MsrB1 (Mm00489121_m1); MsrB2 (Mm00512937_m1); MsrB3 (Mm00622148_m1); and MsrA (Mm01313020).

For histology analysis, 6-month-old wild-type and MsrA knockout mice were perfused intracardially with a fixative solution containing 2.5% glutaraldehyde and 1.5% paraformaldehyde. Both inner ears were dissected, postfixed in osmium, embedded in Araldite, and sectioned at 20 µm on a microtome. Sections were then mounted on microscope slides and spiral ganglion neurons counted.

Results
Except for MsrB2; MsrA, MsrB1, and MsrB3 showed increased levels of cochlear mRNA in 6-month old wild type mice when compared to the same mouse strain at age of 1-month old. Decreased MsrB3 mRNA levels were observed in 1-month-old MsrA knockout mice compared with those of age-matched wild-type mice, but they were recovered by 6 months of age. In contrast, by 6 months of age, MsrA knockout mice failed to increase of MsrB1 mRNA levels, suggesting that MsrA, age, or both might regulate MsrB1 expression in the cochlea.

Semiquantitative analysis of plastic sections of cochlea from 6-month old MsrA knockout mice showed loss of cochlear spiral ganglion neurons by 15% in the 16-26 kHz frequencies region when compared to age-matched control mice.

Conclusion
In this study, we raise the possibility that MsrA represents one component of the protective mechanism that may be responsible for cochlear protection from aging

PS 579

Noncoding Mutations of HGF Cause Human Deafness DFNB39: Confirmation by Mouse Model

Elizabeth Thomason[1]; Julie Schultz[2]; Tracy Fitzgerald[1]; Elizabeth Wilson[1]; Matthew Starost[1]; Thomas Friedman[1]; Robert Morell[1]

[1]National Institutes of Health; [2]GeneDX

Hgf encodes the multifunctional cytokine hepatocyte growth factor (HGF), which is secreted by mesenchymal cells and recognized by the tyrosine kinase receptor MET, expressed by epithelial cells. HGF is critical for cell signaling, cell motility, growth, and development. Noncoding mutations of HGF are associated with nonsyndromic hearing loss (DFNB39) in humans (Schultz et al, 2009). There are multiple isoforms of HGF whose expression, we hypothesize, are influenced by the DFNB39 noncoding mutations of HGF. We have created a mouse model which recapitulates a 10-bp intronic deletion found in some human DFNB39 patients. The 10 base pair deletion is located in intron 5 and founder lines retain a neomycin selection cassette, also located in intron 5 (Hgf tmdel10Neo). A comprehensive phenotypic assessment shows no obvious defects in Hgf tmdel10Neo/del10Neo mice other than cochlear abnormalities. Hearing loss was confirmed by ABR and DPOAE analyses. Hgf tmdel10Neo/del10Neo mice show severe-to-profound hearing loss, while heterozygotes Hgf tmdel10Neo/+ show normal hearing. The hearing phenotype is changed when the Neomycin cassette is removed by crossing to a ubiquitously expressing Cre-recombinase line (Hgf tmdel10*). Hgf tmdel10*/del10* mice show only mild-to-moderate hearing loss. Hgf tmdel10*/del10* mice also demonstrate better resistance to noise-induced hearing loss than their Hgf tmdel10*/+ and Hgf +/+ littermates. A full elucidiation of the HGF isoforms, and their relative abundances, produced from Hgf tmdel10Neo and Hgf tmdel10* alleles will further our understanding of the essential functions of HGF in the human and mouse auditory system.

PS 580

Vestibular schwannomas harbor somatic mutations in multiple genes involved in tumorigenesis

Nathan Schularick[1]; Jed Rasmussen[1]; Rick Nelson[2]; Benjamin Darbro[1]; Girish Bathla[1]; James Clark[1]; Marlan Hansen[1]

[1]University of Iowa Hospitals and Clinics; [2]Indiana University

Background

Mutations in the tumor suppressor gene *NF2* are strongly associated with development of Vestibular Schwannomas (VSs), non-malignant tumors which can result in hearing loss, dizziness, or other cranial nerve deficits. Several observations suggest that additional non-*NF2* somatic alterations may contribute to VS tumorigenesis. To address these observations, we used next generation sequencing to screen for supplementary exonic mutations. We hypothesized that additional somatic DNA lesions important in VS pathogenesis could be elucidated by performing tumor:normal exome sequencing on a cohort of VSs.

Methods

We performed exome sequencing on DNA from 25 VSs with paired peripheral blood samples. Variants identified in the blood leukocytes that were also present in the VSs were subtracted, resulting in a “somatic mutation list” of variants unique to VS tissue. Microarray analysis was also performed to evaluate copy number variants, large chromosomal rearrangements, and as a quality control measure for the HiSeq exome results.

Results

On average, there were 125 (range 22-1038) somatic exonic mutations per VS. 19/25 tumors demonstrated mutations in the *NF2* gene, three of which were from patients with known neurofibromatosis type 2. In addition, several recurring somatic mutations, unique to the VSs, were identified that are: 1) in genes actively transcribed in schwannoma tissues; 2) predicted to be deleterious to protein function; and 3) previously linked to neoplasia and disordered cell growth. Pathway analysis of variants revealed statistically significant enrichment of several pathways implicated in schwannoma tumorigenesis.

Conclusion

These data provide insight into the somatic mutation landscape of VSs and identify additional molecular targets for further research to determine their contribution to schwannoma formation and growth.

Funding

2012 Herbert Silverstein Otology and Neurotology Research Award (ANS/AAO-HNSF) 5 P30 DC010362-03 The Iowa Center for Molecular Auditory Neuroscience (NIH) 5T32DC000040-17? (NIH/NIDCD)

PS 581

Characterization of Lung Fibroblasts from Slc44a2 Mutant Mice

Thankam Nair; Lillian Lu; Bala Naveen Kakaraparthi; Trey Thomas; Pavan Kommareddi; Ariane Kanicki; David Kohrman; Thomas Carey

Kresge Hearing Research Institute, University of Michigan

Background

SLC44A2 (solute carrier 44a2 protein) is abundantly expressed in inner ear supporting cells, lung, leukocytes, kidney, and testis. SLC44A2 is involved in immune-mediated hearing loss, transfusion-related acute lung injury, venous thromboembolism, and as a part of tetraspanin 29 complexes of colon cancer cells. Exons 3-10 encoding the Slc44a2 first extracellular loop were targeted for deletion in an ARHL-resistant FVB/NJ strain (*Cdh23*^{753G}). The FVB/NJ background knockout mice Slc44a2 -/- (KO) display progressive hearing loss, hair cell loss, and spiral ganglion cell loss while heterozygous mice Slc44a2 +/- (HET) exhibit moderate hearing threshold elevation and relatively normal cochlear morphology. In contrast, wild type mice *Slc44a2 +/+* (WT) display normal hearing and normal cochlear morphology.

To understand the functional role of SLC44A2 in an *in vitro* setting, we analyzed lung fibroblast cell lines from Slc44a2 WT, HET, and KO mice.

Methods
Lung samples were harvested from three month-old WT, HET and KO mice and tissue pieces were cultured in Dulbecco's modified Eagle medium containing 10% fetal calf serum (FCS), 50 units/ml penicillin and 50 mg/ml streptomycin at 37°C. Fibroblasts mixed with other types of lung cells proliferated and became confluent in three weeks. Following three passages, 99% of the cells were fibroblasts as verified by an immunofluorescent assay using anti-Vimentin antibody. *Slc44a2* genotypes were verified by RT-PCR of cellular RNA. Proliferation analysis was performed by cell counting and WST-8 proliferation assay.

Results
Vimentin expression was observed in all three cell lines (WT, HET and KO). RT-PCR results demonstrated expression of full-length (3.3 kb) *Slc44a2* transcripts in WTs, truncated mutant transcripts (2.5kb) in KOs and both 3.3 and 2.5 kb transcripts in HETs. Fibroblast proliferation was fastest in KO mice, intermediate in HETs and slowest in WTs. The differences were more evident in early passages (P1-P30) compared to later ones (P50-P70). Differences in cell dissociation during trypsinization were observed among the three genotypes. KO cells dissociated more quickly compared to HET and WT cells.

Conclusion
Slc44a2 protein deletion resulted in a less adherent and more proliferative growth pattern in mouse lung fibroblasts. Our results suggest that SLC44A2 has a key role in normal cell growth and adhesion, and are in agreement with previous observations that HNA-3a antibody bound to Slc44a2 on mice lung endothelial cells, resulting in cadherin degradation and endothelial barrier disturbance (Bayat et al., 2013).

Funding
NIH NIDCD R01DC03686, P30 DC05188

PS 582

Improvement of hearing in A/J mice by Nerve Growth Factor

Lixiang Gao; Ruli Ge; **Fengchan Han**
Binzhou Medical University

Background
A/J mice are a typical mouse model of age related hearing loss. This project was carried out to investigate the otoprotective effects of mouse nerve growth factor (mNGF) on A/J mice.

Study Design
A/J mice at the age of 7 days were randomly divided into 3 groups: a NGF treated group, an injection water (H_2O) treated group and an untreated group (n = 12-15 for each group). NGF was given by intramuscular injection in hips every other day from P7. Otoprotective effects of GNF on A/J mice were observed in a time course manner.

Methods
Auditory-evoked brainstem response (ABR) thresholds were measured in the three groups at age of 3, 4, 6 and 8 weeks, respectively. Histological features of spiral ganglion neurons (SGNs) were observed by HE staining. Whole mount hair cell counts were made at 8 weeks of age. Expression levels of apoptosis related genes were tested by real-time quantitative RT-PCR and Western blot.

Results
The results showed that NGF significantly decreased ABR thresholds in A/J mice as compared with those of the H_2O treated or untreated mice at stimulus frequencies of click, 8-, 16- and 32- kHz at 6 or 8 weeks of age. Moreover, NGF preserved hair cells and SGNs in the cochleae at 8 weeks of age. Further experiments revealed that the expression levels of caspasse-3 in the cochleae of NGF treated mice were inhibited.

Conclusion
NGF showed otoprotective effects by preserving SGNs and hair cells in the cochleae. Inhibition of the apoptotic related pathways was likely involved in the otoprotective process of NGF.

Funding
This project was supported by National Natural Science Foundation of China (No. 81271092, 81570927), Grant for Scientific and Technological Development in Shandong Province (2014GSF118083) and Research Initiation Grant of Binzhou Medical University (BY2012KYQD01).

PS 583

Hearing Loss of Compound Heterozygous Cdh23 Mutant Mice can be Ameliorated by Chemical Chaperone 4-Phenylbutyric Acid

Jing Yuan[1,2]; Bo Li[3]; Juan Hu[4]; Wen Kong[1]; Wenwen Wang[1]; Yu Sun[1]; Li Zhang[3]; Yuzhu Wan[5]; Jessica Pham[6]; Weijia Kong[1]; Qing Zheng[2]
[1]Huazhong University of Science and Technology; [1]Huazhong University of Science and Technology; [2]Case Western Reserve University; [2]Case Western Reserve University; [3]Binzhou Medical University; [4]Xi'an Jiaotong University School of Medicine; [5]Shandong University; [6]Cleveland School of Sciene and Medicine

Hearing loss is one of the most common sensory disorders affecting millions of people. Quite a few genes associated with hearing loss have been found encoding proteins that compose hair bundles, organelles that detect and amplify sound. We previously revealed that mutations of *cadherin 23* (*Cdh23*) contribute in apoptosis and cause hearing disorders like Usher syndrome type 1D (USH1D), non-syndromic autosomal recessive deafness 12 (DFNB12), and age-related hearing loss (AHL) as their role in encoding tip-link in hair bundles is compromised. In our single point mutant model of *erlong* (*erl*) and loss function alleles *waltzer 2J* (v^{2J}), increased endoplasmic reticulum (ER) stress have also been observed to be reduced either by chemical chaperones or knocking out

the gene of the transcription factor C/EBP homologous protein (CHOP). To evaluate these two recessive *Cdh23* mutations, we hybridized them together and generated compound heterozygous mutants. We found earlier (than *erl*) onset of high frequency hearing loss with matching morphological outer hair cell (OHC) loss. We worked through molecular biological analysis to justify these codominant effects which have shown ER stress-induced apoptosis initiated by unfolded protein response (UPR) signaling. Meanwhile, daily treatment with intraperitoneal 4-phenylbutyric acid (4PBA) as a chemical chaperone significantly restored the hearing function and reduced ER stress without causing apparent side effects. We also observed the same impaired UPR and excessive CHOP expression in aged C57BL/6 mice, therefore, proving the universal ER stress in hearing impaired models. As a whole, the data demonstrated that ER stress played a part in inducing hearing dysfunction in *Cdh23* mutant mice and 4PBA as a potential amelioration in the pathological process.

Funding
the China Scholarship Council (No. 201406160073), the National Institutes of Health (R01DC009246), the Foundation of Taishan Scholar (tshw20110515), the Natural Science Foundation (ZR2012HZ004) of Shandong Province, and the National Natural Science Foundation of China (81271085 and 81400467), the Key Project National Natural Science Foundation of China (81230021).

PS 584

A mutated PENDRIN formed intracellular aggregations and caused increase of susceptibilities for cell stress in the inner ear cells induced from Pendred syndrome patients-specific iPS cells

Makoto Hosoya[1]; Masato Fujioka[1]; Kaoru Ogawa[1]; Tatsuo Matsunaga[2]; Hideyuki Okano[1]
[1]Keio university; [2]Tokyo Medical Center

Background
Pendred Syndrome is an autosomal-recessive disease characterized by congenital hearing loss and thyroid goiter. The incidence of the disease is estimated at 7.5 - 10 in 100,000. Pendred syndrome may account for as many as 10% of the cases of hereditary hearing loss, making it most common form of syndromic hearing loss. The deafness is usually seen at the born but can be variable in its expression and, because sometimes the hearing loss appears during childhood and is progressive, understanding pathophysiology of the syndrome is of great importance for the future therapeutics. In 1997, *SLC26A4* was identified as a causative gene of Pendred Syndrome. The gene encodes an anion transporter, PENDRIN and, according to the previous reports based on the mouse studies, the protein exchanges Cl- and HCO3- in the inner ear. Here, we examined the phenotype of inner ear cells derived from Pendred syndrome patients via iPS cells to explore the direct pathophysiological roles of mutated PENDRIN in the syndrome.

Methods
Pendred syndrome/DFNB4 specific-iPS cells were established from three patients' peripheral blood using episomal expression vectors with electroporation. Three germ layers differentiation abilities were confirmed with in vitro embryoid formations. The efficiencies of otic induction abilities were estimated and the lines effectively induced to otic progenitor cells were selected. In the next step, we induced PENDRIN positive inner ear cells from control and disease specific iPS cells via otic progenitors using specific induction medium. Localizations of mutated PENDRIN were examined by immunohistochemistry in these induced cells.

Results
Mutated PENDRIN formed intracellular aggregations in these induced cells from iPS cells established from patients. The phenomenon was not found in control cells.

Discussion
Intracellular aggregations of mutated proteins were observed in neurodegenerative diseases including Huntington's disease, Parkinson's disease and Alzheimer's disease. In those diseases, protein aggregations with mutated proteins cause toxic effects on cell viabilities, directly or indirectly, and resulted in cell death following specific neural symptoms. Our results suggest that those phenomena observed in neurodegenerative diseases may also occur in the inner ear cells of Pendred syndrome patients, which may account for the progressive hearing loss in the patients.

PS 585

Adaptation to Click Trains of the Auditory Brainstem Response in Children

Andrew Dimitrijevic; Lisa Hunter; David Moore
Cincinnati Children's Hospital

Hearing ability is not fully explained by the pure tone audiogram; some individuals with normal clinical pure tone thresholds (≤ 20 dB HL) have impaired speech perception at suprathreshold levels in noisy environments. One important aspect of successful speech perception is sub-millisecond precision of neural encoding of sounds. Auditory neuropathy is associated with reduced neural precision at the level of auditory nerve, and results in severe difficulty with speech in noise. We have previously shown that people with auditory neuropathy show abnormal auditory brainstem responses to click trains (Wynne *et al.*, Brain, 2013). Typically, in adults, the ABR to a train of clicks will adapt after 3-5 clicks, resulting in a stable ABR that shows no further changes in amplitude or latency to clicks further along in the train. Atypical responses are characterized by absent or variable ABRs to successive clicks in the train. The aim of this study was to study the maturation of adaptation to auditory click trains in children. This has not been previously studied to our knowledge.

ABRs using click train stimuli were collected from 11 typically developing children aged 4 to 12 years with normally sensitive pure tone thresholds and 5 normal hearing adults. Stimuli were constructed in trains, each of 10 clicks, 15 ms apart, presented every 250 ms. This paradigm yields 10 individual neural

responses within each train, one response corresponding to each of the individual click positions. Adaptation of the ABR was quantified by measuring amplitude and latency of waves I and V as a function of the click position within the train.

ABRs were observed to all the clicks in the stimulus train in the children. Children showed delayed responses at all click positions compared to adults. An adult-like pattern of ABR adaptation was observed in children. No changes in amplitude/latency of waves I or V were seen after the third click position in the train indicating that the children adapted by the third click. No differences in the rate of adaption were observed as a function of age.

These data demonstrate that the click train ABR paradigm can be recorded in children and suggest that auditory adaptation at the level of the auditory nerve and brainstem is mature at an early age.

PS 586

Minimum Response Levels obtained with Insert Earphones; Behavioural Observation Audiometry Protocol for Infants aged 2-6 Months

Esther Wiersinga-Post; Saskia Haaksma-Schaafsma; Pim Van Dijk
University of Groningen, University Medical Center Groningen

Objective: to obtain ear and frequency specific minimum response levels (MRLs) in infants, with a clinically applicable method of behavioural observation audiometry. The method involves the use of insert earphones and two observers. The second observer was blinded to the stimulus presentation and received instant feedback on his or her performance via an earpiece.

Subjects: 38 infants with normal hearing and normal overall development aged two to six months.

Results: nine infants were excluded for various reasons: two did not accept the insert earphone, three were too fuzzy to test, and four had flat tympanograms. MRLs were successfully obtained in the remaining 29 infants.

With respect to the reliability of the blinded second observer and/or the consistency of the child's behaviour to sound and silence, the various tests differed from each other, as measured by a false alarm rate (SC+). The SC+ was 25% or lower for eleven infants, in between 25% and 45% for ten infants, and above 45% for eight infants. A second session during the same visit, performed after a short break of at least ten minutes, showed a decrease in the SC+ in 77% of the cases. After two sessions, a SC+ of 25% or below was obtained in 38% of the children, 47% of the total number of MRLs (fig. 1).

MRLs decreased significantly with increasing age, from about 65 dB, 50 dB to 40 dB in the two months, four months and six months old infants, respectively (fig. 2). The dependence of MRLs on stimulus frequency was not significant.

Discussion/Conclusion: insert earphone testing is well accepted in the majority of very young infants.

Reliable MRLs, with a SC+ of 25% or below, could be obtained in a significant portion of infants, in two brief testing sessions. The reduction of the SC+ in the second session suggests that performing a second session at the same visit is efficient and effective in obtaining more reliable MRLs in clinical BOA.

Although the procedure described does not provide MRLs that are close to the physiological thresholds of hearing, the information obtained will be useful in the clinical management of young infants. For example, since the MRLs obtained are often better than about 80 dB, this data may be of clinical relevance in important intervention decisions, such as the choice between an acoustic hearing aid or a cochlear implant.

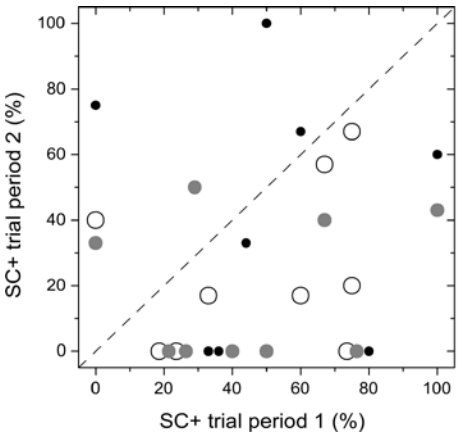

Fig. 1: *False alarm rate (SC+) in MRL trial period 2 compared to trial period 1. Each data point represents one infant (N=26).*

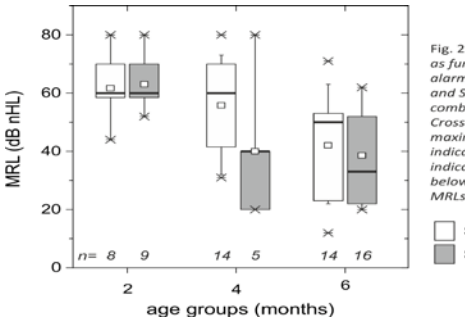

Fig. 2: *Box and whisker plots of the MRLs as function of subject age and false alarm rate (SC+). For each age group and SC+-range, the MRLs were combined across the test frequencies. Crosses indicate the minima and maxima. The small open white squares indicate the averages. The thick bars indicate median values. The values below the bars indicate the number of MRLs included.*

Funding
Rensina Anna Meisner Foundation, Stichting Gehoorgestoord-de Kind, Heinsius Houbolt Foundation.

PS 587

Temporal Modulation Cutoff Frequency in Normal Hearing Infants

David Horn; Caitlin Hutton-Gerhards; Lynne Werner
University of Washington

Introduction

Behavioral measures of temporal processing develop into school-age, although the temporal response properties of the peripheral auditory system mature during infancy. An explanation for this phenomenon is that temporal tasks are affected by non-temporal "efficiency" factors including intensity resolution, attention, memory, and internal and physiologic noise. The cutoff frequency of the temporal

modulation transfer function (TMCF) is a measure of temporal resolution independent of efficiency.. Normal hearing children have mature cutoff frequencies by age 4, but this measure has not been obtained from younger children. In this study, we measured TMCFs for individual normal-hearing infants by varying frequency modulation at a constant modulation depth relative to their low-modulation frequency amplitude modulation (AM) detection threshold. The hypothesis was that 3-month-old infants would have poorer AM detection thresholds than adults but mature TMCFs.

Methods
Three-month-old infants and young adults were tested. All listeners reported normal hearing and passed tympanometric screening. Infants passed newborn hearing screening and had no risk factors for hearing loss. Stimuli were 2-s bursts of Gaussian noise with 15-ms up/down ramps; modulation was introduced 1-s into the burst. Stimuli were presented in soundfield at 65dBA. An observer-based psychoacoustic procedure was used to measure listeners' sensitivity to modulation.For each listener, AM detection threshold at a 10 Hz modulation frequency was measured by varying modulation depth adaptively. Subsequently, the TMCF was estimated by varying the modulation frequency adaptively at a modulation depth 4 dB greater than the 10-Hz AM detection threshold.

Results
Mean AM detection threshold was significantly higher for adults than for 3-month-old infants. In contrast, TMCFs were similar for adults and infants. TMCFs obtained by this two-point method were similar to those reported elsewhere. However significant inter-subject variability existed in both the infant and adult listeners.

Conclusions
Despite immature sensitivity to modulation, the TMCF is adultlike in human infants by 3 months of age suggesting mature temporal resolution by this age. The 2-point method used here appears to be a feasible method for estimating the TMCF in infants and children.

Funding
NIDCD: K23DC013055, R01DC00396, P30DC04661 Seattle Children's Foundation

PS 588

Auditory sequence processing and language skill in mid-adolescence

Timothy Griffiths; Catherine Davison; Sukhbinder Kumar; Faye Smith; Manon Grube
Newcastle University

The relationship between auditory processing and language skill has long been subject of debate. Recent evidence suggests a specific relevance for rhythm as a form of "temporal scaffolding" relevant to both music and language perception and production. Our previous school-based work in over 200 early-adolescent English speakers showed a moderate significant correlation between the perception of short isochronous sequences and language skill (Spearman's rho correlation coefficients of > 0.3, robust against partialing out non-verbal IQ; Grube et al. 2012, 2013). In young adults in contrast, we found a strong and significant correlation with the processing of more complex rhythmic sequences with a roughly regular beat and to a lesser degree for those with a metrical beat (Spearman's rho in the region of 0.6; Grube et al., 2014). The data suggest a developmental shift in the relationship between auditory and language skills toward an increased relevance of more abstract rhythm in older subjects. The present work assesses the correlation between rhythm analysis and language skill in mid-adolescence. Initial analyses (n = 212) reveal moderate but robust and significant correlations with measures of language skill (spelling, reading, non-word reading, rhyme decision, rapid automated naming, spoonerisms) for both the processing of short isochronous sequences and longer, more complex sequences with a roughly regular beat (Spearman's rho correlation coefficients of about .3). No such robust correlations were seen between language skill and the processing of single time intervals or metrical rhythms.The data support the emergence of a developmental change in the relationship between auditory rhythm processing and language skill during adolescence, toward an increase in the relevance of higher-level sequence analysis. On-going work is investigating parallel development in pitch sequence processing.

Funding
Wellcome Trust (UK) Medical Research Council (UK)

PS 589

The Contribution of Contextual Cues to the Development of Speech Recognition in Noise in School-Age Children

Topaz Topper-Viner[1]; Karen Banai[1]; **Hanna Putter-Katz**[2]
[1]University of Haifa; [2]Ono Academic College

Introduction
The processing of speech under degraded listening conditions depends on sensory as well as on linguistic and cognitive factors, but the interaction of these factors over the course of normal development is not well understood. Here we asked whether the use of linguistic context to support speech-recognition in noise improves with age and whether this improvement can account for age-related changes in recognition.

Methods
The ability of 90 normal-hearing children (ages: 6-12 years) to repeat 60 target words embedded in background babble-noise was studied in two different conditions: (1) low predictability sentences (LP) - target words were not predictable from the context of each sentence; (2) high predictability sentences (HP) – target words could be predicted from sentence context. The ability to repeat single words was also evaluated as a baseline. SNR was adapted based on listeners' responses using a staircase procedure and repetition thresholds were calculated for each condition. Naming, verbal memory and non-verbal cognitive skills were also evaluated.

Results
Repetition thresholds improved as a function of age as well as of increasing context (HP < LP < baseline). Furthermore, performance gains associated with sentence context significantly increased with age. Linear regression was used to quantify the contributions of age, sensory acuity (baseline performance) and language skill (naming) to the context effect (threshold difference between the LP and HP conditions). These variables accounted for 19% of the variance in the context effect, with significant contributions of both language skill and sensory acuity.

Conclusions
The current findings show that age-related gains in speech processing under adverse conditions might reflect increases in both sensory and linguistic skills, including the use of linguistic context.

PS 590

Sheep as an Animal Model for Hearing Implants

Martijn Agterberg[1]; X. Frank Walboomers[2]; Andy Beynon[2]; Theo Peters[2]; Joost Zwartenkot[2]; Rishub Verma[3]; Daniel Smyth[3]; Emmanuel Mylanus[2]
[1]Radboudumc, Donders Institute For Brain, Cognition and Behaviour; [2]Radboudumc; [3]Cochlear Technology Centre

Objective
As the developments of acoustic implant technology continues and evolves, the need for a large animal model is increasing. In the present study we investigate whether the sheep skull and cochlea are suitable for testing human hearing implants. Both the bone tissue formation and the functionality of the cochlea are investigated.

Material and method
Skulls of adult sheep cadavers (n=6), and six adult sheep, were used for implantation of bone-conduction hearing implants (n=3) and the Codacs® (n=3). Correct device placement was verified by cone beam CT and histology. Auditory brainstem responses (ABRs) were recorded in anesthetised animals in the surgery room, and in restrained animals at the farm. Histological sections of the osseointegrated bone-conduction device were produced with a modified sawing microtome technique.

Results
Two year old sheep are a good in vivo model for both bone-conduction devices and Codacs®. The sheep middle ear and cochlea are, although smaller, highly similar to the human middle ear and cochlea. With the sawing microtome technique relatively large titanium implants (>3 cm) could be processed. Histological evaluation demonstrated formation of new bone around the screw of the bone-conduction device. Functional ABRs could be recorded in awake animals.

Conclusion
Older sheep are valuable as animal model for the development of new hearing implants especially when larger (human) implants are tested. In vivo implantation of Codacs is complex and the surgery takes >4 hours. Functional measures can be collected in awake animals because sheep can easily be restrained up to 30 minutes without causing stress.

References
Schepbel et al. (2006)
Schnabl et al., 2012
Ter Haar et al., 2010
Eeg-Olofsson et al., 2014

Funding
This work was funded by Cochlear Technology Centre, Mechelen, Belgium

PS 591

Maturation of Auditory Cortical Microstructure is Disrupted in Preterm Infants

Brian Monson[3]; Zach Eaton-Rosen[1]; Simon Warfield[2]; Einat Liebenthal[3]; Terrie Inder[3]; Jeffrey Neil[2]
[1]University College London; [2]Boston Children's Hospital, Harvard Medical School; [3]Brigham and Women's Hospital, Harvard Medical School

Background
The effect of premature birth on human auditory neurodevelopment has been a difficult question to address. Genetic factors and experience with the altered acoustic environment of the neonatal intensive care unit (NICU) are each likely to play a role. Previous work measuring cortical responses suggests that preterm birth is associated with atypical development of auditory cortical processing in infancy, but the responsible neural underpinnings are unknown. Variation in metrics of water diffusion, obtained from diffusion-weighted magnetic resonance imaging (MRI), has proven useful for tracking maturation of cortical gray and white matter microstructure during early human brain development *in vivo*. Here we used diffusion MRI to assess the effect of prematurity on auditory cortical microstructure in infancy and to characterize the maturational timeline of auditory cortex microstructure for preterm infants.

Methods
We analyzed data from 74 infants born very preterm (<30 weeks gestation) and 11 infants born full term who each underwent diffusion MRI at term-equivalent age (38-40 weeks postmenstrual age). We also analyzed data from a subset of very preterm infants who each underwent up to four serial MRI scans during NICU stay (between 26 and 40 weeks postmenstrual age). Values for diffusion metrics of fractional anisotropy and mean diffusivity were obtained from regions of interest (ROIs) placed bilaterally in gray and white matter located within and adjacent to Heschl's gyrus.

Results
The formation of Heschl's gyrus was apparent from approximately 27 weeks postmenstrual age. At term-equivalent age, mean diffusivity in both gray and white matter was significantly higher for the very preterm group, indicating lower tissue density. Between-group differences in fractional anisotropy were observed only for white matter, with values for the very preterm group being significantly lower. Both results point to less mature and/or injured gray and white matter in

Heschl's gyrus for very preterm infants. Similar effects were observed for both hemispheres.

Conclusion
Maturation of auditory cortical gray and white matter microstructure is disrupted by very preterm birth. Results are consistent with a delay in maturation of auditory cortex, although injury cannot be ruled out. The finding of reduced anisotropy in white matter suggests fewer and/or less well organized fiber bundles. Disrupted gray and white matter development might account for abnormal auditory cortical processing previously reported in the preterm population.

Funding
This work was funded in part by NIH grant number R01 HD05709801.

PS 592

Cortical Representation of Bilaterally Presented Sounds in Children with Two Cochlear Implants

Vijayalakshmi Easwar; Michael Deighton; Parvaneh Abbasalipour; Hiroshi Yamazaki; Melissa Polonenko; Blake Papsin; Karen Gordon
The Hospital for Sick Children, University of Toronto

The objective of the present study is to assess effects of simultaneous versus sequential cochlear implantation on cortical binaural processing in children with early onset deafness. Previous studies show that treatment of bilateral deafness with a unilateral CI deprives the auditory system of bilateral auditory stimulation during early development, resulting in an abnormal strengthening of auditory pathways from the first implanted ear. This developmental plasticity of neural pathways from the hearing ear may disrupt the symmetry of binaural pathways, leading to compromised binaural processing. We therefore hypothesized that cortical representation of bilaterally presented sounds in simultaneously implanted children will be symmetrical and similar to age-matched peers, whereas, abnormal binaural processing will be observed in sequentially implanted children.

Participants included 34 bilaterally implanted children; 26 were simultaneously implanted (aged 6.7±1.3 years), and 8 were sequentially implanted (aged 4.35±3.1 years), receiving their second (left) CI after 9.7±3.1 years of unilateral hearing experience with the right CI. Fifteen age-matched normal hearing children were also recruited. Binaural listening experience at test was 4.1±1.0 and 0.56±0.4 years in simultaneously and sequentially implanted groups, respectively. Cortical auditory evoked potentials (CAEPs) were recorded across 64 cephalic electrodes to unilaterally and bilaterally presented stimuli. Biphasic pulses were delivered to electrode #20 (apical end of array) in children with CIs and clicks were delivered through insert earphones in children with normal hearing. The strength and location of stimulus-related activity underlying CAEP peaks were evaluated using the time-restricted artifact and coherent suppression (TRACS) beamformer method.

CAEP waveforms in simultaneously implanted children showed a Pci-N2ci complex during unilateral stimulation as previously reported and the same was observed in response to bilateral stimulation. In sequentially implanted children, a mature CAEP waveform (P1-N1-P2) was observed when the first implanted ear was stimulated and an Nci-Pci waveform was observed when the left ear was stimulated, as previously reported; in the bilateral listening condition, a negative peak at ~100ms was followed by a positive peak at ~150ms. Preliminary analyses indicate activity in both left and right temporal auditory cortices for both peaks in simultaneously implanted children and their normal hearing peers. However, sequentially implanted children showed greater variability with right temporal hemispheric dominance during the negative peak and left temporal hemispheric dominance during the positive peak. Differences in pattern of cortical activity between the groups may be due to chronological age and/or binaural listening experience. This will be further investigated in age-matched normal hearing children.

Funding
Restracomp, Canadian Institute of Health Research

PS 593

A Developmental Analysis of Infant Vocalizations under a Sparse-code Framework

Hiroki Terashima; Shigeto Furukawa
NTT Communication Science Laboratories

Background
The sparse coding model of natural sounds (Lewicki, 2002) related the response characteristics of auditory nerve fibres to sparse codes of human adult vocalizations, supporting the idea of efficient coding. It remains unclear, however, if we can also apply the model during child development. In the present study, we investigated the development of sparse representations of natural voices of human infants and compared them with that of auditory filters.

Method
Natural voices of infants and their parents were taken from the NTT-infant database (Amano et al., 2009), which consists of annotated longitudinal recordings of spontaneous utterances in home environments from five Japanese infants and their parents (three families; from birth to five years old). We divided the recordings into five classes: month 0-20, 21-40, 41-60 (infant voice), adult-to-infant, and adult-to-adult. Their sparse waveform representations were analysed in terms of their centre frequency and tuning sharpness (Q value), following the method of (Lewicki, 2002).

Results
Previous infant studies had demonstrated that, over the development, the auditory filters either gradually increase their sharpness or achieve sharpness comparable to adults at birth. Parallel developmental dynamics would be found in the sparse codes of infants' voice, if the sparse coding model were always applicable during the development. Nevertheless, our results showed that the sparse codes of infants' voices exhibit consistently sharper tuning properties

than those of their parents' voices, suggesting the decrease of tuning sharpness after the recording period. An additional analysis revealed that the sharpness distribution of sparse codes of infants' voices is closer to that of an adult female voice than an adult male voice.

Conclusion
In the early stages of development, the sparse coding model does not explain the relationships between the auditory filter and sparse code of voices: the sparse code of infants' voices shows sharper frequency tuning than both the auditory filter of adults and that of infants. This suggests that the efficiency described by the sparse coding model slowly develops on a ten-year time scale.

PS 594

Expression pattern of Wolframin, the Wolfram syndrome 1 gene (WFS1) product, in Common Marmoset (Callithrix jacchus) inner ear

Noriomi Suzuki[1]; Masato Fujioka[1]; Makoto Hosoya[1]; Naoki Oishi[1]; Takashi Inoue[2]; Hideyuki Okano[1]; Kaoru Ogawa[1]
[1]Keio University; [2]Central Institute for Experimental Animals

Authors

Noriomi Suzuki, Masato Fujioka, Makoto Hosoya, Naoki Oishi, Takashi Inoue, Hideyuki Okano, Kaoru Ogawa

Background
Wolfram syndrome (OMIM: 222300) is an autosomal recessive disorder of the neuroendocrine system, known as DIDMOAD (Diabetes Insipidus, Diabetes Mellitus, Optic Atrophy, and Deafness) syndrome. Patients show mutations in the *WFS1 gene*. The *WFS1* encodes an 890 amino acid protein, called Wolframin, that is predicted to have nine helical transmembrane segments in the endoplasmic reticulum (ER). Wolframin functions in ER calcium homeostasis and unfolded protein responses. Dysregulation of these cellular processes results in the development of ER stress, leading in apoptosis. Hearing loss associated with Wolfram syndrome is typically a high frequency sensorineural hearing loss, although low frequencies may become affected as well (1)(2). Limited literatures describing temporal bone pathology indicate both hair cell loss in the lower basal turn and the atrophy of stria vascularis in the apical turn (3). On the contrary, the expression of Wolframin protein in mice was observed widely and uniformly in the sensory epithelium but was absent in the stria vascularis (4). While *WFS1* knockout mice suffer diabetes, the hearing level of the strain was completely normal. In order to elucidate the discrepancy of the phenotype among species, and to explore the pathophysiology of deafness associated with *WFS1* mutation, we examined expression of Wolframin in the Common Marmoset (*Callithrix jacchus*), non-human primate, inner ear.

Method
Young adult marmosets (n=5) were transcardially perfused with saline followed by fixative with 4%PFA. The fixed temporal bone of marmoset was prepared in the cryosection after decalcification by EDTA. Immunohistochemistry for WFS1 was performed with rabbit anti-WFS1 antibody 1:200 (HPA029128, SIGMA-ALDRICH).

Result
The result revealed strong immunoreactivity in outer hair cells, external sulcus cells, Claudius cells, Hensen cells, spiral ganglion and stria basal cells.

Conclusion
The expression pattern of WFS1 in Common Marmoset inner ear was different from that of mouse. In stria vascularis and organ of Corti where strong immunoreactivity of WFS1 found in Common Marmoset, prominent mutations like atrophy or loss are observed in human inner ear of Wolfram syndrome. The pattern may account for the hearing phenotypes in Wolfram syndrome patients. Common Marmoset would be a powerful and extensive tool for investigating pathophysiology of human auditory disorder that cannot be explained by rodent mutant models.

Reference
(1) Cremers et al. 1977, (2) Higashi et al. 1991, (3) Hilson et al. 2009, (4) Cryns et al. 2003

PS 595

Sub-populations of Mitochondria Characterized in the Vestibular Sensory Epithelium

Anna Lysakowski[1]; Aashutos Patel[1]; Sofia Sobkiv[1]; Vidya Babu[2]; Steven Price[1]; Guy Perkins[3]
[1]University of Illinois at Chicago; [2]Illinois Math and Science Academy; [3]University of California, San Diego

The central hypothesis of the study is that *mitochondria in hair cells and inner ear sensory epithelia are non-homogeneous and that structural and molecular differences they exhibit are related to their differential responses to ototoxic insults, such as aminoglycoside toxicity and noise*. It is likely that due to variations in physical structure and corresponding molecular composition, various sub-populations of hair-cell mitochondria are differentially affected by ototoxic insults, such as aminoglycoside antibiotics and chemotherapeutics. EM tomography and graphic reconstruction methods were used. Our results indicate that there are three different-sized populations of mitochondria in the vestibular sensory epithelium (based upon volume and surface area measurements): large (found in the subcuticular region of central type I hair cells); medium (in hair cells and afferents); and small (in efferent boutons). We are reconstructing several examples of each type to determine the average volume and surface area of each type, and their number and type of cristae (tubular, lamellar or tubulo-lamellar). In addition, we are investigating the number, size and locations of crista junctions (intersections with the inner mitochondrial membrane) in relation to other significant structures within the cell. As one example of our structural findings, we found that in many hair cells, the cristae of mitochondria adjacent to a striated organelle (SO) are polarized toward this organelle (see Figure). This means that these cristae, which are lamellar, align end-on with the striations of the SO and

that the crista junctions (CJs) open towards the SO on that side of the mitochondrion. Crista junctions, which function as barriers to the diffusion of molecules inside mitochondria, (thus concentrating the oxidative phosphorylation complexes that generate ATP) are also thought to be key regulators for release of apoptotic effectors. We are also attempting to characterize the three size sub-populations by ratiometric measurements of mitochondrial potential using JC-1. We conclude that there are significant differences in mitochondrial morphology among these three sub-populations.

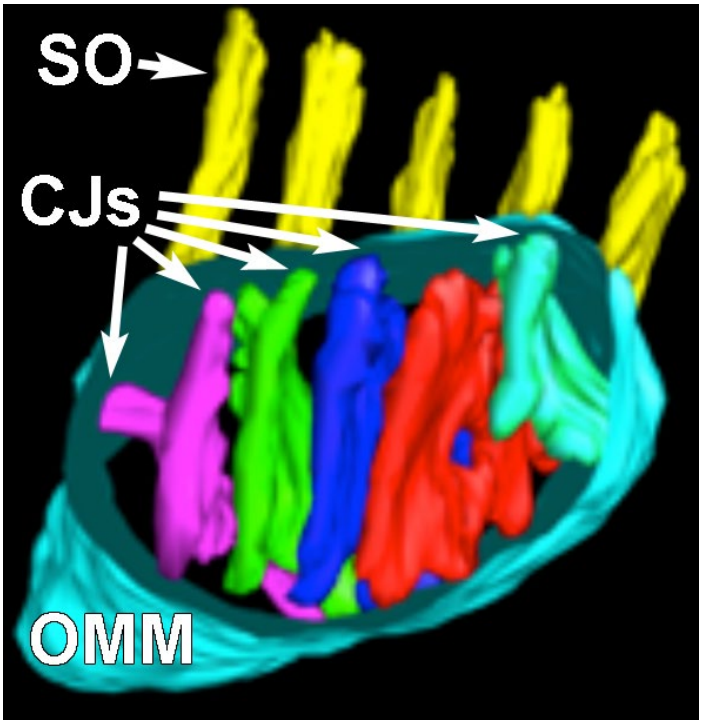

Funding
Supported by NIDCD grant R21-DC013181

PS 596

Physiological Effects of BODIPY-xyloside GAGs on Transduction by the Semicircular Canals

Holly Holman; Vy Tran; Balagurunathan Kuberan; Richard Rabbitt
University of Utah

Background
Proteoglycans and glycosaminoglycans (GAGs) in the central nervous system (CNS) have been shown to be upregulated following nerve injury. An overabundance of GAGs has been reported to inhibit nerve function including causing depression of synaptic transmission. In healthy neuronal tissue, GAGs facilitate modulation of synaptic transmission, neuronal plasticity, and cellular excitability. While characterization of proteoglycans and GAGs in CNS have been well studied, considerably less research has focused on their function in inner ear physiology. Here, we describe the use of a β-D-xyloside to address what the physiological roles of proteoglycans and GAGs are in the vestibular system of *Opsanus tau*.

Methods
To aid in the characterization of these complex and heterogeneous GAGs, we used a newly designed, BODIPY-xyloside (BX). BX, like other β-D-xylosides, interrupts normal proteoglycan post-translational processing by acting as an artificial acceptor for xylosyltransferases. Adding β-D-xylosides to cells and organs results in the production of increased amounts of free GAGs. By conjugating xyloside and BODIPY we are able to elucidate GAG function in a number of inner hair cell processes. We recorded semicircular canal microphonics and single unit afferent neural responses to mechanical and infrared (IR) heat pulse stimuli before and after BX treatment. Micromechanical indentation of the slender membranous duct was applied to mimic physiological head rotation at angular frequencies from 1 to 5 Hz. Spontaneous afferent nerve discharge rates and sensitivity to sinusoidal mechanical stimuli were determined for each neuron using conventional single-unit recordings. Modulation of the voltage in the endolymph relative to the perilymph was recorded using low impedance glass electrodes and lock-in amplification. The microphonic was monitored to measure relative changes in whole-organ transduction current modulation.

Results
Microphonic data indicate that modulation of the net MET current was reduced following BX administration within the first 2 hrs, and recovered slowly over time. As expected, the reduction in the microphonic was accompanied by a reduction in the sensitivity of afferent neurons to the sinusoidal stimulus. The reduction in afferent gain exceeded the microphonic, suggesting BX might have reduced synaptic transmission from hair cells to afferents. Consistent with this, BX treated canals also exhibited partially reduced afferent sensitivity to IR heat pulses applied to hair cells.

Conclusion
Our preliminary results indicate that BX primed GAGs interfere with both mechano-electrical transduction and with transmission from hair cells to afferents, and suggest GAGs play important roles in the physiological function of inner ear sensory hair cells.

Funding
NIDCD R01 DC06685 (Rabbitt); NHLBI P01 HL107152 (Kuberan)

PS 597

Tryptophan-rich basic protein (WRB) mediates membrane insertion of the tail-anchored protein otoferlin and is required for hair cell exocytosis and hearing

Christian Vogl[1]; Iliana Panou[1]; Gulnara Yamanbaeva[1]; Carolin Wichmann[1]; Sara Mangosing[2]; Fabio Vilardi[1]; Artur Indzhykulian[3]; Tina Pangršič[1]; XuDong Wu[3]; Sonja Wojcik[4]; Kelvin Kwan[5]; Blanche Schwappach[1]; Nicola Strenzke[1]; David Corey[3]; Shuh-Yow Lin[2]; Tobias Moser[1]
[1]University Medical Center Goettingen; [2]University of California San Diego; [3]Harvard Medical School, Boston; [4]Max-Planck-Institute for Experimental Medicine; [5]Rutgers University

Background

In eukaryotic cells, the transmembrane recognition complex (TRC40)-pathway mediates the insertion of tail-anchored (TA) proteins into cellular membranes at the endoplasmic reticulum (ER). So far, this pathway has been studied in yeast and cultured mammalian cells, but its function in cells in native tissue remains to be determined. In the present study, we demonstrate that otoferlin, a TA-protein essential for inner hair cell (IHC) exocytosis, critically depends on the TRC40-pathway for membrane insertion.

Methods

To address this, we deleted tryptophan-rich basic protein (Wrb), the receptor for TRC40 on the ER, in hair cells of zebra fish and mice and studied the impact of defective TA-protein insertion on inner hair cell physiology using a range of electrophysiological and immunohistochemical approaches.

Results

In these experiments, *Wrb*-disruption dramatically reduced otoferlin levels in IHCs in a progressive manner, causing a synaptic hearing impairment, while upstream hair bundle morphology and mechanotransduction remained unaffected. In mutant zebra fish, the loss of otoferlin could be restored by transgenic Wrb expression. In IHC-specific *Wrb*-knockout mice, IHCs displayed normal numbers of afferent synapses and Ca^{2+} channels. However, on the ultrastructural level, despite of normal numbers of membrane-proximal synaptic vesicles, we found fewer ribbon-associated vesicles and observed accumulations of large, partially amorphous vesicles in direct proximity to presynaptic ribbons. In line with these findings, electrophysiological recordings of IHC exocytosis and synaptic sound encoding at individual auditory nerve fibers suggest an impaired vesicle replenishment of synaptic release sites in these animals.

Conclusions

In summary, we conclude that the TRC40-pathway is critical for hearing and demonstrate that otoferlin is an essential substrate of this pathway in sensory hair cells.

Funding

Funded by the German Research Foundation through the Collaborative Research Center 889 (projects A2 T.M., A6 N.S., A7 C.W.), the Priority Program 1608 (T.M.&N.S.), the Center for Molecular Physiology of the Brain (FZT-103 T.M.), the Deafness Research Foundation and UCSD Foundation grants (S-Y.L&S.M.) and NIH grants R01-DC000304 and R01-DC002281 (D.P.C).

PS 598

Noise-Induced Alterations of Mitochondria in Auditory Cells

Teresa Wilson; Sarah Foster; Alfred Nuttall
Oregon Health & Science University

Background

Increased oxidative free radical production resulting from loud sound exposure is a key factor in noise-induced auditory hair cell death. The mechanisms that initiate this process are thought to include ischemia/reperfusion injury as well as metabolic overstimulation. In both cases, excessive superoxide radicals are produced by the mitochondria. Despite the importance of auditory hair cells to hearing function, the basic physiology of the mitochondria in these cells is relatively unknown. Further, whether mitochondrial dynamics and spatial localization are altered to respond to increased energy needs of the cells with loud sound exposure has not been well-characterized.

Objective

In this study, our goal was to characterize mitochondrial morphology and spatial distribution in auditory cells under normal and loud sound induced stress conditions.

Methods and Results

To examine mitochondria in outer hair cells (OHCs), $PhAM^{floxed}$ mice were crossed with prestin-$CreER^{T2}$ mice to generate mice that express a mitochondrial-specific version of the Dendra2 fluorescent protein (mito-Dendra2) in the mitochondria in OHCs. For examination of mitochondria in all organ of Corti cells, immunolabeling for the mitochondrial outer membrane protein Tom20 was performed. These mice were exposed to loud sound (98 dB SPL ($PhAM^{floxed}$ x prestin-$CreER^{T2}$ mice) or 106 dB SPL (CBA/CaJ mice) for 2 hours, 8-16 kHz) and the cochlea harvested at 24 and 48 hours following noise exposure. Airyscan and super resolution imaging of mito-Dendra2 and Tom20 fluorescence showed primarily fragmented mitochondria in the OHCs and a mixture of punctate and short rod-shaped mitochondria in the inner hair cells of normal control animals. Following noise exposure, the mitochondria of the organ of Corti cells were examined for alterations in spatial distribution, number, and morphology, and preliminary results demonstrated changes in the distribution of mitochondria in OHCs.

Conclusions

Mitochondria are highly dynamic organelles; the shape, health, and spatial distribution of which are maintained by the conserved activities of mitochondrial division, fusion, motility, and tethering. The presence of cellular stresses typically results in attenuated fusion and stress-induced mitochondrial fragmentation. The presence of fragmented mitochondria in OHCs suggests that the balance of fission and fusion

processes are altered, potentially due to a higher oxidant environment being present in these cells.

Funding
Funding: Supported by grants 5R01DC000105 (ALN) and P30DC005983.

PS 599

Noise-Induced Alterations of Adherens Junction Proteins in the Endothelial Cells of the Cochlear Lateral Wall

Qing Yu; Sarah Foster; Teresa Wilson; Alfred Nuttall
Oregon Health & Science University

Background
The capillaries of the cochlear lateral wall are part of the blood-labyrinth-barrier (BLB) that separates the inner ear fluid from systemic circulation. The BLB controls the exchange of solutes, protein, and water, and plays an essential role in maintaining inner ear homeostasis and the endocochlear potential. Compromise of the BLB's integrity is a contributing factor in various hearing disorders including presbycusis, noise-induced hearing loss, and autoimmune inner ear disease. This crucial barrier's function relies on endothelial cell-cell junctions including those formed by the adherens junction (AJ) proteins. However, the mechanisms which regulate the function of AJs in the cochlear lateral capillaries remain largely unknown.

Objective
In this study, our goal was to characterize the role of AJ protein complexes and the associated signaling pathways in modulating the integrity of lateral wall capillaries under normal and loud sound-induced stress conditions.

Methods and Results
Capillaries of the spiral ligament and stria vascularis of 10 week old CBA/CAJ mice were immunolabeled for VE-cadherin, VEGFR2, β-catenin, and FAK. Subsequent confocal imaging revealed that the fluorescent signals for VE-cadherin and β-catenin overlapped and were clustered at endothelial cell to cell contacts whereas FAK revealed nuclear, cytoplasmic, and focal adhesion distribution without overlap with VE-cadherin. To evaluate the dynamic changes of VE-cadherin and its associated signaling pathway components under stress conditions, we exposed the CBA/CAJ mice to loud sound (106 dB SPL, 8-16 kHz, 2 hours). The following immunofluorescence analysis of the capillaries revealed an increase of specific phosphorylation sites for VE-cadherin, VEGFR2, β-catenin, and FAK in the endothelial cells of noise exposed mice. Super-resolution imaging showed alterations of the AJ proteins at the cell membrane as well as translocation of FAK within the endothelial cells.

Conclusions
Interendothelial junctions are dynamic structures that allow for rapid and specific responses to changes in the perivascular microenvironment. Under a variety of stress-induced conditions, direct phosphorylation of VE-cadherin and its intracellular partners can promote VE-cadherin/β-catenin dissociation, VE-cadherin degradation, and endothelial AJ breakdown. Unraveling the molecular mechanisms and signaling pathways that modulate the function of AJ complexes will contribute to the future discovery of breakthrough therapeutic treatments that maintain inner ear barrier integrity.

Funding
Funding: Supported by grants 5R01DC000105 (ALN) and P30DC005983.

PS 600

Restoration of Cochlear Gap Junction for GJB2 Associated Hearing Loss

Kazusaku Kamiya; Ichiro Fukunaga
Juntendo University

Background
Hereditary deafness affects about 1 in 2000 children and GJB2 gene mutation is most frequent cause for this disease. GJB2 encodes connexin (Cx) 26, a component in cochlear gap junction. We recently demonstrated that the drastic disruption of gap junction plaque (GJP) macromolecular complex composed of Cx26 and Cx30 are critical pathogenesis starting before hearing onset (Kamiya *et al.,* 2014, *J Clin Invest* 124, 1598-1607). To develop the effective therapy for GJB2 associated hearing loss, restoration of gap junction plaque (GJP) macromolecular complex using virus vectors or multipotent stem cells such as induced prulipotent stem (iPS) cells and mescenchimal stem cell (MSC) are expected to rescue the hearing function of GJB2 related hearing loss.

Methods
Mouse induced pluripotent stem cells (iPS) were used for generation of Cx26-expressing cells with proper gap junction plaque between the cells. Adeno associate virus (AAV) were used for the GJB2 gene transfer and restoration of GJP. As animal model of GJB2 related hearing loss, we used two different types of Cx26 mutation as major classification of clinical case. One is a model of dominant negative type, Cx26R75W+ and the other is conditional gene deficient mouse, Cx26f/fP0Cre as a model for insufficiency of gap junction protein.

Results and Conclusion
By diffentiation of iPS cells, we generated the Cx26-expressiong cells with large gap junction plaque as cochlear cells. Cochlear delivery of Gjb2 using AAV significantly improved the auditory responses and development of the cochlear structure of Cx26f/fP0Cre mice (Iizuka, *Hum Mol Genet*, 2015, 24(13):3651-61). Using cell therapy or gene therapy to restore hearing in the mouse models of Gjb2-related deafness may lead to the development of therapies for human hereditary deafness.

Funding
This work was supported in part by research grant from Japan Agency for Medical Research and Development (AMED) of Japan (to K.K.), Takeda science foundation (to K. K.) and The Science Research Promotion Fund for priate school, Japan (to K.K.).

PS 601

Investigating the Weber phenomenon: Intracochlear sound pressure with acoustic and bone conducted stimuli

Renee Banakis Hartl; Nathaniel Greene; Herman Jenkins; Stephen Cass; Daniel Tollin
University of Colorado

Hypothesis: Variation in intracochlear pressure magnitude and phase measurements recorded before and after induced conductive impairments in cadaveric specimens will reflect the acoustic impedance mismatch between the air-filled middle ear space and fluid-filled cochlea, providing a physiologic explanation for the perceptual lateralization of bone conducted sound in conductive hearing loss.

Background
The Weber tuning fork test was first described in the 19th century and remains an important clinical tool of the modern otolaryngologist. A tuning fork applied on the skull at midline will be perceived as louder on the side of a conductive hearing impairment. Though the Weber phenomenon is easily reproducible and widely used clinically, the acoustic basis of this lateralization of sound towards the conductive hearing loss remains poorly understood. It has been proposed that interaural phase or intensity differences resulting from reduced reverse transmission of acoustic signal through an impaired conduction pathway are responsible for the difference in perception, though objective data to support these hypotheses has been difficult to obtain. Here, we sought to quantify the drive to the inner ear directly by measuring ossicular chain velocity concurrently with intracochlear sound pressure levels during air and bone conducted stimulation with and without an induced conductive hearing loss.

Methods
A titanium fixture was surgically implanted at midline on human cadaveric heads and directly connected to a bone conduction transducer. Pure-tone stimuli were delivered via the transducer coupled to custom software. Intracochlear pressure was measured in scala vestibuli and scala tympani using commercially available fiber-optic pressure sensors (FISO Inc.). Stapes capitulum and round window velocities were measured using single-axis laser Doppler vibrometry (Polytec Inc.). Data was collected for air- and bone-conducted stimuli before and after inducing impairments in the conductive system of specimen, including ear canal plugging, middle ear effusion, fixation of the incus, and incudostapedial dislocation.

Results
The induced conductive impairments reduced responses to air-conducted stimuli consistent with prior literature. Intracochlear pressure measures to bone-conducted stimuli revealed alterations to both magnitude and phase after producing conductive impairment in cadaveric specimen. Reduction in velocity of the stapes capitulum relative to the round window membrane was also noted with ossicular fixation and dislocation.

Conclusion
Induced conductive impairments produce altered ossicular velocities and intracochlear sound pressure levels. These results may explain the increased cochlear sensitivity, and will be assessed in the context of previously described theories of sound lateralization towards the impaired ear during the Weber test

Funding
Support: NIH 5T32DC012280-03

PS 602

Correlation of ABR, TM displacement and wideband energy absorbance in otitis media model of chinchilla

Xuelin Wang; Brooke Hitt; **Rong Gan**
University of Oklahoma

Background
Otitis media (OM) is the most common middle ear disease in young children and results in conductive hearing loss. Studies on measurements of tympanic membrane (TM) displacement, wideband energy absorbance (EA), and auditory brainstem response (ABR) have been reported in chinchilla ears at normal and acute otitis media (AOM) conditions. However, how the changes of TM mobility, EA and ABR in OM ears are correlated with each other over the frequencies need further study. The goal of this study is to provide a system analysis of OM mechanism based on experimentally measured data of ABR, TM displacement and EA in AOM model of chinchilla.

Methods
Three groups of data, the elevation of ABR threshold (ΔHL), change of TM displacement (ΔdTM) and alteration of energy absorbance (ΔEA), were gathered from our measurements in the control, intact OM (OM-1), pressure-released OM (OM-2), and pressure-released and fluid-drained (OM-3) chinchillas. We first used Student's t-test to determine the difference between control and OM-1, OM-2 and OM-3 in terms of the ΔHL, ΔdTM and ΔEA. The control vs. OM-1 shows the combined effect from three variables: middle ear fluid (MF), middle ear pressure (MEP), and mechanical properties of tissue (M); control vs. OM-2 indicates the effect of MF + M, and control vs. OM-3 reveals the single effect of M. Next, the statistical analysis was applied between OM-1 and OM-2 results in the effect of MEP; between OM-2 and OM-3 results leading to the effect of MF; between OM-3 and OM-1 revealing the effect of MEP + MF. The relationships between ΔHL, ΔdTM and ΔEA were created with data points at the representative low (f1), medium (f2) and high (f3) frequency ranges.

Results
A group of matrices were derived to quantitatively show the correlation of ΔHL, ΔdTM and ΔEA in relation to middle ear fluid, pressure, and mechanical properties of tissues. The results demonstrated that the reduction of the TM mobility was frequency dependent and proportional to the volume of fluid. The elevation of ABR threshold mainly correlated with the reduction of TM displacement.

Conclusions
A systematic statistical analysis was developed to provide an explanation of the combined fluid, pressure, and mechanical property mechanisms for OM-induced hearing loss. (Supported by NIH R01DC011585)

Funding
This work was supported by NIH R01DC011585

PS 603

Neuroprotective Effects of Regenerating-Agents in Spiral Ganglion Neurons – a Neuropharmacological Approach in Cochlear Implantation

Ariane Roemer; Thomas Lenarz; Athanasia Warnecke
University of Hanover

Background
Immunological processes following cochlear implantation leading to fibrotic tissue formation around the electrode as well as neural retrogression are the most common underling biological factors for low performances in speech recognition.

Heparan sulfate enables fibroblast growth factor (FGF) as well as vesicular endothelial growth factor (VEGF) and tumor growth factor β (TGF- β) to bind and therefor transform in an active state. As these growth factors are known to increase neuronal survival and decrease scarring, heparan sulfate seems like an ideal target for supporting therapies in cochlear implantation.

Methods
Isolated spiral ganglion neurons were incubated with heparan sulfate in different concentrations for 48 hours following DAB-staining and microscopic survival analysis.

Separated spiral ganglia were incubated as whole organs with heparan sulfate for 7 days. Subsequently, the dendrite outgrowth was analyzed in comparison to untreated organs.

Results
We will demonstrate that heparan sulfate analogues increase spiral ganglion neuron survival and neuronal outgrowth of spiral ganglia in vitro.

In addition, we will prove that heparan sulfate - as the main part of extracellular matrix – enables neuronal growth in vitro without any other coating necessary. This supports our matrix-theory, as heparan sulfates induce remodeling processes and may enable neurite outgrowth towards the cochlear implant electrode.

Conclusion
As it is already in clinical use in ophthalmology since years, regenerating agents like heparan sulfate show nearly no side effects and provide therefore an easy to achieve, simple to use and cost-effective pharmacological intervention for the improvement of cochlear implant performance.

Funding
Cluster of Excellence “Hearing4all”

PS 604

Myosin 7a Immunolabeling is Not a Reliable Marker for Hair Cell Viability

Shimon Francis[1]; Elyssa Monzack[1]; Lindsey May[1]; Jonathan Gale[2]; Lisa Cunningham[1]
[1]National Institutes of Health; [2]University College of London

Background
Mechanosensory hair cells (HCs) are susceptible to death from a variety of insults, including noise, ototoxic drugs, and aging. We recently performed a series of live-imaging and fixed-tissue experiments that indicate glia-like supporting cells (SCs) are responsible for clearance of dead hair cells, and perturbation of this activity can result in residual HC “corpses” (Monzack et al., 2015). Myosin7a (Myo7a) is a well-established HC marker and has been widely used in the field to assess HC viability. Our data indicate that Myo7a labels many of these HC corpses. Thus it will be important to establish and characterize a hair cell marker that better reflects the viability of the labeled cell.

Methods
We assessed HC viability in utricle explants from adult mice expressing cytosolic tdTomato in HCs (Atoh1-Cre x Rosa26-tdTomato), and exposed them to the ototoxic drugs cisplatin (30 µg/ml) or neomycin (3 mM). In live-imaging experiments, membrane integrity was assessed using the cell-impermeant dye TOTO-3. Utricles were fixed in 4% paraformaldehyde and probed with antibodies against Myo7a. Confocal microscopy was used to analyze the expression of Myo7a and tdTomato fluorescence.

Results
Viable HCs displayed bright tdTomato fluorescence in their cell bodies and nuclei. Both neomycin and cisplatin resulted in HC death, as indicated by loss of tdTomato fluorescence and uptake of TOTO-3 iodide. These dead hair cells often retained Myo7a immunoreactivity, indicating that Myo7a is not a reliable marker for *living* HCs, especially in the context of impaired SC phagocytic activity, as we observed when hair cells were killed by cisplatin. Up to 40% of HCs that were labelled with Myo7a lacked tdTomato fluorescence and were therefore “HC corpses”.

Conclusions
We have developed an ex vivo model system of the mature mammalian utricle in which tdTomato fluorescence in HCs indicates viability, and its loss signals disruption of membrane integrity and hair cell death. Our data suggest that the well-established HC marker Myo7a, when used alone, is not a reliable indicator that the labeled HC was alive at the time of fixation. Our current experiments are designed to identify other HC markers that better reflect HC viability.

Funding
This work was funded by NIH/NIDCD intramural research program

PS 605

Perilymph proteomic imprint using a new tool with a nanoporous silicon chip.

Eric Boyer[1]; Ali Bouamrani[2]; Akil Kaderbay[1]; Adrien Mombrun[2]; Francois Berger[1]; Sebastien Schmerber[1]
[1]Grenoble University Hospital, Clinatec Cea-Leti; [2]Clinatec Cea-Leti

Background

Hearing loss affects around 10% of entire population and increases with aging. Histological aspects of inner ear impairment could explain most of deafness; nevertheless 25% are currently unexplained. The investigation of the oxidative stress and mitochondrial metabolites in noise-induced hearing loss brought new perspectives for prevention and treatment. Apoptotic pathways and use of apoptotic inhibitor has shown efficiency on long-term protection of the hair cells exposed to oxidative stress induced by ototoxic drugs and traumatic noise. Specific perilymph sampling is impossible in vivo without contamination of cerebrospinal fluid. Our objective is to design a molecular imprint tool of perilymph to analyze it with mass spectrometry in a proof of concept study.

Method

A nanoporous silicon chip (2 mm length, 500 µm large and 300 µm width) is fixed on a medical polyether ether ketone (PEEK) base with a silicon extension cable. The device is surrounded by a retractable PEEK sheath with a sharp distal tip to protect the silicon chip and penetrate the round window membrane.

The surgical procedure was managed on 30 WISTAR rats, 15 healthy rats and 15 rats exposed to ototoxic dose of gentamicin (160 mg/kg/j) during 5 days. We exposed the tympanic bulla by a ventral approach and drilled the bone capsule to have an access to the round window. Then an imprint was done, applying our tool through the round window membrane and insert the silicon chip in cochlea.

The silicon was examined in a MALDI-TOF (Matrix-assisted laser desorption ionization – time of flight) mass spectrometry.

Results

Our results shows a proteinic enrichment of the nanoporous silicon chip instead of a standard inox surface of analysis. The use of a nanoporous surface allows a peptidomic and metabolomic analysis of our perilymph sample. Imprint realization was done easily using our device. We identified a perilymph specific metabolites pattern in the ototoxic model compared to the healthy rats.

Conclusion

This new tool allows a specific perilymph protein analysis. Perspectives are the characterization of the perilymph proteome, the discovery of hearing damage biomarkers and potential treatments and the study of deafness models (i.e. genetic, auto-immune and ototoxic deafness).

Funding

CLINATEC, CEA-LETI. Carnot.

PS 606

Dysregulation of TRPV1 Channel Activity by TNF-α and H2O2 in Noise Induced Hearing Loss

Debashree Mukherjea; Asmita Dhukhwa; Kelly Sheehan; Sumana Ghosh; Vikrant Borse; Sandeep Sheth; Vickram Ramkumar
SIU School of Medicine

Background

Noise induced hearing loss (NIHL) is a global phenomenon. Our laboratory, and those of others, has shown that noise exposure (NE) induces reactive oxygen species generation in the cochlea, which initiates an inflammatory response. We showed up-regulation of inflammatory marker (iNOS) within 2h of NE, followed by additional stress/inflammatory markers such as transient receptor potential vanilloid 1 (TRPV1), NOX3 NADPH oxidase, cyclooxygenase-2 (COX2) and tumor necrosis factor-α (TNF-α). The interaction among these different stress and inflammatory markers is not known. In the current study, we show that two of these markers, namely H_2O_2 and TNF-α, regulate TRPV1 activation which facilitates Ca^{2+} uptake by cochlear cells and perpetuates the oxidative and inflammatory responses initiated by acute NE. Therefore, intervening early in this process by inhibiting ROS, inflammation or TRPV1 could reduce hearing loss.

Method

UB/OC1 cells and HEK293 cells transfected with TRPV1 (HEKVR1) were used for calcium uptake studies by confocal microscopy. Capsaicin, H_2O_2 or TNF-α was used to activate TRPV1 *in vitro*. Wistar rats were used for NIHL studies. Subcutaneous etanercept was used to sequester TNF-α in the rat cochlea. Functional hearing assessment was determined by auditory brainstem recordings (ABRs).

Results

Capsaicin produced a rapid and robust increase in intracellular Ca^{2+} uptake in UB/OC1 and HEKVR1 cells within 30 sec, which returned to baseline values over an additional 30 sec. This response could not be elicited by capsaicin in normal HEK293 cells and was reduced by knockdown of TRPV1 with siRNA. Ca^{2+} uptake could also be induced by H_2O_2 (100 µM) but the onset was delayed and the maximum response was lower compared to capsaicin. Pretreatment of both UB/OC-1 and HEKVR1 cells with TNF-α (100 ng/ml) significantly enhanced the capsaicin response, which did not inactivate over the 5 min period examined. A similar response to H_2O_2 was observed in cells pretreated with TNF-α. These data suggest that inhibition of TNF-α could serve as a useful strategy to reduce TRPV1 channel activity and possibly NIHL. *In vivo* studies indicate the utility of this approach, as etanercept was able to protect against NIHL in rats.

Conclusion

Oxidative stress (produced by H_2O_2) or TNF-α could enhance TRPV1 channel activity and potentiate cell damage/death mediated by this channel in the cochlea, as manifested by NIHL. Abrogation of TNF-α by etanercept reduced NIHL, thereby providing indirect support of this hypothesis. We

propose that subcutaneous etanercept is a potentially useful treatment for NIHL.

Funding
R03DC011621 (DM), R15DC011412 (VR)

PS 607

Screening of anti- and pro-oxidative compounds in mammalian aminoglycoside-induced hair cell loss

Volker Noack; Rahul Jalota; Arwa Kurabi; Daniel Schaerer; Ann Wong; Kwang Pak
University of California, San Diego

Background
A number of prior studies suggest the involvement of reactive oxygen species (ROS) in aminoglycoside (AGS) mediated hair-cell loss. ROS are highly reactive molecules which are primarily generated in mitochondria as a byproduct of cellular respiration. Production can be increased by various forms of cell stress. ROS are involved in cell signaling and metabolism, as well as damage processes that can lead to cell death. In the present study we sought to identify anti-or pro-oxidative molecules which enhance or protect against aminoglycoside induced hair cell death.

Methods
Targeted screening was used to assess the Enzo Redox Library, which consist of 84 anti-or pro-oxidative compounds. Screening was performed in vitro, using microexplants of p3-5 oC from pou4f3/GFP transgenic mice in which hair cells express GFP. The organs were microdissected and the apical turns, insensitive to AGS, discarded. The basal and middle turns were divided into short segments. Each microexplant was placed into a single well of a 96-well tissue culture plate. Triplicate samples were treated with 200 μM of gentamicin (GM) plus three dosages of a test molecule. Three wells each were treated with GM alone, the highest dose of the test compound alone, or only media as controls. The samples were maintained in culture for 72 hours and photographed at the beginning of treatment and then every 24 hours. Test substances that exhibited enhanced survival of GFP+ cells compared to GM alone were flagged as protective. Test substances that showed accelerated GFP+ cell loss, and test-substance-alone wells that exhibited loss of GFP+ cells were flagged as toxic.

Results
The majority of compounds, including many anti-oxidants, had no effect on GM hair cell toxicity. A subset of anti-oxidative substances had a significant protective effect. In addition we observed compounds that enhanced hair cell loss.

Conclusion
Targeted screening was found to be an efficient and productive technique for screening a relatively large number of anti-and pro-oxidative compounds at multiple dosages for effects on mammalian inner and outer hair cells. The results suggest that not all anti-oxidants can protect hair cells from damage, and not all pro-oxidative compounds are harmful.

Funding
Supported by the Resesarch Service of the VA and NIH/NIDCD grant DC000139

PS 608

A Parametric Analysis of Auditory-Nerve Degeneration at the Level of the Auditory Cortex Through Computational Modeling

Christopher Smalt[1]; Thomas Quatieri[1]; Ian Bruce[2]; Jeffery Palmer[1]
[1]MIT Lincoln Laboratory; [2]McMaster University

Background
A common complaint of listeners with normal clinical hearing thresholds is difficulty in understanding speech in noise. Recent animal studies have shown that noise exposure causes selective loss of low spontaneous rate auditory nerve fibers (ANFs), while preserving detection of low level sounds. Furthermore, these studies have observed reduced auditory brainstem response wave-I amplitudes. The goal of this research is to utilize computational models of the auditory periphery and auditory cortex to study the effect of low spontaneous rate ANF loss on the cortical representation of speech intelligibility in noise.

Methods
The auditory-periphery model of Zilany et al. (JASA 2009,2014) is used to make predictions of auditory nerve (AN) responses to speech stimuli under a variety of difficult listening conditions. The effect on normal and reduced low spontaneous rate ANFs is investigated under white noise, reverberation, and multiple talkers. The resulting cochlear neurogram, a spectrogram-like output based on ANF outputs, is then used as a low-auditory-level foundation for two different but related cortical representations of speech: the Spectro-Temporal Modulation Index (STMI; Elihali et al., Speech Comm. 2003) and 2D Fourier Analysis (Wang and Quatieri., IEEE, 2012).

Results
Reducing the number of low spontaneous rate ANFs in the cochlear neurogram results in fewer spikes in each bin of the post-stimulus time histogram per center frequency. This leads to a lower spectro-temporal modulation index (STMI) in poor SNR conditions (reduction of up to 0.2 at 0 dB SNR), while a much lesser or 0 reduction in STMI is observed at high SNRs for supra-threshold sound levels. STMI is a measure of the spectral and temporal modulation energy and is used as a speech intelligibility metric on a 0 to 1 scale. Lower signal energy and blurring is also observed in the output of the temporal modulation filters or “rategram” in poor SNR conditions with simulated ANF degeneration. A 2D Fourier representation of the neurogram is ongoing, and may demonstrate blurring of speaker specific components that increase the difficulty of speaker separation.

Conclusions
Suprathreshold deficits in speech intelligibility, as measured by STMI, may be related to ANF loss or degradation. Using a model that encodes auditory nerve spikes may capture

this effect and the resulting change in modulation domain representation. Further study may lead to strategies to mitigate intelligibility decline by optimizing information at the cortical leve

Funding
This work is sponsored by the Assistant Secretary of Defense for Research and Engineering under Air Force Contract FA8721-05-C-0002. Opinions, interpretations, conclusions and recommendations are those of the authors and are not necessarily endorsed by the United States Government.

PS 609

Plant-Derived Bisbenzylisoquinoline Derivatives Protect Zebra fish Lateral Line Hair Cells from Aminoglycoside Damage

Robert Boney; Matthew Kruger; Allison Coffin
Washington State University Vancouver

Aminoglycoside-induced hearing loss impacts up to 30% of patients that require these drugs, and there are no FDA-approved therapies to prevent this ototoxic side effect. We took advantage of the zebra fish lateral line to identify novel otoprotective compounds from a relatively unexplored source; natural products. Plant-derived compounds are often used in Eastern and alternative medicine and many have active biologic properties, making them an exciting source of new drug leads. Screening a library of 502 natural compounds identified four bisbenzylisoquinoline derivatives: E6 berbamine, berbamine, hernandezine, and isotetrandrine, each of which robustly protected hair cells from aminoglycoside-induced damage. E6 berbamine was highly protective in the sub-micromolar range, making it an ideal target for further optimization. Using the fluorescent aminoglycoside Gentamicin-Texas Red and the vital dye FM 1-43FX we demonstrated that these natural compounds conferred protection by reducing antibiotic uptake into hair cells, similar to other quinoline derivatives that also block the mechanotransduction channel. We then used a Kirby Bauer assay to determine that these natural compounds do not reduce antibiotic efficacy. In addition to these four benzylisoquinoline derivatives, preliminary experiments show that coumarin derivatives also prevent aminoglycoside damage. Quinoline and coumarin have similar structures, but in coumarin rings an oxygen atom takes the place of a nitrogen atom. Coumarin derivatives are roughly three times smaller than our bisbenzylisoquinoline derivatives, which may be advantageous for packaging these compounds for certain drug delivery methods. Together, these natural compounds represent a novel source of possible otoprotective drugs that may offer therapeutic options for patients receiving aminoglycoside treatment.

Funding
This research is funded by R15DC013900 from the NIDCD.

PS 610

Maintenance of the Cochlear Blood-Labyrinth Barrier by Nanoparticle Antioxidant

Fred Pereira[1]; Michelle Seymour[1]; Abigail Wright[2]; E. Loic Samuel[2]; James Tour[2]
[1]Baylor College of Medicine; [2]Rice University

Cisplatin and carboplatin are platinum chemotherapy agents widely used to treat adult and pediatric cancers. Platinum, however, is highly ototoxic to the auditory system; impairing high frequency hearing, and spreading to the lower frequencies with cumulative dosing. Because auditory hair cells do not regenerate, cisplatin-induced hearing loss is permanent. The progressive irreversible side effects of platinum agents greatly impair quality of life and can influence pediatric patients to choose suboptimal dosing therapies. There are no pharmacologic agents that prevent or reverse platinum-induced hearing loss approved by the U.S. Food and Drug Administration (FDA). We urgently need Interventions that reduce platinum toxicity and hearing loss without interfering with the tumoricidal effects so that dose intensity can be maintained or escalated as necessary. In non-dividing somatic cells, platinum compromises mitochondrial function, resulting in production of toxic levels of reactive oxygen species (ROS) that lead to cell death. Cisplatin is proposed to follow a trans-strial trafficking route from strial capillaries to marginal cells, followed by clearance into endolymph, leading to uptake into and demise of the sensory hair cells and non-sensory supporting cells. Cisplatin trauma in the marginal cells and vasculature of the *stria vascularis* disrupts the cochlear blood-labyrinth-barrier (cBLB), which damage cells that maintain the ionic gradients and endocochlear potential (EP) necessary for cochlear hair cell transduction and audition. We have successfully developed novel carbon nanoparticle antioxidants, polyethylene glycol-functionalized hydrophilic carbon clusters (PEG-HCC), which quench ROS, to protect against cisplatin-induced hearing loss in mice. PEG-HCCs given prophylactically after cisplatin treatment maintain ABR thresholds in a dose and time-dependent manner. Cisplatin (8 mg/kg, IP) increased ABR thresholds by an average of 7dB, whereas single prophylactic dose (5 mg/kg, IV 5h post cisplatin) of PEG-HCC attenuated the average threshold change to only 0.6dB, with up to –13dB near the best frequencies (8kHz and 16kHz, (N=2-4 mice per group, ANOVA for Treatment vs. Threshold Change: p=2.82e-06). In addition, within the *stria vascularis*, cisplatin treatment eliminated the presence of the perivascular melanocyte-like macrophages (PVM/Ms) and damaged the cBLB, whereas the majority of PVM/M staining and cBLB integrity was maintained after PEG-HCC treatments. We continue to evaluate these nanoparticle antioxidants in a preclinical animal model to determine their mechanism of protection, and develop an appropriate administration protocol that efficiently protects the auditory system while maintaining cisplatin anti-cancer efficacy.

Funding
John S. Dunn Foundation

PS 611

Characterization of Sestrin2 in the Neonatal Mouse Cochlea

Soledad Levano; Eliane Ebnoether; Alessia Ramseier; Daniel Bodmer
University Hospital Basel

Background

Sensory hair cells of the inner ear can be damaged by ototoxic drugs like gentamicin by production of reactive oxygen species (ROS). Sestrins, a family of stress-responsive proteins, can function as oxireductase and also as inhibitor of the mammalian target of rapamycin complex 1 (mTORC1). Sestrin2 regulates intracellular ROS levels and regenerates reduced peroxiredoxin. Inhibition of mTORC1 induces autophagy by regulating the transcription of autophagy genes. We hypothesized that sestrin2 may protect hair cells from gentamicin-induced oxidative stress.

Methods

C57BL6/J wild type and C57BL6/J sestrin2 knockout mice at P4-P5 were used for our experiments. Gene expression of sestrins was assessed via real-time PCR. Localization of Sestrin2 in mouse cochlea was performed by immunostaining and confocal microscopy. Hair cell damage was performed using different concentrations of gentamicin.

Results

All sestrins were detected in the inner ear compartments. Sestrin2 immunoreactivity was detected in sensory hair cells. High rate of hair cell loss was observed in sestrin2 knockout mice as compared to wild type mice. Currently we are assessing the effect of gentamicin on sestrin gene expression.

Conclusion

Our data provide evidence that sestrin2 plays an important role in gentamicin-induced hair cell damage.

PS 612

Cell Line-Derived Extracellular Vesicles Protect Against Aminoglycoside-Induced Hair Cell Death in Vitro

Andrew Breglio[1]; Lindsey May[1]; Samir El Andaloussi[2]; Matthew Wood[2]; Lisa Cunningham[1]
[1]National Institutes of Health; [2]University of Oxford

Background

The aminoglycoside antibiotics and the chemotherapy drug cisplatin are both very widely used, but their use comes with significant risk for ototoxicity as well as nephrotoxicity. Both aminoglycoside and cisplatin-induced nephrotoxicity can be reduced by exposure to extracellular vesicles derived from cultured human mesenchymal stem cells (huMSCs). Therefore, we sought to examine the potential for cell line-derived extracellular vesicles to protect against ototoxicity from these drugs.

Methods

Conditioned media was collected from four different cell lines in culture: CT26, SW480, HEK 293T, and huMSC. Extracellular vesicles were isolated from this conditioned media via differential ultracentrifugation or ultrafiltration and quantified by nanoparticle tracking analysis. Whole-organ cultures of utricles from adult CBA/J mice were cultured for 24 hours in the presence (or absence) of neomycin (3mM) and purified extracellular vesicles. At the end of culture, utricles were fixed, stained for Myosin 7a, and imaged by confocal microscopy. Densities of surviving hair cells in the extrastriolar region were determined by manual cell counts of five 2500μM2 regions of interest (ROI) per utricle.

Results

Utricles cultured in neomycin had an average of 35.6±4.3 (mean±SD) surviving hair cells per ROI, which was significantly fewer than the 54.2±5.6 observed in control utricles ($p<0.001$). There were significantly more surviving hair cells in utricles co-treated with extracellular vesicles from either the CT26 mouse colon cancer line (52.6±12.7, $p<0.05$) or the SW480 human colon cancer line (45.2±4.0, $p<0.05$), as compared to utricles treated with neomycin alone. Vesicles isolated from HEK 293T or huMSC cells were not protective.

Conclusions

Our results suggest that purified extracellular vesicles from specific cell lines reduce aminoglycoside ototoxicity. The ability of vesicles derived from a particular cell line to protect against ototoxicity may depend upon the nature of the vesicle cargo and/or the efficiency with which they are taken up by cells of the utricle sensory epithelium. Further studies are designed to determine the protein and nucleic acid content of these protective vesicles.

Funding

This work was funded by the intramural program of the National Institute on Deafness and Other Communication Disorders.

PS 613

Synaptic alterations in FVB/n mice in response to acoustic stress

Stephen Paquette; Felicia Gilels; Patricia White
University of Rochester

Acoustic stress has multiple deleterious effects on hearing. To better understand the pathology of acoustic stress and how it correlates to hearing outcomes, we analyzed the effects of acoustic stress on FVB/nJ mice. The effects of acoustic stress on thresholds for auditory brain response (ABR) and distortion product oto-acoustic emission (DPOAE) measurements were characterized. Measurements for ABR thresholds were compared against voltage progressions for ABR waveform peak 1 amplitudes to establish cochlear neuropathy from permanent hearing loss conditions. The effects on pre- and post-synaptic anatomical markers, Ctbp2 and Gria2, were characterized using confocal microscopy and high-power deconvolution rendering. Characterization of the damage effects on synapses was followed using ribbon and receptor patch size comparisons and statistical grouping. Our results show that increasing levels of acoustic stress result in differential damage effects; either an induced cochlear neuropathy condition or a permanent loss of auditory

thresholds is observed depending upon length of acoustic stress treatment. The observed consequence of auditory stress on synapses appears to preferentially impact large ribbons in both noise conditions. The observed effect appears to be a dynamic resizing of synaptic ribbons in the neuropathic condition and location-specific losses of synapses on the pillar side of inner hair cells for the permanent threshold shift condition.

Funding
NIH-T32, Ruth L. Kirchstein Fellowship

PS 614

Therapeutic potential of TrkB agonist for gentamicin-induced hair cell loss in the guinea pig crista ampullaris

Makoto Kinoshita; Chisato Fujimoto; Shinichi Iwasaki; Tatsuya Yamasoba
University of Tokyo

Background
Sensory hair cells (HCs) of the inner ear can be easily damaged by excessive stimulation by ototoxic drugs and by aging. Neurotrophins play the essential role in the development and survival of neurons in the peripheral and the central nervous system. A recent study has shown that transotic administration of BDNF resulted in an increase in type I HCs in the vestibules of guinea pigs damaged by gentamicin (GM) (Kopke et al. 2001). 7, 8-Dihydroxyflavone (7, 8-DHF), a novel small molecule acting as a tropomyosin-receptor-kinase B (TrkB) agonist, activates TrkB and mimics physiological functions of the cognate ligand BDNF. We investigated whether the enhancement of vestibular HC renewal by oral administration of 7, 8-DHF can improve vestibular function in guinea pigs.

Methods
We used 12 albino male guinea pigs (200-250 g) which received GM (40mg/dl, 0.2ml) injection through the cochleostomy. These animals were divided into the following two groups: 1) TrkB group which was orally administrated with 7, 8-DHF (5mg/kg/day) for 28 days after GM injection (n = 6), and 2) sham group which was orally administered saline (n = 6). Before and 28 days after GM injection, each animal was estimated the vestibular function by a caloric test with 5 mL of ice water for 10 seconds. Then it was euthanized immediately. The agarose-embedded cryosections of crista ampullaris were immunostained by the anti-palvalbumin and myosin7a antibody, and observed under a confocal microscope.

Results
Before GM injection, the duration of caloric nystagmus in the TrkB group and the sham group was 97 ± 18.9 and 108 ± 13.4 seconds, respectively. At 28 days after GM injection, the duration of caloric nystagmus in the TrkB group was 24 ± 4.4 seconds, whereas there was no response in the sham group. Histologically, the TrkB group showed more HCs including type I HCs as compared to the sham group, which showed only type Ⅱ HCs.

Conclusion
Our findings suggest that novel small-molecule TrkB agonist can assist neuronal survival. It also facilitates the formation of new calyceal endings on HCs, leading to reappearance of type I HCs in ototoxin-damaged crista. Oral administration of TrkB agonist may be a new candidate for the treatment of vestibular dysfunction caused by ototoxic drugs.

Funding
This research received no specific grant from any funding agency in the public,commercial, or not-for-profit sectors.

PS 615

D-methionine (D-met) Influences Endogenous Antioxidant Activity and Lipid Peroxidation by Dose- and Tissue-Specific Mechanisms

Daniel Fox; Gregory Harpring; Robert Meech; Tim Hargrove; Steve Verhulst; Shelley Tischkau; Kathleen Campbell
Southern Illinois University School of Medicine

Background
D-methionine (D-met) has previously demonstrated otoprotection from noise-induced hearing loss. However, exact protective mechanisms have not been fully elucidated. This study will test dose-dependent D-met influence on endogenous antioxidant enzyme activities and lipid peroxidation.

Methods
Three-year old male chinchillas laniger (n = 5/group) were injected every 12 hours with D-met (25, 100, or 200 mg/kg/dose) or saline starting 48 hours prior to a single steady state (SS) or impulse noise exposure. One hour after noise exposure, cochleae, liver, and serum were collected processed for catalase (CAT), superoxide dismutase (SOD), glutathione reductase (GR) and glutathione peroxidase (Gpx), glutaredoxin 2 (Grx2), and malondialdehyde (MDA) spectrophotometric assays.

Results
CAT assays revealed no significant differences between D-met- and saline- treated groups. Significant serum SOD increases were measured in the 25 mg/kg/dose impulse noise-exposed group. Significant decreases in cochlear SOD were measured in the 200 mg/kg/dose impulse noise-exposed group. Significant decreases in serum and cochlear SOD were measured in the 100 and 200 mg/kg/dose SS noise-exposed group. D-met significantly increased liver GR activity in SS or impulse noise-exposed groups treated with 100 or 200 mg/kg/dose, respectively. D-met also significantly increased serum Gpx activity in the 100 mg/kg/dose impulse noise-exposed group, but decreased cochlear Gpx activity in impulse noise-exposed animals treated with 25, 100, or 200 mg/kg/dose and SS noise-exposed animals treated with 25 or 100 mg/kg/dose. Serum MDA concentrations were significantly ($p \leq 0.05$) decreased in the 25 and 100 mg/kg/dose SS noise-exposed groups. Interestingly, D-met decreased Grx2 activity in the liver 21 days post-SS noise

exposure and also showed a robust and significant Grx2 activity increase in cochlear tissue ($p \leq 0.01$).

Conclusions
D-met administration induced significant dose-dependent changes in endogenous antioxidant enzyme activity and lipid peroxidation levels in multiple tissues from animals exposed to either SS or impulse noise exposures. Lower D-met doses (25 and 50 mg/kg/dose) increased CAT and SOD activity whereas higher D-met doses (100 and 200 mg/kg/dose) tended to increase glutathione enzyme activities. High D-met doses also significantly increased glutaredoxin 2 activity therefore suggesting s-glutathionylation as a potential compensatory mechanism. Thus, D-met influence on endogenous antioxidant pathways and lipid peroxidation is dose-, noise exposure-, and tissue-dependent. Further, results suggest there may be further D-met activity that is beyond D-met's established direct and indirect antioxidant activity.

Funding
Funding: We thank: SIUSOM's Concept Development Award, R01: NIDCD/NIH PI Kathleen Campbell, PhD; and Action on Hearing Loss: Flexigrant; PI: Daniel Fox, MPH, PhD.

PS 616

Mn-SOD affects Noise Induced Hearing Loss

Aynur Turdi; **Makoto Kinoshita**; Chisato Fujimoto; Shinichi Iwasaki; Tatsuya Yamasoba
University of Tokyo

Background
The generation of reactive oxygen species (ROS) is thought to be one of the mechanisms underlying noise-induced hearing loss (NIHL).

Manganese superoxide dismutase (Mn-SOD), one of the antioxidant enzymes acting within the mitochondria, converts toxic superoxide to hydrogen peroxide.

To investigate the pathological role of mitochondrial antioxidant stress in the cochlea, we generated systemic Mn-SOD heterozygous knockout (HET) mice, and investigated hearing loss and hair cell damage after noise exposure.

Material and methods
HET mice were generated by crossbreeding of homozygous Mn- SOD lox/lox mice with the chicken actin promoter-Cre transgenic mice, and their littermate wild-type (WT) C57BL/6 mice were enrolled as controls (N=6, each). Both HET and WT mice were exposed to 120dB SPL 4 kHz octave band noise for 4h. Animals in each group underwent measurements for auditory brainstem responses (ABR) before and 1h, 1, 3, 7, and 14days after noise exposure. At 14days after noise exposure, the animals were euthanized for evaluation of cochlear pathology. The paraffin-embedded cochlear sections were stained with Hematoxylin and Eosin, and were analyzed for an inner/outer hair cell survival rates in the basal, middle, and apical turns of the cochlea.

Results
The mean ABR thresholds at all frequencies, particularly in 4 kHz, were significantly worse on post-noise days 7 and 14 in HET mice compared to WT, although both groups showed similar hearing loss 1h after noise exposure. Histologically, compared with WT mice, outer hair cell damage in HET mice was significantly greater in all, particularly apical ,turns. On the other hand, inner hair cell damage was only slightly greater in the apical turn in HET mice compared with WT mice.

Conclusion
These findings suggest that Mn-SOD has important role to reduce ROS production in hair cell, thereby protecting from NIHL.

Funding
This work was supported by Grant-in-AId for Scientific Research (grant number; 15H06174).

PS 617

HSF1-Mediated Stress Response Activation for Protection Against Noise-Induced Hearing Loss

David Kohrman; Ariane Kanicki; Catherine Martin; David Dolan; Richard Altschuler
University of Michigan

Experimental activation of the classic heat shock stress response through up-regulation of heat shock proteins (HSPs) is very effective in protecting the inner ear from noise induced hearing loss (NIHL) in animal models as well as other traumas such as aminoglycoside- and cisplatin-induced ototoxicity (e.g., J Neurosci 19:10116-10124, 1999; Cell Stress Chaperones 14:427-437, 2009). Conversely, the loss of heat shock pathway induction, through the inactivation of the stress-responsive transcription factor HSF1, results in greater sensitivity to NIHL and ototoxicity (e.g., J Neurosci Res 81:589-596, 2005; JARO 9:277-289, 2008). We are pursuing two parallel approaches to further evaluate the heat shock response as a protective strategy against noise trauma in the cochlea and move closer to an efficient therapeutic method. In one approach, we are taking advantage of a recent screen for molecules that activate HSF1, the transcription factor that is the master regulator of the heat shock response. This screen identified a small molecule (HSF1A; underlined for clarity) that relieves the feedback inhibition of endogenous HSF1 and thus efficiently up-regulates multiple Hsps (PLoS Biology, 8:e1000291, 2010). HSF1A activates HSF1 without causing proteotoxicity, thereby mitigating the cellular pathologies associated with neurodegenerative disease in cultured cell and fruit fly models (Cell Reports, 9: 955–966, 2014). We have demonstrated that systemic delivery of HSF1A to FVB/NJ mice induces multiple Hsp genes in the cochlea, including Hsp70. Notably, systemic delivery of this drug also decreases the threshold shift subsequent to a damaging noise exposure. We are currently treating an Hsf1 null mutant strain and controls to verify that this protective effect against noise is acting through HSF1 activation. In a second approach, we are investigating an alternative mode of heat shock activation through generation of transgenic mice that conditionally ex-

press an activated form of HSF1 (HsfTgAct) in the cochlea and thereby permit a temporary increase in the overall pool of activated HSF1 and promote a more robust heat shock response. We will similarly evaluate the ability of HsfTgAct to protect auditory function from noise trauma.

Funding
NIH-NIDCD R21-DC013185 and P30-DC005188

PS 618

Ginkgo Biloba Flavonols Damage Lateral Line Hair Cells Via Oxidative Stress Mechanisms

Anna Roche; Sarah Neveux; Nicole Smith; Allison Coffin
Washington State University Vancouver

Several drugs, including aminoglycosides and platinum-based chemotherapy agents, are well known for their ototoxic properties. However, the ototoxic potential of most therapeutic compounds is unknown. FDA-approved drugs are not routinely tested for ototoxicity, so their potential to affect hearing often goes unrecognized. This issue is further compounded for natural products, where there is a lack of FDA oversight and the manufacturer is responsible for ensuring the safety of their products. Natural compounds such as herbal supplements are easily accessible and commonly used in the practice of traditional Eastern and alternative medicine. Using the zebra fish lateral line, we screened a natural products library to identify new potential ototoxins. We found that the flavonols quercetin, kaempferol, and isorhamentin, all from the Gingko Biloba plant, demonstrated significant ototoxicity, killing up to 30% of lateral line hair cells. We then assessed the health of the surviving hair cells using the vital dye FM 1-43FX. Mean intensity of FM 1-43FX fluorescence was lower in hair cells treated with quercetin, kaempferol, or isorhamnetin than in the hair cells from untreated fish, suggesting that the health of the remaining hair cells was compromised. We then asked if these flavonols enter hair cells through the mechanotransduction channel, which is the site of entry for many known ototoxins. High extracellular calcium reduces the open probability of the channel and significantly protected hair cells from flavonol damage, implicating the transduction channel as a site of flavonol uptake. Since known ototoxins often activate cellular stress responses, we asked if reactive oxygen species were necessary for flavonol ototoxicity. Co-treatment with the antixodant D-methionine significantly protected hair cells from each flavonol, suggesting that antioxidant therapy could prevent hair cell loss. This research demonstrates the potential for ototoxic damage caused by unregulated herbal supplements and suggests that further supplement characterization is warranted.

Funding
This research is funded by R15DC013900 from the NIDCD.

PS 619

Acute changes in the mouse cochlea after blast injury

Jinkyung Kim; Xiaofang Liu; Zina Jawadi; Nicolas Grillet; John Oghalai
Stanford University

Blast trauma is the most common form injury after a terrorist attack and is a major mechanism of injury to military personnel. Despite numerous studies that have described the consequences of blast trauma on the cochlea, a detailed understanding of how hearing loss occurs after a blast exposure has not been fully understood. Here we studied the acute changes in the mouse cochlea that occur after exposure to a blast wave simulating that of an improvised explosive device. After blast exposure, ABR and DPOAE thresholds in CBA mice were significantly elevated, and only partially recovered over the following seven days. Consistent with this, confocal imaging of whole mount preparations demonstrated a progressive outer hair cell loss within the basal turn within the first 7 days after the blast. To explore this further, we used optical coherence tomography (OCT) to perform noninvasive time-lapse cochlear imaging *in vivo*. This revealed a progressive bulging of Reissner's membrane after the blast, or endolymphatic hydrops, that resolved within 24 hours. To test whether perilymph was mixing with endolymph and causing this phenomenon, we perfused gold nanoparticles through the perilymph. *In vivo* imaging demonstrated complete perfusion of both scala tympani and vestibuli, but no penetration of nanoparticles into the endolymph. Finally, we tested $Tecta^{C1509G/C1509G}$ mice, in which the tectorial membrane is detached from the outer hair cell stereocilia. These mutant mice did not have endolymphatic hydrops or outer hair cell loss after blast exposure. Together, these data argue that stereociliary damage is the inciting factor that leads to post-traumatic endolymphatic hydrops, hair cell loss, and hearing loss.

Funding
This project was funded by NIH-NIDCD DC014450, DC013774, DC010363 and DoD W81XWH-11-2-0004

PS 620

Cortisol Modulates Ototoxic Damage to Lateral Line Hair Cells

Alexander Young[1]; Tamasen Hayward[1]; Erica Crespi[2]; Allison Coffin[1]
[1]Washington State University Vancouver; [2]Washington State University, Pullman

Cortisol is an endogenous glucocorticoid hormone that modulates physiological responses to stressful stimuli. Synthetic glucocorticoids are known to have effects on the auditory periphery. For example, the synthetic glucocorticoid dexamethasone activates cell signaling pathways that promote hair cell survival in response to acoustic trauma in rodents and enhances hair cell regeneration following ototoxic exposure in larval zebra fish. However, less is known about cortisol itself and how the natural stress response impacts the auditory periphery. In this study, we investigated

the effect of exogenous cortisol on hair cells in the zebra fish lateral line as a first step in understanding how physiological stressors modulate hair cell survival. The lateral line is a system of hair cells stereotypically located along the exterior of the fish that are used to detect local changes in fluid dynamics for behaviors such as predator avoidance and prey detection. Using this system, we tested the hypothesis that elevated cortisol levels can modulate hair cell susceptibility to ototoxins. Our findings suggest that acute treatment with cortisol sensitizes hair cells to aminoglycoside damage. This sensitization effect was prevented by co-treatment with a glucocorticoid receptor inhibitor but not by co-treatment with a mineralocorticoid receptor inhibitor, suggesting that cortisol is acting via the glucocorticoid signaling pathway. Future studies will investigate if this sensitization effect is seen in response to endogenous stressors, and how exogenous cortisol treatment affects internal cortisol levels. We will also examine cortisol-mediated modulation of other hair cell toxins. These findings are biomedically relevant because ototoxic drugs are still widely prescribed to patients in hospitals, which may be perceived as a stressful environment. If elevated cortisol sensitizes hair cells to ototoxic damage, we may be able to mitigate these side effects by reducing patient stress.

Funding
This research is supported by a Washington State University Vancouver mini-grant.

PS 621

Neutrophil Hypochlorous Acid Contributes to Cisplatin Ototoxicity

Martin Mwangi[1]; Sung-Hee Kil[2]; David Phak[2]; Hun Yi Park[3]; David Lim[2]; Sung Moon[2]
[1]David Geffen School of Medicine at UCLA; [2]University of California Los Angeles; [3]Ajou University School of Medicine

Background
Cochlear inflammation is involved in cisplatin ototoxicity. Previously, we have demonstrated cisplatin-mediated up-regulation of pro-inflammatory cytokines, which are essentially involved in cisplatin ototoxicity. Besides pro-inflammatory cytokines, chemokines are up-regulated in kidneys from cisplatin-treated animals, which led us to further study a role of chemokines in cisplatin ototoxicity. In our prior study, we demonstrated ERK2/c-Jun-mediated up-regulation of CXCL2, a neutrophil chemoattractant, in cochlear inflammation. Recently, neutrophils have regained attention due to significant contributions to inflammation-mediated tissue injury in a variety of human diseases, but their role remains unclear in cisplatin ototoxicity. Therefore, we aim to determine if neutrophil mediators affect cisplatin-mediated cytotoxicity of auditory sensory cells.

Methods
HEI-OC1 cells were used as an in vitro model of auditory sensory cells, and hypochlorous acid was selected as a model of neutrophil-derived mediators. To generate hypochlorous acid, cells were exposed to myeloperoxidase and hydrogen peroxide. To determine cisplatin-induced CXCL2 up-regulation, RT-PCR analysis was performed. For cell viability analysis, MTT assays were conducted.

Results
We found that HEI-OC1 cells up-regulate CXCL2 upon exposure to cisplatin. MTT assays showed that sodium hypochlorite reduces cell viability of HEI-OC1 cells in a dose-dependent manner. Co-treatment of myeloperoxidase and hydrogen peroxide was found to be cytotoxic to HEI-OC1 cells. Sodium hypochlorite and combination of myeloperoxidase and hydrogen peroxide appeared to augment cisplatin-mediated cytotoxicity of HEI-OC1 cells.

Conclusion
Taken together, myeloperoxidase-mediated hypochlorous acid is involved in cisplatin ototoxicity, but further studies are needed to determine contribution of neutrophils to cisplatin-induced cochlear injury.

Funding
[Supported by NIH DC011862, and Howard Hughes Medical Research Fellowship Grant]

PS 622

Acute Cytoskeletal Changes in Cochlear Outer Spiral Fibers After Noise Exposure

Donna Whitlon; Lyubov Czech; Virginia Smith-Bronstein; Hunter Young; Claus-Peter Richter
Northwestern University

Background
Studies of spiral ganglion nerve fibers after exposure to noise has focused on changes in the type I fibers that connect to the inner hair cells and carry primary auditory information. However, recent studies have suggested that the outer spiral fibers from the Type II neurons, which form long spiral tracts and synapse on 20-30 outer hair cells, play a role in the regulation of the efferent olivocochlear reflex that regulates gain and frequency selectivity in the cochlea. We questioned whether high decibel noise might also cause acute damage to outer spiral fibers.

Methods
We examined the morphology of type II outer spiral fibers in adult guinea pig cochleas 24 hours after exposure to high level noise (120 dB SPL ; 4 hours; 4-8 kHz), using immunohistochemistry with a panel of antibodies directed against different cytoskeletal epitopes.

Results
One antibody directed against cytoskeletal elements allowed us to visualize the full population of outer spiral fibers in unexposed animals. When the animals were euthanized 24 hours after noise exposure, immunoreactivity was observed to collect non-homogeneously in large swellings along the length of the fibers. We have no evidence from immunohistochemistry for compensatory upregulation of other cytoskeletal epitopes.

Discussion
In other regions of the nervous system, the accumulation of cytoskeletal elements in a nerve fiber after insult is characteristic of the initial stages of neurite degeneration. These studies suggest that exposure to high level noise may interfere with the function of the type II spiral ganglion fibers and their effects on the olivocochlear reflex and predispose the cochlea and the contralateral cochlea to damage by subsequent noise.

Funding
Funded by ONR grant #N00014-15-1-2130 and by the Department of Otolaryngology, Feinberg School of Medicine, Northwestern University.

PS 623

The Role of Reactive Oxygen Species and The Protective Effect of D-methionine in Murine Cytomegalovirus-Induced Hearing Loss

Ali Almishaal[1]; Pranav Mathur[1]; Elaine Hillas[1]; Mattia Carraro[2]; Jun Yang[1]; Matthew Firpo[1]; Robert Harrison[2]; Albert Park[1]
[1]University of Utah, Salt Lake City; [2]University of Toronto

Background
Cytomegalovirus (CMV) is the most common infectious cause of congenital sensorineural hearing loss (SNHL). The underlying pathophysiological mechanism of SNHL in CMV is poorly understood and only few clinically effective interventions are available. Numerous studies have indicated that excess production of reactive oxygen species (ROS) plays a significant role in noise-induced hearing loss, ototoxicity, and age-related hearing loss. In the current study, we hypothesize that CMV-induced SNHL may be mediated via an excessive ROS production in the cochlea. Moreover, a potential approach to treatment may consider preventing the imbalance of ROS within the cochlea via the use of antioxidants. Indeed, previous studies in animal models showed a protective effect of antioxidant agents against noise-induced hearing loss. Here, we investigated the expression and distribution of ROS in the cochlea and the protective effect of D-methionine as an antioxidant in a murine CMV-induced SNHL model.

Method
BALB/c mice were inoculated at post-natal day 3 (P3) via intracerebral injection with 2000 pfu murine-CMV engineered to express green fluorescent protein (GFP). At 7 days post inoculation (dpi), the temporal bones were harvested for immunohistochemical analysis to detect the location of the GFP signal, ROS expression, and caspase-3 detection. The ROS level was measured using dihydroethidium (DHE) staining. D-methionine at 400 mg/kg per dose was administered 1 hour before and 1 hour after mCMV-GFP inoculation and continued twice a day for 14 dpi. At P28, the mice underwent hearing tests using distortion-product otoacoustic emissions (DPOAE) and auditory brainstem response (ABR). After hearing tests, the cochleae were harvested for scanning electron microscopy (SEM) and cochleograms.

Results
Consistent with previous findings from our laboratory, mCMV-GFP signal was observed in the spiral ganglion and adjacent to the scala tympani. Immunohistochemistry demonstrated an elevated production of ROS in mCMV-GFP inoculated pups, compared to controls, in the spiral ganglion neurons, stria vascularis, and adjacent to the scala tympani. Furthermore, mCMV-GFP infection induced cell death through activation of caspase-3 in cells expressing GFP. Mice injected with mCMV-GFP showed severe hearing loss while D-methionine administration provided partial hearing protection at all tone frequencies. Morphological analyses revealed that mCMV-GFP inoculation resulted in an extensive loss of outer hair cells (OHCs), which was attenuated by D-methionine treatment.

Conclusion
Our study demonstrates that mCMV-induced SNHL is mediated, in part, by elevated ROS-induced injury to various regions inside the cochlea and that the antioxidant D-methionine provides partial protection against hearing threshold shift and OHCs loss.

PS 624

Quantitative Analysis of the Proteome of Noise-Exposed Mouse Cochlea

Ann C.Y. Wong[1]; Kwang Pak[1]; Ann Hickox[2]; Chelsee Strojny[2]; Allen Ryan[1]; Jeffrey Savas[2]
[1]UCSD, La Jolla; [2]Northwestern University

Excessive acoustic stimulation is known to cause structural and biochemical changes to the sensorineural tissues of the cochlea[1]. This acoustic damage is manifested as Noise-Induced Hearing Loss (NIHL) and is characterized by elevated auditory thresholds. Temporary threshold shift (TTS) is defined as noise-induced increase in thresholds that recovers to pre-noise levels within hours to days, while permanent threshold shift (PTS) reflects permanently elevated thresholds, often determined two weeks after noise exposure. We investigated the effects of increasing noise–exposure levels on the mouse cochlea proteome by high-throughput shotgun proteomics with stable isotope labeling of mammal (SILAM) for quantitative comparisons.

Whole cochleae were harvested from FVB mice raised on a normal diet (^{14}N), and from mice reared on a diet enriched in nitrogen-15 (^{15}N). ^{14}N mice were kept in silence, or exposed to 70, 100 or 105 dB SPL broadband noise centering at 8-16 kHz for 30 minutes under anesthesia prior to sacrifice. Protein was extracted, and individual ^{14}N samples were mixed 1:1 with a pooled ^{15}N sample. The samples were digested with trypsin and analyzed by high-resolution mass spectroscopy to identify peptides and proteins. $^{14}N/^{15}N$ isotopic ratios were used to quantify protein levels across groups. Auditory Brainstem Responses (ABR) on separate groups of noise-exposed mice corroborated TTS or PTS phenotypes. Changes in protein levels associated with noise exposure were interpreted as evidence of new synthesis (increases) or degradation (decreases).

In total, over 7,000 proteins were quantified across all gene ontology groups classified by molecular function and biological process (PANTHER). Many proteins of known cochlear function are represented in the dataset. A variety of gene ontology groups were significantly altered by noise, providing new information regarding the potential mechanisms of NIHL induced by brief noise exposure.

[1] Stockwell CW, Ades HW, Engström H. Patterns of hair cell damage after intense auditory stimulation. Ann Otol Rhinol Laryngol. 1969 Dec;78(6):1144-68.

Funding
Supported by grants from the VA BX001205 and NIH/NIDCD (AFR), Garnett Passe and Rodney Williams Memorial Foundation Research Fellowship (ACYW), NIH/NIDCD R00 DC-013805 (JNS),

PS 625

Effect of Experimental Viremia on the Trafficking of Fluorescent Gentamicin Across the Blood-Brain Labyrinth

William Meier; Zachary Urdang; Jordan Allensworth; Peter Steyger
Oregon Health & Science University

Background
We recently reported that systemic inflammation, similar to that induced by bacterial infections, enhanced cochlear loading of aminoglycosides, and potentiated subsequent ototoxicity (Koo et al., 2015, Science Translational Medicine: 7, 298ra118). Twenty percent of admissions into neonatal intensive care units with clinical signs of inflammation are ultimately diagnosed with viremia or fungal infections, rather than bacterial infections. Nonetheless, these patients are initially empirically treated with antibiotics, including aminoglycosides like gentamicin, until bacterial sepsis is ruled out. In this study, we tested the hypothesis that systemic inflammatory response syndrome triggered by experimental viremia enhances cochlear uptake of aminoglycosides.

Methods
C57Bl6/J mice (4-6wks old) were intravenously injected with saline or synthetic polyinosinic:polycytidylic acid (poly-I:C) as a model of experimental viremia. At 3, 6, 24, or 72 hours after intravenous injection, mice received intraperitoneal injections of gentamicin-Texas Red (GTTR). One hour later, mice were euthanized, systemically fixed and cochlear lateral walls prepared for quantitative confocal microscopy.

Result
Mice with experimental viremia had a marked increase in cochlear lateral wall uptake of GTTR compared to healthy, non-viremic mice. Enhanced GTTR uptake was observed as early as 3 hours after poly-I:C treatment, with decreasing levels of polyI:C-enhanced GTTR uptake at later time points compared to the 3 hour timepoint. Experimental viremia also dilated lateral wall capillaries compared to healthy, non-viremic mice.

Conclusion
We conclude that experimental model of viremia potentiated cochlear lateral wall uptake of GTTR. Our data suggests that systemic inflammation, regardless of etiology, enhances cochlear uptake of aminoglycosides, and potentially ototoxicity, as previously shown for endotoxemia. Thus, generalized systemic inflammation appears to alter blood-brain barrier physiology that can increase the risk of drug-induced ototoxicity of contemporaneously administered aminoglycosides.

Funded by R01 DC004555 (PSS), an American Otological Society Fellowship, and NRSA F30 DC014229-01 (ZDU).

PS 626

Effect of Low Frequency Pulsations on an Inner Ear Fluid Pressure Model

Rick Odland[1,2]; Anna Wilson[1]; Nataniel Helwig[2]; Victoria Jordan[2]; Meredith Adams[2]
[1]Hennepin County Medical Center; [2]University of Minnesota

Background
Audiovestibular symptoms reported by people residing near wind farms may reflect alterations in inner ear fluid pressure in response to infrasound. However, no direct measures of inner ear fluid pressure during low frequency pulsation exposure exist. We hypothesize that low frequency pulsations create a resonance effect and resultant pressure differential between two spaces in fluid communication. Therefore, we aimed to establish a simple bench top model that would allow pressure recording during low-frequency pulsations.

Methods
A model was created using a fluid filled space with 2 chambers on either end. See Figure. A compliant membrane covers the end of the chambers. A valve connecting the two chambers can be adjusted to control resistance. A high frequency response pressure transducer is placed in both chambers. Pulsation is achieved by a mechanical cam shaft device driven by an electric motor. The speed of the motor is controlled by a rheostat and monitored. The model was tested at 5 different frequencies (5, 13, 20, and 37 Hz) and 5 different resistances. Each resistance/frequency setting was tested 3 times. Pressure was recorded by Evolution system. The tracing was continued for 20 seconds or until the pressures stabilized. The average pressure difference over time for each setting was recorded. A 2 factor ANOVA with replication was used to determine statistical significance.

Results
A pressure differential developed between the proximal and distal compartments as soon as the motor was turned on and disappeared when the motor was turned off. There was a trend of greater pressure distally with lower resistance, but this was an irregular function. See Chart. With the valve closed, pressure was higher in the proximal compartment and there was no effect in the distal compartment, as one would expect. The distal pressure increased as the valve was opened at all frequencies except at the 'low resistance' setting, where the apparent trend of decreasing pressure

difference was altered, but only at 13 and 20 Hz. There was a significant interaction between the two variables (P= 0.03)

Conclusion

This preliminary study demonstrates that pulsations in a fluid-filled compartment with compliant membranes can result in a reproducible variation in pressure. The model can be considered to be the oval window, scala vestibuli, helicotrema, scala tympani, and round window in sequence. Low -frequency oscillation may create a pressure differential between scala tympani and scala vestibuli. This complex resonance effect may vary between individuals and symptom states.

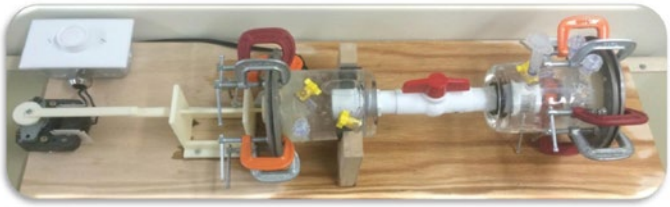

Figure. The model is constucted as a simple tube with a membrane on either end. The the cam shaft device and variable-speed motor on the left caused low-frequency pulsations of the proximal membrane, which are transmitted throughout the space.

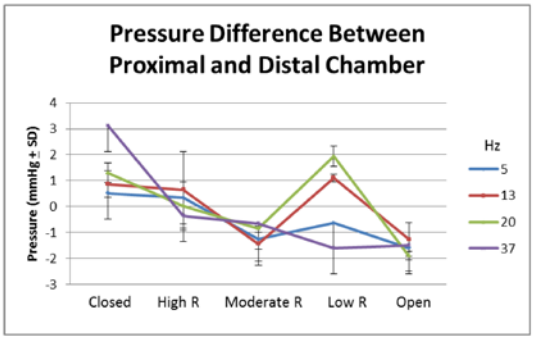

Chart. Graph of the difference in pressure between the proximal and distal chamber measured with the valve between the chambers Closed, set at High, Moderate, and Low resistance, and finally with the valve Open. There is a general trend of increasing distal pressure over the resistances measured at all 4 frequencies. This trend reversed at low resistance but only for 13 and 20 Hz, portending a complicated resonance effect.

Funding

Department of Otolaryngology, Hennepin County Medical Center: Undergraduate Research Opportunity Program, University of Minnesota

PS 627

Effect of Resistance-Compliance Changes in Parallel Fluidic Systems: A Model for Inner Ear Pressure Disequilibrium Caused by Changes in Head Position

Rick Odland[1]; Mark Arnold[2]; Anna Wilson[1]; Meredith Adams[3]

[1]Hennepin County Medical Center; [2]SUNY at Syracuse; [3]University of Minnesota

Background

When two fluid systems, like endolymph and periplymph, are in hydrostatic communication changes in resistance or compliance of either system can transiently affect their equilibrium. Vertigo in the setting of endolymphatic hydrops may result from transient labyrinthine pressure changes, with more compliant membranes suffering greater distension.

We established a physical hydrodynamic model to explore the relationship between the inner ear fluid systems. We aimed to test the effect of two variables, the resistance of fluid flow and membrane compliance, during rotation from horizontal to vertical.

Methods

We constructed a fluid-filled rotating bench-top model of the inner ear (Fig. 1-4). The membrane between the conical structures represented any membrane in hydrostatic communication between the perilymph and endolymph. It was interchanged with a low compliance elastomeric membrane and a compliant membrane. The gate valves adjusted resistance to flow. Fluid pressures were monitored with a fiberoptic transducer tipped pressure monitor placed on either side of the membrane (Fig.1). The model was rotated from 80 degrees to 15 degrees over 15 seconds. Pressure was recorded every second. Five trials with each of the valve settings per membrane were recorded.

Results

Increasing the resistance of one limb of the parallel pathways results in increasing magnitude and duration of pressure differential between the two sides. See Figure Five. With both valves completely open, no pressure differential is seen. With complete obstruction on one side, there is no return to baseline. With intermediate resistance, time to equilibrium increases.

With a change to a more compliant membrane, time to equilibrium peak was delayed. See Figure Six. Resistance was unchanged between experiments. The compliant membrane resulted in a delay to maximum disequilibrium.

Conclusion

Brief periods of disequilibrium were produced by rotation of this parallel fluid pathway model. Increased resistance increased time to equilibrium. Increasing membrane compliance results in a delay to maximum disequilibrium. Changes in resistance or compliance of either side affected the depth and duration of the disequilibrium. Vertigo may be caused by distortion of the membranous labyrinth during a delay in equilibration of endolymphatic and perilymphatic systems, and may be affected by changes in either compliance or resistance (narrowed channels or increase viscosity). This model will allow for further manipulation of resistance and compliance to better understand fundamental physical characteristics of inner ear fluid dynamics.

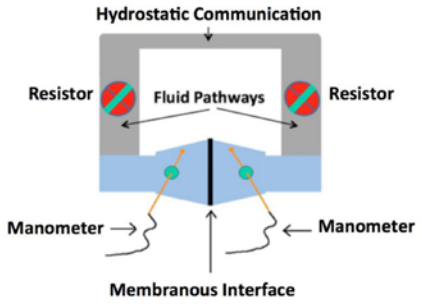

Figure One. Schematic of parallel fluid pathway construct. The two systems have mirror image adjustable resistors, with digital manometers measuring pressure on either side of the compliant membrane. The membranous interface between the two systems can be replaced to change compliance of the system. The fluid pathways are open to atmosphere. The construct can be rotated on an axis about the lower transverse member.

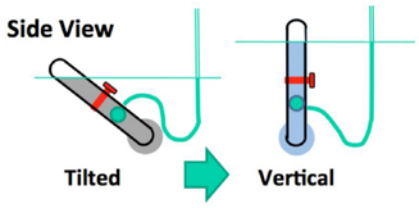

Figure Two. Schematic side view of the Parallel Fluid Pathway Construct. The construct is tilted back to 15 degrees above the horizontal and allowed to come to equilibrium. The fluid manometers measure a lower pressure near the base due to lesser fluid column height. The construct is rotated to a vertical position by a motor. As the construct rotates, pressure at the base will increase, and pressure at the top will decrease. Digital manometers record any differences in pressure between the right and left side. The pressure differential will also deform the membranous interface (See Fig 3)

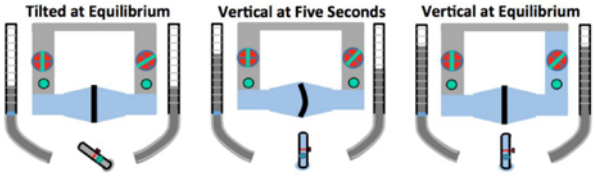

Figure Three. Schematic of the construct at three different times. Manometers are drawn to show relative pressures on each side. In this example, the valve on the right is partially closed to increase resistance to fluid movement. The construct is tilted and allowed to reach hydrodynamic equilibrium. Then the construct is rotated from 15 degrees to 80 degrees over 5 seconds. Initially, pressure on the left base increases immediately, as noted by an increase in the fluid level in the pressure manometer. The increased pressure deforms the membranous interface towards the low-pressure side. As flow continues through the high-resistance right limb, pressure again equalizes and the membrane returns to its midline position. The degree of membrane deformation and the length of the period of disequilibrium are a function of resistance and compliance of the system.

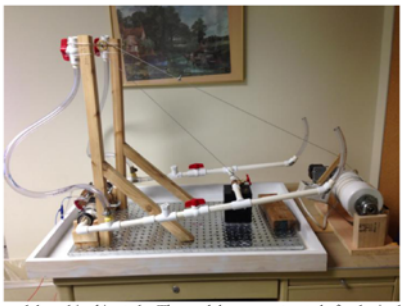

Figure Four. Actual model used in this study. The model was constructed of polyvinylchloride pipe, with gate valves in each limb to change resistance. Using two polycarbonate cups that mated together through a manufactured pressure plate, and the membrane was sandwiched between the pressure plates. The fiberoptic transducer tipped catheters were inserted into the polycarbonate cups. The entire system was filled with water, with an open gate value on the upper crosspiece, and the ends of the tubes were open to atmosphere. The polyvinylchloride piping was rotated by a motor, with the axis of rotation about the low transverse member containing the compliant membrane.

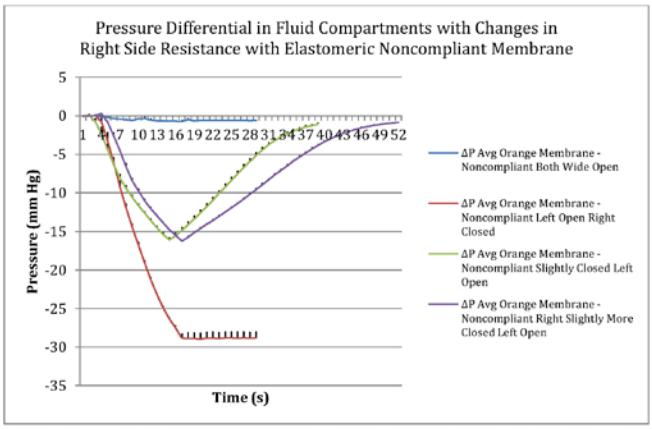

Figure Five. With both values open, no pressure differential between the two sides develops. With one valve closed, pressures diverge and never return to equilibrium. With one value slightly closed, the pressure differential develops and then resolves.

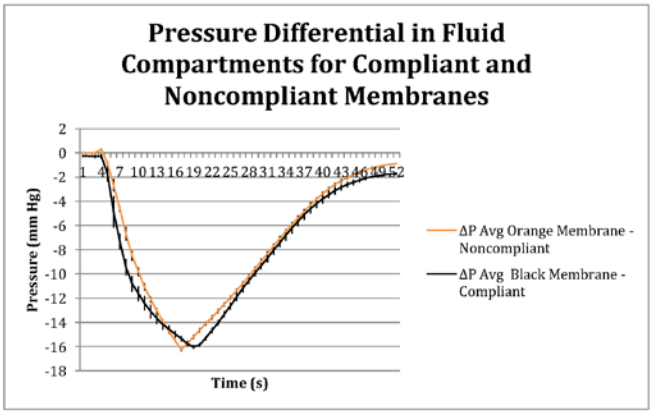

Figure Six. The compliant membrane was slight more delayed in peak differential, demonstrating the effect of the Resistance-Compliance product on time to equilibrium. The return to baseline was affected by several variables.

Funding

This work was supported in part by the Lion's Fund, and in part by the Department of Otolaryngology at Hennepin County Medical Center

PS 628

Cochlear Perfusion with a Viscous Fluid

Yi Wang; Elizabeth Olson

Columbia University

The flow of viscous fluid in the cochlea induces shear forces, which could provide benefit in clinical practice, for example to guide cochlear implant insertion or produce static pressure to the cochlea wall. However, cochlear perfusion with a viscous fluid may damage the cochlea. From a research standpoint, studying the effects of viscous fluid in the cochlea provides data for better understanding cochlear fluid mechanics.

In this work we studied the physiological and anatomical effects of perfusing the cochlea with a viscous fluid. Gerbil cochleae were perfused at a rate of 2.4 µL/min with artificial perilymph (AP) and sodium hyaluronate (Healon, HA) in four different concentrations (0.0625%, 0.125%, 0.25%, 0.5%). The HA was applied in order of increasing concentration as well as viscosity. The perfusion fluid entered from the round window and was withdrawn using a perfusion pump from a hole in the basal scala vestibuli, in order to perfuse the entire cochlea. Compound action potentials (CAP) were measured after each perfusion.

After perfusion with increasing concentrations of HA, the CAP thresholds increased. The threshold elevation after AP and 0.0625% HA perfusion was small or almost zero, and the 0.125% HA was a borderline case, while the higher concentrations significantly elevated CAP thresholds. Histology of the cochleae perfused with the 0.125% and 0.5% HA showed that the Reissner's membrane was torn and the organ of Corti (OC) was distorted. We suspected that these changes were caused by the shear stress produced by the motion of the viscous perfusion fluid. Our results and analysis indicate that the cochlea can sustain, without a significant CAP threshold shift, up to a 0.42 Pa shear stress. In the 0.125% and 0.25% HA perfusion cases, a temporary CAP threshold shift was observed, perhaps due to a changed traveling wave pattern caused by the viscous fluid within the cochlear duct, or to a temporary position shift of the OC. After 0.5% HA perfusion, the character of the CAP waveform changed; in particular, a short latency positive peak (P0) appeared. This P0 was suspected to be a combination of CAP response and increased summating potential (SP) caused by OC distortion or position shift.

Funding
NIH NIDCD R01 DC003130

PS 629

Using a commercially available Optical Coherence Tomography system to measure vibrations within the cochlea

Nathan Lin; Christine Hendon; Elizabeth Olson
Columbia University

I. Introduction
Obtaining vibration measurements of the basilar membrane (BM) and tectorial membrane (TM) simultaneously is vital to understanding hair cell stimulation and the processes leading up to it. This measurement is challenging because the standard method of auditory vibration measurement, heterodyne interferometer, has limited penetration depth.

Spectral Domain Optical Coherence Tomography (SDOCT) system was introduced to the auditory community by the Nuttall and Oghalai labs. In this study, we used a commercial SDOCT system, and applied its functional extension, spectral domain phase microscopy, to simultaneously measure nano-scale vibration of multiple cochlear structures.

II Method
The Thorlabs TELESTO SDOCT system has a central wavelength of ~1325 nm and spectral width >100 nm resulting in an optical sectioning curve with FWHM of ~ 7 um. The system can operate at three sampling rates and the highest, 92 kHz, was used. The object beam was aimed through the round window membrane of just-euthanized gerbils to observe the BM and organ of Corti complex (OCC) surfaces. These structures were identified by their locations in the real time B-scan image obtained with the Thorlabs software. The B-scan's field of view was decreased to obtain an A-scan (a single axial line of the B-scan) that contained the structures of interest. Each A-scan is derived from the magnitude of a spatial-domain Fourier Transform of k-domain data collected by an array of 1024 photodetectors. This results in 512 spatial domain pixels with a spacing of ~5-um within each A-scan axial image. The phase of the A-scan data contains sub-pixel information, including information about motion. A speaker and tube were used to deliver pure tones to the ear canal. Stimulus levels of 74 and 94 dB SPL were used. Repeated A-scans were taken at 92 kHz and the phase of the A-scan phase data used to find the motion of the cochlear structures.

III. Results
The displacement of the BM, OC and round window membrane surfaces we found were consistent with previous motion measurements from our and other's labs. The motions scaled linearly with sound level, as expected post-mortem. The signal:noise level with 0.08s of signal averaging was 0.4nm, which is sufficient for many measurements and will be reduced with the use of a sound booth and increased signal averaging.

IV. Conclusion
This commercial system will allow auditory scientists without expertise in optical system development to perform SD-OCT based inner ear vibration measurements.

Funding
NIH grant R01 DC003130, the Emil Capita Foundation, and Columbia Universityâ€™s Electrical Engineering Department.

PS 631

Experimental pneumococcal meningitis induces rampant cochlear inflammation and neo-ossification in mice

Keiko Hirose; Song Zhe Li
Washington University

Background
Bacterial meningitis is a potentially life threatening infection that frequently affects hearing. Pneumococcal meningitis results in a 50% mortality rate worldwide and 25% chance of profound hearing loss. The mechanism of hearing loss caused by meningitis is not well understood. In human post-mortem studies, degeneration of hair cells and neurons is observed in some, but not all cases of hearing loss after meningitis. In cases of pneumococcal meningitis, ossification of the scala tympani is frequently associated with loss of hearing. We have used a mouse model of meningitis to investigate the process by which hearing is affected by cochlear infection and inflammation.

Methods
Adult mice were injected with $1x10^5$ cfu of streptococcus pneumoniae (type 3) into the cisterna magna. Ceftriaxone was administered IP to mice day 2 and 3 after infection. Mice were evaluated using ABR and micro CT, and perilymph sampling was performed to assess the blood labyrinth barrier integrity at various time points after infection. The inner ears were harvested for histologic analysis.

Results
Hearing loss developed in over 70% of infected animals. Average ABR thresholds after meningitis were 50-60 dB greater than in saline-injected control mice. Rampant inflammation was observed with leukocyte migration and in some animals, overt hemorrhage occurred into the scala tympani. Bacteria and leukocytes appeared to enter the labyrinth through the cochlear aqueduct. The blood labyrinth barrier was profoundly leaky four days after infection and was restored to normal in most animals by 30 days after infection. Some mice demonstrated obstruction of the cochlear aqueduct after infection, associated with fibrosis and ossification of the scala tympani in the basal turn. Cochlear ossification was preceded by entry of both CCR2+ and CX3CR1+ monocytes into the scala tympani. New bone formation was most notable in the basal turn of the scala tympani, which was not consistently the site of the majority of inflammatory cells.

Conclusions
Induction of experimental bacterial meningitis with live pneumococci applied to the cisterna magna caused hearing impairment, cochlear inflammation and ossification of the basal turn of scala tympani in some animals. Cochlear inflammatory monocytes that migrate into the scalae in response to infection are likely precursors to osteoclasts that initiate bone turnover leading to cochlear ossification.

Funding
Study supported by NIH R01 DC001315 (KH)

PS 632

Thickened Strial Capillary Basement Membrane Impairs Diffusion in Alport Mouse.

Edward Doyle III[1]; Grady Phillips[1]; Brendan Smyth[2]; MIchael Anne Gratton[1]
[1]Saint Louis University; [2]Bristol-Myers Squibb

Introduction
Alport syndrome is a genetic disorder of type IV collagen leading to aberrant basement membrane composition. It is associated with glomerulosclerosis and progressive hearing loss. The Alport mouse cochlea is a hypoxic microenvironment. Previously we have shown that Alport mice have upregulated hypoxic inducible factor-1α, are susceptible to noise, and have a reduced endocochlear potential. Furthermore, no difference exists in capillary density or strial area between Alport and wild type (WT) littermates; however, thickness of the Alport strial capillary basement membranes (SCBMs) is significantly increased. Based upon these findings, we hypothesize that the hypoxic microenvironment is due to reduced diffusion capabilities of the thickened SCBMs for molecules diffusing from the strial vasculature into the strial tissue. This hypothesis is substantiated by qualitatively and quantitatively demonstrating that thickened SCBMs have impaired diffusion capabilities.

Methods
7-9wk old 129 Sv/J Col4α3 KO (Alport) and WT mice (3 groups/genotype, 10-15/group) were anesthetized (Avertin (0.4 mg/g BW, IP)). The mouse underwent intra-cardiac injection (200 µl) of unconjugated Rhodamine fluorescent dye (0.04% in sterile saline) followed by 3 minutes incubation.

For qualitative analysis, within 20 minutes, the stria was isolated, flat mounted and subjected to time lapse microscopy every 5 minutes. The images, less identifying information, were reviewed to determine the post-injection time at which fluorescence was detected outside the strial capillaries.

For quantitative analysis, the mouse was transcardially perfused (4ml phosphate-buffered saline (PBS)). The isolated cochleae were perilymphatically perfused (4% paraformaldehyde in cacodylate buffer). Within 20 minutes, the lateral wall (LW) of both cochleae were dissected, placed into 0.5 ml tubes, and frozen in liquid nitrogen. For the 3rd group, spiral ligament only (negative control) was isolated. Each sample was homogenized (PBS); then centrifuged (15 min, 10kg). Fluorescence (550/580) in aliquots (30 µl) of the supernatant and resuspended pellet was quantified (BioTek Neo) in 384 low-volume plates against a standard curve of the fluorescent dye.

Results
The time for dye diffusion from the capillary into strial tissue was approximately 1.5x longer in Alport vs WT stria (38 vs 22 minutes). Fluorescence in supernatant from the LW of Alport mice was significantly lower than that of WT mice, but no difference was noted between genotypes in fluorescence of LW pellets or spiral ligament samples.

Conclusions
The reduced diffusion capability from strial capillaries in the Alport mouse supports our hypothesis that the thickened SCBM is the primary cause of a hypoxic microenvironment in the Alport cochlea.

Funding
Supported by NIH NIDCD DC0042 to MAG

PS 633

Quantification of endolymphatic hydrops after surgical obliteration of the endolymphatic sac using contrast enhanced small animal MRI

Marcus Müller[1]; Julia Mannheim[2]; Andreas Schmid[2]; Hidetaka Kumagami[3]; Bernd Pichler[2]; Hubert Löwenheim[1]
[1]Carl von Ossietzky University Oldenburg; [2]Eberhard Karls University Tübingen; [3]University Graduate School of Biomedical Sciences, Nagasaki, Japan

Surgical obliteration of the endolymphatic sac leads to hydrops of the ductus cochlearis and the sacculus in the labyrinthine membrane. Hydrops is one of the symptoms in Morbus Ménière which is characterized by hearing loss, tinnitus and vertigo. Recent advances in MR imaging have allowed the volumetric quantification of the endolymphatic hydrops and hence allow *in vivo* diagnosis. Guinea pigs underwent a unilateral surgical obliteration of the endolymphatic sac. To quantify volume change of the fluid spaces in the inner ear, guinea pigs were *i.v.* injected with a gadolinium based contrast agent. MR images were acquired at a voxel size of

0.102 x 0.102 x 0.3 mm^3. MR imaging was performed one week before and at regular interval for up to 6 months after obliteration. After the last MRI scan, the inner ear function of the animals was examined using electrocochleography, and inner ears were fixed. One week after obliteration volume of scala media had increased in half of the animals at the expense of the volume of the scala vestibuli (max. 3.1 to 1.5 mm^3). Three weeks after obliteration few animals showed still an increase of the volume of the scala. For one animal that didn't show a volume change in week 1, an increase of volume was detected in week 3 (decrease of scala vestibuli 2.7 to 1.1 mm^3). Some animals, that showed a volume increase in week 1, the volume decreased back to baseline levels. Volume of the scala tympani was stable over time. The electrophysiological examination did not show a significant difference between the control and the obliterated ear. Histological staining showed a good correlation with the MRI results. To our knowledge this is the first *in vivo* study showing the onset of the endolymphatic hydrops one week after surgical obliteration. However, further studies are required to optimize the surgery to obtain a more stable hydrops. Nevertheless, this animal model showed a high potential of being a suitable tool to study potential therapies.

PS 634

Electrogenic transport and K+ ion channel expression by the human endolymphatic sac epithelium

Ji Young Suh[1]; Jin Young Kim[1]; Bo Gyung Kim[2]; Ji Eun Yoo[3]; Jae Young Choi[1]; Sung Huhn Kim[1]
[1]Yonsei University College of Medicine; [2]Sooncheonhyang University College of Medicine; [3]Institute for Human Natural Defense System, Yonsei University College of Medicine

Background
The endolymphatic sac (ES) is a cystic organ that is a part of the inner ear and is connected to the cochlea and vestibule. The ES is thought to be involved in inner ear ion homeostasis and fluid volume regulation for the maintenance of hearing and balance function. Many ion channels, transporters, and exchangers have been identified in the ES luminal epithelium, mainly in animal studies, but there has been no functional study investigating ion transport using human ES tissue. We designed the first functional experiments about electrogenic transport in human ES and investigated the contribution of K+ channels in the electrogenic transport, which has been rarely identified, even in animal studies, using electrophysiological/ pharmacological and molecular biological methods.

Method
Scanning vibrating electrode technique was used for measuring trans-epithelial current from ES epithelium. LC-MS/MS, RT-PCR, and immunohistochemistry was used for detecting protein or transcript expression of human ES tissue.

Results
We identified functional and molecular evidences for the essential participation of K+ channels in electrogenic transport in human ES epithelium. The identified K+ channels involved in the electrogenic transport were KCNN2, KCNJ14, KCNK2, and KCNK6 oupled with the activity of NKCC/Na+, K+ - AT-Pase.

Conclusion
The K+ transport is thought to play an important role in the maintenance of inner ear homeostasis by participating in the regulation of electrogenic transport.

Funding
National Research Foundation of Korea (NRF) grant funded by the Ministry of Education (2013R1A1A2059696) to JYC, and the Basic Science Research Program through the NRF grant funded by the Ministry of Science, ICT & Future planning (2012R1A1A1042980) to SHK

PS 635

Generation of induced pluripotent stem cells from connexin26 conditional knock out mouse

Toru Aoki; Katsuhisa Ikeda; Kazusaku Kamiya
Juntendo University

Objectives
Hereditary deafness affects approximately one in 1600 children. Gjb2 gene encoding connexin26 (Cx26) plays important role in intercellular communication of cochlea Gap junction between the inner ear cells. We previously developed Cx26 knockout mice ($CX26^{f/f}$ P0-Cre) by using Cre-loxP system. In this study, we generated induced pluripotent stem (iPS) cells from $CX26^{f/f}$ P0-Cre mice to reproduce the pathogenesis caused by Cx26 deficiency Our final goal is to produce the inner ear cell-like cells from the patients with GJB2 related hearing loss for drug screening and cell therapy.

Methods
We dissected cochlear fibrocytes of $CX26^{f/f}$ P0-Cre mice and C57BL/6 mice because Cx26 gene is specifically deleted in inner ear of this mouse. These cells were reprogramed to generate iPS cells by using Sendai-virus vector with reprogramming factors, Klf4, Oct3/4, Sox2 and c-Myc, and characterized the pluripotency by alkarine phosphatase (ALP) staining and immunostaining.

Results
Cochlear fibrocytes were dissected from $CX26^{f/f}$ P0-Cre mice and C57BL/6 mice. Cultured cochlea fibrocytes were infected with Sendai-virus (SeV) vector with reprograming genes. iPS cells generated $CX26^{f/f}$ P0-Cre and C57BL/6 inner ear cells were stained with ALP and Oct3/4, Sox-2 and SSEA-1 antibodies as a marker of pluripotency.

Conclusions
In this study, we generated iPS cells from the cochlear fibrocytes of $CX26^{f/f}$ P0-Cre and C57BL/6 mice by SeV vector with reprogramming genes. The ALP staining and immunostaining suggested that the generated cells have a pluripotency as iPS cell. Disease specific iPS cells derived from mutant animal models will be powerful tool for drag screening and cell therapy targeting GJB2 related hereditary deafness.

PS 636

Differentiation of mouse iPS cell into Cx26-positive cell and formation of inter cellular Cx26-gap junction plaque

Ichiro Fukunaga; Kaori Hatakeyama; Toru Aoki; Ayumi Fujimoto; Atena Nishikawa; Katsuhisa Ikeda; Kazusaku Kamiya
Juntendo University

Background

Congenital deafness affects about 1 in 1000 children and more than half of them have a genetic background such as Gap Junction Beta 2 (*GJB2*) gene mutation, the gene encoding the Connexin 26 (Cx26) protein. Recently, we reported that disruption of the Cx26-dependent gap junction plaque (GJP) is associated with the pathogenesis of *GJB2*-related deafness (Kamiya *et al*., *J Clin Invest,* 2014) and the cochlear gene transfer of *Gjb2* using an adeno-associated virus (AAV) significantly improved GJP formation and the auditory function (Iizuka *et al., Hum Mol Genet*, 2015). On the other hand, we developed a novel strategy for inner ear cell therapy with bone marrow mesenchymal stem cells (Kamiya *et al., Am J Pathol,* 2007).

Induced pluripotent stem (iPS) cells can be produced by reprogramming of somatic cells and are capable of self-renewal and differentiation into various types of cells as embryonic stem (ES) cells.

Although, many studies have shown the differentiation of ES/iPS cells into Cx37/40/43/45 expressing cells, the differentiation into Cx26 expressing cells and the Cx26-gap junction formation has not been reported yet. In this study, we developed a new strategy for differentiation of mouse iPS cells into Cx26 expressing cells.

Method

We examined the strategy to induce Cx26 expressing cells with GJP formation from mouse iPS cells using modified methods of previous studies for inner ear differentiations with aggregate formation.

Results

After the aggregate formation in the several differentiation conditions, epithelial like cells were observed at the surface of these aggregates. Notable differences in epithelial formation and thickness were observed among these conditions. In a part of the aggregates, Cx26 positive cells were observed and these cells showed GJP-like formations as cochlear cells.

Conclusion

This is a first report to demonstrate the differentiation of mouse iPS cells into Cx26 positive cells followed by Cx26-GJP formation. By using these Cx26-positive cells, it is expected to establish the inner ear cell therapy for hearing recovery in *GJB2*-related hereditary deafness.

Funding

Japan Agency for Medical Research and Development (AMED) of Japan (to K.K.) The Ministry of Education, Science and Culture (to K.K.) MEXT-support program for the Strategic Research Foundation at Private Universities, 2011â€“2014 (K.I.) Takeda science foundation (to K. K.) The Science Research Promotion Fund for priate school, Japan (to K.K.)

PS 637

Deformation of the Outer Hair Cells and the Accumulation of Caveolin-2 in Connexin 26–Deficient Mice

Takashi Anzai; Kazusaku Kamiya; Katsuhisa Ikeda
Juntendo University Faculty of Medicine

Background

Mutations in *GJB2*, which encodes connexin 26 (Cx26), a cochlear gap junction protein, represent a major cause of prelingual, non-syndromic deafness. The degeneration of the organ of Corti observed in Cx26 mutant–associated deafness is thought to be a secondary pathology of hearing loss. Here we focused on abnormal development of the organ of Corti followed by degeneration including outer hair cell (OHC) loss. Here we investigated the crucial factors involved in late-onset degeneration and loss of OHC.

Method

We analyzed the change in the protein expression and localization in the organ of Corti in our Cx26-deficient mice ($Cx26^{f/f}$P0Cre).

Result

In ultrastructural observations of $Cx26^{f/f}$P0Cre mice, OHCs changed shape irregularly, and several folds or notches were observed in the plasma membrane. Furthermore, the mutant OHCs had a flat surface compared with the characteristic wavy surface structure of OHCs of normal mice. We investigated the factors that contribute to the deformation and degeneration of the organ of Corti of $Cx26^{f/f}$P0Cre mice. Cochleae of $Cx26^{f/f}$P0Cre mice were subjected to proteomic analysis, which revealed an increase in the level and abnormal localization of caveolin-2 (CAV2) in the organ of Corti. Diffuse labeling of CAV2 was observed in the organ of Corti of control mice, but there was remarkable accumulation of CAV2 in $Cx26^{f/f}$P0Cre mice. In particular, this accumulation of CAV2 was mainly observed around OHCs, and furthermore this accumulation was observed around the shrunken site of OHCs with an abnormal hourglass-like shape.

Conclusion

The deformation of OHCs and the accumulation of CAV2 in the organ of Corti may play a crucial role in the progression of, or secondary OHC loss in, *GJB2*-associated deafness. Investigation of these molecular pathways, including those involving CAV2, may contribute to the elucidation of a new pathogenic mechanism of *GJB2*-associated deafness and identify effective targets for new therapies.

PS 638

Induction of iPS cell differentiation into Connexin26 positive cells with gap junction plaques using cochlear feeder cell

Ayumi Fujimoto; Ichiro Fukunaga; Kaori Hatakeyama; Toru Aoki; Atena Nishikawa; Katsuhisa Ikeda; Kazusaku Kamiya
Juntendo University Faculty of Medicine

Objectives

Hereditary deafness affects about 1 in 1600 children and GJB2 gene mutation is most frequent cause for this disease. GJB2 encodes connexin26 (Cx26), a component in cochlear gap junction. Cx26 is mainly expressed in cochlear supporting cells and fibrocytes, and forms large gap junction plaque (GJP) macromolecular complex. To date the differentiation of induce pluripotent stem (iPS) cells into hair cell-like cell have been reported, although the differentiation into cochlear supporting cells and fibrocytes expressing Cx26 is not accomplished yet. To differentiate these cells into cochear cells which is non-neural ectoderm, neural cells are needed to be excluded in the ectodermal differentiation. Our goal is to establish method to differentiation of iPS cells into Cx26 positive cells with proper GJP formation as cochlear cells.

Materials and Methods

The cochlear feeder cells were developed from adult cochlear tissue to support cochlear differentiation. Undifferrentiated mouse iPS cells were cultured in mediums which contain several reagent cocktails on the cochlear feeder cells. Cx26 expression was analyzed by immunohistochemistry. GFP signals controlled by Nanog promotor Nanog-GFP were monitored as an undifferentiated state marker.

Results

The iPS cells proliferated on cochlear feeder cells and showed gradual decrease in expression of Nanog-GFP in all conditions. Remarkable morphological changes among the reagents were observed in about 1-2 weeks. The cells cultured in Reagent B included a number of stroma-like cells. These cells were subcultured, and separated to large cells with strong adhesive property or small cells with low adhesive property. In this small cell culture, a number of the cells forming Cx26-gap junction plaques were observed.

Conclusions

In this study, iPS cells differentiated into neural or non-neural cells depending on the reagent cocktails on cochlear feeder cells. Our method is thought to be effective to establish Cx26 gap junction forming cells similer to cochlear fibrocytes and supporting cells. By establish of this method, it is expected to make disease model cells of patient with hereditary deafness caused by GJB2 gene mutation for the drag screening. Furthermore, the cells are expected to be used also for the cell therapy targeting this disease.

PS 639

Various cochlear gap junction plaque reproduced in human cell line

Kaori Hatakeyama; Katsuhisa Ikeda; Kazusaku Kamiya
Juntendo University

Objectives

The mutations in connexin26 (Cx26), a cochlear gap junction protein, represent a major cause of pre-lingual, non-syndromic deafness, as they are responsible for as many as 50% of such cases in certain population. Recently, we reported that Cx26-dependent gap junction plaque (GJP) disruption occured as the earliest change during embryonic development, results in a drastic reduction in the GJP area and the protein levels in Cx26 mutant mouse models (Kamiya et al., J Clin Invest, 2014;124(4)1598-1607) and Brn4 deficient mice, a model of DFN3 non-syndromic deafness. To elucidate the mechanism of this biochemical change, we developed the molecular live imaging system targeting GJP composed of Cx26 and Cx30. Our final goal is to screen the chemicals to stabilize the cochlear GJPs at the cell borders.

Methods

The cells with the transient expression and stable expression of human wild type Cx26, mutant Cx26 (R75W) and wild type Cx30 were generated with HEK293 and HeLa cell lines.

Results

With our generated connexin expressing cells, we observed various types of GJPs as well as Cx26-mutant mouse cochleae. Our system enabled us to analyze the GJP assembly, trafficking, membrane integration and degradation of GJPs composed of Cx26 and Cx30. In this system, we observed the difference of incorporated gap junction plaque according to the expressed connexin.

Conclusions

These in vitro gap junction constructions will enable the large scale drag screening targeting GJP formation and stabilization for Cx26 associated deafness.

Funding

This work was supported in part by research grant from Japan Agency for Medical Research and Development (AMED) of Japan (to K.K.), Ministry of Education, Science and Culture (to K.K.) and The Science Research Promotion Fund for priate school, Japan (to K.K.).

PS 640

Catecholamines regulate Cx43 expression and endolymphatic homeostasis in inner ear.

Florent Manach[1]; Say Viengchareun[1]; Ingrid Lema[1]; Marc Lombes[2]; Evelyne Ferrary[2]; **Jerome Nevoux**[1]
[1]Paris Saclay University; [2]Inserm

Introduction

Menière's disease is an invalidating disease evolving by crisis, frequently triggered by stress and associating vertigo, deafness and tinnitus. Studies have reported that the plasmatic concentration of epinephrine is higher in patient with a Menière's disease. Ferrary et al have reported also

that potassium concentration is decreased in the endolymph in an animal model of Menière's disease. In the inner ear, beta-adrenergic receptors are present in the endolymph secretory structures, for example the dark cells in vestibule. These data suggest that catecholamine could be implicated in the potassium dysregulation in inner ear that conduct to Menière's disease crisis. The aim of this work is to study the role of catecholamine in potassium regulation and the role of GJA1 in potassium transport in inner ear.

Material and methods
For this purpose, we used the EC5v murine inner ear cell line, previously established in the laboratory, which exhibits functional properties of vestibular dark cells, the human utricular cells in primary culture, harvested during vestibular schwanomma surgery and mice. We studied the Cx43 regulation at the mRNA and protein levels by RT-PCR and Western blot respectively. Standard and confocal fluorescence microscopy was used to localize the subcellular expression of Cx43. Measurement of transepithelial water and potassium transport was performed mesuring tritiated water and rubidium 86 fluxes on EC5v cells cultured on filters. In vivo, in wlid type and Cx43 deleted mice, we investigated with RT-PCR the regulation of Cx43 expression in mice inner ear and heart.

Results
The Cx43 was identified in inner ear by RT-PCR and WB. Cx43 was localized in human utricle and mouse inner ear by immunohistochemistry, and confocal microscopy. Mutant mice presented a delayed and progressive hearing loss. Unidirectional transepithelial potassium fluxes were studied by means of Rb86 transport in murine EC5v vestibular cells cultured on filters, treated or not with isoprotérénol (10-6 M). The inhibitory effect of isoproterenol upon Cx43 expression was assessed in EC5v cells and in vivo in mice.

Cx43 was highly expressed in both endolymph secretory structures of the mouse inner ear, and EC5v cells. We demonstrated that potassium transport, from the basolateral (perilymphatic) to the apical (endolymphatic) compartments, was stimulated by isoproterenol in EC5v cells.

Conclusions
We show for the first time that catecholamines down regulates Cx43 expression in inner ear, and control endolymphatic potassium secretion. These findings should encourage further clinical trials evaluating beta-blockers efficacy in Menière's disease.

Funding
Fondation des Gueules Cassées

PS 641

The Endolymphatic Calcium Concentration Correlates with the Endocochlear Potential rather than with the Endolymphatic pH

Daniel Marcus; Donald Harbidge; Philine Wangemann
Kansas State University

Introduction
Mutations of *SLC26A4* are a common cause of progressive hearing loss. *SLC26A4* encodes pendrin, which is a Cl^-/HCO_3^- exchanger expressed in epithelial cells of the cochlea. Interestingly, cochlear pendrin expression is not necessary for normal development and acquisition of hearing in mice. Pendrin expression, however, is required in the embryonic endolymphatic sac for normal cochlear development (Choi et al., 2011; Li et al., 2013). This raises the question whether cochlear pendrin expression has physiologic relevance in the adult cochlea.

Objective
We raised the hypothesis that HCO_3^- secretion by pendrin raises the pH in endolymph and that lack of pendrin causes acidification and an increase in the endolymphatic Ca^{2+} concentration through inhibition of acid-sensitive Ca^{2+} absorptive pathways. The objective of this study was to determine whether the cochlear pendrin expression affects the endocochlear potential, the endolymphatic pH and the endolymphatic Ca^{2+} concentration in normoxia, hypercapnia and anoxia.

Methods
Experiments were carried out in Tg(-);*Slc26a4*$^{\Delta/+}$ mice that express pendrin in the cochlea and Tg(+);*Slc26a4*$^{\Delta/\Delta}$ mice that lack cochlear pendrin expression. The endocochlear potential (EP), the endolymphatic pH and the endolymphatic Ca^{2+} concentration were measured with double-barrel ion-selective electrodes. Anesthetized animals were artificially ventilated with room air (normoxia; ~20% O_2, ~80% N_2) or with a gas mixture (hypercapnia; 20% CO_2, 20% O_2, 60% N_2) and terminal anoxia was induced by cessation of ventilation.

Results
Hypercapnia resulted in a decline of the EP by 22 mV, an acidification of endolymph by 0.39 pH-units but no change in the endolymphatic Ca^{2+} concentration. In contrast, anoxia resulted in a decline of the EP by 121 mV, an acidification of endolymph by 0.47 pH-units and a 61-fold increase in the endolymphatic Ca^{2+} concentration. No differences were observed between Tg(-);*Slc26a4*$^{\Delta/+}$ and Tg(+);*Slc26a4*$^{\Delta/\Delta}$ mice.

Conclusion
These observations demonstrate a tight correlation of the endolymphatic Ca^{2+} concentration with the EP but not with the endolymphatic pH. The absence of differences between Tg(-);*Slc26a4*$^{\Delta/+}$ and Tg(+);*Slc26a4*$^{\Delta/\Delta}$ mice suggests that pendrin does not control the endolymphatic pH in the adult cochlea.

Funding
NIH-R01-DC012151, Kansas State University

PS 642

Gene-expression Profiling of the Endolymphatic Sac in Slc26a4Δ/+ and Slc26a4Δ/Δ mice

Philine Wangemann[1]; Xiangming Li[1]; Fei Zhou[1]; Keiji Honda[2]; Andrew Griffith[2]
[1]Kansas State University; [2]National Institute on Deafness and Other Communication Disorders

Background
A leading cause of syndromic and non-syndromic hearing loss is mutations of *SLC26A4* that compromise hearing and vestibular function via a pathological enlargement of the inner ear. *Slc26a4*$^{\Delta/\Delta}$ mice recapitulate this enlargement and fail to acquire hearing and balance. The enlargement develops in *Slc26a4*$^{\Delta/\Delta}$ mice between embryonic day 14.5 (E14.5) to E17.5 which coincides with the normal growth phase of the cochlea (Kim & Wangemann 2010). Anatomical truncation experiments have suggested that the enlargement originates from an imbalance of fluid secretion and absorption and that the embryonic endolymphatic sac is the major site of fluid absorption with fluid absorption depending on pendrin. A mechanistic understanding of fluid absorption, however, is lacking. The importance of the endolymphatic sac for the development of hearing is evident from the finding that restoration of pendrin expression solely in the endolymphatic sac is sufficient to prevent enlargement and to restore hearing and vestibular function in *Slc26a4*$^{\Delta/\Delta}$ mice (Li et al., 2013).

Objectives
The objective of this study was to gain a mechanistic understanding of fluid absorption in the endolymphatic sac. We had two hypotheses: (1) Gene expression profiling of the developing endolymphatic sac could support the generation of testable models of ion transport with the goal to identify targets for a pharmacologic manipulation of fluid absorption; (2) Expression levels of ion transport genes engaged in fluid absorption will rise in *Slc26a4*$^{\Delta/+}$ mice.

Methods
Endolymphatic sacs were obtained from *Slc26a4*$^{\Delta/+}$ and *Slc26a4*$^{\Delta/\Delta}$ mice at ages E13.5, E14.5, E16.5 and E17.5. Total RNA was isolated (Qiagen), transcribed into cDNA, amplified, and labeled (Nugen). Gene expression was analyzed on Affymetrix microarrays.

Results
Analysis of the data identified several ion transport genes with rising expression levels in *Slc26a4*$^{\Delta/+}$ mice. Among them, we found pendrin-dependent and pendrin-independent genes. Genes, whose expression levels rose in *Slc26a4*$^{\Delta/+}$ but not in *Slc26a4*$^{\Delta/\Delta}$ mice, included *Cftr, Slc4a9, Clcnkb, Bsnd, Slc4a11, Aqp3,* and *Car3.* Genes, whose expression levels rose in *Slc26a4*$^{\Delta/+}$ and in *Slc26a4*$^{\Delta/\Delta}$ mice, included *Atp6v1b1, Scnn1a*, *Scnn1b, and Car2.* All of these genes are known to be expressed in the renal collecting duct.

Conclusion
The data indicate a model in which that the endolymphatic sac in *Slc26a4*$^{\Delta/+}$ mice absorbs fluid by a model and mechanisms found in the renal collecting duct. Failure of fluid absorption in the endolymphatic sac of *Slc26a4*$^{\Delta/\Delta}$ mice is due to a lack of pendrin expression and a concurrent reduction of expression levels of other ion transport genes.

Funding
NIH-DC012151

PS 643

NaCl secretion in the embryonic vestibular labyrinth drives the enlargement of the inner ear in Slc26a4Δ/Δ mice

Philine Wangemann; Fei Zhou; Daniel Marcus
Kansas State University

Background
Mutations of *SLC26A4* are a common cause of hearing loss associated with an enlargement of the inner ear. *Slc26a4*$^{\Delta/\Delta}$ mice recapitulate the enlargement and fail to acquire hearing and vestibular function. The enlargement develops in *Slc26a4*$^{\Delta/\Delta}$ mice between embryonic day 14.5 (E14.5) and to E17.5 which coincides with the normal growth phase of the cochlea (Kim & Wangemann 2010). Truncation experiments have suggested that the enlargement originates with fluid secretion in the vestibular labyrinth. The site of fluid secretion, however, remained poorly defined and a mechanistic understanding is lacking.

Objectives
The objective of this study was to demonstrate fluid secretion in the embryonic vestibular labyrinth and to determine whether fluid secretion is driven by NaCl or KCl transport. The importance of understanding the mechanism of fluid secretion in the developing inner ear rests with the goal to identify targets for a pharmacological manipulation aimed to restore hearing and vestibular function.

Methods
Preparations of the vestibular labyrinth were isolated by microdissection from embryonic *Slc26a4*$^{\Delta/+}$ and *Slc26a4*$^{\Delta/\Delta}$ mice and maintained for 17-24 hrs in organ culture. These preparations consisted of the anterior part of the utricle with attached anterior and lateral ampulla. Methods were developed to quantify the luminal volume by 3D-confocal microscopy and geometric approximation. Luminal K^+ concentrations and transepithelial voltages were measured with double-barreled K^+-selective electrodes. Expression of the K^+ channel KCNQ1, the $Na^+/2Cl^-/K^+$ cotransporter SLC12A2, and the Na^+/K^+ ATPase subunit ATP1A1 was evaluated by confocal immunocytochemistry.

Results
The luminal K^+ concentration in utricles of *Slc26a4*$^{\Delta/+}$ and *Slc26a4*$^{\Delta/\Delta}$ mice was ~10 mM at embryonic day 16.5 (E16.5) and rose over the next six days to ~90 mM. The initial rise was delayed in *Slc26a4*$^{\Delta/\Delta}$ mice by ~1 day. K^+ concentrations reached 150 mM and 132 mM in adult *Slc26a4*$^{\Delta/+}$ and

Slc26a4$^{\Delta/\Delta}$ mice, respectively. The transepithelial potential at E16.5 was -10 mV in *Slc26a4*$^{\Delta/+}$ and -2 mV in *Slc26a4*$^{\Delta/\Delta}$ mice. Preparations of the vestibular labyrinths isolated at E15.5 from *Slc26a4*$^{\Delta/+}$ and *Slc26a4*$^{\Delta/\Delta}$ mice accumulated fluid at a rate of 1-2 nl/hr leading within 17-24 hrs to a remarkable swelling of these preparations. Strong expression of ATP1A1 was found in vestibular dark cells, the macula utriculi and the cristae ampullaris but no expression of KCNQ1 or SLC12A2 was detected.

Conclusion
These data demonstrate fluid secretion in the embryonic vestibular labyrinth of *Slc26a4*$^{\Delta/+}$ and *Slc26a4*$^{\Delta/\Delta}$ mice and suggest that fluid secretion is driven by NaCl secretion.

Funding
NIH-R01- DC012151

PS 644

Co-release of Glycine and GABA in the Mouse Central Nucleus of the Inferior Colliculus

Lucille Moore; Laurence Trussell
Oregon Hearing Research Center

Background
The central nucleus of the inferior colliculus (ICC) is a nearly obligatory relay station for ascending streams of auditory information. Auditory brainstem regions that project to the ICC release glutamate, GABA and glycine. Glycinergic input originates from the ventral nucleus of the lateral lemniscus (VNLL) and lateral superior olive (LSO), regions important for indicating onset of sound and location of sound in space, respectively. Histological evidence shows that cell bodies in these regions co-express GABA and glycine. This co-expression suggests but does not prove that there is also co-release of these neurotransmitters at their terminals in the ICC. We used ChR2 expression targeted to glycinergic cells to ask whether glycinergic afferents in the ICC co-release glycine and GABA, and if so, whether the responses to the two transmitters are different. Finally, we explored differences between extrinsic GABAergic input from co-releasing terminals and presumed local inhibition.

Methods
Brain slices were made fromGlyT2-Cre;ChR2(H134R)-EYFP mice in which ChR2 expression was restricted to glycinergic neurons. We made whole-cell recordings from the ventrolateral region of the ICC where glycinergic input is more prevalent. With glutamatergic transmission blocked, inhibitory postsynaptic currents (IPSCs) were measured in response to either ChR2 stimulation with blue light or stimulation of fibers with a stimulating pipette.

Results
GlyT2-cre-ChR2 EYFP showed prominent expression of EYFP in somata in brainstem auditory pathways. In the IC, there were extensive fiber labeled but no somata. Stimulating with light while voltage clamping cells at -65 mV evoked IPSCs of +102 to 838 pA. IPSCs had an exponential decay of 3.1±0.4 ms and moderate synaptic depression. Application of 5 uM gabazine blocked 7 to 34% of the IPSC, with the remainder blocked by 500 nM strychnine. Since both antagonists were required to block transmission, both transmitters must have been released by light stimuli. The decay times of the glycinergic and GABAergic components were not significantly different. Similar to ChR2 activation, fiber stimulation evoked IPSCs with a mono-exponential decay of 2.6±0.5 ms.The kinetics of isolated glycinergic and GABAergic IPSCs were also similar for ChR2 activation and fiber stimulation.

Conclusions
At least some portion of the ascending glycinergic input co-releases glycine and GABA. The postsynaptic responses to GABA were smaller than that of glycine but otherwise had similar kinetic features. Future studies will explore the functional significance of co-release from glycinergic afferents and differences among inhibitory inputs within the IC.

Funding
NRSA F31 DC015187-01 ARCS Fellowship NIH RO1 DC004450

PS 645

Long-Lasting Sound-Evoked Afterdischarge in the Auditory Midbrain

Munenori Ono[1]; Deborah Bishop[2]; Douglas Oliver[2]
[1]Kanazawa Medical University; [2]University of Connecticut Health Center

Background
Neural plasticity is one of the central issues in the brain. Neural plasticity has different forms that underlie the various brain functions such as learning, feature extraction, etc. In the central auditory system, different forms of neural plasticity are known to play a critical role in the computation of auditory information. Here, we report a novel neural plastic response in the inferior colliculus, an auditory center in the midbrain of the auditory pathway. A vigorous, long-lasting sound-evoked afterdischarge (LSA) is seen in a subpopulation of both GABAergic and glutamatergic neurons in the central nucleus of the inferior colliculus of normal hearing mice.

Method
Single cell extracellular recordings were obtained using glass pipettes filled with 0.01M PBS (pH 7.4) with 2 % Neurobiotin (4 – 7 MW). To distinguish GABAergic from glutamatergic neurons in vivo, we used VGAT-ChR2-EYFP mice in which inhibitory neurons specifically express Channelrhodopsin-2 in all parts of the neuron. When a light stimulus was delivered to the IC from the brain surface, it evoked spikes in GABAergic neurons, but it suppressed firing in glutamatergic neurons that lacked GAD67.

Results
We found that 20% of glutamatergic (8/40) and 17% of GABAergic (6/36) neurons in the VGAT-ChR2 mice exhibited a long-lasting sound-evoked afterdischarge (LSA) and continued to fire after the sound terminated. We tested 36 GABAergic neurons and 40 presumed glutamatergic neurons for LSA by using long duration, 30- 60s, continuous one-octave noise. The minimum sound duration required to

induce SAD was around 30 s. The discharge after sound was stronger when the response during sound (RDS) was higher and the sound duration was longer. LSA+ neurons had less adaptive firing during sound than LSA- neurons. In response to 30 s sound, both GABAergic and nonGABAergic LSA+ neurons showed more sustained firing during sound than LSA- neurons. The time course of LSA was variable. A peak firing rate occurred 1.0 - 50.1 s after the sound termination. The decays ranged from 0.4 - 235.6 s. LSA was also evoked by discontinuous sound (1 s narrowband noise bursts presented every 2 s, 50 repetitions).

Conclusion
Since the neurons with LSA showed less accommodation than the neurons without LSA, it suggests that the neural mechanism underlying LSA may allow the neurons to fire persistently during a long-duration sound stimuli. LSA might be a byproduct of the neural compensation and be relevant to phantom sound perception.

Funding
NIH grants R01 DC000189 R21 DC013822 UConn Health HCRAC grant 401139UCHC.

PS 646

Intracollicular Inputs to Neurons in Layer 2 of the Lateral Cortex of the Mouse Inferior Colliculus

Alexandria Lesicko; Daniel Llano
University of Illinois at Urbana-Champaign

Background
The lateral cortex of the inferior colliculus contains a network of modules characterized by dense labeling for GAD67 and other neurochemical markers. Previous studies from our laboratory have shown that the inputs to the lateral cortex are patterned, such that somatosensory inputs target the modules while auditory inputs terminate outside these regions. While the topography of extrinsic inputs to the lateral cortex is well defined, the degree and directionality of intrinsic connectivity between neurons in this region remains unknown. In the present study, we sought to characterize the intrinsic inputs to cells in both modular and extramodular regions of layer 2 of the lateral cortex of the mouse inferior colliculus.

Methods
Experiments were performed in brain slices from the GAD67-GFP knock-in mouse to visualize and distinguish between modular and extramodular areas. Voltage and current clamp recordings were collected from layer 2 neurons while potential pre-synaptic sites throughout the ipsilateral colliculus were stimulated using laser photostimulation of caged glutamate.

Results
Preliminary results include a heterogeneous set of input maps. Pre-synaptic stimulation generated both excitatory and inhibitory responses in GAD-positive and GAD-negative cells in layer 2. While most inputs arose from local sites within the lateral cortex, responses from more distal locations were recorded as well.

Conclusions
These preliminary data show that layer 2 cells in the lateral cortex receive a variety of intrinsic inputs. Potential interconnectivity between modular and extramodular regions of the lateral cortex could have important implications for processing of multisensory information in this structure.

PS 647

Neurochemical Modularity in the Developing Mouse Lateral Cortex of the Inferior Colliculus.

Christopher Dillingham; Mark Gabriele
James Madison University

Background
While the layered, tonotopic arrangement of the central nucleus of the inferior colliculus (CNIC) is well-established, less is known about the organization of its neighboring lateral cortex (LCIC). A series of discontinuous neurochemical modules have been described for layer 2 of the LCIC in a host of adult species (Chernock et al., 2004). These modules and their surrounding extramodular domains may serve as an anatomical substrate that interfaces with converging multimodal input arrays (Stebbings et al., 2014). The present study examined the emergence of this periodic modular network in developing mouse.

Methods
In a series of early developmental C57BL/6J mice, immunocytochemical and histochemical stains were performed for glutamic acid decarboxylase (GAD), parvalbumin (PV), acetylcholinesterase (AChE), cytochrome oxidase (CO), and nicotinamide adenine dinucleotide phosphate-diaphorase (NADPH-d). Following fixation, brains were blocked in the coronal plane, cryoprotected, and sectioned at 50µm on a sliding freezing microtome. Brightfield images were captured using a Nikon C1si TE2000 microscope equipped with Nikon Elements software. LCIC modularity reconstructions were performed utilizing a MBF Biosciences Neurolucida system.

Results
Distinct LCIC layer 2 GAD, PV, AChE, CO, and NADPH-d modules were evident in the period preceding hearing onset and up to the latest developmental stage studied, postnatal day 20. This periodic patchy network of discontinuous modules was consistent for all markers, each spanning much of the rostrocaudal dimension of the nascent LCIC. Modular location and relative size in age-matched mice at comparable levels in the coronal plane appeared qualitatively similar for all markers. Extramodular zones, comprised of layer 2 intermodular domains and neighboring aspects of layers 1 and 3, were consistently negative.

Conclusions
As multiple neurochemical stains reveal developing LCIC compartments, a logical next step is to perform co-localization studies to determine the relative degree of modular spatial overlap. Also of interest will be assessing how these neurochemically-defined modules align with similar patchy expression of Eph-ephrin guidance molecules and multimodal modular/extramodular LCIC projection patterns.

Funding
NIH DC012421-01 NSF DBI-0619207

PS 648

GABAergic Inputs to the Superior Colliculus from Brainstem Auditory Nuclei in the Guinea Pig

Jeff Mellott; Brett Schofield
NEOMED

The deeper layers of superior colliculus (SC) receive input from numerous auditory nuclei. Many of these nuclei contain GABAergic cells. We reported previously that GABAergic cells in the guinea pig inferior colliculus (IC) and the nucleus of the brachium of the inferior colliculus (NBIC) project to the SC. However, there are contradictory reports regarding other auditory sources of GABAergic projections to the SC. We examined the overall projection from the auditory brainstem to the SC with a focus on GABAergic cells.

We combined fluorescent retrograde tracers with immunohistochemistry for anti-glutamic acid decarboxylase (GAD) to identify GABAergic cells that project to the SC. We injected red RetroBeads (RB), green RetroBeads (GB) or FluoroGold (FG) into the SC. After 5-7 days for axonal transport, we analyzed retrogradely labeled cells that were GAD^- or GAD^+ in auditory nuclei of the brainstem.

Retrogradely labeled cells were most numerous in the NBIC (39%) and the IC (25%; mostly in IC lateral cortex and rostral pole), with the remainder distributed among the sagulum, the paralemniscal area (PL), the superior paraolivary nucleus (SPN), the dorsal periolivary nucleus, the ventrolateral tegmental nucleus, the lateral and ventral nuclei of the trapezoid body and the intermediate and ventral nuclei of the lateral lemniscus. Each projection had an ipsilateral dominance. Overall, GAD^+ cells constituted 10% of the retrogradely labeled cells. The majority (51%) of such cells were located in the NBIC, with the second largest group (18%) in the IC. Smaller proportions were located in the PL, the SPN and the sagulum. Within individual nuclei, GAD^+ cells always constituted a minority of the retrogradely labeled cells; the highest percentage of retrogradely labeled cells that were also GAD^+ (27%) was observed in the SPN. The dorsal nucleus of the lateral lemniscus (DNLL), a GABAergic nucleus sometimes identified in the literature as a source of substantial input to the SC, rarely contained retrogradely labeled cells in our cases.

We conclude that the guinea pig SC receives input from a diverse set of auditory nuclei throughout the auditory brainstem. GABAergic, presumably inhibitory, projections originate from numerous nuclei, with the NBIC and the IC providing the largest contributions. It is likely that the GABAergic and other projections to the SC play a role in orientation toward acoustic stimuli. The diverse origins of the projections may implicate additional functions associated with the SC, such as defensive behavior or prepulse inhibition of startle.

Funding
NIH DC04391

PS 649

Inhibitory Projections from the Inferior Colliculus to the Medial Geniculate Body Originate from Four Subtypes of GABAergic Cells

Nichole Foster; Jeffrey Mellott; Brett Schofield
Northeast Ohio Medical University

Four subtypes of GABAergic neurons can be distinguished in the inferior colliculus (IC) (Foster et al., 2015). The subtypes are distinguished by the presence or absence of a perineuronal net (PN) and/or a dense perisomatic ring of boutons immunoreactive for vesicular glutamate transporter 2 (VGLUT2). Somatic sizes and distribution within the IC differ across the 4 subtypes. Here, we asked whether all four subtypes of GABAergic neurons project to the medial geniculate body (MG).

We injected a fluorescent retrograde tracer into the MG in adult pigmented guinea pigs. Tissue from each animal was subsequently stained with *Wisteria floribunda* agglutinin to label perineuronal nets (PNs) and antibodies to glutamic acid decarboxylase (GAD, to label GABAergic neurons), neuronal nuclear protein (NeuN, a neuron-specific counterstain), and VGLUT2. In two sections through the IC from each animal, neuronal cell bodies with a visible nucleolus were outlined. Each somatic outline was then classified according to the presence of retrograde tracer and whether it was surrounded by a PN and/or a ring of $VGLUT2^+$ boutons.

Each experiment labeled multiple subtypes of GABAergic cells. Across cases, all 4 subtypes were identified as projecting to the MG. In general, GAD^+ cells that have neither a PN nor a VGLUT2 ring ("GAD-only" cells) were the most numerous subtype labeled by MG injections. The proportions of other subtypes varied considerably between cases. In one case, GAD^+ cells with a VGLUT2 ring but no PN (i.e., "ring-only" cells) were the second most common subtype labeled; this case had no "PN-only" cells. In a second case, PN-only cells were labeled, but "ring-only" cells were not. Such variation likely results from differences in the extent to which the injection sites included different MG subdivisions. This suggests that the different GABAergic subtypes have different patterns of projections to specific MG subdivisions, and supports the supposition that the GABAergic subtypes serve distinct functions.

We conclude that GABAergic projections from the IC to the MG originate from all four subtypes of GABAergic neurons distinguished thus far. The majority are "GAD-only", lacking both a PN and a ring of $VGLUT2^+$ terminals. These cells have small or medium somas. Inhibition supplied to the MG by GAD-only neurons probably plays a different role in auditory processing than inhibition supplied by larger neurons that are surrounded by PNs and rings of $VGLUT2^+$ boutons.

Funding
NIH R01 DC004391 NIH F31 DC014228

PS 650

Corticofugal inputs onto the Projection Neurons in the Peripheral Inferior Colliculus

Kousuke Taki; Yoshinari Aimi; Fuduki Inoguchi; Motoi Kudo
Shiga University of Medical Science

The inferior colliculus (IC) is the midbrain auditory relay-center where bottom-up and top-down flows of information are congested. The top-down element includes corticofugal projection mainly from auditory related area which distributes in the peripheral IC including dorsal cortex (DC) and the external cortex (EC) as well as in the central nucleus. The thalamic target of projection neuron in the DC and EC is widely spread around the medial geniculate body (MG) and involved in the appendant ascending pathway to the wide cerebral regions including amygdala. We designed an investigation to analyze synapse formation between corticofugal projection and projection neuron in the IC with triple labeling of presynaptic and postsynaptic neurons respectively and synaptic marker vesicular glutamate transporter 1 (vGluT1) in order to estimate synapse formation between them. We employed a recombinant Sindbis virus for labeling corticofugal axon with membrane-targeting GFP, and viral injection into the posterodorsal auditory area successfully labeled abundant axons in the IC; more densely in DC and EC. As postsynaptic element, we employed retrograde labeling from the suprageniculate nucleus which is one of the thalamic structures surrounding MG in order to lavel DC and EC neurons effectively. As a result, we found some retrogradely labeled projection neurons in both DC and EN which were contacted with anterogradely labeled corticocollicular projecting axons. In many cases synaptic marker collocalization were positive, which suggested the synaptic formation between them. These results suggest that corticocollicular projection have influence on the main auditory pathway via DC and EN neurons and more directly enhance the parallel ascending pathway formed by themselves.

Funding
This work was supported by JSPS KAKENHI Grant Number 22791593.

PS 651

Correlations Between Morphology and Function in the Guinea Pig Inferior Colliculus

Mark Wallace; Trevor Shackleton; Alan Palmer
MRC

Background
At least five separate functional pathways ascend from the cochlear nucleus towards the forebrain but all have an obligatory relay in the central nucleus of the inferior colliculus. At the same time there are major descending pathways, mainly from the cortex, which terminate primarily in the dorsal/external cortex. We are interested in describing the intrinsic connections and morphology within the central laminae and the external cortex and determining to what degree they form separate channels for functional processing.

Methods
We have used juxtacellular labelling in urethane anesthetized guinea pigs to visualise the cells with biocytin and have analysed their response properties to pure tones. Cells have been reconstructed using Neurolucida software from Microbrightfield and a mechanised stage.

Results
We have previously reported that of 35 filled cells, 15 had a flat or disc-shaped morphology where both the dendrites and the axons were orientated to, and mainly contained within, a single fibro-dendritic lamina of the central nucleus [1]. Here we report the physiological characteristics of the remaining 20 cells that had a stellate morphology. Of the stellate cells, 7 were located in the dorsal/external cortex and had long (> 23 ms) latencies to binaural tone pips at their characteristic frequency. They showed sustained responses and frequency response areas that usually had sideband, or more complicated areas of, inhibition. Their axons were mainly confined to the dorsal/external cortex but two also had axons that spread into the central nucleus and one could be followed to its terminals in a roughly homotopical location on the contralateral side. The remaining stellate cells were located in the central nucleus, had short latencies (< 16 ms) and mainly had “V” shaped or narrow frequency response areas. Six of them had pure onset responses (not seen in the 15 laminar cells we previously reported) and were either large or medium-sized stellate cells. The other 7 stellate cells had sustained responses to pure tones (on-sustained, pauser or phase-locked) and were relatively small. The axons of the stellate cells in the central nucleus always terminated in two or more laminae and some branches also terminated in the dorsal/external cortex.

Conclusion
Despite the diversity in form and functional properties there are some correlations between functional properties and morphology.

References
[1] Wallace, M.N., T.M. Shackleton, and A.R. Palmer. (2012) Morphological and physiological characteristics of laminar cells in the central nucleus of the inferior colliculus. Frontiers in Neural Circuits 6: 55

Funding
Medical Research Council, UK

PS 652

The Spiral Staircase: Tonotopic Microstructure and Cochlear Tuning

Christopher Shera
Harvard Medical School

Fine-grained mapping studies in both cats and rats find a discontinuous, stepwise progression of characteristic frequencies (CFs) along the main tonotopic axis of the central nucleus of the inferior colliculus (CNIC; Schreiner & Langner

1997; Malmierca et al. 2008). Interestingly, the step heights and their variation with CF match estimates of auditory-filter bandwidths (psychophysical and neural critical bands), and the staircase-like map is therefore thought to have deep significance for the analysis and perception of sound.

Does the discontinuous frequency map found in the inferior colliculus originate in the tiered tonotopy of the cochlea?

Mammalian cochlear frequency-position maps are usually thought to be smooth and continuous. Here, however, I combine computational modeling with otoacoustic and basilar-membrane (BM) measurements to argue that although cochlear maps in sensitive ears appear exponential over distances spanning multiple octaves, on smaller scales they manifest a regular staircase-like structure comprising plateaus of nearly constant CF separated by abrupt discontinuities. The height and width of the stair steps are determined by parameters of cochlear frequency tuning and vary with location in the cochlea. As in the CNIC, the step height is approximately equal to the bandwidth of the auditory filter (critical band), and the step width matches that of the spatial excitation pattern produced by a low-level pure tone. Stepwise tonotopy is an emergent property arising from wave reflection and interference within the cochlea, the same mechanisms responsible for the microstructure of the hearing threshold.

Possible developmental relationships between the microstructure of the cochlear map and the tiered tonotopy observed in the inferior colliculus are explored.

Funding
Supported by NIDCD grant R01 DC003687.

PS 653

Optogenetic stimulation of the central auditory pathway

Fei Gao; Alexandra Kadner; Albert Berrebi
West Virginia University

Background
Optogenetics has been used to study many neural systems including memory, motor control, olfaction and the limbic system. However, few recent studies have applied optogenetics to the auditory system. In this ongoing study we explore how neural activity in the inferior colliculus (IC) and superior paraolivary nucleus (SPON) of mice expressing halorhodopsin or channelrhodopsin throughout their brains can be manipulated through laser illumination. Here we report preliminary results from the inferior colliculus.

Methods
The sound evoked responses of IC and SPON in halorhodopsin and channelrhodopsin expressing mice were recorded by using an optrode that permits simultaneous laser illumination and recording from the same site. We carried out similar experiments in both types of mice. The neuronal activity was recorded in response to a total of six stimulus conditions, namely no stimulation, laser illumination alone, a characteristic frequency (CF) tone alone, a noise burst alone, CF tone combined with laser illumination, and noise burst combined with laser illumination. CF tones and noise had a duration of 50 ms and were presented at 20 dB above the studied neuron's threshold in the experiments. To inhibit neural activity in a halorhodopsin expressing mouse, a 532 nm laser (green) was switched on during the entire recording interval. To stimulate neural activity in a channelrhodopsin expressing mouse, a 473 nm laser (blue) was illuminated at the onset of each sound stimulus and lasted for 100 ms.

Results
Illumination of the IC of a halorhodopsin expressing mouse with a 532 nm laser caused a slight reduction of spontaneous activity, as well as reductions of the spike counts in response to tone and noise stimuli by about half. Illumination of the IC of a channelrhodopsin expressing mouse with a 473 nm laser produced a laser evoked response and magnified sound evoked responses. First spike latencies in response to illumination with the blue laser were shorter than those in response to auditory stimulation, and laser evoked spiking continued for the entire period of laser illumination. In the combined laser with tone and laser with noise conditions a large increase of the spike count occurred. We are currently extending our recordings to SPON neurons in both types of transgenic mice.

Conclusion
These results demonstrate a strategy for optogenetics manipulation of the central auditory pathway in mice and lays the groundwork for future applications in auditory research.

Funding
NIH DC-002266 to Albert S. Berrebi

PS 654

Temporal Properties of Inferior Colliculus Neurons to Amplitude-Modulated Infrared and Acoustic Stimulations

Xiaodong Tan[1]; Nan Xia[2]; Yingyue Xu[1]; Hunter Young[1]; Claus-Peter Richter[1]
[1]Northwestern University; [2]Chongqing University

Background
The performance of cochlear implants (CIs) in speech perception is correlated with the ability of detecting the modulation in the acoustic signal. Pulse repetition rates between 250 and 2400 pulse per second (pps) are usually used in CIs, which can minimize the possible interference between the carrier and modulation frequencies. However, the benefit of higher carrier frequency of CIs is still questionable. Novel methods of neural stimulation used in CIs, including infrared neural stimulation (INS), have limited stimulation rates of no more than 200 pps. Whether or not the amplitude-modulated INS can evoke a response different from that evoked by unmodulated stimulation, how and to what degree this low carrier frequency interferes with the amplitude modulation, and whether there is a characteristic frequency dependent change of the temporal modulation transfer function (TMTF), are the questions critical for the future application of INS in CIs.

Method
In this ongoing study, the temporal properties of auditory neurons in the central nucleus of the inferior colliculus (ICC) in response to amplitude-modulated pulsed INS are recorded from cats and guinea pigs. Amplitude-modulated trains of infrared laser pulses with either equal maximum amplitude or equal energy are delivered through a cochleostomy in the basal turn of the cochlea. Amplitude-modulated trains of acoustic clicks are used as control measurements. The response properties of ICC single units are characterized and compared through the analysis of TMTF, group delays to both carrier and modulation frequencies, and firing efficiency.

Results
The pilot results showed that modulated pulsed INS elicited responses of single units in ICC were different from those of unmodulated signals. The TMTFs from the same single units did not show obvious differences in response to INS and acoustic stimulations. The TMTF could vary with the carrier frequency, indicating an interaction between the carrier and modulation frequencies, which will be further investigated.

Conclusion
INS is potentially suitable for encoding amplitude-modulated signals. Interactions between the carrier and modulation frequencies were observed in both INS and acoustic stimulation while its significance in signal coding of CIs is unclear yet. Further investigation is ongoing to address this question as well as the comprehensive TMTF changes in a full picture of ICC neurons with different properties and characteristic frequencies.

Funding
This work is supported by the NIH, R01-DC011855.

PS 655

Age-Related Alteration of Inputs to the Auditory Midbrain Revealed by Current Source Density Analysis

Brent Beck[1]; Elliott Brecht[2]; Joseph Walton[2]
[1]University of Florida; [2]University of South Florida

Current source density (CSD) analysis is an important method of analysis for physiological research that allows one to clearly see the net ionic flow across neural tissue. CSD is the second spatial derivative of a local field potential (LFP), and is typically used to assess auditory processing across laminar of auditory cortex. Significant age-related neural processing occur within the auditory midbrain which can affect auditory processing. We used CSD analysis to study changes surrounding the inputs to the inferior colliculus (IC) in young, middle and old age.

Multi-unit extracellular activity was recorded from the IC using a 16-channel single shank silicon acute penetrating vertical electrode-array on tranquilized young, middle-aged, and old adult CBA/CaJ mice. Neural events (MU activity and LFPs) were acquired and visualized in real-time using the OpenEx software platform. LFPs (1-500Hz) were elicited by tone bursts (25ms duration) and broadband noise bursts presented in the contralateral hemi-field. Tone bursts were presented in from 4-64kHz, at 0-80dB SPL in 5-dB steps, while rate-level function utilized wideband noise, from 0-80dB SPL in 10-dB steps, 50 presentations.

Analysis of the CSD profiles showed that all sinks and sources were significantly reduced by middle-age, especially for high intensity stimuli. In old mice, amplitudes of the sources in response to high intensity stimuli returned to values observed in young mice. This reappearance of maxima was not evident for the peak sink amplitudes (negative deflection of the LFP), or outward flow of negative ions, which showed a significant reduction in middle-age. While in old mice, the peak sinks trended towards a partial return. Similarly, there was a continuous reduction in the threshold of the CSD profiles to both tone and wideband stimuli observed with age.

The main finding of this study indicates significant reductions in excitatory drive, decreases in the negative component of the LFP, which was observed in middle-age and then increases in amplitude for high intensity stimuli with old age. The reduction in input of excitatory activity along the tonotopic axis of the auditory midbrain is also observed in the sustained portion of the CSD profile. The results of the CSD analysis implicate functional declines in synaptic transmission, in the face of minimal hearing loss in middle age, within the IC which then is amplified in older animals. This begs the question, is the rebound of excitatory drive in the older mice a consequence of a loss of inhibition.

Funding
Work Supported by NIH_NIA Grant PO1 AG009524

PS 656

Subcortical decoding of stimulus, group experience, and individuality

Zilong Xie; Rachel Reetzke; Han-Gyol Yi; W. Todd Maddox; Alexandros Dimakis; Bharath Chandrasekaran
The University of Texas at Austin

Auditory subcortical encoding is sensitive to the spectrotemporal patterns within the signal, as well as the listener's acquired experience. Here, we ask whether we can decode information related to stimulus, language experience, as well as individual listener from scalp-recorded electrophysiological responses that reflect auditory midbrain function. Native speakers of Chinese (n = 5) and English (n = 5) passively listened to Mandarin linguistic pitch patterns across five separate days while electrophysiological responses was recorded. A data-driven machine learning algorism, i.e. support vector machine, was used to assess the extent to which stimulus (level pitch vs. rising pitch), group experience (Chinese vs. English), and individual listener (n =10) can be decoded across days from the electrophysiological data. We found that stimulus, group, and individual listener can be successfully decoded from the electrophysiological signals. We also found that stimulus decoding is strongly influenced by long-term linguistic experience, with less precise decoding of the two pitch patterns in English, relative to Chinese listeners. Further, the ability to decode group and individual listener is

stimulus-dependent, with the rising pitch (relative to the level pitch) yielding more precise subcortical decoding accuracies. Notably, decoding accuracies were stable across five days of recording. Our results show that electrophysiological signals from the auditory midbrain contain information related to the stimulus, language experience, and individuality. Neural metrics derived from machine learning can be effective in quantifying these effects on auditory subcortical function.

Funding
This work was supported by the National Institute on Deafness and Other Communication Disorders-National Institutes of Health (Grant R01DC013315 to B.C.) and the National Institute on Drug Abuse-National Institutes of Health (Grant DA032457 to W.T.M.)

PS 659

Masked Tone Thresholds Are Related to Efferent-Induced Linearization of Human DPOAE I/O Functions

Shaum Bhagat; Anusha Yellamsetty
University of Memphis

It is widely accepted that the living, healthy basilar membrane responds to increasing levels of acoustic input by compressing its mechanical output at certain locations across the cochlear partition. Basilar membrane (BM) input-output (I/O) functions at the characteristic frequency in mammalian animal models are characterized by two or three segments that are separated by transitions in response growth rate at the characteristic frequency. Stimulation of medial olivocochlear (MOC) efferent neurons reduces BM sensitivity and increases the slope of BM (I/O) functions in animal models. It has been postulated that MOC efferent neurons play a role in modifying cochlear output to improved detection of signals in noise. Increased linearity of I/O functions at CF associated with activation of MOC efferent neurons can conceivably assist in extending the neural response to the tone above that of noise, leading to an improvement in deteting tones in noise. To test this hypothesis, BM compression was studied indirectly in humans by measuring distortion-product otoacoustic emission (DPOAE) I/O functions in conditions with presentation of contralateral noise. Compression estimates from a three-segment linear regression model applied to the DPOAE functions were derived in order to determine associations with psychophysical measurements of masked tone thresholds. In masking conditions, the tone signal and the noise masker were presented at the same time and were directed to the right ear. Estimation of masked thresholds was provided by a two-interval, two-alternative forced-choice procedure with a two-down one-up adaptive rule. In this study, there were statistically significant associations between DPOAE I/O function slopes and masked thresholds at both 1.0 and 2.0 kHz. At 1.0 kHz, individuals with higher DPOAE I/O function slopes exhibited lower masked thresholds. In contrast to the results seen at 1.0 kHz, data at 2.0 kHz indicated that individuals with lower masked thresholds exhibited lower DPOAE I/O function slopes. When measured with contralateral noise, DPOAE I/O compression slopes were linked to masked thresholds at both frequencies examined in this study. Linearized DPOAE I/O functions presumably reflect linearized BM growth functions under conditions of MOC efferent activation, and this process may have extended the neural response to the signal tone in certain conditions so that it could be more easily heard in the presence of masking noise.

PS 660

Measurements of the Medial Olivocochlear Reflex in Children with Autism and Varying Degrees of Hyperacusis

Uzma Wilson[1]; Kate Sadler[2]; Kenneth Hancock[3]; John Guinan, Jr.[3]; Jeffery Lichtenhan[1]
[1]Washington University School of Medicine; [2]University of Missouri-Columbia; [3]Eaton Peabody Laboratory Harvard Medical School

Children with Autism often have hyperacusis (auditory hypersensitivity) associated with disruptive behaviors in academic and social environments. Adults who have hyperacusis but are otherwise neurotypical (i.e., adults without Autism) have stronger medial olivocochlear (MOC) reflexes than those without hyperacusis (Knudson et al. 2014 *J Neurophysiol*). Several reports suggest that the MOC reflex is normal or weaker in people with Autism but these studies did not control for hyperacusis. We addressed the issue of MOC reflex strength in Autism by measuring the MOC reflex in neurotypical children and children with Autism who have varying degrees of hyperacusis.

We measured the effect of the MOC reflex on transient evoked otoacoustic emissions (TEOAEs) in 17 children with Autism and 13 neurotypical control children. We assessed hyperacusis using an 8-item questionnaire because the loud sounds used to directly measure hyperacusis can upset a child with Autism. TEOAEs were recorded at various click levels without and with contralateral acoustic stimulation (CAS; a 60 dB SPL broadband noise). Linear regression was used to quantify the growth of TEOAE amplitude across sound levels, separately for without and with CAS, for both individual and group data. MOC reflex strength was defined as the difference in dB of the mean TEOAE amplitudes without and with CAS.

The majority of children with Autism reported some degree of hyperacusis, while neurotypical children had fewer than three questionnaire items answered positively for hyperacusis. In children with Autism, the MOC-induced change in TEOAE amplitudes was positively correlated with the number of questionnaire items answered positively for hyperacusis, but not significantly (r = 0.23, p = 0.37). Five children with Autism were combined into a high-hyperacusis group: hyperacusis impacting daily function, with more than seven questionnaire items answered positively for hyperacusis. The remaining 12 children with Autism formed a group with moderate to no hyperacusis group (termed the moderate-hyperacusis group). The MOC-induced changes in TEOAE amplitudes averaged 1.1 dB, 1.7 dB and 2.5 dB for neurotypical, moderate-hyperacusis Autism, and high-hyperacusis Autism

groups, respectively. TEOAE amplitudes without CAS were similar for all three groups.

MOC reflex strength was greatest in children with Autism who reported severe hyperacusis. Children with Autism and moderate or no hyperacusis also had greater MOC-induced suppression, on average, than neurotypical children. Strong medial olivocochlear reflexes in children with Autism may be mediated by hyperacusis, not Autism *per se.* and may be associated with the generalized hypersensitivity in people with Autism.

Funding
McDonnell Center for Systems Neuroscience American Otological Society National Institutes of Health, National Institute on Deafness and Other Communication Disorders (R01 DC005977)

PS 661

The relationship between cochlear efferent activity and morphology in CBA mice

Ji Sun Kong; Shi Nae Park; So Young Park; Sang A Baek
The Catholic University of Korea

Objectives
The outer hair cells receive descending inputs from auditory brainstem structures through medial olivocochlear (MOC) efferent fibers, which has been postulated to play a role in signal detection in noise and protection from noise-induced cochlear damage. Contralateral suppression (CS) of distortion product otoacoustic emission (DPOAE) can reflect medial olivocochlear reflex (MOCR) activity. In the present study, the authors intended to find whether cochlear gradient for the efferent system is present, and investigated the relationship between the morphology of MOC efferent terminals (ETs) and the efferent activity assessed by CS of DPOAE.

Subjects and Method
Sixteen normal hearing ears from 8 CBA mice aged 1 month were used. DP-grams were obtained at 8 points per octave from 6.5 to 35 kHz of f_2 frequency in quiet and in the presence of contralateral acoustic stimulation (CAS) with 55 dB broadband noise. DPOAE change was defined as the signal to noise ratio (SNR) with CAS minus SNR in quiet. Test frequencies were divided into three groups: low (6.5 – 10.8 kHz), middle (11.9 – 23.6 kHz) and high (26 – 35 kHz). Because both suppression and enhancement are supposed to reflect efferent activities, root mean square was used as the representative value of the total DPOAE changes within each frequency group. In whole-mount cochleae, the ETs at the outer hair cell base were made visible by immunofluorescent staining for α-synuclein and examined using confocal laser-scanning microscopy. Specified regions of interest – 8, 16, and 32 kHz – were localized according to a mouse cochlear place-frequency map. For quantitative analysis, we evaluated the diameter of the ETs and the number of them per OHC.

Results
DP-grams demonstrated alternating peaks and dips. Both suppressions and enhancements were observed in one individual at different frequencies, although suppression effects seemed predominant. The middle frequency region having the largest and most clustered ETs exhibited the most active MOCR activity. The base with the smaller size and number of ETs showed similar MOCR activity with that of the middle region. The apex with smaller number of large ETs showed weak efferent activity.

Conclusion
Definite cochlear gradient for the efferent system was not observed. The most active MOCR along with strong morphology of the ETs were found in the middle frequency region where the mouse has the most sensitive hearing

PS 662

Efffects of Contralateral Noise on Spontaneous Otoacoustic Emissions

Vishakha Rawool
West Virginia University

Research Background
Contralateral noise has an effect on spontaneous otoacoustic emissions due to the activation of the medial olivo-cochlear efferent pathway. Such effects can be confounded by the test-retest variability in OAEs, possibility of acoustic crossover of noise to the opposite ear or elicitation of the middle ear acoustic reflex at high noise levels. Control for these confounding variables may provide more accurate documentation of the effects of contralateral noise on spontaneous emissions.

Methods
A participant with seven spontaneous emissions with frequencies of 1.08, 1.31, 1.43, 1.76, 3.45, 3.79, 4.47 kHz in the left ear, participated in the study. Spontaneous emissions were recorded from the left ear with no noise and with noise presented to the right ear at 20, 30, 40, 50, & 60 dB effective masking (EM) levels. The recording was repeated across five trials spread across five weeks, to account for test-retest variability, yielding a total of 210 data points. Spontaneous emissions were recorded after 30 seconds after initiating contralateral noise. A waiting period of at least two minutes was inserted between each recording to allow recovery from the effects of prior noise stimulation. The possibility of crossover of 60 dB EM levels to the contralateral ear was evaluated by establishing air conduction thresholds in the opposite ear at or around the spontaneous emission frequencies in the presence and absence of contralateral masking. No difference in thresholds was apparent, suggesting lack of crossover at these masking levels to the other ear. The possibility of acoustic reflex activation was also ruled out by establishing reflex thresholds with broad-band noise which were recorded well above the 60 dB EM levels. The data was analyzed using a non-parametric technique called Nonoverlap of All Pairs (NAP).

Results
A strong suppression effect was apparent on two emissions (1.43 Hz, 3.45 Hz) with two masking levels: 50 and 60 dB EM. A moderate suppression effect was apparent for the 1.43 Hz emission with 30 and 40 dB EM, for the 3.45 Hz emission with 40 dB EM, and the 3.79 Hz emission with 50 dB EM levels.

The emission at 1.76 Hz showed a moderate enhancement with 30 dB EM. All other effects of contralateral noise were weak showing either enhancement or suppression.

Conclusions
The effects of contralateral noise on spontaneous emissions can be either weak, moderate or strong. When moderate or strong effects are apparent, suppression is more common than enhancement.

PS 663

Determination of Fast Ipsilateral Medial Olivocochlear Reflex Adaptation of Distortion Product Otoacoustic Emissions

Ernst Dalhoff; Dennis Zelle; John Thiericke; Anthony Gummer
University of Tübingen

Introduction
Efferent innervation of the auditory periphery through the medial olivocochlear (MOC) system is supposed to have an inhibitory effect on the nonlinear amplification of sound waves in the healthy cochlea. Therefore, measurements of contralateral suppression or ipsilateral adaptation of distortion product otoacoustic emissions (DPOAEs) due to the MOC reflex are a promising tool to investigate the MOC system in humans. However, previously published studies reported both excitatory and inhibitory MOC reflex effects. Recently, it has been shown that one major factor limiting DPOAEs in assessing the MOC reflex is the interference between the two main components, the nonlinear-distortion and the coherent-reflection component, contributing to the DPOAE (Dalhoff *et al.*, 2014, AIP conference proceedings, in press). There, the ipsilateral MOC reflex adaption was sampled using a sequence of five f_2 pulses during an on-period of the f_1 tone. However, that approach typically requires 20 min measurement time per DPOAE frequency. Here, a more time-efficient paradigm using a two-pulse sequence is introduced enabling the determination of the fast ipsilateral MOC reflex.

Methods
Short-pulse DPOAE sequences were recorded during the on-period of a f_1 tone using a two- and a five-pulse f_2 stimulus array, respectively. Depending on the f_2 sequence, the duration of the f_1 tone was 100 or 350 ms. A pause of length equal to the f_1 tone was included between each stimulus presentation. DPOAEs were acquired at three different frequencies between f_2 = 1 – 4 kHz for four subjects at L_2 = 45 dB SPL and frequency-dependent L_1 values ranging from 59 to 65 dB SPL. The nonlinear-distortion component was extracted in the time domain by sampling the onset of the DPOAE signal (Vetešník *et al.*, 2009). The strength of the MOC reflex adaptation was determined using the extracted nonlinear-distortion components by means of an exponential model for the five-point data or DPOAE level difference for the two-pulse measurement.

Results
Subjects showed inhibitory MOC reflex adaptations. The two-pulse stimulus paradigm yielded similar reflex strengths as compared to the five-pulse paradigm while reducing the measurement time to 1 – 2 min per frequency.

Conclusion
Short-pulse stimulus arrays enable determination of ipsilateral MOC reflex adaptation of DPOAEs without perturbing interference effects. The introduced two-pulse stimulus paradigm represents a time-efficient method to quantify the fast MOC reflex, hence, enabling the use of DPOAEs to indirectly assess the integrity of sensorineural structures beyond outer hair cells.

Funding
Supported by the German Research Council DFG DA 487/3-2.

PS 664

Comparison of Methods for DPOAE Component Separation

Carolina Abdala[1]; **Ping Luo**[1]; Christopher Shera[2]
[1]University of Southern California; [2]Eaton-Peabody Laboratories, Harvard Medical School

Reverse traveling waves are initiated in the cochlea via two different mechanisms: nonlinear distortion and linear reflection. The $2f_1$-f_2 distortion-product OAE (DPOAE) is a mixed emission, including both kinds of energy: distortion from the overlap of the two traveling waves and reflection from coherent wavelets backscattered at the DP place. These two components are affected in different ways by natural and experimental variables such as maturation and aging, activation of the medial efferent reflex, ototoxins like aspirin, and other factors. Therefore, measurement and analysis of the DPOAE in humans should take its dual-source nature into consideration. While offline signal processing is available to separate the total DPOAE into its reflection and distortion components, there has been no systematic investigation into the optimal technique for this purpose. This is important because the distinct phase characteristics of each (i.e., distortion shows approximate phase invariance across frequency whereas reflection shows rapidly varying phase) require differing strategies for their extraction and separation. Here we compare three methods with the eventual goal of providing concrete guidelines for effective component separation of the DPOAE.

DPOAEs were recorded in 15 normal-hearing adults from 0.5 to 8 kHz using upward swept stimulus tones. Offline analyses were conducted to isolate and estimate the distortion and reflection energy contributing to the total DPOAE. Three methods of component separation were applied and compared: (1) A least-squares fitting (LSF) approach using a wide analysis bandwidth to remove reflection energy, followed by a narrow analysis bandwidth to estimate the total DPOAE. The reflection component is estimated as the difference between the two; (2) LSF to estimate the total DPOAE as above, followed by an inverse fast-Fourier transform-based (IFFT) algorithm to separate the two components in the pseudo-time domain based on their phase-gradient delays; and (3) An adaptive approach that refines initial estimates

of reflection and distortion obtained via method #1 above (and/or heterodyning) by using LSF in combination with an ear-specific estimate of the reflection-component delay. Preliminary comparisons among these techniques reveal similarities in their estimates of component amplitude but some systematic differences in component delays. These differences will be described in detail and hypotheses about their origin discussed. Future work to evaluate the efficiency of each method in producing accurate estimates of reflection- and distortion-component amplitude and delay will be considered.

Funding
This work was supported by grants from the NIH NIDCD: R01 DC003552 (CA) and R01 DC003687 (CAS).

PS 665

Large Effects of Ear Canal Half-wave Resonance on Otoacoustic Emissions in Humans Evoked by Forward-Pressure-Compensated Stimuli

Emily Bacalao; Jonathan Siegel
Northwestern University

Introduction
Thévenin calibration of the sound source(s) allows the levels of acoustic stimuli to be specified in terms of the forward-going component of the ear canal pressure (forward pressure level or FPL), greatly reducing standing waves. This is effect can be seen by reduced sensitivity of behavioral thresholds to changes in the depth of insertion of the acoustic probe (Souza, et al, J. Acoust. Soc. Am. 136, 1768-1787, 2014). However, FPL calibration of stimuli does not remove the influence of ear canal acoustics on otoacoustic emissions (OAEs). We measured the effect of intentional changes in probe insertion depth on behavioral thresholds and distortion product otoacoustic emissions (DPOAE) with stimuli calibrated in FPL.

Methods
The Thévenin probe calibration was performed before each test session (Scheperle, et al., J. Acoust. Soc. Am., 124, 288-300, 2008). Békésy tracking behavioral thresholds were measured referenced to forward pressure (Souza, et al, 2014), while distortion product otoacoustic emissions (DPOAEs) were measured using two-tone stimuli (f_2/f_1 = 1.2, L_1, L_2 = 62, 42 dB FPL), f_2 varied in steps from 20 to 1 kHz. The complete set of measurements was performed in each ear of 10 human participants at each of two depths of insertion which differed by ~5 mm. The insertion depth was judged by the frequency of the first half-wave canal resonance. The measurements were repeated in a second test session with insertion depths matched as closely as possible to those from the first test session. The human subjects' protocol was approved by the Northwestern University IRB.

Results
Comparisons were made by subtracting (in dB) FPL-referenced behavioral threshold or DPOAE measurements for either matched insertion depths (i.e., at the two deep or shallow insertion depths from the two test sessions) or for mismatched insertion depths (i.e., deep vs shallow, either within or between test sessions). For behavioral thresholds, there was no statistically-significant difference between matched or mismatched insertion depth conditions indicating little effect of insertion depth, confirming our earlier work (Souza et al., 2014). However, highly statistically-significant changes in DPOAE levels (typically +/- 10 dB) were measured near the frequency of the first half-wave resonance. These changes in each subject could be approximately compensated post-hoc using the change in stimulus FPL at the DPOAE frequency.

Conclusion
OAE levels are strongly influenced by the first half-wave resonance of the ear canal, but may be reasonably-well compensated from the stimulus FPL measured in each ear.

Funding
Supported by a grant to EB by the Undergraduate Research Grants Committee of Northwestern University

PS 666

Temporal Suppression of Clicked-Evoked Otoacoustic Emissions Measured Over a Wide Frequency Range

Karolina Charaziak; Christopher Shera
Massachusetts Eye and Ear Infirmary

Otoacoustic emissions evoked by a click (CEOAEs) can be reduced if the evoking sound is preceded by another ("suppressor") click. This temporal suppression of CEOAEs can provide insights into the dynamics of cochlear nonlinearity. For instance, in contrast to the suppression produced by the memoryless nonlinearities usually employed in cochlear models, CEOAE suppression appears greatest at nonzero (2–4 ms) interclick intervals (ICIs). Existing data suggest that the delay to peak suppression depends on frequency, with low-frequency CEOAE components suppressed maximally at longer ICIs than higher frequency components (at least in the tested range below 5 kHz). Here, we explored the frequency dependence of CEOAE suppression across a wide range of frequencies and ICIs with the goal of illuminating the origin of temporal CEOAE suppression.

We used a version of the "double-click" paradigm (Kemp & Chum 1980) utilizing responses to the test click and combinations of pairs of clicks separated in time. Click waveforms were shaped to give their forward-pressure components a flat spectrum (1–12 kHz). Evoking and suppressor clicks were presented at equal levels (72 dB peFPL) for ICIs from 0–10 ms in 0.1 ms steps. At each ICI, the suppression spectrum was calculated as the Fourier transform of the difference between the averaged responses to the test click and the pairs of clicks. Changes in suppression with ICI were tracked at frequencies corresponding to maxima in the CEOAE spectra determined for each subject. Altogether, suppression was tracked at 131 frequencies (0.8–9.4 kHz) in seven human subjects as a function of ICI. At each frequency, we characterized the suppression curve using two parameters: the ICI at maximal suppression (ICI_{peak})

and the "equivalent rectangular width" (ICI_{width}), a measure of the range of ICIs producing suppression.

Overall, both ICI_{peak} and ICI_{width} decrease linearly with frequency on a log-log scale. For instance, at 1 kHz the suppression width was broad (~6 ms ICI_{width}) and peaked between 2–5.5 ms; near 8–9 kHz, by contrast, the width was narrower (~0.8 ms) and peaked at ~0.5 ms. The frequency dependence of these parameters, when expressed in dimensionless units, is reminiscent of the variation in the sharpness of cochlear tuning estimated from OAE delays. Although the reason ICI_{peak} occurs at nonzero values remains unclear, changes in ICI_{width} with frequency may reflect variations in basilar-membrane impulse-response duration (Kemp & Chum 1980; Verhulst et al. 2014), as observed in animal data.

Funding
Supported by R01 DC003687 and by N00014-12-C-0108 from the US Office of Naval Research.

PS 667

Spontaneous Otoacoustic Emission Measurement with Dual Microphone Technique

Bert Maat; Emile De Kleine; Pim Van Dijk
University of Groningen

Background
Spontaneous otoacoustic emissions are represented by narrow-band acoustic signals generated naturally within the cochlea. They can be measured in the ear canal in the absence of external stimulation with a sensitive microphone. Early studies had found a prevalence of SOAE's in human ears of approximately 40%. When more sensitive microphones were used, the reduction of the noise floor resulted in a prevalence of 60%. Further improved recording techniques resulted in a prevalence of 72% (Talmadge et.al., 1993). Also, it is believed that the mechanisms of SOAE's and TEOAE's are from the same origin, so it is hypothesized that the measured prevalence of SOAE's must be more in concordance with those of TEOAE's and therefore be higher than the recently established 72%.

Methods
To improve the sensitivity of the recording system we used a dual microphone technique to record SOAE's. In normal hearing subjects (n=23, 46 ears) we recorded SOAE's with a probe consisting of two microphones. Averaged power spectra of the combination of the two microphones will decrease the noise floor with 3 dB compared to one microphone. The cross correlation power spectrum of the two microphones will decrease the noise floor up to 10 dB. The averaged power spectra of the two microphones were compared to the cross correlation power spectra.

Results
Preliminary analysis: The recordings did show a significant decrease of the noise floor. Analysis of the SOAE's (criterion > 3dB above noise floor) did not show a significant difference in quantity of emission peaks. However, in the cross correlation power spectra SOAE's were more easily detectable. Further analysis will be conducted to refine the decision criteria of detecting SOAE's.

Conclusion
Since the improvement of the signal to noise ratio did not result in a larger number of SOAE peaks per ear, these results suggests that the current prevalence estimates of SOAE are not limited by microphone or other equipment noise.

C.L. Talmadge and G.R. Long and W.J. Murphy and A. Tubis. New off-line method for detecting spontaneous otoacoustic emissions in human subjects, Hearing research 1993; 71: 170-182

Funding
Heinsius Houbolt Foundation

PS 668

Using Phase of Otoacoustic Emissions Evoked by Swept Tones to Improve Reliability of Hearing Loss Screening

Shixiong Chen; Ning Ji; Guanglin Li
Shenzhen Institutes of Advanced Technology, Chinese Academy of Sciences

Otoacoustic emissions (OAEs) are sound energy emitted by the outer hair cells (OHCs) within the cochlea and could be easily measured by a sensitive microphone placed at the ear canal. The measurement of OAEs has been intensively used as a convenient and noninvasive tool for hearing loss screening in the clinic. However, while both the amplitude and phase of OAE signals carries important information about the healthiness of the OHCs, only the amplitude is currently used and the phase is totally discarded due to insufficient frequency resolution of the clinical tests. In this study, stimulus frequency otoacoustic emissions (SFOAEs) were measured with swept tones of continuous frequencies so that the phase could be obtained in high resolution across a wide frequency range. The amplitude and phase spectra of the swept-tone SFOAEs were compared in human subjects with normal hearing and those with mild hearing loss. The results showed that the phase of swept-tone SFOAEs demonstrated steep gradients as the frequency increased in subjects with normal hearing. The absence of such steep gradients could be used as a sensitive indicator of the occurrence of hearing loss within the corresponding frequency range. Moreover, the phase gradient could be used to identify residual stimulus artifacts that could otherwise be falsely treated as OAE signals when merely checking the amplitude spectrum in conventional tests. The use of swept tones also made it possible to obtain high-definition group delays, which could be used to reflect the goodness of the cochlear tuning and sharpness of the frequency selectivity. This study suggested that incorporating phase information into the clinical protocols of OAE measurements might provide additional information about the functional status of the OHCs and therefore could help improve the reliability of current hearing loss screening.

Funding
National Natural Science Foundation of China under grant # 61302037, National Key Basic Research Program of China under grant # 2013CB329505, Shenzhen Governmental Basic Research Grants under grant # JCYJ20140610152828679

PS 669

Sweep-Tone Evoked Stimulus Frequency Otoacoustic Emissions

Carrick Talmadge[1]; Sri Mishra[2]
[1]University of Mississippi; [2]New Mexico State University

Stimulus frequency otoacoustic emissions (SFOAEs) evoked by low-level pure-tones, are generated via coherent reflection mechanisms and are thought to reflect the functioning of cochlear amplifier gain. As a result, their interpretation is relatively simpler compared to other types of emissions. However, their measurement and analysis are difficult for two main reasons: SFOAEs occur at the same frequency as the evoking pure tones and the recording of SFOAEs takes a relatively long time due to the use of discrete pure tones. Because of these reasons, SFOAEs have not found widespread applications in the clinic or research laboratory, despite their ability to inform about cochlear mechanisms.

Sweep tone SFOAEs have been historically obtained using lock-in amplifiers (e.g., Kemp and Brown, 1984). With this method, the SFOAE was typically isolated from the stimulus tone using a suppressor tone. The use of swept tones in conjunction with digital filters, such as used in this study, date back at least to Long, Talmadge and Shaffer (1994), with several promising reports appearing in the literature (Long et al. 2011; Kalluri and Shera 2013; Henin et al. 2014).

In this study, the influence of several stimulus and recording parameters, such as sweep direction (upward and downward) and sweep rate (16 versus 24 seconds per octave) were explored for defining an optimal test protocol. SFOAEs were recorded from 500 to 4000 Hz in twenty-three normal hearing adults via a suppressor-signal paradigm. Specifically, sweep tones with both primary and suppressor signals were interleaved with measurements of only the primary signal. In this method, the difference of the complex-valued response measured at the primary-signal frequency was subtracted between unsuppressed and suppressed conditions. This difference was equated to the corresponding synchronous evoked otoacoustic emission. In order to cancel the suppressor signal, the suppressor signal was inverted between each consecutive set of signal presentations, that is, an offset of 180° was added to the suppressor signal for every other presentation with a suppressor signal present. The sweep amplitude and phase were analyzed using a least-squared fit method, and the noise floor was estimated using the error of the mean of the sweep amplitude. Overall, the results of this study showed that SFOAEs could be reliably measured using sweep tones in human adults with normal hearing.

Our findings suggest that SFOAEs can be measured rapidly using sweep tones. This will be beneficial in hearing evaluation and for laboratory measurements, such as efferent reflex.

Funding
This work was supported by an Emerging Research Grant from the Hearing Health Foundation and by the Mountain West Clinical-Translational Research – Infrastructure Network under a grant from NIGMS/NIH (1U54GM104944). The content is solely the responsibility of the authors and does not necessarily represent the official views of the sponsors.

PS 670

Natural Combinations of Interaural Time and Level Differences in Realistic Auditory Scenes

Shigeto Furukawa
NTT Communication Science Laboratories

Background
It is reasonable to assume that the functions and mechanisms of the binaural system for processing interaural time and level differences (ITD and ILD, respectively) have been optimized to analyze natural auditory scenes. This study analyzed samples of binaural recordings made under naturalistic conditions to evaluate the correspondence between ITD and ILD representations at an early stage of the binaural system.

Methods
Binaural recordings were made with a dummy-head microphone in quiet rooms (an anechoic room and a small echoic meeting room) and in natural settings (a busy cafeteria, a nature park, and a busy street). In the quiet rooms, we presented speech sound from one or more loudspeakers simultaneously. The recordings at either ear were bandpass-filtered by a gammatone filterbank, half-wave rectified, and lowpass-filtered (passband < 1000 Hz) to simulate the inner ear processing. For each pair of outputs of peripheral channels that matched in the filter center frequency, the iILD, iITD (the peak time in the cross-correlogram), and interaural correlation coefficient (iICC) (the correlation coefficient between the output waveforms at the ITD) were computed. The suffix "i" was used to clarify that the measures are in internal representations. The analyses were made for a running time window with a duration of 50 ms.

Results
Generally, we confirmed that iILD and iITD correlated positively, and the trading ratio, the slope of a line fitted to the iILD-versus-iILD plot, was steeper in high-frequency regions than in low-frequency ones. The trading ratio was smaller for the data recorded in the meeting room than for those in the anechoic chamber. This was likely due to the room's reverberation, which would generally decrease the ILD and make ITD estimates noisy. The difference between rooms was particularly apparent for high-frequency regions (> ~3 kHz). The iICC tended to decrease with filter center frequency, and it was markedly smaller in the meeting room and in natural settings than in the anechoic chamber.

Conclusions
The "natural" trading ratio depends on listening environment. In realistic environments, it is relatively rare for the central auditory system to encounter high interaural correlation particularly in high-frequency channels, which would make high-frequency ITD information less reliable. This could be an ecological explanation of our relative insensitiveness to high-frequency (envelope) ITD information.

Acknowledgments
The author thanks Mr. Michael Wilson for collecting the binaural recording data.

Funding
Supported by JSPS KAKENHI Grant Number 15H05915 (Grant-in-Aid for Scientific Research on Innovative Areas "Innovative SHITSUKSAN Science and Technology").

PS 671

Assessing Changes to Interaural Cues as a Consequence of Open-fit Hearing Aids and Simulated Rooms

Anna Diedesch; G. Christopher Stecker
Vanderbilt University

Interaural time differences (ITD) and interaural level differences (ILD), the major cues for horizontal localization, are susceptible to distortion by multipath acoustics (e.g., reverberation, echoes, and standing waves). Particular styles of hearing aids could additionally interact with sound localization cues. Specifically, open-fit hearing aids mix two copies (processed and unprocessed) with a slight (~2-5 ms) delay.

Here, we assessed binaural recordings of broadband noise using probe-tube measurements on a binaural acoustic manikin. The manikin (KEMAR) was fit with low-gain, Siemens Motion 700 behind-the-ear (BTE) hearing aids programmed with a linear-processing algorithm. Noise reduction, microphone directionality, and feedback suppression options were turned off. Measurements were made using comply foam inserts (containing 0-3 vents) and with open-dome hearing aid coupling. Sounds were presented in three acoustic environments simulated in an anechoic chamber: anechoic, single virtual wall, and simulated room. Simulated direct and reflected sounds were presented from 64 loudspeakers spanning 360º azimuth; twenty-three sound-source azimuths were tested, ranging from ~ -61º to +61º. The virtual wall was 80% reflective (α=0.2) and oriented parallel to the listener's forward gaze, at a distance of 5m to the right; in the simulated room, four virtual walls (α=0.5) were positioned 5m to the left and right, 6.67m in front and 3.33m behind the listening position. Thirteen orders of lateral reflection were simulated.

ITD and ILD were estimated from recordings in a frequency specific manner through binaural cross-correlation and by calculating sound pressure level (SPL) differences between ears within each of 28 band-pass filters (center frequencies 250-8561 Hz).

Results were generally consistent with past studies in that ITD cues became erratic and ILD cues were diminished by increased reflections. Hearing aid effects were less clear, suggesting that in most cases spatial deficits of hearing aid listening will be limited mainly by signal processing (e.g., wide dynamic range compression, directional microphones, etc.) rather than acoustical effects from venting. However, some low-frequency bands showed large ITD distortions, inconsistent with ILD, that are not present unaided. These low-frequency distortions could be particularly relevant to hearing aid users with normal low-frequency thresholds wearing open-fit devices. [Supported by NIH R01-DC011548]

Funding
G. Christopher Stecker's NIH R01-DC011548

PS 672

Osseointegrated Devices Outcomes for Single-Sided Deafness: Implications for Hearing in Noise and Localization ability.

Alexandra Parbery-Clark; Jake Hillyer; Elizabeth Harland; Douglas Backous
Swedish Neurosciences Institute

Introduction
Individuals with single-sided (sensorineural) deafness (SSD) use osseointegrated implants (OIs) to utilize contralateral normal sensory hearing. Speech-in-noise (SIN) and localization is poorer for individuals with sensorineural SSD due to the lack of binaural processing cues which OI devices do not restore. Despite OI users' compromised abilities for both localization and hearing in noise, the relationship between these skills has been largely unexplored. Here, we measured SIN, localization and self-perceived rating of OI device benefit in everyday listening environments in SSD patients with OI devices.

Methods
13 SSD adults with normal contralateral hearing and a minimum of 6 months OI device usage were recruited. SIN was assessed with Bamford-Kowal-Bench sentences (BKB-SIN) presented in surround background noise from an eight speaker array (R-Space). For localization, participants verbally indicated the source speaker (1-8) of the acoustic speech stimulus ("Where am I coming from now?"). Both SIN and localization were assessed with multiple microphone settings (adaptive, fixed directional and omnidirectional) as well as an OI-off condition. Participants completed the Abbreviated Profile of Hearing aid Benefit.

Results
Hearing in noise improves when the speech signal is presented to the normal hearing ear rather than the OI device (+6dB SNR; $p<0.001$) regardless of microphone setting. Localization performance improves with alternate microphone settings ($p<0.05$). Hearing in noise and localization abilities are related: better frontal localization is associated with improved SIN perception ($p<0.01$). Finally, self-perceived benefit with the OI device in everyday settings is highly predictive of objective SIN and localization measures ($p<0.01$).

Conclusions
While SIN and localization remain the primary concerns of SSD populations, OI recipients report device benefit in everyday settings. For improved speech understanding in noise, OI recipients should place the speech signal to their normal hearing ear rather than their OI device. OI patients may also benefit from additional OI device programs (i.e., fixed directional vs. adaptive) for improved localization. Developing objective measures that accurately capture patient's real-world hearing difficulties serve to improve SSD patient care and aid the quantification of auditory training benefits for this population.

Funding
Research supported by Swedish Neuroscience Insititute

PS 673

Precision of Coding of Interaural Delay: Interesting Observations re Age and Hearing-Status

Leslie Bernstein; Constantine Trahiotis
University of Connecticut Health Center

Background
Sound-field and earphone-based discrimination studies demonstrate that sensitivity to changes in interaural temporal disparities (ITDs) declines with increasing reference ITD. At a previous meeting, we described a new paradigm for estimating directly precision of coding of (ITDs) as a joint function of center frequency and ITD magnitude. We now show how that paradigm can provide insight concerning how age and hearing-status relates to, and possibly may affect, coding of ITDs.

Methods
Binaural detection was measured in three conditions. In one, we transformed the classic NoSπ stimulus into an "(NoSπ)τ" stimulus by imposing an ITD on the entire signal-plus-masker waveform. In that condition, errorless internal compensation of external ITDs would yield thresholds both independent of ITD and equal to those obtained under NoSπ. Another condition, (No)±τ(Sπ)τ, was a variant of the "double-delay" condition of van der Heijden and Trahiotis [J. Acoust. Soc. Am. **105**, 388-399 (1999)] in which the masker is the sum of two independent noises, one with an ITD favoring the left, the other with an equal ITD favoring the right. A double-delayed noise has the same interaural correlation as its "single-delayed" counterpart, but its ITD cannot be internally compensated. Thus, detection advantages for (NoSπ)τ re (No)±τ(Sπ)τ reveal relative precision of ITD coding. The third condition, (NoSo)τ, was a control condition having no interaural cues to foster detection. We employed 19 listeners aged 21 to 67 years. All had audiometrically-normal pure-tone averages across the frequencies 500 Hz, 1 kHz, and 2 kHz and none exhibited more than a "slight" loss at 4 kHz (i.e., thresholds <= 25 dB Hearing Level (HL)).

Results and conclusions
As expected, the ordering of thresholds from high to low was (NoSo)τ, (No)±τ(Sπ)τ, (NoSπ)τ. In addition, thresholds obtained using (NoSπ)τ stimuli centered at 500 Hz or 4 kHz increased with ITD. Analyses of the data indicate that 1) older listeners and those with "slight" hearing-loss (10 > HL (dB) < 25) exhibited a relative elevation and "flattening" of the (NoSπ)τ thresholds as a function of ITD; 2) there was no differential effect attributable to hearing-levels at 4 kHz in "monaural" (NoSo)τ conditions. Overall, the data support the hypothesis that even modest hearing-losses can lead to substantial degradations of precision of binaural ITD processing.

Funding
Research supported by GRANT11817268 from the Office of Naval Research (ONR)

PS 674

Relative Perception and Encoding of Sound Location

Andrea Lingner; Michael Pecka; Christian Leibold; Benedikt Grothe
Ludwig-Maximilians-University Munich

The localization and separation of sound sources are crucial for navigation and communication in everyday life. This significance of spatial sensitivity is reflected by the exquisite acuity for localizing a single sound source. Nonetheless, psychoacoustic evidence demonstrated pronounced context-dependency of human sound location, as the presence of a preceding sound source can substantially shift the perceived location of a subsequently presented sound source. These data suggest that neuronal processing of spatial information might be biased for sound source separation rather than absolute localization. It is generally assumed that the location of a sound source is neuronally represented by the relative activity levels of the population of spatially sensitive neurons in each brain hemisphere. However, the coding principles underlying an adaptive representation of acoustic space are not understood.

Here we combined human psychoacoustic testing of sound localization performance and computer modelling of neuronal coding to study the nature of context-dependent spatial sensitivity and its underlying representation. We explored how various acoustic parameters of an adaptor stimulus influenced the spatial perception of a trailing sound. We find pronounced perceptual shifts in sound localization that scaled with the laterality of the adaptor. Moreover, shifts in spatial perception were present at the adaptor location, but increased at more medial locations and extended across the entire hemisphere for highly lateralized adaptors. In addition, we used a second psychoacoustic paradigm to test the effect of the preceding adaptor on sound source separation. We find that the separation ability increases as a function of the test sound locations in the presence of a lateralized adaptor. Finally, to decipher the neuronal code for the relative representation of auditory space, we compared these psychophysical data with the performance of various models of sound localization. Our simulations propose a novel model of sound localization, in which sound source azimuth is estimated based on population vector analysis in both brain hemispheres independently. The two estimates are

then combined to yield a hemispherically balanced estimate of sound source location. Together, our findings emphasize that spatial hearing serves relative separation rather than absolute sound location representation.

Funding
German Center for Vertigo and Balance Disorders (IFB); German Reserach Council (DFG); Bavarian Academy of Sciences

PS 675

Speech Segregation Based On Localization and Equalization-Cancellation Mechanisms

Jing Mi; H.Steven Colburn
Boston University

There are two dominant theories for explaining binaural advantage: Equalization-Cancellation (E-C) theory and localization-based theory. E-C theory features cancelling the noise while the localization-based theory features enhancing the target. In this work, models based on both theories are implemented for speech segregation purposes. For both approaches, in the first step, an additive combination of speech signals is sliced into time-frequency (T-F) units and each T-F unit is assigned to a source location based on interaural time difference (ITD) and interaural level difference (ILD) calculated from corresponding waveforms. Then, for the segregation scheme that emphasizes target enhancement, only the T-F units that are assigned to the target's location get conserved, and other T-F units are set to silence. For the other scheme, which emphasizes masker cancellation, the E-C operation is done for T-F units assigned to maskers' locations in an effort to cancel the dominant noise in those T-F units. In contrast to previous short-time E-C implementations (e.g., Wan et al., 2014), in which the E-C parameters are calculated with the prior knowledge of the target's and maskers' waveforms, the E-C parameters here are obtained from the source assignment in the first step. The results of these two segregation schemes based on interaural differences are compared and analyzed. They are also compared to results from the scheme with optimal E-C operations. [Work supported by NIH/NIDCD: Grant R01 DC00100.]

Funding
NIH/NIDCD: Grant R01 DC00100

PS 676

Salient spatial cues help to assign stimulus components to the target speech

Esther Schoenmaker; Steven van de Par
University of Oldenburg

Background
In a multi-speaker scenario, in which the speech of interest is masked by interfering speech, a spatial release from masking can be observed when the individual talkers are spatially separated. The spatial cues associated with the speaker locations are thought to support grouping and segregation of speech components. It is of interest to know to what degree spatial cues contribute to speech segregation when also monaural cues are available. In this study stimuli were manipulated such that a reduced amount of meaningful spatial cues were available while all monaural cues were preserved.

Methods
Speech from three simultaneous talkers was spatialized with non-individualized HRTFs and presented over headphones to six normal-hearing listeners. Male target speech consisted of sentences from the Oldenburg matrix sentence test and was presented from the front at a global SNR of -8 dB, while ongoing interfering speech from two female speakers was presented from ±60 degrees of azimuth. According to a local SNR criterion, ranging from 0 till +20 dB, spectro-temporal elements of the target speech were presented either from their original location or became collocated with the instantaneously dominant interferer. Hence only the most salient glimpses were presented from the original target location. Target speech intelligibility was measured in dependence of the local SNR criterion and compared to the extreme case of non-manipulated and fully displaced target speech.

Results
Speech intelligibility gradually decreased with increasing local SNR criteria for criterion values larger than 0 dB. Nevertheless, a significant spatial release from masking was found for local SNR criteria up till 16 dB, compared to the situation in which all target speech elements were divided over the positions of the two interfering speakers. For an SNR criterion value of 16 dB, on average only the 4% most salient time-frequency elements of target speech remained at their original position.

Conclusions
The results indicate that the spatial information contained in a small number of very salient glimpses can preserve sufficient location information to support spatial release from masking in a multi-talker situation. These salient glimpses possibly help to assign glimpses to the target speaker which are already grouped based on other cues.

Funding
This work was supported by the DFG (SFB/TRR31 "The Active Auditory System")

PS 677

The Segregation of two Simultaneous Noise Sources in the Free Field

Eric Thompson[1]; Clayton Rothwell[2]; Nandini Iyer[1]; Brian Simpson[1]; Griffin Romigh[1]
[1]Air Force Research Laboratory; [2]Infoscitex

Background
In order to localize two simultaneous sound sources, a listener must first be able to perceptually segregate those sounds into two separate sources. Best, van Schaik, and Carlile (2004, J. Acoust. Soc. Am. 115, pp. 324-336) reported that listeners could perceive two separate sounds presented in virtual space over headphones when they differed in interaural time

differences (ITDs), but listeners generally only perceived one source when the sounds were separated only in elevation. However, free-field cues for the perception of elevation may be more veridical than cues with virtual spatial audio, so the current experiment was designed to test whether there were additional cues available to listeners with free-field presentation that may allow for segregation of two sources that differed in elevation, both when they differed only in elevation, and when they differed in both elevation and in ITD.

Methods
One or two simultaneous 200-ms broadband noise sources were presented to the listeners from randomly selected locations in an anechoic chamber using a spherical array of loudspeakers. The listeners were asked to indicate whether they heard one source our two. Trials were presented in blocks in which the possible speaker locations, all above -45 degrees elevation, were either restricted to the median plane only or unrestricted (i.e. over the full sphere).

Results
When both sources were on the median plane, subjects had difficulty determining whether one or two sources had been presented, with performance near chance levels. Similarly, when the two sources happened to both fall within a plane parallel to the median plane, performance was also near chance, indicating that differences in elevation had little impact on the segregation of the two sources. When the two sources were in opposite left/right hemifields, a left-right angular difference (related to ITD) between the sources of 15 degrees was sufficient for the subject to achieve 85% correct, whereas when both sources were within the same left/right hemifield, a left/right separation of 30 degrees was required to obtain the same level of performance.

Conclusions
These free-field data support earlier findings by Best, van Schaik, and Carlile (2004) with virtual audio presentation; in free-field conditions, a difference in ITD between sources is required for the sources to be segregable. Spectral differences between sources caused by differences in elevation did not enable listeners to perceive two separate sounds. This has important implications for multisource localization, particularly when the sources have similar spectrotemporal properties.

PS 678

Dynamics of Auditory Spatial Attention Gradients

Edward Golob; Jeffrey Mock
Tulane University

Background
The capacity limitations of spatial attention create a dilemma for how attentional resources are allocated over space. Focusing attention on a location pertinent to current goals is vital for intelligent behavior. Yet attention must also be capable of rapid shifts to a different location in response to unexpected sounds that may signal opportunities or threats. Little is known about how the auditory system distributes attentional bias over space to deal with this "stability-flexibility" dilemma.

Methods
Young adult participants (total n=85) performed a sustained attention task by discriminating via button press among white noise stimuli having one of two amplitude modulation rates (25, 75 Hz, 90% depth). Stimuli were delivered using insert headphones, and were presented at 5 virtual locations in the frontal azimuth plane (-90°, -45°, 0° midline, +45°, +90°) by convolving appropriate interaural time, level, and head-related transfer function cues for each location. On most trials stimuli came from a standard location in virtual space (p=.84, either left -90°, midline 0°, or right +90°, tested in separate blocks), but occasionally the location shifted to one of the other four locations (p=.04/location).

Results
For all three standard locations reaction time curves as a function of angular shift distance had an inverted-u shape, with progressive slowing for small shifts followed by faster reaction times for larger shifts (all p's < .01). The amount of slowing was significantly greater when starting at left and midline standard locations relative to the right standard. A follow-up set of two experiments replicated these findings, and also showed that the inverted-u shaped curve was maintained at faster stimulus rates and usually scaled to fit the range of available stimulus locations. Attention to the right standard differed from left and midline by having smaller increases in reaction time following spatial shifts, and the reaction time vs. distance function did not scale to the range of sound locations.

Conclusions
Taken together, these findings suggest at least two mechanisms for auditory spatial attention – a progressively declining top-down bias centered on the standard location, and some form of bottom-up orienting to account for faster reaction times at large shifts. When shifting away from the right side of space attentional shifts were more fluid but insensitive to changes in range, which may reflect overlapping attentional biases to the right side of space.

Funding
This project was supported by NIH grants DC014736 and GM103629 DC014736

PS 679

Comparison of Models for Sound Localization in Normal Hearing- and Cochlear Implant Listeners

Christian Wirtz[1,2]; Joerg Encke[2]; Peter Schleich[3]; Peter Nopp[3]; Werner Hemmert[2]
[1]MED-EL Deutschland GmbH; [2]Technische Universität München; [3]MED-EL, Innsbruck, Austria

Background
The human brain has the remarkable ability to localize spatially separated sound sources in complex acoustic scenarios. This is done by exploiting interaural time- and level

differences (ITDs / ILDs). In the past decades, two different families of models were developed: coincidence or excitation-excitation (EE) family based on Jeffress[1] and the excitation-inhibition (EI) model based on Durlach[2].

Physiological models are inspired by neuronal processing in the lateral- and medial superior olives (LSO and MSO), e.g. [3]. They use the spike responses of the auditory nerve as input signals. For normal hearing listeners, we used a model from Zilany et al. [4] and for cochlear implant listeners a model from Nicoletti et al. [5]. With ANF spike trains as a common physical quantity it is possible, to directly compare NH and CI localization abilities and also to compare CI coding strategies.

Methods

We extended the EE-Model by Lindemann [6] to work with neuronal spike inputs and compared its performance to the MSO model: we determined their spatial accuracy and their localization thresholds with uncorrelated background noise added to the target signals. We also compared NH localization with spike trains predicted by different CI coding strategies.

Results & Conclusion

Although the two models are of different nature, they predicted similar localization thresholds and spatial accuracy, both for NH and CI listeners. The FS4 strategy's localization threshold was only 10 dB below the ones of NH listeners. The CIS strategy failed to convey fine-structure ITD cues.

Funding

This work was funded by a grant from MED-EL Innsbruck, within the Munich Bernstein Center for Computational Neuroscience by the German Federal Ministry of Education and Research (reference number 01GQ1004B and 01GQ1004D) and the DFG "Ultrafast and temporally precise information processing: normal and dysfunctional hearing" SPP 1608 (HE6713/1-1)

PS 680

Extent of Lateralization with Large Interaural Time Differences in Normal Hearing Listeners and Bilateral Cochlear Implant Users

Mathias Dietz[1]; Regina Baumgaertel[1,2]; Hongmei Hu[1,2]; Ben Williges[1,2]; Birger Kollmeier[1,2]

[1]Universität Oldenburg; [2]Cluster of Excellence Hearing4all

For normal hearing listeners, sound localization in the frontal azimuthal half-plane is primarily achieved by neural processing of interaural differences in level and arrival time. While interaural level differences are to some extent also used by bilateral cochlear implant (CI) subjects, encoding of perceptually exploitable interaural time differences (ITDs) by pulse timing is still a topic of ongoing research. The current study is motivated by the fact that CI subjects are able to exploit ITDs when presented with fully synchronized low-rate pulse trains.

In the first part of the study, extent of lateralization for fixed ITDs of up to 3 ms was measured in normal-hearing subjects. Stimuli were either unfiltered or 3-5 kHz band pass filtered click trains, the latter mimicking the perception of CI users, i.e. the absence of any low-frequency temporal fine-structure information. Results indicate that, while unfiltered click trains of 600 µs ITD (corresponding to almost 90° in free-field listening) were lateralized at the ear, filtered click-trains required approximately 1.0-1.4 ms ITD for equally strong lateralization, at least in some subjects.

In the second part of this study, lateralization of low-rate pulse trains was measured using single electrode stimulation in bilateral CI subjects. For the subjects tested so far with the constant rate and constant level pulse trains, a change in lateralization percept with changing ITD could only be measured at rates lower than 200 pulses per second (pps). On average, an ITD of 1.0 ms was required to lateralize the pulse train at the ear.

The results indicate that, if the speech coding allows for sufficiently low pulse rates, ITD enhancement may be beneficial in future binaural CIs to provide improved localization performance. The rate limit of 100-200 pps is, however, even lower than for ITD detection. The results have inspired the development of a signal processing algorithm specific for binaural CIs. Ongoing research is evaluating sound localization performance and speech intelligibility with this new algorithm.

Funding

This work was funded by European Union under the Advancing Binaural Cochlear Implant Technology (ABCIT) grant agreement (No. 304912) and by the DFG Cluster of Excellence Hearing4all.

PS 681

Differences in temporal weighting of interaural time differences between acoustic and electric hearing

Hongmei Hu[1]; David McAlpine[2]; Stephan Ewert[1]; Mathias Dietz[1]

[1]University of Oldenburg; [2]The Ear Institute

Azimuthal sound localization in reverberant environments is complicated by the fact that sound reflections carry interaural differences that can be very different to that from the direct sound. A mixture of direct sound and reflections thus typically result in quickly fluctuating non-stationary interaural differences between the listener's ears. This transforms localization into the challenge of identifying and focusing on the interaural differences of the direct sound source. A highly beneficial auditory processing strategy is to give a high weight to the interaural differences at the onset of the stimulus or at the onset of each modulation cycle. During these onsets, the direct-to-reverberant ratio is typically optimal, and the interaural differences in this short moment are informative on the source location.

In amplitude modulated sounds, such as speech, normal hearing (NH) listeners have indeed a short strongly enhanced sensitivity to interaural time differences (ITDs) during the early rising portion of the modulation cycle, reflecting a higher

weight on temporal read out for that signal portion. Bilateral cochlear implant (CI) listeners can in principle use a similar auditory processing strategy, if carrier phase information is preserved in the pulse timing and if pulse rates are low enough that subjects can perceive ITDs.

Here we compare the temporal ITD read-out weighting of sinusoidally amplitude modulated stimuli between NH and bilateral CI subjects with direct stimulation of a single electrode pair. Experiments were performed with NH and bilateral CI subjects at stimulation rates where subjects are sensitive to carrier ITDs (600 Hz and 200 Hz for NH; 200 pps for CI) and at modulation rates of 8 – 20 Hz. The results indicate that while NH listeners are more sensitive to ITDs applied to the beginning of a modulation cycle, bilateral CI subjects are most sensitive to ITDs applied to the modulation maximum.

The results have implications for future binaural CI processors: If subjects are provided with perceptually exploitable ITD information, this does not necessarily allow them to localize in reverberant and other complex environments.

Funding
This work was funded by the European Union under the Advancing Binaural Cochlear Implant Technology (ABCIT) grant agreement (No. 304912) and the Deutsche Forschungsgemeinschaft (DFG) SFB TRR 31 (B6).

PS 682

Sound Localization by an EAS-CI User: case report

Sebastián Ausili[1]; Martijn Agterberg[2]; Stefan Brill[3]; Emmanuel Mylanus[4]; John van Opstal[2]
[1]Donders Institute of Neuroscience, Radboud University Nijmegen; [2]Radboud University Nijmegen; [3]MED-EL Elektromedizinische Geräte Deutschland GmbH; [4]Radboudumc

ntroduction
Sound azimuth localization of normal-hearing subjects depends on intact binaural processing of ITDs for low-frequency (<2 kHz) and ILDs for high-frequency (>3 kHz) sounds . For subjects with a cochlear implant (CI) is still unclear whether they can gain access to these binaural cues. Several studies demonstrated that not all CI users are capable to localize accurately (Buss et al., 2008; Schleich, Nopp, D'Haese, & D'Haese, 2004; Müller, Schön, & Helms, 2002; Tyler et al., 2002; Gantz et at., 2002). EAS users might have a better representation of ITDs than CI users and EAS users might use ITD as localization cue (Gifford et al., 2014). In the present study, a CI– EAS case was tested on sound localization abilities in a sophisticated setup.

Methods
In the localization tests, the subject had to localize sounds (150 ms) presented in the horizontal direction (azimuth) in a dark, anechoic room by rapid, natural head pointing. Subjects were asked to respond as fast and accurately as possible to the perceived sound location. We measured the result of the earliest bottom--up neural processing stages in the auditory system, with minimal confound from top-down (relatively late, cognitive) factors. To assess the effect of binaural stimulation, the subject was tested during bilateral and unilateral conditions. Absolute sound localization performance of the subject was tested for 3 different sound stimuli: broadband (0.3-20 kHz, ITD&ILD), high-pass (3-20 kHz, ILD), low-pass (0.3-1.5 kHz, ITD). Sound levels were roved over a broad range (50, 60, 70). Each stimulus type was presented from randomly selected locations (homogeneously, but randomly, distributed over a 120 deg range between 60 deg to the left and right), which denies listeners any prior knowledge of upcoming stimulus locations.

Results
As it is shown in Figure 1, results in azimuth are presented according to the type of stimulus described above.

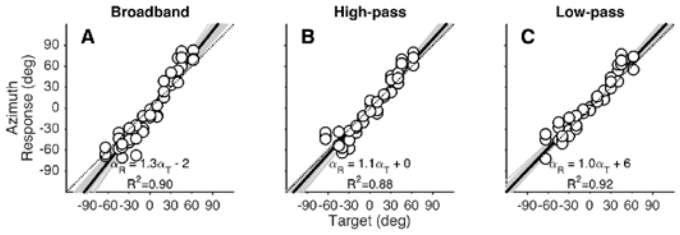

Figure 1. Localization results by CI-EAS subject in azimuth.

This subject demonstrated sound localization abilities close to normal hearing subjects.

Conclusions and Discussion
The almost normal localization abilities of this subject suggest that processing of both ITDs and ILDs is possible. This subject is using EAS (left) and CI (right). In contrast with some literature where CI users cannot perceive ITD cues, this user shows the ability to perceive the interaction between systems (EAS and CI) to detect the sound source location. More studies will be performed on this subject in order to understand better the relation between the two ears, and each ear will be analyzed individually in different conditions (e.g. EAS only).

References
Buss, E., Pillsbury, H. C., Buchman, C. A., Pillsbury, C. H., Clark, M. S., Haynes, D. S., … Barco, A. L. (2008). Multicenter U.S. bilateral MED-EL cochlear implantation study: speech perception over the first year of use. Ear and Hearing, 29(1), 20–32. http://doi.org/10.1097/AUD.0b013e31815d7467

Gifford, R. H., Grantham, D. W., Sheffield, S. W., Davis, T. J., Dwyer, R., & Dorman, M. F. (2014). Localization and interaural time difference (ITD) thresholds for cochlear implant recipients with preserved acoustic hearing in the implanted ear. Hearing Research, 312, 28–37. http://doi.org/10.1016/j.heares.2014.02.007

Müller, J., Schön, F., & Helms, J. (2002). Speech understanding in quiet and noise in bilateral users of the MED-EL COMBI 40/40+ cochlear implant system. Ear and Hearing, 23(3), 198–206. http://doi.org/10.1097/00003446-200206000-00004

Schleich, P., Nopp, P., D'Haese, P., & D??Haese, P. (2004). Head shadow, squelch, and summation effects in bilateral users of the MED-EL COMBI 40/40+ cochlear implant. Ear Hear., 25(3), 197–204. http://doi.org/10.1097/01.AUD.0000130792.43315.97

Van Hoesel, R. J. M., & Tyler, R. S. (2003). Speech perception, localization, and lateralization with bilateral cochlear implants. The Journal of the Acoustical Society of America, 113(3), 1617–1630. http://doi.org/10.1121/1.1539520

PS 683

Short Inter-Pulse Intervals Improve Behavioral ITD Sensitivity in Bilateral Cochlear Implants

Sridhar Srinivasan; Bernhard Laback; Piotr Majdak
Austrian Academy of Sciences

Introduction

Interaural time differences (ITDs) at low frequencies are considered important for sound localization and spatial speech unmasking in the lateral dimension. These so-called fine-structure ITD cues are not encoded in commonly used envelope-based stimulation strategies for cochlear implants (CI). In addition, even under laboratory control of the timing of electric stimulation pulses, ITD sensitivity is poor at the commonly used high pulse rates. The present study aims to determine if and how electrical stimulation can be modified in specific ways to better transmit ITD fine structure cues that result in better ITD sensitivity.

Methods

We measured the ITD sensitivity of bilateral CI listeners when they were presented with unmodulated high-rate (1000 pulses/s) periodic pulse trains overlaid with an additional pulse train at lower rates (50 to 200 pulses/s). The resulting pulse train consisted of periodically occurring pulse doublets having short interpulse intervals (short IPI). The extra pulses were defined by the short-IPI ratio, i.e., a percentage of the regular high-rate interpulse interval (ranging from 6% to 50%) and the short-IPI period, i.e., the interval between the low-rate pulses (ranging from 5 ms to 20 ms). Pulse-trains had a total duration of 600 ms, including 150 ms on- and off-ramps. Participants performed a left/right discrimination task with a zero-ITD reference pulse train. For comparison, the following control conditions were tested: a purely periodic 1000-pps pulse train, a 1000-pps pulse train with binaurally-coherent jitter of pulse timing (Laback & Majdak, 2008, PNAS 105:814-817), and pulse trains with low rates corresponding to the short-IPI periods. All stimuli were adjusted in level to elicit a constant loudness using an adaptive double staircase loudness balancing procedure.

Results & Conclusions

Behavioral ITD sensitivity improved with the introduction of the short-IPI pulses, with the amount of improvement depending on the short-IPI periods and the short-IPI ratios. With certain combinations, the improvement was comparable to that observed in the jittered control condition while the low-rate control conditions elicited maximal improvement in ITD sensitivity. These findings are in line with neurophysiological reports where increased firing rates and improved ITD sensitivity were observed in inferior-colliculus neurons of rabbits upon introduction of pulses with short IPI (Buechel et al., 2015, CIAP W15). Our results indicate that a short-IPI-based stimulation strategy may supplement or even replace the binaurally-coherent jitter stimulation previously proposed.

Funding

Supported by NIH Grant R01 DC 005775

PS 684

Effects of Vocoder Carrier Bandwidths on Binaural Fusion

Abbigail Buente; Justin Aronoff; Melanie Samuels
University of Illinois at Urbana Champaign

Introduction

Individuals with bilateral cochlear implants have difficulty fusing sound from both ears. Differences in the neural populations stimulated in the left and right ear could negatively impact fusion for these individuals. Spectral mismatch between the two ears resulting from different neural survival rates and array insertion depth differences are known to reduce fusion. However, other differences that affect the neural populations stimulated in the two ears may also adversely affect fusion. One such example may be differences in the spread of activation in each ear, which can exist, even with pitch-matched stimulation. The purpose of this study was to determine if differences in the spread of activation for each ear could be detrimentally affecting binaural fusion.

Methods

Ten normal hearing subjects were tested with vocoded speech stimuli. The spread of activation was manipulated by altering the vocoder carrier bandwidths. Carriers were either broadband noises, narrowband noises, or tones. Participants were tested with either the same carrier used for the left and right ear vocoder or different carriers used for each ear. Subjects completed a two-alternative-forced choice task, where they were asked to indicate if they heard a single unitary sound or a different sound in each ear.

Results

Binaural fusion occurred significantly less often when different carriers were used in each ear, with the lowest likelihood of fusion occurring when a tone was combined with a broadband noise.

Conclusions

The results suggest that differences in the spread of activation in each ear has a detrimental effect on fusion. These results suggest that stimulation patterns for bilateral cochlear implant users may need to be altered to reduce the differences in the spread of activation across ears.

Funding

Work supported by NIH/NIDCD R03-DC013380.

PS 685

Effects of Broadening Contralateral Maskers on Masking Functions in Bilateral Cochlear Implant Users

Daniel Lee; Justin Aronoff
University of Illinois at Urbana-Champaign

Background

Contralateral masking functions can provide important insight into how signals presented to the left and right ear interact within the binaural auditory system. Studies have shown that contralateral masking functions are sharper than ipsilateral masking functions in cochlear implant users. This may indicate that the contralateral masker's current spread is sharpened prior to the central auditory system or that it is sharpened due to an interaction between the contralateral masker and probe signal when both are combined centrally. To test these alternatives, contralateral masking functions were compared when using a narrow (masker alone) and a broad (masker-plus-flankers) masker. If no difference is seen between both contralateral masking functions, this would suggest that the masker is being sharpened within the central auditory system where the probe signal and masker interact. In contrast, if a broader masker results in a broader contralateral masking pattern, this could indicate that the central interaction of the masker and probe does not sharpen the contralateral signal and that the peripheral auditory system could be responsible for the relatively sharper contralateral masking function. Considering binaural signal integration in bilateral implant users, it is crucial to understand potential effects of broader contralateral signal and how it could cause unintended channel interaction across ears.

Methods

Masking functions were measured on six bilateral Advanced Bionic cochlear implant users using a simultaneous masking paradigm. A continuous contralateral masker was presented and the level of the probe was adjusted using a modified Bekesy protocol. The broadness of the masker was manipulated by stimulating one masking electrode (masker alone) or the same masking electrode with simultaneous in-phase stimulation of two adjacent electrodes at 10% of the center electrode intensity (masker-plus-flankers). The magnitude of the current presented on the center-masking electrode was held constant across conditions. Masking functions were obtained by measuring probe signal detection thresholds at different regions spanning the entire electrode array in the presence of a consistently placed masker, with the intensity set at the most comfortable loudness level.

Results and conclusions

Results from six bilateral cochlear implant users showed that a broader masking effect occurred with the addition of the flanking electrodes to the central masker. This suggests that the central auditory interaction of signals is not responsible for the sharpened contralateral masking function phenomena. The results suggest that the current shape of signals can impact how signals in the two ears interact in bilateral cochlear implant users.

Funding

Work supported by NIH/NIDCD R03-DC013380

PS 686

Perceptually Aligning Apical Frequency Regions Can Lead to More Binaural Fusion of speech in a Cochlear Implant Simulation

Hannah Staisloff; Daniel Lee; Justin Aronoff
University of Illinois at Urbana-Champaign

Introduction

In bilateral cochlear implant patients, misaligned arrays can cause problems with binaural fusion, localization, and other binaural abilities. Perceptually aligning the left and right electrode arrays is ideal but this is often impossible because of insertion depth differences, causing misaligned apical or basal edges. One option to align the arrays is to disable the electrodes at the ends of the arrays that do not align to anything on the other array. However, this will lead to the input frequency range being allocated to a smaller cochlear region, which could detrimentally affect tasks such as listening to speech in noisy environments. Alternatively, either only the apical or basal ends of the array could be aligned. This would use a larger extent of the electrode array, but could potentially reduce the ability to fuse sounds from the left and right ear into a unitary percept. The goal of this study is to determine whether aligning either the apical or basal portions of the array would be better in terms of binaural fusion.

Methods

Eight normal hearing (NH) listeners were tested in Experiment 1, and nine NH listeners were tested in Experiment 2. For both experiments speech tokens were vocoded and the apical or basal carriers were systematically shifted unilaterally to create a misalignment at one end of the simulated array. For Experiment 2, the vocoder was spectrally inverted. In both Experiments, participants were given a two alternative forced choice task where they were asked to determine if they heard one unitary sound or a different sound at each ear.

Results and Conclusions

For Experiment 1, aligning the apical portion of the simulated arrays led to significantly more binaural fusion. However, when the input was spectrally inverted, aligning the basal portion of the simulated array led to significantly more binaural fusion. The reversal of the effects in Experiment 1 and 2 suggest that the spectral-temporal characteristics of the stimulus may affect which frequency regions are critical for binaural fusion. Given the importance of speech in everyday life, and given that it is dominated by low frequency spectral-temporal modulations, these results suggest that it is more important to perceptually align the apical portions of the array.

Funding

Work supported by NIH/NIDCD R03-DC013380.

PS 687

Developing a Clinically Feasible Pitch Matching Task for Bilateral Cochlear Implant Users

Julia Stelmach[1]; David Landsberger[2]; Monica Padilla[2,3]; Justin Aronoff[1]
[1]University of Illinois at Urbana-Champaign; [2]New York University; [3]University of Southern California

Background

With cochlear implant (CI) users, the left and right arrays rarely stimulate matched cochlear locations due in part to differences in nerve survival and electrode insertion depth. This mismatch can detrimentally affect performance, potentially limiting binaural benefits. One way to address this is by perceptually realigning the two electrode arrays such that a given frequency in the input stimulates perceptually matched locations in the two ears. In order to implement such perceptual realignment clinically, a technique is needed that can be conducted within the time constraints of a clinical visit. This can potentially be addressed by using a pitch matching task if it can be performed in a reasonable amount of time.

Methods

For the current study, an analysis of ten bilateral cochlear implant users' pitch matching data was conducted to determine the minimal number of pitch matches needed to reliably perceptually align the two ears. Reduced sample sets were generated based on 4-16 pseudo-randomly selected pitch matches. Linear fits were found for each reduced sample of data and were compared to the linear fit of the full data set for each participant, to determine how using a particular number of samples would affect which electrodes on the right and left ear would be paired in perceptually aligned maps.

Results and Conclusions

The results indicated that a minimum of six pitch matching samples were sufficient to accurately perceptually align the two ears. With each pitch matching data point requiring approximately one minute to obtain, the pitch matching data needed to perceptually align the two arrays can likely be obtained in less than ten minutes. Thus, this technique could provide a clinically feasible method for perceptually realigning the left and right electrode arrays.

Funding

Funding included: National Organization for Hearing Research, NIH/NIDCD R03-DC-013380, T32DC009975, R01-DC12152 R01-DC001526, R01-DC004993, R03-DC010064

PS 688

Perception of Binaural Level and Timing Cues in Children with Early Bimodal Use Compared to Bilaterally Implanted Children

Melissa Polonenko; Michael Deighton; Parvaneh Abbasalipour; Blake Papsin; Karen Gordon
The Hospital for Sick Children, The University of Toronto

Background

Perception of binaural cues is important for localizing sound and listening in noisy environments. While providing one cochlear implant (CI) and one hearing aid in the non-implanted ear (bimodal hearing) restores access to bilateral sound, delivering sound through two independent devices with substantially different timing delays to the auditory system may compromise binaural hearing development.

Objectives

With these challenges specific to bimodal hearing in mind, we aim to study 1) whether children with bimodal input are able to detect binaural level (ILD) and timing (ITD) cues, and 2) how their performance compares to previously studied groups of bilateral CI users.

Methods

Fifty-three children participated in this study: 28 bimodal users (mean±SD age 12.2±3.2 years) who wore both devices for > 6 months and 25 normal hearing peers (13.0±3.1 years). Previously studied bilateral CI users included 29 simultaneously implanted children (7.4±2.1 years) and 44 sequentially implanted children (13.3±3.4), 28 of whom wore two CIs for <1 year (inexperienced). In a forced-choice task, children indicated on which side of the head they heard bilateral acoustic clicks/electric pulses that varied in ILD or ITD. A generalized linear mixed model with random intercept and slope effects was used to fit binary logistic functions for lateralization and compare slopes across groups.

Results

Bimodal users were able to detect similar changes in ILDs ($p<0.0001$) to simultaneously and inexperienced sequentially implanted children. Yet, they could not detect even very large ITDs up to 3ms as measured by insignificant mean slope of the binary logit functions ($p=0.075$). Slopes of logit functions for ITDs were poorer in the bimodal group than children with longer durations of bilateral CI use but similar to inexperienced sequential CI users. Slopes in the bimodal group and across groups were significantly predicted by length of bilateral device use ($p=0.006$) and inter-device delay ($p=0.009$).

Conclusions\

A balance between levels of acoustic and electric stimuli was obtainable with relatively little bimodal experience. Children with early bimodal use struggle to detect ITDs, and consequently may rely on their ability to detect ILD cues and perhaps other cues or strategies to lateralize sound. However, these children may yet have the potential to develop binaural hearing with their two different devices, considering: 1) lateralization ability correlated with duration of bilateral device use; and 2) though inexperienced sequentially implanted

children were also unable to detect ITDs, children with longer bilateral implant use were sensitive to ITDs.

Funding
Ontario Graduate Scholarship, Canadian Institute of Health Sciences Grant

PS 689

Auditory motion perception of children with bilateral cochlear implants

Keng Moua; Alan Kan; Heath Jones; Ruth Litovsky
University of Wisconsin-Madison

Sound localization performance varies largely in children with bilateral cochlear implants (BiCIs), and can either fall within or outside the range of performance seen in adults with BiCIs. The localization ability of static sounds has been studied in children with BiCIs but their ability to track and locate a moving sound has received little attention. Our previous work has shown that adult BiCI users have increased errors when indicating if a sound source was moving or static, compared to adult normal hearing listeners. In addition, adult BiCI users had difficulty judging the direction of motion for sounds that traversed a large angular range (40°) across azimuth. In this study, we expanded this paradigm to children BiCI users, whose tasks in real world environments requires tracking of moving objects of interest. The use of this auditory motion paradigm may help to better understand sources of variability in static sound localization performance of children with BiCIs.

Adults and children with BiCIs were tested in an auditory motion experiment. Stimuli consisted of white noise tokens which were band pass filtered to match the input frequency range of the Cochlear Ltd processors used by our subjects. Auditory motion was simulated across 37 loudspeakers (5˚ intervals, -90˚ to +90˚ azimuth). Recordings of the stimuli were made with binaural microphones placed in the ears of a KEMAR manikin. Moving and static sound sources were presented in the same 19 target locations (10° intervals, -90° to 90°) for 500 ms. Moving sounds had angular ranges of 10˚, 20°, and 40˚, with velocities of 20˚/s, 40˚/s, and 80˚/s, respectively. All stimuli were presented directly to the auxiliary input ports of the subjects' cochlear implants. Within each of block of trials static and moving sounds of different angular ranges and velocities were randomly presented.

Results to date suggest that children with BiCIs have more difficulty judging whether a sound was moving or static in comparison to adult BiCI users. Sound localization performance was measured using the root mean square (RMS) error. Children with BiCIs had larger RMS errors when locating the start and end locations of a sound source compared to adults with BiCIs in all conditions. The use of an auditory motion paradigm may allow for a comprehensive assessment of the spatial hearing abilities in children with BiCIs.

Funding
NIH-NIDCD (R01 DC003083 & R01 DC008365 to RYL) and NIH-NICHD (P30HD03352 to the Waisman Center)

PS 691

Development of Potent and Selective KCNQ2/3 Potassium Channel Activators as Potential Candidates to Prevent the Development of Tinnitus

Manoj Kumar; Peter Wipf; Thanos Tzounopoulos
University of Pittsburgh

Tinnitus is a neuronal disorder that usually develops after exposure to loud sound. A large portion of the population (5-15%) suffers from chronic tinnitus, which can be a debilitating condition. Despite the high prevalence of tinnitus, no cure is available. Recently our lab showed that noise-induced reduction in KCNQ2/3 channel activity is critical for the induction of tinnitus. Moreover, the FDA approved anti-epileptic drug, retigabine, prevented the induction of tinnitus in mice through activating KCNQ2/3 channels. However, retigabine is not specific for KCNQ2/3 channels and activates KCNQ4 and KCNQ5 channels. To develop more potent and more specific KCNQ2/3 activators we synthesized SF0034, an analog of retigabine, which contains an addition of a fluorine atom at aniline ring. SF0034 is 5 times more potent than retigabine at KCNQ2/3 channels and unlike retigabine, did not activate either KCNQ 4 or KCNQ5 channels. We hypothesized that increasing the number of fluorine atoms at the phenyl ring would increase the potency and selectivity of retigabine analogs. We synthesized a number of analogs by addition of trifluromethyl and pentafluorosulphanyl functional group at position 3 and at position 4 of the phenyl ring of retigabine. We transiently expressed KCNQ2/3 heteromers as well as KCNQ 4 and 5 homomeric channels in CHO cells and tested for potency and selectivity. Two of the newly synthesized analogs are 2-3 times more potent than SF0034, which makes them promising clinical candidates for preventing tinnitus and for treatment of other hyperexcitability-related disorders, such as epilepsy.

Funding
Joint Warfighter Medical Research Program (Grant W81X-WH-14-1-0117)

PS 692

Neural substrates predicting short-term improvement of tinnitus loudness and distress after modified tinnitus retraining treatment

Jae-Jin Song[1]; Shin Hye Kim[1]; Sven Vanneste[2]; Dirk De Ridder[3]; Ja-Won Koo[1]
[1]Seoul National University Bundang Hospital; [2]University of Texas at Dallas; [3]University of Otago

Background
Although the majority of previous studies indicated that tinnitus retraining therapy (TRT) is effective in most patients with tinnitus, neither the exact mechanism of tinnitus improvement nor the predictors of the degree of improvement in tinnitus after TRT are fully understood yet. In this regard, by correlating the degree of tinnitus improvement with pre-TRT resting-state source-localized quantitative electroencephalography

(qEEG) findings, we attempted to find the pretreatment neural substrates of tinnitus improvement.

Method
Thirty-one patients complaining of subjective tinnitus were prospectively enrolled for the TRT program, and their resting-state EEGs were recorded before the initial TRT session. At 3 months after the initial TRT session, source-localized cortical activities were correlated with percent improvement in numeric rating scale (NRS) tinnitus loudness, tinnitus distress, and tinnitus perception.

Results
The enrolled patients showed statistically significant improvements with regard to NRS loudness, distress, and perception 3 months after the initial TRT session. By a median-split approach, we have confirmed that the improvements in NRS loudness, distress, and perception were not affected by the level of hearing loss. Percent improvement of NRS tinnitus loudness was negatively correlated with the activity of the parahippocampus (PHC). Meanwhile, the activity of the insula showed significantly positive correlation with percent improvement of NRS tinnitus distress. Also, the activity of the rostral anterior cingulate cortex (rACC) was positively correlated with percent improvement of NRS tinnitus perception.

Conclusion
The current study may underpin roles of decontexturizing ability of PHC with regard to the improvement of tinnitus loudness, parasympathetic activity control by the insula for tinnitus distress improvement, and noise canceling system for tinnitus perception improvement. The current study has partly replicated classical Jastreboff's neurophysiologic model of tinnitus, and these results may role as a milestone toward patient-tailored application of TRT.

PS 693

Tinnitus Maskers with Customized Spectra Can Be More Efficient than White Noise

W. Owen Brimijoin[1]; Bernd Porr[2]
[1]MRC/CSO; [2]University of Glasgow

Tinnitus can severely affect quality of life, but some sufferers can experience some degree of relief from masking sounds such as white noise. A tinnitus masker is any such sound that is played to lessen the apparent loudness or annoyance of a person's tinnitus, and achieves varying degrees of success. There exist a number of devices that play masking sounds, most often consisting of a pre-set library from which the tinnitus sufferer can select a preferred sound for playback. The method we propose could allow a listener to train a piece of software (or device) to deliver a customized, highly efficient masker or set of maskers for different situations.

The algorithm is based on that found in Brimijoin et al. (2013) where we demonstrated that it is possible to use random noise stimuli to estimate the internal representation of vowel sounds like [a] or [:i]. Analysis of the relationship between listeners' responses and the noise stimuli yielded average signal spectra that closely matched those of actual [a] and [:i] vowels. In our method to estimate efficient tinnitus maskers, the listener is presented with a sequence of noise signals and asked to press a button when their tinnitus becomes more difficult to hear. We used reverse correlation on the listener's responses and the noise stimuli to compute the spectrum of his/her "ideal" tinnitus masker.

Masking strength for these ideal maskers was then evaluated as a function of presentation level and compared to that of white noise and 'worst' maskers (the spectral inverse of the ideal masker). Pilot data suggests that for some listeners our technique did not result in maskers that were any more efficient (effective at lower SPLs) than white noise, but in others the individualized maskers could be at least 12 dB more efficient than white noise. This method shows promise for some patients and could be readily incorporated into current hearing aids, smartphone apps, and/or standalone tinnitus noise generators.

Funding
Work supported by the Medical Research Council (UK) and the Chief Scientist Office (Scotland)

PS 694

Tinnitus Treatment with Digisonic SP Cochlear Implant in Single Sided Deafness Patients.

Michel Hoen
Oticon Medical

Objectives
Recent studies have reported successful reduction of tinnitus after cochlear implantation (CI) in most CI users, but the mechanisms of reduction and the amount of improvement is not fully understood. Especially, the relative role of peripheral and central auditory pathways is not clearly known. This study assessed the effect of CI electrical stimulation on tinnitus in subjects with unilateral tinnitus related to a single-sided deafness (SSD), and relative contributions of peripheral and central auditory pathways in tinnitus reduction.

Methodology
Seventeen subjects showing severe tinnitus with an ipsilateral SSD that was unresponsive to tinnitus treatment were enrolled to receive a CI, all patients met criteria of Sensorineural Hearing Loss (SNHL). CI delivered a continuous white noise stimulation in the first month period and thereafter a conventional stimulation, the outcomes were monitored at 1, 3 and 6 months of CI use. Tinnitus loudness and annoyance were measured with a Visual Analog Scale and tinnitus distress and quality of life were evaluated with tinnitus questionnaires (THI, TRQ and STSS) before and 6 months after implant activation.

Results
Electrical stimulation resulted in a reduction in tinnitus loudness 6 months' post-activation (mean ± SD points; 7.9±0.8 pre-implantation, 4.8±2.9 post-activation) and in annoyance (8.0±.1.4 vs. 4.4±3.0). The Tinnitus Questionnaires revealed a positive effect of CI stimulation with a reduction of THI (77.0±8.4 vs. 39.0±19.9), TRQ (52.5±20.5 vs.32.3±17.2) and STSS scores (12.6±2.1 vs. 8.5±4.4). Moreover, a quick

improvement was noticed in 60% (9/15) of patients only after white noise 1 month period, but a great amount of improvement in 76.9% (10/13) of patients after 1 month of conventional stimulation demonstrated the degree of tinnitus reduction regarding the stimulation modality. Some patients experienced no improvement or exacerbation of tinnitus, 1 patient was withdrawn from the study, no serious adverse event occurred in this ongoing study.

Conclusion

These preliminary results suggest that CIs have a positive effect on unilateral tinnitus resulting from an SSD. But several hypothesis are pending according to the mechanisms by which the CI reduce tinnitus such as habituation, peripheral electrical nerve stimulation or complex cortical reorganization. This study confirms that CI is an effective approach for tinnitus treatment in selected subjects, but further data still necessary to define the optimal stimulation mode.

PS 695

A Balanced Randomised Placebo Controlled Double-Blind Study to Investigate the Efficacy and Safety of AUT00063 versus Placebo in Subjective Tinnitus: Protocol for a Phase IIa Trial

Deborah Hall[1]; Jaydip Ray[2]; Jeannette Watson[3]; Charles Large[3]; Peter Harris[3]

[1]University of Nottingham; [2]Royal Hallamshire Hospital; [3]Autifony Therapeutics Limited

Reduced activity at certain sites in the brain (called "voltage-gated potassium channels") has been linked to hearing problems, like age-related loss of hearing or tinnitus (a 'ringing' or buzzing noise in the ears). AUT00063 is an experimental new medicine that has been developed to improve the action of these specific channels and so treat the brain component of these hearing problems. The main purpose of this study is to try to demonstrate an improvement in the severity of tinnitus after 28 days of treatment with the study medicine or the placebo (dummy drug which does not contain the medication). The first participant was recruited in November 2014, and recruitment will continue at 18 UK sites throughout 2015, with a target sample size up to 152. A clinically relevant interpretation of tinnitus severity relates to the functional impact of tinnitus on daily activities and is measured as a primary outcome using the Tinnitus Functional Index. Secondary outcomes consider the effect on tinnitus loudness. Safety and efficacy will be determined by looking at a number of assessments (physical examinations, blood sampling, hearing assessments, questionnaires, etc.) and in case of any serious medical event during the study. A safety follow-up will be conducted after the treatment period.

Here we present the clinical trial design, and discuss some of the design and implementation challenges that we have had to overcome.

ClinicalTrials.gov Identifier: NCT02315508.

Funding

The study is co-funded by a UK government-backed Biomedical Catalyst award.

PS 696

Inhibition of L-type Calcium Channels for Preventing Noise Induced Hearing Loss and Tinnitus

Ammaar Wattoo; Aaron Apawu; Mirabela Hali; Antonela Muca; Avril Holt

Wayne State University

Background

Increased spontaneous neuronal activity is thought to underlie the pathological changes in tinnitus. Previous studies have demonstrated efficacy of nimodipine, an L-type calcium channel blocker, on reversing these changes in salicylate and quinine induced tinnitus in rat models (Jastreboff, 1991). However, human trials with nimodipine have not consistently demonstrated efficacy as treatment for tinnitus, prompting examination of other calcium channel blockers. In this study, we examined verapamil as a preventative therapy for noise induced tinnitus and hearing loss.

Methods

Male Sprague-Dawley rats (n = 5 - 7/group) were administered verapamil i.p. 15 minutes before a one hour unilateral noise exposure (16 kHz, 106 dB SPL). Hearing thresholds at 12 and 20 kHz were measured using auditory brainstem response (ABR). Gap inhibition of the acoustic startle response (GiASR) was used to assess tinnitus across six frequencies (4, 8, 12, 16, 20 and 24 kHz) at two intensities (45 and 60 dB SPL).

Results

There were no significant differences in hearing thresholds between verapamil and saline groups at any time point or frequency. Within an hour following noise exposure, rats administered verapamil demonstrated enhanced Gap detection at both 45 dB (11.5%, $p < 0.01$) and 60 dB (12.8%, $p < 0.05$, n = 7/group). The effects were more pronounced 24 hours after noise exposure, with rats that received verapamil suppressing their total startle by 18.0% and 20.2% more than controls at 45 dB and 60 dB, respectively ($p < 0.01$, n = 7/group). By five days after noise exposure, rats that received verapamil returned to baseline levels of Gap detection.

Conclusions

Our results demonstrate that verapamil may prevent development of noise induced tinnitus and thus warrants further study. Future studies aim to examine the localization of L-type calcium channels in the central auditory system and explore effects of direct verapamil administration. We also plan to examine whether systemic administration of verapamil prevents synapse loss in the cochlea.

Funding

1I01RX001095-01.U.S Department of Veterans T42 OH008455 National Institute for Occupational Safety and Health, Centers for Disease Control and Prevention

PS 697

Tetrandrine Reduces Behavioral Indications of Tinnitus in Mice.

Hongyan Zuo; Kyle Nakamoto; Debin Lei; Jianxin Bao
Northeast Ohio Medical University

Background

Tinnitus, the perception of a phantom sound, is a common health condition, affecting 10–15% of the general population. Currently there are no FDA-approved drug therapies for tinnitus. Tetrandrine (TET) is a drug approved in China with a long safety history. It is a bisbenzylisoquinoline alkaloid extracted from the root of the herb Stephania tetrandra. Using an improved tinnitus behavioral detection method, we determined that TET diminishes tinnitus-like behavior in a mouse model.

Methods

We used either a salicylate injections (400 mg/kg, i.p.) or unilateral noise exposure (4-25 kHz, narrow band noise, 120 dB, 2h) to induce tinnitus in 2 month old C57BL/6J mice. We used a modified operant conditioning method (Go/No-Go) in a shuttle box to detect tinnitus-like behavior. For the salicylate trials, measurements were made after a salicylate injection or after a salicylate and TET injections. For the noise induction model, measurements were made 2, 4, 8 and 12 weeks after the noise exposure, and also after TET injection.

Results

For the salicylate trials, TET significantly decreased behavioral indications of tinnitus at a dosage of 10 and 30 mg/kg, but no significant changes were observed at a 5 mg/kg dosage. For the noise induced tinnitus trials, TET significantly decreased behavioral indications of tinnitus at a dosage of 60 and 90 mg/kg, but no significant changes were observed at a 30 mg/kg dosage. Both the salicylate and noise trials showed a positive dose-effect relationship of TET on diminishing tinnitus-like behavior. Moreover, there were no significant changes for the “Go” trials, which indicates that TET has no effects on memory functions at these dosages.

Summary

TET diminishes both salicylate and noise induced tinnitus-like behavior in mice, and our finding strongly suggested that TET could be a drug candidate for tinnitus treatment. The effective dosage of TET on salicylate induced tinnitus-like behavior is much lower than on the noise induction model, indicating different cellular or/and molecular pathways underlying these two tinnitus models. We are now studying possible molecular pathways underlying noise-induced tinnitus-like behavior.

PS 698

FEA Model for High Frequency Stimulus of Utricle Receptors

Rachel Craig[1]; Julian Davis[1]; Chris Wong[2]; Ian Curthoys[2]; **Wally Grant**[3]
[1]University of Southern Indiana; [2]University of Sydney; [3]VA Tech

Background

Bone conduction vibration (BCV) and air-conducted sound (ACS) have been shown to selectively activate irregular primary utricle vestibular neurons in the guinea pig over the frequency range for BCV from 100 to 1000 Hz and for ACS from 250 to 2000 Hz (Curthoys & Grant, 2015). These same stimuli are also being utilized for human utricle clinical testing utilizing vestibular-evoked myogenic potentials (VEMP).

Hypothesis

BCV and ACS produce pressure waves in inner ear fluids. These pressure waves cause endolymph fluid displacements when an outlet, such as the round window, allows a fluid displacement path. The pressure waves and fluid displacement activate resonant structures in the otoconial layer (OL) of the utricle. This OL motion induces fluid flow in the striolar region, stimulating hair cell bundles (HCB) that are freestanding or weakly attached to the OL in this region. The OL motion induces fluid velocity flow over HCB creating a drag force acting on the bundle, and displacing Type I HCB in the striolar region. These Type I hair cells generate the irregular afferent signals originating from the striolar region of the utricle.

Detailed finite element (FE) model of the guinea pig utricle is being developed to investigate the natural frequencies of the OL and the potential stimulus by BCV and ACS. Detailed micro-CT images are needed to construct realistic guinea pig FE utricle model. These methods can be extended to human investigation of VEMP.

Methods

Anatomically accurate finite element model of a turtle utricle have been shown to have natural first mode frequency of 363 Hz (Davis & Grant, 2014). Higher mode frequencies are seen in FE models reflect natural frequencies and deflections that arise due to different displacement direction or resonant parts of the utricle-gel layer structure.

Osmium enhanced micro-CT images of guinea pig inner ears are being used to construct a detailed utricle FE model. Detailed dimensional data are taken from these images including: top view shape, thickness, and layer dimensions. The micro-CT images are converted into 3-D FE models, and the dimensional data is utilized for accurate model dimensions. Parameter values for gel, column filament, and otoconial layer modulus, density, and Poisson’s ratio are taken from previous modeling efforts (Davis & Grant, 2014).

Results/Progress

Micro-CT imaging of guinea pig inner ears has been completed. Detailed measurements from these images

have also been completed. Digitized 3-D FE model is under construction.

PS 699

Head Kinematics in Free-Running Chinchillas

Leo Li[1]; Michael Paulin[2]; Jake Smith[3]; Timothy Hullar[4]; Larry Hoffman[3]

[1]University of Michigan; [2]University of Otago; [3]Geffen School of Medicine at UCLA; [4]Oregon Health and Science University

Head movements are coded by sensory epithelia within the vestibular labyrinth and transformed into trains of action potentials transmitted into the central nervous system (CNS). Though a considerable literature exists regarding the neurobiology of this transformation and resulting spiketrains, there is a paucity of information regarding head kinematics made by research subjects during natural ambulatory activities driving this sensory transformation. For many animal research models head-fixing of measurement devices may be problematic due to additional loads of head-mounted sensors and cable tethering that could influence the measurements. The goal of the present research was to assemble and implement a measurement system using off-the-shelf components and wireless data transmission to measure head kinematics in chinchillas during epochs of unrestrained locomotion. We adapted a breakout board with a 9 degree-of-freedom sensor (LSM9DS0; 3 axes each of gyroscope, linear accelerometer, and magnetometer) wired directly to a microcontroller and battery. A Bluetooth module (RF-42) was also wired to the serial data port of the microcontroller for wireless transmission. During recording trials the LSM9DS0 was secured to the head via an array of pins mated with sockets bonded the skull. The microcontroller, RF-42, and battery were carried by the chinchilla in a backpack, and were connected to the sensor via loose wires. Data collection was managed via a Matlab script that logged data transmitted during measurement trials. Raw data from LSM9DS0 gyroscopes and accelerometers were calibrated via a rotatory turntable and Earth-gravity, respectively. These data, along with magnetometer measurements, provided the basis to report head kinematics and the head orientation vectors, the latter of which were derived using the algorithm given by Madgwick et al. Behavioral trials contained periods of ambulatory activity and free standing. While large head movements (>200°/s) were measured during periods of visual exploration, angular head velocities in yaw, pitch, and roll during periods of natural locomotion were more modest in magnitude and appeared to oscillate with gait. Peak-to-peak yaw velocities ranged between -78 and 112°/s, and spectral analyses of these recordings demonstrated the largest amplitudes at frequencies <10 Hz (e.g. approx. 2 and 8Hz). Smaller peaks were clearly evident at frequencies between 10 – 20Hz. Peak angular velocities in pitch tended to exhibit higher magnitudes, while those in roll were smaller. These data provide the foundation for developing behaviorally-relevant stimuli for exploring vestibular sensory circuits, which will aid in understanding the heterogeneity of afferent input to the central nervous system.

Funding
1R01DC014368

PS 699A

Comparative Analyses of Vestibular Epithelia in Bats (Rousettus aegyptiacus) and Mice (Mus musculus)

Kristel Choy[1]; Walter Metzner[1]; Larry Hoffman[2]

[1]UCLA; [2]Geffen School of Medicine at UCLA

By virtue of their flight and echolocation behaviors, bats are acknowledged to be among the most agile of mammals and exhibit characteristics of being “spatiotemporal integration specialists” (Ulanovsky & Moss 2008). While some bat species exhibit adaptations of their cochleae to accommodate increased demands required for echolocation, previous investigations demonstrated the absence of structural adaptations of the vestibular labyrinth that would enhance capabilities for higher performance head movement coding. The objective of this investigation is to determine whether adaptations within cellular components of bat vestibular epithelia (specifically, specimens from Egyptian fruit bats, Rousettus aegyptiacus) may exist to support enhanced capabilities for coding agile (e.g. high frequency) head movements. We focused upon cellular attributes of the crista central zones (CZ) and utricular striola (STR), and compared these findings to parallel measures from mouse epithelia. Anti-calretinin immunohistochemistry was employed to demarcate CZ and STR regions. We used antibodies to oncomodulin (Ocm, aka β-parvalbumin) and Kv7.4 (KCNQ4) as markers in hair cells and calyces, respectively, that are associated with high-frequency stimulus processing. Fluorophore-conjugated phalloidin was used to label stereocilia and epithelial tight junctions, and DAPI was used as a nuclear stain. These additional labels aided in the quantification of epithelial surface areas and hair cell counts. Comparative indices of epitope expression in utricles were determined directly. Indirect indices of epitope expression areas were determined for the cristae; e.g. ratios of total length along the crista apex long axis in which positive immunolabeling was observed and the total apical long axis epithelia length. We found that the striola in mouse and Rousettus were of similar relative size (12.2 and 10.6% relative to total utricular area). However, the area harboring Ocm-positive hair cells, which encompasses the striola, was much larger in Rousettus (20.2%) than that in mouse (12.6%). Much of this relative expansion of the Ocm-positive region was lateral to the line of polarity reversal (in mouse, the vast majority Ocm-positive hair cells were medial to the LPR). The horizontal cristae CZs in mouse and Rousettus cristae exhibited similar relative areas, and the index of Ocm-positive epithelial areas were similar in mouse and Rousettus (64.2% and 66.9%, respectively). Similarly, the crista epithelial areas harboring KCNQ4-positive calyces were also similar in both species. These data suggest that cellular adaptations within the vestibular epithelia may exist to enhance coding fidelity and integration of complex head movements concomitant with flight and/or echolocation.

Funding
UCLA Academic Senate Grant

PS 700

Potassium Regulation at the Type I Hair Cell and Calyx Synapse

Frances Meredith; Katherine Rennie
University of Colorado, Anschutz Medical Campus

Background
A cup-shaped calyx afferent terminal surrounds the mammalian vestibular type I hair cell (HCI), creating a narrow but extensive synaptic cleft between the two cell types. HCI are characterized by a K^+ current, IK_{LV}, active at membrane potentials hyperpolarized to rest. Outward movement of K^+ through this low-voltage-activated channel is thought to significantly increase K^+ concentrations in the synaptic cleft and depolarize the calyx membrane. The presence of ion pumps and K^+ channels on the inner face of the calyx could modulate cleft K^+ concentrations.

Methods
We investigated the impact of altering external K^+ concentration (0-50mM) on calyx properties using patch clamp techniques. Recordings were made from calyces in an intact preparation of the gerbil crista (postnatal days 20-29) (Meredith and Rennie 2015) or from calyces isolated together with their HCI (Rennie and Streeter 2006).

Results
A slowly activating current, I_X, that turned on at -60 mV and persisted in the presence of internal and external cesium and internal QX314 (blocks I_{Na}) was observed in calyx terminals. When external K^+ concentration was increased from 5 to 40mM, peak amplitude increased significantly from a control value of -122pA to -507pA (n=8; P=0.002) and reversal potential shifted from approximately -15 to 12mV (n=8). I_X was completely abolished in 0mM external K^+ but persisted in external barium (0.5mM), 4-AP (0.25mM), Spadin (1µM; TREK channel blocker), E-4031 (10µM; blocks erg channels), XE991 (20µM; blocks KCNQ channels) and ZD7288 (100µM; blocks HCN channels). Nifedipine (20µM), an L-type calcium channel antagonist, reduced I_X by 34% (n=2), suggesting a calcium-dependent component.

In current clamp (performed without internal cesium or QX314), resting membrane potential was initially depolarized (-20 to 20 mV) in high external K^+, but then gradually and spontaneously hyperpolarized until it reached ~ -100mV. Ouabain (1mM) did not block the slow hyperpolarization, suggesting that Na^+/K^+- ATPase was not involved. At -100mV, a sag was observed, returning the membrane to more depolarized potentials and often initiating an action potential. ZD7288 prevented or markedly slowed initiation of the depolarizing sag, suggesting involvement of HCN channels.

Ongoing research will identify the mechanism(s) underlying the tendency of the calyx membrane to hyperpolarize in elevated external K^+, identify the channel underlying I_X and elucidate its role in controlling cleft K^+ concentration. Identifying mechanisms that regulate cleft K^+ concentrations at the HCI/calyx synapse could increase our understanding of the consequences of disrupted ionic homeostasis in vestibular disorders like Meniere's disease.

Funding
Hearing Health Foundation

PS 701

Simultaneous recordings from the calyx and enveloped hair cell in complex calyces of the posterior semicircular canal of the turtle, Trachemys scripta elegans

Donatella Contini; Steven Price; Jonathan Art
University of Illinois at Chicago

Background
In vestibular epithelia, multiple hair cells (HCs) often converge onto a single primary afferent. In primitive vertebrates the HCs synapse onto simple bouton endings. With the advent of amniotes, the afferent complexity increases with the addition of expanded calyceal endings that envelop one or more HCs. Over the course of evolution there is an increased representation of these endings. However, the functional implications of the calyx remain obscure. Our experiments were designed to examine the synaptic and ionic basis of fast excitatory events and a slower modulation of inward, excitatory current in the calyx following depolarization of the hair cell.

Methods
Simultaneous patch–electrode recordings from type I HCs and their enveloping calyx were made with KF/KCl, dye–filled pipettes, in the epithelia of the posterior semicircular canal of the turtle, *Trachemys scripta elegans.* Both pre– and postsynaptic elements were examined in all pairwise combinations of current and voltage clamp, under conditions of ionic substitution, pharmacological block, and mechanical stimulation of the hair cell bundle. Steady–state and instantaneous I–V curves were constructed to analyze changes in conductance and driving force on the presynaptic HC, and the postsynaptic afferent terminal.

Results
Depolarization of HCs from a holding potential of –100 mV demonstrated a large, low voltage activated outward current from –90 mV, that was half–activated at –60 mV. Following depolarization, or mechanical stimulation of the HC ciliary bundle, large, rapid events were elicited in the calyx, that were consistent with conventional excitatory quantal transmission. With HC depolarization there was also a more graded response in the calyx. Both the rapid events and some of the graded response could be blocked by an AMPA receptor blocker CNQX. Calyceal endings held at –100 mV displayed a large inward current, and HC depolarization produced an additional inward current. Much of both the steady level and the HC evoked inward current could be blocked by ZD7288, suggesting that HCN channels in the calyx are also sensitive to the relative concentrations of monovalent ions. Measurement of the instantaneous I–V curve of the HC following prolonged depolarization demonstrated a shift in the reversal potential

consistent with an elevation of [K^+] at the basolateral pole from a nominal extracellular 4 mM to at least 16 mM.

Conclusion
At a minimum, HC transmission to the calyx includes a delicate balance between AMPA mediated events, and potentially depolarizing currents due to changes in monovalent ion concentration.

Funding
This work was supported by NIH-NIDCD, RO1 DC002058

PS 702

Role of low voltage activated calcium current in vestibular afferent neurons discharge

Enrique Soto; Rosario Vega; Maricruz Rangel-Galvan
Benemérita Universidad Autónoma de Puebla

It has been established that the intrinsic properties of neurons (including the expression and density of ion channels in the membrane) significantly contribute to set the discharge pattern in vestibular afferent neurons (VANs). Various channels have been found to be expressed in VANs, among them the low voltage activated (LVA) calcium channels have a differential distribution in the soma of VAN suggesting that they might contribute to differentiate the VANs activity. Thus we decided to study the functional role of LVA calcium current on the frequency and regularity of discharge of the VANs.

Electrophysiological recordings of VANs in primary culture were performed (P7-P10 CII rat) using the perforated patch clamp technique. Nickel and mibefradil were used as blockers of the low voltage activated calcium current.

Current clamp recordings shown that the NAVs express a calcium activated current at low voltages (LVA) that when blocked with 300 μM Nickel, significantly modified the morphology of action potentials (APs) increasing the peak latency and duration at 50%, and decreasing amplitude of AP, and the depolarization and repolarization rates (DR and RR). With the use of mibefradil 2 μM we found a decrease in the AP threshold and in rebound APs an increase in peak latency and decreased amplitude. In neurons with repetitive discharge both Nickel (300 μM) and mibefradil (2 μM) caused a reduction in the number of APs discharge and a decrease in the AP amplitude.

To study the role of LVA calcium current in a dynamical condition sinusoidal current injection was used. We found a group of cells in which AP discharge increased from 117 ± 28 under control condition to 192 ± 33 after Nickel 300 μM. And a group of cells in which AP discharge decreased from 102 ± 23 under control condition to 28 ± 16. This bimodal behavior was similarly found with the use of Mibefradil. To study the regularity of discharge cells were stimulated with Gaussian white noise. The average CV under control was 1.04 and passes to a CV = 1.46 after applying Mibefradil 2 μM (P = 0.06).

These results show that LVA calcium current becomes activated during AP generation and significantly contributes to determine the discharge regularity of these neurons, thus constituting a potential target for neuromodulation and for pharmacological calcium channel blockers.

Funding
This study was supported by grant from Consejo Nacional de Ciencia y Tecnología de México (CONACyT, grant 167052 to Enrique Soto), and by grants from Vicerrectoria de Investigación y Estudios de Posgrado (VIEP-BUAP grants to Rosario Vega and Enrique Soto), and PROFOCIE 2014- and 2015.

PS 703

The vestibular phenotype of loss of Connexin 26 in conditional knock out mice

Min Young Lee; Yohei Takada; Donald Swiderski; Lisa Beyer; Jonie Dye; Megan Wampler; Guoqiang Wan; W. Michael King; Gabriel Corfas; Yehoash Raphael
Kresge Hearing Research Institute, University of Michigan

Background
In the inner ear, connexins are thought to regulate potassium recycling. Connexin 26 and 30 (Cx26 and Cx30, respectively) have been localized to the non-sensory cells of the sensory epithelium in the inner ear. Although Cx26 loss accounts for high proportion of non-syndromic hereditary hearing loss, and its effects in the cochlea are well described, the vestibular phenotype of this mutation is not well characterized.

We have reported that Gjb2-conditional knock out mouse (Gjb2-CKO) exhibits a secondary loss of Cx30 in the peripheral vestibular system. Despite the loss of two connexins, hair cell survival and vestibular function evaluated by rotarod and centrifuge tests did not show differences from wild types (WT). Here we applied other physiological assays and evaluated Gjb2-CKO mice aged 2 to 10 months. We also tested whether the impaired cell-cell communication due to loss of connexins would alter aminoglycoside ototoxicity.

Materials and Methods
Transgenic C57BL/6 mice, in which Sox10-Cre drives excision of the Cx26 gene from non-sensory cells flanking the sensory epithelium of the inner ear (Gjb2-CKO), were compared to age-matched WT. Vestibular functions were tested by VCR (n=7) and VsEP (n=8) in 8 week old animals, and by rotarod in animals older than 20 weeks (n=6). To evaluate the response of the vestibular system to insults, streptomycin was delivered unilaterally into the posterior semicircular canal of seven mice (including both Gjb2-CKO and WT), which were tested by VsEP before and 1 week after the injection. Histology was performed to evaluate hair cells and connexins.

Results
Gjb2-CKO mice that were not exposed to streptomycin did not exhibit hair cell loss up to 20 weeks of age, and performance on rotarod was similar to WT, despite the loss of both connexins. VsEP and VCR showed no significant difference between the two genotypes. After the injection of streptomycin, WT and Gjb2-CKO mice showed abnormal behaviors including head tilt, barrel rolling and absence of

righting reflex. However, VsEP was not affected by unilateral streptomycin injection in either group, suggesting that utricular function is not altered by unilateral lesion and loss of Cx26 or that unilateral stimulation is sufficient to evoke a signal.

Conclusions
Despite the loss of connexins 26 and 30, vestibular function remained unaltered as did survival of the vestibular hair cells. Loss of connexins also did not alter response of vestibular hair cells to treatment with streptomycin.

Funding
Supported by NIH/NIDCD grant P30-DC05188.

PS 704

Single Injection of Antisense Oligonucleotides Rescues Peripheral Vestibular Function in USH1C Mouse Model

Michelle Hastings[1]; Frederic Depreux[1]; Francine Jodelka[1]; Jennifer Lentz[2]; Frank Rigo[3]; Sarath Vijayakumar[4]; Timothy Jones[4]
[1]Rosalind Franklin University of Medicine and Science; [2]Louisiana State University Health Sciences Center; [3]Isis Pharmaceuticals; [4]University of Nebraska-Lincoln

Usher syndrome 1C (USH1C) is associated with profound auditory and vestibular dysfunction. Recent reports (Lentz et al., (2013) *Nature Med*. 19: 345-350) describe dramatic improvements in auditory function and behaviors in USH1C (harmonin) mice following a single systemic administration of a strategically designed antisense oligonucleotide (ASO) designated ASO-29. To further these findings, we sought to better our understanding of the improvements in circling and head-tossing behavior with ASO-29 treatment by directly assessing vestibular function. Vestibular sensory evoked potentials (VsEPs) were used to measure vestibular function directly in ASO-treated mice homozygous for *Ush1c* c.216G>A (216A) as well as mice heterozygous for the variant (WT/216A). Neonatal mice were administered the designed test ASO (i.p. injection) or a control ASO sequence of equal length on day P3, P4 or P5. Four treatment groups resulted: homozygous mutant + control ASO (MC, n = 9), homozygous mutant + ASO-29 (M29, n = 10), heterozygote + control ASO (HC, n = 10) and heterozygote + ASO-29 (H29, n = 10). VsEP measurements were completed at three to five months-of-age (anesthesia: ketamine/xylazine). VsEP latencies (P1, N1), amplitudes (P1-N1) and thresholds were measured. All homozygous mutants receiving control ASO (MS) had absent VsEPs. In contrast all homozygous mutants receiving test ASO-29 (M29) had VsEP responses. Heterozygotes regardless of ASO treatment (HC and H29) had normal VsEPs. Recovery of vestibular function in rescued animals (M29), although dramatic, was not complete. M29 animals had moderately elevated thresholds ($p < 0.001$), prolonged latencies ($p < 0.001$) and reduced amplitudes ($p = 0.001$). There was sufficient recovery to support normal balance behaviors as reported previously. These findings provide the first direct evidence for the rescue of peripheral vestibular function in a mouse model of USH1C.

Funding
Funding: NIH R01 DC012596 (MLH & JJL), Nebraska Tobacco Settlement Biomedical Research Foundation and the Department of Special Education and Communication Disorders, UNL (TAJ)

PS 705

Temporal Discretization Inherent to Continuous Interleaved Sampling Stimulation Causes Negligible Effects on Vestibulo-Ocular Reflex Responses Elicited in Rhesus Monkeys

Peter Boutros; Nic Valentin; Dale Roberts; Kristin Hageman; Chenkai Dai; Charles Della Santina
Johns Hopkins School of Medicine

Background
Stimulation of surviving vestibular afferent neurons can partially restore the angular vestibulo-ocular reflex (aVOR) in animals and humans with profound bilateral vestibular hypofunction (BVH). A common strategy to encode velocity of head rotations is to stimulate vestibular afferents with biphasic current pulses that are pulse frequency modulated (PFM) according to a smooth head velocity-to-pulse frequency mapping. To translate this technique into a commercially viable treatment for BVH, it would be advantageous to use existing cochlear implant (CI) stimulators. Moreover, if the vestibular implant (VI) portion of a combined VI/CI only requires a subset of the stimulator's electrodes, then the remaining electrodes could be implanted in the cochlea and used for hearing restoration. Integrating a PFM-based VI and CI using continuous interleaved sampling (CIS) creates a tradeoff, because temporal discretization inherent to CIS interferes with smooth modulation of pulse frequency. This study investigated the effect of temporal PFM discretization errors on the electrically evoked aVOR.

Methods
One rhesus macaque with BVH due to gentamicin ototoxicity was tested using both a smooth PFM mapping (sPFM) and a mapping corrupted by temporal discretization errors (dPFM) that typify errors that would occur in a VI/CI using CIS. Biphasic current pulses were delivered to individual branches of the left vestibular nerve at varying pulse frequencies to encode virtual sinusoid head motions with peak velocities of 50-400°/s and frequencies of 0.1-5Hz. Responses were assayed using the 3D scleral search coil technique. Stimuli were delivered using a Med El Pulsar CI100 stimulator interfaced with Research Interface Box hardware developed at the University of Innsbruck.

Results
The ratio of aVOR gains produced using each mapping was used in a t-test with the null hypothesis that these ratios come from a distribution with a mean of 1 (i.e., the gains for both mappings were equivalent). The t-test indicated that the null hypothesis could not be rejected at a 5% significance level, suggesting there was no significant difference between VOR gains produced using the sPFM and dPFM mappings ($p=0.233$, CI=[0.893,1.026]).

Conclusions
Temporal discretization errors in stimuli using the dPFM protocol produced negligible effects on the gain of evoked eye movements. This result shows that approximating pulse-frequency modulation of prosthetic vestibular stimuli may not require temporal resolution more precise than what is available within the constraints of a CI running a CIS stimulation protocol on non-vestibular electrodes. This finding provides solid support for development of VI/CIs using minimally-modified stimulator circuitry.

Funding
This work was supported by NIH-R01DC9255. PJB was supported by NIDCD 2T32DC000023-31 through the Johns Hopkins Center for Hearing & Balance.

PS 705A

Characterization of Normal 3D Binocular Chinchilla Otolith-Ocular Reflexes as a Metric to Study Otolith Stimulation using a Multichannel Vestibular Prosthesis

Kristin Hageman; Margaret Chow; Dale Roberts; Pengyu Ren; Peter Boutros; Chenkai Dai; Charles Della Santina
Johns Hopkins University

Background
Research toward a multichannel vestibular prosthesis intended to treat individuals disabled by bilateral vestibular hypofunction has focused on restoring the sensation of rotational motion and angular vestibulo-ocular reflex (aVOR) via stimulation of semicircular canals. Prosthetic stimulation of the utricle and saccule, which normally sense gravitoinertial acceleration, has been relatively unexplored, in part because of challenges posed by their anatomy and relatively small reflexive eye movements. To establish benchmarks against which to compare prosthetically-evoked responses, we characterized 3D binocular otolith-ocular responses (OORs) in normal chinchillas during whole-body translation and static tilt using a new ultra-low noise scleral coil system we developed.

Methods
Normal adult chinchillas were fit with a head post and binocular dual scleral search coils. A 6 degree-of-freedom motion platform was used to perform whole-body translations and tilts in darkness with motion profiles including: (1) 0.1-3 Hz sinusoids at peak acceleration 0.05-3 m/s^2 along lateral/interaural, surge/naso-occipital and heave/supero-inferior axes; (2) 1 Hz, 1-2 m/s^2 peak acceleration sinusoids along oblique angle trajectories within the horizontal and vertical planes; and (3) static tilts from 0-60°.

Results
Coil system noise was reduced to <0.05° from the prior system's 0.63° RMS, allowing detection of previously undetectable OOR responses. Translational VOR eye movements were small (~0.3°-2°) and varied in direction depending on stimulus direction. Sinusoidal movements along the lateral axis produced conjugate eye rotations primarily about the roll axis, while surge produced disconjugate eye rotations approximately aligned with the pitch axis. Movements along oblique angle trajectories in the horizontal plane produced eye rotations about axes between roll and pitch. Responses to heave were highly variable. Static tilts elicited appropriately directed ocular counter-roll with magnitudes similar to those previously reported.

Conclusion
These results demonstrate that 3D OORs of normal chinchillas are small compared to aVOR responses but detectable above the noise floor of our new scleral coil system. In contrast to aVOR responses, which are approximately conjugate and approximately coaxial with head rotation in 3D, OOR responses exhibit a more complex relationship between stimulus and response direction in 3D. Whether OORs comprise a linear, reversible one-to-one mapping from 3D head movement to 3D eye movement, as is approximately the case for the 3D aVOR, is unclear. If they do not, then that will complicate attempts to use prosthetically-evoked OOR responses to infer patterns of nerve activity elicited by prosthetic electrical stimulation.

Funding
This work was supported by NIH-R01DC9255. KNH was supported by NIDCD 2T32DC000023-31 through the Johns Hopkins Center for Hearing & Balance.

PS 706

The role of GABAergic mechanisms in the vestibular oculomotor system in mice

Naoki Shimizu[1]; Scott Wood[2]; Adrian Perachio[1]; Tomoko Makishima[1]
[1]University of Texas Medical Branch; [2]Azusa Pacific University

Background
Systemic administration of a gamma-amino butyric acid (GABA) type B receptor agonist, baclofen, affects various physiological and psychological processes. In the past, the effects on oculomotor system have been well characterized in primates. In humans, baclofen specifically suppresses the high-order vestibular processes, also known as the velocity storage mechanism (VSM) along with the level of motion sickness susceptibility. However, these effects in mice have not been explored so far. Thus we investigated the effects of baclofen on vestibular-related eye movements focusing on the VSM.

Methods
Drug naïve C57BL/6J male mice were used. Other experimental conditions (dosage, routes and onset of recording) were matched with the prior behavioral studies exploring the effects of baclofen in mice. Two rotational paradigms, sinusoidal rotation and counter rotation were employed to stimulate semicircular canals and otolith organs in the inner ear, respectively.

Results
Similar to previous studies during off-vertical axis rotation, there were two components in the steady state eye movement during counter rotation: 1) horizontal nystagmus,

and 2) modulatory eye movements. Each response is considered to be generated by two different neural circuitries; for the horizontal nystagmus, the VSM is responsible. While modulation components arise through tilt VOR pathway. Baclofen significantly reduced the horizontal nystagmus and angular VOR phase with increase in dosage but not modulation components and angular VOR gain.

Conclusions
Vestibular evoked eye movements are largely dissected into two neural circuits in the brain: those composed of simple and direct pathways represented by three-neuron arcs, and those shaping the VSM. The later indirect and multimodal central processes play an important role in self-motion perception and spatial orientation integrating canal and otolith information together with visual and proprioceptive inputs. Here, we revealed that there was a clear distinction in the drug sensitivity showing different involvement of GABA transmission system in the oculomotor pathway in mice. The data corresponded to the previous observations in nodulectomized mice. These findings were consistent with the studies in primates, suggesting a well-conserved nature of GABAergic mechanism in the vestibular oculomotor pathways across lateral-eyed and frontal-eyed animals.

Funding
NIH grant K08DC011540

PS 707

A Fish Larva Vestibulo-ocular Reflex test system with preliminary data

Fangyi Chen; Peng Sun
South University of Science & Technology of China

Zebra fish has been a successful animal model for gene and drug screening. In auditory system, due to its sensitivity to the ototoxicity, zebra fish has certain superior advantage over mouse model in auditory drug screening. An instrument was developed to quantify the vestibulo-ocular-reflex (VOR) of larva zebra fish. Since the vestibular and auditory system shares the same sensory cell, inner hair cell, the study of the VOR function can reflect the hair cell functionality. Therefore, VOR test has been used to evaluate the development of the auditory and vestibular system in fish, frog and other species, where a direct test of the hearing capability is difficult. Many attempts have been made in different labs to build fish VOR test apparatus. However, problems exist in apparatus to hold the fish during the test and image analysis on videos with imperfect illumination. Based on a previous design (Mo et. al., 2010), an improved zebra fish VOR test system was developed to tackle those technical difficulties and produced more reliable results. Rather than simply gluing the fish larva on a cover glass, a plastic fish holder was designed to tightly hold the fish body but also have space for the fish head to move freely. A new algorithm was developed to address the problem that imperfect illumination produces shadows on the fish eye area, which results in false identification. Mechanical and optical systems were redesigned to produce a more compact and stable test system. Preliminary test on zebra fish larva showed that the system had reliably produced VOR results. More tests on zebra fish with gene defects are in progress.

Funding
NSFC 81470701 to F.C

PS 708

Dose-dependent vestibulo-ocular reflex responses and lateral semi-circular canal abnormalities in a mouse model of pendrin deficiency

Yong-Hwi An[1]; Seung Ha Oh[1]; Jun Ho Lee[1]; Ja-Won Koo[2]; Gyu Cheol Han[3]; Byung Yoon Choi[2]
[1]Eulji Medical Center, Eulji University; [2]Seoul National University Bundang Hospital; [3]Gachon University of Medicine and Science, Graduate School of Medicine

Pendrin, encoded by *SLC26A4* gene, is an anion exchanger expressed in the epithelial cells of inner ear. In the absence of pendrin, hearing loss associated with enlarged vestibular aqueduct is observed simultaneously with dizziness and postural imbalance. In this study, we report the quantitative responses of vestibular ocular reflex and anatomical abnormalities of the lateral semicircular canal in pendrin deficient mice strain composed of three distinct genetic conditions; homozygous knockout mice, transgenic mice with doxycycline-inducible expression of *Slc26a4*, and heterozygotes. Hearing and balancing systems were evaluated by auditory brainstem response, rotation test, behavioral observation and histology of the lateral canal. All *Slc26a4* homozygous knockout mice showed total deafness whereas the others had normal hearing, indicating all-or-none phenotype of auditory function. Rotation test exhibited minimal vestibular ocular reflex responses of homozygotes and intermediate responses of heterozygotes and transgenic mice compared to normal controls, implying a pendrin dose-dependent pattern of vestibular dysfunction. Vacuolar replacement and absence of calretinin expression of vestibular hair cells in the lateral canal from homozygotes, but no apparent difference in inner ear architectures among wild-type, heterozygous and transgenic mice were identified. These results suggested that mutations of *SLC26A4* gene in mouse models induce diverse functional deficits of lateral semicircular canals and vestibular diseases with variable manifestations unlike cochlea.

Funding
This research was supported by Basic Science Research Program through the National Research Foundation of Korea (NRF) funded by the Ministry of Education, Science and Technology (2011-0023304 to Choi BY)

PS 709

Vestibular Pathophysiology: Mechanisms and Markers

Raphaelle Cassel[1]; Pierrick Bordiga[1]; Stéphane Besnard[2]; Matthieu Beraneck[3]; Pierre-Paul Vidal[3]; Brahim Tighilet[1]; Christian Chabbert[1]
[1]Aix-Marseille Université; [2]INSERM U1075 Caen; [3]UMR 8119 CNRS Université Paris Descartes

Vestibular pathologies are characterized by unpredictable episodes of vertigo accompanied by postural imbalances and loss of gaze fixation during movement. They are often accompanied by dizziness and nausea. These pathologies can be highly disabling. When recurrent, they may conduct to psychological and social isolation. Because of their high prevalence, vestibular disorders constitute a significant burden to our health care system. Therapeutic solutions to these pathologies lack specificity and efficacy. This relies both on the lack of knowledge of the pathophysiological mechanisms underlying different vestibular disorders and on the lack of biomarkers to discriminate vestibular impairments and properly direct therapeutic approaches. The present project called VERTIDIAG was designed to associate several French research teams expert in the study of vestibular physiology and pathophysiology and displaying multidisciplinary approaches to decipher how a vestibular insult develops into the inner ear and how it governs the heterogeneity of the vertigo symptoms. In turn it ambitions to identify specific biomarkers of the different types and stages of acquired vestibular disorders. The project is based on the development of original animal models of vestibular disorders encountered in human and on the full exploration of the sequence of histological and functional alterations that occur over a one week alter the insult initiation, period that recapitulate the main vertigo symptoms encountered both in human and animal models. Collected data will be used to establish a grid of correlation between etiology and symptomology of vestibular disorders. To ensure best applicability to human pathology, the different stages of the project and exploitation of results will be systematically validated by a board of clinicians expert in human vestibular symptoms. First data will be presented at the meeting.

Funding
AMIDEX FUND - MARSEILLE FRANCE

PS 710

Intra-tympanic Isosorbide for the Treatment of Acute Attack of Endolymphatic Hydrops

Minbum Kim[1], Jae-Hyun Seo[2]
[1]Catholic Kwandong University; [2]The Catholic University of Korea

Objectives
The aims of this study was to investigate the effect of intra-tympanic isosorbide (IT-ISB) on vestibular function at the acute attack model of endolymphatic hydrops

Methods
Forty male guinea pigs were used. Ablation of endolymphatic sac (ES) was performed via suboccipital approach. For the acute attack model, Desmopressin (AVP, 100ug/Kg, SC) was injected 4weeks after ES ablation. For the chronic model, we waited 12 weeks after ES ablation. The change of endolymphatic hydrops was observed in histologic sections. ABR threshold was measured with TDT system, and vestibular function was evaluated with animal rotator. In both models, we compared vestibular function before and after IT-ISB

Results
In chronic disease model, the change of vestibular function was insignificant after IT-ISB, although hydrops was histologically improved. However, symmetry of vestibular function was recovered after IT-ISB in acute attack model, and hydrops was not induced by Desmopressin

Conclusion
After IT-ISB, the improvement of hydrops was observed at the acute attack model as well as chronic model, and the recovery of symmetric vestibular function was observed at the acute attack model. IT-ISB could be a treatment option for the acute attack of Meniere's disease.

Funding
This work was supported by the Basic Science Research Program through the National Research Foundation of Korea, funded by the Ministry of Science, ICT and Future Planning (NRF-2013R1A1A1075990).

PS 712

Longitudinal Efficacy and Impedance Change of Vestibular Prosthesis Electrodes

Chenkai Dai; JoongHo Ahn; Pengyu Ren; Kristin Hageman; Mehdi Rahman; Gene Fridman; Charles Della Santina
Johns Hopkins University

Background
Maximizing the selectivity and efficacy of vestibular nerve branch stimulation is a key goal in development of a multichannel vestibular prosthesis (MVP) intended to restore sensation of 3-dimensional (3D) head movement in individuals disabled by chronic bilateral loss of labyrinthine hair cell function. Long term electrochemical and functional stability of electrodes is essential to achieving this goal. In this study, we evaluated electrode stability by measuring the efficacy of electrical stimulation and impedance for different electrodes in rhesus monkeys over time.

Methods
Electrode arrays were implanted in each semicircular canal in four rhesus monkeys. Vestibular electrically-evoked compound action potentials (eCAPs), 3D vestibulo-ocular reflex (VOR) responses to electrical stimulation, and impedance were measured for each of the implanted electrodes over a time period up to 60 months.

Results
Findings suggest that eCAPs and electrode impedance can remain largely stable for many months after implantation. VOR responses to electrical stimulation remained at similar

initial level and were strongly correlated to eCAPs measured from the same electrode.

Conclusions
MVP electrodes remain stable and effective for long periods of use in nonhuman primates and are likely to exhibit similar long-term stability in humans.

Funding
Funding: NIH-R01DC9255

PS 713

Noisy Galvanic Vestibular Stimulation Provides Sustained Improvement of Body Balance

Chisato Fujimoto; Shinichi Iwasaki; Teru Kamogashira; Makoto Kinoshita; Naoya Egami; Yukari Uemura; Fumiharu Togo; Yoshiharu Yamamoto; Tatsuya Yamasoba
The University of Tokyo

Background
Our group previously reported that most of healthy subjects and patients with bilateral vestibulopathy had imperceptive optimal level of amplitude in noisy galvanic vestibular stimulation (noisy GVS) for 30sec in improving postural stability. However, sustained effect of noisy GVS on improvement of body balance in healthy subjects remains unclear.

Method
Thirty healthy subjects (mean age, 67.0 (± 1.7) years) were recruited. Two experimental sessions, separated by an interval of 7 days according to a cross-over design, were performed. In Session 1, subjects received noisy GVS at their optimal intensity for 30 min twice at 4 h interval, and postural stability was measured after each noisy GVS for 4 h. In Session 2, subjects received noisy GVS at their optimal intensity for 3 h and were monitored without stimuli for 4 h, and postural stability was measured during and after noisy GVS. For each session, posturography was administered with eyes closed on the foam rubber. Normalized ratio (NR) was defined as the ratio of the value of the parameter at the measurement point to that at the baseline. The order of sessions was randomly determined.

Results
In the NRs of the mean velocity (velocity), the envelopment area (area), and the root mean square (RMS) of the center of pressure distance, ameliorating effects on body balance after the cessation of noisy GVS were observed in both Session 1 and Session 2. These aftereffects were strongly observed until 2 h after the cessation and became weaker when 2 h after the cessation was passed. In these 3 parameters, the NRs at 4 h after the cessation of the stimulus of Session 2 were not significantly different than those of the first stimulus of Session 1. In Session 1, further improvement of NRs by the second stimulation over the first stimulation was moderate. However, the second stimulation tended to promote the sustainability of the improvement on body balance. The improvement of NRs at the second post-stimulation period became stronger between 2 h and 3 h after the cessation of the second GVS, and was sufficient until 4 h after the cessation in all the 3 parameters.

Conclusion
Noisy GVS had both post-stimulation and cumulative effects on improvement of body balance.

Research Funding
Ministry of Education, Culture and Technology (25293347; 15K15616) and Ministry of Health, Labor and Welfare (H27-Kankakuki-Ippan-003) of Japan.

PS 714

The Study On Functional Connection Between Locus Coeruleus And Vestibular Nuclei

Jing Wang; Chunfu Dai
Fudan University

Background
The comorbidity of peripheral vertigo and anxiety disorder is very common in the clinical practice, vestibular dysfunction has interaction and influence with anxiety. Locus coeruleus (LC) is one of the most important nuclei mediated anxiety, LC and vestibular nuclei are closely related on the structure. Whether and how the anxious behavior and balance function changed in vestibular damaged mouse after LC intervention?

Method
1) To make LC damaged mouse model, we injected 6 hydroxy dopamine to the right LC and injected saline to the left LC. We observed the damaged effects in different stereotaxic coordinates by means of tyrosine hydroxylase staining 2 weeks later. 2) We injected adeno-associated virus vectors carrying design receptor hM3Dq to the right LC to make LC activated mouse model and activated LC through clozapine-N-oxide (CNO) intraperitoneal injection after 3 to 4 weeks, then observed the active effects of the nuclei through the c-fos staining technology. 3) We detected the anxious behavior and balance function in gentamicin (GT) injected mice after LC intervention and compared with the control group through Elevated plus-maze (EPM), Open-field test (OFT), Light-dark test (LDT) and Rotarod test (RT).

Results
1) The LC damage effects was optimal in coordinates: AP-5.5mm, ML±0.9mm, DV-3.4mm. 2) We saw a large number of black staining nucleus, namely the activated LC neurons, in the virus injection side, and the saline side had no obvious activated LC neurons. 3) EPM proved that the residence time of open arm in GT and GT+LC activated groups were markedly lower than the control group ($p<0.01$), there was statistically difference between GT+LC damaged group and the control group ($0.01<p<0.05$). OFT proved that there were significant differences between GT, GT+LC damaged, GT+LC activated groups and the control group ($p<0.01$). LDT proved that there was statistically difference between GT group and GT+LC damaged group ($0.01<p<0.05$). RT proved that there was no statistically difference in the latency of drop the stick between GT group and GT+LC activated group ($p>0.05$).

Conclusion
This study confirms that LC is closely related to the anxiety caused by the vestibular damage. Damage LC can dramatically reduce the anxiety in vestibular damage mice. The reduce of anxiety can affect the balance function, damage LC can significantly improve the balance ability in the vestibular damage mice, but can't reach the normal level. Activate LC in a short period of time have no significant impact on the balance because they have no cumulative effects.

Funding
This study was supported by 973 project (2011CB504504 [C. F. D]) and National Natural Science Foundation (No. 81070785, 81170909 [C. F. D.]).

PS 715

Cardiorespiratory Responses Induced by Primary Blast Exposure via the Ear Canal in Rats

David Sandlin[1]; Chunming Zhang[2]; John Lippincott[1]; Yue Yu[1]; Courtney Stewart[1]; Jun Huang[1]; Erin Peeden[1]; Hong Zhu[1]; Wu Zhou[1]
[1]University of Mississippi Medical Center; [2]First Affiliated Hospital, Shanxi Medical University

Background
Blast overpressure, such as that produced by explosive devices, is a frequent cause of injury in both military and civilian populations. Primary blast, i.e., the overpressure effect of the blast alone, is believed to cause blast-induced neurotrauma (BINT) through mechanisms such as skull flexion and pressure transmission from the thorax through the great vessels of the neck. However, the ear's role in the mechanisms of primary blast injury remains to be elucidated. We hypothesize that the unprotected ear provides a conduit through which primary blast impacts the brain and results in BINT. To test this hypothesis, we have developed a novel, tabletop blast generator that reliably delivers blast waves exclusively into the ear canal of rats. Using this new model, we examined the effects of primary blast exposure on cardiorespiratory responses in anesthetized rats.

Method
Male Sprague-Dawley rats were anesthetized under isoflurane. The left femoral artery was catheterized for blood pressure monitoring, a piezo-transducer was adhered to the chest to monitor breathing effort, and electrodes were placed subcutaneously to monitor ECG Lead II. A speculum was fixed in the left ear canal; patency was confirmed by otoscope. Baseline recordings of the above parameters were recorded for one minute. Blasts of pressures ranging from 10psi to 300psi were then delivered to the left ear canal, and vital signs were continuously recorded for 5 minutes post-blast. Control rats underwent the same procedures with blast pressure of 0psi.

Results
Exposure to overpressures of 50psi and above resulted in immediate cessation of breathing. However, exposure to overpressures below 50psi resulted in a transient increase in respiratory rate (32% increase) that returned to baseline after ~75 seconds. Exposure to blast overpressures resulted in decreases in heart rate ranging from 72% to 9%, where higher blast pressures caused greater decreases in heart rate. Exposure to blast overpressures also resulted in a drop in blood pressure as great as 30%. PR interval was increased in blast-exposed rats, suggesting a vagal response.

Conclusions
These preliminary data suggest the unprotected ear canal is a potential vulnerability for primary blast overpressure to cause BINT. Drops in blood pressure such as those seen in the present study may result in "blackout" or syncope, symptoms that would impair an individual's ability to seek safety. Ongoing studies employ this animal model to further characterize the ear's role in the acute and chronic effects of primary blast-induced neurotrauma.

Funding
NIH/NIDCD R01DC014930-01 Zhou (PI) 9/01/15-08/30/17 NIH/NEI R21EY025550-01 Zhou (PI) 02/01/15-01/31/20 NIH R01 DC012060-01 Zhu (PI) 5/01/12-04/30/17 NASA UM Subcontract Number 13-07-001 Zhou (PI) 09/01/12-08/31/15

PS 716

Mild Blast Wave Exposure Produces Intensity-dependent Changes in MMP2 Expression Patches in Rat Brains.

Takaki Inui[1]; Carey Balaban[2]
[1]Osaka Medical College; [2]University of Pittsburgh

Background
The prevalence of improvised explosive devices in warfare and terrorism has created unprecedented levels of blast-related traumatic brain injury (bTBI). Mild bTBI can sustain various symptoms, such as tinnitus, hearing loss, post-traumatic balance disorders, and migrainous disorders without overt histological and radiological findings. The etiology of bTBI is poorly understood. This study builds on findings that low level blast overpressure (BOP) exposures initiate gene expression for brain microvascular remodeling in rats. Intravenous coagulation and small venous hemorrhages are prevalent in the inner ear and subarachnoid space. Several authors reported upregulated matrix metalloproteinases (MMPs) in mild bTBI rodent models. This analyzed the MMP2 expression pattern in rat brains after mild (2.7-7.9 psi) or moderate (13-17.5 psi) BOP exposure.

Method
Adult female Sprague-Dawley rats were exposed to single BOP in a dedicated compression chamber under general anesthesia. Brains were harvested at 2, 24 and 72 hours after BOP, and immunopositive MMP2 expression was examined in histological horizontal sections of decalcified heads. The number of the MMP2 positive puncta were counted in cerebrum, brainstem and cerebellum, and were analyzed quantitatively with Metamorph software operating on an optical microscope.

Results

There were no significant changes in the numbers of MMP2-immunopositive patches as a function of post-BOP time in the brainstem, cerebellum or cerebrum. However, differences emerged across brain regions, BOP level and time in (1) the area occupied by immunopositive pixels, (2) the average intensity in a patch and (3) the standard deviation of intensity in a patch. Two hours after BOP, positive pixel areas were larger and more homogeneous in both BOP groups. They decreased in size at 24 hours, then increased in size markedly in the moderate group at 72 hours. Within 72 hours after mild BOP, the within-patch variability resembled normal patches in sham rats.

Conclusions

The MMP2 puncta show graded changes in size and staining intensity after mild and moderate BOP exposure. This pattern is consistent with remodeling responses to coagulation and mild hemorrhage. These neurovascular changes in vestibular and auditory networks may contribute to the neurosensory sequelae of mild bTBI.

SYMP 67

Hyperacusis from the patients and clinicians perspective

Richard Tyler; Brian Pollard
University of Iowa

Hyperacusis is an abnormal, excessive response to sound. There are several types of hyperacusis. In **loudness hyperacusis**, sounds are louder than they would be for normal listener. In **annoyance hyperacusis**, specific sounds become very annoying. In **fear hyperacusis**, patients develop a fear of some situations and often avoid them. In **pain hyperacusis**, certain sounds, even at moderate loudness levels, evoke pain. For example, the clanging of dishes or a passing emergency siren can initiate a pain cycle which may last for hours or days. Hyperacusis is often, but not always, present with hearing loss and/or tinnitus. Primary functions affected include thoughts and emotions, sleep and concentration. A variety of different causes have been identified (e.g. traumatic noise exposure and head and neck injuries, Williams Syndrome, Lyme Disease), but many are unknown. Loudness hyperacusis can be measured directly, and questionnaires are available for annoyance, fear and pain. A variety of symptoms often co-exist. Clearly, as in tinnitus, there are many subtypes of hyperacusis. At present, there are no cures. Counseling and sound therapy can be helpful for many. Counseling (e.g. Hyperacusis Activity Treatment) includes reviews of mechanisms, and strategies to help with sleep and concentration). Sound therapies use wearable partial masking devices providing a variety of background low-level sounds. Understanding individual differences and co-existing symptoms will be an important step to finding cures. A day in the life of a hyperacusis patient will be reviewed!

SYMP 68

The cochlear nerve: type I vs. type II neurons and the phenomenon of hyperacusis

M. Charles Liberman
Harvard Medical School

Cochlear inner and outer hair cells are connected to the brain via a myelinated (Type I) and an unmyelinated (Type II) sensory pathway, respectively. Since the type-II fibers are not only small in caliber, but few in number, their physiological responses have proven difficult to characterize in vivo. Nevertheless, aspects of their neuroanatomy have long suggested that the type-II fibers may be involved in the sensation of auditory pain. This talk will summarize what is known about the peripheral connections and central projections of the type-I vs type-II neurons, and what those data suggests about the relevance of the two pathways to the phenomenon of hyperacusis.

SYMP 69

Auditory nociception, the detection of sounds harmful to the inner ear, is mediated by a non-canonical form of communication from cochlea to brain

Jaime García-Añoveros
Northwestern University

Background

Although cochlear hair cells are specialized for detecting sound-induced vibration, intense and persistent noise will damage and ultimately destroy them [1]. Throughout most of the body, nociceptors of the dorsal root and trigeminal ganglia detect tissue damage (or the physical stimuli causing it) of this sort. However, somatosensory neurons do not innervate the organ of Corti, raising the question of whether its damage goes undetected or whether the cochlea has an alternative, nociceptor-like mechanism. The only sensory neurons innervating the organ of Corti originate from the spiral ganglion, roughly 95% of which innervate exclusively inner hair cells (IHCs). Upon sound stimulation, IHCs release glutamate to activate AMPA-type receptors on these myelinated type-I neurons, which carry the neuronal signals to the cochlear nucleus. The remaining spiral ganglion cells (type IIs) are unmyelinated and contact OHCs. Their function is unknown.

Methods

Using immunoreactivity to cFos, we documented neuronal activation in the brainstem of *Vglut3*$^{-/-}$ mice, in which the canonical auditory pathway (activation of type-I afferents by glutamate released from inner hair cells) is silenced. We exposed *Vglut3*$^{-/-}$ mice (and control *Vglut3*$^{+/+}$ littermates) to ambient, innocuous (80dB), or noxious (120dB) noise, generated cytocochleograms to assess hair cell ablation, and then measured neuronal activity in the cochlear nucleus and other brainstem areas. We also treated similarly CD1 mice at 8 months (with degenerated cochleae but intact vestibular and somatosensory function) and, as control, at 2 months (prior to cochlear degeneration).

Results

In *Vglut3*$^{-/-}$ mice, we found responses to noxious noise, which damages hair cells, but not to innocuous noise, by neurons of the cochlear nucleus, but not in the vestibular or trigeminal nuclei. Noxious noise activated neurons in cochlear nucleus in a pattern consistent with the innervation of type II afferents. The response to noxious noise response originates in the cochlea and not in other areas also stimulated by intense noise (middle ear and vestibule) as it was absent in CD1 mice with selective cochlear degeneration but normal vestibular and somatosensory function.

Conclusions

These data imply the existence of an alternative neuronal pathway from cochlea to brainstem that is activated by tissue-damaging noise and does not require glutamate release from IHCs. This detection of noise-induced tissue damage, possibly by type-II cochlear afferents, represents a novel form of sensation that we term auditory nociception. Such a sensory system may account for the painful sensation in response to noise reported by patients suffering hyperacusis.

SYMP 70

What is the 'Adequate Stimulus' for Type II Cochlear Afferents?

Paul Fuchs; Chang Liu; Elisabeth Glowatzki
Johns Hopkins University School of Medicine

In the mammalian cochlea, acoustic information is carried to the brain by the predominant (95%) large diameter, myelinated type I afferents, each of which is postsynaptic to a single inner hair cell. The remaining thin, unmyelinated type II afferents extend hundreds of microns along the cochlear duct to contact many outer hair cells, but are insensitive to sound. Intracellular recording from the peripheral process *ex vivo* shows that type II afferents are poorly activated by outer hair cell transmitter release. Outer hair cell ribbon synapses are less organized and release glutamate less efficiently in comparison to ribbons of inner hair cells. However, type II afferents are strongly activated when outer hair cells are damaged. This response depends on both ionotropic (P2X) and metabotropic (P2Y) purinergic receptors, binding ATP released from nearby supporting cells in response to hair cell damage. Selective activation of P2Y receptors (by exogenous UTP) increased type II afferent excitability by the closure of KCNQ-type potassium channels, a potential mechanism for the painful hypersensitivity (hyperacusis) that can accompany hearing loss. Type II afferents may be the cochlea's nociceptors, prompting avoidance of further damage to the irreparable inner ear.

SYMP 71

Auditory versus aural nociception: Evidence for partial overlap of cortical activity in humans

Ulf Baumgaertner[1]; Peter zu Eulenburg[2]; Rolf-Detlef Treede[1]; Andre Rupp[1]
[1]Heidelberg University; [2]Munich Technical University

Background

For most painful sensations it has become evident in the past century that they are due to activation of the nociceptive system and not overstimulation of some other sensory system (e.g. tactile or olfactory). The signalling pathways that mediate pain due to intense auditory stimuli (above 120 dB), however, have not been clarified yet.

Methods

We therefore performed a functional magnetic resonance imaging (fMRI) study comparing painful auditory stimuli, non-painful auditory stimuli, and intensity-matched pin-pricks of the earlobes. Sixteen healthy volunteers (8 female, 8 males) with a mean age of 27 years participated in five separate sessions (2xauditory, 2xpin-prick, 1xsomatosensory). The painful auditory stimulus consisted of a 3.2kHz sine tone presented at a level of 130dBA for the duration of the stimulation block (23s) with irregular interruptions of 1s in order to prevent trauma. The auditory control stimulus with the identical position of silent gaps was presented at a level of 75 dB SPL. For somatic nociceptive stimulation, aural pinprick stimuli were applied to the ventral side of the transition zone from the lobule to the inferior helix using a custom-made clip with a 1cm^2 pin-prick area containing 10 sharp plastic pins. Pain ratings to auditory (64/100 ± 3, mean ± SEM) and pinprick stimuli (70/100 ± 4) were similar. fMRI data were acquired with a 1.5 T scanner using echo-planar imaging with a T2*-weighted sequence (TR= 3.3s, TE= 60ms, voxel size= 3x3x4mm) in an experimental standard block design. Analysis was performed with statistical parametric mapping (spm8) in an individually calculated structural reference frame (DARTEL).

Results

Conjunction analysis of painful and non-painful auditory stimuli showed activation of primary and secondary auditory cortex. Subtraction analysis of painful vs. non-painful auditory stimuli showed activation of inferior parietal lobule, supramarginal gyrus, right anterior insula and ventral thalamus. Conjunction analysis of painful auditory and pinprick stimuli showed activation of supramarginal and postcentral gyrus, inferior parietal lobule, rolandic operculum and left posterior insula, i.e. regions considered to be part of the nociceptive network in the brain. The strongest activation was seen in Brodmann area 40, which is equivalent to monkey 7b, where previously nociceptive and visual convergence was described.

Conclusions

These data show activation of the nociceptive network by painful auditory stimuli, but the spatial pattern differed from that induced by somatosensory painful stimulation, suggesting convergent processing of nociceptive and auditory stimuli.

Supported by Deutsche Forschungsgemeinschaft; DFG SFB1158-B05

SYMP 72

The biology of neuropathic pain

Allan Basbaum
University California San Francisco

Neuropathic pain arises from injury to the peripheral or central nervous system and is characterized by ongoing pain and mechanical and thermal (often cold) hypersensitivity (allodynia and hyperalgesia). As local anesthetics are remarkably effective in producing at least temporary relief in many peripheral injury-induced neuropathic pain conditions, attention has focused on regulation of the afferent. Importantly, the primary afferent nociceptor expresses a host of molecules that are not found or are only minimally expressed elsewhere in the CNS. Central sensitization of spinal cord pain processing circuits also occurs after injury. Indeed, NMDA-mediated central sensitization is manifest as increased ongoing activity of dorsal horn pain transmission circuits and their responsiveness to normally innocuous stimulation. The behavioral manifestation of these changes is ongoing pain, allodynia and hyperalgesia. Unfortunately, the widespread expression of the NMDA receptor limited the development of selective antagonists, because of adverse side effects. We take the view that neuropathic pain is an epileptic-like condition resulting from reduced GABAergic inhibitory controls in the dorsal horn of the spinal cord. Consistent with this hypothesis, of course, is the fact that anticonvulsants are among the most effective, or at least the most common, pharmacological approaches to treat neuropathic pain.

An alternative approach to reducing these pathophysiological consequences of injury is to re-establish the inhibitory tone lost in the setting of nerve injury. In recent studies, we have demonstrated that it is possible to restore inhibitory tone by transplanting GABAergic precursor neurons derived from the embryonic cortex into the spinal cord of nerve-injured mice. These precursor neurons develop in the spinal cord, differentiate into GABAergic interneurons and integrate into the host circuitry. Most importantly, peripheral nerve injury-induced mechanical hypersensitivity in a peripheral nerve injury model of neuropathic pain can be completely normalized, within weeks of the transplantation. The approach is also effective in the management of chemotherapy-induced mechanical and thermal (heat) hypersensitivity. With a view to translating these preclinical findings to patients, we have now initiated studies using human pluripotent stem cells modified to assume the properties of GABAergic neurons. Preliminary studies indicate that these cells have the capacity to integrate and influence host circuits. Taken together these studies suggest that a therapy targeted at treating the “disease” of neuropathic pain, namely the pathophysiological alterations in CNS function that are characteristic of this condition, is a viable and novel approach to the management of neuropathic pain.

PD 107

Basilar Membrane and Reticular Lamina Vibrations in Sensitive Mouse Cochleae

Tianying Ren; Wenxuan He
Oregon Health & Science University

Background

Remarkable sensitivity and exceptional frequency selectivity of mammalian hearing depend on a functional cochlear feedback, which uses the outer hair cell-generated force to boost the cochlear partition vibration. The mechanism of how the cochlear feedback works, however, remains largely unknown.

Methods

Young CBA/CaJ mice with normal hearing were used in this study. After the cochlea was surgically exposed, the cochlear partition at the basal turn was visualized through the intact round window membrane. The magnitude and phase of the basilar membrane and reticular lamina vibrations were measured using a custom-built heterodyne low-coherence interferometer at different sound levels and frequencies. The malleus vibration was also measured for estimating transfer functions of the basilar membrane and reticular lamina vibrations. Magnitude and phase relationships between the reticular lamina and basilar membrane vibrations were determined by the ratio of the vibration magnitude of the reticular lamina to that of the basilar membrane and phase difference between the two structures.

Results

The reticular lamina vibration was significantly larger than the basilar membrane vibration not only at the best frequency but also at low frequencies. The phase of the reticular lamina vibration was different from the basilar membrane phase by ~180 degree at very low frequencies, and this difference decreased with frequency and approached zero near the best frequency. The reticular lamina vibration was more sensitive and nonlinear than the basilar membrane vibration. In addition to loss of the sensitivity and nonlinearity, magnitude and phase differences between the reticular lamina and basilar membrane vibration disappeared in postmortem cochleae.

Conclusion

The current results indicate that outer hair cells over the entire region from the base to the best-frequency location can drive cochlear microstructures. Outer hair cells attenuate the cochlear partition vibration near the base and enhance it near the best-frequency location.

Funding

Supported by NIH-NIDCD grant R01 DC004554.

PD 108

Tuning Sharpness of the Human Cochlea

Pim Van Dijk[1]; Geoffrey Manley[2]
[1]University of Groningen; [2]Oldenburg University

Background

Controversy rages as to whether the frequency selectivity of the human cochlea is especially sharp (as indicated

by stimulus-frequency emission delay studies) or not (as suggested by most psychoacoustical studies). We have approached this problem using perhaps the most sensitive technique currently possible, the measurement of suppression tuning curves (STC) of spontaneous otoacoustic emissions (SOAE). There are older data on this topic, but only very few STC within a narrow frequency range and these were collected using different criteria.

Methods
We measured 63 STC in 13 human subjects (12♀and 1♂). After initially establishing individual ear thresholds and the SOAE spectra, we assessed suppression levels by presenting a large raster of tonal frequencies and levels. Suppression contours for 3 and 6dB of suppression were extracted from the SOAE responses at all raster points.

Results
SOAE peaks were studied that had frequencies from 0.62 to 10.91 kHz. The STC of SOAE were very sensitive, being centered ± 0 dB with reference to the ear's threshold and on average with a tip at a frequency 4.5% higher than that of the SOAE peak itself. Frequency selectivity of the STC, measured as the Q3dB, varied remarkably little across frequency, with a mean near 8 across all frequencies. These values lie above the Qerb for Macaque auditory-nerve tuning at low frequencies (<1.5kHz), but well below those at high frequencies. In all species for which both auditory-nerve tuning and SOAE-STC selectivity are available (lizards, barn owl, Macaque), these two measures match closely.

Conclusions
Our data do not support suggestions of exceptionally high frequency selectivity in the human cochlea. Instead, they closely resemble values from most human psychoacoustics studies. At frequencies below a few kHz, human selectivity exceeds the means for auditory-nerve tuning for other mammals (cat, guinea pig, macaque), suggesting that there may be a mild specialization in the most important frequency range for communication. At present, however, the biological significance of the modest frequency selectivity of the human cochlea remains speculative.

Funding
Heinsius Houbolt Foundation

PD 109

Effect of Tectorial Membrane Longitudinal Viscoelasticity on Cochlear Stability

Julien Meaud; Thomas Bowling
Georgia Institute of Technology, Atlanta

Recent experiments with the CEACAM16-null mice have shown that genetic mutations that primarily affect the tectorial membrane (TM) tend to enhance the generation of spontaneous otoacoustic emissions (SOAEs). These experiments suggest that the TM plays an important role in maintaining in the stability of the cochlea since SOAEs are commonly assumed to arise due to the presence of linear instabilities in the cochlea. However, several hypotheses have been proposed regarding the effect of the CEACAM16-null mutation on the TM. In this work, we use a computational model of the mammalian cochlea to examine one of these hypotheses. The model is used to investigate the effect of varying the TM longitudinal viscoelasticity on cochlear stability. The effect of varying the TM properties on the number and statistics of linear unstable modes is analyzed by computing the eigenvalues of linearized models. Furthermore, the effect of varying TM properties on the number, statistics and amplitudes of limit cycle oscillations is studied using nonlinear time-domain simulations. Numerical results demonstrate that stability of the cochlea depends on the TM properties and imply that the observation of enhanced SOAEs in CEACAM16-null might be due to a change in the TM longitudinal viscoelasticity.

Funding
This reseach is funded by startup funds from Georgia Tech.

PD 110

Dispersive Properties of the Cochlear Traveling Wave

Marcel van der Heijden; Nigel Cooper
Erasmus MC

Wave propagation in the cochlea was studied by recording basilar membrane (BM) vibration in the 11-19 kHz region of the gerbil cochlea in response to irregularly spaced tone complexes (zwuis). We directly compared amplitude and phase across pairs of BM locations that were longitudinally separated by 80-300 micrometer, constructing "local transfer functions" as introduced by Ren and coworkers. We analyzed how phase velocity and group velocity depend on stimulus frequency and sound pressure level (SPL). Phase velocity decreased monotonically with frequency. The steepness of this decrease varied with SPL, the steepest dependence occurring at low SPLs. With increasing SPL, the phase-velocity versus frequency curves became shallower, often causing the family of curves to pivot around a single fixed point slightly below the characteristic frequency (CF) of the recording location. This pivoting behavior is consistent with a large body of published single-point BM data on phase shifts evoked by suppressors and SPL variations. Unlike phase velocity, group velocity varied non-monotonically with frequency, showing a minimum at a frequency somewhat below CF. This group velocity dip was deepest (falling to 1 m/s) at low SPLs, and became systematically shallower with increasing SPL. At low SPLs, the ratio of phase velocity to group velocity exceeded 10 in some recordings, indicating an extreme degree of wave dispersion. Loss of sensitivity in the course of an experiment invariably caused the low-SPL propagation characteristics to become less dispersive and coincide with the behavior observed at higher SPLs. This observation suggests an intimate link between wave dispersion and the mechanisms underlying sensitivity. The observed propagation characteristics of the traveling wave as captured in dispersion diagrams (frequency versus wavenumber) contradict the basic predictions of the so-called critical layer absorption proposed for the cochlea by Lighthill. In Lighthill's scheme, the wave comes to a complete

standstill when approaching its resonance point. In the data there is no sign of this indefinite deceleration and, in fact, group velocity shows a regular local minimum rather than the singularity occurring with critical-layer resonance. In view of the generality of Lighthill's analysis, our experimental findings are incompatible with the type of resonance invoked in classical models of cochlear mechanics.

Funding
Supported the Netherlands Organization for Scientific Research (NWO), ALW 823.02.018

PD 111

Does the outer hair cell (OHC) active force boost the basilar membrane (BM) or reticular lamina (RL) motion?

Amir Nankali; Karl Grosh
University of Michigan

An active process is involved in the cochlea that boosts the sound borne vibration of the organ of Corti (OoC) via a compressive nonlinearity in the system which enhances frequency selectivity and sensitivity to low level sounds. The somatic motility of the mechanosensory outer hair cells (OHC) is hypothesized as the key element of the cochlear active mechanism. The OHCs are situated between the basilar membrane (BM) and reticular lamina (RL) inside microstructure of the OoC. The mechanoelectrical properties of these cells allows for conversion of electrical energy, induced by actively maintained ionic imbalance inside the cochlea, into mechanical energy (and vice versa). This process results an active force applied on both the apical and basal ends of the OHCs. In this paper, we use the in vivo experimental data on the OHC extracellular receptor potential together with the displacement of the OoC structural components derived from optical coherence tomographic (OCT) measurements and pressure gradient estimation of the BM velocity to estimate electromechanical energy exchange. The phase relation between somatic force and the BM/RL motions indicate the active power flow direction. A simplified circuit model of the cochlea is introduced in order to approximate the immeasurable quantities (e.g., OHC transmembrane potential). Post processing the experimental data from two separate but related experiments [Fridberger et al. (2004) and Zha et al. (2012)] with our model reveals that the OHC active force dissipates power in the BM side while it amplifies the RL motion. Conversely, another experimental protocol using a single experiment [Dong and Olson (2013)] shows that the OHC active power is generative on the BM side (RL displacement was not available from this experiment). The conflicting data points to the need for concomitant OCT and voltage measurements in order to conclusively determine the applied power.

Funding
Supported by NIH-NIDCD R01-04084 and NIH NIDCD-T32-000011.

PD 112

Outer hair cell stereocilia bundle stiffness and mechanical coherence by horizontal top connectors determined using acoustic frequency modulation atomic force microscopy

Alexander Cartagena-Rivera[1]; Elisabeth Verpy[2]; Christine Petit[2]; Richard Chadwick[1]
[1]National Institutes of Health; [2]Institut Pasteur

Deflection of the mature outer hair cell (OHC) stereocilia bundle results in mechanical opening or closing of mechanoelectrical transduction (MET) channels at the tip of the stereocilia from the middle and short rows and also alters elastic energy in horizontal top connectors, the lateral links that connect adjacent stereocilia both within and between the three rows. Previous study by the Petit lab (Verpy, E. et. al. Nature 456, 255-258) showed that the stereocilin-null mice, that lack horizontal top connectors in OHC stereocilia bundles, becomes progressively deaf from P15. However, at P14, the cochlea sensitivity and frequency tuning are intact, but interestingly suppressive masking and both acoustic and electrical waveform distortions are absent. This unique phenotype suggest that the main source of cochlear waveform distortions may be a top connector-mediated MET channel cooperativity or a mechanical deflection-dependent hair bundle stiffness resulting from constraints imposed by the presence of horizontal top connectors, not only from canonical MET nonlinear behavior. Here we describe a noninvasive, acoustic, and quantitative method to investigate the mechanical stiffness and coherence of stereocilia hair bundles. We developed a theory and formulas for relating hair bundle stiffness to frequency shifts of the phase lag of cantilevers with attached microspheres oscillating at acoustic frequencies. We use the atomic force microscope (AFM) to measure the cantilever frequency shifts at nanometer distances from the stereocilia bundle. Hair bundle stiffness determination of P9-P14 stereocilin-deficient mice with detached tectorial membrane (Strc-/- /Tecta-/- double knockout mice) were used and compared with heterozygous littermate controls (Strc+/-/Tecta-/-). Interestingly, a significant decrease in bundle stiffness was measured when horizontal top connectors were absent. Therefore, the bundle mechanical coherence is affected by the presence or absence of top connectors. Altogether, this finding suggest that interconnected stereocilia by horizontal top connectors provide hair bundle stability and maintenance of coherence in response to mechanical deflection, a vital requirement for hearing integrity.

Funding
Intramural Program of the US National Institute on Deafness and Other Communication Disorders

PD 113

An Arch-Beam Model for the Gerbil Basilar Membrane

Santosh Kapuria[1]; **Charles Steele**[2]; Sunil Puria[2]
[1]India Institute of Technology, Delhi; [2]Stanford University

Background

Models that quantify the basilar-membrane (BM) response typically consider the upper and lower collagen-fiber layers of the BM as a homogeneous 'simple beam model' (SBM), expressing the stiffness as a function of BM width, total thickness, and collagen volume fraction. The SBM resonance frequency predicts the place–frequency cochlear 'map' for several mammals (Olson *et al*., 2012), but not the Mongolian gerbil, prompting several measurements of stiffness vs. deflection that reveal a low initial stiffness plateau followed by a sudden rise, second plateau, and quadratic increase. Submicron BM physiological motions bring into question the relevancy of the second plateau, at deflections of 10–20 μm. In the gerbil, unlike the SBM, the lower fiber layer in the pectinate zone (PZ) forms an arch, making the gap between the two layers unusually large.

Model Formulation

The lower PZ layer is modeled as a shallow circular arch and the upper layer as a beam. The ground substance is modeled as an incompressible gel with uniform internal pressure. In the arcuate zone (AZ), the two layers merge. A tympanic cover layer (TCL) consisting of soft cells on the scala-tympani side is explicitly included, critical for reinterpreting the previous stiffness–deflection measurements. An analytical formulation is developed to predict the large-deflection response of the arch-beam model (ABM) under point-load measurements.

Model Results

The arch buckles with point-load displacements of more than a few lower layer thicknesses. The initial plateau due to TCL compression obscures the buckling in many of the measurements (Olson and Mountain, 1991; Naidu and Mountain, 1998; Emadi et al., 2004), indicating that the reported second-plateau stiffness measurements are far in the post-buckling range. The gel further pushes the upper layer into quadratic stiffening. Pressure loading of the ABM shows good correspondence with the map. Parameter variations show that changing fiber-band thickness longitudinally in the AZ has a significant contribution to the map, while changes to both AZ and PZ are only slight different from AZ alone. The arch height does not cause any significant change in the map. With the AZ width proportional to the BM width, the place–frequency map is governed by the thickness and width of the AZ only.

Conclusions

The gerbil PZ arch stiffens substantially under pressure loading, and the AZ anatomy primarily determines the cochlea's tonotopic organization. The AZ thickness in five gerbilline rodents decreases in thickness from base to apex (Plassmann, 1987) in support of the present findings.

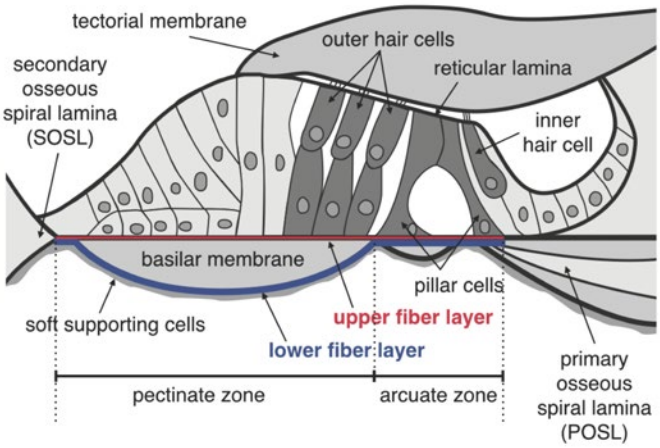

Funding

Work supported by the Fulbright Scholarship fund (SK) and grant No. R01 DC 07910 from the NIDCD of the NIH (SP and CS).

PD 114

Round Window Membrane Achieves Selective Release of Sound Pressure Waves over Quasi-Static Pressure Tuned by Hyperbolic Paraboloid Shape

Hirobumi Watanabe; Anil Lalwani; Jeffrey Kysar
Columbia University

Round window membrane (RWM) is a window selectively releasing sound pressure from the inner ear and holding the perilymph solution within it. To release sound efficiently, the RWM is thin enough to deform flexibly by pressure waves. Furthermore, to maintain the separation of liquid and gas phases of the middle and inner ears for the mechanical conduction and neural transduction of sounds, the RWM must be structurally reliable against static/quasi-static pressure loads of lymph solution. While the semicircular canals align endolymph inertia to deform stereocilia generating sensation of head movement, the RWM must prevent the head movement and perilymph inertia from agitating basilar membrane by immobilization. Recently, our group determined the structure of guinea pig (GP) RWMs as approximately a hyperbolic paraboloid (hyper) which allows us to calculate the compliance. The hyper shape was shown to be extremely effective to provide structural stability against static pressure compared to a flat membrane.

Here, the dynamics of the hyper shape was analyzed to determine the characteristics in releasing sound pressure waves of GPs (hearing frequency: 54~50,000Hz). Finite element modeling was performed to determine eigenmodes and resonant frequencies of RWMs modelled as hyper and flat shells. Steady state dynamic analysis was performed to calculate the vibration dynamics of the whole membranes upon uniform sinusoidal pressure and to determine the volume flow rate and acoustic impedance.

Eigenmode expansion showed that the hyper has no eigenmode in low frequencies but more eigenmodes above 15kHz than the flat shell that has the fundamental frequency at 1.4kHz. The impedance of the hyper was large in low frequencies close to that of water-filled inner ear but was small in broad frequency range above 15kHz and lowest at 26.8kHz reaching the impedance of an air-filled round window niche. Conversely, impedance curve of the flat shell shows a sharp minima with extremely low impedance at 1.4kHz and keep increasing afterwards. Consequently, the impedance of the hyper was 1000 fold greater than the flat shell but became smaller above 15kHz.

These results suggest that the hyper shape effectively immobilizes the quasi-static pressure of perilymph at the large impedance of water and releases sound pressures at meaningful frequencies for GPs more efficiently than at the small impedance of air. While a flat membrane releases sound of a highly specific frequency, the hyper shape allows for releasing sound with non-specific and broad frequency range for guinea pig hearing.

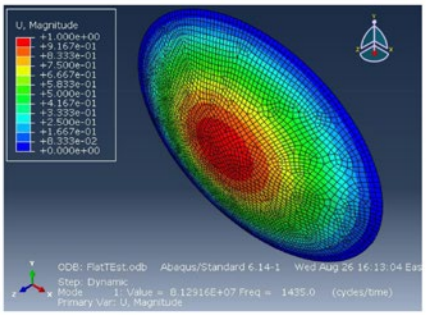

Figure 1. The first eigenmode of the flat elliptical shape at the frequency of 1.4 kHz.

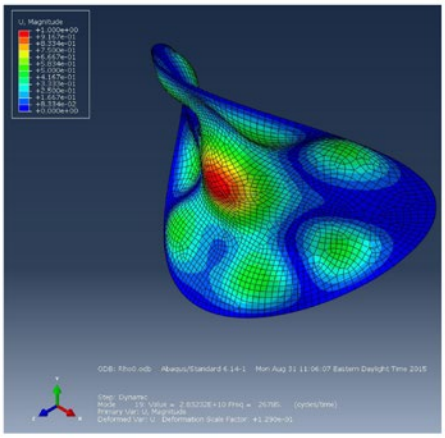

Figure 2. The eigenmode of the hyper shape at the frequency of 26k that showed the minimum impedance.

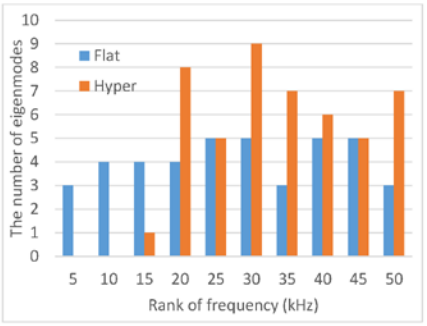

Figure 3. The comparison of the eigenmodes distributions of flat and hyper shapes across the guinea pig hearing frequency range with the bins of 5kHz.

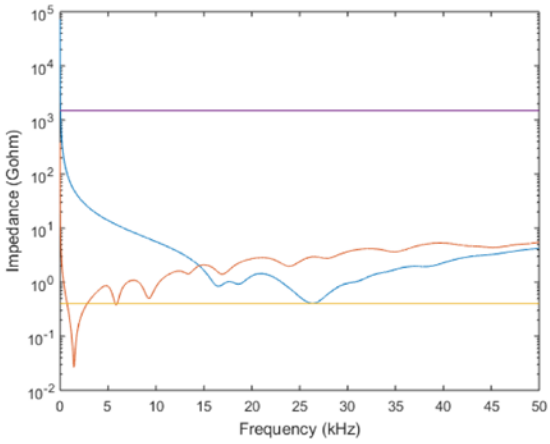

Figure 4. The impedance curves of the flat (orange) and hyper (blue) shapes. The acoustic impedances of an infinite long canal whose diameter is 1 mm filled with air (yellow) and water (purple) are also shown as references.

Funding

Coulter Translational Research Partnerships American Otological Society

PD 99

Classification of the behavior of hair cells operating in a noisy environment

Joshua Salvi; Dáibhid Ó. Maoiléidigh; A. J. Hudspeth

The Rockefeller University

Within the auditory, vestibular, and lateral-line systems of vertebrates, hair cells actively transduce mechanical stimuli into electrical signals that are delivered to the brain. We previously showed that a hair cell's active process can be controlled by the mechanical load applied to its hair bundle. Coupled to different loads, an individual hair bundle may exhibit a wide gamut of behaviors. When a bundle's operating point resides near a transition between behaviors—a bifurcation—the bundle exhibits generic dynamics described by the normal-form equations associated with that type of bifurcation.

To classify the function of a hair bundle one must determine both the proximity of its operating point to a bifurcation and type of bifurcation. Although this type of analysis is described for systems in which fluctuations are negligible, a hair bundle operates in a very noisy environment. We developed a set of tools by which one can classify a system according to the bifurcation near which it operates despite the presence of

substantial noise. We then sought to categorize a bundle's behavior by comparing stochastic simulations of the normal forms of various bifurcations and of a model of hair-bundle motility to the behavior of individual hair bundles with mechanical loads applied by a feedback system.

We found that a hair bundle's behavior falls within one of at least two regimes. For large values of the load stiffness, the bundle operates near a supercritical Hopf bifurcation, achieving high amplification and sharp frequency selectivity in response to periodic stimuli. When the stiffness remains low, the bundle instead approaches a subcritical Hopf bifurcation, providing a graded response to changes in force. The mechanical load might therefore control whether a bundle operates in an auditory or vestibular regime at respectively high or low load stiffness. These results accord with the hypothesis that a hair cell's function depends on its mechanical load and highlight the pertinence of noise in the study of mechanosensory organs.

Funding
This work was supported by the NIDCD (F30DC013468), NIGMS (T32GM07739), and the Howard Hughes Medical Institute.

PD 102

Hair Bundles Are Most Easily Entrained on the Brink of Self-Oscillation

Dáibhid Ó. Maoiléidigh; Joshua Salvi; A.J. Hudspeth
The Rockefeller University

The hair cells of auditory systems evidently behave as active oscillators that are arranged tonotopically such that each cell responds preferentially to sound input at a particular frequency. To ensure that a continuous range of inputs is detected by an auditory system, however, each hair cell must also respond sufficiently well to a band of nearby frequencies. It is therefore important to determine how well a cell responds to inputs near but not at its optimal frequency.

To address this question, we analyzed the response of a generic model of a noisy active oscillator to periodic driving. This active system oscillates spontaneously when one of its parameters, the control parameter, is positive, whereas the system is quiescent for negative values of the control parameter. From the model we predict that the oscillator's phase-locked response and its degree of entrainment to a frequency-detuned stimulus are greatest when the control parameter lies near—but not precisely at—the transition from quiescence to self-oscillation, the location of a Hopf bifurcation.

Because individual hair bundles can behave as active oscillators under appropriate conditions, we tested the model's predictions by observing their responses to periodic stimuli. We employed a feedback system to control the operating point of a bundle, allowing us to coerce a spontaneously oscillating bundle into quiescence or to impel a quiescent bundle into self-oscillation. It was possible to cross a Hopf bifurcation either by changing the constant force applied to the bundle or by adjusting the bundle's load stiffness. As predicted, we found that the phase-locked response and the vector strength peaked for operating points near either bifurcation locus.

These results imply that a hair cell embedded in an auditory organ would optimally detect stimuli within a band of frequencies around its best frequency if the system's operating point were near but not at a Hopf bifurcation. Although hair cells exhibit remarkable frequency selectivity, the sharpness of their tuning is limited so that an auditory system is able to detect a continuous range of frequencies.

Funding
D.O? M. was a research associate and A.J.H. is an investigator of Howard Hughes Medical Institute. J.D.S. is supported by Grants F30DC013468 and T32GM07739 from the National Institutes of Health.

PD 100

The role of stochastic noise and high-order mode-locking in hair cell response

Dolores Bozovic[1]; Michael Levy[1]; Roie Shlmovitz[2]
[1]University of California Los Angeles; [2]St. Jude Medical

Hair cells of the inner ear exhibit a highly nonlinear response to applied signals, and this nonlinearity has been shown to be crucial for achieving the extreme sensitivity of mechanical detection. Under *in vitro* conditions, hair cell bundles can exhibit active motility that can be readily entrained even by very weak stimuli. We model the active motility of hair bundles of the vestibular system with the Adler equation, which describes the phase degree of freedom of bundle motion. We explore the response of the bundles, poised near a bifurcation in the quiescent regime, to applied external signals, in the presence of stochastic noise. The system exhibits stochastic resonance, with active motility of the bundles occurring at a preferential phase of the stimulus cycle. We show that an array of uncoupled hair cells could provide a sensitive detector that encodes the frequency of the applied signal.

We next explore experimentally the response of oscillatory hair bundles to signals significantly higher than that of the innate oscillations. To enable access to higher frequencies of stimulation without mechanically loading the hair bundles, we apply a recently developed technique that uses superparamagnetic particles to actuate the cells. Magnetic nanoparticles are conjugated to bind to the stereovilli of the hair cell and are controlled with an electromagnet to deflect the bundles. This allows for sensitive mechanical control of the position of the stereovilli, without imposing a mechanical load. We apply the technique to study the dynamics of synchronization between spontaneously oscillating hair bundles and an imposed stimulus at increasing frequencies. The evoked response consistently shows regimes of high-order mode-locking, which take the form of Arnold Tongues. Significant areas of overlap occur between synchronization regimes, with the bundle intermittently flickering between different winding numbers. We demonstrate how an ensemble of these noisy nonlinear oscillators could be entrained to detect signals significantly above the characteristic frequencies of the individual cells.

Funding
NIH grant RO1DC011380 and AFOSR grant FA9550-12-1-0407

PD 101

Chloride' influence on prestin kinetics

Joseph Santos-Sacchi; Lei Song
Yale Medical School

The OHC drives cochlear amplification through a voltage-dependent process whereby the motor protein prestin changes conformation resulting in electromotility. The voltage-sensor of prestin can be characterized by measuring nonlinear capacitance (NLC), a consequence of voltage-sensor charge movement within the OHC lateral plasma membrane. Chloride has been observed to play a critical role in prestin's activity, influencing both the operating voltage range and estimated charge movement (Qmax, the total sensor charge moved) as measured by Boltzmann fits to NLC. Typically, NLC is measured by admittance analysis at frequencies near 1kHz. By measuring NLC at various frequencies, we find that NLC frequency dependence is chloride dependent. Derived Qmax markedly rolls off at frequencies above our lowest admittance interrogation frequency of 195 Hz. In order to interrogate lower frequencies, we equivalently integrated voltage step-induced currents. We find that Qmax asymptotes as we increase integration times, indicating that Qmax has been markedly underestimated by high frequency admittance techniques. By fitting our data to the *meno presto* model (Santos-Sacchi and Song, Biol Chem. 289:10823-30, 2014) we arrive at the conclusion that chloride level likely does not influence Qmax, but works by changing the kinetics of prestin's molecular transitions. These observations run counter to current thought, and provide clues about prestin's molecular workings.

Funding
NIH NIDCD DC000273 and DC008130 to JSS

PD 103

Prestin's Non Selective Currents are Mediated by an Auxillary Pathway that is Independent of its Transporter Pathway.

Junping Bai; **Dhasakumar Navaratnam**; Iman Moeini-Naghani; Fang-Yong Li; Sheng Zhong; Shumin Bian; Joseph Santo-Sacchi
Yale University

Prestin, responsible for outer hair cell electromotility and cochlear amplification, belongs to the SLC26 anion transporter family. Recently, prestin was shown to best fir the crystal structure of the distantly related 14 transmembrane bacterial Uric Acid transporter UraA. Recent work has also shown it to conduct the pseudohalide thiocyanate, similar to other anion transporters SLC26a3 and SLC26a6.

Using an inducible cell line we show that 1. Prestin has a non-selective pressure sensitive current that is similar to that demonstrated in the presence of SCN. Noise analysis of Cl- and SCN currents show absent lorentzian properties, consistent with a passive non gated conductance. We also show that mutations of key conserved residues between prestin and UraA, that are critical for transporter functions in UraA, have no effect on SCN currents. In contrast, mutation of several charged residues in the transmembrane domain, which preserved gating charge movement, also decreased SCN currents. We model a potential auxillary pathway that lies between alpha helices that form the inner core and alpha helices in the perimeter of the transmembrane domain, similar to pathways that have been speculated to be present in the electroneutral Na /HCO3 transporter and in the transporters responsible for the neurotransmitters glutamate, GABA, serotonin and dopamine.

Funding
NIH/ NIDCD R01DC 007894 (JSS/DN)

PD 104

Zebra fish Models for the Mechanosensory Hair Cell Dysfunction in Usher Syndrome 3

Suhasini Gopal[1]; Daniel Chen[1]; Shih-Wei Chou[1]; Jingjing Zang[2]; Stephan Neuhauss[2]; Ruben Stepanyan[1]; Brian McDermott Jr[1]; Kumar Alagramam[1]
[1]Case Western Reserve University; [2]University of Zurich

Usher syndrome III (USH3) is characterized by progressive loss of hearing and vision, and varying degrees of vestibular dysfunction. It is caused by mutations that affect the human clarin-1 protein (hCLRN1), a member of the tetraspanin protein family. The missense mutation *CLRN1*^{N48K}, which affects a conserved N-glycosylation site in hCLRN1, is a common causative USH3 mutation among Ashkenazi Jews. The affected individuals hear at birth but lose that function over time. Here, we developed an animal model system using zebra fish transgenesis and gene targeting to provide an explanation for this phenotype. Immunolabeling demonstrated that Clrn1 localized to the hair cell bundles (hair bundles). The *clrn1* mutants generated by zinc finger nucleases displayed aberrant hair bundle morphology with diminished function. Two transgenic zebra fish that express hCLRN1 or hCLRN1^{N48K} in hair cells were produced to examine the subcellular localization patterns of wild-type and mutant human proteins. hCLRN1 localized to the hair bundles similarly to zebra fish Clrn1; in contrast, hCLRN1^{N48K} largely mislocalized to the cell body with a small amount reaching the hair bundle. We propose that this small amount of hCLRN1^{N48K} in the hair bundle provides clarin-1 mediated function during the early stages of life; however, the presence of hCLRN1^{N48K}in the hair bundle diminishes over time because of intracellular degradation of the mutant protein, leading to progressive loss of hair bundle integrity and hair cell function. These findings and genetic tools provide an understanding and path forward to identify therapies to mitigate hearing loss linked to the *CLRN1* mutation.

Funding
This work was supported in part by funds from the Anthony J. Maniglia Endowed Chair, University Hospitals Case Medical Center and NIH (R01-DC010816), to Kumar.N.Alagramam., and by NIH Grant R01-DC009437 to Brian. M. McDermott Jr.

PD 105

Clarin-1 Is an essential structural and functional organizer of the auditory hair cell ribbon synapses

Didier Dulon[1,2]; Samantha Papal[2,3]; Matteo Cortese[2,3]; Alice Emptoz[2,3]; Philippe Vincent[1]; Yohan Bouleau[1]; Saaid Safieddine[2,3]; Paul Avan[4]; **Aziz El-Amraoui**[2,3]; Christine Petit[2,3,5]

[1]Université de Bordeaux; [2]INSERM UMRS1120; [3]Institut Pasteur; [4]Université d'Auvergne; [5]Collège de France

Background

Usher syndrome (USH) is the major cause of hereditary deaf-blindness in humans. Defect in clarin-1, a four-transmembrane glycoprotein, causes USH3A, characterized by a post-lingual progressive deafness and blindness. Structurally, clarin-1 displays some amino acid sequence homology with the Ca^{2+} channel subunit protein 2 (CACNG2) stargazin, a tetraspan protein that has been involved in post-synaptic AMPAR trafficking and clustering. For this reason clarin-1 has been suspected to play a role in the excitatory ribbon synapse junctions between hair cells and cochlear ganglion cells but its precise function still remains uncertain.

Methods

Since constitutive knockout mouse models can sometimes generate abnormal developmental and compensatory effects from which a protein function is difficult to extract,, we generated two clarin-1-deficient mice: one displaying an ubiquitous, early gene inactivation (*Clrn1*$^{-/-}$ constitutive knockout mice) and the other a postnatal, hair cell-specific loss of clarin-1 (*Clrn1*$^{fl/fl}$*Myo15-cre*$^{+/-}$ post-natal conditional knockout mice).

Results

We found that the ubiquitous deletion of clarin-1 at embryonic stages in *Clrn1*$^{-/-}$ mice causes severe hearing loss, which was attributed mainly to the disruption of hair bundle stereocilia. By contrast, the post-natal and hair cell-specific loss of clarin-1 in *Clrn1*$^{fl/fl}$*Myo15-cre*$^{+/-}$ mice leads to a late appearing and progressive hearing loss that mimics the hearing phenotype in USH3A patients. Morpho-functional analyses established that the late hearing deficit in mice arises from pre- and post-synaptic defects at the inner hair cell ribbon synapses. Inner hair cells lacking clarin-1 displayed reduced Ca^{2+}-mediated exocytotic efficiency that was associated with a synaptic F-actin disorganization and abnormal clustering of $Ca_v1.3$ Ca^{2+}channels at the ribbon synapse. Expanded postsynaptic GluA2/3 distribution and afferent nerve fibers degeneration were also observed. Protein-protein interactions indicated that clarin-1 interacts with $Ca_v1.3$ Ca^{2+}channels through its binding to the $Ca_v1.3$ β2 subunit and/or harmonin.

Conclusion

Our results suggest that, in addition to its role in hair bundle formation and functioning, clarin-1 also is necessary for the proper and tight coupling of the Ca^{2+} channel complex to the presynaptic ribbons, and for the correct organization of the AMPA receptors at the postsynaptic region.

Funding

European Union Seventh Framework Programme, under grant agreement HEALTH-F2-2010-242013 (TREATRUSH), LHW-Stiftung, Fondation Raymonde & Guy Strittmatter, Fighting Blindness, FAUN Stiftung, Conny Maeva Charitable Foundation, Fondation Orange, ERC grant 294570-hair bundle, LABEX Lifesenses [ANR-10-LABX-65], "the Foundation Fighting Blindness Paris Center Grant" and the Fondation Voir et Entendre

PD 106

Phosphoinositol-4,5-bisphospate is required for normal cochlea hair cell function

Thomas Effertz; Anthony Ricci

Stanford University

The mammalian auditory organ, the cochlea, utilizes specialized sensory cells, hair cells, to translate sound signals into chemical/electrical signals. The hair cell's sensory organelle is the hair bundle, which consists of three rows of actin filled stereocilia that are arranged in a staircase pattern. Deflections of the hair bundle towards the tallest stereocilia row opens mechano-electrical-transduction (MET) channels that reside at the top of the middle and shortest stereocilia row. How deflections of the hair bundle lead to MET-channel gating is unknown. One could imagine a chain of proteins that propagate the mechanical force or a force relay by the cell membrane. Some data show that the stereocilia cell membrane is compartmentalized, suggesting a biological function for different lipid compositions at different locations (Zhao et al. 2012). We investigated the effect of Phosphoinositol-4,5-bisphospate (PIP2) depletion from rat inner hair cells by blocking PIP2 synthesis with phenylarsine oxide (PAO[TE1]), quercetin, different aminoglycosides, and internal application of PIP2 antibodies. We found a reduction of maximal MET-current, an increase of resting open probability, and a loss of adaptation. A previous study had found similar results in isolated bull frog sacculus hair cells (Hirono et al. 2004). However, the underlying mechanism remained unknown. Using calcium imaging we found that the effect is likely on the channel level and not due to the loss of single transducing stereocilia, which would have explained the reduction of maximal MET-current. The calcium data rather indicates that alterations of single channel properties occurred, such as channel conductance. We also show that using PIP2 in our intracellular solutions protects against the effect of PAO, indicating that the observed effects are directly PIP2 related, as the high concentration of internal PIP2 likely saturates any 2nd messenger cascade. Finally we present two possible explanations for the observed effects. Either the depletion of PIP2 alters global membrane properties/ mechanics (TRP - Hardie & Franze 2012) or PIP2 directly interacts with the channel and functions as a cofactor (Kir2.2 – Hansen et al. 2011).

[TE1]Add pip2 antibody and quercetin

Funding

RO1 DC0003896 NIDCD CoreGrant P30-44992 DFG POst-Doc Fellowship EF100/1-1

PD 115

Sensitivity to the Statistics of Rapid, Stochastic Sequences

Sijia Zhao[1]; Marcus Pearce[2]; Fred Dick[3]; Maria Chait[1]
[1]University College London; [2]Queen Mary, University of London; [3]Birkbeck, University of London

Background

Accumulating work suggests that the human brain is remarkably sensitive to patterns in sound. However, much of the work to date has focused on deterministic (regular) patterns. Here we used psychophysics and EEG to investigate statistical learning of random sequences, the time-scales associated with these processes, and their underlying brain mechanisms.

The experimental paradigm measured behavioural and neural responses to temporally jittered spectral transitions in the fluctuation pattern of random tone-pip sequences. To detect these transitions, listeners had to integrate information over different timescales. By measuring reaction time (RT) and d' to transitions, we infer what - and how much - information about the signal listeners extract.

Methods

In the behavioural experiments (N=20), listeners responded to transitions within stochastic sequences created from 80 50-ms tone-pip sequences (sequence duration 4s). Sequences were too rapid for conscious scanning and thus tapped automatic statistical learning processes.

Tone frequencies were drawn with replacement from a fixed pool of 20 log-spaced values between 200-2k Hz. 50% of trials contained a change in statistics partway through the stimuli, namely a reduction in frequency pool size (from 20 to 10). Conditions differed in the spectral distribution of the reduced tone pool: 10 highest frequency tones (**High**), 10 lowest tones (**Low**), the 10 middle tones (**Medium**), the 10 'edge' frequencies (5 highest & 5 lowest; **Edge**), or were sampled equally from the entire frequency range (**All Bands**). The stimulus set also included STEP stimuli, with the transition being a simple step change in frequency; this condition was used to estimate basic audiomotor RT.

In the EEG experiment (N = 20), passive naïve listeners listened to **High, Medium, Edge** and no-change control stimuli while watching silent videos.

Results

RT and d' measures showed detection was fastest and most accurate to **High** and **Low** spectral transitions (average detection ~11 tones post-transition), followed by **Medium** (~15 tones) and then **Edge** (~18 tones). We compared behavioural data to both statistical simulations and a variable-length Markov chain model.

Preliminary EEG analysis suggested that sustained global field power diverged near the point where statistical information allows for reliable detection of transition consistent with other work in our lab.

Conclusion

Performance reveals that human listeners are tuned to the statistical structure of rapid, random, tone-pip sequences. The tracking of statistical structure and detection of change in statistics occurs automatically, irrespective of attentional focus.

Funding

BBSRC and European Commission supported this study.

PD 116

P1-N1-P2 Responses to Subtle and Overt Vowel Quality Changes in Different Attention Conditions

David Morris
University of Copenhagen

While cortical responses to changes within a sound, like the P1-N1-P2 acoustic change complex are commonly termed 'obligatory,' their precise dimensions can be modulated by the attention state of the subject. This paper explores this modulation in the framework of an EEG study where auditory stimuli, were presented while subjects **i)** attended, **ii)** ignored and watched a film, and **iii)** performed a visual search task. During the visual search task subjects focused their attention on identifying target deviant Japanese Kanji symbols from sets of three. The auditory stimuli consisted of a continuous triphthongal vowel where the second formant changes were either subtle (100 Hz) or overt (1000 Hz). EEG recordings of the responses to these changes were made from 12 normal hearing right-handed participants.

Responses measured from the vertex electrode show that the N1, P2 and N1-P2 response amplitudes increase while the P1 and P2 peak latencies decrease, between the subtle and the overt vowel quality changes. A main effect for presentation condition, which was the task-related level of attention, was observed, but this was restricted to the N1-P2 and absolute P2 response amplitudes and P2 latency. Measures of hemispheric difference, determined from the temporal electrodes showed an asymmetry with larger responses at the right recording site (T8) across all conditions. A significant interaction between presentation condition and vowel formant change was found in the N1c response at the T8 electrode. Otherwise interactions between responses to vowel quality changes and presentation conditions were absent, indicating that the neuroelectrical activity generated in response to the acoustic changes, and that arising from the maintenance of different levels of attention was disparate in the ERPs.

In the design of this study an attempt was made to partial out differences in endogenous attention that can distort results from event-related measurement paradigms. The results demonstrate that a discernible P1-N1-P2 can be measured in response to a subtle vowel quality change, even when the attention of a subject is focused on performing a secondary task. In this way they confirm that the P1-N1-P2 response is obligatory, but not uniform across different attention conditions.

Funding
Innovation Fund, Denmark

PD 117

Sharpening of Frequency Selectivity of the Cortical Representation via Frequency Specific Adaptation and Recovery: Human EEG and Models.

Oscar Woolnough; Jessica de Boer; Katrin Krumbholz; Robert Mill; **Christian Sumner**
MRC Institute of Hearing Research

Background
Adaptation, the reduction in neural responses to repeated stimuli, is a ubiquitous phenomenon throughout sensory systems and is an important aspect of neural coding. Here we test the hypothesis that prolonged adaption increases the frequency selectivity of cortical responses in human EEG recordings, and present a neural model to explain the responses.

Method
Pure tone adapter-probe sequences were presented in which a single probe tone of one frequency was preceded by adapters of a second frequency (frequency difference: 0-, 600-, 1800- cents). Adapters consisted of either a train of 100ms tones (25ms gap), varying in number (1, 2, 3, 6, 9, 15), or a single adapter which varied in duration (100, 225, 350, 725, 1100, 1850-ms). Adaptation was characterized as a reduction of the probe response relative to the response to the probe alone.

Results
In all cases the response to the probe was most strongly reduced when the adapter frequency was closest to the probe frequency. However, the degree of adaptation depended on the temporal arrangement of adapters. At all frequency differences, adaptation of the probe initially grew with increasing numbers of adapters, or adapter duration. At long adapter durations (>400ms), regardless of frequency difference, adaptation was reduced relative to peak values. Adaptation also reduced with >3 repeated adapters, but only when there was a difference in frequency between the adapter and probe. Effectively, the tuning of adaptation became sharper with increasing numbers of adapters, but not with adapter duration.

EEG adaptation tuning was explained by an extension to a model proposed to explain frequency specific adaptation in single neurons (Mill et al. 2011). The model was a two-layer network with convergent inputs, independently adapting synapses and separate non-adapting inputs for onset responses. This model is able to quantitatively reproduce the observed non-monotonic adaptation and sharpening of tuning observed in our EEG responses, and the effects of repeated and prolonged adapters.

Conclusion
The results suggest that adaptation from repeated, but not prolonged stimulation leads to a sharpening of the frequency tuning in auditory cortex, which may serve to emphasize the representation of stimuli that are different in frequency to those that precede it. This may be a natural consequence of a hierarchical network of neurons with independently adapting inputs.

Mill R, Coath M, Wennekers T, Denham SL (2011) A neurocomputational model of stimulus-specific adaptation to oddball and Markov sequences. PLoS Comput Biol 7.

Funding
Medical Research Council, UK

PD 118

Auditory steady-state response to chords: Effect of frequency ratio

Asuka Otsuka[1]; Masato Yumoto[2]; Shinya Kuriki[3]; **Seiji Nakagawa**[1]
[1]National Institute of Advanced Industrial Science and Technology (AIST); [2]Graduate School of Medicine; [3]Tokyo Denki University

Perceptual degree of consonance and dissonance of a chord is varied as a function of frequency ratio between the tones comprised in the chord. Perception of dissonance is attributed to sensation of beats or roughness, which is induced at difference frequency (delta-f) due to interference between adjacent frequency components processed within one auditory filter bank. An earlier study reported that auditory steady-state response (ASSR), phase-locked to the delta-f, exhibited larger activities for dissonant than for consonant chords, suggesting the ASSR as neuronal correlates underlying the sensation of dissonance. However, the ASSR is intrinsically modulated as functions of sound intensity, carrier frequency (fc) and modulation frequency (fm, i.e., delta-f) of a sound. In order to capture the distinct effect of musical cognitive function, such physiological/mechanical characteristics need to be taken into account. Further, it is still unknown if the sensation of consonance is merely an effect of reduced activity. This study therefore investigated the neuromagnetic responses to chords varied in frequency ratio but capable of identical spectral characteristics of fm. The effect of fc was compensated by utilizing a sinusoidally amplitude-modulated chirp tone, which elicited the ASSR at the same fc and fm as the chords without generating any sensation of consonance or dissonance. The spectral energy of all the frequency components was equalized to be flat at 70 dB SPL inside of the ear canals. The single-trial time-frequency analysis showed that the ASSR was larger for the chords with complex frequency ratio. Contrary, the spontaneous activity of alfa frequency band was augmented in a time scale over a second after a diminishment at the stimulus onset for the chords with simple frequency ratio. These results suggest that the sensation of consonance/dissonance is generated interactively between the different neuronal components at relatively longer time interval.

Funding
A part of this research was supported by the Funding Program for Next-Generation World-Leading Researchers provided by

the Cabinet Office, Government of Japan, and Grants-in-Aid for Scientific Research (26282130, 26560320 & 25280063) from the Japan Society for the Promotion of Science (JSPS) for SN.

PD 119

Processing of Temporal and Spectral Cues in the Human Brain during Perception of Speech and Corresponding Non-Speech Signals: An Electrophysiological Study

Nitza Horev; Hillel Pratt
Technion - Israel Institute of Technology

Background:
One of the central questions in speech perception research relates to the uniqueness of the process. That is, to what degree does speech perception depend on a dedicated specialized mechanism and to what degree is it based on general auditory perceptual mechanisms. To address this question we examined how the brain processes linguistically relevant spectral and temporal information compared with the processing of corresponding non-speech signals.

Methods
Auditory Evoked Potentials (AEPs) were recorded from from 61 scalp electrodes during active discrimination of spectral (/ubu/ - /udu/) and temporal (/ubu/ - /upu/) stimulus pairs and their analogous non-speech stimuli. In order to differentiate between acoustic effects and speech-specific effects, AEPs were also recorded during active discrimination of Sine-Wave Speech (SWS) stimulus pairs. SWS stimuli are auditory signals that can be perceived either as speech or non-speech, depending on listeners' expectations about the nature of the stimuli, hence providing a tool to study neural speech specificity using identical acoustic stimuli. Nineteen, healthy, right-handed, Hebrew speakers, participated in two sessions. In the first, "non-speech", session, subjects discriminated spectral and temporal differences in non-speech stimuli and in SWS stimuli, unaware of their speech-like nature. In the second, "speech", session, the same subjects discriminated between spectral and temporal speech pairs and between their SWS counterparts after learning to perceive the SWS as speech.

Results
Perceiving the stimuli as speech, resulted in higher percentages of correct responses and in shorter reaction times. Electrophysiological responses indicated that speech and non-speech perception evoked significantly different voltage differences around the main scalp recorded AEPs peaks. Acoustic differences between speech and analogous non-speech stimuli were reflected in differences in N1 amplitude, recorded 100 ms after stimulus onset, whereas later processing stages were ascribed to the transition to "speech-mode" of processing. sLORETA source estimation revealed stronger activation of auditory cortices to "speech" stimuli at early (around P2b) stages of processing, and at the time of a sustained negativity, stronger activation to "non-speech" stimuli, reflecting later processing stages. Differences were prominent mainly within the right superior temporal cortex and the right prieto-temporal junction.

Conclusion
Our data provide additional evidence for a "speech mode" of processing, which engages different brain mechanisms, distinct from those involved in general auditory (non-speech) processing mode. We suggest that brain specialization for speech processing is not hemisphere- or region-specific, but results from specific and unique activation patterns of distributed neural networks in both hemispheres.

Funding
This PhD research thesis was financially supported by Mr. Herbert Rose and the Technion - Israel Institute of Technology.

PD 120

Electrocorticographic Analyses of the Neural Networks Subserving Speech and Language Perception.

Mitchell Steinschneider[1]; Kirill Nourski[2]
[1]Albert Einstein College of Medicine; [2]University of Iowa

Background
Recent advances human neurobiology have led to extensive modifications of the more classic models pertaining to the neural networks subserving speech and language perception. These modifications include expanding these neural networks to include regions of the non-language hemisphere, the middle temporal gyrus (MTG) and anterior temporal regions of the language-dominant hemisphere, as well as subcortical structures (e.g., Poeppel et al., J Neuroscience 2012).

Methods
To clarify the respective roles of structures within these expanded neural networks, we examined the electrocorticogram (ECoG) recorded simultaneously from auditory and auditory-related cortex, as well as limbic structures, in the dominant and non-dominant hemispheres of the brain. Experimental subjects were neurosurgical patients undergoing evaluation for treatment of medically intractable epilepsy. Subjects gave informed consent prior to their participation, and could rescind consent at any time without jeopardy. Subjects performed the Mini Mental Status Exam (Folstein et al., J Psychiatr Res 1975) and other tasks including digit span, spelling, rhyming, abstract naming, verbal analogies, sentence comprehension, and fund of knowledge. Subjects were also asked to identify favorite items (e.g., favorite food or movie) Analysis focused on high gamma cortical activity, which has been shown to correlate with both neuronal firing rates and hemodynamic responses (e.g., Nir et al., Curr Biol 2007).

Results
Preliminary analyses indicate that language-related tasks produce widespread activation in both hemispheres, including limbic structures. As expected, responses in the superior temporal gyrus tracked the speech envelope bilaterally, with relative suppression occurring during self-

initiated vocalizations. Within the dominant hemisphere, the MTG was prominently activated during tasks requiring the rapid naming of objects (lexical access). While the temporal pole and parahippocampal gyrus were also strongly activated during tasks requiring lexical access, responses were even more prominent during tasks designed to index auditory working memory. Subcortical activity within the amygdala was strongly enhanced when self-initiated speech had a positive emotional valence (e.g., naming one's favorite food or movie). While similar distributions of activation occurred within the non-dominant hemisphere, the most notable responses occurred in the lingual and inferior occipital areas during verbal analogy tasks (e.g., "a pickle is fat, a pencil is…") and in the fusiform gyrus during the digit span test.

Conclusions
The current study demonstrates the proof in principle that direct ECoG recordings can identify the brain regions and their roles in the neural networks underlying speech and language perceptions at both high temporal and spatial resolutions.

Funding
NIH RO1-DC004290, UL1RR024979 and The Hoover Fund

PD 121
Top-down Neural Synchronization during Imagined Acoustic Rhythm

Francisco Cervantes Constantino; Jonathan Simon
University of Maryland, College Park

Background
Perceptual fill-in is one mechanism to overcome missing sensory information, possibly operating by interpolation from context cues. In the form of phonemic restoration, it is a likely candidate at the core of speech intellegibility. This work investigates neural mechanisms of perceptual restoration operating on a time-varying dynamic stimulus: frequency-modulated sounds, which, unlike natural speech signals, can be maximally exploited analytically. Listeners' endogenous neural oscillations associated with perceptual restoration of a template stimulus can be recorded non-invasively with magnetoencephalography (MEG). The time-varying power during these epochs can be correlated with performance in a detection task.

Methods
Auditory steady state responses were recorded from 35 subjects with MEG during presentation of a 60 minute duration rhythmic (5 Hz) pulse train. Brief noise masker probes were pseudo-randomly added. For half of the masker probes, the ongoing rhythmic pulse train was also omitted. Listeners reported, shortly after each probe, whether it had been perceived as rhythmic, or not.

Results
MEG responses showed higher evoked power at the 5 Hz rhythm rate for trials in which the acoustic rhythm was absent but nevertheless perceived than trials for which the acoustic rhythm was present but not perceived. This contrast significantly accounted for variance in detection sensitivity.

Conclusion
We propose that the presence of cortical dynamics synchronized to a sound modulation may lead to the subjective experience of sound as modulated, even in cases where synchronized dynamics is not supported by sensory input - in analogy to some auditory illusions or hallucinations. Moreover, a more faithful synchronization may covary with the vividness of the percept. This implies, at least for modulation rates relevant to human speech communication, top-down synchronization may follow from an internal model formulated to extract meaning from complex sound mixtures, e.g. in the problem of active listening to multiple speakers ('cocktail party' listening). The results also raise the question of contextual interpolation as a common-principled strategy already found in other sensory modes.

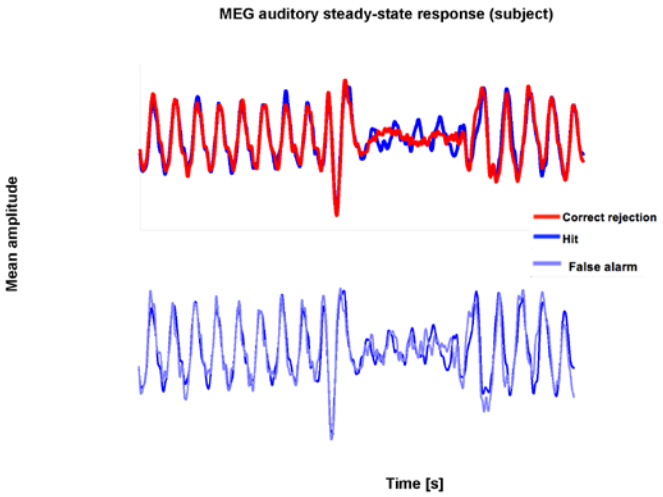

Figure 1. Mean evoked potentials from MEG aSSR-specific virtual sensor in a representative subject (R2141) during noise masker probes. *Top*: A low-amplitude aSSR is observable post noise probe onset (mid-series approx.) during hits (blue) but not during correct rejections (red), in accordance with the presence/absence of a 5 Hz pulse train during the probe. *Bottom*: The average evoked response during false alarm probes (lt-blue) resembles more the aSSR during a hit (blue) than the (acoustic equivalent) average for correct rejections (same as in *Top*), in accordance with the subject's report.

Funding
Support to JZS from NIH R01 DC 014085, R01 DC 008342, and to FCC from CONACYT (Mexico)

PD 122
Exploring the link between music training, auditory processing, statistical learning and reading skills

Pragati Rao Mandikal Vasuki[1]; Mridula Sharma[1]; Katherine Demuth[1]; Joanne Arciuli[2]
[1]Macquarie University; [2]University of Sydney

Introduction
Statistical learning (SL) or the ability to extract distributional cues from incoming data is helpful in word segmentation (Saffran et al., 1996), word reading (Arciuli & Simpson, 2012), and literacy in a second language (Frost et al., 2013). Previous studies have shown better statistical learning in musicians (Francois et al., 2014, Shook et al., 2013). Research has

also shown that proficient music skills are related to better reading outcomes (Anvari et al., 2002). However, a research investigating a combination of these factors in children remains to be undertaken. In this study we investigated the links between music skills, statistical learning and reading outcomes.

Method

Data from 36 children (9-11 years) in an ongoing study is presented here. All participants were assessed on their music skills (melody and rhythm discrimination), auditory processing tasks (frequency discrimination), psychoeducational tests (non-verbal IQ, phonological awareness, reading subtests-WIAT-II). Auditory (aSL) and visual statistical learning (vSL) were assessed using the embedded triplet task based on previous studies (Abla et al., 2008; Arciuli et al., 2012). Information about factors such as parents' education and socio-economic status was also collected.

Results

A preliminary hierarchical regression was conducted with word reading and reading comprehension scores as dependent variables. For word reading, frequency discrimination threshold, aSL and vSL accounted for significant variance after non-verbal IQ and phonological awareness had been entered (full model R^2 =0.47, F (6,35) = 5.33, p<0.005). In case of reading comprehension, rhythm discrimination, aSL, vSL accounted for significant variance after non-verbal IQ and phonological awareness had been entered (full model R^2 =0.44, F (6,35) = 4.76, p<0.005).

Conclusions

Our findings confirm and extend previous findings that statistical learning and frequency discrimination contribute uniquely towards word reading while rhythm discrimination along with statistical learning uniquely contribute to reading comprehension performance in children. Interestingly, both aSL and vSL contribute uniquely towards reading scores indicating that SL may be subject to modality constraints. Recent research indicates that SL is relatively independent from cognitive tasks such as working memory, IQ implying that SL is not a nested cognitive ability (Sigelman et al., 2015). Our results suggest that SL along with rhythm discrimination could help a reader by enabling detection of statistical regularities and thereby efficiently segmenting words for reading. A future model of reading using a larger sample size should encompass factors such as SL, frequency discrimination and music skills to adequately explain variance in reading outcomes.

Funding

Australia Awards Scholarships and HEARing CRC

SYMP 73

Ultra-short Synaptic Delays at a Mature CNS Auditory Synapse

Henrique von Gersdorff

Oregon Health & Science University, Portland

Auditory sensory information is conveyed by neurons specialized to faithfully transmit large amounts of information at high rates. A key event in synaptic transmission is the exocytosis of synaptic vesicles at presynaptic terminals triggered by calcium influx. The calyx of Held synapse in the mammalian brainstem has a "giant" presynaptic terminal with multiple conventional active zones that release glutamate. It plays a pivotal role in the circuitry that computes sound source localization. This nerve terminal can reliably fire at very high frequencies (up to 1 kHz). This ability to spike with high fidelity may be crucial for the task of localizing sound and discriminating pitch. What are the specialized mechanisms that allow the calyx of Held nerve terminal to fire reliably at 1 kHz and for the postsynaptic cell to follow stimulation frequencies near 1 kHz?

To answer this question we are studying neurotransmitter release at this synapse in more mature rodents at physiological temperatures. We are investigating the mechanisms that modulate exocytosis and presynaptic excitability at these calyx-type synapses. We have found that synaptic vesicle fusion probability is reduced during early postnatal development at this synapse because presynaptic action potential half-width is progressively reduced to values of about 130 microseconds. However, vesicle pool size increases dramatically during development to produce a nearly "fail-safe" synapse even near 1 kHz stimulus frequencies.

My lecture will describe recent studies of this synapse that have concentrated on investigating the fundamental mechanisms of spike timing precision at this synapse and the factors that determine the size of the readily releasable pool of vesicles and release probability. I will present a combination of EM tomography data, together with *in vivo* single unit recordings and *in vitro* patch clamp electrophysiological studies of the calyx of Held synapse in postnatal day 30 mice. Using experiments that involve the block of presynaptic Ca^{2+} channels I will show how ultra-short synaptic delays arise during postnatal development.

SYMP 74

Functional and Morphological Continuum at the Calyx of Held Synapse

Lu-Yang Wang

SickKids Research Institute & University of Toronto

The calyx of Held synapse is a critical station converting contralateral excitatory inputs to inhibitory outputs to ipsilateral LSO and MSO to encode interaural timing and level differences (ITD & ILD) as cues for localizing sound in space. We have previously discovered a functional and morphological continuum in the fidelity of neurotransmission at this synapse (Grande & Wang J Neurosci 2011): simple calyces with a few stalks show high release probability (Pr), small readily-releasable pool (RRP) of synaptic vesicles (SVs) and short-term depression (STD), and complex calyces with stalks and additional swellings have low Pr but large RRP and display short-term facilitation (STF) preceding STD. Consequentially, postsynaptic spiking during high-frequency inputs can only be phase-locked near the early onset of stimulation for simple calyx synapses, but fully sustained for complex calyx synapses, suggesting morphological

heterogeneity is one of the important. underpinnings of functional diversity for expanding the dynamic coding range of acoustic information. This talk will present new data with 2-photon Ca2+ imaging, paired patch-clamp recordings and computer simulations to demonstrate how variability in the number of calcium channels and their spatial couplings to SVs in active zones impart the calyx of Held synapse with synaptic heterogeneity and ultimately different phase-locking spike phenotypes.

SYMP 75

A role of myelin in setting structural and functional properties of the auditory nerve terminal

Jun Hee Kim[1]; Emmanuelle Berret[1]; Christopher Kushmerick[2]
[1]University of Texas Health Science Center; [2]ICB Universidade Federal de Minas Gerais

Axon myelination increases conduction velocity and serves to transmit neuronal signals precisely, thus demyelination is associated with neurotransmission dysfunction. Although negative effects of demyelination are generally attributed to conduction failure, accumulating evidence suggests that myelin also regulates structural properties and molecular composition of the axonal membrane. Here, we investigated how myelination affects ion channel expression and function, targeting particularly the last axon heminode, which has been shown to regulate excitability of the calyx of Held terminal. We compared the structure and physiology of normal axons and those of the LES rat, which lacks compact myelin and is a model for central dys-/demyelinating diseases. In normal axons, Na^+ channels clustered in the node and last heminode, but were largely absent from the calyx terminal. Consistent with this, the rise in intracellular Na^+ during action potentials was larger and faster in the heminode than in the terminal. This normal segregation of Na^+ channel expression and dynamics was lost in the calyx of Held terminals from LES rats. Specifically, Na_V-a subunits were dispersed and Na_Vb4 subunit was absent, whereas K^+ channels were increased. Na^+ resurgent and persistent currents were correspondingly reduced and K^+ current was increased, reducing presynaptic excitability and increasing action potential failures in the LES rat. Together these data point to a specific role for compact myelin in dictating protein expression and function at the axon heminode and regulating excitability of the terminal.

SYMP 76

Synaptic Vesicle Release Mechanisms to Support the Initial Stages of Auditory Processing

Samuel Young
Max Planck Florida Institute for Neuroscience

Encoding the onset and modulation of sound at the initial stages of auditory processing requires that synapses respond to rapid and large fluctuations in firing rates over variable timescales, superimposed on a broad range of spontaneous activity. Chemical synaptic transmission relies on a limited number of fusion competent synaptic vesicles (SVs) in the presynaptic terminal, termed the readily releasable pool (RRP); thus sound encoding places great demands on the temporal dynamics of SV release and recycling. Critical to the binaural processing of sound is the calyx of Held, a giant axosomatic glutamatergic presynaptic terminal that arises from the globular bushy cells (GBC) in the cochlear nucleus. The calyx preserves temporal fidelity of the afferent spike train in its patterns of SV release to drive postsynaptic spiking in the principal neurons of the medial nucleus of the trapezoid body (MNTB). The MNTB relays these activity patterns as inhibitory inputs to key binaural cell groups. Due to its experimental accessibility the calyx provides unparalleled opportunities to gain insights into presynaptic mechanisms that support the early stages of auditory processing. Ultimately, the molecular mechanisms that underlie efficient release and replenishment of SVs underpin synaptic integration and sound encoding. A key step in the pathway that regulates temporal dynamics of SV release and recycling within the RRP is priming, the creation of fusion competent SVs that are tightly coupled to voltage gated Ca^{2+} channels (VGCCs) at the active zone (AZ). Using electrophysiological and biophysical methods, in conjunction with mouse transgenic lines and viral vector technology to perturb key synaptic proteins at the calyx, we have begun to uncover the cellular and molecular mechanisms that regulates priming and their impact on SV release replenishment. Here our recent results will be discussed in addition to their potential impact on high-fidelity sound encoding.

SYMP 77

Heterogeneity Across Structural Compartments in the calyx of Held

George Spirou[1]; Dakota Jackson[1]; Paul Holcomb[1]; Henrique von Gersdorff[2]
[1]West Virginia University; [2]Oregon Health and Sciences University

The calyx of Held (CH) is a typically mammalian structure and is one of the largest nerve terminals in the brain. We have studied CH structure in a postnatal day (P)30 mouse at the nanoscale using serial blockface scanning electron microscopy (SBEM) and electron tomography (ET). Using SBEM, we reconstructed a single CH and counted 286 synapses formed with the postsynaptic cell body. The CH consisted of compartments ranging from large irregular shapes to medium and small sized boutons, linked by segments of varying thickness with some as narrow as 150 nm diameter. Large compartments formed more synapses than smaller compartments. We skeletonized the structure, revealing that it has a tree branch organization with no closed loops. The CH contained an internal linking segment that was myelinated. A myelinated branch extended a short distance to innervate the proximal dendrite of an adjacent postsynaptic neuron via a contact area with 17 synapses. ET revealed heterogeneity in the numbers of docked vesicles per active zone. This value averaged 7.2 ± 2.9 and 4.9 ± 2.8 (mean ± sd) docked vesicles in two animals, which was greater than values reported for younger rats. Multi-axis tilt series

permitted high-resolution measurement of free space in the terminal. Approximately one-third of the volume in the first 40 nm thick shell volume adjacent to the AZ was unstained, and considered to be free space. The total number of vesicles in a volume extending 160 nm from the AZ varied nearly seven-fold (22 to 140 vesicles). As previously described, the synaptic vesicle population was confined along the edges of CH compartments, with mitochondria forming a shell around a cytoskeletal core. Collectively, these data argue for tight coupling between Ca^{2+} currents and synaptic vesicle fusion, and specializations to synchronize activation of multiple calyx compartments with heterogeneous structural features.

SYMP 78

Mechanisms and Models of Rapid Synaptic Transmission at the Endbulb of Held

Paul Manis[1]; Luke Campagnola[1]; Ruili Xie[2]
[1]University of North Carolina at Chapel Hill; [2]University of Toledo

The central auditory system utilizes a collection of specific cellular mechanisms to help interpret the rapidly changing features of the acoustic environment. These mechanisms enhance the representation of temporal features on multiple time scales. This presentation will discuss these mechanisms, and examine their representation and consequences in computational models that are used to explore hypotheses regarding the specific roles of different mechanisms.

SYMP 79

Wnt signaling and stem cell control

Roel Nusse
Stanford University

Our laboratory is interested in the growth, development and integrity of animal tissues, with a focus on stem cells. Wnt signaling is widely implicated in stem cell control, as a mechanism to regulate the number of stem cells in tissues, Using various cell labeling methods, we have described novel populations of stem cells in various tissues, including in the liver. In that tissue, we found that hepatocytes that reside in the pericentral domain of the liver demonstrate stem cell behavior. Although these cells are functional hepatocytes, they are diploid and thus differ from the mostly polyploid mature hepatocyte population. They are active in homeostatic cell replacement and therefore distinct from oval cells, which require injury for their induction. Adjacent central vein endothelial cells provide the essential source of Wnt signals for the hepatocyte stem cells and thereby constitute the liver stem cell niche. It is noteworthy that liver cancer is often characterized by loss of function mutations in negative components of the Wnt pathway, including Axin and APC. We suggest that pericentral hepatocyte stem cells, normally controlled by a paracrine Wnt signal, are precursors to liver cancer

SYMP 80

The Role of Wnt/ß-catenin in Adult Taste Bud Homeostasis.

Linda Barlow
University of Colorado School of Medicine

Taste buds are the primary end organs for gustation, or the sense of taste. Most taste buds reside in specialized papillae on the tongue. Fungiform taste papillae, each housing one bud, are distributed throughout the surface of the anterior tongue, while the larger, more specialized circumvallate and foliate papillae each with 100s of taste buds are situated in the posterior tongue. In mice, each taste bud is a collection of ~60 heterogeneous cells, which detect the presence of 5 primary tastes, i.e., sweet, bitter, sour, salt and umami (glutatmate) in the oral cavity. Individual taste qualities are transduced by specific taste receptor cell types that are present in particular ratios in each bud; Type III taste cells are least common and detect sour, while non-overlapping subsets of Type II cells, which together make up ~20% of cells, respond to sweet, bitter or umami. Additionally, Type I cells, which comprise 50% of cells per bud, function as support cells but may detect NaCl. Importantly, all taste cells are rapidly and continually renewed, with a half life of 8-21 days depending on taste cell type. Nonetheless, our sense of taste is remarkably stable. Using inducible molecular genetic tools, we have investigated the role of the Wnt/ß-catenin pathway in the process of taste bud cell renewal in adult mice. We find that ß-catenin function is required for the continual production of new taste cells from taste bud progenitor cells. Further, we find that loss of ß-catenin in taste bud progenitors slows their proliferation and results in a gradual loss in taste function, assessed behaviorally via a limited access taste test. We have also found that ß-catenin influences the fate of newly generated taste cells; ß-catenin gain-of-function, in addition to causing taste progenitors to cease dividing, drives these new daughter cells to become almost exclusively Type I glial cells, with limited induction of Type II taste cells. Thus, ß-catenin functions in taste progenitor cells to regulate both their proliferation and fate selection of post-mitotic daughter cells. Our working model is that ß-catenin levels, in concert with expression of specific co-transcription factors, are crucial for renewal of the precise ratio of taste cell types and for continued taste function throughout life.

SYMP 81

The Wnt-astic Cochlea in Development and Potential for Regeneration

Alain Dabdoub; Joanna Mulvaney; Teppei Noda; Ruishuang Geng
Sunnybrook Research Institute, University of Toronto

Canonical and non-canonical Wnt signaling pathways are essential in multiple developmental processes where specific functional activities of Wnt signaling are context and developmental stage dependent. In the inner ear, canonical Wnt/beta-catenin signaling has been shown to play a major role in several phases of development, including early otic placode specification, proliferation, and cell fate

determination. Furthermore, the non-canonical Wnt/planar cell polarity pathway has been demonstrated to influence cell orientation and convergent extension movements in the cochlear duct, while a role for the non-canonical Wnt/Calcium signaling pathway in the cochlea remains to be determined.

Using genetic fate mapping and Wnt signaling reporter mouse lines, recent studies have demonstrated that canonical Wnt/beta-catenin signaling is active in the developing cochlea; however, specific Wnt signaling components that facilitate this Wnt activity have yet to be identified. We therefore investigated the expression of Wnt signaling molecules including Wnt ligands, Frizzled receptors, co-receptors, and Wnt inhibitors and modulators in the cochlea. We used embryonic day 12 cochlea when canonical Wnt is active, proliferation is occurring and the prosensory region can be analyzed; postnatal day 0, when cellular patterning is complete and exogenous activation of Wnt has been reported to have a response; postnatal day 6, when activation of canonical Wnt signaling has no apparent effect; and adult cochlea.

In canonical Wnt signaling, Wnt proteins bind to Frizzled receptors to bring about context-dependent effects that are contingent on multiple co-receptors and downstream signaling through beta-catenin and Tcf/Lef co-factors. Identification of membrane bound and secreted components of Wnt signaling in the mammalian cochlea is an initial step in functional analyses to understand their role in developmental processes, with the long-term aim of applications in sensory hair cell regeneration. Through gene expression analysis of the developing cochlea, we investigated the presence and location of extracellular components of the Wnt pathway. We have identified Kremen1, a kringle domain containing a single pass transmembrane protein, as a candidate modulator of canonical Wnt signaling during cell fate determination in the developing cochlea. Through gain- and loss-of-function experiments, we determined that Kremen1 is involved in segregation of cells in the nascent organ of Corti, between sensory and non-sensory cell fate.

SYMP 82

Identification of Progenitor Cells in the Cochlea: Lgr5-positive Supporting Cells

Albert Edge
Harvard Medical School

Wnt signaling is required for the differentiation of hair cells during embryogenesis. Wnt stimulates otic progenitors to express transcription factor, Atoh1, which is required for hair cell development. Lgr5, a downstream target of the Wnt pathway and a protein that marks intestinal epithelial stem cells, is expressed in Lgr5-positive cells that gave rise to hair cells based on lineage tracing. Lgr5 continued to be expressed in the postnatal cochlea in a specific subset of supporting cells. In vitro analysis showed that Lgr5-positive cells had distinct phenotypes from the other (Sox2-positive) supporting cells and differentiated to hair cells at a higher rate, consistent with these cells playing a role as hair cell progenitors. The in vitro studies also showed that hair cells did not differentiate from Lgr5-negative cells. Hair cell replacement seen following ototoxic damage in neonatal ears was due to supporting cell transdifferentiation to hair cells, directly, or after cell division in a spontaneous response to damage, without pharmacological intervention. The response to damage was accompanied by Wnt release and was blocked by inhibition of Wnt signaling. Both cell division and hair cell differentiation were increased by treatment with an inhibitor of gamma-secretase. Based on lineage tracing, upregulation of Wnt signaling in the newborn inner ear, even in the absence of damage, specifically targeted the Lgr5-expressing cells, leading to proliferation, and the cells transdifferentiated to hair cells after increasing expression of Atoh1, which was downstream of Wnt. These data suggest that manipulation of signaling pathways increases regeneration of hair cells and that Lgr5-positive cells act as hair cell progenitors in the cochlea.

SYMP 83

Fgf/Notch/Wnt Signaling Interactions Control Progenitor Maintenance and Differentiation During Zebra fish Hair Cell Regeneration

Tatjana Piotrowski; Mark Lush; Andres Romero-Carvajal
Stowers Institute for Medical Research

Deafness due to sensory hair cell loss is one of the most widespread disabilities in the world. In contrast to mammals, all non-mammalian vertebrates regenerate hair cells throughout life. The differences in the gene regulatory network that underlies hair cell regeneration is not well understood, however intimate knowledge of these interactions is crucial for the development of strategies to induce hair cell regeneration and the restoration of a functional sensory epithelium in mammals. Zebra fish possess hair cells in their sensory lateral line system, located superficially in the skin. Our research takes advantage of the accessibility of the lateral line system and utilizes genetic tools and interdisciplinary approaches to investigate the genes and pathways crucial for hair cell regeneration. The ability to manipulate multiple signaling pathways and monitor their impact on cell properties and behaviors in vivo make the zebra fish lateral line system an ideal model for the elucidation and functional characterization of the complex cross-talk between signaling networks. The lateral line sense organs (neuromasts) consist of a central core of hair cells that are surrounded by inner support cells and mantle cells. We developed a powerful assay combining long-term time-lapse analyses, with BrdU/cell fate analyses and in situ hybridization experiments that allows the functional interrogation of signaling pathways. Individual and combinatorial manipulations of the Fgf/Notch/Wnt signaling pathways revealed the interactions underlying the regulation in the balance of progenitor cell self-renewal and differentiation that occur in different compartments of the sensory organs and ensure a life-long ability to regenerate hair cells. Our detailed studies performed at the single cell level provide important new insights into the regulation and behavior of stem cells in vivo and for the design of experiments aimed at triggering proliferation and regeneration of hair cells in the mammalian inner ear.

SYMP 84

Dissecting the Wnt signaling machinery during cochlear development and regeneration

Alan Cheng
Stanford University

Wnt signaling plays diverse roles during development and disease in numerous organ systems. Traditionally, beta-catenin is considered the central mediator of canonical Wnt signaling. By combining different combinations of Wnt ligands and Frizzled receptors, Wnt proteins can also exert effects on Wnt-responsive cells in a beta-catenin-independent manner, via a non-canonical pathway. Recent studies have shown that deletion of beta-catenin during inner ear development inhibits the formation of sensory hair cells. Conversely, stabilizing the protein and thus effectively increasing the levels of beta-catenin not only induces proliferation in the postmitotic cochlear duct, but also formation of extranumerary hair cells. Results from these gain- and loss-of-function experiments point to a role of canonical Wnt signaling in establishing hair cell formation. This contrasts the observed phenotypes of hair cell patterning and convergence-extension defects seen in animals deficient in defined Wnt ligands. It remains unclear how the different components of the Wnt signaling pathway, canonical as well as non-canonical coordinate to regulate hair cell development, patterning and possibly even regeneration. In this talk, I will present work from my laboratory aiming to characterize part of this Wnt signaling machinery in the developing cochlea.

PD 123

Interaural level differences are dominantly evaluated prior to modulation maxima

Bernhard Seeber; Amelia Jiménez Sánchez; Aswin Wijetillake; Marko Takanen
Technische Universitaet Muenchen

Natural sounds, such as speech, comprise amplitude modulations with onsets, offsets and local maxima. When localizing sounds, binaural information is most heavily weighted at sound onsets (Hafter and Dye, 1983) and the salience of interaural time differences (ITD) is greatest at a point prior to modulation maxima (Dietz et al., 2013). However, the precise temporal distribution of perceptual weights for interaural level differences (ILD) remains unclear. Such an investigation has challenges since it is difficult to manipulate ILDs on short timescales without altering the long-term ILD. The aim of the current study was to characterize the temporal weighting of modulated ILDs, while controlling for short- and long-term ILDs. The results demonstrate that ILDs are more effective when conveyed at points prior to modulation maxima.

The efficacy of ILDs conveyed at different phases of the modulation cycle was studied in two experiments: one using a spatial discrimination paradigm and the other measuring lateralization. The stimuli comprised 4-kHz-carrier tones with 50, 100 and 200 Hz SAM. ILDs were applied to specific phases (30°, 60°, 90°, 120° or 150°) of each modulation cycle by scaling the signal with a 1-ms-long Gaussian window. In the first experiment, the introduced short-term ILDs were varied adaptively, while the long-term ILDs were compensated for, to find the threshold for correctly identifying left-right vs. right-left stimulus movements. In the second experiment, the lateralization percepts elicited by short-term ILD adjustments, without long-term compensation, were compared to those elicited by unmodified SAM tones with long-term ILDs of 0, 1, 2, 4, 7 and 10 dB.

The results from both experiments show that concentrating an ILD around positions on the rising flank around 30° to 60° of each modulation cycle yields more efficient lateralization than when the ILD is concentrated in later parts of the modulation cycle. At low modulation rates ILDs placed on the rising flank are also more effective than when placed at 90° in the energetic maximum of the signal. An ILD produced greater lateralization when concentrated on the rising flank than when its energy was spread across the entire stimulus. Hence, ITD- and ILD-based localization seem to share a similar emphasis of binaural cues around modulation maxima, which is useful for localization of speech and other complex sounds in reverberant environments.

Funding
Supported by BMBF 01 GQ 1004B (Bernstein Center for Computational Neuroscience). AJS was supported by an Erasmus studentship.

PD 124

Phase-encoding maps for ILD preferences in the human auditory cortex

Sandra Da Costa
Vanderbilt University Medical Center

Several fMRI studies have used phase-encoding paradigms to highlight topographic representations in various modalities (for review see Engel, 2012), including audition. Here, we apply the phase-encoding approach to study the cortical organization of tuning to spatial hearing cues–specifically, Interaural Level Difference (ILD). Phase-encoding maps of both frequency and ILD preference were acquired in normal hearing subjects at 3T, revealing the cortical organization of preferred ILD within the primary auditory cortex (PAC) and the vicinity of the planum temporale (PT).

First, subjects listened passively to progressions of pure tone bursts (88 to 8000 Hz) presented in 32s-blocks during two 8min runs. This paradigm has been used previously as PAC localizer, based on a gradient of frequency preferences across the Heschl's gyrus (HG). Then in a phase-encoding ILD experiment, participants listened to a series of complex-tone (CT) bursts that progressed slowly in ILD (±21 dB left to right or right to left over 34s). Bursts were presented either (1) alone or (2) in alternation with a competing CT burst at 0 dB ILD. Both conditions were presented in 34s-cycles during runs of 8.5 minutes. We hypothesised that the latter condition would increase ILD selectivity and produce clearer mapping than the former. The phase-encoding analysis was

applied to both experiments to extract cross-correlation maps for preferred frequency and ILD, which were then projected into partially inflated brain surfaces.

Tonotopic mapping (Fig1.A) showed mirror-symmetric gradients of frequency preferences within PAC in an oblique orientation across HG, reproducing previous findings using the same approach (Da Costa et al., 2011; Da Costa et al., 2014) and demonstrating the robustness of the phase-encoding analysis. Cross-correlation results for competing CT bursts (Fig1.B, upper panel) revealed a preference for contralateral ILD within bilateral PAC, consistent with previous single-unit and human imaging studies (Stecker et al., 2005, 2015). Voxels with preference for midline and ipsilateral positions were also found, in PAC and the vicinity of bilateral PT, respectively. These effects were less strong in the non-competing condition (Fig1.B, lower panel).

Our results highlight the cortical organization of ILD preference in individual hemispheres, with consistent contralateral preferences in the both PAC and some restricted ipsilateral preference in both PT. These effects were greater in progressive pairs of competing CT bursts, compared to progressive CT bursts alone.

Funding
This work was supported by National Institute of Health grant R01-DC011548 to G. C. Stecker and by Swiss National Foundation grant P2LAP3-158671 to S. Da Costa.

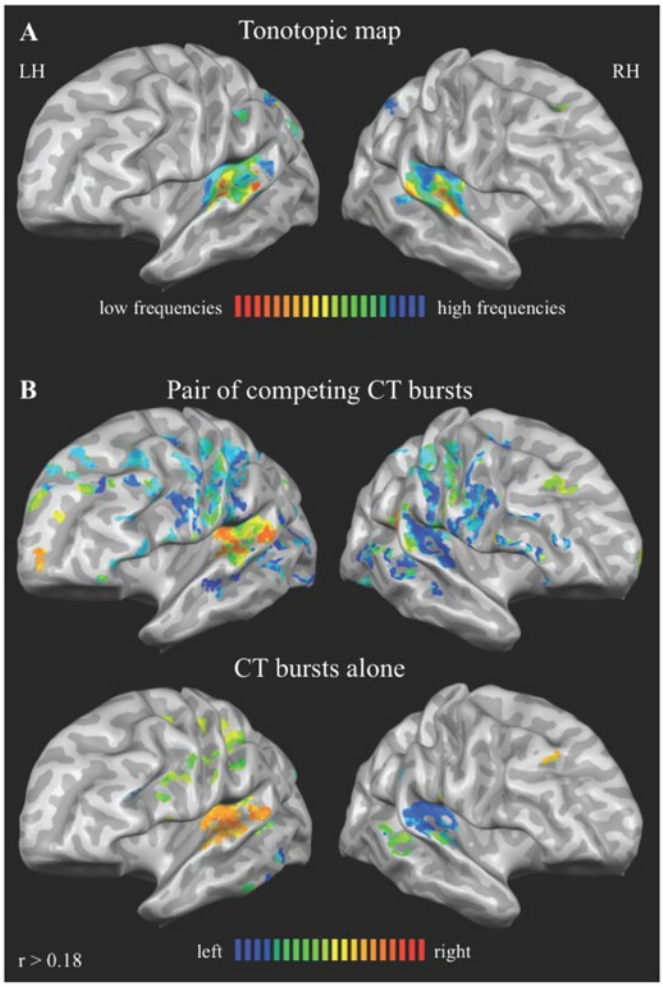

Figure 1. Phase-encoding maps in the human auditory cortex for frequency (A) and ILD preferences (B).

PD 125

Physiology-based engineering solution to the cocktail party problem: spatial sound-source segregation using stimulus reconstruction

Junzi Dong; H. Colburn; Kamal Sen
Boston University

Computational methods for separating single sources of sound in complex, multi-source environments have been intensively studied, and a variety of solutions including microphone arrays, meta-materials, and computational auditory scene analysis algorithms have been proposed. Here we present an engineering solution based on computational models of sound source segregation and stimulus reconstruction for separating sound sources in space using natural binaural inputs. Motivated by the potential to apply the method in modern hearing assistive devices, the model takes realistic binaural speech like those recorded in the binaural inputs of hearing aids. Using these inputs, a sequence of physiology-based computational models of spatial sound-source segregation—including Jeffress-type delay line cross-correlation models and a source selection cortical network model from our previous work—generates a neural output that encodes speech from the desired location. To translate

this neural output back to the acoustic domain, we apply stimulus reconstruction using reconstruction filters derived from training stimuli and neural responses. The final output is a reconstruction of the speech waveform corresponding to the original stimulus in the direction of interest. We quantify the degree of separation and the quality of reconstructed speech, and show that this approach may be a new way to perform sound-source segregation in a method similar to the brain.

Funding
NIH/NIDCD R01 DC00100 NIH/R90 DA 033460

PD 126

ITD Decoding of Complex Sounds in a Model of the Mammalian MSO.

Jörg Encke; Werner Hemmert
Technische Universität München

Mammals locate sound sources in the horizontal plane with two mechanisms. Low frequency sounds are located by exploiting the difference in arrival time between the two ears (interaural time differences ITDs) while for high frequency sounds additional interaural level differences (ILDs) are available. In mammals, the medial superior olive is thought to be the first stage, where ITDs are decoded. In-vivo measurements in gerbils indicate that they use the slope of the ITD-rate function to decode ITDs [Brand2002].

We investigated the robustness of such a strategy by using a spiking neuron network model of the physiological MSO circuit in mammals. The network consists of a Hodgkin Huxley type MSO model which is directly excited by ipsi- and contra-lateral auditory nerve fibers [Zilany2014]. Bilateral inhibition is relayed via globular bushy cells. We also used a feed forward artificial neural network (ANN) as a simplified model of higher processing stages, which compensates level-dependent spike-rate changes. The presented MSO model is able to produce ITD-rate functions consistent with “in-vivo” measurements in the MSO of gerbils [Pecka2003]. This includes the reported shift in the maximum of the ITD - firing rate relationship. By simply using the firing rate difference between the MSO models of both hemispheres, the model could predict the ITD for simple sounds like pure-tones. More complex signals like speech introduced an additional modulation of the firing rates due to changing sound levels. A simple ANN, which was trained on the output of the MSOs and also the firing rates of the primary auditory nerve fibers from the left- and right ear, achieved good prediction for non-stationary sounds like spoken words.

The performance of the system was also robust in noise.

These results indicate that a full Jeffress-like correlation model is not required for robust ITD prediction and that slope-based decoding strategies for ITDs transmit sufficient information.

[Brand2002] Brand, A., et al. (2002). Precise inhibition is essential for microsecond interaural time difference coding. Nature, 417(6888), 543–7.

[Zilany2014] Zilany, M. S. et al. (2014). Updated parameters and expanded simulation options for a model of the auditory periphery. The Journal of the Acoustical Society of America, 135(1), 283–6.

[Pecka2008] Pecka, M. et al. (2008). Interaural time difference processing in the mammalian medial superior olive: the role of glycinergic inhibition. The Journal of Neuroscience : The Official Journal of the Society for Neuroscience, 28(27), 6914–25.

Funding
This work was funded by the German Research Foundation within the Priority Program “Ultrafast and temporally precise information processing: normal and dysfunctional hearing” SPP 1608 (HE6713/1-1) and the German Federal Ministry of Education and Research within the Munich Bernstein Center for Computational Neuroscience (referencenumber 01GQ1004B).

PD 127

Human Performance and a Biophysically-Based Model for ITD Discrimination to Very Low Frequency

Andrew Brughera[1]; Tianshu Qu[2]; Zane Crawford[3]; William Hartmann[3]
[1]Boston University; [2]Peking University; [3]Michigan State University

Background
Sound from an acoustic source located to the side arrives first at the near ear, producing an interaural time difference (ITD), which facilitates sound localization and improves speech reception in noisy environments. Sensitivity to ITD is derived in the left and right medial superior olive (MSO) of the auditory brainstem. MSO neurons receive bilateral excitation via the ventral cochlear nuclei (VCN), and inhibition via the medial and lateral nuclei of the trapezoid body (MNTB and LNTB, contralaterally and ipsilaterally driven, respectively).

Methods
Human discrimination thresholds of interaural time difference (ITD) were adaptively measured for pure tones from 1000 to 39 Hz, and human performance was modeled with a rate-difference display model composed of fitted rate-ITD functions of two identical biophysically-based model MSO neurons with opposite best-ITDs. In the computational model, MSO neurons received realistic excitatory and inhibitory synaptic inputs in terms of number, spike rate, and synchrony. These inputs reflect discharge patterns of bushy cells in the VCN, with spike rates about twice those in auditory nerve (AN) fibers, and synchrony at or above that in the AN. At 150 Hz, a long delay of excitation relative to inhibition contributed to a realistic rate-ITD function in the model, and this technique was continued at lower frequencies. While the use of large axonal delays at very low frequencies remains somewhat conjectural, significant axonal delays in excitatory projections to MSO neurons have been observed physiologically.

Results
With input synchrony similar to the AN, the model matched human ITD discrimination performance down to 125 Hz, and performed somewhat worse than humans by 39 Hz. Realistic best-ITDs may contribute to the matching performance, and an additional explicit model for a VCN neuron driven by three AN fibers suggests a realistic mechanism for maintaining synchrony and increasing spike rate relative to the AN. ITD discrimination in the model at very low frequency was improved by a more rapid transition in spike rate across the physiological range of ITD by head width, via either higher input synchrony or saturated rate-ITD functions. Rate-ITD functions of the model MSO neuron generally matched physiologically measured rate-ITD functions from previous studies, including at the lowest physiologically-measured frequency of 150 Hz.

Conclusion
Overall the model suggests that for a wide range of frequency, a small number of MSO neurons driven by realistic excitatory and inhibitory inputs are sufficient for the ITD sensitivity that is observed physiologically and psychophysically.

Funding
Grant 61175043 from the National Natural Science Foundation of China brought TQ to Michigan State; TQ supported by NIDCD grant DC-00181 and the AFOSRgrant 11NL002. ZDC supported by the Michigan State Professorial Assistant Program and by an Alumni Distinguished Scholarship. AB supported by NIDCD grants DC-00100 and P30-DC04663.

PD 128

In Vivo Whole-Cell Recordings of the Lateral and Medial Superior Olive to Interaural Time Differences of Transients

Tom Franken[1]; Philip Smith[2]; Philip Joris[1]
[1]University of Leuven; [2]University of Wisconsin - Madison

Humans show exquisite behavioral sensitivity to interaural time differences (ITDs) of acoustic transients (Klumpp and Eady, 1956; Hall 1964), but little is known regarding neural responses to such ITDs. The few existing *in vivo* data point to interesting phenomena (Carney and Yin, 1989; Irvine et al., 2001; Joris and Yin, 1995) which call for examination at the intracellular level. In addition, acoustic transients resemble the electrical shock stimuli used in *in vitro* studies of neurons in the superior olivary complex (SOC), so that an *in vivo* intracellular study to click-ITDs offers the prospect of coupling behavior to cellular mechanisms.

Studies of responses of the SOC to acoustic transients are scarce primarily because strong stimulus-locked field potentials hamper spike isolation from single neurons, particularly in the medial superior olive (MSO). We used *in vivo* patch recording techniques to study neurons in the gerbil lateral superior olive (LSO) and MSO. Sub-threshold synaptic and supra-threshold spike responses were obtained in response to monaural and binaural clicks. Approximately half of the neurons recorded were successfully labeled with biocytin and positively identified as LSO or MSO neurons.

In MSO neurons, plots of ITD-sensitivity to clicks were surprisingly shallow, even when these neurons showed clear modulation of spike rate to ITDs of pure tones. Typically a broad peak of increased firing rate was imposed on a general elevation of spike rate, but with little modulation of spike rate within the approximate ecological range of ITDs. The responses to monaural clicks tended to consist of a single EPSP at low stimulus levels, and multiple events at higher SPLs, and these responses often poorly predicted the binaural responses. In contrast, ITD-functions to clicks of LSO neurons frequently displayed steep slopes bordering a trough within which the response was completely suppressed. These slopes could be positioned within the ecological range of ITDs. Comparison of monaural and binaural responses showed a systematic relationship of timing of EPSPs and IPSPs to the spiking response. Remarkably, at a given dB level, the contralateral IPSP could arrive before the ipsilateral EPSP.

We conclude that sensitivity to ITDs of transients is more prominent in LSO than in MSO. This result is consistent with the notion that specializations in the LSO and its afferent neurons, which suggest a role for timing, have evolved to generate spatial sensitivity for a class of stimuli for which an EE-interaction as present in the MSO is poorly suited.

Funding
Supported by a doctoral fellowship of the Research Foundation - Flanders (FWO) to T.P.F., NIH R01 DC012782 to P.H.S. and P.X.J., and grants to P.X.J. from FWO (FWO G.091214N and G.0961.11) and Research Fund KU Leuven (OT/14/118).

PD 129

Perceptual Weighting of Conflicting Interaural Timing Cues by Stimulus Envelope and Fine Structure of Bandpass Noise

Torsten Marquardt; Lee Wah
University College London

Background:
The lateralization of 500-Hz centred bandpass noise with 1.5 ms ITD changes with increasing bandwidth (20 – 400 Hz) from the side of the lagging ear to the side of the leading ear. The weighted image model (Stern et al., 1988) explains this phenomenon based on the pattern produced by the interaural cross-correlogram: Individual modes in this pattern receive greater weighting when they are straighter and/or more central (closer to zero delay). Interpreted in the time course of the above stimulus, the straight mode at the 1.5 ms delay can be attributed to the envelope ITD, and the contradicting -0.5 ms delay position of the most central mode at 500 Hz is associated with the average ITD of the stimulus fine structure. In this study, we varied various stimulus parameters to examine their effect of the relative weighting of ITD in envelope (straightness) and fine structure (centrality).

Method
In a 2 AFC procedure, the stimulus bandwidth was adaptively adjusted by a MLT procedure to the value for which subjects reported lateralization equally to either side. We call this

bandwidth the centring bandwidth, cBW. (Note, however, that the perceptual image was then often reported to be split into two equally strong sources located to either side, their lateralisation presumably based on envelope and fine structure ITD).

Average results for 6 subjects: For the majority of subjects, the cBW was fairly constant across centre frequency (250 – 750 Hz). The cBW increased with decreasing interaural coherence (1.0 to 0.8), but decreased with stimulus level (30 – 70 dB SPL), stimulus duration (0.125 – 2 s), envelope ITD (1.167 – 1.833 ms; IPD of FS fixed to 90°) and crest factor. The cBW had a maximum when the fine structure IPD was near 45° (envelope ITD fixed to 1.5 ms). Deviation of the stimulus ITD of a 500-Hz-centred noise from 1.5 ms in either direction (1.167 – 1.833 ms) lowered the cBW. (Note that this parameter affected both, envelope and fine structure ITD.)

Conclusion
These results will hopefully facilitate the extension/development and validation of binaural models. We argue that these findings are more meaningfully explained in terms of envelope versus fine structure ITD weighting than straightness versus centrality.

R M Stern, A S Zeiberg & C Trahiotis (1988) Lateralization of complex binaural stimuli: A weighted-image model. J. Acoust. Soc. Am. 84 (1), 156 - 65.

Funding
Supported by the Medical Research Council, UK.

PD 130

Modeling the Cochlear Phase Response Estimated in a Binaural Task

Hisaaki Tabuchi[1]; Bernhard Laback[2]; Piotr Majdak[2]; Thibaud Necciari[2]; Katharina Zenke[2]
[1]Austrian Academy of Sciences; [2]Austrian Academy of Sciences, Acoustics Research Institute

Background
The human cochlear phase response is mostly measured by means of the masking effect of harmonic complexes with various phase curvatures on a tonal target, yielding differences in masking of up to 20 dB. There is evidence that signals yielding peaky internal masker representations after passing the cochlear filter produce minimum masking, with the fast-acting cochlear compression as the main contributor to that effect. Thus, in hearing-impaired listeners showing reduced or absent compression, the estimation of the phase response using the masking method might be difficult. The phase response can alternatively be measured by estimating the sensitivity to interaural time differences (ITD) [Tabuchi et al., ASA abstract, 2015]. Here we present model predictions of the experimental results.

Methods
The stimuli were 300-ms Schroeder-phase harmonic complexes ranging from 3400 to 4600 Hz with a 100-Hz fundamental frequency. Left/right discrimination scores were measured as a function of ITD from 25 to 1600 µs, for phase curvature, C, varying from -1 to 1 in seven normal-hearing listeners. The ITD thresholds at 80 percent correct were estimated from psychometric functions. Predictions were based on neural spike simulations from an auditory periphery model [Zilany et al., 2014]. For each ear, the monaural synchronization index (SI) corresponding to the fundamental frequency was computed. The binaural analysis was done by computing a receiver operating characteristic (ROC) cross-correlation between the left- and right-ear period histograms [Prokopiou et al., CIAP abstract, 2015].

Results
ITD thresholds were low around C=0 and increased towards C=±1. An unexpected threshold peak (reduced sensitivity) was consistently observed at C=-0.5. Both the monaural SI and the ROC-based model predicted the general pattern of thresholds across C, but they did not account for the threshold peak. The ROC-based model was also able to predict the effect of the attack and pause durations in signal envelopes [Klein-Hennig et al., 2011].

Conclusion
Low ITD thresholds were observed for phase curvatures similar to those producing minimum masking, suggesting that the ITD method is a promising candidate for estimating the cochlear phase response in hearing-impaired listeners. While the model predictions were generally consistent with the experimental data, further work is required to explain the results for particular phase curvatures.

Funding
[Supported by Austrian Science Fund (FWF), P24183-N24]

SYMP 85

The Onset of Visual Experience Regulates Auditory Developmental Plasticity

Dan Sanes; Todd Mowery; Melissa Caras; Vibhakar Kotak
New York University

The developing nervous system is profoundly influenced by sensory experience. Both sound deprivation and augmented exposure can exert long-lasting effects on auditory processing, particularly during developmental epochs of increased plasticity, called critical periods (CP). However, auditory development is also thought to be influenced by the activity of other sensory modalities. For instance, in congenitally deaf humans, the auditory cortex can become activated by the spared visual and somatosensory modalities. Such findings led us to ask whether the onset of visual experience can regulate the CPs during which the auditory system is most sensitive to the acoustic environment. To address this issue, we first characterized the age range during which a transient period of auditory deprivation can induce cortical deficits. Auditory cortex function was assessed in brain slices obtained from animals reared with bilateral earplugs. Using whole-cell recordings, we measured both membrane and inhibitory synaptic properties, and found that these auditory cortex cellular properties are vulnerable to sound deprivation, but only when the manipulation begins prior to the onset of natural eyelid opening on postnatal day (P)

18. To determine whether auditory perception is vulnerable to transient deprivation during a similar age range, animals were again reared with bilateral earplugs. Fifteen days after earplug removal and restoration of normal thresholds, animals were tested on their ability to detect the presence of amplitude modulation, a temporal cue that supports vocal communication. Animals reared with earplugs from P11-23 displayed elevated amplitude modulation detection thresholds, but an identical duration of deprivation from P23-35 had no effect. Therefore, both functional and behavioral measures demonstrate auditory CPs. To determine whether the onset of visual experience regulates auditory cortex CPs, we manipulated the age of eyelid opening. When eyelids were opened prematurely, the auditory cortex CPs were terminated at an earlier age. That is, after 24 hours of visual experience, auditory deprivation no longer induced deficits of auditory cortex cellular properties. In contrast, delaying eyelid opening caused auditory cortex CPs to remain open for several additional days, such that auditory deprivation induced deficits of auditory cortex cellular properties at a later-than-normal age. Finally, we demonstrated a direct functional projection from visual to auditory cortex that could mediate the cross-modal effects described above. In summary, the onset of visual activity can regulate the precise period during which auditory cortex displays its greatest level of developmental plasticity.

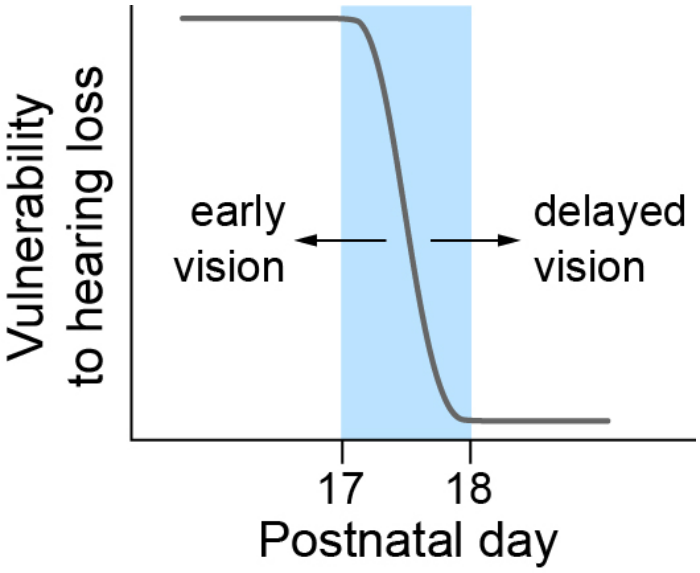

SYMP 86

Development of Auditory-Vocal Perceptual Abilities in Songbirds: Neural and Behavioral Assays

Sarah Bottjer
University of Southern California

Songbirds, like humans, learn the vocal sounds used for communication during a sensitive period of development. Processes of vocal learning between humans and songbirds are strikingly similar: juveniles memorize sounds from adult "tutors" during an auditory memorization phase, and subsequently translate that memory into a motor program by learning to match feedback of their incipient vocalizations (babbling) to the auditory memory of tutor sounds during a phase of sensorimotor integration. Studies of perception in human infants have shown experience-dependent improvements in perception of vocal sounds, which predict later success in speech acquisition. In order to exploit the strength of songbirds as a model system for human speech and provide direct tests of relationships between learning, perception, and their neural substrates, we employed both behavioral and neural assays of discrimination of vocal sounds that can be applied across development. These habituation-dishabituation assays are modeled after procedures used in studies of speech perception in human infants; the same tasks were used at all ages, thus allowing changes in the ability to distinguish vocal sounds to be examined during the period when birds are engaged in the processes of vocal learning from juvenile to adult stages. The results showed that neural tuning in higher-level auditory cortex mirrors behavioral improvements in the ability to make perceptual distinctions of vocal calls as song learning progresses. Thus, separate measures of neural discrimination and behavioral perception yielded highly similar trends during the course of vocal development. Both the behavioral and neural assays showed that adult zebra finches are substantially better than juveniles in their ability to discriminate vocal calls that vary in fundamental frequency. Adults responded to calls that were farthest in frequency from the habituated stimulus as if they were completely different, whereas juveniles demonstrated comparatively low levels of discrimination for calls the same distance away. These results indicate that the ability to discriminate between vocal calls based on fundamental frequency improves with age. Thus as in human infants, the ability to perceive vocal communication sounds may depend on experience with vocal sounds and experience-dependent maturation of neural circuits. In accord with this idea, the timing of this improvement in the ability to distinguish vocal sounds correlates with substantial refinement of axonal connectivity in cortico-basal ganglia pathways necessary for vocal learning in songbirds.

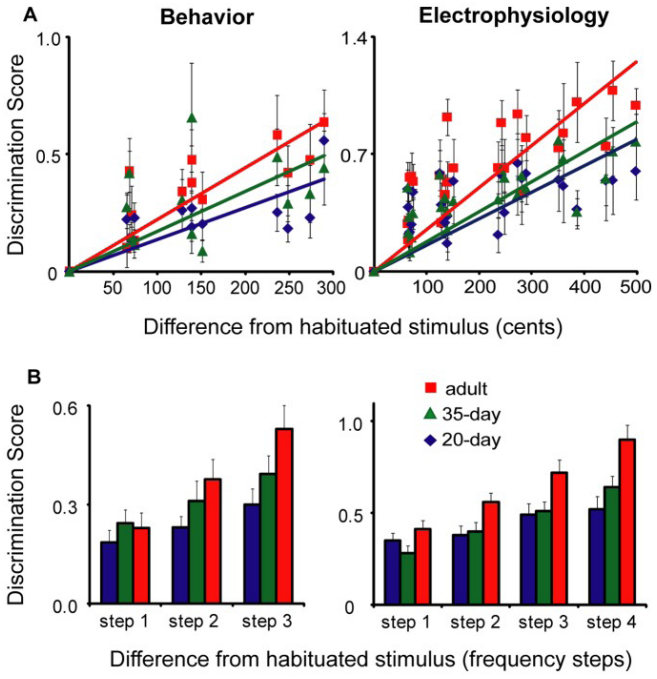

SYMP 87

Perceptual Learning in the Developing Auditory Cortex of Rodents

Shaowen Bao
University of Arizona

The auditory system is remarkably adaptive to the acoustic environment during a “critical period” of heightened plasticity. In this critical period, acoustic exposure has a profound influence on cortical sound representations. The perceptual consequences of this type of developmental cortical plasticity is not entirely clear. Based on the findings that early experience sharpens categorical boundaries of native speech sound perception in humans, we hypothesize that, in a natural acoustic environment, experience-dependent reorganization of cortical sound representations mediates categorical perceptual learning. We tested this hypothesis in a rodent model using a combination of electrophysiological, behavioral and computational approaches.

The nature acoustic environment comprises environmental sounds (e.g., wind blow, water flow…), and animal vocalizations (pup calls and adult encounter calls) and non-vocalization sounds (e.g., from footsteps, wing flaps …). Among those, animal vocalizations are arguably most structured and biologically relevant sounds. They are complex and diverse, but also have some common characteristics. For example, most mammalian vocalization calls are repeated at a temporal rate in the range from 5 to 10 Hz. Within a vocalization bout, the calls are repeated with variations. These statistical structures provide a basis for categorization of animal vocalizations: 1) sounds that are temporally spaced in a bout at 5-10 Hz likely belong to the same category; 2) the differences among individual sounds within a bout likely represent category variability. Electrophysiological and behavioral studies indicate that 1) auditory cortex over-represents sounds repeated at 6 Hz, but not 2 or 15 Hz, and 2) sequential structure between sounds can shape representational and perceptual boundary, where perceptual sensitivity is elevated. These findings support the notion that developmental cortical plasticity may underlie categorical perceptual learning. (The research was supported by National Institute of Health).

SYMP 88

Neuroimaging Reveals Even Rich Acoustic Features are Represented in Auditory Cortex at 3 Months Old

Rhodri Cusack[1]; Conor Wild[1]; Annika Linke[1]; Leire Zubiaurre-Elorza[1]; Charlotte Herzmann[1]; Hester Duffy[1]; Victor Han[2]; David Lee[2]
[1]Western University; [2]London Health Sciences Centre

There is a pressing need for better understanding of the rapid development of infant auditory and language function in the first year, to provide a scientific foundation for pedagogy and to improve clinical care. The fundamental challenge is that using behavioural responses to assess function in preverbal infants is difficult. To circumvent this, we use neuroimaging to provide a new window onto the emergence of infant auditory and language function. With new analysis techniques and modelling, we examine the development of the cortical regions that support speech and auditory processing.

It is known that the hierarchy of regions in adult auditory cortex represents both simple characteristics of sounds (e.g., their envelope and pitch) and more complex spectro-temporal features. Here, we ask how these features develop in infants: are the basic foundations of simple auditory representations built first before more complex acoustic features; or do simple and complex representations develop together? We presented infants at 3 and 9 months with sequences of rich engaging sounds (lullabies), while recording brain activity with functional magnetic resonance imaging (fMRI). To address our core question, we designed a new analysis technique, which brings together the traditional method used to examine neural responses to simple acoustic features (the general linear model), with that used for rich naturalistic stimulation (inter-subject correlation). We combined this with computational modelling of the learning process using a neural network.

We found that the lullabies evoked activity across an area of cortex similar to that seen in adults and, critically, that responses in this region showed sensitivity to complex as well as simple acoustic features even at 3 months. Furthermore, at 3 months the broader speech network was found to be maturely connected, and even regions in the frontal lobe were engaged by the lullabies. Taken together, our empirical and modelling results suggest that by 3 months infants have learnt a subset of complex features in a common way across individuals. By 9 months, this matures to provide a more rounded and flexible representation of complex auditory input.

SYMP 89

Auditory Development from Infancy to Adulthood as Indexed by Auditory Event-Related Potentials in Humans

Laurel Trainor
McMaster University

The auditory system identifies and locates sounding objects, perceives music and decifers speech. The development of these abilities involves a complex interplay between genetically-guided and experience-driven processes. Between birth and one year of age, perception of frequency, pitch, duration, intensity and timbre improve. Also, effects of specific experience are evident and perceptual narrowing is well under way, whereby infants become better at discriminating stimuli that matter in their environment (human faces and voices, native speech categories, native musical structures) and worse at contrasts that do not matter in their environment (animal faces and voices, non-native speech and musical contrasts). Changes in the brain that accompany these developments can be studied in human infants with EEG. Synchronous depolarization of many neurons whose axons point in the same direction results in electrical fields strong enough to be measured at the scalp. Auditory event-related potentials (AEPs) reflect EEG responses to sound events. AEP components from sound onset reflect processing stages. For example P1 (~50 ms) is thought to originate largely in A1, A2 (~100 ms) and P2 (~170 ms) largely in A2. N1 and P2 likely involve communication between auditory cortex and other brain regions supporting top-down attentional modulation of auditory regions. Cortical AEPs in young infants differ morphologically from those of adults and are dominated by slow frontally positive waves. N1 and P2 take many years to mature, reaching maximum amplitude around 10-12 years and diminishing to adult levels around 18 years of age. This AEP developmental trajectory roughly parallels the developmental trajectory of neurofilament expression, which develops first in deeper cortical layers and reaches adult levels in layers II and III around 12 years of age. When an unexpected sound is perceived given the prior context, a mismatch negativity (MMN) component is also seen peaking between about 150 and 250 ms in adults. Mismatch responses do not depend on attention and are seen in very young infants, but manifest initially as slow frontal positivities. An adult-like MMN begins to develop after 2 months of age, with somewhat different developmental trajectories for different sound features and task difficulty. MMN develops over the time period in which perceptual narrowing takes place. The exact relation between AEP development and physiological processes such as myelination, synaptic pruning and neurotransmitter expression are not yet clear. However, AEPs in infancy and early childhood can be used as markers of delayed brain development and various disorders.

PD 139

Actin Core Remodeling at the Stereocilia Tips is Driven by the Mechanotransducer Current

A. Catalina Velez-Ortega[1]; Artur Indzhykulian[1]; Pavel Novak[2]; Oleg Belov[3]; Mary Freeman[1]; Samir Rawashdeh[4]; Yuri Korchev[5]; Gregory Frolenkov[1]
[1]University of Kentucky; [2]Queen Mary, University of London, UK; [3]Research Center for Audiology, Russia; [4]University of Michigan, Dearborn; [5]Imperial College London

Background

Within the adult mammalian hair cell stereocilia, the actin core undergoes active remodeling only at their tips. Interestingly, the tips of mechanotransducing stereocilia often exhibit a “wedge-like” shape, which has been frequently visualized via scanning (SEM) and transmission (TEM) electron microscopy. TEM images show that the wedged stereocilia tips are filled with actin filaments, indicating that stereocilia wedging may be formed by actin remodeling at the tips. Disruption of tip links via chemical or genetic manipulations results in the loss of stereocilia wedging. However, it is still unknown whether the remodeling of the actin core at the stereocilia tips is driven (*i*) by the mechanical tension provided by the tip links or (*ii*) through a signaling pathway triggered by the mechanotransducer current.

Methods

We studied the dynamic changes of the stereocilia tip shape in early postnatal mouse and rat auditory hair cells after (*i*) the disruption of tip links with BAPTA-buffered Ca^{2+}-free medium or (*ii*) the blockage of the mechanotransduction current with known blockers of the transduction channels. We used hopping probe ion conductance microscopy (HPICM) to perform live time-lapse imaging of the same hair cell bundle before and after treatment. Using this technique, we obtained images of the stereocilia tips with nanoscale resolution. For confirmation of major findings, we also imaged chemically fixed samples via conventional SEM.

Results

HPICM imaging showed, for the first time in live cells, the presence of stereocilia wedging (with an X-Y resolution of ~11 nm) in the second row of the inner hair cell stereocilia. We found a marked decrease in the height of stereocilia tip wedges in the cultured organ of Corti explants compared to freshly isolated explants. This result indicates that remodeling of the actin core at the stereocilia tips may be influenced by the extracellular environment. Immediately after the disruption of the tip links with BAPTA, stereocilia wedging remained. However, it was lost by 20 min post-BAPTA and recovered by 3 hours post-BAPTA, in the midst of the tip link regeneration. Blocking of the transduction channels also resulted in significant changes of the stereocilia tip wedging, even though this treatment did not affect the tip links.

Conclusions

Our results indicate that the remodeling of the actin core at the tips of the mammalian auditory hair cell stereocilia is likely to be initiated (or driven) by the inward ionic current through the mechanotransducer channels.

Funding
Supported by NIDCD/NIH (R01DC008861 & R01DC014658)

PD 140

The Stereociliary Paracrystal is a Dynamic Cytoskeletal Scaffold In Vivo

Brian McDermott, Jr.; **Brian McDermott**; Philsang Hwang Hwang; Shih-Wei Chou; Zongwei Chen
Case Western Reserve University School of Medicine

The permanency of mechanosensory stereocilia may be the consequence of low protein turnover or protein renewal. Here we devise a system, using optical techniques in live zebra fish, to distinguish between these mechanisms. We demonstrate that the stereocilium's abundant actin cross-linker, fascin 2b, exchanges, without bias or a phosphointermediate, orders of magnitude faster ($t_{1/2}$ of 76.3 s) than any other known hair bundle protein. To establish the logic of fascin 2b's exchange, we examine whether filamentous actin is dynamic and detect substantial β-actin exchange within the stereocilium's paracrystal ($t_{1/2}$ of 4.08 h). We propose fascin 2b's behavior may enable cross-linking at fast timescales of stereocilia vibration while also noninstructively facilitating the slower process of actin exchange. Furthermore, tip protein myosin XVa fully exchanges in hours ($t_{1/2}$ of 11.6 h), indicating that delivery of myosin-associated cargo occurs in mature stereocilia. These findings suggest that stereocilia permanency is underpinned by vibrant protein exchange.

Funding
This research was supported by National Institutes of Health (NIH) Grants DC009437 (B.M.M.) and the Center for Clinical Research and Technology at University Hospitals Case Medical Center (B.M.M.).

PD 141

Shorter OHC stereocilia rows are deflected by the tallest row during sound stimulation

Pierre Hakizimana; Clark Elliott Strimbu; Anders Fridberger
Linköping University

OHC stereocilia bundles are thought to be deflected by motion differences between the overlaying tectorial membrane (TM), to which the bundles are connected via the tallest row, and the reticular lamina. In isolated TM-free hair cell experiments these stereocilia are commonly deflected either by a stiff probe or a piezoelectric-driven fluid jet. However, it emerged recently that the two techniques produce contradictory results, raising the question of which one of the two was more reliable.

In this work, we used time-resolved confocal imaging to investigate how individual stereocilia are deflected relative to each other by sound in temporal bone preparations from guinea pigs.

We found that acoustically evoked movements of the tallest sterocilia row were significantly higher relative to the shorter stereocilia. Further quantification of the stereocilia movements revealed a phase difference between the tallest row and shorter stereocilia and the inclination of the deflection trajectory was different for the two rows. These results suggest that shorter stereocilia rely on mechanical stimulation from the tallest row, which deflects them via interstereocilia attachments.

We conclude that stimulation methods that indiscriminately stimulate all stereocilia rows are probably not suitable for outer hair cells.

Funding
Tysta skolan foundation LinkÃ¶ping University The Swedish research council

PD 142

Live-imaging of F-actin dynamics reveals mechanisms of homeostasis in inner ear hair cell stereocilia

Meghan Drummond[1]; Melanie Barzik[1]; Jonathan Bird[1]; Dian-Sun Zhang[2,3]; Claude Lechene[2,4]; David Corey[2,3]; Lisa Cunningham[1]; Thomas Friedman[1]
[1]National Institute on Deafness and Other Communication Disorders; [2]Harvard Medical School; [3]Howard Hughes Medical Institute; [4]National Resource for Imaging Mass Spectrometry, Brigham and Women's Hospital

Background
The homeostatic mechanisms of the F-actin paracrystalline core within mechano-sensitive hair cell stereocilia are critical to healthy, lifelong hearing, but are not well understood. A rapid turnover model posits the constant renewal of the central paracrystalline actin core of stereocilia every 24-48 hours by a continuous F-actin treadmill. In contrast, an alternative model proposes long-lived F-actin stereocilia cores, with proteins only in the stereocilia plasma membrane and the distal tip compartment display rapid turn over. To resolve this controversy, we used live cell imaging and fixed cell confocal microscopy to investigate actin dynamics in >400 individual hair cells over time.

Methods
To capture actin dynamics in single cells over time, we biolistically transfected P2-P5 mouse utricle explant cultures with either: (i) EGFP-ß-actin (ii) two forms of mutant EGFP-ß-actin that are unable to polymerize into actin filaments, or (iii) a photoconvertible dendra2-ß-actin. Samples were imaged using live-cell spinning disc confocal microscopy or fixed-cell confocal microscopy. The localization and intensity of fluorescence were evaluated using ImageJ and Volocity software.

Results
Data collected using fixed cell confocal microscopy and analyses of EGFP-ß-actin mutants demonstrated that actin polymerization is required for steady-state tip localization. In 40% of live imaged hair cells, wild-type EGFP-ß-actin was primarily observed at the stereocilia tips for at least 48 hours of live imaging. After 48 hours, we observed elongation of a few individual stereocilia within most hair cell bundles. In the remaining cells that were examined by live-imaging, we recorded stereociliogenesis live for the

first time, showing synchronous uniform incorporation of EGFP-ß-actin into nascent stereocilia. Finally, live-imaging of specific populations of actin in hair cells transfected with photoconvertible dendra2-tagged ß-actin supports F-actin turnover and elongation from the distal tips.

Conclusions
Collectively, our data rule out a rapid F-actin treadmill model as a mechanism of hair bundle homeostasis. In contrast, we find that the paracrystalline core is stable and long-lived with persistent F-actin turnover occurring only at stereocilia tips. The mechanosensory functions within this dynamic zone are under investigation.

Funding
NIDCD Intramural Grant to Thomas B Friedman

PD 143

Primary Cilia Are Not Calcium-Responsive Mechanosensors

Artur Indzhykulian[1,2]; Markus Delling[2,3]; Xiaowen Liu[2,3]; Yaqiao Li[1,2]; Tiao Xie[1]; David Corey[1,2]; David Clapham[2,3]
[1]Harvard Medical School; [2]Howard Hughes Medical Institute; [3]Boston Children's Hospital

Primary cilia are solitary microtubule-based protrusions, generally non-motile, that extend from the surface of cells between cell divisions. Their antenna-like structure leads naturally to the assumption that they sense the surrounding environment, specifically, that they sense mechanical force through calcium-permeable ion channels in the cilium. This hypothesis has been invoked to explain a large range of biological responses, including the planar cell polarity of hair cells, control of left-right axis determination in embryonic development, and adult progression of polycystic kidney disease and some cancers. Here, we report the complete lack of mechanically induced calcium increases in primary cilia, in tissues upon which this hypothesis has been based.

We developed a transgenic mouse, *Arl13b-mCherry-GECO1.2,* expressing a genetically-encoded calcium indicator in all primary cilia. We measured responses to flow in kinocilia of inner ear hair cells, and in primary cilia of cultured kidney epithelial cells, kidney thick ascending tubules, embryonic node crown cells, mouse embryonic fibroblasts, and MLO-Y4 and Ocy454 osteocyte-like cell lines. A swept-field confocal with millisecond frame time helped distinguish Ca^{2+} entry directly into cilia from Ca^{2+} that back-diffused from cytoplasm. The fused mCherry and GECO fluorophores allowed ratiometric Ca^{2+} measurement.

Rapid Ca^{2+} influx specifically into cilia was not observed with physiological—or even superphysiological—levels of fluid flow in any of these cells, suggesting that cilia do not respond to mechanical forces via calcium signaling. Hair cell stereocilia, which accumulate some calcium indicator molecules, do respond rapidly to bundle deflection and thus serve as a positive control. We conclude that the Ca^{2+}-responsive mechanosensor hypothesis of primary cilia should be abandoned.

How might others have observed a Ca^{2+} rise in cilia upon stimulation? Two likely sources of error are insufficient time resolution, in that increased cytoplasmic Ca^{2+} can diffuse into cilia in tens of milliseconds and appear as originating within cilia; and motion-dependent path-length artifacts. Ratiometric measurement—used here—is critical for reducing motion artifacts and inhomogeneous-volume artifacts.

There may still be mechanosensitive responses within primary cilia for physiologically relevant deflections, that occur without changes in ciliary [Ca^{2+}]. Additionally, mechanically released ligands could activate receptors or channels in cilia, or the surrounding cell membrane. However any such mechanosensitive elements do not depend on rapid, stimulus-induced Ca^{2+} entry.

Funding
NIH 5R01 DC000304 to DPC

PD 144

Single-molecule mechanics of a tip-link protein

Tobias Bartsch[1]; Bo Zhao[2]; Ulrich Müller[2]; A. J. Hudspeth[1]
[1]The Rockefeller University; [2]The Scripps Research Institute

The astounding sensitivity and dynamic range of mammalian hearing result from the ear's sensory receptors, the hair cells of the inner ear. Each hair cell features a hair bundle, a cluster of stiff stereocilia, whose deflection causes mechanically gated ion channels to open. One candidate for the mechanical element that converts bundle deflection to a force capable of opening the channels is the tip link, a dimer of dimers of protocadherin 15 and cadherin 23 molecules that connects pairs of adjacent stereocilia. The link's elasticity results both from the elasticity of individual cadherin domains and from the rearrangement of the domains relative to each other, which is stabilized by Ca2+ binding. Although the mechanics of fragments consisting of two cadherin domains apiece from protocadherin 15 and cadherin 23 was recently explored by molecular-dynamics simulations, the mechanical properties of the full-length proteins and their dimers remain unknown.

Using a custom-built photonic-force microscope, we show that the elasticity of the full-length constituents of the tip link can be measured in the physiologically relevant low-force regime by a single-molecule experiment. In our assay thermal forces are exploited to sample the proteins' energy landscapes. Each protein of interest is positioned between a fixed glass substrate and a weakly optically trapped probe nanoparticle, and the three-dimensional spatial probability distribution of the probe's thermal motion is measured with nanometer precision and megahertz bandwidth. The protein's energy landscape can then be computed directly from the measured spatial probability distribution.

Funding
This work was partially supported by a Junior Fellow award from the Simons Foundation to Tobias Bartsch. A. J. Hudspeth is an Investigator of Howard Hughes Medical Institute.

PD 145

Transient Block of Ca2+ Channels by Exocytosed Protons at Mammalian Auditory Hair Cell Ribbon Synapses

Philippe Vincent[1]; Soyoun Cho[2]; Yohan Bouleau[1]; Henrique von Gersdorff[2]; **Didier Dulon**[1]
[1]University of Bordeaux; [2]The Vollum Institute, Oregon Health and Science University

Background

A synaptic cleft pH regulation of presynaptic Ca^{2+} currents has been described at the ribbon synapses of the retina (DeVries et al., 2001; Palmer et al., 2003) and recently in frog auditory hair cells (Cho and von Gersdorff, 2014). However, this proton regulation has never been reported in mammalian auditory inner hair cells (IHCs). To unmask this process in mouse IHCs, we used a physiological pH buffer solution based on bicarbonate. The transient block of Ca^{2+} currents by exocytosed protons will be used as a proxy for exocytosis that mimics the EPSCs to investigate the mechanisms of vesicular release in mouse IHCs.

Methods

Freshly dissected organs of Corti from pre-hearing (P7) and post-hearing (P14-P18) IHCs from controls (*WT* and *Otof* $^{+/-}$) or otoferlin deficient mice (*Otof* $^{-/-}$) were continuously bathed and perfused with a 95% O_2, 5% CO_2 (carbogen) bubbled extracellular solution in the presence of the physiological pH buffer bicarbonate. Ca^{2+} currents and time-resolved changes in membrane capacitance (exocytosis) were recorded in the whole-cell voltage-clamp configuration from IHCs (Vincent et al., 2014).

Results

Using external bicarbonate solutions, Ca^{2+} currents of post-hearing IHCs showed a notch or fast transient block (I_{Ca}TB) right after their peak onset. This I_{Ca}TB was abolished when adding 10 mM HEPES to the external solution, indicating that it was produced by H^+ release. Remarkably, pre-hearing IHCs did not display I_{Ca}TB, suggesting that this regulation requires a tight coupling organization between Ca^{2+} channels and H^+ release sites. When varying external Ca^{2+}, I_{Ca}TB and exocytosis in post-hearing IHCs was best fit with a nonlinear power function with index 3, likely reflecting the cooperativity of the putative Ca^{2+} sensor otoferlin. Indeed, *Otof* $^{-/-}$ IHCs displayed greatly reduced exocytosis and normal Ca^{2+} currents, but no I_{Ca}TB. Remarkably, at a comparably low *Otof* $^{-/-}$ exocytotic response, WT-IHCs displayed significant I_{Ca}TB, suggesting that the lack of otoferlin desynchronized vesicular fusion. Interestingly, I_{Ca}TB in WT-IHCs was also prevented with 5 mM intracellular BAPTA, a fast Ca^{2+} buffer known to desynchronize vesicular release.

Conclusion

Fast proton regulation of Ca^{2+} channels in the sub-ms range occurs at mammalian auditory ribbon synapses. This process likely contributes to the initial extraordinarily fast spike firing adaptation component of the auditory nerve fibers. Furthermore, analysis of the proton regulation greatly favors an otoferlin-mediated multivesicular release and a nanodomain coupling of Ca^{2+} channels to docked vesicles at the synaptic ribbons of mammalian hair cells.

Funding

Fondation Agir pour l'Audition

PD 146

The 133-kDa N-terminal Domain Enables Myosin 15 to Maintain Mechano-Transducing Stereocilia and is Essential for Hearing

Jonathan Bird[1]; Qing Fang[2]; Artur Indzhykulian[3]; Mirna Mustapha[2]; Gavin Riordan[1]; David Dolan[2]; Thomas Friedman[1]; Inna Belyantseva[1]; Gregory Frolenkov[3]; Sally Camper[2]
[1]NIDCD/NIH; [2]University of Michigan; [3]University of Kentucky

Background

How hair cells develop and maintain stereocilia hair bundles is crucial for mechanotransduction and detection of sound. Mutations of *MYO15A* (encoding myosin 15) cause human deafness *DFNB3*. Existing mouse models (*Myo15*^{sh2} & *Myo15*$^{sh2\text{-}J}$) show that myosin 15 is required for stereocilia development. Myosin 15 normally localizes to the stereocilia tips, where it delivers Eps8 and whirlin. There are two major isoforms of myosin 15 which are identical except for an 133-kDa N-terminal domain. Their exact functions remain unclear, since the *Myo15*^{sh2} and *Myo15*$^{sh2\text{-}J}$ alleles affect both isoforms. In this study, we generated an isoform-specific knockout mouse to explore the role of isoform 1 (with the N-terminal extension) in auditory hair cells.

Methods

We knocked-in the p.E1086X (*Myo15*$^{\Delta N}$) nonsense mutation into exon 2, that encodes the N-terminal extension, and is specific to isoform 1. The hearing function of *Myo15*$^{\Delta N/\Delta N}$ mice was assessed by ABR and DPOAEs. Expression of *Myo15* isoforms was measured by qPCR. The localization of isoform 1 protein within the cochlea was detected using immunofluorescence with antibody PB888 specific to the N-terminal extension. The phenotype of *Myo15*$^{\Delta N/\Delta N}$ hair cells was characterized with SEM, TEM, and MET recordings.

Results

Myo15$^{\Delta N/\Delta N}$ mice are profoundly deaf. However, unlike *Myo15*$^{sh2/sh2}$ stereocilia that are abnormally short, *Myo15*$^{\Delta N/\Delta N}$ hair cells develop hair bundles with normal architecture and prominent MET currents. Using PB888 we detected isoform 1 protein at the tips of shorter IHC stereocilia, near the site of MET, from P7 onwards. No PB888 immunoreactivity was detected in *Myo15*$^{\Delta N/\Delta N}$ hair cells, showing that the p.E1086X allele was an isoform 1-null. In *Myo15*$^{\Delta N/\Delta N}$ IHCs, isoform 2 was predominantly concentrated at the tips of the tallest row stereocilia. Consistent with isoform 2 being sufficient to drive stereocilia elongation, we found that Eps8 and whirlin were correctly localized in *Myo15*$^{\Delta N/\Delta N}$ hair cells. Analysis of *Myo15* splicing showed that isoform 2 was the predominant mRNA transcript in P0 cochleae. As hair bundles matured, isoform 1 became the predominant species from P7 onwards. Despite *Myo15*$^{\Delta N/\Delta N}$ hair bundles developing normally in

the absence of isoform 1, we observed degeneration of the actin cytoskeleton specifically in the transducing, shorter row stereocilia. These data indicate that isoform 1 is required to maintain the actin cytoskeleton in this specialized subset of stereocilia.

Conclusions
Our results show that *DFNB3* deafness can occur through two different mechanisms. Isoform 2 is required to assemble the hair bundle, whereas isoform 1 maintains the shorter mechanotransducing stereocilia.

Funding
DC000039-18 and DC000048-18 (JEB, IAB, TBF), R01 DC05053 (SAC, GIF, QF, MM, and AAI), R01 DC008861 (AAI, GIF), P30 DC05188 (DFD), the Hearing Health Foundation (MM) and a University of Michigan Barbour Scholarship and James V. Neel Fellowship (QF).

PD 131

Towards an Efficient Method to Derive the Phase Response in Hearing-Impaired Listeners

Katharina Zenke[1]; Bernhard Laback[2]; Hisaaki Tabuchi[2]
[1]Acoustics Research Institute; [2]Austrian Academy of Sciences

Introduction
Masking experiments suggested that the phase response of the human cochlea has a constant negative curvature. These experiments, however, cannot be well applied to cochlear hearing-impaired listeners who show largely reduced masking effects, probably due to their reduced compression and potentially altered phase responses. These listeners are sensitive to envelope interaural time differences (ITDs) and interaural level differences (ILDs). Recent studies have shown an effect of the phase response of harmonic complexes on ITD thresholds (Tabuchi et al., 2015, ASA abstract). This study is a first step towards a more efficient method to measure the phase response of individual listeners.

Methods
In the first experiment we examined the effects of a signal's phase relations on the ITD-based extent of lateralization. Schroeder-phase harmonic complexes (SPHCs) were used as target stimuli, which are equal amplitude harmonic complexes with constant phase curvatures C. The stimuli consisted of 13 harmonics with a fundamental frequency of 100 Hz falling within an auditory filter centered at 4 kHz. Nine different stimuli with C ranging from -1 to 1 with four different ITDs ranging from 200 to 1600 µs were tested. In a pointing task eight normal-hearing listeners were asked to adjust the ILD of a narrowband pointer stimulus to match the perceived lateral position of the target.

In a second experiment we investigated the potential influence of C on the image width of the SPHC stimuli. In a constant stimuli paradigm participants compared the image width of the SPHC targets to that of narrowband noise stimuli with variable interaural correlations and chose the stimulus evoking the more compact width.

Results
The first experiment revealed a significant dependence of the adjusted pointer ILD on the phase curvature of the targets. In all ITD conditions the extent of lateralization was maximal at Cs around zero, yielding ILD differences of up to 7 dB. Preliminary results of the second experiment showed no systematic effect of C on the perceived image width.

Conclusions
The extent of lateralization of SPHC stimuli systematically depends on their phase curvature. The findings are, however, only partially consistent with ITD thresholds, which seem to be influenced by additional factors, besides the extent of lateralization. Overall, the systematic effect of the phase on ITD-based lateralization could be used to efficiently measure the phase response in hearing-impaired listeners.

Funding
Supported by Austrian Science Fund P24183-N24

PD 132

The TFS-AF Test for Assessing Sensitivity to Interaural Phase: Normative Data

Brian Moore[1]; Aleksander Sek[2]; Andrew Harland[1]; Christian Fullgrabe[3]
[1]University of Cambridge; [2]Adam Mickiewicz University; [3]Institute of Hearing Research

Hopkins and Moore (2010) described the TFS-LF test for rapidly assessing sensitivity to interaural phase (IP, i.e. interaural differences in temporal fine structure, TFS) at low frequencies. On each trial, there are two intervals, each containing four bursts of a sinusoidal tone. The envelopes of all tones are synchronous at the two ears. In one interval, the IP of the TFS is identical at the two ears, while in the other interval the IP alternates between 0 and φ. The subject is asked to indicate the interval in which the tones appear to move within the head. The value of φ is adaptively varied to determine the threshold.

When used to study the effects of hearing loss or age on sensitivity to IP, the frequency is usually fixed, for example at 500 Hz. However, some listeners may be completely unable to perform the task at the selected frequency. This motivated the development of a new version of the test, called the TFS-AF test, where AF stands for "adaptive frequency". In the TFS-AF test, the value of φ is fixed and the frequency is adaptively varied to determine the threshold; performance worsens with increasing frequency, and the task becomes impossible when the frequency is sufficiently high. Results for nine young normal-hearing subjects showed that little practice is required to achieve stable results. With φ set to 90, 165 or 180°, the thresholds for all subjects fell between 920 and 1540 Hz. Thresholds were highly negatively correlated with thresholds obtained using the TFS-LF task.

Normative data were obtained for a large number (>60) of subjects with ages from 60 to 85 years. All subjects had

audiometric thresholds ≤20 dB HL for frequencies up to 1000 Hz and ≤25 dB HL at 1500 Hz. Thresholds tended to worsen with increasing age, and the variability of the thresholds also increased with increasing age. All subjects were able to complete the task except for 3 who were aged 80 years or older.

In summary, the TFS-AF test is more suitable than the TFS-LF test for rapid assessment of sensitivity to IP in large-scale research studies or in the clinic, as a definite threshold measurement can usually be obtained with the former.

Hopkins K, Moore BCJ. Development of a fast method for measuring sensitivity to temporal fine structure information at low frequencies. Int. J. Audiol. 49:940-946, 2010.

Funding
Medical Research Council (UK)

PD 133

Effects of Aging and Bandwidth on the Binaural Masking Level Difference Assessed with Electrophysiological and Psychophysical Measures

Samira Anderson; Robert Ellis; Matthew Goupell
University of Maryland

Introduction
The brain uses interaural level and timing cues to separate the target speech signal from competing signals, but older listeners may have reduced ability to benefit from these cues. One phenomenon that assesses the ability to separate the signal of interest from competing noise is the Binaural Masking Level Difference (BMLD), a phenomenon whereby the listener hears the signal at a lower threshold when the target signal or noise masker is presented out of phase to the two ears than when they are presented in phase. To enhance understanding of the nature of speech-in-noise difficulties experienced by older adults and of the neural mechanisms underlying the BMLD, this study investigated the effects of both aging and bandwidth on perceptual and subcortical measures of the BMLD.

Methods
Participants comprised 15 younger and 15 older normal-hearing adults. Perceptual BMLDs were assessed by obtaining thresholds for a 500 Hz toneburst in quiet and in three interaural phase conditions (NoSo, NoSπ, and NπSo), and in two bandwidths: wideband (WB, 1500 Hz) and narrowband (NB, 50 Hz). The frequency following response (FFR) was recorded to the same 500 Hz toneburst presented in quiet at 55 dB SL and in the noise conditions at -10 dB SNR. BMLDs were obtained by subtracting the perceptual thresholds obtained in the antiphasic conditions (NoSπ and NπSo) from the thresholds obtained in the phasic condition (NoSo), and by subtracting FFR spectral amplitudes of the NoSπ and NπSo conditions from the NoSo condition in both WB and NB.

Results
Behavioral: Perceptual BMLDs were larger in younger than in older adults across conditions. For both age groups, BMLDs in WB are greater than in NB, and BMLDs are greater in NoSπ condition than in NπSo conditions. FFR: Amplitudes in NoSπ conditions were smaller than in NoSo condition for both age groups, consistent with animal studies using single unit recordings in the inferior colliculus. However, these amplitude reductions were smaller in the older adults, possibly due to floor effects as overall amplitudes in the older adults were smaller in all phase conditions. There were no significant correlations among behavioral and FFR measures.

Conclusion
The age-related reduction in perceptual and FFR BMLDs suggests one factor in the older adult's listening difficulties in noisy environments. Older adults appear to have reduced ability to benefit from timing cues as measured by the FFR, possibly due to decreased neural synchronization to auditory stimuli.

Funding
NIH-NIDCD Grant K99/R00 DC010206 (Goupell), P30 DC004664 (Center for Comparative and Evolutionary Biology of Hearing core grant)

PD 134

Modeling the Effect of Peripheral Hearing Disorders on Auditory Localization in Sagittal Planes

Robert Baumgartner; Piotr Majdak; Bernhard Laback
Austrian Academy of Sciences, Vienna

Normal-hearing listeners use monaural spectral cues to localize sound sources in sagittal planes, including up-down and front-back directions. This enables listeners to spatially separate multiple sources in sagittal planes and improves speech intelligibility in multi-talker scenarios. The salience of monaural spectral cues is determined by the spectral resolution and the dynamic range of the auditory system. These factors are commonly degraded by peripheral disorders like outer hair cell (OHC) dysfunction and loss of auditory nerve (AN) fibers. In order to simulate the effects of these disorders on localization performance, we incorporated a well-established model of the auditory periphery (Zilany et al., 2014 JASA 135:283-286) into a recent model of sound localization in sagittal planes (Baumgartner et al., 2014 JASA 136:791-802). First, we evaluated predictions of the resulting localization model against listener-specific localization performance for normal-hearing listeners in various experiments testing the effects of spectral modifications of head-related transfer functions and various sound pressure levels (SPLs). Then, the model was applied on conditions simulating various peripheral disorders while assuming listening in quiet and perfect adaptation of the auditory system to the disorder under test. The predicted localization performance was hardly affected by a moderate OHC dysfunction, but significantly degraded in case of a severe OHC dysfunction. Since cochlear amplification is mainly active at low SPLs, localization of softer sounds was predicted to be stronger

influenced by OHC dysfunction than localization of louder sounds. Furthermore, the model predicted poor localization performance if only high-SR fibers were preserved in the auditory periphery and low- and medium-SR fibers were lost because then the dynamic range of AN responses was too limited to represent spectral cues at various SPLs. The proposed model allows to further investigate the impact of the diverse forms of hearing impairment on sound localization performance.

Funding
FWF P24124

PD 135

Effects of blast exposure and mTBI on the Aurally-Aided Visual Search Performance of walking and standing listeners

Douglas Brungart[1]; Tricia Kwiatkowski[2]; Sarah Kruger[3]; Julie Cohen[2]; Thomas Heil[4]
[1]Walter Reed National Military Medical Center; [2]Henry M. Jackson Foundation; [3]National Intrepid Center of Excellence; [4]Geneva Foundation

Background
Recent reports from audiology clinics within the DoD and VA suggest that service members (SMs) who have suffered traumatic brain injury due to blast may suffer from auditory, visual, and vestibular impairments that place them in the bottom range of normal performance but are not severe enough to result in an abnormal clinical diagnosis in any single sensory modality. This raises the question of how these individuals might perform in complex multisensory tasks that require them to integrate information from multiple sensory systems. Any impairment in multisensory integration could be particularly detrimental for injured Service Members who return to duty and engage in military tasks like dismounted patrols where they must use auditory cues to detect and visually identify targets while maneuvering across the battlefield on foot. In this experiment, blast-exposed SMs with mild traumatic brain injury and healthy control were tested on their ability to identify visual targets, localize sounds, and conduct integrated aurally-aided visual search tasks both while standing and walking in a virtual environment.

Methods
Active duty SMs with and without a history of mTBI were evaluated using the Computer Assisted Rehabilitation Environment (CAREN). The CAREN contains an articulated treadmill surrounded by a 180 degree projection screen with an array of 64 loudspeakers positioned behind it. The testing paradigm required participants to perform the following three tasks both while standing and while walking on the treadmill:

Auditory Localization (AL), where they moved a head-slaved cursor to the perceived location of a pulsed noise target.

Visual Discrimination (VD), where they were asked to identify a visual target presented from a known location.

Aurally-Aided Visual Search (AAVS), where they were asked to use an auditory cue to find and identify a visual target in a field of 264 visually-similar distracters.

Results
There were no significant differences between the mTBI participants and healthy controls either in terms of localization accuracy in the AL task or response time in the VD task. However, there was a significant difference between the response times of the mTBI and control groups in the AAVS task. Contrary to initial expectations, both groups performed significantly better in the AAVS task when they were walking on the treadmill than when they were standing still.

Conclusions
The results of the experiment demonstrate that even high-functioning SMs with mTBI may have difficulties in complex multisensory tasks that cannot be predicted from standard unimodal clinical measures of sensory function.

Funding
This work was supported by the US Army MRMC/CDMRP PH/TBI Awared W81XWH-12-2-0068 . The views expressed in this abstract are those of the authors and do not reflect the official policy of the Department of the Army, Navy, Defense, or United States Government.

PD 136

The Role of the Intactness of Binaural Timing Information in Bilateral Cochlear Implants

Katharina Egger; Piotr Majdak; Bernhard Laback
Austrian Academy of Sciences

Interaural time differences (ITDs) are important for localizing sounds. ITD cues are only suboptimally encoded with current bilateral cochlear-implant (CI) systems which is reflected in a limited sensitivity to ITDs of bilateral CI users. Practical stimulation strategies have to find a compromise between optimal encoding of ITD cues at the individual interaural electrode pairs and the timing limitations imposed by demands from stimulation at adjacent channels. For example, when ITDs require simultaneous stimulation at two electrodes at the same time, the pulses at one of the electrodes have to be slightly shifted or even removed which, in turn, might compromise the ITD cue. Further, due to signal-processing issues, pulses in the stimulation sequence can be missing at one ear but be present at the other ear, compromising the correct representation of the ITD in realistic bilateral signals.

This study addresses the tolerable room for such variations by investigating the potential perceptual degradations due to inaccurate encoding of ITD cues. We hypothesized that, in a pulse train which correctly encodes ITDs, a removal of pulses will reduce lateralization discrimination and larger ITDs will be required in order to detect the correct stimulus side.

Experiments were performed using interaurally coordinated research interfaces. ITD thresholds for unmodulated, 100-pulse-per-second pulse trains presented at a single, pitch-matched, interaural electrode pair were measured. A baseline condition without pulse removal, i.e., a pulse train

which perfectly encodes ITDs, was presented at comfortable loudness. Measurements were performed applying different degrees of bilateral, interaurally uncorrelated pulse removal. Each degree was tested with the same current levels as in the baseline condition, and with stimuli matched in loudness to the baseline condition.

The results provide a link between the inaccurate encoding of ITD cues in terms of pulse removal and the sensitivity to these compromised ITD cues. For large degrees of removed pulses, the removal led to a change in loudness. This in turn can affect ITD sensitivity, similar to previous results showing better ITD sensitivity with increasing current level.

We conclude that inaccurate encoding of ITD cues might deteriorate the sensitivity to ITDs. The tolerable room for pulse-timing variations without significant perceptual degradations and its implications for future stimulation strategies aiming to optimally encode ITD cues in CIs are discussed.

Funding
Supported by MED-EL.

PD 137

Lateralization of Interaural Time Differences with Multi-Electrode Stimulation in Bilateral Cochlear Implant Users

Alan Kan; Heath Jones; Ruth Litovsky
University of Wisconsin-Madison

While sound localization abilities have been demonstrated in bilateral cochlear implant (BiCI) users, this ability does not appear to rely on interaural time differences (ITDs), a cue known to be important for accurate localization in normal hearing listeners. BiCI users demonstrate ITD sensitivity when stimulated on single electrode pairs with synchronized research processors. However, sensitivity to ITDs with multi-electrode stimulation, a prerequisite for good speech understanding, is poorly understood. Recent data show that ITD sensitivity with multi-electrode stimulation is typically on par with single-electrode stimulation, albeit performance can be poorer than that with the single electrode pair that yields best ITD sensitivity. In addition, using electrode pairs along the full length of the electrode array has been shown to yield better ITD sensitivity than just the apical-most electrodes. While these results provide insight into how ITD sensitivity is affected by multi-electrode stimulation, they do not measure the extent of lateralization of perceived auditory images, or whether multi-electrode stimulation can lead to coherent fused auditory images. In the present study, ITD lateralization functions were measured in order to understand how ITDs presented on multiple electrodes are mapped to perceived intercranial locations.

ITD lateralization functions were measured using low rate electrical pulse trains (100 pulses per second) with single and multi-electrode stimulation in eight adult postlingually-deafened BiCI users. Five, pitch-matched electrode pairs that span the length of the array were used. Electrode pairs were stimulated individually, three at a time, and all five together. Various three-electrode configurations were tested: (1) three most basal pairs; (2) three most apical pairs; (3) base-mid-apex electrode pairs; and (4) three electrode pairs that yielded best ITD sensitivity. In multi-electrode configurations, all electrode pairs had the same ITD.

Results showed that lateralization of ITDs with multi-electrode stimulation did not result in poorer range of lateralization compared to single-electrode stimulation. However, significantly poorer lateralization was observed when ITD information was presented on the apical channels compared to spreading ITD information along the whole array. Only one subject indicated perceiving multiple auditory images. These results suggest that multi-electrode stimulation can lead to lateralization of fused auditory images that is comparable to single electrode stimulation. In addition, the present data supports the notion that presenting ITDs in one cochlear region only may not be optimal for maximizing useable ITD cues in multi-electrode stimulation.

Funding
Work supported by NIH-NIDCD (R01DC003083 to RYL) and NIH-NICHD (P30HD03352 to Waisman Center).

PD 138

Proof of Squelch Effect in a Randomized Controlled Trial on Simultaneous Bilateral Cochlear Implantation

Veronique Kraaijenga[1]; Alice van Zon[1]; Yvette Smulders[1]; Gijsbert van Zanten[1]; Wilko Grolman[1]; Robert Stokroos[2]; Nadia Hendrice[2]; Rolien Free[3]; Albertus Maat[3]; Johan Frijns[4]; Emmanuel Mylanus[5]; Wendy Huinck[5]
[1]University Medical Center Utrecht; [2]Maastricht University Medical Center; [3]University Medical Center Groningen; [4]Leiden University Medical Center; [5]Radboud University Medical Center

Background
Binaural hearing provides significant benefits over monaural hearing. The benefits of binaural hearing are most evident in speech-in-noise and localization of sounds and are based upon three principles: the squelch effect, the head shadow effect and the binaural summation effect. The squelch effect is the ability of the auditory system to combine the information from both ears centrally and segregate the speech from the noise by the difference in timing (neural firing) and difference in cues (amplitude) between both ears.

Deaf patients with a unilateral cochlear implant (CI) cannot benefit from the advantages of binaural hearing whilst bilaterally implanted patients are known to profit from the binaural summation and head shadow effect. However, the squelch effect has not been consistently apparent in these patients in current literature. The primairy aim of our study was to investigate the presence of a squelch effect after simultaneous bilateral cochlear implantation (BCI). The secondairy aim was to investigate when a squelch effect becomes present after BCI.

Methods
We conducted a randomized controlled trial (RCT) in multiple tertiary CI centers in order to investigate the benefits of BCI. Deaf adults were randomized to receive bilateral CIs either simultaneously or sequentially. For this study, nineteen simultaneously bilateral implanted patients were included.

Our primary outcome was the squelch effect, measured with the speech intelligibility-in-noise with spatially separated sources test. Sentences were presented from 60° to the left or to the right of the subject and the noise was presented from 60° at the opposite side. Speech perception was measured by averaging the signal-to-noise ratio of the last ten sentences presented, which resulted in the speech reception threshold in noise (SRTn). The bilateral hearing SRTn was compared to the situation in which the CI at the noise side of the head was turned off in a patients' best performing situation.

Results
One year after BCI the SRTn of the bilateral CI situation was not significantly different from the SRTn with the contralateral CI off. Two years after BCI the SRTn differed significantly between the bilateral CI situation (2.5dB) and when turning the contralateral CI off (4.1dB) (p<0.01).

Conclusions
Our RCT shows that BCI is effective in difficult hearing situations such as in spatially separated sounds and localization of sound. The current study shows that simultaneously bilateral implanted patients developed a squelch effect after two years. The squelch effect was not yet apparent after 1-year of follow up.

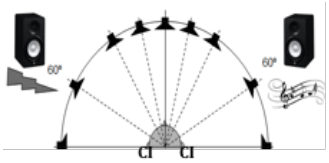

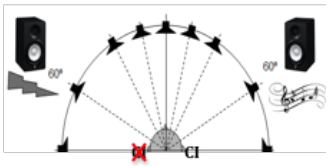

Funding
Wilko Grolman receives non-restrictive funds from Cochlear, MedEl, Advanced Bionics and Oticon.

PS 717

Network receptive field modeling reveals extensive integration and multi-feature selectivity in auditory cortical neurons

Nicol Harper[1]; Oliver Schoppe[2]; Benjamin Willmore[1]; Zhanfeng Cui[1]; **Jan Schnupp**[1]; Andrew King[1]
[1]University of Oxford; [2]Technische Universität München

Sensory neurons are commonly characterized using the receptive field, which describes the stimulus characteristics upon which their response linearly depends. Although this approach has a long and distinguished history, the simplicity of the receptive field leads to substantial limitations in the complexity of neural processing it can capture. In primary auditory cortex, receptive fields are often little more than a dot in frequency-time space. In reality, the response of a neuron is a consequence of the network of neurons to which it is connected, where each neuron is a nonlinear unit. Here, we reveal some of this complexity by describing neural responses to natural sounds using a nonlinear feedforward network model (a network receptive field). We show that primary auditory cortical neurons integrate in a complex non-linear manner over a substantially larger spectrotemporal domain than is seen in their receptive fields derived using standard approaches. The network receptive field, a parsimonious network whose output is found to integrate over up to 7 nonlinear units, each with its own spectrotemporal receptive field, consistently better predicts neural responses to natural sounds than conventional receptive field models. Notably, network receptive fields reveal many nonlinear aspects of auditory processing hidden from standard analyses. They reveal separate excitatory and inhibitory units with different non-linear properties, and the interaction of the units captures important operations such as gain control and conjunctive feature selectivity. The conjunctive effects, where neurons respond only if several particular features are present together, enable increased selectivity for specific complex spectrotemporal structures, and may constitute an important stage in the sound recognition. In conclusion, we demonstrate that fitting auditory cortical neural responses with network models gives substantially improved predictive power and reveals key non-linear aspects of cortical processing.

Funding
Supported by the Wellcome Trust (WT076508AIA) the BBSRC (BB/H008608/1) and Action on Hearing Loss (PA07)

PS 718

Frequency Selectivity of Neurons in the Ferret Auditory Cortex measured using Notched Noise Masking

David Merry; Toby Wells; Peyman Adjamian; Alan Palmer; **Christian Sumner**
Institute of Hearing Research

Background
Frequency selectivity describes the ability to resolve the individual frequency components in sound, and is a fundamental feature of hearing. It is crucial for most auditory tasks such as identifying sounds, separating auditory objects, and understanding speech. The ability of the auditory system as a whole can be measured through the behavior of a subject, whereas the ability of neurons to be informative can be measured by observing their spiking activity when presented with an external stimulus.

Methods
We examine the neural correlates of frequency selectivity using a notched noise masking paradigm. Although typically associated with behavioral measurements we instead utilized it to examine multi-unit neuronal response in the ferret's primary auditory cortex (A1). Neuronal responses to stimuli were recorded while the ferret was anesthetized or awake. Results were compared to previous behavioral studies, and to peripheral measurements of tuning in the auditory nerve (AN).

Results
Neuronal tuning in A1 of awake ferrets resembles estimates of frequency selectivity measured perceptually reasonably well. They are also similar to tuning in AN, although A1 bandwidths are more heterogeneous across units of similar characteristic frequency. These would suggest that frequency selectivity is established at the periphery, is maintained to the level of A1, and this ability is reflected in perception. However, pure tone tuning in the same units is broader. In contrast, units recorded in the ferret A1 under anesthesia had better frequency selectivity, or sharper tuning, compared with A1 units recorded under awake conditions, and perceptual and AN tuning.

Conclusions
The bandwidths of A1 neurons measured using notched noise masking matches cochlea and perceptual tuning in an awake preparation. However, this tuning does not appear to be an immutable property of auditory neurons.

Funding
Medical Research Council, UK

PS 719

Monkey Business in the Cat Auditory Cortex

Lauren Javier; Justin Yao; **John Middlebrooks**
University of California, Irvine

Background
Well-isolated single units recorded in the auditory cortex of awake marmosets exhibit spectral and temporal coding properties that are rarely, if ever, seen in other popular experimental preparations, including anesthetized cats. Those properties might represent specialization for reception of the marmoset's sophisticated vocal repertoire, or it might be that failure to observe those properties in other preparations is due simply to differences in experimental technique.

Methods
We recorded from auditory cortex in awake passively listening cats implanted with chronic recording arrays (Modular Bionics). Activity was recorded from well-isolated single units and from multiples of two or more undifferentiated units. Pure-tone stimuli, varied in frequency and pressure level, were used to measure frequency response areas (FRAs). Temporal coding was assessed using trains of clicks or 20-ms noise bursts, varied in presentation rate. The present sample size is small compared to published reports, but each of the following observations is supported by examples of well-isolated single units and by additional multi-unit recordings.

Results
We observed a variety of FRAs, including the V shapes that are commonly observed in anesthetized-cat cortex as well as level-tolerant I and O shapes that are rarely seen. The O-shaped FRAs were restricted both in frequency and level. Level-tolerant bandwidths were as narrow as ~1/6 octave, much narrower than is seen in anesthetized conditions. Single- and multi-unit recordings showed no systematic difference in spectral sensitivity, suggesting that nearby neurons share similar spectral properties. Preferred tones often elicited sustained responses lasting throughout or even beyond the 100-ms tone durations, whereas less-preferred tones elicited only onset responses like those that are typical of anesthetized conditions. About half of units showed sustained responses synchronized to trains of clicks or noise bursts, with some synchronizing to rates >40 s^{-1}, much higher than the 10-20 s^{-1} rates at which sustained responses are lost in anesthetized conditions. Other units showed minimal responses to clicks at low rates, but fired in a sustained manner to click rates 50 s^{-1} and greater, with responses generally peaking at click rates around 160 s^{-1} and declining at higher rates.

Discussion
The results demonstrate that the remarkable spectral and temporal sensitivity observed in awake marmosets is not limited to marmosets or to single-unit recording. Those properties are present in cats, and possibly other species, but apparently must be studied in unanesthetized conditions.

Funding
RO1 DC 000420

PS 720

Thalamocortical Long-term Potentiation in the Adult Mouse in vivo: Involvement of NR2A Subunits

Lingzhi Kong; Michael Zeeman; Xiuping Liu; Jun Yan
University of Calgary

The auditory cortex is continuously shaped by learning and experience, even throughout adulthood; this plasticity is known to be input-specific, i.e. to the sound frequency. Long-term potentiation (LTP) has been shown to be induced by the tetanic stimulation of the whole auditory thalamus or thalamocortical pathway with high-level currents and long-impedance electrodes however, such potentiation is obviously non-specific. Here, we firstly measured the frequency and amplitude receptive field of the cortical and thalamic neurons using pure tones and the cortical and thalamic neurons with the same characteristic frequency are considered in one point-to-point thalamocortical projection. We then electrically stimulated the thalamic neuron and recorded the field excitatory postsynaptic potential (fEPSP), and compared the fEPSP before and after the tetanic stimulation of the thalamic neuron. The tetanic stimulation successfully increased the amplitude of the ES-evoked cortical fEPSPs for more than forty minutes, therefore thalamocortical LTP was induced. When an antagonist preferring NMDA receptor NR2A subunit (NVP-AAM077) was applied to the auditory cortex 10 min before the above procedures, the LTP was not shown by tetanic stimulation of the thalamic neuron. These findings suggest that the NR2A plays an essential role in the thalamocortical LTP in the adult auditory cortex.

Funding
the Canadian Institutes of Health Research (MOP274494), the Natural Sciences and Engineering Research Council of Canada (Discovery Grant), Alberta Innovates Health Solutions and by funds from the Campbell McLaurin Chair for Hearing Deficiencies at the University of Calgary.

PS 721

Spectral tuning of short-term plasticity in auditory cortex

Ivar Thorson; Zachary Schwartz; **Stephen David**
Oregon Health and Science University

Perception of behaviorally relevant signals (*e.g.*, vocalizations) often requires integrating acoustic information over hundreds of milliseconds or longer, but the latency of sound-evoked activity in auditory cortex typically ranges over a much shorter duration. The ability of cortex to encode sounds in their broader spectro-temporal context has been attributed to modulatory phenomena, such as stimulus-specific adaption and contrast gain control. The current study tested whether short-term synaptic plasticity (STP) can provide a mechanism for such contextual influences on cortical responses to complex natural sounds.

Single-unit activity was recorded from core (A1) and belt (dPEG) cortex of awake ferrets during presentation of a large battery of natural sounds. Encoding properties were first characterized using a standard linear-nonlinear spectro-temporal receptive field model (LN STRF). LN STRFs where then compared to variants of the STRF that incorporated a simple STP mechanism (depression and/or facilitation) prior to the linear filtering stage. In two model variants, STP was applied globally to all incoming spectral channels or locally to subsets of the inputs. For the majority of neurons, STRFs incorporating locally tuned STP predicted neural activity as well or better than the LN STRF and the global STP STRF. These results suggest that cortical neurons integrate inputs over multiple spectral channels, each in a different adaptation state determined by the preceding sensory context. The time course of STP varied across neurons, but was generally stronger for excitatory channels than inhibitory channels. STP effects typically recovered over 100-1000 ms, a timescale consistent with previously reported contextual phenomena. Spectrally and temporally heterogeneous adaptation, subserved by STP or a mechanism with similar dynamics, may support representation of the diversity of spectro-temporal patterns that occur in natural sounds on behaviorally relevant timescales.

Funding
NIH R00DC010439

PS 722

Task-driven A1 plasticity in the temporal domain during performance of a click-rate discrimination task

Martin Averseng[1]; Diego Elgueda[2]; Jonathan Fritz[2]; Shihab Shamma[1]; Yves Boubenec[1]
[1]Ecole Normale Superieure; [2]University of Maryland

Studying changes in neuronal responses induced by task-engagement is crucial to understanding how the brain processes inputs to match behavioral demands in a changing environment. As the subject engages in auditory discrimination tasks, information is converted from an external physical acoustic stimulus to a neural spectrotemporal representation and then to an abstract and task-relevant representation observable through subjects' decisions. This process involves behavior-dependent plastic changes in neuronal responses that have already been reported in auditory primary cortex (Fritz et al. 2003). In conditioned avoidance discrimination tasks involving pure tones, several studies in the primary auditory cortex (A1) have reported task-relevant plasticity in receptive field (RF) tuning, as responses to sounds near the target tone frequency were enhanced compared to other frequencies. Previous findings have focused on task-dependent RF changes in the spectral domain. Here we describe similar task-relevant plasticity in the temporal domain during discrimination of periodic click rates.

We analyzed A1 extracellular recordings from two adult ferrets trained to discriminate low and high rate click trains, during passive sound presentation and active behavior conditions. We reconstructed the phase-locked component of neuronal responses using a non-linear stimulus reconstruction method successfully used in recent auditory studies (Pasley et al., 2012) to analyze recorded neuronal responses. This method performs a linear filtering of the neurophysiological data and reconstructs the incoming stimulus, thus providing a visualization of the stimulus representation as it is encoded in the neuronal population. We assessed changes in the neural encoding using reconstructed data from the passive and active conditions.

We found that the global quality of phase-locked encoding was substantially degraded for all stimuli during behavior, due to an increase in the spontaneous firing rate and a decrease in evoked firing rate of the A1 neuronal population. However, we observed that temporal adaptation of the neuronal response to the target click-train stimulus was specifically reduced during behavior, while adaptation to the non-target click-train stimulus was left unchanged (compared to the passively listening condition). This resulted in enhanced response to the targets in the second half of target click trains. This enhanced response to behaviorally relevant click rates reveals RF plasticity in the temporal domain that is similar to the behaviorally driven RF plasticity in the spectral domain that we have previously described.

In summary, we demonstrated that A1 neuronal adaptation can be modulated not only by behavioral states, as previously shown, but also to match behavioral requirements.

PS 723

Developmental Laterality Change in Auditory Cortex of Normal Hearing Rats

Doo Hee Kim[1]; Su-Kyoung Park[2]; Mun Young Chang[3]; Min Young Lee[4]; Seung-Ha Oh[3]
[1]Seoul National University; [2]Hallym University Medical Center; [3]Seoul National University Hospital; [4]Kresge Hearing Research Institute

Background
The maturation of cochlear of a rat is finished 2 to 3 weeks after birth, then the auditory cortex starts to configure based on acoustic stimulus. However, currently electrophysiological

responses of auditory cortex, in the early stage right after the acoustic stimulus are not completely understood. The aims of this study are to investigate the laterality changes of auditory cortices after birth and to speculate the critical period of early postnatal auditory cortex development in rat.

Methods
Eighteen SD rats with normal hearing were used to observe the activity of auditory cortex using multi-unit recording. The neuronal activity was obtained from the bilateral auditory cortices at the age of 3, 4, 5, 8, 10 and 12 weeks. After the surgical exposure of auditory cortex, 4x4 microelectrode arrays were inserted 4 times for each hemisphere (total 64 units). Auditory stimulation (Gaussian white noise, 100 ms length) was generated and introduced to the right ear every 685 ms during recording. The acquired data was processed and peri-stimulus time histogram (PSTH) was formulated. From the PSTH, sum of evoked spikes, peak amplitude and onset/peak latency were analyzed.

Results
The sum of evoked spikes was larger in the ipsilateral auditory cortex between 3 to 7 weeks after birth. However, at postnatal 8 week, the sum of evoked spikes was larger in contralateral auditory cortex. The peak amplitudes of the contralateral cortex increased rapidly at 5 week, decreased at 7 week and increased again at postnatal 8 week. The peak latency showed variable results before 8 week, but contralateral shorter latency was observed after 8 week. The onset latency also showed noticeable shorter latency after 8 weeks of age.

Conclusion
The contralateral dominance of auditory cortex was observed after 8 weeks of age. Before postnatal 8 weeks, ipsilateral dominance or even response between ipsilateral and contralateral cortex were found. These results might indicate that the critical period of rats would be within postnatal 7 weeks.

Funding
This research was supported by grant number 04-2014-0210 from the SNUH Research Fund.

PS 724

Depth Specific Developmental Changes in Neural Noise Correlation Profiles in the Mouse Auditory Cortex

Muneshwar Mehra; Sharba Bandyopadhyay
IIT Kharagpur

There are profound changes in sensory cortical neural circuitry during development based on sensory experience. Synaptic connections are pruned and new connections are formed to a great extent during early stages. The final broad connectivity patterns and strengths determine the functional properties of such circuits. Noise correlation (NC) between responses of pairs of single units is a measure of functional connectivity and is known to play a role in population encoding. In this study we investigate the nature and spatial patterns of NC between simultaneously recorded pairs of neurons in the primary auditory cortex at different stages of development, following ear canal opening. Changes in NC over the above time period are quantified in a depth specific manner, using neuronal pairs from superficial (II/III), input (IV) and deeper (V/VI) layers.

Single unit activity in response to brief (50-100 ms) tone pips and noise pips at multiple sound levels were collected simultaneously from multiple neurons from the auditory cortex of developing mice (C57BL6 male and female, ages: postnatal day 13-42, P13-P42) serially from multiple depths (grouped in superficial, input and deeper layers: 0-400, 400-600 and above 600 microns). Units were confirmed to be in the primary auditory cortex (A1) based on latency. Only neurons with clear best frequency (BF) were included in further analyses. Noise correlations were calculated between simultaneously recorded pairs of neurons. The relative location of the neurons was obtained from the respective electrode locations.

NC profiles (mean NC as a function of distance between the pair of neurons) decrease with distance in all groups. While middle layer profiles stabilize early, superficial and deeper layer profiles keep changing till later ages showing further changes in circuit in these depths. Analysis of the profiles along rostro-caudal (across tonotopic axis) and medio-lateral (within isofrequency axis) show differential changes across age and depth.

We conclude that average connectivity between neurons in different layers in the auditory cortex is shaped differently through development allowing mature circuits to compute different aspects in a layer specific manner. The NC profiles essentially provide a way to understand how different features in parallel channels (different frequencies or other aspects within the same iso-frequency sheet) are combined and how they develop during early hearing. Network models based on such connectivity profiles lead to better understanding of development of A1 circuits.

Funding
Wellcome Trust-DBT India Alliance, IIT Kharagpur Internal Funds

PS 725

Influence of sensory activity on the development of subplate neuron circuits

Xiangying Meng[1]; Patrick Kanold[1]; Joseph Kao[2]
[1]University of Maryland, College Park; [2]University of Maryland School of Medicine

Subplate neurons (SPNs) are among the earliest generated neuronal population in the cerebral cortex. They provide a transient excitatory relay of thalamic information to layer 4. Ablation studies have shown that SPNs play an instrumental role in the establishment and refinement of early thalamocortical and intracortical circuits.

Sensory experience, esp. sensory deprivation, has a profound influence on cortical development. Since SPNs are the first cells to receive sensory activity, sensory deprivations

could alter SPN function. This altered SPN function could influence the developing cortical circuits, and thereby cortical development, even past the duration of the sensory disruption. Thus, we here test if sensory experience influences SPN circuits and function by using a genetic deafness model and investigating if synaptic circuits associated with SPNs in the auditory cortex (ACX) are disrupted.

To investigate synaptic circuits onto SPNs we use laser-scanning photostimulation (LSPS) in thalamocortical slices of ACX from TMC1/TMC2 double-knockout mice at postnatal days 10-15. We compare the spatial pattern of excitatory inputs to SPNs in cells from genetically deaf mice with those in normal controls. Our analysis suggests that the pattern of excitatory inputs to SPNs in cells from genetically deaf mice is altered. These results indicate that early sensory experience might sculpt SPN circuits and thereby potentially alter subsequent development.

Since in humans the effects of deafness on SPNs would happen in utero before deafness can be diagnosed even at the earliest possible diagnosis cortical circuits could have already been affected by deafness.

Funding
R01 DC009607, R01 GM056481

PS 726

Uncaging the Auditory Cortex: Using Laser Photo-stimulation to Characterize Inputs into the Mouse Corticocollicular System

Bernard Slater[1]; Stacy Sons[1]; Daniel Llano[2]
[1]University of Illinois, Urbana Champaign; [2]University of Illinois

Background
In the auditory cortex, the projections leaving the cortex heavily outweigh those entering the cortex. In the corticocollicular system, neurons in cortical layers 5 and 6 project to the inferior colliculus. These projections have been shown to have a wide variety of effects when stimulated *in vivo*. Very little is currently known about nature of the inputs from the rest of the auditory cortex onto these cells. To investigate these inputs, we use laser photo-uncaging of glutamate to stimulate the cells that synapse onto the layer 5 and layer 6 corticocollicular cells. Here we examine the spatial activation profiles of cells from layer 2/3 to layer 6 with laser stimulation as well as the effect on pre-identified layer 5 and layer 6 corticocollicular neurons.

Methods
Mice postnatal days 25-40 were used in accordance with the University of Illinois IACUC. Thalamocortical brain slices were obtained at 300um. Using a visualized IR-DIC electrophysiological rig, cells from various layers of the cortex were recorded in a cell attached manner. A UV laser was utilized to photo-stimulate MNI-glutamate in a tight grid over the attached cell. Prior to layer 5 and 6 identified corticocollicular recordings, animals were injected with a retrograde tracer. Pre-identified cells were then recorded in a whole cell patched configuration then stimulated with a larger grid covering the area from the white matter to the pia.

Results
Cells recorded in different layers of the cortex show variety of stimulation patterns with attached recordings. Activation of individual cells varied, some only spiking when the cell itself or proximal apical dendrite was stimulated, others responded more widely with spikes arising from stimulation of basal dendrites. In identified layer 5 and layer 6 corticocollicular recordings, cells show spatial differences in their respective input maps with layer 5 having broader inputs in general than layer 6.

Conclusions
Cells in the mouse auditory cortex have varied response profiles to laser photo-stimulation; this will therefore impact the spatial resolution of input maps to the corticocollicular cells in layer 5 and layer 6. Layer 5 and layer 6 have been shown to have different electrophysiological properties and there is evidence that they differ in the nature of their inputs. Differences in these properties will likely then play different roles in modifying ascending information at the IC. These differences may explain the varied results seen in the inferior colliculus during *in vivo* stimulation of the auditory cortex.

Funding
F31 DC013501 R01DC013073

PS 727

Emergence of Spatial Stream Segregation in the Ascending Auditory Pathway

Justin Yao[1]; Peter Bremen[2]; John Middlebrooks[1]
[1]University of California, Irvine; [2]Radbound University Nijmegen

Background
Listeners are capable of disentangling multiple competing sequences of sounds that originate from distinct sources. This stream segregation is aided by differences in spatial location between the sources. We have described a possible substrate of spatial stream segregation (SSS) in the auditory cortex of anesthetized cats, where cortical neurons exhibit SSS by synchronizing preferentially to one of two sequences of noise bursts that alternate between two source locations. The mechanisms leading to those cortical responses are unknown. Here, we examine the emergence of SSS along the tectal and thalamocortical auditory pathways in the rat.

Methods
Extracellular recordings were made in anesthetized rats from the inferior colliculus (IC), the nucleus of the brachium of the IC (BIN), the medial geniculate body (MGB), and primary auditory cortex (A1). Stimuli consisted of interleaved sequences of 5-ms broadband noise bursts that alternated between two source locations with burst presentation rates of 5 to 40 bursts per second (bps). In a separate set of experiments, we applied pharmacological agents topically over the surface of cortical area A1 to assess the consequences of GABA receptor blockage on forward suppression. We tested 3 different types of GABA receptor antagonists that targeted specific pre- or

post-synaptic GABA-A or GABA-B receptors: Gabazine, CGP 36216 hydrochloride, and 2-Hydroxysaclofen. Stimuli for the drug tests consisted of sequences of 5-ms noise bursts at rates of 1 to 40 bps.

Results

At stimulus presentation rates of 5 and 10 bps, at which human listeners report robust SSS, neural SSS was weak in the central nucleus of the IC (ICC), it appeared in the BIN and in about two thirds of neurons in the ventral MGB (MGBv), and was prominent in A1. Cortical SSS reflects the spatial sensitivity of neurons enhanced by forward suppression. The GABA receptor blockers showed no significant effects on cortical forward suppression, although overall increases in spike rates indicated that the drugs were applied in adequate doses. The demonstration that forward suppression in A1 does not result from GABA-ergic inhibition at the cortical level indicates that cortical forward suppression, and the resulting enhanced SSS, might reflect synaptic depression at the thalamocortical synapse.

Conclusion

Our results highlight brainstem mechanisms that culminate in SSS at the level of the auditory cortex where auditory streams are segregated as distinct mutually-synchronized neural populations.

Funding

Funding: R01-DC000420 and F31-DC013013

PS 728

Across-Electrode Variations in Rate Discrimination and Gap Detection in Cochlear Implant Users

Stefano Cosentino[1]; **Robert Carlyon**[2]; John Deeks[1]; Wendy Parkinson[3]; Julie Bierer[3]

[1]Medical Research Council; [2]Cognition and Brain Sciences Unit; [3]University of Washington

Rate-discrimination experiments for pulse trains presented to single electrodes have revealed two findings that may underlie the poor pitch perception experienced by cochlear implant (CI) users: (i) The smallest change in pulse rate that can be detected at low rates (e.g. 100 pps) is typically larger than the corresponding frequency DL for pure tones in normal hearing, and (ii) above some limit – typically 300 pps – further increases in pulse rate are undetectable. Both the rate DL at low rates and the "upper limit" can vary across electrodes in a given listener. Here we compare across-electrode and across-subject variation in these two measures with the variation in performance on another temporal-processing task, gap detection, in order to explore the limitations of temporal processing in CI users

Rate discrimination was measured in 4-5 electrodes in each of 10 Advanced Bionics CI users. In each two-interval trial a single electrode was stimulated with two 200-ms pulse trains that differed only in pulse rate. Thresholds were measured using two interleaved adaptive tracks, corresponding to standard rates of 100 and 400 pps. The signal always had a rate higher than the 100-pps standard and lower than the 400-pps standard. Thresholds were defined as the signal rate averaged over the last four "turnpoints" of the corresponding adaptive track, and were expressed as a ratio relative to the corresponding standard rate. Gap detection was measured for 1031-pps 400-ms stimuli using an adaptive procedure, as described by Bierer *et al* (JARO 2015), and for the same electrodes and listeners as for the rate discrimination measures.

Across-electrode correlations between tasks were calculated in two ways. When across-listener differences were removed, the correlation between gap detection and rate discrimination at 400 pps ("Rate400") was of borderline significance ($r=0.33, p=0.06$), but neither measure correlated with rate discrimination at 100 pps ("Rate100"). Rate400 thresholds, averaged across electrodes, correlated significantly with gap detection across subjects ($r=0.90$, $p<0.001$), and, importantly, this correlation was significantly larger than that between Rate100 and gap detection ($r=0.43$, n.s.). The results are consistent with the upper limit of rate discrimination sharing a common basis with gap detection; it may be that, when rate discrimination breaks down at high rates, listeners cannot detect the gaps between successive pulses. The results also suggest that rate discrimination at lower rates is limited by a different mechanism.

Funding

This work was supported by the MRC (MC-A060-5PQ70) and by Action on Hearing Loss (MC-A060-5PQ75).

PS 729

Measured Lateral Position as a Function of Stimulus Interaural Level Difference and Overall Level

Nathaniel Spencer; **Christopher Brown**

University of Pittsburgh

Auditory dynamic range tends to decrease with severity of hearing loss. Hearing devices amplify and compress sounds, so that intensity changes for broad ranges of source intensities can be encoded, even when auditory dynamic range is small. Sound sources away from the mid-saggital plane give rise to interaural differences in time (ITDs) and in level (ILDs). These interaural differences play fundamentally-important roles for a wide variety of different everyday binaural listening tasks. However, sources like speech are modulated and thus vary over time in monaural level. Recent attention has been directed to the possibility that lateral position judgments based on ILDs for a bilateral cochlear implant user might be level-dependent (1). The purpose of the current study was to explore some of the potential factors underlying level-dependence of lateral position judgments in bilateral device users. Lateral position judgments by normal-hearing listeners were measured for different ILDs, for harmonic complex stimuli. ILDs were varied from -15 to 15 dB in 1 dB steps, and were obtained by attenuation. Three different dynamic range regions were studied: high overall stimulus levels, where stimuli might be compressed by features such as device-independent automatic gain

control (AGC), a middle range, and lower overall stimulus levels, at which the level at the far ear may be near or below threshold. Compression was applied using a threshold of 60 dB SPL, and inaudibility was simulated with expansion. The inaudibility threshold was 30 dB for four conditions in which the pre-AGC-stage inputs at the higher channel (i.e., the ear ipsilateral to the sound source) varied among 80, 65, 50 and 40 dB SPL in long-term average level. In a fifth condition, the inaudibility threshold was 40 dB SPL for stimulus levels of 50 dB SPL at the higher stimulus-level ear. Preliminary measurements were made with un-modulated harmonic complexes of 67 Hz fundamental frequency, and filtered to one octave in bandwidth around center frequencies of 500 Hz, 1 kHz or 2 kHz. Preliminary data suggest that response angles for normal-hearing listeners changed less rapidly with stimulus ILD, as stimulus level increased (Figs 1,2,3). This is consistent with level-dependent decreases in the slopes of the stimulus ILD/mean presented ILD functions (Fig. 4). Such level-dependent changes might be problematic for any kind of a bilaterally-aided, hearing-impaired listener for which dynamic range is compromised.

1) Goupell M.J. et. al. (2013), J. Acoust. Soc. Am. 133, EL101-107.

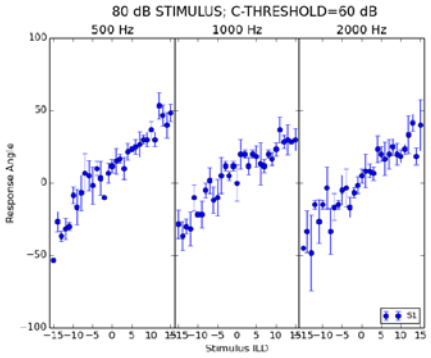

Figure 1: Stimulus ILD/Response Angle functions for a normal-hearing listener, for 80 dB stimulus level.

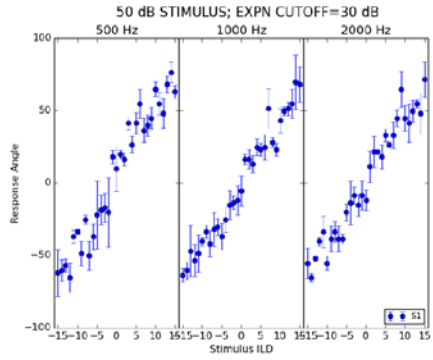

Figure 2: Stimulus ILD/Response Angle functions for a normal-hearing listener, for 50 dB stimulus level, 30 dB expansion/inaudibility cut-off.

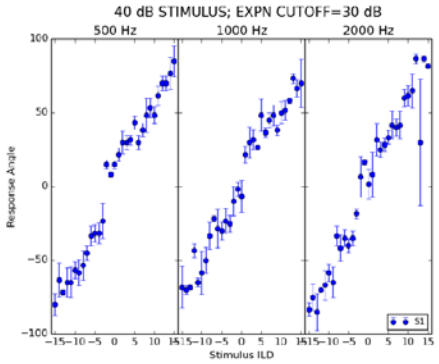

Figure 3: Stimulus ILD/Response Angle functions for a normal-hearing listener, for 40 dB stimulus level, 30 dB expansion/inaudibility cut-off.

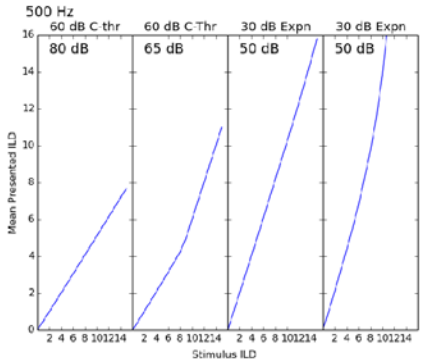

Figure 4: Stimulus ILD/Mean Presented ILD functions as a function of stimulus level for 500 Hz center frequency, with 30 dB expansion/inaudibility cut-off.

Funding
NIH; NIDCD; Brown RO1-008329

PS 730

The Effect of Interaurally Interleaved Channels on Speech Reception in Simulated Cochlear Implant Listening

Ann Todd[1]; Justin Aronoff[2]; Hannah Staisloff[2]; David Landsberger[1]
[1]New York University; [2]University of Illinois at Urbana-Champaign

Background

Speech reception in noise by listeners with cochlear implants (CIs) is thought to be limited in part by channel interactions caused by large spread of excitation from electrical stimulation. In listeners with bilateral CIs, one way to reduce channel interactions is to interleave channels between the two ears (e.g., stimulate odd channels in the left ear and even channels in the right ear). With interaurally interleaved channels, channel interactions can be reduced because there are larger distances between channels in each ear, while the total number of spectral channels is maintained collectively across both ears. However, when interleaved processing has been implemented for CI users, improvements in speech perception performance have been inconsistent. These inconsistencies may be caused by variability across listeners in neural survival and in the extent of interaural mismatch in electrode insertions.

In the current study, we examined the effect of interaurally interleaved channels on speech reception in noise. We used an acoustic model of CI stimulation with normal-hearing listeners in order to control for subject-specific factors. We hypothesized that interaurally interleaved channels would improve speech reception due to reduced channel interactions relative to diotic stimulation (stimulation presented from all channels in each ear) when spread of excitation was simulated.

Methods

Speech reception accuracy was measured at a fixed signal-to-noise ratio using a closed-set speech test. The speech-in-noise stimuli were processed using a 16-channel noise vocoder. Spread of excitation was simulated to represent electrical current attenuation rates of 4 dB/mm, 3 dB/mm, and 2 dB/mm. Performance was examined in diotic, monaural, and interaurally interleaved conditions. In the diotic and monaural conditions, each of 16 channels was presented in both ears or in one ear, respectively. In the interaurally interleaved conditions, eight odd channels were presented on the left and the eight even channels were presented on the right.

Results and Conclusions

Preliminary results suggest that listeners show poorer performance with greater amounts of simulated spread of excitation. Further data will be collected to evaluate the effect of interleaved channels on speech reception for each level of simulated spread of excitation. Results from the experiment are expected to provide insight into the variability in improvements from interleaved processing with CI users.

Funding

Support provided by NIH grants R01 DC012152 (Landsberger) and R03 DC013380 (Aronoff).

PS 731

Spatial Specificity and Temporal Acuity of Cochlear Implant Stimulation as a Function of Pulse Rate

Mahan Azadpour; Mario Svirsky
New York University School of Medicine

Higher rates of stimulation in cochlear implants (CIs) can encode more rapid temporal envelope variations, but they also impair detection of changes in stimulation level. We recently showed that the latter effect is associated with greater perceptual or internal variability (i.e. trial-to-trial variations in perceived loudness) when stimulation rates are higher. The present study further investigated CI users' temporal acuity and spatial specificity as a function of pulse rate. This was done using a psychophysical forward masking paradigm, in which a probe stimulus is presented following a masker stimulus. Since neural activity due to the masker stimulus persists after its offset and may still be present during probe presentation, probe detection is expected to be influenced by the variability of this neural activity. Thus, based solely on greater internal variability of higher rate stimuli, it is predicted that probe detection and the associated measure of temporal acuity would become poorer as masker rate is increased. However, neurophysiological studies in implanted animals suggest that probe detection improves at higher masker rates (Kirby and Middlebrooks, 2010), perhaps because neural excitation due to probe stimulus is enhanced. Spatial specificity, in contrast, is predicted to become poorer at higher masker rates as evidenced by animal neurophysiological studies. For example, Middlebrooks (2004) observed that the threshold of cortical responses to an electric pulse delivered to an intracochlear electrode is reduced when the pulse is preceded by a subthreshold pulse on a nearby electrode, and the reduction in cortical thresholds was more pronounced at shorter time intervals between the two pulses. This observation suggests that higher rates of interleaved stimulation provided by intracochlear electrodes cause greater channel interaction than lower rates.

The above predictions were evaluated by comparing psychophysical temporal and spatial forward masking patterns obtained with loudness-balanced maskers of 500 and 3000 pulses-per-second. For each masker rate, temporal acuity was estimated from the pattern of detection thresholds of a single-pulse probe stimulus at various masker-probe delays. Spatial specificity was estimated from the pattern of probe thresholds obtained with equally-loud maskers at various masker-probe distances. Preliminary results are consistent with predictions from animal studies, and confirm that both measures of temporal acuity and spatial specificity are influenced by stimulation pulse rate. These results provide important information on how pulse rate affects perceptual abilities that are known to underlie speech perception by CI users.

Funding

This study was supported by the National Organization for Hearing Research (NOHR).

PS 732

Mandarin Tone and Vowel Recognition in Reverberation with Cochlear Implants

Xin Luo[1]; Pavel Zahorik[2]; Yi-ping Chang[3]
[1]Arizona State University; [2]University of Louisville; [3]Children's Hearing Foundation in Taiwan

Introduction

Reverberation has been shown to adversely affect consonant and sentence recognition with cochlear implants (CIs). Among the acoustic cues distorted by reverberation, formant frequencies (important for vowel recognition) may be blurred, and amplitude modulations at the fundamental frequency (important for pitch perception) may be flattened. However, it remains unclear how CI performance in Mandarin tone and vowel recognition may change with reverberation. To answer the question, this study tested the effect of reverberation on Mandarin tone and vowel recognition of CI users, with reverberation time and prior exposure to the reverberant environment as the variables.

Methods
Ten native Mandarin-speaking CI users aged between 11 and 23 years participated in this study. Six Mandarin vowels (/a/, /o/, /e/, /i/, /u/, and /ü/) were produced in four Mandarin tones (Tone 1: high-flat, Tone 2: mid-rising, Tone 3: low-falling-rising, and Tone 4: high-falling) by a male and a female talker. To test the effect of reverberation time, the stimuli were processed by virtual acoustic techniques to simulate four rooms with broadband reverberation time of 0, 0.3, 0.6, and 1s, respectively. In the blocked-room presentation condition, the room was fixed within a block of trials, to provide consistent exposure to a reverberant environment. In the mixed-room condition, the room was randomly varied from trial to trial, to limit consistent room exposure.

Results
The results showed that CI users' Mandarin vowel recognition was not significantly affected by the reverberation time or the presentation condition. For Mandarin tone recognition, the effect of presentation condition was still not significant. However, the effect of reverberation time approached significance, and there was a significant interaction between the reverberation time and presentation condition. Interestingly, in the mixed-room condition, Mandarin tone recognition was significantly better with the 0.3 s and 0.6 s reverberation time than with the 0 s reverberation time (i.e., an anechoic environment). Compared to the mixed-room condition, the blocked-room condition significantly improved Mandarin tone recognition only with the 0 s reverberation time.

Conclusions
When the reverberation time varied across trials, CI users' Mandarin tone recognition improved with moderate degrees of reverberation. This effect was not observed when CI users had consistent exposure to each reverberation time in the blocked-room condition.

PS 733

Longitudinal Assessment of Spectral Ripple Discrimination and Speech Perception Evolution in Cochlear Implant Users

Alejandro Lopez Valdes[1]; Myles Mc Laughlin[1]; Laura Viani[2]; Peter Walshe[2]; Jaclyn Smith[2]; Lesley Flood[2]; Richard Reilly[1]
[1]Trinity College Dublin; [2]Beaumont Hospital

Introduction
Psychoacoustic studies have shown that cochlear implant (CI) users' ability to discriminate spectrally-rippled noise stimuli correlates reasonably well with their speech perception. Non-linguistic tests utilizing spectral ripple have been proposed to be useful for evaluation of CI performance. However, little is known about the evolution of spectral ripple discrimination (SRD) over time after the implantation and its relationship with speech perception rehabilitation. Here, we evaluate longitudinally the evolution of SRD and speech perception in quiet and noise for adult CI users.

Methods
Nine adult CI users attended research sessions, during their first year of rehabilitation, at dates indicated by the clinic (switch-on, one week, one month, two months, three months, six months, nine months and one year after switch-on). Behavioural SRD thresholds were measured using a two-alternative forced-choice paradigm. Speech perception in quiet and talker-babble noise (10dB SNR and 5dB SNR) was measured using AzBio sentences. Stimuli were presented unilaterally, at most comfortable level as indicated by the participant and sent directly to the CI speech processor via the auxiliary input cables.

Results
Repeated measures ANOVA indicates that there is a significant time effect in the evolution of SRD ($F_{(7,56)}$=6.65, p-value<0.0005) and speech perception in quiet and in noise at 10dB SNR ($F_{(7,16.21)}$=4.45, p-value<0.01; $F_{(6,55.82)}$=3.16, p-value=0.01). However, speech perception in noise at 5dB SNR showed a slight improvement over time that did not reach statistical significance ($F_{(7,41.66)}$=1.54, p-value>0.1). Post-hoc tests using the Bonferroni correction revealed that there is an increase in SRD at all sessions compared to the switch-on session, however, statistically significant changes only occur two months after implantation and onwards. Statistically significant changes for speech perception occur one year after implantation for the quiet condition and in noise at 5dB SNR. Pearson's correlation analysis revealed that SRD at one week after switch on has a strong and significant correlation with speech perception in quiet (r=0.878, p-value=0.002) and in noise at 10dB SNR (r=0.707, p-value=0.05). SRD at one week after switch-on also correlated with speech perception in quiet up to nine months after implantation (r=0.835, p-value=0.038).

Conclusion
Longitudinal assessment of SRD and speech perception indicated that the SRD progression is faster than speech perception in quiet and in noise for adult CI users. SRD even at one week after switch-on showed promising potential estimating speech perception abilities longitudinally. This opens the prospect of using SRD as an objective metric to estimate future speech perception abilities in CI users.

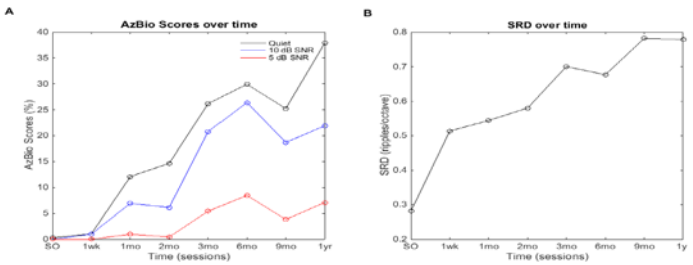

(A) AzBio scores during the first year after implantation showing slower progression and lower scores for the noise condition (blue and red traces). **(B)** Spectral ripple discrimination scores during the first year after implantation showing an increasing tendency and faster progression than the speech perception depicted in (A)

Funding
This research was funded by Cochlear Ltd., and under the Programme for Research in Third-Level Institutions and co-funded under the European Regional Development fund.

PS 734

The Trade-off Relationship Between Spatial Tuning and Multipulse Integration in Human Subjects with Cochlear Implants

Ning Zhou
East Carolina University

Background

Guinea pig studies have shown a correlation between the slope of the function relating psychophysical detection thresholds to pulse rate (known as multipulse integration) and the spiral ganglion cell density near the tested stimulation sites. If this relationship holds true in human subjects with cochlear implants, we hypothesize that multipulse integration should reduce (i.e., become shallow sloped) with focused stimulation, because focused stimulation restricts spread of excitation and effectively reduces the number of participating neurons. The effect of electrode configuration on multipulse integration however should depend on spatial tuning of the stimulation site. The effect of focused stimulation on multipulse integration should only be expected for stimulation sites with broad activation.

Methods

Multipulse integration was measured at multiple stimulation sites using two pulse rates (160 pps and 640 pps) with phase duration of 75 us in a monopolar stimulation mode (MP1+2) and bipolar stimulation mode (BP+N). In the bipolar stimulation mode, the separation of the reference and active electrodes was systematically varied as specified by N in BP+N. Forward-masked spatial tuning curves were also measured for these stimulation sites in a monopolar stimulation mode (MP1+2).

Results

The slopes of the multipulse integration functions were shallower when stimulation mode was changed from MP1+2 to BP+0, consistent with the idea that multipulse integration is dependent on neural density. However, the effect was only seen for stimulation sites that were measured with broad tuning in the monopolar stimulation mode. At those sites, the slope of multipulse integration became increasingly shallower as the focus of stimulation increased (i.e., increased N in BP+N). At stimulation sites measured with sharp tuning, multipulse integration tended to be shallow in the monopolar stimulation mode and the effect of focused stimulation was minimal.

Conclusion

These results suggested a trade-off relationship between spread of excitation and multipulse integration. Stimulation sites with sharp tuning tended to have poor multipulse integration. A broad activation supported good multipulse integration, but the integration at these sites reduced when the focus of stimulation increased.

Funding

Work was supported by the Hearing Health Foundation

PS 735

Does Rate or Place Affect Interaural Timing Difference Sensitivity in Children Who Use Bilateral Cochlear Implants?

Erica Ehlers; Alan Kan; Ruth Litovsky
University of Wisconsin-Madison

Children who are profoundly deaf routinely receive bilateral cochlear implants (CIs). One of the motivations is the provision of access to binaural cues, namely interaural time and level differences (ITDs, ILDs), to improve spatial hearing abilities. Our studies with low rate stimulation of 100 pulses per second (pps) suggest that bilaterally implanted children generally have sensitivity to ILDs, whereas sensitivity to ITDs is weak or absent. Lack of ITD sensitivity may arise from numerous factors. For example, clinical speech processing strategies provide stimulation at rates too high for encoding ITDs. However children hear amplitude modulated stimuli, and may be sensitive to the ITDs in the envelopes. In addition, prior studies with children used pitch matching to identify electrode pairs for testing, in order to account for possible differences in electrode insertion depth across the ears. Although pitch matching has been used successfully in adults, it may not be appropriate for children if they have learned pitch through their clinical maps (c.f. Reiss et al., 2008).

Children ages 9-17 (N=9) with bilateral Cochlear Nucleus CIs participated. Binaural sensitivity was evaluated by measuring ITD just-noticeable-differences (JND) thresholds. ITDs were imposed on stimuli with pulse rates of 1000 Hz whose amplitudes were modulated at a rate of 100 Hz, which is more akin to what children may be hearing on a daily basis. Performance was compared with unmodulated stimuli at rates of 100 or 1000 Hz. Another novelty in this study was the implementation of a direct pitch comparison (DPC) task, where subjects directly compared the perceived pitch of different interaural pairs of electrodes, which was intended to provided a more accurate and sharper estimate of interaural pitch matching.

Results showed that for children who have ITD sensitivity at 100 pps, comparable performance was achieved with high-rate, amplitude-modulated stimulation. Furthermore, the pitch matched electrode pair typically yielded the lowest ITD JND, in line with results from adults with bilateral CIs. However, the majority of children continued to show an absence or weak sensitivity to ITDs, suggesting that neither the rate of stimulation nor the choice of interaural electrode pair can account for the observed lack of ITD sensitivity. This suggests that other factors such as poor maturation of the binaural system due to lack of acoustic experience may be contributing to the deficit in ITD sensitivity.

Funding

Work funded by NIH-NIDCD (R01DC8365) and in part by NIH-NICHD (P30HD03352)

PS 736

Envelope Interactions in Multi-channel Amplitude Modulation Frequency Discrimination by Cochlear Implant Users

John Galvin[1]; Sandra Oba[1]; Deniz Başkent[2]; Monita Chatterjee[3]; Qian-jie Fu[1]
[1]University of California, Los Angeles; [2]University of Groningen; [3]Boys Town National Research Hospital

Previous cochlear implant (CI) studies have shown that single-channel amplitude modulation frequency discrimination (AMFD) can be improved when coherent modulation is delivered to additional channels. It is unclear whether the multi-channel advantage is due to increased loudness, multiple envelope representations, or to component channels with better temporal processing. Comparing perception of envelope interference to that of coherent modulation may shed light on how modulated channels can be combined. In this study, multi-channel AMFD was measured in CI subjects using a 3-alternative forced-choice, non-adaptive procedure ("which interval is different?"). For the reference stimulus, the reference AM (100 Hz) was delivered to all 3 channels. For the probe stimulus, the target AM (101, 102, 104, 108, 116, 132, 164, 228, or 256 Hz) was delivered to 1 of 3 channels, and the reference AM (100 Hz) delivered to the other 2 channels. The spacing between electrodes was varied to be wide or narrow to test different degrees of channel interaction. Results showed that CI subjects were highly sensitive to interactions between the reference and target envelopes. However, performance was non-monotonic as a function of target AM frequency. For the wide spacing, there was significantly less envelope interaction when the target AM was delivered to the basal channel. For the narrow spacing, there was no effect of target AM channel. The present data were also compared to a related previous study in which the target AM was delivered to a single channel or to all 3 channels. AMFD was much better with multiple than with single channels whether the target AM was delivered to 1 of 3 or to all 3 channels. For very small differences between the reference and target AM frequencies (2-4 Hz), there was often greater sensitivity when the target AM was delivered to 1 of 3 channels versus all 3 channels. The present results suggest that multiple envelope representations may contribute to the multi-channel advantage observed in previous AMFD studies. The different patterns of results for the wide and narrow spacing suggest a peripheral contribution to multi-channel temporal processing. Because the effect of target AM frequency was non-monotonic in this study, adaptive procedures may not be suitable to measure AMFD thresholds with interfering envelopes. Envelope interactions among multiple channels may be quite complex, depending on the envelope information presented to each channel and the relative independence of the stimulated channels.

Funding
John Galvin, Sandy Oba, and Qian-Jie Fu were supported by NIH grant DC004993. Monita Chatterjee was supported by NIH grant R01 DC014233. Deniz Başkent was supported by VIDI grant 016.096.397 from the Netherlands Organization for Scientific Research (NWO) and the Netherlands Organization for Health Research and Development (ZonMw)

PS 737

The impact of asymmetric stimulation rates on auditory grouping and binaural sensitivity in bilateral cochlear implant listeners

Tanvi Thakkar; Alan Kan; Ruth Litovsky
University of Wisconsin-Madison

Patients with bilateral cochlear implants (BiCIs) navigate through noisy environments by utilizing the monaural head shadow which arises from having two implants, but their ability to segregate and group auditory objects in multi-source environments remains largely unknown. Normal-hearing (NH) listeners can do this task well due to a facilitation from binaural processing or perceptual grouping of auditory objects. Auditory object formation in NH listeners incorporates a multi-dimensional space whereby grouping cues provides the perception that a specific auditory stream emanates only from one source. In contrast, BiCI users are exposed to the same incoming acoustic cues but the cochlear implant processing that encodes these cues may interrupt the mechanism of auditory grouping. In addition, inputs to the binaural system in patients with BiCIs may be asymmetric, leading to further degradation of auditory object formation. Good auditory object formation is likely to be a prerequisite for spatial hearing in NH listeners. However, the spatial hearing abilities of patients with BiCIs may be impacted by interrupted auditory object formation due to cochlear implant processing and interaural asymmetries. In this study, we examined the extent to which differences in the rate of stimulation across the ears contribute to poor auditory object formation, and in turn its impact on interaural time difference (ITD) sensitivity. Differences in average rate of stimulation across the ears can arise due to independent cochlear implant processing, or clinical mapping decisions that lead to different pulse rates being chosen for each ear.

BiCI subjects were presented with diotic and dichotic stimuli consisting of a constant amplitude pulse train at a pitch-matched, single electrode pair. The stimulation rate was fixed at a base rate in one ear, while being varied proportional to the base rate in the contralateral ear. Subjects participated in two tasks. In Task 1, subjects listened to a single interval and reported whether they heard one or two streams. In Task 2, ITD sensitivity was measured in a two interval, two alternative forced choice task.

The results measured the range of permissible interaural rate disparity for maintaining binaural auditory object formation and its effect on ITD sensitivity. These results have clinical relevance for choosing rates of stimulation across the ears in BiCI users and for designing new speech processing strategies in order to maximize perceptual grouping and binaural sensitivity.

Funding
Work supported by NIH-NIDCD (R01DC003083 to RYL) and NIH-NICHD (P30HD03352 to Waisman Center).

PS 738

Cochlear Implant Angular Insertion Depth and Detection of Musical Sound Quality Deterioration Due to Bass Frequency Removal

Alexis Roy[1]; Richard Penninger[2,3]; Monica Pearl[4]; Waldemar Wuerfel[3,5]; Patpong Jiradejvong[6]; Courtney Carver[4]; Andreas Buechner[3,5]; Charles Limb[6]
[1]Harvard University; [2]Med-El Corporation; [3]Cluster of Excellence Hearing4all; [4]Johns Hopkins University School of Medicine; [5]Medical University Hannover; [6]University of California San Francisco

Objective

Many cochlear implant (CI) users report poor musical sound quality. This may be partially attributed to the fact that CI arrays are unable to reach the most apical regions of the cochlea that encode low frequencies. This results in electrode-place mismatch between the frequencies transmitted by a given electrode and the corresponding cochlear location in which this electrode maximally stimulates. Longer electrode arrays that reach more apical regions of the cochlea may improve musical sound quality perception by decreasing electrode-place mismatch of low frequencies. The purpose of this study was to assess the effect of apical cochlear stimulation, as measured by angular insertion depth, on musical sound quality discrimination.

Methods

Standard (31.5mm, n=17) and medium (24mm, n=8) array Med-El CI users and NH listeners participated. Imaging confirmed the angular insertion depth of the implanted array. Participants completed a musical discrimination task in which they were presented with a real-world musical stimulus (labeled reference) and randomized test versions of the reference, which included a hidden reference, stimuli with increasing amounts of low frequency removal (200-, 400-, 600-, 800-, 1000-Hz highpass filters of the reference), and anchor (1000-1200Hz bandpass filter of reference). Participants provided sound quality ratings for each test stimulus. Scores for each CI users were calculated based on how much their ratings differed from NH listeners for each stimulus version.

Results

Medium array and standard users had significantly different angular insertion depths of 389.4±64.5 and 583.9 ± 78.5 degrees, respectively ($P < 0.001$). A significant Pearson's correlation was observed between angular insertion depth and the hidden reference scores ($P < 0.05$).

Conclusion

CI users with deeper angular insertions better perceived low frequency musical information, such that they could make sound quality discriminations that more closely resembled those of NH controls. This is the first study to assess the effect of angular insertion depth on musical sound quality discrimination. These findings suggest that more apical cochlear stimulation improves low frequency perception of musical stimuli, which may in turn provide a more satisfactory musical listening experience.

Funding

Research grant from Med-El corporation. Research grant from Advanced Bionics Corporation for unrelated work.

PS 739

Cochlear Implant Simulations in Cochlear Implant Patients with Contralateral Normal Hearing

Jeroen Peters; Ruben van Eijl; Anne Wendrich; Huib Versnel; Koenraad Rhebergen; Wilko Grolman
University Medical Center Utrecht

Background

It is unknown what a cochlear implant (CI) sounds like. Although vocoder software programs can mimic the signal processing of sounds in a CI processor, these simulations still sound different than what CI users actually hear. Traditional CI patients cannot point CI professionals in the right direction of what their implant sounds like. However, recently patients with single-sided deafness have been implanted. Their contralateral normal hearing (NH) enables them to compare the sound of their CI to simulations played to their NH ear.

Methods

Seven patients with variable etiologies, CI experience (2-12 months) and duration of deafness (2-10 years) participated in this experiment. The participants performed a forced-choice-experiment comparing the original sound file to vocoded simulations of those sound files. Loudness was balanced across stimuli. First, original sound files (sentence spoken by female/male speaker; guitar/piano music) were played to the CI ear alone via a loudspeaker, with the NH ear masked with broadband noise. We asked them to identify the gender of the speaker (or sort of instrument), and to repeat the sentence. Subsequently, two vocoded sound files were played to the NH ear alone (CI off) via a loudspeaker. Patients indicated which of these two vocoded sound files had the highest similarity to the original sound file that was played to their CI ear alone. They rated the similarity of sounds with a grade 1-10 out of 10. We randomly varied the orders of vocoder scripts, carriers (noise vs. sine) and frequency bands.

Results

Most patients were able to recognize the gender of the speaker and to repeat the sentence correctly, whereas it appeared hard to recognize the music instrument. For most stimuli and patients, a noise carrier generally resulted in the highest grades for similarity (i.e. 8-9 out of 10). Most patients preferred the widest frequency bandwidth (0-8000 Hz). On average, the music fragments received lower grades of similarity than the speech files.

Conclusions

Vocoders that have been widely used in psychophysical research could simulate sounds perceived by a cochlear implant reasonably well. We have obtained a fairly good idea of the sound of a CI, which we will play during our presentation. However, we should be aware that bilaterally deaf subjects may perceive their CI quite differently than our single-sided deaf participants.

Funding
Part of the costs of this study is funded by Cochlear Ltd. as a non-restrictive research grant.

PS 740

Voice emotion communication by listeners with cochlear implants

Monita Chatterjee[1]; Julie Christensen[1]; Aditya Kulkarni[1]; Mickael Deroche[2]; Sara Damm[1]; Adam Bosen[1]; Mohsen Hozan[1]; Charles Limb[3]
[1]Boys Town National Research Hospital; [2]McGill University; [3]University of California, San Francisco

Background
Relatively little is known about voice emotion communication by children, particularly those with cochlear implants (CIs). We hypothesize that voice emotion recognition by children with CIs will be partially related to their sensitivity to changes in complex harmonic pitch. We further hypothesize that voice emotion production by children with CIs will differ in acoustic features from the productions of children with normal hearing. A comparison of particular interest is between children with CIs and post-lingually deaf adults with cochlear implants, two groups that bring different auditory experiences to the table, but listen with the same device.

Methods
Participants are children with normal hearing and with CIs, adults with normal hearing and adults with CIs. Tasks include harmonic pitch discrimination, voice emotion recognition (*identify one of five emotions*), and voice emotion production (*say the same sentences in a happy and a sad way*).

Results
Children with CIs showed significantly poorer performance in voice emotion recognition than children and adults with normal hearing, but their performance was similar to that of adults with CIs. For children with CIs, voice emotion recognition scores were significantly correlated with complex harmonic pitch discrimination thresholds. Acoustic analyses of the productions showed that children with CIs produced smaller contrasts in mean voice pitch, spectral centroid and intensity than their normally hearing peers. Post-lingually deaf adults with CIs showed production patterns that were closer to the normally hearing population, but they, too, produced smaller intensity differences between happy and sad emotions. Further analyses of the variances of these parameters are ongoing and will be presented.

Conclusions
These results show that children with CIs have significant deficits in both voice emotion recognition and production, compared to normally hearing peers. This suggests that rehabilitation efforts should emphasize these aspects of speech perception and production, as emotional communication is an important aspect of social development and quality of life. We also conclude that emotional speech production is largely driven by acoustic experiences in childhood, but that device limitations still constrain emotional communication after deafness, as observed in voice emotion recognition and some aspects of voice emotion production in post-lingually deaf adults with cochlear implants.

Funding
Work supported by NIH/NIDCD grants R01 DC004786-08S1, R21 DC011905, R01 DC014233, T35 DC008757, and P30 DC004662.

PS 741

Forward modulation interference in cochlear implant listeners

Aditya Kulkarni; Monita Chatterjee
Boys Town National Research Hospital

Background
Envelope coding is important for cochlear implant (CI) listeners. Modulation detection interference has been reported in CI listeners when the interferers are simultaneously presented with the target. Previous work in NH listeners has shown modulation interference in forward masking (Wojtczak and Viemeister, J. Acoust. Soc. Am. 118(5), 3198-3210). Here, we report on adult CI listeners' sensitivity to amplitude modulation (AM) under conditions of forward masking by steady-state and AM maskers.

Methods
Single-channel 50 Hz AM detection thresholds are measured in adult post-lingually deaf users of Cochlear Corp™ devices, in the presence of forward maskers presented 1) on the same or different electrodes 2) with and without AM (50 Hz) 3) with and without a synchronous cueing stimulus on a remote channel. The masker-signal onset delay was varied. The masker and target were both fixed at syllable-like durations of 300 ms.

Results
Preliminary results in four CI listeners indicate varying levels of forward modulation detection interference, generally decaying with increasing masker-signal delay. No effects of the remote cueing signal have been observed as yet.

Conclusions
Recovery from forward masking may extend beyond the audibility of the target, and influence the auditory system's ability to encode target features such as temporal envelope, particularly when the masker is also modulated. These results are broadly consistent with previous findings in normally hearing listeners. Ongoing experiments will investigate effects of masker AM rate and depth and target duration.

PS 742

Spectral Resolution and Across-Channel Intensity Resolution in School-age Children Versus Adults: Effects of Age and Cochlear Implant Use

David Horn[1]; **Daniel Dudley**[1]; Kavita Dedhia[2]; Ward Drennan[1]; Kaibao Nie[1]; Jay Rubinstein[1]; Lynne Werner[1]
[1]University of Washington; [2]Emory University

Introduction

Spectral resolution matures during infancy in normal-hearing (NH) children (Spetner-Olsho, 1990) while intensity resolution develops through school-age (Maxon & Hochberg, 1982; Hall & Grose, 1990). Both factors are important for speech understanding in cochlear implant (CI) listeners and may be useful markers of CI candidacy and clinical device efficacy. The present study investigates whether development of these factors is affected by implant use.

Methods

Four groups of 10 participants were tested: NH adults, postlingually-deafened CI adults, NH children, and children with CIs implanted prior to age 2. Both groups of adults and children were matched for chronological age ranging from 41 to 79 for adults and from 10-15 years for children. Testing was conducted in soundfield in a sound booth at 61 - 65dBA. CI listeners were tested with their best ear only using clinical processors and settings. Tests included spectral ripple discrimination (SRD) and spondee identification in speech-shaped steady state noise (SRT). In SRD, listeners chose which of three noises contained a 90-degree phase difference in the spectral envelope. Ripple density was varied adaptively. Five ripple depths from 5dB to 30dB were tested in random order. The logarithmic equation SRT Threshold = B * ln (Ripple Depth/A) was used to fit individual listeners' data. The slope (B) was taken as the measure of spectral resolution and the x-intercept (A) was taken as a measure of across-channel intensity resolution.

Results

Mean SRD threshold improved with increasing depth and individual data was successfully fit to the logarithmic function for all but one participant. ANOVA demonstrated significant main effects of hearing loss (NH better than CI) on both spectral and intensity resolution as well as on SRT. Children showed better SRT scores than adults. Children and adults showed similar spectral and intensity resolution. No significant interactions between age and hearing loss were observed on any measure. Spectral resolution was significantly correlated with SRT for CI listeners but not for NH listeners. Correlations between intensity resolution and SRT were not significant for either group.

Conclusions

CI users had poorer spectral and across-channel intensity resolution than NH listeners, but school-age children in both the NH and CI groups had adultlike resolution on both measures. For CI listeners, spectral resolution is correlated with speech perception in noise in children and adults.

Funding

NIDCD: K23DC013055, T32DC000018, R01DC010148, R01DC00396, P30DC04661 Seattle Children's Foundation Gifts from Estate of Verne Wilkins and Motors Northwest

PS 744

Simplifying and speeding-up psychoacoustic measures of tinnitus

Christophe Micheyl[1]; Swapan Gandhi[2]; Adriana Goyette[1]; Shareka Pentony[1]; Sridhar Kalluri[2]
[1]Starkey Hearing Technologies; [2]Starkey Hearing Research Center

Background

Psychoacoustic measurements of tinnitus using traditional psychoacoustic techniques (e.g., method of adjustment) can be tedious and have low test-retest reliability. Moreover, current clinical guidelines for measuring tinnitus using an audiometer are particularly inefficient. Here, we describe a new approach for measuring psychoacoustic characteristics of tinnitus, including pitch, timbre, and loudness.

Method

The approach, using an efficient Bayesian adaptive paired-comparison procedure combined with a psychoacoustic model for automatically adjusting spectral stimulus parameters, was evaluated in 12 patients (13 ears). Each patient performed at least two, and usually three, runs of the adaptive procedure, including measurements of tinnitus pitch, timbre, and loudness.

Results

Complete tinnitus measurements could be obtained relatively quickly (mean test time less than 7 min.), with no preliminary training needed. Test-retest reliability was usually good; in particular, differences in the measured tinnitus pitch across consecutive tests was usually within the limited precision of the adaptive procedure (one third octave or less).

Conclusion

The new proposed approach for measuring psychoacoustic characteristics of tinnitus appears to be acceptably fast and reliable for use in clinical or research applications.

Funding

Work funded by Starkey Hearing Technologies.

PS 745

Early aging noise exposure increases loudness - a novel animal model of hyperacusis

Ana'am Alkharabsheh; Wei Sun; Fen Xiong; Richard Salvi; Sethilvelan Manohar; Guangdi Chen
University State of New York, University at Buffalo

Background

The neural mechanisms that give rise to hyperacusis, a reduction in loudness tolerance, are largely unknown. Some reports suggest that hyperacusis is linked to childhood hearing loss; however, the evidence for this is largely circumstantial. In order to rigorously test this hypothesis, we exposed rats

to intense noise shortly after the onset of hearing and then measured their loudness growth functions in adulthood using reaction time - intensity functions (RT-I), a metric which has been used in both human and animal studies to measure loudness growth, loudness recruitment and hyperacusis.

Methods
Eight postnatal day 16 rats were divided into two groups. Four in the Noise Group were exposed to narrow band noise (12 kHz, 115 dB SPL, 2-4 hours) and four were in the Control Group. All rats were trained on RT-I functions. RT-I functions were obtained to narrow band noise bursts centered at 2, 4, 12 kHz and measured over a broad range of intensities. The auditory brainstem response (ABR) was used to evaluate hearing thresholds and a comparison of ABR threshold in the noise-exposed and control animal was used to gauge the hearing loss in the Noise Group.

Results
The Noise Group showed a mean 30-40 dB hearing loss compared to the Control Group at frequency 4 kHz and above. Interestingly the reaction times in the Noise Group were much shorter than the Control Group at suprathreshold levels, behavior indicative of hyperacusis. The average reaction times in the Noise Group (n = 4) were 92.8 ± 4.8 ms, 84.2 ± 4.5 ms, 79.7 ± 6 ms at 2,12, and 4 kHz (90 to 110 dB SPL) versus 289.4 ± 5 ms, 275.6 ± 39.8 ms and 215.81 ± 34.9 ms for the Control Group respectively. The averages RT at low intensities were similar for either Groups or the Nosie Group shows longer RT.

Conclusion
Our results indicate that noise-induced hearing loss induced near the onset of hearing leads to a significant reduction of reaction time to suprathreshold sounds, behavior indicative of hyperacusis. Our results are consistent with clinical reports suggesting that hearing loss at an early age is a significant risk factor for hyperacusis.

PS 746

Tinnitus Characteristics in Patients with Menière's Disease and Normal-Hearing Subjects after Exposure to Intense Low-Frequency Sound

Margarete Ueberfuhr[1]; Lutz Wiegrebe[1]; Eike Krause[2]; Robert Gürkov[3]; Markus Drexl[1]
[1]Ludwig-Maximilians University; [2]Grosshadern Medical Centre, University of Munich; [3]Medical Centre, University of Munich

Tinnitus is one of the three classical symptoms of Menière's disease (MD) along with hearing loss and vertigo. Previous studies indicate that tinnitus in

MD patients is usually low-frequency and of the 'roaring' type, which is uncommon in tinnitus patients with other underlying pathologies. A tinnitus of similar quality, however, was reported to occur for a short duration (90 sec) in healthy, normal-hearing subjects after presentation of an intense low-frequency tone.

The study aims to describe tinnitus percepts regarding loudness and pitch/timbre with a psychophysical procedure. Subjects consisted of two groups:

1. normal hearing subjects with a transient tinnitus percept unilaterally evoked by exposure to an intense low-frequency tone (120dB SPL, 30Hz, 90s).
2. tinnitus patients with unilateral MD.

Subjects were asked to match their tinnitus percept to stimuli which were presented contra-lateral to the affected ear and consisted of sinusoidal tones of different frequencies and noises shaped by filters with adjustable slopes. Subjects could alter the selected matching tone in real-time regarding loudness and frequency content, so that it resembled their tinnitus best.

Transient tinnitus after low-frequency tone exposure occurred in all normal hearing subjects. About half of the subjects matched their tinnitus to noise, the other half to a sinusoidal tone with the majority (94%) below 2 kHz. Adjusted noises showed mainly either positive slopes above +5 dB per octave (hissing) or negative slopes below -5 dB per octave (roaring). 48% of all subjects reported a tinnitus with multiple components including pure tones and noise.

MD patients described tinnitus of either high-pitched tonal character above 3 kHz or a roaring noise with slopes below -5 dB per octave. Sound pressure levels of stimuli matching the perceived tinnitus predominantly fell into the range between 5-20 dB SL for both groups.

Results suggest that:

i) transient tinnitus after low-frequency tone exposure differs from tinnitus e.g. present in noise trauma because of its low-pass character;

ii) high-pitched tinnitus in MD patients might point to a later stage of disease or comorbidity;

iii) roaring tinnitus in both groups might be specific to an elevated endocochlear potential causing an increase in transmitter release of hair cells and firing rate of auditory nerve fibers (rate tinnitus);

iv) further research is needed to investigate whether similar tinnitus percepts in both groups are due to the same tinnitus-generating mechanism in MD patients and after low-frequency stimulation.

Funding
This work was funded by a grant (01EO1401) from the German Ministry of Science and Education to the German Center for Vertigo and Balance Disorders (IFB), project TRFII-6 to L.W. and M.D.

PS 747

Evaluation of an Acoustically Cued Tactile Startle Stimulus to Evaluate "Tinnitus" in Mice

Andrea Lowe[1]; Elliott Brecht[1]; Edward Lobarinas[2]; Joseph Walton[1]

[1]University of South Florida; [2]University of Texas at Dallas

A previous study has shown that temporary unilateral hearing loss in rats can result in a false positive indication of tinnitus when using gap pre-pulse inhibition of an acoustic startle (GPIAS). This was primarily due to a reduction in the startle response amplitude elicited by the acoustic startle stimulus; a limitation that can be overcome by using a tactile startle elicitor, such as an air-puff (Lobarinas 2013). Here we evaluated the efficacy of using a tactile startle-eliciting-signal (SES), an air-puff, in measures of noise and gap pre-pulse inhibition (PPI) in both a tinnitus and unilateral hearing loss model.

Preliminary testing was performed on young adult CBA/CaJ mice to determine the ideal air pressure to elicit reliable and repeatable startle responses. Startle amplitudes increased as a function of psi from 4 to 15, then decreased at 20psi, suggesting an optimal air pressure setting of 15psi. PPI was then evaluated using either 110dB Gaussian broadband noise bursts or rapid air puffs. For gap-PPI testing, both startling stimuli were imbedded into either a continuous 70dB broadband or narrowband noise (width of 1000 Hz, centered at 12, 16, or 20 kHz) presented with or without a 50ms silent gap, 100ms before the SES. A control noise PPI (NPPI) condition, with a 20ms noise burst presented 60ms before the SES, was used to determine pre-pulse salience. Testing conditions included baseline, unilateral hearing loss (cotton/silicone earplug with approximately 30dB attenuation), 2h post-salicylate (250 mg/kg i.p.) and a 48h post-salicylate washout.

Relative to baseline, the unilateral hearing loss condition showed significant amplitude decreases (51%) for the acoustic SES gap-PPI trials, resulting in altered PPI results. In contrast, there was no significant startle reduction for the air-puff SES, and these gap-PPI results remained unchanged. Under NPPI, there was also a significant amplitude decrease in the unilateral hearing loss condition for only the acoustic trials, though no significant differences in NPPI were induced for either acoustic or air-puff stimuli. Following salicylate treatment, startle amplitudes were increased for both the acoustic and air-puff trials, which returned to baseline levels during the washout condition. However, there were no differences in gap-PPI or NPPI between the acoustic and air-puff SES. These results highlight potential sources of error when using PPI as a function of hearing loss or other "tinnitus" inducing conditions that alter overall startle amplitude.

Funding

Supported by NIH-NIA Grant P01 AG009524

PS 748

Development and Validation of an Appetitive Operant Conditioning Model to Screen Rats for Noise-Induced Tinnitus

Krystal Beh; Marei Typlt; Greg Sigel; Ashley Schormans; Daniel Stolzberg; Brian Allman

University of Western Ontario

Background

In order to accurately screen laboratory animals for noise- or drug-induced tinnitus, it is important that the chosen behavioral paradigm be resilient to the hearing loss that often accompanies tinnitus induction, and closely replicate the conditions under which humans experience tinnitus (i.e., people perceive a steady noise or tone in quiet conditions). To that end, we previously established a novel, two-alternative forced choice appetitive behavioral paradigm that was optimized for the simultaneous recording of neural activity in rats temporarily experiencing salicylate-induced tinnitus. We investigated whether this behavioral paradigm was also capable of screening rats for tinnitus in the hours, days and/or weeks following intense noise exposure.

Methods

Sprague-Dawley rats were trained to nose-poke the left feeder trough during various steady narrow-band noises, and the right feeder trough during amplitude-modulated noise or quiet trials (speaker off). Correct feeder choices were reinforced with a food pellet. In subsequent testing sessions (i.e., following noise/sham exposure), performance during quiet trials were neither reinforced nor punished so as to avoid biasing the test day results. To further develop and validate our original paradigm, rats were screened for the presence/absence of tinnitus (1) immediately after intense 15-minute tone exposure (12 kHz tone at 115 dB SPL) or sham, or (2) up to two weeks after a one-hour intense tone exposure (12 kHz tone at 115 dB SPL) or sham.

Results

Following sham exposures, rats correctly chose the right feeder during quiet trials, even when they had experienced a substantial layoff from training. Conversely, after the 15-minute noise exposure, all rats (n=10) mistakenly went to the left (steady noise) feeder during the quiet trials indicating the rats perceived a steady phantom sound (i.e., tinnitus). Their tinnitus was transient, however, as all rats returned to normal baseline performance 24 hours post-exposure. As predicted, approximately 50% of rats screened positive for tinnitus one week following the hour-long noise exposure.

Conclusions

Collectively, these data suggest that our appetitive operant conditioning model is able to reliably screen rats for both acute and chronic noise-induced tinnitus, as the paradigm appears resilient to the associated hearing loss, and the learned behavior does not extinguish when a testing session occurs several days after tinnitus induction. Future experiments will record neural activity in behaving rats in an effort to investigate the neural correlates of acute and chronic noise-induced tinnitus.

Funding
CIHR Open Operating Grant

PS 749

Animal behavioral model for the emotional response to tinnitus

Amanda Lauer; Gail Larkin; Aikeen Jones; Bradford May
Johns Hopkins University

Tinnitus-related anxiety (TRA) is often more debilitating than the perception of phantom sound. The underlying mechanisms of this important hearing disorder remain poorly understood, in part, because tinnitus and anxiety have proven difficult to characterize in laboratory animals. Here, we report our ongoing efforts to develop an objective behavioral model for the emotional response to tinnitus. Laboratory rats were trained to drink from a water spout during periods of silence and to suppress the behavior during periods of sound. After the completion of training, tinnitus was induced by sound exposure or salicylate intoxication. Rats were subsequently classified tinnitus-positive if they began to drink during certain sound presentations. We assume this rapid, frequency-dependent loss of suppression behavior occurred because the rats heard a similar phantom sound during the silent water reinforcement periods. We have verified this interpretation by simulating tinnitus in untreated rats with actual sounds. The anxiety state of tinnitus-positive and tinnitus-negative rats was measured with behavioral assays that included open field exploration and social interaction tests. Independent studies have confirmed that anxious rats show less exploration and reduced interactions. Treatment with either sound exposure or salicylate produced high-anxiety phenotypes relative to untreated controls. In the case of sound exposure where tinnitus-positive outcomes (67%) were mixed with tinnitus-negative outcomes (33%), tinnitus-positive rats showed less exploratory behavior than tinnitus-negative rats. All sound-exposed rats showed fewer social interactions than normal controls. These results suggest the open field test is a selective measure of TRA, while the social interaction test may reflect general consequences of hearing loss. This unique phenotype represents a new animal model for future studies of neuropathology in the brain's pathways for sound and emotion.

Funding
Tinnitus Research Consortium, Action on Hearing Loss

PS 750

FMRP in the development and afferent influence of the auditory brainstem

Yuan Wang
Florida State University

The goal of the research is to identify the roles of fragile X mental retardation protein (FMRP) in the development and afferent regulation of the auditory brainstem. FMRP is an mRNA-binding protein that regulates the synthesis of selected proteins. Absence of FMRP results in fragile X syndrome (FXS), characterized by intellectual deficits and sensory dysfunction. FMRP is highly expressed in auditory brainstem neurons in birds, gerbils, primates, and humans.

In the chicken brainstem, we confirmed 6 variants of FMRP proteins. RT-PCR revealed differential expression levels of these variants in both developing and mature systems. Immunocytochemistry using a specific antibody to the chicken FMRP further demonstrated the distribution of FMRP in nucleus magnocellularis and laminaris (NM and NL), comparable to the mammalian cochlea nucleus and medial superior olives. Following surgical ablation of one cochlea, we detected rapid (within hours) and dramatic increases in FMRP immunoreactive in some but not all afferent-deprived neurons. Importantly, the neurons with enhanced FMRP eventually died while the neurons with a consistent level of FMRP survived. These observations support the hypothesis that FMRP is required for normal development and involved in afferent-dependent plasticity of the neurons in this circuit. We are currently examining the subcellular distribution pattern of FMRP during the circuit development as well as the effect of FMRP knockdown on NM and NL development.

Funding
NIDCD (R01 DC013074); Florida State University

PS 751

Maturation of Voltage-Gated Sodium Channel Properties in the Avian Cochlear Nucleus Magnocellularis

Hui Hong; Brooke Feinstein; Jason Sanchez
Northwestern University

Background
Auditory neurons generate ultrafast and temporally precise action potentials (APs), a function critical for normal hearing. Fundamental to this AP generation are voltage-gated sodium (Nav) channels. Previous immunohistochemistry studies in the avian cochlear nucleus magnocellularis (NM) suggest that developmental changes in Nav channel subtypes may differentially regulate AP generation. However, the functional maturation of Nav channels remains largely unexplored. To address this, we characterized the maturation of Nav channel properties in the avian NM.

Method
Voltage clamp recordings were obtained from chicken embryos (E) at days E10-12, E14-16, and E19-21. Voltage steps of varying magnitude were injected into NM neurons, and isolated Nav currents were recorded during application of voltage-dependent potassium channel blockers tetraethylammonium (TEA, 3 mM) and 4-aminopyridine (4-AP, 30 μM). Nav channel properties (amplitude, density, conductance, kinetics, reliability, and inactivation) were characterized and compared across developmental periods.

Results revealed that the amplitude of Nav currents significantly increased with maturation. From E10 to E16, changes in amplitude were consistent with an increase in channel density but not channel conductance. In contrast, from E16 to E21, Nav channel conductance became

significantly larger with minimal variation in channel density compared to immature neurons, suggesting developmental changes in Nav channel subtypes. We also found significant changes in Nav channel kinetics with maturation. The rise and fall rate of Nav currents became faster and the maximum amplitude half width became smaller. Surprisingly, Nav current jitter increased with maturation. These results suggest that larger and faster Nav currents are susceptible to poorer reliability. Finally, we characterized the development of Nav channel inactivation properties and found that from E10 to E16, NM neurons have similar inactivation membrane voltages. In contrast – and despite variations in Nav channel amplitude, density, conductance and kinetics – mature NM neurons contain Nav channels that inactivate at more negative membrane voltages than immature neurons.

In conclusion, we report that NM neurons develop large Nav currents due in part to differential changes in channel density and conductance. Coincident with an increase in Nav current size is a decrease in Nav current reliability, possibly as a consequence of changing kinetics, inactivation properties and channel subtypes. Together with our previous research, we suggest that the development of voltage-gated potassium channels may operate to offset maturational changes in Nav channel properties in order to maintain ultrafast and temporally precise AP generation in the avian NM.

Funding
School of Communication, Knowles Hearing Research Center. Northwestern University

PS 752

Cleaved Caspase-3 is Necessary for the Development and Innervation of the Chick Nucleus Laminaris

Sarah Rotschafer; Michelle Allen-Sharpley; Karina Cramer
University of California, Irvine

Caspase-3 is a cysteine protease typically associated with apoptosis. Recent studies have suggested that caspase-3 also contributes to cell differentiation, migration, and development of cell morphology. Loss of caspase-3 in mouse models severely affects auditory function and cochlear morphology. Here we have investigated the role cleaved caspase-3 plays in the development and innervation of the chick auditory brainstem. We previously showed that expression of cleaved caspase-3 follows the spatial and temporal development of the chick auditory brainstem, with caspase-3 first expressed in auditory axons of the VIIIth nerve, then in *n. magnocellularis* axons projecting to *n. laminaris* (NL), and subsequently in dendrites of NL neurons. We also demonstrated that blocking caspase-3 cleavage with the tetrapeptide Z-DEVD-FMK disrupts lamination of NL. NL neurons in Z-DEVD-FMK injected embryos failed to form the single-neuron thick lamina characteristic of NL, and the cell-free dendritic zone of Z-DEVD-FMK injected embryos suffered intrusion from non-neuronal cells. Because cleaved caspase-3 was notably expressed in axons innervating the ventral portion of NL during development, we investigated whether blocking caspase-3 activation affected axonal targeting within NL, and whether targeting errors might be associated with the degree of NL disorganization. To examine axonal targeting, we injected rhodamine dextran amine (RDA) into the auditory midline-crossing axons of E10 sham, control, and Z-DEVD-FMK injected embryos. Rather than terminating at the ventral dendrites of NL neurons as in our sham and control groups, the majority of Z-DEVD-FMK injected embryos showed axon tracts deviating into and through the neuronal layer of NL. Because NL neurons are normally arranged in a tightly grouped sheet one single-cell thick, the R^2 coefficient of a line fit to the spatial arrangement of NL cells is a useful measure of the degree of neuronal disorganization within NL, with lower values describing greater disruption of the NL lamina. We compared R^2 coefficients in control embryos, Z-DEVD-FMK injected embryos with axonal targeting errors, and Z-DEVD-FMK injected embryos without axonal targeting errors. We found that Z-DEVD-FMK injected embryos with axonal targeting errors had significantly lower R^2 coefficient values than Z-DEVD-FMK injected embryos without axonal targeting errors or control embryos. Loss of cleaved caspase-3 in developing axons is thus correlated with poor NL lamination. These results suggest that axon targeting and NL morphogenesis are closely linked developmental processes that likely involve two-way communication between growing axons and their targets.

Funding
National Institutes of Health, National Institute for Deafness and Other Communication Disorders Institutional Training Grant T32DC010775

PS 753

Tonotopic Differences in Membrane Properties Underlie Different Computational Strategies for Phase-Locking in the Chick Cochlear Nucleus

Stefan Oline; R. Michael Burger
Lehigh University

Auditory stimuli are processed in parallel frequency-tuned circuits, beginning in the cochlea. Auditory nerve fibers (nVIII) impart 'tonotopic' organization onto nucleus magnocellularis (NM), a division of the cochlear nucleus specialized for phase-locking. NM neurons receive subthreshold inputs that, even when phase-locked to tones, arrive with temporal jitter. Ideally, these neurons exclude poorly timed inputs while preserving responsiveness to signals over a broad range of stimulus intensities. Though all NM neurons function to preserve or improve temporal precision, membrane properties differ along the tonotopy, and thus may confer computational specificity. Further, the integrative properties of the membrane must adapt to depressing excitatory synaptic inputs (Zhang and Trussell 1994; Oline and Burger, 2014), and summation of inhibitory inputs (Howard and Rubel, 2010) that change dynamically with the acoustic environment. We investigated NM neurons' tolerance to time varying input across the tonotopic axis to a range of stimulus conditions. For individual neurons, a changing acoustic environment is manifest by changes in baseline

resting membrane potential (RMP). We manipulated RMP within its physiological range while injecting currents as either frequency modulated 'chirp' or ramp stimuli designed to probe sub- and superthreshold responses to input, respectively. At rest, all NM neurons regardless of characteristic frequency (CF) preferred slower inputs, exhibiting low-pass response features. Low CF neurons remained low-pass at all RMPs. In contrast, high CF responses shifted dynamically from low-pass to band-pass during periods of mild depolarization. Surprisingly, in both LCF and HCF neurons, the minimum *rate* of depolarization sufficient to evoke spiking remained constant in all conditions, indicating that 'slope threshold' is a robust intrinsic characteristic. This suggests that the optimal excitatory input for each NM neuron is invariant, even when confronted with dynamically changing input conditions. Further, this requires that the voltage-gated channels underlying membrane excitability are poised to respond to a restricted range of input parameters that is specified by tonotopic position. Together, these data suggest NM neurons maintain temporal precision by using different computational strategies along the tonotopy. Low CF neurons depend on summation of many small inputs over a broad integration period, and do not show membrane selectivity adaptation. In contrast, high CF neurons dynamically adjust their integrative properties according to RMP. Remarkably, the robust slope thresholds exhibited by all NM neurons arise despite highly dynamic combinations of input timing, synaptic depression, and inhibition, each of which are known to contribute to highly precise membrane selectivity.

PS 754

Hyperpolarization-activated Cation Conductances are Tonotopically Distributed in the Chick Cochlear Nucleus

Lashaka Jones; Stefan Oline; R. Michael Burger
Lehigh University

Auditory stimuli are processed in parallel frequency-tuned circuits, beginning in the cochlea. Auditory nerve fibers (nVIII) impart 'tonotopic' organization onto nucleus magnocellularis (NM), a division of the cochlear nucleus specialized for phase-locking. Phase-locking precision is required for sound localization via a coincidence detection process in nucleus laminaris (NL), the sole target of NM output. While NM is a superficially homogenous structure, a large number of physiological properties vary systematically along the tonotopic axis. For example, low voltage-activated potassium currents (K_{LVA})(Fukui & Ohmori, 2004), length of the spike initiation zone (Kuba & Ohmori, 2009), number of synaptic inputs, and resting potential, all vary tonotopically. NL neurons exhibit similar tonotopically arranged features including expression of hyperpolarization-activated cation channels (HCN), the channels that underlie I_h currents. HCN channels contribute to membrane excitability and resting potential. In NM, we demonstrated that membrane input selectivity also varies systematically along the tonotopic axis (Oline and Burger, companion abstract). An unresolved question is whether HCN channels may contribute to this selectivity gradient. As a first step, we have investigated whether HCN channels are indeed tonotopically distributed in NM as they are in NL. To examine I_h currents, we measured membrane responses using whole cell voltage clamp protocols in the presence or absence of the HCN antagonist ZD7288, and a cocktail of pharmacological agents to block synaptic or other voltage gated conductances. Our data show that the magnitude of I_h current is larger in low characteristic frequency (CF) neurons in comparison to high CF neurons. Interestingly, the activation voltage for both populations of NM neurons appears to be well matched to the resting membrane potential within that population where low CF neurons tend to rest at more depolarized potentials while high CF neurons rest at more hyperpolarized potentials. This further suggests that low and high CF neurons express a different compliment of HCN channel subunits, or are differentially modulated by endogenous modulators of HCN activity, or a combination of both. An intriguing unresolved question is to what extent HCNs contribute to setting the resting membrane potential, and more importantly, whether HCNs contribute to NM neurons' selectivity for particular input characteristics across the tonotopic axis.

PS 755

A Model of Sodium Channel Inactivation and Spike Threshold Adaptation in the Avian Cochlear Nucleus

Susan Lubejko[1]; Sara Soueidan[1]; Bertrand Fontaine[2]; **Katrina MacLeod**[1]
[1]University of Maryland; [2]University of Leuven

Single neurons operate in functional modes which range on a spectrum from coincidence detection (CD) to broad time scale integration. These properties determine how a neuron transmits information. In the auditory system, highly specialized CD neurons require rapidly fluctuating inputs to fire. However, a subset of repetitively firing neurons in the avian cochlear nucleus are also sensitive to the timing of input fluctuations, responding with increased firing rates to larger fluctuations and more reliable firing (Kreeger, Arshed & MacLeod, 2012, *J. Neurophys. v108(10):2794*). The intrinsic properties underlying this sensitivity is not understood, but may arise from the dynamics of spike initiation. We assessed the hypothesis that spike threshold adaptation is related to the operating modes of cochlear nucleus neurons by recording from avian cochlear nucleus angularis (NA), the brainstem area responsible for early sound intensity and spectrotemporal coding. To investigate intrinsic mechanisms, we made whole cell patch clamp recordings in brain stem slices in vitro and used direct, white noise 'fluctuating' current injections into the repetitively firing NA neurons. By systematically varying the mean step and noise variance, the resulting FI curves resolve repetitively firing neurons in NA into two groups: those that responded to increased stimulus variance with increased firing (coincidence detectors, CDs) and those that did not (integrators).To determine whether sodium channel inactivation could explain the CD-like behavior in NA neurons, we explored a neuronal model that included adaptive spike initiation derived from sodium channel dynamics (Platkiewicz & Brette, 2010, *PLoS Comp*

Biol 6:e1000850). The model was optimized to match firing patterns responding to a range of noisy stimuli. The resulting parameters that relate to the voltage dependence of the sodium inactivation curve, as well as the kinetics of inactivation, were different in the CD-like versus integrator cell types: the critical voltage of the steady state threshold function of the CD neurons was hyperpolarized by >8 mV and the time constant of the recovery from inactivation to be more than two-fold longer. This finding demonstrates that spike threshold adaptation could rely on sodium channel dynamics, although this does not preclude a role for low threshold K+ channels which may contribute even in repetitively spiking neurons. These data suggest that the intrinsic properties of cochlear nucleus neurons are crucial to their ability to encode input fluctuations that characterize in complex sound stimuli.

Funding
This work was supported by a NIDCD/NIH grant DC100000 to KMM.

PS 756

GABA-B receptor modulation of synaptic input to the avian cochlear nucleus angularis

Stefanie Eisenbach; Sara Soueidan; Katrina MacLeod
University of Maryland

The two cochlear nucleus divisions of the avian auditory brainstem serve divergent functions, but receive a common descending inhibitory feedback from a third order brain stem nucleus. Cochlear nucleus angularis (NA), which encodes intensity, projects to the superior olivary nucleus (SON). The SON in turn sends a feedback signal to both NA and cochlear nucleus magnocellularis (NM), as well as NM's target, nucleus laminaris (NL). Release of GABA affects NM and NL via direct ionotropic receptors, but may also modulate inputs with presynaptic inhibition via GABA-B receptors ($GABA_BR$). While inhibition at NM and NL circuits may influence interaural time difference coding, the role of the inhibitory feedback to NA is as yet unclear. In this study, we investigated whether the synaptic inputs to cochlear nucleus angularis is similarly affected by $GABA_BR$ modulation.

Whole cell patch clamp recordings were made from NA neurons in brainstem slices from embryonic day 17-18 chicken (Gallus gallus). Extracellular electrical stimulation evoked postsynaptic currents (PSCs) under voltage clamp. Excitatory, glutamatergic PSCs or inhibitory (mixed glycine/GABA) PSCs were pharmacologically isolated in separate experiments. Agonist (baclofen) or antagonist (CGP52432) against the GABA-B receptor were bath applied.

The $GABA_BR$ agonist baclofen profoundly suppressed both excitatory and inhibitory synaptic inptus. Single evoked EPSCs and evoked IPSCs were both reduced to ~10% of control by 20 μM baclofen. To determine whether the effect had a presynaptic locus, we measured spontaneous excitatory or inhibitory synaptic currents (sEPSCs and sIPSCs). Baclofen significantly decreased the frequency of sEPSCs and sIPSCs to 64.9% and 29.5% of control, respectively ($p=0.0047$ and $p=0.049$). In contrast, no change in the amplitude of spontaneous currents were observed. Nor were changes observed in postsynaptic input resistance or holding currents, suggesting no postsynaptic $GABA_BR$ contribution to reduced evoked EPSCs/ISPCs or sEPSCs/IPSCs. At inhibitory synapses, blockade of $GABA_BR$ with the antagonist CGP52432 resulted in a significant increase the evoked IPSC amplitude. However, short-term plasticity during stimulation with short trains was not systematically altered. These results suggest that both excitatory and inhibitory synapses in the avian cochlear nucleus angularis can be strongly modulated via presynaptic metabotropic $GABA_BR$. At inhibitory synapses, basal, sponaneous release of GABA may be at sufficient levels to tonically suppress release. The modulation of excitatory and inhibitory inptus of NA neurons via $GABA_BR$ activation appears to parallel that in NM and NL.

Funding
This work was supported by NIDCD/NIH grant DC100000

PS 757

Synaptic Transmission in the Endbulb Synapse of Mice Lacking GluA3 AMPA receptor subunit

Flora Antunes; Karl Kandler; Maria Rubio
University of Pittsburgh

AMPA-type glutamate receptors (AMPARs) mediate fast excitatory synaptic transmission in the CNS including the cochlear nucleus. AMPARs are tetrameric ion channels formed as combinations of four subunits (GluA1-4). The exact receptor subunit composition determines the physiological properties of AMPARs including their kinetics. GluA3-containing AMPARs are Ca^{2+} permeable, have large single-channel conductance and fast kinetics. GluA3-containing AMPARs are expressed by bushy cells (BCs) in the cochlear nucleus and, together with GluA4, are believed to enable the fast and precise synaptic transmission at the endbulbs of Held synapses.

Here, we examined the contribution of GluA3 to the kinetic properties of evoked and spontaneous EPSCs at the endbulb-BC synapse, using GluR3-KO (P17-P22) and age-matched wild type mice. Our results show that the absence of GluA3 had no significant effect on the kinetic properties of evoked and spontaneous EPSCs in BCs. However, in GluA3-lacking neurons, endbulb-elicited EPSCs exhibited lower short-term depression in response to high frequency stimulation (300 Hz). We hypothesize that the endbulb-BC synapse compensates for the lack of GluA3 through incorporation of GluA4 subunits which have been shown to lower synaptic short term depression at the calyx of Held in the medial nucleus of the trapezoid body (Yang et al., 2011). As synaptic depression can improve BCs temporal firing (Yang and Friedman, 2011) we tentatively predict an impaired ability of BCs in GluR3-KO to precisely encode temporal information.

Funding
NIH/NIDCD 013048 (MER); NIH/NIDCD 04199 (KK)

PS 758

Endogenous ATP Tunes Bushy Cell Action Potentials and Temporal Discharge Pattern Depending on the Tonotopic Position

Tamara Radulovic; Sasa Jovanovic; Jana Nerlich; Rudolf Rübsamen; Ivan Milenkovic
University of Leipzig

Background

Neuronal activity is essential for development of topographically ordered connections in sensory systems. In the developing auditory system, the precise pattern of spontaneous activity before hearing onset provides an instructive signal for structural refinement of the prominent inhibitory MNTB-LSO circuit. While the inner hair cells trigger APs in the auditory nerve fibers, the endogenous release of ATP in the ventral cochlear nucleus (VCN) conspicuously modulates the activity at the first central synapse of the afferent auditory pathway. ATP facilitates firing of bushy cells through cation-permeable P2X2/3 receptors that mediate cytosolic calcium signaling and protein kinase C activity. These effects of ATP engage bushy cells but not multipolar cells and in the former diminish with maturity. Here we determine the contribution of endogenous purinergic modulation to the AP properties and to the fine temporal structure of bushy cell discharges.

Methods

We used both in vivo- and acute slice-recordings to determine how the P2X2/3R affect the fine temporal profile of AP discharges in bushy cells of the VCN. The responsiveness of VCN neurons was assessed along the tonotopic axis with in vivo juxtacellular recordings combined with iontophoretic drug applications. Slice recordings were conducted in parasagittal VCN slices. Experiments were performed on Mongolian gerbils, aged P13-23 for in vivo-, and P4-16 for slice recordings.

Results

In vivo extracellular recordings conducted shortly after hearing onset in combination with iontophoretic drug applications revealed that P2X2/3R shape the fine temporal pattern of spontaneous activity in bushy cells. Endogenous activation of P2X2/3 receptors increases the incidence of inter-spike-intervals ranging 10-100ms, shortens the EPSP-AP transition time, and generates broader APs. In slice recordings, the APs evoked by synaptic stimulation of the endbulb inputs were prolonged upon a brief puff-application of the P2X2/3 agonist. The longer EPSC tau-decay can account for the observed effects. The area of the VCN in which the bushy cells are affected by ATP signaling progressively decreased during development to finally cover characteristic frequencies below 10kHz.

Conclusion

The endogenous ATP release facilitates AP generation and determines the fine temporal structure of bushy cell discharges by shortening the inter spike intervals during spontaneous activity. With maturity, the P2X2/3R-mediated effects are specifically constrained to the low-frequency region of the anterior VCN. These results point to the potential role of purinergic signaling in early establishment of the tonotopic gradient.

Funding

DFG grants MI 954/3-1, MI 954/2-1

PS 759

Functional Properties of Spherical Bushy Cells Assessed by Spectro-Temporal Receptive Fields

Christian Keine[1]; Bernhard Englitz[2]; Jörg Encke[3]; Werner Hemmert[3]; Rudolf Rübsamen[1]
[1]University of Leipzig; [2]Radboud University Nijmegen; [3]Technische Universität München

Spherical Bushy Cells (SBC), located in the anteroventral cochlear nucleus (AVCN), are second-order neurons of the afferent central auditory system. SBCs provide the input to different downstream nuclei of the sound localization circuitry, namely the medial and lateral superior olive. While SBCs receive their main excitatory input directly from auditory nerve fibers (ANF) through giant synaptic terminals, the endbulbs of Held, they are also targeted by acoustically activated inhibitory inputs. This inhibition is mediated by γ-aminobutyric acid (GABA) and/or glycine. The physiological role of this input still remains elusive. Previous *in vitro* and *in vivo* studies showed a remarkably slow inhibitory dynamics which suggests a gain control as the major function of this inhibition. This assumption can be tested in *in vivo* studies by analyzing the neurons' responses in complex acoustic environments and direct comparison to the neurons' ANF input.

In the present study, we aimed for an *in vivo* characterization of acoustically evoked inhibition and its potential contribution to signal processing using complex settings of excitatory and inhibitory acoustic stimulation. Loose-patch *in vivo* recordings in ketamine-xylazine anesthetized gerbils (P30-P60) were performed in the rostral AVCN. The input-output function was assessed by analyzing the overall ANF input as well as the EPSPs that failed or succeeded in generating a postsynaptic action potential. We used temporally orthogonal ripple combination (Klein et al., 2000, J Comput Neurosci) and dynamic random chord (Ahrens et al., 2008, J Neurosci) acoustic stimulation. Both stimuli are spectrally (3 Octaves) and temporally (2-100 ms) rich and thus suited to co-activate the excitatory and inhibitory inputs in a large variety of different combinations. The experimental results were compared to *in silico* data using a Hodgkin & Huxely type SBC model. The model was excited by a single ANF from a model of the auditory periphery (Zilany et al., 2014, J Acoust Soc Am), while sideband inhibition was implemented by a set of interneurons with different center frequencies. We estimated spectro-temporal receptive fields of SBCs, including an arbitrary input scaling, separately for the excitatory ANF inputs, as well as the SBC output spikes. This allowed us to compare the transfer properties and thus the function of inhibition at the SBCs. We conclude that the inhibitory inputs on SBCs shaped both their spectral and temporal response properties, rendering them temporally and spectrally more precise.

Funding
DFG RU 390/19-1, RU 390/20-1, HE 6713/1-1, Marie Sklosowska Curie Fellowship 660328

PS 760

Characterization of Multiple Encoding Properties of Single Units in the Guinea Pig Cochlear Nucleus

Arkadiusz Stasiak[1]; Boris Gourévitch[2]; Stefan Bleeck[3]; Ian Winter[1]
[1]University of Cambridge; [2]University Paris-Sud, Orsay; [3]University of Southampton, UK

Background
It is well accepted that auditory neurons at central stages of auditory pathways are sensitive to a multidimensional space of acoustic parameters characterised by spectro-temporal interaction. However, it remains unclear how spectro-temporal modulations, which are characteristic of environmental and communication sounds, are processed or transformed through different types of units within the cochlear nucleus (CN). Here, we report the responses of single units in the CN to a novel, multi-parameter stimulus, the Random Double Sweep (RDS, Gourévitch B. 2015). The RDS can probe: i) frequency tuning; ii) frequency-modulation-sweep direction and velocity selectivity; iii) frequency interactions; iv) temporal properties of neurons such as adaptation. Spectro-temporal receptive fields (STRFs) obtained from RDS stimuli were used to test response predictions.

Methods
Recordings were made from single units in the cochlear nucleus (CN) of normal hearing, urethane-anaesthetised, pigmented guinea pigs. Units were recorded extracellularly with low impedance glass-coated tungsten electrodes. The RDS stimulus was composed of two uncorrelated random sweeps (bandwidths 1-20kHz) at 3 different sound levels (in intervals of 20 dB above threshold) for 180 seconds. Response parameters were extracted by reverse correlation of the spike times and the RDS stimulus.

Results
We observed distinct STRF patterns reflecting sweep velocity tuning and temporal modulation tuning in different unit types of the CN. On average, onset (ON), primary-like with notch (PN) and chopper units have clear sweep-direction preferences, often robust across sound levels. Recordings from the dorsal CN show pauser-buildup (PB) and type IV units with a complex interaction between excitation and suppression. Predictive power is low, but best for ON and PN units and weaker for type IV units. In general, STRFs for all types of units tend to become more similar as sound level decreases, but prediction performance remains unaltered.

Conclusions
The diverse pattern in spectro-temporal tuning preferences between different unit types might indicate that CN neurons preprocess some specific sound features different immediately after the auditory nerve. Neuronal tuning preferences were mostly sound level-invariant. This is important for maintaining salience of acoustic cues in spite of modulation of absolute level by distance, reverberation or masking. Overall, the relatively weak prediction performance for most unit types indicates that RDS stimuli are unable to characterize the full response pattern of single units in the CN.

Funding
Acknowledgements This work supported by a research grant from EPSRC UK (RP09203).

PS 761

Responses to Sinusoidal Frequency Modulation in the Guinea Pig Ventral Cochlear Nucleus

Nihaad Paraouty[1]; Arkadiusz Stasiak[2]; Christian Lorenzi[1]; Ian M. Winter[2]
[1]Ecole Normale Supérieure; [2]Physiological Laboratory, University of Cambridge, UK

Background
Many psychophysical studies have investigated the detection of sinusoidal frequency-modulation (SFM) and on the type of sensory information it predominantly relies on: temporal-envelope (ENV) resulting from cochlear filtering, or temporal fine-structure (TFS) cues conveyed by changes in the neural phase-locking pattern over time, or a combination of both. Few neurophysiological studies have addressed this issue and data is still lacking regarding the relative strength of ENV and TFS coding in auditory neuron responses to SFM. This work aimed at characterizing the responses of ventral cochlear nucleus (VCN) neurons to SFM tones presented at various modulation depths and sound levels.

Methods
Single-units in normal-hearing anaesthetized pigmented guinea pigs were recorded extracellularly using tungsten-in-glass microelectrodes. Stimuli were 1-second SFM tones played at the unit's best frequency (BF), at modulation rates of 2, 5 and 10 Hz and modulation depths of 2, 4, 8, 16, and 32 % relative to BF. All stimuli were presented at positive and negative polarities and at several sound levels.

Results
VCN responses to SFM varied as a function of sound level, bandwidth and unit type. Shuffled correlogram analyses were carried out in order to assess the relative strengths of ENV and TFS coding. For small modulation rates (≤5Hz) and small modulation depths (≤16%), low-CF units showed weak temporal ENV coding but high phase-locking to TFS. In comparison, high-CF units generally followed the stimulus ENV for most conditions. The transition region over which temporal coding changes from being dominated by TFS coding to ENV coding was around 1-2 kHz.

Conclusion
The results are consistent with the notion that FM is encoded via neural phase-locking to TFS cues for low carrier frequencies and modulation rates, and via neural phase-locking to ENV cues at high carrier frequencies. The results also sug-

gest weaker phase-locking to TFS in guinea pigs compared to other species.

Acknowledgements
Work supported by ANR-Heart, ANR-11-0001-02 PSL, ANR-10-LABX-0087, Entendre-SAS & DFG FOR 1732 (TPE).

Funding
Work supported by ANR-Heart, ANR-11-0001-02 PSL, ANR-10-LABX-0087, Entendre-SAS & DFG FOR 1732 (TPE).

PS 762

Cholinergic Modulation of Excitability in Spherical Bushy Cells of the Mammalian Anteroventral Cochlear Nucleus

David Goyer[1]; Stefanie Kurth[1]; Christian Keine[2]; Rudolf Rübsamen[2]; Thomas Kuenzel[1]
[1]RWTH Aachen University; [2]University of Leipzig

Low frequency spherical bushy cells (SBC) receive direct input from the auditory nerve via the Endbulbs of Held, forming an integral part in the pathway of sound source localization in the azimuth. Recent data have shown that inhibition changes SBC input-output function by tuning excitability in a stimulus-dependent manner. Also, cholinergic innervation in the cochlear nucleus has been shown before. Two sources have been identified: Collaterals of the olivocochlear bundle originating in the superior olivary complex, and top-down projections from the tegmentum have been shown anatomically. We hypothesize that cholinergic modulation plays an additional role in fine-tuning of SBC excitability.

Whole cell patch clamp recordings from SBC were obtained from P15-25 gerbils (Meriones unguiculatus). Local application of 1mM Acetylcholine (ACh) or 500µM Carbachol caused a transient depolarization of 3.73mV (±0.54mV) caused by an inward current of -73.58µA (±22.74µA, tau-weighted=461ms ±117ms), due to activation of alpha7 subtype nicotinic receptors. Additionally, repeated ACh applications (10sec interval) tonically depolarized the resting membrane potential (RMP) to values of RMP+5.61mV (±1.36mV) which was driven by muscarinic ACh-Receptors and lasted minutes. SBC hyperpolarized under Atropine/Tolterodine block, indicating a tonic activation of muscarinic receptors already at rest.

Application of ACh was then combined with electrical stimulation of auditory nerve fibers, triggering synaptic SBC activation through the endbulbs of Held. Under these conditions, SBCs showed an increased firing probability. To further validate these findings, we performed in-vivo recordings from SBCs with iontophoretic application of Carbachol. Carbachol iontophoresis caused a significant increase of spontaneous spike rate (mean 139±7%, $p<0.01$, $n=24$), which was in agreement with the in vitro findings.

We tested the functional relevance in-silico and found that cholinergic enhancement of excitability increases SBC output rate without a loss in temporal precision of SBC output. Through collaterals of the OCB this would work in a stimulus dependent manner. Furthermore, responses to any auditory stimuli will be enhanced, if they are temporally aligned with acute nicotinic activation. It thus seems possible that the cholinergic projections originating in the tegmentum could modulate the SBCs input-output function based on saliency or behavioral context of the stimuli.

This work was funded by German Science Foundation's (DFG) Priority Program PP1608: "Ultrafast and Temporally Precise Information Processing: Normal and Dysfunctional Hearing"

PS 763

Intrinsic Membrane Properties of Bushy cells in the Cochlear Nucleus during Age Related Hearing Loss

Ruili Xie
University of Toledo

Background
Bushy cells in the cochlear nucleus are among the very first neurons of the central auditory system to receive peripheral inputs from the auditory nerve. They are specialized to encode fine temporal cues of the sound, which are essential in the performance of auditory tasks like azimuthal sound localization and speech perception. Such fine temporal processing in the central auditory system is impaired during age related hearing loss. Our study showed that at the endbulb of Held, the synapse between the auditory nerve and the postsynaptic bushy neuron, synaptic transmission is compromised in aged CBA/CaJ mice with profound hearing loss. It is unclear, however, whether the intrinsic membrane properties of bushy neurons are also changed during age related hearing loss.

Method
We studied the membrane properties of bushy neurons using young (1 month old) and aged (25 to 30 months old) CBA/CaJ mice. Auditory brainstem responses reveal significant hearing loss in the aged group. We performed whole-cell patch clamp recording from bushy neurons in parasagittal brain slices containing cochlear nucleus. Hyperpolarizing and depolarizing current steps were injected to drive membrane potential changes under current clamp mode. Depolarizing current injections at different ramp slopes were also used to assess the rate of depolarization threshold in bushy neurons.

Results
We compared the membrane properties of the bushy neurons recorded from young and aged mice. Bushy neurons in aged mice are more depolarized (by 0.95 mV on average) in resting membrane potential than those in young mice ($p = 0.0303$). There is a trend that the membrane input resistance of bushy neurons is higher in aged mice than in young mice, however, the different is not significant ($p = 0.0579$). There is no difference in the membrane time constant of bushy neurons between two mice groups. In response to ramp current injections, bushy neurons from both groups showed no difference in either the rate of their depolarization threshold, or the integration window for action potentials.

Conclusion
We conclude that despite of slightly depolarized resting membrane potential, the intrinsic membrane properties of bushy neurons in the cochlear nucleus remain largely unchanged in aged mice at the end of their life span. These bushy neurons have the same rate of depolarization threshold and integration window, which suggest that bushy neurons in aged mice can trigger functional outputs like those in young mice upon same auditory inputs.

Funding
Supported by NIDCD grant R03 DC013396 (R. Xie).

PS 764

Effects of Noise Exposure on Detection of Sound Features in vivo by Units in the Cochlear Nucleus.

Tenzin Ngodup; Matthew Xu-Friedman
University at Buffalo, SUNY

In the auditory system, noise exposure has been well-established to change the properties of neurons at various high-level stages, such as cortex and inferior colliculus. Recently, we discovered that non-damaging noise exposure changes fundamental characteristics of auditory nerve fiber (ANF) synapses onto bushy cells (BC) in the anterior ventral cochlear nucleus (AVCN). This suggests there may be additional unrecognized changes at the start of the auditory pathway that improve acuity. We tested how prolong exposure to non-damaging noise could affect processing of sound at BCs and ANFs. We reared mice in constant, non-damaging noise for a week, and performed single unit *in vivo* recordings of responses of ANFs and BCs to tones of varying intensity in both quiet and noisy backgrounds. We measured tone thresholds from BCs and ANFs from control and noise-reared animals in the presence and absence of masking noise. We found that in the presence of masking noise both BCs and ANFs from control animals had higher thresholds and greatly reduced dynamic range. By contrast, BCs and ANFs from noise-reared animals had little or no change in threshold and dynamic range. These results suggest that changes in properties of BCs and ANFs after noise exposure enhance their responses to tones in masking noise. As both the BCs and ANFs adapt to noisy sound conditions, it appears adaptations in the cochlea are primarily responsible for this enhanced sound acuity.

Funding
National Science Foundation grant 1208131 to M.A.X.-F., and the Dalai Lama Trust Fund to T.N..

PS 765

Synaptic Plasticity at Connections between T Stellate Cells in the Ventral Cochlear Nucleus

Xiao-Jie Cao; Donata Oertel
University of Wisconsin, Madison

T Stellate cells of the ventral cochlear nucleus convey information about the envelope of acoustic energy that falls within their narrow tuning curves and as a population they convey information about the spectrum of sounds. T Stellate cells project farther and more widely than any other of the principal cells of the cochlear nuclei, innervating the lateral superior olive, and medial olivocochlear efferent neurons, ventral nucleus of the lateral lemniscus, the inferior colliculus, and the thalamus. The present study is aimed at understanding what the excitatory inputs are that feed into this important pathway. It has long been known that T stellate cells receive input from a small number of type I auditory nerve fibers. T Stellate cells also receive input from other T stellate cells through local collaterals that terminate within roughly the same isofrequency lamina as the dendrites. Dual recordings confirm that action potentials in one T stellate cell can evoke EPSCs in nearby T stellate cells (Cao and Oertel, 2015, ARO Abstract). Those connections were unexpectedly weak, however. In only 5 of 27 pairs did presynaptic action potentials evoke EPSCs and when they did, the probability that a presynaptic action potential evoked EPSCs was low, less than 20%. We therefore tested whether synapses between T stellate cells can be potentiated by pairing postsynaptic depolarization with presynaptic firing. After recordings were established in two nearby T stellate cells that were aligned within the same isofrequency lamina, depolarizing current evoked action potentials in one cell while the second was held at -65 mV to record EPSCs. In each of the pairs, presynaptic action potentials evoked no EPSCs. Then one cell was depolarized to +30 mV while action potentials continued to be evoked in the other. Within less than 2 sec, reversed EPSCs were observed at +30 mV. Upon return of the postsynaptic voltage to -65 mV, EPSCs continued to be evoked by presynaptic action potentials. The magnitude and duration of potentiation varied with the duration of postsynaptic depolarization. Potentiated synaptic connections were observed in all 4/4 pairs tested, suggesting that the probability of neighboring T stellate cells being connected is high. Even after potentiation, the probability that presynaptic spikes evoked EPSCs did not exceed 25%. Our results indicate that T stellate cells contact one another through synapses that are potentiated by pairing of postsynaptic depolarization with presynaptic firing.

Funding
This work was funded by a grant from NIH DC00176.

PS 766

Theoretical Predictions of Cochlear Nucleus Receptive Fields from Auditory Nerve Fiber Responses to Natural Sounds

Aquib Jawed; Sharba Bandyopadhyay
IIT Kharagpur

Sparse coding and efficient coding of natural stimuli have been applied to understand neuronal properties. For example sparse coding has been shown to predict primary visual cortex simple cell receptive fields. Efficient coding of natural sounds has also been theoretically shown to accurately predict filtering properties of auditory nerve fibers (ANFs). In this study we use natural sound spectrotemporal information preserving criteria to theoretically predict receptive fields of

cochlear nucleus neurons based on ANF response to a large database of natural sounds.

We start with a large ensemble of natural sounds and use an ANF model (Carney et al) to obtain spiking responses of an array of ANFs with different best frequencies (BF). These ANF responses serve as the inputs to the cochlear nucleus. Receptive fields of theoretical cochlear nucleus principal neurons are estimated by optimizing a spectro-temporal information preservation criterion, at a variety of time scales. We explicitly introduce inhibitory inter neuronal inputs on principal cells along with inputs from the wide array of ANFs.

Sideband inhibition commonly observed in most VCN cell types is directly predicted by the optimization principle used. The predicted receptive fields for different time scale information match well with that of observed ventral cochlear nucleus (VCN) specific neuronal types, their response properties. Further analysis based on other criteria are also used to understand coding principles used in the auditory pathway. Such approaches can be extended to study stimulus transformations from one stage to another stage in the auditory pathway and help better understand functional neuronal organization principles followed.

Funding
Wellcome Trust DBT India Alliance

PS 767

A Rat Model to Study Ictal and Postictal Disordered Breathing and Potential Interventions to Prevent Death

Hamid Arjomandi; Ko Nakase; Richard Kollmar; Joshua Silverman; Krishnamurthi Sundaram; Mark Stewart
SUNY Downstate Medical Center

Background
Obstructive apnea due to laryngospasm may contribute to sudden unexpected death in epilepsy (SUDEP). Laryngospasm during seizures is often evidenced in humans by stridor. “Pulling” against such a closed airway may result in acute pulmonary edema and impaired gas exchange. Pulmonary edema is, in fact, the most common autopsy finding in patients with SUDEP. Here we report the use of a rat model to study laryngospasm and disordered breathing ictally and postictally, which can be used to develop practical emergency interventions.

Methods
Adult male Sprague-Dawley rats were anesthetized with urethane. Head-out plethysmography and quantitative video laryngoscopy were performed to assess baseline respiration and vocal cord motion. Simultaneous ECG and pulse-oximetry recordings were collected throughout each experiment. Each animal underwent surgery to place a tracheotomy tube. In the experimental group, the tracheotomy tube was then completely obstructed until respiratory arrest, followed by chest compression to resuscitate. A subgroup of experimental rats had their lungs inflated with either oxygen or nitrogen at the time of obstruction.

Results
All experimental animals went into respiratory arrest within two minutes after the onset of tracheal obstruction (60-135 s, mean=91.2 s). Oxygen saturation dropped as low as 20% during the obstruction, but recovered rapidly during resuscitation. Post-resuscitation, however, there was a second severe drop in oxygen saturation that recovered much more slowly and sometimes incompletely over 15 minutes. If the lungs were inflated during the period of airway obstruction, the desaturation during obstruction was delayed and decreased (more so by oxygen than by nitrogen), and the second drop after the obstruction did not occur.

Conclusion
We used a rat model to explore the respiratory consequences of complete airway obstruction such as that caused by laryngospasm during seizures. Post-obstruction desaturation may be related to acute pulmonary edema, but this is a work in progress. The results from the use of lung inflation during obstruction help define the kinetics of desaturation and suggest that this model might be useful for testing interventions that may be developed into practical emergency tools.

Funding
Supported by multiple sponsors’ award from SUNY Downstate to Dr. Stewart

PS 768

Overview of the University of Miami Children’s Hearing Program

Kari Morgenstein; Fred Telischi; Simon Angeli; Michael Hoffer; Andrea Green
University of Miami

Background
Hearing loss is the most common birth defect impacting 12,000 children each year. With the implantation of newborn hearing screenings, we are able to identify and provide intervention earlier than ever before. The University of Miami Children’s Hearing Program (UM CHP) was developed to ensure that children with hearing loss are identified early and provided comprehensive family-centered care. UM CHP strives to ensure that all children with hearing loss are able to meet their full potential.

Methods
Currently, we have a unique interdisciplinary team that consists of a program coordinator, pediatric audiologists, auditory-verbal therapists, ENT physicians, and a psychologist. In the near future, we will be adding several additional healthcare professionals to our team including a social worker, deaf educator, and music therapist. This will allow us to provide children with hearing loss comprehensive care in one location, likely decreasing the no show rate and stress on parents by having to take their children to multiple locations for various therapies. Within CHP, all families receive a personal phone call 48 hours before their scheduled appointment time to remind them of their appointments, answer their questions, and help facilitate any issues with getting to their appointments.

All children undergo a detailed case history and obtain a comprehensive hearing evaluation. If a hearing loss is confirmed, patients are seen by an ENT physician, receive a speech and language evaluation, discuss intervention options with the family, are given subjective questionnaires, and undergo a comprehensive review of the child's educational performance. In addition to this standard protocol, CHP offers hearing assistive technology evaluations, vestibular testing, auditory processing evaluations, a hearing device loaner bank, extensive counseling and parent support, community outreach, advocacy, a mentor program, and various activities for our patients and their siblings to participate in.

Results

The UM CHP saw 3,600 children in FY 2015.

- 1,600 children received audiological evaluations
- 93 diagnostic ABRs
- 246 hearing aid fittings
- 32 bone conduction device fittings
- 57 children have benefited from the CHP loaner bank ensuring that no child is without sound for an extended period of time.
- 150 distinct children received auditory verbal therapy, however, we had 860 appointments performed by our speech therapy team to ensure children with hearing loss are getting the proper therapy to be able to learn and develop spoken language.
- 7 presentations and educational advocacy events
- Decreased appointment wait times from two-three months to three weeks to one month.
- Since methods mentioned above have been implemented, the no show rate of our program has decreased significantly by 27%.

Conclusions

UM CHP is a unique resource for children with hearing loss and their families. Our goal is to offer all children with hearing loss enhanced opportunities to lead healthy and productive lives. By creating a model that other institutions will replicate, this program will impact children across the country and around the world.

PS 769

Inner Ear Structures Damage During Cochlear Implantation. Analysis of Insertion Forces, Cone Beam CT and Electron Microscope Images in Temporal Bone Specimens.

Daniele De Seta[1,2,3,4]; Guillaume Kazmicheff[2]; Renato Torres[2]; Jean Loup Bensimon[5]; Evelyne Ferrary[2,6]; Olivier Sterkers[2]; Yann Nguyen[2]

[1]Hospital Pitié Salpêtrière; [2]Sorbonne University Pierre et Marie Curie; [2]Sorbonne University Pierre et Marie Curie; [3]INSERM UMR S 1159; [4]Sapienza University of Rome; [5]Imagerie Medical Paris; [6]INSERM

Objective

To study the forces during cochlear implant (CI) insertion and correlate with cochlear anatomy and inner ear traumatism.

Study Design

Twelve fresh frozen temporal bones were implanted at constant speed with the aid of a motorized insertion tool. The MedEl flex 28 array was used in this study. During the insertion the data of the force applied to the cochlea was recorded with a 6-axes force sensor. The maximal peak of force, the force momentum, the sudden rise of the force and the smoothness of the curve were calculated and studied. Pre- and post-implantation Cone Beam CT scans were performed in order to study the cochlear anatomy and the position of the electrodes array within the cochlea. Scanning Electron Microscope acquisitions and histologic study defined the degree of traumatism caused by the array insertion. Force metrics were finally compared with pre- and post-implantation radiological images and correlated to inner ear traumatism.

Results

The radiologic images showed a translocation rate of 42% (5/12) from the scala tympani to scala vestibule. The position of 6 apical electrodes and 4 basal electrodes was not possible to be defined. The mean maximal peak of force was in 72.55 mN (range 38-139). The histological analysis showed 7 electrode arrays correctly positioned in the scala tympani and confirmed a translocation in 5 specimens (42%); the scalar translocation occurred always in the basal turn between160° and 200°. The elevation of the basilar membrane occurred in 2 cases, the rupture of basilar membrane in 2 cases and a fracture of the osseous spiral in 3 cases. The insertions with a scalar translocation had a maximal peak of force significantly higher than the insertions without inner ear structures damage ($p<0.05$, Student t test). A peak of force superior to 0.1 N was always associated with scalar translocation.

Conclusion

The area at the opposite of the round window (180° region), where the straight electrode arrays impact the lateral wall, represents the site at major risk for translocation. A peak force limit of 100 mN would be a good safety parameter to ensure quality of insertion into the scala tympani.

Funding

This work has been partially funded by MEDEL.

PS 770

Patients with Normal Auditory Thresholds but Difficulty Listening in Noisy Environments: Willingness to Complete Auditory Training

Brent Spehar; **Jeffery Lichtenhan**
Washington University in St. Louis

Background

There are no treatment options for patients with normal audiograms who complain about their ability to listen in noisy environments. Hearing aids and assistive listening devices, for example, are based on fitting strategies calculated for auditory thresholds and are thus not appropriate in these patients. However, we hypothesize that Auditory Training may be a treatment option for this group of underserved patients. It is clear that Auditory Training can help improve listening in noise ability for patients with severe to profound hearing losses or after cochlear implantation. As an initial step of recruiting subjects to address our hypothesis, we determined the prevalence of patients seen at our university hospital with normal audiograms and difficulty listening in noise.

Method

We used an established database of all patients seen by our Otolaryngology Department to identify those with normal auditory thresholds. We used a telephone-based, 14-item questionnaire designed to assess these people's degree of difficulty listening in the noisy environments, and willingness to be a participant to determine the extent to which they can benefit from Auditory Training.

Results

A total of 11,938 hearing tests were recorded between January 5, 2012 and August 27, 2015. Bilateral, normal pure tone threshold averages (PTAs) at mid-frequencies (0.05, 1, and 2 kHz) were found in 2,654 patients. We successfully contacted 474 of these people who were willing to complete the questionnaire. The number of people with normal PTAs and difficulty listening in noisy environments was 159, 70% of whom were willing to complete an Auditory Training program. When we considered only those patients with normal PTAs in both mid- and high-frequency (3, 4, 8 kHz) ranges, the number of these patients with difficulty listening in noise was 97, 74% of whom would complete Auditory Training.

Conclusions

These results can guide recruitment expectations for studies on the increasingly popular condition of "hidden hearing loss" – degraded performance on difficult tasks such as listening in noise despite normal performance on simple tasks like detecting pure-tone thresholds (Schaette & McAlpine 2011). Of the hearing tests performed at our institution over a 44 month period, 0.93% of the patients had normal mid-frequency PTAs, difficulty listening in noisy environments, and would complete Auditory Training. However, only 0.35% of all patients had normal PTAS in both mid- and high-frequency regions, difficulty listening in noisy environments, and would be a study participant.

PS 771

Evaluating the Effectiveness of Interventions to Prevent or Treat Hearing Disorders

Thais Morata[1]; Lena Wong[2]
[1]National Institute for Occupational Safety and Health; [2]University of Hong Kong

Otolaryngologists and other healthcare professionals have to make decisions involving prevention or treatment of hearing disorders on a routine basis. In order to adopt an evidence-based practice (EBP), such decisions should be guided by high-quality scientific knowledge. While there is consensus that EBP is a desired approach, it is not always clear what is meant by the term and what has to happen to claim that your practice is evidence-based. Unfortunately, there is a misconception that evidence supporting effectiveness can range from a "success story" based on a single example to high quality evidence involving formalized testing through cross-sectional or, better yet, prospective experimental design. A stronger quality and quantity of evidence than a single case study in a specific environment with a specific group of affected individuals is required for practices to be accepted as evidence-based. In this presentation we will describe the principles of EBP as they apply to the evaluation of interventions to prevent or treat hearing disorders. We will introduce approaches used for intervention effectiveness research, systematic reviews of the literature, the Cochrane Systematic reviews, and discuss strategies for the collection of evidence about different interventions. Examples will be provided on the best available evidence using different types of interventions for treatment of hearing loss, such as cochlear implants, and prevention of noise-induced hearing disorders. We will highlight where further evidence is needed, and recommend how further evidence should be collected and applied in the clinic.

Disclaimer: The findings and conclusions in this abstract have not been formally disseminated by the National Institute for Occupational Safety and Health and should not be construed to represent any agency determination or policy.

PS 772

Auditory Assessment Using the Pupillary Dilation Response

Avinash Bala[1]; Elizabeth Whitchurch[2]; Katherine Fitch[1]; Terry Takahashi[1]
[1]University of Oregon; [2]Humboldt State University

Hearing assessment is easy in cooperative children and adults, but is more difficult in people, such as infants, who cannot provide a reliable voluntary response. Here, we report results that suggest that the pupillary dilation response (PDR) may be useful in assessing hearing in the latter population.

While many phenomena can produce changes in pupil diameter, the term pupillary dilation response refers to a novelty-elicited dilation - one of a suite of autonomic responses that comprise the orienting response (OR). The PDR is a short-latency, multi-component response in which a quick dilation is followed by a brief constriction and then

a prolonged dilation. The fast dilation resists habituation but the prolonged component habituates rapidly upon repeated exposure to a stimulus. The PDR is briefer and has a shorter latency than the pupil dilation evoked by sustained attention or intense cognitive effort.

We measured pupil size before and after the presentation of an auditory stimulus, and simultaneously asked the subjects (normal hearing; >18 yo) to signal tone detection by button press. We show that we can estimate auditory thresholds at multiple frequencies in a single session that lasted 20 to 40 min. Detection thresholds were derived from response-intensity functions, which could be reliably derived from as few as 4 or 5 iterations. Single-session thresholds derived using the PDR are at least as sensitive as that derived from voluntary responses. Further, lower sound levels - at which subjects have not yet signaled detection - evoke a detectable change in pupil size, suggesting that under the right conditions, PDR-based assessment may be more sensitive.

The data described above were collected using a commercial eye-tracker. There are unavoidable limitations in optimization and flexibility when assessing pupil size using proprietary equipment designed for measuring eye-saccades. To overcome these issues, we designed a custom system for pupillometry, which can be scaled down economically for multiple uses. Results from the new system obtained in adults and infants are also presented, and contrasted with pupil size measurements from an eye-tracking system.

Funding
Translational Research Grant (2008; Innovation and Entreprneurship Program, University of Oregon) Incubating Interdisciplinary Initiatives (I3) Award (2015; University of Oregon)

PS 773

The effect of the transducers on paediatric thresholds estimated with Auditory State-Steady Responses

David Bakhos[1,2]; Villeneuve Alexandre[1,2]; Soo Kim[1,2]; Philippe Bordure[3]; Emmanuel Lescanne[1,2]; Jean-Marie Aoustin[2]; John Galvin[4,5]
[1]Université François-Rabelais de Tours; [2]CHU de Tours; [3]Nantes university; [4]Division of Communication and Auditory Neuroscience, House Research Institute; [5]University of California Los Angeles, David Geffen School of Medicine Department of Head and Neck Surgery

Background
The objective of this study was to investigate the usefulness of auditory steady state responses (ASSRs) for estimating hearing thresholds in young children, compared with behavioural thresholds. The second objective was to investigate ASSR thresholds obtained with insert earphones versus supra-aural headphones to determine which transducer produces ASSR thresholds most similar to behavioural thresholds measured with supra-aural headphones.

Method
This study was performed in two French ENT paediatric centres. We included children aged from 6 to 60 months who underwent ASSR (Eclipse) following behavioural audiometric testing. In their regular clinical practice, one centre used insert earphones and the other used supra-aural headphones to measure ASSR thresholds. Twenty-nine participants (58 ears) were included: 12 children (24 ears) in the insert group and 17 children (34 ears) in the supra-aural group. There was no significant difference in age between the two groups according to the results of a Mann Whitney test (p=0.14; U=68). First behavioural thresholds were compared to the raw physiological ASSR thresholds (nHL). Next, behavioural thresholds were compared to estimated ASSR thresholds (eHL) using table correction v.101. To compare behavioural and ASSR thresholds, Pearson's correlation and linear regression was performed at each frequency for each group. Paired t-tests were also performed on the behavioural and ASSR data.

Results
No general anaesthesia was used to perform ASSR. In the present study, strong correlations between behavioural and ASSR thresholds were observed for each test frequency and with either insert earphones or supra-aural headphones. In the insert group, the Pearson correlation was stronger than that in the supra-aural group, as indicated by a positive z value.

Conclusion
When behavioural thresholds are difficult to obtain, ASSR may be a useful objective measure that can be combined with other audiometric procedures to estimate hearing thresholds and to determine appropriate auditory rehabilitation approaches.

PS 774

Condensed Execution Model for Clinical Research Studies into the Daily Practice

Constanza Pelusso; Anthony Etzel; Hillary Snapp; Michael Hoffer; Fred Telischi; Liu Xiu
University of Miami

Introduction
Research in otolaryngology is essential for continued improvement in health care. However, clinical research is inherently subject to problems with protection of human subjects, bias, data collection, data analysis and reporting. This has led to an increase in regulation for clinical research practices by federal bodies. Understanding the fundamental differences between clinical practice and clinical research is essential to improve clinical research performance and reduce noncompliance. Problems are especially prevalent in clinical researchers with predominantly clinical practice experience who are not given appropriate levels of guidance and mentorship in responsible conduct of research.

Goal
To identify the pitfalls and oversights commonly associated with clinical research practices and to improve clinical research methods by implementing a condensed execution model that can be easily incorporated into daily clinical practice.

Methods
A survey was conducted of four different groups of health care providers (postdocs, residents, fellows and practitioners) in the department to identify 1. gaps in knowledge related to responsible clinical research, 2. common violations in study practices, 3. areas at risk for noncompliance.

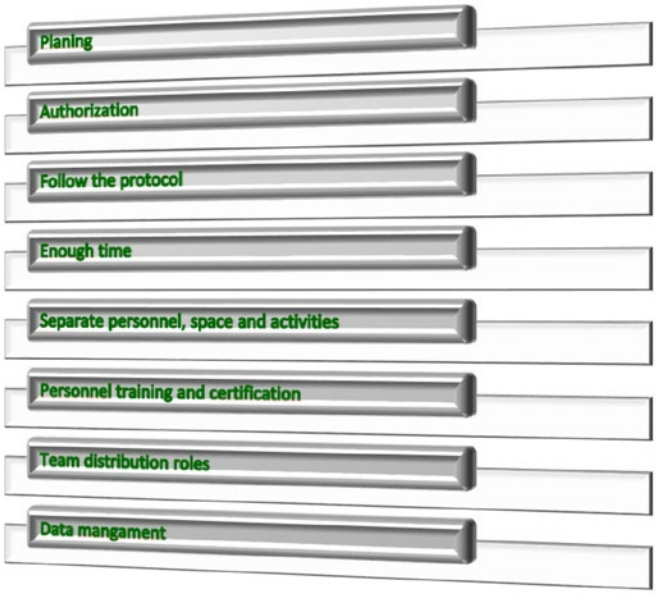

Results
Survey results indicated key areas of weakness in responsible conduct of research. Preliminary data suggest that condensed training models support improved protocol compliance and reduction in study violations.

Conclusions
Clinical researchers who are exposed to appropriate training in responsible conduct of research have reduced incidence of non-compliance with FDA, GCP, OHRP, NIH and HIPAA guidelines. Emphasis on key concepts related to consent, data management, protection of humans subjects, and ethics improved initiation of IRBs thereby reducing administrative support and delays in study execution.

Funding
University of Miami, Miller School of Medicine, Otolaryngology Department

PS 775

Measurement of the Compound Action Potential in Intraoperative Electrocochleography in Cochlear Implant Patients

William Scott; Christopher Giardina; Tatyana Fontenot; Andrew Pappa; Douglas Fitzpatrick
University of North Carolina, Chapel Hill

Electrocochleography (ECochG) is being increasingly explored for use in the field of cochlear implantation (CI) to determine residual cochlear health in CI patients and to assess damage during electrode insertion. Being able to separate the nerve and hair cell contributions to ECochG could help clarify this data. The compound action potential (CAP) is well-established to be of neural origin and may help to characterize nerve activity. Its recognizable shape and predictable location at the onset and offset of stimuli make it an intuitively useful surrogate for nerve activity in ECochG. Since the CAP should signify the persistence of nerve activity, its presence should correlate with better outcomes.

Intraoperative round window ECochG was performed in adult and pediatric subjects undergoing CI. Responses to tone bursts of multiple frequencies were recorded; from these responses CAP amplitude was measured. Adult patients were then assessed with CNC word scores 6 months post-implantation.

Less than half of CI subjects had a measurable CAP at any frequency, although the majority had good outcomes based on CNC word scores. The presence of a CAP was found to correlate with CNC word scores, but this relationship was quite weak. Previous work in our lab has shown that ECochG-TR(the sum of spectral magnitude of significant harmonics across frequencies) correlates with outcomes in CI patients. When added into multivariate analysis with the ECochG-TR, neither the presence nor amplitude of CAP improved the correlation. In addition, a substantial percentage of CI patients that showed no evidence of a CAP did show strong evidence of an auditory nerve neurophonic (ANN), another component of ECochG of neural origin.

The strong CNC scores and the presence of the ANN in many cases with weak or no CAP suggest that despite the lack of CAP, these subjects had residual nerve activity. Therefore, the CAP alone is not sufficient to define the contribution of the nerve to ECochG in this population. Measuring the CAP in CI patients is challenging because almost all have some degree of nerve damage, and many hear only at low frequencies where the CAP becomes difficult to characterize. Measurements of the ANN may be able to be used in conjunction with the CAP to make a more accurate assessment of nerve activity, which will better define the physiology of CI patients and may help predict outcomes.

Funding
NIH Grant 5 T32 DC 5360-12, MED-EL Coproration

PS 776

Optimizing Cell Ingrowth into Biomimetic 3D-Printed Tympanic Membrane Grafts

Nicole Black[1]; Elliott Kozin[2]; Max Colter[1]; Michelle Walsh[1]; Aaron Remenschneider[2]; Jennifer Lewis[1]
[1]Harvard University; [2]Eaton Peabody Laboratory, Massachusetts Eye and Ear Infirmary

Background
Contemporary techniques in tympanic membrane (TM) reconstruction utilize autologous grafting material, such as muscle fascia and/or cartilage. Variable surgical outcomes may be due, in part, to intrinsic defects in the graft materials or poor integration with the surrounding external auditory canal (EAC) and remnant TM. As a consequence, many patients experience re-retraction and re-perforation of the

TM and thus require revision surgery. In an effort to address these limitations, we have created biomimetic TM grafts via 3D printing technology. We hypothesize that by specifying scaffold architecture and infill contents, cellularization of grafts can be optimized, potentially improving graft integration and wound healing for 3D printed TMs.

Methods

Filamentary extrusion 3D printing was used to create TM grafts with rapidly tunable fiber arrangements from biocompatible polymers: polydimethylsiloxane (PDMS), polycaprolactone (PCL), and flexible polylactic acid (PLA). 3D printed scaffolds were infilled with a biologic hydrogel matrix composed of varying concentrations of fibrin, collagen, and basic fibroblast growth factor (bFGF). PDMS molds were 3D printed to mimic the circumferential arrangement of cells in the EAC. These molds were infilled with a fibrin hydrogel containing green fluorescent protein (GFP)-expressing human neonatal dermal fibroblasts (HNDFs). Infilled TM grafts (n=3) were overlayed onto the molds. Cellular ingrowth was determined by confocal laser microscopy, tetrazolum assay (MTS), and Masson's trichrome stain.

Results

All TM grafts supported fibroblast confluence by one month. Cell viability was confirmed for up to four months in culture. PCL grafts supported the greatest fibroblast adhesion, allowing cells to be channeled into the interior of the graft along the radial fiber axes. After 32 days, GFP fluorescence on PCL grafts infilled with 40 mg/mL fibrin and 1.4 mg/mL collagen was 85% and 118% greater than PDMS and PLA grafts, respectively. Additionally, an MTS assay confirmed that PCL grafts containing 10 ug/mL bFGF in the infill exhibited 30% greater fibroblast proliferation than those without bFGF. Higher scaffold fiber counts improved fibroblast confluence over the entire TM graft. Masson's trichrome stain confirmed the presence of extracellular collagen in the TM grafts.

Conclusion

3D printed TM grafts can become populated by HNDFs from their circumference. Increased cell motility and proliferation can be optimized by adjusting graft polymeric skeleton material, fiber arrangement, hydrogel infill material, and growth factor presence. In the future, TM graft scaffold degradation rates will be selectively tuned to match cellular proliferation rates, allowing the resorption of the graft to parallel native tissue ingrowth.

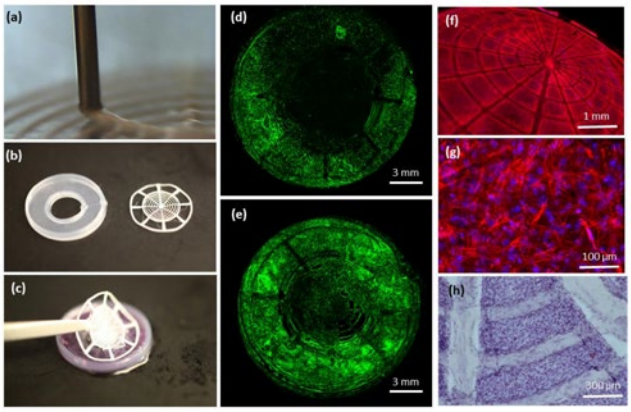

Figure 1: Schematic of 3D printed TM graft fabrication and *in vitro* HNDF ingrowth from their circumference. Filamentary extrusion 3D printing of a tympanic membrane graft skeleton with PLA at 20 wt% in HFIP (a). The final 3D printed PDMS cell mold and final PLA 8C/8R TM graft (b) are infilled with fibrin and HNDFs into the mold and a fibrin/collagen/bFGF infill in the TM graft. The TM graft is overlayed on top of the mold so that only the noninfilled border region is in contact with cells. Day 32 HNDF ingrowth on PLA 8C/8R grafts infilled with 30 mg/mL fibrin, 1.4 mg/mL collagen without growth factors (d) and with 10 ug/mL bFGF (e) (green; GFP). Day 94 PDMS 8C/16R graft infilled with 40 mg/mL fibrin, 1.4 mg/mL collagen, and 10 ug/mL bFGF demonstrating cell proliferation over the entire TM grafts (f) and a 40x magnified section (g) fixed and stained with Alexa Fluor Molecular probes (red; actin, blue; nuclei). Day 134 PDMS 8C/16R graft infilled with 40 mg/mL fibrin and 0.5 mg/mL collagen fixed and stained with Masson's Trichrome (blue; collagen, red; cytoplasm, black; nuclei) (h).

PS 777

Auditory Profile and Common Audiological Functional Parameters (CAFPAs): From Diagnostics to Machine-Learning-based Evidence

Birger Kollmeier[1,2]; Thomas Lenarz[1,3]; Anna Warzybok[1,2]; Marc Schädler[1,2]; Sabine Haumann[1,3]; Thomas Brand[1,2]; Jörg Lücke[1,2]

[1]Cluster of Excellence Hearing4All; [2]Universität Oldenburg; [3]Medical University Hanover

Introduction

How well should the various audiological findings best be represented and how can this information be used to characterize the individual hearing problem of each patient – preferably in a way which is independent from his or her native language? This contribution reviews the approach and models developed in the Cluster of Excellence Hearing4All (Oldenburg/Hannover) to unite the diverse audiological databases, e.g. from the hearing research and clinical institutions in Oldenburg and in Hannover in a more abstract, comprehensive way than the previously defined "auditory profiles".

Method

A set of "common audiological functional parameters" (CAFPAs) has been defined that serves as an abstract representation of the most important audiological characteristics of each patient. The CAFPAs include, e.g., sensitivity loss in different frequency regions, distortion component and compression loss at low and high frequencies, central and binaural loss, cognitive and socio-economic component of the hearing loss. These CAFPAs have been defined in order to make non-consistent and non-complete audiological data accessible for methods of machine learning, such as, e.g. Bayesian nets. Since speech recognition tests in noise are the most crucial outcome parameter, the multilingual matrix test (Kollmeier et

al., 2015 Int. J. Audiol. online first) is used which is suitable not only for comparisons across different clinics but also across languages. The individual Speech Recognition Thresholds (SRT) in stationary and in fluctuating noise were predicted using the audiogram and an estimate of the internal level uncertainty as parameters following the Automatic Speech Recognition (ASR) approach by Schädler et al. (2015, Int. J. Audiol. Online first)

Results
Using such statistical methods, a data-driven audiological classification for different classes of hearing loss becomes possible. Estimates of the "typical" hearing loss and suprathreshold distortion components in combination with ASR-based speech recognition prediction allow to predict the individual performance for the closed-set Matrix sentence recognition test in different languages.

Conclusions
A consistency check across the different audiological input and outcome measures becomes possible by using auditory models adapted to the individual hearing impairment. The concept of a more abstract representation of audiological diagnostical information in combination with speech recognition prediction methods and other machine learning approaches appears to be promising for further research in diagnostical and rehabilitative audiology.

Funding
DFG, EXC 1077 Hearing4All

PS 778

3-Dimensionally Printed Biomimetic Grafts for Treatment of Tympanic Membrane Perforations

Elliott Kozin[1]; Nicole Black[2]; Michelle Walsh[2]; Jeffrey Cheng[1]; Max Cotler[2]; Jennifer Lewis[2]; John Rosowski[1]; Aaron Remenschneider[1]
[1]Eaton Peabody laboratory, Massachusetts Eye and Ear Infirmary; [2]Harvard University

Introduction
Tympanic membrane (TM) perforations affect more than 30 million individuals each year, affecting sound conduction to the middle ear. Previous attempts have been made to use non-autologous and synthetic materials, including human fascia, chitosan, hyaluronic acid and silk fibrin to facilitate office based TM perforation repair; however, they have not achieved clinical adoption due, in part, to limitations in graft design and scaffold architecture. Recent advances in 3-dimensional (3D) printing now allow the creation of structures with impressive complexity on a micron scale. We hypothesize that a 3D printed biomimetic graft can be successfully designed, fabricated, and tested with *in vitro* and *in vivo* models of TM perforations.

Methods and Materials
3D printed graft design was based on the ultrastructure of the human fibrous TM. Fabrication of grafts was performed with direct ink writing using a custom-designed, multi-material 3D printer. AeroBasic G-code was used to digitalize designs and produce grafts in varying fiber arrangements from polydimethylsiloxane (PDMS), flex polylactic acid (PLA), and polycaprolactone (PCL) through 100μm nozzles. Once printed and cured, grafts were uniformly infilled with bovine fibrin hydrogel to obtain a continuous membrane. Grafts of varying fiber counts were subjected to dynamic mechanical analysis (DMA) to study the elastic and failure point properties of each material. Results were compared to cadaveric human temporalis fascia, which served as a control. Graft placement feasibility was then trialed in cadaveric human and chinchilla models.

Results
Biomimetic TM grafts with organized fiber architecture reflecting the human eardrum can be designed and produced using a biologic 3D printer. Print materials and scaffold architecture influence the specific mechanical properties of each TM graft. Higher fiber counts result in greater force requirements for constant displacement. 3D printed TM grafts do not undergo the hysteresis seen in human temporalis fascia. Novel 3D graft design can facilitate basic surgical underlay techniques through the ear canal in cadaveric specimens.

Conclusions
3D printing technologies can facilitate the production of biomimetic grafts at anatomically relevant scale. Grafts have mechanical properties that are resilient over time compared to autologous tissue. These data have implications for the clinical application of 3D printed grafts and future animal studies to demonstrate their efficacy.

Funding
American Otological Society Research Grant

PS 779

Extracochlear Detection of Trauma during Insertion of a Cochlear Implant

Christopher Giardina; Tatyana Fontenot; Craig Buchman; Kevin Brown; Harold Pillsbury; Douglas Fitzpatrick
UNC Chapel Hill

The large variance in speech perception outcomes with cochlear implants (CIs) remains a substantial and frustrating issue for patients and clinicians alike. The reasons for this variance are largely unknown. Recently, by measuring residual cochlear physiology just before implantation using electrocochleography (ECochG), we found differences in the overall magnitude of the ongoing response were able to account for 40-50% of the variance in speech perception outcomes in adults. A substantial portion of the remaining variance may be due to surgical trauma to the cochlea, especially when the implanted electrode traverses from scala tympani into scala vestibuli. Recent improvements in post-insertion imaging reveals a strong correlation between improperly placed electrodes and poor speech perception outcomes.

Surgeons currently have no intraoperative feedback on whether trauma is occurring. Such feedback could be used

to warn the surgeon in time to change the insertion approach and ameliorate the damage, to identify when irreversible trauma has occurred which could dictate the insertion depth chosen, and to identify electrode location relative to residual surviving hair cell and neural elements. Reductions in trauma and better electrode placement will in turn lead to improved outcomes. The goal of this study was to monitor changes in cochlear physiology using specific extracochlear electrodes, acoustic stimuli, recording and analysis during implant surgeries. The hypothesis tested here is that reductions in response with an extracochlear electrode during insertion are indicative of surgical trauma.

Intraoperative ECochG responses from a fixed location on the promontory were recorded to 500 Hz suprathreshold tones before, during, and after electrode insertion in human subjects. ECochG was successfully collected in all participants. On average, the responses at 500 Hz increased after opening the round window, remained relatively stable during initial implantation of the electrode, and reduced toward the end of the insertion. Interestingly, some responses declined but then rebounded with further insertion.

Intraoperative ECochG is a sensitive method for detecting electrophysiologic changes during implantation and shows promise in identifying and minimizing trauma. However, a drop in ECochG power is not sufficient to conclude that damage has occurred, since in some cases the responses recovered.

Funding
NIH T32: 5T32DC5360-12 MED-EL Corporation Advanced Bionics Corporation

PS 780

High signal on 3D FLAIR, a predictable factor for progression to Meniere's disease in Sudden Hearing Loss

Joong Ho Ahn; Sang Hun Lee; Chan Joo Yang; Jeong Hyun Lee
University of Ulsan College of Medicine, Asan Medical Center

Objective
Three-dimensional fluid-attenuated inversion recovery (3D-FLAIR) image in MRI has recently been developed to detect high concentrations of protein or hemorrhage. Other articles have previously reported that 50% of patients with sudden hearing loss show high signals in the affected inner ear on 3D-FLAIR MRI. However, the relationship between 3D-FLAIR findings and hearing prognosis is unclear. The aim of study was to evaluate the relationship between the results of 3D-FLAIR MRI and prognosis (especially progression to Meniere's disease) in sudden hearing loss.

Materials and Methods
Retrospective chart review of a clinical data from August 2011 to December 2014, 450 patients diagnosed as unilateral sudden hearing loss and performed temporal bone MR within 2weeks from the onset of hearing loss.

Hearing loss type was divided to 4 group: Low tone loss, high tone loss, flat, profound. The low-tone loss type meets the following criteria: the average hearing level at 250, 500 and 1 kHz is at least 10 dB worse than that at 2, 4, and 8 kHz. 8 patients were categorized as low tone loss. Profound type was defined as the average hearing level at 500Hz, 1kHz and 2kHx was worse than 90dB. Whirling type vertigo was checked by chart reviewed. Meniere's disease was evaluated according to the 1995 AAO-HNS criteria. And high signal intensity on FLAIR image was checked by radiologist.

Result
Among the 450 patients, high signal intensity on 3D-FLAIR image was observed in 75 patients. Age, sex, affected ear was no difference between high signal group and no signal group. In audiogram, high signal group showed worse result. (p=0.047) But final audiogram and recovery was no statistical difference. High signal intensity was more frequently observed in profound hearing loss. (p=0.000) In cases of High signal on FLAIR image, the more patients had experienced vertigo attack. (p=0.010) And high incidence of positive on FLAIR image was observed in Meniere group. (p=0.026)

Conclusion
If a patient had high signal intensity on FLAIR, it tend to have worse hearing and the likelihood of vertigo attack could increase. In cases of High signal on FLAIR image, the more patients had experienced vertigo attack and had tendency of high incidence on patients of Meniere's disease. Positive findings on FLAIR image might be considered as predictable factor for Meniere's disease in sudden hearing loss patients.

PS 781

Hidden Hearing Loss in Young Adults: Audiometry, Speech Discrimination and Electrophysiology.

Michael Epstein[1]; Sandra Cleveland[1]; Haobing Wang[2]; M. Charles Liberman[2,3]; **Stéphane Maison**[2,3]
[1]Bouvé College of Health Sciences, Northeastern University; [2]Massachusetts Eye & Ear Infirmary; [3]Harvard Medical School

Most research on noise-induced or age-related hearing loss has focused on threshold elevation and the loss of sensory cells that typically causes it. Recent animal work suggests that synapses between hair cells and cochlear nerve terminals are the most vulnerable elements of the inner ear (Kujawa and Liberman, 2015). We hypothesize that acoustic overexposure in humans causes cochlear neuropathy before it elevates audiometric thresholds and that electrophysiological recordings that allow comparison of the hair-cell summating potential (SP) to auditory nerve action potential (AP) could be a useful diagnostic tool.

To test this, we recruited college-age subjects, aged 18-26, with "normal hearing". Subjects included those reporting minimal exposure to loud music and others (from a local music school) who were exposed regularly without hearing protection. Cochlear function was assessed by threshold audiometry (250 Hz – 16,000 Hz), DPOAEs (L_2= 55 dB SPL,

L_1=65 dB SPL, f_2 varied from 500 Hz to 12,000 Hz) and ABRs recorded from Tiptrodes in response to 100μs clicks of alternating polarity, at 94.5 dBnHL and 9.1 Hz. NU-6 word recognition scores were assessed at 35 dB HL in absence or presence of noise at 5 and 0 dB SNR, as well as on two time-compressed NU-6 word lists (45% or 65% compression with 0.3 sec reverberation).

All subjects had similar, and normal, audiometric thresholds (< 20 dB HL) from 250 Hz to 8,000 Hz; however, high-exposure subjects had poorer thresholds (10 to 20 dB) from 8,000 – 16,000 Hz. DPOAEs were not significantly different between groups. While absolute and inter-peak latencies of all ABR waves were normal and similar across groups, a significant increase in the SP/AP ratio was observed in high-exposure vs. low-exposure subjects (0.25 ± 0.02 vs. 0.43 ± 0.03, respectively). No difference in performance for word recognition in noise was observed between groups, however the high-exposure subjects performed significantly worse on the 45% time-compressed NU-6 word list with reverberation.

Electrophysiological results are consistent with a selective loss of cochlear-nerve fibers in the high-exposure group and suggest that SP/AP ratios could be useful in early detection of cochlear neuropathy. Poorer performance in word recognition under challenging conditions also suggests that primary neural degeneration is a key contributor to hearing impairments in those with sensorineural hearing loss.

PS 782

Murine Cytomegalovirus (mCMV) Time-Course of Early (day 1-15) Inner Ear Infection.

Mattia Carraro[1]; Elaine Hillas[2]; Matthew Firpo[2]; Albert Park[2]; Robert Harrison[3]
[1]University of Toronto; [2]University of Utah, Salt Lake City; [3]The Hospital for Sick Children

Introduction
Cytomegalovirus (CMV) is an important cause of congenital hearing loss. This virus is estimated to account for at least 20% of sensorineural hearing loss (SNHL) in young children. Of interest is the possibility of treatment with antiviral therapy. The exact mechanisms for CMV induced hearing loss remain unknown, and there is no clear evidence of the first viral targets on entry into the temporal bone. It is clearly important to determine the migratory pathway of the virus, to assess the first effected structures, and to potentially identify approaches to prevent and treat this common infection.

Methods
We used Balb/C mice inoculated 3 days after birth with murine cytomegalovirus (mCMV-GFP) via intra-cerebral injection in the right hemisphere with 2000 pfu. We harvested the temporal bones at days 1, 2, 3, 5, 7, and 14 post-injection and imaged the cochleae to detect the location of the virus.

In order to evaluate the GFP signal, we fixed and stained the samples with a GFP-Trap® conjugated with Atto488/561 and with Phalloidin-Alexa561/633. Then we cleared the cochleae with the HQFix protocol and imaged them with light sheet fluorescence microscopy (LSFM). The post-processing of the images was done with Fiji, Imaris Bitplane and Arivis 4G.

Results
We have previously demonstrated that a week after infection mCMV-GFP signal can be detected in the spiral ganglion and adjacent to the scala tympani. At four weeks of age auditory brainstem and otoacoustic emission measures indicate a moderate to severe and sometimes a profound hearing loss.

From whole mount images we provide more detailed assessments of the viral migratory pathway and can define the first cochlear structures to be targeted. Regarding vascular degeneration we have shown that the stria vascularis is first affected followed by capillary networks in spiral limbus and in spiral ligament structures.

Conclusion/Discussion
The vasculature of the cochlea appears to be one of the most important migratory pathways for the cytomegalovirus. The developing cochlear bone, especially towards the apex, seems to be one of the first effected structures, perhaps the primary target in mCMV pathogenesis.

Funding
Canadian Institutes of Health Research (CIHR). University of Toronto Harry Barberian Scholarship Fund. Triological Society.

PS 783

The Chorda Tympani Degenerates during Chronic Otitis Media: an Electrone Microscopy Study

Katarina Holm; Magnus von Unge
Center for Clinical Research, Uppsala Universitet, County Hospital Västerås

Background
The most important nerve of taste, the chorda tympani nerve, runs uncovered through the middle ear. This location predisposes it to become affected by bacterial toxins, enzymes and mechanical damage in various forms of middle ear pathology, such as chronic otitis media and cholesteatoma. A difference between inflammatory diseases, such as chronic suppurative otitis media and cholesteatoma, and noninflammatory diseases, such as otosclerosis, regarding taste disturbance preoperatively and symptoms postoperatively have been noticed. The present study aims to investigate ultrastructural changes of chorda tympani in different forms of inflammatory middle ear disease, such as chronic suppurative otitis media and cholesteatoma, as compared with normal.

Methods
Five chorda tympani specimens were collected from healthy middle ears of patients subjected to surgery for acoustic neuroma to be used as normal controls, and five from middle ears with chronic otitis media or cholesteatoma where the nerve could not be saved during the operation. Light microscopy and electron microscopy were used to identify signs of pathological processes.

Results
Ultrastructural changes that implicate inflammatory changes and degeneration were found in all five nerves from ears with chronic otitis media and cholesteatoma. There were signs of proliferation of connective tissue of the endoneurium, disorganization and demyelination of axons, vacuolar degeneration of the axons, myelin sheath disintegration and edema. As a sign of regeneration capacity there was occurrence of sprouting in CTN from ears with inflammatory diseases.

Conclusion
Chorda tympani nerves from ears with chronic inflammatory middle ear disease exhibit structural signs of deterioration that correlates well to taste disturbances.

There were signs of nerve regeneration that could explain the ability of taste recovery.

PS 784

Changes in G-protein expression in a murine model of acute otitis media

Daniel Schaerer[1]; Kwang Pak[2]; Arwa Kurabi[1]; Nicholas Webster[1]; Bickler Stephen[3]; Allen Ryan[1]
[1]University of California, San Diego; [2]VA Medical Center, La Jolla; [3]Rady Children Hospital of San Diego

Background
Otitis media (OM) is the most common disease of childhood indevelope d countries and accounts for more than 5 billion dollars in healthcare costs annually in the US. The middle ear undergoes extensive changes during OM and the molecular mechanisms that underlie these changes are not fully understood. However the relatively small numbers of G-proteins, which are important regulators of cellular events, represent a common pathway for many immune and inflammatory processes.

Methods
The middle ears of 320 WBxB6 F1 hybrid mice were inoculated with non-typeable Haemophilus influenzae (NTHi) to induce OM or PBS (sham control). Two independent samples were generated for each time point and condition, from initiation of infection to resolution. Middle ear mRNA was profiled on Affymetrix mouse 430 2.0 whole-genome microarrays. G-proteins with human analogs were analyzed for significant changes in expression.

Results
12 G-proteins with human analogs were found to undergo significant changes in the murine OM model. Differences in gene expression levels were observed primarily in α subunits, but also in β and γ. Gα13, involved in Rho family GTPase signaling, showed consistently increased expression throughout acute OM. The largest increase in expression (6.6-fold increase at 24 hrs) was in Gγ12, involved in the regulation of various ion channels and phosphoinositide-3-kinase. The largest decrease (-4.4 fold decrease at 48 hrs) was seen in Gαz, which negatively regulates the production of cAMP.

Conclusions
Our findings demonstrate that expression of multiple G-proteins is altered significantly in mice during acute OM, enhancing select intracellular signaling pathways. Further research is needed to determine the downstream effect of these changes and their clinical implications.

Funding
(Supported by NIH grants DC000129, DC006279, DC012595 and the VA Research Service.)

PS 785

Comparative Uptake Parameters of Contrast Agents Across the Blood Perilymph Barrier and Intrastrial Fluid-blood Barrier in the Mouse Inner Ear Using Ultra High Field MRI

Göran Laurell[1]; S. Allen Counter[2]; Cecilia Engmér Berglin[3]; Sahar Aski[3]; Peter Damberg[3]
[1]Uppsala University; [2]Harvard University; [3]Karolinska Institutet

Background
The Gadolinium (Gd) paramagnetic contrast agent has been successful especially to enhance MRI visualization of the cochlea. The objective of the present study was to determine the most effective Gd contrast agent for low signal-to-noise ratio and maximal visualization of the in vivo cochlea measuring the temporal and spatial parameters involved in drug uptake across the inner ear barriers.

Method
Gadoteric acid (Dotorem®), Gadobutrol (Gadovist®), Gadodiamide (Omniscan), Gadopent acid (Magnevist®) were administered intravenously (IV) using the tail vein of Balb/C mice. High resolution T1 images of drug uptake was acquired with a horizontal 9.4 T Varian Agilent magnet equipped with a 12 cm inner diameter gradient system with maximum gradient strength of 1000 mT/m . Signal intensity was used as a metric of drug delivery and distribution to the perilymphatic and endolymphatic spaces.

Results
The four contrast agents penetrated the perilymphatic compartments of the cochlea with increase concentration and minimal variability over a period of 95 minutes. The Gadoteric acid (Dotorem®) complex was found to be the most effective and efficient Gd compound in terms of rapid morphological enhancement and analysis of the temporal and spatial uptake in the perilymphatic space of the cochlea in T1 weighted images. Gadobutrol (Gadovist®) was similarly effective in morphological visualization of the mouse inner ear over time, but slightly less efficient. Gadodiamide (Omniscan®) and Gadopent acid (Magnevist®) were least efficient in penetrating the perilymphatic spaces of the mouse inner ear. The ultra-high field MRI showed no penetration of the intrastrial fluid-blood barrier.

Conclusion
Doterem had greater efficacy as a contrast agent for enhanced visualization of the perilymphatic spaces of the inner ear

labyrinthine in the mouse, including the scala tympani and scala vestibuli of the cochlea, and the semicircular canals of the vestibular apparatus. Minimal, if any Gd contrast agent crossed the blood-intrastrial barrier of the filled scala media. These finding may inform the clinical application of Gd compounds in patients with inner ear fluid disorders.

Funding
Foundation Afa Insurande and Tysta Skolan

PS 786

Rat Model of Chronic Tympanic Membrane Perforation: Ventilation Tube with Mitomycin C and Dexamethasone

Allen Yu-Yu Wang[1]; Yi Shen[1]; Lawrence J Liew[1]; Jeffrey T Wang[1]; Magnus von Unge[2]; Marcus D. Atlas[1]; Rodney J Dilley[1]
[1]The University of Western Australia; [2]Akershus University Hospital and University of Oslo, Norway

Background
Numerous clinical studies have shown that long-term ventilation tube (VT) treatment may increase the likelihood of chronic tympanic membrane perforation (TMP) development in patients. Overall in clinical settings, the rates of persistent TMPs in long-term VT treatment range between 10% and 30%. To date there are no reported experimental use of VT to create a chronic TMP animal model. Hence, the aim of this study was to evaluate the efficacy of VT treatment or VT treatment in combination with topical mitomycin/dexamethasone (M/D) in creating a rat chronic TMP model, compared to spontaneous healing.

Methods
Thirty male Sprague-Dawley rats underwent myringotomy of the right tympanic membrane (TM) and were divided into three experimental groups: spontaneous healing (myringotomy control), VT-only treatment for two weeks, VT treatment for two weeks in conjunction with topical application of M/D (VT-M/D). All TMs were regularly assessed by otoscopy for ten weeks and then animals were sacrificed for histological evaluation.

Results
In the VT-M/D group, seven out of ten (70%) perforations were patent at ten weeks (mean patency, 57.9 days; $P < .01$). VT-only group had two out of ten (20%) perforations patent at ten weeks (mean patency, 26.5 days; $P < .01$), while all the perforations from the myringotomy control group were closed by day nine (mean patency, 7.2 days). Histologically, the perforations patent at week ten depicted a stratified squamous epithelial rim, a thickened keratinocyte layer around the perforation edge as well as increased collagen deposition and macrophage infiltration.

Conclusions
Chronic TMP in a rat model was successfully created by VT-only treatment and the efficacy was increased in combination with topical application of M/D. This model may be utilized for further investigation of pathogenic factors and testing of bioengineered grafts or therapies.

TABLES

Table 1
Number of patent tympanic membrane perforations at different time points.

Group	0 d	1 d	3 d	5 d	7 d	9 d	14 d	15 d	17 d	19 d	21 d	23 d	25 d	28 d	35 d	42 d	49 d	56 d	63 d	70 d
Myringotomy control (N = 10)	10	10	10	10	1	0	0	0	0	0	0	0	0	0	0	0	0	0	0	0
VT (N = 10)	10	10	10	10	10	10	7	4	3	2	2	2	2	2	2	2	2	2	2	2
VT-M/D (N = 10)	10	10	10	10	10	10	10	10	10	9	8	8	8	8	8	8	7	7	7	7

D – days; VT – ventilation tube; M/D – mitomycin C/dexamethasone.

Table 2
Summary of tympanic membrane perforation patency duration.

Group[a]	Minimum TMP patency duration (days)	Maximum TMP patency duration (days)	Mean TMP patency duration (days ± SEM)
Myringotomy control	7	9	7.20 ± 0.2
VT	14	70	26.50 ± 7.3[b]
VT-M/D	19	70	57.90 ± 6.6[c]

[a] $P < 0.05$, Groups were compared by one-way ANOVA
[b] $P < 0.05$, Myringotomy control vs. VT (t test)
[c] $P < 0.05$, Myringotomy control vs. VT-M/D (t test)

TMP – tympanic membrane perforation; SEM – standard error of the mean; VT – ventilation tube; M/D – mitomycin C/dexamethasone; ANOVA – one-way analysis of variance.

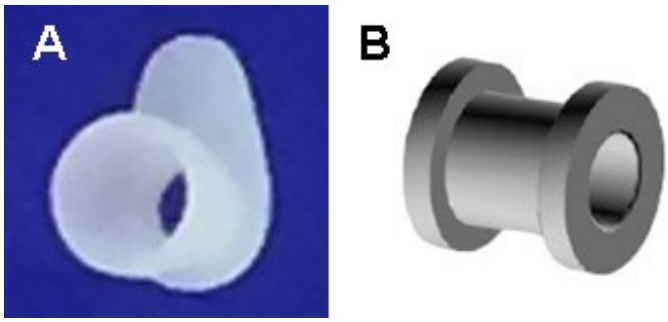

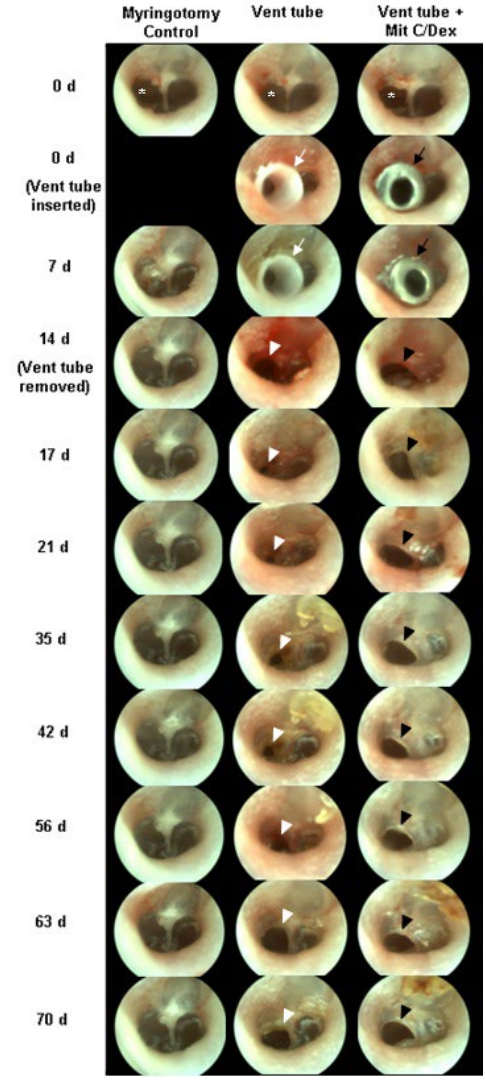

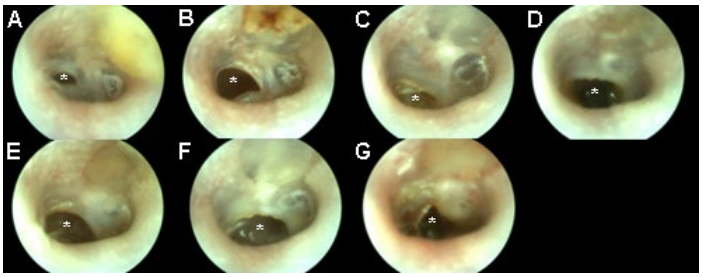

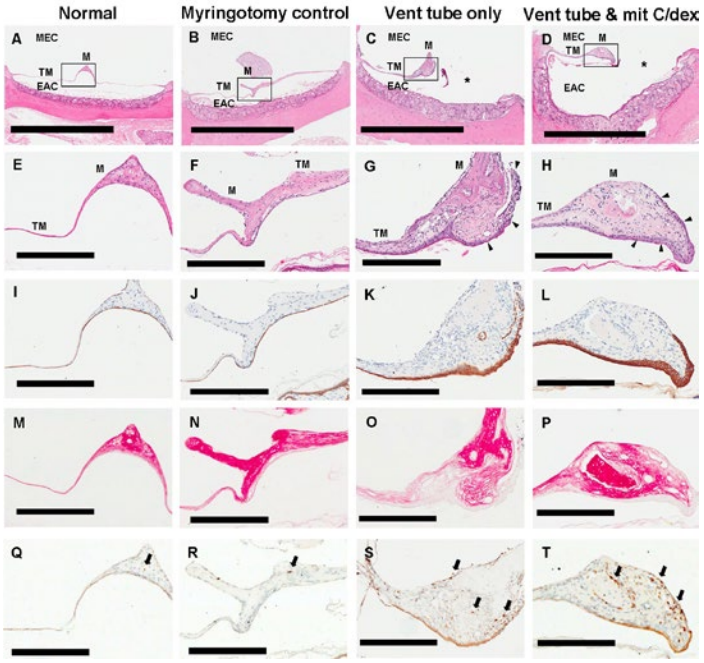

Funding
The University of Western Australia Scholarship, Garnett Passe & Rodney Williams Memorial Foundation and the National Health and Medical Research Council of Australia.

PS 787

A Three-dimensional Volumetric Analysis of the Epitympanum and Tympanic Isthmus in Patients with Retraction Pockets

Rafael Monsanto; Henrique Pauna; Omer Hizli; Geeyoun Kwon; Michael Paparella; Sebahattin Cureoglu
University of Minnesota

We analyzed the volume of the epitympanic space and area of the tympanic isthmus in temporal bones with retraction pockets to temporal bones with chronic otitis media and normal cases, to investigate any differences in bony volume and tympanic isthmus area among these groups. We performed a three-dimensional reconstruction and measurements of the bony epitympanum in 16 temporal bones containing retraction pockets, 16 with chronic otitis media without retraction pockets and 16 temporal bones within normal limits to compare the epitympanum volume and tympanic isthmus area among the groups. The mean bony volume of the epitympanum was 40.55±7.14 mm3 in the retraction pocket group, 50.03±8.49 mm3 in the chronic otitis media group and 48.03±9.16 mm3 in the normal group. The volume of anterior, lateral and medial compartments in temporal bones with retraction pockets were smaller when compared to the other groups ($p<0.05$), as well as the total epitympanic volume ($p<0.05$). The tympanic isthmus area was significantly smaller in retraction pockets group (8.11 ±2.44 mm2) when compared to chronic otitis media without retraction pockets (9.82±2.06 mm2) and normal (10.66±1.78 mm2) groups ($p<0.05$). Our data indicate that temporal bones with retraction pockets have a smaller epitympanic volume and TI area compared to chronic otitis media and normal

groups. The fact that the tympanic isthmus area is smaller in the retraction pocket group supports the assumption that a blockage in the aeration pathways to the epitympanum could create a tendency for selective dysventilation, creating negative pressure and resulting, ultimately, in retraction pockets and cholesteatoma.

Funding
The study was supported by the National Institute on Deafness and Other Communication Disorders (NIDCD), U24 DC011968-01; the International Hearing Foundation; the Starkey Hearing Foundation; and the 5M Lions International.

PS 788

Hearing changes after intratympanically applied steroids for therapy of sudden hearing loss: A metaanalysis using mathematical simulations of drug delivery protocols

Arne Liebau[1]; Olivia Pogorzelski[1]; Alec Salt[2]; Stefan Plontke[1]
[1]Martin Luther University Halle-Wittenberg; [2]Washington University in St. Louis

Objective
To establish optimal local drug delivery protocols for the treatment of patients with idiopathic sudden sensorineural hearing loss (ISSHL).

Data Sources
Controlled and uncontrolled studies with intratympanic application of glucocorticoids for ISSHL.

Study Selection
A total of 51 studies with 61 treatment groups between January 2000 and June 2014 were selected based on description of protocols with respect to drug concentration, dosing regimen (i.e. start, number and time intervals of treatment), and outcome parameters sufficiently detailed for analysis with the computer model.

Data Extraction
Cochlear drug levels were calculated based on the concentration and volume of glucocorticoids applied, the time the drug remained in the middle ear, and on the specific timing of injections.

Data Synthesis
A validated computer model of drug dispersion in the inner ear fluids was used to calculate cochlear glucocorticoid drug levels resulting from specific clinical delivery protocols. Dosing in the cochlea and parameters of the delivery protocol were compared with changes of hearing sensitivity and final outcome. Time courses were quantified in terms of the maximum concentration (Cmax) and the area under the curve (AUC) of the drug at specific cochlear locations.

Conclusions
There was no influence of applied drug concentration, application time, number of injections, interval between injections, duration of treatment, total local dose (quantified as AUC) or Cmax on outcome. This calls into question the importance of the application protocol, and perhaps the effectiveness on intratympanic glucocorticoid therapy for ISSHL in general.

Change in pure tone average (PTA) might not be an adequate outcome parameter to assess effectiveness of the intervention, since it appears to depend on initial hearing loss. Final PTA might be used as an alternative parameter when comparing different clinical reports.

Further efforts should be made towards standardization of outcome parameters and publication of outcomes in individual patients in clinical studies with interventions to improve hearing.

PS 789

Hearing loss in a novel polygenic mouse model of Type II diabetes mellitus

Krysta Gasser Rutledge[1]; Brendan Smyth[2]; Flint Boettcher[3]; Michael Anne Gratton[3]
[1]Washington University in St. Louis; [2]Bristol-Myers Squibb; [3]Saint Louis University

Type II diabetes mellitus (T2DM) affects 8.3% of the global population. Recent epidemiological literature consistently demonstrates a correlation with hearing loss (HL). Currently, most mouse T2DM models are based upon the C57Bl6 strain, which demonstrates HL during young adulthood due to a well-documented mutation in Cdh23. Our lab has shown that the HL in T2DM mice on a C57 background is more severe than that of age-matched C57 controls; however, the influence of an interaction between early age-related HL and diabetes-related HL cannot be easily ascertained. The TallyHo mouse, a relatively new model of T2DM, accurately mimics human T2DM showing gradual onset of disease with less obesity and metabolic dysfunction than other T2DM models. This mouse is NOT based upon the C57Bl6 background. This pilot project sought to determine 1) onset of HL in the TallyHo mouse and 2) associations(s) between blood chemistry biomarkers for diabetes and onset of the HL.

Auditory brainstem response testing and blood chemistry analysis were completed in male experimental (n = 15 TallyHo) and background strain control mice (n = 12 Swiss Webster) from 5 – 22 weeks of age with sacrifice at 5 and 13 – 14 weeks of age. The ABR was evoked by tone burst stimuli (8 – 40 kHz at octave intervals) and used to determine auditory threshold. Blood was collected and analyzed for glucose and lipid panel levels (CardioCheck+, PTS Diagnostics), HbA1C levels (A1CNow+, PTS Diagnostics), and insulin levels (ELISA Kit, Chrystal Chem). Repeated measures ANOVA followed by Holm-Sidak multi-comparisons were conducted on threshold shift and blood chemistry biomarkers. The 40 kHz threshold and HbA1C levels were significantly elevated from baseline values at 9 weeks of age ($p < 0.015$). By 11 – 13 weeks of age, a functionally significant threshold shift (> 10 dB) existed at 40 kHz as well as 24 and 32 kHz ($p < 0.021$). Moreover, at 13 weeks, a simple linear regression revealed a significant, positive relationship between auditory threshold (24, 32 kHz) and either HbA1C or blood glucose levels. The

blood chemistry values approximate those reported in current literature. Histological analysis is ongoing.

This pilot study shows that 1) the TallyHo mouse is an appropriate model for study of T2DM-related HL, 2) HbA1C is an early biomarker of said HL, and 3) further study could explore the potential ability of statins in lowering of blood glucose levels in addition to prevention/alleviation ofT2DM-related HL in the TallyHo model.

Funding
Supported by the American Academy of Audiology/American Academy of Audiology Foundation Research Grants Program awarded to KLGR and NIH-NIDCD DC006422 to MAG

PS 790

The Pathway and Damage in Vestibular System after Intratympanic Gentamicin Administration

Qianru Wu; Yibo Zhang; Chunfu Dai
Fudan University

Background
Intratympanic injection of gentamicin (ITG) is widely applied for controlling refractory vertigo in patients with Meniere's disease. However, a complication of disequilibrium is observed in some patients immediately after ITG. This symptom will alleviate due to compensation in majority of some patients. We aimed to explore the pathway of gentamicin and the damage in the vestibular system after ITG and to explore the mechanism underlying disequilibrium.

Methods
（1）Four guinea pigs were sacrificed 3 days after ipsilateral intratympanic injection (IT) of 100ul gentamicin (5mg/ml). Ultrathin sections of vestibular semicircular ampulae were harvested to immunostain with gentamicin antibody and 15nm colloidal gold, and then observed under transmission electron microscope (TEM). （2）Four guinea pigs were sacrificed 3 days after ipsilateral IT of 100ul gentamicin (30mg/ml). Immunofluorescent staining and TEM were used to explore the uptake of gentamicin and the ultrastructural changes in vestibular ganglion (VG) respectively. （3）Four guinea pigs were sacrificed respectively 3days after ipsilateral IT of 100ul gentamicin (60 mg/ml). We labeled vestibular efferent neuron (EVE) with anti-gentamicin antibody following by DAB staining. The ultrastructural changes in EVE were observed under TEM. Guinea pigs under IT of saline served as control.

Results
（1）TEM revealed concentrated damages within the afferents and efferents of partial type I & II vestibular hair cells. Colloidal gold were observed mainly in efferents of type II hair cells. （2）Negative gentamicin Immunofluorescence labeling was observed in VG cells. Moreover, we did not find significant damage in VG cells under TEM. （3）Bilateral EVE showed damages at 3 days under TEM.

Conclusion
This study demonstrated that gentamicin mainly traveled through the vestibular efferent system. In other words, gentamicin was firstly taken up by vestibular efferent synapses, trafficked along the vestibular efferent nerve, and finally located in the bilateral EVE after ITG. The damage of EVE may relate to vestibular disequilibrium. However, whether a long-term compensation of the damaged EVE is related to the alleviation of disequilibrium remains to be comfirmed.

Funding
The National Natural Science Foundation (No. 81300826)

PS 791

Enhanced Auditory Steady State Responses in Subjective Idiopathic Tinnitus

Zahra Ghasemahmad[1,2,3]; Saeid Mahmoudian[4,5]; Saeid Farahani[1]; Shohreh Jalaei[1]
[1]Tehran University of Medical Sciences; [2]Northeast Ohio Medical University; [3]Kent State University; [4]Iran University of Medical Sciences; [5]Iranian Center for Auditory Science and Tinnitus

Introduction
Tinnitus is the sensation of sound in one or both ears without any external stimulation. Although tinnitus is associated with noise exposure, hearing loss, and some medications, the etiology of tinnitus in patients with Subjective Idiopathic Tinnitus (SIT) is often undetectable. Auditory Steady State Responses (ASSR) at different modulation frequencies (MFs) originate from different sources in the auditory pathway and provides a good tool for studying tinnitus. In the current study we used ASSR at three MFs to identify the sites of problems in these patients who also have normal hearing.

Methods
23 normal and 19 patients (aged 25-45 years) with SIT were enrolled in this study. SIT subjects were selected from tinnitus patients that were referred to the Ear, Nose and Throat Research Centre at Hazrat Rsoul Hospital, Tehran. Immitance audiometry, auditory brainstem responses and pure tone audiometry along with a close check of the patients' medical history were performed to rule out the possibility of any obvious cause of tinnitus. All the patients and normal participants underwent ASSR at three modulation frequencies (20, 40 and 80 Hz) and the results were compared across patients and controls.

Results
There was no significant difference between ASSR thresholds recorded from either contralateral or ipsilateral side to the tinnitus ear between right and left lateralized tinnitus. Also ASSR thresholds were not statistically different for any of the three MFs between the right and left ear ($p>.05$). When we compared the contralateral and ipsilateral ASSR thresholds between tinnitus and the normal hearing group, the differences in thresholds were statistically significant at most of the carrier and modulation frequencies ($p<.05$).

Conclusion
Based on the previous literature, the whole auditory system can be studied using the ASSR method, with the auditory cortex being most sensitive to lower MFs (12-40 Hz) and

brainstem to higher MFs (80Hz). Changes in patients' thresholds for most of the modulation and carrier frequencies identify multiple possible anatomical sources of dysfunction in SIT patients. This is in line with previous research showing enhanced auditory MLRs (which is equivalent to 40 Hz ASSR) in tinnitus patients. The significance of this study is that we focused on multiple MFs while eliminating the effect of any known contributing factor to enhanced thresholds. This study opens a new avenue for studying the source of tinnitus in SIT patients.

Funding
Tehran University of Medical Sciences

PS 792

Restoration of Auditory Thresholds in the VGLUT3 Knockout Mouse by Fetal Gene Transfer to the Developing Inner Ear

Lingyan Wang[1]; Beth Kempton[1]; Han Jiang[1]; Rebecca Seal[2]; Omar Akil[3]; Lawrence Lustig[4]; John Brigande[1]
[1]Oregon Health and Science University; [2]University of Pittsburgh; [3]University of California, San Francisco; [4]Columbia University

Background
Inner hair cells release the excitatory neurotransmitter glutamate at the first synapse in the auditory pathway. Glutamate is loaded into inner hair cell synaptic vesicles by vesicular glutamate transporter 3 (VGLUT3). A missense mutation in the human VGLUT3 gene, SLC17A8, has been associated with the progressive high-frequency hearing loss observed in autosomal dominant DFNA25. Targeted disruption of VGLUT3 in mice leads to profound congenital deafness. Adeno-associated virus (AAV)-mediated transfer of VGLUT3 to inner hair cells at postnatal day 1-3 (P1-3) restores wild-type auditory thresholds for at least 7 weeks after which thresholds variably elevate. Spiral ganglion neuron number, ribbon synapse morphology, and startle responses of postnatally-treated VGLUT3 mutants deviate significantly from wild-type values. We hypothesize that fetal gene transfer of VGLUT3 to the developing inner ear will restore late embryonic VGLUT3 expression and effect more comprehensive therapeutic recovery.

Methods
An AAV1 vector encoding mouse VGLUT3 at 5.3 X 10^{13} genome equivalents/mL was microinjected into the embryonic day 12.5 (E12.5) VGLUT3 knockout otic vesicle. VGLUT3 and Myosin 7a expression were assessed by cochlear whole mount immunofluorescence at P22. Auditory brainstem response (ABR) testing was conducted monthly from P40-340.

Results
Whole mount cochlear immunofluorescence analysis indicates that >80% of inner hair cells express VGLUT3 with off-target expression detected in outer hair cells, spiral ganglion neurons, and supporting cells at P22. In a cohort of 30 injected VGLUT3 knockout embryos, 16 mice demonstrated ABR thresholds and 14 mice were deaf at P40. Of the 16 responders evaluated at 8, 16, and 32 kHz, 7 mice presented ABR thresholds at 20-50 dB SPL (high responders) and 9 presented thresholds at 55-85 dB SPL (intermediate responders) for at least one tested frequency at P40. Three of the 7 high responders retained thresholds through 300 days and then transitioned to intermediate responder status. Three mice retained intermediate responses through 340 days.

Conclusion
A single dose of AAV1-VGLUT3 at E12.5 can restore auditory thresholds in 22% of injected mice to near wild type levels at P40 and 10% of the mice retain high responses for 340 days. The data suggest that improvements in temporal and spatial control of fetal gene expression may further enhance therapeutic outcomes. We conclude that fetal gene therapy to the developing mammalian inner ear holds promise as a treatment modality for congenital deafness.

Funding
NIH R01DC008595; NIH R01DC014160

PS 793

Manipulation of Wnt/Beta-Catenin Pathway in the Embryonic Periotic Mesenchyme

Sara Billings; Nina Myers; Elvis Huarcaya Najarro; Alan Cheng
Stanford University

Background
Emerging evidence suggests that the periotic mesenchyme provides signaling cues for hair cell development in the embryonic cochlear duct. While Wnt-active cells have been reported to reside both within the cochlear duct and in the surrounding periotic mesenchyme, the roles of canonical (beta-catenin-mediated) Wnt signaling in dictating their behavior has not been investigated in detail. Previous studies have examined the effect of Wnt pathway manipulation in periotic mesenchyme on early development of the inner ear (before E10.5), but the role of this pathway at later stages remains unclear.

Methods
Using Axin2 as a reporter of active Wnt signaling, we manipulated Wnt-active cells in the embryonic cochlea at E12.5 with an inducible Cre allele driven by the Axin2 promoter. Axin2-positive cells were fate-mapped using the Rosa26R-loxP-stop-loxP-tdTomato mouse strain as a Cre reporter, and the Ctnb1-exon3/flox allele was used to over-activate the Wnt pathway.

Results
Fate-mapping of Axin2-positive cells at E12.5 resulted in labeling of periotic mesenchymal areas at E19.5, including tympanic border cells, spiral ligament, spiral limbus, modiolus and the mesenchymal layer of Reissner's membrane. Labeling is most robust in the periotic mesenchyme, with occasional labeled cells observed inside the cochlear duct. Manipulation of Wnt/beta-catenin signaling in Axin2+ cells led to defects throughout the cochlea. Overactivation of the pathway led to excess proliferation and formation of clusters of cells we termed foci. These foci were found primarily in

the modiolus and spiral ligament, but were also observed in the organ of Corti. Regardless of location, most foci appear proliferative and express Ki67 and also express the beta-catenin target LEF1. In the cochlear duct, foci have a heterogenous expression pattern of Sox2, Prox1, and Sox9. Conversely, foci in the periotic mesenchymal regions lack Sox9 expression, but frequently express the epithelial marker E-cadherin.

Conclusion
Wnt/beta-catenin signaling exerts differential effects on proliferation and cell fate in the developing cochlear duct and periotic mesenchyme.

Funding
California Institute for Regenerative Medicine RN3-06529 NIDCD/NIH RO1DC013910 Akiko Yamazaki and Jerry Yang Faculty Scholarship

PS 794

Seeking Evidence for the Role of Canonical Wnt/β-Catenin Signaling in Radial Axis Patterning of Chicken Basilar Papilla

Ankita Thawani[1]; M. Scott[1]; Vidhya Munnamalai[1]; Ulrike Sienknecht[2]; Donna Fekete[1]
[1]Purdue University; [2]Carl von Ossietzky University Oldenburg

Similar to the mammalian organ of Corti, the auditory organ in the bird, called the basilar papilla (BP), has 2 mechanosensory hair cell populations that are differentially innervated by afferent versus efferent axons. In the BP, tall hair cells are found on the neural (or medial) side and short hair cells on the abneural (or lateral) side. Sienknecht and Fekete (2008) published a comprehensive Wnt expression study, in part to search for candidate Wnts that are present at the right time and place to influence the specification of hair cells types across the BP. One candidate molecule, *Wnt9a*, is expressed adjacent to the neural edge of the prosensory BP. When Wnt9a is overexpressed, the entire BP assumes a phenotype that is normally confined to the neural half of the organ. This suggests that Wnt9a may function as a morphogen to pattern the radial axis. If so, then the normal sensory organ should show evidence for a gradient in Wnt signaling. We begin by looking at a readout for canonical Wnt/β-catenin signaling in controls and Wnt9a-infected specimens.

RCAS/Wnt9a retrovirus is injected into the right embryonic day 3 (E3) otocyst. At E5-E7, tissue is collected and processed either as sections through the head or as BP whole mounts. During canonical Wnt signaling, β-catenin is phosphorylated at a specific tyrosine residue and translocates to the nucleus to function as a transcriptional co-activator. An antibody designed specifically against this phosphorylated epitope is used to map the expression of nuclear-localized β-catenin, while Serrate 1 and neurofilament immunolabeling identify the sensory BP. Viral capsid protein immunolabeling and *Wnt9a* in-situ hybridization are used to detect infected cells.

Control E6 BPs have higher β-catenin fluorescence intensity on the neural side, supporting the hypothesis that Wnt9a is functioning as a morphogen. Mitotic cells are particularly well labeled. At E7-7.5, spatial variations in β-catenin intensity are less apparent. By E7, Wnt9a-infected BPs are wider and have more mitotic cells. Moreover, nuclear β-catenin levels are moderately increased.

In summary, a mild radial gradient of nuclear-localized β-catenin is consistent with a role for canonical Wnt signaling in giving radial axis information to the undifferentiated BP. And yet, despite the obvious phenotype induced by Wnt9a delivery, the observed overexpression of nuclear β-catenin was less robust than expected. Perhaps the responsiveness of the BP to secreted Wnt ligands is being restrained, for example by the presence of secreted inhibitors or receptor availability.

Funding
This work was funded by the National Institutes of Health (http://www.nih.gov/ R01DC002756 to D. M. F.; P300CA023168)

PS 795

Sequential retraction segregates SGN processes during target selection in the cochlea

Noah Druckenbrod; Lisa Goodrich
Harvard Medical School

Background
A growing axon encounters a variety of potential synaptic partners within its target tissue but eventually targets a single cell or a subset of the whole. Efforts to understand how specificity within the target region is achieved have been a major goal and multiple cellular mechanisms that contribute to specificity throughout the nervous system have been identified. However, it has been challenging to define how and when these mechanisms influences behavior as an axon transitions between targeting and refinement. In the mature cochlea, spiral ganglion neurons (SGNs) form stable synapses with either IHCs or OHCs but not both. Here, we took advantage of this stereotyped and simple wiring pattern to gain insights into the cellular and molecular events that direct processes towards their correct synaptic partners.

Methods
We utilized a sparse fluorescent label for live imaging and 3D-reconstructions. We quantified the changes in morphology and growth behavior that occur as individual SGN peripheral processes grow within the three-dimensional structure of the cochlea and are later refined. To explore the role of Epha4-signaling in SGN growth and targeting behaviors, we developed SGN-specific Epha4 knockout animals. To further specify the signaling pathway, a chemical allele in which Epha4 kinase activity can be rapidly blocked was introduced

Results
SGN terminals are segregated prior to birth. SGNs do not target both hair cells during postnatal refinement but radial fibers transiently extend extra branches around IHCs before

resolving into a single contact around P6. Live imaging of SGN dynamics at fetal stages reveal that shortly after arriving to the target region at E16, many SGNs fail to enter the OHC region, most have targeting biases away from the OHC-region and instead remain active in IHC regions. By E18, neurites within the IHC region continue to explore but the OHC region becomes even less permissive to SGN invasion. However, we have identified a cellular mechanism by which neurites invade, persist, and grow within the E18 OHC-region via invading a specific 3D-domain of the target space. We have also found that Epha4-signaling contributes specifically to local growth within this 3D-domain.

Funding
Funding was provided by the NIDCD (R01 DC009223 to LVG), the NINDS (T32 NS007484 to NRD), a John and Virginia Kaneb Fellows Award (LVG), and a Mahoney Fellowship (NRD).

PS 796

Disorganizing the Organ of Corti to Reveal Principles of Innervation Development

Israt Jahan; Ning Pan; Jennifer Kersigo; Bernd Fritzsch
University of Iowa

Backgrounds
Age-related sensorineural hearing loss progressively deprives the ear of hair cells (HCs) and neurons. Hearing restoration will need to resolve mechanisms that reorganize the organ of Corti (OC) HCs (inner, IHC and outer, OHC) AND their specific innervation by two distinct types of afferent fibers (type I and II spiral ganglion neurons) and efferent fibers (LOC, Lateral and MOC, Medial Olivo-Cochlear neurons). Nearly all past research has only provided correlative evidence of fiber sorting to HC types. Going beyond this correlation requires novel models that selectively lose specific HCs or have disarranged HCs to uncouple place principles from molecular principles of specific HC attractions. Essentially, we like to understand if IHC receive their specific innervation because they are near the habenula perforata or because they are molecularly distinct to attract their specific innervation. Partially untangling cell type from topology is possible with recent mouse models with changes in number, type and distribution of HC.

Methods and Results
We worked on the following deaf mutants with altered HCs: We generated a novel compound mutant by combining the self-terminating Atoh1 conditional null mouse with misexpression of the neuronal bHLH gene, Neurog1 (Atoh1-Cre; Atoh1$^{f/kiNeurog1}$). This mutant mouse has a nearly normal complement of HC in a disorganized OC. Despite the rescue of most HCs, these mice are deaf. Importantly, HC survive for up to 9 months and allow establishing sorting of afferents to HC types that are not regularly distributed, missing or replaced by HC-like differentiated pillar cells. Our data reveal that type I afferents project to OHC in gaps of IHCs. This is also profound in cases of IHC-like transformation of OHCs in Neurod1 null mice using Pax2-Cre. To further test this ability of Type I fibers to home onto IHC or, in cases of absence of IHCs to OHCs, we investigated another mouse model: the Bronx-Waltzer mutant, which results in loss of almost all IHCs with normal OHCs. In these mice most afferents survive and project massively to the only remaining HC, OHCs.

Conclusions
Our data suggest that afferents types innervate specific HC types even if abnormally distributed. We also show that afferents follow a hierarchy and innervate OHC if they are unable to home onto IHCs. Combined these data provide a very different, molecular based preference of afferents to specific types of HCs that has not been recognized in past descriptive studies unable to untangle place from HC type.

Funding
This work was supported by National Institute on Deafness and Other Communication Disorders (NIDCD) (R03 DC013655 to IJ) and Hearing Health Foundation (Emerging Research Grant to IJ) and the P30 core grant for support (DC 010362).

PS 797

Investigating the Development of Cochlear Lateral Supporting Cell Subtypes by Single Cell mRNAseq

Michael Kelly; Joseph Burns; Kathryn Ellis; Joseph Mays; Robert Morell; Matthew Kelley
NIH

The lateral, or abneural, domain of the organ of Corti represents a distinct population of cells, marked by unique morphological, molecular, and functional characteristics. Supporting cells from the lateral domain include inner and outer pillar cells and Deiters cells, which have unique and highly stereotyped three-dimensional architectures that are likely essential for proper auditory mechanics. Little is known about the transcriptional program that directs the unique differentiation of these cell types. Furthermore, while a shared developmental lineage for lateral supporting cells and all other sensory cells of the organ of Corti has been hypothesized, limited direct evidence exists to support this assumption. Here, we utilize single cell RNA sequencing (mRNAseq) to explore the transcriptional differentiation of these specialized cell types.

Mouse cochlea epithelia from E16, P1 and P7 samples were enzymatically and mechanically dissected to enrich for sensory and adjacent non-sensory cells. The Fluidigm C1 system was used to capture single cells from each dissection and to generate amplified cDNA libraries that were sequenced on an Illumina platform. Because developmental gradients exist along the longitudinal axis of the cochlear duct, apical and basal turns of the cochlea were separated and processed in parallel so that differentiation-dependent transcriptional changes could be reliably identified. Lateral supporting cells were identified by sample clustering and by expression of known markers, such as *Fgfr3* and *Prox1*. Differentiation trajectories for each cell type were modeled using transcriptional profiles across each developmental timepoint.

In comparison to medial supporting cells, which share gene expression profiles with non-sensory cells, lateral supporting cells display distinct transcriptional profiles at all timepoints examined. These results suggest that the lateral supporting cells may represent an early-specified domain of cells that are distinct from the medial sensory region. Moreover, expression analysis of lateral supporting cells across timepoints identifies previously uncharacterized components of the Wnt signaling pathway in the development of this region. Differentiation trajectory models were consistent with known basal to apical developmental gradients.

Overall, these results suggest that the lateral domain of the organ of Corti may represent a unique developmental lineage important for increased auditory sensitivity and frequency discrimination. Validation of other component genes and pathways identified from the differentiation trajectory models is ongoing and we are performing genetic lineage tracing to determine at what point a separate lateral sensory domain may arise.

Funding
This project was supported by funds from the Intramural Program at NIDCD to M.W.K. (DC000059).

PS 798

Crosstalk of the Wnt pathway with other signaling pathways to pattern the mammalian cochlea.

Vidhya Munnamalai; Donna Fekete
Purdue University

The promise of Wnts for stimulating regeneration in the cochlea has created a surge of interest in the Wnt pathway in recent years. Activating the Wnt pathway has been shown to stimulate proliferation and increase the differentiation of distinct cell populations in the organ of Corti. However, the mechanisms that determine these cell fates are not well understood. Our objective is to investigate how Wnts can influence patterning across the radial axis in the developing cochlea at various stages of development by exploring the regulation of downstream genes.

To study patterning, we culture embryonic mouse cochleas and activate the Wnt pathway using an *in vitro* pharmacological approach. Cochleas are harvested at E12.5 and cultured for 6 days *in vitro*. Wnt activation on different days produces different phenotypes of the organ of Corti, as detected by immunofluorescent labeling. We use microarray, in situ hybridization and/or RT-qPCR to evaluate spatial and temporal changes. This approach reveals transient changes in gene expression that are most likely to initiate a cascade leading to the eventual alterations in cell fates observed on day 6.

Within a few hours of Wnt activation, we find expression changes in genes belonging to several signaling pathways: FGF, Notch and BMP. Furthermore, these fold-changes vary with the timing of drug treatment. For example, *Jagged1*, a known Wnt target gene, is highly upregulated in response to Wnt activation on day 0 and day 5 *in vitro*. However, on day 1 the increase in *Jag1* expression is less robust. One explanation is that on day 1, a second Wnt target gene is upregulated that incoherently feeds forward to limit *Jag1* transcription. If present, this response may globally activate a gene network that normally serves to influence local patterning in the cochlea. Temporally discordant results are also seen for other signaling pathways in response to Wnt activation, with accumulating evidence that these pathways can crosstalk.

In summary, a complete understanding of the mechanisms underlying cell fate acquisition in the embryonic cochlea must take into account the responsiveness to the major signaling molecules, changes over time. This information may offer insights on the full potential of manipulating the Wnt pathway to stimulate regeneration in the damaged adult cochlea.

Funding
NIDCD R01DC002756

PS 799

Age-regulated Function of Autophagy in the Mouse Inner Ear

Sara Pulido[1]; Rocío de Iriarte Rodríguez[2]; Isabel Checa[2]; Marta Magariños[2,3,4]; **Isabel Varela-Nieto**[2,3,5]
[1]CSIC-UAM; [2]Instituto de Investigaciones Biomédicas, CSIC-UAM; [3]CIBERER, Unit 761, Instituto de Salud Carlos III; [4]Universidad Autónoma de Madrid; [5]IdiPAZ, Instituto de Investigación Sanitaria

Background
Autophagy is a highly conserved catabolic process essential for vertebrate embryonic development and adult homeostasis. Autophagy induction has been reported to resolve inflammation, to ameliorate ageing and to protect from neurodegeneration. In the inner ear, autophagy has been reported to play roles in chicken otic neurogenesis and in the response to otic injury in the adult mouse (1,2). Here, we will discuss the role of autophagy in late cochlear development and functional maturation.

Methods
Animals. For this study two mouse strains have been used (HsdOla:MF1*129/Sv and HsdOla:MF1).

RT-qPCR. Autophagy genes TaqMan® probes were used and referred to Rplp0 and 18S rRNA as the endogenous housekeeping genes. The estimated gene expression was calculated as $2^{-\Delta\Delta Ct}$.

Western blotting. Autophagic flux was assessed by measuring the levels of microtubule associated protein light chain 3-II (LC3-II) and sequestosome 1 (SQSTM1/p62).

Statistical analysis. ANOVA or Student t-test were carried out with SPSS v19.0 to compare gene expression in the organs, time points and genotypes of each strain. Post hoc analyses included the Bonferroni test. Results were considered significant at $p < 0.05$.

Results
Autophagy machinery genes *(Becn1, Atg4b, Atg5 and Atg9)* were expressed in the mouse cochlea, vestibular system and brainstem cochlear nuclei, although with different expression levels and temporal patterns. Gene expression was up-regulated from perinatal to adult ages in the cochlea of two mouse strains. Protein levels of LC3-II and p62 confirmed that autophagic flux was increased with age. Immunohistochemistry revealed that LC3B was mainly localized in the neurons of the spiral ganglion. *Cox2*, an inflammation marker, showed the same temporal expression profiles as those obtained from autophagy transcripts. In contrast, no evident association with IGF-1 deficiency was observed.

Conclusion
Our data suggests that autophagy is regulated with age in the cochlea and that it plays a role in the functional maturation of the mouse inner ear.

References

1. Aburto MR et al. (2012) Cell death & disease 3: e394.
2. Taylor RR et al. (2008) JARO 9:44-64.

Funding
This work was supported by an Spanish grant from the Ministerio de Economia y Competitividad (SAF2014-53979-R) and European FP7-PEOPLE-IAPP-TARGEAR.

PS 800

Foxg1Cre-mediated Overexpression of Neurod1 Disrupts Normal Inner Ear Development

Ning Pan[1]; H. Joyce Li[2]; Andrew Leiter[2]; Israt Jahan[1]; Jennifer Kersigo[1]; Bernd Fritzsch[1]
[1]University of Iowa; [2]University of Massachusetts Medical School

Background
Mammalian inner ear development is highly regulated through temporal, spatial, and quantitative control of gene expression. Previous studies using mouse models with loss-of-function gene alterations have established that three proneural basic helix-loop-helix (bHLH) transcription factors (Atoh1, Neurod1 and Neurog1) play crucial roles in regulating cell fate decisions and differentiation during neurosensory development. More detailed studies have demonstrated extensive cross-regulations between these bHLH genes. In particular, Neurod1 inhibits both Atoh1 and Neurog1 through negative feedback loops to regulate differentiation of neurons and hair cell types and thus play a central role in the gene regulatory network that controls the neurosensory cell fate determination. This essential function of Neurod1 is underscored by several recent reprogramming studies using viral induction that reveal the ability of Neurod1 to drive neuronal differentiation in various models, indicating its potential in regenerative medicine.

Methods
To further elucidate the functions of Neurod1 in ear neurosensory development, we developed a genetically engineered gain-of-function mouse model that induces overexpression of Neurod1 using the Cre-loxP recombination system. We combined this mouse line with a $Foxg1^{Cre}$ line to drive Neurod1 overexpression in presumptive otic vesicles and characterized the effects on the ear development.

Results
Using *in situ* hybridization, we first confirmed $Foxg1^{Cre}$-induced Neurod1 overexpression in the otic vesicle, as well as the telencephalon, the olfactory epithelium, and parts of the eye. The overexpression of Neurod1 in the early developing otic vesicle seemed to completely disrupt inner ear development, leading to mice without any ears. Otocyst cells prematurely exposed to a differentiation-inducing bHLH factor underwent cell death, shown by activated Caspase 3 immunostaining. In addition, the expression of several neurosensory patterning genes such as Pax2 and Sox2 was rapidly altered in the mutant embryos.

Conclusions
We show that $Foxg1^{Cre}$-mediated Neurod1 overexpression massively affects otocyst cell fate, eliminating the developing ear through apoptosis. We propose that Neurod1 acts to drive differentiation at whichever state of decision making a cell is in, but precursors at this early stage are unable to respond to Neurod1 with proper differentiation. Therefore, the state of decision making ultimately determines the outcome elicited by Neurod1, which is cell death if expressed prematurely. Further studies using this novel gain-of-function mouse model will provide important insights into spatiotemporal regulation of key regulators and molecular mechanism underlying cell fate determination of the neurosensory precursors in the inner ear.

Funding
This work was supported by NIH grants P30 DC 010362 and R03 DC 013655. We also acknowledge the financial support of the Office of the Vice President for Research at the University of Iowa.

PS 801

The Role of canonical Wnt/β-catenin signaling in the establishment of planar cell polarity of the vestibular maculae in vitro

Dong-Dong Ren[1,2,3]; Xiao-Yu Yang[1,2,3]; Xin-Wei Wang[1,2,3]; Rui Ma[1]; Fang-Lu Chi[1,2,3]
[1]Eye & Ent Hospital of Fudan University; [2]Shanghai Auditory Medical Center; [3]Key laboratory of Hearing Science, Ministry of Health

Background
Planar cell polarity(PCP) is a special kind of cell arrangement regularity. Vestibular maculae present the best well known cell polarity in three levels of anatomical organization. As we all know that Wnt signaling is critical for inner ear development, previous our study has demonstrated that the precursors of hair cells proliferate and differentiate in accordance with the

polarity of hair cell bundle establishment. Therefore, the aims of this study are to explore the role of canonical Wnt/β-catenin signaling in the establishment of the PCP of the vestibular maculae in vitro.

Method

1) RT-PCR to detect expressions of Wnt correlated genes in the dissected E13.5 and E18.5 mouse utricles. RNA-seq sequencing is adapted to E13, E13.5, E14, E15, and P1 utricles. Highly expressed genes that associated with differentiation and polarity are selected, especially Wnt pathway correlated ones. 2) Wnt/β-catenin pathway inhibitor IWP2 and typical Wnt pathway activator Licl is added in the E13.5 utricles respectively in vitro, while DMSO is added into control group. We use scanning electron microscopy(SEM) and immunostaining to observe the directions of planar cell polarity of hair cells after treatment for 5 days. 3) Real-time PCR to detect the changes of Wnt related genes expression and the core PCP genes expression in the utricle epithelium after Wnt pathway inhibitor/activator treatment in vitro.

Results

1): On E13.5 and E18.5, the Wnt related genes, Wnt5a, Wnt7a, Wnt11, β-catenin and Frizzed are all expressed. 30 Wnt pathway differential genes are discovered. Among them, the up-regulated genes correlated with Wnt signal pathway as the development postponement are: Apc, Axin2, Camk2d, Csnk2a2, Ctbp1, Fzd1-8, Mapk8, Rac1, Rock1, Smad4, Wif1, which are mainly correlated with the typical pathway.2) Compared with the control group DMSO, the polarity of hair cells is disordered in the outer side of the borderline after IWP2 treatment, with the decrease of Axin2、Wnt5a, Wnt7a, Wnt11 ,WiF1 and Frizzled and increase of c-myc. On the other hand, the borderline LPR position is changed and the polarity obviously disordered after Licl treatment, with the decrease expression of apc, Axin2, Camk2d, Frizzled and the increase expression of Wnt5a, Wnt7a, Wnt11 and Wif1.

Conclusion

There are differences in the Wnt pathway related genes expressions in the different stages of the utricles polarity formation procedure. It is discovered that controlling the typical Wnt pathway can affect the formation of utricles polarity with the downregulation of Axin2.

Funding

Supported by NSFC 81271084?81420108010 to F.C, 81000413 , 81370022,81570920 to D.R.? Training Program of the Excellent Young Talents of the Shanghai Municipal Health System(XYQ2013084) to D.R. Innovation Project of Shanghai Municipal Science and Technology Commission (11411952300) to F.C.

PS 802

Differentiation of Utricular Hair Cell Sub-Types Follows a Distinct Spatiotemporal Pattern

Stephen McInturff; Joseph Burns; Matthew Kelley
NIDCD/NIH

Introduction

Vestibular organs in the inner ear detect head movements and acceleration through mechanosensitive hair cells (HCs). Two sub-types of HCs have been described in the vestibular organs of mammals, birds, and reptiles: Type I and Type II. Classically, the definitions of these sub-types have been based on differences in afferent innervation, morphology, and physiology. Unlike the cochlea, where the differentiation of cells has been extensively described, our understanding of HC development in the vestibular epithelium is extremely limited.

Methods

Using existing single-cell RNA-Seq data, we identified potential new markers for Type I and Type II HCs in the adult (>P60) mouse utricle. Markers were validated by correlating marker expression with synapse type (calyx for Type I or bouton for Type II). To determine the developmental timing of hair cell formation, utricular progenitor cells were marked using *Atoh1*^{CreERT2}*; R26R*^{tdTomato} or *Plp1*^{CreERT2}*; R26R*^{tdTomato} mice induced with tamoxifen at specific embryonic time points. Subsequent analysis of adult utricles using sub-type-specific antibody-labeling provided information on the pattern and timing of hair cell formation within the utricle.

Results

We identified several antibody markers that specifically label Type I or Type II HCs in the striolar and extrastriolar regions of the adult mouse utricle. Using these novel markers, we have begun to determine the timing of HC sub-type differentiation at the molecular level. Type II markers are expressed in all HCs in the utricular epithelium until the second postnatal week, when they appear to become downregulated in Type I HCs. At least one Type I marker is detectable in a subset of HCs on the medial side of the utricle as early as E16.5 and spreads laterally to cover the whole extrastriola by P0, before entering the striola after the first postnatal week. Ocm, a known marker of striolar Type I's, is also detectable as early as E16.5. Preliminary results from lineage tracing experiments indicate that the first HCs in the utricle arise in the striola and the medial region between E12.5 and E13.5 and that the vast majority of these early hair cells differentiate into Type I's.

Conclusions

Type I HCs may begin to differentiate much earlier than previously thought, and striolar and extrastriolar Type I HCs may be more distinct at young ages than in adults. Surprisingly, differentiation of Type II's might occur after Type I's as adult Type II's appear less derived and retain many of the markers expressed by immature HCs.

Funding
This project was supported by funds from the Intramural Program at NIDCD to M.W.K. (DC000059)

PS 803

Role of CCCTC-Binding Factor (CTCF) in the Mammalian Inner Ear

Jeong-Oh Shin; Youn-Wook Chung; Ji-Hyun Ma; Hyoung-Pyo Kim; Jinwoong Bok
Yonsei University College of Medicine

Background
The inner ear is comprised of diverse cell types specialized to convert sound waves into electrical stimuli and convey the signals to the brain. These cells include mechanosensory hair cells and their associated ganglion neurons as well as various non-sensory components such as tectorial membrane and otic fibrocytes. How these specialized cells develop in coordination with their neighbors has been rigorously investigated during the past decades. Now, we have relatively good understanding as to how certain signaling pathways dictate specific differentiation programs at the right time and place by regulating expression of genes important for specific cellular differentiation and development. Recent advancements of epigenetics, however, demonstrated that in addition to the classical views of "genetic" regulations, "non-genetic" regulations such as conformational changes of chromatin structures induced by histone and DNA modifications are also important for animal development and function.

Methods
As an effort to understand how the epigenetic regulations contribute to inner ear development and function, we examined inner ear-specific (*Pax2-Cre; Ctcf$^{lox/lox}$*) or hair cell-specific (*Gfi1-Cre; Ctcf$^{lox/lox}$*) conditional knockouts of *Ctcf*, a well-known epigenetic regulator.

Results
Inner ears of *Pax2-Cre; Ctcf$^{lox/lox}$* mutants showed that gross morphogenesis was severely disrupted, such that anterior and lateral semicircular canals and cristae were absent and the cochlear duct was shortened and malformed. Gene expression and immunofluorescence analyses indicated that neurogenesis was severely compromised and hair cell differentiation occurred prematurely in a disorganized pattern. Microarray analyses of the *Pax2-Cre; Ctcf$^{lox/lox}$* otocysts confirmed that genes associated with early neurogenesis including *Neurog1* were significantly downregulated. Consistently, we found several CTCF putative binding sites in the *Neurog1* promoter region in the mouse genome, and confirmed that CTCF binding induced a DNA looping between the enhancer and the promoter sequences of the *Neurog1* in P19 cell line. Unlike *Pax2-Cre; Ctcf$^{lox/lox}$* mutants, *Gfi1-Cre; Ctcf$^{lox/lox}$* mutants were viable and displayed normal hair cell differentiation. However, *Gfi1-Cre; Ctcf$^{lox/lox}$* mutants exhibited progressive hearing loss when examined by ABR test. DPAOE measurements and scanning electron microscopy confirmed that the hearing loss is mainly due to degeneration of the hair cells, suggesting that CTCF function is required for hair cell maintenance.

Conclusion
Our data suggest that CTCF plays crucial roles in inner ear development and function. We are currently investigating the mechanisms by which CTCF regulates inner ear morphogenesis, neurogenesis, and hair cell maintenance.

PS 804

Wnt9a influences hair cell development in the auditory epithelium of chickens

Ulrike Sienknecht
Carl von Ossietzky University Oldenburg

During development the inner ear has to set up a regime that controls and coordinates the different well orchestrated spatial and temporal events. In the forming auditory epithelium (BP), developmental gradients come into place along which: (1) the mitotic production of cells, (2) cell fate specification, and (3) cytodifferentiation, the structural maturation of cells take place.

Endogenous Wnt9a is transcribed briefly within the BP of chickens at embryonic day (E)4.5 and has vanished a few hours later at E5 (Sienknecht and Fekete 2009). The transient expression of Wnt9a preceding hair cell (HC) development make this gene a potential regulator of cell proliferation in the forming BP. Its dose may also trigger cells to become postmitotic and initiate differentiation.

The experimental approach for testing this hypothesis was to overwrite the naturally restricted expression of Wnt9a in chicken embryos.

Excessive and long-term stable expression of Wnt9a was obtained by retrovirus-mediated transfection. Otocysts were injected with RCAS-Wnt9a virus at E3. Embryos were then harvested at different stages of development between E5 and E16. Hair cell development was monitored by immunolabelling with anti-HCS-1 (otoferlin).

Excessive Wnt9a caused: (I) a delayed HC development in the BP, (II) disruptions of the developmental gradients across the organ primordium, and resulted (III) in super numerous HCs.

In control ears HCS-1 immunoreactivity was first detected in the distal end of the BP as early as E7 (s31), which replicated earlier reports (Goodyear et al. 2010). By E8 untreated BPs were plentiful of HCs that populate the sensory primordium with the exception of the most proximal part.

The auditory primordium of ears that excessively expressed Wnt9a lacked any HCs until the first HCS-1 positive cells became visible in the distal BP by E8 (s34). Furthermore, in Wnt9a ears, the developmental gradients were disrupted and led to various BP phenotypes: (a) a broadened sensory epithelium with densely packed HCs, and BPs with variously sized regions of either (b) sparsely distributed, or (c) entirely missing HCs.

The data suggest that Wnt9a is crucial in the control of cell proliferation and the transition to cytodifferentiation in the developing auditory epithelium.

Moreover, it will be discussed whether the local timing of cell cycle exit and the onset of cell differentiation is instrumental for a cell's fate discriminating (vestibular vs. auditory and tall vs. short HCs).

Funding
Funding support was provided by the Carl von Ossietzky University Oldenburg.

PS 805

Interaction of the bHLH Transcription Factor Atoh1 with the Zn Finger Transcription Factor Gfi1 in the Production of Sensory Hair cells

Lynn Powell[1]; John Devane[2]; Andrew Jarman[1]
[1]University of Edinburgh; [2]University of Freiberg

We present data from our investigation of transcription factors from two families that are essential for differentiation and survival of sensory hair cells in the inner ear. These factors are Atoh1, a bHLH transcription factor, and Gfi1, a Zn finger transcription factor of the GPS protein family. Atoh1 mutant mice lack all sensory hair cells in the inner ear while misexpression of Atoh1 results in the production of ectopic sensory hair cells. Gfi1 mutant mice initially specify cochlea hair cells but they are disorganised and are lost shortly prior to or soon after birth by apoptosis. Work in our laboratory on the *Drosophila* homologues of these two proteins, Atonal and Senseless, demonstrated a direct interaction between the two that lead to synergistic activation of target genes essential during neurogenesis. Gfi1 is generally known as a transcriptional repressor whereas Senseless has a dual role as both transcriptional co-activator and repressor. Hence we decided to test whether Gfi1 can function as a coactivator of Atoh1 activity.

Here we present results from studies of the vertebrate Gfi1 and Atoh1 proteins in mammalian tissue culture and in zebra fish to test the hypothesis that these two proteins work synergistically in sensory hair cell production through direct interaction.

Using morpholino knockdown in zebra fish embryos we demonstrate a role for the Gfi1 homologue Gfi1ab in sensory hair cell development in the neuromasts of the lateral line. Gfi1ab morphants have reduced numbers of neuromasts, and remaining neuromasts have a disorganised structure and a reduced number of hair cells. This phenotype can be rescued by coinjection of Gfi1 mRNA. Furthermore, at low levels of Gfi1 mRNA that are not sufficient to give rescue alone, we have demonstrated that coinjection of Atoh1 mRNA results in rescue of the Gfi1ab morphant phenotype. These results are consistent with a genetic interaction between Gfi1 and Atoh1 during sensory hair cell development *in vivo*.

Investigation of the two factors in cultured P19 cells provides evidence for their physical interaction. Gfi1 enhances the Atoh1 transcriptional activation of a luciferase reporter gene in mammalian cells in the absence of a Gfi1 DNA binding site. Results of a GST pull-down assay provide further evidence of a direct interaction between the two factors. We propose therefore that direct interaction between Atoh1 and Gfi1 results in synergistic activation of target genes during sensory hair cell production.

Funding
This work was supported by MRC grant no. MR/L021099

PS 806

Adaptor protein-3 complex is required for Vangl2 membrane targeting and planar cell polarity of the inner ear

Cristy Tower-Gilchrist; Stephanie Zlatic; Victor Faundez; Xi Lin; **Ping Chen**
Emory University

Planar cell polarity (PCP) refers to coordinated polarization of neighboring cells along a planar axis. PCP signaling is essential in development and in tissue function. Defects in PCP result in a range of developmental anomalies and diseases in the inner ear, the kidney, the lung, the heart, the brain, the vascular system, and the spinal cord. Some of the PCP proteins are asymmetrically sorted across the planar polarity axis in the mammalian inner ear to regulate coordinated hair cell polarity and cochlear duct extension. However, the cellular and molecular machinery that regulates the asymmetric localization of these proteins is not clear. We documented Vangl2 association with early and recycling endosomes as evident by colocalization with endosomal markers Rab5, and Rab4a and Rab11a, respectively. In addition, we show that Vangl2 biochemically interacts with adaptor protein-3 complex (AP-3) and is contained in the same compartment as AP-3. Furthermore, knockdown of AP-3 endogenous levels or chemical blocking of endosomal pathways in cultured cells resulted in disruption of Vangl2 localization at the cell membrane. In mice, we observed reduced membrane localization of Vangl2 in AP-3 deficient cochleae. More importantly, noticeable PCP defects include deformation of hair cell stereociliary bundles and disorganization of cell patterning along the basal region of the cochlea suggesting convergent extension deficits. We examined the vestibular of AP-3 deficient mice and revealed a disruption in polarity in hair cell orientation in the posterior cristae. AP-3 deficient mice are deaf and balance deficient, which is consistent with the morphological abnormalities. These findings strongly suggest that AP-3 mediated endosomal pathways are essential for the targeting of core PCP proteins.

Funding
NIH RO1 DC 005213 NIH F32 DC012702

PS 807

Roles of inhibitor of differentiation and DNA-binding proteins in Developing Cochlear Epithelium

Susumu Sakamoto; Tomoko Tateya; Koichi Omori; Ryoichiro Kageyama
Kyoto University

The family of inhibitor of differentiation and DNA-binding (Id) proteins, including Id1 to Id4, is a group of evolutionarily conserved molecules, which play important regulatory roles in organisms ranging from Drosophila to humans. Id proteins are small polypeptides harboring a helix-loop-helix (HLH) motif, which are known to mediate dimerization with other basic HLH proteins, primarily E proteins. Because Id proteins do not possess the basic amino acids adjacent to the HLH motif necessary for DNA binding, Id proteins inhibit the function of heterodimers between E proteins and tissue-specific bHLH proteins. The roles of Id proteins in the growth and differentiation of the cochlear epithelium during development are not fully elucidated. We previously investigated the spatiotemporal expression pattern of Id proteins in the developing mouse cochlea. Id1, Id2 and Id3 were expressed in the prosensory domain and it suggested that these Ids were involved in the development of cochlear sensory epithelium.

The purpose of this study is to clarify the roles of these Ids in the development of cochlear sensory epithelium by both gain- and loss-of-function experiments. We performed overexpression experiments and majority of prosensory cells transfected with Id1, Id2 or Id3 expression plasmids were fated to be supporting cells.

Because Id1, Id2 and Id3 are expressed in similar patterns within the cochlea, there may be functional redundancy among these Ids. However, targeted deletion of even two of Ids was reported to result in embryonic lethality. To overcome the limitations of functional redundancy, we are generating conditional double-mutant mice. We will report the phenotypes of single and double-mutant mouse cochleae and discuss the roles of Ids in the cochlear epithelium during development.

PS 808

Comparing Retroviral Vectors to Tol2 Transposase Technology for Delivery of Short-hairpin RNAs to the Developing Chicken Inner Ear

M. Scott[1]; Michelle Stoller[2]; Kaidi Zhang[3]; Ankita Thawani[1]; Vidhya Munnamalai[1]; Donna Fekete[1]
[1]Purdue University; [2]University of Utah; [3]Georgetown University

The developing otic cup gives rise to vestibular and auditory organs of the inner ear. Due to the ease of *in ovo* manipulations and gene transfer to the otic cup, the chicken embryo is an excellent model to study genes involved in inner ear development. Long-term overexpression of protein-encoding genes in the chicken inner ear is routinely done using RCAS retroviral vectors, and more recently using Tol2-mediated gene transfer. We seek to complement these gain-of-function approaches with knockdown experiments, and are comparing these two transduction methods. Our goal is to deliver short-hairpin RNAs (shRNAs) that are converted into small-interfering RNAs (siRNAs). As a test case, we are targeting *Wnt9a* by creating siRNA vectors based on an intronic design previously used for microRNA (miRNA) overexpression.

Artificial introns carrying one of three *Wnt9a* siRNA hairpins, or pre-miRNA hairpins, were inserted into RCAS. For the Tol2 expression vectors, introns were placed upstream of GFP, with gene expression driven by a CAG promoter. In both types of vectors, we expect the transcribed intronic sequences will be converted into either siRNAs or miRNAs by the endogenous miRNA processing machinery. High-titer RCAS-shRNA virus was injected into the otocyst at embryonic day 3 (E3). Tol2-shRNA-GFP vectors were co-electroporated with a transposase-encoding plasmid into E2 otic cups. Sections through E7 cochlear ducts were processed for immunostaining to detect either viral capsid protein (RCAS infections) or GFP expression (Tol2 electroporations). *In situ* hybridization (ISH) was used to detect miRNA and *Wnt9a* transcripts. Real-time quantitative polymerase chain reaction (RT-qPCR) was also used to measure *Wnt9a* transcripts.

Following injection of RCAS-shRNA viruses, we confirmed robust virus infection of the cochlear duct. However, neither RT-qPCR nor ISH showed a detectable knockdown of *Wnt9a* transcripts using RCAS-siRNA. Similarly, ISH detected little to no miRNA overexpression. We suspect that this problem is related to retroviral transcript processing of the shRNAs. For Tol2-transposase delivery, GFP expression revealed successful targeting of the cochlear duct and ISH detected transcribed miRNAs in adjacent sections. We will use RT-qPCR and ISH of tissue sections to evaluate and quantify whether Tol2-siRNAs are able to reduce *Wnt9a* transcripts.

In summary, we find RCAS to be unreliable to express either siRNAs or miRNAs in the chicken cochlea. In contrast, following Tol2-mediated gene transfer, transcribed intronic pre-miRNA hairpins are efficiently processed into mature miRNAs. We are currently testing whether Tol2 can similarly be used to express siRNAs *in ovo*.

Funding
This work was funded by the National Institutes of Health (http://www.nih.gov/ R01DC002756 to D. M. F.; F31DC011687 to M. L. S.; P300CA023168).

PS 809

Development of Tone-Evoked Neuronal Population Responses in Auditory Cortex

Krystyna Solarana; Zac Bowen; Ji Liu; Daniel Nagode; Daniel Winkowski; Patrick Kanold
University of Maryland College Park

Early experiences of the world are fundamental in shaping the structural and functional organization of the brain, and neuronal connections are established and modified based

on the sensory stimulation we encounter. Sensory input is particularly relevant for the proper maturation of the auditory cortex (ACX), which requires exposure to behaviorally relevant acoustic stimuli during the critical period of auditory development. Previous studies have shown that artificially manipulating environmental sounds during early postnatal life results in wide-scale restructuring of topography in adult rodents, yet little is known how ACX organization develops in normally-reared pups during ear opening and throughout the critical period window. Here we investigated how the functional responses and spatial tuning distribution of ACX neurons change and mature in different cortical layers during early hearing development. We used *in vivo* two-photon calcium imaging in one to three-week old Thy1-GCaMP6s mice and measured fluorescent responses of ACX neuronal populations in thalamorecipient layer 4 and supragranular layers 2/3 in response to amplitude-modulated tones. We measured response changes on an individual neuronal level (response amplitude, frequency selectivity, sound level threshold) and on a population level (best frequency variability, signal and noise correlations), and found that significant changes occur during the critical period that are reflective of specific modifications in feed-forward and intracortical connectivity as the circuit is refining. A greater understanding of the complexity and plasticity of ACX during development will provide insight into the critical relationship between early sensory experience and the maturation of fine-scale cortical organization.

Funding
This work was supported by NIDCD F31DC013951 (K.L.S)

PS 810

Highly Patterned Spontaneous Activity in the Developing Mammalian Auditory System In Vivo

Adam Lombroso[1]; Alexandra Gribizis[1]; Han Chin Wang[2]; Yingxin Zhang-Hooks[2]; Travis Babola[2]; Dwight Bergles[2]; Michael Crair[1]
[1]Yale University; [2]Johns Hopkins University

Spontaneous activity is a common feature of developing sensory systems. In the visual system, waves of spontaneous activity generated in the retina propagate to the thalamus and cortex before the retina is visually responsive. This patterned spontaneous activity helps to define neuronal pathways in the ascending visual system. In the developing auditory system, bursts of activity initiated within the cochlea before hearing onset may play a similar role in refining auditory system neural circuits. However, relatively little is known about the spatial and temporal patterns of this spontaneous activity in the ascending mammalian auditory system, and its role in development remains to be defined. To examine developmental changes in this sensory-independent activity and determine the mechanisms responsible, we imaged global changes in neuronal activity in the developing inferior colliculus (IC) and auditory cortex (A1) in awake neonatal mice using genetically encoded calcium indicators (GECIs). The IC plays a central role in the ascending auditory system, receiving input from auditory brainstem nuclei and relaying this activity to the MGN and eventually A1. We observed bands of activity in neonatal IC that were highly correlated between hemispheres and with activity in the ipsilateral auditory cortex. These activity bands were stationary (they did not propagate across the IC), their orientation was consistent with tonotopic bands previously observed using anatomic and functional (electrophysiological) techniques, and they depend on input from the cochlea. Spontaneous bands of activity become more frequent, more refined, and of shorter duration as animals aged. By examining the source of this spontaneous activity and changes in its spatial and temporal properties during development, we hope to understand the role this early activity plays in preparing the auditory system for the onset of hearing.

PS 811

The Effect of Pulsed Electric Fields on the Electrotactic Migration of human Neural Progenitor Cells and the Involvement of Intracellular Calcium Signaling.

Hisamitsu Hayashi[1]; Fredrik Edin[1]; Hao Li[1]; Yatsuji Ito[2]; Helge Rask-Andersen[1]
[1]Uppsala University Hospital; [2]Gifu University Graduate School of Medicine

Background
Profound sensorineural hearing loss is often caused by impaired hair cell function in the sensory organ of the cochlea. It results in alteration in the auditory nerve stimulation and signaling to the brain. Neural stem cell transplantation to the inner ear could be an option for the regeneration of auditory neurons and hair cells to restore hearing and improvement of the efficacy of cochlear implant in individuals with restricted neural potential. Pulsed current electric fields (EFs) have demonstrated potentially beneficial cellular effects on proliferation, protein synthesis and differentiation in cultured fibroblasts, keratinocytes and macrophages. The EF potentially allows stem cell to migrate toward the designated site and differentiate into neural cell. The present study puts its focus on the influence of mono-directional pulsed EF on electrotactic migration and differentiation of human neural progenitor cells (hNPCs) in vitro.

Methods
We applied the mono-directional pulsed EF with a strength of 250 mV/mm to immortalized hNPC for 6 hours. The EF was applied to the cells in a handmade electrotactic chamber via agar salt bridges and Ag/AgCl electrodes. An electric circuit was completed by connecting the electrodes to a pulsed stimulator. An inverted microscope equipped with an incubator was used for time-lapse video recordings. The distance of cell migration was measured as the length between the starting and final position of the migrating cell. The cell tracking rate was calculated from the full distance of cell migration in a given time period.

Results
The migration distance parallel to the EF of the hNPCs exposed to pulsed EF was significantly greater compared with the control not exposed to the EF. Pulsed EFs, however, had less of an effect on the migration of the differentiated hNPCs. Repetitive exposure of hNPCs to pulsed EF for 18 hours enhanced the differentiation into neuronal marker-positive cells. To investigate the role of Ca^{2+} signaling in electrotactic migration of hNPCs, pharmacological inhibition of Ca^{2+} channels in the EF-exposed cells revealed that the electrotactic migration of hNPCs exposed to calcium channel blockers was significantly lower compared to the control group.

Conclusion
The findings suggest that the pulsed EF has unique potential to migrate stem cell to the designated site and differentiate it.

Funding
This study was supported by ALF grants from Uppsala University Hospital and Uppsala University and by the Tysta Skolan Foundation, Swedish Deafness Foundation. Our research is part of the European Community 7th Framework Programme on Research, Technological Development and Demonstration. Project acronym: NANOCI. Grant agreement no: 281056.

PS 812

Role of Perinatal Corticotropin Releasing Factor Receptor 1 Expression in Generating Mature Cochlear Nucleus Organization

Kathleen Yee[1]; Le'Andrea Mitchell[2]; Sorbor Jaryan[3]; Douglas Vetter[1]
[1]University of Mississippi Medical Center; [2]Tougaloo College; [3]Mississippi College

Background
To build on the extensive understanding of the morphology and physiological response properties of cochlear nucleus (CN) neurons, we are interested in how early developmental events impact the structural organization of the CN. In contrast to a large body of literature that has focused predominantly on gene expression *at* and *during* hearing onset as well as in association with hearing loss/dysfunction, work in our lab aims to understand how gene expression prior to the onset of hearing effects mature CN structure.

We have previously shown that corticotropin releasing factor (CRF), a neuropeptide that is involved in the systemic stress response and has modulatory effects on glutamatergic neurotransmission in the nervous system, is expressed in the auditory periphery (Graham et al. 2010). As CRF is expressed by spiral ganglion (SG) neurons and its peripheral process is involved in signaling in the cochlea (Graham et al, 2010), we were interested in examining whether corticotropin releasing factor receptor 1 (CRFR1) might be important in signaling at the first auditory brain region, the CN. Indeed, Justice et al. (2008) used a CRFR1 BAC transgenic mouse line that expresses GFP under the control of CRFR1 promoter and enhancer elements (R1-GFP mouse line) to show that CRFR1 is expressed in dorsal and ventral adult CN. Adding to these findings from the adult state, we have previously reported that by using the R1-GFP mice, a dynamic spatiotemporal expression of CRFR1 is revealed between postnatal day 0 through 10 months of age.

Methods/Results/Conclusions
We report here that in embryonic day 16.5 R1-GFP mice CN, there is robust expression of CRFR1 as revealed by immunohistochemical localization of the GFP transgene. We previously reported that GFP expression in the molecular and granule cell layers is detectable through at least 4 weeks of age. Additionally, we now show that at early postnatal stages, GFP-positive neurons with migratory phenotypes can be observed within the molecular and granule cell subdomains. At perinatal stages, there is broad GFP expression throughout the CN in developing neurons, including those that are migratory. To determine whether loss of CRFR1 expression could affect mature CN structure, we have examined the CN in constitutively null CRFR1 mice. Examination of general overall histological organization of the CN shows aberrant organization of the molecular and granule cell layers. Deviation of cell position from normal in CRFR1 null mice likely alters circuitry and auditory processing in the cochlear nucleus

Funding
University of Mississippi Medical Center Office of Research

PS 813

Feasibility of autologous auricular chondrocytes as donor for the tissue-engineered reconstruction of auricular defect

Jeong-Hoon Oh; Yoon Hee Kwon; Ki-Hong Chang; Byung Guk Kim
The Catholic University of Korea

Background and purpose
Tissue engineering of autologous cartilage offers a potential alternative. Large quantities of autologous neo-cartilage have been generated from a small fragment of nasal septal cartilage using alginate-recovered chondrocyte (ARC) method, but these tissue-engineered nasal septal constructs do not possess the biomechanical and biological properties of native tissue yet. Furthermore, the elastin content and innate curvilinear shape of auricular cartilage render the septal cartilage inferior for the auricular reconstruction. The aim of this study was to evaluate the feasibility of autologous human auricular cartilage as a donor for the reconstruction of auricular defect using ARC method.

Materials and method
Human auricular and nasal septal chondrocytes were isolated, and then expanded in monolayer culture. At confluency, a re-differentiation to the chondrocytic phenotype with production of functional cartilaginous extracellular matrix (ECM) was induced by ARC method. Next, the re-differentiated cells and ECM were incubated to form neo-cartilage. The constructs were terminated for assessment of their morphological,

histochemical, biochemical, and biomechanical properties and compared.

Results
Using the Real-Time quantitative polymerase chain reaction and the enzyme-linked immunosorbent assay, the expression of the aggrecan and collagen I was not significantly different between the constructs from auricular and septal chondrocytes. However, the composition of collagen II and elastin was much higher in the auricular cartilage constructs. The tensile and bending properties were higher in the auricular cartilage constructs.

Conclusion
The neo-cartilage construct from human auricular cartilage tissue showed higher composition of collagen II and elastin, representing the highly tensile and elastic properties of auricular cartilage. Auricular chondrocytes may be superior to be used as a donor for the tissue-engineered auricular reconstruction.

PS 814

Non-coding RNA Expression Profiling in Developing Mouse Otocysts and Human Embryonic Spiral Ganglion Neurons

Miho Matakatsu[1]; Joel Fontanarosa[1]; Cassing Hammond[1]; Linda Ernst[1]; John Kessler[2]; Yasukazu Nakamura[3]; Akihiro Matsuoka[1]
[1]Northwestern University; [2]Department of Neurology and Pharmacology; [3]National Institute of Genetics

Introduction
Defining genes involved in neuronal cell-type specification during vertebrate otic neural development have been relatively well-elucidated whereas non-coding transcripts such as miRNAs are emerging as important regulators. The precise mechanism by which miRNAs regulate otic neuronal development has yet to be determined. For this purpose, we used next generation sequencing to characterize whole transcriptomes in an early developing otocyst in a mouse model system and a human fetus.

Methods
Otic-placodes and otocysts from mouse embryos at the embryonic age 8.5 (E8.5), 9.5 (E9.5) and 10.5 (E10.5) were microdissected and isolated. After rRNA depletion, 40 ng of transcripts were used for 200bp single-end reads RNA sequencing on Ion-Proton™ platform. Human fetal tissues were transferred in RNAlater on ice to maintain RNA Integrity Number (RIN) > 8.0. Spiral ganglions were isolated from the cochlea and 200-400 ng of total RNAs were extracted for the RNA sequencing. For miRNA whole transcriptome assay, spiral ganglions were laser microdissected from a series of formalin-fixed, paraffin-embedded (FFPE) tissue sections. Duplicated 2,258 miRNA expressions were examined on HTG EdgeSeq System™.

Results
About 25M reads depth of mouse E8.5 placode and E8.5 peri-placodal transcript data were sufficient to confirm previously characterized otic developmental transcripts as well as differential expressing genes. Twenty-one hundreds of miRNA species were identified from spiral ganglions of a 55-day old fetus. A temporal measurement of non-coding RNAs in spiral ganglions will be discussed.

Conclusions
Uncovering landscape of otic developmental non-coring RNAs would provide us with a useful tool to address subsequent molecular mechanisms in developing otic neuronal cells. The information will eventually provide guidance in re-programming induced pluripotent cells for otic neuronal differentiation.

Funding
NIH K08, Knowles Leadership Fund

PS 815

Determining Crosstalk of Calcium signals between Hair Cell Synapses during the Development of the mammalian Inner Ear

Marcelo Moglie[1]; Paul Fuchs[2]; Ana Belén Elgoyhen[1]; Juan Goutman[1]
[1]Instituto de Investigaciones en Ingeniería Genética y Biología Molecular, INGEBI; [2]Johns Hopkins School of Medicine

Background
Before the onset of hearing (in altricial rodents, postnatal day 14) cochlear inner hair cells (IHCs) fire sensory-independent action potentials, crucial for the normal development of the auditory pathway. Ca^{2+} influx through voltage-dependent Ca^{2+} channels triggers the release of glutamate to afferent dendrites of the auditory nerve, determining an excitatory role for Ca^{2+} ions. At this stage, IHC are also innervated by efferent cholinergic neurons, projecting from the brainstem. At this synapse Ca^{2+} has an inhibitory functional endpoint. The entry of Ca^{2+} through α9α10 cholinergic receptors activates SK2, Ca^{2+}-dependent potassium channels, producing hyperpolarization, and modulating IHCs electrical activity. Segregation of Ca^{2+}'s excitatory versus inhibitory effects within IHCs appears as a functional demand within a very small diffusional space. The aim of our work was to investigate this phenomenon at the cellular level.

Methods
IHC were 3D reconstructed from ultra-thin serial section electron micrographs. Electrophysiological recordings were combined with Ca^{2+} imaging measurements in IHCs from P9-P11 mice to investigate Ca^{2+} dynamics during synaptic currents evoked by efferent axon electrical stimulation. IHC afferent bouton currents were recorded in whole-cell patch clamp configuration while stimulating efferent synapses.

Results
Electron-micrographs of IHC exhibited thin near-membrane cisterns juxtaposed to efferent synaptic contacts, similar to those described in mature OHC. In addition, close proximity between these cisterns and synaptic ribbons was observed.

Imaging experiments showed an average of 2.4 Ca^{2+} entry hotspots per IHC, using efferent fibers electrical stimulation. During single synaptic events, these hotspots were spatially segregated from those observed after IHC depolarizations (average minimal distance = 2.0 mm). In contrast, trains of stimuli at different frequencies, and ACh applications, evoked global Ca^{2+} signal increases.

Surprisingly, recordings from afferent boutons showed that exogenous applications of ACh produced a strong increase in the frequency of EPSCs, presumably due to release triggered by Ca^{2+} influx through α9α10. This was reproduced by electrical stimulation of efferent fibers with trains at high frequencies (80 Hz), which also inhibited IHC. In contrast, stimulation at lower frequencies produced a decrease in afferent pathway activity. Consequently, trains of stimuli at these frequencies produced either partial (2–10 Hz), or complete (20 Hz) inhibition of IHC action potential firing.

Conclusions
Both morphological and Ca^{2+} imaging data provide evidence for a close proximity between afferent and efferent synapses in developing IHC. Physical barriers, imposed by synaptic cisterns and/or strong Ca^{2+} buffering in IHC prevent efferent to afferent synaptic crosstalk only at low frequency stimulation.

Funding
ANPyCT to ABE, FIRCA-NIH 1R03TW009403-01 (to Elisabeth Glowatzki and JG) and R01 DC001508 (to ABE and PF)

PS 816

Effects of disrupting ATP production at auditory hair cell synapses

Karina Leal; Henrique von Gersdorff
Oregon Health and Science University

Background
The hair cell afferent ribbon synapses are specialized for fast and precise synaptic transmission. In response to continuous stimulation these synapses have the ability to recruit new vesicles for exocytosis with little fatigue. At presynaptic vesicle release sites, ATP consumption and production is highly regulated in response to synaptic activity. Presumably, mitochondrial ATP production via oxidative phosphorylation is the chief source of cellular energy. Hair cells contain an abundance of mitochondria with estimates of greater than 1000 mitochondria per hair cell. Here, we investigated the contribution of ATP and mitochondrial respiration to synaptic transmission at the auditory hair cell synapse of the adult bullfrog amphibian papilla.

Methods
Amphibian papillae (AP) were dissected from adult bullfrogs. The AP were stretched out and split with fine micro-tools to expose hair cells and afferent fibers perfused with artificial perilymph. Whole-cell patch clamp recordings and membrane capacitance measurements were preformed with a double EPC9/2 patch-clamp amplifier. Data analysis was performed with Igor Pro software and Excel.

Results
Using whole-cell paired recordings of a hair cell and afferent fiber, we found that hair cell synapses maintain robust exocytosis in the absence of ATP provided by the patch pipette measured by presynaptic capacitance changes. This data suggest that local ATP production by mitochondrial respiration may supply continuous ATP for synaptic transmission. To test the contribution of presynaptic mitochondrial ATP production to sustain synaptic transmission, we dialyzed hair cells with oligomycin, an inhibitor of mitochondrial ATP synthase, in the presence of ATP-gamma-S to further out compete endogenous ATP. Inhibition of mitochondrial respiration in hair cells greatly reduced presynaptic capacitance changes and excitatory postsynaptic current (EPSC) amplitude during repeated stimulation. However, in preliminary results, blocking glycolysis had little effect on presynaptic capacitance measurements, suggesting that mitochondrial ATP production plays a critical role in supporting continuous release. We also find that inhibition of ATP production impairs the synchronized component of the EPSCs in hair cell afferent fiber paired recordings.

Conclusion
Our results indicate that hair cells maintain copious exocytosis by producing large amounts of ATP from mitochondria. ATP is required for vesicles recruitment and plays a role in maintaining the readily releasable pool of synaptic vesicles at hair cell synapses.

Funding
NIDCD R01-DC004274, Tartar Trust Fellowship

PS 817

Localization of the Reversed Polarity Mechanotransducer Channels in Cochlear Hair Cells

Maryline Beurg; Adam Goldring; **Robert Fettiplace**
University of Wisconsin-Madison

Two types of mechanotransducer (MT) currents have been described in cochlear hair cells: a conventional MT current evoked by displacements of the bundle towards its tallest edge, and an MT current evoked by bundle displacements in the opposite direction, termed a reversed polarity current. Conventional MT channels are located at the bottom end of the tip links but the reverse polarity MT current persists after severing the tip links with BAPTA, suggesting a different localization for this channel. The reverse polarity channels show similar pharmacology to the conventional MT current (block by calcium, amiloride, FM1-43 and dihydrostrepmycin). Here we investigated the properties and localization of reverse polarity MT channels using cell-attached patch recordings on cochlear outer hair cells (OHC) of neonatal mice, supplemented by detection of calcium influx with Fluo5F indicator using swept-field confocal imaging (Beurg et al. 2009). To map the reverse MT channels, single-channels were recorded in cell-attached mode on the apical surface around the base of the hair bundle. Currents were evoked by applying suction through the patch pipette. Mechano-sensitive single channels could be elicited on the apical surface of

Tmc1:Tmc2 double mutant OHCs. Single-channels currents were only evoked in response to membrane suction (pull), and were not activated either without suction or with a positive stimulus (push). The mean single channel conductance was 58 ± 4 pS in 1.5 mM $CaCl_2$. In reduced calcium (0.07 mM) saline, the mean conductance increased 1.5 fold to 86 ± 6pS, as with conventional MT channels. The reversal potential was about 0 mV as expected for a non-selective cationic channel. Reverse polarity MT currents can also be generated in wild-type mice after BAPTA exposure (Kim et al. 2013). Before BAPTA application, no mechanically-evoked channels were present on the apical surface of wild type OHCs, but they appeared a few minutes after BAPTA exposure with a mean conductance of 61 ± 6 pS in 1.5 mM $CaCl_2$. The apical surface of the OHC was confirmed as the main site of calcium entry during reverse polarity MT currents using calcium imaging. In summary, the electrophysiological properties of the reverse polarity MT channels closely resemble the conventional MT channels and are concentrated on the apical plasma membrane of the hair cell. We propose they most likely reflect insertion of new channels before their transport to the transduction complex.

Funding
Grant RO1 DC01362 from the NIDCD

PS 818

The Calcium Permeability and Adaptation of the Transducer Current is Affected by the M412K Point Mutation in TMC1

Laura Corns[1]; Stuart Johnson[1]; Corné Kros[2]; **Walter Marcotti**[1]
[1]University of Sheffield; [2]University of Sussex

Background
The transduction of sound stimuli into electrical signals by hair cells relies on mechanoelectrical transducer (MET) channels that open in response to hair bundle deflection. Despite the importance of this channel, its molecular identity is still uncertain. Recent studies have showed that the transmembrane channel-like protein isoforms 1 (TMC1) and 2 (TMC2) are the candidate subunits of the MET channel (Kawashima et al., 2011 J. Clin. Invest. 121:4796-4809; Pan et al., 2013 Neuron 79:504-515), although there is also evidence pointing to a more accessory subunit role (Beurg et al., 2014 J. Gen. Physiol 144:55-69). *TMC1* mutations in humans cause either profound congenital deafness or progressive hearing loss, the latter of which can be modelled by the mutant mouse *Beethoven*. The *Beethoven* (*Bth*) mutant mouse has a single dominant missense mutation of a methionine to a lysine at position 412 of *TMC1* (Kurimaet al., 2000 Nat. Genet. 30:277–284; Vreugde et al., 2002 Nat. Genet. 30:257-258). In this study we have used the *Bth* mouse to provide further evidence for a direct role of TMC1 and TMC2 in MET in mouse outer hair cells (OHCs).

Method
OHCs from *Bth* mice were studied in acutely dissected organs of Corti using whole cell patch clamp recordings. MET currents were elicited by applying mechanical steps or saturating 50 Hz sinusoids using a piezoelectric driven fluid jet placed close to the hair bundles. All experiments were performed in accordance with the UK Home Office regulations.

Results
Bth mice showed a reduced Ca^{2+} permeability of the MET channel of OHCs without affecting the maximum size of the MET current (range tested P2-P11). We also found that the M412K mutation reduces the affinity for the MET channel blocker dihydrostreptomycin (DHS) by an order of magnitude when applied extracellularly (Marcotti et al., 2005 J. Physiol. 567:505-521). Surprisingly, the Ca^{2+}-dependent adaptation of the MET channel, which is used to reset its operating range, was more pronounced in the homozygous mutant OHCs.

Conclusions
Our findings show that the *Bth* mutation has functional consequences for Ca^{2+} permeability, Ca^{2+} adaptation and DHS binding. We propose that the positively charged lysine in the *Bth* mutation in *Tmc1* causes a reduced affinity of a binding site in the channel's vestibule for Ca^{2+} ions and DHS and is located near this site. This implies that TMC1 is an integral component of the MET channel in hair cells.

Funding
The Wellcome Trust

PS 819

Afferent Synaptic Structure in Cochlear Outer Hair Cells of Rats and Mice

Pankhuri Vyas[1]; Chang Liu[1]; Rodrigo Monodero[2]; Hakim Hiel[1]; Mohamed Lehar[1]; Elisabeth Glowatzki[1]; Paul Fuchs[1]
[1]Johns Hopkins University School of Medicine; [2]University of Southern California

Background:
Each type II cochlear afferent is postsynaptic to many outer hair cells (OHC). Transmission from each OHC occurs by infrequent vesicular release, producing receptor potentials of only a few millivolts (Weisz et al., 2009, 2012, 2014). It is of interest to determine what structural features underlie this modest transmission. Each outer hair cell possesses 2-3 synaptic ribbons at which vesicles cluster to release glutamate onto postsynaptic type II afferent boutons. Additional type II boutons contact OHCs but without presynaptic ribbons, as reported for several species (cat- Dunn and Morest 1975; Pujol et al. 1980; adult rat- Lenoir et al. 1980, Pujol et al. 1980; human, Nadol,1983)

Methods
The arborization of individual type II afferent neurons in the young rat cochlea was quantified by *posthoc* processing after intracellular filling with biocytin. In separate experiments, antibodies to CtBP2 and postsynaptic proteins, including the AMPA receptor GluA2 were used to quantify functional synaptic contacts in young and mature rats. Serial thin-section electron micrographs from the middle turn of 3-week-old mouse cochleas were used to reconstruct ribbon-associated and ribbon-less type II afferent contacts on OHCs.

Results
Innervation patterns were examined for 15 biocytin-filled labeled type II afferents located at the apical turn of the young rat cochlea (P7-P9). Among these, 8 had a single spiral process from which extended on average 17 short branches with bouton endings. The other 7 had two (6) or three (1) spiral processes. In most cases, only one of the processes gave off terminal branches.

Antibodies to CtBP2 and GluA2 revealed juxtaposed immunopuncta for approximately half the type II terminals (enumerated by PDS-95 label – the remainder had neither ribbons, nor GluA2 patches). Using serial TEM, thirty-five afferent boutons were examined on 26 OHCs among which 18 were associated with presynaptic ribbons. OHC synaptic ribbons had similarly-sized central cores, but fewer, more heterogeneous vesicles than found at IHC ribbons (Weisz et al., 2012) (Fuchs and Glowatzki, 2015, Hearing Research in review).

Conclusion
Type II afferents form multiple terminal contacts with 10-20 OHCs. Approximately half these contacts are associated with presynaptic ribbons, and include postsynaptic clusters of AMPA receptors. Functional roles for ribbon-less contacts are unclear but these may be 'silent synapses' analogous to those found on central neurons.

Funding
This study was supported by NIH/NIDCD 5R01DC011741-02 to PF and EG, and P30 DC005211 to the Center for Hearing and Balance

PS 820

The Roles of Espins in Hair Cell Stereocilia: Site-directed Mutagenesis of the Espin Actin-bundling Module

Lili Zheng[1]; Dina Beeler[2]; **James Bartles**[1]
[1]Northwestern University Feinberg School of Medicine; [2]University of Illinois at Chicago

Background
The analysis of jerker mice has demonstrated that espin actin-bundling proteins are required for the widening, differential elongation and stabilization of hair cell stereocilia. A hallmark of the espins is their carboxy-terminal 116-residue peptide, the actin-bundling module, which is required for actin filament bundling in vitro and microvillar elongation in transfected epithelial cells. Our prior deletion mutagenesis studies implicated candidate actin filament-binding peptides at the amino- and carboxy-terminal ends of the module. Here, we refine and extend our analysis of structure-activity relationships for the espin actin-bundling module.

Methods
Scanning alanine mutagenesis was used to identify key motifs and residues in the espin actin-bundling module. Recombinant His-tagged espin proteins were expressed in *E. coli* and purified using Ni-NTA agarose. Actin filament binding and bundling activities were compared by cosedimentation. Targeting and microvillar elongation by pEGFP-C2 espin constructs was examined in transiently transfected LLC-PK1-CL4 epithelial cells.

Results
Among the amino acid residues we found to be required for espin-mediated microvillar elongation were three conserved tryptophans. The first and third tryptophans (W1 and W3) were uncovered the candidate actin filament-binding peptides at opposite ends of the actin-bundling module. However, the second tryptophan (W2) was detected in a cluster of required residues in the middle of the module. Mutation of W2 to alanine blocked microvillar elongation, yet had no obvious effect on actin filament bundling in vitro. This suggested that a peptide in the central part of the actin-bundling module is also required to drive the elongation of microvilli. Visual inspection revealed the amino acid sequences around W1, W2 and W3 to be curiously similar, raising the possibility that the actin-bundling module could actually contain three related actin filament-binding peptides. Accordingly, mutation of all three tryptophan residues to alanine was necessary to decrease actin-filament bundling activity to baseline and prevent GFP-espin from accumulating in microvilli.

Conclusions
By scanning alanine mutagenesis of the espin actin-bundling module, we identified three relatively similar tryptophan-containing residue clusters required for espin-mediated microvillar elongation in transfected epithelial cells. Beyond the clusters expected at the two ends of the actin-bundling module, we found an additional cluster in the middle of the module. The amino acid sequence similarity of the clusters suggested that there are three actin filament-binding peptides in the espin actin-bundling module. This multivalency could help explain some unique properties of espins, such microvillar elongation and the over-twisting of actin bundle filaments at low stoichiometry.

Funding
Supported by NIH R01 DC004314 from the National Institute on Deafness and Other Communication Disorders to JB.

PS 821

Altered Distribution of the Tip Link-Channel Linker Protein, LHFPL5, suggests Mislocalisation of Transduction Channels in Protocadherin 15-Deficient (av3J) and BAPTA-Treated Mouse Hair Cells

Shanthini Mahendrasingam[1]; Robert Fettiplace[2]; Kumar Alagramam[3]; **David Furness**[1]
[1]Keele University; [2]University of Wiscopnsin-Madison; [3]Case Western Reserve University

The hair-cell mechanoelectrical transduction channel (MET) is connected to the tip link by LHFPL5 (aka TMHS). LHFPL5 occurs at stereociliary tips, binds PCDH15 and regulates tip-link assembly (Xiong et al, 2012, Cell, 151:1283-1295.). In LHFPL5 mutations, expression of TMC1, a putative MET subunit, and MET current is lost in the bundle (Beurg et al., 2015 PNAS 112:1589-1594.). Transducer polarity is reversed

when tip links are missing in av3J mice, which lack PCDH15 (Alagramam et al 2011, PLoS One 6(4):e19183.) and BAPTA-treated hair cells (Kim et al., 2013, J Gen Physiol. 142:493-505.), possibly due to mislocalisation of the METs. Given its association with TMC1, we hypothesised that LHFPL5 would be mislocalised in similar situations.

Distributions of LHFPL5 were investigated in mice from: (i) P3 – P12 wild type (WT); (ii) P3 av3J homozygous and heterozygous; and (iii) BAPTA treated P3 – P6 WT. Cochleae were fixed using 4% paraformaldehyde, some including 0.1% glutaraldehyde. For BAPTA treatment, cochleae were exposed to 5 mM BAPTA (5 mins) before fixation 0 to 5 minutes afterwards. Immunofluorescence, pre- and post-embedding immunogold LHFPL5 antibody labelling was carried out. LHFPL5 knockouts lacked labelling, confirming antibody specificity.

Immature hair bundles contain several rows of ranked stereocilia with central unranked stereocilia, with all except the tallest four (IHCs) and three (OHCs) ranked rows being resorbed by P12. Immunofluorescence showed LHFPL5 expression in WT to P12, and in av3J and BAPTA treated hair bundles. With immunogold EM, LHFPL5 was found predominantly at the tips of all except the tallest ranked stereocilia, and in P3 – P7 WT, it was associated with lateral and ankle links. In av3J mice, the distribution was altered: in heterozygous IHCs 37% of ranked and less than 2% of unranked stereocilia tips were labelled, whereas in homozygotes only 11% of ranked compared with 16% of unranked tips were labelled. In OHCs, the distributions differed in that a substantially higher proportion of shortest row tips labelled amongst ranked stereocilia in the homozygotes (60%) compared with the heterozygotes (8%). In BAPTA experiments, tip labelling was also reduced from 30% in controls to 9% after treatment in OHCs.

These results suggest LHFPL5 distribution is altered in av3J hair bundles, perhaps corresponding to mislocalisation of the MET. In BAPTA treated bundles, tip labelling was reduced, but as yet no other change has been quantitatively defined. This may explain loss of the normal current, perhaps unmasking a reversed current.

Funding
Supported by funding from the BBSRC

PS 822

Towards the Hair Cell Proteome: Identifying Key Hair Cell Proteins through Mass Spectrometry-Based Proteomics

Ann Hickox[1]; Ann Wong[2]; Kwang Pak[2]; Chelsee Strojny[1]; Allen Ryan[2]; Jeffrey Savas[1]
[1]Northwestern University; [2]University of California San Diego and Veterans Administration Medical Center

Hair cells are highly specialized, comprising sensitive mechanotransduction apparati at their apical surfaces and precise neurotransmission machinery at the basal poles. Known and yet-unidentified proteins subserve these functions and are required for normal hearing and balance. Owing to the cells' post-mitotic state, irreparable damage to proteins can underlie permanent noise-induced or ototoxic insult resulting in functional impairment. Here, we use an unbiased, "bottom-up" proteomic approach aimed at identifying the complete set of proteins highly enriched in hair cells, to highlight potential future therapeutic targets.

To identify novel proteins enriched in cochlear and vestibular hair cells, we analyzed inner-ear extracts from mice selectively expressing GFP in hair cells driven by the pou4f3 gene promoter (Masuda et al. 2011). Three sample types were collected from *Pou4f3-GFP* mice (P4-P7, both sexes): (1) inner ears (IE; n = 3 pups), comprising whole inner ear structures isolated from bone; (2) sensory epithelia (SE; n = 25 pups), comprising micro-dissected cochlear and vestibular epithelia; and (3) hair cells (HC; n = 132 pups), isolated by FACS, totaling nearly 200,000 GFP-expressing auditory and vestibular hair cells. Following tryptic digestion, peptides were analyzed by reversed-phase liquid chromatography coupled to tandem mass spectrometry (LC-MS/MS). Protein identification based on acquired tandem mass spectra was performed using ProLuCID and DTASelect2 within Integrated Proteomics Pipeline-IP2.

We identified over 11,000, 5,000, and 6,000 proteins in IE, SE, and HC samples, respectively, with over 3,000 proteins identified in common across samples. Enrichment of known hair cell proteins in HC compared to IE and SE samples (e.g. otoferlin, myosin-6), together with identification of low-abundance proteins in HC only (e.g. stereocilin, espin) indicates successful purification of hair cell proteins in the HC sample. We found strong agreement between our hair-cell proteomic library and published hair-cell transcriptomic data in regards to gene identification, but with differing protein- and mRNA rank abundances. We successfully identified homologous proteins associated with nearly half of known human hereditary deafness genes. Furthermore, we identified new HC proteins not previously cataloged by transcriptomic approaches.

Using an unbiased, shotgun proteomic approach, we generated an inner-ear protein library, from which we identified proteins strongly enriched in mammalian cochlear and vestibular hair cells across stereocilia, cell membrane, and synaptic compartments. Combined analyses of proteins detected only in purified hair cells, proteins with high rank-abundance, and newly identified proteins at this developmental stage, together may contribute to future development of therapeutics for impaired hearing and/or balance.

Funding
NIDCD R00 DC-013805 (JNS), VA Research Service BLS Grant BX001295 (AFR), GPRWMF (ACYW).

PS 823

Do Prestin Isoforms Persist within the Cochlea to Affect Charge Movement?

Varun Sreenivasan; Vivek Rajasekharan; **Brenda Farrell**
Baylor College of Medicine, Houston

Introduction. Prestin-associated voltage sensors exhibit charge movement, *q* in response to changes in cell membrane potential. Summed over all participating atoms, *q* is the product of each atom's charge and the relative distance it moves within the dielectric thickness of the membrane. The quotient of *q* and a Boltzmann, $\kappa_B T$ (κ_B: Boltzmann's constant T: temperature) is the voltage sensitivity, α of the sensor. It is determined experimentally for a large number ($N > 10^4$) of sensors by measuring the voltage-dependent capacitance of an outer hair cell (OHC) or a prestin-transfected cell with electrophysiological techniques. **Experimental Observation.** Last year we presented data that showed α is higher in OHCs that originate from the basal region of the cochlea when compared to cells from the apical region, and that α increases monotonically with the characteristic frequency of the OHC. This relationship was observed only for OHCs isolated from our colony of pigmented guinea pigs, and not for cells extracted from albinos. In addition, when comparing OHCs across the cochlea, we observe that the total charge measured for each OHC is inversely proportional to α (cf. directly proportional) suggesting that the sensors may not act independently. **Explanation.** Prestin is the fifth member of solute carrier family 26 where *SLC26A5a* of *Homo sapiens,* also known as isoform X1 of *Cavia porcellus,* is the dominant variant. Three less common isoforms were reported in humans with two different variants predicted to exist in the domestic guinea pig. We hypothesize that isoforms of prestin coexist and their arrangement within an oligomer vary to account for the gradient of α, where a component of an oligomer translates a different fraction of *q* and the measured voltage sensitivity <α> represents the ensemble average. Specifically, we suggest mixtures of homomers and heteromers of the isoforms are found within the lateral wall membrane and this mixture varies across the cochlea for OHCs. **Method**.To test this we first establish whether mRNA of the predicted isoforms is found in the apical and basal regions of the cochlea by reverse transcription of mRNA and amplification of gene products by the polymerase chain reaction. To detect the isoforms we design primers that bind to exons flanking the missing exons. **Result**. We detect splice variants in cochlea tissue. This data will be discussed with respect to experimental measurements of charge movement.

Funding
Supported by NIDCD RO1DC00354 and Bobby R. Alford Department of Otolaryngology Head and Neck Surgery

PS 824

Distribution and Function of a8β1 Heterodimer in Inner Ear.

Marisa Zallocchi; Duane Delimont; Dominic Cosgrove; Edward Walsh; JoAnn McGee
Boys Town National Research Hospital

Background
Although the apical expression of integrin α8β1 (ITGA8) heterodimer in hair cells was demonstrated more than 10 years ago, little is known regarding ITGA8 function in the inner ear. In that early work, ITGA8 mutant mice showed hair cell bundle abnormalities as early as embryonic day 18, loss of FAK (focal adhesion kinase)-apical localization, and perturbations in the distribution of ITGA8 ligands and other components related to the inner ear extracellular matrix. Although ITGA8 was present in both types of hair cells (auditory and vestibular hair cells) morphological defects in the ITGA8 mutant mouse were only observed in the hair cells of the utricle.

Method
Whole mount organ of Corti and vestibular system specimens were immunostained for different cilia/stereocilia markers plus ITGA8 and prepared for confocal imaging or super-resolution structure illumination microscopy. Physiological measurements (ABRs) were done in ITGA8 mutant and control littermates.

Result
ITGA8 is developmentally regulated in the inner ear, with hair cells showing robust expression of ITGA8 between E18 to P3. By P6 we were unable to detect ITGA8 with our antibody preparation. Confocal microscope analysis in the organ of Corti showed ITGA8 is localized at the hair cell bundle and kinocilia in the outer hair cells while it is only present in the kinocilia in the inner hair cells. Super-resolution structure illumination microscopy showed ITGA8 has a similar distribution in crista, utricle and saccular hair cells where it is expressed all along the kinociliary plasma membrane. Preliminary physiological studies (ABR) suggest that ITGA8 mutants may exhibit auditory deficits.

Conclusion
The presence of the α8β1 heterodimer in the hair cell bundles together with possible auditory deficits observed in the ITGA8 mutants suggest a putative involvement for this integrin in the formation/maturation of the stereocilia. Since ITGA8 localizes all along the kinocilia, it may also be playing a role in ciliogenesis, planar cell polarity and/or in the regulation of signaling molecule activation.

Funding
NIH grants R01 DC004844 to DC and 1P30GM110768 to EJW. Health grant 5P20RR018788 and the Tobacco Settlement Fund from the State of Nebraska To MZ

PS 825

Role of Follistatin in the apical cochlear patterning

Hei Yeun Koo; Jihyun Ma; Jeong-oh Shin; Harinarayana Ankamreddy; Jinwoong Bok
Yonsei University

Background

The vertebrate cochlea is tonotopically organized, such that hair cells located in the base respond to high frequency sounds and their counterparts towards the apex progressively respond to lower frequencies. Recent studies suggest that the tonotopic organization is established by a temporal cascade of molecular events that is initiated by a decreasing apex-to-base gradient of Sonic hedgehog (Shh) signaling both in birds and mammals. In the chicken basilar papilla, *Bmp7* appears to be a key downstream target of Shh in mediating the tonotopy. In the mouse organ of Corti, however, the downstream mediators of Shh are not known. A likely candidate is *Follistatin* (*Fst*), which encodes an antagonist for Bmp/TGFβ signaling. The expression pattern of *Fst* is in a similar apex-basal gradient in the developing mouse cochlea as the gradient of Shh signaling and *Fst* expression is regulated by Shh as well. Here, we investigated the role of *Fst* in the tonotopic organization of the mammalian cochlea using *Fst* knockout mouse embryos.

Methods

We examined the inner ears of *Fst* knockouts (KOs) and inner ear-specific conditional knockouts (*Pax2-Cre; Fst$^{lox/lox}$;* cKOs) using the paint-fill technique, in situ hybridization, and immunostaining.

Results

In *Fst* KOs, the cochlear length was largely normal, yet its apical end displayed a slightly irregular shape based on paint-filled specimens. Within the cochlear duct, an extra row of outer hair cells was evident only in the apical cochlear region and these hair cells appeared more mature than those in the wild type, based on hair bundle morphology and onset of *Atoh1* expression. Importantly, genes that are preferentially expressed in the apical cochlea such as *Msx1* and *Efnb2* were abolished or down-regulated in *Fst* KOs, respectively. These results suggest that apical cochlear patterning is disrupted in the absence of Fst function. Since the neonatal lethality of *Fst* KOs precludes hearing function analyses, we generated inner ear-specific *Fst* cKOs, which are viable and closely recapitulate the cochlear phenotypes of *Fst* KOs. We are currently examining hearing function of *Fst* cKOs by measuring ABR and DPOAE.

Conclusion

Our data suggest that Fst is required for proper organization and differentiation of hair cells in the cochlear apex and is an important downstream mediator of the Shh signaling in the apex to facilitate tonotopy of the mammalian cochlea.

Funding

This work is supported by the BK 21 PLUS Project for Medical Science, Yonsei University

PS 826

Primary cilia mediates Shh signaling to control cochlear elongation and hair cell differentiation

Kyeong-Hye Moon[1]; HongKyung Kim[1]; Ji-Hyun Ma[1]; Jeong-Oh Shin[1]; Sun Myoung Kim[2]; Ping Chen[2]; Doris Wu[3]; Hyuk Wan Ko[4]; Jinwoong Bok[1]
[1]Yonsei University College of Medicine, Seoul; [2]Emory University School of Medicine; [3]National Institute on Deafness and Other Communication Disorders; [4]Dongguk University College of Pharmacy, Goyang

Background

The primary cilium serves as a signaling center for several cellular pathways important for animal development and homeostasis including Sonic hedgehog (Shh), Wnt, and PDGF. Defects in the primary cilium are associated with a range of genetic disorders known as ciliopathies, which include hearing loss. Previous studies showed that ciliary defects resulted in shortened cochlear duct and abnormal hair cell polarization. While the hair cell polarization defect is attributed to defective planar cell polarity (PCP) signaling, the cause for shortened cochlear duct remains unclear. Given the role of Shh signaling in cochlear patterning and growth, we analyzed Shh signaling in inner ears of three different ciliary mutants, *Broad-mined* (*Bromi*) mutant, *Intestinal cell kinase* (*Ick*) knockout (KO), and conditional knockout of *Ift88* (*Pax2-Cre; Ift88$^{lox/lox}$, Ift88* cKO), which all display a shortened cochlear duct.

Methods

Bromi, *Ick* KO, and *Ift88 cKO* cochleae were assessed for (1) the length of the cochlear duct, (2) Shh signaling based on *Patched1* (*Ptc1*) and *Msx1* expression patterns, and (3) maturity and pattern of sensory hair cells in the organ of Corti based on phalloidin staining and *Atoh1* expression.

Results

As previously reported, *Ift88* cKO mutants lack the primary cilium. Both *Bromi* and *Ick* mutants showed abnormal morphology and increased length of the cilium, respectively. All three mutant cochleae showed a shortened cochlear length, with *Bromi and Ift88* cKO cochleae more severe than that of the *Ick* KO. Our results indicate that Shh signaling was compromised in the cochlea of these mutants. First, all three cochleae showed a reduction in *Ptch1* expression, which is a direct readout of Shh signaling. Second, the expression of a bona-fide apical cochlear marker, *Msx1*, was reduced or absent, suggesting that the patterning of the apical cochlear region is compromised. Third, *Bromi* and *Ift88 cKO* developed ectopic sensory patches containing vestibular-like hair cells in the Kölliker's organ, which is also a phenotype associated with reduced Shh signaling. Fourth, hair cell differentiation in these cochleae was premature, consistent with phenotypes found in *Shh* mutants.

Conclusion

Taken together, our results underscore the complexity of ciliary mutants and the importance of disrupted Shh signaling in contributing to the cochlear phenotypes of ciliary mutants.

Funding
This work is supported by the Brain Korea 21 PLUS Project for Medical Science, Yonsei University

PS 827

Prestin Oligomerization and Function

Richard Hallworth
Creighton University

Tetramerization is ubiquitous in the SLC26 family of proteins, including mammalian and non-mammalian prestins, but the role of oligomerization is unclear. Evidence for cooperative interactions is lacking, so it has been assumed that the sub-units operate independently. In this study, I studies the stoichiometry of several prestin mutations with substantial changes in the membrane potential peak of non-linear capacitance, both hyperpolarizing (C1, D154N) and depolarizing (499, D342Q). Using single-molecule imaging to determine stoichiometry, I found show that each of these four mutations separately reduces the oligomerization state of prestin from the tetramer to the dimer state. Thus the observations suggest that the tetrameric oligomerization of prestin is a requirement for correct function.

Funding
Phillip E. Heflin Auditory Research Fund

PS 828

Presynaptic Mechanisms of Heterogeneous Information Transfer to the Auditory Nerve

Mantas Gabrielaitis[1]; Tobias Moser[2]; Fred Wolf[1]
[1]Max Planck Institute for Dynamics and Self-Organization; [2]University of Goettingen

Background
Spiral ganglion neurons (SGN), which are postsynaptic to inner hair cells (IHC), differ strongly in their responses to sound stimuli. Variable spiking thresholds, dynamic ranges, spontaneous and maximum rates were reported for SGNs innervating the same tonotopic position of the cochlea. This phenomenon is believed to underlie the remarkable ability of the mammalian auditory system to encode sound intensities over many orders of magnitude with a high precision. One of the hypothesis states that the heterogeneity of SGN responses is, at least partially, due to differences in the organization of the presynaptic active zones of the ribbon synapses between IHCs and SGNs. Currently available data on presynaptic heterogeneity, however, has not yet directly quantified its significance for the diverse coding properties of SGNs.

Methods
In this work, we tested the presynaptic hypothesis of the apparent SGN heterogeneity by mathematical modeling. To this end, we constructed a biophysical model of the IHC ribbon synapses which took into account all main aspects of the presynaptic active zone organization relevant to the neurotransmitter release. Among them were presynaptic active zone topography, kinetics of the presynaptic Ca2+ channel gating, dynamics of the presynaptic Ca2+ signals, Ca2+ binding to the Ca2+ sensor of exocytosis and synaptic vesicle replenishment. Phasic response properties of SGNs were described by a refractory counter model. Using this model, we studied steady-state responses of SGNs to pure tone bursts well below the characteristic frequencies, thus avoiding complications arising from the the nonlinearity of the basilar membrane dynamics. Rate-level functions (RLFs) of SGNs were considered as their quantitative response characteristics.

Results and Conclusions
We found that variation of the presynaptic parameters in a reasonable range could quantitatively reproduce measured RLFs from a population of cat SGNs in a detail. The modeling revealed the origin of the well-known tight relations between the spike thresholds, dynamic ranges and spontaneous rates. Our results showed that SGNs with a full range of spike thresholds, as well as other aspects of RLFs, can be hosted by the same IHC. Though, any chosen RLF could be reproduced by different sets of presynaptic parameters. This suggests a possibility of different molecular mechanisms to the presynaptic response heterogeneity. We furthermore found that variation of postsynaptic excitability could in principle contribute to the apparent heterogeneity of SGN responses to sound. However, additional modeling of in vivo spike patterns strongly suggested that this contribution is marginal.

PS 829

Activity-induced ultrastructural changes at wild-type and mutant inner hair cell ribbon synapses

Rituparna Chakrabarti; Susann Michanski; Sangyong Jung; Tobias Moser; Carolin Wichmann
Institute for Auditory Neuroscience and InnerEarLab, University Medical Center Göttingen

Background
The ribbon synapses of the cochlear IHCs transmit acoustic information at hundreds of Hz with temporal precision over long periods of time. This is achieved by high rates of presynaptic exocytosis (Moser and Beutner, 2000). The exocytotic mechanism(s) in IHC ribbon synapse are still poorly understood. It was proposed, that different synaptic vesicle (SV) pools of the ribbon synapses mediate distinct kinetic phases of release (Lenzi and von Gersdorff, 2001). A small population of membrane proximal SVs contribute to the rapid phase of exocytosis (fusion of the readily releasable pool, RRP), while the slower component of exocytosis (sustained release) is mediated by vesicle replenishment, potentially involving ribbon-tethered SVs, and subsequent fusion (Nouvian et al., 2006).

Method
Here we used electron microscopy to study presynaptic vesicle dynamics upon 15 min high K^+ stimulation. We employed high pressure freezing/freeze substitution (HPF/FS) in order to obtain close to native state preservation and fast immobilization of the samples combined with electron tomography for high Z-resolution. Parameters such as size, shape, and number of SVs were analyzed for different activity states (inhibitory and stimulatory). Additionally we studied the tethering of vesicles and provide evidence that tethers are involved in vesicle replenishment.

Important Results
We observed that, ≤80 nm around the ribbon a mesh of short multiple tethers and inter-connectors bring SVs closer to the ribbon upon stimulation potentially allowing SVs to be transported along the ribbon during continued stimulation. Membrane proximal vesicles at the active zone (AZ) mostly displayed single tethers to the membrane, which appeared longer upon stimulation. In addition to IHCs of wild-type mice, we also investigated the role of proteins involved in exocytosis such as rab-3 interacting protein 2α (RIM2α) and otoferlin in tethering. RIM2α single KOs (*RIM2aSKO)* exhibited reduced RRP and sustained exocytosis (Jung et al., 2015), whereas, exocytosis was nearly abolished otoferlin KOs (*Otof*$^{-/-}$) (Roux et al., 2006). *Pachanga* mutants (*Otof*$^{Pga/Pga}$), carrying a missense mutation in C_2F domain of otoferlin, showed impaired replenishment of the RRP (Pangršič et al., 2010). Ultrastructurally, *RIM2αSKO* exhibited a reduced fraction of membrane-tethered SVs, while tether lengths were unaltered (Jung et al., 2015). Deletion of otoferlin led to a loss of short vesicle tethers to the membrane (Vogl et al., 2015). Preliminary data from *Otof*$^{Pga/Pga}$ mutants indicate an altered filamentous meshwork at the base of the ribbon.

Funding
This work has been supported by the Deutsche Forschungsgemeinschaft (DFG) through the Collaborative Research Center 889, project A7, Cellular Mechanisms of Sensory Processing

PS 830

Regulation of Hair-cell Ribbon Synapse by Intracellular Calcium Stores

Hiu-tung Wong[1,2]; Katie Kindt[2]
[1]Johns Hopkins University; [2]NIH

Background
Sensory hair cells rely on specialized ribbon synapses to coordinate as well as facilitate rapid and sustained vesicle release. Calcium plays a critical role in signaling for synaptic vesicle release at the ribbon synapse. Additionally, previous studies have shown that the synaptic ribbon structure is sensitive to local calcium concentration during a critical period of development. While the majority of calcium influx is though the L-type calcium channel cav1.3, several sources of calcium including endoplasmic reticulum (ER) and mitochondria may actively modulate calcium concentration to modulate hair cell function, as well as synapse development. We aim to investigate how organeller calcium stores regulate ribbon synapse formation and function in order to produce rapid and sustained release at the sensory hair cell syanpse

Methods
To study the effects of calcium stores on ribbon synapse development, we examined hair cells in the zebra fish lateral line. Lateral line hair cells in the superficial neuromast organ resemble mammalian vestibular hair cells in structure and are easy to access for pharmacology, stimulation and visualization. Our work utilizes transgenic zebra fish lines that express mitochondria or ER targeted, fluorescent calcium sensors to visualize calcium dynamics in hair cells. In addition, our work uses pharmacology to disrupt ER-mitochondrial calcium cycling in the developing hair cells, and immunofluorescence staining of the synaptic ribbon

Results
Our preliminary findings on organellar calcium stores are twofold. (1) We have found that in response to mechanical stimulation of the hair bundle, there is heightened mitochondrial calcium import. Mitochondrial import occurs at the basal end of hair cells, near synaptic ribbons. (2) Pharmacological inhibition of mitochondrial or ER calcium uptake in developing hair cells causes an overall increase in synaptic ribbon morphology. This was observed as an increase in Ribeye protein, the main constituent of the synaptic ribbon. This result is consistent with previous findings that calcium influx, mediated by the ribbon-associated calcium channel $Ca_v1.3$, can influence synaptic ribbon development.

Conclusion
The results from this study demonstrate that mitochondrial calcium stores are active when hair cells are mechanically activated, at sites near ribbon synapses. In addition our results indicate that organeller calcium stores play a role in fine tuning synaptic ribbon morphology during hair-cell development. The functional significance and mechanism underlying these phenomena remains unclear.

Funding
NIDCD

PS 831

NRF2 is a target for prevention of noise-induced hearing loss by reducing Oxidative damage of cochlea.

Yonei Honkura[1]; Tetsuaki Kawase[1]; Yukio Katori[1]; Hozumi Motohashi[2]
[1]Tohoku University Graduate School of Medicine; [2]Tohoku University, Development, Aging and Cancer

Background
One of the major mechanisms of high intensity noise-induced hearing loss (NIHL) has been considered as an increase of oxidative stress in cochlea based on the observation that the cochlear blood circulation is impaired during noise exposure. Thus, the noise exposure experiment is a model of cochlear ischemia-reperfusion injury.

A transcription factor NRF2 is a master regulator of numerous detoxifying and antioxidant genes in response to oxidative and electrophilic stresses. NRF2 is constantly ubiquitinated by KEAP1, resulting in the rapid degradation of NRF2. In the activated condition, stabilized NRF2 is translocated into the nucleus, bind to antioxidant/ electrophile response elements, and activates the transcription of cytoprotective genes encoding detoxification enzymes (e.g., NAD(P)H dehydrogenase quinine 1 [Nqo1]), antioxidant enzymes (e.g., heme oxygenase-1 [Ho-1] and thioredoxin reductase 1 [Txnrd1]), and enzymes for glutathione synthesis (e.g., glutamate-cysteine ligase, catalytic subunit [Gclc] and glutamate-cysteine ligase, modifier subunit [Gclm]). Although

previous studies showed that NRF2 contributes to the protection from oxidative stress in various organs, NRF2 funcion in the cochlea has not been clarified. 2-cyano-3,12 dioxooleana-1,9 dien-28-imidazolide (CDDO-Im) is a potent inducer of NRF2. Pretreatment with CDDO-im has been shown protective from inflammatory insults and chemical toxicity in other organs. However, the protective effect of CDDO-Im in cochlea has not been tested.

Method
To elucidate whether NRF2 protects inner ear against oxidative stress, we performed noise exposure experiments and CDDO-Im administration experiments, using wild type mice and *Nrf2*$^{-/-}$ mice, by ABR, RT-PCR, 4-HNE immunohistochemistry, immunoblotting, and metabolome analysis.

Results
We demonstrated that CDDO-Im protects inner ear against oxidative stress induced by noise exposure in an NRF2-dependent manner.

Conclusion
High NRF2 activity is beneficial for cochlear protection from noise- induced injury and suggested that NRF2 is a target for the prevention of NIHL.

Funding
JSPS KAKENHI grant number 24390075 MEXT KAKENHI grant number 23116002 Takeda Scientific Foundation

PS 832

The protective effects of sildenafil on neuroprotection and cognitive dysfunction in noise-induced stress

Huerxidan Sikandaner; Min Jung Kim; So Young Park; Dong Won Yang; Shi Nae Park
College of Medicine, The Catholic University of Korea

Background
The cognitive effects of stress are known to be profound. Noise exposure has been well characterized as an environmental stressor, and auditory and non - auditory effects of noise have been well established. Sidenafil, an inhibitor of phosphodiesterase (PDE5) affects signaling by elevating cGMP, which is the second messenger involved in the process of neuroplasticity. In the present study, the effect of sildenafil on cognitive function and neuroprotection in noise-induced and memory-related behavior alterations were investigated.

Subjects and Methods
Mice were exposed to noise for 4 hours every day up to 14 days at 110dB SPL. Mice were divided into four groups; control, sildenafil only, noise only, and noise with sildenafil. The control mice received saline and test mice received sildenafil (15 mg/kg) orally 30 minutes before noise exposure. All mice were age-matched. Behavioral assessments were performed using novel object recognition (NOR) test and radial-arm maize (RAM) test. Similarly, the stress levels and cognitive dysfunction were analyzed through western blot, flow cytometry using single-cell suspension of hippocampus, or immunohistochemistry of whole brain and cochlea. Hearing levels were also tested before and after noise exposure using auditory brainstem response.

Results
Sildenafil treatment reduced the cognitive dysfunction caused by noise exposure. NOR test showed that discrimination index and the time spent on novel object increased in sildenafil treated mice compared with noise-exposed group. However, in RAM test, there were no differences of trends in learning curves for all parameters among all groups; total trial time, working memory error, reference memory error, and correct entry ratio. Flow cytometry analysis of single-cell suspensions of hippocampus showed increased BDNF expression and decreased Hsp70 and P-tau levels in sildenafil group compared with noise-exposed group. Our data suggest that sildenafil has protective effect in mouse brain against noise-induced stresses.

Conclusion and implications
Mice exposed to noise exhibited hippocampus-dependent memory deficits, whereas sildenafil-treated mice showed suppressed cognitive dysfunction along with the decrease in 'tau' phosphorylation, Hsp70 expression, and BDNF down-regulation. Our data further strengthen the potential effects of sildenafil as the therapeutic agent for cognitive dysfunction.

Funding
Hanmi Pharmaceutical Co., Ltd.(5-2014-D0259-00004)

PS 833

Noise and Stress: Evaluation of stress in blood, cochlea and brain in the animal model of noise induced hearing loss

Sang Gyun Jin; Min Jung Kim; Shi Nae Park; So Young Park; Ji Sun Kong; Sang Won Yeo
College of Medicine, The Catholic University of Korea

Objective
Noise is known as a living environmental stimulator which can induce not only hearing problem due to damage of the cochlea but also elevation of stress responses in the body. In the present study, we tried to prove our hypothesis that acute noise stress induces changes of stress hormones in the blood as well as hearing alteration.

Materials and Methods
Male C57BL/6 mice aged 1 month were used. Experimental mice were exposed to 110 dB sound pressure level of white noise for 60 minutes. Hearing levels, architecture of the organ of Corti (OC), and the levels of representative stress hormones (NE and 5-HIAA) in the serum were compared between the experimental and control groups by various morphological and molecular biologic methods.

Results
The noise-exposed mice showed higher levels of ABR threshold shifts at all test stimuli and decreased DPOAE responses at almost all test frequency regions. OC degeneration by light microscopy was extensive in the noise

exposed group compared to controls. Post-noise serum levels of NE measured by high-performance liquid chromatography (HPLC) demonstrated no significant differences between the groups. Mean value of serum 5-HIAA of the noise exposed group was lower than that of controls.

Conclusion
Noise induced OHC dysfunction and damage of the OC, while serum concentrations of the hormones were not changed significantly. Further study is needed with different protocols to investigate the relationship between noise stress and the expression of blood stress hormones as well as their potential diagnostic roles as stress markers after noise exposure.

PS 834

Age-related hearing loss in TrpV1 knockout mice

Hongzhe Li; Anastasiya Johnson; Meiyan Jiang; Peter Steyger
Oregon Health & Science University

Background
Several transient receptor potential (TRP) channels including TRPV1 are located on hair cell membranes. The gating mechanisms of these channels are associated with cellular stress, inflammation, and cytoplasmic uptake of aminoglycosides. Thus, TRPV1 channel may serve as a functional target that links acoustic trauma and enhanced aminoglycoside trafficking. TrpV1 mutant mice have no apparent hearing loss as young adults. Here, we assessed the hearing sensitivity of TrpV1 mutant mice compared to their littermate controls as they age.

Methods
TrpV1 mutant mice (B6.129X1-Trpv1^{tm1Jul}/J, stock #3770) were crossed with C57Bl/6 (JAX stock #0664) to generate F1 offspring, and then backcrossed with the initial TrpV1 mutant mice to generate experimental animals. Animals were housed in a Specific Pathogen Free-modified room, without further treatment, at ambient noise. Auditory brainstem responses to a broad frequency range, from 4 to 48 kHz, were measured at multiple age points, including week 7, 11 and 18. Cochlear and kidney tissues were collected to confirm that the presence or absence of TRPV1 expression, using immunofluorescence.

Results
At 7 weeks of age, the auditory sensitivity in TrpV1 mutant mice was comparable to their heterozygous littermates. By 11 weeks of age, mutant TrpV1 mice exhibited evident high frequency hearing loss, with 30-to-40 dB elevated thresholds between 24-48 kHz, compared to littermate controls. At 18 weeks of age, high frequency hearing sensitivity worsened in both groups of mice, and this age-related progressive hearing loss was further expedited in TrpV1 mutant mice compared to littermate controls.

Conclusions
TRPV1 channels unlikely play any pivotal role during auditory development, manifested by normal hearing sensitivity in juvenile TrpV1 mutant mice. Mice with a B6 background typically begin exhibiting age-related hearing loss around 12 weeks of age in this strain. This early onset of hearing loss is expedited in mutant TrpV1 mice. Further research is required to determine the otoprotective role of TRPV1 channel in maintaining auditory sensitivity as mice age, and whether TrpV1 functionality exacerbates aminoglycoside-induced ototoxicity.

Funding
Funded by R01 DC012588 (PSS) and W81XWH1410006 (HL).

PS 835

Lack of PEX5 gene induces hearing impairment

Jae-Young Lim[1]; Joon No Lee[1]; Min Soo Kim[1]; Jinwoong Bok[2]; Soo Kyung Koo[3]; Se-Jin Kim[1]; Myriam Baes[4]; Seong-Kyu Choe[1]; **Raekil Park**[1]
[1]Wonkwang University; [2]Yonsei University; [3]Korea National Institute of Health; [4]KU Leuven

Peroxisomes are subcellular organelles that are involved in various metabolic reactions, including fatty acid oxidation, bile acid synthesis, plasmalogen biosynthesis, and detoxification of reactive oxygen species. Mutations in genes involved in peroxisome biogenesis or peroxisomal function cause inheritable genetic disorders. Notably, a sensory deafness has been known as one of the clinical symptoms associated with peroxisome defects, such as Zellweger syndrome, infantile Refsum disease, acyl-CoA Oxidase deficiency and D-bifunctional protein deficiency. However, the mechanism of hearing loss caused by peroxisome dysfunction is unclear. Since Pex5 plays an important role in peroxisome biogenesis and its function, we generated cochlea-specific PEX5 knockout (KO) mice to test the role of peroxisomes in auditory system. We find that PEX5 deficiency in cochlea causes hearing loss by measuring auditory brainstem response, though overall morphology of inner ear seems normal. The results from Scanning electron microscopy demonstrates that kinocilium is mispositioned in outer hair cells and stereocilia bundles in outer and inner hair cells abnormal, which in turn may be tightly linked to a severely damaged mechanotransduction activity of hair cells in Pex5-deficient cochlea. Interestingly, we also find neurite degeneration in spiral ganglion neurons of Pex5 KO mice, probably due to dysfunctional neuronal activities. Finally, reduction of peroxisome number and diffused staining of Catalase in PEX5 KO mice are consistent with the proposed role of Pex5. All together, our results suggests that there might be tight relationship between peroxisomes and hearing function.

Funding
This work was supported by the National Research Foundation of Korea [NRF] grants funded by theKorea government MEST No. 2014M3A9D8034463 and No. 2011-0030130.

PS 836

Combination of SLOT and Immunohistochemistry to Define Complex Morphological Phenotype Changes in Cochlear Structures, Exemplary Shown on Cav1.3 Knock-Out Mice

Jennifer Schulze[1]; Lena Nolte[2]; Stefan Lyutenski[1]; Nadine Tinne[2]; Tammo Ripken[2]; Marc Willaredt[3]; Hans Gerd Nothwang[3]; Thomas Lenarz[1]; Athanasia Warnecke[1]
[1]Hannover Medical School; [2]Laser Zentrum Hannover e.V.; [3]Carl von Ossietzky University Oldenburg

Overview

The present study focuses on the identification of morphological differences of $Ca_v1.3$ knock-out mice in comparison to wild type mice by application of different methods. $Ca_v1.3$ knock-out mice lack the voltage-gated L-type Ca^{2+} channels $Ca_v1.3$. This channel controls vesicle fusion and subsequent neurotransmitter release from cochlear inner hair cells to afferent auditory nerve fibers. $Ca_v1.3$ knock-out mice display a developmental failure of cochlear structures. This study aimed at the characterization of early and late stage of the degenerative process in the inner ear in order to identify suitable time-point for therapeutic interventions concerning preservation of hair cell function and regeneration of the auditory nerve.

Methods

Wild type mice and knock-out mice were used for the isolation of the cochleae and fixed by immersion of PFA (4%). For immunocytochemistry, the cochleae were dissected into basal, medial and apical sections and these were stained with CtBP2, Otoferlin and DAPI for counting the number of synaptic ribbons per inner hair cell. For scanning laser optical tomography (SLOT), decalcification, dehydration, optical clearing and antibody staining of the whole cochlea were performed. For visualization of myelinated nerve fibers, the cochleae were stained with osmium.

Results

Coupling of SLOT and immunocytochemistry allowed the overview of whole cochleae to show specific anatomical structures and selective mapping of cellular structures (hair cells and afferent nerve fibers respectively). Accordingly, the number of synaptic ribbons in the $Ca_v1.3$ knock-out mice is decreased along the different cochlear turns compared to wild type mice as shown previously. The decrease starts around postnatal day (P) 9 in the basal and medial turn of the cochlea and around P20 in the apical turn. A slightly reduced myelination and density of afferent auditory fibers was shown by osmium staining of the cochlea at P18

Conclusions

This study reveals that SLOT is a suitable tool in the field of otology for *in toto* visualization of the internal structure of the cochlea. By means of the different methods, we showed that the degenerative processes start as early as P9 in the basal and medial turn of the cochleae of $Ca_v1.3$ knock-out mice and proceed to the apical turn at about P20.

Funding

Cluster of Excellence “Hearing4all”

PS 837

Influence of a Mitotic Inhibitor on Neurons and Cell Ratio of the Spiral Ganglion Neuron Culture In Vitro

Jana Schwieger[1]; Karl-Heinz Esser[2]; Thomas Lenarz[1]; Verena Scheper[1]
[1]Hannover Medical School; [2]University of Veterinary Medicine Hannover Foundation

Background

Sensorineural deafness is mainly caused by damage of hair cells followed by degeneration of the spiral ganglion neurons (SGN). Cochlear implants (CI) can replace the function of lost hair cells and stimulate the SGN electrically. The benefit of the CI depends on the number and excitability of the SGN. Current research focuses on the identification of potential drugs for treatment of SGN. Therefore, *in vitro* tests are performed on spiral ganglion cells (SGC), including all kinds of cell types located in the Rosenthal’s canal.

One difficulty with these *in vitro* cultures is long-term cultivation, due to overgrowth of the SGN by non-neuronal cells. Another issue is the influence of these non-neuronal cells on neuroprotection and neuritogenesis in culture, which affects the evaluation of a direct effect on neurons by tested factors. A mitotic inhibitor such as Cytarabine (AraC) may reduce growth of dividing cells, addressing these issues. We investigated if AraC treatment allows for increased cultivation time of SGN without affecting the neuronal vitality.

Methods

Dissociated SGC from neonatal rats were cultivated for 4 and 7 days with and without AraC and addition of fetal calf serum (FCS) or neurotrophic growth factors (NTF; brain-derived neurotrophic factor (BDNF) and neurotrophin 3 (NT3)). By immunocytochemistry the different cell types of the SGC culture were identified. We analyzed the number of all cultivated cells, the number of SGN, and the ratio of neurons related to the plated cell population. Additionally the neurite outgrowth and soma diameter were observed to evaluate the effect of the inhibitor on SGN vitality.

Results

The total cell number in culture was significantly reduced in all conditions after 7 days of cultivation with AraC while the proportion of neurons was significantly increased, especially with addition of NTF. There was no significant difference in the number of neurons after 4 and 7 days of cultivation when adding AraC and the effect of the NTF was not significantly reduced. Neurite length and soma diameter of the analyzed neurons was not significantly affected by AraC treatment. The ICC showed a nearly complete removal of fibroblasts and an effective reduction of glial cells.

Conclusion

The addition of AraC is an effective tool to reduce the non-neuronal cell population and raise the number of SGN in

SGC culture, without negative effects on the neurons. AraC allows for long-term cultivation of SGN and for investigation of drug effects on SGN with reduced glial support.

Funding
This project is funded by the EC project NeuEar: "Neurotrophic Cochlear Implant for Severe Hearing Loss" and the German Research Foundation project "Development of an implant-linked alginate matrix for cell-mediated neuronal protection".

PS 838

Investigating the Route of Entry of Cisplatin into Mouse Cochlear Hair Cells

Sian Kitcher; Nerissa Kirkwood; Molly O'Reilly; Emma Kenyon; Alaa Abdul-Sada; John Spencer; Guy Richardson; Kros Corné
University of Sussex

Background
Cisplatin is a very effective cytostatic agent used in the treatment of many forms of cancer, however a degree of permanent hearing loss has been reported in the majority of treated patients. Although cisplatin has been shown to selectively damage the sensory hair cells of the cochlea, its route of entry into these cells has been the subject of much debate, with one suggested pathway being through the mechanoelectrical transducer (MET) channels.

Methods
To investigate this question we have recorded MET currents from mouse outer hair cells (OHCs), both before and during cisplatin exposure, using the whole-cell configuration of the patch clamp technique. Bundle stimulation was achieved using a fluid jet driven by a piezoelectric disc. Alongside this, we have explored the morphological effects of cisplatin on organotypic cochlear cultures prepared from wild type (CD-1) mice and *Myo7a*^{6J} mice with a myosin 7a deficiency that compromises MET channel function.

Results
Our preliminary electrophysiological data suggested that cisplatin was a permeant blocker of the hair cell MET channel. Further investigations, however, revealed that the majority of cisplatin preparations tested (including powder forms from several different sources as well as clinical grade cisplatin in solution) have no effect on the MET currents even at millimolar concentrations. Nonetheless, we have identified a related platinum (II) complex, tetraammineplatinum (II) chloride, that does show a voltage dependent block of the MET currents. In contrast, our investigations with organotypic cochlear cultures have revealed that most preparations, in addition to being globally cytotoxic, have a specific effect on hair-cell morphology within 24 hours that is not seen in cultures prepared from homozygous *Myo7a*^{6J} mutants.

Conclusions
Although homozygous *Myo7a*^{6J} hair cells failed to react morphologically in the same way as heterozygous *Myo7a*^{6J} or wild type CD1 hair cells in response to prolonged exposure to cisplatin, the drug does not appear to interact directly with the MET channels. This raises the possibility that a compound related to cisplatin or a decomposition product may be responsible for the damage to these cells. Further experiments with certain platinum complexes will be carried out in an attempt to identify the mechanisms of cisplatin ototoxicity.

Funding
Supported by Action on Hearing Loss and the MRC

PS 839

Mechanism of Protective Effect of Low Level Laser on HEI-OC1 cells after Gentamicin-induced Ototoxicity

So-Young Chang; Chung-Ku Rhee; Phil-Sang Chung; **Jae Yun Jung**
Dankook University

Background
Recently low level laser (LLL) irradiation has been showing its possible therapeutic role in cochlear hair cells using animal models. Mechanism study encompassing from ATL production level to the caspase activity are necessary for further clinical usage. We investigated adenosine triphosphate (ATP) production, nitric oxide (NO), reactive oxygen species (ROS) production and apoptosis related proteins after aminoglycoside administration both in no LLL and LLL condition

Methods
The HEI-OC1 cells used in this study were maintained in DMEM with 10 % FBS at 33℃ under 5 % CO_2 in air. The cells ($2.5X10^3$ cells/well) were incubated with two fold diluted gentamicin (GM, Sigma, US) for 24 h, and the dose -dependent effects of GM were measured using a MTT assay. Based on MTT assay results as a function of GM concentration, two different concentrations (6.6 and 13.1mM) were chosen for further analysis to see the effects of LLL irradiation on ototoxicity with given concentration. The ATP assay, NO and ROS production in HEI-OC1 cells were measured immediately, 1 hour and 2 hours after laser irradiation. Bcl2, BAX, p-JNK and caspase-3 were measured using western blot.

Results
GM treatment showed decreased ATP production in a dose dependent manner. But laser irradiation restored ATP level in GM damaged cells up to as same level as control. GM resulted in ROS increase in dose dependent manner. But ROS decreased dramatically with LLL even in higher GM concentration. BAX, p-JNK and caspase-3 showed elevated protein level after GM treatment. LLL showed decreased BAX, p-JNK and caspase 3.

Conclusion
GM treatment decreases cell survival and ATP synthesis in auditory hair cell line. LLL irradiation facilitates hair cell survival after gentamicin damage in vitro. This rescue seems to be achieved by increasing ATP productions and reducing ROS generations and anti-apoptotic mechanism.

Funding
This research was supported by Leading Foreign Research Institute Recruitment Program through the National Research Foundation of Korea (NRF) funded by the Ministry of Education, Science and Technology (MEST) (2012K1A4A3053142).

PS 840

Noise-induced hearing loss due to pejvakin defect: from pathogenesis to treatment

Sedigheh Delmaghani[1]; Jean Defourny[1]; Asadollah Aghaie[2]; Maryline Beurg[3]; Didier Dulon[3]; Nicolas Thelen[4]; Isabelle Perfettini[1]; Tibor Zelles[5]; Anais Meyer[1]; Alice Emptoz[1]; Marc Thiry[4]; Saaid Safieddine[1]; Jean-Pierre Hardelin[1]; Paul Avan[6]; Christine Petit[1]
[1]Institut Pasteur; [2]Institut de la Vision; [3]Université de Bordeaux, Neurosciences Institute; [4]University of Liege; [5]Hungarian Academy of Sciences; [6]Laboratoire de Biophysique Sensorielle, Université d'Auvergne

Mutations of *PJVK*, which encodes pejvakin, a protein of unknown function present only in vertebrates, cause the DFNB59 recessive form of sensorineural hearing impairment. In the first patients described, the impairment was restricted to neurons of the auditory pathway, as demonstrated by the combination of abnormal auditory brainstem responses (ABRs) with decreased wave amplitudes and increased inter-wave latencies. However, some DFNB59 patients were found to have a cochlear dysfunction, as shown by an absence of the otoacoustic emissions (OAEs). These patients had truncating mutations of *PJVK*, whereas the previously identified patients had missense mutations (p.T54I or p.R183W). However, the identification of patients also carrying the p.R183W missense mutation but lacking OAEs refuted any straightforward connection between the nature of the *PJVK* mutation and the hearing phenotype. The severity of deafness in DFNB59 patients varies from moderate to profound, and may even be progressive in some patients, suggesting that extrinsic factors may influence the hearing phenotype.

We investigated the role of pejvakin, with the aim of determining the origin of the phenotypic variability of the DFNB59 form of deafness. Our study of *Pjvk* knockout mouse models and of patients revealed an unprecedented hypervulnerability of auditory hair cells and neurons to sound-exposure, accounting for phenotypic variability. We found that pejvakin is a peroxisome-associated protein involved in the oxidative stress-induced proliferation of this organelle. Pejvakin-deficient mice revealed the key role of peroxisomes in the redox homeostasis of the auditory system and in the protection against noise-induced hearing loss.

Funding
This study was supported by grants from Louis-Jeantet Foundation, ANR – NKTH "HearDeafTreat" 2010-INTB-1402-01, Humanis Novalis-Taitbout, Réunica-Prévoyance, BNP Paribas, and French state program ''Investissements d'Avenir'' (ANR-10-LABX-65).

PS 841

D-Tubocurarine is a Permeant Blocker of the Hair Cell's Mechano-Electrical Transducer (MET) Channel

Molly O'Reilly; Nerissa Kirkwood; Marco Derudas; Emma Kenyon; Sian Kitcher; Simon Ward; Guy Richardson; Corné Kros
University of Sussex

Background
Aminoglycoside antibiotics (AGs) provide an effective treatment against serious bacterial infections including tuberculosis and septicaemia. Alongside their therapeutic actions, however, these compounds are ototoxic. They enter the hair cells of the inner ear via the mechano-electrical transducer (MET) channels and once inside the cell trigger mitochondrial dysfunction and the initiation of the apoptotic cascade. Here we investigate d-tubocurarine (d-TC), a compound that acts as an otoprotectant *in vitro* by competing for entry through the MET channel (Alharazneh *et al*., 2011 PLoS One 6:e22347).

Methods
In order to assess the protective capacity of d-TC we tested the compound in two model assays: 1) a 1 hour zebra fish assay to assess whether d-TC protected against neomycin-induced death of hair cells pre-loaded with the fluorescent marker YO-PRO-1 in the lateral line system and 2) a 48 hour cochlear assay – simultaneously applying gentamicin together with various concentrations of d-TC, to establish a dose-response relationship. Furthermore we carried out electrophysiological recordings to establish the interaction of d-TC and several related compounds with the MET channel, by observing the effect of these compounds on the MET currents.

Results
Our results confirmed the protective efficacy of d-TC both in the zebra fish and cochlear culture assays. In the zebra fish assay complete protection against 6.25 μM neomycin was seen at d-TC concentrations above 12.5 μM. In the cochlear cultures d-TC was found to be protective against 5 μM gentamicin at concentrations of 25 μM and above. Electrophysiological recordings revealed that d-TC acts as an open channel blocker, rapidly and reversibly blocking the MET channel with a half-blocking concentration of 2.2 μM in the presence of 1.3 mM Ca^{2+} at -104 mV. Interestingly, we found that the block was released at extreme hyperpolarised potentials, indicative of d-TC being a permeant blocker of the MET channel. Of the five related compounds tested, two were highly toxic at 50 μM, one showed no block of the channel at 100 μM and the remaining two behaved as permeant blockers of the MET channel, similar to d-TC.

Conclusions
In this study we have demonstrated that d-TC, a previously reported non-permeant blocker of the MET channel, does in fact act as a permeant blocker. To act as an effective otoprotectant ideally we require a high-affinity, non-permeant blocker of the MET channel, so this provides the first step towards synthesising a suitable compound.

Funding
Supported by the MRC

PS 842

Effect of Novel Peptide Vaccine GV1001 on Aminoglycoside-Furosemide Ototoxicity Model

Shin Hye Kim; So Young Kim; Gaon Jung; Jae-Jin Song; Byung Yoon Choi; Ja-Won Koo
Seoul National University Bundang Hospital

Background
Cell penetrating peptide GV1001 has been under investigating as an anticancer agent. It derived from the active site of the human telomerase reverse transcriptase. Recently, it has also demonstrated antioxidant and anti-inflammatory effects during clinical trial. In this study, we tested if GV1001 shows rescue effect on hearing in aminoglycoside-furosemide ototoxicity mouse model.

Methods
The ototoxicity mouse model (C57BL/6, female, 5 weeks, 15-25 g) was made by intraperitoneal injection of kanamycin (1000 mg/kg) followed by furosemide (100 mg/kg) in 30 minutes. Twenty-four mice were divided into 3 groups: GV1001 group, dexamethasone group, saline group. GV1001 (10 mg/kg) was subcutaneously administered at 1, 2, and, 3 days after intraperitoneal injection of kanamycin and furosemide. Hearing thresholds were measured at 8, 16, 32 kHz before injection, at day 7 and at day 14. Cochlea was harvested and imaged with confocal Laser scanning microscopy to analyze hair cell damage. Intact hair cell proportion was defined as intact hair cell count/total hair cell count (%). Hearing thresholds and hair cell damage of GV1001 group were compared with those of dexamethasone (15 mg/kg) and saline groups. For the statistical analysis, ANOVA test performed to compare the continuous variable among the GV1001, saline, dexamethasone groups; the p-values less than 0.05 were considered significant.

Results
GV1001 treated mice showed lower mean hearing thresholds (8kHz: 56dB, 16kHz: 54dB, 32kHz: 65dB) than those of dexamethasone (8kHz: 70dB, 16kHz: 69dB, 32kHz: 75dB) or saline groups (8kHz: 89dB, 16kHz: 94dB, 32kHz: 98dB) at day 14 with statistically significance on high frequency (between saline and GV1001, p=0.051 on 16 kHz, p=0.040 on 32kHz). GV1001 treated mice showed higher intact hair cell proportions (apex: 65%, middle: 62%, base: 61%) than those of dexamethasone (apex: 39%, middle: 41%, base: 40%) or saline groups (apex: 11%, middle: 0%, base: 0%) with statistically significance on middle and basal turn of cochlea (between saline and GV1001, p=0.022 on middle, p=0.023 on base).

Conclusions
GV1001 showed fewer threshold shifts with less hair cell damage than dexamethasone and saline control in kanamycin-furosemide ototoxicity mouse model when it was given 1 day after kanamycin-furosemide treatment.

Funding
Basic Science Research Program through the National Research Foundation of Korea funded by the Ministry of Education (Grant 2011-0010166)

PS 843

Differential Effects of Four Pharmaceutical Interventions for Noise Induced Hearing Loss

Yan Yu; **Megan Kobel**; Bing Hu; Hui Li; Jianxin Bao
Northeast Ohio Medical University

Background
Noise-induced hearing loss is the most common cause of hearing loss worldwide and poses a large financial and psychosocial burden. While promising otoprotective agents, mainly based on modulating oxidation signaling, are in preclinical studies, no FDA approved drugs exist for NIHL. Currently, one effective way in clinical trials of otoprotective agents is to test NIHL protection from an exposure inducing only temporary threshold shift (TTS). Its underlying assumption is that this protection will translate to noise exposures inducing a permanent threshold shift (PTS). The relationship between TTS and PTS has been a topic of study for many years, but recent studies discovering long-term synaptic damage after low-level noise exposure emphasizes the importance of examining this relationship. In this study, we set to determine whether there are any correlations between protection of TTS and PTS by otoprotective agents targeting identified major signaling pathways underlying NIHL.

Methods
Ten groups of two-month old CBA/CaJ mice were used in this study: two noise exposure x five drug treatment groups. Two noise models were established: one inducing a large PTS (110 dB SPL, 4-25 kHz, 30 min), and the other inducing a pure TTS (90 dB SPL, 4-25 kHz, 2 h) without synapse damage. Animals were administered saline, zonisamide, ebselen, methylprednisolone, or tetrandrine through intraperitoneal injection before noise exposure. Dosages were determined through our previous studies or through pilot studies. ABR thresholds, wave I amplitude, and DPOAEs were measured before exposure and 1-2 hours, 24 hours, and 2 weeks post-exposure.

Results
No clear correlation between TTS and PTS were found among the four different otoprotective agents. For zonisamide, protection for both TTS and PTS was observed but no DPOAE protection was detected for either noise exposure. For tetrandrine, protection of TTS, PTS and DPOAEs for both noise exposures was seen. For methylprednisolone, protection of PTS was not detected, but protection of TTS as well as DPOAE amplitude was seen in both noise exposure models. Preliminary testing of ebselen showed significant PTS protection and TTS studies are being completed.

Conclusion
This study demonstrates that protection against a noise exposure inducing TTS does not always correlate to PTS protection. Due to the popularity of the TTS only model for

clinical development of otoprotective agents, our studies strongly suggest the importance of other models with PTS for future clinical studies in this field.

PS 844

Co-Localization of WDR1 and Actin in HEI-OC1 Cells

Henry J. Adler[1]; Meiyan Jiang[2]; Peter S. Steyger[2]
[1]State University of New York at Buffalo; [2]Oregon Health & Science University

Background

WD40 repeat protein-1 (WDR1) interacts with actin and its binding partners in several cell types, including healthy and challenged auditory hair cells in birds and mammals. These interactions could provide insight into the mechanisms of inner ear protection, cellular repair and/or immunological responses to stress. Previously, we reported a compact region of WDR1 expression, adjacent to the nucleus of COS7 cells that is co-localized with the Golgi body.

Since COS7 cells lack epithelial polarity, potentially obscuring the role of WDR1 in stress response to cytotoxic drug treatment *in vitro*, we chose differentiated HEI-OC1 cells because of their structural similarity to inner ear supporting cells. We tested the hypothesis that a distinct region of WDR1 expression is localized adjacent to the nucleus of HEI-OC1 cells, and that actin is co-localized with WDR1 expression.

Method

HEI-OC1 cells were differentiated for two weeks at 39°C with 10% CO_2, prior to exposure to 5 or 10 µM gentamicin for 1 hr at 22°C, and subsequent recovery in drug-free media for 0, 1, 3, or 6 hours at 39°C before fixation. The cells were subjected to WDR1 immunofluorescence and phalloidin labeling followed by confocal microscopy.

Results

HEI-OC1 cells generally exhibited distinct, compact regions of WDR1 expression adjacent to their nuclei as well as weaker, diffuse WDR1 immunofluorescence throughout the cytoplasm. Phalloidin labeling revealed filamentous actin localization at the cellular periphery. Interestingly, a cluster of short actin filaments is present within the compact region of WDR1 expression in ~50% of control cells. Immediately after gentamicin treatment, the percent of cells expressing these short actin filaments within the distinct region of WDR1 expression dropped to ~30%, before increasing during the recovery period to being present in as many as 86% of treated cells. The higher gentamicin concentration reduced the prevalence of these short actin filaments.

Conclusion

The presence of a distinct, compact region of WDR1 expression next to the nucleus of HEI-OC1 cells is similar to that in COS7 cells. Further studies to analyze the relationship between WDR1 and several organelles are needed to determine if WDR1 expression is associated with Golgi bodies in HEI-OC1 cells. The localization of short actin filaments to compact regions of WDR1 expression in HEI-OC1 cells provides further insight to the potential contributions of WDR1 to actin remodeling in normal and stressed cells.

Funding

Funded by NIH-NIDCD grants R01 DC04555 (PSS) and P30 DC05983 (OHSU)

PS 845

Targeted Depletion of MAPK1, Using siRNA-loaded Nanoparticles, Protects Auditory Cells Against Cisplatin-Induced Cytotoxicity

Ibrahima Youm; Matthew West; Xiaoping Du; Richard Kopke
Hough Ear Institute

Background

Ototoxicity represents a major adverse side-effect of the widely-used anticancer drug, cis-diamminedichloroplatinum-II (cisplatin, CDDP). While many signaling pathways have been implicated in the pathophysiology of cisplatin-induced ototoxicity, the mitogen-activated protein kinase (MAPK) pathway is thought to play a central role in potentiating the apoptotic effect of cisplatin on cochlear hair cell loss. The objective of this work was to test the effect of targeted knockdown of MAPK1 (ERK2) on enhancing the viability of inner ear cells exposed to toxic levels of CDDP, using small interfering RNAs (siRNAs).

Methods

Cochlear cell lines (IMO-2B1 and HEI-OC1) were pre-incubated with or without escalating doses of MAPK1 siRNA transfection complexes prior to exposure to an ototoxic dose of CDDP (25µM). The protective effect of targeted knockdown of MAPK1 siRNA on CDDP-induced cytotoxicity was then evaluated, using standard cell viability assays. To enhance the potential clinical utility and *in vivo* stability of these small inhibitory molecules, *siMAPK1* was encapsulated within poly(lactide-co-glycolic acid) (PLGA) nanoparticles (NPs), which are non-toxic to inner ear tissues at high concentrations. Cytotoxicity and cellular uptake profiling were conducted with these NP formulations, and the therapeutic efficacy of the *siMAPK1* NPs against CDDP-induced cytotoxicity was evaluated.

Results

Prophylactic depletion of MAPK1 with lipofection-mediated transfection of target-specific siRNAs resulted in marked protection of auditory cell lines against CDDP-induced apoptosis. Encapsulation of *siMAPK1* within clinically-safe PLGA-based NPs resulted in a formulation that exhibited significant, dose-dependent protection of auditory cell lines against cisplatin exposure. These PLGA NPs were validated as non-toxic and were shown to be taken up by auditory cells through a multi-faceted regime, including receptor mediated endocytosis. Ongoing experimentation to validate the efficacy of this therapeutic agent in organotypic cultures is currently underway.

Conclusions
Targeted, local RNAi-mediated depletion of the key cell signaling factor, MAPK1, using a non-toxic PLGA NP formulation, may represent a promising therapeutic strategy for limiting the ototoxic side-effects associated with the systemic administration of cisplatin, thus enhancing the positive clinical attributes of this antineoplastic agent.

PS 846

Effect of Noise Trauma to an Implanted Cochlea with Residual Hearing

Adrien Eshraghi; Jonathan Roell; Ayca Baskadem Yilmazir; Jorge Bohorquez; Rasim Yilmazer; Carolyn Garnham; Mateo Guardiolla; Jeenu Mittal
University of Miami

Background
Delayed loss of residual hearing post cochlear implantation remains a major concern still completely not understood for patients implanted with an electro-acoustic or hybrid cochlear implant device. Noise trauma can cause mechanical and metabolic damages within the inner ear. One hypothesis is that the cochlear implant patients may be more vulnerable to noise-induced trauma thereby losing the residual hearing post high intensity sound exposure. The objective of this study is to assess the effect of noise trauma to an implanted cochlea with residual hearing and evaluate the effects of a dexamethasone-eluting electrode for prevention of loss of residual hearing post noise trauma.

Methods
Young adult guinea pigs are used as the animal model for cochlear implantation. A cochleostomy is performed and the cochlear implant electrodes with or without dexamethasone eluting properties are inserted. Unoperated contra-lateral ears were used as controls. Hearing and hair cell function tests are performed on animals post surgery. At day 7 post implantation, guinea pigs will be subjected to acoustic trauma for 2 hours at 120dB at a continuous tone of 6-10 kHz. Hearing tests are performed at day 1, 7, 14, 30, 90 post noise trauma.

Results
After noise trauma, the average ABR threshold shifts from baseline tended to be higher in the control group than both EIT and DXM-EIT groups. Average ABR threshold shifts from baseline tended to be less on day 30 in DXM-EIT than EIT alone or EIT-non eluting groups.

Conclusion
The dexamethasone-eluting implants shows promising results for protection of residual hearing post implantation even in cases of significant noise trauma.

Funding
MED-EL Corporation, Innsbruck, Austria to Dr. AA Eshraghi

PS 847

Dynamics of Superoxide Generation and STAT1 Phosphorylation in Acute versus Chronic Models of Gentamicin-Induced Outer Hair Cell Death

Peng Jiang[1]; **Michael Brenner**[2]; Amrita Ray[3]
[1]University of Michigan, Kresge Hearing Research Institute; [2]University of Michigan; [3]University of MIssissippi

Introduction
Reactive oxygen species (ROS) have been implicated in gentamicin-induced hearing loss, and signal transducer and activator of transcription-1 (STAT1) has been shown to mediate stress-induced inflammation and apoptosis in the inner ear. Gentamicin therapy is given in acute or lengthy regimens and is thought to accumulate in hair cells. This study therefore compared acute and chronic models of gentamicin injury, investigating patterns of STAT1 phosphorylation at tyrosine 701 (Tyr^{701}) and serine 727 (Ser^{727}) in relation to reactive oxygen species generation.

Methods
Two models of gentamicin therapy where compared: an acute, high dose model (50 µm for 4 to 24 hours) and a chronic, low dose model (4 µm for 72 hours). Patterns of STAT1 phosphorylation were investigated in P2 to P3 neonatal murine organ of Corti explants. Gentamicin was administered alone or in combination with 50 µm epigallocatechin gallate (EGCG), an antioxidant and STAT1 inhibitor. Cochlear explants were then stained with rhodamine and fluorescent-labeled phalloidin. Cytocochleograms were performed, and confocal microscopy images were taken to quantify Tyr^{701} and Ser^{727} P-STAT1 fluorescence. Superoxide production was evaluated with DHE, and mitochondrial membrane potential assays were used to evaluate effects of gentamicin on hair cell mitochondrial integrity.

Results
The chronic model demonstrated ascending hair cell death in a base-to-apex gradient, preceded by superoxide production and Ser^{727} STAT1 phosphorylation. Acute (50 µm) gentamicin induced accelerated injury to outer hair cells and supporting cells with earlier STAT1 activation relative to chronic condition ($p<.01$). Tyr701 STAT phosphorylation peaked at 4 hrs but was only significant in the acute regimen. Gentamicin dissipated mitochondrial membrane potential and enhanced phosphorylation at STAT1 ser^{727} after both acute (50 µM; 16 hrs; $p<.001$) and chronic (4µM; 72 hrs; $p<.01$) treatment. A 50 µM EGCG pretreatment attenuated chronic gentamicin-induced oxidative stress, inhibited Ser^{727} phosphorylation ($p<.01$), and protected from gentamicin toxicity with 55 ± 4.7% versus 10 ± 6.7% outer cell loss ($p < .0001$).

Conclusion
Gentamicin damaged outer hair cells after activation of STAT1, generation of oxidative stress, and dissipation of the mitochondrial membrane potential, culminating in outer hair cell death. Pretreatment with EGCG in a chronic gentamicin regimen conferred outer hair cell protection, suppressed

superoxide production, and decreased phosphorylation of Ser^{727}. The chronic gentamicin injury model demonstrates classic morphology seen *in vivo*, likely reflecting the more physiological model of injury. The patterns of STAT1 phosphorylation and superoxide production suggest presence of common pathways and treatments for drug-induced ototoxicity.

Funding
1K08DC012535-03

PS 848

Modulation of the STAT1/STAT3 Signaling Pathway by Epigallocatechin 3-Gallate (EGCG) Protects Against Cisplatin Ototoxicity

Vikrant Borse[1]; Tejbeer Kaur[2]; Debashree Mukherjea[1]; Kelly Sheehan[1]; Sandeep Sheth[1]; Asmita Dhukhwa[1]; Sumana Ghosh[1]; Srinivasan Tupal[1]; Leonard Rybak[1]; Vickram Ramkumar[1]
[1]SIU School of Medicine; [2]Washington University

Backgroun:
Cisplatin is a commonly used chemotherapeutic agent for multiple solid tumors. However, cisplatin-induced neurotoxicity, nephrotoxicity and ototoxicity hamper its use in clinical setting. Although, neurotoxicity and nephrotoxicity can be prevented, there is no cure for cisplatin ototoxicity. Recently, we have shown that reactive oxygen species (ROS) mediated activation of signal transducer and activator of transcription 1 (STAT1) by cisplatin, leads to cochlear inflammation and apoptosis of cochlear hair cells. This loss of cochlear hair cells due to cisplatin is responsible for permanent hearing loss. In this study, we determined the efficacy of epigallocatechin gallate (EGCG), as a STAT-1 inhibitor, to protect against cisplatin ototoxicity in male Wistar rats.

Methods
Organ of Corti-derived cells (UB/OC-1) were cultured and treated with cisplatin in the presence and absence of EGCG to determine effects on STAT1 and STAT3 activity and cell apoptosis. Male Wistar rats (200-250g) were treated with oral EGCG (100mg/kg), followed by cisplatin (11mg/kg, i.p.). Auditory brainstem responses (ABRs), scanning electron microscopy (SEM) and cochlear whole mount studies were performed to assess hearing loss and outer hair cell (OHC) morphology. Lactate dehydrogenase (LDH) and Annexin V assay were performed to assess cisplatin mediated cytotoxic effect and apoptosis. Western blots were performed to determine STAT1, STAT3 activation and apoptotic proteins expression. University of Michigan squamous cell carcinoma (UMSCC) 10B cells were used to examine potential antitumor interference by EGCG.

Results
Results from UB/OC-1 cells shows that EGCG significantly inhibited cisplatin-induced Ser^{727} STAT1 phosphorylation. EGCG decreased the levels of pro-apoptotic proteins (p53, cleaved caspase-3 and Bax), but increased the levels of anti-apoptotic proteins (Bcl-2, Bcl-xL) in UB/OC-1 cells. EGCG also reduced cisplatin-induced Annexin V immunolabeling of UB/OC1 cells. Interestingly, EGCG significantly reversed cisplatin-induced inhibition of Tyr^{705} STAT3 phosphorylation in UB/OC-1 cells. Inhibition of STAT3 by pharmacological agent (STATTIC) or STAT3 siRNA sensitized UB/OC-1 cells to cisplatin, suggesting that reversal of STAT3 inhibition by EGCG could mediate cytoprotective property. *In vivo* studies showed that oral EGCG significantly protected animals from cisplatin-induced ABR threshold shift at all frequencies tested and reduced OHC damage in the basal turn of the cochlea. Furthermore, EGCG potentiated cisplatin-induced cell killing of UMSCC 10B cells by inhibiting Bcl-XL, suggesting an additional potential benefit of this drug against these cancer cells.

Conclusions
In conclusion, this study shows that oral EGCG could potentially reduce cisplatin ototoxicity, while potentiating its chemotherapeutic efficacy.

Funding
Funding: This study was supported by NIH grants RO1DC002396 (LPR), R03DC011621 (DM), R15DC011412 (VR) and R01CA166907 (VR) and by Excellence in Academic Medicine grant from SIU School of Medicine.

PS 849

Treatment of Cisplain-induced Ototoxicity by a Combination of HPN-07 and NAC

Wei Li[1]; Jianzhong Lu[1]; Donald Ewert[1]; Xiaoping Du[1]; Robert Floyd[2]; Richard Kopke[1]
[1]Hough Ear Institute; [2]Oklahoma Medical Research Foundation

Background
Cisplatin is a frequently-used effective antitumor drug. However, its use is limited by its side effects, such as ototoxicity. The formation of reactive oxygen species (ROS) is thought to play a key role in causing hearing loss. Our previous studies have demonstrated that a novel combination of the antioxidants 2,4-disulfonyl alpha-phenyl tertiary butyl nitrone (HPN-07) and *N*-acetylcysteine (NAC) successfully reduced noise- and blast-induced hearing loss. The purpose of this study was to determine if the combination of HPN-07 and NAC could also reduce cisplatin-induced ototoxicity.

Methods
Long Evans rats were administered cisplatin by slow intravenous infusion at escalating dose levels (13, 14, 15 and 16 mg/kg). The antioxidants NAC and HPN-07 were delivered at an equimolar ratio by i.p. injection at a dose of 600/600 or 900/900 mg/kg 1 hour before and 1, 6, and 24 hours after cisplatin injection. Hearing levels were evaluated by ABR analysis before and at 72 hours after cisplatin administration. Hair cell counts were performed on fixed cochlear tissues following the terminal ABR test.

Results
A dose-dependent effect of cisplatin on hearing loss was observed in our analyses. Based on these results, a series of experiments were conducted using a fixed cisplatin dose

of 15 mg/kg to determine the optimal drug dose and timing of antioxidant delivery relative to cisplatin administration. From this analysis a dose of 600/600 mg/kg HPN-07/NAC administered one hour prior to the initiation of cisplatin infusion achieved the maximum protective effect based on ABR threshold shift reduction for a 15 mg/kg dose of cisplatin. Using this treatment paradigm, the antioxidant formulation achieved maximal therapeutic efficacy when the ototoxic dose of cisplatin was reduced to a dosage of 13 mg/kg, as supported by ABR measurements and hair cell counts.

Conclusions
These studies demonstrated that administration of an antioxidant formulation consisting of HPN-07 and NAC could significantly reduce the ototoxic effect of cisplatin *in vivo*. Information regarding the critical timing of initial drug treatment relative to the administration of cisplatin has important clinical implications regarding the treatment efficacy of antioxidants for reducing ototoxicity among cancer patients.

Funding
This work was supported in part by a grant from Otologic Pharmaceutics, Inc.

PS 850

Caffeine Consumption Exacerbates Cisplatin-Induced Hearing Loss in the Rat

Sandeep Sheth; Kelly Sheehan; Srinivisan Tupal; Sumana Ghosh; Vikrant Borse; Asmita Dhukhwa; Michelle Lowy; Debashree Mukherjea; Leonard Rybak; Vickram Ramkumar
Southern Illinois University School of Medicine

Background
Permanent hearing loss is one of the serious side effects of the anti-cancer drug, cisplatin. Recent studies suggest that cisplatin produces ototoxicity by initiating an inflammatory process through activating the transcription factor, signal transducer and activator of transcription (STAT1), which are negatively regulated by the adenosine A_1 receptor (A_1AR). A_1ARs are expressed in the cochlea where they attenuate hearing loss produced by cisplatin, in part by inhibiting STAT1 activity. Caffeine, a widely consumed substance present in coffee, soda and energy drink, is a non-selective antagonist of the A_1AR. We reasoned that caffeine intake could antagonize the endogenous protective role of the A_1AR in the cochlea and potentiate hearing loss induced by cisplatin. In the current study, we demonstrate that caffeine exacerbates cisplatin-ototoxicity in a rat model.

Methods
Auditory brainstem responses (ABRs) in naïve male Wistar rats were recorded before and 3-days following cisplatin (11mg/kg), oral caffeine (15mg/kg) and transtympanic *R*-PIA (1μM), treatment to assess hearing loss. Cochlea were then isolated for whole mount preparation to check for the loss of OHCs using myosin VIIa staining. The effects of caffeine and cisplatin were also studied on cochlear explant cultures from neonatal mice and UB/OC-1 cells for hair cell loss and phospho-STAT1 levels. qRT-PCR was performed on UB/OC-1s to study expression of *iNOS, COX-2* and *TNFα*.

Results
Oral administration of caffeine significantly exacerbated cisplatin-induced hearing loss in rats at 32, but not at 8 or 16 kHz, as determined by ABRs. Exacerbation of OHC damage by caffeine was also observed in whole mount preparations. In *in vitro* studies using cultured hair cells (UB/OC-1), caffeine enhanced cisplatin-induced killing. This effect of caffeine was associated with enhancement of STAT1 activity over that observed with cisplatin. Caffeine also enhanced cisplatin-induced expression of STAT1 regulated genes, such as *iNOS, COX-2* and *TNFα*. These effects of caffeine were completely reversed by *R*-PIA, an A_1AR agonist.

Conclusion
Our findings indicate that a single dose of oral caffeine sensitizes the cochlea to cisplatin inhibiting the endogenous protection afforded by the A_1AR. These studies point to a possible drug-drug interaction between caffeine and cisplatin and suggest that caffeine consumption should be avoided or reduced in cancer patients on a chemotherapeutic regimen containing cisplatin.

Funding
This study is supported by the grant from American Hearing Research Foundation awarded to Dr. Sandeep Sheth

PS 851

Oxidative stress in the guinea pig model of electrode insertion trauma followed by noise trauma

Jonathan Roell; Christopher O'Toole; Noah Shaikh; Carolyn Garnham; Jeenu Mittal; Adrien Eshraghi
University of Miami

Background
Cochlear implantation causes direct tissue trauma, but also generates molecular events that may initiate programmed cell death (PCD) via various mechanisms such as oxidative stresses, release of pro-inflammatory cytokines, activation of the caspase pathway which can result in apoptosis and generation of pro-apoptotic signal cascades within the damaged tissues of the cochlea which can lead to a loss of residual hearing. The objective of this study is to dissect the molecular mechanisms involved in oxidative stress of sensory cells post electrode insertion trauma (EIT) and EIT followed by noise-induced trauma.

Methods
EIT was performed in guinea pigs by cochleostomy and unoperated contra-lateral ears were used as controls. Noise trauma was performed to the guinea pigs 1 week after EIT for 2 hours at 120dB at a continuous tone of 6-10 kHz. ELISA for different enzymes involved in oxidative stress and PCD such as SOD, catalase, glutathione reductase or glutathione peroxidase was performed at 0 hr, 2 hr, 6hrs, 12hrs and 24hrs both post-EIT and noise trauma.

Results
We observed in animals with only EIT an increase in catalase activity in the trauma ear compared to the control. There

was no significant change in SOD, glutathione reductase or glutathione peroxidase. The changes in these enzymes post noise trauma are similarly analyzed.

Conclusion
Oxidative stress plays an important role in hearing loss following EIT. Oxidative damage may result from overproduction and/or lack of clearance of ROS/RNS by the scavenging mechanisms. Enzymatic defenses are comprised of agents that catalytically remove ROS, such as SOD, catalase, glutathione reductase or glutathione peroxidase. A better understanding of the mechanisms involved in oxidative stress can help us determine the best method for preventing loss of sensory cells.

Funding
MED-EL Corporation, Innsbruck, Austria to Dr. AA Eshraghi llowed by noise trauma

PS 852

Neuroprotective Mechanisms of Therapeutic Hypothermia and Preservation of Residual Function Following Electrode Implantation

Ilmar Tamames[1]; Esperanza Bas[1]; Jessie Truettner[1]; Fred Telischi[1]; Dalton Dietrich[1]; Curtis King[2]; Abhishek Prasad[1]; Suhrud Rajguru[1]
[1]University of Miami; [2]Lucent Medical Systems

Background
Mild to moderate hypothermia is a promising neuroprotective intervention when induced during or after a central nervous system injury. When localized and administered prior to trauma, these effects may be enhanced with little adverse effects on other biological phenomena. Here we studied the efficacy of localized therapeutic hypothermia applied to the cochleae and brain in reducing residual functional loss associated with electrode insertion trauma. Furthermore, we studied for changes in gene expression in normothermic and hypothermic cochleae implanted with cochlear implant analog to delineate the underlying neuroprotective mechanisms.

Methods
In chronic experiments, the auditory brainstem responses (ABRs) were recorded from anesthetized to assess their hearing function before and after cochlear implantation. Changes in hearing following electrode insertion trauma were tested in response to 0.5-32 kHz pure tone pips between three groups: control cochleae, normothermic and hypothermic cochleae. At the conclusion of the trials, inner ears were harvested for histology. Furthermore to assess changes in gene expression at various time points following implantation, we used pathway specific gene arrays for oxidative stress and inflammatory cytokines and receptors. Each array included 84 different genes with 5 house-keeping genes for normalization and 7 RT-PCR controls. Gene expression was compared for implanted animals in three groups: control, normothermic-implanted and hypothermia-treated implanted animals.

Results
Results suggest that therapeutic hypothermia provided during cochlear implantation significantly reduced associated trauma and prevented residual functional loss. Preliminary data from rats showed that electrode insertion caused a significant increase in expression of pro-inflammatory cytokines and chemokines and downregulation of anti-apoptotic Bcl2. Trauma upregulated the pro-inflammatory cytokines IL-1β, IL-11, Il17-a and TNF-α several folds above the levels found in control cochleae. Hypothermia comparatively limited the upregulation of these cytokines. Additionally a significant increase was observed for chemokines and their receptors at 48 hours and Ccl11, Ccl12 and Ccl17 at 48 hours post trauma. Hypothermia significantly limited upregulation of these factors, which are known to play an active role in the acute phase inflammatory response. We also observed an increase in expression of Bcl-2 with hypothermia, which can inhibit both apoptosis and necrosis.

Conclusion
Therapeutic hypothermia affects pathways leading to apoptosis, inflammation and free radical production. Previous studies have shown that hypothermia may also influence neurogenesis, gliogenesis and angiogenesis after injury. Our preliminary results suggest that it is likely that the neuroprotective effects of hypothermia cover multiple factors.

Funding
1UL1TR000460 (Pilot Award to SMR) and 1R21DC014324 (SMR)

PS 853

Effect of growth factors on the re-innervation of hair cells by spiral ganglion neurons and neural stem cell-derived neurons

Jeong Han Lee; Ebenezer Yamoah
University of Nevada, Reno

Previous studies have demonstrated that one of the early signs of hearing loss is alterations hair cell (HC)-spiral ganglion neuron (SGN) synapse. Re-innervation and the mechanisms thereof would be an important step in restoring hearing. The objective of this study was to test whether; 1) SGNs and neural stem cell-derived neurons can establish functional synaptic connections after denervation: 2) Growth factors including BDNF, and NT3 as well as growth promoting factors, such as can increase neurite outgrowth and promote synapse formation: 3) Neural stem cell (NSC)-derived neurons use similar mechanism to establish synapse with HCs: 4) There are age-dependent alterations in the mechanisms of HC-SGN re-innervation.

The neural stem cells from the sub-ventricular zone of the lateral ventricle can differentiate into functional SGNs. NSCs were co-cultured with organ of Corti obtained from P3 mice. At Day 2, the NSCs grew neurite toward the sensory epithelium. At Day 7, neurites of NSCs-derived neurons elongated toward HCs and established functional synapses.

We used a GsMTx4, tarantula toxin, to produce complete SGN loss, and then transplanted new SGNs from different cochleae. In the presence of growth factors, re-innervated of de-afferentted HCs was enhanced. In contrast, in the absence of growth factors neural outgrowth did not lend itself for re-innervation. However, application of small direct current (DC) sufficed to promote neurite growth and migration NSCs to form functional synapse with HCs. The electrotactic response was both time and voltage dependent. NSC-derived neurons can provide a model for studying regeneration, re-innervation, and synaptic plasticity

Funding
R01 DC0100386; DC007592; DC003826

PS 854

Recovery from Noise Exposure in an Outbred Mouse Model

Edward Walsh; Amanda Branch Woods; JoAnn McGee
Boys Town National Research Hospital

Inbred strains of mice have been commonly, if not exclusively, employed in murine studies of noise-induced hearing loss (NIHL). However, interest in the use of outbred animal strains is on the rise, most notably when considering toxicological and pharmacological interventions. One significant concern related to the use of outbred strains is the expectation that highly variable genotypes will produce diverse phenotypic populations and reduced statistical sensitivity for a given sample size, requiring the use of large study groups. Although this view is pervasive in the scientific community, relatively few comparative studies have actually been considered. To assess the suitability of using outbred mice to study the impact of noise exposure and recovery from NIHL, mice representing the NMRI outbred strain were exposed to an octave band of white noise centered on 11.3 kHz for 1 hr. Exposure level was varied to determine the energy required to produce a consistent and significant hearing deficit; a permanent hearing loss was achieved using a noise band that was delivered at 103 dB SPL. Auditory brainstem responses (ABRs) were used to assess the degree of hearing loss immediately following exposure and to track recovery from temporary hearing loss. Immediately following noise exposure, threshold at the center frequency of the exposure band, 11.3 kHz, was, on average, 101 dB SPL +/- 4.8 dB, 79 dB higher than control, baseline values. This finding was compared to the outcome of exposing CBA/J inbred mice to the same noise band. At equivalent exposure energies, CBA/J mice were notably less sensitive to noise exposure than NMRI cohorts. When exposed to a 3 dB higher level of noise energy, thresholds in CBA/J mice were elevated by 63 dB at 11.3 kHz, 16 dB lower than that observed in NMRI mice immediately following exposure. Furthermore, the degree of permanent hearing loss at 11.3 kHz was nearly 10 dB lower for CBA/J relative to NMRI cohorts (i.e., average threshold shifts of 28 dB versus 36 dB, respectively) at the end of one post exposure week. Based on these results, we tentatively conclude that outbred NMRI mice are more vulnerable to noise exposure than inbred CBA/J mice, although overall outcome variability was similar, suggesting that concerns related to the need for large sample sizes to achieve equivalent statistical power may be unfounded.

Funding
This work was supported by the Office of Naval Research Grant N000141410562 and NIH Grant P30 GM110768-01.

PS 855

Murine “Mini Ears” for Phenotypic High-Content Screening

Mirko Jaumann[1]; Aurélie Dos Santos[1]; Marcus Mueller[2]; Hubert Loewenheim[2]
[1]University of Tübingen Medical Center; [2]University of Oldenburg

In vitro models to study ototoxicity, otoprotection or otoregeneration have utilized inner ear cell lines, zebra fish, and to a certain extent whole organ culture. Since cell lines and non-mammalian models for ototoxicity may behave distinct from primary cells in response to drug treatment, we developed an *in vitro* standardized assay for ototoxic drug screening derived from murine organ of Corti progenitor cells, representing “Mini Ears”.

We isolated cells from the postnatal day 0 organ of Corti of NMRI mice that are known to give rise to stem cell derived otospheres (Oshima et al., 2007, J Assoc Res Otolaryngol). From these spheres, differentiated epithelial islands - “Mini Ears” - populated with hair- and supporting cell-like cells can be obtained. Primary cells were cultured in a proliferative environment for 5 days in vitro (DIV). With the removal of the growth factors, plating on 96-well plate format, and pursued culture for 14 DIV in adherent conditions, the spheres differentiate into prosensory cell patches. The “Mini ears” were fixed, immunohistochemically stained, and automatically analyzed using an ImageXpress Micro XLS High-Content Screening microscope (Molecular Devices).

Varying culture conditions and testing markers for hair and supporting cell–like cells, we found reproducible conditions for the generation of “Mini-Ears”. A fully automated data acquisition algorithm that identifies, images, and analyses “Mini Ears” with no user intervention for up to 5 different markers and z-stacks was established. Using the inducible reporter mouse line Fgfr3-iCreER^{t2}, proliferation could be monitored selectively in specific sub types of supporting cells. The assay now provides a screening platform to conduct “Mini Ear” based high-content screening for ototoxicity, otoprotection, and oteroregeneration.

Funding
The research leading to these results has received funding from the European Communityâ€™sSeventh Framework Programme under grant agreement No. 603029 (Project OTOSTEM).

PS 856

Modeling Acquired and Genetic Hearing Loss using Induced Hair Cells from Direct Cellular Reprogramming

Louise Menendez; Suhasni Gopalakrishnan; Juan Llamas; Litao Tao; Welly Makmura; Neil Segil; Justin Ichida
University of Southern California

Hearing loss affects 360 million people worldwide, with loss of hair cells within the cochlea being a major cause. For research purposes, it is difficult to obtain these specialized cells for in vitro studies because they are fragile and very few in number. Our goal for this project is to use direct cellular lineage conversion to generate an in vitro model of these cells in order to study the cellular mechanisms that underlie their vulnerability. We are a using transcription factor based cellular reprogramming approach. RNA sequencing data obtained from primary hair cells allowed us to identify a set of transcription factors that could be used to reprogram somatic cells towards a hair cell fate. Viral transduction of these factors was used to reprogram mouse embryonic fibroblasts and human iPSC derived fibroblasts resulting in the generation of hair cell-like cells. The induced hair cells express an Atoh1 driven GFP reporter and show immunostaining for MyosinVI, Myosin VIIa, parvalbumin in addition to having polarized phalloidin staining. Our aim is to use this in vitro model of hair cells to study genetic and ototoxic vulnerabilities.

Using these induced hair cells we have conducted pilot studies to test their ototoxic vulnerability. A survival experiment was performed with longitudinal tracking of ototoxin induced hair cell death. The induced hair cells, positive for Atoh1 driven GFP, were robotically imaged twice a day after the addition of gentamicin, a known ototoxic antibiotic. The time-lapse video was used to quantify the number of GFP positive cells surviving following treatment. The results demonstrated a clear dose dependent decrease in the survival of induced hair cells in the presence of gentamicin.

In separate experiments, we have used Crispr/Cas9 genome editing technologies to engineer human iPSC lines with a mutation known to cause sensorineural hearing loss, DFNA2. The mutation is a common point mutation found in the KCNQ4, voltage-gated potassium channel, which is essential for hair cell function. This cell line will allow us to make induced hair cells with the mutation and study the cellular mechanisms involved in hair cell degeneration. Similarly we are using this genome editing technology to make iPSC lines with other common mutations linked to deafness in order to identify the pathogenic mechanisms. Together, we hope our induced hair cells will provide a high throughput system for studying cellular mechanisms of both acquired hearing loss due to ototoxic vulnerability and genetically inherited vulnerabilities.

Funding
CIRM- Regenerative Medicine Initiative Thank you to the Sidgmore Family Foundation and the Hearing Health Foundation to N.S.

PS 857

Toward a Nonhuman Primate Model of Noise Induced Hearing Loss

Jane Burton[1]; Samantha Hauser[1]; Justin Watson[1]; Michelle Valero[2]; Troy Hackett[1]; Ramnarayan Ramachandran[1]
[1]Vanderbilt University; [2]Massachusetts Eye and Ear Infirmary

Noise induced hearing loss affects many individuals in the human population. Several animal models have been used for peripheral and some central characterization of the effects of noise induced hearing loss. The purpose of this experiment was to characterize the peripheral and central effects of noise induced hearing loss in nonhuman primates, an animal model phylogenetically close to humans.

Physiological characterization of auditory function was obtained in four monkeys (*Macaca mulatta*) by measuring auditory brainstem responses (ABRs) and distortion product otoacoustic emissions (DPOAEs). ABRs were measured for click and toneburst stimuli (500-32000 Hz) using a soundfield speaker. DPOAEs were measured at 1.15, 1.20, 1.22, and 1.25 frequency ratios and 65/55 and 70/70 level ratios (500-8000 Hz, 8 points per octave) bilaterally. After obtaining baseline measures, each monkey was exposed to a 50 Hz bandwidth of sound centered at 2 kHz for four hours under anesthesia. Many sound levels were tried, with a noise level of 146 dB SPL spectrum level ultimately used to create permanent noise induced hearing loss. ABRs and DPOAEs were measured periodically following each deafening to document progression, improvement, or stability of physiological measures of auditory function over time. Monkeys were euthanized 8 weeks after their 146 dB noise exposure, and the brain and cochleae extracted for further analysis.

No long-term changes could be measured in physiological measures of auditory function following exposure to 108, 120, or 140 dB SPL noise when compared with baseline measures. Exposure to the 146 dB SPL noise created permanent and consistent changes to both DPOAEs and ABRs, indicating permanent loss of outer hair cell (OHC) function and impairment of the auditory brainstem pathway. ABR toneburst thresholds and waveform latencies were increased, with the largest measured threshold changes above 2 kHz. DPOAEs were absent across all frequencies and conditions tested, with greater DP amplitude variability at low frequencies with the 70/70 level ratio conditions. Cochlear histology showed widespread OHC, but minimal inner hair cell, loss. The basal-most region lacked a discernable organ of Corti. These effects were accompanied by a frequency specific reduction in the number of ribbon synapses, with the peak a half octave above the impairment frequency.

These results highlight similarities in the effects of noise induced hearing loss across species and provide a baseline for ongoing investigations of behavioral, neurophysiologic, and genomic correlates of noise induced hearing loss in macaques.

PS 858

Effective Stimulus to the Cochlear: Intracochlear Pressure Measurement

Jae Hoon Sim[1]; Flurin Pfiffner[1]; Lukas Prochazka[2]; Ivo Dobrev[1]; Dominik Péus[1]; Adrian Dalbert[1]; Christof Röösli[1]; Alexander Huber[1]
[1]University Hospital Zurich; [2]Streamwise

Background

Recent measurements of stapes motion have shown that there are rocking-like as well as piston-like spatial components that influence cochlear activation. However, the mechanism of cochlear activation by the rocking-like stimulation from the perspective of cochlear dynamics has not been clarified. Measurements of intracochlear pressure with different types of stimulation may help to reveal the mechanism of cochlear activation by the rocking-like motion, to supplement the intracochlear pressure measurements made by other researchers that were limited to acoustic stimulation in the ear canal.

Methods

Intracochlear pressure with controlled motion of the stapes was measured in fresh human temporal bones. The desired motion patterns of the stapes were produced by direct stimulation on the stapes using a custom-made magnet-coil driving system. Simultaneous measurements of the electromagnetically induced 3-D motion of the stapes and intracochlear pressure were made using laser Doppler interferometry (LDI) and a custom-made intracochlear pressure sensor, respectively.

Results

The magnitude ratio of the intracochlear pressure to the piston-like motion with the rocking-like motion dominant was larger than the corresponding ratio with the piston-like motion dominant, indicating that the rocking-like motion also generates the intracochlear pressure.

Conclusion

The rocking-like motion as well as the piston-like motion generate the intracochlear pressure and thus contribute considerably to the cochlear activation.

Funding

This work supported by a SNF project 320030-153396, and partially by a project â€œNew receiver technology for totally implantable cochlear implantsâ€ funded by Cochlear Ltd.

PS 859

Origins of Carhart's Notch - Middle-Ear Mass or Oval-Window Impedance?

Namkeun Kim[1]; Stefan Stenfelt[2]
[1]Incheon National University; [2]Linkoping University

Background

In 1950, Carhart showed about 15 – 20 dB depressed hearing thresholds (called 'Carhart's Notch) at 1 – 2 kHz for bone-conducted (BC) stimulation in otosclerosis patients. Many researchers have studied the origin of Carhart's Notch (CN) and proposed that CN is primarily caused by loss of the middle-ear (ME) inertia due to stiffening of the stapes annular ligament. However, those studies could not distinguish between the loss of the ME inertia and the increase of the oval window (OW) impedance caused by stiffening of the stapes annular ligament. Therefore, in order to distinguish the effects of those two factors, we developed a computational framework.

Methods

A three-dimensional finite element (FE) model of a human middle ear coupled to the inner ear was devised. In the model, the stapes annular ligament was stiffened to simulate otosclerosis, which efficiently block the ME inertia to the cochlea. In order to implement the pseudo OW impedance, we manipulated the model as following in order: 1) removing all the ME components except the stiffened stapes annular ligament and stapes footplate, 2) changing the density of the stapes footplate to a value close to zero, and 3) re-assigning the complex Young's modulus of the stapes footplate to an impedance similar to a normal ME structure.

Results

When removing the ME inertia by stiffening the stapes annular ligament, about 15 dB hearing loss was observed from 0.1 kHz to 0.4 kHz worsening to 40 dB hearing loss at 1.1 kHz and diminishing to about 25 dB at 3 kHz to 6 kHz . When the the stiffening of the stapes annular ligament was applied together with the pseudo OW impedance, a hearing loss of 30 dB appeared at 1.3 kHz while the low (below 0.4 kHz) and high frequency (above 3 kHz) losses were limited to 0 – 5 dB.

Conclusions

Stiffening of the stapes annular ligament causes both the loss of the ME inertia and increses the ME impedance. The loss of the ME inertia gave rise to hearing loss at about 1 – 2 kHz (called Carhart's Notch) while the increase of the OW impedance gave hearing loss at low (below 0.4 kHz) and high (approximately 3 kHz – 6 kHz) frequencies.

Funding

This research was supported by Basic Science Research Program through the National Research Foundation of Korea (NRF) funded by the Ministry of Science, ICT & Future Planning (201501660001).

PS 860

Bone conduction hearing is affected by superior canal dehiscence

Xiying Guan; Song Cheng; John Rosowski; Hideko Nakajima
Harvard Medical School, Massachusetts Eye & Ear

Background

Third-window lesions such as superior canal dehiscence (SCD) can cause a variety of auditory and vestibular symptoms (e.g. autophony and hyperacusis). In some, SCD causes unusually low audiometric bone conduction (BC) thresholds (hypersensitive BC). Such abnormal BC thresholds often normalize after successful surgical repair of SCD, suggesting a restoration of physiological cochlear fluid mechanics and sound transduction. However, surgery-induced sensorineural

hearing loss could also explain a post-operative increase in BC thresholds. By measuring intracochlear pressures in fresh cadaveric human temporal bones, we study the effect of SCD on the cochlear input pressure drive in response to BC sounds, and compare our results to previous studies of SCD and air-conducted (AC) sound.

Methods
Intracochlear pressures in scala vestibuli (Psv) and scala tympani (Pst) at the basal turn of 4 fresh human cadaveric ears were measured using micro-fiberoptic sensors. SCD was simulated by creating a small defect in the lateral aspect of the superior semicircular canal. Intracochlear pressures in the frequency range of 0.1-10 kHz evoked by a bone-anchored hearing aid (BAHA) were measured before and after opening the dehiscence.

Results
Post-dehiscence BC-evoked Psv and Pst both increased at low frequencies (f < 700 Hz). Psv was increased by as much as 15 dB due to SCD. A smaller increase (5-10 dB) was observed in Pst. The pressure drive across the cochlear partition (Psv-Pst) was increased by 5-10 dB over the same low frequency range. SCD did not affect the BC-evoked intracochlear pressures at higher frequencies. AC-evoked pressures decreased with SCD similar to our previous studies. Repairing the SCD by hermetically sealing with soft material generally returned the AC-evoked pressures to normal values, however, BC-evoked pressures required additional hard material to return the BC-evoked pressures to their normal values.

Conclusion
Our data suggest that hypersensitivity to low-frequency BC sounds in patients with SCD is due to dehiscence-induced acoustic/mechanical changes within the inner ear. In air conducted sounds, SCD decreases intracochlear pressures. In contrast, BC-induced Psv and Pst both increase in SCD as does their difference, consistent with observations of hypersensitive BC. Unlike AC, BC requires a hard material for repairing the SCD to return pressures to their normal values. Mechanism of such changes will be further investigated. This study is supported by NIH/NIDCD R01DC013303.

Funding
This study is supported by NIH/NIDCD R01DC013303.

PS 861

Acoustic Activation of the Semicircular Canals

Marta Iversen[1]; John Carey[2]; Charley Della Santina[2]; Wu Zhou[3]; Hong Zhu[3]; Richard Rabbitt[1]
[1]University of Utah; [2]Johns Hopkins School of Medicine; [3]University of Mississippi Medical Center

Introduction
Single-unit afferent recordings demonstrate that the semicircular canals become highly sensitive to acoustic stimuli if a window (simple model of dehiscence) is introduced into the bony canal wall. Sensitive afferents phase lock action potentials to oval window acoustic stimuli and in many cases demonstrate slow excitatory increases in discharge consistent with sound-induced deflection of the cupula, typically toward the dehiscence. Changes in afferent discharge rate follow a time-course similar to the mechanical lower-corner frequency present during angular motion stimuli. We hypothesize that the slow component occurs during acoustic stimulation because nonlinear compression and dilation of the membranous labyrinth leads to partially rectified endolymph volume displacement. To investigate this hypothesis, afferent responses in a chinchilla model of superior canal dehiscence were compared to a 3D biomechanical model of sound induced cupula motion.

Methods
A morphologically descriptive finite-element model was constructed based on micro-MRI and CT data. The model included the complete bony labyrinth and a subdomain of the membranous labyrinth. The Navier-Stokes equations were solved to examine compressional waves and flow in endolymph and perilymph. Mechanical rectification of the membranous labyrinth was also simulated. The mechanical displacement of the cupula in the superior canal was computed in both the intact and dehiscent labyrinth.

Results
Simulations predict that the acoustic pressure distribution in the intact bony labyrinth is dominated by an evanescent wave trapped in the vicinity of the oval and round windows. The evanescent pressure wave and associated flow is likely responsible for the weak acoustic activation of canals observed in the intact condition. In the dehiscent labyrinth, the pressure distribution extended into the superior canal. In the absence of rectification, simulations predict a small sound-driven streaming flow in the inhibitory direction inconsistent with experimental data. Simulations that included rectification predicted sound-driven endolymph displacement toward the dehiscence that built to a maximum following a time constant of ~6.4s (vs. 11.7s for rotational stimuli in the intact canal).

Conclusion
Based on compressible fluid mechanics within the intact bony labyrinth, the semicircular canals would be expected to respond very modestly to acoustic stimulation of the oval window. With dehiscence, simulations predict the mechanical response will increase ~100 fold in magnitude and the slow time constant governing cupula deflection will decrease ~50%. Results support the hypothesis that excitatory afferent responses observed in the dehiscent semicircular canal arise from a mechanical rectification and sound-driven endolymph displacement.

Funding
Funding: Support was provided by the NIH R01-DC006685 (Rabbitt) and NIH R01-DC012060 (Zhu).

PS 862

Both Fast and Slow Pressure Waves Affect Cochlear Mechanics in the Vestibule Space

Wenxiao Zhou[1]; Yanju Liu[1]; C Geisler[2]; **Jong-Hoon Nam**[1]
[1]University of Rochester; [2]University of Wisconsin-Madison

Background

In the fluid-filled cochlea, sound pressure waves travel toward the apex slowly (< 100 m/s), interacting with transverse vibrations of the cochlear partition. Most existing theories assume that the fast pressure wave (symmetric pressure component across the cochlear partition) does not contribute to cochlear mechanics. However, there are observations that are incongruent with the slow wave theory—little to no onset latency to click in the cochlear base (e.g., Temchin et al., 2012), which was ascribed to the fast pressure waves (Recio-Spinoso & Rhode, 2015). We hypothesized that fluid-structure interactions in the large 3-D vestibule at the base (as opposed to the 1-D tubular fluid space in the middle to apical turns) reveals the effect of fast compressive waves.

Methods

A recent cochlear model (Liu et al., 2015) was modified to incorporate the effect of the large sound port (SP) representing the vestibule space. The assumption of anti-symmetric pressure distribution across the cochlear partition was relaxed. The model solved three physical domains simultaneously—solid, fluid and hair cell electro-mechanics. The cochlear partition was represented by a 3-D finite element model with detailed organ of Corti structures. The fluid domain was discretized with a finite difference scheme. Known physiological properties were incorporated to represent the hair cell mechano-transduction and electro-motility.

Results

A series of pure tone stimuli and an impulse were simulated with different SP configurations—when the SP is at the basal end, and when the SP ranges the vestibule region along the cochlear length. When the hair cells were active (comparable to small sound stimulation), the responses were similar despite different SP configurations. However, when the hair cells are passive (comparable to loud sound stimulation), there were qualitative differences. The conventional model agrees with the traveling wave theory with onset latency increasing gradually along the entire cochlear length. For the model with the vestibule, the onset latency stayed zero in the basal region, but increased gradually in the middle to apical region.

Conclusions

Our model simulations suggest that, due to the large 3-D vestibule, the effects of fast compressive waves and slow traveling waves co-exist in the base of the cochlea. Due to the fast compressive waves, there is virtually no onset latency to loud sound stimuli in the basal turn of the cochlea.

Funding

Supported by NSF CMMI 1233595 and NIH R01 DC014685 to JN

PS 863

Wave Propagation in a Simplified 1D Cochlear Model

Samiya Alkhairy[1]; Christopher Shera[2]
[1]MIT; [2]Eaton Peabody Lab, Mass Eye and Ear Infirmary

To lay the groundwork for studying various forms of coupling in the cochlea, we examine wave propagation in a simplified 1D model in which the partition is coupled by fluid inertia. We obtain results applicable to the analysis of experimental data from the model's perspective. Using scalae pressure and BM velocity data from Dong and Olson in gerbil we derive an idealized, qualitative expression for the partition impedance near the traveling-wave peak. Using this idealized partition impedance we investigate several properties of wave propagation in a one-dimensional transmission-line model of the cochlea in which adjacent segments of the partition are coupled by the motion of the scalae fluids.

In particular, we:

a. Derive approximate expressions for the wavenumber, differential pressure, and BM velocity. Whereas the pressure has the form of a traveling wave, the BM velocity is better thought of as a "filtered wave", rather than a true traveling wave.

b. Investigate the relationship between forward- and reverse-propagating solution components. In general, the pressure components are antisymmetric (i.e., the wavenumbers have the same magnitude but opposite sign) and the nature of the velocity components depends on the partition impedance. For the idealized partition impedance, the velocity components are also approximately antisymmetric.

c. Derive approximate expressions for the quality factor and group delay that characterize the frequency tuning of BM velocity. Those expressions relate global response characteristics to parameters of the wavenumber and BM impedance.

Funding

Supported by T32 DC00038 and R01 DC003687.

PS 864

Investigating the spatial variations of distortion products in the cochlear fluids using a computational model

Thomas Bowling; Julien Meaud
Georgia Institute of Technology

Distortion product otoacoustic emissions (DPOAEs) are generated due to outer hair cell nonlinearities when the cochlea is stimulated by two primary tones of frequency f_1 and f_2. While DPOAE measurements are a common clinical and research tool, whether DPOAEs propagate from their site of generation to the middle ear as fast compressional wave through the cochlear fluids or as a slow wave on the basilar membrane is still debated. A physiologically based computational model of the gerbil ear is used to study the propagation of DPOAEs in the cochlea. This model includes

a nonlinear model of the cochlea, formulated in the time-domain and based on the finite element method, and a lumped parameter model of the middle ear. The cochlear model includes two ducts and the fluid is modeled in three dimensions. Numerical simulations are used to investigate the spatial variations of the intracochlear pressure. Results demonstrate that while the pressure is fully three-dimensional close the f_2 and DPOAE best places, the pressure becomes one-dimensional at more basal locations. Simulations are compared to direct measurements for model validation. The implications of the spatial variations of the pressure at the DP frequency regarding the fast wave and slow wave hypotheses are discussed.

Funding
This research is funded by National Science Foundation grant # CMMI-1536830.

PS 865

Effects of Heavy Beads on Distortion Product Otoacoustic Emissions in Gerbil

Xiangming Zhang[1]; **Wei Dong**[1,2]
[1]VA Loma Linda Healthcare System; [2]Loma Linda University Healthcare

Background
Generation of distortion product otoactoustic emissions (DPOAEs) has been summarized into nonlinear distortion and linear coherent reflection theories (Shera and Guinan, 1999). Nonlinearity in cochlear responses is the fundamental element in generation of DPOAEs. The coherent reflection is based on the non-perfectly smooth array of the cochlear partition. The current study seeks to advance our understanding of the generation of DPOAEs by modifying the mass and/or the stiffness of the basilar membrane (BM) using heavy beads (4.26g/cc). Basilar membrane velocity and ear canal pressure responses to two-tone stimulation were simultaneously measured. Effects of heavy beads on the BM responses as well as on the DPOAEs were analyzed.

Methods
Experiments were performed in anesthetized young adult gerbils. The care and use of the animals were approved by the Institutional Animal Care and Use Committee of Loma Linda VA Healthcare System (IACUC). The left pinna was removed and the bulla was opened to expose the cochlea. Basal turn BM velocity responses to single- and two-tone stimulation were measured using Laser Doppler Vibrometer (OFV 5000). Simultaneously, ear canal pressure responses close to the tympanic membrane were measured using Sokolich probe tube microphone.

Results
30 gerbils were used in this study and consistent results were shown across animals. Heavy beads influence on cochlear mechanics was demonstrated by the BM responses to single- and two-tone stimulation recorded at different longitudinal locations. Comparing before and after placement of heavy beads, effects on the BM velocity responses were found to stay local. Any apical heavy beads, or beads more than 200 micrometers away, seemed to have little effect on the BM responses. However, at distances within 100 micrometers, the heavy beads increased the BM response magnitude and shifted the phase-frequency curve to higher frequencies. Influence of heavy beads could be explained within the framework of mass and stiffness effects on the traveling wave. Two-tone responses were also compared pre- and post-delivery of these heavy beads. The variations both in intracochlear distortion product (DP) and in ear canal DPOAE were consistent with the BM property change regarding the generation of DPOAEs.

Conclusions
Heavy bead effects on cochlear mechanics appeared to be local. The change in the DPOAE suggested that the generation of DPOAEs was consistent with the prediction of the two-source theory.

Funding
NIDCD R01DC011506

PS 866

Physiologically Based Simulation of MOC Effect on SFOAEs

Maria Berezina-Greene; Christopher Shera
Harvard Medical School

In guinea pigs, reducing the gain of the cochlear amplifier via electrical stimulation of medial olivocochlear (MOC) efferents results in both inhibition *and* enhancement of stimulus-frequency otoacoustic emissions (SFOAEs). Here, we test the hypothesis that this unexpected effect of MOC activation can be explained by the coherent reflection theory (CRT) of OAE generation combined with the patchy innervation patterns of individual MOC efferent fibers revealed by anatomical studies (Brown 2014). According to CRT, SFOAEs are generated by coherent wave scattering from micromechanical irregularities along the cochlea. We hypothesize that activation of MOC fibers changes the pattern of irregularities by reducing the gain of the amplifier at the sites of fiber innervation. Altering the pattern of irregularities changes wave scattering within the cochlear region affected by MOC activation and, we hypothesize, can result in either increased cancellation or addition of wavelets, producing either overall inhibition or enhancement of SFOAEs.

In the real ear, spatial variations in the forces produces by outer hair cells (OHCs) may be an important source of mechanical irregularity. In the model, these variations can be simulated by varying the gain and frequency tuning of the oscillators in different longitudinal sections of the cochlea partition (Zweig and Shera 1991). In this work, we assume that MOC activation reduces the amplifier gain and tuning sharpness of the innervated oscillators. Simulated innervation patterns were chosen to replicate those exhibited by MOC fibers, as reported for guinea pigs (Brown 2014). The augmented model can be used to generate SFOAES both with and without the activation of a variable number of MOC fibers and at variable fiber attenuations.

The model produces SFOAE vs frequency functions that qualitatively resemble those measured in guinea pigs, both with and without MOC activation. In particular, the simulated MOC effect shows both inhibition and enhancement of SFOAEs. The measured MOC effect on SFOAEs in guinea pigs can be matched quantitatively when as few as six MOC fibers are activated within the 0.5 to 8 kHz region of the cochlea explored by the measurements. Overall, our results indicate that coherent reflection model, augmented with anatomically realistic patterns of MOC innervation, can produce physiologically realistic MOC effects on SFOAEs.

Funding
Work supported by NIDCD grant R01 DC003687.

PS 867

Introducing global coupling to nearest-neighbor models of SOAE generation

Christopher Bergevin
York University

While the existence of spontaneous otoacoustic emissions (SOAEs) provides the most salient evidence for an "active" ear, the underlying generation mechanisms are still not well understood. Both wave-based and local oscillator-based frameworks have been studied, but common ground between them remains unclear (e.g., standing waves versus frequency plateaus; Epp et al. MoH 2014). The present study sought to gain further insight (e.g., role of waves for dynamically coupling elements together) by focusing on a relatively simpler ear that exhibits robust SOAE activity, that of a lizard. The approach taken here is two-fold. First, a theoretical foundation is developed that combines active nonlinear oscillators (Vilfan & Duke, 2008, Biophys. J. 95:4622-4630) with global coupling via the rigid papilla (Bergevin & Shera, 2010, JASA 127:2398-2409). This framework is explored computationally and solved in the time domain. Second, we report some recent OAE data collected from lizards focused on characterizing dynamics of SOAE activity (e.g., response to clicks, tone bursts). The purpose is to use such data as a qualitative benchmark for assessing the validity of the model. While the large parameter space coupled with the nonlinearity introduces challenges, initial findings indicate that the model is capable of capturing some features apparent in SOAE data (e.g., the generation of peaks) but not others (e.g., limited dynamic range, width of peaks). It was also observed that oscillators within a "cluster" (i.e., plateau) exhibit relatively complicated motions and poor phase coherence, indicating the need to better characterize the biomechanical relevance of a cluster.

Funding
Natural Sciences and Engineering Research Council of Canada (NSERC) Discovery Grant

PS 868

Relevance of OAEs in Echolocating CF-Bats

Hendrikus Duifhuis
University of Groningen

The 2nd half turn of the *Rinolophus* cochlea maps the echolocation frequency range. It is characterized with very sharp neural tuning (Q_{10dB} > 100) and an exceptionally detailed cochlear frequency map. The structural transitions from stapes to the 1st half turn in the cochlea, from half turns 1 to 2, and from 2 to 3 have provoked some unsolved questions. If the first half turn (~4mm) would act as an acoustic interference filter (Duifhuis & Vater, 1985) in a linear passive cochlea, then acoustic power in the echolocation frequency band would dissipate at the edge from half turns 1 to 2. However, half turn 2 is clearly active in the entire echolocation range, with a frequency mapping of approx. 0.1 octave over 2 mm. In *R. ferrumequinum* the bony ring in the spiral lamina in the 1st turn has been proposed to play a role in this 'magic' process. However, an alternative interpretation, in line with other more recent findings would be that *active* processes in the (healthy) cochlea compensate for the damping. In other words, in the healthy cochlea the net damping would be negligible at low levels [implying no damping at low levels, but nonlinear growth at higher levels, thereby also generating distortion products, but not necessarily SOAEs]. The mechanism is even more plausible in bats that have significant SOAEs [e.g., *Pteronotus*].

We will demonstrate that a regular travelling wave at RF (the Resting Frequency of the echolocation frequency range) will be generated if the local damping vanishes (at least at low levels). Without the damping reduction -without active processes- the RF-frequencies do not set up a traveling wave. Instead they are dissipated at the entrance of the 2nd cochlear half turn.

-H. Duifhuis and M. Vater (1985) On the mechanics of the horseshoe bat cochlea, in: Proceedings MoH 1985, (Springer), pp 89-96

-M. Vater, A.S. Feng and M. Betz (1985). An HRP-study of the frequency-place map of the horseshoe bat cochlea: Morphological correlates of the sharp tuning to a narrow frequency band, J.comp.Physiol.157, 671-686

-M. Vater and M. Kössl (2011). Comparative aspects of cochlear functional organization in mammals. Hearing Res. 273, 89-99.

Funding

PS 869

Transient Emissions Induced by High-Frequency "Suppressors" in a Cochlear Model with No Roughness

Yi-Wen Liu
National Tsing Hua University

Background

Transient-evoked otoacoustic emissions (TEOAEs) have been regarded as a result of coherent reflection from the characteristic places of individual spectral components. The suppression tuning of TEOAEs should therefore provide an estimate of the breadth of cochlear filters. Recent experiments (Siegel and Charaziak, 2014), however, found that OAEs evoked by a tone burst could be inferred even when the suppressor frequency (f_{sup}) is three times higher than that of the probe (f_p). This finding seems to contradict with the coherent reflection theory, which predicts that TEOAEs are generated near the best place (BP) of the probe. The aim of the present work is to provide a computational framework for an alternative explanation --- the emissions might have been generated, instead of being suppressed, by the high-frequency suppressor due to an impedance mismatch it creates near its BP.

Method

An iterative approach that involves quasi-linearization is developed to predict the change in characteristic impedance for any small perturbation when a strong steady tone is present. The change in impedance depends on the level of the suppressor (L_{sup}) due to nonlinearities in outer hair cell transduction. The longitudinal variation of the impedance causes traveling waves to reflect partially. This approach should be applicable for any transmission-line model of cochlear mechanics with localized instantaneous nonlinearities. A previously developed model (Liu 2014) is adopted. This model does not include roughness, so coherent reflection is not expected.

Results

Numerical experiments have been conducted with f_{sup} = 7-14 kHz, L_{sup} = 60 dB SPL and f_p = 2-4 kHz. Typically, the characteristic impedance decreases by as much as 30% near the suppressor's BP. Consequently, the probe gets reflected near the BP of the suppressor, and the magnitude of the reflected component reaches 20 dB below that of the forward-going component in the cochlea. When exiting through the middle ear, it gives rise to an emission at approximately 40 dB below the stimulus in the ear canal. The group delay (<1 ms) decreases when f_{sup} increases. These results agree qualitatively with experiments. Comparison against time-domain simulation also validated the accuracy of the present calculation.

Conclusion

Results suggest that, while we mean to suppress transient OAE with a suppressor tone, its very presence might induce an emission through nonlinear scattering when the suppressor's frequency is higher than that of the probe. This wave-scattering mechanism complicates the interpretation of TEOAE data from existing experiments.

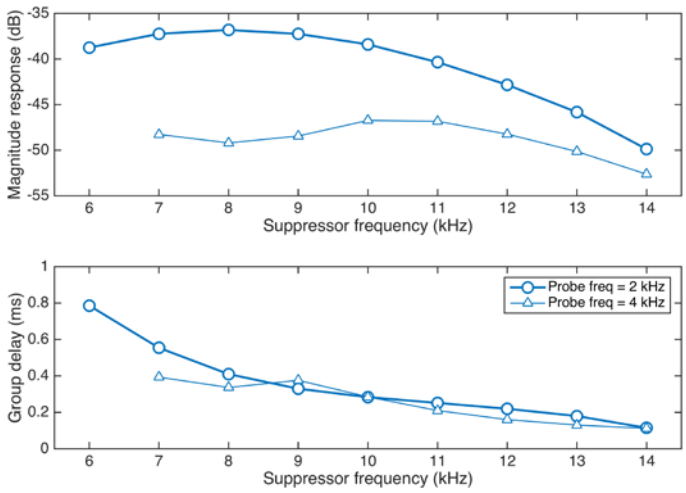

Figure 1: the magnitude and group delay of the TBOAE, predicted by the model, as a function of suppressor frequency. The probe frequency is 2 or 4 kHz.

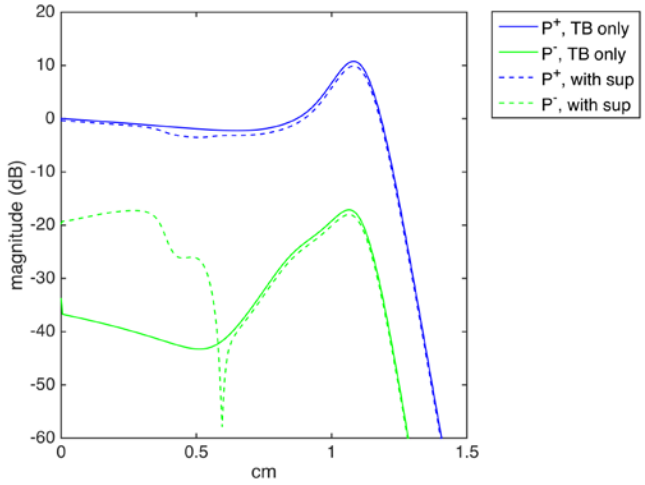

Figure 2: Decomposing the 4-kHz traveling waves into the forward-going (P+) and the backward-going (P+) components. Results with tone-burst (TB) only vs. with the suppressor are shown for comparison.

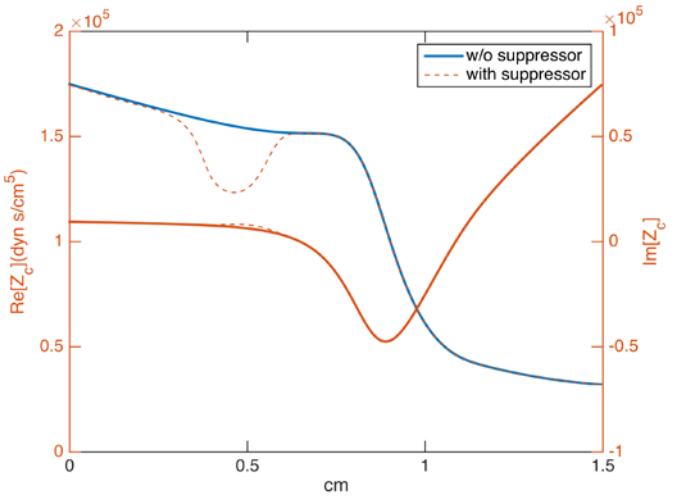

Figure 3: Spatial variation of the characteristic impedance (Zc) for the 4-kHz probe. When a 9-kHz suppressor is present, the real-part of Zc decreases significantly near the 9-kHz best place.

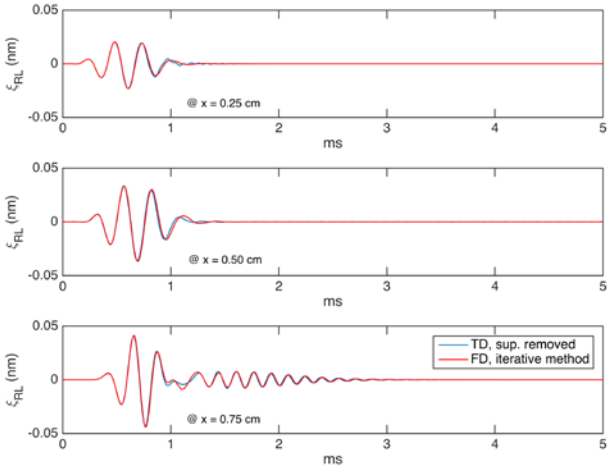

Figure 4: Comparison of results obtained from the frequency-domain (FD) iterative approach against time-domain (TD) simulation with suppressor removed.

Funding
Ministry of Science and Technology, Taiwan (Grant No. 103-2221-E-007-085-MY2).

PS 870

Transient Induction of Deafness by Optogenesis Targeting the Endocochlear Potential in the Inner Ear

Mitsuo Sato[1]; Fumiaki Nin[1]; Taiga Higuchi[1]; Satoru Uetsuka[1]; Takamasa Yoshida[1]; Masatsugu Masuda[2]; Takahisa watabe[3]; Sho Kanzaki[3]; Kaoru Ogawa[3]; Katsumi Doi[4]; Hirohide Takebayashi[1]; Kenji Tanaka[3]; Hiroshi Hibino[1]
[1]University of Niigata; [2]University of Kyorin; [3]University of Keio; [4]University of Kinki

Introduction

More than ten percent of world population currently suffer from hearing loss, which is primarily caused by disorders in the inner ear in both congenital and acquired conditions. In the latter, some cases that show reversibility at the early stage become irreversible and finally result in refractory hearing loss. To develop new drugs and therapeutic strategies for the disease, creation of model animals that mimic reversible sensorineural hearing loss (SNHL) in human is crucial. In the present study, we have accessed this issue by using optogenetics.

There are three target tissues for SNHL in the cochlea; spiral ganglion neurons, hair cells and stria vascularis. Of these, the stria vascularis is an epithelial tissue that maintains a highly positive potential of +80 ~ +120 mV in the endolymph. This called endocochlear potential (EP) maximizes the sensitivity of the hair cells. The loss of the EP induces deafness. We have optogenetically dysfunctioned the stria.

Methods

We used a bigenic approach involving a tet-inducible promoter system. We generated transgenic mice with a cell type-specific promoter driving a tetracycline-controlled transcriptional activator (tTA) expressing allele. We also generated transgenic mice with the tTA-dependent promoter (tetO) driving the expression of channelrhodopsin-2 (ChR2), a blue light-gated, nonselective, cation channel. And then, we performed crosses between mice from the two sets to obtain animals expressing ChR2 (Tanaka KF, et al : Cell Rep. 2012).

Results

Measurement of auditory brainstem response revealed that hearing threshold of the double transgenic mice was increased by ~20 dB when their cochleae were exposed to blue light. Histological assays detected that, of multiple cell types in the stria, only intermediate cells expressed ChR2. Electrophysiological experiments demonstrated that the illumination sharply reduced the EP by 25 mV in a few seconds. Upon cessation of the light exposure, the EP was completely recovered within 5 minutes. The extent of the EP reduction depended on duration and intensity of the illumination.

Conclusions

We have described temporal control of deafness accompanied by the EP reduction in the ChR2-expressing mice. The mice may serve useful tools to study reversible or transient hearing disorders.

PS 871

Using fNIRS to study Neuroplasticity and Speech Perception in Cochlear Implant Users

Xin Zhou[1]; Adnan Shah[1]; Abd-Krim Seghouane[1]; Ruth Litovsky[2]; Colette McKay[1,3]
[1]The University of Melbourne; [2]The University of Wisconsin-Madison; [3]The Bionics Institute of Australia

Auditory speech understanding varies among cochlear implant (CI) users. Peripheral factors including etiology, duration of deafness, onset of deafness, and CI experience can only explain some (~20% of the variance). Imaging studies have shown that in adult CI users, central neuroplasticity occurs after post-lingual deafness and that neural response measures could be correlated with CI outcome. Deaf patients might adopt different communication strategies, which can affect the type and degree of neuroplasticity that occurs as a result of deafness. The aim of this experiment was to use a non-invasive imaging technique to explore where in the brain neuroplasticity has occurred in CI users, and to investigate the correlation between neuroplasticity and speech understanding. We hypothesized that the brain activation pattern of CI users to auditory or visual speech is different from that in normal-hearing people, and that functional near-infrared spectroscopy (fNIRS) can reveal these differences. We further hypothesized that the brain activation to speech in at least one region of interest in CI users is related to their auditory speech understanding performance after implantation.

Participants were 15 post-lingually deafened adult CI users with varying auditory speech understanding ability, and a group of age-matched normal-hearing controls. Three measures were made in this study. First, brain activation was measured using fNIRS while participants performed lip-reading and auditory speech listening tasks. Second, auditory speech understanding was measured in quiet and in background noise. Third, lip-reading ability was measured with visual-only stimuli.

Results were compared between the two groups in order to identify brain “regions of interest,” i.e., areas of activation that differentiated the CI group from the normal-hearing group. In addition, the correlation between activation in the regions of interest and auditory speech understanding ability was computed. Experimental results verified the hypothesis that fNIRS could reveal the neuroplasticity in CI users that is correlated with their auditory speech understanding.

Funding
Supported by a Melbourne University PhD scholarship to ZX, a veski fellowship to CMM, an Australian Research Council Grant (FT130101394) to AKS, the Australian Fulbright Commission for a fellowship to RL, the Lions Foundation, and the Melbourne Neuroscience Institute.

PS 872

Late Maturation of the Response to Perceptual Training on a Non-Native Phonetic Categorization Task

Beverly Wright[1]; Julia Huyck[2]; Nicole Marrone[3]
[1]Northwestern University; [2]Kent State University; [3]University of Arizona

Introduction
Many auditory skills improve with practice, enabling optimization of normal and disordered auditory capacities. To investigate how the requirements for effective training change during development, we have been comparing learning outcomes between adolescents and young adults trained with the same regimens. We previously documented that training regimens that yield learning reliably in young adults can fail to do so in adolescents, suggesting that the response to perceptual training has a long developmental course. In those investigations, the trained task was the detection or discrimination of simple sounds and the training regimen required performance of the trained task throughout each training session. Here we asked whether late maturation of the response to perceptual training extends to a categorization task with speech stimuli and to more varied training regimens.

Methods
We trained different groups of normal-hearing adolescent (~12 years) and young adult (~22 years) native-English speakers on a non-native phonetic-categorization task along a voice-onset-time continuum using one of three training regimens: (1) Task Only: Task performance (240 trials/day). (2) Task+Sound Only [written task]: Task performance (120 trials/day) alternating every 60 trials with stimulus-exposure alone while performing a written symbol-to-number matching task (120 trials/day). (3) Task+Sound Only [visual task]: As in (2) but with a visual picture-repetition task instead of a written task during the periods of stimulus-exposure alone. Each regimen consisted of a pre-test, training phase, and post-test on each of two consecutive days.

Results
All three training regimens were less effective in adolescents than young adults. Starting performance did not differ between the two age groups. Young adults improved with all three regimens, and learned twice as much with the Task+Sound Only [written task] regimen as the Task+Sound Only [visual task] and Task-Only regimens. Adolescents improved only half as much as adults on the Task+Sound Only [written task] regimen, and did not improve at all with the other two regimens.

Conclusions
These results extend the previous evidence that the response to perceptual training has a long developmental course to a new task (categorization) and more complex stimuli (speech syllables), and demonstrate that it is possible to quantify differences in the effectiveness of various perceptual training regimens during development. That adolescents learned with one regimen suggests that their failure to learn with the others may arise from immaturity of specific learning processes

rather than of general capacities needed for learning. Thus, training regimens could be optimized by keeping development in mind.

Funding
NIH: NIDCD

PS 873

Population Receptive Field Mapping of the Auditory Cortex and Subcortex in People with Absolute Pitch

Larissa McKetton; Kevin DeSimone; Keith Schneider
York University

Introduction
Using high-resolution functional magnetic resonance imaging (fMRI), recent studies have been able to measure in detail the tonotopic organization of the human auditory cortex. However, the exact orientation of primary gradients of Heshl's gyrus (HG) are still debated, which has led to various interpretations of the locations of the primary auditory cortex and surrounding fields. Auditory subcortical structures such as the inferior colliculus and medial geniculate nucleus (MGN) remain less studied, as they are harder to resolve due to their small size. Population receptive field (pRF) analysis is a relatively recent method to study the organization of sensory areas in the brain. It involves fitting a model to each fMRI voxel to best explain its responses to a variety of stimuli. In our study we use the pRF methodology to measure the organization of the auditory cortical and subcortical structures. Our subject population is composed of people with absolute pitch, a musical skill in which people can identify isolated notes without a reference note.

Methods
Each participant had their cortex and subcortex scanned at 1.5 x 1.5 x 2 mm^3 resolution using a Siemens Trio 3T MRI scanner and 32-channel head coil at the York MRI Facility. We stimulated the auditory system using pure tone logarithmic chirp sweeps modified from De Martino *et al* (2012) to conduct tonotopic mapping and tuning bandwidth maps of the auditory cortical and subcortical regions using fMRI. We analyzed the data using an adaptation of the population receptive field (pRF) technique developed by Dumoulin and Wandell (2008), used initially for retinotopic mapping. The pRF approach can also be used to estimate different neuronal population quantities such as sound frequencies in auditory cortex. Our model treated the pRF underlying each voxel's response as a one-dimensional Gaussian function of frequency providing an estimated sensitivity function for each voxel with a given center, or preferred frequency, and standard deviation, or tuning bandwidth.

Results
Both eccentricity and angle information was derived from the 1D Gaussian models and plotted on the unfolded cortical surface for each hemisphere in each subject. Using our analysis technique, we were able to obtain reliable tonotopic and tuning bandwidth maps within the auditory cortex and subcortex in humans.

Conclusions
Our data has helped reveal the variability and consistencies of auditory processing pathways in normal human controls. This technique can be applied to studying differences in special populations with auditory processing such as absolute pitch.

Funding
The authors acknowledge the following funding sources, the Natural Sciences and Engineering Research Council of Canada (NSERC), the Dorothy Pitts Research Fund (NG).

PS 874

Effects of Hearing Loss on Auditory and Visual Cognitive Processing in Older Adults

Kristina Backer; Kate McClannahan; Kelly Tremblay
University of Washington

Background
With age, many people experience progressive sensorineural hearing loss (SNHL), resulting in partial auditory deprivation. Previous research, in both animals and humans, has demonstrated that SNHL can induce changes along the auditory pathway from the cochlea to auditory cortex. However, much less is known about how SNHL in older adults may impact cognitive processes beyond auditory cortex, such as attention and memory, and if these putative cognitive effects are auditory-specific or also extend to other sensory modalities. Thus, the goal of this study was to examine how SNHL in older adults affects cognitive processing of both auditory and visual stimuli, using electroencephalography (EEG).

Methods
To assess auditory and visual cognitive processing, normal hearing (NH) and SNHL participants performed a computer-based task, during EEG recording. On each trial, a stimulus array comprising two sounds and two pictures (corresponding to four different objects) was presented. Before or after the stimulus array, participants were cued (via visually-presented symbols) to attend and remember only pictures (Visual Cue) or only sounds (Auditory Cue). At the end of each trial, one picture or sound was presented, and participants judged if it was "Present" or "Absent" in the stimulus array. EEG analyses were time-locked to the visually-presented cues to examine cognitive processing independent of audibility.

Results
The SNHL group responded more slowly on both Auditory and Visual Cue trials than the NH group. Furthermore, EEG analyses revealed group differences in sustained potentials following both Auditory and Visual Cues, occurring 500 ms and later after cue onset.

Conclusion
These results suggest that SNHL affects higher-level cognitive processes, beyond auditory cortex, that are important for speech understanding, especially in acoustically-adverse environments.

Funding
Funding from NIH-NIDCD (T32 DC005361: awarded to KCB and KSM; P30 DC004661: supported participant recruitment), internal departmental funding (KLT), the Virginia Merrill Bloedel Hearing Research Travel Scholar Award (KLT), and the American Academy of Audiology Foundation Student Investigator Research Grant (KSM) supported this research.

PS 875

Change Deafness is Reduced but not Eliminated by Practice

Vanessa Irsik; Joel Snyder
University of Nevada, Las Vegas

Background
There is a growing literature on auditory change detection which suggests that listeners often miss rather large changes in their environment, a phenomenon now referred to as *change deafness*. Recent reports suggest that failures to notice auditory changes frequently occur due to unsuccessful encoding (Gregg, Irsik, & Snyder, 2014). Efforts to improve encoding ability have been reported in the visual domain, and suggest that visual detection failures, or *change blindness*, can be ameliorated using training with feedback (Gaspar et al., 2013). However, it remains to be shown to whether *change deafness* can likewise be reduced or eliminated through training. One reason that encoding failures may occur in the auditory domain is that listeners may struggle to segregate and fuse the correct features for each co-occurring sound. The central aim of the current study was to improve encoding and reduce change deafness by training individuals to better individuate co-occurring sounds.

Methods
Participants completed change detection trials during a pre-test, a training activity, an immediate post-test, and a second post-test 12 hours later. During each trial participants heard two auditory scenes separated by a 350 ms silent interval, after which they were asked to make a same/different judgment. Each scene was composed of six 1,000 ms band-passed filtered white noise rhythms, with each stream consisting of a different rhythm. The training activity involved either testing and receiving detailed feedback on performance, testing without feedback with short inter-trial intervals, testing without feedback with longer inter-trial intervals (to match the trial onset with those receiving lengthy feedback), or a control condition where listeners watched a documentary instead of training. During detailed feedback, listeners were told the correct response and reheard both the individual changed sound in isolation and the entire change detection trial.

Results
Those who received detailed feedback during training improved significantly across test sessions, and showed a 14-point reduction in percent error from the pre-test to post-test two. Both groups that tested without feedback (average error reduction= 8%) as well as the control group (error reduction = 9%) had reduced error across test sessions, but to a lesser extent.

Conclusions
All groups showed significant improvement; however, receiving detailed feedback resulted in the greatest error reduction. In summary, change deafness was reduced, but not eliminated, as a result of training or testing. Future studies should address the benefit of additional training and the longevity of observed perceptual enhancements.

Funding
Supported by Army Research Office grant W9IINF-I2-I-0256

PS 876

Neural Correlates of Auditory-Tactile Integration

Juan Huang[1]; Tianxu Wu[2]; Xiaoqin Wang[1]
[1]Johns Hopkins University; [2]Tsinghua University

Previous studies have shown that concurrently presented auditory and tactile stimulation can be integrated. A recent study from our lab has provided evidence of auditory and tactile integration in music meter perception even if when stimuli from the two modalities are not presented simultaneously. How the brain accomplishes this integration still remains mostly unknown. In this study, we examined the neural correlates of auditory and tactile integration. Event Related Potentials (ERPs) were recorded from 15 human subjects while they were presented with uni-modal auditory, uni-modal tactile, or bi-modal music note sequences. Results showed that when a stimulus sequence contained meter structure, steady-state evoked responses (SSERs) reflecting the rhythm frequency was significantly enhanced in bi-modal conditions than in uni-modal conditions. Such bi-modal enhancement in SSERs was not observed in sequences with the same rhythm frequency but without meter structure. In addition, the phase coherence of SSERs in bi-modal condition is greater in bimodal conditions than in uni-modal conditions. Comparing with the uni-modal stimulation, bi-modal stimulation produced ERPs with significantly shorter latencies and larger amplitudes, indicating that the brain can integrate auditory and tactile stimuli when both are presented. In summary, this study shows that the auditory-tactile integration significantly enhances the neural processing of meter structure. These findings help further understand how the brain processes temporal patterns of sensory inputs and performs multi-modal integration.

PS 877

Responses to Social Vocalizations in the Mouse Basolateral Amygdala

Emily Hazlett; Jasmine Grimsley; Jeffrey Wenstrup
Northeast Ohio Medical University

Mice emit vocalizations in many different behavioral contexts. During a variety of social interactions, adult male and female mice emit song composed of ultrasonic vocalizations (USVs), with features and emission patterns that differ with context. Mice also emit broadband vocalizations with warbled and chaotic harmonics (noisy calls) and with harmonic stacks (LFH calls). Noisy calls are typically emitted by isolated mice, while LFH calls are emitted by female mice during mating

and by both sexes in response to distress. We have shown that the basolateral amygdala (BLA) contributes to analysis of LFH meaning by integrating information from several senses. This study assesses responsiveness of BLA neurons to other social vocalizations and other auditory stimuli.

Using wireless technology, we recorded spiking activity and local field potentials (LFP) from 13 awake, free-moving, adult CBA/CaJ mice with custom multi-electrode implants. Responses to social vocalizations were tested using 40 repetitions each of a range of vocal stimuli including nine USV syllables, the noisy call, and the LFH call. These stimuli were presented at a rate of 1/s in both randomized and repeated, or blocked, patterns. We also obtained responses to broadband noise (BBN) and to pure tones over a range of frequencies and levels.

Responsiveness to vocal stimuli was assessed for 63 neurons in the BLA. Of these, all were presented with the randomized stimulation pattern and 40 were also presented with the repeated pattern. Overall, 27% (17/63) of neurons responded to vocalizations and 16% (10/63) responded to BBN. Frequency response areas were typically disorganized, but tended to be high threshold with best responses below 30 kHz. Neurons were highly selective to vocalizations under these recording conditions, on average responding to 1.4 of 11 vocalizations presented (SD = 0.63). Vocalizations were more likely to evoke a response in a randomized presentation pattern (24%, 15/63) than in a repeated pattern (8%, 3/40). Across presentation patterns, only one neuron responded to a USV, whereas 41% (7/17) of vocalization-responsive neurons responded to the noisy call and 88% (15/17) responded to the LFH call. LFP responses to acoustic stimuli were comparable in selectivity and frequency tuning to the single unit data.

These results show that mouse BLA responses to social vocalizations are highly selective and depend on the temporal patterning of stimuli. Further, these results suggest that the mouse BLA may respond preferentially to negative vocalizations.

Funding
R01 DC00937

PS 878

Comprehensive Comparison of Various Deafening Methods

Ina Shehu[1]; Julia King[2]; Mario Svirsky[2]; Robert Froemke[2]
[1]Hunter College, New York; [2]New York University, School of Medicine

Disabling hearing loss affects 360 million people worldwide, has a number of etiologies, and can be classified in numerous of ways (WHO, 2015). In order to examine the neural basis of hearing loss and potential for hearing recovery, it is critical to utilize consistent methods of inducing and measuring hearing loss in animal models. Currently, many methods exist to induce hearing loss in rodents, but it is unclear on how they compare with one another.

We are comparing common deafening methods in adult rats using three independent hearing assessments: physiological, by measuring auditory brainstem responses (ABRs); behavioral, by using a frequency-recognition go/no-go task (Froemke et al, 2013; Martins and Froemke, 2015); and anatomical, by examining cochlear histology. Following acquisition of a baseline ABR and behavioral performance, we examine deafness induced by four different procedures: malleus removal (Tucci et al., 1999), physical cochlear trauma (Lu et al., 2005), or intracochlear (Murillo-Cuesta et al., 2009) or systemic ototoxic drug administration (Hartley et al., 2010). In normal hearing animals, baseline ABRs had normal waveforms and typical thresholds. Baseline behavioral performance indicated that animals were proficient at identifying the target tone while avoiding foil tones and that this task could assess behavioral hearing thresholds, which were comparable to click ABR thresholds (behavior: 36±2 dB SPL, ABR: 35±3 dB SPL, $p>0.8$).

Following surgery, behavioral performance and ABRs were re-assessed. While ABR waveforms were abolished up to 90 dB SPL following either malleus removal or cochlear trauma (before: 35±2 dB SPL, after: nonresponsive, $p<0.01$), behavioral responses were not equally decimated. Animals with malleus removal were able to perform the task (d' before: 1.64±0.2, d' after: 1.46±0.4, $p>0.05$), although their behavioral hearing thresholds increased (before: 33±5dB SPL, after: 47±6 dB SPL, $p<0.05$). In contrast, animals with cochlear trauma were unable to perform the task (d' before: 1.87±0.06, d' after: 0.08±0.1, $p<0.01$) and we were not able to assess behavioral hearing thresholds (before: 36±5dB SPL, after: nonresponsive, $p<0.01$). Initial histologic comparison of the cochleae from all animals does not show gross pathology (e.g., fibrosis); we are currently quantifying changes in hair cell, spiral ganglion neuron, and peripheral nerve counts to see if these changes can account for the degree or type of hearing loss (Kopelovich et al., 2015). Together these data indicate that ABRs and auditory behavior assess different aspects of hearing loss. Comprehensive hearing loss assessment is therefore critical to inform the choice of deafening method.

Funding
NIDCD, NYU Grand Challenge

PS 879

Development of Context Dependence in the Mouse Auditory Cortex

Sharba Bandyopadhyay; Muneshwar Mehra
IIT Kharagpur

Preceding stimulus history affects the responses of auditory cortical neurons. Long range (several seconds) temporal effects in auditory cortex is hypothesized to be a potential neural substrate for auditory processing that requires integration over timescales of seconds or longer, such as stream segregation, stimulus specific adaptation and deviance detection. In this study we specifically investigate auditory cortical single unit responses to a tonal sound (D, deviant) in the midst of a series of broadband noise tokens (S, standard) or a broadband sound (D) in the midst of a series of

tone tokens (S). By comparing the responses of the D sound presented by itself and in the context of S we can investigate the context dependence of responses. The development of context dependence is studied here, from early hearing stages to young adults in a depth specific manner, using single units from superficial (II/III), input (IV) and deeper (V/VI) layers.

Single unit activity in response to brief (50-100 ms) tone pips and noise pips at multiple sound levels and to SS…SDS…S kind of stimulus sequences were collected simultaneously from multiple neurons from the auditory cortex of developing mice (C57BL6 male and female, ages: postnatal day 13-42, P13-P42) from multiple depths (grouped in superficial, input and deeper layers: 0-400, 400-600 and above 600 microns). Units were confirmed to be in the primary auditory cortex (A1) based on response latency and frequency tuning observed across multiple electrodes/units. A context dependence index (CDI) is defined based on responses of D in the context of S and responses of D by itself to quantify context dependence in populations of neurons.

Across the populations of neurons at different depths and different ages we find a wide variety of types and strengths of context dependence. We observe strong context dependence (stronger responses to D in context of S as opposed to D itself) of tonal sounds in deeper layers to be present at early ages, which is absent in superficial layers. However, the opposite effect is observed in terms of context dependence of broadband noise sounds, with strong context dependence in superficial depths developing. Development of such differential processing of tonal and noise stimuli is related to observed circuitry development in A1.

Funding
Wellcome Trust DBT India Alliance Grant to SB, CSIR Fellowship to MM, IIT Kharagpur Internal Funds to SB

PS 880

The Differential Effects of Adult-Onset Noise-Induced Hearing Loss on Laminar Processing in Multisensory and Auditory Cortical Areas

Ashley Schormans; Marei Typlt; Brian Allman
University of Western Ontario

Background
Complete or partial hearing loss results in an increased responsiveness of neurons in the auditory cortex to visual and/or tactile stimuli (i.e., crossmodal plasticity). Our recent work has demonstrated that the multisensory cortex—an area which is capable of integrating audiovisual stimuli—also shows an increased responsiveness to visual stimuli following partial hearing loss. In the present study, we investigated the effect of noise-induced hearing loss on laminar processing in multisensory and auditory cortical areas.

Methods
Adult male Sprague-Dawley rats (n=6) underwent an auditory brainstem response (ABR) test to determine their baseline hearing levels, followed by a bilateral noise exposure (0.8-20 kHz at 120 dB for 2 hours). Two weeks later, hearing levels were reassessed, and acute electrophysiological recordings were performed under ketamine/xylazine anesthesia. In vivo extracellular electrophysiological recordings were made with a 32-channel electrode that was inserted perpendicular to the cortical surface so as to record across all cortical layers simultaneously in the lateral extrastriate visual cortex (V2L), and then the dorsal auditory cortex (AuD). For each penetration, computer-generated auditory (noise burst), visual (light flash) and combined audiovisual stimuli were delivered, and the associated local field potentials (LFPs), and spiking activity were compared to that of age-matched controls (n=6).

Results
Noise exposure increased the ABR click threshold 17±3 dB. Despite adjusting the sound intensity to account for each rat's hearing level, analysis of the averaged rectified current source density (AVREC) revealed a 50% reduction of peak amplitude in V2L to auditory and audiovisual stimuli in noise-exposed rats, as well as an increased peak amplitude to visual stimuli. In contrast, AuD showed increased peak amplitudes of 25% to auditory and audiovisual stimuli in noise-exposed rats. Current source density (CSD) analysis showed increased sink amplitudes to visual stimuli and decreased sink amplitude to auditory and audiovisual stimuli across most cortical layers in V2L. Conversely, following noise exposure, AuD showed increased sink amplitudes in only the granular layer to auditory and audiovisual stimuli.

Conclusions
The degree and nature of crossmodal plasticity differed across cortical areas; the multisensory area, V2L, showed a decrease in auditory input across all cortical layers, whereas the predominantly auditory area, AuD, showed increased auditory input in the granular layer following adult-onset noise-induced hearing loss.

Funding
NSERC Discovery Grant & CIHR Open Operating Grant

PS 881

Visual Deprivation Enhances the Excitability of Layer 3/4 Pyramidal Neurons of Primary Auditory Cortex

Toshio Suzuki; Hideki Kawai
Soka University

Visual deprivation leads to crossmodal changes in auditory cortex. Recently, it was reported that dark rearing of mice enhanced thalamocortical inputs from auditory thalamus to thalamo-recipient layer (layer 3/4) neurons of primary auditory cortex (A1) Here, we investigated whether intrinsic properties of layer 3/4 pyramidal neurons change due to enculation. We examined passive neuronal properties in sighted and enucleated mice and changes in intrinsic excitability due to high frequency firing (HFF) stimulation.

We recorded membrane potentials in the current-clamp mode using auditory thalamocortical slices prepared from

mice enucleated or sham-operated at postnatal day 15, and reared for 8-11 days. In response to +100 pA depolarizing current injections, first after-potentials were more depolarized in enucleated mice compared with sighted mice. In sighted mice, most neurons (24 out of 25 neurons) demonstrated regular spiking (RS) patterns, while one neuron showing initial "doublet spiking (DS)" (>30 Hz inter-spike interval of initial two action potentials, and first after-potential peak is higher than spike threshold.). Meanwhile, in enucleated mice, 8 out of 26 neurons (31%) showed DS firing patterns with the rest having reduced afterhyperpolarization, suggesting that visual loss leads to increases in neuronal excitability. Comparing intrinsic properties of RS neurons in the sighted mice (sighted RS), DS neurons of enucleated mice (blind DS) showed lower spike threshold, shorter onset latency, and larger spike amplitude with an increase in hyperpolarization-induced depolarizing ("sag") potentials.

We then tested the effect of HFF (15 times at 40 Hz for 10 min at 0.25 Hz) on neuronal properties for possible long-term changes in intrinsic excitability. After HFF stimulation, resting membrane potential (RMP) increased for at least 25 min in sighted RS neurons as well as blind RS and blind DS neurons. Although spike onset latency decreased in any neuron types, the number of action potentials did not increase, perhaps due to elevated spike threshold. We did observe, however, differences in RMP during HFF stimulation. While RMP rapidly declined ~2 mV within initial 1 min in all neuron types, subsequent changes in RMP differed among them. Thus, the decreased RMP persisted for the rest of 10 min HFF in sighted RS and blind DS, but it recovered in blind RS neurons.

Overall, visual deprivation resulted in increased excitability in layer 3/4 neurons with more depolarized first after-potentials and increased doublet spiking, while RMPs in blind RS showing recovery following their reduction during HFF.

Funding
Japan Society for the Promotion of Science (No. 23500402)

PS 882

Frequency Modulation Discrimination by CBA/CaJ Mice

Laurel Screven; Micheal Dent
University at Buffalo

Introduction
The ability to communicate with others implies a fundamental understanding of differences in the vocalizations that are created. In mice, acoustic communication includes vocalizations that differ in many characteristics, including frequency and duration. Mice are able to vocalize in ultrasonic frequency ranges, with many of their vocalizations in the 60-80 kHz range. Mice produce ultrasonic vocalizations (USVs) in social situations but the function of these vocalizations is still somewhat unclear (Hanson & Hurley, 2012). Additionally, there has been little work done to show that mice are able to differentiate between their vocalizations (but see Neilans et al., 2014). Some of the most common vocalizations mice produce sweep upwards in frequency (upsweeps). Mice also produce downsweeping vocalizations (downsweeps). Consequently, it is expected that the mice should not have difficulty differentiating between artificial frequency modulated stimuli within the same frequency range as their natural calls. Determining the ability of mice to discriminate between these stimuli will expand the current knowledge about acoustic communication in mice.

Methods
In the present study, the mice were trained and tested using operant conditioning procedures and positive reinforcement to discriminate between artificial upsweeps and downsweeps. Multiple stimulus frequency ranges and durations were tested in a nose poking task. The animals were required to respond when they heard a change in the repeating background.

Results
The mice had difficulty discriminating between background and target upsweeps and downsweeps when the stimuli occupied the same bandwidths, even when the stimuli also differed in duration. However, when the sweeps occupied different frequency ranges, discrimination performance improved. For example, when the repeating background downsweep ranged from 80 to 60 kHz, it was much more difficult for the mouse to discriminate a target sweeping from 60 to 80 kHz than 50 to 80 kHz. Overall, bandwidth, not sweep direction or duration, appeared to be the primary cue for discrimination.

Conclusions
These results collected using artificial stimuli created to mimic natural USVs indicate that the bandwidth of vocalizations may be much more important for communication than the frequency contour of the vocalizations. This was surprising given the seeming complexity of many of the ultrasonic vocalizations of mice, and the many categories of vocalizations created by researchers attempting to understand acoustic communication in mice.

Funding
This work was supported by NIH DC012302.

PS 883

Echo-acoustic Flow Guides Flight in Bats

Kathrin Kugler
Ludwig Maximilian University of Munich

Common to all airborne animals is the need to react fast and correct to rapid changes in their environment during flight. Visually guided animals tackle this challenge by evaluating optic flow, generated by their movement through structured environments.

Echolocating bats flying in complete darkness cannot make use of optic flow; they can navigate solely by echolocation, i.e. the auditory analysis of self-generated sounds. In contrast to vision, echolocation provides explicit distance information through the analysis of echo delay.

Here we show that bats exploit echo-acoustic flow to navigate rapidly through narrow passages. Specifically, we find that bats' navigation between lateral structures is significantly

affected by the echo-acoustic salience of those structures, independent of their physical distance. This is true despite the stroboscopic nature of echolocation which interferes with a motion percept and although echolocation, unlike vision, provides explicit distance cues.

The results demonstrate that sensory flow elicited by self motion is a ubiquitous principle for guidance of flight in the animal kingdom, independent of the fundamentally different peripheral representation of flow information across the senses of vision and echolocation.

Funding
The study was funded by a grant of the Deutsche Forschungsgemeinschaft (DFG) WI 1518/12-1 to L.W..

PS 884

Probing the Behavioral and Physiological Mechanisms Underlying Vocalization Discrimination in the Common Marmoset (Callithrix jacchus)

Michael Osmanski; Xiaoqin Wang
Johns Hopkins University

The common marmoset is a small, arboreal New World primate with a rich vocal repertoire. Several different classes of vocalizations have been described for this species and there is evidence that many of these vocalizations serve roles in group maintenance, individual identification, territorial defense, and other behaviors. However, we know surprisingly little about how these vocalizations are actually perceived by these animals and even less about the primary acoustic features that define particular call types. Further, almost nothing is known about the neural underpinnings of vocal perception in marmosets. We began to address these questions by training marmosets using operant conditioning techniques to discriminate among several variants of both natural and artificial vocalizations.

Marmosets were first trained to discriminate within- and between-class variants of their species-specific vocalizations (i.e., twitter, phee, etc). Results show that marmosets took longer to correctly discriminate within-class vocalizations (e.g., twitters vs. twitters) compared to between-class vocalizations (e.g., twitters vs. phees). We analyzed response latencies derived from this task using multidimensional scaling (MDS) procedures, which arrange those latencies into a multidimensional space that reflects their underlying perceptual organization. The resulting MDS representation shows distinct clusters of vocal stimuli that correspond to previously defined call types for this species.

We then created a series of virtual vocalizations for each call type that monotonically deviated away from the mean population value for a single acoustic parameter (e.g., dominant frequency, FM rate, etc.). Results from behavioral experiments utilizing these stimuli showed that marmosets appeared insensitive to changes in a single acoustic parameter for a given call type over a range of ~1–2 SD of the population mean for that call type. Furthermore, marmosets showed less sensitivity to variations in their species-specific vocalizations compared to similar variations in simpler stimuli (e.g., pure tones, sFM tones, etc.), which suggests potential specializations for vocal perception by marmosets.

Finally, we examined changes in neural activity across auditory cortex including putative core (A1 and R) and lateral belt auditory fields while marmosets engaged in a discrimination task or passively listened to the same stimuli. Our results showed significant changes in stimulus-evoked firing rates during active behavior compared to passive listening, including a suppression of onset responses along with increases in sustained activity during task engagement.

Funding
Supported by NIH grants DC003180 to XQW and DC013150 to MSO

PS 885

Psychoacoustic Estimates of Cochlear Gain Reduction at 2 and 4 kHz

Kristina Milvae; Elizabeth Strickland
Purdue University

The medial olivocochlear reflex (MOCR) is a physiological mechanism that reduces cochlear gain in response to ipsilateral, contralateral, and bilateral sound. This reflex is hypothesized to maintain sensitivity to changes in incoming sound. However, the amount of gain reduction across frequency is not known for human listeners. The temporal effect is a psychoacoustic measure thought to reflect a decrease in cochlear gain. It is the improvement in threshold for a short tone as it is delayed from the onset of a masker. The temporal effect is larger for higher frequencies than for lower frequencies. However, the temporal effect may be confounded by suppression when measured using simultaneous masking. Gain reduction has been estimated at 4 kHz using forward masking, which avoids the effects of suppression. Because the MOCR is sluggish, the input-output function of the cochlea can be estimated using sequential maskers and signals that are short enough that the MOCR will not be active during the presentation of the signal. A precursor can be presented before the masker to activate gain reduction during the presentation of the signal. This technique has not yet been used to explore cochlear gain reduction at frequencies below 4 kHz, and is the focus of this research project. Young adults with normal hearing participated in this experiment. Growth-of-masking (GOM) functions were measured to estimate the basilar membrane input-output function at 2 and 4 kHz. For a fixed masker level on the linear portion of the GOM function, threshold was re-measured with the addition of preceding pink noise. The amount of cochlear gain reduction was estimated as the difference in signal threshold with and without preceding sound. For the same listeners, a second gain reduction estimate was measured as the change in signal threshold with a precursor when the masker was replaced by a silent gap. Comparisons of results across frequency and methods will be discussed.

Funding
NIH(NIDCD): 5T32DC000030-24

PS 886

Evaluation of the mismatch waveform elicited by amplitude modulated auditory stimuli as an objective measure for temporal discrimination abilities to aid future Cochlear Implant fitting

Saskia Waechter[1]; Alejandro Lopez Valdes[1]; Cristina Simoes-Franklin[2]; Laura Viani[2]; Richard Reilly[1]
[1]Trinity College Dublin; [2]National Cochlear Implant Programme, Beaumont Hospital

Introduction

Extensive research has been performed to explore temporal auditory processing abilities. However, to date no reliable objective measure has been determined for temporal auditory discrimination abilities. Such an objective measure may be of importance for the fitting process following cochlear implantation, especially in infants, who are unable to provide feedback. This study aims to investigate the mismatch waveform (MMW) elicited by changes in amplitude modulation depth (AMD), as a representative, objective measure for temporal discrimination abilities.

Methods

Ten young, normal-hearing adults participated in a study comprising both psychoacoustic and neurophysiological paradigms. Auditory stimuli were presented monaurally to the left ear at 65dB SPL and consisted of amplitude modulated and unmodulated noise. The modulation frequency was set to 8Hz and the AMD was varied.

A psychoacoustics (PA) paradigm probed the AMD detection ability for specific AMDs (10%-100%) and monitored the percentage of correct responses for each, resulting in a 2nd order temporal modulation transfer function (TMTF). Stimuli were presented individually and the participant decided whether it was modulated or unmodulated.

Electroencephalography (EEG) data was acquired via a single-channel set-up and an auditory unattended oddball paradigm. Modulated (deviant, 10%) and unmodulated (standard, 90%) stimuli were presented for 4 AMDs (100%, 75%, 50% and 25%).

Results

The results of the PA task show a 2nd order TMTF with high-pass characteristics with the drop-off located below 25%. A one-way ANOVA revealed statistically significant differences between AMDs for PA task ($F_{(5,54)}$=37.78, p<0.001). Tukey comparisons then determined that the 10% and 12.5% AMD conditions were significantly different from all other conditions (25%-100%).

A one-way ANOVA revealed a significant difference for the MMW areas between AMDs for early responses (110-310ms; $F_{(3,36)}$=17.44, p<0.0001). Post-hoc Tukey comparisons showed MMW area values for 100% AMD were significantly different to all other conditions. No significant differences were observed for the late responses (310-450ms; $F_{(3,36)}$=2.03, p=0.127).

Conclusion

Our results suggest that the changes observed via the MMW paradigm at different AMDs do not correspond with the second order TMTF observed from the PA paradigm. Further investigation into the cause of this discrepancy needs to be carried out. Due to the significant decrease in MMW area with decreasing AMDs there is no direct relationship to the constant behavioural data between 25% and 100% AMD. This limitation hinders the possibility to use MMWs as a neurophysiological measure of AMD detection.

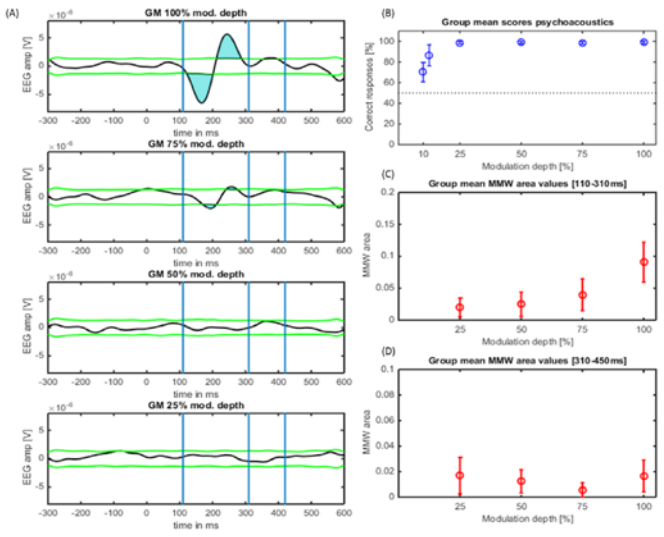

Figure 1: (A) Neurophysiological data showing the mismatch waveform (MMW) for the group average and the MMW areas exceeding the noise floor (green) for differing AMDs; (B) the TMTF (PA) depicting the group average and error bars indicating the standard deviation of the scores for each AMD; the group mean MMW area values with error bars depicting the standard deviation for each AMD for 110-310ms (C) and 310-450ms (D)

Funding
This research was funded by Cochlear Ltd.

PS 887

The effects of gain reduction on suppression measured as a function of age

Erica Hegland; Elizabeth Strickland
Purdue University

Background

Understanding speech in noise becomes more difficult as people get older, even if their audiometric thresholds remain within the normal range. One reason for this difficulty may be reduced cochlear nonlinearity. Two-tone suppression is one measure of cochlear nonlinearity. Previous work has supported the idea that suppression may decrease with age, but it can also decrease with maskers and suppressors long enough to elicit gain reduction, which may be due to the medial olivocochlear reflex (MOCR). Rather than using a long masker and suppressor, gain reduction may be better studied using a precursor presented prior to a short masker and suppressor. A fixed-level precursor should result in a fixed amount of gain decrease, while the gain decrease from a long masker and suppressor may vary with frequency and level. In the present experiment, suppression was measured

using a forward masking paradigm with short maskers and suppressors. Suppression was measured with and without the addition of a precursor.

Methods
Younger adults (age 18-29) and older adults (age 60+) with audiometric thresholds within the normal range at 2 kHz were tested. The signal was a 10-ms, 2-kHz tone, fixed at 20 dB SL. Threshold was measured for a 20-ms forward masker at 1.2, 2, and 4 kHz. Masker threshold at 2 kHz was also measured with a 20-ms low-side suppressor (1.2 kHz) and a high-side suppressor (2.4 kHz) and with an additional 50-ms precursor. The precursor was either broadband noise or a tone at 1.2, 2, or 2.4 kHz. Masker threshold at 2 kHz was also measured for a 70-ms masker with and without a 70-ms suppressor. Gain reduction was estimated by measuring the change in a forward-masked signal threshold with and without a noise precursor. Each participant also completed a noise questionnaire and the Patient Self-Assessment of Communication (SAC).

Results
Suppression was estimated as the difference in masker threshold with and without a suppressor. Estimates of suppression with the 20-ms masker and suppressor were greater than estimates with a 70-ms masker and suppressor. Suppression estimates also decreased with a broadband noise precursor, and with an on-frequency, 2-kHz precursor.

Conclusions
Results suggest that suppression estimates are lower with longer suppressors and with the addition of a precursor. Group and individual differences in amounts of suppression, gain reduction, questionnaire responses will be compared.

Funding
Research supported by NIH(NIDCD) F31 DC014359

PS 888

Detecting Variations in Music by Pupil

Hsin-I Liao; Makoto Yoneya; Shigeto Furukawa; Makio Kashino
NTT Communication Science Laboratories

Our previous study found that pupil reflects subjective salience, as well as loudness, of sounds (Liao et al., 2015). The sounds used in the previous study were presented shortly (500-ms) in discrete frequency (10-s ISI). Considering that pupillary response is sustained, in the current study, we further examine whether the reflection of pupillary response in auditory salience can be accumulated and revealed in continuous and yet structural auditory stimuli, e.g., music.

Participants listened to 15 episodes of music while their pupillary responses were recorded. The episodes were consisted of three genres: classic, jazz, and rock. Each episode was presented for 90 s in randomly assigned order. In the first session, participants rated concurrently while listening how rich in variation the episode became, by sliding a rating bar continuously in the range of 0~10. In the second session, the participants listened to the same 15 episodes again but were not involved in any task.

The pupil diameter data obtained from both sessions was time-aligned to the rating data obtained from the first rating session, and segregated between the period when the rating score was above 7 and below 3. Results showed that in both sessions, mean pupil diameter was larger during the period when the participants (once) considered the episode was richer in variation (i.e., above 7) than monotonous (i.e., below 3). The results cannot be explained by mere loudness change, since when the pupil diameter data was clustered by the sound pressure levels of the episodes, the pupillary response pattern differed depending on the task involvement. When the pupil diameter data was time-locked to the rating change moments, the pupil size increased when the rating was about to change, regardless whether the rating score increased or decreased. Moreover, this pupillary dilation response to the change moment was only observed in the first rating session, but not in the second passive listening session.

Pupillary dilation response reflects rating change, which is presumably related to motor command and/or decision-making. Most importantly, pupil dilates during the richer-in-variation moments in music, which is independent of task involvement, and cannot be explained by merely acoustical amplitude change. The underlying mechanism could be due to an automatically implicit variety assessment in the auditory environment.

Reference
Liao, H. I., Kidani, S., Yoneya, M., Kashino, M., & Furukawa, S. (2015). Correspondences among pupillary dilation response, subjective salience of sounds, and loudness. *Psychonomic Bulletin & Review.* doi: 10.3758/s13423-015-0898-0

PS 889

Auditory pitch perception and the audio-motor loop

Hadrien Jean[1]; Laurent Demany[2]; Daniel Pressnitzer[1]
[1]Laboratoire des Systèmes Perceptifs (CNRS UMR 8248), École normale supérieure; [2]Institut de Neurosciences Cognitives et Intégratives d'Aquitaine (CNRS UMR 5287), Université de Bordeaux

Extensive perceptual training improves performance on various kinds of pitch tasks (Micheyl et al., 2006). Here, we present preliminary data investigating whether the implication of the audio-motor loop during training could lead to faster improvements on pitch discrimination and identification, for normal-hearing listeners.

Based on recent results for visual training (Deveau et al., 2014), we developed a tablet-based auditory training game. Participants controlled in real time the pitch of a continuously-playing pure tone and had to find the position corresponding to the highest possible frequency. This position varied randomly from trial to trial and was not marked by any visual cue. Scores were allocated based on accuracy and speed of response, and visual plus auditory feedback was provided.

For pre-test and post-test evaluation, we used the roving dual-pair paradigm of Semal & Demany (2006). For each trial, participants heard four pure-tones split into two pairs. One pair contained identical tones and the other pair contained different tones. In the "Detection" task, listeners had to report the pair containing different frequencies. In the "Identification" task, listeners had to report the direction of the largest frequency-change they had heard. Tones were roved between 400 Hz and 2400 Hz for each pair. Two pre-test measurements were performed for both Discrimination and Identification, followed by 30 mn of auditory game training, followed by two post-test measurements. Baseline improvement was evaluated by comparing the first and second run within the pre-test or post-test sessions. Training was evaluated by comparing pre-and post-test measures across the training phase. Ten participants completed one such 1 h session. Participants generally improved slightly, but preliminary analysis did not reveal any benefit of the short training phase over baseline improvement, neither for the detection nor for the identification tasks. In the auditory training game, however, listeners were unexpectedly accurate: for all listeners, the average frequency error was smaller than the detection and identification thresholds measured in the dual-pair paradigm.

Further experiments will extend the amount of training, and explore whether the apparent advantage of pitch estimation using the audio-motor task is due to task demands, experimental apparatus, or a real audio-motor bonus possibly mediated by attention. The results could have implications for future training regimens offered to users of hearing aids or cochlear implants.

Deveau, J., Ozer, D. J., & Seitz, A. R. (2014). Improved vision and on-field performance in baseball through perceptual learning. Current Biology, 24(4), R146–R147.

Micheyl, C., Delhommeau, K., Perrot, X., & Oxenham, A. J. (2006). Influence of musical and psychoacoustical training on pitch discrimination. Hearing Research, 219(1–2), 36–47.

Semal, C., & Demany, L. (2006). Individual differences in the sensitivity to pitch direction. The Journal of the Acoustical Society of America, 120(6), 3907–3915.

PS 890

Effect of Moderate Musical Practice on Frequency Discrimination and Speech-in-Noise Perception

Wouter Schaake; Marc Lammers; Koenraad Rhebergen; Wilko Grolman; **Huib Versnel**
University Medical Center Utrecht

Background

Musicians generally show improved auditory perception relative to non-musicians as demonstrated for pitch discrimination (Micheyl et al., Hear Res 219:27-36, 2006) and speech-in-noise perception (Parbery-Clark et al., Hear Res 302:121-131, 2013). Clear advantages have been found for highly trained musicians, including professionals. In the current study we examine listening benefits in young adults with moderate practice in playing musical instruments.

Methods

Participants were 41 normal-hearing young adults (between 18 and 27 years of age) with varying musical background. Musical expertise was scored by multiplying the average incidence of musical practice per week with the total years of active musicianship. Based on this score 20 subjects classified as musician (score≥20) and 21 subjects as non-musician (score<10). Two experiments were performed. First, frequency discrimination was performed using pure tones with reference frequencies of 250, 1000, and 4000 Hz in a 3-interval 2-alternative forced choice paradigm. Sounds were presented over a headphone in three separate aural conditions: right ear, left ear and both ears. Second, speech reception threshods (SRTs) were measured in free-field speech-in-noise tests using Dutch standardized sentences.

Results

For each of the nine conditions (3 frequencies, 3 aural conditions) frequency discrimination thresholds were lower, on average by a factor of 1.6, for musicians than for non-musicians (repeated measures ANOVA, $p<0.05$). Notably, we observed a significantly lower threshold for the left ear than for the right ear ($p<0.01$), and an additional advantage when listening with both ears. The left-ear advantage did not depend on amount of musical practice. The SRT was slightly lower, on average 0.5 dB, for musicians than for non-musicians, which was not significant ($p>0.1$). The SRTs were not significantly correlated to the frequency discrimination thresholds.

Conclusion

Advantages of practising music for frequency discrimination not only apply to highly trained individuals but also to individuals who play their musical instrument a few times a week. The advantage for speech-in-noise perception was small but comparable to effects described in literature. The left-ear advantage for frequency discrimination may be ascribed to right-hemisphere specialization for pitch processing (Hyde et al., Neuropsychologia 46:632–639, 2008).

PS 891

A continuous paradigm for pitch discrimination

Mathilde de Kerangal; Dorothée Arzounian; Alain de Cheveigné
CNRS / ENS

Studies that measure frequency discrimination often use 2, 3, or 4 tones per trial. Here we investigate a 1 tone per trial task in which each tone is judged relative to the previous tone. Potential advantages are a greater yield (number of responses per unit time), and a more uniform history of stimulation for the study of context effects, or to measure cortical responses. We compare the new 1-tone task relative to a classic 2-tone task with similar parameters. Stimuli were pure tones of duration 100 ms and frequency close to 1 kHz. Between-tone frequency differences were of random sign,

and a magnitude determined according to a 4-track adaptive rule. 14 subjects (7 musicians, 7 non-musicians) participated in 3 experimental sessions, each including 6 blocks of 120 trials. In the first session the subjects performed the 1-tone and 2-tone tasks in interleaved blocks to control for order effects. In the second session they performed the 1-tone task and a variant of that task in which alternate frequency steps were fixed at 1 semitone. In the third session they performed the 2-tone task, and a variant of that task in which the first tone of each pair was set to 1 kHz. The main results were: (1) Thresholds did not differ significantly between the 1-tone and 2-tone tasks. (2) Thresholds did differ between the two variants of the one-tone task, showing a deleterious effect of inserting relatively large steps in the frequency sequence. (3) Thresholds also differed significantly between the two variants of the 2-tone task, showing an advantage for the fixed frequency standard. There was no indication that results were more variable with either task. In an additional session, EEG responses were gathered from 7 subjects performing both tasks. Event-related potentials were comparable between tasks. Overall, we found no reason not to use the new task in lieu of the classic task.

Funding
EU H2020 ICT2014-1, grant number 644732

PS 892

Amplitude-Modulation Detection in Noise: Relation to Subcomponents of Peripheral Hearing Loss

Sarah Verhulst; Anoop Jagadeesh; Manfred Mauermann; Frauke Ernst
Oldenburg University

Recent physiological evidence suggests that noise exposure and aging can reduce the number and types of auditory-nerve fibers responsible for a robust coding of sound to the auditory brainstem. Even though a temporal coding deficit associated with auditory-nerve and brainstem processing has been linked to degraded amplitude-modulation detection in listeners with normal audiometric thresholds, it is not clear how these supra-threshold hearing deficits interact with the outer-hair-cell-loss component of hearing loss. As listeners with elevated audiometric thresholds likely suffer from a mixture of peripheral pathologies, it is important to understand which of the hearing deficits is perceptually more dominant in specific listening conditions.

The present study separated cochlear mechanical hearing deficits derived from DPOAE growth functions from brainstem coding fidelity measures (ABR and EFR) in listeners with normal and mildly-sloping audiograms, and compared these metrics to psychoacoustic amplitude-modulation (AM) detection performance. Specifically, we adopted a differential paradigm in which we tested how badly various types of masking noises impact AM detection performance. The fixed-level wideband noise masker condition was designed to inform about how auditory filter widening and coding fidelity impact AM detection performance. In the second, narrowband masker (40Hz), condition, we expected performance to be limited by temporal coding fidelity within a single auditory filter.

AM detection thresholds to 65 and 70 dB SPL, 100-Hz-modulated 4-kHz pure tones were measured in 18 listeners in the quiet and two masker conditions. Two stimulus configurations were considered for the elevated-threshold group: in the first, stimulus levels were adjusted according to equal sensation level (SL); in the second, stimulus levels were kept constant. AM detection performance in quiet was similar for both the elevated-threshold and normal-threshold group when stimuli were presented at equal SL. For that same condition, AM thresholds were significantly more robust against the broadband noise in the elevated-threshold group. However, for the fixed level condition, AM detection was significantly worse in the elevated-threshold group and the broadband noise degraded AM detection more in the normal-hearing group. The narrowband masker impacted both groups similarly in the equal SL condition, but had nearly no effect on the elevated-threshold group when stimuli were presented at fixed levels. We are currently further relating the psychoacoustic results to the recorded physiological metrics to elucidate which subcomponents of peripheral hearing loss are responsible for AM detection performance in the different masker conditions.

Funding
DFG Cluster of Excellence EXC 1077/1 â€œHearing4allâ€

PS 893

Auditory Context Effects During Processing of Mistuned Harmonic Tones: Behavioral and Electrophysiological Evidence

Breanne Yerkes; David Weintraub; Joel Snyder
University of Nevada, Las Vegas

Perceptual decision making is determined both by current available sensory information and prior immediate context. Two context effects have been identified across several modalities: a contrastive effect that is dependent upon physical features of the prior stimulus and a facilitative effect that is dependent upon perception of the prior stimulus. These effects are not well studied within the auditory domain and it unclear how these effects influence perception during different auditory scene analysis tasks. In this experiment, we recorded event-related potentials (ERPs) while participants completed a concurrent sound segregation task using a paradigm in which trials contained a manipulated context stimulus, followed by a test stimulus that remained constant and ambiguous. Stimuli consisted of harmonic complex tones. The context stimulus was mistuned by 0%, 2%, or 16% and the test stimulus was always mistuned by an ambiguous 2%. After each stimulus presentation, participants indicated whether they heard the tone as one or two objects. Preliminary results revealed an effect of prior perception (facilitative) on current perception and when the context was perceived as two objects there was an effect of prior stimulus (contrastive). ERPs showed an object-related negativity (ORN) and a later positive response (P400) during the context, replicating previous ERP results on mistuned harmonic processing. During the test,

larger mistuning percentages presented during the context elicited greater negative amplitudes beginning at around 400ms post-stimulus onset (effect of prior mistuning). In addition, the topographies associated with current mistuning during the context and prior mistuning during the test were distinct, suggesting additional or separate mechanisms when processing the current and prior stimulus. Taken together, these results provide the first evidence that context effects are present during a concurrent sound segregation task; they also provide clues about how current and prior information are used to organize sounds in auditory cortex.

Funding
National Science Foundation BCS-1026023

PS 894

Evaluating Spatial-hearing Abilities with Item Response Theory

Christophe Micheyl[1]; Adriana Goyette[2]; Harvey Abrams[2]; Sridhar Kalluri[2]; Simon Carlile[2]
[1]Starkey Hearing Research Center; [2]Starkey Hearing Technologies

Background
Questionnaires are often used by clinicians and researchers to assess the difficulties experienced by hearing-impaired individuals, or the benefits of hearing aids, in real-life situations. Unfortunately, subjectivity and response biases can limit the reliability and usefulness of questionnaire data. Moreover, questionnaire selection is rarely based on quantitative or statistical arguments, in large part, because detailed comparisons of results across questionnaires that use different answer formats (such as numeric response scales vs. multiple-choice verbal answers) are rare. Here, we illustrate how Item Response Theory (IRT) can be used to design, analyze, and compare spatial-hearing questionnaires.

Method
78 participants, including individuals with normal hearing, unilateral, asymmetric, or symmetric hearing loss, hearing-aid wearers and non-wearers, completed both a new online spatial-hearing questionnaire and the spatial subscale of the Speech Spatial and Qualities of Hearing Questionnaire (SSQ, Gatehouse and Noble, 2004).

Results
Data analyses using a probabilistic (Bayesian) IRT model showed: (a) statistically significant correlations between spatial-hearing abilities inferred across the two questionnaires, even after taking into account the limited precision of inferences at the individual level; (b) statistically significant differences in inferred spatial-hearing abilities between the normal-hearing group and other participant groups with impaired hearing; some of these group differences were expected based on previous findings. Importantly, the patterns of group differences were not the same for the different spatial abilities, and were not always consistent across the two questionnaires. In particular, clearer differences among the normal-hearing and hearing-impaired groups were observed for spatial selective attention for the new questionnaire, compared to the spatial subscale of the SSQ; conversely, for distance perception, the spatial SSQ subscale was more discriminant than the new questionnaire. In addition, the IRT model yielded quantitative estimates of the difficulty and discriminating ability of each question.

Conclusion
IRT models provide a useful tool for the design and the evaluation, or validation, of questionnaires in hearing science and audiology.

Funding
Work funded by Starkey Hearing Technologies.

PS 895

Change Deafness is Due to Both Capacity Limits and Memory Loss

Melissa Gregg[1]; Vanessa Irsik[2]; **Joel Snyder**[2]
[1]University of Wisconsin, Parkside; [2]University of Nevada, Las Vegas

Background
Change deafness, the inability to notice changes to auditory scenes, has the potential to provide insights about sound perception in busy situations typical of everyday life. While several causal factors have been proposed as contributing to change detection failures, the contribution of memory capacity and memory loss remains unclear. The current study aimed to determine whether change deafness to simple and complex sounds is due to the capacity of processing multiple sounds or loss of memory for sounds over time by manipulating the number of sounds in each scene and the delay interval between scenes.

Method
On each trial, participants heard two auditory scenes separated by a silent interval, after which they made a same/different judgment. Auditory scenes contained multiple auditory objects and were created using either complex sounds (recognizable, unrecognizable) or simple sounds (tone rhythms, noise rhythms). Scene size and the delay interval were also manipulated. Scenes could contain 2, 4, or 6 objects. The silent interval could last from 0 to 6000 ms.

Results
For all sounds, change detection performance worsened as scene size increased. However, change detection to the complex sounds did not deteriorate much as the interval between scenes increased up to 2000 ms, but did deteriorate substantially when the interval between scenes was extended to 6000 ms. For simple sounds, in contrast, change detection performance suffered even for very short intervals but was most accurate at 0 ms delays.

Conclusions
These results suggest that although capacity for processing for both complex and simple sounds is limited, complex sounds stored in memory are not lost except when memory must be stored for several seconds.

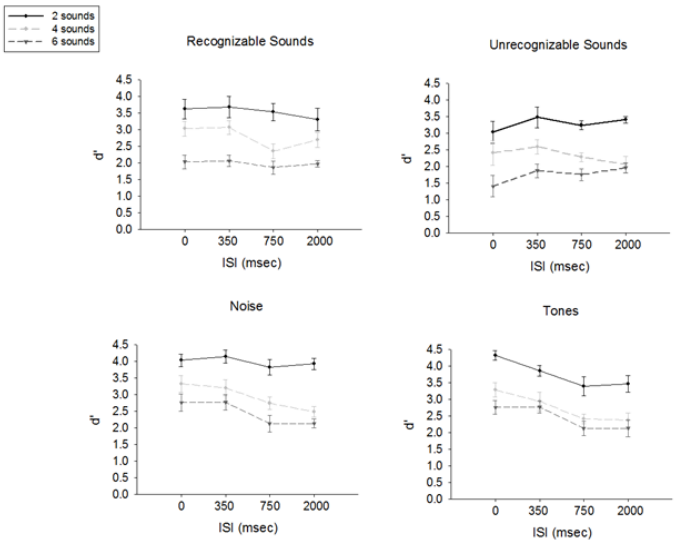

Funding
Supported by Army Research Office grant W9IINF-I2-I-0256

PS 896

Musical rhythms induce long-lasting beat perception in musicians and non-musicians

Karli Nave; Erin Hannon; Joel Snyder
University of Nevada, Las Vegas

People are exposed to rhythmic stimuli on a daily basis, whether from observing others moving, listening to music, or listening to speech. Humans easily perceive a beat (a quasi-isochronous pattern of prominent time points) while listening to musical rhythms, as evidenced by experiments measuring synchronized tapping or perceptual judgments. However, most previous studies have limited their focus to perception of simple, unmusical stimuli. Information found in more complex stimuli appears to influence beat perception, including not only rhythmic features, but also pitch features. The aim of the present study was to investigate auditory perception of beat in musical rhythms. Experiment 1 tested adult participants, who completed a beat matching task. Participants heard a piano stimulus, consisting of a musical excerpt followed by a beat-ambiguous rhythm. This rhythm could be perceived as having one of two patterns of beats: 1) the beat occurs on every other event, or 2) the beat occurs on every third event. When a drum stimulus began to play, participants indicated whether "the drummer" was matching or not matching the "piano player". Accurate performance meant subjects had to perceive the beat in the musical excerpt and also maintain perception of the beat throughout the ambiguous rhythm, despite having no surface evidence to reinforce that perception. Results indicated that participants perceived the beat of the musical excerpt and maintained that perception when the musical rhythm became ambiguous. Musicians performed better than non-musicians, suggesting a benefit of musical experience for beat perception. Importantly, after removing the musicians from the sample, non-musicians were able to maintain the perceived beat of the original musical excerpt throughout the ambiguous stimulus. Experiment 2 tested participants who completed the same task with one exception: the drummer could enter at one of four different times during the stimulus, essentially varying the amount of time over which participants had to maintain beat perception despite the ambiguous pattern. Results showed that participants perceived the beat of the music and maintained it equally well for 0, 2, 4, or 8 measures of the ambiguous stimulus. Overall these results provide additional evidence for perception and long-lasting memory for musical beat.

PS 897

Creation and rendering of interactive virtual acoustic environments for audiology: Requirements and limitations

Giso Grimm; **Volker Hohmann**
Universität Oldenburg

The increasing complexity of recent hearing devices requires novel evaluation methods that include the assessment of their interaction with the acoustic surroundings as well as with the user behavior (environment-device-user loop). This has led to an increasing attention on virtual acoustic environments and spatial reproduction methods in the past years. Limitations of virtual acoustic environments can occur at different layers. The multi-channel audio reproduction introduces spatial aliasing, which may depend on the underlying reproduction method and spatial resolution of the system. This spatial aliasing may limit the reliably usable bandwidth and the size of the listening area. The methods of acoustic simulation, e.g., room acoustics, Doppler shift or air absorption, may affect the spatial perception of virtual acoustic environments. Finally it is unclear to what extent simulated complex every-day environments are suitable to predict the real-life benefit of hearing devices.

This study presents a time-domain simulation method and summarizes the limitations of virtual acoustic environments. Results indicate that for applications with multi-channel hearing devices the reproduction method is the limiting factor. With sufficient spatial resolution the acoustic simulation can provide a valid perception of space, and complex virtual acoustic environments may predict the differences between hearing aid benefit as measured in the laboratory and as experienced in real-life.

Funding
Supported by DFG research grant FOR1732 „Individualisierte Hörakustik".

PS 898

Round-window Delivery of Neurotrophin 3 Regenerates Cochlear Synapses after Acoustic Overexposure

Jun Suzuki[1]; Gabriel Corfas[2]; Leslie Shinobu[3]; M. Charles Liberman[1]
[1]Harvard Medical School; [2]University of Michigan; [3]Decibel Therapeutics LLC.

Introduction
Loss of synapses between hair cells and cochlear nerve fibers, contributes to the sensory impairment in noise-

induced, age-related and drug induced hearing loss, and may contribute to tinnitus generation. Since the cell bodies and central axons of disconnected spiral ganglion neurons (SGNs) can survive for months to years, there may be a long therapeutic window for restoration of cochlear function. Prior studies have shown that cochlear delivery of neurotrophins, i.e. NT-3 and/or BDNF, can prolong SGN survival and elicit SGN neurite extension after drug induced hair cell destruction. Furthermore, using transgenic overexpression of NT-3 by supporting cells we have shown partial synapse regeneration and cochlear functional recovery after noise damage (Wan et al., 2014: Elife Oct 20;3). To test if exogenous NT-3 can be used as a drug, we evaluated the effects of round-window NT-3 application in CBA/CaJ mice after noise exposure causing synaptic damage without hair cell loss.

Methods
Baseline cochlear function was measured by auditory brainstem responses (ABRs) and distortion product otoacoustic emissions (DPOAEs) at 6 wks of age. Mice were then assigned to one of four experimental groups: (1) normal (no trauma, no surgery), (2) vehicle (poloxamer) only, (3) low-dose NT-3, and (4) high-dose NT-3. Mice in groups 2-4 were exposed to octave-band noise (8-16 kHz) for 2 hrs at 98 dB SPL at 7 wks of age, and round-window administration of drug/vehicle was performed 24 hrs after exposure. Final ABRs and DPOAEs were measured 9 days later, and the cochleas were removed for histological analyses. Hair cells and cochlear nerve synapses were counted by confocal microscopy of wholemounts immunostained with anti-myosin 7a, CtBP2, and GluA2.

Results
In every ear with vehicle only or with low-dose NT-3, we saw the expected 50% loss of synapses and 50% decrement in suprathreshold amplitude of ABR wave 1. In half the ears with high-dose NT-3, we saw almost complete regeneration of pre- and post-synaptic elements coupled with almost complete recovery of suprathreshold response amplitude for ABR wave 1.

Conclusions
Round-window administration of NT-3 in mice can regenerate cochlear nerve synapses after acoustic overexposure, along with near-complete recovery of cochlear neural output. Given that round-window drug application is achievable in humans by transtympanic injection, this result suggests a therapeutic strategy for hearing restoration in noise-induced and age-related hearing loss.

Funding
Research supported by grants from the NIDCD, including R01 DC 0188 (MCL), R01 DC04820 (GC and MCL) and P30 DC05209 (MCL), as well as by a gift from Decibel Therapeutics.

PS 899

Examination of the Effect of Neurotrophic and Growth Factors on Neurite Outgrowth of Human Induced Pluripotent Stem Cell-derived Neurons

Desislava Skerleva[1]; Hiroe Ohnishi[1]; Stefan Stoyanov[2]; Norio Yamamoto[1]; Juichi Ito[3]; Takayuki Nakagawa[1]
[1]Kyoto University; [2]Medical Institute-Ministry of Interior, Sofia, Bulgaria; [3]Hearing Communication Medical Center, Shiga Medical Center Research Institute

Cochlear implantation is the only available solution for patients with profound hearing loss. But the loss of spiral ganglion neurons is reported to interfere with cochlear implants performance (Starr et al. 1996, Valero et al. 2012). Establishment of induced pluripotent stem (iPS) cells gives us the exciting opportunity to investigate their role in the field of regenerative medicine for inner ear diseases and to confirm the effects we observe in animal experiments in future translational studies.

In this study we investigate the effect of IGF-1, BDNF and NT-3 on neurite outgrowth of human induced pluripotent stem (hiPS) cell-derived neurons.

Human iPS cell line labeled with green fluorescent protein (201B7-GFP) was differentiated into neural stem cells (Ishikawa et al. 2015) which were cultured on U-bottom low adhesion plate for preparation of neurospheres. After transferring and differentiation into neurons on Matrigel-coated plates for 7 days with or without additional neurotrophic or growth factors, the neurospheres were stained with anti-β III tubulin antibody and assessed by ImageJ plug-in NeuriteJ (Torres-Espin et al. 2014).

Neurospheres contained βIII-tubulin and neurofilament positive cells. A protocol for assessing the neurite outgrowth of human iPS cells was established.

PS 900

Using Multi-Electrode Arrays to Stimulate and Record from Stem Cell-Derived Sensory Neurons in vitro

Bryony Nayagam[1]; Abdullah Alshawaf[2]; Wanzhi Qui[2]; Stan Skafidas[2]; Mirella Dottori[2]
[1]Bionics Institute; [2]University of Melbourne

Background
In severe cases of sensorineural deafness where the numbers of hair cells and auditory neurons are significantly depleted, stem cell-derived neurons may provide a potential source of replacement cells. In the absence of functional hair cells, these stem cell-derived neurons would require appropriate depolarization from a cochlear implant in order to precisely relay sound information to the brainstem. Unlike acoustic stimulation, electrical stimulation of the auditory nerve causes significantly higher firing rates in auditory neurons. This raises important considerations for the development of a stem cell replacement therapy, including: can stem cell-derived neurons faithfully transmit electrical signals to the target neurons in the

cochlear nucleus, and will they be able to respond to the high stimulus rates delivered by a cochlear implant? As a first step, we are investigating whether electrical stimulation of stem cell-derived neurons using multi-electrode arrays (MEAs), can improve overall firing rates of these neurons *in vitro*.

Methods
We utilised our previously published protocols to derive functional sensory neurons from human stem cells. These stem cell-derived neurons were cultured on MEAs (Multichannel Systems, Germany) for up to five weeks *in vitro* and exposed to five minutes of electrical stimulation (800mV, 0.5Hz) twice a week. Following experimentation, cultures were fixed and stained using a cohort of neurosensory markers. *Results*: Stem cell-derived neurons generated action potentials in response to membrane depolarization, and expressed a cohort of sensory- and neural- specific markers. *In vitro* electrical stimulation of stem cell-derived neurons using MEAs produced a maximum average array-wide rate of 170.2 spikes/second after five weeks of culturing. In contrast, stem cell-derived neurons cultured on MEAs for five weeks, but without any stimulation, showed a maximum array-wide spike rate of 70.05 spikes/second. By comparing the electrical properties of stem cell-derived neurons with mammalian auditory neurons before/after electrical stimulation *in vitro*, we can determine the physiological similarity between these two populations.

Conclusion
In vitro electrical stimulation may assist in the functional maturation of stem cell-derived sensory neurons in vitro. This has important implications for developing a combined stem cell/cochlear implant therapy for severe-to-profound sensorineural hearing loss.

Funding
This work is sponsored by the Garnett Passe and Rodney Williams Memorial Foundation, the National Health and Medical Research Council of Australia, The Australian Research Council, and The University of Melbourne.

PS 901

A Nanofiber Guided Approach for Cochlear SGN Regeneration with Human Neural Precursors

Sandra Hackelberg[1]; Samuel Tuck[2]; Arjun Rastogi[2]; Christina White[2]; Liqian Liu[1]; Diane Prieskorn[1]; Ryan Miller[1]; Long He[1]; Susan DeRemer[1]; Che Chan[2]; Joseph Corey[2]; Josef Miller[1]; Robert Duncan[1]
[1]University of Michigan, Ann Arbor; [2]VA Ann Arbor Healthcare Center (VAAAHC), Ann Arbor

Loss of function of spiral ganglion neurons (SGN) can be based on noise damage, aging, infections, blast exposure and skull fractures or genetic defects. The resulting impairment of auditory signal transduction can lead to hearing loss and compromise success of cochlear implants. Since mammalian SGNs lack the ability to spontaneously regenerate, alternative strategies must be implemented. A replacement of human SGNs with pluripotent stem cells must secure functional integration in order to improve patient hearing. In a study utilizing mouse embryonic stem cells, we have previously demonstrated the guidance of neurons by nanofibers (Purcell et al., 2012). Subsequent experiments using human embryonic stem cell (hESC) derived neural precursors (NPCs) confirmed the ability of nanofibers to foster neuron alignment (Hackelberg et al, ARO 2015). Here, we are testing the potential of a nanofiberous scaffold to guide the integration of human NPCs into the auditory nerve area of guinea pigs.

To evaluate the feasibility of the approach, the longevity of neurons in the scaffolds and the response of the host tissue were examined. To this end, we have seeded NPCs on electrospun PCL/PLLA nanofiber bundles and cultured them enclosed in an implantable PCL scaffold. Initial seeding density on fiber bundles was about 5000 cells/mm^2, approximately 50% of the density found on adjacent polystyrene coverslips. After one week in culture, cell numbers were about 700/bundle (size ca 1.5 x 0.2 mm). Attachment could be observed up to 6 weeks post seeding. The NPCs showed uptake of the fluorescent dextran fluoro-ruby, making it a promising tool for tracing of the cells in vivo. To test the interaction of the nanofiber supported NPCs with host tissue, surgical methods have been established to implant the scaffolds into the internal auditory meatus of live guinea pigs. Pre implantation, guinea pigs were deafened by ouabain injection into the scala tympani. Deafening was confirmed by auditory brainstem response (ABR) measurements to acoustic clicks, which showed up to 80 dB threshold shifts. Histological sections of the cochlear modiolus showed a massive loss of SGNs. Next, sham operated animals were compared to control. Preliminary results show minimal inflammatory responses, consistent with the biocompatible properties of the utilized material. We find that empty (NPC free) scaffolds allow for infiltration of endogenous cells into the scaffold core. Assessment of NPC survival and differentiation will inform further optimization of scaffolds and implantation protocols and reveal whether nanofibers are indeed beneficial for NPC integration.

Funding
Supported by DOD Grant W91ZSQ2136N601 to R Keith Duncan and P30 DC005188

PS 902

3-D culture of auditory neurons

Fredrik Edin; Hao Li; Yu Zhang; Helge Rask-Andersen
Uppsala University

Normal hearing is conveyed through the ossicular chain to the cochlea where the vibrations are translated into an electrical signal by the 3500 inner hair cells. Inner hair cell loss is irreversible and can cause sensorineural deafness which cannot be ameliorated using normal hearing aids. Bypassing the non-functioning or missing inner hair cells and electrically stimulating the auditory neurons (spiral ganglion, SG) directly, cochlear implants (CI) can restore some sense of hearing. Current CI technology has peaked in terms of number of possible channels that can be perceived by the user as the resolution cannot be increased without causing cross-talk. By

stimulating axonal outgrowth and eliminating the anatomical gap between CI and neurons, the number of channels could be increased thus providing a better sound perception.

As an *in vitro* model, human vestibular ganglia (VG) were retrieved with ethical permission during skull base surgery removing life threatening tumors. Mouse SG neurons were isolated from P8 mice. Tissues were 3-D cultured as explants in extracellular matrix gels.

We found that neurites from human VG and mouse SG explants were able to grow into Matrigel, but also fibrin and hyaluronic acid based gels. Our findings suggest that gels may be injected into scala tympani during CI insertion to stimulate axonal outgrowth and minimize the anatomical gap between SG neurons and CI electrodes. This will reduce the cross-talk between stimulation channels, and opens up the possibility to increase the number of stimulation points and hence a better resolution of sound from CI.

Funding
Acknowledgements: This study was supported by ALF grants from Uppsala University Hospital and Uppsala University and by the Foundation "Tysta Skolan", Swedish Deafness Foundation (HRF). Our research is part of the European Community 7th Framework Programme on Research, Technological Development and Demonstration EU-FP7-NMP-2011-Small-5 "NANOCI", Project no: 281056.

PS 903

Directing Differentiation of Human Embryonic Stem Cells Toward Placode-Derived Spiral Ganglion-Like Sensory Neurons

Akihiro Matsuoka[1]; Augusta Fernando[2]; Miho Tanaka-Matakatsu[2]; Kazuaki Homma[2]; Tammy McGuire[2]; Ljuba Lyass[2]; John Kessler[2]
[1]Northwestern University; [2]Northwestern University Feinberg School of Medicine

Background
Stem cells are promising candidates for the regeneration of spiral ganglion neurons (SGNs), which would have wide-ranging applications in the treatment of sensorineural hearing loss (SNHL). The ability to selectively control the differentiation of human embryonic stem cells (hESCs) into SGNs would be a significant step toward stem cell replacement therapy for SNHL. Encouraging recent studies suggest that a stem cell replacement therapy be feasible for the loss of human SGNs. There have been also encouraging progresses and findings in developing a few protocols that generate glutamatergic sensory-type neurons that may mimic human SGNs, however, a protocol for generating cells that have a human-SGN phenotype has yet to be developed.

Method and Results
We have established an efficient protocol for generating cells with cellular and molecular characteristics of human SGNs. Furthermore, these cells preferentially formed a synaptic connection with an appropriate target in an organotypic co-culture with a rat brainstem slice, demonstrating regional characteristics of human SGNs in the developmental hindbrain. Collectively, these observations suggest that our protocol generates cells that closely replicate the genotypical and phenotypical characteristics of human SGNs. This study also characterizes the signaling pathway that generates human SGNs and also demonstrated that they are similar to murine SGN development.

Conclusion
Availability of our protocol should accelerate a clinical pathway for a stem cell replacement therapy in the inner ear in conjunction with a cochlear implant in the near future.

Funding
1. NIH K08 DC13829 01 2. The American Otological Society 3. The Triological Society and the American College of Surgeons

PS 904

Regeneration of Afferent Hair Cell Synapses in the Mouse Cochlea after Glutamate Toxicity

Wei Hsi (Ariel) Yeh; Albert Edge
Harvard University

Auditory neuropathy has both genetic and non-genetic causes. Noise-induced synaptic damage at hair cells that signal to neurons results in hearing loss. Over fifteen percent of Americans between the age of 20 and 69 suffer from noise-induced hearing loss (National Institutes of Health). To study the effects of neuronal degeneration in the cochlea, we characterized a model of neuronal degeneration in which the cochlea is exposed to exogenous glutamate receptor agonist, kainate, resulting in synaptic loss. Results of immunohistochemistry in neonatal cochlear explants exposed to kainate showed 1) postsynaptic density loss; 2) loss of peripheral fibers. Presynaptic ribbons were preserved after kainate. Quantification of the extent of neural regeneration at time points after kainate exposure showed: at 5 hours most fibers had retracted and regeneration of new fibers had been initiated; at 24 hours regeneration was more distinctive – more fibers innervated inner hair cells; and at 72 hours regeneration had reached a maximum. Next, we compared several gene expressions, i.e., neurogenesis genes, at these time points to identify genes that could enhance regeneration in adult ears. Finally, the qPCR results support our findings and hypotheses.

Immunohistochemistry results: quantification and preliminary 200X confocal images

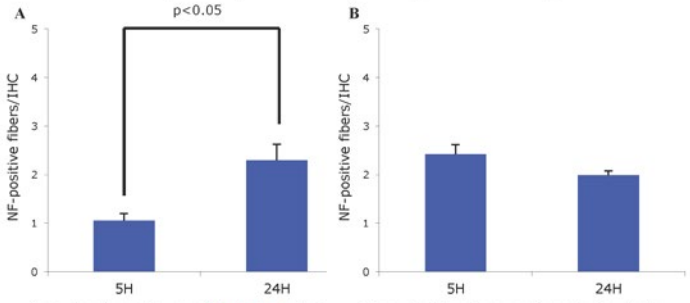

A: counts of type I neurons in **kainate** explants B: counts of type I neurons in **control** explants

Table 1: numbers of neuron counts through image processing in *Matlab*

Conditions	Average of Neurons per IHC	Standard Error
5hour control	2.42	0.20
5hour after treatment	1.05	0.15
24hour control	1.98	0.10
24hour after treatment	2.29	0.33

Table 2: preliminary organ of Corti. images (Neurofilament; CtBP2; PSD-95)

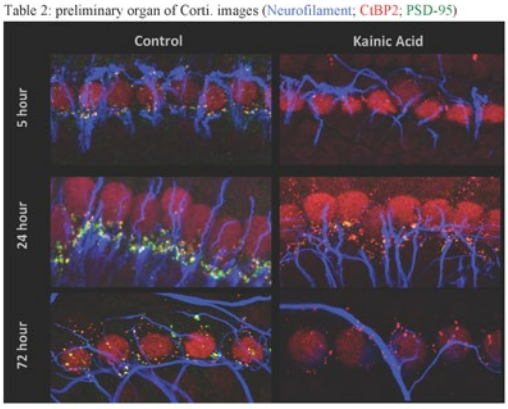

Funding
Harvard University Graduate Program, Speech and Hearing Bioscience and Technology

PS 905

Macrophage Response to Ototoxic Injury of Zebra fish Lateral Line Neuromasts

Mark Warchol; Sarah Garbo; Angela Schrader
Washington University School of Medicine

Background

Macrophages are recruited into hair cell epithelia after injury, but the nature of the interaction between macrophages and hair cells remains unclear. Larval zebra fish are transparent, so their lateral line neuromasts are an advantageous system in which to investigate the injury-evoked activity of macrophages. We have used a transgenic fish line that expresses YFP in macrophages to examine the response of macrophages to ototoxic injury caused by exposure to either neomycin or cisplatin. Additional studies characterized the effects of anti-inflammatory drugs on the process of hair cell regeneration.

Methods

Studies of macrophage activity used the MPEG1:YFP transgenic line, in which YFP is expressed in all macrophages and microglia. Fish (7-8 dpf) were treated in either 50 µM neomycin (30 min) or 1 mM cisplatin (4 hr). Both treatments induced a nearly-complete lesion of lateral line hair cells. Fish were examined at 0, 1, 2 and 24 hours after ototoxic injury and all macrophages within a 25 µm radius of the three most-posterior neuromasts (P9, P10, P11) were quantified. Other studies examined the effects of immunosuppression on hair cell regeneration. Larval fish (AB strain, 6 dpf) were pretreated with ibuprofen, dexamethasone or sodium salicylate, exposed for 30 min. to neomycin and then allowed to recover for 48 hr. Immunosuppressents were present during the entire treatment period. Control fish were treated identically, but were not exposed to immunosuppressants. Hair cells were immunolabled and quantified.

Results

Macrophages were commonly observed in the vicinity of unlesioned neuromasts and occasionally extended pseudopodial processes into the sensory region. Shortly after exposure to neomycin or cisplatin, macrophages often entered the neuromasts and appeared to engulf hair cell debris. Notably, however, the numbers of macrophages located within 25 µm of lesioned neuromasts did not differ from that observed in undamaged neuromasts. This suggests that phagocytosis may be conducted by 'local' macrophages, rather than macrophages that are recruited from other regions. We also observed nearly identical numbers of regenerated hair cells in fish that were incubated in immunosuppressant drugs throughout the processes of injury and regeneration, vs. those in control fish.

Conclusions

Macrophages enter neuromasts and phagocytose hair cell debris after ototoxic injury, but such injury does not increase the number of macrophages in the near vicinity of neuromasts. Treatment with immunosuppressing drugs does not inhibit hair cell regeneration, suggesting that inflammation is not a critical component of the regenerative process in the lateral line.

Funding
NIDCD R01DC006283

PS 906

Mesenchymal Stem Cells Produce a Wound Healing Activity for Cells of the Tympanic Membrane

Rodney Dilley; HuanTing Ong; Sharon Redmond; Robert Marano
Ear Science Institute Australia

tympanic membrane (TM) is subject to injury from trauma or middle ear infections. It has a high regenerative capacity but in some patients fails to heal and develops a chronic perforation, which may attract surgical treatment. Stem cell therapies are beginning to be explored experimentally as alternatives, after initial success with embryonic stem cells and mesenchymal stem cells in animal models. We have been developing knowledge about the repair of tympanic membrane with human models *in vitro*. In the present study we investigated the paracrine effects of human adipose-derived mesenchymal stem cells (ADSC) on wound healing mechanisms with human TM keratinocytes and a transformed epidermal keratinocyte cell line (HaCaT). Conditioned media

from ADSC were collected to assess paracrine activity on keratinocyte proliferation by MTT assay and on keratinocyte migration by scratch assay. The ADSC were further assessed for cytokine expression in a wound healing PCR array. Hypoxic conditions (<0.1% O_2) were applied to ADSC to generate contrasting effects on cytokine expression and these conditioned media were further evaluated for effects on wound healing. hTM keratinocyte proliferation was stimulated by serum over 24 and 48 hours. In conditioned media from ADSC cultures, the keratinocytes also increased in cell number, and further significant increases were seen in conditioned media from hypoxic cells. Cell migration responses were similarly increased in conditioned media and again a significantly greater increase was seen in media from hypoxic cells. HaCat keratinocyte proliferation and migration were similarly affected by ADSC conditioned media. The ADSC expressed a range of wound healing cytokines and under the stringent serum-free and hypoxic conditions they further up-regulated several important candidates (e.g. VEGF, MMP9, Tissue Factor, PAI-1) and down-regulated others (e.g. CXCL5, CCL7, TNFa), which may be secreted and contribute to the activity of conditioned media. Further experiments will identify whether such candidates may be useful in regulating hTM keratinocyte wound healing as an alternative or adjunct to surgical therapies for tympanic membrane repair.

PS 907

Bone Marrow-derived Stem Cells for Treating Tympanic Membrane Perforations

Stefania Goncalves; Esperanza Bas; Bradley Goldstein; Simon Angeli
University of Miami Ear Institute

Background

Tympanic membrane perforations(TMP) are one of the most common health problems in the world. Although up to 94% of acute perforations heal spontaneously, many become chronic TMPs and require surgical intervention. Without treatment, chronic TMPs may be complicated by infection, otorrhea, pain, conductive hearing loss, and reduced quality of life. Therefore, we sought to test the hypothesis that cell-based therapy utilizing bone marrow mesenchymal stem cells (BM-MSC) could provide an alternative treatment strategy for certain perforations, in a mouse model.

Methods

In vitro: under sterile conditions, commercially used scaffolds [i.e. Gelita-Spon (GS), Merocel, EpiDisc (ED)] were cut in small pieces of 2.54x2.54x2.54mm, placed in a 24-well plate and incubated with mouse BM-MSC expressing green fluorescent protein (GFP) at a density of 5 x 104 cells per well and incubated in an atmosphere of 5% CO2 at 37 °C with alpha-DMEM with 20% fetal bovine serum and 1% penicillin-streptomycin. After 72 hours plates were taken to the confocal microscope for imaging. Same procedure was performed for the in vivo application. In vivo: 32 mice of variable gender and weighing 20 – 30 grams were divided into 4 groups [i.e. control(n=9), GS(n=9), ED(n=10) and no scaffold(NS; n=5)]. Ear canal and tympanic membrane were examined under a surgical microscope after anesthesia with ketamine(100 mg/kg) and xylazine(5 mg/kg). Bilateral 50% TMPs were performed using a sterile 27-gauge needle. 6-8 hours after injury, BM-MSC-GFP embedded within GS or ED were soaked in PBS and then topically applied on the right ears and scaffolds alone on the left ears. The control group did not receive treatment. After 7 days, animals were euthanized and bullas were harvested, fixed with 4% paraformaldehyde for later immunostaining and visualization under confocal microscopy.

Results

In vitro: GS and ED allowed healthy growth of BM-MSC-GFP within and on top of the scaffolds; in vivo: 100% of Control TMPs remained open after 7 days of trauma. 100% of TMPs in the GS and NS groups showed partial healing. 60% of TMPs treated with BM-MSC-GFP using ED as a scaffold showed complete healing (** Pearson = 0.0086). Furthermore, those TMPs treated with BM-MSC-GFP showed a thicker healing neotympanum when compared with the control ears (* p< 0.05).

Conclusions

Cell based therapy is a promising alternative to otologic surgery in those patients that are not surgical candidates. Further studies will assess longer recoveries as well as treatment of chronic dry perforation models.

PS 908

Highly Efficient Delivery of Functional Protein with a Peptide into Mammalian Inner Ear in vivo

Yilai Shu[1]; Yong Tao[1]; Margie Li[2]; Zhengmin Wang[3]; Huawei Li[3]; David R Liu[2]; Zheng-Yi Chen[1]
[1]Massachusetts Eye and Ear Infirmary, Harvard Medical School; [2]Harvard University; [3]Fudan University

Introduction

Lack of efficient delivery into mammalian inner ear remains a major barrier to the studies of mammalian inner ear. We have previously demonstrated direct protein delivery into mammalian hair cells using a super-positively charged GFP (+36 GFP) as a carrier. We report here the study of a 13-residue peptide, aurein 1.2, which substantially increased protein delivery into multiple mammalian inner ear cell types *in vivo*.

Method

To evaluate the ability of aurein 1.2 to increase the efficacy of cationic protein delivery *in vivo*, we delivered aurein 1.2–+36–GFP protein fused with Cre recombinase (aurein1.2-+36GFP-Cre) at 5 μM, 22.5 μM and 50 μM to P1 cochleas of Cre reporter transgenic mice that express tdTomato upon Cre-mediated recombination. The tissues were harvested five days later for analysis. +36–GFP protein fused with Cre recombinase at corresponding concentration were injected as control. We evaluated hair cells and supporting cells of cochlear and utricle, as well as in the auditory nerve and spiral ligament for td Tomato signal by immunolabeling. We

compared delivery methods including cochleostomy and round window.

Results: Microinjection of aurein 1.2–+36–GFP-Cre to P1 Rosa-tdTomato$^{f/f}$ cochlea resulted in tdTomato (tdT+) signal in 96%, 58%, 6% and 87%, 75%, 30% of cochlear Outer and Inner hair cells at 50μM, 22.5 μM and 5 μM, respectively. We found wide-spread tdT+ signals in the cochlear supporting cells, hair cells and supporting cells of utricular cells, auditory nerve and spiral ligament. In contrast, +36 GFP–Cre treatment resulted in low levels of recombination only in 4% of cochlear hair cells at high concentration (50 μM), but not in any cochlear supporting cells, utricle cells, auditory nerve or spiral ligament. We quantified the number of hair cells after aurein 1.2–+36–GFP-Cre injection and found most hair cells survived, with the exception that at the highest concentration (50 μM) tested, there were 8% outer and 19% inner hair cells loss. Compared to cochleostomy, injection through the round window membrane produced a similar tdT+ labeled cells with fewer cell loss.

Conclusion

The peptide aurein 1.2 fused with a supercharged protein (+36 GFP) dramatically expanded the delivery of proteins into wide range of mammalian inner ear cell types *in vivo* with improved efficiency. This technology should enable to study of inner ear protein functions. The system can be developed to carry unlimited combinations of proteins in biophysiology study and be used as protein-based therapy including regeneration and genome editing in mammalian inner ear.

Funding

The work was supported by US National Institutes of Health(R01 DC006908), the Bertarelli Foundation, and the David-Shulsky Foundation.

PS 909

The Influence Of Fluid Flow And Surface Topography On Primary Inner Ear Hair Cells in Vitro

Else Frohlich[1]; Will McLean[2]; Danielle Lenz-Kasher[2]; Abigail Spencer[1]; Brett Isenberg[1]; Albert Edge[2]; **Erin Pararas**[1]
[1]Draper Laboratory; [2]Massachusetts Eye and Ear Infirmary

The sensory hair cells (HC) of the inner ear are easily damaged with excessive stimulation, which results in permanent decrease in hearing sensitivity. HC physiology, including differentiation, functional mechanisms, and response to toxicity are poorly understood due to the challenge of studying them outside the body. Inner ear progenitor cells have shown promise to treat hearing loss but are difficult to culture and differentiate in a controlled manner. Microfabricated *in vitro* tissue models provide well-controlled systems that more accurately mimic the *in vivo* environment. An *in vitro* platform that supports primary HC viability, attachment and replication of the *in vivo* architecture of the inner ear is needed to better culture and study HCs. In this work we have begun to explore the effect of controlled mechanical stimuli, such as surface topography and fluid flow, on primary inner ear progenitor cells *in vitro*. Cell populations were generated by targeting known signaling pathways with a combination of molecules to differentiate the progenitor cells into HCs. Micro-and nano-patterned substrates served as a cell culture platform to investigate the influence of surface topography on cell adhesion, morphology and differentiation. The platforms were coupled with microfluidic channels to administer fluid flow to the system. Progenitor cells were seeded at varying densities on three types of surface topographies: 5 μm grid, 800 nm grooves and control surfaces to allow maximal cell survival and confluency. HCs were differentiated over 10 days, fixed, stained and imaged for HC-specific markers of differentiation. In microfluidic devices, time lapse videos were taken under varying flow-induced shear stresses to investigate cell attachment on different surface topographies. Cells seeded and differentiated under flow were labeled for differentiated markers and compared to statically-grown HC populations. It was found that grid patterns significantly influence cell attachment under static conditions, and also under flow conditions. After 10 days of static culture, approximately 30% more HC remained on grid substrates compared to control substrates. Similarly, under flow rates up to 3 dynes/cm^2, 90% of cells remained on the grid compared to less than 10% of cells on the other substrates. Increased cell adhesion due to topography allows more robust assays to be developed *in vitro* as well as flow conditions to be established to control spatial differentiation of cells for tissue engineering applications.

Funding

This work was supported by NIH NIDCD Grant 5 R01 DC13909-2.

PS 910

Embossed nanotopography and printed electrodes for integrated monitoring of in vitro hair cell activity

Abigail Spencer[1]; Else Frohlich[1]; Will McLean[2]; Danielle Lenz-Kasher[2]; Peter Lewis[1]; Albert Edge[2]; **Erin Pararas**[1]
[1]Draper Laboratory; [2]Massachusetts Eye and Ear Infirmary

Mechanoelectrical transduction is the phenomenon by which hair cells translate the mechanical energy of a sound wave into an electrochemical signal that can be interpreted by the auditory nerve. This response is quantified by measuring individual hair cell receptor potentials using patch-clamping. However, this method has serious drawbacks in that it is a tedious and sensitive process that provides data on individual cells and cannot deliver real-time measurements of a hair-cell colony in a fully enclosed flow device. Therefore, we fabricate planar electrodes onto which we culture progenitor cells to execute real-time monitoring of hair cell functional responses to stimuli. A nickel mold patterned with nanotopographical features was used to emboss 1.2mm-thick clear polystyrene. These patterns include features as small as 700nm checkboards and 800nm grooves, up to 10um-wide channels. A hydraulic Carver Auto Series Press was used to emboss these patterns to a depth of approximately 750nm into the polystyrene. Then, using the Optomec Aerosol Jet 300 Series, we printed silver and gold

electrodes on nanotopographically-patterned substrates. The Optomec atomizes a wide variety of inks, most relevantly those comprised of conductive nanoparticles and organic solvents. This aerosol stream is then directed through a nozzle, allowing for focused printing with 25µm trace-width precision. This system allows us to print small features that will cause minimal change to the substrate pattern, but also geometries large enough to easily probe or wire bond (e.g., 2mm x 2mm pads). Furthermore, our conductive traces have submicron trace thickness, preserving the nanotopography of the substrate. The nature of the aerosol jet also means we can print electrodes that conform to the substrate independent of patterning. Finally, our laser sintering capabilities allow us to sinter the conductive gold or silver ink on the polystyrene without damaging the substrate while achieving less than ten times the bulk resistivity of the pure metal. This technique results in a topographically patterned substrate that supports the differentiation of inner ear progenitor cells into hair cells and incorporates an integrated circuit capable of detecting the typical resting potential of the hair cells, as well as the change in receptor potential as the hair cells reacts to stimuli, monitoring healthy hair cell activity.

Funding
This work was supported by NIH NIDCD Grant 5 R01 DC13909-2.

PS 911

Speech Perception in Noise in Unilateral Cochlear Implant Patients with Contralateral Routing of Signal

Hillary Snapp; Suhrud Rajguru; Michael Hoffer; Xue Liu
University of Miami

Background
Bilateral profound sensorineural hearing loss (PSNHL) affects nearly 1.2 million Americans. Treatment of PSNHL remains challenging and often involves unilateral treatment via cochlear implant. However, despite the considerable benefits achieved through implantation, deficits inherently associated with monaural listening remain. Individuals with a severe unilateral hearing impairment largely lose the ability to understand speech in reverberant or noisy environments. This is due to the loss of auditory cues provided through binaural hearing. Studies show that contralateral routing of signal (CROS) technology is successful in improving speech perception in noise for individuals with unilateral PSNHL. We propose that non-invasive wireless CROS technology is capable of providing similar benefit in the unilateral cochlear implant population and may provide an alternative to bilateral implantation in those individuals who do not have access to such treatment.

Methods
To investigate performance of speech perception in noise in individuals with bilateral PSNHL who are unilaterally treated by cochlear implant, stimuli were presented in a sound booth utilizing four speech/noise configurations (Figure 1a). After presentation of each stimulus, subjects were asked to identify the key words in sentences with varying levels of background noise for the unaided condition (unilateral cochlear implant only) and aided condition (cochlear implant plus CROS device). Performance outcomes analyzed for change in benefit for the unilateral cochlear implant vs cochlear implant plus CROS condition.

Results and Conclusion
A prospective clinical trial was conducted to compare the performance of the unilateral cochlear implant condition in individuals with bilateral PSNHL with the cochlear implant plus CROS condition. Statistically significant improvements were observed for the cochlear implant plus CROS condition over the cochlear implant only condition for tasks of speech perception in noise. Hearing data including audiometry, speech in noise measures and subjective outcomes will be presented. Implications for use, candidacy criteria, and expected outcomes will be discussed. These results indicate the use of CROS stimulation in unilateral cochlear implant recipients provides increased benefit and an additional rehabilitative option for this population when bilateral implantation is not possible.

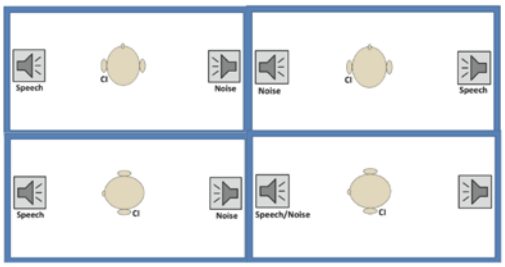

Figure 1. A schematic of the experimental setup demonstrating the four speech in noise configurations evaluated.

Funding
Study was supported in part by Advanced Bionics, LLC

PS 912

Simulating Speech Recognition of Listeners with Impaired Hearing using an Automatic Speech Recognition System: Modelling Supra-threshold Deficiencies with Level Uncertainty

Marc René Schädler; Anna Warzybok; Thomas Brand; Birger Kollmeier
Carl von Ossietzky Universität Oldenburg

Introduction
Which information is needed to complement the pure tone audiogram in order to accurately predict speech reception thresholds (SRTs) in noise for listeners with impaired hearing? To answer this question, a framework which is able to simulate speech recognition in noise of listeners with normal hearing and accurately predict reference-free SRTs in several noise conditions (Schädler et al., in press) was enhanced to perform simulations for listeners with impaired hearing.

Method
Reference-free, i.e. not depending on any reference measurement, SRTs were predicted by simulating the

German matrix sentence test (Wagener et al. 1999) with an individually adapted automatic speech recognition (ASR) system. In a first experiment, the effect of the absolute hearing thresholds, determined from 200 individual audiograms, was implemented into the feature extraction stage of the ASR system. The recognition results were compared to empirical data and speech intelligibility index (SII) based predictions form the literature. For a second experiment, in extension to the pure tone audiogram based simulations, a supra-threshold deficiency, modelled by a level uncertainty u_L in the feature extraction stage of the ASR system, is postulated. The values for the individual supra-threshold deficiency u_L were determined from the respective other noise condition by choosing u_L to match the empirical and predicted SRTs.

Results

The results show that the loss of sensitivity described by the individual pure tone threshold explains only 40% of the empirically observed variance in a stationary and 50% in a fluctuating noise condition. Taking into account pure tone threshold and individual supra-threshold hearing deficiency, 67% and 76% of the empirically observed variance can be explained in the stationary and the fluctuating noise condition, respectively.

Conclusions

The study concludes that the individual audiogram describes the impaired hearing incompletely and should be complemented with a description of individual supra-threshold hearing deficiencies to improve the prediction accuracy. The accurate simulation of human speech recognition, using sub-optimal signal processing in order to model impaired hearing, could enable simulations under aided conditions. The suitability of this approach for aided performance prediction should be assessed in future work.

Funding

This work was supported by the Deutsche Forschungsgemeinschaft SFB/TRR 31 “The active auditory system” and the Cluster of Excellence Grant “Hearing4all”.

PS 913

Contributions of Pictorial and Dynamic Visual Cues to Audiovisual Speech Reception in Noise

Jonathan Venezia; Leon Wojno; Robert Sandlin; Gregory Hickok; Virginia Richards
University of California, Irvine

Background

Viewing a speaker’s facial movements substantially improves speech reception in noise. Visual speech conveys information via pictorial cues (e.g., detailed facial configurations) and dynamic cues (e.g., time-varying trajectories of facial effectors). Dynamic cues provide correlated information (e.g., lip motion is correlated with the acoustic envelope over time) while pictorial cues convey linguistic distinctions such as place of articulation that are present but may be corrupted in the auditory signal. Here, we measure the influence of pictorial and dynamic cues on audiovisual speech reception.

Methods

We produced an audiovisual version of the Hearing in Noise Test (AV-HINT) comprising 250 short sentences produced by a single female talker. The video and audio signals were manipulated to reduce the influence of pictorial and dynamic cues. To reduce the influence of pictorial cues, videos were blurred with a Gaussian low-pass filter (cutoff = 5.5 cycles/face). To reduce the influence of dynamic cues, temporal modulations from 3-7 Hz were filtered from the acoustic envelope. Lip movements are maximally coherent with the acoustic envelope at 3-7 Hz, so the latter manipulation reduced the effective presence of correlated visual/acoustic information. Speech reception was assessed in two groups of eight normal-hearing listeners in four conditions: unfiltered audio, filtered audio, unfiltered audiovisual, and filtered audiovisual. One group was presented with blurred videos and the other with clear videos. Performance was quantified via an adaptive procedure that varied the signal-to-noise ratio (SNR; -25 dB to +20 dB) to estimate the psychometric function (PF).

Results

The PF provided two measures of performance: (1) SNR at 65% correct performance, (2) maximum audiovisual advantage (AV-A) in % correct. For (1), there were significant effects of presentation modality ($p < 0.001$; 3-4 dB improvement in AV vs. A) and envelope filtering ($p < 0.001$; 7 dB decrement due to filtering), but no interaction between the two, and there was no effect of blurring. For (2), there was a marginal effect of filtering ($p = 0.076$; reduction of AV advantage from 38% to 32%), but no effect of blurring and no interaction between the two.

Conclusion

Crucially, the audiovisual advantage was largely preserved (3.5 dB, 31% correct) in the condition with blurred videos and filtered audio (i.e., with reduced influence of pictorial and dynamic cues). Thus, the data suggest the benefit conferred by audiovisual speech is not due only to simple pictorial and dynamic cues.

Funding

NIH T32 DC 010775-05 NIH R21 DC 013406

PS 914

Audiovisual speech perception at varying levels of perceptual processing

Kaylah Lalonde; Lynne Werner
University of Washington

Listeners can use visual speech to help understand auditory speech in noise. There are multiple mechanisms that could account for these benefits, including using the visual speech to reduce uncertainty as to when auditory speech will occur, using the correlations between the envelopes of auditory and visual speech, and accessing internal visual or multimodal speech representations. In order to assess the contribution of these mechanisms to visual speech enhancements, this study assesses auditory-only, and audiovisual speech perception on three tasks varying in the level of perceptual processing

required to complete them: detection, discrimination, and identification. Of special interest is the development of audiovisual perception; in the current study adults were tested in a procedure closely matched to a procedure used to test infants. Participants are tested in a sound-attenuating booth facing a 27-inch monitor with an insert earphone in their right ear. They listen to a continuous speech-shaped noise, raise their hand when they hear a "signal," and receive visual feedback for correctly identifying signals. In the detection task, a signal is the presentation of a speech sound. In the discrimination task, a signal is a change from one speech sound to another. In the recognition task, a signal is a change from one speech category to another speech category. Half of the trials are no-signal trials on which no speech sound (detection), no speech sound change (discrimination), or a speech sound from a non-target category (recognition) occur. In auditory-only conditions, participants see a still image of the talker throughout testing. In audiovisual conditions, participants see either matched or mismatched video images. In the match condition, the video image of the talker matches the auditory target on each signal trial. In the mismatch condition, the video image of the talker producing a different speech sound is presented with the auditory target on each signal trial. Preliminary data lead us to expect that adults will detect, discriminate, and identify speech in noise better in audiovisual than auditory-only conditions. While reductions in temporal uncertainty are expected to improve performance in all tasks, access to visual speech representations is expected to be useful only in discrimination and identification. Finally, if adults use the correlations between the envelopes of auditory and visual speech to obtain benefits, we expect that benefits will be greater for the audiovisual match condition than the audiovisual mismatch condition.

Funding
NIH NIDCD T32 DC005361, NIH NIDCD R01 DC000396

PS 915

How Voice Familiarity Facilitates Speech Intelligibility in Multi-talker Situations

Ysabel Domingo; Emma Holmes; Ingrid Johnsrude
University of Western Ontario

Background
The ability to separate one voice from a mixture is crucial for successful communication. An experiment by Johnsrude et al. (2013), using the Coordinate Response Measure procedure (Bolia et al., 2000) and a two-voice mixture, showed that listeners more accurately reported the colour and number spoken by a target voice when either the target or masker voice was familiar, compared to when both voices were novel. However, it is unclear whether this improvement reflects better segregation of concurrent speech streams, or whether listeners simply encoded all coordinates and used familiar-voice information to decide which to report (template-matching). The current experiment used a larger stimulus set to determine whether familiar-voice cues in fact aid stream segregation.

Method
Eighteen participants were recruited in pairs, who were friends or siblings. Each participant recorded 480 sentences from the BUG corpus (Kidd et al., 2008), in which sentences are of the form NAME VERB NUMBER ADJECTIVE NOUN (e.g., "Bob bought two big bags"). In the main task, participants were asked to report all four subsequent words spoken by the talker who said a specified name (e.g., Bob or Pat) in the presence of a masking phrase in a different voice. Three conditions were presented: (1) In the Familiar Target condition, the target talker was the participant's partner and the masker talker was an unfamiliar participant; (2) In the Familiar Masker condition, the target was an unfamiliar participant and the masker was the participant's partner; and (3) in the Unfamiliar Baseline condition, both talkers were unfamiliar. Within each condition, stimuli were presented at four target-to-masker ratios (TMRs; -6, -3, 0, and +3 dB). Accurate identification of all four words in the target sentence was required for a trial to be scored correct.

Results
We found a significant main effect of TMR, with more accurate performance at +3 dB than at the other TMRs. Listeners were significantly more accurate at reporting the target sentence in the Familiar Target condition than in the other two conditions. Performance was significantly poorer in the Familiar Masker condition than in the Unfamiliar Baseline condition, perhaps because the familiar talker was more distracting than an unfamiliar talker.

Conclusion
These results are consistent with the idea that familiar-voice cues aid perception of masked speech. However, we cannot conclude that this benefit is due to facilitation of segregation, since a template-matching strategy would also result in better intelligibility of a target.

Funding
Funding source: CIHR Title: From sound to meaning: The neural and functional bases of speech perception

PS 916

Using the Discourse Comprehension Test (DCT) to Explore Auditory Gist

Nandini Iyer; Eric Thompson; Brian Simpson
Air Force Research Laboratory

Background
The purpose of this research was to investigate whether listeners can extract "auditory gist" from multiple simultaneous talkers when two messages were presented dichotically. Cherry (1953) showed that listeners are able to process only simple attributes of the unattended speech signals (change of speech to tones, change from male to female), suggesting that listeners may be able to capture only the broad statistical properties of an unattended message. When listeners were asked to respond to information presented to two ears simultaneously (Broadbent, 1958; Best et al., 2006), there was a substantial cost associated with responding to both streams (especially if listeners had to report the order in which they

were presented). More recently, Harding et al (2008) have argued that listeners are able to rapidly process the auditory information without any understanding of the actual content of each individual message.

Methods
40 listeners participated in the experiment. Listeners heard two randomly-selected DCT stories, one in each ear, and responded to 8 questions in 4 different listening conditions: a) Directed Attention: Listeners heard two stories, one in each ear and were directed to listen to one of those; b) Undirected attention/Single ear: Listeners heard two stories and were asked questions about the story presented in one ear; c) Undirected attention/Both ears: Listeners heard two stories but were asked questions about both stories four questions from each story. d) Misdirected attention: Listeners were asked to direct their attention to one ear but were asked questions about the story presented in the unattended ear. In order to evaluate if I performance would be influenced by the misdirected attention condition, listeners randomly received the misdirected attention as the first or last block of trials in the experimental conditions.

Results
The data indicate that listeners obtain best performance in the listening condition where they are asked to direct their attention to a particular story; not surprisingly, performance is significantly worse in condition where listeners were instructed to attend to one ear but asked questions about the story played in the unattended ear (Misdirected attention condition). Remarkably, there was relatively little decrease in performance in the undirected conditions, compared to the directed attention conditions.

Conclusion
The results are consistent with studies of visual gist processing, suggesting that global features, rather than details, are perceived even before attention is focused on the auditory streams.

PS 917

Does Sound Source Diffuseness Affect Speech Recognition in Noise?

Meital Avivi-Reich[1]; Bruce Schneider[2]
[1]Interdisciplinary Center (IDC), Herzliya; [2]University of Toronto Mississauga

The variety and nature of auditory scenes have changed significantly over the years due to the growing use of electronic amplification and surround sound systems. When amplification is used, sound sources often are presented over more than a single loudspeaker, creating a more diffused auditory image of the original sound source. In contrast, in natural settings, sound sources typically have a compact image emanating from the actual source location. As amplification becomes more common, it is important to understand how the changes it creates in the auditory scene may affect one's ability to communicate in it. The goal of the current study was to investigate how the degree of compactness of a speech target affects speech recognition in the presence of diffused masker.

Younger and older native-English and younger nonnative-English listeners were asked to repeat grammatically correct but semantically anomalous sentences with three target words in each (e.g., "A *rose* can *paint* a *fish*"). The target sentences were presented either over three loudspeakers (diffused image), or over a central loudspeaker only (compact image). Under both conditions the target sentences as well as the masker, were perceived as emanating from the center. Target sentences were presented with either one of three types of masking stimuli: steady-state speech-spectrum noise, 12-talker babble, or competing same-gender speech. Correct repetition was recorded and scored for analysing.

The results provide strong evidence that a contrast between the diffuseness of the target and that of the masker can provide a release from masking. The amount of release found when there was a contrast in diffuseness between target and masker was similar in all three groups.

Funding
This work was supported by a Canadian Institutes of Health Research grant (MOP-15359) awarded to Bruce Schneider

PS 918

Mismatch Negativity Responses Predict Speech Intelligibility in Quiet and Noise

Tess Koerner; Yang Zhang; Peggy Nelson
University of Minnesota, Twin-Cities

Background
Successful speech communication requires the extraction of relevant acoustic cues from insignificant background noise. The pre-attentive auditory mismatch negativity (MMN) represents a potential clinical tool for evaluating the neural processing of speech, however, little is known about whether MMN measures correlate with higher sentence-level speech perception abilities in noise. This study evaluated the effect of background noise on the neurophysiological processing of consonant and vowel changes in noise using MMN latency, amplitude, and spectral power measurements. It was designed to investigate whether variations in these objective measures of cortical speech processing recorded at the segmental level can be used to predict behavioral sentence recognition across quiet and noise listening conditions.

Methods
The MMN was recorded from 15 normal-hearing participants using a double oddball paradigm with the CV syllable /ba/ as the "standard" stimulus and the two CV syllables /da/ and /bu/ as "deviant" stimuli in quiet and in a four-talker speech-babble at a -3 dB SNR. In addition to analyzing averaged MMN latencies and amplitudes, time-frequency analysis was completed to evaluate EEG power in the theta frequency band. Behavioral data included percent correct phoneme detection and response time, as well as percent correct IEEE sentence recognition in quiet and noise.

Results
Background noise increased MMN latencies, decreased MMN amplitudes, and decreased EEG power in the theta frequency band. Results revealed that the addition of background noise had a differential effect on the pre-attentive processing of consonant and vowel changes, such that noise had a greater affect on the neural processing of the more salient vowel change. Correlational analysis revealed that variations in the MMN were able to predict changes in behavioral speech perception abilities across listening conditions.

Conclusions
These results have important implications regarding the use of the speech-evoked MMN as an objective measure for assessing and predicting speech perception abilities across quiet and noise listening conditions. In addition, using time frequency-analysis to evaluate power in the theta band provided an additional measure to evaluate pre-attentive auditory discrimination in quiet and in noise. Future research will focus on whether these brain-behavior correlations are significant in clinical populations, such as those with hearing loss.

Funding
University of Minnesota, NIDCD R01-DC008306, Capita Foundation

PS 919

Developmental Sex Differences for Speech Processing in Early Childhood

Kali Woodruff Carr; Sebastian Otto-Meyer; Travis White-Schwoch; Elaine Thompson; Evan Davies; Jessica MacLean; Nina Kraus
Northwestern University

Background
During early childhood, the central auditory system develops rapidly, impacting a child's access to valuable speech information important for language learning. Speech comprises multiple layers of acoustic information (e.g., frequency content and timing cues) that can be neurophysiologically assessed in a listener. Sex differences have been observed in auditory processing throughout life. However, it remains unclear whether sex differences in neural speech processing are present during early childhood, and, if so, how they intersect with maturation. Here, we report how speech processing develops at ages critical for language learning, revealing similarities and differences in development between males and females for processing specific acoustic cues.

Methods
We conducted a three-year longitudinal assessment of 100 young children ages 3-7, evaluating neural processing of speech by eliciting subcortical and cortical auditory-evoked responses.

Results
We discovered rapid maturation of speech processing during early childhood, with divergent neurodevelopmental trajectories for processing select acoustic features between the sexes. Females had more robust spectral representation and earlier neural processing of sound onsets, which improved between the ages of 3 to 7. Males had smaller and later neural representation of these signals, with delayed or static development. Other aspects of sound processing, such as precise tracking of the stimulus envelope and inter-trial consistency, developed similarly between males and females.

Conclusions
There are distinct developmental trajectories of neural speech processing for different acoustic cues between the sexes in young children. Spectral and temporal feature encoding develops rapidly in this age range for females, but remains static in males, possibly developing later in childhood than in females. We discuss our results in the context of language-based learning disabilities (e.g., autism, dyslexia, and specific language impairment), which may be characterized as developmental delays and are more prevalent in males.

Funding
Supported by NIH (RO1 HD069414) and the Knowles Hearing Center of Northwestern University.

Funding
Supported by NIH (RO1 HD069414) and the Knowles Hearing Center of Northwestern University.

PS 920

Auditory Development in Early Childhood: Individual Differences in Perception and Neural Processing of Speech in Noise

Elaine Thompson; Kali Woodruff Carr; Travis White-Schwoch; Sebastian Otto-Meyer; Evan Davies; Jessica MacLean; Nina Kraus
Northwestern University

Background
During early childhood, careful listening in myriad learning environments (e.g., gym classes, crowded lunchrooms, and bustling classrooms) requires clear perception of speech in noise.Though speech-in-noise perception plays an integral role in child development, little is knownabout the biological underpinnings that support this critical process. Even less is known about theorigins of wide inter-individual variability observed in children's perception of speech in noise. We hypothesize speech-in-noise perception variability is rooted in individual differences in auditory neurodevelopment.

Methods
We followed a cohort of 66 preschoolers, ages 3 – 5 y longitudinally, assessing their perceptionof words in noise and neural processing of sound (brainstem responses to speech).

Results
Distinct profiles of year-to-year change in the ability to perceive speech in noise were observed. Many children improved in their word-in-noise perception abilities; about half of these childrenmatured to the point where they could understand words when they were quieter than the noise,whereas the other half started with poorer performance but still improved by the same magnitude. Other children deviated from this trend; some "late bloomers" caught up to their peers, whileother children showed a developmental decrease in their

speech perception skills. Individualtrajectories in speech-in-noise perception were paralleled by distinct maturational trajectories ofneural processing of sound (spectral and temporal aspects of neural activity).

Conclusion
We show a relationship between maturation of the neural processing of speech cues and theability to perceive words in noise in young children. These results are consistent with evidencefrom older children and adults wherein neural processing of spectral cues of speech supportspeech-in-noise perception, and suggest this link emerges developmentally. We reveal that individual differences in central auditory processing development may contribute to unique maturational paces.

Supported by NIH (RO1 HD069414) and the Knowles Hearing Center of Northwestern University.

Funding
Supported by NIH (RO1 HD069414) and the Knowles Hearing Center of Northwestern University.

PS 921

Neurofeedback as a Tool to Increase Voice Discrimination in Cochlear Implant Users

Annika Luckmann[1,2]; Jacob Jolij[1]; Etienne Gaudrain[3]; Deniz Başkent[1,2]
[1]University of Groningen; [2]University Medical Center Groningen; [3]Lyon Neuroscience Research Center

Cochlear implant (CI) users report difficulties understanding speech in noisy environments. Perception of speech in noise, especially in presence of background masker voices, heavily depends on the perception of vocal characteristics, namely the fundamental frequency (F0) and the vocal tract length (VTL). Previous literature has already shown that, due to degradations in transmitted speech cues via the CI, F0 perception in CI users is weaker than that of normal hearing. Recent research (Fuller et al, 2014; Gaudrain & Başkent, 2015), however, showed that they had even more difficulty perceiving VTL. It was observed that participants reported to hear both female as well as male speakers in a gender categorization task, but looking at their performance it became clear that VTL cues were neglected and many error were made. One of the main questions that remains is, therefore, whether CI users do not receive any VTL cues, or whether they do but these are not used efficiently. The goal of this study is to investigate if training can improve the perception of one or both of these vocal cues, given the degraded speech transmission of CIs.

The training paradigm focuses on perceptual learning through neurofeedback. Neurofeedback is an online feedback method, in which neuronal oscillations, measured with EEG, are used to give real-time feedback to participants. In this case, we will focus on an event-related potential (ERP) that is commonly used to investigate whether a target stimulus was perceived, called the P300.

In the present study, the stimuli will be triplets of syllables (see Gaudrain & Başkent, 2015). The target will deviate in either VTL or F0 from the standard stimulus. To individualize the training, a pretest will be given to the subjects, measuring their just noticeable difference for both F0 and VTL. On the basis of these individual discriminatory thresholds, the stimuli for each participant for the actual experiment will be produced. This ensures that they are trained at a stimulus level that is neither too difficult nor too easy. Participants will be presented with a stream of triplets and if a target is perceived, the participant receives encouraging visual feedback. A repeated measurement of thresholds post training will show the learning effect. To also investigate transfer of learning to speech, we will test speech-on-speech perception pre- and post-training. Results from normal hearing participants tested with acoustic simulations of CIs, and CI participants will be presented.

Funding
The authors are supported by the BCN-Brain Research Institute of the University of Groningen, a Rosalind Franklin Fellowship from the University Medical Center Groningen, University of Groningen; and the VIDI Grant No. 016.096.397 from the Netherland Organization for Scientific Research (NWO).

PS 922

On the Relation Between Objective Measures and Hidden Hearing Loss

Jaime A. Undurraga[1,2]; Richard Windle[1]; Priya Pransveswaran[1]; Macarena Bowen[3]; David McAlpine[1]; Roland Schaette[1]
[1]University College London; [2]Macquarie University; [3]University of Chile

Background
Sensorineural hearing loss (SNHL) leads to degeneration of hair cells and auditory nerve fibers (ANFs). The standard view of HL assumes that hair cells and ANFs degenerate proportionally, and the latter indistinguishable with respect to the type of fibers. HL is clinically assessed by means of pure tone audiograms (PTAs). However, animal data have demonstrated that even moderate levels of noise exposure can lead to auditory neuropathy directly, selectively damaging high-threshold, low-spontaneous rate (LSR) ANFs, before any damage to hair cells is evident. Because of their higher thresholds, loss of LSR fibers is not evident in the PTA, and therefore potentially contributes to supra-threshold hearing problems, - so-called 'hidden hearing loss' (HHL). This idea is supported by the fact that human listeners with normal PTA often report hearing difficulties when listening speech in noisy environments. Data from animal models suggest that some aspects of HHL may be revealed through the use of objective measures. However, there is little evidence as yet supporting a link between hearing difficulties and objective measures in humans listeners.

Methods
Auditory brainstem responses (ABRs) and auditory steady-state responses (ASSRs) were obtained from 19 listeners.

ABRs were obtained at 100, 90, and 80 ppeSPL. ASSRs were obtained using a carrier frequency of 4 kHz modulated at 41 Hz and presented at 80 dB SPL (at 100% modulation) and several modulation depths. PTAs, vowel-consonant-vowel (VCV), speech-in-noise (QuickSIN) tests, noise exposure questionnaires and the abbreviated profile of hearing aid benefit (APHAB) were obtained from all participants. Additionally, objective measures of temporal binaural processing are being obtained and will also be presented in the meeting.

Results

Preliminary analyses indicate that the ratio of ABR waves V and I (V/I) obtained at high intensities increases for subjects in cases where HHL is suspected. This is in line with a compensating gain at the level of the auditory brainstem, perhaps as the early as the level of the cochlear nucleus. The ABR V/I ratio was independent of PTAs and age, but correlated significantly with speech-in-noise tests, VCV test and QuickSIN. Hearing difficulty scores measured using APHAB and reported noise exposure also correlated significantly. ASSR amplitude as a function of modulation depth was partially correlated with ratios of ABR waves V/I and with APHAB scores.

Conclusions

The data demonstrate significant correlations between objective measures and hearing difficulties in otherwise normal-hearing listeners. These measures provide potential clinical tool to assess HHL.

Funding

The research leading to these results has been partially funded by the Action on Hearing Loss Flex grant award number 166868.

PS 923

Establishment of a Ferret Behavioral Model for Speech Perception

Daniel Duque[1]; Shihab Shamma[2]; Jonathan Fritz[1]

[1]University of Maryland; [2]University of Maryland École Normale Supérieure

Receptive communication relies on the ability to hear, segregate and recognize discrete elements comprising ongoing speech, and requires learning sound-to-meaning associations (e.g., memories). Such memories may be stored in associative cortices and retrieved when an acoustic memory template is matched by a sound input. Encouraged by results of a previous study (Mesgarani et al., 2008), demonstrating neuronal responses in ferret primary auditory cortex are sufficiently diverse to encode and discriminate phoneme classes, and recent behavioral studies on phoneme discrimination in ferrets (Bizley et al., 2013, 2015) we initiated a new study to explore the neural mechanisms by which the auditory system encodes human words.

Six ferrets were trained to recognize target words that cued the availability of liquid reward. The single target word for each animal, composed of a unique sequence of three distinct synthetic consonant-vowel phonemes, was maintained throughout training. Along with the target word, different distractor words were played during training. Some of these words were easy to distinguish from the target word and others were more difficult to segregate (some phonemes in the distractor words were identical to the phoneme components in the target word). As all the phonemes have the same length and the same consonant-vowel configuration, words can be identified by their phoneme composition and phoneme sequence order, but not by the duration of the word.

Their discrimination rate was highest for the distractor words that presented no phoneme overlap with the target word and intermediate for distractor words with one or two phoneme overlap with the target. Ferrets could differentiate distractor words that shared the first one or two phonemes with the target word, proving that they were attending not only to the presence of specific phonemes in making their decision but were also seeking to match the complete phoneme sequence in the whole word. Moreover, ferrets were also order-sensitive and responded preferentially to correctly ordered sequences and did not respond to distractor words composed of the same phonemes in a different order. Further work is required to understand if ferrets either perceive such words as a given sequence of phonemes or recognize the entire pattern as a whole (Warren and Ackroff, 1976). This behavioral study of phoneme sequence discrimination will be useful in future neurophysiological studies in the behaving animal, to understand the neural basis for representation of complex sound sequences, and to provide an animal model for speech perception.

Funding

Financial support was provided by NIH/NIDCD-R01-DC00577 and R00-DC010439 to Shihab Shamma and Jonathan Fritz. Daniel Duque held a fellowship from AGAUR (Generalitat de Catalunya) in the frame of the EU COFUND Marie-Curie program (2014BP-A00226) and a fellowship from the Erasmus Mundus ACN program.

PS 924

Whistling in the dark: the mouse vocal production mechanism

Elena Mahrt[1]; Coen Elemans[2]; David Perkel[3]; Christine Portfors[1]

[1]Washington State University Vancouver; [2]University of Southern Denmark; [3]University of Washington

In social contexts, mice emit complex ultrasonic vocalizations that often contain frequency modulation, harmonics, and sudden jumps in frequency. These vocalizations are often altered in mouse models of genetically linked human communication disorders. Autism *ProSAP1/SHANK2* mice, for example, emit vocalizations that are lower in peak frequency. However, it is not known whether the vocal output of these mice differs because of changes in auditory processing or peripheral vocal production mechanisms. One such vocal production mechanism that could differ is the control of laryngeal movement. Improving our understanding of how mouse vocalizations are produced can help us understand the mechanisms that contribute to acoustic differences in

mouse models of communication disorders. Previous studies have suggested that mice produce ultrasonic vocalizations using an aerodynamic whistle mechanism rather than by vocal fold vibration, but this has not been directly tested. To address this, we recorded ultrasonic vocalizations emitted by mice in normal air and in less dense air (heliox). We found that the fundamental frequency of mouse vocalizations emitted in heliox increased significantly, indicating that mice use a whistle mechanism.

To determine how the mouse larynx produces ultrasonic whistles, we used novel *in vitro* high speed videography and ultrasound recordings of excised mouse larynges. We made three main observations. First, excised mouse larynges produced ultrasounds that were acoustically similar to *in vivo* mouse vocalizations. Second, systematic removal of oropharyngeal and laryngeal tissue suggested that only glottal opening and the base of the epiglottis are necessary for ultrasound production. This indicates that mice are not using a two-hole-tone whistle mechanism as expected from other animals that produce whistles, but rather may be using a whistle mechanism not yet described in a biological system. Finally, we observed in our high speed videography recordings that the fundamental frequency of ultrasounds increased with increases in glottal area, which is driven by increases in subglottal air pressure. Sudden changes in glottal air velocity contribute to jumps in frequency and the presence of harmonics. Our findings provide an increased understanding of how mice produce their ultrasonic vocalizations. This can help determine whether changes in vocal production mechanisms contribute to acoustic differences exhibited by mouse models of communication disorders.

Funding
This project was funded by NSF IOS 1257768 to CVP.

PS 925

Top-down Processing of Auditory Signals along the lifespan

Hanna Putter-Katz[1]; Nitza Horev[1]; Hillel Pratt[2]
[1]Ono Academic College; [2]Technion - Israel Institute of Technology

Introduction
Categorical perception (CP), considered specific to speech, refers to a mode of perception in which subjects can only discriminate between stimuli that they identify differently. Sine-wave speech (SWS), in which speech formants are replaced by 3 tones, can be perceived either as speech or non-speech, depending on listeners' expectations about the nature of the stimuli. Therefore SWS provides a tool to study perceptual mechanisms specific to speech or non-speech sounds using identical acoustic stimuli. The present study compares the categorical perception of SWS signals based on temporal and spectral cues, before and after they were perceived as speech in young and older listeners.

Methods
SWS signals were modeled after two speech continua: [1] Voicing (temporal) continuum, which varied in stop-closure duration, ranging from /ubu/ to /upu/. [2] Place of articulation (spectral) continuum, which varied in F2 onset frequency, ranging from /ubu/ to /upu/. Thirty young and thirty older subjects listened to each continuum and identified and discriminated the stimuli twice: first as naive listeners, and then after being exposed of the speech-like nature of the SWS signals.

Results
For all subjects perceiving the very same stimuli as speech was associated with steeper identification functions and better discrimination of stimuli that straddle the category boundary compared to when they were perceived as non-speech. This effect was more prominent for the spectral /ubu/-/udu/ SWS stimuli than for the temporal /ubu/-/upu/ stimuli for the younger listeners. However, this effect was not found in the older subjects.

Conclusions
Our results showing categorical perception to emerge only when the signals were perceived as speech, provide additional evidence for a mode of processing for speech which is distinct from processing other (non-speech) sounds. Moreover, this perceptual mode is more critical in aging subjects as they have to rely more on top-down processes due to less efficient bottom-up processing of auditory information.

PS 926

Speech Intelligibility and Melody Recognition are Differentially Affected by Degraded Amplitude and Phase Spectra Information

Sierra Broussard; Gregory Hickok; Kourosh Saberi
University of California, Irvine

Background
Differences in speech and music processing have become increasingly apparent through neuroimaging, behavioral, and clinical population studies. A clear example of these processing differences is electric hearing. Cochlear implants transmit impoverished signals to the auditory cortex, which maintains speech intelligibility but renders music nearly unrecognizable. In order to fully understand these processing differences, it is useful to investigate how a signal's amplitude and phase spectra affect standard units of language, such as phonemes and syllables, and structures in music such as note tempo and melodic pitch.

Methods
The current study investigated how amplitude and phase information differentially contribute to speech intelligibility and music recognition. Listeners in our experiment heard either degraded sentences and identified words or they heard degraded melodies and performed a same-different judgement. Each stimulus was degraded by first dividing it into segments; then for each segment, the amplitude and phase spectra were decorrelated independently relative to those of the original segment. Finally, segments were recombined into their original full length to present to the listener. We used three segment lengths: 30 ms (*phoneme length condition*),

250 ms (*syllable length condition*), and full stimulus length (*non-segmented condition*).

Results
If the stimulus is not segmented before decorrelation, phase spectrum information is most helpful for both speech intelligibility and music recognition. For the syllable length condition, speech becomes unintelligible when the phase spectrum correlation is 0.4 or less, even when the amplitude spectrum is unaltered. Conversely, music only becomes unrecognizable in the syllable length condition when the amplitude spectrum correlation is below 0.5. In the phoneme length condition, speech is unintelligible whenever the amplitude spectrum is completely decorrelated, while music is recognizable as long as the phase-spectrum correlation is 0.8 or higher.

Conclusions
These results not only support recent findings that phase spectrum information is more critical to speech intelligibility at longer time segment lengths, but also delineate the range of amplitude and phase correlations necessary for melody recognition.

Funding
Research supported by NIH.

PS 927

In What Way is Air Conducted Sound an Otolithic Stimulus?

Ian Curthoys[1]; Wally Grant[2]
[1]University of Sydney; [2]Virginia Tech

Background
Air-conducted sound (ACS) and bone conducted vibration (BCV) are widely used to test utricular and saccular function but the frequencies used (500Hz - 1000Hz) are above the upper frequency cut-off of the mechanical response of the otoliths to linear acceleration (Dunlap and Grant 2014). Furthermore there is no linear acceleration in ACS. So how do ACS and BCV generate otolithic responses, such as VEMPs? We sought to answer that by recording guinea pig single primary neurons with irregular resting discharge, identified as originating from the striola of the utricular macula or saccular macula or central superior semicircular canal crista by staining and tracing, using an superior semicircular canal dehiscence (SCD) to increase fluid displacement.

Results
Normally irregular afferents from the anterior canal do not respond to 500Hz short tone burst ACS and BCV – at least up to 135dB SPL ACS or 3g BCV. However continuous recording from such canal afferents while an SCD was made showed that after this SCD the afferent was activated and phase locked to the ACS stimulus even at very high frequencies (up to 3000Hz). This was not due damage because: after the SCD the neurons still responded to pitch angular acceleration and if the SCD was resealed the activation and phase locking disappeared.

An SCD enhances fluid displacement (Rosowski et al) and these results imply that this enhancement was sufficient to make a previously non-responsive irregular canal afferent, respond. These data are evidence that ACS works by causing fluid displacement (as Young et al 1977 suggested), which causes the short stiff hair bundles of type I receptors to be deflected and so the afferent neurons to be activated and phase-lock to the stimulus.

If after SCD the ACS stimulus (e.g 1000Hz) is maintained for seconds, then following the initial excitation, most neurons are progressively silenced and then return to resting rate slowly after stimulus offset. The silencing is very fast (1 sec) after 2000Hz, slower at lower frequencies. This response pattern may be due to the cupula being deflected by an “impedance pump” mechanism since regular neurons from that canal show similar patterns of progressive silencing and return without the early activation of irregular afferents.

Conclusion
Sound is an otolithic stimulus because it activates otolithic afferents, not by linear acceleration, but by fluid displacement deflecting the receptor hair bundles of type I receptors. Phase locking shows that each cycle is the effective stimulus.

Funding
Garnett Passe and Rodney Williams Memorial Foundation

PS 928

5MHz Pulsed Ultrasound Activates Vestibular Otolith Organs

R. Schrumm; M. Iversen; D. Christensen; D. Parker; M. Fereck; **R. Rabbitt**
University of Utah

Background
The primary function of the otolith organs is to sense gravito-inertial acceleration in 3D, and to transmit spike trains encoding the direction, amplitude, timing, and frequency to the brain. The bandwidth is remarkably broad and extends from gravitational to auditory signals. Auditory sensation by otolith organs is ancestral dating back to primitive fish, and underlies VEMP methods currently used in the clinic to assess otolith function. Here, we report that otolith organs also respond to ultrasound, and that responses are likely due to the acoustic radiation force imparted by ultrasound on the otolithic mass.

Methods
A focused ultrasound transducer directed dorsal to ventral was used to deliver 5MHz (0.5-1000 kPa) energy packets (20-1000μs, repetition rates 0.1 to 2000 s^{-1}) to the utricle, saccule or crista ampullaris in the oyster toadfish. Single-unit afferent responses were recorded and analyzed for vector strength and discharge rate. A finite-element (FE) model was used to estimate the acoustic radiation force. The otolith was modeled as a rigid solid supported by an elastic gel layer, immersed in a compressible viscous fluid.

Results
Saccular afferents responded robustly, with high vector strength, phase locking to each ultrasound packet. Responses of utricular afferents were weaker, and responses of semicircular canal afferents were rarely detectable. The lack of robust responses in semicircular canal afferents, and sensitivity to the direction of the ultrasound wave, ruled out heat as the primary mechanism of activation. This led to the hypothesis that acoustic radiation force might be responsible. FE simulations supported the hypothesis. The radiation force is rectified, so the sinusoidal 5MHz ultrasound generated a nonzero average force in the direction of the incident wave. Equivalent acceleration is nonlinear and was predicted to reach a 12g (g=gravity) for 1000-kPa incident ultrasound, and 0.003g for 1-kPa.

Conclusion
Results show that 5MHz ultrasound activates otolith organs, evoking action potentials in primary afferents with high vector strength. Afferent responses were sensitive to the direction of the ultrasound wave and occurred primarily in otolith organs, consistent with an acoustic radiation force origin. FE simulations show ultrasound stimuli >1 kPa can generate a physiologically detectable acoustic radiation force, and higher-power ultrasound stimuli can exceed 1g equivalent acceleration. Focused ultrasound provides a new means to selectively activate vestibular otolith organs for applications in basic science and in clinical assessment.

Funding
NIDCD R01 DC006685 (Rabbitt)

PS 929

Comparing the low-voltage-activated conductances of vestibular type I hair cells across zones of the mouse utricle

Koh Koizumi[1]; Omar Ramírez[1]; Kazuo Ishikawa[2]; Ruth Eatock[1]
[1]University of Chicago; [2]Akita University

In mammals and other amniotes, vestibular sensory epithelia have two major classes of hair cell, type I and type II, which differ in the afferent terminals they receive, cell shape, and ionic conductances. Type I hair cells are enclosed by a large calyceal afferent terminal and have a low-voltage-activated conductance (gK,L) that is open at resting potential. The reported voltage dependence of gK,L can differ substantially across or even within preparations, though it is always quite negative. One factor when calyces are present is K+ accumulation in the synaptic cleft on the apparent voltage dependence (Lim et al. 2011, Exp Brain Res 210:607). Another possible factor is epithelial zone, given that many features of the epithelia and afferents differ sharply between zones. To investigate this possibility, we have recorded with the whole-cell patch clamp method from type I hair cells in identified zones in semi-intact utricular epithelia from CD-1 mice (postnatal days 11 to 26). The bathing medium was modified L-15, the pipette solution was KCl-based with 5 or 10 mM EGTA, and recordings were made at 22-26°C.

The epithelium of the mammalian utricle comprises a central striola (S) and a surrounding extrastriola with lateral and medial parts (LES and MES). Striolar type I cells were significantly larger (1-way ANOVA, $p<0.05$) than extrastriolar hair cells, as indicated by their capacitances: 5.2±0.3 pF (16 S cells) vs. 4.3±0.3 pF (14 LES cells) and 3.7±0.2 pF (10 MES cells). Resting potentials were similar across zones, with a mean of −82±1 mV for the pooled cells (n=40). All type I cells had gK,L. In contrast to reports from younger mice, no cells with gK,L had clear HCN currents.

Activation curves showing the steady-state voltage dependence of gK,L were generated from tail currents at −40 mV following protocols designed to reduce K+ accumulation effects. Averaged activation curves differed with zone: maximal conductance was largest in striolar cells, in proportion to surface area, and gK,L was half-activated at −92±0.3 mV, a significantly more negative value than the midpoints of extrastriolar curves: −83±0.3 mV (LES) and −83.0±0.5 mV (MES). The more negative the activation range of this low-voltage-activated conductance, the more negative the resting potential and the smaller the cell's input resistance and receptor potential.

Funding
Supported by NIDCD R01DC012347

PS 930

Analysis of Synaptic Density of Utricular Hair Cells in Neonatal Wild-Type and Otoferlin-Deficient Knockout Mice

Katerina Oikonomou; Larry Hoffman; Felix Schweizer; Ivan Lopez
University of California, Los Angeles

In both mature and immature mammalian hair cells, neurotransmitter release is predominantly initiated by Ca+2 influx via voltage-dependent Ca+2 channels. Otoferlin, a large multi-C2 domain transmembrane protein located at the active zone of hair cells, has been shown to participate in Ca+2-dependent exocytosis. Although spontaneous exocytosis is preserved in otoferlin-deficient knockout (Otof-/-) mice, stimulus-induced transmitter release is severely attenuated (Dulon et al., 2009). Therefore, this animal represents an outstanding model for exploring the role of natural stimuli in the development and plasticity of synapses within vestibular hair cells. In the present study, we explored the distribution of synapses in vestibular hair cells from utricles in neonatal wild-type (WT) and Otof-/- mice, investigating their distribution in type I and II hair cells across the major topographic regions of the utricle.

We used anti-CtBP2 (C-terminal binding protein 2) to label the presynaptic ribbon and anti-GluR2 (glutamate receptor subunit 2) to identify the postsynaptic receptor. We defined a quantifiable synapse as a locus of close apposition of both CtBP2 and GluR2 immunopositive punctae. Type I hair cells were distinguished by the presence of postsynaptic calyces immunolabeled with anti-β3-tubulin. Stereocilia were labeled with fluorophore-conjugated phalloidin, which was used to navigate utricular topography (e.g. the line of polarity reversal). The ratio of type I to II hair cells from the WT mice was

found to be 1.36:1 while that from the Otof-/- mice was 1.24:1. Synapse density in both WT and Otof-/- utricles was calculated as the ratio of synapse and hair cell counts. We found that the average synapse density across topographical regions of WT utricles was 11.8 synapses/hair cell in type I hair cells and 3.8 synapses/hair cell in type II hair cells. The average synapse density of Otof-/- utricles was 3.6 synapses/hair cell in type I hair cells and 2.6 synapses/hair cell in type II hair cells. Specifically, synapse density was significantly lower in striolar (p=0.01) and medial extrastriolar (p=0.006) regions of the Otof-/- utricles compared to the WT. The number of total synapses was also quantified and found to be remarkably lower in Otof-/- striolar regions (p=0.009) than in the WT. Lastly, fewer isolated CtBP2-positive punctae were found in Otof-/- striolar (p=0.026) and medial extrastriolar (p=0.015) regions compared to WT. These data suggest that the distribution of maturing ribbon synapses in utricular hair cells may be dependent upon stimulus-evoked exocytosis, either directly or indirectly via afferent modulation and centrifugal efferent activity.

Funding
NASA grant NNX13AL99G

PS 931

Localization of CRFR1 in the Vestibular End Organs of Mice: A Possible Protective System Utilizing CRF-mediated Signaling

Ryan Guyton; Kathleen Yee; Courtney Stewart; Hong Zhu; Wu Zhou; Douglas Vetter
Univ. Mississippi Medical Center

Background
A large proportion of people experiencing noise-induced hearing loss also show signs of vestibular dysfunction. While the effects of noise on the auditory system have been well studied, the effects of noise on the vestibular system are not well understood. Recent research revealed a novel, potentially protective, signaling system in the cochlea based on corticotropin releasing factor (CRF) and its receptors. In the cochlear CRF signaling system, hair cells express CRF and the CRF receptors CRFR1 and CRFR2 are localized in surrounding support cells. Studies of cochlear function show these receptors have complimentary roles in balancing optimal hearing sensitivity with protection against noise-induced hearing loss. Additionally, activation of CRFR2 in cells harvested from the organ of Corti prevented oxidative stress and cell death pathway activation, indicating this system mitigates metabolic injury. Here we seek to determine whether a similar signaling system exists within the vestibular end organs. Establishing a similar signaling pathway to that shown in the cochlea may indicate the existence of a system involved in mitigating noise-induced damage to vestibular end organs that can be functionally tested as a potentially protective system.

Methods
CRFR1-GFP transgenic mice (Justice et al., 2008; n=9) were perfused and the inner ears extracted, sectioned and processed for dual-label immunohistochemistry for GFP and the hair cell marker myosin VIIa. Sections containing semicircular canal cristae and otolith maculae were analyzed using confocal microscopy.

Results
We found expression of CRFR1 in support cells surrounding the hair cells of the cristae and maculae. We also found a non-homogenous CRFR1 expression pattern in neurons of Scarpa's ganglion and vestibular nerve fibers, suggesting CRF signaling between vestibular hair cells and particular vestibular afferent fibers. The type of afferent fiber (calyx, dimorphic, or bouton) involved in vestibular CRF signaling, as well as expression of CRF or related peptides by various hair cell types, is currently being examined.

Conclusions
These results provide evidence supporting the existence of a novel CRF peptide signaling system involving both afferent fibers and support cells of the vestibular end organs. The role of this signaling system in possibly protecting vestibular end organs from noise-induced damage will be investigated using combinations of constitutive and conditional, cell specific gene ablation techniques. This research could lead to novel drug targets useful for protecting vestibular function either in populations exposed to intense sounds, and/or to the aging population, which typically experiences a decline in vestibular function later in life.

Funding
Supported by NIH R01DC012060 (HZ), and UMMC Office of Research (DEV)

PS 932

Effects of an H4 Receptor Antagonist on Mammalian Vestibular Sensory Evoked Potentials

Choongheon Lee; Timothy Jones
University of Nebraska-Lincoln

H4 receptor antagonists, such as JNJ7777120, are novel pharmacological agents that suppress vestibular activity (Desmadryl et al., 2012. Brit. J. Pharmacol. 167, 905-916) and thus may be useful for intervention and management of vestibular disorders. Although it is thought that H4 antagonists act on the vestibular system, it is uncertain whether they act on the vestibular system centrally, peripherally or both. Our specific aim here was to determine the effects of JNJ7777120 on peripheral vestibular function as measured using vestibular sensory evoked potentials (VsEPs). This included the evaluation of the effects of a single drug dose as well as multiple drug doses over time.

To evaluate macular function, VsEPs were measured in anesthetized C57BL/6J mice at 5 minute intervals (stimulus level: +6dBre:1.0g/ms) and threshold was determined at 20 minute intervals before and after intraperitoneal drug/vehicle administration. In the progressive multiple dose (PMD) protocol, mice received 4 incremental doses of JNJ7777120 (0.03 ml volume, 20, 40, 80, and 160 mg/kg) or vehicle (100%DMSO), where successive doses were separated by

20 minutes. In the single dose (SD) protocol, mice received a single dose of JNJ7777120 (0.1 ml volume, 160 mg/kg) or vehicle in order to characterize drug effects over a period of up to 120 minutes. Response threshold, onset latencies (P1 & N1) and amplitudes (P1-N1) for peripheral components of the VsEP were quantified and used for evaluating functional changes (brain temperature was held at 36.0 ± 0.2 ºC).

P1-N1 amplitudes increased following drug administration in both protocols (RM ANOVA; PMD: $p < 0.0001$; SD: $p = 0.023$), but not following vehicle administration alone. Similarly, amplitude regression slopes (amplitude vs time) were significantly different for treatment and vehicle groups (PMD: $p = 0.002$; SD: $p = 0.023$). In addition, peripheral latencies and vestibular thresholds decreased following drug treatment in the SD procedure ($p = 0.003$ and $p = 0.044$, respectively) but not in the vehicle group or in the PMD group.

The effects of JNJ7777120 on the VsEP, although modest in magnitude, clearly indicate that the drug is acting on peripheral vestibular sensors following systemic administration. The effects observed suggest that JNJ7777120 administration leads to a more precise synchronization of primary afferent spike discharge at the onset of responses to transient stimuli. Although H4 receptor antagonists reportedly shorten tonic responses to sustained stimuli, it appears that vestibular onset responses to transient stimulation are somewhat enhanced.

Funding
Supported by the American Academy of Audiology (AAA) and AAA foundation Research Grants Program, by the Nebraska Tobacco Settlement Biomedical Research Foundation and by funds from the Department of Special Education and Communication Disorders, UNL.

PS 933

Eye movement Evoked by Frequency Modulated Infrared Neural Stimulation of Vestibular System

Weitao Jiang
University of Miami

Background
Bilateral vestibulopathy in patients leads to postural instability and chronic disequilibrium. Infrared neural stimulation (INS) has been investigated as an alternative neurostimulation modality that does not require direct contact with neural tissue and has been shown to produce significant post-synaptic afferent responses in the vestibular system. In the present study, we investigated the eye movements evoked by frequency modulated pulsed infrared stimulation of the vestibular system and carried out histopathological analysis.

Method
All procedures were carried out according to procedures approved by the University of Miami Institutional Animal Care and Use Committee. Eye movements were recorded in Long-Evans rats anesthetized with ketamine (44 mg/kg) and xylazine (2.5 mg/kg). The animal was placed in a custom-designed modified Kopf stereotaxic frame that allows delivery of head rotations in pitch, roll, and yaw planes tracked using rotary potentiometers. A head post was cemented to the skull to secure the animal's head during stimulation and recording procedures. Eye movements were measured using a video-based eye tracking system (ISCAN inc, Woburn, MA) and a custom MATLAB program was used for analysis. Frequency modulated infrared stimulation (1863nm, 200µs, 250pps, different radiant exposures and modulated between 0.05-1Hz) was delivered to the vestibular endorgans approached by drilling away the dorsal bony wall of the utricle just caudal and medial to the bony casing of the anterior canal ampulla. Changes in blood pressure and heart rate during INS were also measured to characterize vestibular regulation of the vestibulosympathetic reflex. Histological and immunostaining analysis of the vestibular endorgans and brain were carried out following the acute experiments.

Results
We observed significant in-torsion followed by sinusoidal movements of the ipsilateral eye evoked by frequency modulated infrared pulses. Depending upon the modulation frequency, amplitude of oscillating eye movement ranged from 1 to 7º. At lower modulation frequencies (0.05-0.25Hz), we observed significant eye movements. As anticipated, an increase in the stimulation frequency was matched by a corresponding increase in the magnitude of the eye movement response. Though at modulation frequencies greater than 0.5 Hz, we failed to observe clear oscillatory eye movements.

Conclusions
As an encouraging finding, we observed that significant eye movements continued to be evoked by the infrared stimulation after 30+ minutes of continuous stimulation. This suggests the feasibility of INS as a potential long-term functional replacement of absent vestibular function. Future experiments will focus on optimizing the parameters of infrared neural stimulation and improved surgical approach.

Funding
1R01DC013798-01A1

PS 934

Using Imaging Techniques to Locate the Rhesus Vestibular Nerve for Single Unit Recording

Shiyao Dong; Pengyu Ren; Paul Bottomley; Philippe Gailloud; Jeffrey Trost; Charles Della Santina; Chenkai Dai
Johns Hopkins School of Medicine

Background
Accurate targeting is required for single unit recording from the vestibular nerve of alert rhesus monkeys, which is a powerful but technically challenging technique. Stereotactic guidance based on atlas coordinates has long been successfully employed by investigators experienced in that technique; however, the small size of the vestibular nerve, long distance to the nerve from the recording chamber craniotomy, and variation in cranial anatomy combine to make recording from the vestibular nerve difficult. We explored 3D multiplanar computed tomography (CT), optical coherence tomography

(OCT) and ultrasound (US) to facilitate targeting the vestibular nerve.

Methods
In NN adult rhesus monkeys, bilateral recording chambers were implanted on the skull using stereotactic techniques. A guide tube containing a tungsten microelectrode was inserted via a craniotomy along the axis of each recording chamber, advanced toward the presumed location of the porus acusticus, and left in place while a CT scan was performed (voxel size 0.4x0.3x0.3mm). Multiplanar 3D reconstructions yielded images perpendicular and parallel to each chamber's axis. A notch in the recording chamber served as an azimuth reference for reconstruction and placement of an XY stage. Distance from the chamber axis (i.e., the stereotactic estimate of porus acusticus location) and the true target location was measured from the CT reconstructions. Alternate techniques for image guidance, including use of small caliber OCT and US imaging units passed through the guide tube, were also evaluated.

Results
For the 8 chambers (4 monkeys) examined, the distance between the chamber axis and true porus acusticus location was 0.5±0.19 cm, and the distance from the craniotomy dural surface to the porus was 3.54±0.26 cm. Systems designed for intravascular OCT and US provided additional information with high spatial resolution around the tip of a probe inserted through the guide tube, but application of these techniques to single-unit recording in our setting was complicated by their side-viewing design.

Conclusions
Although small sample size and lack of randomization precluded statistically robust comparison between techniques, CT-based image guidance proved to be a simple and useful complement to traditional stereotaxis. Atlas-based stereotaxis, CT, OCT and US offer complementary advantages and disadvantages for targeting cranial nerves. Adaptation of intravascular OCT and US systems for intracranial or intrathecal imaging of cranial and spinal nerves may hold promise for intraoperative guidance in minimal-access rhizotomy and other clinical procedures that require precise spatial targeting of neural structures through narrow channels.

Funding
This work was supported by NIH-R01DC9255 and NIH-R01DC2390

PS 935

Effects of cochleostomy on peripheral vestibular organ and vestibular nucleus activity: an animal research

Myung-Whan Suh[1]; Yong-Ho Park[2]
[1]Seoul National University Hospital; [2]Chungnam National University

Dizziness and vertigo frequently occur after cochlear implantation (CI) surgery, particularly during the early stages. It could recover over time but some of patients suffered from delayed or sustained vestibular symptoms after CI. This study used rat animal models to investigate the effect of unilateral cochleostomy on the vestibular organs over time. Twenty seven Sprague Dawley rats underwent cochleostomy to evaluate the postoperative changes in hearing threshold, gain and symmetry of the vestibular ocular response, overall balance function, number of hair cells in the crista, and the c-fos activity in the brainstem vestibular nucleus. Loss of vestibular function was observed during the early stages, but function recovered partially over time. Histopathological findings demonstrated mild peripheral vestibular organ damage but not significant. Increased c-fos immunoreactivity in the vestibular nucleus, observed in the early stages after cochleostomy, decreased over time. Cochleostomy is a risk factor for peripheral vestibular organ damage that can cause functional impairment in the peripheral vestibular organs. Altered vestibular nucleus activity may be associated with vestibular compensation and plasticity after unilateral cochleostomy.

Funding
This work was supported by a 2013 Chungnam National University Hospital Research Fund.

PS 936

Directional change in spontaneous nystagmus in the rat after potassium chloride injection into the tympanic cavity

Takefumi Kamakura[1]; Tadashi Kitahara[2]; Makoto Kondo[1]; Yasumitsu Takimoto[1]; Yusuke Ishida[1]; Yukiko Nakamura[1]; Arata Horii[3]; Takao Imai[1]; Hidenori Inohara[1]; Shoichi Shimada[1]
[1]Osaka University Graduate School of Medicine; [2]Nara Medical University; [3]Niigata University Graduate School of Medical and Dental Sciences

Background
Ménière's disease is an inner ear disease characterized by episodic vertigo, fluctuating hearing loss and tinnitus, and spontaneous nystagmus beating in an ipsilateral direction and then changing to a contralateral direction is observed. These symptoms have been reproduced in animal experiments by increasing the potassium ion concentration of the perilymph surrounding the nerve branches to the vestibular and cochlear areas.

Method
We allocated twenty-six rats to four groups and injected potassium chloride (KCl) solution or distilled water into the tympanic cavity of the right ear, and monitored spontaneous nystagmus. Group 1 (n = 10) received saturated (3.4 M) KCl solution, Group 2 (n = 10) received 2 M KCl, Group 3 (n = 3) received 1 M KCl, and Group 4 (n = 3) received distilled water.

Results
After KCl injection into the tympanic cavity, rats in Groups 1 and 2 showed spontaneous ipsilateral beating (irritative) nystagmus, followed by contralateral beating (paralytic)

nystagmus. In Group 3, we observed spontaneous nystagmus but its direction was not stable. Rats in Group 4 showed no nystagmus.

Conclusion
These nystagmus changes of rats were the same as those of guinea pig in the previous report and similar to those of acute attack of Ménière's vertigo. Our results demonstrate the availability of a rat nystagmus model of acute Ménière's attack.

Funding
This study was supported by a Grant-in-Aid for Scientific Research, Grant Number 23791894, from the Japan Society for the Promotion of Science (JSPS).

PS 937

Development of murine model of benign paroxysmal positional vertigo and changes of protein expression after otoconia detachment

Hong Ju Park; **Ji-Won Lee**; Chan Joo Yang
University of Ulsan College of Medicine

Background
Mammalian ears contain thousands of small particles called otoconia that sense linear acceleration and gravity. In human, detachment of these structures and subsequent entrapment in the semicircular canals can result in benign paroxysmal posi

PS 938

Identification of common candidate auto-antibody and antigen with a molecular weight of 68 KDa in bilateral sudden hearing loss and Meniere's disease: A preliminary study

Jeon Mi Lee[1]; Jin Young Kim[2]; Jae Young Choi[1]; Sung Huhn Kim[1]
[1]Yonsei University College of Medicine; [2]Institute for Human Natural Defense System, Yonsei University College of Medicine

Background
In the previous study (, we demonstrate autoimmune reaction in bilateral sudden hearing loss (BSHL) and Meniere's disease (MD) by proteomic analysis and western blotting. The commonly identified Ag-Ab reaction in the study was detected in the molecular weight of 68 kDa. In this study, we tried to investigate the identity of autoantibody and antigen with a molecular weight of 68dKa commonly found in BSHL and MD patients by molecular biologic method.

Method
Immunoprecipitation with serum samples of BSHL and MD (each n = 2) and membranous labyrinth of cochlea and vestibule of C57BL/6 mouse was performed. After immunoprecipitation, the samples were subjected to sodium dodecyl sulfate gel electrophoresis on an 8-16% Tris/Glycine gel and stained with Coomassie Brilliant Blue. Bands corresponding to the molecular weight 68kDa was excised and digested, then LC-MS/MS was performed to identify protein constituent in the bands.

Results
Most commonly identified proteins after LC-MS/MS were immunoglobulin (Ig) variants (82%). Most Igs were non-specific, but the specific immunoglobulins (31% of Ig variants) to viruses, hair cell cilia, cellular structures, signal transduction pathways, and ion channels were identified. These antibodies can be candidates for the autoimmune reaction. The other proteins (18%) corresponded to the hair cell cilia, cellular structural proteins, synaptic organelles, ion channels, enzymes, and proteins involved in the signal transductions. These findings indicate that there should be circulating auto-Abs for the inner ear autoimmune reaction in the patients with BSHL and MD.

Conclusion
We identified candidate auto-Abs and Ags with a molecular weight of 68dKa for the autoimmune reaction in the patients with BSHL and MD. Narrower targeting using large population of patients will be needed in the near future and this enables elucidating the mechanism and site of the autoimmune-related hearing loss and MD.

PS 939

Peripheral Vestibular Pathology in Mondini Dysplasia

Serdar Kaya; Fatima Kaya; Michael Paparella; Sebahattin Cureoglu
University of Minnesota

Background
Mondini dysplasia is the most common type of cochlear malformations (more than 50%). It is one of the most common reasons of congenital genetic sensorineural hearing loss. Mondini dysplasia can be described as an inner ear disease including various type of bony and membranous anomalies, such as flat cochlea, short cochlear duct, large endolymphatic duct and sac, hypoplastic modiolus, large, small or absent semicircular canals, immature or missing vestibular sense organs and nerves, and deficient interscalar septum.

Objective
The purpose of this study is to evaluate the changes of peripheral vestibular sensory epithelia in Mondini dysplasia.

Material-Methods
The study material consisted of 15 human temporal bones with Mondini dysplasia and 15 age-matched controls. Sensory epithelium consists of the saccular and utricular macula, and the epithelium of the cristae of the 3 superior, lateral, and posterior semicircular canals. We assessed the sensory epithelium of the human vestibular system includes type I, type II, and total number of hair cells. Comparisons were made between Mondini dysplasia and control groups.

Results
In Mondini dysplasia, the hair cell densities of the crista of the superior semicircular canal including type I (p = 0.001) and type II (p = 0.009) hair cells and total hair cells (p =

0.001) significantly decreased ($p < 0.05$). There was a significant difference in type I ($p = 0.009$), type II ($p = 0.005$), and total hair cells ($p = 0.001$) of the crista of the posterior semicircular canal ($p < 0.05$). In terms of the crista of the lateral semicircular canal, significant correlation was obtained in type I ($p = 0.015$) and total hair cells ($p = 0.018$), but there was no significant difference in type II hair cells ($p > 0.05$). The density of type II ($p = 0.001$) and total hair cells (p = 0.004) in the saccular macula was significantly lower than in controls, but no significant difference in type I hair cells ($p > 0.05$). There was significant difference in type II (p = 0.018) and total hair cells (p = 0.001) in the macula of the utricle, but no significant correlation was found in type I hair cells compare to control group ($p > 0.05$).

Conclusion
Loss of vestibular hair cells may end up with vestibular dysfunction in patients with Mondini dysplasia.

Funding
The study was supported by the National Institute on Deafness and Other Communication Disorders (NIDCD), U24 DC011968-?01; the International Hearing Foundation;the Starkey Hearing Foundation; the 5M Lions International; and TUBITAK (Turkey).

PS 940

MicroRNA expression in the rat vestibular nucleus after unilateral labyrinthectomy

Mun Young Chang[1]; Young Kook Kim[2]; Myung-Whan Suh[3]; Yu-Jung Hwang[3]; Jeong-Sug Kyong[3]; Jun Ho Lee[1]; Seung-Ha Oh[1]; Moo Kyun Park[1]; Young Ho Kim
[1]Seoul National University College of Medicine; [2]Chonnam National University; [3]Seoul National University Hospital;

Background
Vestibular compensation is the functional recovery that follows unilateral peripheral vestibular lesions, which is a good model for the neuroplasticity of the central nervous system. Several experimental studies have been performed to identify the cellular and molecular mechanisms involved in vestibular compensation. MicroRNA is a important regulator of biological processes. MicroRNA expression in vestibular compensation has not been reported yet. In the present study, we investigated microRNA expression in rat vestibular nucleus after unilateral labyrinthectomy.

Method
First, we identified the course of behavioural recovery after unilateral labyrinthectomy. A total of 10 male Sprague–Dawley rats, 7 weeks old, were randomly divided into two groups, sham-operated group (n=5) and unilateral labyrinthectomy group (n=5). In the sham-operated group, tympanic membrane, malleus and incus were removed and no inner ear injury was made. Behavioural scores, including nystagmus, postural asymmetry and rotaroad score, were measured at baseline, 4 hours, 1, 2, 3, 4 days,1, 2, 3, 4, 6 and 8 weeks post-operation in all rats. Second, we utilized microarray methods to reveal expression of microRNAs in rat vestibular nucleus. Twenty four rats were randomly divided into two groups, sham-operated group (n=12) and unilateral labyrinthectomy group (n=12). Six rats of each group were sacrificed at 4 hours and 3 days post-operation, respectively. Then vestibular nucleus tissue was harvested and microarray analysis was performed. Third, we used quantitative RT-PCR methods to verify the microarray results. 50 rats were randomly divided into two groups, sham-operated group (n=25) and unilateral labyrinthectomy group (n=25). Five rats of each group were sacrificed at 4 hours,1, 2, 3 and 4 days post-operation, respectively. Then vestibular nucleus tissue was harvested and quantitative RT-PCR was performed.

Results
The behavioural recovery of the unilateral labyrinthectomy group reached the highest level on 3 days post-postoperation. Microarray results showed that nine microRNAs were more than 1.2-fold up-regulated (p-value < 0.2), and one miRNA were more than 1.2-fold down-regulated (p-value < 0.2) in the unilateral labyrinthectomy group compared to the sham-operated group. The quantitative RT-PCR results indicated that miR-219a-5p and miR-218a-5p could be involved in vestibular compensation.

Conclusion
We suggested that miR-219a-5p and miR-218a-5p might be regulators in vestibular compensation. This study could pave the way for the study which identifies the role of microRNA in the neuroplasticity of the central nervous system.

PS 942

Relationship Among Visual Dependence, Balance, and Spatial Orientation and Abnormal Loading of the Labyrinth in BPPV

Helen Cohen[1]; **Maitreyi Nair**[2]; Ajitkumar Mulavara[3]; Jacob Bloomberg[4]; Haleh Sangi-Haghpeykar[1]
[1]Baylor College of Medicine; [2]Saint Thomas' Episcopal High School; [3]Universities Space Research Association; [4]NASA/ Johnson Space Center

People with benign paroxysmal positional vertigo are thought to have otoconial particles displaced from the utricle into the posterior semicircular canal. This change in the inertial load distributions of the labyrinth on one side has the potential to affect spatial perception. Using general linear mixed models, we compared 23 healthy controls to 18 people with unilateral BPPV on the Romberg test on complaint foam, the rod-and-frame test and a mental rotation test. In normals, but not BPPV subjects, balance scores were moderately correlated with visual dependence, suggesting that reliance on visual cues affects balance as well as orientation to the visual vertical. BPPV and control subjects did not differ on the mental rotation task, suggesting that this cognitive function was unimpaired by BPPV. The side of impairment was strongly related to the side of perceived bias in visual vertical determined by BPPV subjects, indicating the relationship between otolith unloading and simultaneous canal loading and spatial orientation perception.

Funding
Supported by NIH grant DC009031, and by a grant from the National Space Biomedical Research Institute through NASA NCC 9-58.

PS 943

The VOR Interacts with Saccade Main Sequence: Data from the Baltimore Longitudinal Study of Aging

Eric Anson; Sascha du Lac; Michael Schubert; Yuri Agrawal
Johns Hopkins School of Medicine

Background
Saccade peak velocity and amplitude have a well described relationship, known as the main sequence (Bahill et al., 1975). The main sequence relationship holds true for point to point gaze shifts and has also been observed during optokinetic nystagmus (Garbutt et al., 2001). Saccades are a primary compensatory strategy for stabilizing gaze in individuals with reduced vestibulo-ocular reflex (VOR) function (Schubert and Zee, 2010). Individuals with a deficient VOR display two types of compensatory saccades: 1) covert saccades which occur during head motion; 2) overt saccades which occur after head motion stops. It is not currently known whether both classes of saccades follow a main sequence relationship between peak velocity and amplitude.

Methods
202 subjects from the Baltimore Longitudinal Study of Aging were recruited for this experiment. Vestibular function was measured for the horizontal VOR using the EyeSeeCam video Head Impulse Test (vHIT) system. Participants sat 1.25 meters from a visual fixation target on the wall. Each subject received 10-15 small amplitude (15-20^0) head impulses to the right and left. HITs with compensatory saccades were identified and absolute peak velocity, relative peak velocity (accounting for VOR eye velocity), and amplitude of the first saccade was measured. Relative peak velocity was calculated as the difference between eye velocity (non-zero for covert saccades) when the saccade started and peak velocity.

Results
The main sequence for absolute peak velocity and saccade amplitude did not differ between overt and covert saccades. However, using relative peak velocity only overt saccades retain their main sequence relationship. Covert saccades do not demonstrate the same main sequence relationship when peak velocity is normalized to account for underlying eye velocity from the VOR.

Conclusion
The main sequence for compensatory saccades that correct for a deficient VOR depends on the timing of the saccade with respect to underlying head and VOR eye movements. Our data suggest that either covert saccade main sequence is distinct from that of other saccades, or in generating the covert saccade, the brain considers the underlying eye velocity when executing covert saccades such that the relative increase in eye velocity is sufficient to result in a typical main sequence.

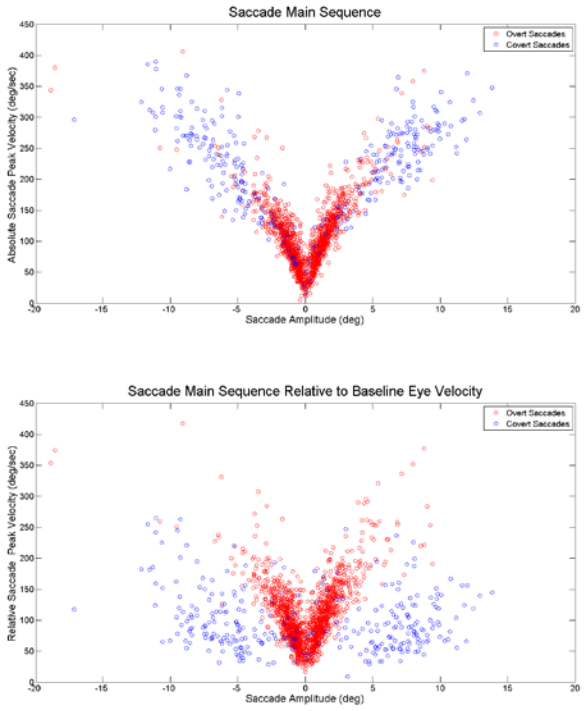

Funding
NIDCD K23 DC013056 (Y. Agrawal, PI) and NIDCD T32 DC000023 (E Anson)

PS 944

Evidence that Perception uses Distinct Signal Processing for Decision-Making

Dan Merfeld; Faisal Karmali
Harvard Medical School

Perception can be attended in different ways. For example, when the vestibular system transduces self-motion, subjects can focus on different aspects of the perception. More specifically, during rotation, humans can focus on the amount of rotation perceived, or the perceived direction of rotation. Different perceptual features utilize different neural pathways that likely include signal processing appropriate to the perception of interest. For example, high-pass filter characteristics have been described for perception of rotational velocity (1), for perceptual thresholds during a direction recognition task demonstrate (2,3,4), as well as for semicircular canal afferent signaling (5). Some authors have suggested that each of these filters is distinct, while others have suggested that some may reflect the same underlying processing. To investigate this issue, we measured both the magnitude of perceived angular yaw rotation and perceptual yaw rotation direction recognition thresholds in a population of 8 human subjects on a low-vibration rotator. Thresholds were measured by asking subjects to report whether they perceived a leftward or rightward rotation when rotated using cosine velocity profiles at different frequencies. As reported before, we found that thresholds increased as frequency decreased. As for earlier studies a high-pass filter time constant consistent

with the data was determined using generalized linear model fits. Magnitude of perceived rotation was measured by rotating the same subjects using 50 deg/s velocity steps and asking them to press a button every time they rotated through 90 deg. All subjects demonstrated an exponential decay in perceived angular velocity. We found the average time constant for magnitude estimation was 24 s, while the average time constant for direction recognition was 1.2 s. These values are substantially and significantly different t-test, $p<0.001$). These results suggest the existence of a high-pass filter specifically for the decision-making process, which is distinct from other high-pass filtering for vestibular sensation and perception.

1. Bertolini et al. 2011, J Neurophysiol 105.1: 2097223.
2. Grabherr et al. 2008 Exper Brain Res 186.4: 6777681.
3. Soyka et al. 2011 Exp Brain Res 209.1: 957107.
4. Coniglio et al. 2014 J Assoc Res Otolaryngol 15.2: 3057317
5. Goldberg et al. 1971 J Neurophysiol 34:635–660.

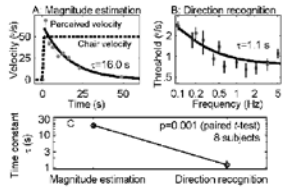

Figure 1: (A) Magnitude estimation in one typical subject, showing the velocity step rotation (dashed line), perceived rotation (dots) and exponential fit with 16 s time constant (line). (B) Thresholds from one subject (dots) showing high-pass filter characteristics (line) with a 1.1 s time constant. (C) Magnitude estimation vs. thresholds across subjects.

PS 945

Mathematical and Experimental Analysis of Galvanic Correction of Output Vestibular Signals

Tamara Alexandrova[1,2]; Vladimir Aleksandrov[1,2]; Rosario Vega[1]; Maribel Reyes[1]; Alicia Ángeles[1]; Octavio González[1]; Enrique Soto[1]

[1]Universidad Autónoma de Puebla; [2]Moscow State University

It is known that during the conditions of orbital flight astronauts experience problems related to dysfunction of vestibular system that leads to increased delay of the gaze stabilization (E. S. Tomilovskaya, M. Berger, F. Gerstenbrand, I.B. Kozlovskaya, 2006). Considering the importance of this function for the different operations performed in an orbit, both in and out of the space ship, studying the possibility of the correction of signals from vestibular end organs is of relevance for elimination of these dysfunctions. Works in which galvanic stimulation of peripheral apparatus of vestibular system was applied are used, generally with correction of a vertical posture on Earth. Simulations of the vestibular dysfunction in astronauts after orbital flight with use of galvanic stimulation was carried out by researchers of NASA (S.T. Moore, V. Didla, Y. G. MacDougall, 2011). We propose a new approach to the study of functional alterations of the vestibular system in orbital flight conditions.

1. Using of the mathematical model of the primary afferent neuron activity which has been previously presented by us (Patent US 2014/0081346A1) for the analysis of the influence of the entrance information from the micro accelerometers established on the astronaut's helmet.
2. Creation and use of the algorithm of a galvanic signal structure for vestibular end organs stimulation using mathematical analysis of the model (p.1). This algorithm allows the number of spikes increasing from afferent vestibular neurons with small amplitudes of a periodic galvanic current.
3. Use of the experimental data that analyze the possibility of influence of vestibular galvanic stimulation on the movement of the eyeballs relative to the head.
4. It is necessary to have the information on the forecast of the astronaut head turn in orbital flight from the micro accelerometers for the space orientation improve. The experiments at 3-D panoramic stand of MSU made by us showed that it is possible.

Funding

Supported by the Russian Foundation for Basic Researches (project 13-01-00515) and BUAP- VIEP Project 2015.

PD 162

A new function of cochlear efferent neural system: Control of gap junctional coupling between cochlear supporting cells to regulate hearing sensitivity

Hong-Bo Zhao; Yan Zhu

University of Kentucky Medical Center

It is well-known that descending cochlear efferent nerve system provides feedback to hair cells in the cochlea to regulate hair cell activity and hearing function. This is also the only known function of the cochlear efferent system. Here, we report a new function of the cochlear efferent system, which can control gap junctional coupling between cochlear supporting cells thereby regulating hearing sensitivity. The cochlear efferent system has innervations with outer supporting cells (Deiters cells and Hensen cells). We found that application of efferent neurotransmitter acetylcholine (ACh) reduced gap junctional coupling between outer supporting cells. Moreover, the second messenger system is a common downstream cell signaling pathway for most neurotransmitters. We found that application of the second messenger c-AMP and c-GMP could also regulate gap junctional coupling between supporting cells. However, application of glutamate, which is a putative neurotransmitter of synapses between hair cells and afferent auditory nerves, had no significant effect on gap junctions. Finally, we found that deficiency of gap junctional coupling between outer supporting cells could reduce hearing sensitivity. These data demonstrate that the cochlear efferent system can control gap junctional coupling between supporting cells. These data also reveal a new mechanism of the cochlear efferent system that can control inner ear gap junctions to regulate hearing sensitivity.

Funding

This work was supported by NIDCD DC 05989

PD 163

Hearing Circadian Rhythms: From Central Circuits to Hair Cells

Christopher Cederroth[1]; Vasiliki Basinou[1]; Jung-Sub Park[1]; Gabriella Lundkvist[1]; Stephan Michel[2]; Barbara Canlon[1]

[1]Karolinska Institutet; [2]Leiden University Medical Center

Physiological functions are regulated in a temporal manner by the circadian system that integrates environmental cues (light, feeding). Theses physiological responses are orchestrated by the suprachiasmatic nucleus (SCN) that synchronizes central and peripheral rhythms through endocrine signaling, appetite and temperature. Recently, the cochlea and the inferior colliculus have been shown to harbor a molecular clock machinery unraveling a potential role of the circadian system in regulating auditory physiology. Mice were found to be more vulnerable to noise-induced hearing loss (NIHL) at night compared to day. The capacity to recover from a noise trauma in a temporal manner appears to be regulated though the diurnal control of neurotrophin activation. Using PER2::Luciferase-reporter mice and gene expression, we were able to reveal that the cochlear clock can be modulated by noise-exposure *in vivo* or pharmacological interventions *in vitro* with dihydroxyflavone (DHF), a selective TrkB receptor agonist. DHF administration was able to prevent night NIHL. Bilateral SCN ablations were found to have little impact on regulating the day/night differences in NIHL suggesting that the circadian regulation of this response is independent of the SCN. To gain insight on the cellular mechanisms that generate the PER2::LUC rhythms, we adapted a method to track oscillations in the cochlea at the single-cell level. Radial and longitudinal gradients of PER2::LUC oscillations were apparent and these findings may provide novel insights in cochlear function. Understanding the mechanisms underlying circadian regulation of the auditory system will improve our understanding of NIHL and provide new insights into auditory dysfunctions and preventive strategies.

Funding

AFA Insurance Company, Swedish Medical Research Council, National Institute on Deafness and other Communication Disorders of the National Institutes of Health, National Research Foundation of Korea grant, Knut and Alice Wallenberg KAW2008.0149, Karolinska Institutet, Tysta Skolan, Hörselforskningsfonden, Lars Hiertas Minne, Magnus Bergvalls, Lee och Hans Österman and Wenner Gren Stiftelse.

PD 164

Scanning Laser Optical Tomography (SLOT) of the Decalcified Cochlea: An Imaging Technique for Visualization of the Human Intracochlear Soft Tissue

Omid Majdani[1,2]; Saleh Mohebbi[1]; Jose Andrade[1]; Athanasia Warnecke[1]; Thomas Rau[1]; Thomas Lenarz[1]; Lüder kahrs[3]; Nadine Tinne[4]; Georgios Antonopoulos[4]; Heiko Meyer[4]; Tammo Ripken[4]

[1]Hannover Medical School; [2]Excellence Cluster Hearing4all; [3]Leibniz University Hannover; [4]Laser Zentrum Hannover e.V.

Research background

Scanning Laser Optical Tomography (SLOT) is an equivalent method to computed tomography, but instead of radiation, light will be transmitted through a translucent object. The absorption and autofluorescence of the intracochlear structures are used as contrast media. To make the cochlea translucent, a combined chemical and mechanical decalcification protocol was developed: after thinning down of the outer walls of the labyrinth organ to 300 µm thickness, the chemically decalcified cochlea was made translucent using methylsalicylate and benzylbenzoate (MSBB).

SLOT imaging was applied to visualize the membranous intracochlear structures.

Methods

Five temporal bones from our body donation program were harvested and the labyrinth including the cochlea and the semicircular ducts was cut as a block out of it. After drilling the surrounding bone around the otocapsule, the labyrinth block was treated with EDTA (20%) for decalcification. In order to accelerate the chemical decalcification, the outer parts of the cochlea, which were softened through its exposure to the EDTA-solution, were removed with a surgical drill. This process was applied in iteration on daily basis. To prevent any violation to the membranous parts of the cochlea, the thickness of the remnant bone around the cochlea was measured repetitively using Optical Coherence Tomography (OCT). Once the thickness of the outer wall was about 300µm, the probes were exposed to MSBB for at least two days to make them translucent.

Results

SLOT images were acquired in all cases. The three intracochlear scalae, the basilar membrane and the Reissner membrane as well as the stria vascularis were visualized.

Conclusion

This study introduces SLOT as an ideally suited tool in the field of otology for in toto visualization of human intracochlear structures.

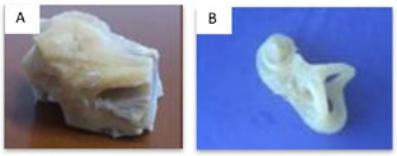

Fig. 1: Decalcification of the cochlea: A: cutting the cube of labyrinth out of the temporal bone specimen. B: Decalcified Cochlea

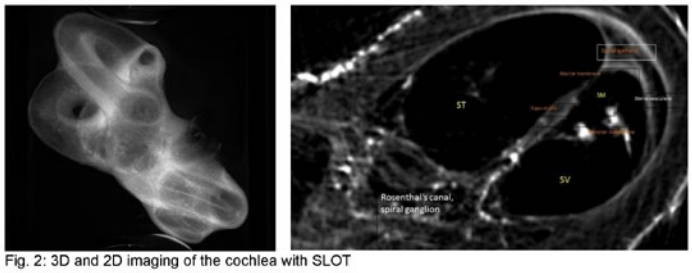

Fig. 2: 3D and 2D imaging of the cochlea with SLOT

Funding
This Project has been founded by the German Science Foundation (Deutsche Forschungsgemeinschaft, DFG) as a subproject of the Excellencecluster “Hearing4all”

PD 165

Expression and Functional Roles of the Anion Exchanger AE2 in the Cochlear Duct

Jeong Han Lee[1]; Choongryoul Shin[1]; Xiao-Dong Zhang[2]; Wei Chun Chen[2]; Grady Phillips[3]; Adnan Hussaini[3]; Michael Anne Gratton[3]; **Ebenezer Yamoah**[1]
[1]University of Nevada, Reno; [2]University of California, Davis; [3]Saint Louis University

The existence of anion exchangers and the specific isoforms expressed in HCs and the organ of Corti is unclear The anion exchange protein AE2 have been suggested to play unspecified role/s as both anion exchangers (Cl^-/HCO_3^- exchangers) and anchor/motility proteins for maintaining the shape and volume of outer hair cells (OHC) following high-frequency stimulation. The SLC4 family consists of 10 genes (*SLC4A1-5*; *SLC4A7-11*). AE2 is encoded by the *SLC4A2* gene. Here, we aimed to characterize AE2 expression and explore its functional role. First, we confirmed AE2 expression in OHCs using both immunofluorescence and immunoelectron microscopy (IEM) in mature cochlea from wild type (WT) mice. AE2 expression was also seen in supporting cells of the organ of Corti and the spiral ligament. Interestingly, IEM showed the highest AE2 density in the Deiter’s cell.

Since AE2 KO mice die at weaning, the loss of AE2 was explored in P14-21 AE2 knockout (KO), heterozygotes and WT mice. ABR and DPOAE testing was followed by examination of cochlea ultrastructure with transmission and scanning electron microscopy (TEM, SEM). ABR thresholds in the AE2 KO were elevated by ~60-70 dB at P21. The DPOAE was absent in AE2 KO mice compared to WT and heterozygote mice. Although by way of SEM, both AE2 KO and heterozygote mice showed a normal complement of IHC and OHCs along the cochlear length, TEM showed pathological features in the organ of Corti of both genotypes. Notably, many OHC had a dark, dense cytoplasm while others had a very light cytoplasm void of organelles but with large vacuoles similar to lytic necrosis. Degenerating synapses were evident at the IHC and OHCs. Dark slender crystal spicules consistent with calcium oxalate were noted within cells as well as in the intercellular spaces.

Taken together, the results imply a physiologic role of AE2 in the cochlear homeostasis, and OHC functions.

Funding
R01 DC0100386; DC007592; DC003826

PD 166

Desensitization-Resistant AMPA Receptors in Auditory Afferent Fibers of the Bullfrog Amphibian Papilla

Gang Li; Adolfo Cuadra; Daniil Frolov; **Geng-Lin Li**
University of Massachusetts Amherst

In the auditory periphery, sensory signals are transferred from hair cells to afferent fibers through AMPA receptor-mediated synaptic transmission. Under physiological conditions, hair cells release neurotransmitter glutamate constantly at a high rate, even in the absence of acoustic stimulation. While this could cause profound desensitization of AMPA receptors in most central neurons, it does not seem to be the case for auditory afferent fibers. Here in the bullfrog amphibian papilla we show that even with strong presynaptic depolarizations, the charge of excitatory postsynaptic current (EPSC) rises linearly with the presynaptic capacitance change for progressively longer depolarizations from 50 to 500 ms. This linear relationship persists in the presence of 50 μM cyclothiazide, a desensitization blocker for AMPA receptors. Meanwhile, 20 μM glutamate, when applied through bath perfusion, induces a sustained current of ~200 pA and reduces the amplitude of spontaneous EPSCs by ~30%. Lastly, whole-field uncaging of 2 mM Rubi-Glutamate induces a peak current of ~1.5 nA, which decays to ~700 pA with a time constant of ~15 ms. This slow and incomplete desensitization can be sufficiently characterized by a kinetic model with a slow desensitization rate constant and a fast resensitization rate constant. We conclude that AMPA receptors in auditory afferent fibers are desensitization-resistant, which allows sensory signals to be transferred continuously over a broad dynamic range in the auditory periphery.

Funding
This study was supported by a NIH/NIDCD R00 award (DC010198) and a university startup to G.-L. L.

PD 167

Electrophysiological responses of zebra fish lateral line afferent neurons to white noise stimulation

James Liao[1]; William Stewart[1]; Otar Akanyeti[1]; Jamie Theobald[2]
[1]Whitney Lab for Marine Bioscience, University of Florida; [2]Florida International University

Assessing how sensory systems respond to complex stimuli is important to understanding how animals initiate and modify diverse behaviors. In the flow-sensitive lateral line system of fishes, clusters of hair cells called neuromasts lie on top of the skin and deflect to the slightest flow. Previous work has measured the responses of lateral line afferent neurons to simple sine wave deflections of individual neuromasts. However, natural stimuli are more complex and can elicit non-linear responses. To address this, we measured the responses of afferent neurons to a mechanical white noise stimulus applied to a single neuromast. This approach deflects the neuromast with different displacements, velocities, and accelerations randomly through time. Using 4-6 day post fertilization wild-type zebra fish larvae (n = 20), we simultaneously stimulated a single neuromast, video-tracked its deflection, and made extracellular recordings of the connected afferent neuron. Preliminary results show that the elicited afferent spikes are reproducible. When a neuromast was stimulated with a 10 second train of white noise, we found that 75% of the spiking pattern from the afferent neuron was reproduced across all repeated trials (n = 19). The timing of these spikes was reliable, exhibiting a mean jitter of less than 1 ms (0.6±0.1 ms = mean±1 SD). When we compared the motion of the neuromast that immediately preceded each spike, we found considerable variation, indicating that the time history of deflection and spiking are critical to afferent firing. On-going analyses focus on identifying the components of the stimulus that are most important to the afferent neuron.

Funding
NIDCD NIH RO1 DC 010809 to JCL NSF IOS 1257150 to JCL

PD 168

Zebra fish as a Vertebrate Model for Sensorineural Hearing Loss

Zhongmin Lu[1]; Alexandra DeSmidt[2]; Bing Zou[3]; M'hamed Grati[3]; Denise Yan[3]; Rahul Mittal[3]; Qi Yao[2,3]; Michael Richmond[2]; Steven Denyer[2]; Xue-Zhong Liu[3]
[1]University of Miami; [2]University of Miami Coral Gables Campus; [3]University of Miami Miller School of Medicine

Background
Three hundred and sixty million people in the world suffer from hearing loss. Genetic causes account for the majority of congenital hearing loss. The zebra fish (*Danio rerio*) has become a valuable vertebrate model for human hearing disorders because of many advantages in genetics, embryology, and *in vivo* visualization. We have investigated auditory functions of zebra fish orthologs of several new human deafness genes such as *SLC22A4*, *OTOGL*, *FAM65B*, *DCDC2, and PRPS1*. In this study we report results from morphant and mutant zebra fish generated by employing antisense mopholino-induced knockdown of *prps1* and CRISPR/Cas9-mediated mutations in *myo7aa*.

Methods
Zebra fish (wild-type AB, mutant Casper, and transgenic *Et(krt4:GFP)^{sqet4}*) were used in this study. We first identified zebra fish orthologs of candidate human genes and then determined expression of the genes in the inner ear using whole mount *in situ* hybridization and RT-PCR with cDNA from sensory epithelia of otolith organs. We subsequently used antisense morpholinos (Gene Tools, LLC) that targeted intron-exon junctions of the genes to knock down their functions. sgRNA and Cas9 protein (PNA Bio Inc.) were injected into zebra fish embryos at the one-cell stage to create targeted modifications of the candidate genes. Phenotypic analyses of the inner ear of morphants/mutants were conducted using light and confocal microscopy. Finally, hearing function of morphants/mutants was assessed using microphonic potential recording from hair cells in the inner ear.

Results
We identified two zebra fish orthologs (*prps1a* and *prps1b*) of human *PRPS1* and found that PRS-I is highly conserved in vertebrates. Both *prps1a* and *prps1b* were expressed in the inner ear of zebra fish. Two splice-blocking antisense morpholino oligonucleotides caused exon-2 skip and intron-2 retention of *prps1a* and exon-2 skip and intron-1 retention of *prps1b* to knock down functions of the genes, respectively. Morphants had smaller areas of otic vesicles and otoliths, fewer inner ear hair cells, and lower microphonic response amplitude and sensitivity than control zebra fish. Therefore, *prps1* knockdown resulted in significant sensorineural hearing loss in zebra fish. Some preliminary data showing a proof of concept of CRISPR/Cas9-based genomic mutations in *myo7aa* will also be presented and discussed.

Conclusions
We conclude that the *prps1* genes are essential for hearing in zebra fish. This is the first study using an *in vivo* animal model for human DFNX1, which helps us understand the biology of non-syndromic sensorineural hearing loss. Applications of CRISPR/Cas9 combined with morpholino gene knockdown in hearing research provide new insights into the pathology of genetic deafness.

Funding
This work was supported by the National Institute of Deafness and Other Communicative Disorders of the National Institutes of Health [R21DC009879 to Zhongmin Lu; R01DC05575, R01DC012546 and R01DC012115 to Xue-Zhong Liu], University of Miami Provost Research Awards, and College of Arts and Sciences Gabelli Fellowship to Zhongmin Lu.

PD 169

Molecular Chaperone Mediated Rescue of p.H723R Pendrin

Jinsei Jung; Mei Huang; Michelle Suh; Jae Young Choi
Yonsei University, College of Medicine

Background

Mutations in *SLC26A4* gene encoding pendrin, are responsible for hearing loss with enlarged vestibular aqueduct (EVA). The most common hereditary hearing loss-related mutation in Korea and Japan is p.H723R, which leads to defects in protein folding and cell surface expression. Here, we show that H723R-pendrin can be rescued to the cell surface via the HSP70 co-chaperone DNAJC14-dependent unconventional trafficking pathway.

Method

To find the candidates that were relevant t o the unconventional traffikcing of misfolded pendrin, we performed tandem affinity purification (TAP) assay with mass spectrometery and small interfering RNA screening.

Results

Blockade of ER-to-Golgi transport or activation of ER stress signals induced Golgi-independent cell-surface expression of H723R-pendrin and restored its cell-surface Cl^-/HCO_3^- exchange activity. Proteomic and short interfering RNA screenings with subsequent molecular analyses showed that Hsc70 and DNAJC14 are required for the unconventional trafficking of H723R-pendrin. Moreover, DNAJC14 upregulation was able to induce the unconventional cell-surface expression of H723R-pendrin.

Conclusion

These results indicate that Hsc70 and DNAJC14 play central roles in ER stress-associated unconventional protein secretion, and are potential therapeutic targets for diseases arising from transport defects of misfolded proteins, such as Pendred syndrome.

Funding

the National Research Foundation, the Ministry of Science, ICT & Future Planning, Republic of Korea

PD 147

Using A Large Biomedical Database, AudGenDB, to Characterize the Prevalence of Hearing Loss and Otitis Media in Down Syndrome Patients

E Bryan Crenshaw III[1,2]; Lezhou Wu[1]
[1]The Children's Hospital of Philadelphia; [2]Perelman School of Medicine at the University of Pennsylvania

Advances in information technology have opened new avenues of research into the causes of congenital hearing impairment. Nonetheless, many obstacles impede the realization of these new research directions, including the need to identify patient cohorts, develop a rich dataset of clinical characteristics, and navigate the regulatory mechanisms necessary to protect patient privacy. Importantly, much of the information and materials necessary to pursue these new research directions has been collected, but remains isolated in disparate – often obsolete - clinical data systems. To overcome the obstacles to acquiring clinical research data, a biomedical-computing infrastructure that collects information from several clinical data sources and integrates them into a central relational database has been developed, which is called the Audiological and Genetic Database (AudGenDB). To further enhance the utility of this database, an intuitive, powerful web-based user interface that can build complex queries of data across datasets from several clinical disciplines has been developed (http://audgendb.chop.edu). AudGenDB currently contains anonymized data from nearly 100,000 patients, including 4.4 million diagnoses, ~186,000 audiograms, and ~106,000 tympanograms. To demonstrate the power of using databases of this size, we have examined the prevalence of hearing loss and otitis media in Down Syndrome patients, an uncommon condition occurring in about 0.15% of births in the US. At the time of our analyses, the database contained records for 1253 patients with Down Syndrome. Using data in AudGenDB, we characterized with great precision and high statistical significance changes in tympanometric and audiometric values in these patients compared to normative values from the database. They had reduced external canal volumes, lower median static admittance values, and a broader peak pressure distribution. In addition, we demonstrated an increased prevalence of both conductive and sensorineural hearing loss. Finally, we've characterized in fine detail the temporal changes in the prevalence of otitis media during childhood. These data demonstrate the power of using a large biomedical database to characterize the hearing health of patients with conditions that occur with low incidence in the population.

Funding

Research funded by NIDCD grant R24 DC012207.

PD 148

The Audiological and Genetic Database Project: A Large Biomedical Informatics Platform for Hearing Research

Jeffrey Pennington[1]; Byron Ruth[1]; Jeffrey Miller[1]; Aaron Masino[1]; Joy Peterson[1]; John Germiller[1]; Ian Krantz[1]; Tamar Gomes[2]; Derek Stiles[2]; Juliana Manganella[2]; Margaret Kenna[2]; John Lee[3]; **Linda Hood**[3]; E Bryan Crenshaw III[1,4]
[1]The Children's Hospital of Philadelphia; [2]Boston Children's Hospital; [3]Vanderbilt University; [4]Perelman School of Medicine at the University of Pennsylvania

Recent developments in research and clinical practice have improved detection of childhood hearing impairment, the ability to ameliorate its impact on social and cognitive development of children, and the understanding of the genetic basis for hearing impairment. Newborn screening programs detect hearing loss at an early age, and the advantages of early detection and intervention are well documented. Hearing aids and cochlear implants are profoundly important for speech and language rehabilitation, and appropriate assessments of these outcomes are crucial for developing

evidence-based guidelines for use and quantification of benefit. Genetic analyses hold the promise of improved early detection and diagnosis, prediction of outcomes of therapies, and development of new therapies to reverse hearing impairment. These technologies are already widely used in the clinical setting, potentially providing a plethora of data that could serve to further improve diagnosis and describe the outcomes of therapy. However, most of these data are recorded in disparate written records, clinical systems, or database formats that are incompatible and, if in different institutions, often unknown to each other, and therefore difficult to compare or to use effectively in large-scale studies. To overcome these difficulties, researchers at The Children's Hospital of Philadelphia (CHOP) initiated the AudGenDB project. This project extracts, transforms, and loads data from these disjointed, incompatible information sources into a single relational database, and subsequently provides a powerful, web-based user interface (UI) for querying these data. Here, we describe AudGenDB 2.0, which has been improved by expanding the range and complexity of data within the database, In addition, with the acquisition of data from other institutions, namely Vanderbilt University Medical Center (VUMC) and Children's Hospital Boston (CHB), the scope and reach of the data resource continues to grow. AudGenDB 2.0 represents the next step in building a national network for the exchange of patient-oriented data to facilitate research in pediatric hearing health.

PD 149

Cytomegalovirus (CMV)-associated Hearing Loss – Findings from the NIDCD CHIMES Study

Suresh Boppana[1]; Shannon Ross[1]; April Palmer[2]; Amina Ahmed[3]; Pablo Sanchez[4]; Marian Michaels[5]; David Bernstein[6]; Kristina Feja[7]; Audra Stewart[8]; Karen Fowler[1]
[1]University of Alabama at Birmingham; [2]University of Mississippi Medical Center; [3]Carolinas Medical Center; [4]Ohio State University and Nationwide Children's Hospital; [5]University of Pittsburgh and Children's Hospital of Pittsburgh; [6]University of Cincinnati and Cincinnati Children's Medical Center; [7]Saint Peter's University Hospital; [8]University of Texas Southwestern Medical School

Background
CMV is the most frequent cause of congenital infection in the U.S. Congenital CMV infection (cCMV) is a leading non-genetic cause of sensorineural hearing loss (SNHL) however, data from population-based studies in which newborns are screened for both hearing and CMV are not available. The objective of the study is to determine the prevalence of CMV-associated SNHL at birth and at 4 years of age and whether newborn hearing screening (NHS) identifies majority of newborns with CMV-associated SNHL.

Methods
In addition to routine NHS, infants born at seven hospitals in the U.S. were screened for CMV as part of the NIDCD-sponsored CMV and Hearing Multicenter Screening (CHIMES) study. Infants who did not pass NHS or who tested positive for CMV underwent diagnostic audiologic evaluations to confirm SNHL. CMV-positive infants were enrolled in follow-up to monitor hearing outcome during the first 4 years of age.

Results
Between 2007 and 2012, of the 100,332 newborns screened for CMV, 99,942 infants were also screened for hearing. Overall cCMV prevalence was 0.5% (95%CI, 0.4-0.5%) and SNHL at birth occurred in 7.6% of CMV-infected infants. NHS in this cohort identified 57% of all CMV-related SNHL that occurred in the neonatal period. Overall, CMV-associated SNHL (SNHL at birth and late-onset loss) occurred in 12.0% of children with cCMV by 4 years of age. Significantly more CMV-positive infants did not pass NHS than CMV-negative infants (7% vs 0.9%, $p<0.0001$). Among CMV-positive infants, SNHL was confirmed in 65% of infants who did not pass NHS and 3.9% who passed NHS. SNHL occurred in 8.8% of children with asymptomatic and in 41.0% with symptomatic cCMV infection. After onset of loss, a majority of CMV-infected children with SNHL experienced progression. Infants born to non-Hispanic Black women <20 years of age had the greatest risk for cCMV and accounted for 45% of all CMV-associated SNHL.

Conclusions
Targeted CMV screening, which is currently being considered in many hospitals and in some states (Utah, Connecticut, and Illinois) will identify approximately 60% of infants with CMV-associated SNHL at birth. However without universal newborn CMV screening, a significant proportion of infants with CMV-associated SNHL at birth and all infected children with asymptomatic cCMV who develop late onset hearing loss will be missed. Infants of teenage Black women are at the greatest risk for cCMV and congenitally infected infants, especially those without other clinical findings are at risk for late-onset SNHL.

Funding
National Institutes on Deafness and Other Communication Disorders

PD 150

The Mechanics of Cochlear Homeostasis: Re-evaluation of the "Servo-Null" Animal Model Technique for Direct Measurement of Cochlear Chamber Pressures

Eric LePage; Paul Avan
Universite d'Auvergne

There are two ways to assess fluid pressures in cochlear chambers, indirect and direct. Indirect methods attempt to find a physiological effect which changes with applied pressure, e.g. phase of the distortion product, and attempt to calibrate that effect against externally applied changes in pressure, e.g. due to body tilt. The direct approach is to develop an animal model in which a pressure transducer is directly connected to a cochlear chamber. The "servo-null" approach was developed in the 1960s to cope with tiny vessels. The tip of a glass micropipette is introduced into the test chamber and as the pressure changes, a servo mechanism tracks

that pressure, adjusting external pressure sources to null electrolyte movement within the tip of the micropipette, outputting the value of that matching pressure to a recording device. The tip is also used to measure independently the electric potential. The use of glass micropipettes to measure pressure is indeed an order of magnitude more complex than using them to measure electric potential. Overpressure has long been suspected responsible for ruptures of Reissner's membrane in Meniere's attacks. Despite 40+ studies which have used this approach in the expectation of revealing pressures required to rupture, none have shown that the pressure in perilymph, nor in endolymph, nor the difference between them is remarkable. We have been studying this technique for five years, using both bench testing and its use in the cochleae of some 80 Mongolian gerbils, entering scala tympani via the round window then sequentially scala media through the basilar membrane. This presentation focuses upon a review of the literature and is followed by an assessment of the experimental results in the hindsight of a delineation of the strengths and weaknesses of the methodology. We find that seals are vitally important. The servo-null approach was not designed for any system in which frequency-dependent electric potentials exist which could interfere with the measurement. The commercial system is not supplied with any data on the characteristics of the device nor micropipettes and lacks any indication of whether the servo-system is indeed phase-locked. It was not designed for a biological system in which conceivably there is internal active homeostatic regulation of pressure. It does not mean that the device, short of redesign, is unusable. Maybe the lack of obvious progress is not because of lack of inspired experimental design and care so much as the need to revise the question?

PD 151

Roll Vection in Migraine Patients Using Inertial Nulling and Certainty Estimate Techniques

Mark Miller; Benjamin Crane
University of Rochester

Background

Vection is an illusory perception of motion that can occur when a visual motion is presented in the majority of the visual field. We used both certainty estimate (CE) and inertial nulling (IN) techniques to study the effect of visual stimuli on roll perception in humans with and without migraine.

Method

Nineteen human subjects were recruited, ten with typical migraine and nine controls. A visual star-field stimulus consistent with clockwise or counterclockwise roll motion was presented for 1 or 8s. For the IN method, an inertial nulling stimulus was delivered during the final 1s of the visual star-field stimulus. Subjects reported the overall perceived direction of motion during the final 1s of the stimulus. The magnitude of inertial motion was varied based on previous responses to find the point of subjective equality (PSE) at which clockwise (CW) and counter-clockwise (CCW) responses were equally likely to be perceived. For the CE trials, the same durations of visual motion were used but without inertial motion and subjects rated their certainty of motion on a scale of 0-100.

Results

For IN trials, the overall difference in PSE between 1s and 8s subjects is significant ($p=0.03$)[BC1] . Additionally, migrainers had a greater deviation in IN studies in the 8s than 1s ($p=0.01$), but controls did not ($p=0.72$). The variance among migraine subjects at the 8s ($\sigma^2=2.32$) was much greater than controls ($\sigma^2=0.35$) in IN nulling trials. Two-way ANOVA by population and duration was significant for duration and subjects matching for both CE and IN trials, and the interaction between the two approached significance in the IN trials ($p=0.06$). The correlation between CE and IN was small across all trials. Interestingly, the correlation between clockwise and counterclockwise studies was modest in the IN trials ($r=0.44$), whereas the correlation for CE was unusually high ($r=0.97$).

Conclusion

IN is a useful tool in measuring vection in the roll plane. The marked difference in correlation between clockwise and counterclockwise studies between IN and CE studies highlights the fact that CE studies may be less sensitive to variations in observed motion due to the nature of the reporting tool. Perception of roll rotation in migraine subjects was more influenced by visual roll relative to controls. However, there was substantial variation between subjects.

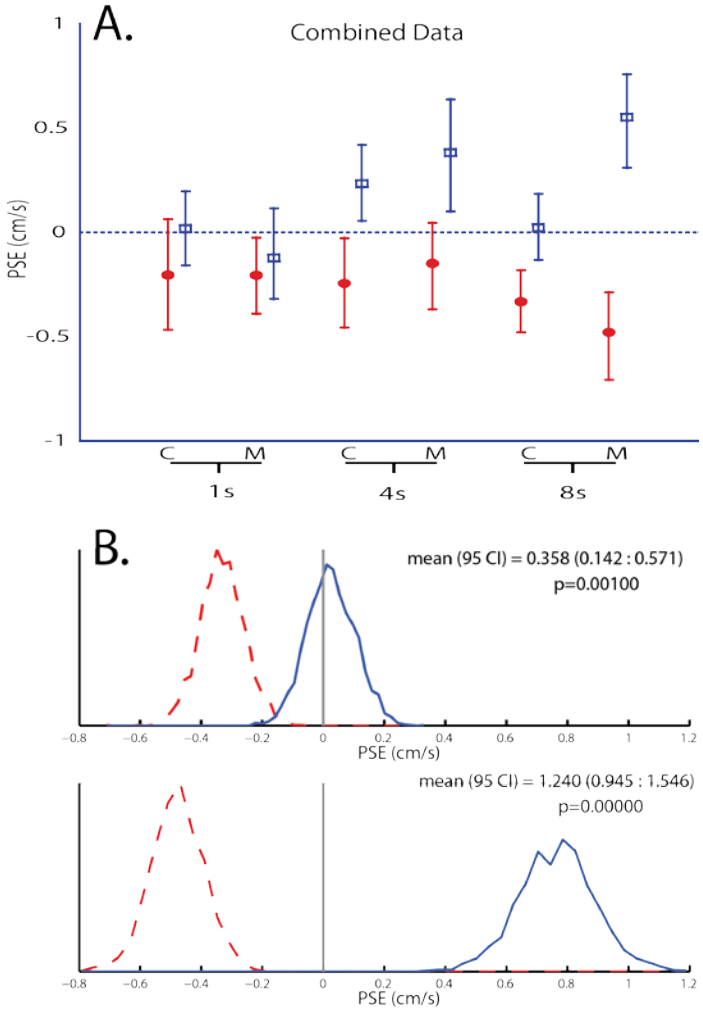

Figure 1: Panel A: Combined subject data by population and trial. Counterclockwise visual stimuli are represented with filled red circles, clockwise visual stimuli are represented by blue open squares. A positive PSE indicates that neutral motion would be perceived as clockwise self-motion. Error bars represent 95% CI. Panel B: 8s histogram comparing combined controls and migrainers response using a random resampling of responses. Responses from all subjects were included. Responses collected with counterclockwise visual stimuli are represented with a dashed red line, clockwise visual stimuli responses are represented with a solid blue line.

Funding
This work was supported by NIDCD K23 DC011298, R01 DC013580, P30 DC005409, and T32 DC009974, and a Triological Career Scientist Award, as well as a University of Rochester School of Medicine Office of Medical Education Research Grant.

PD 152

Bone Marrow-Derived Progenitor Cells in Human Cochlea Implantation

Athanasia Warnecke; Ariane Römer; Ulrike Köhl; Stephan Kloess; Christine Falk; Sabine Haumann; Omid Majdani; Thomas Lenarz
Hannover Medical School

Background

Neuronal degeneration as well as immunological reactions to foreign body hamper the performance of cochlear implants. Therefore, modulation of immunological processes in order to reduce scar formation and to optimize nerve-electrode-interaction may improve clinical outcome.

Progenitor cells are well-known sources of growth and immune factors suppressing inflammatory processes, which can be provided to the inner ear at appropriate amounts.

Methods

Three patients with bilateral severe hearing loss were treated. They were unilaterally implanted with a cochlear electrode previously and had chosen a second cochlear implant surgery on the other side. Due to different conditions, all patients were in danger of a substandard outcome on the second side and were, therefore, given the opportunity of progenitor cell transplantation. Surgery was performed without complications in our clinic according to Hannover CI standard procedure. Bone marrow was obtained by sternal puncture. The mononuclear cell fraction (MCF) consisting of progenitor cells was separated from blood immediately by centrifugation and re-suspended in plasma. The cell-coating of the cochlear implant electrode was performed with fibrin glue by a dipping procedure – leaving a thin coat of progenitor cells on the surface. Thereafter, the electrode was implanted into the cochlea. A model electrode was also coated with MCF for parallel in vitro testing.

In addition, a preliminary protocol for *cell-release* assessment of those enriched $CD45^-$ cell fractions including mesenchymal stromal cell (MSCs), their secretome and for identification of $CD45^+$ cells was developed using a single platform 10-colour flow cytometric panel.

Results

The patients' acceptance to the salvage treatment was high without postoperative problems. Initial fitting was performed six weeks after surgery showing excellent results.

In vitro, we demonstrated successful coating of the electrode-surface with good cell survival over two weeks. The release of different cytokines and growth factors and the neuroprotective effects on spiral ganglion neurons was shown in cell culture-conditions.

Conclusion

Implantation of progenitor cells in otology shows a high potential. It was very well tolerated and promising audiological results were obtained during initial fitting.

Our in vitro-experiments showed neuroprotective effects of the MCF on spiral ganglion neurons as well as the release of cytokines and growth factors involved in vascular remodeling. Thus, we propose this procedure as a promising protocol for protection of residual inner and outer hair cells in future clinical applications.

Consequently, progenitor cells are about to open the door to improved speech perception and maintenance of residual hearing in cochlear implantation.

Funding
Cluster of Excellence "Hearing4all"

PD 153

Minding species gaps in the cochlea: non-human primate and patient derived- hiPSc models for the study of hereditary hearing loss

Masato Fujioka[1]; Makoto Hosoya[1]; Noriomi Suzuki[1]; Hideyuki Okano[1]; Tatsuo Matsunaga[2]; Kaoru Ogawa[1]
[1]Keio University School of Medicine; [2]National Institute of Sensory Organs, National Tokyo Medical Center

The rodent model has been contributed to the study of hereditary hearing loss. Particularly, gene modification technology (e.g. knock-out, knock-in, transgenic) is a powerful tool for investigating phenotypes of diseases in detail to understand the pathophysiology. However, there are diseases of which mouse models cannot recapitulate human phenotypes, for example Pendred syndrome/DFNB4 H723R mutation in SLC26A4 gene. To circumvent such a pitfall and to further understand intractable cochlear sensorineural hearing loss, we have been investigating the physiology/ pathophysiology of monogenic, bilateral, gradual but fluctuating deafness using common marmoset (Callithrix jacchus), a non-human primate, and human iPSC technology. In the talk I will introduce our data showing differential expression pattern of deafness genes in the cochlea of marmoset in comparison with that in mouse. Also, I will present an example revealing human phenotypes of disease-state cochlear cells derived from patients harboring mutations in the SLC26A4 gene. We anticipate that the combination of non-human primate experiments and iPSC-based in vitro model may be useful for translational studies investigating the pathogenesis of other forms of hereditary deafness, and idiopathic hearing loss, to identify new treatments for these conditions.

PD 154

Tympanic Membrane Damage Induced by Blast Overpressure – A Study in Head Block Attached with Human Temporal Bones

Rong Gan; Don Nakmali; Kyle Smith; Kegan Leckness; Zachary Yokell
University of Oklahoma

Introduction
Mechanical damage to middle ear components in blast exposure directly causes hearing loss, and the rupture of tympanic membrane (TM) is the most frequent injury of the ear. However, it is unclear how the severity of TM damage is related to the overpressure level and impulse wave direction. This paper reports the recent study in "head block" attached with human temporal bones and exposed to blast. The hypothesis is that the threshold for TM rupture is directly related to blast overpressure level and the orientation of the head w.r.t. blast wave. The goal is to investigate the relationship between the TM damage and impulse noise intensity and direction.

Methods
A "head block" attached with human temporal bone and mounted with two pressure sensors was developed. One sensor was inserted near the TM (P1) and another was behind the TM inside the middle ear (P2). The blast pressure was monitored by the third sensor placed at the ear canal entrance (P0). The "head block" was exposed to blast inside the test chamber in our lab at three setups: blast wave from the top of the head, lateral to the ear, and front of the face. 13-15 temporal bones were tested in each setup. Pressure waveforms were recorded and the TM rupture thresholds were determined. The impulse pressure energy spectra analysis of waveforms was then performed to calculate signal energy flux over frequency bands. Finally, the 3D finite element model of human ear was used to predict the distributions of stress in the TM.

Result
Measurements from all temporal bones show that the blast overpressure P0 induced the highest peak pressure P1 and a much lower pressure P2. There was no significant difference of waveforms between three setups, but there were some differences in peak pressure ratio of P1 to P0 and the TM rupture threshold, as well as the distribution of impulse energy flux over 10 octave frequency bands. The finite element modeling results predicted the location of maximum stress in the TM caused by blast waves.

Conclusions
The experimental setup for monitoring impulse wave transduction from the ear canal to middle ear is successfully completed along three blast directions w.r.t. the head. The TM damage thresholds are identified and the results suggest that the ear canal and pinna play an important role for overpressure transmitted into the middle ear. (Supported by DOD W81XWH-14-1-0228 and NIH R01DC011585)

Funding
Research was supported by DOD W81XWH-14-1-0228 and NIH R01DC011585.

PD 155

Intracochlear Drug Delivery through the Oval Window in Fresh Cadaveric Human Temporal Bones

Woo Seok Kang[1]; Kim Nguyen[2]; Charles McKenna[2]; William Sewell[1]; Michael McKenna[1]; David Jung[1]
[1]Massachusetts Eye and Ear Infirmary; [2]University of Southern California

Background

Otosclerosis is a bone remodeling disorder that affects the otic capsule, inhibits movement of the stapes, and presents as a conductive hearing loss. Larger otosclerotic lesions can involve the cochlea and may result in an overlying sensorineural hearing loss due to involvement of the cochlear endosteum and spiral ligament.

Bisphosphonates bind to bone minerals and inhibit osteoclast activity to treat a variety of metabolic bone diseases. We have previously demonstrated that zoledronate, a nitrogen-containing bisphosphonate, can arrest the sensorineural hearing loss seen in cochlear otosclerosis. We have also shown that, in animals, local delivery of bisphosphonate into the cochlea can dramatically increase delivery efficiency without incurring ototoxicity. In the present study, a fluorescently labeled bisphosphonate compound (6-FAM-ZOL) was introduced into the human cochlea through the oval window and its distribution within the temporal bone was quantified.

Methods

In three fresh human temporal bones, we introduced 1 µL of 10 µg/µL 6-FAM-ZOL via the oval window and the scala vestibuli using a micropipette after lifting the stapes footplate. We compared these specimens to control specimens treated with artificial perilymph alone. Specimens were processed, embedded into methylmethacrylate, and ground to the mid-modiolar axis. Images were collected using a Leica TCS-SP2 confocal microscope to generate maximum fluorescence images and fluorescence levels were quantified using ImageJ.

Results

Strong fluorescent signal was observed in the bony wall of the vestibular capsule and the cochlea. We found 6-FAM-ZOL to be distributed up to the apical cochlear turn. In specimens treated with 6-FAM-ZOL, we identified a strong baso-apical gradient of fluorescent signal along the lateral cochlear wall and the modiolus both in the scala vestibuli and in the scala tympani. For both the lateral wall and the modiolus, a significant dose effect (6-FAM-ZOL vs artificial perilymph) was observed both in the scala vestibuli and the scala tympani (all $p < 0.05$). There was no significant effect of scalae location (scala vestibuli vs scala tympani) either in the lateral wall or in the modiolus.

Conclusion

Bisphosphonate introduced via the oval window and the scala vestibuli in the human cochlea can be delivered up to the apical cochlear turn at significant levels in both the scala tympani and the scala vestibuli. Interscalar communication is likely to play an important role in determining patterns of drug delivery in the inner ear.

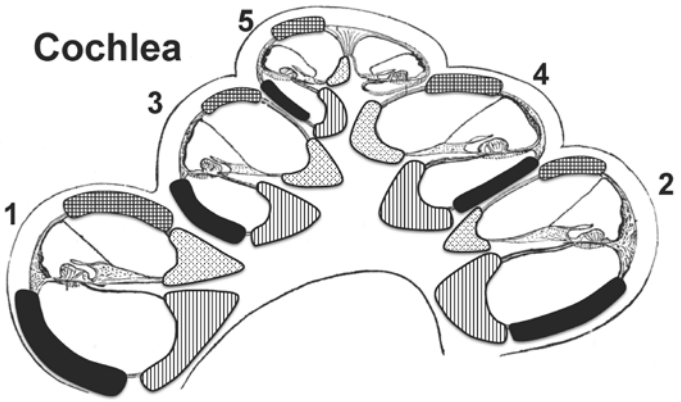

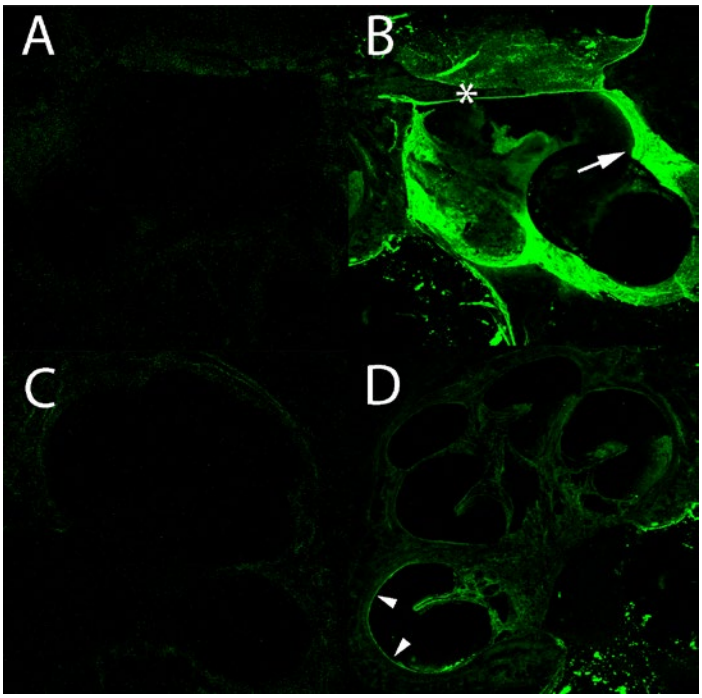

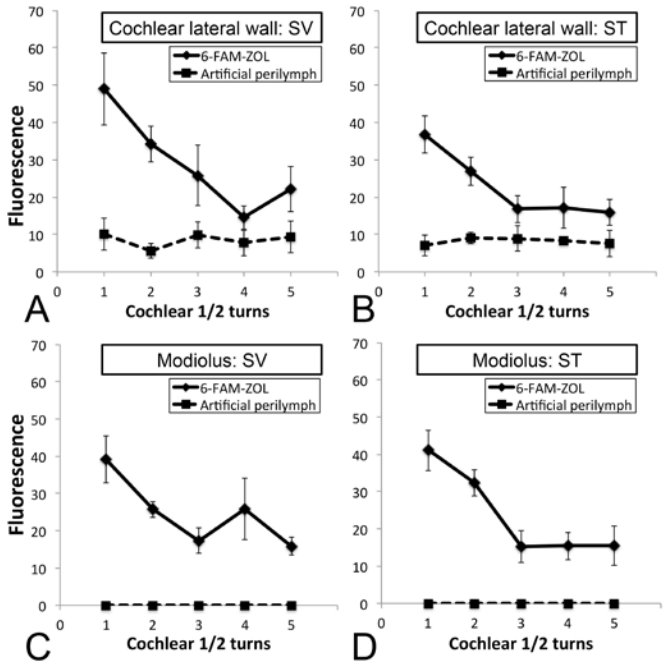

Funding
This work was supported by NIH NIDCD Grant R01 DC009837.

PD 156

Protein Transduction Therapy Via the Round Window in Guinea Pigs

Hiroki Takeda[1]; Takaomi Kurioka[2]; **Ryosei Minoda**[1]; Takeshi Matsunobu[2]; Kunio Mizutari[2]; Turu Miwa[1]
[1]Kumamoto University; [2]National Defense Medical College

It is important to develop effective and safe methods for drug delivery into the inner ear to establish treatment modalities for inner ear diseases. Cell-penetrating peptides (CPPs) are short sequences of amino acids that facilitate the penetration of conjugated cargos across mammalian cell membranes. Generally, simple polyarginine peptides induce significantly higher cell penetration rates among CPPs. 'X-linked inhibitor of apoptosis protein' (XIAP) is the most potent member of the inhibitors of apoptosis (IAP) family. XIAP enhances the survival signal directly by forming a complex with TAB1/TAK1 via its BIR1 domain. Cooper et al. demonstrated the successful protective treatment effect of XIAP against cisplatin-mediated ototoxicity using an AAV vector that was injected into the scala tympani of the cochlea. When considering the clinical application of AAV-based XIAP treatment, the direct injection of viral vectors into the scala tympani, which is part of the perilymphatic space, may cause inner ear damage, and the direct injection of therapeutic molecules into the perilymphatic and endolymphatic spaces of the cochleae has not been performed clinically because of this risk. Thus, the need exists for a simpler and safer strategy to administer therapeutic molecules such as XIAP into the cochleae. CPP-based treatment may be such a treatment modality.

We first examined the safety and efficacy of protein transduction using a CPP consisting of nine arginines (9R-CPP) via the round window niche. Second, to examine the feasibility of 9R-CPP-based treatment via the round window, we performed 9R-CPP-based XIAP treatment against noise-induced hearing loss in guinea pigs in vivo.

Consequently, a peptide consisting of nine arginines ('9R') effectively delivered enhanced green fluorescent protein (EGFP) into guinea pig cochleae via the round window niche without causing any deterioration in auditory or vestibular function. A second application 24 h after the first prolonged the presence of EGFP. To assess the feasibility of protein transduction using 9R-CPPs via the round window, we used 'X-linked inhibitor of apoptosis protein' attached to a 9R peptide (XIAP-9R). XIAP-9R treatment prior to acoustic trauma significantly reduced putative hearing loss and the number of apoptotic hair cells in the cochleae. Thus, the topical application of molecules fused to 9R-CPPs may be a simple and promising treatment strategy for inner ear diseases.

PD 157

Exosome-associated AAV as a highly efficient vector platform for cochlear hair cell gene delivery

Bence Gyorgy[1,2]; Cyrille Sage[1]; Deborah Scheffer[1]; Artur Indzhykulian[1]; Dakai Mu[3]; Xandra Breakefield[3]; Casey Maguire[3]; David Corey[1,2]
[1]Harvard Medical School; [2]Howard Hughes Medical Institute; [3]Massachusetts General Hospital

Introduction

In recent gene therapy trials, adeno-associated virus (AAV) vectors for diseases such as blindness and hemophilia were found to be safe and effective. Gene therapy for hearing and balance disorders is not as advanced, because gene delivery into the cochlea (particularly to sensory hair cells) is generally less efficient. Indeed, recent studies using AAV (Akil et al., 2012; Askew et al., 2015) showed almost exclusively inner hair cell (IHC) transduction. Here we show that exosome-associated AAV vectors (vexosomes) outperform regular AAVs in hair cell gene delivery *in vitro* and *in vivo,* virally transducing inner as well as outer hair cells (OHC).

Methods

Vexosomes from media of AAV-producing cells (293T) were harvested by ultracentrifugation. For *in vitro* cochlear transductions, we explanted organs of Corti from P1 CD1 mice. Conventional AAV1 vectors or AAV1 vexosomes, encoding GFP, were added to the culture medium to determine the extent of transgene delivery and expression. For *in vivo* studies, we injected vectors at P1 into the scala media through cochleostomy or into the scala tympani through the round window membrane (RWM). To study whether vexosomes can rescue a disease phenotype *in vitro*, we explanted organs of Corti from P1 *Tmhs/Lhfpl5* knock-out mice, which lose mechanotransduction (and hearing and balance) by P5. Cultures were transduced with vexosomes encoding TMHS (tetraspan membrane protein of hair cell stereocilia) and restoration of function was assessed by accumulation of FM1-43 dye, which is trapped inside functional hair cells.

Results
In vitro, AAV1-vexosomes led to 80% transduction of IHCs and OHCs, while regular AAV1 was able to transduce only up to 30% of IHCs and OHCs at equivalent genome copies per cell. *In vivo*, vexosomes also outperformed regular AAV. Delivered by cochleostomy, AAV1-vexosomes transduced 63.7±6.5% and 30.0±9.8% of IHCs and OHCs, respectively, whereas AAV1 transduced only 35.8±0.7% and 16.7±1.9% (mean fraction of transduced cells from two experiments with 10 animals in each group). Delivered by RWM, AAV1-vexosomes transduced 88.0±2.2% and 25.2±10% of IHCs and OHCs, whereas AAV1 transduced 75.0±4.4% and 15.6±0.4% (two experiments). Importantly, AAV1-vexosomes encoding TMHS were able to restore FM1-43 accumulation in ~60% of TMHS KO hair cells *in vitro*, apparently rescuing mechanotransduction.

Conclusion
Exosome-associated AAV is a powerful gene delivery system to the mammalian cochlea *in vitro* and *in vivo*. Therefore they may be utilized to study hair cell physiology *in vitro*, and—in the future—for *in vivo* gene therapy.

PD 158

Effect of Locally Applied Dexamethasone on Spiral Ganglion Neuron Density and Function in Vivo

Verena Scheper[1]; Thomas Lenarz[1]; Timo Stöver[2]; Gerrit Paasche[1]
[1]Hannover Medical School; [2]Goethe Universität, Frankfurt

Background
A cochlear implant directly stimulates the spiral ganglion neurons (SGN), the primary auditory neurons. Fibrous tissue growth around the electrode array may occur after cochlear implantation. Research showed that the glucocorticoid dexamethasone (DEX) can reduce tissue growth as well as loss of residual hearing. Up to now little is known about the effect of local DEX treatment on SGN. Therefore the effect of locally applied DEX on SGN survival and electrophysiological responsiveness was investigated.

Methods
Normal hearing guinea pigs were systemically deafened and after three weeks implanted with an electrode-micropump system. Four experimental groups were unilaterally treated with A) artificial perilymph (AP), B) AP and electrical stimulation (ES; biphasic charge balanced pulses, 100 µsec per phase, 250 Hz at a 40% duty cycle, 8 dB above the electrical response threshold, 24h a day for 27 days), C) dexamethasone (DEX, 100 ng/ml), D) DEX + ES. All animals were sacrificed 4 weeks after implantation. In both electrically stimulated groups electrically evoked auditory brainstem responses (eABR) were measured after implantation and before sacrificing the animals. SGN density was evaluated on paraffin embedded specimens.

Results
DEX did not affect the SGN density compared to the control group. When stimulating the animals electrically, an already described protective effect of ES is observed (AP versus AP+ES $p<0.05$). This effect is even stronger when DEX is simultaneously applied (AP versus DEX+ES $p<0.01$). The eABR threshold of AP+ES treated animals did increase over time compared to the threshold measured directly after surgery, whereas the threshold of DEX+ES treated animals decreased within the same timeframe.

Conclusion
In the concentration and treatment duration used in this study DEX had no negative effect on the SGN density. Applied simultaneously with electrical stimulation it resulted in even better hearing thresholds and SGN survival. Based on these results DEX seems to be a safe drug for local inner ear treatment of peri-implant fibrosis in cochlear implant patients.

Funding
EC funded Project BioEar.

PD 159

Transtympanic Delivery of Antisense Oligonucleotides in Murine Model of Usher Syndrome

Christopher Tran[1]; Abhilash Ponnath[1]; Mette Flaat[1]; Francine Jodelka[2]; Frank Rigo[3]; Michelle Hastings[2]; Jennifer Lentz[1]
[1]Louisiana State University Health Sciences Center - New Orleans; [2]Rosalind Franklin University of Medicine and Science; [3]Isis Pharmaceuticals, Inc.

Usher syndrome (Usher) is an autosomal recessive disorder that consists of sensorineural hearing impairment, variable vestibular dysfunction and delayed-onset retinitis pigmentosa. Type 1 Usher syndrome (USH1) is characterized by congenital profound sensorineural hearing loss and vestibular areflexia, with adolescent-onset retinitis pigmentosa. Mutations in the *USH1C* gene account for approximately 6-8% of USH1 cases, however, the *USH1C* c.216G>A (216A) mutation is responsible for nearly all USH1 cases in the Louisiana Acadian population. The 216A mutation creates a cryptic splice site that results in a truncated mRNA and harmonin protein, a protein essential for normal hair cell development and function. We created a knock-in mouse model of USH1C containing the c.216G>A mutation, and showed that systemic treatment with antisense oligonucleotides (ASOs) targeting the 216A mutation rescues hearing and vestibular function when given early in life. The purpose of this study was to test the effects of ASO delivery locally to the ear on hearing rescue. Trans-tympanic injection in neonatal mice was developed, and 216AA mice and littermate controls were treated with ASOs. Hearing and vestibular function were assessed by auditory-evoked brainstem response (ABR) and circling behavior, respectively. Normal external ear, tympanic membrane morphology and hearing was observed in 1 month old wild type mice that received trans-tympanic saline or control ASO injections within the first three weeks of life. Although mice younger than 7 days had a particularly underdeveloped middle ear, a trend towards low frequency hearing rescue was observed in 216AA mice with gelfoam-mediated topical 216A-targeted ASOs placed at the external

tympanic membrane. Trans-tympanic membrane injection in neonatal mice is a safe and a minimally invasive way to administer ASOs.

Funding
NIH/NIDCD 1R01DC012596

PD 160

Neurotrophic Encapsulated Cell Device for Co-Implantation with Cochlear Implants: Neuroprotective Effects In Vivo

Wiebke Konerding[1]; Heike Janssen[1]; Peter Hubka[1]; Jana Schwieger[1]; Anandhan Dhanasingh[2]; Pavel Mistrik[2]; Jenny Ekberg[3]; Thomas Lenarz[1]; Lars Wahlberg[3]; Jens Tornøe[3]; Andrej Kral[1]; Verena Scheper[1]
[1]Hannover Medical School; [2]MED-EL, Innsbruck, Austria; [3]NsGene

In patients with sensorineural hearing loss (SNHL), cochlear implants (CI) are bypassing the affected hair cells and electrically stimulate the auditory nerve. To prevent the degeneration of spiral ganglion neurons (SGN), as is common in SNHL, treatment with neurotrophic factors (NTF) has been shown to be effective both *in vitro* and *in vivo*. As a means for delivering NTF to the human inner ear, an encapsulated cell (EC) device has been developed. We tested the long-term functionality of the EC devices using human retinal cells (ARPE-19), genetically engineered to produce glial cell line-derived neurotrophic factor (GDNF). The device was tested either with or without additional application of electrical stimulation (ES) via a CI. We assessed SGN cell survival and electrophysiological responsiveness of the auditory system in an animal model of SNHL.

Neonatally deafened cats (daily s.c. injection of neomycin) were implanted unilaterally, 2-3 months after confirmed deafness, with an EC device and a CI into the scala tympani. The animals were assigned to 3 treatment groups: (1) control group (ARPE-19 parental cells), (2) GDNF group (ARPE-19 cells producing GDNF), and (3) ES group (GDNF producing cells + chronic ES). ES was applied via environmental acoustic exposure through a human speech processor 4 h/day, 5 days/week. Auditory brainstem responses (ABR) to ES of the acutely implanted, treated and untreated ear were measured and both cochleae were harvested for histology, 6 months following implantation. The GDNF production from explanted EC devices was measured via enzyme-linked immunosorbent assay (ELISA) and compared to preimplantation production levels. Electrophysiologic results were correlated with histological assessment of SGN density in the Rosenthal's canal. The results were compared to those of acutely deafened cats.

The EC devices usually ceased GDNF production before the end of the study period. In one animal GDNF production was still evident after 6 months of implantation. Preliminary electrophysiologic (ABR) and histologic results did not reveal significant differences between the 3 treatment groups; detailed analyses are pending. The viability of encapsulated cells is discussed in light of fibrous tissue formation within the scala tympani. Further modifications of the devices or pharmacological support of the implant ingrowth are necessary for functional long-term application.

Funding
Funded by the European Union EC project NeuEar

PD 161

Nanoparticle-mediated inner ear steroid delivery mitigates ototoxicity from cisplatin treatment.

Didier Depireux[1]; Bharath Ramaswamy[1]; Benjamin Shapiro[1]; Andrea Apolo[2]
[1]University of Maryland, College Park; [2]National Cancer Institute

Background
Cisplatin is still the antineoplastic drug of choice for several cancers, particularly urogenital cancers, and as a radiosensitizer, particularly in head and neck cancers.

However, it is very toxic to the kidneys, to the inner ear and to the nervous system. While the nephrotoxicity is well controlled and mitigated by "hyper-hydrating" the patients, no such option exists to prevent the hearing loss and tinnitus which almost always develop in the typical patients. Steroids are known to mitigate the ototoxicity, but they interfere with the efficacy of the cisplatin.

In a mouse model, we sought to study whether actively steering steroid-eluting magnetic nanoparticles into the cochlea during cisplatin treatment can reduce the ototoxicity of the cisplatin while preserving its antineoplastic effect.

Method
We adopted the cisplatin model of Roy et al (PMID:24216513), which established a cisplatin and hyper-hydration regimen which reliably induces severe hearing loss with very little mortality. Coincident with the cisplatin delivery, we magnetically pushed into the left of the mice biocompatible nanoparticles loaded with prednisolone phosphate. The prednisolone phosphate diffuses from the particles over several days, but being confined to the cochlea, it does not interfere with the cisplatin efficacy. The right ear is left intact. Otoxocity is measured via ABRs and post-mortem cytocochleograms.

Results
We measured ABRs at several time points during the cisplatin treatment. We observed a gradual degradation of the hearing thresholds at high frequencies (32kHz) where no threshold was measurable in any non-treated ear by the end of the injections. In treated ears, saline-injected ears displayed the same hearing loss as the non-treated ear, with complete loss of outer hair cells in the basal turn of the cochlea. Mice treated with intratympanic methyldprednisolone showed a reduced outer hair cell loss, but non-measurable hearing thresholds at the highest frequency. Mice treated with steroid-eluting nanoparticles showed a mild hearing loss and only minimal out hair cells loss in the basal turn.No significant hearing loss was measured at the lowest frequency of hearing, and no

significant hair cell loss was seen in the apical turn in any group.

Conclusion

Treating patients with intra-cochlear steroid-eluting nanoparticles offers the possibility of mitigating or eliminating the hearing loss and tinnitus in patients undergoing cisplatin therapy, in a way that does not interfere with the antineoplastic effect of cisplatin. The same nanoparticles can be used to deliver other therapies, biologics, siRNA and other agents of interest.

Funding

NCI-UMD seed fund

PD 170

Pitch-Responsive Cortical Regions in Subjects with Congenital Amusia

Sam Norman-Haignere[1]; Philippe Albouy[2]; Anne Caclin[2]; Nancy Kanwisher[1]; Josh McDermott[1]; Barbara Tillmann[2]
[1]MIT; [2]CNRS

Congenital amusia is a lifelong deficit in music perception thought to reflect an underlying impairment in the perception and memory of pitch. Prior studies have suggested that amusia stems from impaired connectivity between auditory cortex and downstream areas of frontal cortex. However, it remains unclear whether impairments in the coding of pitch in auditory cortex also contribute to the disorder, in part because prior studies have not measured responses from the cortical regions most implicated in pitch perception in normal individuals. We addressed this question by measuring fMRI responses in 11 subjects with congenital amusia and 11 non-musician control subjects to a stimulus contrast that reliably identifies pitch-responsive regions in normal individuals: harmonic tones vs. frequency-matched noise. Surprisingly, we found that amusic individuals with substantial pitch perception deficits nonetheless exhibited clusters of pitch-responsive voxels that were comparable in extent, selectivity, and anatomical location to those of control participants. Our results are consistent with the hypothesis that amusics' pitch deficits arise from impaired connectivity between auditory and frontal cortex, rather than impaired responses to pitch in auditory cortex. These findings suggest parallels between amusia and other neurodevelopmental disorders, such as dyslexia and prosopagnosia, which may also stem from impaired connectivity between core sensory areas and downstream cortical regions.

Funding

Grant from the "Agence Nationale de la Recherche" (ANR) of the French Ministry of Research (ANR-11-BSH2-001-01) to Barbara Tillmann and Anne Caclin, CNRS fellowship to Philippe Albouy, NRSA Research Fellowship to Sam Norman-Haignere

PD 171

Low Frequency Auditory Synchronization Deficiencies in Schizophrenia

Krishna Puvvada[1]; L Hong[2]; Jonathan Simon[1]
[1]University of Maryland, College Park; [2]University of Maryland School of Medicine

Background

Schizophrenia is a severe and often disabling brain disorder. A hallmark feature of schizophrenia is auditory hallucinations, which is present in most patients sometime during the course of illness. Auditory evoked potentials measured using electroencephalography (EEG) show consistent abnormalities in patients, especially the auditory steady state response (ASSR). Traditionally ASSR studies in schizophrenia have focused on 40 Hz responses (gamma band) due to its strength and its hypothesized role in synchronizing local neural networks. Recent studies indicate that neural coding at slow frequencies (2-8 Hz) is most critical for perception of speech and other natural sounds, and so may play an important role in auditory hallucinations. Hence, we hypothesize that the abnormalities in neural responses at slow rates will serve as better indicators of schizophrenic population than responses at 40 Hz.

Methods

EEG responses to click trains at different frequencies (2.5 Hz, 5 Hz, 10 Hz, 20 Hz, 40 Hz) were recorded from 137 schizophrenia patients, 117 normal controls and 60 first-degree relatives. The stimuli consisted of 75 trials of click trains consisting of 15 clicks at the appropriate frequency. Data is recorded using 64-channel EEG. Working memory of the subjects was also assessed.

Results

EEG responses were analyzed in terms of both phase locking factor (PLF) and ASSR power. Both PLF and ASSR power show substantially better differentiation between patients and controls at 2.5 Hz compared with all other frequencies. ASSR power at 2.5 Hz shows significant group separation between patients and first-degree relatives of patients who have increased vulnerability to schizophrenia, where as ASSR power at 40 Hz showed significant separation between relatives and controls. ASSR power at 2.5 Hz also showed significant correlation with working memory.

Conclusion

SSR abnormalities can be observed in schizophrenic patients not only in faster gamma range neural responses but also in slower rates. Recent studies suggested that the ability to activate delta during cognitive tasks represent the ability to inhibit other irrelevant activities. The positive correlation of 2.5 Hz ASSR power with working memory might be indicative of this, as 2.5 Hz ASSR is a test of capacity to activate delta band. The fact that 2.5 Hz ASSR shows group separation between patients and relatives suggest that it is indicative of expression of psychosis where as 40 Hz ASSR deficit in relatives compared to controls suggest that it is a possible vulnerability biomarker.

Funding
NIH support from R01DC014085 to JZS and R01MH085646 to LEH, and a seed grant from the University of Maryland to JZS and LEH.

PD 172

Differential effect of transient developmental hearing loss on cortical and striatal synapses.

Todd Mowery; Vibhu Kotak; Dan Sanes
New York University

Background
Critical periods have been studied almost exclusively in the primary sensory pathways, yet deprived animals can display behavioral deficits that are not solely attributable to sensory processing. Using a cortico-striatal brain slice preparation, we explored whether transient developmental hearing loss differentially affects inhibitory synapse function in layer V pyramidal neurons and their medium spiny neuron targets in striatum.

Methods
Whole-cell voltage-clamp recordings were obtained from layer V ACx pyramidal neurons and ACx-recipient medium spiny neurons (MSN) in cortico-striatal brain slices from gerbils that experienced transient mild hearing loss. Earplugs were inserted bilaterally on postnatal day (P) 11 and removed on P35; thus the animals experienced normal hearing from P35 until the day of recording (P86). Inhibitory post synpatic current (IPSC) properties in layer V pyramidal neurons from animals that were earplugged (n=20) were compared to those recorded from age-matched layer V controls (n=26). Likewise MSNs from earplugged animals (n=12) were compared to those recorded from age-matched MSN controls (n= 15).

Results
We found that IPSCs were significantly enhanced in ACX layer V pyramidal cells. Spontaneous (s) IPSC amplitudes were larger [mean ± SEM: control; -39.4 ± 2.1 pA vs. transient earplug: -52.8 ± 5.9 pA; $p < .05$], sIPSC frequencies were greater [control: 11.8 ± 0.9 Hz vs. transient earplug 15.4 ± 1.5 Hz, $p < .05$], and SIPSC decay time constants were faster [control: 9.5 ± 0.6 ms vs. transient earplug: 7.1 ± 0.8 ms, $p < .05$). In contrast, the medium spiny neurons of transiently earplugged animals had sIPSC amplitudes that were significantly smaller [mean ± SEM: control; -25.1 ± 3.6 pA vs. transient earplug: -12.7 ± 1.0 pA; $p < .05$), sIPSC frequencies that were significantly lower [control: 15.2 ± 2.7 Hz vs. transient earplug 3.77 ± 1.3 Hz, $p < .01$] and sIPSC time constants that were significantly slower [control: 22.2 ± 2.7 ms vs. transient earplug: 30.1 ± 3.3 ms, $p < .05$).

Conclusion
These results suggest layer V pyramidal neurons and the medium spiny neurons that receive projections from them are differently sensitive to transient hearing loss. Taken together with our finding that IPSCs are reduced in layer 2/3, these results suggest that each layer of the network may be responding to changes in its afferent population. This could have implications for the etiology by which individuals recovering from transient developmental hearing loss have normal hearing thresholds and yet display non-sensory deficits.

Funding
NIH R03DC014807 (TMM)

PD 173

Layer Specificity of Intracortical Microstimulation of the Auditory Cortex In Vivo

Mathias Voigt; Andrej Kral
Hannover Medical School

Previous attempts at developing cortical implants for sensory restitution relied mostly on stimulation of the cortical surface. One reason for the unsatisfactory outcome could be the high spread of synchronous activity evoked by such stimulation using relatively high currents. Intracortical microstimulation (ICMS) using penetrating electrodes would allow a much more focused activation of local networks. Recent technical developments made an *in vivo* combination of simultaneous electrical stimulation and extracellular recordings possible. This was used to assess the effects of focused ICMS on a local auditory cortical network.

We stimulated the primary auditory cortex of adult guinea pigs under ketamine/xylazine anesthesia electrically (charge-balanced, cathodic-leading, biphasic single pulses in monopolar configuration; return electrode in the neck muscles), using single electrodes of a 16 channel, linear multi-electrode Neuronexus array. Evoked activity was recorded from the remaining 15 electrodes in parallel. By varying stimulation parameters (current, pulse duration and stimulation layer) of focal ICMS, the ability to evoke auditory-like columnar response patterns could be investigated.

Local field potentials as well as multi-unit responses evoked by ICMS increased systematically with increasing current and pulse duration in 5 animals. Stimulation thresholds were found to vary in the range of 12–28 μA_{pp}, lowest thresholds were observed for granular and supragranular layers. Chronaxies obtained for stimulation of different layers were in the range of 290–780 µs, demonstrating a predominant activation of axons and dendrites. Consistent columnar response patterns were observed in all animals. These patterns were consistently dependent on the stimulated layer. Current source density profiles evoked by auditory pure tone stimulation and ICMS were quantitatively compared using cross-correlations. Columnar activation most closely resembling the activation by auditory stimuli was achieved by stimulation of middle layers. After the experiments, histological analysis of the cortex using Nissl and cytochrome oxidase excluded any current-induced damage.

The stimulation layer of ICMS has a significant influence on the activation of local neural networks in the primary auditory cortex. Stimulation of the thalamo-recipient granular layer IV leads to response patterns most similar to physiological columnar activity. Using such a focused, layer-specific,

low-current ICMS approach could improve the specificity of elicited percepts by cortical implants, compared to the more unfocused surface stimulation used previously.

Funding
Supported by Deutsche Forschungsgemeinschaft (Cluster of Excellence Hearing4all)

PD 174

The Adult Auditory Cortex is more Resistant than Suspected to Long Lasting Daily Exposure to Environmental Noise: A Study in the Sprague Dawley Rat.

Florian Occelli; **Jean-Marc Edeline**; Boris Gourevitch
CNRS UMR 9197 & University Paris-Sud

Background
Over the last decade, several studies have suggested that non-traumatic noise exposures (<85dB) strongly impact functional properties in the adult auditory cortex (ACx) such as the tonotopy or the ability to follow fast amplitude modulations (Norena et al 2006; Zhou & Merzenich 2012; Zhen 2012; review in Gourévitch et al 2014). Here, we aim at determining what are the consequences of long-term exposure (3-18months) on functional properties of ACx neurons in Sprague Dawley rats. We used a real-world noise with a flat spectrum between 0.1 and 40kHz and a large range of amplitude modulation. We tested, on the same animals, ABR audiograms, behavioral performance in a go/no-go behavioral task, and neuronal activity in primary auditory cortex.

Methods
Separated groups of rats were submitted to 3, 6, 12 or 18 months of noise exposure (80dB, 8h/day) in a dedicated room; age-matched control rats were housed in a standard colony room. ABR were tested before and after exposure. Neurons were recorded in the ACx of Ketamine/Xylazine anesthetized rats using arrays of 16 electrodes inserted in the tonotopic field A1. Frequency response areas (FRA) were quantified by presenting gamma tones from 0.1-36kHz at 75-5dB. The responses to amplitude modulated sounds as well as conspecific and heterospecific vocalizations in absence or presence of background noise were also obtained.

Results
At the behavioral level, there was no difference between the performance of exposed and control rats whatever the age. Using ABRs, we found that 6 and 12 months of noise exposure induced a temporary threshold shift immediately after exposure but no sign of permanent hearing loss 3 weeks after the end of exposure. The mean Q10 and Q20 values were similar in exposed and control animals and so were the cortical thresholds in all frequency bands. Temporal and Depth MTFs showed similar patterns in control and exposed rats and the responses to natural vocalizations provided similar responses in both groups. Tonotopy did not seem modified by the long-term exposure.

Conclusions
Auditory cortex neurons seem more resistant than expected to long-lasting noise exposure. Our data, obtained with a "real-world noise" which was already shown to have little impact on ACx activity (Pienkowski et al 2013), suggest that not all types of noise exposure impact the properties of ACx neurons.

Funding
Funding Supported by CNRS and University Paris-Sud.

PD 175

Changes in Neuroanatomical Connections to the Second Auditory Cortex (A2) in Early- and Late-Deaf Cats

Blake Butler; Stephen Lomber
University of Western Ontario

Background
When one sensory modality is absent, compensatory advantages are behaviorally evident in remaining modalities. These advantages are thought to be the result of recruitment of cortical areas that typically process stimuli from the missing modality. For example, evidence suggests that auditory areas contribute to enhancements in the visual domain following deafness. Interestingly, while the fractional volumes occupied by many fields of cat auditory cortex are diminished following hearing loss, the second auditory cortex (A2) undergoes an expansion in deaf animals; however, the nature of the changes in neural connectivity that underlie this expansion remains unknown. Thus, this study sought to examine how thalamo-cortical and cortico-cortical projections to A2 are altered following deafness.

Methods
A retrograde neuronal tracer (BDA) was deposited into A2 in hearing cats, and cats ototoxically deafened shortly after birth (early-deaf) or following auditory maturity (late-deaf). Coronal sections at regular intervals were observed under a bright field microscope and all neurons showing positive retrograde labeling were counted. Labelled neurons were assigned to functional cortical and thalamic areas according to previously documented criteria. The proportion of labelled neurons in each area was determined in relation to the total number of labeled neurons in the ipsilateral hemisphere. ANOVAs and posthoc tests were performed to identify changes in labelling patterns.

Results
Following the onset of hearing loss, changes in the pattern of labelled projections to A2 are observed both within the auditory modality and between sensory modalities. The nature of these changes depends on the age at which hearing loss occurred. Interhemispheric projections were not assessed in the current study for reasons of animal conservation, but previous anatomical studies suggest that commissural connections account for a very small proportion of the total number of neurons projecting to fields of cat auditory cortex.

Conclusions
In total, our results show that the patterns of thalamo-cortical and cortico-cortical projections to the second auditory cortex are altered following hearing loss, and that the nature of these changes is related to the age at the onset of deafness.

Funding
This research is supported by the Canadian Institutes for Health Research, the Natural Sciences and Engineering Research Council of Canada, and the Canada Foundation for Innovation.

PD 176

Dexamethasone Regulation of Neuroinflammation after Traumatic Noise Exposure

Ksenia Varakina[1]; Bhavishya Suprapaneni[2]; Linda Mattiace[2]; Ana Kim[1]
[1]New York Eye and Ear Infirmary; [2]New York Medical College

Steroids remain the only medical treatment for noise induced hearing loss (NIHL), although mechanism of its action is largely unknown. NIHL is thought to result in loss of peripheral inner ear cells either by necrosis or apoptosis, followed by secondary degeneration of central auditory neurons. Microglia plays a central role in modulating neuroinflammation thru secretion of pro-inflammatory cytokines and reactive oxidative species. They influence astrocyte activity, express phagocytic capability, and play key roles in synaptic pruning. Less well known is the effect of peripheral injury on glial cell types in the central auditory system. Sensory deafferentation experiments have illustrated a role for microglia and astrocytes in the auditory brainstem. Presently, little is known about microglia and astrocytes within the retrocochlear auditory centers. The purpose of our study was to examine the role of microglia and astrocytes in response to noise trauma in key brainstem auditory centers - 8th nerve, cochlear nucleus (CN), and the superior olivary complex (SOC). CBA mice were treated with nothing, or intra-tympanic saline or dexamethasone (Dex) prior to acoustic trauma. Hearing function, assessed by auditory brainstem response (ABR), showed mice pretreated with Dex have significantly better hearing recovery than animals pretreated with saline or nothing ($p<0.05$). Neuroinflammatory characteristics were assessed using IBA1 staining for microglia and GFAP for astrocytes. NIHL mice showed an increase in IBA positive cells in the 8th nerve, CN, and SOC at day 1 ($p<0.05$), whereas Dex pretreated mice showed no significant increase in cell numbers in all three areas after noise exposure. On day 14, there was no significant difference between all groups. In contrast, there was no GFAP positive cell count difference after NIHL. In addition to cell counts, microglia cell morphology changed dramatically in the NIHL animals 1 day after trauma up to day 3. Thereafter, cell processes reverted back to baseline by day 14. Astrocyte morphology changed after NIHL as well. Mice pretreated with Dex showed similar astrocyte and microglial cell shape to the control mice, while those pretreated with saline remained the same to the untreated NIHL group. This study presents a novel mechanism of NIHL. Gaining better understanding into the mechanism of steroid action in treating NIHL will lead to the development of specific therapeutic target sites. In addition, it is critical to preserve auditory architectures such as the 8th nerve, CN, and SOC neurons for future interventions in cases of reversible NIHL.

Funding
Dept of Otolaryngology New York Eye and Ear Infirmary of Mount Sinai

PD 177

Oxytocin Enables Maternal Behavior by Balancing Cortical Inhibition

Bianca Marlin; Mariela Mitre; James D'Amour; Moses Chao; Robert Froemke
New York University

Oxytocin is important for social interactions and maternal behavior. However, little is known about when, where, and how oxytocin modulates neural circuits to improve social cognition. Here we describe a fundamental mechanism by which oxytocin enables pup retrieval behavior through enhancing responses to infant distress calls in left primary auditory cortex.

We performed behavioral, anatomical, and physiological experiments to determine how oxytocin controls maternal responses to pup calls. Naive virgin females initially do not retrieve pups in distress. We tested when virgin females first expressed retrieval behavior after interacting with dams and pups. We found that oxytocin (pharmacologically-applied or optogenetically-released) accelerated the time to first retrieval, expression of retrieval behavior required left but not right auditory cortex, and expression of retrieval behavior was accelerated by oxytocin in left auditory cortex. We made new antibodies specific to the mouse oxytocin receptor, and found that oxytocin receptors were preferentially expressed in left auditory cortex. Electron microscopy revealed oxytocin receptors at synapses, including inhibitory terminals on excitatory neurons.

Pup calls are known to evoke more activity in auditory cortical neurons of mothers compared to those of naive virgin females. We performed in vivo whole-cell recordings to examine auditory cortical responses in both virgins and dams. We made current- and voltage-clamp recordings to measure spiking and synaptic responses to pup calls. Neural responses to pup calls were lateralized, with co-tuned and temporally-precise responses to pup calls in left primary auditory cortex (AI) of maternal but not pup-naive adults, and not right AI. Importantly, pairing calls with oxytocin (pharmacologically or optogentically) enhanced call-evoked responses by balancing the magnitude and timing of inhibition with excitation in virgins, transforming the virgin state to a maternal state. Oxytocin rapidly reduced IPSCs, and subsequently strengthened of EPSCs during and after pairing. Finally, a form of inhibitory plasticity seemed to emerge over hours, improving excitatory-inhibitory balance. These findings suggest that oxytocin, paired with social

stimuli, can modify neural circuits to increase the salience of social cues. Our study provides a potential biological basis for the lateralization of vocal processing in left auditory cortex and the emergence of experience-based social behaviors.

Funding
NIDCD (DC009635), a McKnight Scholarship, a Pew Scholarship, a Sloan Research Fellowship, and a Whitehead Foundation Fellowship (R.C.F.); a Skirball Institute Collaborative Research Award (M.V.C. and R.C.F.); and NIMH (T32; B.J.M.)

PD 186

Combined Blast- and Concussion-Induced Tinnitus and Hearing Loss in Rats

Jinsheng Zhang[1]; Hao Luo[1]; Edward Pace[1]; Dalian Ding[2]; Richard Salvi[2]; Anika Meggo[1]; Marwan Marwan Boulis[1]; Caleigh Lin[1]; Srinivasu Kallakuri[1]
[1]Wayne State University; [2]The State University of New York at Buffalo

Blast and concussion are frequently encountered incidences among combat personnel. The trauma-induced co-morbidities include tinnitus, hearing loss, mild traumatic brain injury (mTBI) and posttraumatic stress disorder. We have previously reported that blast alone induces tinnitus, which is accompanied by temporary threshold shift but chronic degradation in wave 1 amplitude in ABR measurements. The impacted animals also showed early onset hyperactivity in the dorsal cochlear nucleus (DCN) and inferior colliculus (IC), and delayed hyperactivity in the auditory cortex (AC), but with a complex time course. In this study, we explored the impact of combined blast and concussion on tinnitus, hearing loss and related TBI. Nineteen rats were subjected to two blasts at 22 psi in the left ears and to one concussion via a weight-drop (2 meter height), with 8 rats undergoing sham procedures. Two months after the combined blast and concussion, 15 rats showed tinnitus (tinnitus$^{(+)}$) and 4 rats did not (Tinnitus$^{(-)}$). ABR data showed significant elevation of hearing thresholds in both tinnitus$^{(+)}$ and tinnitus$^{(-)}$ rats, but with more threshold elevation in tinnitus$^{(+)}$ than tinnitus$^{(-)}$ rats. One interesting finding was increased ABR wave 1 amplitude in the unexposed right ears of tinnitus$^{(+)}$ and tinnitus$^{(-)}$ rats, though amplitude increased more in tinnitus$^{(+)}$ rats. Cochlear histology revealed that combined blast and concussion caused significant loss of both inner hair cells (IHCs) and outer hair cells (OHCs) in the left ears, predominantly in the middle- and high-frequency regions of the cochlea. Electrophysiologically, we found increased spontaneous firing in the DCN, but decreased spontaneous firing in the IC and AC in both tinnitus$^{(+)}$ and tinnitus$^{(-)}$ rats. MRI data showed increased apparent diffusion coefficient (ADC) and fractional anisotropy (FA) values in the left DCN, but decreased ADC and FA bilaterally in the IC and AC of tinnitus$^{(+)}$ rats. Taken together, compared to blast alone, combined blast and concussion generated greater and more chronic impact on tinnitus and hearing, as well as central changes. The induced neurophysiological and anatomical changes in the auditory centers may help explain the underlying mechanisms of tinnitus and its associated mTBI.

Funding
This work was supported by the U.S. Department of Defense (Grant award #W81XWH-11-2-0031).

PD 187

Changes of neuronal activities in the auditory pathway on a rat tinnitus model induced by laser-induced shock waves

Katsuki Niwa[1]; Kunio Mizutari[1]; Toshiyasu Matsui[1]; Satoko Kawauchi[1]; Takeshi Matsunobu[2]; Shunichi Sato[1]; Yasushi Satoh[1]; Akihiro Shiotani[1]; Yasushi Kobayashi[1]
[1]National Defense Medical College; [2]New Tokyo Hospital

Background
Auditory deficiency, such as hearing loss or tinnitus, is one of the most frequently observed consequences after blast injuries. However the mechanisms of blast-induced hearing loss and tinnitus have been still unknown.

We have established an animal model of sensorineural hearing loss (SNHL) by laser-induced shock wave (LISW). Utilized this model, we conducted tinnitus evaluation by gap detection test. We analyzed relationship between tinnitus and neuronal activity of the rat brain.

Method
SD rats were exposed to LISWs generated by irradiating a laser target with a nanosecond Nd:YAG laser pulse at 2.25 J/cm^2. We evaluated tinnitus repeatedly using gap detection test up to 4 weeks accompanied by hearing functional measurement. Gap detection test is one of objective tinnitus evaluation tests utilizing startle reflex. Histological analysis at the organ of corti was performed at 4 weeks after the LISW exposure. In addition, we evaluated the cochlear nucleus (CN), inferior colliculus (IC), medial geniculate body (MGB), auditory cortex (AC) and amygdala. Brain expression of c-Fos and Arc/Arg3.1, which are neuronal activity markers, was evaluated by immunohistochemistry,.

Results
The ABR thresholds were elevated 1 day after LISW exposure. The threshold shifts at higher frequencies remained up to 4 weeks. Tinnitus at high frequencies aroused 1 or 2 weeks after LISW exposure, and tended to fade away by 4 weeks. The number of c-Fos or Arc/Arg3.1 positive cells at the CN, IC, MGB, AC and amygdala were drastically increased compared to normal rat brain immediate after LISW exposure. The number of c-Fos or Arc/Arg3.1 positive cells at the AC remained increased 4 weeks after LISW exposure, whereas other part decreased.

Conclusion
This research revealed that LISWs can replicate acute phase tinnitus accompanied with SNHL. Although neuronal activities in the CN, IC, MGB and amygdala were increased immediately after inner ear damage, they were dramatically down regulated. However in auditory cortex, neuronal activities were remained higher level at 4 weeks after LISW exposure. These results indicate that there are dramatic neuronal activity changes in acute phase tinnitus. We

speculated that these neuronal activity changes might lead to central plasticity for tinnitus perception. Also, the balance between excitatory neuron activity and inhibitory neuron activity at the AC was thought to be directly related with tinnitus generation and disappearance.

PD 188

Neurochemical Profiles from the Auditory Cortex of Rats with Behavioral Evidence of Tinnitus: Assessment with High Resolution Magic-Angle Spinning Proton Magnetic Resonance Spectroscopy

Avril Genene Holt; Matthew Galloway; Farhad Ghoddoussi; Anthony Cacace
Wayne State University

Based on advancements in tinnitus research over the last 3 decades, it is reasonable to suggest that a prominent theory of tinnitus neuropathology subsumes a neurochemical basis. This view is consistent with converging evidence that partial or complete peripheral deafferentation from acoustic trauma results in a cascade of changes in the peripheral and central nervous system that induces an imbalance between inhibitory and excitatory inputs to auditory neurons at various levels in the auditory pathways.

Male Sprague Dawley rats were divided into noise-exposed and non noise-exposed groups; auditory thresholds and Gap detection assessments were determined for each group both before and after exposure to a tone (16 kHz, 106 dB SPL, 1 hr). Neurochemical profiles were determined one month after noise-exposure with high resolution magic angle spinning proton magnetic resonance spectroscopy (HR-MAS 1 H-MRS) at 11.7T *ex vivo*. Frozen tissue samples (4–7 mg) were placed into a zirconium rotor containing 8 µL of buffer (pH = 7.4), then into a Bruker 11.7T Avance 500 MHz spectrometer maintained at 4°C, spun at 4.2 kHz, at a spatial orientation of 54.7° (the magic angle) relative to the longitudinal magnetic field (B_o). Tissue spectra were acquired with a Carr-Purcell-Meiboom-Gill (CPMG) echo train acquisition sequence. Concentrations of MR visible metabolites were corrected for tissue weight and were expressed as nmol/mg tissue weight.

Using HR-MAS 1 H-MRS, we obtained unbiased neurochemical profiles of intact auditory cortex tissue from noise-exposed animals with behavioral evidence of tinnitus. We found significant increases in alanine (ALA, +41%) and glutathione (GSH, +43%) as well a decrease in glycerophosphorylcholine (GPC, -19%) and their corresponding ratios to total creatine. Although the absence of changes in glutamate, glutamine, and GABA argue against putative lesions in the auditory cortex of noise-exposed animals, elevated ALA is consistent with increased transamination of pyruvate (i.e., the end-product of glycolysis) or increased decarboxylation of aspartate. Similarly, increases in GSH, the major antioxidant in the brain, may represent a compensatory response to cellular oxidative stress. Decreases in GPC, generated during the production of inflammatory mediators from membrane phospholipids, may reflect decreased production of inflammatory lipids or increased demand for GPC in membrane phospholipid biosynthesis. Overall, the results suggest neuroplasticity as measured by ^{1}H-MRS in auditory cortex from an animal model of noise-induced tinnitus, possibly associated with disrupted pyruvate metabolism, oxidative stress, and membrane phospholipid turnover. Future studies will focus on neurochemical changes in other brain regions-of-interest.

Funding
Grant 1I01RX001095-01U.S. Dept. of Veterans Affairs to AGH Grant T42 OH008455 from the National Institute of Occupational Safety and Health, Center for Disease Control and Prevention

PD 189

Neuronal Activity in a Model of Noise Induced Tinnitus: A Longitudinal Study

Avril Holt[1]; Farhad Ghoddoussi[1]; **Antonela Muca**[1]; Aaron Apawu[1]; Mirabela Hali[1]; Sharowynn Wilson[1]; Anthony Cacace[2]; Bruce Berkowitz[1]
[1]Wayne State University School of Medicine; [2]Wayne State University

Background
Tinnitus, "ringing in the ears", is the number one service related disability for Veterans. Currently, no objective biomarkers exist for tinnitus. We have previously demonstrated that both noise- and drug-induced tinnitus result in behavioral deficits in Gap inhibition of the acoustic startle reflex (GiASR) 48 hours following tinnitus induction. Manganese-enhanced MRI (MEMRI) uses the paramagnetic manganese (Mn^{2+}) ion, a contrast agent and calcium channel probe, to assess calcium channel linked neuronal activity. Tinnitus has been associated with increases in neuronal activity, and we have previously reported increases in Mn^{2+} uptake in the inferior colliculus (IC) following acute tinnitus induction. We tested the hypothesis that enhanced manganese uptake (MEMRI) will be positively correlated with Gap detection deficits (GiASR) over time.

Methods
In male Sprague Dawley rats, Mn^{2+} uptake was assessed in 12 regions of interest (ROIs) from MEMRI data (n = 10/group) before, and 1, 28, and 84 day(s) following acoustic trauma (16 kHz, 106 dB SPL, 1 hour). ASR testing was performed twice per week in the same animals across six frequencies (4, 8, 12, 16, 20 and 24 kHz). Each animal was administered a non-toxic dose of 66 mg/kg of $MnCl_2$ (i.p) 24 hours prior to each imaging session (7T Clinscan). In a subgroup of rats, Mn^{2+} clearance from ROIs was measured after 1, 14, 28, 42 and 84 day(s).

Results
All animals had unimpaired pre-pulse ASR responses before and after noise exposure. Deficits in Gap detection were evident in noise animals at all time points except the first week after noise exposure (20 kHz, 60 dB). In contrast to our previous findings in acute models of tinnitus, later time points in this study demonstrated supernormal Mn^{2+} uptake in the paraflocculus at 4 (14% greater) and 12 (7% greater) weeks. Twelve weeks following noise exposure the IC and medial

geniculate body also exhibited significant increases in Mn^{2+} uptake. The clearance rate of Mn^{2+} was found to be similar between subdivisions of the IC at all examined time points.

Conclusions

The present data further strengthen our hypothesis that chronic tinnitus without permanent hearing loss is associated with increases in calcium channel linked neuronal activity. Differential uptake in brain regions may have initially been associated with hearing loss and later with tinnitus, paralleling the progression of a temporary threshold shift. These results suggest the need for longitudinal assessment of tinnitus progression using MEMRI and GiASR biomarkers when evaluating therapeutic intervention.

Funding

Grant 1I01RX001095-01 U.S. Dept. of Veterans Affairs Grant T42 OH008455 from the National Institute for Occupational Safety and Health, Centers for Disease Control and Prevention

PD 190

Hyperacusis and tinnitus: A challenge for age dependent hearing loss?

Lukas Rüttiger; Dorit Möhrle; Marlies Knipper
University of Tübingen

Progressing loss of auditory sensation is a major problem of aging populations. In humans, loss of hearing function can be observed through increased thresholds, altered sound processing of temporally and spatially modulated auditory stimuli, but also through abnormal perception of above-threshold sounds or phantom perceptions, like hyperacusis and tinnitus (for review see Knipper et al., 2013).

Previous studies on the rodent had already demonstrated the degeneration of auditory fibres following mild auditory trauma (Kujawa and Liberman 2009, Furman et al. 2013, Rüttiger et al., 2013, Singer et al., 2013) and over age (Sergeyenko et al. 2013).

We here challenge the question if a mild auditory trauma induces hyperacusis or tinnitus in differentially aged animals. Hyperacusis and tinnitus sensation were tested using a behavioral approach (Rüttiger et al. 2003), and hearing function was studied using auditory evoked brainstem responses (ABR) and otoacoustic emissions (DPOAE). To gain insight into the central brainstem function above-threshold responses to click and frequency specific stimuli were analysed in detail for fibre recruitment and latencies of ABR wave deflections (wave amplitudes and latencies). Results from behavior studies on differentially aged rats, before and after auditory overstimulation, are presented in correlation with individual hearing functions and morphological specifications of the hair cell molecular phenotype and hair cell ribbon loss.

Funding

Supported by Action on Hearing Loss, RNID G45 (Rü)

PD 191

Reflex-Based Gap Measurement of Tinnitus in Humans: Results of a Preliminary Study

Jeremy Turner[1,2,3]; Deb Larsen[1]
[1]SIU School of Medicine; [2]OtoScience Labs; [3]Illinois College

Since 2006 researchers have been using gap-based startle reflex approaches in the attempt to quantify tinnitus in animal models and humans. This test, referred to as the Gap Test (or gap prepulse inhibition of acoustic startle; GPIAS), makes use of the startle reflex and the fact that stimuli presented approximately 100ms before a startle pulse will inhibit that reflex automatically. Under normal (non-tinnitus) conditions, silent gap cues placed 100ms before a startle will inhibit the reflex as a function of the salience of the silent gap cue. The Gap Test is based on the premise that tinnitus specifically disrupts one's ability to hear silence and that when tinnitus is present the silent gap cue has a reduced signal-to-noise, thereby degrading the capacity for silent gap cues to inhibit the reflex. Human subjects with tinnitus and hearing-matched controls were tested for gap inhibition of eye-blink startle reflex using background sounds that were 5 and 15 dB above threshold. Data from several dozen subjects will be reviewed and we will highlight the relative merits and shortcomings of this reflexive technique for auditory assessments, hearing loss, hyperacusis, and tinnitus.

Funding

Grant support provided primarily by the Tinnitus Research Consortium to Southern Illinois University School of Medicine, but also through a Neurosensory Research Award from the US Department of Defense Psychological Health and Traumatic Brain Injury Program to OtoScience Labs.

PD 192

Towards a Global Consensus on Outcome Measures for Clinical Trials in Tinnitus

Deborah Hall
University of Nottingham

Introduction

In Europe alone, over 70 million people experience tinnitus. Despite its considerable socioeconomic relevance, progress in developing successful treatments has been limited. The European Union has approved funding to create a pan-European tinnitus research collaboration network (2014–2018). The goal of one working group is to establish an international standard for outcome measurements in clinical trials of tinnitus. This is the COMiT initiative (Core Outcome Measures in Tinnitus). Importantly, this would enhance tinnitus research by informing sample-size calculations, enabling meta-analyses and facilitating the identification of tinnitus sub-types, ultimately leading to improved treatments. Clinical effectiveness is judged according to change in primary outcome measures, but because tinnitus is a subjective condition, the definition of outcomes is challenging and it remains unclear which distinct aspects of tinnitus (i.e. 'domains') are most relevant for assessment. The development of a minimum outcome reporting standard would go a long way to addressing these problems. And COMiT is

open to all those stakeholders across the globe who wish to actively participate in the initiative. Agreeing the domains that contribute to tinnitus severity (i.e. '*what'*) is the first step towards achieving a minimum outcome reporting standard for tinnitus that has been reached via a methodologically rigorous and transparent process.

Methods And Analysis

Deciding what should be the core set of outcomes requires a great deal of discussion and so lends itself well to international effort. This presentation lays out the RoadMap for COMiT to define a Core Domain Set for clinical trials of tinnitus (Trends in Hearing. 2015;19:1-7). We start our project with two systematic reviews to establish existing knowledge and practice: One reflects the views of professional stakeholders and will establish which outcome domains and outcome instruments have been measured in recent registered and published clinical trials. The other represents people who experience tinnitus and will summarise the findings of narrative syntheses of qualitative data to establish which domains are important to these stakeholders. We present observations from the first systematic review which has identified 228 individual clinical trials on tinnitus since July 2006. Our systematic review protocols are registered on PROSPERO (International Prospective Register of Systematic Reviews): CRD42015017525 and CRD42015020629.

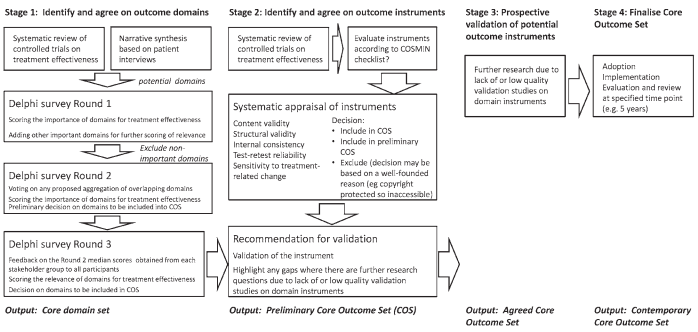

Funding

This project is funded by EU COST Action BM1306.

PD 193

Development of Dual-Targeted Nanoparticles for Delivery to Tinnitus Affected Brain Regions

Magnus Bergkvist[1]; **Avril Holt**[2]; Stephanie Curley[1]; Mirabela Hali[2]; Yuchuan Ding[2]; Anthony Cacace[3]; James Castracane[1]
[1]SUNY Polytechnic Institute; [2]Wayne State University School of Medicine; [3]Wayne State University

Tinnitus is a prevalent problem in our society and currently there are no effective treatments for this condition. Even after a single exposure to a high-level noise, resulting in a temporary or permanent hearing loss, tinnitus has been linked with neuronal hyperactivity in different regions of the brain. Targeting susceptible brain regions via delivery of theranostic nanoparticles (NPs) will facilitate diagnostic localization and provide a delivery device to help alleviate tinnitus symptoms. Fundamental challenges for reaching this goal are detection of brain regions that demonstrate neuronal hyperactivity following tinnitus onset and delivery of functional nanoparticles to these regions. Since direct brain injection is not a viable delivery option in humans, the initial challenge is to design NPs that cross the blood brain barrier (BBB). Thus a dual-targeted system is needed that 1) remains stable during systemic administration and 2) crosses the BBB to facilitate localization and treatment.

A protein-based NP platform (based on the MS2 capsid) has been designed, developed, and produced in order to increase the likelihood of crossing the BBB, adipocyte protein 2 (AP2) is being explored as a target ligand. This 19 amino acid peptide derived from proteins, binds and transports over the BBB using the low density lipoprotein receptor-related protein 1 (LPR1). AP2 with a C-terminal cysteine and an N-terminal FAM label was conjugated to the MS2 capsid using a heterobifunctional crosslinker, resulting in ~32 AP2/ particles.

In these initial experiments, NPs were examined both *in vitro* and *in vivo* to allow characterization and modification. For in vivo studies, anesthetized adult male Sprague Dawley rats were used to introduce NPs into the 4thventricle of the brain stereotaxically. A 2.4x10^14 NP/mL stock was diluted 1:40 before delivery. In another case NPs were diluted 1:60 and delivered to the internal carotid artery to maximize delivery to the brain. Following the injection (1 or 3 hours) 40 µm frozen sections were collected and imaged using fluorescence microscopy to track NP distribution.

In vitro, the AP2 conjugated MS2 capsids were able to bind to LPR1 containing HepG2[MB1] cells *in vitro*, and *in vivo* the NPs successfully crossed the BBB. Future studies will build on these results and optimize NP concentration, load and deliver therapeutics/imaging agents, and explore over expressed receptor targets to promote delivery to specific brain regions. The AP2 conjugated MS2 capsids with fluorescent tags are good candidates for delivering compounds to brainstem neurons for alleviation of tinnitus.

Funding

1R21DC013895-01A1

PD 178

Discrimination of Relative Motion in the Azimuth Plane

William Yost
Arizona State University

Relative motion of objects can be a potent cue for segregating visual objects. This study investigated the relative motion of sound in the azimuth plane; specifically the ability of listeners (twelve listeners) with normal hearing to discriminate the direction of sound rotation. Four sets of sounds were studied: speech utterances (one-word numbers between one and twelve, spoken by one of six female or six male talkers), a 250-Hz fundamental tone and its higher harmonics, a 250-Hz fundamental tone and its higher harmonics but with the second harmonic mistuned to 613 Hz, and tones with frequencies chosen randomly between one and two critical bands (ERBs) above 250 Hz and its higher harmonics.

Three, four, or six sounds were presented and each sound was presented from a different, equally-spaced loudspeaker around a twenty-four loudspeaker azimuth array in a sound-deadened room. In Experiment I, one of the sounds in each set was rotated around the loudspeaker array in either a clockwise or counterclockwise direction. The rotating sound was never presented from the fixed location of any of the other (non-rotating) sounds. Listeners could not discriminate the direction of rotation of any of the harmonics of the 250-Hz fundamental frequency harmonic sequence. No Listener achieved more than 67% accuracy in discriminating the direction of rotation of the second, mistuned harmonic (613 Hz). No listener was better than 71% accurate in discriminating the direction of rotation of any of the tones presented with random frequencies. Listeners were nearly all 100% accurate in discriminating the direction of one speech sound (a spoken number) relative to the fixed location of the other speech sounds. These trends were almost independent of the number (3, 4, 6) of sounds. In Experiment II all of the sounds rotated and listeners were to indicate the direction of rotation of all of the sounds. The results were essentially the same as they were for Experiment I. All listeners reported that they could determine the direction of rotation of the speech sounds in Experiment II only because they could attend to one sound and follow its rotation. No listener reported that there was a perception that all of the speech sounds were rotating in Experiment II. The results will be discussed in terms of the role relative motion may play in segregating sound sources as opposed to other cues that might be responsible for sound source segregation.

Funding
Research supported by an AFOSR grant

PD 179

Zwicker Tones: a Musical Pitch Percept?

Hedwig Gockel[1]; Robert Carlyon[2]
[1]Medical Research Council; [2]MRC-Cognition and Brain Sciences Unit

Periodic sound waves produce periodic patterns of phase-locked activity in the auditory nerve. It has been argued that this temporal code is the basis for our sensation of pitch, and, specifically, that musical pitch, i.e. pitch in its strictest sense, requires phase locking. The aim of the present study was to assess whether a musical pitch can be heard in the absence of phase locking, using Zwicker tones (ZTs).

A ZT is a faint, decaying tonal percept that can arise following the presentation of a band-stop broadband noise (Zwicker, 1964). The pitch is within the frequency range of the band-stop. Several findings indicate that ZTs are unlikely to be produced mechanically at the level of the cochlea and, therefore, there is unlikely to be phase locking to ZTs in the auditory periphery. A crucial question, therefore, is whether ZTs can evoke a musical pitch.

In stage I of the experiment, musically trained listeners adjusted the frequency, level, and decay time of an exponentially decaying sinusoid so that it sounded similar to the ZT they perceived following a broadband noise, for various band-stop positions. In stage II, the same listeners adjusted a sinusoid in frequency and level so that its pitch was a specified musical interval below that of either a preceding ZT or a preceding sinusoid, and so that it had the same loudness as the preceding tone. For each listener the reference sinusoid corresponded to their adjusted sinusoid from stage I. Listeners selected appropriate frequency ratios for ZTs, but the standard deviations of the adjustments were larger for the ZTs than for the equally salient sinusoids by a factor of 1.1-2.2. This is smaller than the corresponding ratio (of 1.6-11.7) previously reported for 10-kHz and 1-kHz reference tones (Burns &Feth, 1983). The results suggest that a musical pitch may exist in the absence of peripheral phase locking.

References

Burns, E. M. and Feth, L. L. (**1983**) “Pitch of sinusoids and complex tones above 10kHz” in *Hearing – Physiological Bases and Psychophysics*, edited by R. Klinke and R. Hartmann (Springer, Berlin), 327-333.

Zwicker, E. (**1964**) “Negative afterimage in hearing” J. Acoust. Soc. Am. **36**, 2413-2415.

Funding
Work supported by intramural funding from the MRC.

PD 180

Relation between Speech Perception in Cochlear Implant Users and Intensity Discrimination Within and Across Channels

Colette McKay; Natalie Rickard; Katherine Henshall
Bionics Institute

The psychophysical deficits that underlie poor speech perception in cochlear implant (CI) users have been studied using methods that probe the ability of CI users to detect changes in spectral shape. Performance on the ‘spectral ripple test’ - the ability to differentiate spectrally-rippled noise from its spectral inverse with increasingly dense ripples - has been correlated with speech understanding, suggesting that poor spectral resolution may underlie poor speech understanding. On the other hand, other studies have shown that speech understanding is more correlated with the ability to detect spectral ripples with very low ripple density, suggesting that the ability to detect spectral-shape shifts across broad frequency ranges was more important than spectral resolution. Since within-channel intensity discrimination has not been found to be correlated with spectral ripple detection, it was hypothesised in this experiment that ability to detect across-channel changes in relative intensity is correlated with speech understanding. It was also hypothesised that within- and across-channel intensity discrimination rely on different neural mechanisms and are thus not correlated.

Ten experienced adult CI users participated in the experiment. Speech understanding was tested using CNC words in quiet and CUNY sentences in multi-talker babble. Within-channel intensity discrimination was tested using 500-ms

duration pulse trains of rate equal to the per-electrode rate in their clinical speech processor, and an adaptive 3IFC task. Across-channel intensity discrimination was tested using dual-electrode stimuli, in which pulses alternated between two nearby electrodes (10, 13) or two distant electrodes (3, 20). Stimuli had the same per-electrode rate and duration as before. A 4IFC task was used to test ability to distinguish the stimulus with equal loudness on the two electrodes from equally-loud stimuli where the relative current levels were shifted by various amounts: increasing the current on one electrode by a fixed amount and decreasing the current on the other electrode by the same amount, and *vice versa*. This task was done with level jitter, limiting within-channel cues.

Results of within-channel intensity discrimination did not vary greatly among participants, whereas those with poor speech understanding found it very difficult to perform the across-channel intensity difference task. Preliminary data suggest a strong relationship between cross-channel intensity discrimination and speech understanding.

Funding
The Bionics Institute acknowledges the support it receives from the Victorian Government through its Operational Infrastructure Support Program

PD 181

A Potential Role of Phase-Locking Cues in the Perception of Logarithmic Frequency Sweeps

Carolyn McClaskey[1]; Daniel Cramer[2]; Kourosh Saberi[1]
[1]University of California, Irvine; [2]Oberlin College

Background
The dynamic changes in frequency that are ubiquitous in our auditory environment are important for many aspects of speech perception: formant transitions consist of rapid short-duration frequency sweeps, while slower changes in frequency are an important part of speech intonation, prosody, and lexical tones. Studies of both frequency sweeps and frequency modulated (FM) stimuli suggest two complementary mechanisms underlying the perception of changes in frequency: one that operates optimally at slow rates of change and is based on phase-locking to the temporal fine structure of the stimulus, and one that uses spectral energy cues and which is optimal for especially rapid rates of frequency change. The goal of the current study was to investigate the complementary role of these two mechanisms and, in particular, to examine the role of phase-locking cues in the perception of frequency sweeps that more closely parallel those of speech prosody and tonal languages.

Methods
We tested sweep direction identification for logarithmic sweeps with low rates of frequency change and small extents of frequency change, referred to here as transition span. In a single interval direction-identification task, listeners were presented with a unidirectional frequency sweep and reported whether it moved up or down. Sweeps were uniformly varied along the two dimensions of rate and transition span: the rate of frequency change was varied between 0.0147 and 0.1667 octaves/second, and the transition span was varied between 0.1 and 0.5 semitones; all stimuli were at least 50ms in length. Listeners' sensitivity (d') was quantified using signal detection theory methods and compared across conditions.

Results
As expected, our results show that direction sensitivity significantly increases with increasing transition span, and subjects are better at identifying upward sweeps than downward ones. Results furthermore show a strongly significant decrease in sensitivity as the rate of frequency change increases, suggesting that phase-locking cues – which are adversely affected by such rapid rates of change – may play a role in the current task.

Conclusions
Our data suggest that the perception of dynamically changing frequency, and especially the perception of slow-moving frequency sweeps at low frequencies, is partially reliant on phase-locking cues.

Funding
Funding was provided by a pre-doctoral NIH grant through the UCI Center for Hearing Research

PD 182

The perception of vocal characteristics in children with normal hearing or cochlear implants

Deniz Başkent[1]; Jacqueline Libert[1]; Deborah Vickers[2]; Etienne Gaudrain[3]
[1]University of Groningen, University Medical Center Groningen; [2]University College London, The Ear Institute; [3]CNRS, Lyon Neuroscience Research Center

Voice characteristics provide important cues for many speech-related tasks, such as gender categorization, vocal emotion perception, and perhaps most importantly, speech perception in the presence of competing voices. These are the very tasks that are known to be difficult for cochlear implant (CI) users. Most related research with normal-hearing (NH) or CI listeners has focused on voice fundamental frequency (F0), which was shown to be crucial for these tasks, but more weakly perceived by CI users than NH individuals. More recently, Smith et al. [2005, JASA 117:305–18] have shown the importance of another voice characteristic: the vocal tract length (VTL; related to speaker size). Subsequent work from our group has indicated that while CI users have difficulty in utilizing F0, they are even more limited at VTL perception [Fuller et al. 2014, JARO 15:1037-48].

The present study aimed to further understand factors potentially contributing to this limitation, by exploring F0 and VTL perception in NH children and children with CIs. We hypothesized that children may learn to utilize F0 before VTL cues because of exposure to exaggerated F0 cues in infant-directed-speech, and acquisition of VTL cues may come later, due to the necessity for exposure to multiple talkers. This hypothesis, hence, implies a hierarchy in processing the two vocal cues in normal hearing. We further hypothesized

that children with CIs may be better at processing voice cues than adult-implanted CI users, implying that these perceptual cues could be learned.

NH and CI children, between the ages of 5 and 14, participated in the study. Three experiments conducted, each measuring an aspect of voice characteristics perception (JNDs for F0, VTL) or a speech-related perception task that closely relates to voice characteristics perception (speaker gender categorization, emotion identification).

Preliminary results showed a trend for impaired perception of voice characteristics in CI children compared to NH children. NH children had smaller JNDs than CI children for both voice characteristics. Gender categorization and emotion identification performance was also better in NH children. While results followed the expected pattern, more data is being collected to statistically confirm our initial findings and to clarify the developmental trajectories.

Overall, the perception of voice characteristics seems to be impaired in CI children, but more data is needed to confirm the specific hypotheses. Differences found between NH and CI children were smaller than differences found between NH and CI adults, potentially reflecting the beneficial effects of early implantation.

Funding
This work was supported by VIDI grant 016.096.397 from the Netherlands Organization for Scientific Research (NWO), from a Rosalind Franklin Fellowship from University of Groningen, and from the Heinsius Houbolt Foundation.

PD 183

The Contribution of Interaural Cues to Spatial Release from Masking

Heath Jones[1]; Sean Anderson[1]; Alan Kan[1]; Matthew Winn[2]; Ruth Litovsky[1]
[1]University of Wisconsin; [2]University of Washington

Understanding speech in noisy environments can be demanding, particularly for individuals with hearing impairment even with the use of hearing aids or cochlear implants. For listeners with normal hearing, source segregation can be enhanced if spatial cues are available. Specifically, speech intelligibility increases when target and masking sources are spatially separated compared with situations in which both sources originate from the same location, a benefit known as spatial release from masking (SRM). For situations where target speech occurs in the presence of multiple maskers that are spatially distributed, monaural head shadow benefits are greatly reduced and listeners need to rely more heavily on binaural cues (interaural time and level differences; ITDs and ILDs). Presently, there is conflicting evidence about the contribution of individual binaural cues to SRM; thus, it is unclear how to best approach improving the deficits observed in hearing-impaired individuals. The current study investigated the contribution of each binaural cue to SRM by using a pupil dilation measure as novel index of listening effort.

Normal hearing participants were tested on sentence recognition of a target male talker in the presence of a two same-sex talkers. Testing was conducted in both the free-field and virtual acoustic space (VAS) created individually for each listener. Speech reception thresholds were obtained using an adaptive tracking procedure for two target/maskers configurations: 1) Co-located; target/maskers presented from the center location at 0°; 2) Symmetrically separated; target at 0° location and maskers symmetrically distributed at ±90° locations. Listening effort was assessed by measuring changes in pupil diameter relative to baseline levels recorded prior to stimulus presentation for signal-to-noise ratios that produced 50% sentence intelligibility. For VAS conditions, a minimum-phase approximation of measured individualized head-related transfer functions (HRTFs) was used. In order to isolate the contributions of ITDs and ILDs to SRM, the magnitude and phase responses of the HRTFs were independently manipulated, respectively. Findings from this study have implications concerning how best to address the SRM deficits observed in hearing-impaired individuals. Knowledge about whether a particular spatial cue increases SRM or reduces listening effort can help guide the development of hearing assistance devices aimed at enhancing speech understanding in every day social settings.

Funding
Work supported by NIH-NIDCD (R01-DC003083) and NIH-NICHD (P30-HD03352).

PD 184

A Fast And Accurate Technique To Measure The Highest Audible Frequency

Odile Clavier[1]; Catherine Rieke[2]; Chris Brooks[1]; Douglas Brungart[3]; Abigail Fellows[2]; Jay Buckey[2]
[1]Creare; [2]Dartmouth College; [3]Wlater Reed National Military Medical Center

Background
The American Academy of Audiology advocates the use of extended high-frequency testing to improve sensitivity to the effects of ototoxic drugs. Such threshold testing can be time consuming. An alternative, reduced protocol based on the highest audible frequency (HAF) has been recommended. The HAF is the highest frequency at which a patient can hear tones at 100 dB SPL. The HAF is used to set the sensitive range of ototoxicity (SRO) (the seven 1/6th octave frequencies at and below the HAF) which is monitored throughout treatment. However, finding the HAF requires an extended audiogram at baseline.

Methods
The Fixed-Level, Frequency Threshold (FLFT) test was designed to search for the highest frequency at which a pure tone set at fixed level can be heard. In a study designed to investigate behavioral and objective measures of hearing for ototoxic effects, we compared the FLFT test against a standard high frequency audiogram. In this study, the FLFT follows a B**é**k**é**sy-like tracking algorithm: a continuous pulsating tone is presented to the subject, at fixed level, but with increasing or decreasing frequency (1/12th octave step

size). The subject is asked to press the button as long as the pulsating tones are heard, and to release it otherwise. While the button is pressed, the frequency increases, otherwise, it decreases. The subject is presented with the pulsating tones until 6 reversals occur. The last 6 reversals are averaged, and the nearest 1/6th octave is used as the HAF.

Results
Normal-hearing subjects performed a standard extended audiogram from 500Hz and 20 kHz and the FLFT at their baseline visits. During subsequent visits, subjects were tested over the SRO and also performed the FLFT. Number of visits varied from 1 to 5, with the median number of visits equal to 4. The value of the nearest 1/3rd octave obtained for the HAF using the FLFT and that obtained with the audiogram were identical in 82% of subjects and within 1/3rd octave for all subjects (N=17 at the time of this abstract). The median time to complete the FLFT was 26 seconds, versus 7 minutes and 28 seconds for the extended audiogram. Repeatability of the FLFT was excellent with a mean standard deviation across tests equal to 340 Hz (using the 1/6th octave result returned by the FLFT).

Conclusion
The FLFT is an efficient searching algorithm for the highest audible frequency and could shorten baseline testing for ototoxicity studies.

Funding
The research was funded by the US Army Medical Research and Materiel Command (SBIR contract W81XWH-13-C-0194) and the Office Naval Research (N00014-14-1-0250)

PD 185

Investigating speech on speech masking using pointillistic speech

Kameron Clayton[2]; Jayaganesh Swaminathan[1]; Gerald Kidd, Jr.[1]
[1]Boston University; [2]Harvard University

Background
Pointillistic speech is created by generating a time-frequency matrix of pure tone "points" derived from the original speech stimulus. Previous work has shown that pointillistic speech is intelligible, even though the stimulus is degraded, when measured in a closed-set identification format with syntactically correct sentences. Based on the observation that sparse representations of pointillistic speech remain intelligible, the current study examined the intelligibility of one of two concurrent talkers when the talkers were represented pointillistically in mutually exclusive (orthogonal) time-frequency bins, limiting the energetic overlap of the talkers. First, we examined whether three methods that produce release from masking for natural speech (i.e., sex differences, spatial separation, and time reversal) were effective with pointillistic stimuli. Second, we examined the importance of preserving instantaneous frequency information in producing release from masking that is due to a sex difference between talkers.

Methods
Natural speech was bandpass filtered into 16 logarithmically-spaced frequency bands between 100 Hz- 8000 Hz. In each band the average instantaneous frequency and envelope was extracted for 10-ms time windows from the Hilbert analytic signal. "Points" were created by replacing the original waveform for each time-frequency bin with a gated pure-tone that was specified by the average instantaneous frequency and amplitude. The target and masker sentences were selected from a laboratory designed (closed-set) speech corpus. Bin drops were imposed on both target and masker so that fifty percent of each signal remained.

Results
Group mean results revealed significant release from masking when the maskers were: 1) from a different sex talker; 2) time reversed and 3) spatially separated from the target. In the second experiment, when frequency was fixed at the band center frequency (akin to tone-vocoded speech), no release from masking was observed for the different-sex maskers. However, when average instantaneous frequency was provided, there was a significant enhancement in performance in the different-sex masker case when the 50% bin drop was implemented and the target and masker alternated in 10-ms time slices rather than as random time-frequency bins.

Conclusions
Overall, these results suggest that conditions that provide listeners release from masking are preserved in some pointillistic representations. Release from masking due to a sex difference between talkers is dependent on the presence of average instantaneous frequency information. Lastly, the organization of the pointillistic representation of the speech (randomly drawn or ordered by time-slice alternation) appears to have a significant impact on performance.

Funding
AFOSR and NIDCD

PD 210

A Functional Role for Distortions Produced by the Hearing Organ

Anders Fridberger[1]; Tianying Ren[2]; Sripriya Ramamoorthy[2]; Yuan Zhang[2]; Thomas Lunner[1]; Brian Moore[3]; Nuttall Alfred[2]
[1]Linköping University; [2]Oregon Health & Science University; [3]University of Cambridge

Speech, music and animal communication calls contain many different frequencies that change rapidly over time. Yet, studies have shown that a single component of this complex mixture, the slowly varying envelope, is sufficient for accurate speech recognition, at least in quiet conditions. Direct evidence for this comes from cochlear implant users, most of whom get very good speech recognition when only a few frequency bands of envelope information are presented through the implanted electrode.

Frequency components corresponding to the envelope are not found in the sound-evoked vibrations of the basilar

membrane, but they are clearly present in the discharges of the auditory nerve. How can the auditory nerve encode information absent from the basilar membrane, which provides the stimulus that drives the nerve?

To answer this question, we recorded basilar membrane motion and electrical potentials inside the organ of Corti in anesthetized guinea pigs, using three-component stimuli. By varying the phase of the center tone, the envelope of the stimulus changes although the magnitude spectrum remains the same.

Outer hair cell extracellular receptor potentials, but not basilar membrane vibrations, showed large changes that were dependent on center-tone phase. When the envelope was flat (center-tone phase 90 degrees) the electrical f2-f1 distortion product was undetectable. With a peaked envelope (center-tone phase 0 or 180 degrees), the level of the f2-f1 distortion product increased drastically, sometimes becoming larger than the response to the primaries. All the other distortion products also showed statistically significant changes dependent on the center-tone phase. We propose that the electrical distortion products produced by the hair cells allow the auditory nerve to transmit information about envelope shapes to the brainstem. Thus, distortion products produced by the cochlea are not just a by-product of sensory transduction but actually help to encode features of the stimulus that are essential for communication.

Funding
Supported by the Swedish Research Council (K2014-63X-14061-14-5), Torsten Söderberg foundation, Strategic research area for systems neurobiology (Region Östergötland), Linköping University, and NIH-NIDCD (R01 DC-004554 and R01 DC 000141).

PD 211

Age and objective measures of functional hearing abilities.

Hamish Innes-Brown[1]; Renee Tsongas[2]; Colette McKay[2]
[1]KU Leuven; [2]Bionics Institute

Aims
People with impaired hearing often have difficulties in hearing sounds in a noisy background. This problem is partially a result of the auditory systems reduced capacity to process temporal information in the sound signal. In this study we examined the relationships between perceptual sensitivity to temporal fine structure (TFS) cues, brainstem encoding of complex harmonic and amplitude modulated sounds, and the ability to understand speech in noise. Understanding these links will allow the development of an objective measure that could be used to detect changes in functional hearing before the onset of permanent threshold shifts.

Methods
We measured TFS sensitivity and speech in noise performance (QuickSIN) behaviourally in 34 normally hearing adults with ages ranging from 18 to 63 years. We recorded brainstem responses to complex harmonic sounds and a 4000 Hz carrier signal modulated at 110 Hz. We performed cross correlations between the stimulus waveforms and scalp-recorded brainstem responses to generate a simple measure of stimulus encoding accuracy, and correlated these measures with age, TFS sensitivity and speech-in-noise performance.

Results
Speech-in-noise performance was positively correlated with TFS sensitivity, and negatively correlated with age. TFS sensitivity was also positively correlated with stimulus encoding accuracy for the complex harmonic stimulus, while increasing age was associated with lower stimulus encoding accuracy for the modulated tone stimulus.

Conclusions
The results show that even in a group of people with normal hearing, increasing age was associated with reduced speech understanding, reduced TFS sensitivity, and reduced stimulus encoding accuracy (for the modulated tone stimulus). People with good TFS sensitivity also generally had less faithful brainstem encoding of a complex harmonic tone.

Funding
Supported provided by the National Health and Medical Research Council of Australia (Early Career Research Fellowship #1069999 to HIB). The Bionics Institute acknowledges the support it receives from the Victorian Government through its Operational Infrastructure Support Program. HIB is support by a Marie Curie Pegasus Fellowship from the FWO.

PD 212

Objective Predictors of Listener Susceptibility to Reverberant Distortion

Paul Reinhart; Pamela Souza
Northwestern University

Background
Reverberation in an environment distorts speech acoustics and can significantly decrease speech intelligibility, especially for individuals with hearing impairment. However, an individual's audiogram does not entirely predict how reverberation will affect speech intelligibility. Previous research has suggested that there are suprathreshold influences including age, cognitive, and psychoacoustic factors which may further modify one's ability to perceive reverberant speech. However, these measures are highly intercorrelated with one another. These intercorrelations hinder our ability to generalize findings across studies. The purpose of this study was to investigate a comprehensive set of individual factors which can be used to predict listener intelligibility across a range of reverberant conditions.

Methods
Participants included older individuals with age-related, sensorineural hearing loss. Reverberant speech intelligibility was assessed using sentences that were processed using virtual acoustic techniques to simulate reverberation representing a range of real-world listening environments. Four predictor variables were additionally collected from all of the subjects: pure-tone average, age, working memory, and gap detection. Pure-tone average was quantified as the binaural average of

audiometric thresholds at .5, 1, and 2 kHz. Age was quantified as chronological age in years. Working memory is a cognitive process involved in the simultaneous storage and processing of information. Working memory was assessed using a reading span test. Gap detection is a psychoacoustic ability related to a listener's sensitivity to gaps in the temporal envelope of a signal. Gap detection was assessed using an adaptive 3-AFC paradigm with a broadband noise carrier.

Results

The four predictors (pure-tone average, age, working memory, and gap detection) were all correlated with one another ($p<0.01$). Predictors were entered into a step-wise linear regression model in order to examine which variables uniquely predict speech intelligibility, while accounting for intercorrelation and redundancy of the predictor variables. A separate regression model was developed to predict speech intelligibility at each of the reverberation times tested. Each regression model was significant ($p<0.01$); however, the predictors that were retained vs. excluded from each model varied across reverberation time conditions.

Conclusions

Our data suggest that there are suprathreshold considerations which predict reverberant speech intelligibility. Moreover, some suprathreshold abilities become more important for speech intelligibility under reverberant conditions. That is, certain abilities may have minimal impact when listening to undistorted speech, but may be taxed more heavily when listening to reverberant speech. Overall, these findings clarify the reasons for variability among individuals in reverberant speech intelligibility. [Work supported by NIH]

PD 213

Top-down Repair of Interrupted Speech for Bimodal Users

Jeanne Clarke[1]; **Etienne Gaudrain**[2]; Deniz Başkent[1]
[1]University of Groningen, University Medical Center Groningen; [2]Lyon Neuroscience Research Center, CNRS

The benefit from top-down repair of interrupted speech differs in cochlear implant (CI) users than that of normal-hearing (NH) listeners. The poor pitch perception commonly reported in CI listeners might contribute to this difference. Previous studies from our lab have shown that simulating electro-acoustic stimulation (EAS) yielded better intelligibility of interrupted speech than simulating electrical stimulation alone (CI only). In a more recent study we showed that the addition of F0 to CI simulation improved top-down repair in the spectral resolution range of CI users. We thus expected to observe similar benefit with bimodal CI users wearing a hearing aid (HA) in the contralateral ear where low frequency information, richer in voice pitch cues, can be transmitted.

We tested twelve bimodal users in two hearing modes: CI only, and CI and HA together. The top-down repair of speech was measured with the phonemic restoration (PR) paradigm. The participants listened to sentences periodically interrupted with silent intervals or with these intervals filled with noise bursts (0dB SNR), at an interruption rate of 1.5 Hz, with 3 duty cycles (DC: 50%, 62.5% and 75% of speech vs. interruption). Intelligibility was measured as the proportion of correctly identified words. The PR benefit was measured by the increase in intelligibility when the silent interruptions were filled with noise.

Group analysis results showed an effect of duty cycle on intelligibility. As expected, presenting more speech (at longer DC) led to better interrupted speech intelligibility. However, no PR benefit was observed, even at the higher DC where it was previously shown that CI users benefited from PR [Bhargava et al. 2014, Hear. Res. 309:113-23]. Unexpectedly again, adding the HA to the CI led to no bimodal benefit.

As we observed large variability in participants' scores, further analysis are still needed to evaluate the effect of the different variables on top-down repair mechanisms at the individual level.

Funding

This work was supported by VIDI grant 016.096.397 from the Netherlands Organization for Scientific Research (NWO), from a Rosalind Franklin Fellowship from University of Groningen, and from the Heinsius Houbolt Foundation.

PD 214

Enhanced Recognition Memory for Acoustically Degraded Sentences

Ingrid Johnsrude; Harrison Ritz; Spencer Arbuckle; Conor Wild
University of Western Ontario

Background

Participants' long-term memory for auditory word lists is poorer when speech is degraded than when speech is clear (e.g., Murphy, Craik, Li, & Schneider, 2000; Wingfield, Tun, & McCoy, 2005). A common interpretation is that effortful perception compromises memory encoding because these processes share a finite pool of cognitive resources. In apparent contrast, other researchers have observed that memory is better for text words that were presented masked rather than clear during the study phase (e.g., Nairne, 1988; Hirshman, & Mulligan, 1991; Mulligan, 1996). Mulligan and colleagues suggest that semantic compensatory processes, which recover degraded inputs, also enhance memory encoding (Mulligan, 1996). Here, we describe two experiments in which we examine whether acoustically degraded sentences (which are semantically richer than single words) are remembered better than clear sentences.

Methods

In both experiments, participants (n = 22; n=27) heard 108 everyday sentences that were either clear or noise-vocoded (NV; Shannon et al., 1995), making a yes/no gist-perception decision after each. In Experiment 1, sentences were either clear or 6-band NV. In Experiment 2, sentences were clear, 6-band NV, or 12-band NV. Matched lists of sentences were assigned to conditions in a counterbalanced fashion across participants, and sentences were presented in a pseudorandom order. After all sentences were presented, a surprise recognition test was administered with text versions

of trial sentences and matched foils. In an independent sample, word-report scores for 12-band NV and clear speech were similar and >98%. Word-report scores for 6-band NV speech were poorer but still high (92%).

Results
Gist decision scores during the study phase were similar to word-report scores obtained in a pilot sample. Recognition memory (d') was significantly better for both 6-band NV (Experiment 1: d' = 1.70, p = .004; Experiment 2: d' = 1.36, p = .03) and 12-band NV (Experiment 2: d' = 1.41; p = .003) sentences than for clear sentences (Experiment 1: d' = 1.15; Experiment 2: d' = 1.14).

Conclusion
Recognition sensitivity was superior for degraded than for clear sentences, even when degraded sentences were matched for intelligibility to clear speech (i.e., 12-band NV). The semantic context available in sentences may lend itself to compensatory processes that enhance memory (Mulligan 1996). Further study is required to determine whether this memory benefit persists under more naturalistic challenges to clarity (such as masking speech or hearing impairment) and whether it persists in older individuals who may have reduced cognitive resources.

Funding
Supported by a Canadian Institutes of Health Research operating grant (MOP 133450) and Natural Sciences and Engineering Research Council Discovery grant (327429-2012) to IJ, and by the University of Western Ontario.

PD 215

Which Tests of Central Auditory Processing Best Differentiate Among Individuals with and without Blast Exposure and/or Traumatic Brain Injury?

M. Lewis[1]; Frederick Gallun[1]; Garnett McMillan[1]; Heather Belding[1]; Serena Dann[1]; Melissa Papesh[1]; Michele Hutter[1]; Marjorie Leek[2]
[1]VAPORHCS; [2]Loma Linda VAMC

Background
Previous work by Gallun, Diedesch, Kubli, Walden, Folmer, Lewis, McDermott, Fausti & Leek (2012) demonstrated that individuals with blast exposure may have more difficulty on tests of central auditory processing (CAP) as compared to age- and hearing-matched individuals without blast exposure. This is consistent with clinical reports of some Veterans reporting greater difficulties processing auditory information than might be expected from their pure-tone hearing test results.

Gallun and colleagues are building upon this earlier work to determine the degree to which deficits on tests of CAP are likely to result from exposure to high-intensity blasts, as well as from non-blast related traumatic brain injury (TBI). Here, we report information as to which specific CAP tests best differentiate these patient populations from individuals without a history of blast-exposure or TBI.

Methods
Three groups of individuals are being evaluated on a large, comprehensive auditory test battery. These three groups are: (1) Veterans with exposure to high intensity blast waves within the past 10 years; (2) Veterans and non-Veterans with non-blast-related TBI; and (3) a control group of participants statistically matched in age to the blast-exposed group with no history of blast-exposure or TBI.

For the purposes of the present analysis, only the following CAP tests were considered: Frequency Patterns Test (Musiek & Pinheiro, 1987), Dichotic Digits Test (Musiek, 1983), Staggered Spondaic Word Test (Katz, 1998), the SCAN-A (Keith, 1995), the Words-In-Noise test (Wilson, 2003), the (modified) Quick Speech-In-Noise test (standard, with reverberation, and with reverberation and compression; Brungart, Sheffield, & Kubli, 2014), the Time Compressed Speech Test (Wilson, Preece, Salamon, Sperry, & Bornstein, 1994), the Gaps-In-Noise test (Musiek, Shinn, Jirsa, Bamiou, Baran, & Zaida, 2005), and a newly-created spatial release from masking test (Gallun, Diedesch, Kampel, & Jaiken, 2013).

Results
Preliminary analyses revealed that the Frequency Patterns Test showed the most variability among the three groups, followed by the SCAN-A, the Time Compressed Speech Test, and the Staggered Spondaic Word test. The (modified) Quick Speech-In-Noise test, the Words-In-Noise test, and the spatial-release from masking test showed the least variability among groups.

Conclusions
These early findings suggest that the Frequency Patterns Test may hold good promise as a clinical test for discriminating among these patient populations. Further analyses will clarify the potential value of this test.

Funding
VA RR&D

PD 216

Multilingual Matrix Sentence Recognition Tests: Providing a common Ground for Multi-Center Audiological Studies

Birger Kollmeier[1]; Anna Warzybok[1]; Sabine Hochmuth[1]; Maria Boboshko[2]; Ruth Bentler[3]; Melanie Zokoll[1]
[1]Cluster of Excellence Hearing4All & Universität Oldenburg; [2]St. Petersburg Pavlov State Medical University; [3]University of Iowa

Introduction
The difficulty of understanding speech in noisy environments is not very well reflected by pure tone audiogram findings. To better understand a patient's problem, it is necessary to assess his or her communication ability in noisy environments. This might also help to assess possible supra-threshold distortions that occur in the auditory system as a result of hearing impairment, independent from the sensitivity loss assessed by the tone audiogram or speech audiometry in quiet. Hence, speech recognition tests in noise have become

more and more important in audiological diagnostics in recent years. So-called 'matrix sentence tests' use a closed-set format and comprise syntactically fixed, semantically unpredictable sentences (e.g. "*Peter kept two green toys*"). Providing a vocabulary of only 50 words (10 alternatives for each position in the sentence), matrix sentence tests are suitable for speech perception testing without losing the usability for repeated speech perception testing with the same patient. In a multilingual society where each patient should be tested with her or his native language, experimenters that do not understand the test language may still supervise the test if its closed-set response format is used. Meanwhile matrix sentences tests developed according to common minimum quality standards for speech intelligibility tests are available for 15 different languages (i.e., in Swedish, German, Danish, Dutch, American English, British English, French, Polish, Turkish, Spanish, Italian, Persian, Arabian, Finnish, and Russian) together with a varying degree of supportive data. The common quality standards result in a high homogeneity of the speech materials and test lists employed what yields steep test-specific intelligibility functions and high test efficiency.

Methods
This contribution presents matrix sentence test data of two multi-center studies in the USA and Russia investigating the different influence of hearing ability on the SRT in quiet and noise. Data include adaptively estimated speech reception thresholds (SRTs), i.e. the sound pressure levels or signal-to-noise ratios (SNR) yielding 50% speech intelligibility, as well as correlations between hearing ability and SRT.

Results
The common quality standards applied during their development resulted in efficient and reliable tests with high comparability across the languages. Data emphasize the high potential of matrix sentence tests to disentangle the contribution of possible supra-threshold distortions to a certain hearing loss from that of the pure loss in sensitivity.

Conclusions
The Matrix test format has been shown as a sensitive diagnostic tool suitable for multilingual comparisons.

Funding
DFG, Cluster of Excellence 1077 Hearing4All

PD 217

Stimulus Repetition and Training-Session Length: Contributing Factors to the Perceptual Learning of Time-Compressed Speech and its Generalization?

Karen Banai[1]; Yizhar Lavner[2]
[1]University of Haifa; [2]Tel-Hai College

Background
The recognition of acoustically degraded speech which is charactersitic of many listning situations, is a challenge even for young, normal-hearing listeners. Although the ability to recognize such speech improves markedly following multi-session training, the generalization of this training-induced learning to new untrained tokens is often quite limited. Here we tested the hypothesis that stimulus repetition during training promotes token-specific learning and thus limits the generalization of learning to untrained tokens. We also asked whether the length of each training session influences the perceptual learning of time-compressed speech and its generalization to untrained tokens and to a new untrained talker.

Methods
Four groups of listeners (n = 9-11 per group) received four sessions of training on the semantic verification of time-compressed sentences. Subsequently, the recognition of time-compressed speech was compared between trained and untrained listeners using three test conditions (trained sentences, untrained sentences, and untrained talker). The contributions of both training-session length and training-set size were assessed by training listeners for either brief (60-trial) or long (240-trial) sessions with a training-set size of either 60 or 240 different sentences.

Results
At test, listeners from all trained groups significantly outperformed untrained listeners on all three conditions. With brief training sessions, less learning of the trained sentences and weaker transfer to an untrained talker were observed with the large than with the small training set, but training-set size had no effect on the generalization of learning to untrained tokens. With longer training sessions, the contribution of training-set size was minimal.

Conclusions
Stimulus repetition during training may have promoted item-specific learning, especially with brief training sessions. This specificity contributed to the recognition of training-set sentences produced by a new talker, but had little effect on the ability to recognize untrained sentences. The current findings are inconsistent with earlier reports on the contribution of stimulus variability (particularly talker variability) to the perceptual learning of speech and suggest that not all forms of variability are created equal.

Funding
This work was supported by the National Institute of Psychobiology in Israel.

PD 194

Isolation of Myosin VIIA Protein Complexes from Purified Hair Cell Stereocilia

Clive Morgan[1]; Jocelyn Krey[1]; M'hamed Grati[2]; Peter Barr-Gillespie[1]
[1]Oregon Health and Science University; [2]University of Miami Miller School of Medicine

Mutations in myosin VIIA (MYO7A) can lead to either non-syndromic deafness (DFNA11) or to Usher Syndrome (USH1B). MYO7A executes its vital role in the mechanosensory stereocilia of inner ear hair cells. Initially implicated in ankle-link positioning, other experiments have suggested a role in mechanotransduction. MYO7A was the

first protein involved in hair-cell mechanotransduction to be identified by genetics. Whilst mouse genetics, interaction, and localization experiments suggest that CDH23, USH1C, and USH1G interact with MYO7A at the upper tip-link density, there is no direct biochemical evidence for this or any other MYO7A complex in stereocilia.

We have developed a high-throughput method for stereocilia isolation using the monoclonal antibody D10, which allowed us to immunoprecipitate rare protein complexes from stereocilia detergent extracts. In combination with immunoaffinity purification using an anti-MYO7A monoclonal antibody, we found that MYO7A interacts tightly with several scaffolding proteins, including PDZD7 and GIPC3. We confirmed that these interactions are direct using immunoprecipitation of expressed proteins in tissue-culture cells. Moreover, we found that MYO7A is also in a protein complex including ADGRV1 (aka GPR98 and VLGR1); PDZD7 likely mediates this interaction. We also determined that a substantial amount of MYO6 co-precipitates from chick stereocilia with MYO7A, although this interaction is weak when tested in tissue-culture cells. Finally, we showed that USH1C, USH1G, and CDH23 co-precipitate from chick stereocilia with MYO7A, confirming the presence in tissue of this complex. These experiments show not only that MYO7A participates in both tip-link and ankle-link complexes, but that MYO7A participates in other stereocilia protein complexes. Further studies will help to clarify these distinct roles of MYO7A in the hair bundle. Moreover, our new high-throughput purification method will allow characterization of other protein complexes from stereocilia, expanding our ability to biochemically characterize hair-bundle function.

Funding
This work was supported by NIH grants R01 DC002368 and P30 DC005983 to PGBG. We also received support from the following core facilities: mass spectrometry from the OHSU Proteomics Shared Resource (partial support from NIH core grants P30 EY010572 & P30 CA069533; Orbitrap Fusion S10 OD012246)

PD 195

Severe Hair Bundle Anomalies that Differ with Hair Cell Type are Associated with Disruption of SorCS2.

Andy Forge[1]; Ruth Taylor[1]; Sally Dawson[1]; Michael Lovett[2]; Angela Laws[1]; Dan Jagger[1]
[1]University College London; [2]Imperial College London

Background
Behavioural anomalies suggesting an inner ear disorder were observed in a colony of transgenic mice from a non-ear related project. Evidence suggested that the disorder was likely to be the result of gene disruption by a randomly inserted transgene construct.

Methods
The sensory epithelia of the inner ears of mice aged from postnatal day 1 to 12 months were assessed by SEM, TEM and immunohistochemistry. Whole genome DNA sequencing and gene expression analysis by qPCR were used to identify the disrupted gene.

Results
In all sensory patches there were severe hair bundle anomalies and stereocilia were shorter than normal, but of normal width. Bundles on OHC, were mis-oriented and mis-shapen but stereocilia were graded in height with, in early postnatal animals, the kinocilium positioned behind the longest stereocilia, regardless of bundle orientation. Bundles on IHC were generally rounded with shorter stereocilia around the circumference and longer ones in the centre; kinocilia were located eccentrically in a close-to-normal position. Macular hair cell bundles were round with stereocilia slightly graded in height towards the centrally located, long kinocilium. Hair bundles in cristae appeared less affected; stereocilia were graded in height in one direction, in some case surrounding a centrally positioned kinocilium. No ABR could be elicited from affected animals at any sound pressure level tested. With ageing in affected animals, while stereocilia on IHC and in utricles became fused and elongated, as occurred in unaffected age-matched mice, on OHC stereocilia were lost by apparent retraction into the cell. Whole-genome sequencing demonstrated that in affected animals the transgene had interrupted the *SorCS2* (Sortilin-related VPS-10 domain containing protein) locus. Real-time-qPCR demonstrated that homozygous mutant mice had disrupted expression of *SorCS2* RNA in cochlear tissue. Immunohistochemistry showed SorCS2 to be expressed in the sensory epithelia of wild-type animals.

Conclusion
SorCS2 is a proneurotrophin receptor that is involved in growth cone collapse through regulation of actin dynamics (Deinhardt et al 2011, Sci Signalling 4, 202). The present results suggest that SorCS2 may play a role in hair bundle orientation and formation which is explored in a companion poster (Jagger et al. this meeting). They also suggest that details of the molecular machinery regulating hair bundle formation and orientation, and perhaps stereociliary maintenance, differ between hair cell types. In addition the results highlight the potential unintended consequences of gene insertion strategies.

Funding
Action on Hearing Loss (AoHL) Rosetrees Trust

PD 196

Ground Control of Stereocilia Elongation during Hair Cell Differentiation

Basile Tarchini; Abby Tadenev; Nick Devanney
The Jackson Laboratory

Sensory perception in the inner ear relies on the proper shaping of the brush of movement detectors at the surface of hair cells, the stereocilia bundle. Using the mouse model, we previously showed that the asymmetric V-shaped or semi-circular edge of the bundle is first defined when microvilli covering the apical membrane in undifferentiated cells become excluded from a new region polarized in the plane.

This 'bare zone' is labeled and expanded by mInscuteable-LGN-Galphai, a protein complex mostly recognized for its role in orienting the mitotic spindle. In time, select microvilli grow into stereocilia adopting graded heights across the bundle, with the row directly abutting the bare zone being the tallest. The resulting staircase-like architecture is widely conserved among all vertebrates and considered instrumental for direction-sensitivity to sound stimuli, but remains largely unexplained at the molecular level.

Our work introduces and supports the idea that the staircase-like architecture of the stereocilia bundle in the vertical axis is established by recycling planar polarity information along the horizontal axis. In addition to regulating microvilli placement at the apical membrane, we show that the mInscuteable-LGN-Galphai complex directly controls stereocilia elongation in the tall row. When this protein complex is disrupted, postnatal stereocilia are stunted, forming an immature-appearing bundle with only a shallow staircase pattern. Interestingly, similar defects have been reported in the absence of Myosin XV, Whirlin and EPS8, three proteins restricted to stereocilia unlike mInscuteable-LGN-Galphai. Based on evidence for sub-cellular communication between distinct apical compartments, we propose that early planar asymmetry of protein enrichment at the bare zone is used as a reference for specific enrichment of LGN-Galphai in adjacent protrusions, promoting the elongation of the tallest row. In turn, the tallest row has been shown to influence the height of shorter rows via oblique tip-links interconnecting stereocilia across rows. Our studies have the potential to explain in molecular detail how multiple levels of cytoskeletal polarity are implemented and integrated during hair cell differentiation in order to build the mechanosensory compartment of hair cells.

Funding
The Jackson Laboratory; Assistant Professor start-up

PD 197

Molecular Pathophysiology in a Mouse Model of Usher Syndrome, Type IC

Bifeng Pan[1]; Selena Heman-Ackah[2,3]; Yukako Asai[1]; Alice Galvin[1]; Artur Indzhykulian[3]; **Gwenaelle Geleoc**[1]
[1]Boston Children's Hospital; [2]Beth Israel Deaconess Medical Center; [3]Harvard Medical School

Ush1c.216G>A mice carry a cryptic splice site mutation found in French-Acadian USH1C patients that favors expression of a truncated, 135 amino-acid (harmonin-135), form of the protein harmonin and reduced expression of full-length harmonin (Lentz et al. 2007; 2010). Humans homozygous for the Ush1c.216G>A mutation suffer severe hearing loss and retinal degeneration, which is recapitulated in the mouse model as early as one month of age. Interestingly, homozygous Ush1c-null mice have a less severe phenotype (Tian et al. 2010), which raises the possibility that harmonin-135 may outcompete full-length harmonin for binding partners and thereby disrupt function. To investigate this possibility we assessed hair cell and auditory function in heterozygous Ush1c.216G>A mutant mice and in mice transfected with a viral vector encoding harmonin-135.

Analysis of heterozygous Ush1c.216G>A mice revealed normal hearing, hair cell transduction and hair bundle morphology at P8 and P18. RT-PCR confirmed expression of mRNA encoding the truncated protein. We conclude the Ush1c.216G>A mutation does not cause dominant loss-of-function when expressed in heterozygotes.

Next, we wondered whether there might be a dose-dependent effect, with harmonin-135 outcompeting the full-length protein when expressed higher levels. To investigate this possibility, we generated adeno-associated viral vectors (AAV) to overexpress harmonin-135 together with green fluorescent protein (GFP) as a transfection marker. One microliter of AAV2/1.CMV.eGFP Harm-135 (1.9E^14 gc/ml) was introduced through the round window membrane of wild-type C57BL/6J mice at P0-P1. Injection efficiency was assessed in post-mortem tissue and revealed viral transduction of IHCs along the entire length of the cochlea. Some of the injected mice were euthanized at P5 and their cochleas were excised and maintained in culture up to 14 days (~P19). MET currents, recorded from GFP-positive and GFP-negative control IHCs, did not differ significantly and were similar to wild-type. Auditory brainstem responses (ABR) were recorded in control and injected mice at P28-P30. There were no statistically significant differences in ABR thresholds between control and injected mice. Lastly, we assessed hearing thresholds in 8-week old heterozygous and homozygous Ush1c.216G>A mice and confirmed normal thresholds were maintained in heterozygous mice.

The results suggest that harmonin-135 does not compete with full length harmonin and supports the hypothesis that reduced expression of full-length harmonin is the most likely cause of deafness in Ush1c.216G>A patients. If so, gene augmentation with the full-length harmonin may be a viable strategy for compensation of the Ush1c.216G>A mutation in USH1C patients.

Funding
This work was supported by a donation from Kids-B-Kids and a subaward from the Foundation Fighting Blindness (PI: Luk Vandenberghe). S.H.A.also received a diversity fellowship from BIDMC that partially supports this work.

PD 198

Functional Interactions between Pcdh15a and Itga8 in Zebra fish Hair Cells

Marisa Zallocchi; Oluwatobi Ogun
Boys Town National Research Hospital

Background
Usher syndrome (USH) is a genetically heterogeneous disorder affecting neurosensory cells in the inner ear and eye. We recently demonstrated an *in vivo* interaction between clarin-1 (USH3A) and the ortholog for the mouse protocadherin15 (USH1F), protocadherin-15a (Pcdh15a), in fish hair cells. Absence or decrease in clarin-1 protein-activity (clarin-1 morphants) produces alterations in Pchd15a distribution at the apical aspect of hair cells with the concomitant reduction in mechanotransduction channel

activity. Defects in vesicle recycling and/or endocytosis were also observed. Expression and a putative role in stereocilia/kinocilia development have been demonstrated for integrin α8β1 (Itga8) heterodimer more than 10 years ago. Here we present novel data demonstrating an interaction between Pcdh15a and Itga8 that leads to activation of downstream signaling and, show that this signaling is required for normal hair cell function.

Methods
Zebra fish morphants and/or mutants were assayed for vesicle recycling impairment and by the presence of Pch15a/Itga8 interactions by confocal, super-resolution structure illumination microscopy and proximity ligation assay. Pull-down and western blot studies were also performed.

Results
Pcdh15a and Itga8 are expressed in the stereocilia in neuromast and ear hair cells. Co-immunoprecipitation studies and proximity ligation assays suggest an interaction between these two proteins at the apical aspect of hair cells. Decrease or absence of Pcdh15a or Itga8 results in absence of the reciprocal protein demonstrating interdependency in complex formation. Morphants/mutants for both Pcdh15a and Itga8 have vesicle recycling/endocytosis impairment with a reduction in kinocilia length and defective ribbon synapse formation. Some of these effects can be rescued if we co-inject Itga8 morphants with constitutive active Rhoa, suggesting that Itga8 signals through this small GTPase. Mechanotransduction channel activity is also reduced in the Itga8 morphants, determined by FM1-43 uptake and this defect can also be rescued by co-injection with constitutive active Rhoa.

Conclusions
There is a Pcdh15a/Itga8 protein complex that functions in hair cells regulating vesicle recycling/endocytosis and the formation of hair cell specialized structures through activation of the Rhoa signaling cascade.

Funding
Health grant 5P20RR018788 and the Tobacco Settlement Fund from the State of Nebraska.

PD 199

Using Larval Zebra fish as an In Vivo Model System to Study Otoferlin, a Protein Expressed in the Sensory Hair Cells and Essential for Hearing.

Paroma Chatterjee[1]; Murugesh Padmanarayana[1]; Nazish Abdullah[2]; Robert Tanguay[1]; Katie Kindt[3]; Colin Johnson[1]
[1]Oregon State University; [2]Weill Cornell Medical College, New York City; [3]NIDCD/NIH, Bethesda

Paroma Chatterjee, Murugesh Padmanarayana, Nazish Abdullah, Robert L. Tanguay, Katie S. Kindt, Colin P. Johnson

Introduction
Sensory hair cells convert mechanical motion into chemical signals. Otoferlin, a six-C2 domain transmembrane protein linked to deafness in humans, is hypothesized to play a role in exocytosis at hair cell ribbon synapses. To date, however, otoferlin has been studied almost exclusively in mouse models, and no rescue experiments have been reported.

Methods
Zebra fish larvae were used in this study. RT-PCR, *in situ* hybridization and immunohistochemical labeling were used for studying expression of otoferlin. Otoferlin morphants were generated using splice-blocking morpholinos. Ribbon synapse morphology of otoferlin morphants were examined by whole-mount immunohistochemical labeling of hair cell synaptic proteins including ribeye and the synaptic vesicle marker Vglut3. Furthermore, the endocytotic marker mCLING (Rizzoli et al, 2014) was used to examine vesicle uptake and recycling. The calcium imaging experiments were done as described in (Kindt et al, 2012). Rescue experiments were done with full length and truncated forms of mouse otoferlin constructs.

Results
In our previous study (Chatterjee et al, 2015) we found that larval zebra fish has two otoferlin genes, otoferlin a and otoferlin b. Expression of both isoforms occurs early in development and is restricted to hair cells and the midbrain. Immunofluorescence microscopy revealed localization to both apical and basolateral regions of hair cells. Knockdown of otoferlin, resulted in hearing and balance defects, and a 'circling' phenotype associated with a looping and circular swimming pattern. Further, otoferlin morphants had uninflated swim bladders. In more recent experiments with otoferlin morphants we observed changes in hair cell presynaptic structures; namely changes in ribeye distribution and VGlut3 localization. Calcium imaging experiments shows no significant changes in fluorescence signal between morphants and control, suggesting that otoferlin morphants do not exhibit mechanotransduction defects. However, uptake of the mCLING dye is less in the morphants compared to controls indicating the possibility of defective vesicle uptake and recycling. Rescue experiments conducted with mouse otoferlin restored hearing, balance, and inflation of the swim bladder. Remarkably, truncated forms of otoferlin retaining the C-terminal C2F domain also rescued the otoferlin knockdown phenotype, while the individual N-terminal C2A domain did not.

Conclusion
We conclude that otoferlin plays an evolutionarily conserved role in vertebrate hearing and that truncated forms of mouse otoferlin can rescue hearing and balance. We also predict that otoferlin may play a role in pre-synaptic ribbon formation by modulating vesicle trafficking.

Funding
This work was supported by funds from Oregon State University and NIH P30 000210.

PD 200

Wbp2 is required for normal glutamatergic synapses in the cochlea and is crucial for hearing in Mice and Humans.

Annalisa Buniello[1]; Neil Ingham[1]; Morag Lewis[1]; Andreea Huma[2]; Raquel Martinez-Vega[3]; Oliver Houston[4]; Tanaya Bardhan[4]; Stuart Johnson[4]; Izabel Varela-Nieto[3]; Jacqueline White[2]; Huigun Yuan[5]; Walter Marcotti[4]; Karen Steel[1]
[1]King's College London; [2]Wellcome Trust Sanger Institute; [3]Instituto de Investigaciones Biomédicas, CSIC-UAM; [4]University of Sheffield; [5]Chinese PLA General Hospital

Steroid hormones are known to be implicated in normal auditory function, and estrogen signalling protects against noise-induced hearing loss. In order to investigate the functional link between hormonal signalling and hearing impairment and identify new targets for therapies, we used Wbp2-deficient mice as a genetic tool. *WBP2* encodes the WW domain-binding protein 2, which is phosphorylated before translocating into the nucleus where it acts as a transcriptional coactivator for the estrogen and progesterone receptors *ESR1* and *PGR*.

Auditory Brainstem Response (ABR) thresholds were raised at high frequencies as early as 4 weeks of age in the *Wbp2*-deficient mice and progressively increased and extended to lower frequencies by 14, 28 and 44 weeks old, indicating progressive hearing loss. Wbp2-deficient mice also show progressive abnormal emissions at high frequencies after recording of distortion product otoacoustic emissions (DPOEs) at 4 and 20 weeks of age. Interestingly, while the gross and cellular structure of the mouse mutant inner ears showed no obvious damage or degeneration up to 30 weeks old, confocal imaging performed at postnatal day 14 (P14), 4 and 8 weeks showed swollen nerve endings below inner hair cells, which is sign of glutamate excitotoxicity. Ribbon synapses showed abnormal morphology after double labelling with pre- and post-synaptic markers (CtBP2 and Glur2/3) in the mutants at 4 weeks of age, and these results were confirmed by transmission electron microscopy (TEM). We built up a pathway to understand the mechanistic link between the loss of Wbp2 and progressive hearing loss, and our data suggest that the phenotype is associated with reduced expression of *Esr1*, *Esr2* and *Pgr* in the cochlea, leading to disruption of expression of key post-synaptic proteins such as Shank3 and Psd-95.

Finally we report the cases of two children with severe to profound sensorineural hearing loss, each carrying two different point mutations in heterozygosis in the *WBP2* gene.

This study describes a new gene involved in the molecular pathway linking hearing impairment to hormonal signalling, and provides new therapeutic targets.

Funding
Wellcome Trust

PD 201

Gene Therapy Restores Auditory and Vestibular Functions in a Mouse Model For Usher Syndrome

Alice Emptoz[1]; Omar Akil[2]; Vincent Michel[1]; Andrea Lelli[1]; Typhaine Dupont[1]; Sylvie Nouaille[1]; Ménélik Labbe[1]; Elodie Ey[1]; Didier Dulon[3]; Lawrence Lustig[4]; Christine Petit[1]; **Saaid Saffieddine**[1]
[1]Institut Pasteur//INSERM UMRS 1120, Paris; [2]University of California, San Francisco; [3]Université de Bordeaux II; [4]Columbia University School of Medicine

Hearing impairment is a major concern and a serious burden for Public Health. The early-onset forms of severe deafness are mostly genetic in origin. Current clinical approaches to remedy hearing loss include hearing devices and cochlear implants. These solutions are still far from ideal especially in noisy environments. We investigated gene transfer as a therapeutic strategy to restore inner ear defects in a mouse model of Usher syndrome of type 1G (USH 1G), a human disease characterized by congenital profound deafness, vestibular dysfunction, and retinitis pigmentosa. We used the *Ush1g*$^{-/-}$ mutant mice defective for sans, a scaffold protein required for the maintenance of the stereocilia tip-links in the auditory hair cells. We chose the adeno-associated virus (AAV) as presently one of the most promising gene transfer systems. The murine Ush1g cDNA flanked by an IRES eGFP reporter cDNA sequence was subcloned into the AAV2 genome. Viral particles expressing mUsh1g-IRES-eGFP were produced in the AAV2/8 configuration. The viral particles were delivered to the cochlea through the round window membrane of *Ush1g*$^{-/-}$ mice at P2-P3. The hearing function of these mice was assessed by auditory-evoked brainstem response (ABR) recordings at different sound frequencies. The structure and function of the transduced hair cells were probed using scanning electron microscopy and mechanoelectrical transduction (MET) current measurements, respectively. Finally, several behavioral tests were used to evaluate the rescue of vestibular function, including circling behavior analyzed with a tracking software system and swimming tests.

Our results showed that a single and unilateral cochlear injection of the recombinant viral particles restored the normal shape of hair cell stereocilia bundles in *Ush1g*$^{-/-}$ mice. In addition we observed a complete recovery of auditory and vestibular hair cell-MET in response to mechanical stimulation of hair cell bundles in treated *Ush1g*$^{-/-}$ mice, and a complete rescue of the vestibular function. Finally ABR recording of mice that underwent *Ush1g* gene therapy showed typical ABR waveforms, indicating significant recovery of the hearing function.

Our results show that intracochlear gene transfer is a promising therapeutic approach to cure genetic forms of human deafness with or without balance defects.

Funding
FRM, European Union Seventh Framework Programme, under grant agreement HEALTH-F2-2010-242013

(TREATRUSH), LHW-Stiftung, Fondation Raymonde & Guy Strittmatter, Fighting Blindness, FAUN Stiftung, Conny Maeva Charitable Foundation, Fondation Orange, ERC grant 294570-hair bundle, LABEX Lifesenses [ANR-10-LABX-65], “the Foundation Fighting Blindness Paris Center Grant” and the Fondation Voir et Entendre

PD 202

In-vitro Analysis of Intrinsic and Synaptic Contributions to Adaptation in the Avian Central Nucleus of the Inferior Colliculus

Thomas Kuenzel; Sebastian Malinowski; Stefanie Kurth; Hermann Wagner
RWTH Aachen University

Response adaptation occurs in the avian inferior colliculus (IC) and is thought to play a role in complex auditory functions like echo-suppression or direction selectivity. However, magnitude and time-constant of adaptation varies considerably between recording sites and reports. In-vivo recordings also did not yet address cellular mechanisms of adaptation nor rigorously distinguished between different physiological sources. Notably, one study in the barn owl IC reported a double-exponential recovery from adaptation suggesting two mechanisms with distinct temporal profiles (Singheiser et al., 2012). We hypothesize here that rapid adaptation may be mediated by intrinsic ion channel properties of the IC neurons and longer-lasting adaptation may be attributed to synaptic short-term plasticity.

We tested this by performing whole-cell patch clamp recordings from neurons in the central IC in acute chicken embryonic (E20) brain slices. We first performed a detailed biophysical characterization of chicken IC neurons. Then, intrinsic adaptation was elicited by injection of current stimuli with varying inter-stimulus intervals. Action potentials were counted and analyzed in detail. Properties of synaptic inputs were examined by recording postsynaptic events in the chicken IC neurons after electrical stimulation of ascending auditory axons. Neurons were filled with biocytin during recordings and their dendritic fields were visualized with confocal microscopy.

We found that chicken central IC neurons can be distinguished by their responses to depolarizing current injection. 71% of the neurons fired tonically, 29% of the neurons fired phasically. These response groups could not be matched with the anatomical groups established in the IC of the chicken by Niederleitner & Luksch (2012). Overall, IC neurons of the chicken showed remarkable biophysical homogeny despite their diverse morphological appearance. However, intrinsic adaptation was more pronounced and recovered more rapidly in phasic firing neurons (exponential time constants of 10.7ms for phasic vs. 16.1ms for tonic neurons at room temperature). In the next step we recorded excitatory synaptic events upon electrical stimulation of ascending axons. Postsynaptic events showed pronounced depression even at inter-event intervals in the range of seconds, which could account for long-lasting reduction in input strength.

We thus conclude that in the central IC of the chicken fast adaptation in the millisecond range can indeed be explained by intrinsic ion channel properties and long-lasting adaptation could be caused by synaptic short-term depression.

Funding
This work is funded by German Science Foundationâ€™s (DFG) Priority Program PP1608 “Ultrafast and temporally precise information processing: Normal and dysfunctional hearing”.

PD 203

Seasonal Changes in Auditory Responses and Distribution of Androgen and Estrogen Receptors in the Central Auditory System of the Bat

Ellen Covey; Kimberley Miller; Leah Ogier
University of Washington, Seattle

Many temperate species adapt to seasonal environmental changes by altering their endocrine status, which triggers behaviors such as breeding, nesting, or food storage. Corresponding changes in auditory processing have been shown in amphibians, fish and birds, but few mammals. *Eptesicus fuscus* is typical of temperate zone bats in that both sexes undergo seasonal behavioral changes. Acoustic communication plays a key role in many behaviors such as male mating vocalizations in the fall, and mother-infant communication vocalizations in summer. Auditory processing might be expected to reflect these marked seasonal changes in communication behavior.

To explore the possibility that seasonal changes in hormonal status could drive functional plasticity in the central auditory system of a mammal, we used single-unit recording in awake bats to examine the responses of 673 neurons in the inferior colliculus (IC) at different seasons, and immunohistochemistry to map the distribution of alpha estrogen (ERA) and androgen (AR) receptors throughout the central auditory system of *Eptesicus*.

The average first-spike latency of IC neurons in females more than doubled in spring compared to other times of year, whereas in males it remained relatively stable year-round. Latency jitter for both sexes was higher in winter and spring than in summer or fall. The percentage of simple discharge patterns (sustained and transient) was higher in males than females in spring and higher in females than males in the fall. In females, the percentage of short-pass duration tuned neurons doubled in summer and remained elevated through fall and early winter. In males, the percentage of short-pass duration tuned cells increased in spring and the percentage of band-pass duration tuned cells doubled in the fall.

Both AR and ERA are found throughout the cochlear nuclei and medial nucleus of the trapezoid body of both sexes throughout the year, but labeling in the medial and lateral superior olives and medial geniculate is sparse or absent in all seasons. The nuclei of the lateral lemniscus and inferior

colliculus appear to express AR and ERA in a sexually dimorphic and/or seasonally plastic manner.

These findings indicate that there are seasonal changes in response characteristics of IC neurons in *Eptesicus*, especially in temporal response properties and duration sensitivity. Moreover, the pattern of changes is different in males and females, suggesting that hormone-driven plasticity in the IC and some lower brainstem structures adjusts central auditory processing to fit the characteristics of the vocalizations specific to seasonal, sex-specific behavioral patterns.

Funding
NIH Grants DC-00607 and DC-00287; NSF Grant IOS0719295; UW Royalty Research Fund Grant.

PD 204

Glycinergic and GABA-mediated Inhibition on Stimulus-Specific Adaptation (SSA) in the Inferior Colliculus (IC) of the Anesthetized Rat.

Yaneri Ayala[1]; Colleen Gabel[2]; Manuel Malmierca[1]
[1]University of Salamanca; [2]Massachusetts Institute of Technology & University of Salamanca

Background
SSA is a response decrease to repetitive sound frequencies that does not generalize to the sensitivity to rare sounds. Although $GABA_A$-mediated inhibition exerts a gain control, the question remains whether or not local inhibition mediated by receptors other than $GABA_A$, or by the combined activation of several receptors, is responsible for SSA.

Methods
We performed microiontophoretic injections of $GABA_B$ and glycinergic antagonists alone or combined with gabazine ($GABA_A$ antagonist). Extracellular single-unit spikes evoked by rare and repetitive sounds were recorded before and during the pharmacological manipulation. The SSA level was estimated by the common-SSA index (CSI), whose positive values indicate that the repetitive sounds evoke a smaller response than the rare ones. A Wilcoxon Signed-Rank test was performed to test for significant drug effects. Median values are reported.

Results
The $GABA_B$ antagonist CGP35348 (20 mM) decreased CSI from 0.41 to 0.3 (p=0.02, n=13), while the specific antagonist for presynaptic $GABA_B$ receptors, CGP36216 (10 mM), increased CSI from 0.45 to 0.48 (p=0.003, n=20). While CGP35358 did not alter the population evoked-response, CGP36216 decreased the response for the deviant (p=0.01) and standard tones (p=0.01). The blockage of the glycinergic receptors (strychnine 20 mM, n=24) failed to affect SSA (p=0.87). This may be partially explained by the finding that strychnine exerted a weak but significant increase in SSA of neurons with low baseline CSIs (0.44, n=8, Bootstrapping, C.I. 95%), but decreased SSA levels in neurons with high baseline CSIs (0.84, n = 7). Combined injections of CGP35348 with other antagonists elicited a stronger decrease in CSI; CGP35348: 26%, CGP35348+Gabazine: 50% (n=10), CGP35348+Gabazine+Strychnine: 47% (n=13). A progressive increase in the sound-evoked responses was observed when more receptors were simultaneously blocked (Figure 1). Finally, disinhibition revealed SSA spiking responses to previous subthreshold sound frequencies (n=3).

Conclusions
Our data show that SSA neurons may exhibit pre- and postsynaptic $GABA_B$ receptors, which differentially affect the excitation-inhibition balance. *In vitro* studies suggest presynaptic $GABA_B$ receptors are expressed throughout the IC, while dorsal cortex neurons expressed both pre- and postsynaptic receptors. The decrease in the neural spiking elicited by CGP36216 contrasts with the general idea that glutamatergic excitation in IC is modulated by presynaptic $GABA_B$ receptors, and suggests they might be also affecting the GABAergic or glycinergic inhibiton. Finally, the persistence of SSA under combined injections of antagonists indicates that SSA is not shaped exclusively by the recruitment of inhibitory inputs within the local network.

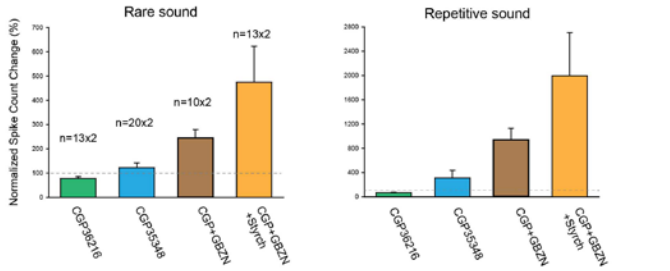

Figure 1. Normalized change in the sound-evoked response to rare and repetitive sounds in IC neurons. Percentages higher than 100 indicate an increase in the neuron´s spiking while those lower than 100 indicate a response decrease. Two pure tones were presented for each neuron as rare and repetitive stimulus. Data displayed as mean ± SEM.

Funding
This project was funded by the MINECO grant BFU201343608-P and the JCYL grant SA343U14 to M.S.M. Y.A.A. held a CONACyT (216106) and a SEP fellowship.

PD 205

Task-Related Plasticity in the Inferior Colliculus of the Marmoset Monkey

Sean Slee; Stephen David
Oregon Health and Science University

The marmoset monkey is a promising new non-human primate model for studying auditory behavior. In this study, we tested whether receptive field properties in the inferior colliculus (IC) of marmosets undergo changes during auditory behavior, similar to our previous findings in IC of the ferret. We trained a marmoset to detect a pure tone target embedded in a background of random spectral shape (RSS) distractor stimuli. The level of the tone was manipulated to vary task difficulty. The marmoset was able to accurately perform this task over the 4 octaves of sound frequency tested (1.25-20 kHz). As the level of the tone was decreased, we found a small but significant decrease in the hit rate and a comparatively large increase in the false alarm rate.

We measured the effects of task engagement by simultaneously recording electroencephalograms (EEGs) and single neurons in the IC. Neural responses to both targets and RSS distractors were compared between conditions when the marmoset was passive or performed the detection task. The target frequency was placed near the best frequency (BF) of the neuron under study. EEG power spectra remained stable between conditions, confirming that the level of arousal was similar in the passive and active states. During task engagement spike responses to the RSS distractors were suppressed in about half of the neurons. The median global gain change (-15%) in these neurons was comparable to our previous study in the ferret (median=-20%).

Responses to the RSS distractor stimuli were also used to fit linear and nonlinear spectral weighting models. RSS weights were tuned around BF for most neurons in the central nucleus of the IC. In about 1/3 of these neurons we found a significant decrease in the RSS weight at BF (target frequency) during task engagement. The median weight change (-25%) was also similar to previous measurements in the ferret (-32%). Finally, we computed the discrimination index (d') between the distributions of neural responses to the target and distractor stimuli in both behavioral conditions. We found that most IC neurons can discriminate between the task stimuli (d'>1) but discrimination *does not* improve during task engagement. These preliminary results suggest that although the IC is significantly modulated during task engagement, improvements in neural discrimination are not consistently observed in single neurons.

Funding
Sean Slee (DC012124) Stephen David (DC010439)

PD 206

Midbrain-based decoding of vowel and speaker information in humans

Bharath Chandrasekaran; Zilong Xie; Han-Gyol Yi; Rachel Reetzke
The University of Texas at Austin

Here we ask to what extent information related to 'what' is being said, and 'who' is speaking can be decoded using single-trial scalp-recorded EEG and machine learning metrics. We measure an evoked component called the frequency-following response (FFR), which reflects ensemble activity of neuronal populations in the auditory brainstem and midbrain that phase-lock to the auditory stimulus. These sustained components can be elicited from scalp-electrodes and encode stimulus related information with high temporal and spectral precision. Previous studies have typically utilized thousands of trials to gauge FFRs to vowel and speaker information. Our aimed to classifying speech based on 'who' is taking and 'what' is being said on a single-trial basis using the FFRs. Participants (n=15, age range: 18-35) underwent a subcortical electroencephalography (EEG) session where the FFRs to two English vowels (/a/ and /u/) produced by two native English speakers were collected. Sentence recognition in noise was also assessed in the same participants in a separate session. Consistency of subcortical encoding was assessed using a machine learning approach, where an observer-independent classifier based on the support vector machine algorithm was trained to differentiate responses to the two vowels across the two speakers or the two talkers across the two vowels on a single-trial basis. The classifier was then tested on an independent set of trials. The classifier trained to differentiate vowels performed significantly above chance level (50%), 95% CI [76 %, 85%]. The classifier trained to differentiate speakers also performed significantly above chance level (50%), 95% CI (77%, 87%). Further, vowel classification accuracy significantly predicted speech perception performance in noise [β = 6.492, SE = 2.394, $\chi 2$ (1) = 4.625, p = 0.032]. In contrast, speaker classification accuracy was not associated with speech perception in noise. These data indicate that the integrity of vowel encoding as assessed using the machine learning approach is associated with expertise in speech processing under challenging listening environments, indicating a strong brain-behavioral correspondence. Our results provide first evidence of the utility of data-driven approaches in deciphering information related to speaker identity and content single-trial FFR.

Funding
(Grant R01DC013315 (NIH) to B.C)

PD 207

'Unjittering' midbrain activity boosts the representation of speech formant structure

Travis White-Schwoch[1]; Trent Nicol[1]; Catherine Warrier[1]; Daniel Abrams[2]; Nina Kraus[1]
[1]Northwestern University; [2]Stanford University

Jitter, or timing variability, occurs naturally in biological systems. Converging perceptual and neurophysiological studies motivate a hypothesis that excessively-jittered neural coding contributes to difficulties in speech understanding, particularly in challenging listening environments, and that jitter specifically targets the neural coding of fine-grained speech features (for example, the temporal changes that convey the contrast between the sounds /b/ and /d/). An important test of this hypothesis is to examine whether more synchronized neural activity would, across multiple trials, produce a specific enhancement in the neural representation of high-frequency speech features such as formants. To address this question, we measured *in vivo* extracellular activity from central nucleus of inferior colliculus to speech sounds in guinea pigs. We determined the timing discrepancy between each response trial and unjittered the activity by correcting for these timing differences prior to averaging the near-field multiunit responses. *Whereas unjittering minimally affected coding of the fundamental frequency, correcting for timing variability amplified higher-frequency spectral amplitudes up to tenfold.* This activity reflects coding of formant features in the speech signal and is consistent with the hypothesis that jitter disrupts the intelligibility of these particular speech features. The specificity of this effect was confirmed across multiple stimuli that varied parametrically in spectral structure. Additionally, we ran a series of biologically-plausible simulations to determine how each 0.1 millisecond

increase in jitter blurs spectral coding; these simulations confirmed that increasing the degree of jitter progressively reduces spectral coding of the formants while leaving the fundamental frequency relatively unaffected. A parallel experiment in human listeners shows that formant coding in the central auditory system relates to everyday listening skills—scalp responses to the same speech sounds were elicited in children, and the strength of responses to formant features, but not the fundamental frequency, related to tests of auditory processing. Together, these results establish that jitter specifically targets the neural processing of fine-grained speech cues, such as formants, but may spare the processing of voicing cues. Our results are consistent with evidence from clinical populations that degraded coding of fine-grained temporal cues disrupts speech perception, particularly in adverse listening conditions. Moreover, these results are consistent with models of auditory processing that propose orthogonal neural mechanisms underlie the coding of voicing (fundamental frequency) and formant (harmonic) cues in speech, and suggest a role for subcortical systems in this dichotomy.

Funding
Supported by NIH R01 DC01510 & R01 HD069414

PD 208

Dopamine Receptor Distribution in Key Auditory Brain Regions

Aaron Apawu; Brittany Adams; Bozena Fyk-Kolodziej; Mirabela Hali; Avril Holt
Wayne State University

Background
Dopamine (DA), a multi-modal neurotransmitter, has also been implicated in auditory processes. We have previously shown that direct administration of DA antagonist into the inferior colliculus (IC) may provide protection from noise induced hearing loss and enhance Gap detection. However, the role of DA neurotransmission in auditory function is not fully understood. Binding of DA to membrane bound receptors elicits diverse signaling responses that can be either excitatory or inhibitory depending on the class (Type 1 or Type 2) of DA receptor mediating the response. Therefore, the distribution of DA receptors across auditory brain regions is key to understanding the role of DA neurotransmission in auditory processes. In the present work, we examine the localization and expression of DA receptor subunits (Drd1, Drd2, Drd3, Drd4, Drd5) across auditory brain regions.

Methods
Protein and mRNA were isolated from the auditory cortex (AC), cochlear nucleus (CN), and IC of adult male Sprague Dawley rats (n = 10). In addition to Western blotting, real time RT-PCR was performed with hypoxanthine phosphoribosyltransferase 1 (HPRT1) as the housekeeping gene. Immunocytochemistry was used to determine the distribution of DA receptors in sections through the AC, IC, and the medial geniculate body (MGB). Images were examined using fluorescence microscopy.

Results
Both protein and gene expression studies demonstrated the presence of D1- and D2-like DA receptors throughout the AC, CN, IC, and the MGB. Gene expression data demonstrated the highest level of Drd1 expression in the AC while expression in dorsal CN (DCN), ventral CN (VCN), and IC, was less than half of AC values. For Drd2, the IC exhibited the highest expression level, followed by the AC, VCN and then DCN. The most prominent Drd3 expression was in the DCN with the lowest expression in the AC. There was no differential expression of Drd5 across the regions tested. Immunocytochemistry data showed localization of D1-like receptors primarily on dendrites and cell bodies while D2-like receptors were localized to axon terminals in the AC, IC, and MGB.

Conclusions
Both the D1 and the D2 families of the DA receptors are found in the AC, CN, IC, and MGB suggesting that neurons in the AC, IC and MGB may be regulated by DA. Future studies will examine noise induced changes in DA receptor levels and identify the origin of auditory related dopaminergic pathways.

Funding
Grant 1I01RX001095-01U.S. Dept. of Veterans Affairs to AGH NIH DC007733 (to AGH)

PD 209

Dynamics of short-term experience-dependent plasticity in human subcortical auditory function

Rachel Reetzke; **Zilong Xie**; Han-Gyol Yi; W. Todd Maddox; Alexandros Dimakis; Bharath Chandrasekaran
The University of Texas at Austin

A plethora of recent evidence suggests that subcortical function is malleable to short-term auditory experience. Here we examined subcortical decoding of linguistically relevant pitch patterns using electrophysiological and machine learning methods, in order to understand the dynamics of short-term experience-dependent plasticity in subcortical auditory function. We trained native English listeners to categorize Mandarin pitch patterns in a single training session. We collected frequency-following responses (FFRs) before, during, and immediately after training. Meanwhile, previous studies suggest that sleep is critical for consolidation of learning as well as learning-related neuroplastic changes. The second goal of our study was to examine the role of sleep in consolidating the Mandarin pitch patterns and in shaping training-related subcortical plasticity. To this end, we also collected FFRs from each listener on a second day, which was immediately followed by a generalization task to categorize Mandarin pitch patterns produced by speakers different from the training task. We utilized a data-driven machine learning algorithm, i.e. support vector machine, to test whether subcortical differentiation of Mandarin tones (level pitch *vs.* rising pitch) from FFRs can be modulated by training-induced behavioral relevance. Our results showed that subcortical differentiation of pitch patterns remained unchanged during and immediately after training. Differentiation spontaneously

improved after participants were brought back on a second day, and the extent of subcortical differentiation related to the retention of pitch patterns. These findings suggest that auditory subcortical responses to pitch patterns are enhanced when clear behavioral relevance (via training) is established; however, the enhancement may not be evident until after at least a day of sleep-related consolidation.

Funding
This work was supported by the National Institute on Deafness and Other Communication Disorders-National Institutes of Health (Grant R01DC013315 to B.C.) and the National Institute on Drug Abuse-National Institutes of Health (Grant DA032457 to W.T.M.)

ADDENDUM TO THE
ABSTRACTS OF THE 39TH ANNUAL MIDWINTER MEETING OF THE

PRES SYMP 5

Gene Therapy for Hearing and Balance defects: How close are we ?

Christine Petit [1,2,3,8], Alice Emptoz[1,2,3], Sedigheh Delmaghani,[1,2,3] Omar Akil[4] , Paul Avan [5,6], Lawrence Lustig[7], and **Saaid Safieddine**[1,2,3]

[1]Unité de Génétique et Physiologie de l'Audition, Institut Pasteur, 75015 Paris, France

[2]UMRS 1120, Institut National de la Santé et de la Recherche Médicale (INSERM), 75015 Paris, France

[3]Sorbonne Universités, UPMC Université Paris 06, Complexité du Vivant, 75005 Paris, France

[4] Otorinolaringology-Head & Neck Surgery, University of California San Francisco, 2380 Sutter Street, San Francisco

[5]Laboratoire de Biophysique Sensorielle, Université d'Auvergne, 63000 Clermont-Ferrand, France

[6]UMR 1107, Institut National de la Santé et de la Recherche Médicale (INSERM), 63000 Clermont-Ferrand, France

[7]Columbia University School of Medicine and New York Presbyterian Hospital, New-York

[8]Collège de France, 75005 Paris, France

Since the initial report on hearing restoration by cochlear gene transfer in a mouse mutant defective for vesicular glutamate transporter-3 (VGLUT3-/-), a growing number of studies tackle similar objectives in the perspective of developing inner ear gene therapy in humans. This presentation will focus on our main approaches to inner ear gene therapy, including the prevention of noise-induced hearing loss and the restoration of balance in vestibulopathies.

The first issue was addressed upon the finding that the mutations in the gene encoding pejvakin (Pjvk) result in an hypervulnerability to sound in mice and humans caused by a marked oxidative stress; this stress develops as a consequence of the defect in the adaptive peroxisome proliferation in response to noise exposure. The results of a comparative analysis of the prevention of noise-induced hearing loss by anti-oxidant drugs and adeno-associated virus (AAV) gene transfer of the murine Pjvk cDNA in Pjvk-/- mice will be discussed.

The second issue was addressed in a mouse model for Usher syndrome of type 1G (USH 1G), that is characterized by congenital profound deafness, vestibular dysfunction, and retinitis pigmentosa. This gene encodes Sans, a scaffolding protein expressed in the cochlear and the vestibular hair-bundles. The results of the cure of hearing and vestibular disorders of Ush1g-/- mutant mice by an recombinant AAV2/8 carrying the Ush1g cDNA will be presented with a special focus on the vestibulopathy of the syndrome.

NOTE: The presenting author has changed to *Saaid Safieddine.

PD 71

A Mutation in SLC22A4 Encoding an Organic Cation Transporter Expressed in the Cochlear Strial Endothelium Causes Human Recessive Non-Syndromic Hearing Loss DFNB60

M'hamed Grati[1]; Mariem Ben Said[2]; Bing Zou[1]; Imen Chakchouk[2]; Qi Ma[1]; Qi Yao[1,3]; Bouthaina Hammami[4]; Denise Yan[1]; Rahul Mittal[1]; Abdelmonem Ghorbel[4]; Lingling Neng[5]; Mustafa Tekin[1,6]; Xiao Rui Shi[5]; Saber Masmoudi[2]; Zhongmin Lu[3]; Mounira Hmani[2]; Xuezhong Liu[1,6]

[1]Department of Otolaryngology, University of Miami Miller School of Medicine; [2]Laboratoire Procédés de Criblage Moléculaire et Cellulaire, Centre de Biotechnologie de Sfax, Université de Sfax; [3]Department of Biology, University of Miami; [4]Service Otorhinolaryngologie, Hôpital Universitaire Habib Bourguiba, Sfax, Tunisia; [5]Oregon Hearing Research Center, Department of Otolaryngology/Head and Neck Surgery, Oregon Health & Science University; [6]Dr. John T. Macdonald Foundation Department of Human Genetics, and John P. Hussman Institute for Human Genomics, University of Miami

Introduction

The high prevalence/incidence of hearing loss (HL) in humans makes it the most common sensory defect. The majority of the cases are of genetic origin. Non-syndromic hereditary HL is extremely heterogeneous. Genetic approaches have been instrumental in deciphering genes that are crucial for auditory function.

Goal

Mapping and identification of the gene causing ARNSHL in a large consanguineous Tunisian family (FT13), and characterization of the function of the encoded protein.

Methods

We used NADf chip to screen for common North African HL-causing mutation in FT13. We performed genome-wide linkage analysis to map the causative gene. We performed whole-exome sequencing on patient DNA to identify homozygous variants in genes within the determined locus that would cause the disease. We screened a cohort of small Tunisian HL families searching for additional patients carrying the same variants. We studied the targeting properties of candidate proteins in cell lines and performed immunofluorescence on rat inner ear preparations to study their tissue and cellular localization. We used morpholino-based gene knockdown, live imaging, immunofluorescence, and electrophysiological recordings to study auditory function of the orthologous genes in zebra fish.

Results

We first excluded the implication of known North-African mutations in deafness in family FT13. We then assigned the deafness gene locus to a 12.8 Mb critical region on ch:5q23.2-31.1, corresponding to DFNB60 locus. Moreover, we uncovered aminoacid substitution p.Cys113Tyr in a novel protein SLC22A4 (OMIM#604190), as the cause of ARNSHL DFNB60. Besides, screening a cohort of 71 Tunisian HL

families led to uncover a deaf proband of consanguineous parents that is homozygous for p.Cys113Tyr. This patient carried a homozygous microsatellite marker haplotype bordering SLC22A4 gene locus that was identical to that transmitted within FT13, indicating that this mutation is ancestral. SLC22A4 transports various compounds including organic cations, such as physiological carnitine, and naturally occurring potent antioxidant ergothioneine. Within tissues, carnitine facilitates fatty-acid transport into mitochondria to enter ß-oxidation for energy production. Using immunofluorescence, we demonstrate that Slc22a4 is expressed in the stria vascularis (SV) endothelial cells of adult rat and mouse cochlea and targets their apical plasma membrane. These observations were corroborated by finding Slc22a4 transcripts in our RNA-seq library from purified primary culture of mouse strial endothelial cells. Finally, slc22a4 disruption in zebra fish causes sensorineural HL.

Conclusions

We present SLC22A4 as an organic cation transporter of the SV that is essential for hearing, and its mutation causes DFNB60 form of HL.

Research Funding

The National Institutes of Health: R01DC005575, 2P50DC000422-Sub-Project 6432 and R01DC012115 to X.Z.L.; R21DC009879 and the University of Miami Provost Research Award to Z.L.; R21DC012398 and R01DC010844 to X.R.S.; R01DC009645 to M.T.; the International Centre for Genetic Engineering and Biotechnology and Ministry of Higher Education and Research of Tunisia to S.M.

NOTE: Additional authors and affiliations have been added.

PD 60

Hypervulnerability to sound-exposure through impaired adaptive proliferation of peroxisomes

Sedigheh Delmaghani[1]; Jean Defourny[1]; PD 60

Hypervulnerability to sound-exposure through impaired adaptive proliferation of peroxisomes

Sedigheh Delmaghani1; Jean Defourny1; Saaid Safieddine1; Paul Avan2; Christine Petit1

1Institut Pasteur; 2Laboratoire de Biophysique Sensorielle, Université d'Auvergne

A deficiency of pejvakin, a protein of unknown function, causes a strikingly heterogeneous form of deafness. Pejvakin-deficient (Pjvk-/-) mice also exhibited variable auditory phenotypes. Correlation between their hearing thresholds and the number of pups per cage suggested a possible harmful effect of pup vocalizations. Direct sound or electrical stimulation showed that the cochlear sensory hair cells and auditory pathway neurons of Pjvk-/- mice and patients were exceptionally vulnerable to sound. Pjvk-/- cochleas displayed features of marked oxidative stress and impaired anti-oxidant defenses. We showed that pejvakin is associated with peroxisomes, and is required for the oxidative stress-induced proliferation of these organelles. In Pjvk-/- hair cells, peroxisomes displayed structural abnormalities after the onset of hearing. Noise-exposure of wild-type mice rapidly upregulated Pjvk cochlear transcription, and triggered peroxisome proliferation in hair cells and primary auditory neurons. Our results reveal that the anti-oxidant activity of peroxisomes protects the auditory system against noise-induced damage. Pjvk gene transfer can rescue auditory dysfunction in Pjvk-/- mice.

Funding

This study was supported by grants from Louis-Jeantet Foundation, ANR – NKTH "HearDeafTreat" 2010-INTB-1402-01, Humanis Novalis-Taitbout, Réunica-Prévoyance, BNP Paribas, and French state program "Investissements d'Avenir" (ANR-10-LABX-65).

[1]; Paul Avan[2]; Christine Petit[1]

[1]Institut Pasteur; [2]Laboratoire de Biophysique Sensorielle, Université d'Auvergne

A deficiency of pejvakin, a protein of unknown function, causes a strikingly heterogeneous form of deafness. Pejvakin-deficient (*Pjvk*$^{-/-}$) mice also exhibited variable auditory phenotypes. Correlation between their hearing thresholds and the number of pups per cage suggested a possible harmful effect of pup vocalizations. Direct sound or electrical stimulation showed that the cochlear sensory hair cells and auditory pathway neurons of *Pjvk*$^{-/-}$ mice and patients were exceptionally vulnerable to sound. *Pjvk*$^{-/-}$ cochleas displayed features of marked oxidative stress and impaired anti-oxidant defenses. We showed that pejvakin is associated with peroxisomes, and is required for the oxidative stress-induced proliferation of these organelles. In *Pjvk*$^{-/-}$ hair cells, peroxisomes displayed structural abnormalities after the onset of hearing. Noise-exposure of wild-type mice rapidly upregulated *Pjvk* cochlear transcription, and triggered peroxisome proliferation in hair

cells and primary auditory neurons. Our results reveal that the anti-oxidant activity of peroxisomes protects the auditory system against noise-induced damage. *Pjvk* gene transfer can rescue auditory dysfunction in *Pjvk*$^{-/-}$ mice.

Funding
This study was supported by grants from Louis-Jeantet Foundation, ANR – NKTH "HearDeafTreat" 2010-INTB-1402-01, Humanis Novalis-Taitbout, Réunica-Prévoyance, BNP Paribas, and French state program ''Investissements d'Avenir'' (ANR-10-LABX-65).

NOTE: The presenting author has changed to *Saaid Safieddine.

SYMP 21

One Woman's View of Deafness and the Impact of Science, Policy and Culture on Achieving Her Career Goals

CANCELLED

Claudia Gordon
U.S. Department of Labor

Overview
Claudia Gordon will provide an overview of her journey that has led her to where she is today, not only as the Chief of Staff for the Department of Labor's Office of Federal Contract Compliance Programs (OFCCP), but also as an independent deaf woman of color on a mission to promote inclusion and access for individuals with disabilities in our society. Ms. Gordon suddenly lost her ability to hear at the age of eight. Placed in isolation and stigmatized, two years would pass before she emigrated to the U.S. and was enrolled at a school for the deaf. A whole new world opened up for her once she learned to communicate in American Sign Language. When Ms. Gordon expressed an interest in furthering her education and becoming a lawyer, she was advised that she might not do as well in a hearing environment. Undeterred, she attended Howard University and subsequently American University Washington College of Law (WCL). During her time at Howard University and WCL, she had access to sign language interpreters for her classes, and this is still her preferred mode of communication.

Ms. Gordon has served as a senior policy advisor with the U.S. Department of Homeland Security's Office for Civil Rights and Civil Liberties, staff attorney for the National Association of the Deaf Law and Advocacy Center and Vice-President of National Black Deaf Advocates, Inc. Ms. Gordon is also a member of the Gallaudet University Board of Trustees. As a member of the Obama Administration since 2009, she initially served as Special Assistant to the Director of OFCCP and is now OFCCP's Chief of Staff. OFCCP enforces the civil rights of applicants and employees of companies benefitting from government contracts. Notably, in 2013 – 2014 she conducted a temporary assignment with the White House Office of Public Engagement as an Associate Director where she served as liaison to the disability community, advising on disability policies. She was awarded the Department of Homeland Security Secretary's Gold Medal, and the Paul G. Hearne Leadership Award, both for her work with the disabled community.

Ms. Gordon will speak about the numerous challenges faced along her journey, her resiliency and deep commitment to advancing equality of opportunity for people with disabilities. "People with disabilities are defined not by our limits but by our potential. With the right tools and support from the scientific community as well as our policymakers, anything is possible."

NOTE: SYMP 21 has been cancelled.

PS 142

Minimal Basilar Membrane Motion in Lowfrequency Hearing

Anders Fridberger[1]; Rebecca Warren[1]; Sripriya Ramamoorthy[2]; Nikola Ciganovic[3]; Yuan Zhang[2]; Teresa Wilson[2]; Tobias Reichenbach[3]; Alfred Nuttall[2]

[1]Linköping University; [2]Oregon Health & Science University; [3]Imperial College

Low-frequency hearing is critically important for speech and music perception, but no mechanical measurements are available from inner ears with intact low-frequency parts. These regions of the cochlea may function in ways different from the extensively studied high-frequency regions, where the sensory outer hair cells produce force that greatly increases the sound-evoked vibrations of the basilar membrane. We used laser interferometry in vitro and optical coherence tomography in vivo to study the low-frequency part of the guinea pig cochlea, and found that a minimal portion of the basilar membrane was moving in response to sound stimulation. The motions that were present had smaller amplitude and different dependence on stimulus frequency than vibrations measured near the mechanosensitive stereocilia. These measurements show a radically different mechanism for detecting low frequencies that help to explain why low-frequency hearing is so resistant to potentially damaging sound levels.

NOTE: This poster has been added to the meeting.

PS 325

Simultaneous Multigene Mutation Detection in a Multi-Ethnic Cohort of Patients with Sensorineural Hearing Loss Through MiamiOtoGenes Panel

Denise Yan[1]; Demet Tekin[1]; Guney Bademci[2]; Joseph Foster II[2]; F.Basak Cengiz[2]; Abhiraami Kannan-Sundhari[1]; Shengru Guo[2]; Rahul Mittal[1]; Bing Zou[1]; Mhamed Grati[1]; Rosemary I. Kabahuma[3]; Mohan Kameswaran[4]; Akeem O. Lasisi[5]; Gabrielle N. Manzoli[6]; Kiyoko A. Sandes[6]; Angelina X. Acosta[6]; Ibis Menendez[2]; Claudia Carranza[7]; Temis M. Felix[8]; Reza Maroofian[9]; Andrew H. Crosby[9]; Saber Masmoudi[10]; Susan H. Blanton[1,2]; Mustafa Tekin[1,2]; Xue Zhong Liu[1,2]

[1]Department of Otolaryngology, University of Miami Miller School of Medicine, Miami, FL 33136, USA; [2]Dr. John T. Macdonald Department of Human Genetics, University of Miami Miller School of Medicine, Miami, FL 33136, USA; [3]Department of Otorhinolaryngology, Steve Biko Academic Hospital, University of Pretoria, Cnr Malan and Steve Biko Road, Gezina, Pretoria, South Africa; [4]Madras ENT Research foundation (MERF) No-1,1st Cross Street,Off. II Main Road, Raja Annamalai Puram, Chennai, Tamil Nadu 600028, India; [5]Department of Otorhinolaryngology, College of Medicine, University of Ibadan, Ibadan, Nigeria. [6]Gonçalo Moniz Research Center (CPqGM), Oswaldo Cruz Foundation (FIOCRUZ), Salvador, Bahia, Brazil [7]Institute for Research on Genetic and Metabolic Diseases, INVEGEM, Guatemala. [8]Serviço de Genética Médica, Hospital de Clinicas de Porto Alegre, Brasil [9]Institute of Biomedical and Clinical Science, University of Exeter Medical School, RILD Wellcome Wolfson Centre, Exeter, UK [10]Laboratoire Procédés de Criblage Moléculaire et Cellulaire, Centre de Biotechnologie de Sfax, Université de Sfax, Sfax, Tunisie

Background

Genetic causes of hearing loss are very heterogeneous. Thus far, more than 66 genes have been characterized for nonsyndromic hearing loss. In addition approximately 150 genetic loci have been mapped, and it is estimated that the number of genes could reach 300, equivalent to 1% of all human genes. Extreme genetic heterogeneity of deafness combined with striking variations in the distribution of causative variants in different ethnic groups has made genetic diagnosis expensive and time consuming using traditional methods.

Methods

We took advantage of the SureSelect target capture system (Agilent; https://earray. chem.agilent.com/suredesign/) to develop a custom capture panel (MiamiOtoGenes) to contain all exons, 5' UTRs and 3' UTRs of 180 known and candidate deafness causing genes. A target size of approximately 1.158 MB comprising 3494 regions was designed to include genes associated with both syndromic and nonsyndromic hereditary hearing loss. We undertook a targeted sequencing of the 180 genes in a multi-ethnic cohort (South American consisting of Brazilian, Guatamalan, Tunisian, Nigerian, indigenous South African, Turkish, Iranian, Indian, South Florida multi-ethnic

patients) of 360 GJB2 mutation–negative probands. Hearing loss (HL) was congenital or prelingual-onset with a severity variant from mild to profound. The Genomes Management Application (GEMapp; https://secureforms.med.miami.edu/hihg/gem-app) was used for data filtering. Single-nucleotide variants (SNVs), insertion/deletions (INDELS) and copy-number variations (CNVs) were determined. Computational functional prediction algorithms [ClinVar; American College of Medical Genetics and Genomics (ACMG) guidelines] and conservation scores (PHASTCONS, GERP) were also applied.

Results

Overall, the mutation detection rates for a likely pathogenic variant are high, at 55% to 75%, for South American, Indian, Tunisian, Turkish, Iranian, Indian, South Florida groups. In contrast, the pickup rates for Nigerian, indigenous South African are currently low, with only approximately 14% to 50% of probands have sequence changes identified as a probable cause of deafness. There are no predominant recurring mutations in the selected genes within ethnic groups. The lower rate of mutations found amongst sub-Saharan African patients may be indicative of the link of infectious disease to deafness.

Conclusion

Our study highlights the utility of next generation sequencing techniques combined with functional studies analysis tools to provide insight into the etiology of a genetically heterogeneous human disorder such as deafness. Furthermore our data indicate that a deafness gene based panel may be a more cost effective way of assessing genetics of hearing loss in a particular population.

Funding

The work is supported by NIH R01DC012115, R01DC005575, R01DC009645 and the University of Ibadan TETFund Grant.

NOTE: Additional authors and affiliations have been added.

PS 338

Transcription Analyses of Sensory Epithelia in the Inner Ear of Zebra fish

Rahul Mittal[1]; Lingyu Wang[2]; Qi Yao[1,2]; M'hamed Grati[1]; Bing Zou[1]; Denise Yan[1]; Zhongmin Lu[2]; Xuezhong Liu[1]

[1]Department of Otolaryngology, University of Miami Miller School of Medicine, Miami, FL, 33136, USA; [2]Department of Biology, University of Miami, Coral Gables, Miami, FL, 33146, USA

Background

The transcriptome is the set of all RNA molecules, including mRNA, rRNA, tRNA, and other non-coding RNA transcribed in one cell or a population of cells. (In our study, we primarily focus on the mRNA.) Transcriptome analysis can provide crucial information that will help in understanding the genetic mechanisms that control differentiation, proliferation, senescence, metabolism, morphology, and function of a cell or tissue under normal and pathological conditions. Recently, zebra fish model is gaining increasing attention for the study of the development and function of the vertebrate inner ear. The aim of this study is to examine the differential gene expression in saccular, utricular, and lagenar maculae of zebra fish, which helps us to understand the molecular basis underlying functional differences among three otolith organs.

Methods

Sensory epithelia were carefully dissected out from the saccule, utricle and lagena of adult transgenic zebra fish (Et(krt4:GFP)sqet4). Total RNA per sample was prepared using the Ovation Pico WTA System V2 and yielded cDNA product that was fragmented and labeled using the Encore Biotin Module according to the manufacturer's protocol. Affymetrix Zebra fish Gene 1.0 ST Array were scanned using GeneChip Scanner 3000 7G system. Following quality control, the signal estimates were uploaded for differential expression analysis to the Affymetrix Transcriptome Analysis Console (TAC). The results were statistically analyzed using ANOVA and p values <0.05 were considered significant.

Results

We observed that there was differential expression of genes in the saccule, utricle and lagena. We uncovered hundreds of differentially expressed genes in the three otolith organs. Some of these differentially expressed genes are related to the otolith development and balance in zebra fish, or related to the deafness in human. However, some of the genes were conserved among all three otolith organs. Uniquely expressed genes accounted for <10% of all genes in either otolith organ. Gene ontology and pathway enrichment analyses also provided insights into the gene expression signatures of each otolith organ.

Conclusions

The present study provides a dataset that will help in identifying and exploring the role of deafness and balance related genes. It will help in validating the utilization of zebra fish as a model to study human auditory and vestibular disorders. Morphants and mutants would help in deciphering the physiological effects of these genes in hearing and balance functions.

Funding
This work was supported by NIH/NIDCD grants R01DC012546, R01DC121125, and R01DC005575.

NOTE: Additional authors and affiliations have been added.

PS 657

Dual Rate Codes for the Pitch of Harmonic Complex Tones in the Auditory Midbrain of Unanesthetized Rabbit

Yaqing Su[1,2]; Daniel Goodman[3]; Bertrand Delgutte[1,4]
[1]Massachusetts Eye & Ear; [2]Boston University; [3]Imperial College London; [4]Harvard Medical School

Background
The pitch of harmonic complex tones plays an important role in auditory scene analysis and speech and music perception. hile the coding of pitch in the auditory nerve and cochlear nucleus is well understood, and pitch-selective neurons have been found in marmoset auditory cortex, little is known about how the peripheral codes are transformed into pitch selectivity at intermediate stages of processing. To address this gap, we studied the coding of harmonic complexes in the inferior colliculus (IC) of unanesthetized rabbits.

Method
We recorded from single IC units of three rabbits in response to tone complexes with equal amplitude harmonics and varying fundamental frequency (F0). Two stimulus paradigms were used to assess the coding of pitch based on resolved and unresolved harmonics, respectively. In the first paradigm, F0 was varied so that the ratio of the neuron's characteristic frequency (CF) to F0 ranged from 0.5 to 5.5. These stimuli were usually presented at 30, 45 and 60 dB SPL per harmonic. In the second paradigm, F0 was varied from 26 Hz to 1792 Hz. Temporal envelope cues to pitch were manipulated by altering the phase relationships among the harmonics: Cosine phase (COS) gives strong envelope cues at F0, random phase gives weak envelope cues, while alternating sine-cosine phase (ALT) doubles the envelope repetition rate.

Results
Using the first paradigm, some high-CF neurons (> 3.3 kHz) showed prominent peaks in firing rate when a low-order (up to 7_{th}) harmonic of F0 coincided with the CF, thereby providing rate-place cues to resolved harmonics. This rate-place code was available for higher F0s (> 750 Hz) and appeared to be more robust across stimulus levels than the rate-place code in the auditory nerve of anesthetized animals. With the second paradigm, the firing rates of many neurons peaked for a specific F0 that was unrelated to the CF. While such rate tuning to F0 was observed for both COS and ALT stimuli, the peak for ALT often occurred roughly one octave lower than the peak for COS, suggesting the tuning was dependent on envelope repetition rate.

Conclusion
Two complementary rate codes to the pitch of harmonic complexes are available in IC neuron activity: A rate-place code to the frequencies of resolved harmonics for higher F0, and a non-tonotopic rate code to the envelope repetition rate at lower F0 that is presumably created centrally through transformation of temporal cues in the periphery.

PS 658

Visualizing Population Model Responses of Peripheral, Brainstem and Midbrain Neurons to Complex Sounds

Laurel Carney; Langchen Fan; Natalia Galant; Zejin Li; Braden Maxwell; Danika Teverovsky; Thomas Varner
University of Rochester

Complex sounds are represented by the pattern of discharge rates across the population of auditory-nerve (AN) fibers. This representation is transformed as the information ascends the auditory pathway. There are several ways in which the fine-structure and envelope temporal properties are altered. At low stimulus frequencies (< 600-700 Hz), in the anteroventral cochlear nucleus (AVCN), the synchrony of primary-like response type neurons to the fine-structure of stimuli is enhanced, but at high frequencies their synchrony is reduced. Temporal envelope cues, or amplitude fluctuations, in the stimulus are encoded by fluctuations in the instantaneous discharge rates of AN responses. The neural representations of these envelope cues are shaped by narrowband filtering in the auditory periphery. The AN neural fluctuations are further shaped by nonlinearities such as rate saturation and synchrony capture. All types of AVCN neurons across all frequency channels have enhanced synchrony to the neural fluctuations. This enhanced synchrony to the neural fluctuations increases contrasts in the amplitudes of fluctuations across frequency channels. These contrasts set up differences in discharge rates at the level of the inferior colliculus (IC), where neurons are tuned to low-frequency fluctuations of their inputs. Visualization of these envelopebased contrasts for complex stimuli requires population responses of actual or model neurons. We have developed software to display the responses of the Zilany et al. (2014, JASA 135:283-286) AN model, and simplified models for AVCN and IC neurons (Carney et al., 2015, eNeuro 2:e0004- 15). Contrasts in the fluctuations across frequency channels provide a basis for coding complex sounds. Visualizing responses at several stages of the ascending pathway to stimuli from classic psychophysical studies provides insight as to the cues that are available to listeners based on neural fluctuations. We will illustrate responses to several stimulus paradigms including tones in bandlimited noise and notchednoise maskers, profile analysis stimuli, and stimuli with steep spectral slopes, such as those used in studies of edge pitch and pinna cues.

NOTE: This poster has been added to the meeting.

PD 136

The Role of the Intactness of Binaural Timing Information in Bilateral Cochlear Implants

Katharina Egger; **Piotr Majdak**; Bernhard Laback
Austrian Academy of Sciences

Interaural time differences (ITDs) are important for localizing sounds. ITD cues are only suboptimally encoded with current bilateral cochlear-implant (CI) systems which is reflected in a limited sensitivity to ITDs of bilateral CI users. Practical stimulation strategies have to find a compromise between optimal encoding of ITD cues at the individual interaural electrode pairs and the timing limitations imposed by demands from stimulation at adjacent channels. For example, when ITDs require simultaneous stimulation at two electrodes at the same time, the pulses at one of the electrodes have to be slightly shifted or even removed which, in turn, might compromise the ITD cue. Further, due to signal-processing issues, pulses in the stimulation sequence can be missing at one ear but be present at the other ear, compromising the correct representation of the ITD in realistic bilateral signals.

This study addresses the tolerable room for such variations by investigating the potential perceptual degradations due to inaccurate encoding of ITD cues. We hypothesized that, in a pulse train which correctly encodes ITDs, a removal of pulses will reduce lateralization discrimination and larger ITDs will be required in order to detect the correct stimulus side.

Experiments were performed using interaurally coordinated research interfaces. ITD thresholds for unmodulated, 100-pulse-per-second pulse trains presented at a single, pitch-matched, interaural electrode pair were measured. A baseline condition without pulse removal, i.e., a pulse train which perfectly encodes ITDs, was presented at comfortable loudness. Measurements were performed applying different degrees of bilateral, interaurally uncorrelated pulse removal. Each degree was tested with the same current levels as in the baseline condition, and with stimuli matched in loudness to the baseline condition.

The results provide a link between the inaccurate encoding of ITD cues in terms of pulse removal and the sensitivity to these compromised ITD cues. For large degrees of removed pulses, the removal led to a change in loudness. This in turn can affect ITD sensitivity, similar to previous results showing better ITD sensitivity with increasing current level.

We conclude that inaccurate encoding of ITD cues might deteriorate the sensitivity to ITDs. The tolerable room for pulse-timing variations without significant perceptual degradations and its implications for future stimulation strategies aiming to optimally encode ITD cues in CIs are discussed.

Funding
Supported by MED-EL.

NOTE: The presenting author has changed to *Piotr Majdak.

PS 743

Simulating Cochlear Pathology in a Distributed-Diameter Auditory Nerve Population Model

Gabrielle (Elle) O'Brien; Jay Rubinstein
Department of Otolaryngology Head and Neck Surgery University of Washington

In theory, comparing the neural coding deficits associated with different cochlear pathologies could inform the development of new cochlear implant stimulation strategies optimized for individual listeners. To this end, we demonstrate modifications that simulate pathology in a previously published biophysical computational model of a population of myelinated fibers with normally distributed diameters. This model has been shown to accurately describe temporal response characteristics of single fibers in acutely deafened felines and predict discrimination of Schroeder-phase and sinusoidally amplitude modulated stimuli. Presently, we simulate three distinct cochlear pathologies in the model. First, we evaluate the effects of removing randomly selected fibers from a population of 30,000 auditory nerve fibers on temporal characteristics such as population latency, relative spread, and jitter. The combined population response is analogous to the electrically evoked compound action potential. The random removal of fibers describes a cochlear trauma that does not preferentially affect any subpopulation. Second, we compute the same temporal response measures in a population where small diameter fibers are preferentially removed, simulating the selective neuronal death characteristic of acoustic overexposure (Furman et al. 2013). Finally, we modify the myelinated internodes of the cable model by increasing the membrane capacitance and decreasing the transversal resistance of these segments. We demonstrate the effects of the coordinated manipulation of these two parameters on axonal conduction velocity in a single fiber and select a parameter set that best describes physiological demyelination. In this new model for a demyelinated auditory nerve fiber, we quantify the chronaxie and absolute and relative refractory periods. Taken as a whole, these manipulations of the computational model provide a toolkit for exploring the effects of cochlear pathology on complex stimulus coding.

NOTE: This poster has been added to the meeting.

PS 799

Age-regulated Function of Autophagy in the Mouse Inner Ear

Sara Pulido[1]; Esperanza Bas[6]; Rocío de Iriarte Rodríguez[2]; Isabel Checa[2]; Marta Magariños[2,3,4]; **Isabel Varela-Nieto**[2,3,5]
[1]CSIC-UAM; [2]Instituto de Investigaciones Biomédicas, CSIC-UAM; [3]CIBERER, Unit 761, Instituto de Salud Carlos III; [4]Universidad Autónoma de Madrid; [5]IdiPAZ, Instituto de Investigación Sanitaria; [6]Department of Otolaryngology, University of Miami - Miller School of Medicine

Background

Autophagy is a highly conserved catabolic process essential for vertebrate embryonic development and adult homeostasis. Autophagy induction has been reported to resolve inflammation, to ameliorate ageing and to protect from neurodegeneration. In the inner ear, autophagy has been reported to play roles in chicken otic neurogenesis and in the response to otic injury in the adult mouse (1,2). Here, we will discuss the role of autophagy in late cochlear development and functional maturation.

Methods

Animals. For this study two mouse strains have been used (HsdOla:MF1*129/Sv and HsdOla:MF1).

RT-qPCR. Autophagy genes TaqMan® probes were used and referred to Rplp0 and 18S rRNA as the endogenous housekeeping genes. The estimated gene expression was calculated as $2^{-\Delta\Delta Ct}$.

Western blotting. Autophagic flux was assessed by measuring the levels of microtubule associated protein light chain 3-II (LC3-II) and sequestosome 1 (SQSTM1/p62).

Statistical analysis. ANOVA or Student t-test were carried out with SPSS v19.0 to compare gene expression in the organs, time points and genotypes of each strain. Post hoc analyses included the Bonferroni test. Results were considered significant at $p < 0.05$.

Results

Autophagy machinery genes *(Becn1, Atg4b, Atg5 and Atg9)* were expressed in the mouse cochlea, vestibular system and brainstem cochlear nuclei, although with different expression levels and temporal patterns. Gene expression was up-regulated from perinatal to adult ages in the cochlea of two mouse strains. Protein levels of LC3-II and p62 confirmed that autophagic flux was increased with age. Immunohistochemistry revealed that LC3B was mainly localized in the neurons of the spiral ganglion. *Cox2*, an inflammation marker, showed the same temporal expression profiles as those obtained from autophagy transcripts. In contrast, no evident association with IGF-1 deficiency was observed.

Conclusion

Our data suggests that autophagy is regulated with age in the cochlea and that it plays a role in the functional maturation of the mouse inner ear.

References
1. Aburto MR et al. (2012) Cell death & disease 3: e394.

2. Taylor RR et al. (2008) JARO 9:44-64.

Funding
This work was supported by an Spanish grant from the Ministerio de Economia y Competitividad (SAF2014-53979-R) and European FP7-PEOPLE-IAPP-TARGEAR.

NOTE: Additional author and affiliation has been added.

PS 883

Echo-acoustic Flow Guides Flight in Bats

Kathrin Kugler[1]; Wolfgang Greiter[2]; Harald Luksch[2]; Uwe Firzlaff[2]; Lutz Wiegrebe[1]
[1]Department Biology II, LMU Munich, Großhaderner Str. 2, 82152 Planegg-Martinsried; [2] Chair of Zoology, TU Munich, Liesel-Beckmann-Str. 4, 85350 Freising-Weihenstephan

Common to all airborne animals is the need to react fast and correct to rapid changes in their environment during flight. Visually guided animals tackle this challenge by evaluating optic flow, generated by their movement through structured environments.

Echolocating bats flying in complete darkness cannot make use of optic flow; they can navigate solely by echolocation, i.e. the auditory analysis of self-generated sounds. In contrast to vision, echolocation provides explicit distance information through the analysis of echo delay.

Here we show that bats exploit echo-acoustic flow to navigate rapidly through narrow passages. Specifically, we find that bats' navigation between lateral structures is significantly affected by the echo-acoustic salience of those structures, independent of their physical distance. This is true despite the stroboscopic nature of echolocation which interferes with a motion percept and although echolocation, unlike vision, provides explicit distance cues.

The results demonstrate that sensory flow elicited by self motion is a ubiquitous principle for guidance of flight in the animal kingdom, independent of the fundamentally different peripheral representation of flow information across the senses of vision and echolocation.

Funding
The study was funded by a grant of the Deutsche Forschungsgemeinschaft (DFG) WI 1518/12-1 to L.W.

NOTE: Additional authors and affiliations have been added.

PS 941

Both stimulus strength and rate alter the responding patterns of non-determinant learning procedures in vestibular nucleus.

Gyutae Kim[1]; Sangmin Lee[1]; Kyu-Sung Kim[2]; EunHae Jeon[2]; Hyeon-min Shim[1]
[1]Inha University; [2]Inha University Hospital

Background

The vestibular system is known as one of the most dynamic areas for the non-determinant learning procedures, habituation and sensitization, which the responding intensity decreases or increases, respectively. In general, the neuronal responding intensity changes depending on the stimulus characteristics (strength, type, rate, etc.). However, it is elusive if there is any dominant stimulus factor over others to change the neuronal responding intensity. Here, we investigated the effects of stimulus characteristics, comparing the slopes of habituated or sensitized responses.

Method

We used the galvanic vestibular stimulation (GVS) as a main stimulus type, and all the neuronal activities were recorded in the vestibular nucleus, originated from the lateral vestibular afferents. The obtained data were filtered (bandpass, 0.3-5 kHz) and stored at a sampling rate of 40 kHz (Plexon, US). For a control response, a multiple set of GVS (100μA DC) with a 3-second stimulation and a 60-second resting period (type I stimulation) was applied on the animal's temporal bone and around its muscle. The responding effect by strength or rate was induced by increasing the interval of resting period (120-second) (type II stimulation) or the DC amplitude (200μA DC) (type III stimulation), respectively.

Result

Fifteen neuronal responses from seven healthy guinea pigs (509-604g, males) were recorded by a single tungsten electrode (5-12 MΩ). In each neuron, three slopes by type I, II, and III stimulations were calculated, and each slope was computed by using a linear regression on the multiple averaged firing rates during GVS. The comparison between the slopes during type I and II showed more than half of neurons (9/15, 60%) changed their responding slopes after type II, and the same amount of neurons (9/15, 60%) changed their responding slopes after type III. Seven neurons (47%) changed their slopes in both type II and III, and two neurons (13%) showed no changes in both stimulations.

Conclusion

Based on the data population, we concluded that both stimulus strength and rate of GVS affected the non-determinant learning processes of a neuron. Due to the low modification of neural information in the vestibular nucleus, the changes in neuronal responding intensity were relatively small. However, the conclusion was convinced even after excluding the data with a small slope (absolute value of slope<1). [This research was supported by Basic Science Research Program through the National Research Foundation of Korea (NRF) funded by the Ministry of Education (2010-0020163) and the Ministry of Science, ICT & Future Planning (NRF-2013R1A2A2A04014796).]

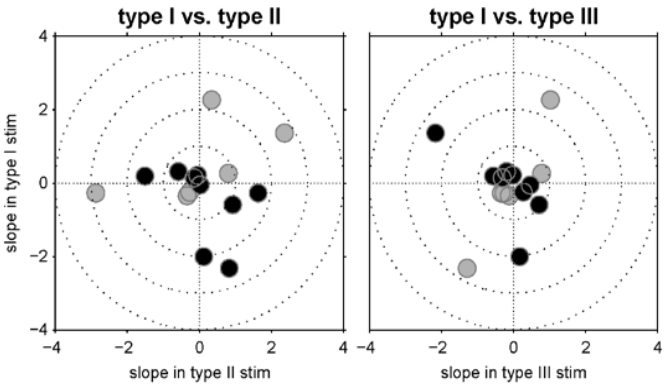

PD 145

Transient Block of Ca2+ Channels by Exocytosed Protons at Mammalian Auditory Hair Cell Ribbon Synapses

Philippe Vincent[1]; Soyoun Cho[2]; Yohan Bouleau[1]; Henrique von Gersdorff[2]; Didier Dulon[1]
[1]University of Bordeaux; [2]The Vollum Institute, Oregon Health and Science University

Background

A synaptic cleft pH regulation of presynaptic Ca^{2+} currents has been described at the ribbon synapses of the retina (DeVries et al., 2001; Palmer et al., 2003) and recently in frog auditory hair cells (Cho and von Gersdorff, 2014). However, this proton regulation has never been reported in mammalian auditory inner hair cells (IHCs). To unmask this process in mouse IHCs, we used a physiological pH buffer solution based on bicarbonate. The transient block of Ca^{2+} currents by exocytosed protons will be used as a proxy for exocytosis that mimics the EPSCs to investigate the mechanisms of vesicular release in mouse IHCs.

Methods

Freshly dissected organs of Corti from pre-hearing (P7) and post-hearing (P14-P18) IHCs from controls (*WT* and *Otof* $^{+/-}$) or otoferlin deficient mice (*Otof* $^{-/-}$) were continuously bathed and perfused with a 95% O_2, 5% CO_2 (carbogen) bubbled extracellular solution in the presence of the physiological pH buffer bicarbonate. Ca^{2+} currents and time-resolved changes in membrane capacitance (exocytosis) were recorded in the whole-cell voltage-clamp configuration from IHCs (Vincent et al., 2014).

Results

Using external bicarbonate solutions, Ca^{2+} currents of post-hearing IHCs showed a notch or fast transient block (I_{Ca}TB) right after their peak onset. This I_{Ca}TB was abolished when adding 10 mM HEPES to the external solution, indicating that it was produced by H^+ release. Remarkably, pre-hearing IHCs did not display I_{Ca}TB, suggesting that this regulation requires a tight coupling organization between Ca^{2+} channels and H^+ release sites. When varying external Ca^{2+}, I_{Ca}TB and exocytosis in post-hearing IHCs was best fit with a nonlinear power function with index 3, likely reflecting the cooperativity of the putative Ca^{2+} sensor otoferlin. Indeed, *Otof* $^{-/-}$ IHCs displayed greatly reduced exocytosis and normal Ca^{2+} currents, but no I_{Ca}TB. Remarkably, at a comparably low *Otof* $^{-/-}$ exocytotic response, WT-IHCs displayed significant I_{Ca}TB, suggesting that the lack of otoferlin desynchronized vesicular fusion. Interestingly, I_{Ca}TB in WT-IHCs was also prevented with 5 mM intracellular BAPTA, a fast Ca^{2+} buffer known to desynchronize vesicular release.

Conclusion

Fast proton regulation of Ca^{2+} channels in the sub-ms range occurs at mammalian auditory ribbon synapses. This process likely contributes to the initial extraordinarily fast spike firing adaptation component of the auditory nerve fibers. Furthermore, analysis of the proton regulation greatly favors an otoferlin-mediated multivesicular release and a nanodomain coupling of Ca^{2+} channels to docked vesicles at the synaptic ribbons of mammalian hair cells.

Funding

Fondation Agir pour l'Audition

NOTE: The presenting author has changed to *Philippe Vincent

PD 200

Wbp2 is required for normal glutamatergic synapses in the cochlea and is crucial for hearing in Mice and Humans.

Annalisa Buniello[1]; Neil Ingham[1]; Morag Lewis[1]; Andreea Huma[2]; Raquel Martinez-Vega[3]; Oliver Houston[4]; Tanaya Bardhan[4]; Stuart Johnson[4]; Izabel Varela-Nieto[3]; Jacqueline White[2]; Huigun Yuan[5]; Walter Marcotti[4]; **Karen Steel**[1]
[1]King's College London; [2]Wellcome Trust Sanger Institute; [3]Instituto de Investigaciones Biomédicas, CSIC-UAM; [4]University of Sheffield; [5]Chinese PLA General Hospital

Steroid hormones are known to be implicated in normal auditory function, and estrogen signalling protects against noise-induced hearing loss. In order to investigate the functional link between hormonal signalling and hearing impairment and identify new targets for therapies, we used Wbp2-deficient mice as a genetic tool. *WBP2* encodes the WW domain-binding protein 2, which is phosphorylated before translocating into the nucleus where it acts as a transcriptional coactivator for the estrogen and progesterone receptors *ESR1* and *PGR*.

Auditory Brainstem Response (ABR) thresholds were raised at high frequencies as early as 4 weeks of age in the *Wbp2*-deficient mice and progressively increased and extended to lower frequencies by 14, 28 and 44 weeks old, indicating progressive hearing loss. Wbp2-deficient mice also show progressive abnormal emissions at high frequencies after recording of distortion product otoacoustic emissions (DPOEs) at 4 and 20 weeks of age. Interestingly, while the gross and cellular structure of the mouse mutant inner ears showed no obvious damage or degeneration up to 30 weeks old, confocal imaging performed at postnatal day 14 (P14), 4 and 8 weeks showed swollen nerve endings below inner hair cells, which is sign of glutamate excitotoxicity. Ribbon synapses showed abnormal morphology after double labelling with pre- and post-synaptic markers (CtBP2 and Glur2/3) in the mutants at 4 weeks of age, and these results were confirmed by transmission electron microscopy (TEM). We built up a pathway to understand the mechanistic link between the loss of Wbp2 and progressive hearing loss, and our data suggest that the phenotype is associated with reduced expression of *Esr1*, *Esr2* and *Pgr* in the cochlea, leading to disruption of expression of key post-synaptic proteins such as Shank3 and Psd-95.

Finally we report the cases of two children with severe to profound sensorineural hearing loss, each carrying two different point mutations in heterozygosis in the *WBP2* gene.

This study describes a new gene involved in the molecular pathway linking hearing impairment to hormonal signalling, and provides new therapeutic targets.

Funding
Wellcome Trust

NOTE: The presenting author has changed to *Karen Steel

Effects of Round Window Occlusion on Intracochlear Pressures

Yew Song Cheng; Xiying Guan; Daniel Lee; John Rosowski; Hideko Heidi Nakajima
Harvard Medical School, Massachusetts Eye & Ear

Background
Reinforcement of the round window (RW) has gained attention recently as a minimally invasive surgical treatment for superior canal dehiscence (SCD). It is theorized that SCD symptoms are improved by decreasing the compliance of the RW. Clinical outcomes from such procedures are varied and the effects of RW manipulations on inner ear fluid mechanics are not fully understood. Here, we quantify the effects of RW reinforcement on intracochlear fluid pressures in fresh human cadaveric temporal bones in baseline-normal state and in simulated SCD conditions.

Method
To measure intracochlear pressures in scala vestibuli (PSV) and tympani (PST), micro-optical fiber pressure sensors were positioned in the respective spaces at the base of the cochlea. Graded reinforcement of the RW was performed using perichondrium, followed by cartilage and then dental impression material in a step-wise fashion. PSV and PST in response to air-conducted sound stimulus in the frequency range of 25-10,000 Hz were measured at baseline and after each incremental reinforcement of the RW. Next, a small defect was created along the lateral aspect of the superior canal to simulate an SCD. Graded reinforcement of the RW was repeated with corresponding measurements of intracochlear pressures.

Results
In the normal temporal bone, RW reinforcements resulted in a graded increase in PSV, PST, and differential pressure across the cochlear partition (Pdiff) in the lower frequencies (f<500 Hz). Pdiff is a measure of cochlear input pressure drive, which provides an estimate of hearing (Pdiff = PSV - PST).

After the creation of an SCD, RW reinforcement resulted in a small increase in PSV (<5dB) around 500 Hz. A variable increase in PST (5-20 dB) at frequencies between 200-1000 Hz was observed. Together, this resulted in small variable increasing or decreasing (5-10 dB) change in Pdiff between 200-600 Hz.

Conclusion
Reinforcing the RW in a normal temporal bone causes a graded increased in PSV and PST. Contrary to current theories, this resulted in an increase in Pdiff.

With an SCD, the effects of RW reinforcement were markedly diminished. The effect on Pdiff is small, frequency band limited and variable across the temporal bones.

Research Funding
Yew Song Cheng, BM. BCh., is funded by the American Otological Society Research Training Fellowship.

Author Index

MANCHESTER GRAND HYATT SAN DIEGO
1 Market Place
San Diego,CA 92101, USA

+1 619 232 1234 **TELEPHONE**
+1 619 239 5678 **FAX**

manchestergrand.hyatt.com

GRAND | HYATT®

FLOOR PLAN

All Floors

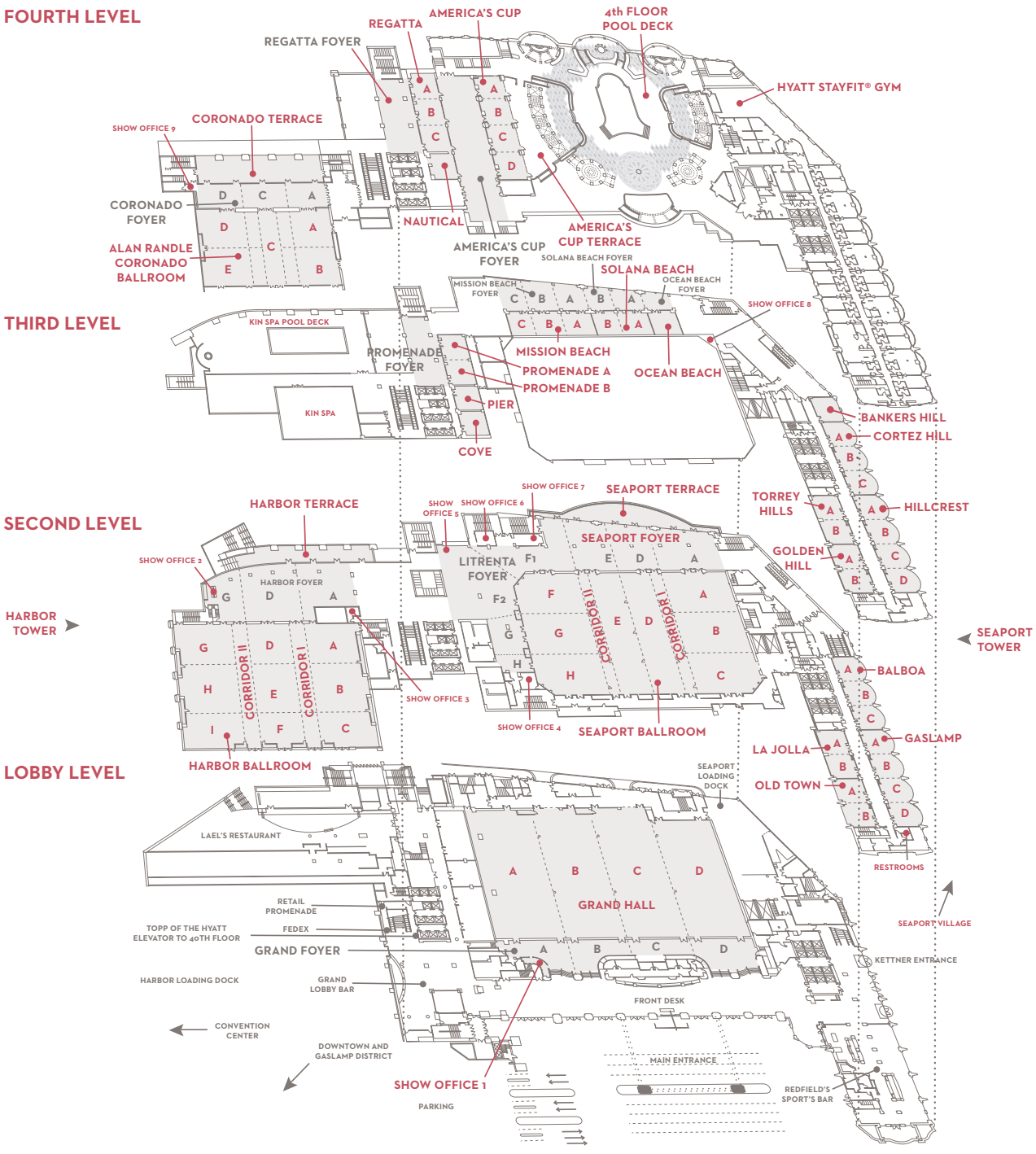

SAVE THE DATES

February 11-15, 2017
40th Annual MidWinter Meeting
Baltimore Marriott Waterfront
Baltimore, Maryland, USA

February 10-14, 2018
41st Annual MidWinter Meeting
Manchester Grand Hyatt
San Diego, California, USA

February 9-13, 2019
42nd Annual MidWinter Meeting
Baltimore Marriott Waterfront
Baltimore, Maryland, USA

Association for Research in Otolaryngology
19 Mantua Road
Mt. Royal, NJ 08061 USA
www.aro.org